A. No. 891
Class. No.
Sh. No. 13 ~~22~~

A TREATISE ON MODERN PHYSICS

ATOMS, MOLECULES, NUCLEI

SCIENTIFIC PUBLICATIONS

BY

The Indian Press, Ltd.

1. A Treatise on Heat by M. N. Saha, D.Sc., F.R.S., and B. N. Srivastava, M.Sc., (in Press) being the thoroughly revised edition of the authors' Text Book of Heat.

2. Heat for Junior Students by M. N. Saha, D.Sc., F.R.S., and B. N. Srivastava, M.Sc., Second Edition (in Press).

A TREATISE
ON
MODERN PHYSICS

ATOMS, MOLECULES AND NUCLEI

VOLUME I

BY

M. N. SAHA, D.Sc., F.R.S.
Professor of Physics, Allahabad University

AND

N. K. SAHA, M.Sc.

LIBRARY

THE INDIAN PRESS, LTD.
ALLAHABAD AND CALCUTTA

1934

IIA Lib.

Printed and Published at The [illegible] Press [illegible]
[illegible]

PRINTED IN INDIA
All rights reserved

TO

SIR JAGADISH CHANDRA BOSE, D.Sc., F.R.S.,

THE PIONEER OF SCIENTIFIC RESEARCH IN INDIA

PREFACE

The object of the present treatise and of the companion volumes which it is intended to publish at an early date is to give a concise, up-to-date and self-contained account of the wonderful series of discoveries which make up the present-day Atomic Physics. As is well-known, progress in this direction began with Röntgen's discovery of X-rays in 1894. This great discovery supplied mankind not only with a new light for looking into opaque matter, but also inspired the Physicists with the novel, nay then almost the revolutionary, idea that beyond the knowledge of physical phenomena accumulated up to 1894, there were other vast fields as yet unexplored. Part of the new ground has since been broken by the active participation of the most acute scientific brains of the contemporary world. Our intention has not been merely to chronicle these discoveries, but rather to present the new knowledge as a consistent story and a logical system of thought. In imposing upon ourselves this task, we have not been unmindful of the great difficulties before us. For the discoveries which make up the new knowledge have often followed without any logical order or sequence, and the developments of underlying thought which are intended to bring order into the system have undergone violent and abrupt changes within short intervals of time. And as very often happens in the first days of exploration, those who have actively participated in these activities, as well as those who have merely kept an intelligent watch on the progress of events, have been equally puzzled by the vicissitude of ideas leading to speculation as well as to work.

It will be acknowledged that it is no easy matter to present an account of the new knowledge when the issues in many cases are still uncertain. The treatment given in the following pages is the result of twelve years' experience of the senior author in lecturing to the B.Sc. (Hons.), and M.Sc. students in Physics of the Allahabad University, and earlier at the Calcutta University. The subject-matter is arranged to cover a course for two years, the easier and more descriptive portions being reserved for the first year. It is needless to add that the teaching programme has to undergo substantial changes almost every year, but the underlying skeleton of this book has remained unchanged, at least for some time. The plan of teaching as outlined in these pages has been found to be quite successful with the students with whom the senior author had come into contact and he hopes that others also will find his scheme workable. We have attempted to make the book as much self-contained as possible without making it too bulky or technical.

It was at first intended to include chapters on Molecular Physics, Interaction between Matter and Light, Wavemechanics and Nuclear Physics, but as the book had already become bulky, it was decided to incorporate these chapters in a second volume. Most of these chapters are almost ready. Messrs. D. S. Kothari of the University of Delhi and Ram Nivas Rai of the Allahabad University are engaged in writing a volume on mathematical physics which, it is hoped, will serve as a more elaborate mathematical supplement to the two volumes.

We feel it our pleasant duty to express our indebtedness to such treatises as Sommerfeld's classical work *Atombau und Spektrallinien*; Pauling and Goudsmit's *Structure of Line Spectra* whose treatment we have closely followed in many places; to the articles by Grotrian and Laporte on Spectroscopy in the *Handbuch der Astrophysik*; also to various volumes of the *Handbuch der Physik and Handbuch der Experimental physik* for several important articles; to Siegbahn's *Spektroskopie der Röntgenstrahlen*, 1931; and to Rutherford, Chadwick and Ellis's *Radiations from Radioactive Substances*, 1930.

THE PHYSICAL LABORATORY,
ALLAHABAD UNIVERSITY.
OCTOBER, 1934.

THE AUTHORS

ACKNOWLEDGMENT

It is a pleasure to acknowledge our grateful thanks to our numerous friends and colleagues who have rendered help in the preparation of the book.

Chapters I and II were critically reviewed by my colleague Prof. S. Bhargava, who helped us also with many valuable suggestions.

Chapters VI and XI.—In the preparation of these two chapters on X-rays we received invaluable help from Mr. J. B. Mukherjee, M.Sc., who was mainly responsible for the preparation of the tables, charts and figures, and accounts of modern works on the subject, as well as of the technical information contained in these chapters. Dr. B. B. Ray of Calcutta favoured us with criticism of the plan and with many other helpful suggestions.

Chapters XII and XIV—on Spectra of Elements. In the preparation of these chapters, we received great help from Mr. L. S. Mathur, M. Sc., research scholar, who wrote and rewrote many of the sections, checked the calculations, collected and arranged the data given in these chapters.

Chapter XIII—on Critical Potentials—was partly written and arranged by Mr. G. C. Mukherjee, M.Sc.

Chapter XV—on Magnetism and its Theories. This chapter owes a good deal to Dr. D. P. Ray Chaudhuri of the University College of Science, Calcutta, who favoured us with many helpful criticisms, valuable suggestions and supplied many useful data.

Besides the above-mentioned friends, we have to express our thanks to Prof. D. S. Kothari, Ph.D. (Cantab.), Head of the Department of Physics, Delhi University, and to Mr. Ram Nivas Rai, M. Sc., Junior Lecturer in the Allahabad University, for many helpful criticisms and suggestions, and to Mr. A. N. Tandon, M. Sc., Empress Victoria Scholar, for help in preparing the index.

It is feared that in spite of the care taken, there have been many errors and omissions. The authors will feel grateful if such errors and omissions are pointed out to them.

We further gratefully acknowledge our indebtedness to the authors and publishers of the following books for permitting us to reproduce the diagrams noted below:—

E. Rutherford, *Radioactive Substances and their Radiations:* Chap. I, Figs. 20a, 27 ; Chap. IV, Figs. 5, 6, 7, 11.

E. Rutherford, J. Chadwick and C. D. Ellis, *Radiations from Radioactive Substances:* Chap. IV, 8, 13, 17, 18, 14, 15, 26 ; Chap. I, 10.

J. J. Thomson and G. P. Thomson, *Conduction of Electricity through Gases:* Chap. I, 17, 17a ; Chap. II, 13 ; Chap. III, 9, 11, 12.

F. W. Aston, *Mass-Spectra and Isotopes:* Chap. III, 5, 6, 7 ; Chap. VII, 6.

Handbuch der Physik: Chap. II, 8, 11, 12, 14, 16; Chap. III, 8, 10; Chap. IV, 6, 10, 19, 29, 30; Chap. V, 4a, 4b, 5, 15.

Hand buch der Experimental physik: Chap. V, 12; Chap. VI, 8, 13, 29, 30, 31, 32, 33, 38, 39, 43, 47, 48b, 50, 61, 63, 68; Chap. XI, 24, 26, 27, 32, 33, 34, 35, 36.

E. Back and A. Landé, *Zeemaneffekt und multiplet-struktur :* Chap. X, 2, 7, 11a.

A. Sommerfeld, *Atombau und Spektrallinien* ; Chap. X, 9a, 9b ; *Atomic Structure and Spectral Lines :* Chap. VII, 17a ; Chap. XI, 4.

M. Siegbahn, *Spektroskopie der Röntgenstrahlen :* Chap. VI, 2, 44, 45, 48a, 52, 60 ; Chap. XI, 2, 5, 6, 7, 9, 10, 11, 12, 23.

E. C. Stoner, *Magnetism and Atomic Structure:* Chap. X, 8 ; Chap. XV, 11, 12, 13. *Magnetism:* Chap. XV, 17.

E. N. da C. Andrade, *Structure of the Atom :* Chap. X, 4, 9.

A. Ruark and H. Urey, *Atoms, Molecules and Quanta :* Chap. XIII, 15.

K. Honda, *Magnetic Properties of Matter :* Chap. XV, 4, 5, 6, 19.

J. H. Van Vleck, *Electric and Magnetic Susceptibilities :* Chap. XV, 18.

Handbuch der Astrophysik : Chap. VIII, 10 ; Chap. IX, 5 ; Chap. XII, 6, 10, 11, 12, 14, 15 ; Chap. XIII, 28, 29.

Ergebnisse der exakten Naturwissenschaften : Chap. V, 8, 9, 10, 11, 13; Chap. XIV, 15, 16 ; Chap. XIV, 22.

J. Franck and P. Jordan, *Anregung von Quantensprungen durch Stösse :* Chap. XIII, 1, 2a, 2b, 5, 6.

G. Hevesy and F. Paneth, *A Manual of Radioactivity :* Chap. IV, 1, 2, 3, 4, 15.

G. Hevesy, *Chemical Analysis by X-rays and its Applications :* Chap. VI, 53 ; Chap. XII. 16.

Townsend, *Electricity in Gases ;* Chap. I, 14, 18.

P. Foote and F. Mohler, *The Origin of Spectra :* Chap. VII, 5, 11 ; Chap. VIII, 3, 8.

R. W. Wood, *Physical Optics ;* Chap. VII, 3, 4.

W. H. Bragg and W. L. Bragg, *X-rays and Crystal Structure :* Chap. VI, 10, 15, 16, 26, 27.

Du Bridge and Hughes, *Photoelectric Phenomena :* Chap. V, 3.

Clarke, *Applied X-rays ;* Chap. VI, 23.

A. Fowler, *Report on Series in Line Spectra :* Chap. VII, 1; Chap. VIII, 1, 2, 5a ; Chap. IX, 3.

Zeitschrift für Physik : Chap. IV, 14a, 14b, 28a, 28; Chap. VI, 49, 74 ; Chap. IX, 19, 20, 21, 23; Chap. XIII, 33, 37 ; Chap. XIV, 17, 18, 20, 20, 23.

Proceedings of the Royal Society of London ; Chap. III, 13 ; Chap. V, 14; Chap. VIII, 4 ; Chap. XI, 22, 28 ; Chap. XIII, 34, 38.

Reviews of Modern Physics : Chap. II, 1; Chap. VIII, 2 ; Chap. 17, 18a, 18, 19, 20, 21.

Philosophical Magazine and Journal of Science : Chap. II, 4.

Annalen der Physik : Chap. VI, 62 ; Chap. VII, 8, 9, 14.

Physical Review : Chap. XI, 30, 31 ; Chap. XIII, 23, 24, 25, 26.

Journal of the Optical Society of America: Chap. VI, 66, 67.

Proceedings of the Physical Society of London : Chap. VI, 64.

Philosophical Transactions of the Royal Society of London : Chap. XIV, 1, 2

CONTENTS

VOLUME I

PAGE

PREFACE vii

ACKNOWLEDGMENT ix

CHAPTER I. Ionisation of Gases 1

" II. The Electron 39

" III. Positive Rays 81

" IV. Elementary Radioactivity 109

" V. Nature of Light 174

" VI. Röntgen Rays 204

" VII. Bohr's Theory of the Spectrum of Hydrogen 319

" VIII. Spectra of the Alkali Metals: the Doublet Spectra 361

" IX. Spectra of Elements of Group II . . . 380

" X. Zeeman Effect 391

" XI. X-ray Spectra 431

" XII. Periodic Classification and Principles of Atom Structure 525

" XIII. Critical Potential of Elements . . . 590

" XIV. Complex Spectra 676

" XV. Magnetism and its Theories 770

APPENDIX: Auxiliary Notes 823

Table of Physical Constants 831

AUTHOR INDEX 833

SUBJECT INDEX 840

LIST OF PLATES

		PAGE FACING
PLATE I :	Positive ray parabolas for H, O, Hg, Ne and CO; The positron track.	86
" II :	Tracks of α-rays from ThC+C′; The curved α-ray tracks in strong magnetic field. . .	143
" III :	Tracks of β-rays from RaD, and of γ-rays from RaC in magnetic field; Relative intensities of modified and unmodified lines in Compton scattering phenomena. . . .	163
" IV :	Laue-spots for ZnS; X-ray diffraction pattern for powder, and for liquid ethyl alcohol. .	250
" V :	Grating diffraction spectra of X-rays; X-ray diffraction pattern by slit; The Balmer lines of hydrogen in Sirius and Vacuum tube; Spectra of Zeta Tauri showing Balmer lines in absorption.	321
VI :	Lines of Pickering-Series (ζ-Puppis); Emission and Absorption spectra of sodium. . .	333
" VII :	Absorption of principal lines of alkalies; H, K and *g*-lines of Ca; Spectra of Zn, Cd and Hg.	374
" VIII :	The diffuse triplet of Ca; Stern-Gerlach-photograph for Ag; Absorption spectrum of Ca vapour; Zeeman effect for singlet (Cd), doublet (Na) and triplet (Zn) spectra. . .	396
" IX :	Paschen-Back effect for oxygen-triplet; X-ray spectra of Hafnium.	427
" X :	Stark-effect for hydrogen and helium lines . .	658
" XI :	Spectra of galactic Nebulae	748
" XII :	Spectra of Mn, and of Fe; Spectra showing the hyperfine-structure of Bi λ4722 and of Tl λ5351 (isotope effect); Zeeman effect in the hfs-spectra of Bi λ4722	752

CHAPTER I

PHENOMENON OF IONISATION OF GASES

1. Electrical Conductivity of Gases.—A gas in its normal state is one of the best insulators of electricity. But it has been known for a long time that under certain circumstances gases may acquire considerable amount of electrical conductivity, for example, when it is illuminated by ultra-violet light, or when it is in the neighbourhood of a heated body. To the early workers there appeared some doubt whether this phenomenon might not be due to leakage through stands of the vessel which enclosed the gas.

Thus Elster and Geitel* showed in 1899 that absolutely dry air possessed certain amount of electrical conductivity. Their apparatus is shown in Fig. 1. The apparatus is essentially an electroscope with aluminium leaves L, standing on an ebonite support B. This is enclosed within a glass flask containing perfectly dry air. Z is the metallic part which carries the leaves, and Y is the metallic mantle completely surrounding Z.

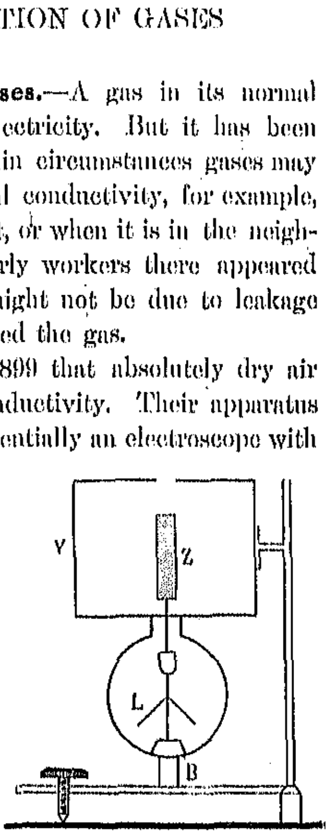

Fig. 1
Elster and Geitel's electroscope.

Z was charged to a potential of about 200 volts. The leaves then diverged due to the repulsion of the electrical charges on them. On standing for some time a slow rate of fall of the leaves was noticeable. The fall is due to loss of charges from the leaves, and this again must be ascribed to conduction across the air surrounding the electroscope, and perhaps partly to the leakage through the ebonite support. The experiment was not very conclusive, as it failed to distinguish between actual conductivity of the enclosed air and the leakage through the insulating parts.

---

* J. Elster and H. Geitel, *Phys. Zeits.*, 1, 11, 1899.

This point was made clear by later works. Extended investigations by Geitel,* C. T. R. Wilson† and others showed that real electrical conductivity could be imparted to an otherwise nonconducting gas by various agencies. A typical experiment (Fig. 2) performed by C. T. R. Wilson which is described below will probably make the matter clear.

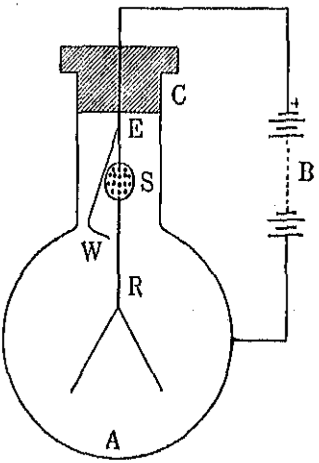

Fig. 2
C. T. R. Wilson's apparatus for testing the conductivity of air.

A	is a spherical vessel, the inside being coated with silver.
C ...	An ebonite plug closing its mouth.
S ...	A block of sulphur.
R ...	A brass rod carrying a pair of gold leaves.
E ...	A brass rod passing through the ebonite C, and carrying S at one end. It is connected to the positive terminal of the battery B. The negative terminal is attached to the vessel.
W ...	A wire which can be manipulated by means of a magnet from the outside, so as to make it touch R at will.

A constant difference of potential is always maintained between E and the silver face of the vessel by means of the battery B. The gold leaf system is charged to the same potential as E by bringing in contact with it the iron wire W by means of a magnet. On breaking the contact the leaves become insulated, and they diverge under mutual repulsion of electrical charges on the leaves.

Since the gold leaf system has a small electrical capacity, a small change of the electrical charge on it is likely to produce a considerable change in its potential, and hence in the divergence of the leaves. Under normal conditions of the enclosed gas, the leaves are found to collapse very slowly when observed under the microscope. But on passing ultra-violet light through the gas the leaves were found to collapse rather rapidly.

---

* H. Geitel, *Phys. Zeits.*, **2**, 116, 1900.

† C. T. R. Wilson, *Proc. Camb. Phil. Soc.*, **11**, 32, 1900; *Proc. Roy. Soc.*, **68**, 151, 1901.

The interpretation of the above observations is simple. It is apparent that any conduction across the sulphur plug will tend to restore the potential of the leaves, and maintain their divergence steady. Since the leaves are otherwise in a perfect state of insulation, leakage of charge must have occurred across the enclosed gas. In fact, both Geitel and Wilson found that the normal leakage varied as the volume of the vessel, amounting to 10^{-8} V units per sec., at atmospheric pressure, where V denotes the volume. Since the rate of leakage is normally extremely slow, the gas must be regarded as an almost perfect insulator under normal conditions; but when exposed to the action of ultra-violet light and certain other agencies to be mentioned presently the gas acquires considerable conductivity, and the charge on the gold leaves gets neutralised and they rapidly collapse. If the external agent be withdrawn, it is seen that the conductivity diminishes, until finally it reaches normal value.

2. The Ionisation Hypothesis.—To account for this acquired conductivity, it was postulated by J. J. Thomson[1] and others, that air when subjected to these agencies (ultra-violet light, X-rays, etc......) becomes ionised, that is, particles containing negative and positive charges are produced throughout the volume of the gas, so that when it is placed between two electrodes connected to negative and positive terminals of a source of E.M.F. the positive carriers are attracted to the negative electrode and the negative carriers to the positive, thus gradually neutralising the charges on the leaves. The acquired conductivity of the gas is due to the movement of the carriers. These carriers of electricity are called *ions*, and the phenomenon is known as *ionisation*. The agency which is responsible for the ionisation of the gas is known as the *ionising agent*. On removing the ionising agent, the fresh supply of ions is cut off, and those already present gradually lose themselves by mutual collisions.

3. The Various Ionising Agents.—Besides ultra-violet light and heated bodies many other ionising agents have been discovered since 1895. Such are, for example, X-rays radiations from radioactive bodies (α, β, γ rays), flames, chemical action, etc. The study of ionisation due to radiations, from radio-active bodies is illustrated in the following experiment. The apparatus used is shown in Fig. 3 and described below.

A and B are two parallel plates kept within a closed chamber from which they are insulated by means of sulphur plugs *s*, *s*. Sulphur plugs are used because sulphur is found to be a very good insulator.* The gas of which the ionisation is to be investigated is enclosed in the chamber.

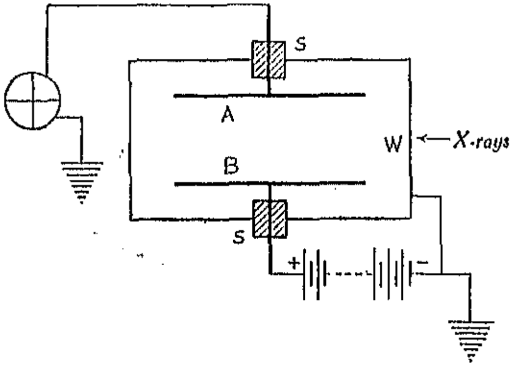

Fig. 3. The Ionisation chamber.

The measuring instrument may be a quadrant electrometer, or electroscope, or some other equivalent apparatus. For the present we take it to be a quadrant electrometer Q. One pair of quadrants is connected to A, and the other pair of quadrants is earthed. A difference of potential is, therefore, maintained between A and B which can be easily measured by means of a potentiometer. The body of the closed chamber is earthed so as to shield A and B against the action of any stray electrostatic field.

The ionising agent may be placed either on the plate B, as in the case of substances like Thorium or Uranium, or it may be put outside and the radiation allowed to pass through the window W.

The gas particles are broken up into positive and negative ions by the action of the ionising agent, and the ions of appropriate sign are attracted to the electrode A, which instantly shares its charge with the electrometer. A difference of potential is thus established between the two pairs of quadrants of the electrometer which consequently causes a deflection of the needle. As more and more charges accumulate on the plate A, the difference of potential, and hence the deflection of the electrometer needle gradually increases. The movement of the ions between the two plates is equivalent to a current flowing between them. This is known as the *ionisation current.* The rate of change of deflection of the electrometer is a measure of

---

* A comparison of the insulating power of a number of substances is given in the following table.

Paraffin ...	500	Mica ...	90	Rubber ...	200	Quartzglass ...	5000
Sulphur ...	1000	Glass ...	66	Porcelain ...	3	Wood (Mahogany)	0·4

For comparison the insulating powers of a few good conductors are given below:

Bismuth ...	10^{-10}	Manganin ...	$3{\cdot}8\times10^{-10}$
Ironsulphide ...	$1{\cdot}12\times10^{-15}$	Copper ...	$1{\cdot}5\times10^{-20}$

The values are in units of 10^{14} ohm^{-1}.

the current, and of the intensity of ionisation. The details of measurement of the ionisation current are given in §4.

The closed chamber described above, in which the phenomenon of ionisation takes place is known as the *ionisation chamber*. Under different forms the ionisation chamber is very frequently used in radio-metric measurements.

The ionisation due to other agents may also be studied by experiments similar to those described above. Such studies have made it clear that though ionisation is produced by all the different agents mentioned above, there is a considerable difference regarding their mode of action. While the ionisation produced by X-rays and ultra-violet radiations are found to be uniform throughout the volume of the ionisation chamber, that due to radioactive radiations are unsymmetrical, being strongest near the plate containing the active substance, and it gradually diminishes at greater distances from the plate. This interesting result, as we shall see later, has led to closer investigations on the passage of radioactive radiations through gases.

4. Use of Electrometer and Electroscopes for the Measurement of Ionisation Currents.—The amount of current to be measured in such experiments is extremely small and may be of the order of 10^{-13} to 10^{-15} amperes. If very strong ionising agents are available, a sensitive galvanometer may be used. But for currents of the order of 10^{-13} to 10^{-15} amperes the quadrant electrometer and electroscopes are found to be the only apparatus which can be used.

We shall now explain how the ionisation current can be quantitatively estimated from the rate of deflection of the needle as described in §3. The adjustments and calibrations necessary for this purpose are as follows.

(1) *The constancy of zero reading.*—Initially, the needle of the electrometer must be symmetrically situated between the two pairs of quardants. To ensure this, both the pairs of quadrants, as well as the needle, are earthed. Then the needle is insulated, and a charge given to it by connecting it to a source of high potential. If the conditions are satisfactory, *the needle remains undeflected.* Otherwise, this condition is attained by levelling the base of the instrument, and adjusting the torsion of the suspending fibre. This being done, the needle will return to the same zero reading always after deflection, and equal and opposite charges to the quadrant will produce equal deflections on either side of zero.

(2) *Calibration of the deflection for voltage.*—For calibrating the instrument, the plate A (Fig. 3) and one pair of quadrants are raised to

definite voltages which can be measured by a potentiometer, and the deflections are plotted against the potential. According to the elementary theory of the quadrant electrometer, with a high potential on the needle, the deflection of the instrument should be directly proportional to the difference of potential applied between the two pairs of quadrants. This can be seen from the expression[2]

$$\theta = K(V_1 - V_2)\left(V - \frac{V_1 + V_2}{2}\right) \quad . \; . \; . \; . \; . \; . \; . \; . \; (1)$$

where $V_1 - V_2$ is the difference of potential between the two pairs of quadrants, V is the potential of the needle, K the constant of the instrument and θ the deflection. When V is very high compared to potential of the quadrants,

$$\theta = K(V_1 - V_2)V \quad . \; . \; . \; . \; . \; . \; . \; . \; . \; . \; . \; . \; (2)$$

i.e. $\theta \propto V_1 - V_2$, when V = constant ;

and $\theta \propto V$, when $V_1 - V_2$ = constant.

In practice these results are found to be only approximately true. An actual calibration curve being plotted, the potential for any deflection may be immediately obtained from it.

The potential to which the electrometer needle is to be charged also requires careful selection. Though according to simple theory (eqn. 2) the deflection for a constant potential of the quadrants should be proportional to the voltage of the needle, in reality this is far from being true. The movement of the needle between the charged quadrants causes a variation in the electrostatic field acting between the needle and the quadrants. This is due to the distorsion of the lines of force between the two systems on account of motion of the needle. This gives rise to an additional couple depending upon the potential of the needle and other minor factors. The couple may be either in the direction or in opposition to the restoring couple due to the torsion of the fibre. The actual nature of the variations of the deflection with the potential of the needle is shown in Fig. 4, in which the curve *ab* corresponds to the case of the additional couple aiding the torsional couple, and the curve *c* represents the opposite case. The mathematical theory[3] of the correction is given in Makower and Geiger's "*Practical Measurements in Radioactivity*," Chapter 1.

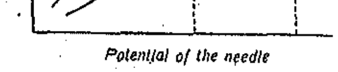

Fig. 4
Sensitiveness of Quadrant electrometer.

In the measurement of currents, in addition to the distorsional couple, a new couple caused by the reaction of the charges set up on the quadrants by the motion of the charged needle arises. This is called the inductional couple and its action is analogous to the damping effect of a loop of wire on the moving coil of a galvanometer. To avoid this it is advisable to keep the needle potential fixed throughout, and to use the same part of the scale.

(3) *Capacity of the electrometer.*—It will be seen just now that in order to measure currents with quadrant electrometers, absolute determination of its capacity is necessary. For this purpose, the needle is connected to a source of high voltage, and the two pairs of quadrants are connected to the two terminals of a cell of e.m.f. E. An amount of charge q_1 flowing from the battery collects on the quadrants. Due to this the deflection of the needle rises steadily from o to θ within a time t_1 which is noted. Now a standard condenser having the capacity C_0 is connected in parallel to the two pairs of quadrants. Using the same cell, now a longer time t_2 is required for getting the same deflection θ. Let a charge q_2 collect on the quadrants in this case. If C be the capacity of the electrometer,

$$q_1 - it_1 = CE$$

$$q_2 = it_2 = (C+C_0)E$$

where i denotes the corresponding current. We thus get

$$C = \frac{C_0 t_1}{t_2 - t_1}$$

which gives the capacity.

After these adjustments connections are made to the ionisation chamber as stated in §3. The needle will at once show a deflection, which will remain steady if no ionising agent be present, or if there is no leakage. But usually, there is always a small leakage present. This should be observed first and allowed for in subsequent readings. Then the chamber is exposed to the action of the ionising agent. The deflection will now change more rapidly depending upon the strength of the ionising agent. This is due to the fact that a current passes to the insulated plate, and begins to charge this and the pair of quadrants connected to it.

If C=capacity of the electrometer plus the plate connected to it, $=V$ the potential acquired by it at any instant t due to a charge Q imparted by the ions, the ionisation current

$$i = \frac{dQ}{dt} = C\frac{dV}{dt} = C\frac{V_1 - V_2}{t}, \quad . \quad . \quad . \quad . \quad . \quad (3)$$

where V_1 = potential at the beginning, and V_2 = potential at the end of t seconds. If V be measured in volts, C in centimeters (e. s. units of capacity), and t in seconds,

$$i = \frac{1}{300}\,\frac{C(V_1-V_2)}{t}\ \text{electrostatic units}$$

$$= \frac{10}{300\times3\times10^{10}}\,\frac{C(V_1-V_2)}{t}\ \text{amperes}$$

$$= 1{\cdot}11\times10^{-12}\,\frac{C(V_1-V_2)}{t}\ \text{amperes.}\quad\ldots\ldots\quad(4)$$

In modern types of electrometers (Dolezalek, Wulf, Lindemann and Compton types) the capacity is extremely small, of the order of 10 cms. So the sensitiveness is very great. Thus a Dolezalek electrometer gives a deflection of about 1000 divisions per volt, at the rate of one division in 10 seconds.

An arrangement of apparatus for the use of electroscope in ionisation experiments is shown below in Fig. 5.

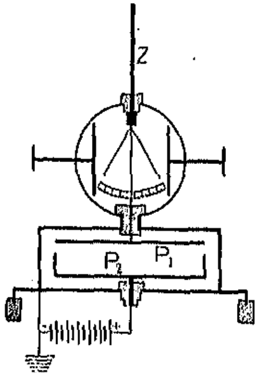

Fig. 5
Arrangement for using the Electroscope.

Z = Rod for charging the gold leaves.
P_1 = Upper plate of the ionisation chamber, which is in metallic contact with the gold leaves.
P_2 = Lower plate, on which the active substance is spread. It is connected to the positive pole of a battery, the negative of which together with the body of the ionisation chamber is earthed.

Thus a difference of potential is maintained between P_1 and P_2, and as the ionisation current flows between them, the leaves of the electroscope receive additional charges, under which they continually diverge. The rate of movement of the leaves can be read on a scale behind them through a suitable window by means of a telemicroscope. As in electrometers, the natural leakage of the instrument must be allowed for, and a calibration curve may be used.

The above arrangement is known as the "Ionometer". The change in potential occurring in a given interval of time can be known from the change in deflection of the leaves during the interval.

The sensitiveness of the electroscopes is also very great. Thus in most cases they give a deflection of about 200 divisions per volt, at the rate of one division in 10 seconds. In an actual experiment, a brass electroscope of volume one litre showed a fall of potential of 6 volts in one hour. Its capacity was one centimeter. So the ionisation current according to eqn. (4) was

$$i=\frac{1{\cdot}11\times10^{-12}\times6}{3600}$$

$$=1{\cdot}9\times10^{-15}\text{ amperes.}$$

This is the order of the current measurable by an electroscope or an electrometer. The electroscope has a smaller capacity than an electrometer; the former is therefore more current sensitive than the latter. But the voltage sensitiveness of the two instruments is in the reverse order.

5. Other Types of Electrometers and Electroscopes.—Many special forms of electrometers and electroscopes have been devised by various workers for special purposes. We shall give a brief account of the most important of them.

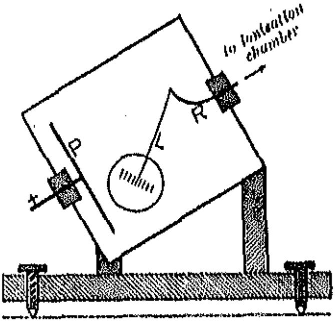

Fig. 6. The Tilted Electroscope.

Electroscopes: (1) The Tilted Electroscope.—A particularly sensitive electroscope was devised by C. T. R. Wilson* for measuring ionisation currents which are so feeble that they do not admit of accurate measurement by electrometers. This is known as Wilson's 'tilted" electroscope, and is shown in Fig. 6. A single foil of a thin gold leaf L is attached to a conducting rod R. The whole is mounted inside a brass chamber through sulphur insulation. An insulated plate P is placed close to the opposite wall of the chamber and charged to a constant potential (generally 200 volts). The entire chamber is kept in an inclined position relative to the base, and the angle of inclination is adjustable. For a given potential of the plate and a certain critical inclination of the chamber the gold leaf is particularly unstable. A little below this point the instrument has the maximum sensitiveness. In a particular experiment with a potential of 207 volts on the plate, the critical tilt was found to be 30°.

After adjusting the tilt of the instrument the gold leaf is earthed and a microscope provided with a scale in the eye-piece is focussed on the leaf so that it rests on the zero position of the scale. The leaf is then insulated, the source of potential to be measured is connected to R and the movement of the leaf is noted.

---

* C. T. R. Wilson, *Proc. Camb. Phil. Soc.*, **12**, 135, 1903.

(2) *Wulf's Electroscope.*—A modified form of electroscope shown in Fig. 7 has been used by Wulf* in his investigations on atmospheric ionisation. In this (see Fig. 7) the gold leaves are replaced by a double quartz fibre LL coated with silver to make it conducting. The quartz fibre is fixed on an insulating support S and its lower ends are stretched together by a quartz bow B. The source of potential (one plate of the ionisation chamber) is brought in contact with the fibres. This causes a movement of the fibres that can be observed under a microscope. This arrangement is specially suitable for measuring ionisation current at sea, as the movement of the fibres remains unaffected† by the motion of the ship.

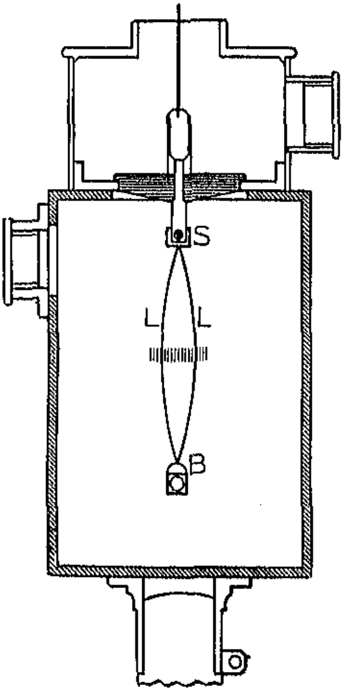

Fig. 7. Wulf's Electroscope.

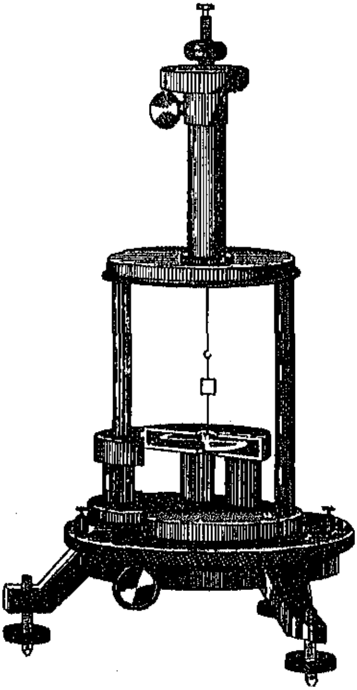

Fig. 8. Dolezalek Electrometer.

Other forms of sensitive electroscopes have been designed for the measurement of ionisation current due to radioactive radiations. These are known as α, β and γ-ray and emanation electroscopes, and they will be described later in the chapter on Radioactivity.

---

* Wulf, *Phys. Zeits.*, 8, 246, 537, 780, 1907; 9, 1090, 1910.

† Simpson and Wright, *Proc. Roy. Soc.* A, 85, 175, 1911.

Electrometers.—The electroscopes described above, though very sensitive, are limited in their range of application. In this respect the electrometers are very useful, as they can be used for a large range of currents. Like electroscopes the electrometers have also received various modifications in the hands of different workers. The important among these are:—

(1) *The Dolezalek Electrometer.*—The sensitive form of quadrant electrometer commonly used in ionisation measurements is that devised by Dolezalek.* The instrument is shown in Fig. 8. In this the needle is made of silvered paper and is consequently very light. It is suspended by a fine quartz fibre, and lies fairly close to the quadrants. Generally the sensitiveness of a quadrant electrometer increases to a maximum for a critical potential of the needle, and then it decreases with further rise of potential (see curve, Fig. 4). In order to take advantage of this condition the needle is charged to the critical potential. On account of lightness of the needle and its closeness to the quadrants, it acts as its own damper. The sensitiveness attained is very high, *viz.*, the order of several thousand divisions per volt.

(2) *Compton Electrometer.*—A. H. Compton† has designed an electrometer (Fig. 9) which is essentially a Dolezalek electrometer of which the needle NN is slightly tilted along its axis, and one pair of quadrants Q is a little below or above the plane of the other. These modifications have been found to greatly enhance the sensitiveness of the instrument which amounts to as much as 15,000 mm. per volt. The tilt and the elevations introduced are so slight that these do not materially affect the uniformity of scale deflection, or rapidity of taking readings. On account of increased sensitiveness, the instrument is, however, rather difficult to handle, except in the hands of experienced workers.

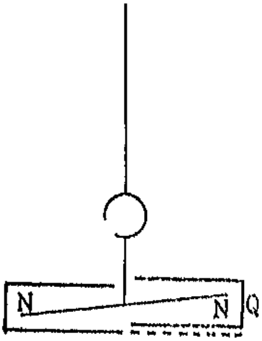

Fig. 9
The Compton Electrometer.

(3) *The Lindemann Electrometer.*—The Lindemann Electrometer‡ is, perhaps, the most convenient form of electrometer with a sensitivity in no way inferior to the Dolezalek type of instrument and yet requiring practically no adjustments which are often so cumbersome with the latter. Besides being sensitive and handy, it has the further advantage of possessing a very small capacity (usually about one or two centimeters) and a very low period, so that it is very sensitive not only to very low potentials but also to very minute currents, and may be used in cases

---

* F. Dolezalek, *Verh. d. D. Phys. Ges.*, 3, 18, 1901. *Ztschr. f. Instr.* 21, 345, 1901.

† A. H. Compton, *Phys. Rev.*, **14**, 58, 1919.

‡ Lindemann, *Phil. Mag.*, **47**, 577, 1924.

where rapidly varying potentials or currents are to be detected. Further, the Lindemann Electrometer gives readings which are practically quite independent of tilt, neither the sensitivity nor the position of zero being appreciably affected by this process.

The principle of the instrument is more or less the same as that of the quadrant electrometer. It consists of four cross-connected plates (Fig. 10) A, A and B, B with planes perpendicular to the plane of the paper; the needle NN, which has the shape of a very thin cylindrical pointer, is suspended at its centre O on a *torsion fibre* in such a way that it can rotate between the plates, that is to say, the torsion fibre is placed perpendicular to the needle and parallel to the plane of the plates and therefore perpendicular to the plane of the paper. It is fixed at both ends on the tips of a rigid U-shaped frame (not shown in the diagram). The whole thing is enclosed inside a small cylindrical brass box provided with two holes on the plane faces covered with microscope cover-slides through which to observe the deflections of the needle. This box may be mounted on a vertical stand with its plane faces vertical, and the motions of the end-point of the needle may conveniently be observed with a suitable microscope also attached to the stand. It is, therefore, evident that since no mirror is attached to the needle and it is itself very light, the moment of inertia of the moving parts is extremely small. Hence, in order to increase the sensitivity of the instrument we may use a very small torsional couple without any danger of allowing the period to become large, which, in these instruments, is of the order of a few hundredths of a second.

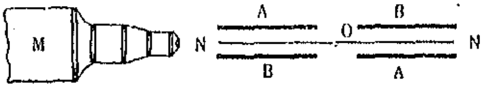

Fig. 10. The Lindemann Electrometer.

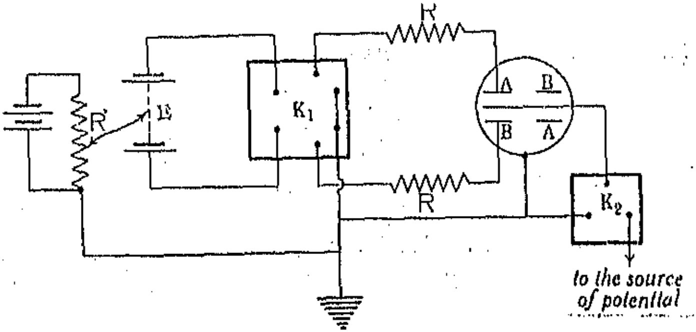

Fig. 11. Arrangement for using the Lindemann Electrometer.

Use.—The mode of using the electrometer is illustrated in the adjoining diagram (Fig. 11). Potential to the plates A, B is applied by means of a battery E through very high safety resistances R, R (about one megohm).

With the help of the commutator K_1, we may charge the *plates* or earth them as we please. Similarly, the *needle* may be either earthed or connected to a given source of potential by means of the key K_2. The rheostat R′ serves to make slight adjustments in the value of the potential of one pair of quadrants B B. It is important to note in this connection that under ideal conditions the needle, if earthed, should not deflect, if the plate A is as much above as B is below the potential of the needle. But owing to some such cause as imperfect symmetry of the needle with respect to the plates the relative potentials of the latter with respect to the needle will have to be adjusted by changing the potential of the middle point of the battery, in order to bring the needle back to the zero position. When this is done the instrument is ready for use. The sensitivity of the electrometer may be varied within wide limits by changing the value of the field. Of course, the observed deflections will depend on the magnifying power of the microscope, but it is claimed that potentials as low as $\frac{1}{4,500}$-th of a volt may be detected.

(4) *The String Electrometer.*—The electroscopes and electrometers described so long are not suitable for measuring rapidly varying ionisation currents, for, the slow movement of the needle cannot keep pace with the high frequency of alternation of the currents. A single fibre electrometer has been devised by Laby,* Elster and Geitel† and others‡ for this purpose. The principle of this instrument is shown in Fig. 12. A single platinized quartz fibre L is suspended centrally between two parallel metal knife-edges K,K which are charged to equal and opposite potentials (about 200 volts). On giving a rapidly varying charge to the fibre it vibrates with some frequency due to the attraction and repulsion of the knife edges. The movement can be reproduced on a revolving photographic plate. This electrometer is specially useful for studying the rapidly discontinuous ionisation due to the emission of α and β rays from radio-active bodies.

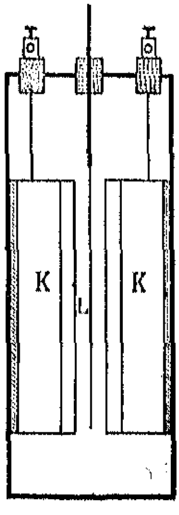

Fig. 12
The String Electrometer.

A comparison of different types of electrometers and electroscopes described above has been shown in the following table 1.

---

* Laby, *Proc. Camb. Phil. Soc.*, 15, 106, 1909.
† Elster and Geitel, *Phys. Zeit.*, 10, 664, 1909.
‡ Lutz, *Phys. Zeit.*, 9, 100, 1908.

Table 1.

COMPARISON OF THE SENSITIVENESS OF DIFFERENT TYPES OF MEASURING INSTRUMENTS.

Instrument	1 Scale Division =Volts	Method of Observation	Capacity
Wilson's tilted electroscope.	5.10^{-3} ...	Micrometer microscope	A few cms.
Elster and Geitel electroscope	3.10^{-3} ...	Microscope ...	2 cm.
Wulf electroscope ...	1.1 ...	Microscope with scale.	3—4 cm.
Dolezalek electrometer.	1.10^{-3} to 1.10^{-4}	Telescope with scale.	50 cm.
String electrometer ...	1 ...	Microscope ...	4—10 cm.
Compton electrometer	6.10^{-4} ...	Telescope ...	
Lindemann electrometer.	4.10^{-4} ...	Microscope ...	1—2 cm.

6. Nature of Ionisation : Variation of Ionisation-Current with Voltage.

We shall now return to a closer study of the phenomenon of ionisation of gases treated in § 3. It has been explained there that in order to observe the current due to ionisation, it is necessary to apply a steady potential difference between the plates of the ionisation chamber. The magnitude of the ionisation current is found to vary in a characteristic manner with the variation of the applied potential. This is illustrated by the curve in Fig. 13, in which the ordinate represents the ionisation current and the abscissa

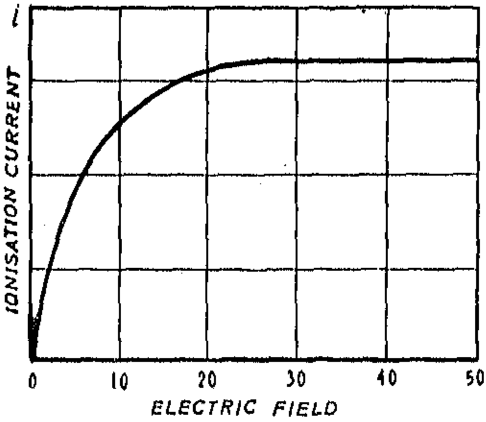

Fig. 13

Variation of ionisation current with potential.

the applied voltage. It is found that at first the current increases almost linearly with the voltage, then the rate of increase slows down and ultimately a steady value is reached, after which the current does not further increase with increase of the potential difference. At this stage the current is said to be *saturated*. This effect is illustrated by the horizontal part of the curve in Fig. 13.

The phenomenon receives a simple explanation on the ionisation theory. The action of the ionising agent is to break the gas particles into negative and positive ions throughout the volume of the ionisation chamber, and thus to produce ions at a definite rate. But the ions are constantly moving about within the chamber and are frequently colliding with one another during their motion. As a result, some of the positive and negative ions are recombining into neutral gas particles. So before the application of the electric field the number of ions produced per unit volume gradually increases, but finally an equilibrium is attained when the number of fresh ions produced per second is exactly equal to the number lost by recombination. When the electric field is applied, the positive ions begin to move towards the negative plate, and the negative ions to the positive. If the applied voltage is very small, the ions would take a considerable time to reach the plates, during which most of them will be lost by recombination. So the ionisation current will be very small. On increasing the difference of potential the ions will gain in speed, the recombination will be less, and consequently the ionisation current will increase. This process will go on until the applied potential is so large that as soon as the ions are formed, all of them are immediately removed to the plates and there is scarcely any time for recombination. Further increase of potential cannot increase the current any further. This corresponds to the constant saturation current.

Besides the rate of recombination, and the velocity of the ions, the saturation potential depends also upon a number of other conditions. Thus the saturation voltage increases with the increase in the distance between the plates, and for a given distance between the plates, it increases with the intensity of ionisation, and for a given intensity of ionisation it diminishes rapidly with the lowering of the gas pressure between the plates. The fall in the value of the saturation voltage with fall of pressure is due to two causes. Firstly, the lowering of pressure decreases the ionisation; and secondly, the velocity of the ions increases which diminishes the rate of recombination. Both these factors cause the saturation to take place at a lesser voltage.

Townsend* and von Schweidler† have shown that at *very low* pressure the nature of the variation of ionisation with potential is very different from that at ordinary pressure (*e.g.*, one atmosphere). The curve in Fig. 14 represents the nature of the variation of current for air at a pressure of 2 mm. due to ionisation by X-rays. It is observed that within a certain limiting voltage the phenomenon is similar to ordinary ionisation at one atmosphere pressure. This is exhibited by the part OAB of the curve. But as the voltage increases beyond this critical value (corresponding to B) the ionisation current increases, at first slowly, but very soon very rapidly, until the current is so great that a spark passes between the two electrodes. The minimum potential at which the spark passes is known as the *Sparking Potential.* To explain this phenomenon Townsend assumes that if at a very low pressure the applied potential exceeds a certain limit, the ions begin to move so fast that they ionise by their impact the air molecules which they encounter in their way. This phenomenon is called the *ionisation by collisions.* At first only the negative ions take part in the process on account of their greater efficiency in this respect. The fresh ions cause a slow increase in the ionisation current. But if the potential is still further increased the positive ions also take part in the process and the ionisation current increases very rapidly. This is shown by the part BC of the curve. Finally, the conductivity of the gas becomes so great that electric charges actually jump from one electrode to another, just as they pass through a conductor. Here the sparking commences.

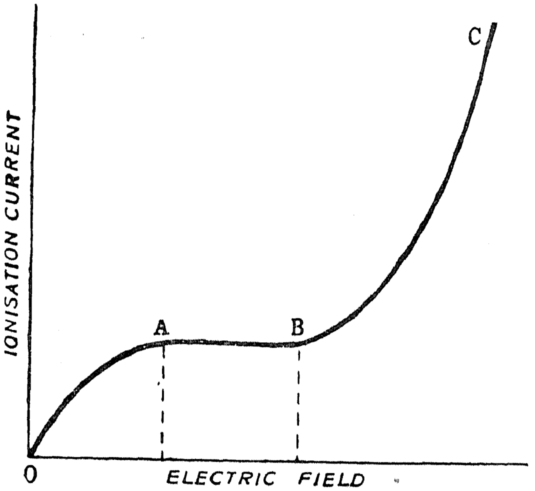

Fig. 14. The complete ionisation curve.

It has been found that sparking potential is directly proportional to the pressure of the gas. Thus for air at atmospheric pressure it is about 30,000 volts per cm.; while at a pressure of 1 mm. it may be as small as 40 volts per centimetre. The exact law of the variation of sparking potential with pressure has been given by Paschen,* who, as the result of a large number of observations, concluded that the sparking potential is a function only of the product of the distance between the electrodes (the sparking distance) and the pressure of the gas, or, in other words, of the mass of the gas in unit area between the electrodes. This is known as *Paschen's law*.

---

* Townsend, *Phil. Mag.*, **1**, 79, 1901 ; **3**, 557, 1902.

† Von Schweidler, *Wien Bericht.*, **108**, 273, 1899.

7. On the Physical Nature of the Ions.—So long we have been talking of the '*ions*' in a rather loose fashion. We have not definitely stated whether they are molecules, or clusters of molecules, or something smaller than molecules. The early investigators started with similar vague ideas, which became clearer as detailed investigations were carried out on the motion, diffusion, and the charges carried by the ions. So we shall begin with a brief account of these early investigations and then see what light they throw on the physical nature of the ions.

Mobility of Ions.—When the space in which ions are formed is subjected to a uniform e.m.f. the ions are subjected to a force eX, where X is the field strength. The equation of motion would be

$$m\frac{d^2x}{dt^2}+c\frac{dx}{dt}=eX$$

where $c\frac{dx}{dt}$ is a frictional term, which opposes motion. If this be rather small, and can be neglected, the motion becomes accelerated. If, on the other hand, $c\frac{dx}{dt}$ is large, we can neglect $m\frac{d^2x}{dt^2}$ and the motion becomes uniform. Actual observations showed that the motion of the ions is uniform and proportional to the applied field. Thus the second assumption is correct. In this case, the final velocity

$$V=\frac{dx}{dt}=\frac{eX}{c}=kX \quad . \quad . \quad . \quad . \quad . \quad . \quad . \quad . \quad (5)$$

is found to be proportional to the field-strength; and to the velocity observed when $X=1$, the term '*mobility*' is applied. Thus in equation (5) k stands for mobility of the ions. The reason for this kind of motion is that the 'ions' are large clusters of molecules, and, as they move through the gas, their motion is impeded by large forces of viscosity. The mobility can be experimentally determined in various ways, of which two are described below :—

---

* Paschen, *Wied. Ann.*, **37**, 79, 1889.

(*i*) *Rutherford's Method.*—Rutherford* determined the interval required for the ions moving under a known electric field to travel a given distance directly by the following arrangement (Fig. 15).

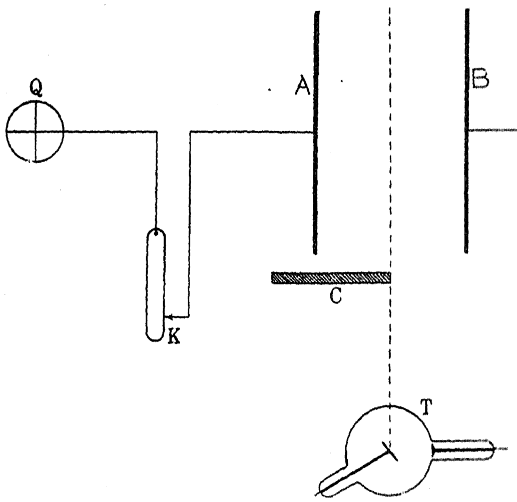

Fig. 15. Rutherford's arrangement for the determination of mobility of ions.

A, B is a pair of parallel metal plates enclosing the gas under investigation.

E is a battery whose positive terminal is connected to B, and the negative terminal is earthed.

K is a make and break key, which may be of the form of a moving pendulum, that closes the circuit between the plate A and a quadrant electrometer Q at one point of its path of oscillation.

T is an X-ray tube. It generates X-rays at a known regular interval, on account of the making and breaking of the secondary circuit of a transformer which feeds the tube by a similar pendulum arrangement.

C is a thick screen of lead, so placed between the plates and the X-ray tube that the gas in one-half of the space only between the plates can be exposed to the action of X-rays.

Thus X-rays are being produced intermittently, and the electrometer circuit is also being closed and opened at regular intervals. The time elapsing between the two processes: (1) the switching-on of the X-ray tube circuit, and (2) closing of the electrometer circuit, can be adjusted. But in order that the electrometer may give any deflection the time interval between the two processes must be at least equal to that required for the ions to travel from the dotted plane to the plates. In actual experiment the time interval is gradually increased. If t = the critical time interval, $2d$ = distance between the plates, and V = the applied potential, the mobility of the ions is given by

---

* E. Rutherford, *Phil. Mag.*, (5) **44**, 429, 1897.

$$k = \frac{d}{t} \div \frac{V}{2d}$$

$$= \frac{2d^2}{Vt} \text{ cm./volt per cm.}$$

In one of Rutherford's experiment, $t = 0{\cdot}36$ sec., $V = 220$ volts, $d = 8$ cm. These give $k = 1{\cdot}6$ cm. per sec.

(*ii*) *Langevin's Method.*—Rutherford's method has now been replaced by a more accurate method due to Langevin* (1903). The principle of this method may be understood from Fig. 16.

A, B is a pair of parallel plates as in Rutherford's experiment.

T is a X-ray tube. A single instantaneous flash of X-rays from T ionises the air between the plates.

A potential difference is maintained between A and B. At some convenient interval after exciting the flash the direction of the applied electric field across A, B can be reversed by means of suitable switches. Suppose k_1 = mobility of the positive ions, k_2 = mobility of negative ions, and X = the electric field. Suppose now that starting with A at the positive potential and B at the negative, the field is reversed after t seconds from the flash. By this time all the positive ions within a distance k_1Xt from the original negative plate B have reached the latter. If A = area of the plate and n = number of ions per c.c., the number of positive ions thus reaching B is nAk_1Xt. Similarly the number of negative ions reaching A by this time is nAk_2Xt. There will thus be left $2nAd - nAk_2Xt$ negative ions in the space between A, B at the instant when the field is reversed. On reversal this number will reach the plate B, imparting to it a total negative charge

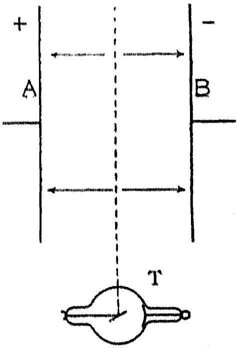

Fig. 16
Langevin's arrangement.

$$Q = e\,(2nAd - nAk_2Xt) - enAk_1Xt_1$$

If the interval after which the reversal occurs is gradually lengthened, the net amount of negative charge Q will diminish, more and more, firstly due to the diminution in the number of available negative ions in the space at the time of reversal, and, secondly, due to increase in the number of positive ions already deposited on B before reversal. The diminution of Q takes place in a linear relation with time t. This is represented by the straight line AB in Fig. 17. Very soon the number of positive ions reaching B before reversal exceeds the number of negative ions reaching it after reversal, and Q becomes positive (over PB). Let us assume that the negative ions move faster than the positive. Then ultimately it becomes so large that all the negative ions reach A before reversal, and the charge at B after reversal is only due to the positive ions reaching B before reversal. So further increase of t does not increase the positive value of Q as rapidly as before. This brings a sharp bend in the curve (at B) denoting a sudden change in the rate of change of Q. The subsequent course of the curve follows BC. The sharp change evidently occurs when $nAd - nAk_2Xt = 0$. Calling the value of t corresponding to this t_2, we get

---

* Langevin, *Ann. de Chim. et de Phys.*, **28**, 289, 1903. *Comptus Rendus.*, **134**, 646, 1902.

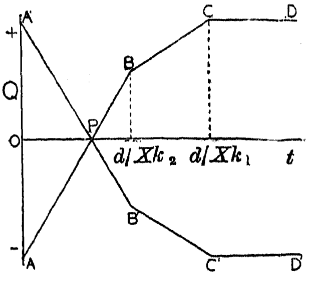

Fig. 17
Graphical representation of expected results.

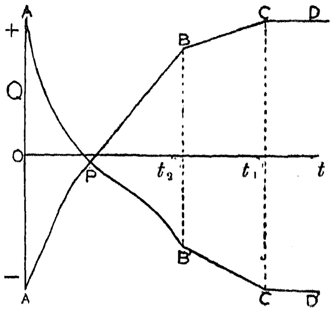

Fig. 17a
Experimental Curve.

$$k_2 = \frac{d}{Xt_2} \quad . \; . \; . \; . \; . \; . \; . \; . \; . \; . \; . \; . \quad (6)$$

On further increasing the interval after which the reversal occurs a time will come when not only all the negative charges reach A, but also all the positive ions will reach B before reversal. From this instant onward Q will remain constant (over CD). At this point (at C) there will be another sharp bend in the curve. This corresponds to $nAd - nAk_1tX = 0$. Calling this value of time t_1 we get

$$k_1 = \frac{d}{Xt_1} \quad . \; . \; . \; . \; . \; . \; . \; . \; . \; . \; . \; . \quad (7)$$

Since t_1 and t_2 can be known from the graph accurately, k_1 and k_2 can be calculated. A similar curve $A'B'C'D'$ is obtained corresponding to the charge at A. On account of non-uniformity of ionisation the experimental curves are not exactly symmetrical, but still sharp bends are obtained which permit of the determinations of k_1 and k_2 with accuracy.

The experimental curve is given in Fig. 17(a). A table containing Langevin's values of mobilities is given below. k^+ denotes the mobility for the positive ion, and k^- that for the negative.

Table 2.

COEFFICIENTS OF MOBILITY OF IONS.

Gas	Molecular Weight	k^+	k^-
Hydrogen (dry) ...	2	6·7	7·95
" (moist) ...	—	5·30	5·60
Air (dry)	—	1·36	1·87
" (moist)	—	1·36	1·51
Carbon monoxide ...	28	1·10	1·14
" dioxide ...	44	0·81	0·85
Sulphur "	64	0·44	0·41
Carbon tetrachloride ...	154	0·30	0·31
Pentane	72	0·36	0·35

The methods employed by different workers (Zeleny,* Wellisch† and others) are sometimes widely different. But the results obtained are generally in agreement. It will be seen from the table that the velocities of the negative ions are generally greater than those of the positive. This fact was first pointed out by Zeleny. Experiments have been performed with ionising agents other than X-rays. They show that the ions produced by X-rays, uranium radiations, or some other agents move with identical velocities. It has been found that introduction of water vapour into the ionisation chamber has a marked effect in diminishing the mobility, specially that of the negative ion.

Langevin‡ has observed that the mobility of the ions considerably increases with the decrease of pressure of the gas. The effect is shown in Fig. 18 taken from subsequent works of Lattey.* It may be noted that for the positive ions the mobility increases linearly with the fall of pressure, but for the negative ions the increase in mobility beyond a certain range of pressure is much more rapid.† These results have important bearings on the nature of the ions, and will be discussed in § 10.

---

* Zeleny, *Phil. Trans. Roy. Soc. A*, **195**, 193, 1900.

† Wellisch, *Phil. Trans. Roy. Soc. A*, **209**, 249, 1909.

‡ Langevin, *loc. cit.*

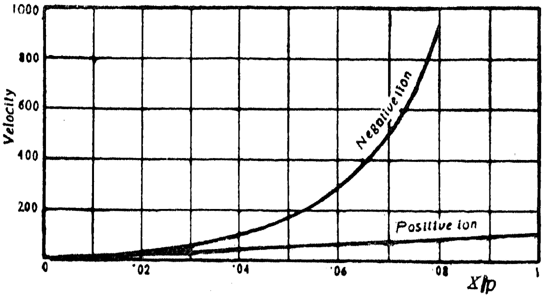

Fig. 18. Variation of mobility with pressure.

8. Diffusion of Ions.—The ions, like the ordinary molecules of gases, diffuse to sides in passing through narrow spaces. Thus it is a common experience that an ionised gas when allowed to pass through any porous material like cotton wool, loses its conductivity. This is due to the fact the ions diffuse to the sides of the material in their passages through the fine pores, and the sides being oppositely charged by induction, neutralise the charges of the ions. Townsend‡ experimentally studied the effect of diffusion of ions by allowing a stream of ionised gas to pass through a number of narrow metal tubes, and examining the conductivity of the gas before and after passage through the tubes. In this way the proportion of the positive or the negative ions abstracted from the beam in the process was obtained. From this the number of ions diffused per second across unit area at right angles to the direction of motion was calculated. This number is called the *coefficient of diffusion* and is denoted by D. The coefficient of diffusion of a number of gases is shown in the following table. Column IV represents the coefficients of inter-diffusion of some gases into carbon dioxide. The significance of these values will be clear in §10.

---

* R. T. Lattey, *Proc. Roy. Soc., A*, **84**, 173, 1910.
R. T. Lattey, H. T. Tizard, *Proc. Roy. Soc. A*, **86**, 349, 1912.

† An idea of the variation of mobility with pressure for positive and negative ions may be formed from the following typical data :—

p—(cm of Hg)	142·0	76·0	41·5	20·0	7·5
k^+	0·75	1·60	2·61	5·44	14·76
k^-	0·90	1·70	3·31	7·34	21·86

‡ Townsend, *Phil. Trans. Roy. Soc. A*, **193**, 129, 1899.

Table 3.

COEFFICIENTS OF DIFFUSION OF IONS.

Gas	D for + ions	D for − ions	Observer	Coefficients for inter-diffusion into air	Observer
Air (dry) ...	·028	·043	Townsend	...	
„ (moist) ...	·032	·035	„		
Oxygen (dry) ...	·025	·0396	„	·17778	Loschmidt
„ (moist) ...	·0288	·0358	„		
Carbon dioxide (dry)	·023	·026	„	·142	
„ (moist)	·0245	·9255	„		
Hydrogen (dry) ...	·123	·190	„	·634	
„ (moist)	·128	·142	„		
Nitrogen (dry) ...	·029	·0414	Selles	...	

Experiments showed that in all cases the negative ions diffused faster than the positive ions. Further, it was found that the *coefficients of diffusion of different gases were proportional to their mobilities.* This result follows from simple application of the principles of kinetic theory[6] to the motion of ions. Let n = number of ions per cubic centimetre of the gas. By the above definition of the coefficient of diffusion, the number of ions which in one second cross a unit area placed at right angles to the axis of x is $D\frac{dn}{dx}$. We can, therefore, regard the ions as moving along the axis of x with a mean velocity of $\frac{1}{n}D\frac{dn}{dx}$. If p = partial pressure of the ions at any constant temperature T, $p=n\beta T$, where β = gas constant. The pressure p is, therefore, proportional to n. Supposing U = velocity of the ions, we have then

$$U=\frac{D}{p}\frac{dp}{dx} \quad . \quad . \quad . \quad . \quad . \quad . \quad . \quad . \quad . \quad (8)$$

But $\frac{dp}{dx}$ = the force acting along the x-axis on unit volume of the gas. Therefore it follows from (8) that if the ions are placed in an electric field X acting along the axis of x they will acquire a velocity in this direction, which can be obtained by substituting $\frac{dp}{dx}=Xen$. That is,

$$U=Xen\frac{D}{p} \quad . \quad . \quad . \quad . \quad . \quad . \quad . \quad . \quad (9)$$

Since the ratio $\frac{n}{p}$ =constant, if $\tilde{n}$ be the number of ions per c. c. at this temperature at atmospheric pressure P, we have $\frac{n}{p}=\frac{\tilde{n}}{P}$. Hence

$$U= Xe\ D\frac{n}{P} \quad . \ . \ . \ . \ . \ . \ . \ . \quad (10)$$

Thus the mobility of the ions can be expressed as

$$k=\frac{U}{X}=D\frac{\tilde{n}e}{P} \quad . \ . \ . \ . \ . \ . \ . \ . \quad (11)$$

This shows that k will be proportional to D, the coefficient of diffusion of the ions.

9. Charge on the Ions.—Townsend compared the charge carried by a gaseous ion with that by a hydrogen atom obtained in the electrolysis of water or dilute acids in the following manner.

In electrolysis it is known that one gm.-atom of hydrogen is liberated by the passage of 9645 e. m. units of electricity. Assuming that each H-ion carries the charge e', and there are N atoms in a gm.-atom of hydrogen,

$$\begin{aligned} Ne' &= 9645\times3\times10^{10} \text{ e. s. units.}\\ &= 2{\cdot}89\times10^{14} \text{ e. s. u.}\end{aligned}$$

In one experiment on gaseous ionisation it was found that $D={\cdot}128$, $k=5{\cdot}3$ cm. per volt per cm. for the positive ion of moist hydrogen gas at 15° C and 760 mm. pressure. From equation (11) we get therefore,

$$e=\frac{kp}{D\tilde{n}}=\frac{k\beta T}{D}$$

and

$$\begin{aligned} Ne &= \frac{kRT}{D}\\ &= \frac{5{\cdot}3\times300\times8{\cdot}3\times10^{7}\times288}{{\cdot}128}\\ &= 2{\cdot}97\times10^{14} \text{ e. s. units.}\end{aligned}$$

Therefore $\frac{e}{e'}=1{\cdot}03$ which is very nearly equal to unity. Almost the same ratio is obtained for the ions of any other gas with proper values of k and D. This shows that *the charge carried by an ion of all gases, both positive and negative, is the same as that contained by an hydrogen atom in electrolysis. We shall further see in the next chapter* *that the absolute measure of this charge is the most elementary unit of electricity and is equal to* $\mathbf{e} = 4{\cdot}77 \times 10^{-10}$ *e. s. units.*

10. Mass of the Ions.—Important evidences regarding the mass of the positive and the negative ions are obtained from two sources,—(1) the rate of diffusion of ions, and (2) the variation of the mobility of ions with pressure.

It has been found (*vide* Table 3) that the coefficient of diffusion of the negative ions is always greater than that for the positive ions of the same substance. This would indicate that in general the positive ions are heavier than the negative ions. The coefficient of diffusion of ions for any gas has also been compared with the coefficient of *inter-diffusion* of the *molecules* of the same gas into those of any other gas. Thus the positive ions in moist CO_2 have the coefficient of diffusion ·0245, and the coefficient of inter-diffusion of CO_2 into air is ·14. According to the kinetic theory of gases the rate of inter-diffusion of two gases is inversely proportional to the square root of the product of the masses of their molecules. From this it appears that a positive ion of CO_2 is many times heavier than a neutral molecule of the same gas. Results on the inter-diffusion of negative ions for CO_2 as well as for other gases lead us to similar conclusions. From these evidences it follows that an ion at ordinary pressures consists of a central charged particle which attracts round itself a cluster of neutral gas molecules, and is set in motion as a whole.

The above conclusion is not, however, fully supported by the results of ionic mobility. It has been stated in §7 that on lowering the pressure the mobility of the positive ions linearly increases. This can be readily attributed to increase in mean free paths of the ion and we need not assume that there is any change in their mass. For negative ions, however, the mobility increases much more rapidly with fall of pressure than can be accounted for simply by assuming that the mean free path increases. It is, therefore, believed that the negative ion consists actually of a group of molecules with a central charged particle, as suggested by the study of inter-diffusion of ions, and the group gradually disintegrates into smaller clusters as the pressure is lowered.

11. Mechanism of Ionisation.—It is now well known that atoms of all substances contain extremely small negatively charged particles called *electrons* having a mass nearly 2000 times smaller than that of a hydrogen atom. These electrons play an important part in the phenomenon of ionisation. It is believed that the action of the ionising agent is to expel an electron from the molecule of the gas, so that the latter is left with an excess of positive charge, and constitutes the nucleus of a positive ion. The latter may then attract round it a number of neutral gas molecules forming a cluster. At ordinary pressure the electron, soon after its release, attaches itself to a neutral gas molecule, giving to it its negative charge. This negatively charged molecule behaves as a negative ion at ordinary pressures. But at very low pressures the liberated electron can very rarely find a partner, as the number of gas molecules is extremely few. So the electron exists in free state, and forms the majority of the negative ions at low pressures. Evidences also show that under special circumstances it is possible that a number of neutral gas molecules cluster round the positively charged gas molecule as centre, and the entire group behaves as a positive ion.

12. Photographing the Ions: C. T. R. Wilson's Cloud-Chamber Method and its Modifications.—Some experiments will now be described which verified in a direct way the hypothesis of the production of charged ions throughout a gas due to the action of ionising agents. The method is based upon the property that the ions under certain conditions can serve as nuclei for the condensation of water drops, a property which has been utilized for rendering the individual ions visible, as well as for counting the number of ions.

It has been long known, that if air saturated with water vapour be suddenly expanded, a cloud consisting of small globules of water is formed. This is due to the fact that on account of adiabatic expansion, the temperature falls considerably and the space becomes supersaturated with water vapour. The excess is condensed as particles of water forming the cloud. It was however shown by Aitken that if the air were perfectly dustfree (as can be easily done by passing it through glasswool), no cloud is formed even when the space is considerably supersaturated. The explanation is as follows: When no dust particles are present, the excess of water vapour finds no surface on which it can deposit itself. Small particles which are formed due to the concentration of a number of water molecules at one point evaporate rapidly, since, as Lord Kelvin had shown, the saturated vapour pressure over a surface of such small·curvature is much larger than that over a flat surface. The relation[7] giving the difference of vapour pressures over a curved and a plane surface is

$$ln\frac{p'}{p} = -\frac{2S}{r}\frac{M}{\rho RT} \quad . \; . \; . \; . \; . \; . \; . \; . \; . \; (12)$$

or

$$p = pe^{-\frac{2S}{r}\frac{M}{\rho RT}} \quad . \; . \; . \; . \; . \; . \; . \; . \; (13)$$

Here p' = saturated vapour pressure over a surface of radius of curvature r. The curvature is to be taken positive if the surface is concave to the space, negative when it is convex, S = surface tension, ρ=density, M=the molecular weight and T=the absolute temperature.

For a spherical water drop at 27°C, if r=1 $\mu\mu$

$$\frac{2S}{r}\frac{M}{\rho RT} = \frac{2\times 73}{10^{-7}}\frac{18}{8{\cdot}30\times 10^{7}\times 300} = 1{\cdot}05.$$

Since r is negative, over a drop having the radius 10^{-7}cm., $p' > 2p$ nearly. Hence the drops evaporate as soon as they are formed, even if the supersaturation pressure be more than double the saturation pressure.

The experiments* of R. von Helmholtz, Richarz and Lenard showed that even when the air is completely dustfree, condensation may be produced by expansion, provided that the space was exposed to X-rays or other ionising agencies like ultraviolet light or flames. Extended investigations by C. T. R. Wilson showed that the ions postulated by J. J. Thomson to account for the acquired electrical conductivity of a gas serve as centres of condensation of molecules of water round them. In fact a charged nucleus acts as a centre of condensation for a smaller degree of saturation than an uncharged nucleus. For, on account of a charge e, the system has a potential energy proportional to $\frac{e^2}{r}$ which diminishes with increase of r †; since the potential energy of any system tends to become minimum, a drop formed round such a nucleus acquires an extra stability on account of the charge. C. T. R. Wilson found that if V_1 be the initial volume of air, V_2 the volume after expansion, the negative ions act as centres of condensation when $\frac{V_2}{V_1} > 1{\cdot}25$, and the positive ions act when the ratio is greater than 1·31. When the ratio exceeds 1·35, a dense cloud appears even in the absence of all nuclei. By confining the expansion within narrow limits, ions possessing only one kind of charge can be rendered visible as fine drops of clouds. Thus when the ratio of the final to the initial volume lies between 1·25 to 1·38, the first stage of (rain-like) condensation sets in. This stage is due to the condensation on negative ions. When the ratio exceeds this limit, a much denser form of cloud appears, which is due to condensation on *positive ions*. These are shown in Table 4:

---

* For an account of R. von Helmholtz's experiments on the condensation of steam in a space subjected to point discharge, see J. J. Thomson and G. P. Thomson's *Conduction of Electricity through Gases*, p. 310.

† For a theory of condensation on charged drops, see Thomson and Thomson, *loc. cit.*, p. 325.

Table 4

Gas.	RAIN-LIKE CONDENSATION.		CLOUD-LIKE CONDENSATION.	
	Final/Initial Volume.	Super-saturation.	Final/Initial Volume.	Super-saturation.
Air	1·252	4·2	1·375	7·9
Oxygen . . .	1·257	4·3	1·375	7·9
Nitrogen . . .	1·262	4·4	1·375	7·9
Hydrogen . . .	—	—	1·375	7·9
Carbonic acid . .	1·365	4·2	1·53	7·3
Chlorine . . .	1·30	3·4	1·44	5·9

The third and the fifth columns represent, in rain-like and cloud-like condensations respectively, the ratio of the pressure of the water-vapour actually present in the space to the saturation pressure at the same temperature.

A later form of C. T. R. Wilson's* apparatus is shown in Fig. 19. A B is the expansion chamber which is completely closed and cylindrical in shape, 16·5 cm. in diameter, and 3·5 cm. in height. The base B is a movable platform equivalent to a piston working within water-tight joints at the bottom. The space below B may be put in communication with a highly evacuated vessel D by opening a valve C which is pulled from outside. W, W are two wooden blocks inside B and they serve only to reduce the air space within the chamber. On opening the valve C, the platform A suddenly drops down, (until it is arrested by rubber pads) causing a sudden expansion of the volume of the chamber.

---

* C. T. R. Wilson, *Proc. Roy. Soc. A*, **87**, 277, 1912.

An X-ray tube, and an illuminating spark are so arranged that the sudden drop of the platform excites the two in quick succession, and the drops of clouds formed on the ions along the X-ray tracks are simultaneously illuminated and can be instantaneously photographed. The process can be repeated by re-evacuating the vessel D by means of a pump. By employing the radioactive radiations as ionising agents in place of X-rays, the track of a single α or β-ray can also be photographed in a similar way. In many cases it is necessary to study the picture of the tracks in space ; for this purpose stereoscopic photographs of the tracks are taken by using two cameras at right angles.

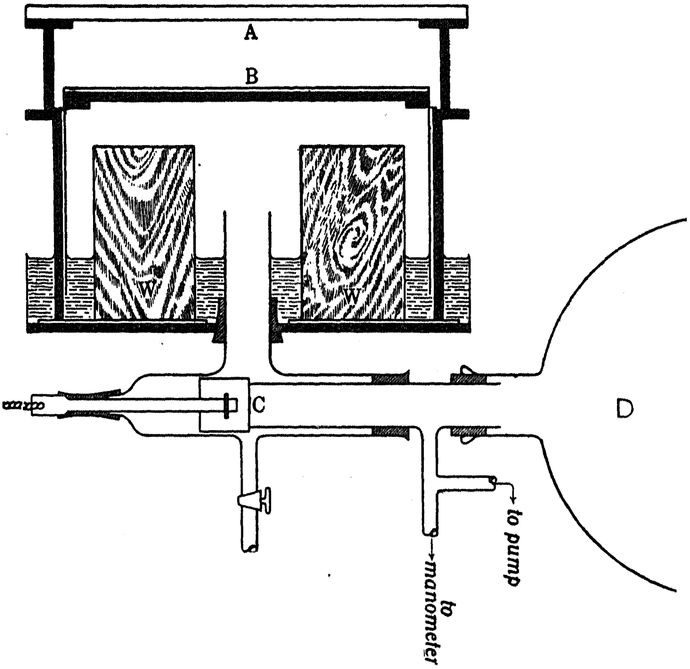

Fig. 19. C. T. R. Wilson's cloud-chamber apparatus.

In photographing some rare phenomena of collision of α-particles with atomic nuclei (*vide supra*) it becomes necessary sometimes to obtain about a million photographs of the tracks, out of which one may be successful. In such experiments Wilson's method, in which the state of supersaturation of the space inside the chamber cannot be prolonged, proves rather inconvenient. For such works

Shimizu* devised an automatic apparatus in which expansions may be rapidly repeated maintaining supersaturation for hours together, and a continuous series of photographs of the track can be obtained. Shimizu's apparatus is shown in Fig. 20.

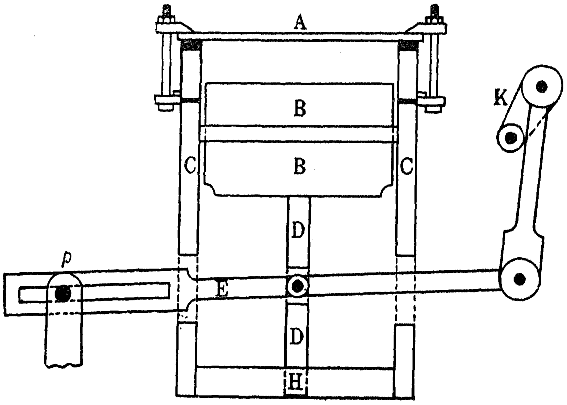

Fig. 20. The Shimizu Expansion chamber.

A is a circular glass plate which forms the top of the cloud chamber.

B is the piston sliding along the walls of the brass cylinders CC.

D is the piston rod which finds its way through a hole H in the base of the apparatus.

E is a horizontal rod passing through D and pinned to the latter. One end of E is connected to a horizontal shaft K which is driven by a motor by means of an *arm and a link*. The other end of E is fixed by a pin *p* which acts as a fulcrum. Thus as the shaft rotates, E executes a rocking motion, and the piston a reciprocating motion, the extent of which is controlled by the position of the pin *p* so as to produce the suitable supersaturation. The operation may be continued as long as necessary without interruption.

By means of a rotating commutator an electric field is temporarily established over the air-space in the chamber. This field serves to remove all the ions generated between two successive supersaturations, and the field is withdrawn every time at the instant when supersaturation occurs, because otherwise the ions on a track of the ray will be pulled apart by the electric-field and distort the appearance of the track.

The moments of admitting the ionising rays into the chamber, exciting the illumination, and opening the camera for photography are regulated by a number of shutters.

Shimizu has also developed a method for obtaining simultaneous photographs of two images of the track viewed in two directions at right angles to each other on a moving film; by this means the orientation of the track in space can be determined. Shimizu's method has in general been employed by Blackett, Harkins and Ryans, Auger and Perrin and others in their numerous investigations on rare and complicated collision phenomena due to the passage of α and β-rays.

---

* T. Shimizu, *Proc. Roy. Soc. A*, **99**, 425, 1921.

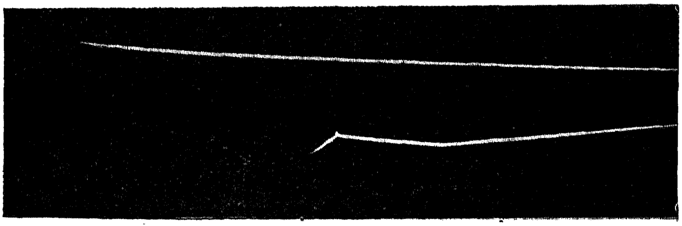

Fig. 20a. Track of α-particles.

Blackett* has shown that in Shimizu's method, though very efficient for continuous photography of the α-ray tracks for a long time, the tracks obtained are not as sharp and well-defined as in Wilson's original method. The excellent definition of the track evidently requires very sudden expansion which was a characteristic of the original method. So in his own researches he used a modified Shimizu apparatus in which the reciprocating mechanism was replaced by simple spring action. This combines with the merit of sudden expansion of Wilson's original design the mechanism of repeating it as frequently as required. The modified part (only the spring action) is shown in Fig. 21. The speed of expansion is regulated by the tension of the spring A, and the amount of expansion by the adjustable screw B. The various operations, *viz.*, the occurrence of expansion, the admission of α-rays, the illumination, and opening of the film camera were carefully timed. It was found best to obtain photographs just when the expansion was completed.

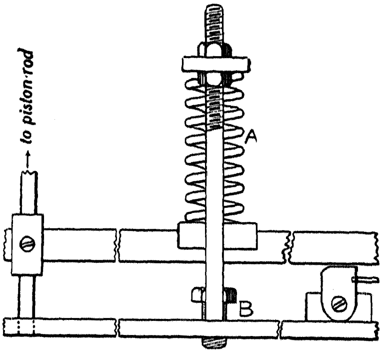

Fig. 21
Blackett's apparatus.

The "cloud chamber" experiments described above are of very wide applicability in the study of complex radiometric phenomena. A typical photograph of two α-ray tracks from Radium obtained by this method is shown in Fig. 20a. The abrupt bending near the end of one of the tracks is remarkable. Its significance will be clear in Chap. IV. The photographs obtained in numerous other cases will be given in their proper places later on.

---

* P. M. S. Blackett, *Proc. Roy. Soc. A*, **102**, 294, 1922.

13. Electrical Counters.—A very sensitive method of detecting the presence of single charged particles was first successfully attempted by Rutherford and Geiger* in the year 1908. They fired a beam of α-rays (which are positively charged particles emitted by radioactive substances like U) through a very narrow opening into a cylindrical ionisation chamber with a central wire electrode, the gas in the chamber being reduced to a pressure of about 4 cms. The cylinder was charged to high negative potential of several hundred volts and the wire was connected to a sensitive quadrant electrometer. The entrance of each α-particle produced ionisation in the chamber which, owing to the low pressure and the strong electric field, multiplied itself several thousand times and caused the electrometer needle to be deflected appreciably. Thus the number of kicks of the electrometer needle gave the number of α-particles entering the chamber.

Four years later, Rutherford and Geiger modified their apparatus by using a cylindrical chamber with a hemispherical end, a rod with a spherical knob at its end serving as the central electrode (Fig. 22). The quadrant electrometer was replaced by a string electrometer so that a larger number of α-particles could be detected as soon as they entered the chamber. In such experiments, the string electrometer is preferred as it possesses no lag.

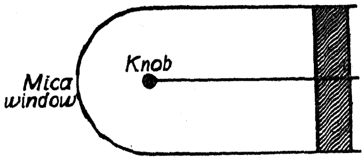

Fig. 22

But the two types of counters described above were not sensitive enough for detecting β-particles, and Geiger†, in the year 1913, devised an apparatus by which it was possible to count β-particles as well. His apparatus is described below.

The Geiger Point-Counter.—It consists essentially of a cylindrical brass chamber (Fig. 23) one end of which is closed by a disc DD and to the other end is fitted an ebonite or hard rubber plug C.

---

* E. Rutherford and H. Geiger, *Proc. Roy. Soc. A*, **81**, 141, 1908.
† H. Geiger, *Verh. D. Phys. Gesell*, **15**, 534, 1913.

Through this plug passes a wire WW ending in a fine needle point W. At the centre of the disc is bored a small hole B so that it lies just in front of the "point." This counter works well even at atmospheric pressure. Although the arrangement of electrical connections used by various experimenters has varied, yet the one which we give below (Fig. 24) illustrates fully the working of the apparatus.

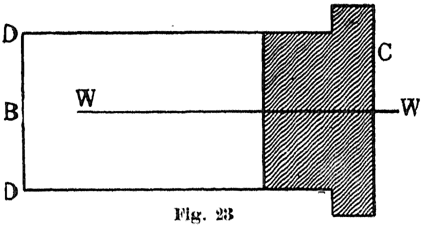

Fig. 23
The Geiger Point-Counter.

The cylinder is connected to the positive pole of a source of a very high potential (up to 2000 volts), while the point electrode is joined to a string electrometer and is at the same time earthed through a very high resistance R (of the order of 10^{10} ohms). When some source of α or β-particles is brought in front of the hole, the string of the electrometer is deflected intermittently, each deflection signalising the entrance of a particle into the chamber. Thus it is possible to find out definitely the rate of emission of the particles from a given sample of a radioactive substance. When an α-particle or a β-particle reaches the very strong field near the point, it starts a point discharge ("Spitzentladung") which gives rise to a flow of electric charge sufficient to cause an appreciable deflection of the electrometer. By the time another rush of current takes place, this charge leaks away to the earth through the high resistance.

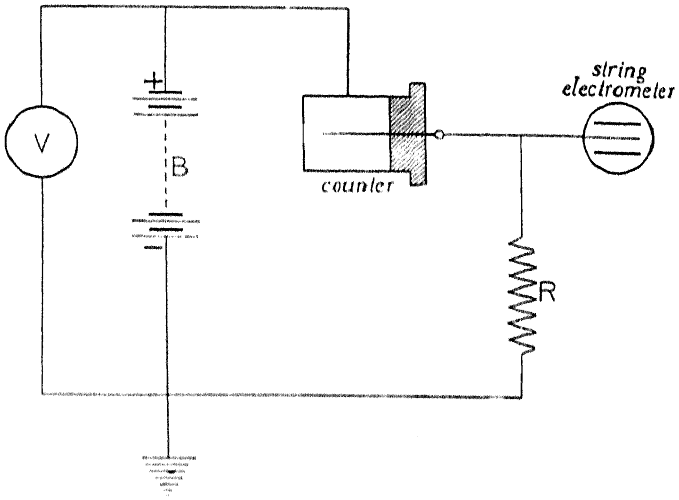

Fig. 24. Arrangement for using the Point-Counter.

Instead of using an electrometer for detection, various other devices such as telephone-receivers, electroscopes and very sensitive galvanometers have been used. The modern method is to employ some sort of a vacuum tube amplifier and then to use a loud speaker or some self-recording device, *e.g.*, a sensitive relay. An example of a very simple arrangement of this type is shown in Fig. 25. The positive pole of the anode battery is connected to the plate of the triode, while the negative pole is joined to the filament and earthed through a sensitive relay R which operates a local circuit L.C. actuating the chronograph pen P. In this way we are able to obtain a permanent record of the α-particles or β-particles. Usually a three-stage vacuum tube amplifier is quite sufficient for this purpose. Very recently an "Automatic Adding and Registering Machine" has been devised by Neufeldt and Werner* to be used with Geiger Counters.

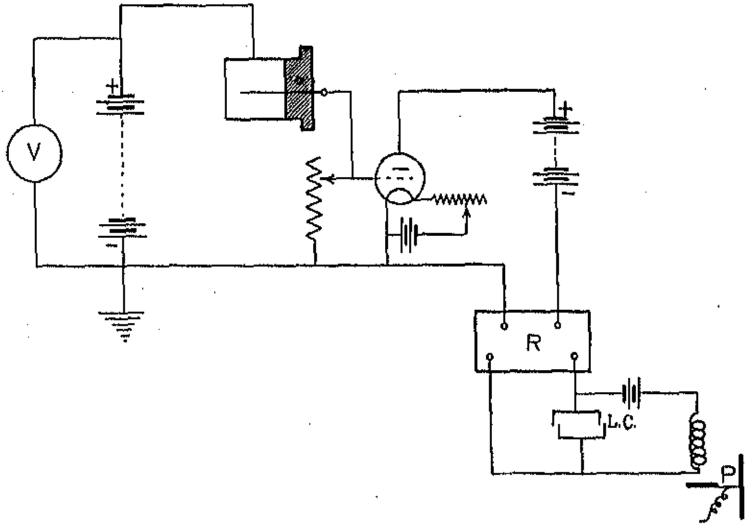

Fig. 25. The use of amplifier in Geiger Counter

One very important fact about Point Counters which is not very well understood is that their successful operation is very much dependent on the nature of the point employed and the point requires careful preparation and preservation in order that it may perform its function properly for some length of time; otherwise it may work only for a few hours and then be rendered useless. Another difficulty experienced while working with counters is caused by the appearance of "stray discharges" or "natural disturbances," *i.e.*, discharges even when evidently there is no radioactive substance in the neighbourhood. They may be due to the α-particles from the emanation in the air, or radiations from the material of the counting chamber, or penetrating γ-radiations from the earth and other sources, and also to imperfect needle points. The results of researches carried so far, though not very definite seem to lead to the conclusion that very fine platinum points or very minute platinum globules thoroughly cleansed with alcohol and carefully heated are most suitable for use in Point Counters.

---

* Neufeldt and Werner, *Phys. Zeits.*, 32, 453, 1931.

The effect of the sizes of the chamber and the point, of their material shape and disposition, and the influence of the gas inside the chamber, and its pressure, etc., have been investigated by several experimentors, but their individual results are so inconsistent with each other that it is very difficult to say anything definitely about them. And the various observers have built different theories—none too satisfactory to explain the phenomena observed by others—on the basis of their own observations. As an example of these controversies may be mentioned the fact that while Kutzner* explains the principle of action of the counter by supposing the formation of a layer on the chamber surface, Geiger† thinks that a layer is formed not on the chamber but on the surface of the point; but Emelius‡ explains it as a purely ionisation phenomenon. And yet another worker, Curtiss§, thinks that a layer of gas is definitely formed round the point. But whatever may be the processes occurring inside the chamber, the counter in the hands of expert observers has been, up till now, a very useful instrument for various kinds of measurements in radioactivity.

Since the Geiger counter can detect individual α-particles and β-particles, it should be able to detect γ-rays and X-rays also, for they produce secondary electrons when they fall on matter; and in fact, the counter has been utilised successfully for this purpose. On the same principle ultraviolet light can also be detected with the help of a Geiger counter. Further, this instrument has been employed for counting and determining the range of H-particles‖, and for counting slow electrons¶.

---

* Kutzner, *Zeits. f. Phys.*, 23, 117, 1924.
† H. Geiger, *Zeits. f. Phys.*, 27, 7, 1924.
‡ Emelius, *Proc. Camb. Phil. Soc.*, 22, 676, 1925.
§ L. F. Curtiss, *Phys. Rev.*, 31, 1060, 1928.
‖ Schmutzer, *Phys. Zeits.*, 28, 245, 1927.
¶ Hornbostel, *Ann. d. Phys.* (5), 8, 991, 1931.

14. The Geiger Tube Counter.—In 1928, Geiger and Müller* described a new form of counter now sometimes known as the Geiger-Müller Tube-counter. It is many times more sensitive than the Point-Counter and has therefore been used to detect the radiations from substances which show only very weak radioactivity. Thus with the help of this tube counter, it has been possible to detect the radioactivity of Potassium and Rubidium, also of Beryllium and Samarium. This apparatus (Fig. 26) consists of a cylindrical metal chamber along the axis of which is stretched a fine wire passing through hard rubber plugs which close the tube air-tight, and the chamber is exhausted to a pressure of about 4 or 5 cm. Although Geiger and Müller originally believed that the counter would give intermittent discharges due to the rays only if the central wire be coated with a semi-insulating layer, it has now been definitely established that even a bare well-polished wire serves the purpose equally well, and that no such preparation of the wire as is necessary in the case of the "Point" in a Point-Counter is needed here. But it has been found that the Tube-Counter does not work properly if even traces of moisture are present in the counter. The gas used has therefore to be dried thoroughly by passing through sulphuric acid and P_2O_5. Many of the difficulties which are met with in the case of point counters are experienced with tube counters as well and the same remarks apply as regards the results of various workers in this field. But while the operation of the tube counter is not affected by the nature of the surface of the wire, it is certainly influenced by the nature of the inner surface of the chamber walls. On the basis of these observations L. F. Curtiss† has proposed a theory which claims to be consistent with the present-day conceptions about ionisation. Whether this theory will stand the test of further experiments it is very difficult to say.

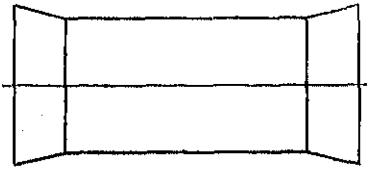

Fig. 26. The Tube Counter.

The method of using the Tube Counter is very much similar to that described for the Point Counter, except that in this case the counter is made negative with respect to the central electrode. An amplifier and loud speaker or some self-recording device are usually employed to detect the impulses. But the form of the counter as well as the experimental arrangements differ widely to suit the particular end in view. This type of counter, on account of its greater sensitivity, has been very much more useful than the Point-Counter. It has been utilised in the magnetic spectrograph* in connection with investigations on the X-ray photoelectrons where it replaces the usual photographic plate. Use has also been made of a modified form of the Geiger Tube Counter in measuring very minute quantities of radium† (even as small as 10^{-6} mg.). But perhaps by far the most important application of the Tube Counter has been in experiments on Cosmic Rays.

---

* Geiger and Müller, *Phys. Zeits.*, **29**, 839, 1928.

† L. F. Curtiss, *Bureau of Standard Journal*, **5**, 115, 1930.

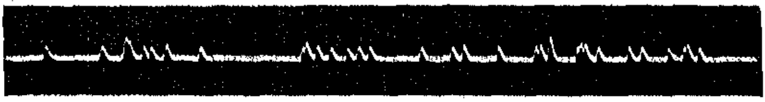

Fig. 27. A Record of the Geiger-Counter.

A typical photograph of the Geiger Counter record of α-ray is shown in Fig. 27. In this α-rays enter the chamber at a rate of 600 per minute. The sharp kinks indicate the entrance of each α-ray into the chamber.

References to Books:

1. J. J. Thomson and G. P. Thomson—*Conduction of Electricity through Gases* (3rd. Ed.), Chap. II, § 10.

2. J. H. Jeans—*The Mathematical Theory of Electricity and Magnetism*, Chap. IV, § 123.

3. Beattie—*Electrician*, Aug. 12, 1910.

Geiger and Makower—*Practical Measurements in Radioactivity*. Chap. I.

4. Graetz—*Elektrizität und Magnetismus*, Band I, pp. 141-42.

5. J. A. Crowther—*Ions, Electrons and Ionising Radiations* (1927), Chap. V, §§ 26 to 30.

Townsend—*Electricity in Gases*, Chap. IX, § 225.

6. J. J. Thomson and G. P. Thomson—*loc. cit.*, Chap. II, § 26.

Townsend—*loc. cit.*, Chap. III, § 84.

7. M. N. Saha and B. N. Srivastava—*A Text Book of Heat* (1st Ed.), Chap. V, § 22.

---

* Neufeldt, *Phys. Zeits.*, 30, 494, 1929.

† Watson and Van der Akker, *Phys. Rev.*, 37, 1631, 1931.

Books Recommended :

On the Measurements of Ionisation Current by Electrometers and Electroscopes—S. Meyer und F. von. Schweidler, *Radioaktivität*, Chap. V.

On the Principles and Theories of Electrometers and Electroscopes
—Geiger and Makower, *Practical Measurements in Radioactivity*, Chap. I.
—A. Gray, *Absolute Measurements in Electricity and Magnetism.*
—E. Rutherford, *Radioactive Substances and their Radiations*, (1913), Chap. III.

On the Phenomena connected with Motion of the Ions—Mobility, Diffusion, Recombination, and Ionisation by Collision.
—Rutherford, *loc. cit.* (1913), Chap. II.
—Townsend, *Electricity in Gases*, Chaps. IV, V, VI, VIII, IX.
—J. J. Thomson and G. P. Thomson, *Conduction of Electricity through Gases*, Chaps. II, III.
—K. Przibram's article, "*Die Ionen in Gasen*" in *Handbuch der Physik*, Bd. XXII, Chap. IV.

On the Methods of Photographing the Ions
—Rutherford, Chadwick and Ellis, *Radiations from Radioactive Substances* (1931), Chap. II, § 12d.

—Townsend, *loc. cit.*, Chap. VII.

On the Electrical Counters—Rutherford, Chadwick and Ellis, *loc. cit.*, Chap. II, §12a.

CHAPTER II

THE ELECTRON

15. Introduction—Earlier Theories of Matter.—The electrical theory of matter, which is discussed in this book, may be said to form a logical extension of the atomic theories* of matter which were elaborated during the nineteenth century and which dominated scientific thought for over fifty years. But historically, the subject grew from studies on the ionisation of gases of which a brief account has been given in Chapter I. It will now be profitable to begin with a short review of the atomic theories.

The idea that all matter in the Physical World is made up of atoms, *i.e.*, "small elementary particles with very characteristic properties" is a very old one, and can be found in the literary records of many ancient culture-people.* These atoms were also conceived as elements, and a hundred and fifty years ago, the belief was universal that this polygot world was made up of five fundamental elements, *viz.*, "Earth, Air, Water, Fire, and Aether." There was no idea regarding the size, shape or mass of these atoms, except that they were conceived in some vague way to be infinitely small.†

---

* The founder of one of the six systems of philosophy in India, *viz.*, the Vaisheshika, propounded in remote antiquity a form of the atomic theory, and was nicknamed 'Kanad' or the Atomeater by the rival metaphysicians, because he based his philosophy of the World on small particles. In Greece, a form of the atomic theory was put forward in the fifth century B.C. by Leucippus and Democritus. These atoms were conceived as small, indivisible particles, infinite in number, capable of various shapes and sizes.

Empedocles affirmed the existence of four elements to which a fifth was added later. The first four were earth, air, fire, and water, and the fifth was aether. The same belief is found also amongst the Hindus, but it is not definitely known with whom it first originated. It is also not clear whether the elements were conceived as 'principles,' or as 'atoms.'

† This explanation of Nature persisted amongst men of science up to the end of the eighteenth century, when the strictly quantitative and experimental study of Nature was initiated by Lavoisier. The rationalistic methods of Lavoisier still dominate scientific thought and are responsible for the extraordinary expansion of our knowledge of the Physical World within the last hundred and fifty years.

The time-honoured belief in the five elements received a rude shock towards the end of the eighteenth century. It was shown with the aid of the newly discovered Voltaic pile, that one of these ancient elements, *viz.*, water can be decomposed into two elementary and simpler gases, Hydrogen and Oxygen. Following this discovery, chemists and physicists went on discovering one elementary substance after another till, when a census was taken, it was found that their number could not be limited by the magical properties of any particular integer. By the time Dalton formulated his 'Atomic Theory' to explain chemical combination, and Clausius and Maxwell were busy in finding out definite values for the number and size of different atoms, their total number had reached well over fifty. But the human mind refuses to believe in complexity; so before long, philosophers began to ponder whether the so-called chemical elements were at all elementary, whether they might not turn out to be composed of some more elementary stuff. The most sensational effort was made by Prout; he thought that hydrogen was the elementary atom, and other atoms were merely its condensation products. But experiments showed that the weights of atoms were not integral multiples of the weight of the H-atom and Prout's theory failed to live through. In the nineteenth century, scientists with a few exceptions, notably the astronomer Sir Norman Lockyer, continued to believe in the non-divisibility of the atom.

But in 1896, the atom was definitely shown to be capable of further subdivision.

16. Studies in Electricity.—Side by side with the advance in our knowledge of the atom, other groups of physical phenomena, *viz.*, electricity, magnetism, light and heat began to receive greater attention. They were first studied as isolated groups, but discoveries were soon made which showed that these different groups of phenomena are all interconnected. Thus Oersted's discovery that a wire carrying a current creates a magnetic field about itself showed for the first time, that an intimate connection exists between Electricity and Magnetism, and later, it led to momentous discoveries in Electromagnetism. Weber and Kohlrausch's discovery that the ratio between the electrostatic and electromagnetic units of *electricity* is equal to the velocity of light showed for the first time that light is an electromagnetic phenomenon (*Vide* Note 1).

The first intimate connection between atomic theories and electricity was revealed by Faraday's discovery of the laws of Electrolysis. These laws, interpreted in the light of atomic theories, led to the conclusion, that in solutions the electrolytes split up into ions or charged particles of opposite signs, which can be separated by the passage of an electric current. The ions are simply atoms, or groups of atoms (*compound radicles*) endowed with a definite quantum of electricity, or some multiple of it. Thus if we suppose that the H-ion is charged with the amount of electricity e, the bivalent Ca-ion in solution has double this amount of charge, the Al-ion which is usually trivalent has treble the amount. The laws of electrolysis thus clearly led to the fact that electricity in ions occurs in integral multiples of an elementary quantum e. Helmholtz showed in 1881 that we can make a fair estimate of this charge if we have a knowledge of the number of atoms N in a gram-atom (the Avogadro-Loschmidt number), for,

$$Ne = 9645$$

i.e., the charge carried by a gram-atomic equivalent of N atoms is experimentally found to be 9645 electromagnetic units.*

But at this time this elementary charge could not be isolated, nor could it be shown that it formed part of the atom.

17. Isolation of the Electron—Phenomena in a Discharge Tube.

—The isolation of the elementary negative charge was first effected by studying the phenomena of discharge of electricity through a vacuum tube, and can be illustrated by a number of experiments. We proceed to describe them below.

Take a simple discharge tube, that is, a cylindrical glass tube about 20 cm. long and 3 cm. in diameter, fitted with two aluminium electrodes, and connect it to a high vacuum pump. Connect the two electrodes to the two terminals of an induction coil, or any other source of high voltage, say forty thousand volts.

At first it is difficult for any discharge to pass through. Then at a pressure of about 10 mm., discharge begins to pass, which takes the form of red streamers. Let us now observe the change in the nature of the discharge as the pressure begins to diminish.

---

* For the determination of the number N from the kinetic theory of gases, see Saha and Srivastava's *Text Book of Heat*, p. 732

The different stages are:—

(*a*) When the pressure of the enclosed air falls down to about 4 mm. of mercury, a dark discharge passes through the tube with slight luminous effect at the two electrodes. These are the *negative* and the *positive glows* at the cathode and the anode respectively.

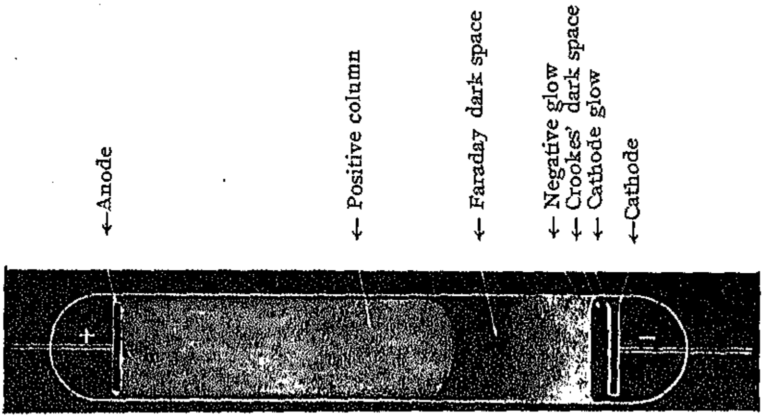

Fig. 1. A typical glow discharge in air at a pressure of 1 mm.

(*b*) At a pressure of about 1·65 mm., a long conspicuous column of uniform pink glow starts from the anode and occupies the greater part of the tube. It is called the *positive column* and is separated from the negative glow by a dark region known as the *Faraday dark space.* With a potential difference of 680 volts across the tube and about 6 milliamperes current through it, this general appearance persists up to a pressure of 0·8 mm; only at this lower limit, the negative glow is cleared out of the cathode surface, by a narrow dark region, known as the *Crookes' dark space.*

(*c*) As the exhaustion still continues, at a pressure of 0·37 mm. and a current of about 1 milliampere through the tube, the uniform luminosity of the positive column is broken up into pink coloured *striations,* separated by short dark regions. The number of these striations gradually increases with the reduction of pressure, until at about 0·24 mm., of pressure, the striations appear over the whole of the positive column; this latter however contracts in length and the Crookes' dark space, the negative glow and the Faraday dark space occupy more space than before. The glass walls of the tube begin to fluoresce at this stage.

(*d*) At still higher rarefaction, when the pressure becomes as low as 0·1 mm. the positive column recedes to the anode, and finally disappears; the Faraday dark space is also pushed to the positive electrode and the negative glow and Crookes' dark space fill the whole tube. At this stage, luminous streaks are seen to come out of the cathode, normal to its surface. These are *Cathode rays*. Continuing the exhaustion still further to 0·02 mm., luminosity which is to be found at the end of the Crookes' dark space disappears and first the electrodes, then the whole tube begins to shine; this is the well-known stage preliminary to the emission of X-rays. At a still higher vacuum, it is impossible to send a discharge through the tube. This is known as the *no discharge stage.* When this stage is reached, the pressure is about 10^{-4} mm. of mercury.

With a fixed pressure inside the discharge tube, if the distance between the anode and the cathode be gradually decreased, the same series of phenomena, *viz.*,—at first the contraction of the positive column and the Faraday dark space, and then expansion of the Crookes' dark space and negative glow towards the anode—are observed, and finally the Crookes' dark space may be made to occupy the whole tube.

These effects depend, besides on the pressure of the gas, and distance between the electrodes, upon the nature of the gas, size and shape of the tube and the electrodes, purity of the contained gas and numerous other factors. The voltage required to send a discharge through the tube is mainly dependent upon the gas pressure. It decreases as the pressure is gradually reduced from its ordinary value, until it reaches a minimum; for pressures lower than this, the voltage again increases, and finally rises to a very high value.

These phenomena depend entirely upon the power of conducting electrical charges acquired by the space inside the discharge tube at a very high vacuum. It is believed, that at the state of high rarefaction, when most of the nonconducting air molecules have been removed from the tube, electrons are ejected from the surface of the cathode due to the intense electric field in its vicinity. They travel with very great velocity acquired under the high potential difference, and *ionise* the few air molecules encountered in their way. It is these ions which are mainly responsible for the acquired conductivity, and they owe their origin directly to the free electrons emitted from the cathode.

18. Distribution of Electric Field and Conductivity in the Discharge Tube.—To explain the above interesting phenomena observed in a discharge tube, it is necessary to determine the distribution of electric field, and the number of ions present at each point, along the path of the discharge. The distribution of electric intensity has been investigated by J. J. Thomson and others. The usual method employed is to insert two auxiliary, fine platinum wire-electrodes separated by a fixed distance, at different parts along the discharge, and to find out the difference of potential between them by means of a quadrant electrometer. This is directly proportional to the electric field. At the cathode and the anode, however, where ions of only one sign naturally predominate, the result given by this method becomes uncertain. Therefore, a second method has been devised by J. J. Thomson.* In this (Fig. 2) a narrow beam of cathode rays is passed between two subsidiary electrodes, C', A' contained in a side-tube T, in a direction at right angles to that of the main discharge CA. In traversing any part of the main discharge, the beam suffers a deflection proportional to the electric field over this part (see §21). The deflection can be read by receiving it on a screen placed inside another side-tube T' opposite to T, and it directly gives a measure of the electric field. The method is specially useful in determining the field near the electrodes.

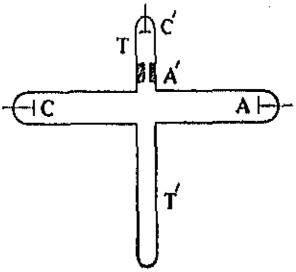

Fig. 2
Apparatus for the determination of electric field in discharges.

The actual distribution of the field changes with change of pressure in the discharge tube. The general nature of the distribution however remains the same. A typical distribution, first obtained by Graham † in a nitrogen discharge tube at 0·63 mm. pressure, and later on confirmed by Wilson, is shown graphically in Fig. 3, in which the shaded parts represent the luminous regions in the discharge tube from cathode to anode, and the ordinate at each point of the curve above represents the electric field at the corresponding point of the tube.

It will be seen that at the cathode the electric field is very large, which diminishes rapidly over Crookes' dark space and reaches a minimum on the cathode side of the negative glow. The large change of potential over the Crookes' dark space is known as the *Cathode fall of potential*. It has been thoroughly investigated by Aston and Watson.‡ Beyond the Crookes' dark space, the field rises a little, but falls again in the Faraday dark space. Towards the end of the latter, the field begins to rise rapidly, reaching a high value at the beginning of the positive column. Over the striations, the field rapidly fluctuates rising to a maximum at the region of a maximum brightness, and *vice versa*. The field then goes on increasing abruptly up to the anode.

---

* J. J. Thomson, *Phil. Mag.*, **18**, (6), 441, 1909.
† W. P. Graham *Weid. Ann. d. Phys.*, **64**, 49, 1898.
‡ F. W. Aston, *Proc. Roy. Soc.*, **79**, 80, 1907.
F. W. Aston and H. E. Watson, *Proc. Roy. Soc.*, **86**, 168, 1912.

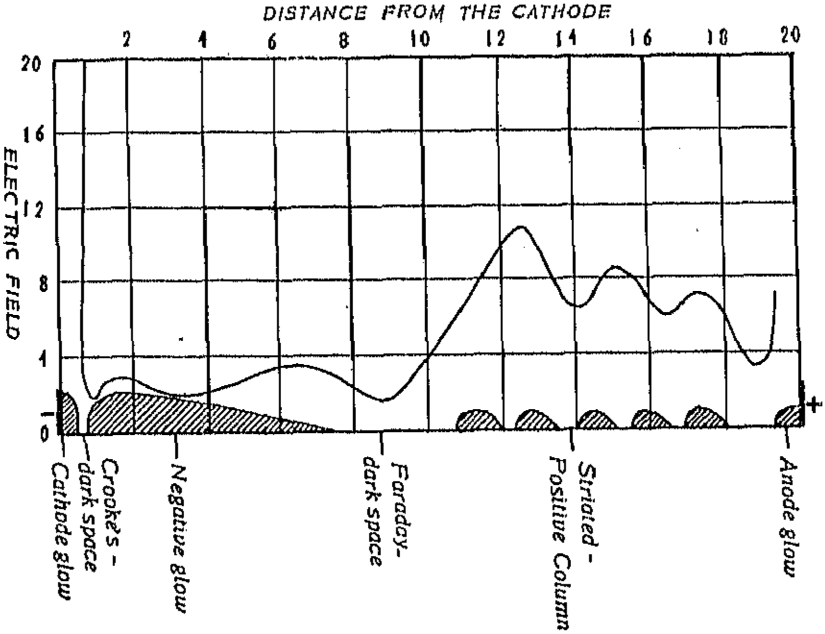

Fig. 8. Distribution of Electric field.

The distribution of conductivity along the path of discharge has been investigated by H. A. Wilson, B. Van der Pol, and others. Wilson's* method is a modification of the usual method for determining the distribution of electric field by means of subsidiary electrodes. The two wire electrodes have been replaced by small plate electrodes, placed on either sides of the discharge, with their planes parallel to the discharge. They can be shifted from region to region along the path of the discharge, and applying a small difference of potential across them, the current between them at each point can be determined. This current is a direct measure of the number of ions present, that is, the conductivity along the discharge. In this method, there is however the great difficulty, that the actual distribution of conductivity may be considerably modified by the secondary ionisation which may occur between the cross-electrodes under the applied difference of potential. The result obtained therefore becomes rather doubtful.

---

* H. A. Wilson, *Phil. Mag.*, 49 (5), 505, 1900.

The difficulty has been eliminated in the method devised by Van der Pol.* The apparatus used is shown in Fig. 4. FC is the discharge tube held vertically by means of ebonite supports H, K, between the condenser end of a parallel wire-system A B D of a Lecher bridge. At B the two ends of the Lecher system are freely connected to a Duddel thermogalvanometer E. Initially, without any discharge in the tube, a stationary wave is induced in the pair of parallel wires by tuning them to a Hertzian oscillator. When steady state is reached, the thermogalvanometer indicates a maximum current in the Lecher system. On starting the discharge, the space between the wires at the point acquires some amount of conductivity. So energy is absorbed in this region, and the thermogalvanometer would indicate a smaller steady current. The latter current is a measure of the conductivity in the particular region of the discharge tube between the wires. By means of pulleys, the tube may be slid along its length, and the conductivity at its various parts may be tested in this way.

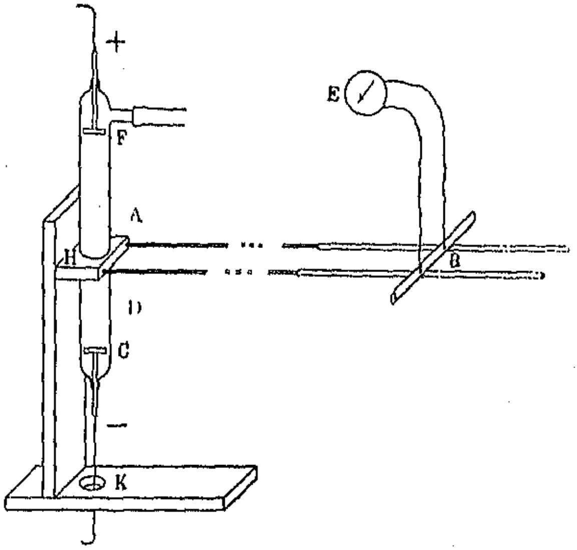

Fig. 4. Van der Pol's apparatus.

The general characteristic of the distribution of conductivity is exhibited in Fig. 5, adopted from Van der Pol's paper. The ordinates of the curve represent deflection of the galvanometer, and hence are inversely proportional to the conductivity of the discharge tube. It will be seen that the conductivity gradually increases up to a point in the negative glow, where it reaches the maximum. In the Faraday dark space, the

---

* B. Van der Pol, *Phil. Mag.*, 38 (7), 352, 1919.

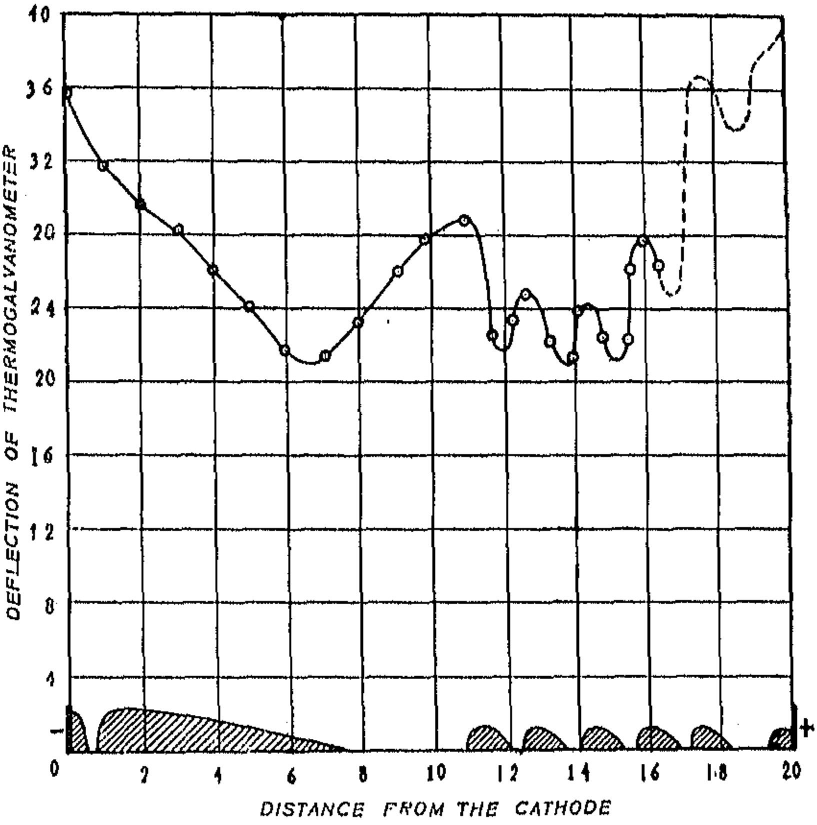

Fig 5. Distribution of conductivity.

conductivity gradually decreases towards the positive column. Over the striations, the conductivity fluctuates, the minimum of conductivity occurring at the negative point near the brightest part of each stria. In regions very close to the electrodes, the conductivity is practically zero. It may be remarked here that these results are just the reverse of those obtained by H. A. Wilson. But in view of uncertainty in the latter's experiment, Van der Pol's results are accepted as correct. Moreover, it has been pointed out by J. J. Thomson, that as the brightest parts of the striations correspond to maximum electric fields, ions are expected to move fast across these parts, giving the least accumulation of ions, and therefore minimum conductivity in these regions.

In recent times attempts have been made to investigate theoretically the distribution of potential and the numerous secondary collision phenomena taking place in a discharge tube. The task is indeed very difficult, because, say, in the case of investigation of the distribution of potential, one has got to consider the superposed effect of the space charge due to the moving ions and the electrons, and the charges on the electrodes. Besides, the nature of the distribution changes with the space of the electrodes, the state of vacuum and numerous other factors. A full account of these investigations has been given by I. Langmuir and K. T. Compton in an article "Electrical discharges in gases" published in two parts in the *Review of Modern Physics,* Vol. 2, No. 2, p. 123 and Vol. 3, No. 2, p. 191.

19. Nature of the Cathode Ray Discharge.—The above investigations throw important light on the nature of discharge phenomena at low pressures. At some definite pressure and at a constant difference of potential, a steady current flows between the electrodes. Thus the motion of ions is continuously taking place in a discharge tube, and in the absence of any other external source of ionisation, the ions must be produced constantly by the process of collision of positive and negative ions with gas molecules. But how is the action set up? Supposing the action to be initiated by cathode particles, how do the latter originate? To decide this point, a series of experiments were performed by Villard.* It is well known that the electric field near the cathode is very strong. According to Villard's theory, the positive ions, near the cathode acquire very great velocity in the intense electric field, and they impinge on the metallic cathode with great momentum, resulting in the emission of cathode rays or electrons from the cathode itself. On account of strong repulsion, the cathode particles are now thrown forward with high velocity and they produce ions by collision in course of their fast motion. The electric field in the region beyond the cathode is considerably weak, so that the positive ions are accumulated here in large number. The accumulation of positive ions near the negative electrode maintains the strong electric field near the cathode and accounts for the *cathode fall of potential* over the Crookes' dark space.

Now it has been seen that the distribution of the electric field over the region between the cathode and the anode is not uniform, the brightest parts of the discharge being in general places of weakest fields. This will cause non-uniformity in the production of ionisation. In regions of strong field, there will be intense ionisation, while, in places of weak fields, ions will accumulate and there will be no appreciable ionisation by collisions. These conclusions are in excellent agreement with the results of experimental investigations of the distribution of the number of ions along the path of the discharge, as already stated, that is, the points of maximum concentration of ions are those which correspond to minimum fall of potential. It is generally believed that the regions in which ionisation by collision takes place are marked by luminous effects, while dark regions are characterised by absence of appreciable ionisation. This accounts, in a general way, for the appearance of bright and dark spaces in the discharge tube. It is quite possible that the physical processes giving rise to striations (at low pressures) are but repetitions of those occurring in the Faraday dark space.

---

* Villard, *Journ. de Physique,* (3) **8**, 1, 1899.

We shall now turn our attention to the study of Cathode Particles.

20. Nature of the Cathode Particles.—Sir W. Crookes* early realised that these cathode particles were something much finer than the atoms, and gave to them the rather imposing name of *protyles* or *the fourth state of matter*. But their real nature was not elucidated till long afterwards; and very often gave rise to heated controversies. The following are the chief observations which led to final elucidation of their physical nature:

(1) The cathode rays are found to produce a bluish phosphorescent light on screens made of Willemite, which is a sulphide of Zinc. Such screens are often used to detect their presence. The side of the cathode ray tube away from the cathode is often impregnated with these substances, and the pencil of cathode rays is limited by a number of perforated diaphragms. (See description of the Braun tube, Fig. 8.) In the earlier experiments, observations were carried without any diaphragms.

(2) They travel in straight lines (Goldstein).

This can be easily demonstrated by holding a sheet of aluminium in the path of the cathode ray stream in a Braun tube. A sharp shadow of the sheet is thrown on the opposite wall of the tube.

(3) They are deflected by magnets (Plücker).

This can be easily shown by holding a bar magnet near the tube (Fig. 8), when it is found that the luminous spot shifts its position.

(4) They possess considerable momentum and energy.

---

* W. Crookes, *Phil. Trans.*, (1879—1885).

This is readily shown by inserting a light frictionless aluminium wheel set on a smooth rail in the path of the cathode rays. The wheel begins to move with the cathode ray particles under their impact.

This property of cathode rays is very often used for melting very refractory substances in modified forms of the discharge tube known as cathode ray furnaces. The refractory substance is placed in a crucible of magnesia or silicia, and placed within the discharge tube in such a way that the beam of cathode rays can be directed on it. As the rays are stopped, they deliver their whole energy to the refractory matter which i thereby heated and ultimately melts.*

(5) They can pass through thin sheets of matter.

This property was first discovered by Lenard† who showed that if one end of a cathode ray tube (see Fig. 6) is closed by a thin diaphragm of aluminium, the rays can still be detected outside. This property, instead of helping in the elucidation of the problem, gave rise to the erroneous view that the cathode particles were a kind of electro-magnetic waves like light or the waves used in wireless telegraphy.

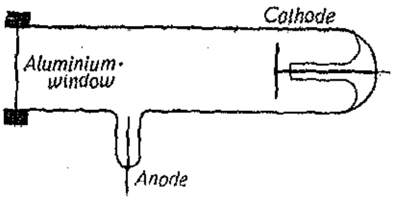

Fig. 6. Lenard's electron tube.

(6) They carry negative charge and are deflected by an electrostatic field. This property of cathode rays was demonstrated by Perrin in 1895 in the following manner.

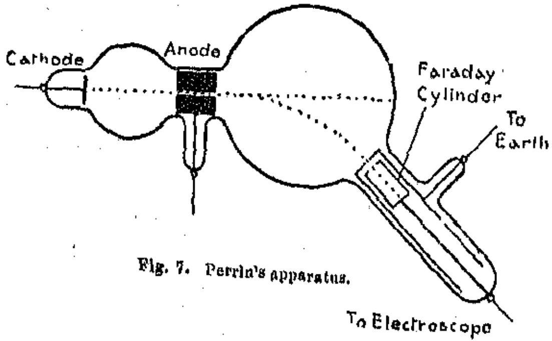

Fig. 7. Perrin's apparatus.

Perrin ‡ took a long discharge tube (Fig. 7) with its anode perforated longitudinally to open into a large glass tube. The latter contained an insulated Faraday cylinder* inclined at an angle. A beam of electrons proceeding from the cathode was led through the anode. It was deflected by applying a suitable magnetic field, to pass into the Faraday cylinder. The latter was connected to a quadrant electrometer which showed a negative charge.

---

* The refractory element tungsten (m. p. 3500°C) was first melted by this method.

† P. Lenard, *Ann. d. Phys.*, 52, 23, 1894.

‡ Perrin, *C. R.*, 121, 1130, 1895.

Quantitative study of these electrical and magnetic deflexions led to determination of $\frac{e}{m}$ (ratio of charge to mass), and of the velocity of these particles.

The movement of an electron under the joint actions of electric and magnetic field is often conveniently studied in an apparatus known as the Braun tube† (Fig. 8).

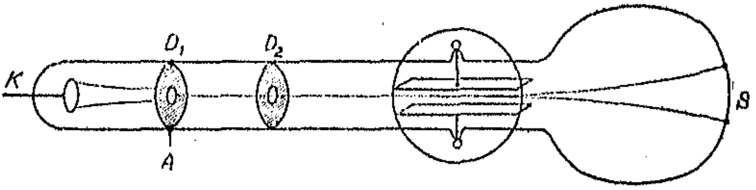

Fig. 8. The Braun tube.

A narrow beam of cathode rays rendered parallel by the diaphragms D_1, D_2, is passed between two parallel plates which are connected to the opposite terminals of a battery. The beam is deflected by the electric field and falls on a willemite screen *S*, and is detected by blue phosphorescent light it produces on the screen. Now applying a magnetic field in a suitable direction, the behaviour of the electron may be observed on the same screen.

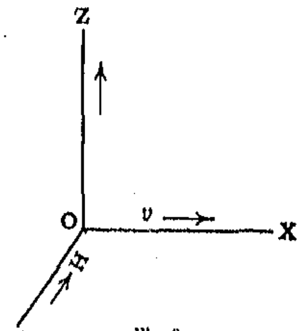

Fig. 9.

21. Elementary Mathematical Treatment of Motion of Electrons.—Let the initial direction of motion be represented (Fig. 9) by the x-axis, and let the electric force be applied along the *z*-axis (vertical), and the magnetic field be along the *y*-axis (perpendicular to the plane of the paper). We first suppose that the fields are applied separately, and then consider their joint action. We have thus three cases:

---

* Faraday Cylinder: A metallic cylinder used for collecting charges.

† J. J. Thomson, *Phil. Mag.*, 44, 293, 1897.

(*a*) There is only an electrostatic field of strength Z.

The particle is now subjected to a constant vertical force eZ and therefore to an acceleration $f = \frac{eZ}{m}$. At O it is projected horizontally with the velocity v. The problem is therefore analogous to the flight of a particle under the gravitational field of the earth. The orbit is a parabola with the latus rectum $l = \frac{2v^2}{f} = \frac{2mv^2}{Ze}$, with O as apex. It can be analytically represented by $x^2 = \frac{2mv^2}{Ze} . z$

Analytically the equations of motion are

$$m\frac{d^2z}{dt^2} = eZ, \qquad m\frac{d^2x}{dt^2} = 0, \quad m\frac{d^2y}{dt^2} = 0 \quad . \quad . \quad . \quad . \quad (1)$$

Hence $\frac{dy}{dt} = \text{const} = 0$, $y = 0$, the motion takes place in the xz-plane.

$$\frac{dx}{dt} = \text{const} = v, \qquad x = vt. \quad . \quad . \quad . \quad . \quad . \quad . \quad (1a)$$

$$\frac{d^2z}{dt^2} = \frac{eZ}{m}, \quad \frac{dz}{dt} = \frac{eZt}{m}, \qquad z = \tfrac{1}{2}.\frac{eZ}{m}t^2 \quad . \quad . \quad (1b)$$

Eliminating t between (1a), and (1b), we have

$$x^2 = \frac{2mv^2}{Ze} \cdot z \quad . \quad . \quad . \quad . \quad . \quad . \quad . \quad . \quad (2)$$

This is the equation of a parabola with its axis along the z-axis. At the apex it can be replaced by its circle of curvature with the radius mv^2/Ze.

(*b*) The electron is subjected to a magnetic field of strength H applied along the y-axis.

The action of the magnetic field on the *moving charge* is just equivalent to that on an element of current. The student has learnt in elementary electrodynamics that the force exerted by H on an element of wire ds carrying a current i is $ids \sin\theta H$, where θ is the angle between i and H, and it is perpendicular to both. In the present case, the charge 'e' moving with the velocity u in the xz-plane is just equivalent to a current $\frac{eu}{c}$ and the force on it $= \frac{Heu}{c}$, and this force is perpendicular to H, therefore it is in the xz-plane, and it is always perpendicular to the current, *i.e.*, to the trajectory.

It is known from dynamics that under these conditions, the trajectory is a circle of which the radius can be found from the relation

$$\frac{mu^2}{r} = \text{force} = \frac{Heu}{c}$$

or

$$r = \frac{muc}{He} \quad \ldots\ldots\ldots\ldots \quad (3)$$

$$u = \text{initial velocity} = v.$$

(c) When both electric and magnetic fields act simultaneously, the orbit will be more complicated. A treatment of this general case will be found in J. J. and G. P. Thomsons' *Conduction of Electricity through Gases.* There it is shown that the orbit is a cycloid or a trochoid, but for all practical purposes, we can deduce correct results from experimental works by assuming that they act separately.

Suppose now in the Braun tube, we first apply the electrostatic field Z, and observe the deflection. Then we apply the magnetic field and bring the spot back to the zero point. The radii of curvatures ρ of the two trajectories will then be equal and opposite. We have

$$\frac{mvc}{eH} = \frac{mv^2}{Ze} = \rho \quad \ldots\ldots\ldots\ldots \quad (4)$$

from which

and

$$\left.\begin{aligned} \frac{v}{c} &= \frac{Z}{H} \\ \frac{e}{mc} &= \frac{Zc}{\rho H^2} \end{aligned}\right\} \quad \ldots\ldots\ldots\ldots \quad (5)$$

These formulæ give us $\frac{e}{mc}$ as well as v.

J. J. Thomson * employed equation (5) to determine $\frac{e}{mc}$ and v for the negative ions of a number of gases. The results of these first determinations were, however, not very accurate. He obtained a mean value of $\frac{e}{mc} = 7{\cdot}7 \times 10^6$, and observed an approximate constancy of $\frac{e}{mc}$ for all the gases examined by him. This value of $\frac{e}{mc}$ is, as we know now, too low. It is found that except in some exceptional cases (*vide* § 29)

$$\frac{e}{mc} = 1{\cdot}77 \times 10^7 \quad \ldots\ldots\ldots\ldots \quad (5a)$$

---

* J. J. Thomson, *Phil. Mag.*, (5), **44**, 293, 1897.

while $\frac{v}{c}$ may have all values from $\frac{1}{300}$ to nearly unity. This value of $\frac{e}{mc}$ was first obtained by Kaufmann in 1897.

22. Kaufmann's determination of $\frac{e}{mc}$.—We shall see in Chap. III that when a particle of mass m and charge e traverses a distance x through a transverse magnetic field H, it suffers a deflection

$$\delta = \frac{e}{mv}\int_0^d\left[\int_0^x H dx\right]dx = \frac{eH}{mv}K_1 \quad . \quad . \quad . \quad . \quad . \quad (6)$$

where d = distance of the screen from the origin. The quantity under the integral sign depends only on the value of the applied field and the geometry of the apparatus and may be taken equal to a constant K_1. The corresponding deflection due to an electric field E is

$$\left.\begin{aligned}\delta' &= \frac{e}{mv^2}\int_0^d\left[\int_0^x E dx\right]dx\\ &= \frac{eE}{mv^2}K_2\end{aligned}\right\} \quad . \quad . \quad . \quad . \quad . \quad (7)$$

If the direction of H is parallel to that of E, the deflection δ will be at right angles to δ'.

Kaufmann applied this theory directly to the determination of $\frac{e}{mc}$. He performed two sets of experiments, one of which we describe below.

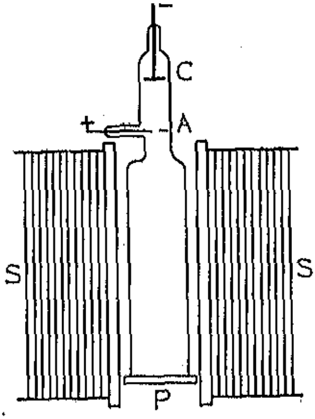

Fig. 10
Kaufmann's apparatus.

The principle of Kaufmann's* earlier experiment is illustrated in Fig. 10. C and A are the cathode and the anode of a discharge tube, between which a difference of potential V is applied. The anode is perforated at the centre, so that the cathode particles coming to A pass into the lower part of the apparatus. A strong magnetic field H is applied over the region from A to P by means of solenoid SS in such a way that lines of force are in the plane of the paper, but perpendicular to the direction of the discharge. On traversing the magnetic field the particles are deflected normally to the plane of the paper. If δ = deflection, we have

---

* W. Kaufmann, *Weid. Ann.*, **61**, 544, 1897.

$$\delta = \frac{He}{mv} \cdot K_1 \quad . \; . \; . \; . \; . \; . \; . \; . \; . \; . \quad (8)$$

P is a photographic plate, and δ can be measured from the trace of the deflected beam on it. Again assuming the velocity v to be acquired under a total fall of potential V, we obtain

$$Ve = \tfrac{1}{2} mv^2 \quad . \; . \; . \; . \; . \; . \; . \; . \; . \; . \; . \quad (9)$$

This assumption is valid, if the loss of energy by molecular collision is negligible. This was found true at low pressures, as the same amount of deflection was produced with different pressures of air in the discharge tube. From (8) and (9)

$$\frac{e}{m} = \frac{2V\delta^2}{H^2 \; K_1^{\,2}} \quad . \; . \; . \; . \; . \; . \; . \; . \quad (10)$$

The integral in equation (6), and hence the constant K_1, was determined by careful investigation of magnetic field between A to P. By this method Kaufmann obtained $\frac{e}{mc} = 1{\cdot}77 \times 10^7$ for cathode rays.

23. Maximum Velocity of Electrons.—In a discharge tube, the velocity of the electron is really determined by the potential difference between the cathode and the anode, according to the law

$$\tfrac{1}{2} mv^2 = eV \quad . \; . \; . \; . \; . \; . \; . \; . \; . \; . \quad (9a)$$

i.e., kinetic energy acquired by the cathode particle is equal to the work done as it falls through a potential difference V.

$$v = \sqrt{\frac{2eV}{m}} = \sqrt{\frac{2 \times 1{\cdot}77 \times 10^7 \times 3 \times 10^{10}}{300}} \,.\, \sqrt{V}$$

when the potential is expressed in volts, for, 1 volt = $\frac{1}{300}$ e. s. unit. Therefore

$$v = 5{\cdot}92 \times 10^7 \,.\sqrt{V} \text{ cm./sec.} \quad . \; . \; . \; . \; . \; . \quad (11)$$

This formula holds as long as $v < c$, the velocity of light (*vide* § 28).

All cathode particles do not possess the velocity given by (6), because some originate in the middle of the tube, others lose velocity by collision. The velocity given by (6) represents the maximum velocity attainable in a discharge tube.

Again, when subjected to a magnetic field H, the path of the electron is ρ, given by equation (4) as

$$H\rho = \frac{mvc}{e} \quad . \; . \; . \; . \; . \; . \; . \; . \; . \quad (12)$$

The product of maximum velocity $v_{max.}$ given by (9a) and $H\rho$ is therefore a measure of kinetic energy of the electrons. The velocity and kinetic energy of the electrons corresponding to given differences of potential are shown in the following table taken from Gräetz's *Handbuch der Electrizität und Magnetismus,* Vol. III, page 135.

Table 1.

Potential (Volts).	Velocity × 10^{-8} (cm. sec.$^{-1}$)	$H\rho$	Kinetic energy × 10^{12} (ergs.)
0·5	0·418	2·39	0·785
1·0	0·592	3·38	1·57
2·0	0·836	4·78	3·14
3·0	1·025	5·86	4·71
4·0	1·183	6·76	6·25
5·0	1·323	7·56	7·85
6·0	1·449	8·28	9·42
7·0	1·566	8·95	10·1
8·0	1·673	9·56	12·6
9·0	1·775	10·14	14·1
10·0	1·871	10·69	15·7
20·0	2·646	15·12	31·4
100·0	5·920	33·80	157·0
300·0	10·250	58·60	471·0

For laboratory methods of determining $\frac{e}{m}$ see Appendix, Note 2.

24. The Elementary Quantum of Electricity.—The formula (5) gives us the ratio between e and m. Unless we can find out either e or m separately, no further progress in the study of the electron is possible. We shall describe in the next section how 'e' has been determined. But before this was done, it was found that the cathode particle, though it was first isolated in such an artificial medium as a vacuum tube, is in itself not so rare, but is given out in almost all chemical and physical processes. Thus it was early observed that when a body was heated, it could discharge an electroscope placed in its neighbourhood. It is now known that all bodies, when they are sufficiently heated, emit electrons which make the air near it conducting and help in the discharge of electroscopes. (This phenomenon is treated under *Thermionics*.)

It was found in the last century that when a metal plate is illuminated by ultraviolet light, an electroscope placed in its neighbourhood gets easily discharged and the plate, if insulated, is found to be positively charged (*Hallwachs*). This has been proved to be due to the liberation of electrons by light *(photo-electrons)* from the metallic plate. In all these and other cases, e.g., *radio-activity, chemical reactions,* the nature of these negatively charged particles has been studied by using the method described here and $\frac{e}{mc}$ has always been found to have the value given by (5*a*).

All these considerations point out that *the cathode particle or the electron is a universal constituent of all matter.*

25. Mass of the Electron.—Before the charge on the electron was measured with any certainty, some physicists had come to the conclusion that the fundamental quantum of electricity, as we obtain in electrolysis, is identical with the charge carried by the cathode particle. On this assumption we can compare the mass of the electron with that of the hydrogen atom. Thus we have from electrolysis

$$\frac{Ne}{c} = 9645 \quad . \; . \; . \; . \; . \; . \; . \; . \; . \; (13)$$

where e = charge carried by a monovalent ion, say H^+, and $Nm_H = 1$.

Hence $$\frac{e_H}{cm_H} = 9645 \text{ e.m. units.}$$

For the cathode particle $\frac{e}{cm} = 1{\cdot}773 \times 10^7$ e.m. units.

Supposing that $e_{\mathrm{H}} = e$, we have

$$\frac{m}{m_{\mathrm{H}}} = \frac{9645}{1{\cdot}773\times10^{7}} = \frac{1}{1847}$$

Thus the electron is found to be nearly 2000 times lighter than the smallest atom known up to the year 1896.

But the hypothesis that the charge on the cathode particle is equal to the charge carried by monovalent ions in solution required confirmation.

26. Determination of the Charge on the Electron—Millikan's Method.—The measurement of the charge on the electron proved to be a rather long and protracted affair, and we shall omit here the account of the earlier historical experiments carried out at the Cavendish Laboratory by Townsend, J. J. Thomson, H. A. Wilson and others. A short account is given at the end of the chapter. We proceed to the description of Millikan's* experiment which proves that electricity produced by friction on very small particles always occurs in integral multiples of the elementary quantum $e=4{\cdot}774\times10^{-10}$ e. s. units.

The essential parts of the apparatus (Fig. 11) are two plane parallel plates of brass M and N forming a parallel plate condenser and separated by a distance of 0·5 to 0·8 cm. One plate is connected to earth, the other charged to a high-potential which may be as large as 1000 volts. There is thus a vertical electrostatic field in the space between M and N. A is an atomiser containing oil which opens over the vertical orifice P in the upper plate; when the atomiser is blown, small particles (10^{-2} cm. in diameter) of oil enter into the condenser space through P. In the process of atomisation, they are charged with electricity by friction. In the condenser space they are subjected to the vertical forces (i) gravity$=mg$, (2) electrical force$=qZ$, where q=charge, Z= field strength. The electrical force can be made to oppose the force due to gravity by manipulating a reversing key. The particle is illuminated from the sides by means of light coming from a strong source (a high power glow lamp), and focussed exactly on the centre by lenses. The oil drop is then observed by means of a small telescope provided with three horizontal cross-wires. The drop appears

---

*R. A. Millikan, *Phys. Rev.*, 2, 136, 1913.

as a luminous point in the field of view, and is seen to go up or down, and the velocity can be reduced to any small value by adjusting the field strength. The charge can now be deduced from these observed velocities in the following way :—

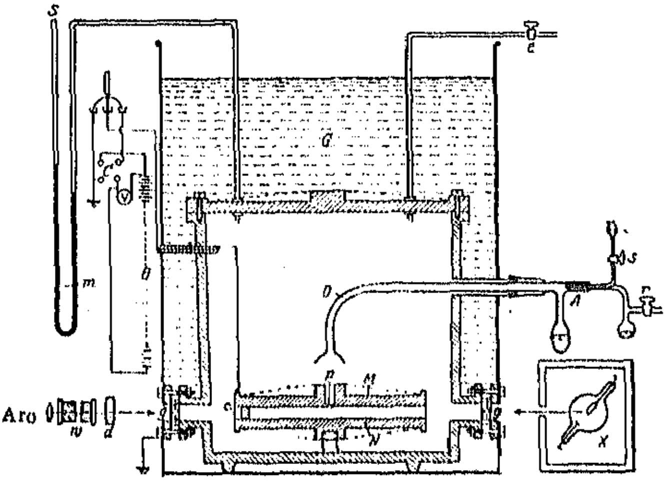

Fig. 11. Millikan's apparatus.

Since the particle is moving in a viscous medium, the force F required to maintain it in motion with the *steady* velocity v is, according to a fundamental theorem by Stokes,*

$$F = 6\,\pi a\mu v \quad . \quad . \quad . \quad . \quad . \quad . \quad . \quad . \quad . \quad . \quad (14)$$

where μ = coefficient of viscosity of the medium, a = radius of the particle. Let v_1 = velocity when an e. s. field Z is working on the particle urging it upwards. Then we have

$$6\,\pi a\mu v_1 = e_n Z - mg \quad . \quad . \quad . \quad . \quad . \quad . \quad . \quad . \quad (15)$$

$$6\,\pi a\mu v_2 = mg \quad . \quad . \quad . \quad . \quad . \quad . \quad . \quad . \quad . \quad . \quad (16)$$

when v_2 = velocity of free fall when the electric field is not applied, and e_n = charge on the particle.

From (15) and (16), we have

$$\frac{v_1 + v_2}{v_2} = \frac{e_n Z}{mg} \quad . \quad . \quad . \quad . \quad . \quad . \quad . \quad (17)$$

---

* For the deduction of Stokes' law from hydrodynamical principles, see Lamb, *Hydrodynamics*, Chap. XI, § 338.

Now e_n can be obtained if m, the mass of the oil drop, can be known.

Generally the oil drop is so small that its mass can be obtained only indirectly. This can be done from (16). Let ρ be the density of oil, and σ the density of air. We have

$$6\,\pi a\mu m v_2 = mg = \frac{4\pi a^3}{3}\,g\,(\rho-\sigma)$$

from which $a = \left(\frac{9\mu v_2}{2g\rho}\right)^{\frac{1}{2}}$, neglecting σ in comparison to ρ.

and $$e_n = \frac{4\pi}{3}\left(\frac{9\mu}{2g}\right)^{\frac{3}{2}}\frac{g}{Z}\,\frac{(v_1+v_2)v_2^{\frac{1}{2}}}{(\rho-\sigma)^{\frac{1}{2}}} \quad . \; . \; . \; . \; . \quad (18)$$

Sometimes the particle under observation may pick up new charges from the neighbouring air. This is particularly facilitated if the air is ionised by X-rays, or by the presence of a speck of radioactive matter in the lower condenser plate. Let $e_{n'}$ be the new charge, and let the particle now move with the velocity v'_1.

Then we have

$$e_n = \frac{mg}{v_2 Z}(v_1 + v_2) \quad . \; . \; . \; . \; . \; . \; . \; . \; . \; . \quad (19)$$

$$e_{n'} = \frac{mg}{v_2 Z}(v'_1 + v_2) \quad . \; . \; . \; . \; . \; . \; . \; . \; . \; . \quad (20)$$

We have now

$$e_{n'} - e_n = \frac{mg}{Zv_2}(v'_1 - v_1) = \frac{mgd}{Zv_2}\left(\frac{1}{t'_1} - \frac{1}{t_1}\right) \quad . \quad (21)$$

Now $$v_1 = \frac{d}{t_1}, \qquad v'_1 = \frac{d}{t'_1}$$

where d = distance between the crosswires, t_1 = time of passage between the two wires.

Now if $e_{n'} - e_n = pe$, where p is an integral number, we have

$$\frac{1}{t'} - \frac{1}{t_1} = \frac{Zv_2}{mgd}\,e\,p \quad . \; . \; . \; . \; . \; . \; . \; . \quad (22)$$

i.e., the differences $\frac{1}{t'_1} - \frac{1}{t_1}$ will be integral multiples of a common factor. That this is the case is shown in the following table, adopted from Millikan's "*The Electron,*" Chap. IV, p. 75.

Table 2

t_1 (Sec.)	t'_1 (Sec.)	$\frac{1}{t_1}$	$\frac{1}{t'_1}$	$\pm\left(\frac{1}{t'_1}-\frac{1}{t_1}\right)$	p	$\frac{1}{p}\left(\frac{1}{t'_1}-\frac{1}{t_1}\right)$
80·708	22·366 22·390 22·368	·01236	·04470	·03234	6	·005390
22·366 22·390 22·368	140·565	·04470	·00719	·03751	7	·005348
140·565	79·600	·007192	·01254	·005348	1	·005348
79·600	34·748 34·762 34·846	·01254	·02870	·01616	3	·005387
34·748 34·762 34·846	...	·02870	...	...	...	...
29·286 29·236	137·308	·03414	·007268	·026872	5	·005375
137·308	34·638	·007268	·02884	·021572	4	·005393
34·638	22·104 22·268	·02884	·04507	·01623	3	·005410
22·104 22·268	500·1	·04507	·00200	·04307	8	·005384
500·1	19·704 19·668	·00200	·05070	·04870	9	·005421
19·704 19·668	77·830 77·806	·05070	·01285	·03794	7	·005420
77·830 77·806	42·302	·01285	·02364	·01079	2	·005395
42·302	...	·02364	...	...	...	...

27. Ehrenhaft's Hypothesis of Sub-electrons.—Ehrenhaft* carried out the same kind of experiments as Millikan did, but with particles of a much smaller size. These particles were formed by blowing a draft of air against an arc maintained between metallic electrodes. Very small particles from 10^{-4} to 10^{-6} cm. in diameter could thus be obtained. Ehrenhaft did not find consistent values of the elementary charge as Millikan did, but his values were very often much less than Millikan's value of e. He was led to the conclusion that "sub-electrons," or electrical charges less than that carried by electrons exist.

---

* Ehrenhaft, *Phys. Zeits.*, **11**, 619, 940, 1910.

Ehrenhaft's hypothesis of sub-electrons did not find much credence amongst the physicists, and Millikan*, Bär† and others have pointed out that his results are due to two sources of error in his experiments:—(i) on account of the extreme smallness of the particles, their sizes cannot be determined by an application of Stokes' Law, for this holds only when the size of the particle is large compared to the mean free path of the gaseous molecules amongst which the particle is moving. In Ehrenhaft's case the size, 10^{-5} and 10^{-6} cm., is of the same order as the mean free path, *viz.*, 10^{-5} cm. In such cases, the apparent value of the viscosity has to be corrected according to a formula given by Cunningham‡. This is

$$\mu = \frac{\mu_0}{1+A\frac{l}{a}} \quad . \; . \; . \; . \; . \; . \; . \; . \; . \; . \; . \; . \; . \quad (23)$$

where $\mu =$ corrected value, and $\mu_0 =$ ordinary value of viscosity, $A =$ a constant, and l = mean free path of molecules. This gives at once the corrected velocity

$$v_2 = \frac{2}{9} \frac{ga^2}{\mu_0}(\rho-\sigma)\left(1+A\frac{l}{a}\right) \quad . \; . \; . \; . \; . \; . \; . \; . \quad (24)$$

Hence the absolute value e_n in terms of the apparent value e_{n_1} is given by

$$e_n = \frac{e_{n_1}}{\left(1+A\frac{l}{a}\right)^{\frac{3}{2}}} \quad . \; . \; . \; . \; . \; . \; . \; . \; . \; . \; . \quad (25)$$

or

$$e_n^{2/3}\left(1+A\frac{l}{a}\right) = e_{n_1}^{2/3} \quad . \; . \; . \; . \; . \; . \; . \; . \; . \quad (26)$$

To apply this correction, a large series of e-values for different values of $\frac{l}{a}$ are experimentally obtained by varying either the pressure or the size of the drops. A graph is then plotted with $\frac{1}{ap}$ as abscissa, where

---

[*] R. A. Millikan, *Phys. Zeits.*, **12**, 161, 1911; *Phys. Rev.*, **32**, 394, 1911.

[†] R. Bär, *Ann. d. Phys.*, **67**, 157, 1922.

[‡] Cunningham, *Proc. Roy. Soc. A*, **83**, 360. 1910.

p = pressure of the gas, and $e_1^{\frac{2}{3}}$ as ordinates (Fig. 12). The graph becomes a straight line, from which both e_n and A can be obtained from the relation (26), using the conditions: (1) when $\frac{1}{ap} = 0$, $e_n = e_{n_1}$,

$$\text{(2) when } e_{n_1} = 0, \quad A = -\left(\frac{l}{a}\right)^{-1} = -\frac{1}{lp}\left(\frac{1}{ap}\right)^{-1} = \frac{1}{lp}\cdot\frac{1}{\text{OB}}.$$

Introducing this correction, Millikan found that Ehrenhaft's results gave more consistent values of e. The second source of error is due to the assumption that the atomised particles have the same density as the solid metal. It is quite probable that during arcing, the metal is oxidised, or becomes porous.

A typical set of data giving the absolute value of e is shown in the following table 3 which has been taken from one of Millikan's papers*

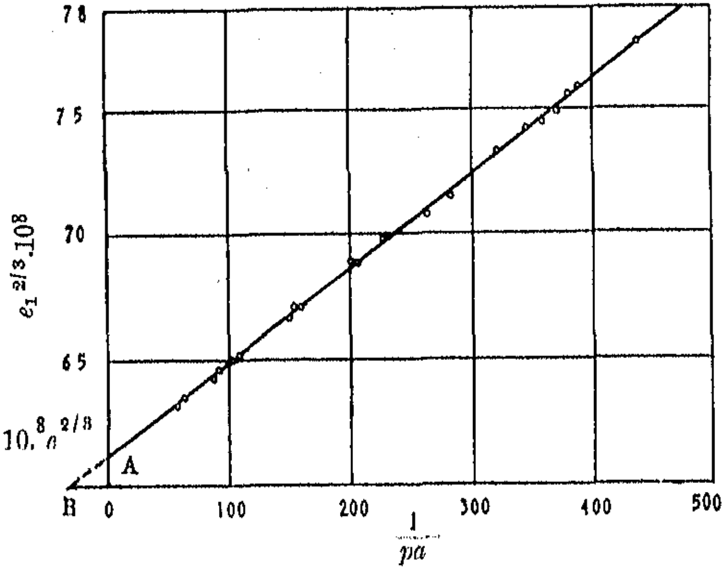

Fig. 12

These data are for oil particles in air, and correspond to the straight line in Fig. 12.

---

* R. A. Millikan, *Phil. Mag.*, 34, 1, 1917.

Table 3

Number.	Potential (Volts)	Time of free fall t_2 (sec.)	v_2 (cm./sec.)	Number of free electrons n	$a \times 10^5$	p (cm. of Hg.)	$\frac{1}{pa}$	$\frac{l}{a}$	$e_1.^{\frac{2}{3}} 10^8$	$e^{\frac{2}{3}} 10^8$
1	6650	16·50	0·06194	7—13	23·40	74·49	57·45	0·04111	63·21	61·03
2	6100	16·76	·06099	8—11	23·22	75·00	75·5	·04115	63·204	61·03
3	5308	19·73	·05180	7—15	21·34	74·49	63·0	·04509	63·54	61·16
4	4132	37·82	·02703	4—6	15·33	75·37	86·7	·06205	64·27	60·97
5	4661	40·09	·02521	3—6	14·84	75·00	90·6	·06484	64·63	61·21
6	4111	51·53	·01983	3—4	13·05	75·77	101·3	·06502	65·02	61·16
7	5299	51·48	·01985	2—5	13·05	74·98	102·4	·07329	65·07	61·20
8	6661	56·06	·01823	2—3	12·50	75·40	106·3	·07608	65·13	61·11
9	6082	59·14	·01728	1—4	12·17	75·04	109·7	·07850	65·19	61·05
10	4077	57·46	·01779	3—8	12·34	75·67	107·3	·07680	65·21	61·16
11	4663	16·58	·06165	10—12	22·72	29·26	150·6	·10780	66·70	61·01
12	4661	29·18	·03502	5—7	17·08	36·61	160·1	·1146	67·12	61·07
13	4687	18·81	·05432	8—10	21·26	30·27	155·6	·1114	67·14	61·26
14	4651	47·65	·02145	2—7	13·20	36·80	206·4	·1477	68·90	61·11
15	4648	32·72	·03129	4—6	15·92	31·35	200·7	·1437	68·97	61·39
16	3393	18·34	·05572	12—16	21·11	20·58	227·8	·1630	69·88	61·27
17	4669	46·82	·02294	2—4	13·12	29·10	262·4	·1878	70·85	60·94
18	4691	26·62	·03819	5—7	17·32	20·54	281·4	·2014	71·60	60·98
19	3339	14·10	·07249	15—19	23·00	13·24	321·4	·2297	73·34	61·20
20	4682	39·24	·02605	3—5	14·00	20·72	345·4	·2472	74·27	61·22
21	3350	18·30	·05585	10—13	20·47	13·62	359·1	·2570	74·54	60·97
22	3370	43·88	·02329	3—6	13·17	20·47	371·5	·2659	75·00	60·97
23	3381	46·90	·02179	3—6	12·69	20·74	380·6	·2724	75·62	61·24
24	3345	19·65	·05201	9—12	19·65	13·12	388·5	·2781	75·92	61·24
25	3344	26·76	·03819	6—9	16·57	13·80	438·3	·3137	77·74	61·18
									Mean=61·129	

The above values of $e^{\frac{2}{3}}$ have been computed on the basis that the viscosity of air is $\mu=0·0001824$, and the absolute value of electronic charge corresponding to the mean value $e^{\frac{2}{3}}=61·126$ comes out to be

$$e = 4·774 \times 10^{-10} \text{ e. s. units.}$$

Experiments have also been performed on droplets of mercury in air, and on drops formed out of shellac in air. Taking the average of a large number of data for a variety of substances, and calculating the most probable error, the value of the elementary quantum of electricity as obtained from Millikan's experiments is

$$e = (4·774 \pm 0·005) \times 10^{-10} \text{ electrostatic units.}$$

27a. On the Absolute Value of *e*—Recently much controversy has been taking place regarding the exact absolute value of the elementary electronic charge e, specific electronic charge $\frac{e}{m}$, and some other fundamental physical constants, *e.g.*, Planck's constant h and others, which we shall come across later.

R. T. Birge* made a critical study of the different experimental methods, of methods of calculation and their probable errors in case of thirteen fundamental physical constants including the above. He recalculated their values by using the most up to date and reliable values of all *auxiliary constants,* avoiding any approximate formulae, and taking weighted mean of values of the same constant obtained by different methods.

Thus, as stated before, Millikan's value of electronic charge is

$$e=(4{\cdot}774\pm0{\cdot}005)\times10^{-10} \text{ e. s. units.}$$

This was calculated on the basis of the following values: viscosity of air $\mu=0{\cdot}0001824$, and $c=2{\cdot}999\times10^{10}$ cm. sec.$^{-1}$. Birge recalculated it, taking $\mu=0{\cdot}00018227$ (value of 1917-determination), Michelson's† value of velocity of light, $c=(2{\cdot}99796\pm0{\cdot}00004)\times10^{10}$ cm. sec.$^{-1}$, and recalculating all electrical quantities in international units, he obtains

$$e=(4{\cdot}768\pm0{\cdot}005)\times10^{-10} \text{ e. s. units}$$

In recent years, other independent methods for the accurate determination of e have been developed. These are based upon the relation (see appendix) $Ne=9648\pm0{\cdot}7$ e.m. units of electricity, where N stands for the Avogadro number. N has been determined accurately (i) from an estimation of lattice constant of crystals by Wadlund‡ (ii) from the absolute determination of the wavelength of K_α line of Cu, (iii) by Bäcklin§, from that of K_α line of Al and (iv) by Bearden§§ from K and K_β lines of Cu. Their values of e are as follows:

Wadlund ..... $e=(4{\cdot}776\pm0{\cdot}0003)\times10^{-10}$

Bäcklin ..... $e=(4{\cdot}793\pm0{\cdot}015)\times10^{-10}$

Bearden ..... $e=(4{\cdot}825\pm\quad)\times10^{-10}$

---

* R. T. Birge, *Phys. Rev. Suppl.,* **1**, 1, 1929.

† A. A. Michelson, *Astr. J.,* **65**, 1, 1927.

‡ A. P. R. Wadlund, *Proc. Nat. Acad. Sci.,* **14**, 588, 1924; *Phys. Rev.,* **32**, 841, 1928.

§ E. Bäcklin, *Absolute 'Wellenlängenbestimmungen der Röntgen Strahlen, Upsala Dissertation,* 1928.

§§ J. A. Bearden, *Proc. Nat. Acad. Sci.,* **15**, 528, 1929.

Birge considers the last two values much too high, and holds that being pioneer works, they are open to unsuspected errors, and rejects them. Taking the weighted mean of Millikan's and Wadlund's values, he gives the most probable value of the electronic charge as

$$e=(4{\cdot}770\pm0{\cdot}005)\times10^{-10} \text{ e. s. units}$$
$$=(1{\cdot}5910\pm0{\cdot}0016)\times10^{-20} \text{ e. m. units.}$$

W. N. Bond,* on the other hand, has started discussions on the values of the fundamental constants from an entirely different point of view. It had been long suspected that some primary relation exists between the fundamental constants e, c and h. Attacking the problem by the method of dimensions, it is found that the product $\frac{hc}{e^2}$ is a pure number, the same quantity occurs in Sommerfeld's fine-structure constant (Chap. VII) as $\alpha = \frac{2\pi e^2}{ch}$. Eddington † has obtained from considerations of quantum mechanics that

$$\frac{hc}{2\pi e^2} = 137. \quad . \quad . \quad . \quad . \quad . \quad . \quad . \quad . \quad . \quad . \qquad (27)$$

Bond starts his calculations of e and h on the supposition that Eddington's relation is correct.

Birge has pointed out that the determination of Planck's constant h from any experimental data is equivalent to the estimation of a constant A in an equation of the form

$$h=A\,e^{n} \quad . \quad . \quad . \quad . \quad . \quad . \quad . \quad . \quad . \quad . \qquad (27a)$$

where n has the values 1, $1\frac{1}{3}$, $1\frac{2}{3}$, 2, etc. . . . according to the method used. Thus in Eddington's relation

$$A = \frac{2\pi}{c}.137$$
$$n=2$$

Now if we choose any particular value of A permanently, and can assign to e its correct value, then since the values of h given by different methods should be fundamentally the same, we hope to obtain a value of h from equation (27a) which will not vary *systematically* with the value of the index n. Bond has chosen $A=\frac{2\pi}{c}\cdot 137$ and by trial has found that the particular value of e, for which the h-values corresponding to the different values of n lie unsymmetrically about a mean value of h. This method gave him the following values for e and h:—

---

* W. N. Bond, *Phil. Mag.*, **10**, 994, 1930.

† Eddington, *Proc. Roy. Soc. A*, **126**, 696, 1930.

$$e=(4{\cdot}779\pm0{\cdot}0017)\times10^{-10} \text{ e. s. units.}$$

$$h=(6{\cdot}559\pm0{\cdot}0046)\times10^{-27} \text{ erg. sec.}$$

Further, from this consideration, Bond finds no justification for rejecting Bäcklin's and Bearden's values of e, as Birge has done. It will be noticed that Bond's value of e calculated on the assumption of Eddington's relation is nearer Bäcklin and Bearden's values than Millikan's. The two sets of values, however, are widely different, which leaves the situation very uncertain.

28. $\frac{e}{mc}$ for very swift electrons — Kaufmann's experiment.—It was found by Kaufmann* that for very swift electrons, such as β-rays from RaC, which are projected with velocities nearing the velocity of light the value of $\frac{e}{mc}$ was not constant, but decreased rapidly. In one of Kaufmann's experiments, $\frac{e}{mc}$ was found to have as small a value as $1{\cdot}1\times10^7$ e. m. units. We describe below Kaufmann's experiment which led to this important discovery.

The apparatus used is shown in Fig. 13.

R . . . is a small speck of Ra within a vacuum chamber.

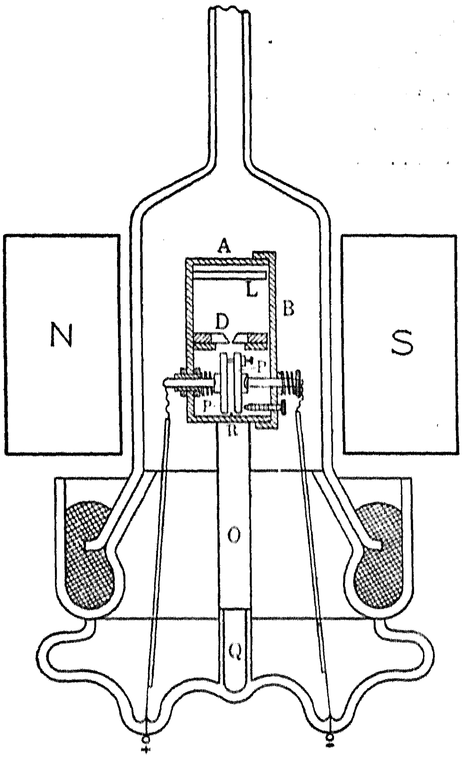

Fig. 13. Kaufmann's apparatus.

P, P. . . are a pair of plates about 1·5 mm. apart. A difference of potential of about 6700 volts is applied across them.

---

* W. Kaufmann, *Göttingener Nachr.*, 1901—1903; *Ann. d. Phys.*, **19**, 487, 1906.

D... is a diaphragm in front of the space between P, P.

L... is a photographic plate, situated perpendicular to the plane of P, P.

N, S... are the poles of a strong electromagnet giving a magnetic field over the region from the source R to L.

β-rays from Ra pass between P, P and are acted on by the electric field. They are led out of the plates through D and finally strike the photographic plate L. During the whole of the journey from R to L, the rays are acted on by the magnetic field whose lines of force are parallel to those of the electric field. At the beginning of the experiment, both the fields are withdrawn, and a spot corresponding to the direct beam is obtained on L. Then the fields are applied and the particles are deviated. The two deflections are at right angles to each other, the electric deflection being parallel to the plane of the paper, and the magnetic deflection above or below the plane. They can be both found from the positions of the deflected and undeflected traces on L. These have been expressed in (6) and (7) as

$$\delta = \frac{e}{mv}\int_0^d \left[\int_0^x H dx\right] dx$$

$$\delta' = \frac{e}{mv^2}\int_0^d \left[\int_0^x E dx\right] dx$$

which give both v and $\frac{e}{mc}$. Thus each point of the trace on the photographic plate gives $\frac{e}{mc}$ corresponding to a definite velocity v. A few of Kaufmann's results are shown in the following table which clearly indicates a variation of $\frac{e}{mc}$ with v.

Table 4

$v \times 10^{-10}$	$\frac{e}{mc} \times 10^{-7}$
2·83	·63
2·72	·77
2·59	·95
2·48	1·17
2·36	1·31

Since β-rays from RaC possess velocities almost up to the velocity of light, the deflected points will be distributed on a continuous curve on the photographic plate reaching almost the origin. If again, the electric field be reversed during the experiment, a second branch of the curve will be produced, which is the image of the first corresponding to the points of equal and opposite electric deflections. It easily follows that if $\frac{e}{mc}$ were constant for all β-rays, the two branches of the curve (Fig. 14a) would meet, and have a common tangent at the undeflected point. The experimental curve is shown in Fig. 14 (b) which clearly shows that the two branches do not touch. The obvious conclusion from this result is that $\frac{e}{mc}$ depends upon the velocity of the particle.

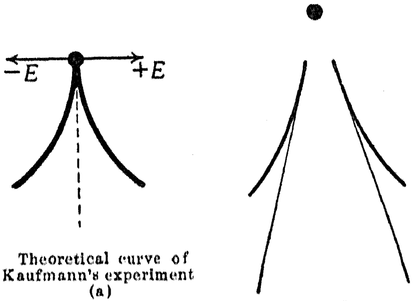

Theoretical curve of Kaufmann's experiment (a)

Experimental curve. (b)

Fig. 14

It was pointed out by Kaufmann and J. J. Thomson that these results can be explained by assuming that while e remains constant, m, the mass of the electron, is not constant, but varies with the velocity. Various expressions have been found for the variation of the mass of the electron with velocity. According to Abraham, the electron in motion behaves as a rigid sphere. On this hypothesis of *rigid electrons*, Abraham* obtained the following formula for the variation of mass with velocity.

$$m = \frac{3}{4}\frac{m_0}{\beta^2}\left[\frac{1+\beta^2}{2\beta} \cdot \ln\frac{1+\beta}{1-\beta} - 1\right] \quad . \; . \; . \; . \; . \; (28)$$

where m_0 = rest-mass, $\beta = \frac{v}{c}$. According to Lorentz, a contraction occurs in the dimension of the electron in the direction of the motion in the ratio $\sqrt{1-\beta^2} : 1$. On this hypothesis of *contractile electrons*, Lorentz* obtained the following expression for the variation of mass with velocity

$$m = \frac{m_0}{\sqrt{1-\frac{v^2}{c^2}}} \quad . \; . \; . \; . \; . \; . \; . \; . \; . \; . \; . \; (29)$$

---

* For the derivation of Abraham and Lorentz-formulae, see Lorentz, *Theory of Electrons*, Chap. V.

This expression was also deduced independently from the principle of Special Relativity by Einstein, and is generally referred to as the *Lorentz-Einstein*[*] *formula.*

A large number of experiments were carried out by Bucherer, Guye, and others to decide between the two rival formulae. The Lorentz-Einstein formula was found to be correct. We describe below Bucherer's experiments. In this, the method of crossed fields, explained in greater detail in Chap. III was used.

29. Bucherer's Experiment.—The main purpose of Bucherer's[†] experiment, as stated above, was to decide between the Abraham *rigid electron* and the Lorentz *contractile electron.* The experimental arrangement used for this purpose is shown in Fig. 15. A parallel plate condenser with two circular plates A, B very close to each other was taken. A small speck of RaF was placed at R, the centre of the lower plate. The condenser was connected to opposite terminals of a battery, and the whole was placed inside a co-axial cylinder C D which was evacuated. The cylinder was kept between the poles of a rectangular solenoid, so that the magnetic lines of force were parallel to the plates of the condenser, and perpendicular to the plane of the paper. A photographic film was inserted all along the circumference of the cylinder.

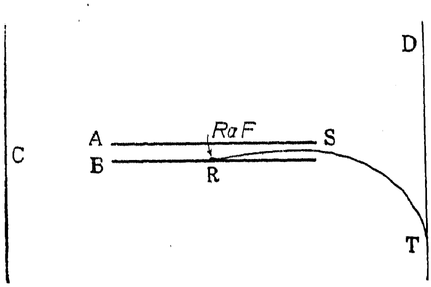

Fig. 15. Arrangements of Bucherer's experiment.

On withdrawing the magnetic and electric fields, at first β-particles from RaF were ejected in straight lines between the plates, and struck the photographic film so as to produce a complete circular trace on it in the plane of the condenser. Now suppose the fields are applied. Let a particle start with a velocity v in a direction θ with the magnetic field. If the magnetic and electric fields are not properly compensated, it will be arrested by either of the plates A, B. It will be able to pass out of them, when the fields have satisfied the condition

$$Xe = Hev \sin\theta c \quad . \; . \; . \; . \; . \; . \; . \; . \; . \quad (30)$$

---

[*] Einstein, *Ann. d, Phys. V*, **17**, 1905.

[†] A. H. Bucherer, *Ann. d. Phys. IV*, **28**, 513, 1909.

Thus a particle escaping in a direction θ possesses a velocity

$$\left.\begin{aligned} v &= \frac{X}{H\sin\theta} \\ \text{or} \qquad \beta &= \frac{X}{cH\sin\theta} \end{aligned}\right\} \quad \ldots\ldots\ldots (31)$$

In Bucherer's experiment, the electric and magnetic fields are so arranged that $\frac{X}{cH} = \frac{1}{2}$, so that

$$\sin\theta = \frac{1}{2\beta} \quad \ldots\ldots\ldots\ldots\ldots (32)$$

What happens when a β-particle comes outside the plates? Here a particle is acted upon by the magnetic field alone, and is deflected in a spiral path, and strikes the cylinder at a distance z, below the circular trace. We can get an idea of z, the amount of deflection for different particles coming out in different directions as follows. From the relation (32) we have, when

$$\theta=30^\circ,\quad \beta=1,\quad v=c,\quad z=0$$

$$\theta=\frac{\pi}{2},\quad \beta=\tfrac{1}{2},\quad v=\tfrac{1}{2}c,\quad z=\text{maximum}$$

$$\theta=150^\circ,\ \beta=1,\quad v=c,\quad z=0.$$

For, the radius of curvature of the deflected path is proportional to the mass of the particle, which becomes infinite when $v=c$. Hence the particle travels undeflected; in other words, in the directions of 30° and 150°, the particles directly meet the undeflected circular trace. The particles suffer a maximum deflection in a direction midway between them, that is, at $\theta = 90^\circ$. In other directions, the deflections have intermediate values. No particle can escape from between the plates in a direction for which θ lies outside the range 30° and 150°. For when $\theta>150^\circ$ or $\theta<30^\circ$, $v>c$, which is an impossible velocity for any material particle. On unrolling the film, the traces show the appearance given in Fig. 16. The central

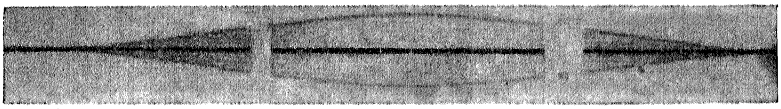

Fig. 16

Traces of the electron in Bucherer's experiment.

line corresponds to the undeflected circular trace, and the deflected traces corresponding to the applications of direct and reversed fields are on either sides of it.

At the point corresponding to the maximum deflection, the path of the particle is circular, so that we can calculate the radius of curvature r in terms of z. If r be the radius of curvature of the circle and a the distance between the photographic plate and the nearest end of the condenser we have

$$z = \frac{a^2}{2r-z}$$

We therefore get $\frac{mv^2}{r} = Hev$ or $m = \frac{He}{2v}\left(z+\frac{a^2}{z}\right)$

Using the Lorentz-Einstein formula $m = m_0\,(1-\beta^2)^{-\frac{1}{2}}$ we obtain

$$\frac{e}{m_0} = \frac{2v}{H} \cdot \frac{z}{a^2+z^2} \cdot \frac{1}{\sqrt{1-\beta^2}}$$

$$= \frac{2cz}{H\,(a^2+z^2)} \tan\,(\sin^{-1}\beta) \quad . \quad . \quad . \quad . \quad . \quad (33)$$

Since $\beta = \frac{1}{2}$, hence $\tan\,(\sin^{-1}\beta) = \frac{1}{\sqrt{3}}\cdot$ We have using the Abraham formula

$$m = \frac{3}{4}\,\frac{m_0}{\beta}\left[\,\frac{1+\beta^2}{2\beta}\,ln\,\frac{1+\beta}{1-\beta}-1\,\right],$$

$$\frac{e}{m_0} = \frac{2\,cz}{H\,(a^2+z^2)}\left[\frac{3}{4\beta}\cdot\frac{2\delta-\tanh 2\delta}{\tan 2\delta}\right] \quad . \quad . \quad . \quad (34)$$

where $\delta = \tanh^{-1}\beta$.

Thus the absolute values of $\frac{e}{m_0}$ can be calculated from the experimentally observed maximum deflections corresponding to different values of β by means of the formulæ (33) or (34). The relative constancy of the values calculated from the two formulæ allows to decide between them. The data obtained are shown below;

Table 5

$\beta = \frac{v}{c}$	H (*gauss*)	z (*mm*)	$\frac{e}{mc} \cdot 10^{-7}$ (Lorentz)	$\frac{e}{mc} \cdot 10^{-7}$ (Abraham)
·3173	104·55	16·37	1·752	1·726
·3787	115·78	14·45	1·761	1·733
·4281	127·37	13·50	1·760	1·723
·5154	127·55	10·18	1·763	1·706
·5154	127·55	10·35	—	—
·6870	127·55	6·23	1·767	1·642

The above results show that the Lorentz-Einstein formula agrees closely with the experimental observations, while the values calculated from the Abraham formula do not satisfy the experimental values.

30. Early Determinations of *e*.—The earliest determination of the absolute value of the electronic charge was due to Townsend* in 1897. His experiment, though not very accurate and based on assumptions not quite free from objections is interesting, as it utilised practically all the principles underlying all subsequent accurate determinations of *e*.

It is well-known that the gases liberated during electrolysis at the two electrodes of a voltameter carry electric charges of positive and negative signs with them. Townsend showed that when these gases were led into a chamber saturated with aqueous vapour, they formed a stable cloud in the chamber due to the condensation of water vapour round the ions. On standing, the cloud was seen to settle slowly under the force of gravity with a constant limiting velocity. He assumed that each cloud drop was formed round a single gaseous ion, and observed the limiting velocity of fall of the cloud-top by means of a microscope. From this he calculated the radius of a single drop by using Stokes' law

$$v = \frac{2}{9} \frac{ga^2}{\eta} (\rho - \sigma) \quad . \quad . \quad . \quad . \quad . \quad . \quad . \quad . \quad . \quad . \quad (35)$$

where ρ = density of water, σ = density of the gas, η = viscosity of the air, and a = radius of each drop. The mass of the single drop m was then calculated from the relation

$$m = \frac{4}{3} \pi a^3 \rho \quad . \quad . \quad . \quad . \quad . \quad . \quad . \quad . \quad . \quad . \quad (36)$$

---

*Townsend, *Proc. Cam. Phil. Soc.*, 9, 244, 1897.

Now the cloud was completely absorbed in bulbs of known weight containing drying agents like concentrated sulphuric acid. The increase of weight of the bulbs gave the mass of the whole cloud M. Thus we obtain the number of waterdrops forming the cloud, *viz.*, $n = \frac{M}{m}$.

Finally, the total charge carried by the cloud was measured by means of a quadrant electrometer. If E be the total charge, the charge on each gaseous ion is given by $e = \frac{E}{n}$. Townsend obtained by this method, values of e ranging from $2{\cdot}4 \times 10^{-10}$ e. s. units, to $3{\cdot}1 \times 10^{-10}$ e. s. units with ions of different gases.

The main sources of inaccuracy in the above experiment are the assumptions:—

(1) That each drop was formed round a single gaseous ion.

(2) That the drops were all of the same size.

(3) That the continuous evaporation of the drops had no effect on the mass of the drops.

(4) That Stokes' law of free fall was valid for such small droplets.

(5) That the velocity of the drops was not disturbed by convection currents in the gas.

J. J. THOMSON'S EXPERIMENT.

The next attempt for the determination of e was due to Sir J. J. Thomson* in 1898. His method closely resembled that of Townsend, except that a different method for the formation of cloud was adopted. He used, in fact, C. T. R. Wilson's cloud chamber (*vide* Chapter I).

The charged ions were formed in the cloud-chamber itself by some ionising agent, such as X-rays. The mass of a single droplet was calculated by precisely the same method as by Townsend. The total mass of the cloud was calculated from observations of the temperature of the chamber before expansion, and the minimum temperature attained during expansion. Let T_1, T_2 be the two temperatures and ρ_1 and ρ_2 the corresponding saturated vapour densities of water vapour. Then from the known volume of the chamber, the masses M_1, M_2 of aqueous vapours saturating it before and after expansion are calculated. Now assuming that the excess of vapour in the lower temperature has condensed into cloud, the total mass of the latter is given by $M_1 - M_2$. Following this method Thomson obtained values of the electronic charge ranging between $5{\cdot}5 \times 10^{-10}$ to $8{\cdot}4 \times 10^{-10}$ e. s. units. It will be noticed however that the main objections to Townsend's method all existed in Thomson's determination, and moreover the value of total mass of the cloud was more uncertain here.

---

* J. J. Thomson, *Phil. Mag.*, **46**, 528, 1898.

Wilson's Balanced Drop Method

Thomson's method was ingeniously modified by H. A. Wilson[*] in 1903, so as to eliminate some of the sources of errors. Firstly he placed inside the chamber two horizontal brass plates 3·5 cm. in diameter and about 8 mm. apart. Waterdrops were condensed round charged ions between the plates as before, and the mass of the individual drops was determined in the same way by applying Stokes' law. Secondly an electric field was then applied between the plates, the upper plate being connected to the positive potential and the lower plate earthed. The electric force thus created attracted the negatively charged drops upwards against gravity, and by suitable adjustment of the electric field, it was possible to balance the two forces and keep the drop suspended at any position between the plates. When this condition was attained, we have the relation

$$Xe = mg \qquad \ldots\ldots\ldots\ldots \qquad (37)$$

where $X =$ the applied electric field. Now m being known as before, e was easily calculated. The method was decidedly an improvement over the previous ones, as it avoided the uncertainties involved in the calculation of the mass of the cloud. Taking the mean of a large number of observations, Wilson gave the final value of e to be $4{\cdot}77 \times 10^{-10}$ e. s. units.

The method is, however, still open to the same serious objections as are mentioned under Townsend's experiment, and they have been largely eliminated by the elegant improvement due to Millikan, described in §26.

31. Dimensions of the Electron.—In the previous paragraphs, we have given an account of the experimental determination of the charge, and mass of an electron. Nothing has been said regarding its dimensions, except that we have implicitly assumed it to be a mere geometrical particle. But the particle is merely the pure mathematician's abstraction, it has got no other physical basis except simplicity to recommend it. From very early times, there has been a tendency to regard the electron as a spherical body of extremely small radius with either a uniform volume or surface-distribution of electricity. Such a picture cannot evidently be strictly correct, for the parts of the electron would repel each other, and the electron would disappear in an explosion unless there be certain 'hidden forces' balancing the forces of repulsion. The conditions of stability of the electron have not yet been elucidated, but a number of results was obtained from classical electrodynamics, which were interpreted in interesting fashions. Some of these are given below in brief outline :—

---

[*] H. A. Wilson, *Phil. Mag.*, 5, 429, 1903.

(I) All mass is electrical.

Experiments described in §§ 28, 29, have proved that the mass of the electron is not invariable but varies with the velocity according to (II, 29). To a physicist of the nineteenth century accustomed to regard the principle of conservation of mass as an absolute truth, this result would have appeared extremely strange. But the way was prepared by painstaking studies in classical electrodynamics. J. J. Thomson showed in 1885, that when an electrified sphere of radius a moves with the velocity v in a medium having the permeability μ, it creates in the surrounding space an e. m. field, whose strength varies as the velocity. On account of this field, there is a storage of energy which can be obtained by integrating the energy-density over the whole space. The additional energy was shown by J. J. Thomson to be equal to

$$E = \frac{2}{15} \frac{\mu e^2 v^2}{a c^2} \quad . \quad . \quad . \quad . \quad . \quad (38)$$

Thomson illustrated the apparent increment in inertia by giving a hydrodynamical analogy. When a spherical body is set in motion in a liquid with the velocity v, it produces motion in the liquid, and the total energy of this motion can be calculated with the aid of hydrodynamical principles. This 'additional energy' causes an apparent increase of inertia of the material body which, in the case of the spherical body, is equivalent to the mass of the displaced liquid. In the present case, we may regard the charged particle as generating moving lines of magnetic force in the aethereal fluid and these moving lines of force cause the apparent increase in inertia.

The electrodynamics of moving spherical charges were further considered by Lorentz and Abraham. For a detailed account of these works, special treatises ought to be consulted.* But a brief outline may be given here.

Let a spherical charge e move (Fig. 17) with the velocity u, u being much smaller than c. Then the moving charge is equivalent to a current $\frac{eu}{c}$. The magnetic field at a distance r due to the moving charge is

---

* See Lorentz, *Theory of Electrons*, p. 210.

$$H=\frac{eu}{c}\,\frac{\sin\theta}{r^2} \quad . \; . \; . \; . \; . \; . \; . \; . \quad (39)$$

where r = OP, XOP = θ, the direction of H being perpendicular to the plane of the paper.

The total e. m. energy associated with the motion is

$$E=\frac{1}{8\pi}\iiint H^2\,d\Omega = \frac{1}{8\pi}\,\frac{e^2u^2}{c^2}\iiint\frac{\sin^2\theta}{r^4}\,d\Omega \quad . \; . \; . \quad (40)$$

The integration taking place over the whole space exterior to the electron, *i.e.*, from $r=a$ to $r=\infty$. The total energy then comes out to be

$$E=\frac{1}{3}\,\frac{e^2u^2}{ac^2} \quad . \; . \; . \; . \; . \quad (41)$$

This may be put equal to $\frac{1}{2}mu^2$, where m is the mass of the electron. We have

$$m=\frac{2}{3}\,\frac{e^2}{ac^2} \quad . \; . \; . \; . \; . \quad (42)$$

According to this theory, the whole mass is supposed to be of electrical origin. If the hypothesis be correct, we obtain from (42) an estimate of the radius of the electron. We have

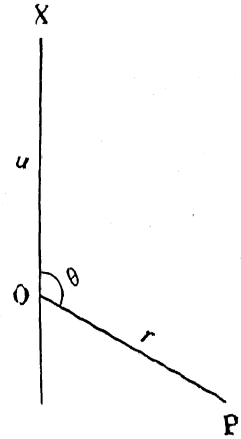

Fig. 17.

$$a=\frac{2}{3}\,\frac{e^2}{mc^2} \quad . \; . \; . \; . \; . \; . \; . \; . \; . \; . \; . \; . \; . \; . \quad (43)$$

$$=1{\cdot}9\times10^{-13}\text{ cm.}$$

The above proof is correct only if u be small compared to c, the velocity of light. When this assumption can no longer be made, the calculations become very much involved, and original sources must be consulted. Supposing that in course of motion the electron continues to remain spherical (*hypothesis of rigid electrons*), Abraham deduced (28) for the value of the mass. Lorentz, on the other hand, showed that the calculations become much simpler if we assume that the diameter of the sphere is contracted in the direction of motion as $\sqrt{1-v^2/c^2}:1$ (*hypothesis of contractile electrons*). He arrived at the formula (29), which as mentioned above, was independently deduced by Einstein from the Special Theory of Relativity and has been found to agree with experimental results.

32. The Rotating Electron.—Abraham further proved that the spherical electron may be supposed to be rotating about an axis passing through its centre. In such a case, it will possess an intrinsic magnetic moment, and will behave like an elementary magnet. He calculated the value of the magnetic moment μ as well as that of the mechanical moment Ω and found that the ratio of the two moments

$$\frac{\mu}{\Omega}=\frac{e}{mc} \quad . \quad . \quad . \quad . \quad . \quad . \quad . \quad . \quad . \quad . \quad . \quad (44)$$

The hypothesis of "Rotating Electrons" has been revised in recent years by Goudsmit and Uhlenbeck to explain duplicity phenomena in Spectroscopy (*vide* Chap. X). But on the other hand it attributes to the electron certain properties which are scarcely comprehensible. For, on this hypothesis it comes out (*vide loc. cit.*) that the peripheral velocity of the rotating electron is several hundred times larger than the velocity of light. This is a great difficulty which has not yet been overcome.

33. The Electron as Wave.—Finally, we may mention at this place the far-reaching discovery of De Broglie that an electron, moving with the velocity v may be regarded as a bundle of waves of mean length

$$\lambda=\frac{h}{mv} \quad . \quad . \quad . \quad . \quad . \quad . \quad . \quad . \quad . \quad . \quad . \quad (45)$$

moving with the wave velocity $u=\frac{c^2}{v}$, but with the group velocity v.

This subject will be taken in much greater detail in a subsequent chapter.

34. The Atom of Positive Electricity—The Proton.—After the atom of negative electricity was finally isolated and its charge and mass measured, it was natural that the atom of positive electricity should be looked for. But no exact counterpart to the electron was found up to 1933. The smallest positively charged particles so far found possessed the same charge as the electron, but its mass was equal to that of the hydrogen atom and it is therefore 1847 times heavier than the electron. It is in fact identical with the nucleus of the hydrogen atom (see Chap. III). It was supposed that this was the smallest atom of positive electricity, and to this the name of '*Proton*' was given.

35. The Positron.—But quite recently several investigators seem to have satisfactorily established the existence of the *positron*, which has got a positive charge equal to that of the electron and the same mass as the electron. It is thus the exact positive counterpart to the electron. The Proton, according to I. Curie and F. Joliot, is composed of the *neutron*, a neutral mass having almost the same weight as the H-atom, and a *positron*. For details see Chap. III and the last chapter on *Nuclear Physics*.

THE CANAL RAYS.

In the discharge tube, positively charged particles occur along with electrons. Godstein found in 1886 that if the cathode be perforated, and the discharge tube prolonged on the side away from the cathode (*vide* Fig. 1, Chap. III), a system of charged particles is found to proceed in a straight line from the cathode in a direction opposite to those of the electrons. He gave to these the name of " *Canal Rays*, 'Kanal'" being the German word for channel. These canal rays have characteristic colour, and J. J. Thomson found that the mineral willemite which is a silicate of zinc, phosphoresce brightly when exposed to these rays. Later experiments by Wien and Thomson showed that these particles are positively charged, but possess as large masses as the atoms and molecules of the residual gas within the tube. They are in fact identical with atoms or molecules which have lost some electrons. The experimental methods for studying them will be described in Chap. III.

Books Recommended.

On the Phenomena in a discharge tube:

—Kaye, *X-rays*, Chap. I.

—Townsend, *Electricity in Gases*, Chap. XI.

—Crowther, *Ions, Electrons and Ionising Radiations*, Chap. VI.

—Langmuir and Compton's article in *Reviews of Modern Physics*, Vols. 2 and 3 (1931).

On the determination of $\frac{e}{m}$ for cathode rays:

—J. J. Thomson and G. P. Thomson, *Conduction of Electricity through Gases*. Chap, VI,

—*Handbuch der Physik,* Band XXII, W. Gerlach's article, Chap. I. B.

On the Mathematical treatment of the motion of cathode rays under Electric and Magnetic fields:

—J. J. Thomson and G. P. Thomson, *loc. cit.*, Chap. V.

On the determination of 'e':

—R. A. Millikan, *The Electron* (1916).

—Perrin, *Les Atomes* (English Translation *Atoms*) (1923).

—*Handbuch der Physik, loc. cit.*

On the determination of $\frac{e}{m}$ for swift β-rays:

—*Handbuch der Physik, loc. cit.*

—Richardson, *Electron Theory of Matter*, Chap. XI.

On the Dimensions of the Electron:

—Lorentz, *Theory of Electrons.*

CHAPTER III

POSITIVE RAYS

36. Experimental Study.—In Chapter I, we have already mentioned the circumstances leading to the discovery of Positive Rays.

The experimental methods for the study of the positive rays were evolved by W. Wien* and J. J. Thomson. It was found that the positive rays were deflected by a magnetic field in a direction opposite to that of the electrons, but the deflections were rather too small. The method of *crossed fields* which is used for finding out the value of e/m for electrons was not found suitable for this case, and a fresh method was worked out in which the fields were kept parallel. This method had already been applied by Kaufmann for finding out e/m for β-rays (electrons from radioactive bodies which sometimes move with velocities approaching c) and is generally known as the *method of parallel fields*.

We describe below J. J. Thomson's apparatus in which his classical experiments were done.

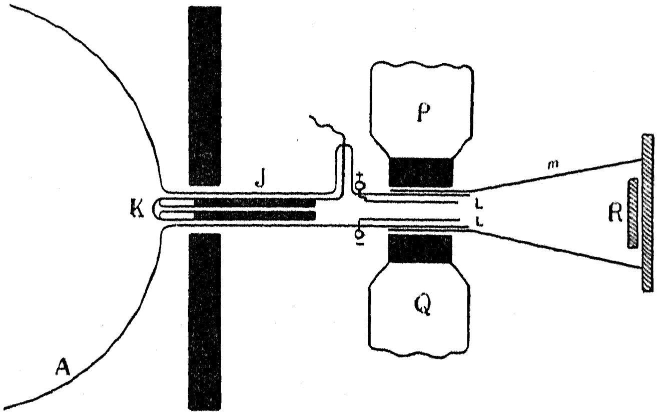

Fig. 1
J. J. Thomson's positive ray apparatus.

---

* Wien, *Verh. d. Phys. Gesell.*, **17**, 1898.

A ... is a large glass flask in which the discharge takes place. It has a side tube containing cocoanut charcoal in liquid air.

K ... is the cathode, made of a rod of soft iron with aluminium end, and pierced axially by a fine hole through which the positive rays enter into the space to the right. Sometimes the diameter of the hole is 0·1 of a mm.

P,Q ... Pole-pieces of an electromagnet.

L, L ... Pieces of soft-iron with plane faces between which the electric field is applied. They are enclosed in an ebonite box.

J ... Water jacket for cooling.

R ... A carrier containing the photographic plate which is exposed to the positive rays.

Thus both the electric and magnetic fields are applied parallel to the plane of the paper. On running the discharge tube, positive ions move towards the cathode and finally a fine pencil of rays pass through its narrow bore. They are then subjected to the simultaneous action of the electric and the magnetic fields between L, L and their deflected traces photographed at R.

To obtain good results, the whole apparatus is to be carefully evacuated. If the vacuum in the discharge tube becomes too high, no discharge can pass through it, while, if the vacuum is insufficient, the positive ions will suffer frequent collisions with neutral gas molecules and the latter may pass through the cathode and strike R instead of the positive ions, and thus give rise to unexpected and puzzling results. On the other hand, the pressure on the camera side may be as low as possible. This is effected by additional exhaustion of this part through a side tube. The extremely narrow bore of the cathode serves to maintain the difference of pressure on either side of it. The cocoanut charcoal in liquid air contained in the side tube serves to regulate the pressure of the discharge tube.

37. Theory of the Method of Parallel Fields.—It is clear from the description of the above apparatus that the pencil of charged particles is projected along the axis of the tube (say the x-axis) with the initial velocity v. This velocity may vary within wide limits. The electric and magnetic fields E and H are both applied vertically along the axis of z. The electrostatic deflection is along the z-axis—let us denote it by z. The magnetic deflection is along the y-axis, as the deflecting force is parallel to this axis. The particles are received on a plane parallel to the yz-plane. Let us now find out the displacements. Let e and m denote the charge and mass of the particles in general.

(a) THE ELECTROSTATIC DEFLECTION.

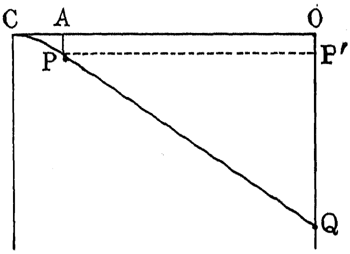

Fig. 2
Deflection of positive rays in electric field.

Let CO represent the axis of the tube (x-axis), O be the central point on the plate where undeflected particles fall on the plate, OA the length of the electric field.

Let CO $= l$, CA $= a$.

Then as proved in §21, Chap. I, the particle describes a parabola up to CP and then flies off at a tangent to the parabola and hits the plate at Q. We have

$$z = \text{OQ} = \text{OP}' + \text{P}'\text{Q}$$
$$= \text{AP} + \text{P}'\text{Q}$$

Since the parabola is given by

$$x^2 = \frac{2mv^2}{Ee} \cdot z \quad \dots\dots\dots\dots \quad (1)$$

and the x-coordinate of P $= a$, AP the z-coordinate of P is obtained by putting $x = a$ in (1). We have

$$\text{AP} = \frac{Ee}{2mv^2} . a^2$$

Now P′Q $= wt$, where w = z-component of the particle-velocity at P, and t is its time of flight from P to the plate. We have

$$w = \frac{Ee}{m} \cdot \frac{a}{v}, \quad t = \frac{l-a}{v}$$

as $\frac{Ee}{m}$ = vertical acceleration, $\frac{a}{v}$ = time of flight from C to P.

Therefore, $$\text{P}'\text{Q} = \frac{Ee}{mv^2} a\,(l-a)$$

Hence we have

$$\left. \begin{aligned} z &= \frac{Ee}{mv^2} \left\{ \frac{a^2}{2} + a\,(l-a) \right\} \\ &= \frac{Ee}{mv^2} A, \quad \text{where } A = a\left(l - \frac{a}{2}\right) \end{aligned} \right\} \quad \dots\dots \quad (2)$$

(*b*) THE MAGNETIC DEFLECTION.

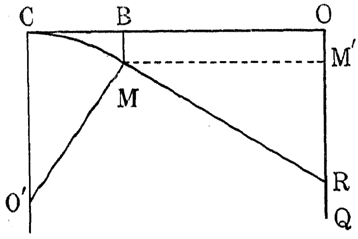

Fig. 3.
Deflection of positive rays in magnetic field.

Let COR represent the xy-plane, OR representing the y-axis. In this case the particle describes a circle with radius $\rho = \frac{mvc}{eH} = \text{CO}'$, and centre O′.

Let CB$=b$ represent the length of the magnetic field. The particle describes segment of a circle up to M, and then flies in a tangent to the circle to hit the plate at R.

Hence

$$y = \text{OR} = \text{OM}' + \text{M}'\text{R}$$
$$= \text{BM} + \text{M}'\text{R}$$

Now $$\text{BM} = \frac{\text{CB}^2}{2\rho} = \frac{b^2}{2\rho}$$

$$\text{M}'\text{R} = \text{MM}' \tan\theta$$
$$= (l-b)\sin\theta, \text{ when } \theta \text{ is small.}$$
$$= (l-b).\frac{b}{\rho}$$

Therefore $$y = \frac{1}{\rho}\left[\frac{b^2}{2} + b\,(l-b)\right]$$

$$\left.\begin{aligned} &= \frac{eH}{mvc} b\left(l-\frac{b}{2}\right) \\ &= \frac{eH}{mvc}.B \end{aligned}\right\} \quad \ldots\ldots\ldots\ldots \quad (3)$$

where $$B = b\left(l-\frac{b}{2}\right).$$

When both the fields are simultaneously applied we have

$$x = \frac{eE}{mv^2}.A, \qquad A = a\left(l-\frac{a}{2}\right) \quad \ldots\ldots\ldots \quad (2a)$$

$$y = \frac{eH}{mvc}.B, \qquad B = b\left(l-\frac{b}{2}\right) \quad \ldots\ldots\ldots \quad (3a)$$

The positive particles may have any velocities from maximum to zero. Hence the trace of the particles on the plate is obtained by eliminating v between (2a) and (3a). We get

$$y^2 = \frac{B^2H^2}{Ac^2E} \cdot \frac{e}{m} z \quad \ldots\ldots\ldots\ldots \quad (4)$$

$$\frac{v}{c} = \frac{y}{z} \cdot \frac{EA}{HB} \quad \ldots\ldots\ldots\ldots \quad (5)$$

(4) is the equation of a parabola in the yz-plane with its axis parallel to the z-axis. But the whole parabola is not described, only a part of it is described. For, the maximum velocity of the particles is given by

$$\tfrac{1}{2} mv^2 = eV$$

where V is the potential difference in the tube. These particles fall through the whole potential difference between the anode and the cathode. Hence the minimum value of z is given by

$$z_{min.} = \frac{EA}{2V}$$

and since the particles have only one kind of charge, y has only one sign. So only a trace like p. (Fig. 4) is described. By reversing H, we get p', the image of p below the z-axis. If the electrostatic field is reversed, we can have the trace to the left of the y-axis.

A number of Thomson's parabolas are shown in Plate I (Fig. 5).

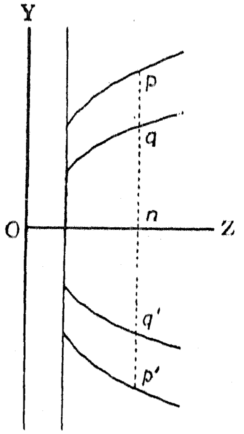

Fig. 4
Ideal Positive ray Parabola.

38. Positive Ray Parabola.

—In Fig. 5 and the following figures (Figs. 6, 7, Plate I) the deflection due to the magnetic field is vertical, while that due to the electrostatic field is horizontal. The central point corresponds to undeflected particles.

A particular parabola is due to particles possessing the same value of e/m and these particles have retained their charges throughout the whole of their journey through the electric and magnetic fields. Each point on a particular parabola corresponds to a definite velocity, and the velocity of the particles is according to (5) proportional to the tangent of the angle joining the origin to this point. Hence the points nearest the axis correspond to the highest velocity of the particles as given by equation (5), and the points further away correspond to decreasing velocities. The parabola is not of uniform brightness; which shows that the velocity distribution of the particles is not uniform.

The lines joining the origin to the parabolas which sometimes appear on the plates are due to particles which get charged or discharged within the fields. This is proved by shortening the fields, when these lines disappear. For explanation of other details, see original papers, or J. J. Thomson's *Positive Rays of Electricity.*

The outermost parabolas are those which have the largest latus rectum, and hence the smallest value of e/m. For the outermost parabola in Fig. 5, e/m was found on calculation to be 9645 and it has been ascribed to H^+, *i.e.*, due to hydrogen atoms which have one positive charge. Once one parabola on a plate is correctly assigned, the e/m for others can be identified by comparison, and then their origin can be looked for. Thus in Fig. 5, parabolas have been ascribed to $H_2{}^+$, O^{++}, O^+, $O_2{}^+$, Hg^+. For the parabolas ascribed to oxygen the e/m values were found to be $\frac{1}{8}$, $\frac{1}{16}$, $\frac{1}{32}$ of e/m_H, hence they were identified with O^{++}, O^+, $O_2{}^+$, respectively. We thus observe that the oxygen-molecule in the discharge tube may have a single plus charge, may be broken up into atoms each with one plus charge, or two plus charges. This is a general phenomenon, and the Hg-atom has been found with sometimes as many as eight positive charges (*vide* Plate I, Fig. 7). *But the hydrogen atom was never found with more than one plus charge.* This fact was one of the bases of the assumption made by Bohr that the H-atom cannot contain more than one nuclear positive charge (*vide* Chap. VII).

Besides positively charged particles we may have negative charges only, *e.g.*, $\overline{H}$ (Fig. 5).

Fig. 6 is interesting. In this experiment the tube contained some residual Ne-gas, whose atomic weight as determined in the laboratory is 20·2. A parabola corresponding to $m=20$ was obtained, but just below this a fainter parabola corresponding to $m=22$ was just visible. As there is no element having the atomic weight 22, it was supposed that the parabola 22 is due to an isotope of Neon (*vide supra*) with the atomic weight of 22. The investigations at this point were taken up by F. W. Aston and are described in the following sections.

39. Applications of the Positive Ray Method to the Study of Isotopes.—The greatest triumph of positive ray analysis has been achieved in its application to the problem of isotopes, *i.e.*, of *atoms possessing different weights, but having the same chemical and*

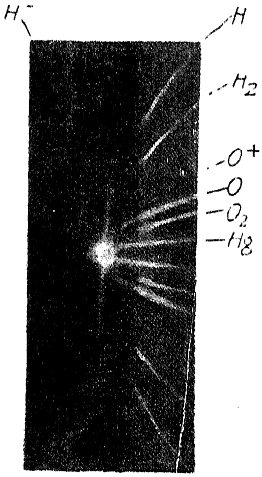

Fig. 5. Positive-ray Parabolas
(*p.* 86)

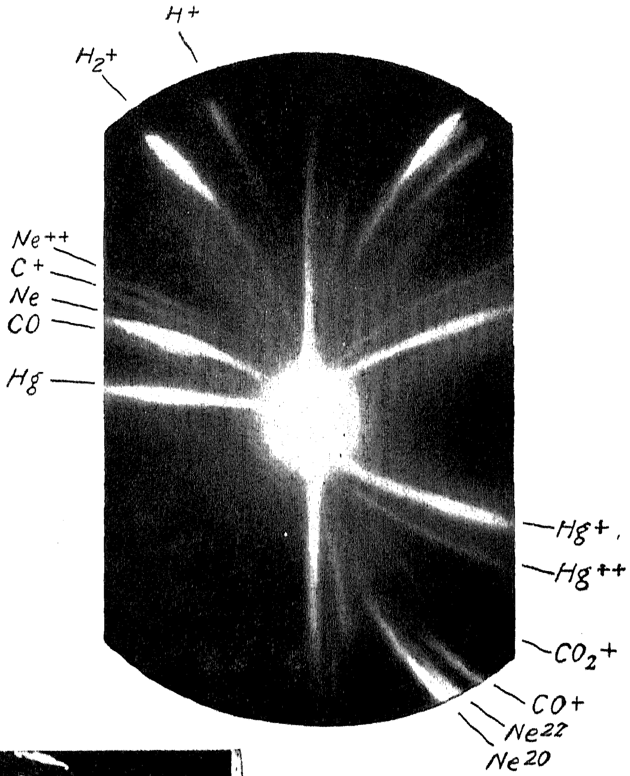

Fig. 6. Positive-ray Parabolas showing the neon isotopes.
(*p.* 86)

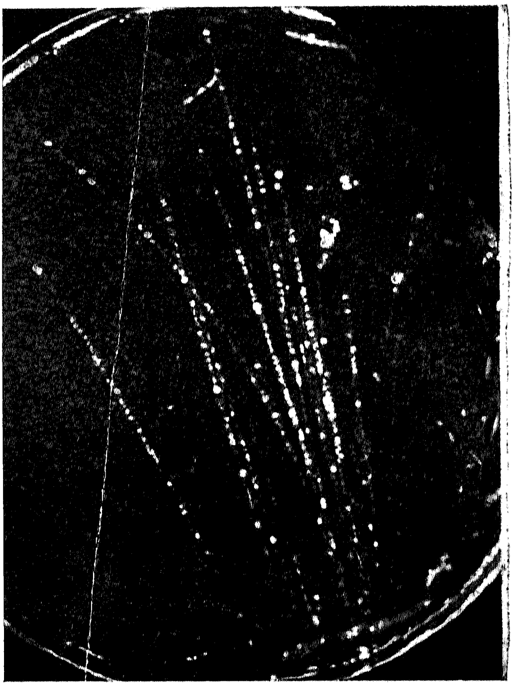

Fig. 13. The Positron track: The faint line with gradual curvature to the right is due to the positron. The tracks curved in the opposite direction are due to electrons.
(*p.* 100)

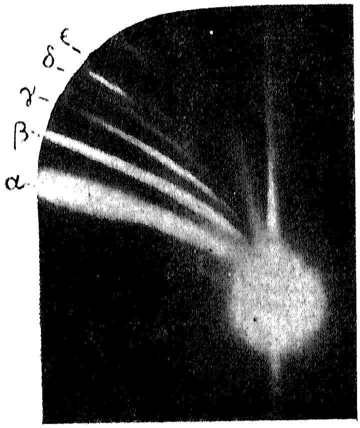

Fig. 7. Parabola showing multiply-charged mercury ions.
(*p.* 86)

physical properties. In Chap. I, we have described in brief Prout's search for a fundamental atom. Prout's hypothesis came to grief, because Dumas and Stas, in their fundamental researches on the determination of atomic weights proved that many atoms had weights which were not integers but involved fractions. Thus Cl was found to have the weight 35·5, Iodine 128·1, and Neon 20·2. Prout tried to explain these on the hypothesis that the half-hydrogen atom, or the quarter-hydrogen atom was the fundamental atom, but such attempts could be regarded only as artificial. So throughout the nineteenth century the belief became universal that the weights of atoms were not in general integral.

But the whole aspect of the question was changed in the beginning of the twentieth century. Evidences began to pour from different directions which showed that a belief in the constancy of the weight of the atom could no longer be maintained. First of all, no positive unit of electricity having a mass smaller than that of the H-atom could be found in either the discharge tubes, or in other experiments where a breaking of atoms is expected. Hence if atoms are formed of protons and electrons, their masses ought to be, apart from the small masses ascribed to electrons, integral multiples of the mass of the H-atom. Secondly from studies in radioactivity (IV, §§ 61,62) it was found that if we take the two chief radioactive groups, one headed by Uranium, and the second by Thorium, and trace the radioactive changes in the two groups, we find that the end products in both cases are lead, but closer scrutiny (*vide* Chap. IV) shows that while Pb from U can have an atomic weight of 206, Pb from Th has the weight 208. Ordinary Pb was found to have the A. W. 207·22. It has been supposed that Pb in Uranium-bearing minerals may differ considerably in its A. W. from Pb from Thorium-bearing mineral. This was actually found to be the case. Hönigschmidt found that Thorium-lead extracted from Ceylon-Thorianite had an atomic weight of 207·77, while Richards and Lambert found that the Uraniolead from Norwegian Clevite had an atomic weight of 206·08, in striking agreement with theory. Both these types of lead had identical chemical and physical properties, and could not be separated from one another by any chemical or physical means. Their spectra were also found to be identical.

On certain other basis which will be more fully discussed in Chap. IV Soddy and Fajans developed their theory of *isotopes.* This was a term coined by Soddy to denote the different forms of the same elements which like U-lead, and Th-lead have identical chemical and physical properties but differ in atomic weights. It was supposed that all elements which showed fractional atomic weights were mixtures in fixed proportion of different isotopes, the weight of each of which was integral.

Thus Neon has an atomic weight of 20·2. Positive ray analysis quoted in §37 however showed that Neon gives two parabolas having the atomic weights 20 and 22. It is therefore probable that Neon consists of two isotopes Ne_{20} and Ne_{22} mixed in different proportions. We may therefore assume that

$$Ne = Ne_{20}\ 90\% + Ne_{22}\ 10\%.$$

As most elements show atomic weights involving fractions, they may be supposed to consist of a number of isotopes each having some integral weight but mixed in different proportions. The discovery of a general and powerful method for the separation and quantitative estimation of these isotopes has been the crowning achievement of F. W. Aston's long-protracted labours. The parabola method described above gives also a means for separating these isotopes.

It has been found that the parabola method is specially suitable for the mass analysis of light elements. Aston* has extended this method to the determination of the isotopes of Li, and G. P. Thomson† to the case of Be. In these cases only the method of production of positive ions was improved. They employed a hot anode discharge tube with perforated cathode, and phosphates or sulphates of the metals were deposited on the anode. The anode consisted of a strip of platinum which was electrically heated and gave out metal ions. The device was first introduced by Gehrcke and Reichenheim and the streams of particles were called by them *Anode rays*. Lithium gave two parabolas and was thus found to be composed of two isotopes Li^7 and Li^6, while Be was proved to be a simple element of mass 9. (*vide* however *supra*).

40. The Mass-Spectrograph.—Aston found that Thomson's method of analysis of positive rays, though almost ideal for a general survey of masses and velocities, was not suitable as an instrument of precision, and required too long exposures. For precision measurements, the parabolas must be very fine. Though this can be achieved by taking long, fine bores, the procedure is not without its disadvantages, for the intensity falls off as the fourth power of the diameter of the bore, and exposures with narrow beams become unusually long. For removing this and other defects, he was led to devise another apparatus* in which particles possessing the same *e/m*, but differing widely in velocity and direction can be focussed on a single point. The plan of the apparatus is shown in Fig. 8, and the actual apparatus in Fig. 9. The description of the apparatus is given below.

---

* Aston and G. P. Thomson, *Nature*, Feb. 24, 1921.

† G. P. Thomson, *Phil. Mag.*, **42**, 857, 1921.

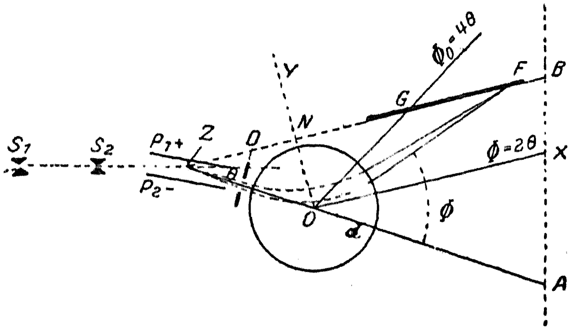

Fig. 8. Plan of Aston's Mass-Spectrograph.

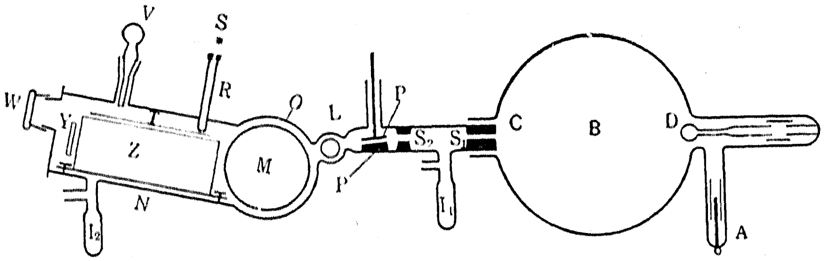

Fig. 9. Aston's Mass-Spectrograph.

S_1, S_2	... are two narrow slits of special construction, through which the positive rays pass.
P_1, P_2	... parallel plates for applying the electrostatic field.
D	... a diaphragm; the rays enter the space obliquely, diverge, and a wide beam is allowed to pass through D.

---

* Aston, *Phil. Mag.*, **38**, 709, 1919.

O ... the centre of the circular pole-pieces. The magnetic field is applied perpendicular to the plane of the paper so that the magnetic deflection is parallel to the plane of the paper. This deflection is in the opposite direction to that of the electrostatic field.

In Fig. 9, B is the discharge tube in which the rays are produced. S_1, S_2 are the slits, and P, P the plates. The diaphragm is placed near L. The magnetic field is applied at M. Z is a pair of earthed plates which protects the beam of rays from the action of any stray electrostatic field. T is the photographic plate which can be manipulated by a rod working through the ground glass joint V. The beam of rays can be thrown on the willemite screen Y and its intensity examined through the window W. S is a source of light from which a fine bean can be thrown on T and thus a fiducial spot can be obtained from which measurements are to be made.

For practical purposes, we may suppose that the rays diverge from O. Let θ be the electrostatic deflection of a set of particles of velocity v, φ their magnetic deflection from the initial direction $S_1 S_2$. We have then,

$$\theta = \frac{aEe}{mv^2}, \quad \varphi = \frac{bHe}{mvc} \quad . \quad . \quad . \quad . \quad . \quad . \quad . \quad . \quad . \quad (5a)$$

Hence $\theta v^2 =$ constant, $\varphi v =$ constant for all rays having the same e/m, and deflected within small angle.

We have from (5a)

$$\frac{\delta\theta}{\theta} + \frac{2\delta v}{v} = 0, \qquad \frac{\delta\varphi}{\varphi} + \frac{\delta v}{v} = 0$$

So that

$$\frac{\delta\theta}{\theta} = 2\frac{\delta\varphi}{\varphi} \quad . \quad . \quad . \quad . \quad . \quad . \quad . \quad . \quad . \quad . \quad . \quad . \quad (6)$$

Suppose we have a beam diverging from Z. Let ZO be the central beam (passing through O, which makes an angle θ with S_1S_2D the line of slits). Let the extreme beam through D make an angle $\theta+\delta\theta$ with S_1S_2D. Then at O, the half breadth of the beam is $b\ \delta\theta$. From O, the central beam diverges through φ, *i.e.*, the angle AOF, and the extreme beam through $\varphi + d\varphi$, and let the two beams meet at F. Then from simple geometry we find that the angle between the rays at F is $\delta(\varphi-\theta)$.

Since the rays are supposed to come to a focus at F, we have

$$b\ \delta\theta = r\delta(\varphi-\theta), \text{ where } r = \mathrm{OF}$$

Hence with the aid of (6), we have

$$r\ (\varphi-2\theta) = 2b\theta \quad . \quad . \quad . \quad . \quad . \quad . \quad . \quad . \quad . \quad . \quad (7)$$

It is now easy to see that if we draw a line ZP_1, so that $PZS = SFO$, then it can be easily proved that ZP is the locus of the point (r, φ), *i.e.*, all particles having the same value of e/m, whatever the value of v may be, are focussed on some point in ZP. To prove this we draw a line OQ parallel to ZP through O. Let OQ cut ZP at Q. Then we have $\angle FOQ = \varphi - 2\theta$, and $OF\,(\varphi - 2\theta) = OZ.\,QO$.

Thus (7) is fulfilled.* F lies on the photographic plate, where it produces a narrow trace like that of a broad spectral line. The value of e/m corresponding to any such trace can be determined by comparison with known reference lines.

41. Methods of Comparison.†—In actual practice absolute determination of m/e is not necessary. By using gases like O_2, CO_2, CH_4, etc., as impurities with the experimental gas, a number of reference lines corresponding to C^{++} ($m/e = 6$), O^{++}(8), O^{+}(16), C^{+} (12), CO^{+}(28), $CH_2{}^{+}$ (14), $CH_3{}^{+}$(15), $CH_4{}^{+}$ (16), etc., are obtained. Some of them can be seen in the mass spectra reproduced in Fig. 10, from Aston's papers. The behaviour of these gases is previously known from the parabola method; so their lines can be easily identified. Then a calibration curve is drawn with the distance of the different lines from a fiducial point as a function of the mass. This can be used in ascertaining the mass-number corresponding to any new line.

For greater accuracy certain other methods have also been used by many workers. One of these, known as the *method of coincidence* consists in obtaining two sets of mass-spectra for the same substance, (1) with definite values E and H for the electric and magnetic fields, (2) with different values E' and H' for them. Let V, V' be the potentials corresponding to E and E'. The new values V', H' are so adjusted that a mass m' photographed under the second condition occupies the same position as that due to a mass m under the first condition. Then since the electric and magnetic deflections for the two lines have been interchanged, we have

$$\rho e = \frac{mv}{H} = \frac{m'v'}{H'}$$

and

$$\frac{mv^2}{m'v'^2} = \frac{V}{V'}$$

---

* The full mathematical analysis of the theory of the apparatus has been given by R. H. Fowler (*Phil. Mag.*, 1922). Here we have adopted an approximate theory.

† For an account of the methods of measurement of mass-spectra, see Aston's *Isotopes* (1923), Chap. V, p. 55.

Hence
$$\frac{m'}{m} = \frac{V}{V'}\left(\frac{H'}{H}\right)^2 \quad \ldots\ldots\ldots\ldots \quad (8)$$

Thus the ratio of m to m' is known. If one of them be a standard line, the other can be found.

A modification of the above method has also been largely used. In this the magnetic field is kept constant, and only the electric field is changed from V to V' in the second exposures, as in the method of coincidence. If the conditions

$$\frac{m'}{m} = \frac{V}{V'} \quad \ldots\ldots\ldots\ldots \quad (9)$$

be satisfied, coincidence of m' and m will occur. Thus the line C (12) under 320 volts will occupy the same place as O (16) under 240 volts. If in any case the coincidence is not exact, the amount of difference can be easily determined even from a rough calibration curve. The condition that the magnetic field should be maintained constant is a great disadvantage of this method. But still this is the only method applicable for masses far removed from reference lines in the spectrum, and with mass ratio as large as 3 : 1.

A special method of great accuracy, known as the *method of bracketing**, has been used by Aston for analysing the isotopes of hydrogen and helium. In this three exposures are taken instead of two, using potentials V, $2V-h$ and $2V+h$ respectively, where h is a small difference of potential. This method is specially suitable for analysing isotopes of mass ratio 2 : 1, for example, H_2^+ and H^+ or H_2^+ and He^+.

It is clear that if $m' : m = 2 : 1$, the two lines for m corresponding to $2V-h$ and $2V+h$ will lie symmetrically on either sides of the line for m' corresponding to V, and the two m-lines thus form a *bracket* with the m'-line. The method is applicable even when the ratio is not exactly double, and its exact value can be determined from the calibration curve.

Using very narrow slits and apparatus of suitable dimensions, Aston has obtained in his works on mass spectrography a resolving power dm/m of 1 in 130, and an accuracy of the order of 1 in 1000 in the determination of mass-number.

42. Explanation of the Spectra.—A number of typical mass-spectra obtained by Aston has been reproduced in Fig. 10. Oxygen and carbon which were formerly supposed to be elements with single isotopes having the exact weights of 12 and 16 have now been found

---

* Aston, *Phil. Mag.*, 39, 621, 1920.

(see §43) by other methods to possess other isotopes in minute quantities, having the atomic weights 17 and 18 for O, and 13 for C.

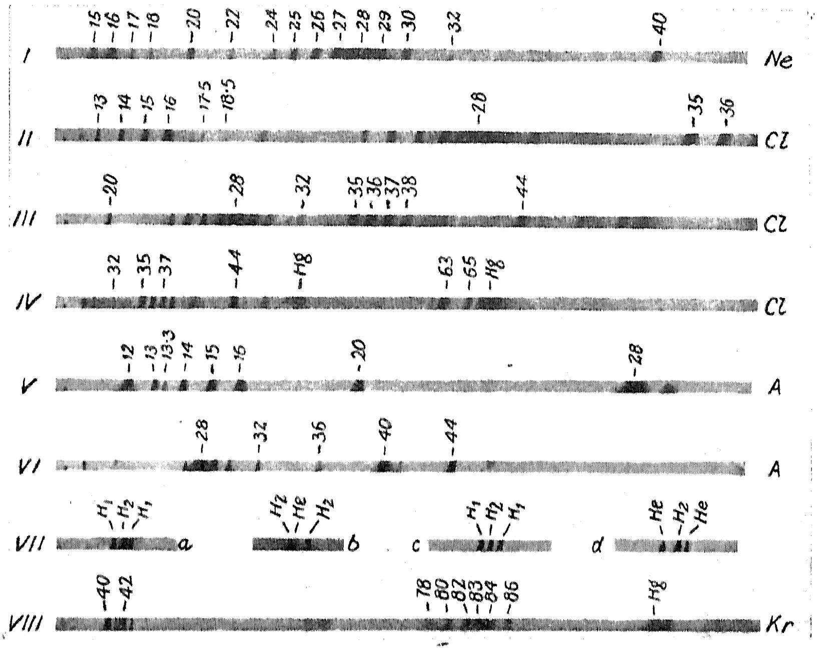

Fig. 10. Mass-Spectra of Elements (*Aston*).

The main isotopes have almost exact integral values. So these elements, their atoms and molecules, and their compounds with each other and hydrogen are generally used as reference lines. Thus here we have got the following reference lines :—O_2^+(32), O^+(16), O^{++}(8), C^+(12), CO^+(28), C^{++}(6), CO_2^+(44); C^+(12), CH^+(13), CH_2^+(14), CH_3^+(15), CH_4^+(16) or O^+(16) (see spectrum *V*); C_2^+(24), C_2H^+(25), $C_2H_2^+$(26), $C_2H_3^+$(27), $C_2H_4^+$(28) or CO^+(28), $C_2H_5^+$(29), $C_2H_6^+$(30) (see spectra *I* and *II*).

Coming to the actual results of experiment, we find that Ne was the first element to show clearly isotopes. Ne showed two isotopes Ne^{20} and Ne^{22}. Next Cl was examined. The result is shown in spectra *II*, *III* and *IV*. A group of four lines 35, 36, 37, 38 occurs in spectrum *III*. Of these the lines 35 and 37 are isotopes of Cl, and 36, 38 are attributed to HCl. The corresponding second order lines (*i.e.*, for nuclei with two positive charges) 17·5 and 18·5 (due to Cl^{++}) occur in spectrum *II*. The isotopes of Argon are exhibited in spectra *V*, *VI*. The strong line at 40 in spectrum *VI* shows that it is the main constituent of the element. In spectrum *V*, the lines 20 (for A^{++}) and 13·33 (for A^{+++}) correspond to the same constituent in second and third orders. A very faint line 36 in spectrum *VI* is attributed to a second isotope of argon A^{36}.

But the corresponding second and third order lines 18 and 12 are absent in spectrum *V*. This is due to the presence of H_2O (18) and C (12) as impurities in the gas. It is well-known that the gas krypton cannot be completely freed from argon. The neverfailing presence of a line 36 in the mass-spectra of Kr confirms the above conclusion.

The result of mass analysis of hydrogen and helium is very interesting. The method of bracketing has been used for these two substances. It will be seen in spectrum *VII* (*a* and *c*) that when comparing H_2^+ and H^+, the bracket is perfectly symmetrical. The potentials used in these exposures were 250, 488 and 512 volts respectively. This proves that within the limit of experimental error, the mass of H_2 is exactly double that of the hydrogen atom. Spectrum *VII* (*b*) and (*d*) show the results of comparing H_2^+ with He^+. Helium atom has a mass approximately twice that of hydrogen molecule. So the same three sets of voltages are used. The bracket is here however unmistakably asymmetrical. In (*b*), He^+ has been bracketed by the two H_2^+-lines, and it is seen that both the H_2^+-lines in the bracket have shifted to the side of increasing mass scale, compared to their symmetrical positions about the He^+-line. But in (*d*) where the H_2^+-line is bracketed by two He^+-lines, the shift of the He^+-lines is in the reversed direction. The nature of these asymmetries clearly indicates that the mass of the H_2-molecule is greater than half that of He-atom.

It is remarkable that neither the hydrogen nor the helium atom gives any second order spectra (spectra due to particles having double charges). This behaviour of hydrogen agrees with Bohr's picture of the structure of the hydrogen atom as consisting of a single electron revolving round a single positive charge. Further the absence of of He^{++} is attributed to the fact that the energy required to remove two electrons from it is extremely high (nearly 80 volts). In some of the photographs a mass H_3^+ has been identified. It was also observed by J. J. Thomson in the parabola method. Recently, an isotope* of the H-atom has been found having a mass of 2, and a charge of one. H_3 may be a molecule formed of the isotopes H^2 and H.

---

* H. C. Urey, F. G. Brickwedde and G. M. Murphy, *Phys. Rev.*, **40**, 1, 1932; **39**, 164, 1932.

The last spectrum *VIII* in (Fig. 10) is for krypton. A characteristic group of five isotopes 80, 82, 82, 83, 84, 86 is clearly seen in the photograph. A faint line at 78 is also visible. The group of five lines in the second order Kr^{++} has been reproduced in the left of the same spectrum.

The method of mass spectrograph has also been applied by Aston† to the study of the isotopes of the alkali metals Na and K. The device for the production of ions ordinarily employed in such experiments was however found unsuitable in the cases of Na and K on account of the ambiguity due to multiply charged ions which are very often present in this method. So a Gehrcke and Reichenheim hot anode discharge tube was fitted to the mass spectrograph. Na showed the most unambiguous result, namely that it was a simple element of mass 23, and K was found to be composed of two isotopes of masses 39 and 41.

Besides the substances discussed, a number of other substances has also been subjected to mass analysis. The results in brief are shown in table 1, §44. For a full account of these analyses, Aston's '*Isotopes*' (1923), pp. 71 to 89, also later publications must be consulted.

43. Dempster's Method.

—A focussing method for the determination of e/m. alternative to Aston's mass spectrograph, has been developed by Dempster* and used with great success in several lines of investigation. The apparatus employed is shown in Fig. 11. The source of ion in this experiment is usually a volatile salt of the metal, or the metal itself when it can be easily evaporated.

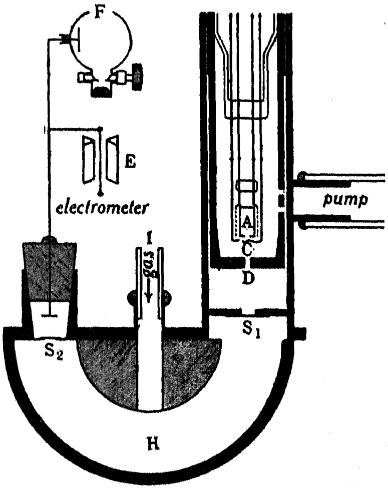

Fig. 11. Dempster's Apparatus.

---

* Aston, *Phil. Mag.*, **42**, 436, 1921.

† Dempster, *Phys. Rev.*, **11**, 316, 1918.

A ... is a hollow anode coated with the given salt. It is then electrically heated.
C ... is a platinum cathode, the electrons from which bombard the anode A.
S_1, S_2 ... are two slits.
F ... is a Faraday cylinder.
E ... is an electrometer.
I ... is the inlet for the substance, if it is a gas.

Charged particles are emitted from the heated anode bombarded by the electrons from the cathode, and they diffuse out through D with a slow velocity. A potential of the order of 800 to 1000 volts is applied between D and S_1. So the particles come out through S_1 as a narrow diverging beam. The particles are then subjected to a suitable magnetic field applied at right angles to the plane of the paper. Those with the same velocity and e/m are bent into a semicircular path and are finally brought to a focus on S_2. The charge is collected by the Faraday cylinder F which is connected to the electroscope E. If the substance be a gas, it is directly introduced at I, and bombarded by electrons from the platinum cathode C.

The great advantage of the method is that particles which emerge at S_1 making slight angles with the normal to S_1, come to a point focus at S_2 after having approximately described semicircles. This is due to the fact that the particles possess identical velocity and mass. If V = applied potential, H = the magnetic field, 2ρ = diameter of the semicircle,

$$He\rho = mvc$$

and

$$\tfrac{1}{2}mv^2 = Ve$$

therefore,

$$\frac{e}{mc^2} = \frac{2V}{H^2\rho^2} \quad \ldots\ldots\ldots \quad (10)$$

By altering the accelerating voltage, particles having different values of e/m can be brought to focus at S_2, and their e/m determined by equation (10).

The method of analysis used by Dempster is both simple and accurate. The magnetic field is kept constant. By suitable changes in the electric field, particles of different masses are brought to a focus at S_2 and the ionic charges indicated by the deflections of the electrometer are noted. Usually when the focussing is not obtained, the ionic current is very small, but for certain voltages corresponding to maximum concentration of ions the current suddenly rises to maximum. Thus for Mg three distinct maxima were observed at 953, 914 and 879 volts. According to (10) the masses of the ions are inversely proportional to the applied voltages. As in every case a maximum due to N_2^+ ($m=28$) was present at 817 volts, the masses corresponding to other voltages could be obtained by comparison. The masses were plotted against ionic currents. The curve obtained is shown in Fig. 12 taken from Dempster's original paper. Thus Mg shows three isotopes of masses 24, 25 and 26 corresponding to the three maxima A, B, C. The maximum D at $m=28$ corresponds to N_2^+. The height of the ordinates at each point shows the relative number of the isotopes present in the atom.

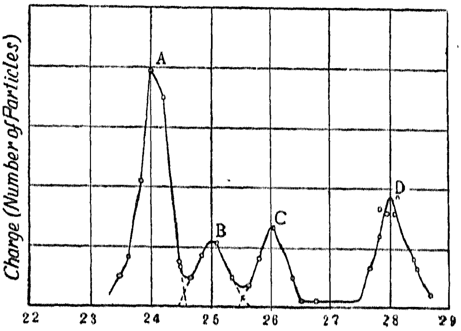

Fig. 12
Dempster's Mass analysis for Mg.

Besides Mg, this method was also applied by Dempster* to Ca, Zn and K. He discovered the isotopes 40, 44 of Ca; 64, 66 and 68, 70 of Zn, and confirmed the isotopes of Li and K found by other observers.

More recently Dempster's method has been employed by Bainbridge† to a very critical analysis of the isotopes of Na, K and Li, and he has confirmed in general the previous results of Aston, Thomson and Dempster. He has determined also exact masses of some of the isotopes of Be and Ne and his results are regarded as of high degree of accuracy.

44. Discussion of Results.—The results of mass analysis of elements so far investigated are given in table 1 at the end of this chapter. The isotopes of each element have been given in their decreasing order of abundance where otherwise not mentioned. In other cases the relative abundances have generally been calculated from the intensity measurement of the mass-spectra of elements by Aston and others. Column 4 of the table gives the exact atomic weights of the isotopes, and column 5 those of the nuclei. The latter values are obtained by subtracting the masses of Z electrons from the atomic weights in column 4.

---

* Dempster, *Proc. Nat. Acad. Sci.*, 7, 45, 1921.

† K. T. Bainbridge, *Jour. Frank. Inst.*, 212, 317, 1931.

A few isotopes given in the table have been recently reported from the study of the isotope-effect of band spectra (see Chap. XX). These are Be^8, C^{13}, N^{15}, O^{17}, O^{18}, Ne^{21}*, Cl^{39}, Cl^{40} and others to be found in the table. Their relative proportion compared to the main isotopes is however extremely small. Thus O^{18} occurs in the proportion of 1 in 630 and O^{17} in proportion of 1 in more than 3000. From a scrutiny of the number and weights of the isotopes of different elements in the table, the following conclusions have been arrived at :—

(1) The atomic weights of isotopes are all very nearly integers.

(2) Elements of even atomic number have generally more numerous isotopes than those of odd atomic number. Elements of odd atomic number have not yet been found to possess more than two isotopes (*vide* however chlorine which is an exception).

(3) Isotopes having even mass number occur more frequently than those of odd mass number; further, those having their mass number divisible by 4 are more frequent than those with mass number not divisible by 4.

N.B.—It is supposed that the mass of an isotope is wholly due to the protons it contains, and the mass of a proton is taken to be unity. On this basis the mass of an isotope is numerically equal to the number of protons it contains. This number is known as the *mass number* and is denoted by A. On the other hand the atomic number Z of an element is equal to the units of effective positive charge of its nucleus. So if A=mass number of an isotope, Z=its atomic number, it must contain $N=A-Z$ number of electrons in the nucleus. Thus for Li^7, $A=7$, $Z=3$, so that $N=4$, while for Li^6, $A=6$, $Z=3$, therefore $N=3$. These simple ideas are based on the assumptions that the electrons and protons exist in the nucleus in free states. There are however grave doubts regarding the validity of this assumption. In fact it is now fairly certain that there are no free electrons in the nucleus. This question will be discussed later in the chapter on *Nuclear Physics*.

---

* Hognes and Kvalnes, *Nature*, **122**, 441, 1928.

Isotopes containing even number of electrons (N) in the nucleus occur more frequently than those containing odd number of electrons.

(4) Mass number of an isotope is always either equal to or greater than twice its atomic number ($A \geqq 2Z$), so that the number of free electrons in the nucleus is either equal to or greater than the atomic number ($N \geqq Z$). It follows also then that $A \leqq 2N$, *i.e.*, the number of protons can never exceed twice the number of electrons.

(5) The number of isotopes for any single element is not very large, and their mass-number vary within narrow limits.

The full significance of all these conclusions have not been completely understood, but some of them are clear. Thus the whole number rule of the weights of isotopes seems to indicate that the atomic nuclei of all elements are built up of the elementary constituents protons and electrons. Further, the rule of divisibility of mass number by 4 indicates that in most nuclei the protons may have a tendency to occur in groups of 4. We shall discuss the question further in the chapter on *Nuclear Structure.*

44a.—The Discovery of the Positive Electron (Positron).— It is likely that the reader of this book has heard of *Cosmic rays* which are a kind of penetrating radiation of ultraterrestrial source coming in equal intensity from all parts of the sky and possess the remarkable property of discharging electroscopes even when these are protected by thick lead-shields (*vide* for details chapter on *Nuclear Physics*). The question whether this radiation consists of corpuscles or photons, has been the subject of much investigation in the past couple of years. While light is being thrown on this fundamental problem only recently (they are now almost proved to be super-gamma-rays), these researches have led quite unexpectedly to another discovery of foundamental importance, *viz.*, to the discovery of a particle *positively* charged and possessing a *charge and mass*—which so far as can be judged from the present preliminary investigations are *equal to that of the electron.* This new particle is styled the "*positron*".

At the California Institute of Technology C. D. Anderson,* while using a vertical Wilson cloud chamber (of 15 cms. diameter), which is traversed by a horizontal magnetic field of about 15000

---

*C. D. Anderson, *Science*, **76**, 238, 1932 ; *Phys. Rev.*, **43**, 491, 1933; **44**, 406, 1933.

gauss, to observe the tracks of particles associated with cosmic rays,* found (August, 1932) that some of the tracks had a curvature (due to the magnetic field) of such a sign that assuming the particles to be moving downwards—as presumably the particles liberated by the cosmic rays actually do—the charge on the particle must be *positive*. Yet the ionisation along the track was much smaller than that to be expected for a proton of the same velocity and corresponded to that of a particle of much smaller mass. It was improbable that it could be a proton, but might it not be an electron moving upwards which in the magnetic field would have the same curvature as a positive particle moving downwards? A plate of lead 6 mm. thick was placed in the middle of the chamber so that the corpuscles had to pass through this plate. The particle loses energy in passing through the plate, and thus its track would show different curvatures on the opposite sides of the plate—the direction of motion of the particle being obviously from the side of lesser curvature to that of the greater. In this way Anderson found the direction of motion of the particles and showed that there existed particles of positive charge having a much smaller mass than the protons. He fixed an upper limit for the proper mass of the positron to be about 20 times that of the electron.

A repetition of these experiments by Blackett and Occhialini† at Cambridge has fully confirmed this discovery, the magnetic field in their experiments was much inferior to Anderson's (2000 to 3000 gauss), but they improved on his method in one important respect. By placing two Geiger counters—one above and the other below the chamber—they so arranged that the track of any particle which fired both the counters was automatically photographed. Very recently a deflection of the positrons in electro-static field has also been reported. A Wilson chamber photograph of the positron-track obtained by Blackett and Ochialini is reproduced in Plate I, Fig. 13. The velocity of the positron is very nearly equal to that of light, and hence in accordance with the Lorentz-Einstein formula, the mass is enormously increased in motion. There is no reason to believe that the rest-mass of the positron is different from that of the electron.

---

*This method of taking Wilson photographs of cosmic ray tracks in a magnetic field was initiated by Skobelzyn (*Zs. f. Phys*, **43**, 354, 1927; **54**, 686, 1929) who was the first to observe electrons of enormous energy released by cosmic rays.

† Blackett and Occhialini, *Proc. Roy. Soc. A*, **139**, 699, 1933.

Almost simultaneously with the work of Blackett and Occhialini, Meitner* showed that positrons can be produced by the bombardment of the nucleus by neutrons, and Anderson † and Curie-Joliot ‡ showed that they are produced by bombardment of the nucleus by penetrating gamma-rays from ThC$''$. In such cases, the electron and the positron are produced in pairs. It is suggested that the gamma-rays split up under the action of the nucleus into two fundamental electric particles of opposite signs.

It may be mentioned that the existence of the positron was predicted in 1931 by Dirac§ from speculations based on his relativistic theory of the electron. The discovery of the positron thus lends a great weight to the importance to physics of his rather abstruse and abstract ideas. For details reference must be made to his original papers.

Books Recommended.

J. J. Thomson, *Rays of Positive Electricity* (1913), Longmans Green. *Positive Rays of Electricity*, 2nd Ed. (1921).

W. Wien, *Handbuch der Radiologie*. Bd. 4, Leipzig, (1917).

Handbuch der Physik, Bd. XXII.

Aston, *Isotopes* (1923), (1931).

---

* L. Meitner and Philipp, *Naturwiss.*, **21**, 286, 1933.

† Anderson and Neddermeyer, *Phys. Rev.*, **43**, 1034, 1933.

‡ I. Curie and F. Joliot, *Journ. Phys. Radium*, **4**, 494, 1933.

§ Dirac, *Proc. Roy. Soc. A*, **126**, 360, 1930; **133**, 60, 1931.

See also Fermi's article, *Quantum Theory of Radiation*, in *Review of Modern Physics*, Vol. 4, § 16.

APPENDIX TO CHAPTER III

Table 1. Isotopes of Elements.

Atomic Number	Element	Mass Number	Weight of Atom* ($O_{16}=16$)	Weight of Nucleus†	Mean Atomic Wt. (Scale O=16·000)	Relative Abundance‡	Reference
1	H	1	1·00778	1·00724	1·0078	4500 [1d]	[1] Urey, Brickwedder and Murphy, *Phys. Rev.*, **39**, 164, 1932.
	(Deuton)	2 [1]	2·01363 [1a]	2·01309		~1	[1a] Bainbridge, *Phys. Rev.*, **44**, 57, 1933.
2	He	4	4·00216	4·00108	4·002		[1b] Costa, *Ann. d. Phys.*, 4, 425, 1925.
3	Li	6 [1b]	6·012	6·0104	6·940	6	[1c] Cockcroft and Walton, *Proc. Roy. Soc. A*, **137**, 229, 1932.
		7 [1b, 1c]	7·012	7·0104		94	[1d] Bleakney and Gould, *Phys. Rev.*, 44, 265, 1933.
4	Be	8 [2]			9·02	1 } [2]	[2] Watson and Parker, *Phys. Rev.*, **37**, 167, 1931.
		9	9·0155 [2a]	9·01334		2000	
5	B	10	10·0135	10·0108	10·826	22	[2a] Bainbridge, *Phys. Rev.*, **43**, 367, 1933.
		11	11·0110	11·0083		78	

* Taken from Smekal, *Quantentheorie,* Kap. 6, Mott's article, *Wellenmechanik und Kernphysik,* p. 794.

† On the basis of mass of the electron m_e = ·00054.

‡ Aston, *Proc. Roy. Soc. A*, **126**, 511, 1930; **130**, 302, 1931; *Nature*, **123**, 313, 1929.

Table 1.—(Contd.)

Atomic Number	Element	Mass Number	Weight of Atom ($O_{16}=16$)	Weight of Nucleus	Mean Atomic Weight (O=16)	Relative Abundance	Reference
6	C	12 13^3	12·0036 $13·0039^3$ $13·0045^{3b}$	12·00036 13·00066 13·00126	12·000	400 1 ^{3a}	[3] King and Birge, *Nature*, **124**, 182, 1929.
7	N	14 15^4	14·008 $15·007^{4b}$	14·0042 15·0032	14·008	346 1	[3a] King and Birge, *Astr. Jr.*, **72**, 19, 1930.
8	O	16 17^5 18^5	16·000 $17·0029^{4b}$ $18·0065^{4b}$	15·99568 16·99858 18·00218	16·000	630 $<·189$ 1 ^{5a}	[3b] Chadwick, Constable and Pollard, *Proc. Roy. Soc.* A, **130**, 463, 1931.
9	F	19	19·0000	18·99514	19·00		[4] N. Naudé, *Phys. Rev.*, **36**, 333, 1930.
10	Ne	20 21 22 $(23)^6$	$19·9967^6$ $21·9947^{6a}$	19·9913 21·9893	20·183	93·7 1 9·75 Ne^{20} : Ne^{23} = 2000 : 1^6	[4b] Birge, *Phys. Rev.*, **37**, 841, 1931.
11	Na	23			22·997		[5] Giaque and Johnston, *Nature*, **122**, 318, 1929 ; **123**, 831, 1929.
12	Mg	24 25 26			24·32		[5a] Same as [6].
13	Al	27			26·97		[6] Kallmann, and Lasareff, *Zs. f. Phys*, **80**, 237, 1933.
14	Si	28 29 30	27·9818	27·97424	28·06		
15	P	31	30·9825	30·9744	31·02		[6a] Bainbridge, *Phys. Rev.*, **43**, 423, 1933.

Table 1.—(Contd.)

Atomic Number	Element	Mass Number	Weight of Atom ($O_{16}=16$)	Weight of Nucleus	Mean Atomic Weight (O=16)	Relative Abundance	Reference
16	S	32 33 34			32·06		
17	Cl	35 37 ·39[7] (40)[6]	34·983 36·980	34·9738 36·9708	35·457	6000 1850 1 $Cl^{35}:Cl^{40}=1:10^{-5}$	[7] Hettemer and Böhme, *Naturwiss.*,19,252,1931. [6] () The round bracket denotes uncertain value.
18	A	40 36	39·971 35·976	39·9612 35·9662	39·94		
19	K	39 41*			39·10	94·8 5·2	* The radio-active nuclei are marked with asterisk.
20	Ca	40 44			40·07		
21	Sc	45			45·10		
22	Ti	48 49			47·90		
23	V	51			50·96		
24	Cr	50 52 53 54	51·948	51·935	52·01	4·9 81·6 10·4 3·1	
25	Mn	55			54·93		
26	Fe	56 54			55·84		
27	Co	59			58·94		

Table 1.—(Contd.)

Atomic Number	Element	Mass Number	Weight of Atom ($O_{16}=16$)	Weight of Nucleus	Mean Atomic Weight (O=16)	Relative Abundance	Reference
28	Ni	58	57·942	57·927	58·69		
		60					
29	Cu	63			63·57		
		65					
30	Zn	64	63·937	63·9208	65·38	48·0	
		65				2·5	
		66				25·9	
		67				5·3	
		68				17·1	
		69				0·85	
		70				0·38	
31	Ga	69			69·72		
		71					
32	Ge	74					
		72					
		70					
		73					
		75	74·934	74·9168	72·60		
		76					
		71					
		77					
33	As	75			74·96		
34	Se	74			79·2	1·8 [8]	[8] Aston, *Proc. Roy. Soc. A*, **132**, 487, 1931. In this paper Aston gives also the isotopes and their relative abundance for Os, Ru, Tl, Ge, Re, Cl.
		76				20	
		77				17·4	
		78	77·937	77·9186		50·1	
		80	79·941	79·9226		100	
		82				19·5	
35	Br	79	78·929	78·91	79·916	50 [8]	
		81	80·926	80·91		50	

Table 1.—(Contd.)

Atomic Number	Element	Mass Number	Weight of Atom ($O_{16}=16$)	Weight of Nucleus.	Mean Atomic Weight (O=16)	Relative Abundance	Reference
36	Kr	78	77·926	77·9065	82·9	0·4	
		80	79·926	79·9065		2·5	
		82	81·927	81·9075		11·8	
		83	82·927	82·9075		11·8	
		84	83·928	83·9085		56·8	
		86	85·929	85·9095		16·7	
37	Rb	85			85·44	3 [9]	[9] Aston, *Proc. Roy. Soc. A*, **134**, 571, 1932. This paper also contains data for Li, Cs, Sc. * Radioactive nuclei are marked with asterisk.
		87*				1	
38	Sr	86			87·63	12 [9]	
		87[9]				8	
		88				100	
39	Y	89			88·92		
40	Zr	90			91·22		
		94					
		92					
		96					
42	Mo	92			96·0	14·2	
		94				10·2	
		95				15·5	
		96				17·8	
		97				9·6	
		98	97·945	97·9223		23·0	
		100	99·945	99·9223		9·8	
47	Ag	107			107·880		
		109					
48	Cd	114			112·41	See below†	
		112					
		110					
		113					
		111					
		116					
49	In	115			114·76		

† The proportion of the even isotopes (taken together) to the odd isotopes is 77 to 23.

Table 1.—(Contd.)

Atomic Number	Element	Mass Number	Weight of Atom ($O_{16}=16$)	Weight of Nucleus	Mean Atomic Weight (O=16)	Relative Abundance	Reference
50	Sn	112				1·07	
		114				0·74	
		115				0·44	
		116				14·19	
		117			118·70	9·81	
		118				21·48	
		119				11·02	
		120	119·912	119·885		27·04	
		121				2·96	
		122				5·03	
		124				6·19	
51	Sb	121				100 [8]	
		123			121·77	78·5	
52	Te	128	127·936	127·908			
		130			127·5		
		126	125·937	125·909			
53	I	127	126·932	126·903	126·932 to 126·92		
54	Xe	124				0·1	
		126				0·1	
		128				2·3	
		129				27·1	
		130			130·2	4·2	
		131				20·7	
		132				26·4	
		134	133·929	133·8998		10·3	
		136				8·8	
55	Cs	133	132·933	132·9033	132·81		
56	Ba	135 [9]				8 [9]	
		136			137·36	12	
		137				15	
		138	137·916	137·8857		100	
57	La	139			138·90 to 138·92		

Table 1.—(Contd.)

Atomic Number	Element.	Mass Number	Weight of Atom ($O_{16}=16$)	Weight of Nucleus	Mean Atomic Weight (O = 16)	Relative Abundance	Reference
58	Ce	140 142			140·13		
59	Pr	141			140·92		
60	Nd	142 144 146 (145)			144·27		
74	W	182 183 184 186 [8]	184·00	183·96	183·96	74·8 57·1 100 99 [8]	
80	Hg	196 198 199 200 201 202 204	200·016	199·973	200·61	0·1 9·9 16·4 23·8 13·7 29·3 6·8	* The radioactive nuclei are marked with asterisk.
81	Tl	203 205 207* 208* 210*	203·036 205·037	202·982 204·983	204·30	30 70	
82	Pb	203 204 205 206 207 208 (209) 210* 211* 212* 214* [10]	208·010	207·9657	207·22	0·04 1·50 0·03 27·75 20·20 49·55 0·85 0·08 [10]	[10] Aston, *Proc. Roy. Soc. A*, **140**, 535, 1933.
83	Bi	209 210* 211* 212* 214*			209·00		

CHAPTER IV

ELEMENTARY RADIOACTIVITY

SECTION I

45. Discovery and Nature of the Phenomenon.—The story of the discovery of the phenomenon known as Radioactivity forms one of the most interesting scientific romances of the nineteenth century. The discovery of X-rays by Röntgen in 1895, and the unexpected properties possessed by them created the most intense interest throughout the scientific world. It led to an exhaustive investigation of various substances with the expectation of finding out some which under ordinary circumstances, might emit radiations similar to X-rays. Since the production of phosphorescence is one of the most characteristic properties of X-rays, substances which are phosphorescent under ordinary conditions were attempted first. But most of these experiments gave negative results. A chance observation was however made by Prof. H. Becquerel of Paris (1896) who placed a phosphorescent uranium compound on a photographic plate wrapped in black paper. It was found on development that a faint image of the solid was produced on the plate. At first Becquerel was inclined to connect this phenomenon with phosphorescence, but further experiments brought to light the unexpected result that *phosphorescence had no connection whatsoever with the phenomenon*, and as a matter of fact all compounds of uranium (whether phosphorescent or not) produced the same effect to a degree depending upon the thickness of the layer employed and the proportion of uranium present in the compound. Conducting experiments under different conditions, it was found that the effect could not be influenced by varying the temperature or the state of aggregation (solid, solution or crystal) of the substance emitting these radiations or the presence or absence of other radiations in the surroundings, or any chemical or physical changes of the most drastic nature. These considerations led clearly to the conclusion that these radiations could not be regarded as due to something like emission of energy which had been conserved in the substance in consequence of its exposure to a source of light, but they were undoubtedly associated with some specific property of the substance Uranium.

46. Some Properties of the Radiations.—In addition to these properties of the radiations, it was observed by Becquerel, and later on by Mme Curie that the emission of radiation from Uranium was persistent, did not undergo any change in intensity or nature with the lapse of time. Attempts were then directed to observe reflection, refraction and polarisation of these radiations, but the results were inconclusive. But they discovered that like X-rays, these radiations possessed the important property of ionising a gas, *i.e.*, when they were allowed to pass through air which is ordinarily nonconducting, they rendered it conducting. Thus when a charged electroscope is brought near a gas subjected to the action of radioactive radiations, it rapidly loses its charge. The effect is illustrated by the experiment described in (I, §3). These experiments can be made quantitative and the apparatus can be utilised to find out the quantity of radioactive matter in a mineral. In the hands of the Curies, this method led to the discovery of the wonderful element Radium.

47. Discovery of Radium.—So far the nature of the radiations from U was quite unknown. For a long time, they were known as Becquerel rays. The next step was to find out whether these radiations were confined to U or were possessed by other substances. Of the 80 elements known till then, it was found by G. C. Schmidt, and M. Curie in 1898, that the next heaviest element thorium emitted radiations similar to those of U. The ordinary elements potassium (Campbell, 1907) and rubidium were also found to be feebly radioactive. But the most intense interest was created by the discovery of Radium, which was the culmination of an extensive series of systematic researches carried out by P. and Mme Curie. They began these researches with the object of finding out whether all Uranium-bearing minerals emitted Becquerel rays in proportion to their Uranium-content. They estimated the radioactive property by measuring the ionisation with an electroscope as described before (I, § 4). They found that while in most minerals the intensity of Becquerel rays was proportional to their U-content, a particular sample known as Pitch-Blende from a mine at a place called

Joachimsthal in Czeckoslovakia showed four times more activity in proportion to its U-content than ordinary uranium. They thought that the increased activity was due to the presence of an unknown element in the mineral, possessing more intense radioactive properties than U, in minute proportions. Guided by this conviction, they set to themselves the task of isolating this *active matter*. The principle used was very simple, though the struggle was epic. They started with 30 tons of the mineral, and went on separating the constituents by applying the methods of group separation used in chemistry. After a separation was effected, the two parts were tested separately for radioactivity. Generally one part was found to be inert, the other active. The active part was taken and again subjected to group analysis. Proceeding in this way, they found that most of the activity was due to a residue which was separated with barium. As barium itself was not active, they were led to the conclusion that the activity was due to a higher homologue of the group comprising Ca, Sr and Ba. The residue was converted into a chloride, and the active substance was separated from barium by fractional crystallisation. To this unknown element, they gave the name of Radium. Only 2 milligrams of radium were extracted from 30 tons of pitchblende.

But though the quantity was extremely small, it was found to account for almost the whole of the activity possessed by the original pitchblende. Thus weight for weight radium was found to be nearly million times more active than uranium, *i.e.*, 1 mg of radium produced as much ionisation as about 10^6 mg of U.

Later researches proved that radium had an atomic weight of 226, and filled a vacant place (No. 88) in the Periodic Table. As noted already, it is divalent, and belongs to the group Ca, Sr, Ba.

The discovery of radium is a landmark in the history of science. It placed for the first time in the hands of investigators a substance with the aid of which the study of this interesting phenomenon could be carried much further.

48. Other Radioactive Bodies.—Following the discovery of radium from pitchblende, this mineral was subjected to more critical examination for detecting the presence of any other active substance which may possibly be present in it. The idea was immensely fruitful, as it led to the discovery of several radioactive bodies such as, actinium, polonium, ionium and radiolead.

Actinium was obtained by Debierne in 1899, precipitated with elements of iron group from U-residues. Later on (1900), the same substance was discovered by Giesel from pitchblende and separated with the rare-earth element lanthanum. It was found that actinium emits a radioactive emanation whose activity dies out in a few seconds from its separation. Hahn and Soddy discovered independently in 1917 that actinium is always associated with another active substance *Protoactinium*, which is believed to be the parent of Ac.

Polonium was first separated by Mme Curie in 1898 from U minerals and named after her mother country Poland. It was found to possess the striking property that its activity is not permanent like that of Uranium, Radium or Thorium, but the substance decayed in activity in a few months. The radiations emitted by this substance was seen to produce very intense ionisation, but the ionisation ceased beyond a few millimeters from the source. Polonium is however many times more active than Radium.

Besides these elements, a large number of other radioactive substances including an isotope of lead (radio-lead) and some gases (radium emanations) were discovered. They were however not very permanent in activity. It is well-known that they originate from the disintegration of one or other of the active substances already mentioned. Even the elements U, Ra and Po are perhaps genetically related to each other. We shall return to these in §§60, 61 of this chapter.

49. On the Physical Nature of Radiations from the Radioactive Bodies.—The discovery of radium placed in the hands of investigators a very powerful and convenient material for the further study of the Becquerel rays. It was shown by Le Bon and Rutherford that the radiations are complex in nature, and consist of three different types, to which the names α, β, and γ-rays were given.

(1) The α-rays : The α-rays are very easily stopped by obstacles; even $\frac{1}{10}$ mm. of Al-screen is sufficient to cut off the α-rays. This is shown by an abrupt fall of the ionising powers of the radiations—in fact the ionisation is reduced to one hundredth part of its value. This shows that α-rays are mainly responsible for the ionisation of the gas. Later researches (see §§ 68, 69) showed that α-rays are positively charged particles, having its mass equal to four times the mass of a hydrogen atom, and its charge equal to twice the charge on the electron. It is in fact identical with the helium atom which has lost two electrons. The velocity with which the α-particles are emitted

is found to vary from $1{\cdot}4 \times 10^9$ to $1{\cdot}7 \times 10^9$ cm. per sec., depending upon the source, but the velocity of α-rays emitted in a particular disintegration has always the same value.

(2) The β-rays: Even after the α-particles are cut off, it is found that the residual radiation possesses a small ionising power. This is due to the β-particles. These particles were found to be identical with electrons, but possessing enormous velocities which sometimes may be as high as ·98 c. The β-rays are completely cut off by one cm. of Aluminium.

(3) The γ-rays: Even after the β-rays are cut off, there are rays which cause some ionisation, about $\frac{1}{10000}$ part of the original amount. Sometimes even very thick sheets of matter do not completely stop them. They are named γ-rays, and have been found to be not corpuscular at all, but electromagnetic in nature like light and X-rays. In fact they are only a penetrating form of X-rays.

The proper choice of the thickness of the absorbing medium, therefore, gives us a means of isolating one particular kind of radiation to the exclusion of others.

The fundamental difference in the nature of the three types of rays is clearly exhibited by their deflections in the magnetic field.

Suppose a quantity of radium is placed inside a thickwalled lead cylinder with a narrow opening which allows the radiations to pass upwards in a straight line. On applying a strong magnetic field at right angles to the plane of the paper, the α-rays are slightly deflected to one side, the β-rays suffer much greater deflection in the opposite side, and the γ-rays pass undeviated (Fig. 1). From the direction of the magnetic field and deflection of the rays, the nature of the charges carried by α and β rays can be determined.

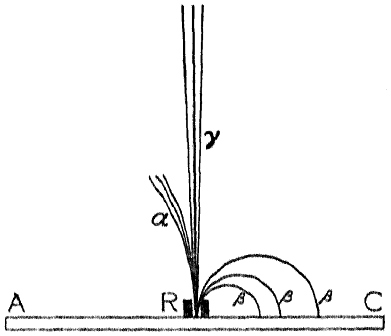

Fig. 1. Magnetic Deflection of α, β, and γ-rays.

50. Characteristic Properties of α, β, γ-rays.—The three kinds of radiations emitted from a radioactive substance have some characteristic properties common to them. Thus they all ionise the gas by which they are surrounded, they can penetrate different thicknesses of matter, they produce photographic action and show many physical, chemical and physiological actions. As instances of the latter properties, it may be cited that α-rays very rapidly decompose water; an ordinary piece of soda glass, if exposed for a long time to the radiations from a radioactive substance, is coloured deep violet, and by continued exposure is almost blackened. The property of producing ionisation is mainly responsible for these physical and chemical changes. If animal bodies are exposed to these radiations, they produce irritation and burns, and sometimes painful sores difficult to heal are produced as in the case of X-rays. This is mainly due to the penetrating power of these rays. The photographic action of the β and γ-rays is very pronounced. The α-rays are comparatively inactive in producing photographic effect on ordinary plates.

Another conspicuous property of these radiations is their heating effect. It was first pointed out by Curie and Laborde in 1903 that a quantity of radium always maintains itself at a higher temperature than the surrounding air. It has been estimated that one gm. of radium produces about $8{\cdot}7 \times 10^5$ calories of heat in a year.

One important property possessed by α and β rays is that when they are allowed to fall upon zinc sulphide or barium-platino-cyanide screens, they produce luminous spots of short durations upon them. On observing the surface of the screen by means of a magnifying glass, a larger number of scintillations distributed all over the surfaces are seen. This property was used by Wm. Crookes in an instrument called the "Spinthariscope" for making the α-particles visible. It consists of a small speck of Ra placed before a zinc sulphide screen which is carried at one end of a short tube, the other end of which carries a magnifying glass. On viewing through the glass in a dark room against a dark background, the screen is found to be full of bright specks of light, which are constantly flashing out and disappearing.

The ZnS screen is specially sensitive to α-rays, and the barium-platinocyanide screen to β-rays.

51. Simple Measuring Instruments in Radioactivity.— The property of the radioactive radiations which is commonly made use of in studying the strength and activity of active matters is their power of ionisation. Evidently the simplest instrument that can be designed on this principle is a pair of insulated plates, between which sufficient difference of potential is maintained by a battery; a galvanometer is connected to one of the plates, and one terminal of the galvanometer together with one pole of the battery is earthed. The full arrangement has been shown (I, §3). The saturation current recorded by the galvanometer gives a measure of the activity of the radioactive substance.

This simple arrangement, however, becomes insensitive for the small ionisations produced by α, β and γ-rays. So special apparatus, based on the above principle, have been designed for the three types of radiations according to their relative power of ionisation. These are known as the α-, β-, and γ-ray electroscopes respectively.

(1) *The α-Ray Electroscope*: This instrument, commonly used in experiments on α-rays, consists of an ionisation chamber (Fig. 2) AB on the lower plate of which the radioactive substance is put; while the upper plate A is connected to a metal rod C which passes through an insulating plug S and carries a thin metal leaf L. The leaf and the part of the rod above the ionisation chamber are enclosed in a second chamber. At first the rod C is charged to a high potential, the upper plate and the leaf being charged at the same time to the same potential. The leaf will be deflected on account of mutual repulsion of the charges on C and L. Initially, the deflection of the leaf is calibrated for different potentials given to it. Now if the potential applied be sufficient, the upper plate and the leaf acquire a corresponding extra potential due to the charge deposited by the ions. This causes a change in the deflection of the leaf. The method of calculation of ionisation current is the same as in Chap. I, § 4.

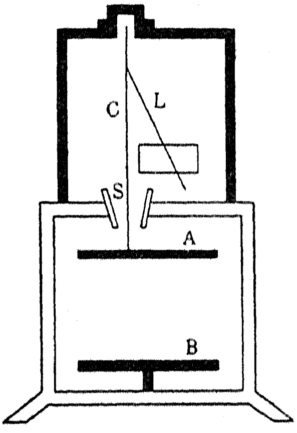

Fig. 2. The α-ray electroscope.

This ionisation in fact is due to all the three types of radiations from the substance. But the effect due to α-rays being many times greater than those due to β and γ rays, the ionisation may be considered to be due to α-rays alone.

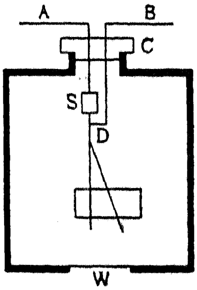

Fig 3. The β and γ ray electroscope.

(2) *β- and γ-ray Electroscopes*: The ionisation produced by β-rays is much smaller than that by α-rays. Hence the instrument designed for the β-rays should have greater sensitiveness. This is achieved by reducing the capacity of the system by a reduction of the size, so as to include the ionisation chamber inside the measuring chamber itself. The instrument is shown in Fig. 3. The chamber is a thickwalled lead vessel provided with an aluminium window W at the bottom, which is of such a thickness as to cut off the α-rays completely but transmit the β and γ rays through it. The radioactive

substance is placed below W. In other respects the instrument resembles the α-ray electroscope. The same instrument can be used as γ-*ray electroscope*, only now the Al-window is replaced by one of such a thickness as to cut off both α and β rays, and allow only γ-rays to pass through. The α-ray electroscope has also been modified into a form, in which the ionisation chamber is an air-tight vessel provided with stopcocks so as to enclose the active substance if it is a gas, *e.g.*, radium emanation. The chamber itself is connected to the earth and forms the lower plate of the ionisation system. The other arrangements are as usual. This is known as the *emanation electroscope* (Fig. 4).

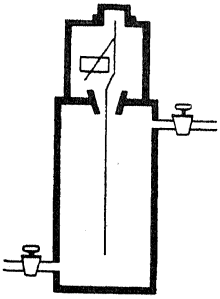

Fig. 4. The emanation electroscope.

Besides the electroscopes, electrometers are also widely used for radiometric measurements. An account of important types of electroscopes and electrometers employed for this purpose has been already given in Chap. I.

52. Other Properties of Radioactive Bodies.—The spontaneous emission of the charged particles α- and β-rays, with extremely high velocity from these heavy atoms was a matter of extreme surprise to the contemporary physicists. They were at a loss to find out the origin and source of this inexhaustible and uncontrollable source of energy. Further studies showed that the property of emitting these radiations is entirely *atomic*, thus confirming the early observations of Becquerel. Thus radium emits the same type of radiation whether it occurs in the form of chloride, bromide, or sulphate, and the intensity is always proportional to the radium content of the compound. Secondly, the properties were found to be entirely unaffected by the most violent physical changes. Madame Curie and K. Onnes found that the intensity of the radiations from radium retained the same value from the temperature of liquid air up to 1500°C. Thirdly, radium was found to produce heat continuously ; in fact one gm. of radium was found to produce heat at the rate of nearly 100 gm. calories per hour. We shall discuss this question in greater detail (§ 81) later.

53. Growth and Decay of Radioactivity.—In 1900, a further discovery of great value was made regarding the nature of radioactive processes. Sir Wm. Crookes found in 1900 that by a single chemical process (precipitating solution of a U-salt in ammonium carbonate, and then dissolving the precipitate in an excess of the reagent) a small residue was left which was found to be photographically many hundred times more active, weight for weight, than the uranium from which it was separated. This and other results, taken by themselves, pointed to the conclusion that the activity of U was not so much due to the element itself, but primarily to some other substance associated with it and possessing different chemical properties. To this substance the name UX was given. To avoid interference from α-rays when examining its activity, the substance under examination was always wrapped up in an Al-foil 1/10 mm. thick which completely cut off the α-rays. On removing the Al-foil, however, before or after the separation of the residue, U was always found to give a strong ionisation (due to α-ray emission), but the ionisation produced by UX alone was found to be negligible. This indicated that UX probably did not emit α-rays.

The observation was repeated by Becquerel who showed that the active substance is precipitated along with $BaCl_2$, mixed up with barium sulphate. The precipitate was found to contain all the activity, while the original U was found to be almost inactive. The inactive U and the active substance contained in Ba were then left aside for a year and again tested for photographic activity. Now the surprising observation was made that *inactive U had regained its activity, while Ba (or the active matter contained in it) had completely lost all activity.*

The same observation was made by Rutherford and Soddy who, working with Th, isolated minute quantities of an active substance which they called ThX from analogy to Crookes' UX. Using the ionisation method, they found that in course of a month ThX lost all activity while the original Th regained its activity. The matter was then quantitatively studied. The residue and the inactive matter were taken separately, and their activities were then plotted against time. The curves obtained are shown in Fig. 5.

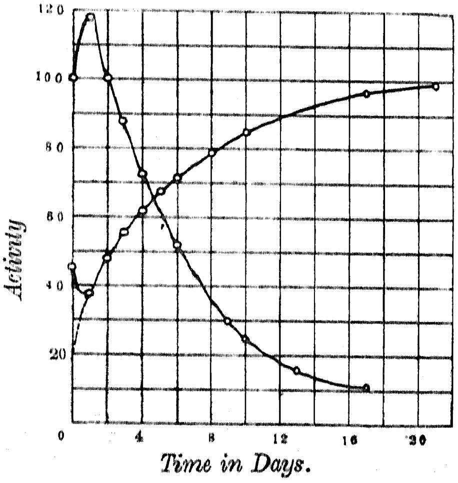

Fig. 5. Decay and Recovery curves.

The final activity of Th, and the initial activity of ThX are taken as 100. The ordinates represent the activities determined by the ionisation current, the abscissa represents the time in days. Both curves are irregular for the first two days, after which they become regular. It will be easily seen from the curves that the percentage proportion of activity regained by Th in any given interval is approximately equal to the percentage of activity lost by ThX during the same interval.

It is found that the decay curve can be represented by the mathematical formula

$$I = I_0 e^{-\lambda t} \quad \ldots\ldots\ldots\ldots \quad (1)$$

where I_0 is the initial activity of ThX and I the activity after a time t; while the curve of growth can be represented by the complementary curve

$$I = I_0(1 - e^{-\lambda t}) \quad \ldots\ldots\ldots \quad (2)$$

The constant λ has the same value in both cases.

54. Rutherford and Soddy's Theory of Spontaneous Disintegration of Radioactive Bodies.—These facts were explained by the hypothesis of spontaneous disintegration which was formulated by Rutherford and Soddy in 1902. The hypothesis postulates :—

(1) Atoms of every radioactive substance are constantly breaking up into fresh radioactive products with the emission of α, β and γ rays. The new product has entirely new chemical and radioactive properties.

(2) The process is spontaneous and of the type known in chemistry as *monomolecular*, *i.e.*, the rate of breaking cannot be influenced by foreign agencies, but depends entirely on the *law of chance*.

Thus if we take N atoms of ThX, and if we suppose that the number dN breaks up in time dt, then $\frac{dN}{dt}$ is the rate of breaking. According to the above postulates we should have

$$\frac{dN}{dt} = -\lambda N \quad \ldots\ldots\ldots\ldots \quad (3)$$

where λ is a constant characteristic of the disintegration. The solution of (3) is

$$N = N_0 e^{-\lambda t}$$

and

$$\frac{dN}{dt} = -\lambda N_0 e^{-\lambda t} \quad \ldots\ldots\ldots \quad (4)$$

The ionisation is proportional to $\frac{dN}{dt}$, hence (4) explains the decay curve of ThX.

55. Life of the Atom.—The Half-value Period.—It is clear that if the active substance be left to itself then after lapse of sufficient time, it will completely disappear. Now some atoms have disappeared in time t, others in time $t+dt$.... etc. We can therefore talk of the average life of the atom. This is

$$\tau = \int_0^\infty \frac{t\,dN}{N_0} = \int_0^\infty \frac{t\,N(t)\,\lambda\,dt}{N_0} = \frac{1}{\lambda} \quad \ldots\ldots \quad (5)$$

The average life is thus inversely proportional to the decay constant λ.

Half-value Period.—The half value period T is defined as the time in which the quantity of radioactive matter falls to half its initial value. We have

$$N_0 \; e^{-\lambda T} = \frac{N_0}{2}$$

Hence $$T = \frac{ln\ 2}{\lambda} = \cdot 6931\ \tau \quad \ldots\ldots\ldots \quad (6)$$

For explaining the decay curve of ThX we supposed that ThX spontaneously breaks up and transforms itself into an inactive substance. Let us now see how it is produced from the mother substance, *viz.*, Th.

Experiments have shown that the activity of ThX is due to α-rays. Th also emits α-rays, and the percentage proportion of activity lost by ThX is almost equal to that gained by Th in any given time. Hence we suppose that Th is also breaking up spontaneously producing ThX*, though its rate of decay is much more slower. Let us now consider a system initially consisting of P_0 thorium atoms. Let the system contain after a time t, P thorium atoms and Q ThX atoms, each breaking up according to its own rate. This picture corresponds to the inactive Thorium which is left to itself to recover its activity. We have

$$\frac{dP}{dt} = -\lambda_1 P$$

$$\frac{dQ}{dt} = \lambda_1 P - \lambda_2 Q$$

The second equation is modified because $\lambda_1 P$ atoms of ThX are produced per sec. by the breaking up of Th, and $\lambda_2 Q$ atoms of ThX disappear by the breaking up of ThX. We suppose that Th is not produced from anything more fundamental, and the product of ThX is inactive. λ_1 is a very small quantity while λ_2 is very large.

---

* ThX has however now been found not to be the direct product of Th, but there are a number of intermediate products.

In the steady state, *i.e.*, after the lapse of sufficient time, we shall have constant activity, *i.e.*, the rate of production of ThX from Th is just equal to the rate of breaking up of ThX. Hence $dQ/dt = 0$.

or
$$\lambda_1 P = \lambda_2 Q \quad . \quad . \quad . \quad . \quad . \quad . \quad . \quad . \quad . \quad . \quad (7)$$

or
$$P/Q = \lambda_2/\lambda_1 = \tau_1 : \tau_2$$

or in the steady state, the number of atoms of Th: the number of atoms of ThX $= \tau_1 : \tau_2 =$ Life of Th : Life of ThX.

When the steady state has not been reached as in Crookes' experiment, we have

$$P = P_0 \, e^{-\lambda_1 t}$$

and
$$\frac{dQ}{dt} = \lambda_1 \, P_0 \, e^{-\lambda_1 t} - \lambda_2 Q.$$

Solving this equation and using the condition that initially $Q = 0$, we have

$$Q = \frac{\lambda_1 \, P_0}{\lambda_2 - \lambda_1} \left(e^{-\lambda_1 t} - e^{-\lambda_2 t} \right) \quad . \quad . \quad . \quad . \quad (8)$$

Since λ_1 is very small compared to λ_2, we have approximately

$$Q = \frac{\lambda_1 \, P_0}{\lambda_2} \left(1 - e^{-\lambda_2 t} \right) \quad . \quad . \quad . \quad . \quad . \quad . \quad (9)$$

This gives the number of ThX atoms present after a time t. Now the activity is proportional to the number of ThX-atoms breaking up, *i.e.*, to $\lambda_2 Q$. Hence activity varies as

$$\lambda_1 P_0 \left(1 - e^{-\lambda_2 t}\right) = Q_0 \left(1 - e^{-\lambda_2 t}\right).$$

Or, denoting activity by I, we have

$$I = I_0 \left(1 - e^{-\lambda_2 t}\right) \quad . \quad . \quad . \quad . \quad . \quad . \quad . \quad . \quad (10)$$

Thus eqn. (10) explains the recovery curve of Rutherford and Soddy. We find that the curve represented by (10) is complementary to the curve represented by (4). This can also be verified from Fig. 5.

56. Extension to Successive Disintegrations.—The condition that ThX on breaking up is converted into an inactive compound, may not be in general true. In fact Rutherford proved by studying the disintegration products of Ra that the disintegration may successively be continued up to 7 or 8 members. We shall now give a brief account of his experiments.

RADIOACTIVE EMANATIONS AND INDUCED RADIOACTIVITY.

The early workers on radioactivity were much puzzled by two phenomena, *viz.*, (1) They found that the radioactivity of Th or Ra depended to some extent on the presence of air currents in the neighbourhood of the source. Thus taking a tube containing Th, if an air current is blown across it, most of the activity is found to be carried away by the current. (2) The so-called *induced radioactivity*. It was found that if a knife be exposed for sometime to Ra, Th or Ac, its surface becomes highly radioactive. But it was soon discovered that the term 'Induced radioactivity' by which this phenomenon was sometimes designated was misleading, as the activity was found to be due to the deposit of some very highly radioactive matter coming from the source.

It was shown that both phenomena can be accounted for satisfactorily by supposing that all sources of radioactivity give out highly radioactive gases which, on coming into contact with a knife, or better with a positively charged surface, deposit further highly radioactive solid matter. For an account of experiments clearing up these points, see Chap. IX and X of Rutherford's *Radioactive Substances and Their Radiations* (1913).

57. Properties of Radium Emanation.—The properties of Ra-Emanation have been studied in great detail by several investigators. It has been shown that Ra-emanation is a radioactive gas of high molecular weight (222), which is chemically analogous to the inert gases He, Ne, A, Kr and Xe, and forms the element 86 in the periodic classification. It is much more highly radioactive than Ra from which it is produced, and it is found to decay with an average life of 5·56 days. It emits α, β and γ-rays, but these are not wholly due to Ra-Em, but to its products of disintegration which are called Ra A, B, C, D, E, F. Only these products emit γ-rays, which are not due to Ra-Em. *Hence the amount of Ra Em within a sealed tube can be estimated by measuring the γ-ray activity of the content of the tube.*

The radium emanation has been found to be the immediate disintegration product of Ra. As Ra (at. wt. = 226) emits an α-particle, it is converted to Ra-Em. (at. wt. = 222). The number of Ra-Em. atoms produced by a gm. of radium is equal to the number of α-particles emitted by radium within the same time. This has been found to be $q = 3{\cdot}4 \times 10^{10}$ per sec. per gm. of Ra (*vide supra*).

One Curie of Emanation.—If we take one gm. of freshly prepared radium and seal it in a tube, then Ra will go on evolving RaEm, which will reach an equilibrium value after a sufficient length of time. According to (7) the number N atoms of Emanation present in equilibrium with 1 gm. of Ra is given by $N = q/\lambda$. Since $\lambda = 2{\cdot}085 \times 10^{-6}$sec.$^{-1}$, $N = 1{\cdot}63 \times 10^{16}$. *The volume of this gas under N. T. P. comes out to be 0·59 cubic millimeters with a mass of* $5{\cdot}81 \times 10^{-6}$ *gm.* According to international agreement*, it has been decided to designate this unit as *one Curie. The practical unit is equal to* 10^{-10} *Curie which is sometimes known as one Eman.*

58. Disintegration of Ra-Emanation.—The activity of Ra Em and its active deposits (*vide* table 1) was studied by Rutherford and his pupils for α, β and γ-rays, jointly and separately, and found to be very complex. We cannot enter here into a detailed description of the various experiments by which the experimental observations were explained, but we shall state only the results. Among other facts it was discovered by Soddy and Boltwood that radium is not by itself the parent substance to start the series of successive changes, but it is genealogically connected to Uranium. This element, after a series of α, β transformations gives birth to radium, which continues the process still further. The entire series is therefore known as the *Uranium-Radium series.* This series is illustrated in chart I. The various products of transformation have been separated by employing the methods of chemical and physical analysis where possible, and in most other cases by the method of radioactive recoil. The latter method depends upon the fact that when a radioactive element emits, say an α-particle, in a backward direction, it itself recoils in the forward direction with a velocity inversely proportional to its mass. If m_1, v_1 be the mass and velocity of the emitted α-particle, m_2, v_2 the corresponding quantities for the radioactive element, we have $m_1v_1 = m_2v_2$, v_2 being directed oppositely to v_1. The recoil atom in its motion ionises the surrounding gas, and it is found that in this process it loses a few of its electrons and becomes positively charged. So by applying a suitable potential difference between the source and an insulated plate placed above it, it is possible to get the recoil atom deposited on the plate. By this method it has been found possible to collect in many cases the individual radio-elements in a pure state.

---

* Radiology Congress, Brussels, 1910.

CHART I.—URANIUM-RADIUM SERIES

$M = 4n+2$

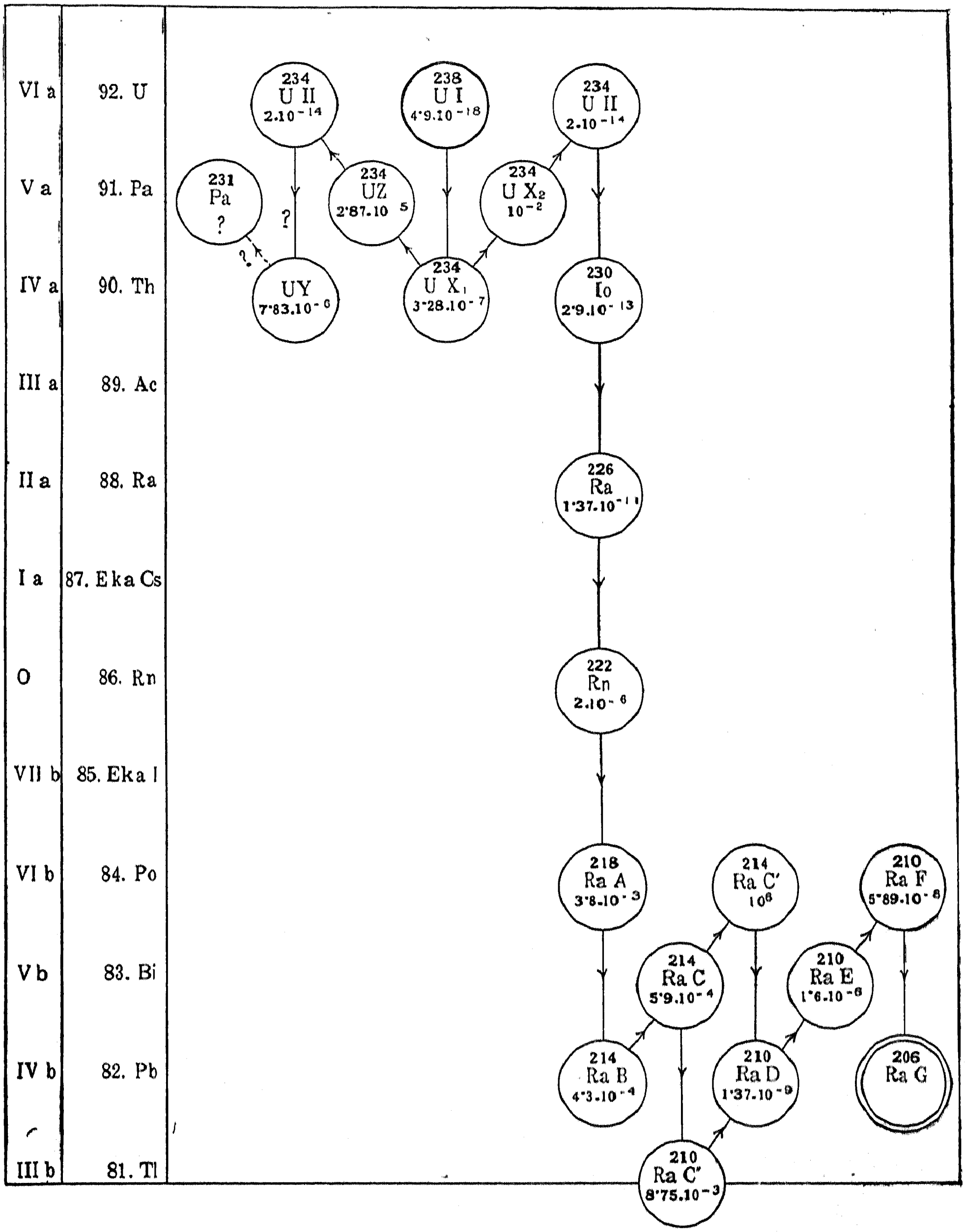

The vertical arrows denote α-ray transformations, and the diagonal arrows β-ray transformations. $T = 0{\cdot}6931/\lambda$ sec. For more accurate λ-values see table 1.

One year = 3·15. 10^7 sec.; 1 day = 8·64. 10^4 sec.; 1 hr. = 3600 sec.

CHART II.—ACTINIUM AND THORIUM SERIES.

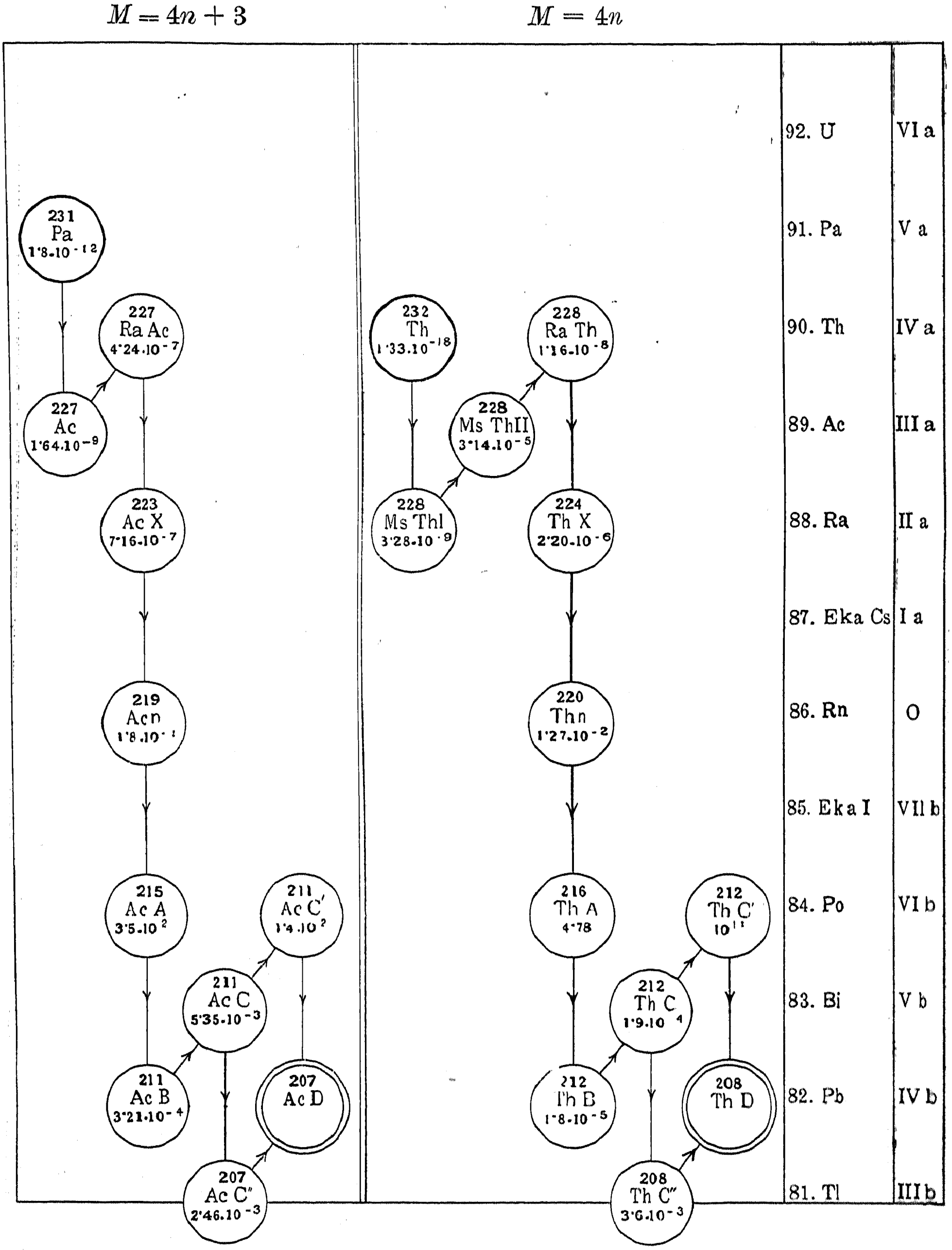

The vertical arrows denote α-ray transformations, and the diagonal arrows β-ray transformations. $T = 0{\cdot}6931/\lambda$ sec. For more accurate λ-values see tables 2 and 3.

One year = 3·15. 10^7 sec.; 1 day = 8·64. 10^4 sec.; 1 hr. = 3600 sec.

Table 1.—Radioactive Constants of U-Ra Series.

Element		Atomic number Z	Mass number M	Type of disintegration.	Decay constant λ*. (sec.$^{-1}$)	Half-value period T	Extrapolated Range at 15°C, 760 mm. R †	Energy of α-particle E_α 10^{-6} e.v.	Energy of disintegration (with recoil) $E 10^{-6}$ e.v.
Uranium I	UI	92	238	α	$4{\cdot}9.\ 10^{-18}$	$4{\cdot}5.10^{9}$ years	2·70 cm.	4·12	4·19
Uranium X$_1$	UX$_1$ ...	90	234	β	$3{\cdot}275.\ 10^{-7}$	24·5 days	...	...	...
Uranium X$_2$	UX$_2$ ...	91	234	β	$1{\cdot}013.\ 10^{-2}$	1·14 min.	...	...	...
Uranium Z	UZ	91	234	β	$2{\cdot}87.\ 10^{-5}$	6·7 hours	...	...	...
Uranium II	UII	92	234	α	$7{\cdot}4.\ 10^{-14}$	3.10^{5} years	3·28	4·626	4·75
Uraninm Y	UY	90	?	β	$7{\cdot}83.\ 10^{-6}$	24·6 years	...	...	...
Ionium	Io	90	230	α	$2{\cdot}6\ \ 10^{-13}$	$8{\cdot}3.10^{4}$ years	3·194	4·545	4·67
Radium	Ra	88	226	α	$1{\cdot}373.\ 10^{-11}$	1600 years	3·389	4·744	4·85
Radon	Rn	86	222	α	$2{\cdot}097.\ 10^{-6}$	3·826 days	4·122	5·441	5·53
Radium A	Ra A ...	84	218	α	$3{\cdot}79.\ 10^{-3}$	3·05 min.	4·722	5·972	6·07
Radium B	Ra B . .	82	214	β	$4{\cdot}31.\ 10^{-4}$	26·8 min.	...	...	...
Radium C	Ra C ...	83	214	αβ	$5{\cdot}86.\ 10^{-4}$	19·7 min.	4·145†	5·44	5·55
Radium C′	Ra C′ ...	84	214	α	10^{6}	10^{-6} sec.	6·971	7·683	7·82
Radium C″	Ra C″ ...	81	210	β	$8{\cdot}75.\ 10^{-3}$	1·32 min.	...	...	...
Radium D	Ra D ...	82	210	β	$1{\cdot}00.\ 10^{-9}$	22 years	...	...	...
Radium E	Ra E ...	83	210	β	$1{\cdot}60.\ 10^{-6}$	5·0 days	...	...	...
Radium F	Ra F (Polonium)	84	210	α	$5{\cdot}886.\ 10^{-8}$	136·3 days	3·925	5·253	5·36
Radium G or Uranium-Lead	Ra G U-Pb ...	82	206	Stable	...	...	...	...	...

* The λ values have been taken from the *Report of the International Radium-standards Commission*, Brussels (1930).

† The ranges given are the values obtained by Geiger, *Zs. f. Phys.*, **8**, 45, 1922 (*vide* table 5). The value for RaC is due to Rutherford and others (*Proc. Roy. Soc. A*, **129**, 211, 1930). These values have been considerably modified in a recent determination by Rutherford (*Proc. Roy. Soc. A*, **139**, 617, 1933) using a new method of annular magnetic field.

Table 2.—*Radioactive constants of Ac-series.*

			Atomic number Z	Mass number M	Type of disintegration	Decay constant λ (sec.$^{-1}$)	Half-value period T	Extrapolated Range at 15°C,760 mm. R_α	Energy of α-particle E_α 10^{-6} e. v.	Energy of disintegration (with recoil) E. 10^{-6} e. v.
Protactinium	Pa	...	91	231	α	·686. 10^{-12}	3·2. 10^4 yrs.	3·673 cm.	5·013	5·12
Actinium	Ac	...	89	227	β	1·64. 10^{-9}	13·4 yrs.	...	...	...
Radioactinium	Rd Ac	...	90	227	α	4·24. 10^{-7}	18·9 days	4·676 cm.	5·923	...
Actinium X	AcX	...	88	223	α	7·16. 10^{-7}	11·2 days	4·369	5·659	...
Actinon	An	...	86	219	α	0·177	3·92 sec.	5·789	6·819	7·03
Actinium A	AcA	...	84	215	α	3·74. 10^{2}	2.10^{-3} sec.	6·584	7·405	7·53
Actinium B	AcB	...	82	211	β	3·21. 10^{-4}	36·0 min.	...	...	...
Actinium C	AcC	...	83	211	$\alpha\beta$	5·35. 10^{-3}	2·16 min.	5·511	6·610	6·70
Actinium C′	AcC′	...	84	211	α	1·4. 10^{2}	5.10^{-3} sec.(?)	6·5	7·32	7·46
Actinium C″	AcC″	...	81	207	β	2·43. 10^{-3}	4·76 min.	...	...	...
Actinium D (Actinium Lead Ac-Pb)	AcD	...	82	207	Stable	...	...	...	...	...

Table 3.—Radioactive constants of Th-series.

			Atomic number Z	Mass number M	Type of disintegration	Decay constant λ (sec.$^{-1}$)	Half-value period T	Extrapolated Range at 15°C,760 mm. R_α	Energy of α-particle E_α 10^{-6} e. v.	Energy of disintegration (with recoil) E 10^{-6} e. v.
Thorium	Th	...	90	232·1	α	1·33. 10^{-18}	1·65. 10^{10} yrs.	2·59*	3·98	4·06
Mesothorium I	Ms Th I	...	88	228	β	3·28. 10^{-9}	6·7 days.	...	...	...
Mesothorium II	Ms Th II	...	89	228	β	3·14. 10^{-5}	6·13 hrs.	...	...	...
Radiothorium	Ra Th	..	90	228	α	1·16. 10^{-8}	1·90 yrs.	4·019	5·347	5·43
Thorium X	Th X	...	88	224	α	2·20. 10^{-6}	3·64 days.	4·354	5·645	5·73
Thoron	Thn	...	86	220	α	1·27. 10^{-2}	54·5 sec.	5·063	6·244	6·33
Thorium A	Th A	...	84	216	α	4·95	0·145 sec.	5·683	6·737	6·84
Thorium B	Th B	...	82	212	β	1·82. 10^{-8}	10·6 hours	...	...	...
Thorium C	Th C	...	83	212	αβ	1·91. 10^{-4}	60·5 min.	4·787	6·015	6·18
Thorium C′	Th C′	...	84	212	α	10^{11}	10^{-11} sec.(?)	8·617	8·617	8·97
Thorium C″	Th C″	...	81	208	β	3·61. 10^{-3}	3·20 min.	...	...	..
Thorium D or Thorium Lead	Th D Th-Pb	..	82	207·77	Stable	..	...	...	...	...

* The range of Th is due to G. H. Henderson and J. L. Nickerson, *Phys. Rev.*, **36**, 1344, 1930. Geiger's value is 2·90 cm.

59. Explanation of the Chart.—The whole process of radioactive transformation is schematically represented in charts I and II. The circle round UI (chart I) represents the Uranium atom, and so on for various other products of the series. The series in chart I is the *Uranium-Radium* series. The name of each product in symbol, its atomic weight and the decay constant λ are enclosed within the circle representing the element. Elements in the same horizontal row have the same atomic number as indicated in the extreme left. The transformation from one element to another is always brought about by spontaneous disintegration, which is marked by the emission of an α or a β-particle, and very often the β-ray disintegration is accompanied by the emission of γ-rays. The vertical arrows in the scheme denote α-ray disintegrations, while the diagonal arrows represent β-ray disintegrations. Since an α-particle has a mass $4m_H$ and a charge $+2e$, and a β-particle a negligible mass, and a charge $-e$, a product of α-ray transformation is displaced two units downwards on the atomic number scale, and loses in mass by four units; and a product of β-ray transformation possesses equal atomic weight with the parent atom, but is displaced one unit upward on the atomic number scale. Thus we have for uranium I, atomic weight=238·18 and atomic number=92, and for uranium X_1 which is its immediate α-ray disintegration product, atomic weight=234 and atomic number=90. The same relations may be verified between radium and radon (which is also called radium emanation) the α-ray disintegration product of Ra. Again for radium B, atomic weight=214 and atomic number=82, and for its immediate β-ray transformation product RaC′ the corresponding quantities are 214 and 83 respectively.

The constants for the various products of the series, with their full names and symbols are given in table 1. The type of disintegration each product undergoes is shown in column 4. The decay constants and half-value periods are shown in columns 5 and 6. In case of α-ray disintegrations, the extrapolated ranges of α-rays (R_α) are given in column 7. The energy of the α-particle, and that of the disintegration with recoil are respectively given in columns 8 and 9 of the table. It will be seen that T which is a measure of stability of the element varies between $4·5 \times 10^9$ years and 10^{-6} seconds and λ varies from $4·9 \times 10^{-18}$ to 10^6, for radioactive processes so far known.

Chart II represents other two series of the radioactive family, *viz.*, the actinium and the thorium series. They will be discussed in § 61. The three series begin with the atomic weights $4n+2$, $4n+3$ and $4n$ respectively, where n denotes an integer.

60. The U-Ra Series.—We shall now discuss the chart in greater detail. The transformation of U to UX is attended with the expulsion of an α-particle. The element UX now undergoes a β-ray transformation in two different ways :

$$(1)\quad \underset{\beta}{\overset{90}{UX_1}} \rightarrow \underset{\beta}{\overset{91}{UX_2}} \rightarrow \underset{\alpha}{\overset{92}{UII}} \rightarrow \underset{\alpha}{\overset{90}{Io}} \rightarrow \underset{\alpha}{\overset{88}{Ra}}$$

$$(2)\quad \underset{\beta}{\overset{90}{UX_1}} \rightarrow \underset{\beta}{\overset{91}{UZ(?)}} \rightarrow \underset{\alpha}{\overset{92}{UII}}$$

These are represented by the two diagonal branches starting from UX_1. The first of the two branches is the main series of changes to which 99·65 % of UX_1 contribute, while only 0·35 % of UX_1 takes part in the second. Both of these give the ultimate product UII ; the intermediate products of the two branches, UX_2 and UZ* (?), are chemically identical, but they differ widely in their half-value periods (1·14 min. and 6·7 hrs. respectively). The product UII is an α-ray body like UI itself. In fact the two are chemically inseparable and differ only in atomic weights. It was at one time thought, as the result of an observation by Boltwood, that UI emits two α-particles instead of one ; but now it is known that the second α-particle comes not from UI, but from UII, which is thus transformed into a new element *Ionium*. In 1907, the element ionium was first isolated by Boltwood, who showed that this was the parent of radium.

We now come to radium and its family. The genealogical relation of Ra with U has been clearly shown in the above discussion. The disintegration product of Ra is radium-emanation, or radon a gas whose property has been discussed in § 57. Further products of the series are :

$$\begin{tikzcd}
 & & & & & \underset{\alpha}{\overset{84}{RaC'}} \arrow[r] & \underset{\beta}{\overset{82}{RaD}} \arrow[r] & \underset{\beta}{\overset{83}{RaE}} \arrow[r] & \underset{\alpha}{\overset{84}{RaF}} \arrow[r] & \overset{82}{RaG} \\
\underset{\alpha}{\overset{88}{Ra}} \arrow[r] & \underset{\alpha}{\overset{86}{Rn}} \arrow[r] & \underset{\alpha}{\overset{84}{RaA}} \arrow[r] & \underset{\beta}{\overset{82}{RaB}} \arrow[r] & \overset{83}{RaC} \arrow[ur, "\beta"] \arrow[dr, "\alpha"'] & & & & & \\
 & & & & & \underset{\beta}{\overset{81}{RaC''}} \arrow[r] & \overset{82}{RaD.} & & &
\end{tikzcd}$$

The elements RaA, RaB, RaC are characterised by short lives, while RaD, RaE, RaF possess quite long lives. The breaking up of RaC is interesting. It is a dual disintegration of both α and β types, shown by the two branches of the above scheme. 99·96 % of the total amount of RaC breaks up with the expulsion of a β-particle giving RaC′, which again breaks up with the expulsion of an α-particle and forms RaD. On the other hand 0·04% of RaC undergoes α-ray disintegration giving the product RaC″, which finally breaks up after emitting a β-particle and forms RaD. Thus the sequence of transformation in one branch is reversed compared to that in the other.

---

* UZ was discovered by Hahn in 1921.

The element RaD has the atomic number 82 and is identical in chemical properties with Pb. RaD is therefore identified with *Radio-lead*, discovered in uranium minerals in 1901. Further, it has been found that RaF is identical with the element polonium discovered by Mme. Curie in 1898 (*vide* §48). The last product of the series is RaG which is inactive. It is again identical with ordinary lead. But for indicating its origin, it is commonly described as *Uranio-lead.*

It should be remarked here that the positions of the products UZ and UY[*] in the table are not very certain. The same remarks apply to the transformation UII→Pa. This is indicated by the sign of interrogation against them. In fact the production of Pa having an atomic weight 231 and atomic number 91 from UII having the atomic weight and number 234 and 91 seems highly improbable, unless we assume the emission of a particle of mass 3 and charge + 1 at one stage. There is yet no proof of the existence of such a particle from any other source. It is therefore supposed that Pa originates from an isotope of U called *Actino-uranium*[†] having atomic weight 235 and atomic number 92. The process may be

$$92\overset{\alpha}{\mathrm{U}}(235)\rightarrow 90\mathrm{U}\overset{\beta}{\mathrm{Y}}\ (231)\rightarrow 91\ \mathrm{Pa}\ \overset{\alpha}{(231)}\rightarrow 89\ \overset{\beta}{\mathrm{A}}\mathrm{c}\ (227).$$

The process is then continued to the Ac-series.

61. Actinium and Thorium Series.

—Besides U-Ra series, there are two other series of successive disintegrations. These are the Th-series and Ac-series one of which (Th) at least is unrelated to the other two. They are represented in chart II and their constants are given in tables 3 and 2. As they are given on exactly the same lines as U-Ra series, they require no further explanation. It is rather striking to note that here again dual disintegrations of both α, β types occur in Thorium C and Actinium C, each of which breaks up into two distinct ways. These are shown separately in schemes A and B below.

---

[*] UY was discovered by Antonoff in 1911.

[†] Western and Ruark, *Phys. Rev.*, **44**, 675, 1933. See however, Gratias and Collie, *Proc. Roy. Soc. A*, **139**, 567, 1933.

There is but one difference that while in U-Ra and Th series, in the dual disintegration of "C" products, it is the β-disintegration branches which are main lines of products, in the Ac series, the α-disintegration

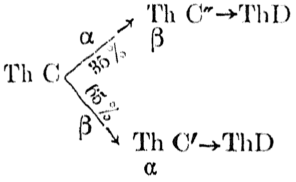

(A)

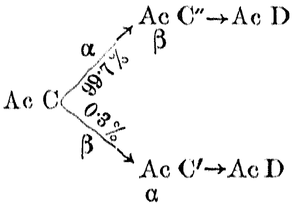

(B)

branch predominates. The final products ThD and AcD of the two series are again inactive and identical with Pb (82). They are described as *thorio-lead* and *actinio-lead* respectively. It may be mentioned here that recently Aston* has verified the three important isotopes of Pb 206, 207 and 208, and a very faint isotope 210 (RaD?) by the mass-spectrograph.

It remains now to discuss if the element Ac is genealogically related to the U-Ra series. This is an interesting question, but unfortunately the position is not very certain. According to one view the element UY which is possibly a branch product of UX_1 (see chart I) is the parent of the Ac-series, and the newly discovered element Protactinium is the intermediate product between UY and Ac. Extreme weakness in activity of Ac and its products has again led to another view that Ac has its origin in an isotope of U occurring in a relatively small proportion. This hypothesis has already been discussed at the end of § 60.

62. Soddy and Fajans' Displacement Law: Radioactive Isotopes.—With the clearing up of the ideas of successive transformations, attempts were made to study the physical and chemical properties of the products in greater detail in order to fix their positions in the periodic table. It was very soon found that many radioelements could not be separated from each other or from some common element by the methods of chemical analysis. Thus McCoy and Ross found that Rd Th (Radiothorium) and Th were chemically inseparable, and so also were Ra and MsTh (mesothorium) as pointed out by Soddy and Marckwald. Similarly in spite of numerous investigations Ra D has not been separated from Pb with which it occurs in the analysis of U-minerals. This early led to the view* that the two elements of each such pair, a parent and a product, *e.g.*, RdTh and Th, or RaD and Pb, do not differ at all in their chemical properties, that is, they must be placed in the same vertical column in the periodic table. What is then the connection between the chemical property of a product and the ray emitted by the parent element? This question first occurred to Soddy and Fajans, and was satisfactorily answered by them.

---

* Aston, *Proc. Roy. Soc.* A. **140**, 535, 1933.

From a scrutiny of the chemical properties of the successive products of a disintegration series, Soddy and Fajans arrived at results of wide generalisation. They can be stated as follows :—

(*a*) When a radioactive atom emits an α-particle, it is converted to another element whose valency is less than that of the parent substance by 2, or its place in the periodic classification is shifted by two places to the left. Thus Ra on emitting an α-particle is converted to RaEm. The valency of Ra is 2, the valency of RaEm is zero. The atomic number of Ra is 88, that of RaEm is 86. The atomic weight decreases by 4 in this process.

(*b*) When a radioactive atom emits a β-particle, it is converted to a new element whose valency is greater than that of the parent substance by 1. The place in the periodic table is shifted by one position to the right. Many examples will be found in charts I, and II. The products of the three series can all therefore be placed in their respective positions in the periodic table, as shown in charts I and II.

A scrutiny of the charts shows that there are many radioactive elements in the same horizontal row, and therefore possessing the same chemical properties, but having entirely different atomic weights, *e.g.*, in the group marked IIa, we have Ra, ThX, AcX, MsTh, all having the atomic number 88 and they are all divalent.

This raises the possibility that atoms having the same chemical properties may have different weights. Such atoms are said to form *isotopes*. Thus RaB, RaD are all isotopes of lead.

SECTION 2

PROPERTIES OF α-RAYS

63. Nature of α-Particles.—Of the three kinds of radiations from a radioactive substance, the γ-rays have been found to be

---

*Soddy, *Trans. Chem. Soc.*, **99**, 72, 1911.

electromagnetic in character like light, while α and β rays have been found to be charged material particles. The β-rays are very light and from the direction of their deflection in a magnetic field were early found to possess a negative charge. But evidences regarding the nature of α-rays could not be obtained so easily. This was partly due to their photographic inactivity compared to the β-rays and partly to the fact that they were unaffected by ordinary magnetic fields which were sufficient for causing deflection of the β-particles. It is now known that this was due to the greater mass of the α-particles. The earliest attack on the problem was due to Rutherford in 1903. He allowed the α-rays from radium to pass through a large number of parallel vertical slits G, separated by a distance of 1 mm. into an evacuated chamber V containing a charged gold leaf B. (*Vide* Fig. 6). The effect was the rapid collapse of the leaf, due to the ionisation of the air by α-rays. But on applying a strong magnetic field parallel to the slits, a marked diminution in the rate of collapsing was noticed. Evidently some of the α-particles are deviated from their course and prevented from entering the chamber. In order to avoid the absorption of α-rays in the gas RaEm emitted by Ra, a steady flow of hydrogen was maintained through the apparatus which removed the emanation.

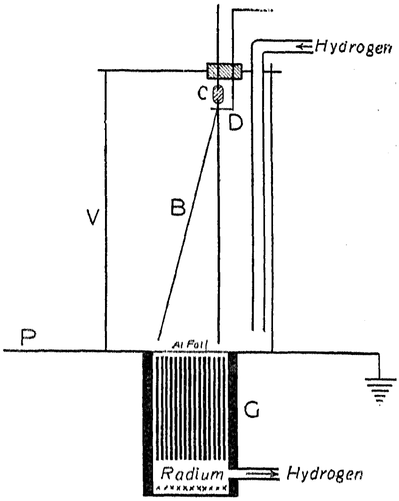

Fig. 6. Magnetic deviation of α-rays.

64. Magnetic Deflection of α-Rays.—Accurate measurement of magnetic deflection of α-rays was made by Rutherford and Robinson* in 1914. They found that ordinarily a radioactive substance gives α rays of wide range of velocities which render the magnetic deflection uncertain, and a homogeneous source of α-rays was essential for any precision measurement. For this purpose they took a platinum wire which had been exposed for a long time to the radioactive gas radon and had thus obtained a thin deposit of RaA, RaB, RaC over it. The α-rays from such a wire at A (Fig. 7) were allowed to pass through a narrow slit at B parallel to the wire (perpendicular to the plane of the paper) and received on the photographic plate C. The enclosing chamber was evacuated. A strong uniform magnetic field, parallel to the slit, was applied by means of a large electromagnet, which deviated the α-ray beam to one side as shown in Fig. 7. Two deflected bands due to direct and reversed magnetic fields were obtained on the photographic plate. If $2d$ = distance between the bands, b = distance between the source and the slit, a=distance between the slit and the plate and ρ = radius of curvature of the beam, we have, when d is small

---

* Rutherford and Robinson, *Phil. Mag.*, 28, 552, 1914.

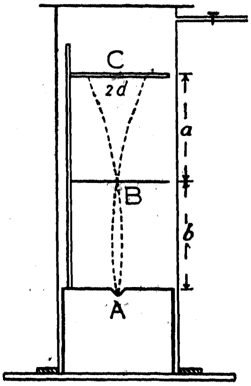

Fig. 7. Magnetic deflection of α-rays.

$$2\rho d = (a + b)\, a$$

Taking E = charge carried by an α-particle and M = its mass, and u = the velocity of the α-particle, we have

$$\frac{Muc}{E} = H\rho = \frac{Ha(a+b)}{2d} \quad . \quad . \quad . \quad . \quad (11)$$

where H = the applied magnetic field. Using a = 6·54 cms., b = 6·618 cms., the deflection was $2d$ = 13·63 mm. for a field of 6236 gauss. In this way a mean value of $\frac{Muc}{E} = 3{\cdot}983 \times 10^5$ was obtained. An actual photograph of curved α-ray tracks in a high magnetic field is shown above in Plate II (Fig. 8). This is due to Kapitza*.

65. Deflection of α-Rays under Electric Field.—The electric deviation of α-particles was measured with precision by the same authors† in 1914. At a distance suitable for obtaining appreciable electric deflection the intensity of α-rays from the wire-source being too weak, they used for the source a thinwalled α-ray tube filled with radon. A uniform difference of potential was maintained between two large strips of silvered glass plates A B (Fig. 9) with their planes vertical and parallel to each other. The α-ray tube S was held centrally near one end of the plates, the other end of which carried a narrow mica slit L. The whole was enclosed in an evacuated glass tube closed at the ends. The α-rays from S on passing between the two plates traversed the electric field and were received on the photographic plate P. Two bands were obtained, one on reversing the electric field, and the other with direct field. If D = the deflection of a band from the centre under a potential difference V between the condenser plates, l = distance of the photographic plate from the end of the condenser plates and d = the distance between the plates, then

---

* Kapitza, *Proc. Roy. Soc.*, **106**, 602, 1924.

† Rutherford and Robinson, *loc. cit.*

$$\frac{Mu^2c}{E} = \frac{8\,V\,l^2}{(D-d)^2} \quad . \quad . \quad . \quad (12)$$

With an electric field of 2000 volts and the distance between the condenser plates about 4 mm., it was found that the value of $\frac{Mu^2c}{E}$ was of the order 6×10^{14}.

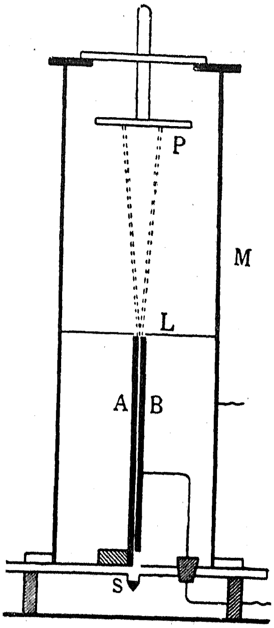

Fig. 9. Electric deflection of α-rays.

66. $\frac{E}{M}$ **for α-rays.**—From combined observations of the electric and magnetic deflections, the value of E/M for α-particles can be calculated using the equations (11) and (12). In actual experiment, the source is a mixture of three substances Radon, Ra A and Ra C, so that the plate shows for magnetic or electric experiment three bands on either side of the central band. The results calculated for the three substances from these have been shown in Table 5.

Table 5. E/M for α-rays.

Source of rays.	Experiment	$\frac{Muc}{E}$	$\frac{Mu^2c}{E}$	$\frac{E}{Mc}$
Ra C	1	$3{\cdot}555 \times 10^5$	$6{\cdot}083 \times 10^{14}$	4813
	2	3·555	6·110	4826
Ra A	1	2·941	4·174	4824
	2	2·941	4·185	4837
Radon	1	2·717	3·560	4822
	2	2·717	3·563	4826

The values of E/M for the α-particles from the three sources are found to be constant within the limits of experimental errors. The results of a few accurate determinations for Ra C gives a mean value 4820. For the hydrogen ion $\frac{e}{m_H}=9650$, which is nearly double the value for α-particles. This opens out three possibilities, namely, (1) $E=e$, $M=2m_H$, (2) $E=\frac{e}{2}$, $M=m_H$, (3) $E=2e$, $M=4m_H$. Again Briggs* calculated the ratio for the helium nucleus and has obtained a value 4826. This agreement lends evidence in favour of the last possibility, which makes an α-particle identical with a doubly charged helium ion (*i.e.*, He^{++} —nucleus). The question was finally settled by an actual determination of the charge carried by a single α-particle simultaneously by Regener, and by Rutherford and Geiger. The experiment consists of two parts. In the first part, the total number of α-particles emitted from a radioactive substance per gram per sec. is obtained, and in the second part, the total charge carried by the α-particles is determined.

67. Counting the α-particles.—This was done almost simultaneously by Regener, and Rutherford and Robinson. Regener's† apparatus is extremely simple and is shown below (Fig. 10).

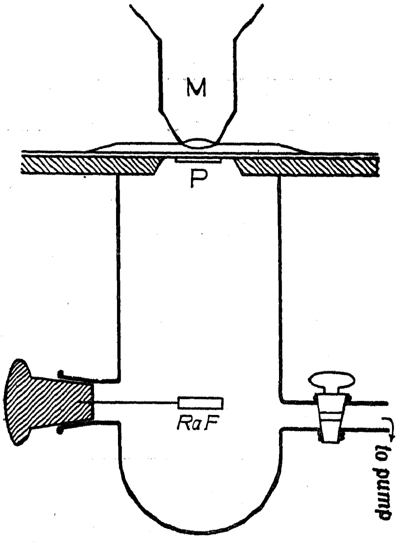

Fig. 10. Regener's apparatus.

In this method, the number of scintillations produced on a sensitised screen by α-particles is counted. As sensitive screen, Regener used a thin crystal plate of zinc blende, or a diamond crystal plate P of ·1 mm. thickness; the scintillations are observed by a microscope M (magnification 170, aperture $f/1{\cdot}40$). The radioactive source is a thin preparation of polonium (RaF) which gives only α-particles. These go out through a definite solid angle and are received on the plate. The total number of α-particles emitted per sec. can be easily calculated by counting the number of scintillations in a definite time. Independent evidence has shown that each α-particle produces only one scintillation on a diamond plate.

---

* Briggs, *Proc. Roy. Soc. A*, **118**, 549, 1928.

† Regener, *Verh. d. D. Phys. Ges.*, **19**, 78, 351, 1908.

Let R be the distance of RaF from the crystal plate, f=surface of the crystal, n'=number of scintillations observed in time t, then n the number emitted per sec. is given by

$$n = \frac{n'}{t} \cdot \frac{2\pi R^2}{f}$$

Using R=127 mm. Regener obtained in an experiment n=3·935×10^5.

The amount of radioactive substance present can be determined from its γ-ray activity. So the number of α-particles emitted by the source per gm. per second can also be calculated. This is an important physical constant, and for Ra the value of this quantity is Q=3·5×10^{10}

If the total charge carried by the n α-particles now be determined, the charge on one α-particle e_α would be obtained on dividing the total charge E by n. Thus using E=3·77. 10^{-4} (see §68),

$$e_\alpha = 9{\cdot}58\times10^{-10} \text{ e. s. units} \pm 3\%$$

from which it is apparent that the charge carried is *2×charge on the electron.*

Electrical methods of counting, which depend upon the ionising power of α-rays at low pressures, were subsequently developed by Rutherford and Geiger. An account of these methods and their further developments by Geiger have already been given (I, §13).

68. Charge on an α-particle.—We now proceed to the method of determination of charge of an α-particle. This was done by Rutherford and Geiger* (1908) by measuring the total charge carried by a definite number of α-particles emitted within a given solid angle. The constant Q, that is, the number of α-particles emitted per second per unit gramme of the active substance was known by the methods in § 67. To determine the corresponding charge, the apparatus in Fig. 11

---

*Rutherford and Geiger, *Proc. Roy. Soc. A*, **81**, 141, 1908.

was employed. A known amount of radioactive substance Ra C was placed at R. The α-rays first pass through the Al foil B and then fall upon the plate CA, the lower portion of which is covered with a thin Al foil. The whole apparatus is placed in a strong magnetic field which deflects the β-particles from Ra C, as well as δ-particles (recoil electrons), so that they do not disturb the measurements. The apparatus is highly evacuated, and the current between CA and B measured. The number of α-particles falling on the plate per second is known from the γ-ray activity of Ra C (§ 67).

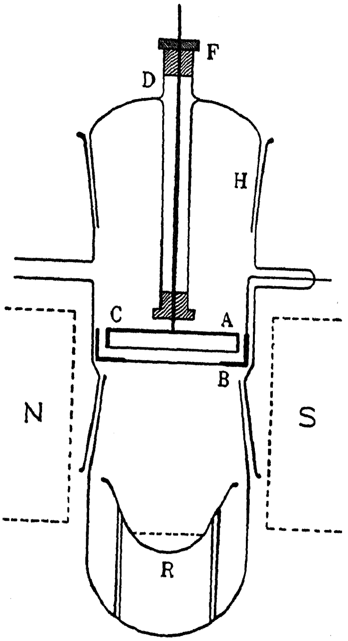

Fig. 11. Arrangement for measuring the charge on an α-particle.

The strong magnetic field completely eliminates the effect due to β and δ-rays and charges the upper plate positively whatever may be the charge on B. The plate B is first given a positive potential $+V$, then a negative potential $-V$. Let i_1 and i_2 be the observed currents in the two cases and i_0 be the current due to the residual ionisation of gas. Then

$$i_1 = ne_\alpha + i_0$$

$$i_2 = ne_\alpha - i_0$$

where n=number of α-particles falling on the upper plate per sec., e_α = charge on each of them. Thus, we have

$$nE = \frac{i_1 + i_2}{2}$$

n can be obtained as in § 67. Thus the charge carried by an α-particle can be calculated. The value obtained in this way is

$$e_\alpha = 9{\cdot}30 \times 10^{-10} \text{ e. s. units.}$$

But the charge on an electron is $e = 4{\cdot}77 \times 10^{-10}$ e. s. u., which is very nearly equal to half the above value. From this it is apparent that the *charge carried by an α-particle is twice the charge on an electron.*

69. The α-particle and the Helium atom.—From § 68, we have thus

$$e_\alpha = 2e$$

and
$$\frac{e_\alpha}{m_\alpha c} = 4823 = \frac{e}{2m_H c}$$

Hence
$$m_\alpha = 4m_H$$

i.e., the mass of the α-particle is four times the mass of the H-atom.

From these measurements, it appears that the mass of the α-particle is equal to the mass of the helium atom. This gave rise to a strong suspicion that there was very intimate connection between α-rays and helium. The suspicion was further strengthened by the knowledge, that almost all radioactive minerals contain a certain quantity of helium. This receives an easy explanation if we suppose that the helium is of radioactive origin, and is formed due to the conversion into helium of α-particles emitted through ages.

The identity of α-particles with helium was definitely demonstrated by Rutherford and Royds* by the following experiment (Fig. 12).

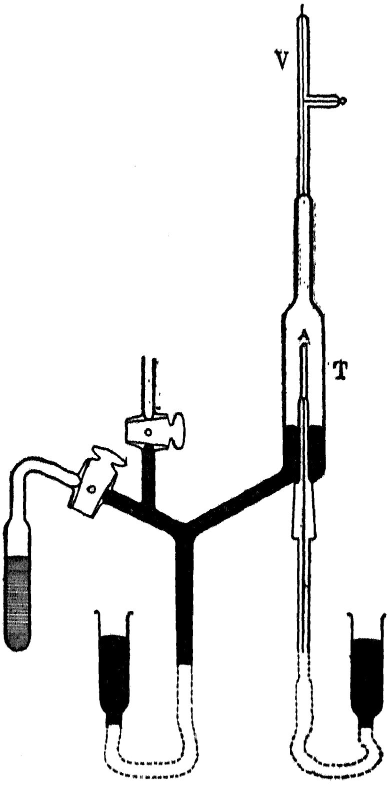

Fig. 12. Rutherford and Royd's Apparatus.

A is a thin glass tube less than ·02 mm. thick. It was surrounded by a wider tube T, which ends in the capillary V. Within A we have about 100 millicuries of radium emanation. T was evacuated. The α-particles of the emanation and other active deposits flow through the glass surface of A into the outer tube T, and stick to the surface of T. In process of time the α-particle diffuses into the volume of T, and can be collected in V for spectroscopic examination by raising the mercury. After two

---

*Rutherford and Royds, *Phil. Mag.* 17, 281, 1909.

days, the yellow line of helium D_3 was visible, and in a few days all the lines appeared strongly in the spectrum.

Blank experiments were performed to show that ordinary helium introduced in A could not diffuse through the glass walls.

It may be mentioned that the α-particle is not quite identical with the normal He-atom, but it is equivalent to the He-atom which has lost two electrons. We shall see later that it is identical with the *helium nucleus.*

70. Absorption of α-particles in their passage through matter—the Range of α-particles.—It has been already mentioned that α-rays from Ra are completely absorbed by a thickness of a few cms. of air. The thickness of Al required to stop completely α-rays of a definite velocity is much less, and in fact the thickness depends entirely on the nature of the absorbing medium. The earlier studies on the absorption are due to Rutherford and Mme Curie, but a thorough experimental and theoretical study of the absorption of α-rays by matter is due to Bragg and Kleeman (1904). Bragg explained the mechanism of the absorption process as follows :

The α-rays from a thin layer of radioactive substance are emitted with a definite velocity. But as they are allowed to traverse through matter, they gradually transfer their kinetic energy to the neighbouring molecules by collision with them, and are ultimately completely stopped. The energy thus lost is expended in producing ionisation in the medium. When the α-particle has lost most of its energy, it may capture one or two electrons and get neutralised. The ionisation, therefore, ceases completely beyond a certain distance from their source when the α-rays lose all their energy and probably get neutralised. This limiting distance is called the *Range of the α-particles.* Bragg arrived at this conclusion from an experimental study of the ionisation of an α-particle at different points of its track.

The method employed by Bragg for this investigation was quite simple. He took a thin pencil of homogeneous α-rays from a radioactive substance. Two parallel metal gauzes separated by a small distance were then placed at any point of the pencil of rays. By applying a suitable p. d. across the gauzes, and shifting the gauzes at different parts of the pencil along its length, the saturation current between them was measured. This gave directly the ionisation produced by the α-rays at different points of their track. The form of the ionisation curves for α-rays from Po and Ra C$'$ as obtained by

I. Curie by this method is shown in Fig. 13, in which distances from the source have been plotted as abscissæ and the corresponding ionisation observed as ordinates. It is seen that the ionisation at first increases with the distance along the track of the rays, it then reaches a maximum and then suddenly drops almost to zero. The distance corresponding to the zero ionisation gives the range of the α-particles. Thus for Po, the range is 3·84 cm. and for Ra C′, it is 7 cm. from the curves.

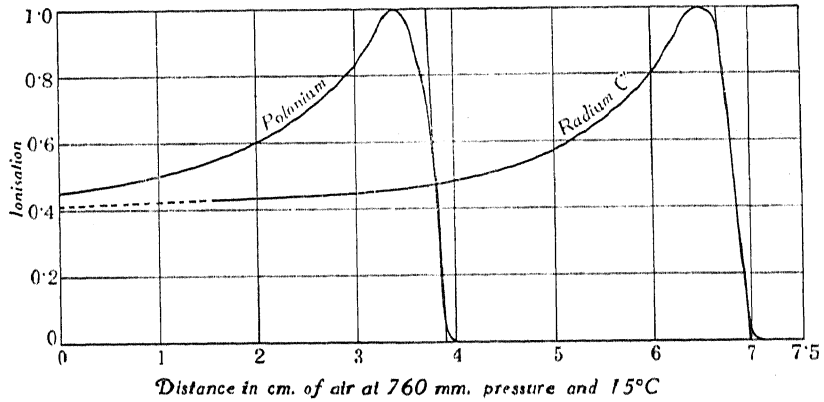

Fig. 13. Ionisation Curves for α-particles

It will be observed that the end of the ionisation curve where it approaches the abscissa terminates in a pronounced tail. This part of the curve has been more carefully investigated by Henderson,* Marsden and Perkins†, Feather and Nimmo‡ and others. It is now clear that the actual range of the particles should be determined by extrapolating the straight line part of the end curve and observing where it cuts the abscissa. The range thus obtained is known as the *extrapolated range*. The point where the tail cuts the x-axis determines the *maximum range* of α-rays. The tail actually represents a more complicated phenomenon known as *straggling*, and it is supposed to be due to α-rays behaving in a complicated way at the end of its track, though during the initial stages, the behaviour of all α-rays is identical.

It is to be noticed, that the picture of absorption presented above differs fundamentally from that of cathode-ray absorption where, on account of the lightness of the cathode rays, they are continually arrested in numbers at every point of the beam, and finally are completely stopped. In the case of α-rays, the phenomenon refers to each of the individual particles, the number of particles projected from the source proceeds undeviated each to the end of its range, and the cessation of ionisation is due to a gradual loss of energy of each particle.

---

* Henderson, *Phil. Mag.*, **42**, 538, 1921.

† Marsden and Perkins, *Phil. Mag.*, **27**, 690, 1914.

‡ Feather and Nimmo, *Proc. Camb. Phil. Soc.*, **24**, 139, 1928.

The range of α-particles depends strictly on the velocity with which they are projected from the source. The actual relation existing between the range R and velocity v was investigated by Geiger in 1910, who expressed it by the formula

$$v^3 = aR \quad . \quad . \quad . \quad . \quad . \quad . \quad . \quad . \quad . \quad . \quad (13)$$

where a=a constant. This formula was found to hold approximately over a wide range of velocities up to ·5 of the maximum velocity. Below this limit the photographic as well as the scintillation methods usually employed become insensitive and the observation is complicated by the effect of large angle scattering of α-rays, which will be discussed just now. Accepting Bragg's assumption that the ionisation produced in the passage of rays is proportional to their loss of energy, we have, since

$$v^2 \propto R^{\frac{2}{3}}$$

and $$E \propto R^{\frac{2}{3}}$$

therefore, $$\frac{dE}{dR} \propto R^{-\frac{1}{3}} \propto \frac{1}{v}$$

Thus the ionisation produced by an α-particle at any point in its track is inversely proportional to its velocity at the point. This gives also a method for the determination of total ionisation produced by α rays from their range.*

The range of α-particles can be reduced by placing a uniform screen of some material over the source. Thus α-rays from RaC have a range of 7·06 cm. of air at 20°C and 760 mm. pressure. Suppose the range is reduced to 5 cm. by inserting a uniform Al-screen over RaC of a few mm. thickness. The air equivalent of the range by which it is reduced (2·06 cm. in the present case) is called the *stopping power* of

---

* For recent works on this subject see H. Ziegert, *Zs. f. Phys.*, **46**, 668, 1928.

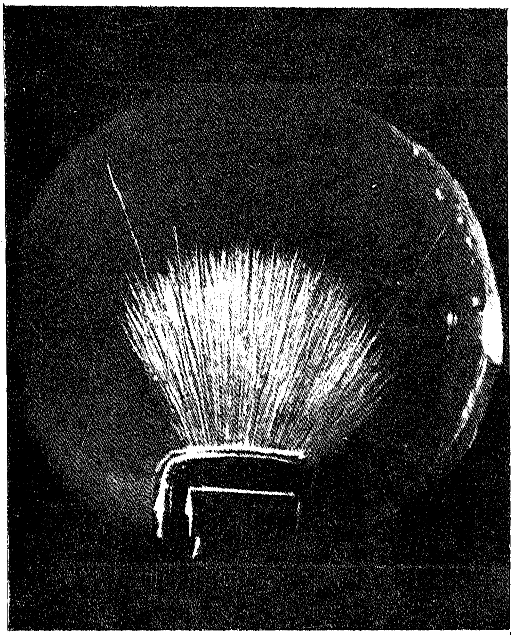

Fig. 15. Tracks of α-particles from ThC+C′ showing particles of ranges 8·6 cm., 9·5 cm., and 11·5 cm.

(p. 143)

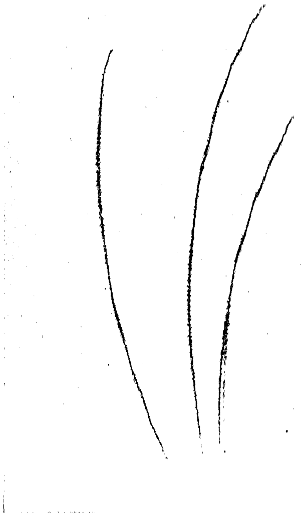

Fig. 8. The curved tracks of α-particles in strong magnetic field (*Kapitza*).

(p. 134)

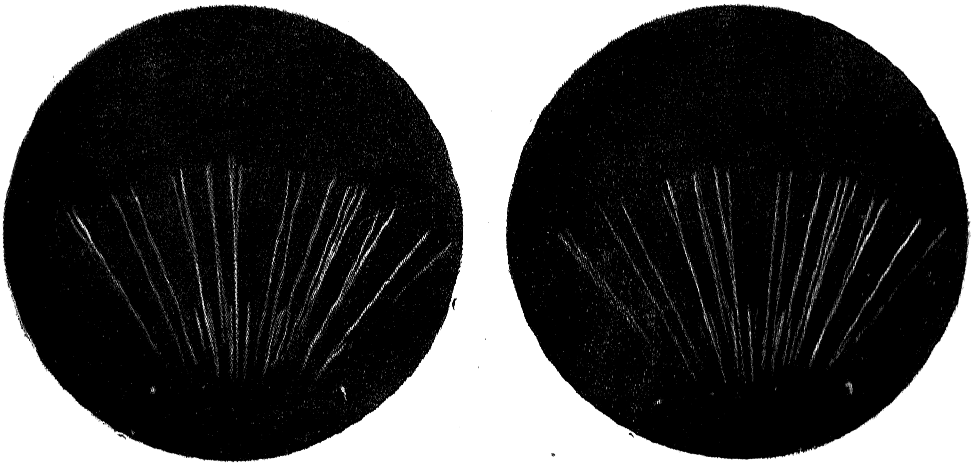

(a) (b)

Fig. 14. Tracks of α-particles from ThC+C′, showing particles of ranges 4·8 and 8·6 cms.

(p. 143)

the material (Al), and it depends upon the thickness of the screen and atomic weight of its material.

71. Direct Determination of the Range.—The soundness of these views regarding the passage of α-rays through air is very beautifully illustrated in C. T. R. Wilson's method of actually rendering the path of individual rays visible (I, §12). Some of the photographs of the α-ray tracks in air are shown in Plate II, Figs. 14 (*a*), (*b*) and (15). These are for α-rays from ThC and have been taken from the original papers of Meitner and her co-workers. It will be seen that the tracks terminate abruptly beyond a certain distance, which clearly shows the ranges of the particles.

It has already been explained (§61) that ThC undergoes a dual disintegration of (α, β) type according to the scheme

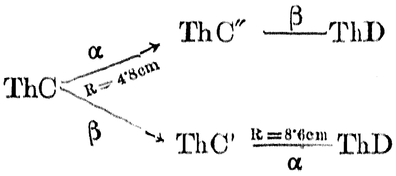

The α-ray from ThC itself has a range of 4·8 cm. The β-ray product ThC′ also emits an α-ray having the range 8·6 cm. Fig. 14 (*a*), (*b*) is a stereoscopic Wilson cloud-chamber photograph of α-ray tracks from ThC obtained by Meitner and Freitag. It clearly shows two groups of tracks corresponding to the α-rays of the two types. Besides these, Rutherford and Wood* and later Meitner and Freitag† have observed another rare group of α-rays from ThC+C′ having the range 11·5 cm. The latter‡ have detected also a new group of α-rays of range 9·5 cms. The number of both of these groups of long range α-particles is extremely small as is apparent from the disintegration hypothesis. In fact Meitner has estimated that out of 10^6 α-particles from ThC+C′, about 200 particles have a range of 11·5 cm. and only 70 have the range 9·5 cm. Fig. 15 represents these rare phenomena as observed by the cloud-chamber method§. The two very long tracks on the extreme left and right are of 11·5 cms. range, and the shorter one is of 9·5 cms. range.

---

* E. Rutherford and A. B. Wood, *Phil. Mag.* (6), **31**, 379, 1916.
† Meitner and Freitag, *Zs. f. Phys.*, **37**, 481, 1926.
‡ Meitner and Freitag, *loc. cit.*
§ Meitner, *Naturwiss.*, **12**, 634, 1924.

Similarly long range α-rays have also been detected from RaC*. The origin of these rays has been a subject of much discussions which throw light on the problem of nuclear structure. It will be discussed fully in the chapter on *Nuclear Physics.*

Quantitative measurements of the range of α-particles have also been made from these photographs. The results obtained are in good agreement with those of other methods.

72. Other Methods for the Determination of the Range.—

Besides the ionisation method and cloud-chamber method, the scintillation method has also been sometimes employed for the determination of range. The method is practically the same as that of counting α-particles by the spinthariscope (§50), only the distance of the screen is made variable. This method however becomes unworkable when a very weak source of α-particles is available.

GEIGER AND NUTTALL'S METHOD.

For such cases a method originally employed by Geiger and Nuttall† is useful. This is illustrated in Fig. 16. A spherical glass bulb A is coated inside with silver. The active substance in the form of a thin film is deposited at B the centre of the bulb, at one end of a metal rod R. On applying a high potential between A and B. the ionisation current between them for any pressure inside the bulb can be noted by an electroscope. Observations are made at different pressures of air in the bulb. The result obtained is shown by means of the curves in Fig. 17, in which the pressures are plotted along the x-axis and the corresponding ionisations along the y-axis. It will be seen that the curves take a sharp turn at one point, after which they are parallel to the x-axis. At low pressures, the ionisation increases directly as the pressure. But for a certain critical pressure the ionisation is maximum and does not change with further increase of pressure. At this critical pressure, the α-particles just stop at the side of the bulb, so that they have produced the maximum ionisation possible before actually touching the sides of the bulb. The radius of the bulb then gives the range at the

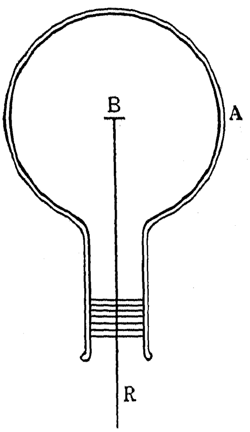

Fig. 16. Geiger and Nuttall's apparatus

---

* Philipp, *Zs. f. Phys.* 52, 759, 1929.

† Geiger and Nuttall, *Phil. Mag.,* 22, 613, 1911; 23, 445, 1912.

critical pressure. Since the range is inversely proportional to pressure,

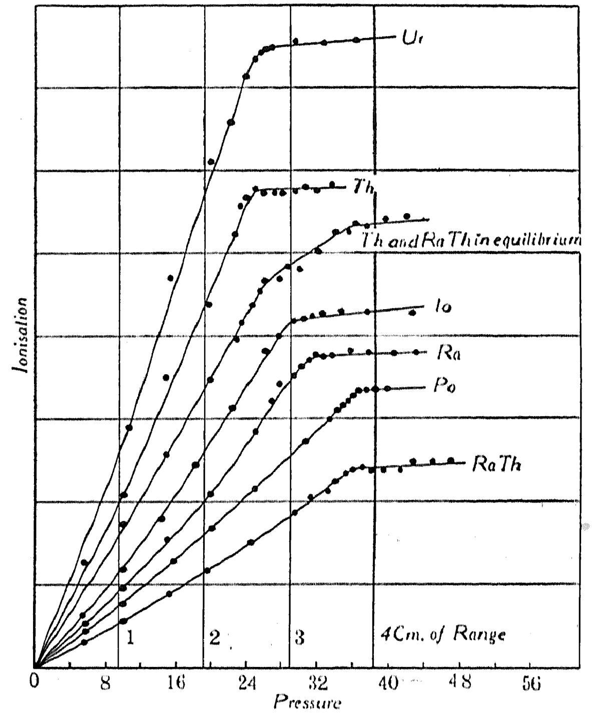

Fig. 17.

the range at N. T. P. can also be deduced from that at the critical pressure.

GEIGER'S METHOD.

This original method of Geiger and Nuttall (1912) has been modified by Geiger* (1921) so as to obtain greater accuracy in the determination of the range. The principle of the method can be understood from Fig. 18.

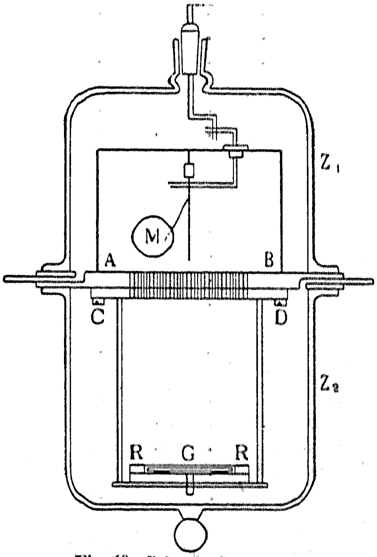

Fig. 18. Geiger's Apparatus.

R, R...is the plate on which the active matter is deposited. The latter is wrapped up in a thin film of mica so as to prevent the escape of any active gas from it.

Z_2 ...is the lower chamber.

Z_1 ...is the upper chamber which encloses an electroscope M.

AB ...is the metal plate which separates Z_1 from Z_2. It is perforated at right angles to its plane by boring about 500 holes each 15 mm. long and 3 mm. in diameter.

---

* Geiger, *Zs. f. Phys.*, **8**, 45, 1921.

CD ...is the lower face of AB. It is covered by means of a thin sheet of mica so that Z_1 and Z_2 can be separately exhausted.

A pressure of about 3 to 6 mm. is maintained in Z_1. α-rays from the source pass through the holes and ionise the gas in Z_1, the amount of ionisation being recorded by the electroscope. The ionisation in Z_1 is observed for different pressures in Z_2.

At very low pressures, the α-particles lose very little energy in passing from the source to AB, hence the main part of their tracks lies in Z_1 where they produce very strong ionisation. On increasing the pressure in Z_2, the residual track of α-rays, as well as the ionisation in Z_1 gradually diminishes. So by this means the end part of the ionisation curve (Fig. 13) can be very accurately studied. At a critical pressure of air in Z_2, the α-particles are just stopped at AB, so that the ionisation produced in Z_1 is almost zero. The distance between AB and RR gives the range of the α-particles at this pressure.

Table 5.—Range of α-particles.

Radioactive element	Range in cm. at 15°C R	Velocity in cm. per sec. $v = a\sqrt[3]{R}$.	Velocity in cm./sec. calculated by Briggs.	Energy in electron-volts.
Uranium I	2·73	1·401 × 10^9	1·391 × 10^9	4·049 × 10^6
Uranium II	3·28	1·495	1·492	4·626
Ionium	3·194	1·479	1·479	4·545
Radium	3·389	1·511	1·511	4·744
Radon	4·122	1·618	1·618	5·441
Radium A	4·722	1·695	1·695	5·972
Radium C′	6·971	1·922	1·922	7·683
Radium F	3·925	1·590	1·590	5·253
Protactinium . .	3·673	1·552	1·553	5·013
Radioactinium . .	4·676	1·683	1·688	5·923
Actinium X	4·369	1·645	1·650	5·659
Actinon	5·789	1·807	1·810	6·819
Actinium A	6·584	1·886	1·887	7·405
Actinium C	5·511	1·777	1·783	6·610
Thorium	2·90	1·435	1·437	4·231
Radiothorium	4·019	1·600	1·604	5·347
Thorium X	4·354	1·643	1·648	5·645
Thoron	5·063	1·728	1·733	6·244
Thorium A	5·683	1·796	1·800	6·737
Thorium C	4·787	1·696	1·701	6·015
Thorium C′	8·617	2·063	2·052	8·761

By using this method Geiger has determined and re-examined the range of α-particles from many elements of the radioactive series. A full list of his determinations is given in Table 5. The method failed only in the cases of UI and UII which are very weak sources of α-rays.

The range of α-particles from UI and UII have recently been determined by Laurence* by using Blackett's cloud-chamber method with minor modifications. The results of the determination of Geiger, Laurence and others have been compiled in Table 5. It gives the ranges for all the radioactive elements belonging to the three series. The ranges observed are given in column 2. The velocity of α-rays calculated by using the Geiger formula (3) is shown in column 3. The velocities directly determined by Briggs† for the α-rays of known *E*/*M* from different substances are also given in column 4 for comparison. Column 5 gives the energies of α-rays calculated from formula (1, 9) expressed in electron-volts.

73. Relation between Velocity of Emission of α-rays and Life of Radioactive Atoms.—It was early observed that there seemed to exist some intimate relationship between the velocity with which α-particles are expelled in a radioactive disintegration, and the life of the atom which by its disintegration emits the α-rays. Thus Radium C′, which is an extremely shortlived product, emits α-rays of high velocity (and therefore of large range *viz.*, 6·97 cm.) while U which is an extremely longlived product emits α-rays of much smaller velocity (the range =2·73cm). The data regarding the range of α-particles, and λ, the radioactive disintegration constant, were first collected by Geiger and Nuttall‡, and *log* λ was plotted against *log R* (*vide* Fig. 19). It was found that the products belonging to any

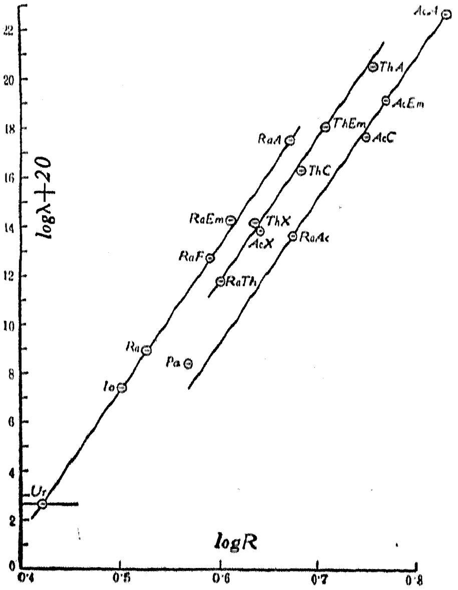

Fig. 19. Relation between the range and disintegration constant for α-rays.

---

* Laurence, *Phil. Mag.*, **5**, 1027, 1928.
† Briggs, *Proc. Roy. Soc.*, A, **118**, 549, 1928.
‡ Geiger and Nuttall, *Phil. Mag.*, 22, 613, 1911; **23**, 439, 1912.
Geiger, *Zs. f. Phys.* **8**, 45, 1921.

radioactive series very nearly fell on one straight line. Swinne* has shown that the relation can be approximately expressed by a formula of the type

$$log\,\lambda = a + b\,E \quad . \; . \; . \; . \; . \; . \; . \; . \; . \quad (14)$$

where E=energy of the α-particle.

The relation is however only approximately true. Applying the formula Jacobsen and Barton found that RaC′ should have a life of order 10^{-8} sec., while the actual life was experimentally found to be of the order 10^{-6} sec.

In recent years, the Geiger-Nuttall relationship has been made the starting point of very interesting speculations regarding the origin of radioactive transformations from a wave-mechanical point of view. This subject will be taken up in the chapter on *Nuclear Physics.*

74. Path of a Particle Under a Central Force.—Article 75 dealing with the large angle scattering of α-particles will not be intelligible to the general student unless he has a clear knowledge of the path of a particle moving under a central force. The student can obtain this knowledge by consulting any book on dynamics, but for the sake of ready reference, the whole theory is worked out in these notes.

Let '*m*' denote the mass of the particle and r, θ (Fig. 20) denote its polar coordinates. The equations of motion are given by :—

$$\left.\begin{aligned} m\,(\ddot{r} - r\dot{\theta}^2) &= F \\ \frac{m}{r}\,\frac{d}{dt}\,(r^2\dot{\theta}) &= 0 \end{aligned}\right\} \quad . \; . \; . \; . \; . \; . \; . \; . \; . \quad (15)$$

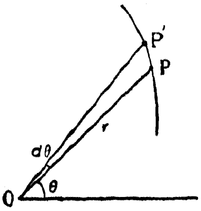

Fig. 20.

The terms on the left hand side represent mass × radial and cross-radial accelerations. The second terms are put equal to zero, because the force is central. We have therefore

$$r^2\dot{\theta} = \text{constant} = A. \quad . \; . \; . \; . \; . \; . \; . \; . \quad (16)$$

This is Kepler's second law of planetary motion.

To find out the form of the orbit, we should eliminate t from (15) with the aid of (16). We have

$$\frac{d\theta}{dt} = \frac{A}{r^2} = Au^2, \text{ where } u = \frac{1}{r} \quad . \; . \; . \; . \; . \; . \; . \quad (16')$$

With the aid of this relation, it can be proved that

$$\frac{dr}{dt} = -A\,\frac{du}{d\theta}, \qquad \ddot{r} = -A^2u^2\,\frac{d^2u}{d\theta^2}$$

---

* Swinne, *Phys. Zs.,* **13**, 14, 1912.

and $$-r\dot{\theta}^2 = -A^2u^3$$

$$v^2 = \left(\frac{dr}{dt}\right)^2 + r\left(\frac{d\theta}{dt}\right)^2 = A^2\left[\left(\frac{du}{d\theta}\right)^2 + u^2\right] \quad . \quad . \quad . \quad (17)$$

Again $A = pv$, where p=perpendicular distance from the origin on the direction of projection. We have

$$\frac{1}{p^2} = \frac{v^2}{A^2} = \left[\left(\frac{du}{d\theta}\right)^2 + u^2\right] \quad . \quad . \quad . \quad . \quad . \quad . \quad . \quad . \quad . \quad (18)$$

Substituting these expressions in (15), we obtain

$$\frac{d^2u}{d\theta^2} + u = -\frac{F}{mA^2u^2} \quad . \quad . \quad . \quad . \quad . \quad . \quad . \quad . \quad . \quad . \quad (19)$$

Now when the force varies inversely as the square of the distance we can put

$$F = \mu\, mu^2$$

where μ=force per unit mass. It is positive when the force is repulsive, negative when it is attractive.

The equation can then be written as

$$\frac{d^2u}{d\theta^2} + u = -\frac{\mu}{A^2} \ldots \text{(Force repulsive)} \quad . \quad . \quad . \quad . \quad (19A)$$

$$= \frac{\mu}{A^2} \ldots \text{(Force attractive)} \quad . \quad . \quad . \quad . \quad (19B)$$

We shall first take the case of attractive forces. We have then, multiplying (19B), by du and integrating

$$\left(\frac{du}{d\theta}\right)^2 + u^2 = \frac{2\mu u}{A^2} + B \quad . \quad . \quad . \quad . \quad . \quad . \quad . \quad . \quad . \quad . \quad (20)$$

or from (17),

$$v^2 = 2\mu u + BA^2$$

or $$\tfrac{1}{2}mv^2 - \frac{\mu m}{r} = \tfrac{1}{2}BmA^2 \quad . \quad . \quad . \quad . \quad . \quad . \quad . \quad . \quad . \quad . \quad (21)$$

This is the law of conservation of energy, for $\frac{1}{2}mv^2$ is the kinetic energy at any point, and $-\mu\, mu = -\mu m/r$ is the potential energy at the distance r. The theorem merely states that the sum of the potential and kinetic energies remains constant during motion.

Now to find out the orbit, we can write equation (20) in the form :—

$$\left(\frac{du}{d\theta}\right)^2 = B + \frac{2\mu u}{A^2} - u^2$$

$$d\theta = \frac{du}{\sqrt{B + \dfrac{2\mu u}{A^2} - u^2}}$$

$$= \frac{du}{\sqrt{\left(B + \dfrac{\mu^2}{A^4}\right) - \left(u - \dfrac{\mu}{A^2}\right)^2}}$$

Integrating, we obtain

$$\theta = \cos^{-1}\left(u - \frac{\mu}{A^2}\right) \Big/ \sqrt{B + \frac{\mu^2}{A^4}} + const.$$

or

$$u - \frac{\mu}{A^2} = \sqrt{B + \mu^2/A^2}\,.\ \cos(\theta + \alpha) \quad . \quad . \quad . \quad (22)$$

The equation to a conic section is of the form

$$u = \frac{1 + e\cos\theta}{l} \quad . \quad . \quad . \quad . \quad . \quad . \quad . \quad . \quad (23)$$

when referred to its focus.

Hence comparing we find that the orbit is a conic section with the following characteristics :—

$$\frac{1}{l} = \frac{\mu}{A^2}, \quad or\ A^2 = \mu l$$

and

$$e = l\sqrt{B + \frac{1}{l^2}}\ or\ Bl^2 = e^2 - 1, \quad B = \frac{e^2 - 1}{l^2} = \pm\frac{1}{la}$$

where the plus sign refers to a hyperbola, the minus sign to an ellipse. $\alpha = \infty$ denotes a parabola. We have

$$B = \pm\frac{1}{la}$$

The equation of conservation of energy therefore becomes

$$v^2 - 2\,\mu u = \pm\frac{\mu}{a}$$

or

$$v^2 = \mu\left(\frac{2}{r} \pm \frac{1}{a}\right) \quad . \quad . \quad . \quad . \quad . \quad . \quad . \quad . \quad . \quad (24)$$

Hence the orbit is ellipse, parabola or hyperbola according as

$$v^2 \lesseqgtr \frac{2\mu}{r}$$

Thus from the initial velocity of projection and initial distance, we obtain a. The latus rectum is given by $A^2 = \mu l$. Thus the orbit is completely defined.

REPULSIVE FORCE.

In this case, the equation of motion is

$$\frac{d^2u}{d\theta^2} + u = -\frac{\mu}{A^2}$$

The equation (20) now takes the form

$$\left(\frac{du}{d\theta}\right)^2 = B - \frac{2\,\mu u}{A^2} - u^2$$

$$d\theta = \frac{du}{\sqrt{\left(B + \frac{\mu^2}{A^4}\right) - \left(u - \frac{\mu}{A^2}\right)^2}}$$

or integrating

$$u = -\frac{\mu}{A^2}\left[1 - \frac{\sqrt{B+\mu^2/A^4}}{\mu/A^2}\cos(\theta + \alpha)\right]$$

or $$u = \frac{1}{l}\Big[e\cos(\theta + \alpha) - 1\Big] \quad . \; . \; . \; . \; . \; . \; . \; . \; . \; . \; . \quad (25)$$

where $l = \frac{\mu}{A^2}$, $Bl^2 = e^2 - 1$ as before, or $B = \frac{1}{la}$

The equation of energy is now

$$v^2 = -2\mu u + BA^2$$

or $$\tfrac{1}{2}mv^2 + \frac{\mu m}{r} = \tfrac{1}{2}BmA^2 = \frac{1}{2}\frac{\mu m}{a} \quad . \; . \; . \; . \quad (26)$$

Equation (25) represents the branch of a hyperbola with the centre of force as the outer focus. For

$$e\cos\theta - 1 > 0, \quad e > 1 \text{ and } \cos\theta > \frac{1}{e}$$

or $$\theta \text{ lies between } \quad \pm\cos^{-1}\left(\frac{1}{e}\right).$$

The constants of the hyperbola can be easily determined. Let V be the velocity at infinity, *i.e.*, when $r = \infty$. Then from (26), we have

$$\tfrac{1}{2}mV^2 = \frac{1}{2}\mu\frac{m}{a}$$

therefore, $$a = \frac{\mu}{V^2}$$

It is therefore clear that if a particle P is projected (Fig. 21) with the velocity V from infinity towards a centre of repulsion S, along the line PO, then it will describe the hyperbola PAP′ to which PO is an asymptote, it will curve round and pass on to the other asymptote OP′.

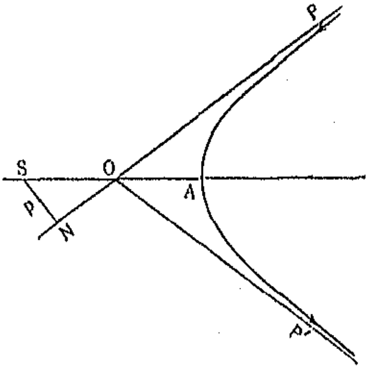

Fig. 21.

The constants of the hyperbola are

a = semi-transverse axis = μ/V^2
b = semi-conjugate axis = SN

and the angle of deflexion $\varphi = \pi - 2\theta$ as the particle is deflected from the line PO to OP′.

Hence we have

$$\tan\frac{\varphi}{2} = \frac{a}{b}$$

$$\varphi = 2\tan^{-1}\frac{a}{b} = 2\tan^{-1}\frac{\mu}{bV^2}$$

The distance of nearest approach

$$SA = a\,(1 + \sec\theta) = 2b\,\frac{1 + \tan\varphi/4}{1 - \tan\varphi/4} \quad . \quad . \quad . \quad . \quad . \qquad (27)$$

Equation (27) makes it clear that for a definite particle velocity and a given field of force, the distance of nearest approach is a function of φ or θ only. For example, when

$$\theta = 0, \quad \varphi = \pi, \quad SA = 2a$$
$$\theta = \pi/4, \quad \varphi = \pi/2, \quad SA = 2{\cdot}41a$$

Thus as θ changes from 0 to $\pi/2$, φ varies from π to 0, and the distance of nearest approach is minimum (equal to $2a$) when $\varphi = \pi$, that is, the collision is end-on.

We shall now consider the application of these theorems to the problem in hand.

75. Scattering of α-Rays—The Structure of the Atom.—

The α-particle is a concentrated particle of electrified mass possessing for its size enormous energy, and it was early expected that much information regarding the internal structure of atoms would be afforded if they were bombarded by α-particles, and the results could be properly interpreted. This hope was fulfilled beyond the limits of expectation.

It was early observed that as a straight pencil of α-rays is passed through matter, it becomes more and more diffuse. Thus Rutherford found that if particles through a narrow slit were received on a photographic plate through an evacuated vessel, the image of the slit was sharply defined. If, however, the vessel were filled with air, or if thin sheets of metal were placed in the way, the image became diffuse. The diffusivity increased with the increasing thickness of the obstacle and with increasing atomic weight. This phenomenon is known as *scattering.*

A general explanation of scattering was given by J. J. Thomson, and gave rise to the first speculations regarding the structure of atoms out of positive and negative electricity. The scattering is certainly due to the fact that α-particles are deviated from their straight course as they pass through matter. As the particles are charged, the deviation must be due to some electrical field. The atom as a whole is neutral, and therefore as long as an α-particle passes at a sufficient distance from the atom, its course should remain straight. But the case will be otherwise if some of the α-particles are to pass through the inside of atoms, as some of them are sure to do. Thomson supposed that the atom consisted of a positive core having about half or one-third the radius ascribed to the atom. All the positive electricity was supposed to be spread over this sphere, and the negative electricity in the form of electrons was supposed to be describing orbits about this. The electrical field inside such an atom, at a distance r, would be equal to Ze/r^2 due to the positive charge, minus the field due to the electrons. As the electrons must be more or less uniformly distributed, their fields would largely cancel each other, or amount to only a small fraction of the field due to the positive core. As the α-particle passes at a distance r from the centre of the core, it would be subjected to this repulsive force, and deflected from its straight path. In this way, Thomson could account for small angle scattering of α-rays. In some cases, the deflexion may be large owing to successive scattering by a number of atoms, but the chances of such scattering is limited to only a small fraction of α-particles.

But according to this model the deflecting field can never be larger than $2Ze/b^2$, where b is the radius of the positive core of electrification hence the scattering can never exceed a certain maximum value which, as calculation shows cannot be larger than 2° to 3° in the case of heavy atoms, if we suppose that 'b' is comparable with the radius of the atom. But Geiger and Marsden made the very striking observation that the angle of scattering can, in a small number of cases, be as great as 90° or even higher. They used for this purpose the scintillation method of observing particles in which even individual particles can be detected. The number of such particles is extremely small, *viz.*, 1 in about 10000 (using a platinum radiator), but even this small number is decisive. The large deflexions tell us that b must be much less than half or one-third a, in fact according to Rutherford, it should be 10^{-4} to 10^{-5} times the radius ascribed to atoms. The positive electricity is thus regarded as concentrated in a very small volume having a radius of the order of 10^{-12} cm. and the electrons are supposed to revolve round the nucleus. The picture is analogous to that of the solar system; the nucleus may be compared to the sun which occupies the centre of the system. The electrons may be compared to the planets describing orbits, the only difference being that they have all equivalent mass and charge. This planetary theory of the atom was suggested by Nagaoka in 1904, but to Rutherford and his coworkers belong the credit of establishing it on sure experimental foundation.

For a proper understanding of the works of Rutherford, the student must take the trouble of understanding the theory of planetary orbits of which an account has been given in the previous section.

76. Mathematical Theory of Large Angle Scattering.—We may now suppose that the nucleus of positive electricity is represented by S in Fig. 21, and the α-particle is projected from infinity along the direction PO. The perpendicular distance SN = b, may then vary from a certain minimum value, *viz.*, the radius of the nucleus to x. 10^{-8} cm, which is the diameter of the atom. The repulsive force is $2Ze^2/r^2$ where $+Ze$ is the positive charge on the nucleus. The electrons are distributed in layers about the nucleus, and they will attract the α-particle, but as they are distributed symmetrically, we may suppose that these forces largely cancel each other. Then the α-particle will be deflected along PAP′, *i.e.*, from the branch PO it will be deflected to OP′. Applying the results of §74, we obtain

$$\mu = \frac{2Ze^2}{m_a}, \quad a = \frac{2Ze^2}{m_a u^2}$$

where m_a = mass of the α-particle, u its velocity of projection.

The angle of deflection

$$\varphi = 2 \tan^{-1} \frac{2Ze^2}{m_a u^2 b} \quad . \quad . \quad . \quad . \quad . \quad (28)$$

The distance of nearest approach is

$$d = 2b \, \frac{1+\tan \varphi/4}{1-\tan \varphi/4} = \frac{2Ze^2}{m_a u^2} (1+\operatorname{cosec} \varphi/2) \; . \quad . \quad (29)$$

This is minimum for end-on collision and is equal to $4Ze^2/m_a u^2$.

The expressions show that the particles having the smallest value of b are most deflected. The upper limit of deflection is given by the smallest value of b, and this can be identified with the radius of the nucleus. Conversely, if we have some data regarding the largest deflection, and the values of Z, m_a and u, we can form an estimate of the value of the upper limit to the value of b.

In an experiment on large angle scattering with Pt, the data were as follows :

$$\frac{2e}{m_a} = 4800 \times 3 \times 10^{10} \text{ e. s. units}$$

$u = 2 \times 10^9$ cm/sec, for α-particles from RaC.

$e = 4{\cdot}77 \times 10^{-10}$ e. s. units

Rutherford assumed in his first researches that $Z=100$ for Pt. Then we obtain

$$\varphi=2\tan^{-1}\frac{1{\cdot}73\times10^{-12}}{b}$$

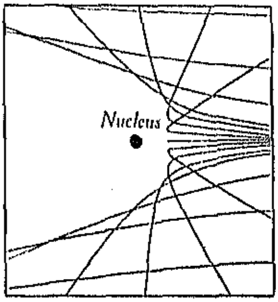

Fig. 22. Paths of the deflected α-particles.

Hence φ cannot have a large value unless b is of the order of $1{\cdot}73\times10^{-12}$. Then the distance of nearest approach

$$d=\frac{2Ze^2}{m_a u^2}\,(1+\operatorname{cosec}\varphi/2)$$

$$=1{\cdot}73\times10^{-12}\,(1+\operatorname{cosec}\varphi/2)$$

An idea of the ideal scattering for different distances of approach will be found in the accompanying diagram (Fig 22).

Thus the radius of the nucleus comes out to be about 10^{-5} times the atomic radius (10^{-8} cm.)

77. Experimental Verification of the Nuclear Theory.—

Though relation (28) can be used for a rough verification of the nuclear theory, Rutherford and his coworkers planned a number of well-thought out experiments for its complete test. These experiments are described in the following section. We give here a brief outline of the mathematical work underlying these experiments.

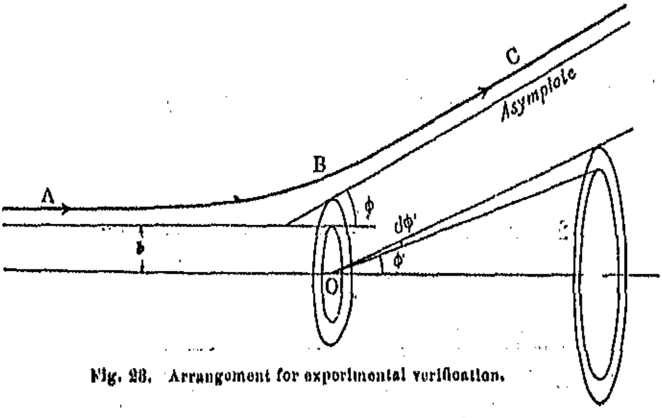

Fig. 23. Arrangement for experimental verification.

Let O be the scattering nucleus (Fig. 23), ABC the path of the α-particle, b the distance of the nucleus from its initial line of motion; and ϕ the angle through which the α-particle is deflected by the field of the nucleus.

For a homogeneous beam of α-rays and a foil of the given scattering metal, φ is a function of b only; in other words, the α-particle, the distance of the initial line of motion of which from the nucleus is b, will be deflected through an angle φ, and the α-particle whose distance is $b+db$ will be deflected through an angle $\varphi+d\varphi$, so that the α-particles whose b's lie between b and $b+db$, will be deflected through an angle lying between φ and $\varphi+d\varphi$.

If the scattering foil has the thickness t, and contains n atoms per unit volume, the probability of an α-particle being aimed so as to pass some nucleus at a distance between b and $b+db$, is $2\pi bdbnt$, since a unit area of the foil contains nt atomic targets. This particle will naturally be deflected through an angle lying between φ and $\varphi+d\varphi$.

Now, suppose for a moment that a unit sphere is described with O as centre. The particles deflected through angles lying between φ and $\varphi+d\varphi$ fall on an area $2\pi \sin\varphi\, d\varphi$ of the sphere. This is equal to $4\pi \sin\frac{\varphi}{2}\cdot\cos\frac{\varphi}{2}\cdot d\varphi$. The chance of a particle falling on unit area of this region will be evidently

$$\frac{2\pi nt\,bdb}{4\pi \sin\frac{\varphi}{2}\cdot \cos\frac{\varphi}{2}\cdot d\varphi}.$$

Now $$\tan\frac{\varphi}{2}=\frac{2Ze^2}{m_\alpha u^2}\cdot\frac{1}{b}$$

or $$db=\frac{2Ze^2}{m_\alpha u^2}\cdot\tfrac{1}{2}\operatorname{cosec}^2\frac{\varphi}{2}\cdot d\varphi$$

or $$2\pi\, nt\, bdb=\pi nt\left[\frac{2Ze^2}{m_\alpha u^2}\right]^2\cdot\frac{\cos\frac{\varphi}{2}}{\sin^3\frac{\varphi}{2}}\cdot d\varphi$$

Hence $$\frac{2\pi\, nt\, b\, db}{4\pi \sin\frac{\varphi}{2}\cos\frac{\varphi}{2}d\varphi}=\left[\frac{2Ze^2}{m_\alpha u^2}\right]^2\frac{nt}{4\sin^4\frac{\varphi}{2}}.$$

The mathematical working of the theory is due to Rutherford (*Phil. Mag.*, **21**, 669, 1911).

If, therefore, a small screen of area A is set up at a distance r from O, so as to receive particles at an angle φ, the number received per second is

$$\left[\frac{2Ze^2}{m_a u^2}\right]^2 \frac{AQnt}{4r^2 \sin^4\frac{\varphi}{2}}, \quad . \quad . \quad . \quad . \qquad (30)$$

where Q is the number of particles falling on the scattering foil per second.

On this theory then, it is to be expected, that the number of particles scattered through an angle φ should be proportional to

(1) $\operatorname{cosec}^4 \frac{\varphi}{2}$

(2) thickness of scattering foil, *i.e.*, nt

(3) central charge $(Ze)^2$.

(4) $\frac{1}{[m_a u^2]^2}$.

78. Description of the Experiments.—These conclusions were verified by Geiger and Marsden* in an elegant series of experiments carried out with the aid of the following apparatus.

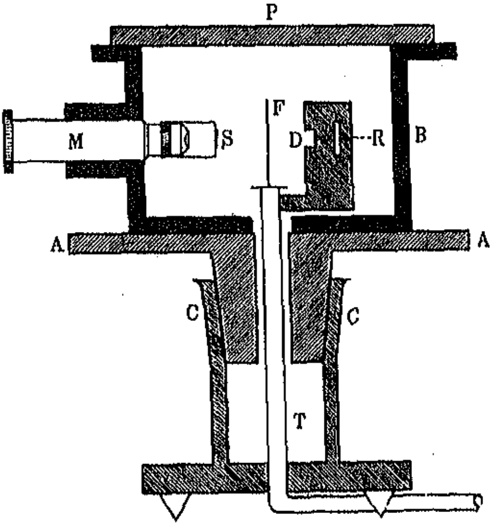

Fig. 24. Geiger and Marsden's apparatus.

B . . . a cylindrical metal box. This contains the following.

R . . . the source of α-particles, which is a tube filled with radon.

F . . . the scattering foil mounted on a tube T which is kept fixed. The apparatus can be evacuated through T.

S . . . zinc sulphide screen fixed to M, on which α-particles impinge and produce scintillations.

M . . . microscope for viewing the scintillations.

---

* Geiger and Marsden, *Phil. Mag.*, 25, 604, 1913.

A . . . a graduated circular platform fixed to B.

C . . . an air-tight joint on which AB can be rotated, while FR remains fixed.

P . . . ground glass plate closing B.

By rotating A, S is placed at different angles to the primary direction of the beam of α-particles. Observations were taken between 5° and 150°.

Foil of any thickness and material could be placed in place of F. Gold, silver and platinum were used.

The results of the experiment are shown in Table 6.

Table 6.—Variation of Scattering with angle.

Angle of Scattering φ	$\text{Cosec}^4 \frac{\varphi}{2}$	SILVER		GOLD	
		Number of Scintillations *N*	$\frac{N}{\text{Cosec}^4 \frac{\varphi}{2}}$	Number of Scintillations *N*	$\frac{N}{\text{Cosec}^4 \frac{\varphi}{2}}$
150°	1·15	22·2	19·3	33·1	28·8
135	1·38	27·4	19·8	43·0	31·2
120	1·79	33·0	18·4	51·9	29·0
105	2·53	47·3	18·7	69·5	27·5
75	7·25	136	18·8	211	29·1
60	16·0	320	20·0	477	29·8
45	46·6	989	21·2	1435	30·8
37·5	93·7	1760	18·8	3300	35·3
30	223	5260	23·6	7800	35·0
22·5	690	20300	29·4	27300	39·6
15	3445	105400	30·6	132000	38·4
30	223	5·3	0·024	3·1	0·014
22·5	690	16·6	0·024	8·4	0·012
15	3445	93·0	0·027	48·2	0·014
10	17330	508	0·029	200	0·0115
7·5	54650	1710	0·031	607	0·011
5	276300	...	...	3320	0·012

The second conclusion regarding the variation of scattering with the thickness of the scattering foil was then tested by Geiger and Marsden.* In this case a homogeneous source of α-rays was essential. For this they used Ra B and Ra C. The apparatus employed is shown in Fig. 25.

---

* Geiger and Marsden, *loc. cit.*

A . . . a brass-ring closed by two glassplates B, C.
R . . . source of α-rays (Ra B & C).
O . . . opening for the entrance of α-rays. It is closed by a thin sheet of mica.
D . . . diaphragm.
S . . disc carrying the scattering foil F. It can be rotated about its axis, so as to expose foils of different thickness to the path of α-rays.
Z . . . ZnS screen placed at a fixed angle to the incident beam.

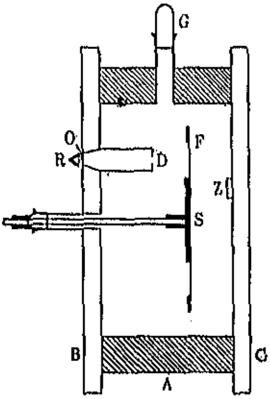

Fig. 25. Variation of Scattering with atomic weight.

The apparatus was evacuated. The number of scintillations per second was counted after placing the ZnS screen at an angle of about 25° to the direction of the incident beam. Observations with different meterials showed that the number of α-particles scattered was proportional to the thickness of the foil, as long as it was not so thick as to reduce substantially the velocity of α-rays on passing through it.

The variation in the amount of scattering with change of velocity of the α-rays was also examined with the same apparatus. To reduce the velocity, absorbing screens of different thickness was inserted between the source and the opening O. The Geiger relation $v^3 = aR$ was employed to calculate the velocity, from the observation of range. The number of α-particles scattered per second was found to vary inversely as the fourth power of the velocity.

79. Chadwick's Measurement of Nuclear Charge.—For all the above experiments relative measurements were quite sufficient. But for finding out Z, the nuclear charge, it is necessary to make absolute measurements, *i.e.*, taking any element, the number of α-particles scattered on a definite surface through a known angle has to be counted, and compared with the total number of α-particle emitted directly from the source (*vide* equation 30). This was done by Geiger and Marsden (*loc. cit.*) using thin foils of Au, Sn, Ag, Cu, Al, C. The number of α-particles Q emitted was obtained by measuring the γ-ray activity of the source. The other quantity n was obtained as described above, and then (30), gave the value of Z. It was found to be about ½ the atomic weight.

All this was done before the nuclear theory was firmly established.

In 1912, Bohr utilised the nuclear theory to explain the spectrum of hydrogen in particular (*vide* Chap. VII) and of the other elements in general. Since this time, the soundness of the nuclear theory of the structure of the atom has been so thoroughly established, as a result of many converging lines of evidence, that it is now regarded as the cornerstone of new physics, and starting point for further investigations. Van der Broek* was the first to suggest that Z is exactly equal to the atomic number, *i.e.*, the number expressing the serial position of the element in the periodic classification. Thus H has the atomic number 1, He has 2, Na 11, and Au 79. The suggestion was brilliantly verified by Mosley's classical work on the measurement of the wavelength of the K-series of X-ray characteristic lines of elements (see Chap. XI). In 1920, Chadwick† showed that the atomic number can be directly determined from scattering experiments, by improving the earlier methods.

Improvement was effected in the two following respects :—

(1) Increasing the fraction of scattered rays relative to the number incident.

(2) Measuring the scattered and incident beam on the same screen under the same conditions.

The apparatus used is shown in outline in Fig. 26 and in full in Fig. 27. The scattering foil AA is in the form of an annular ring, R is the source of α-rays, and S the ZnS screen, so placed that RP=PS. D is a diaphragm and L is a thick lead screen which can be used to cut off completely the direct beam RS from the screen, or can be removed to allow direct beam to fall on it. This enables Q to be

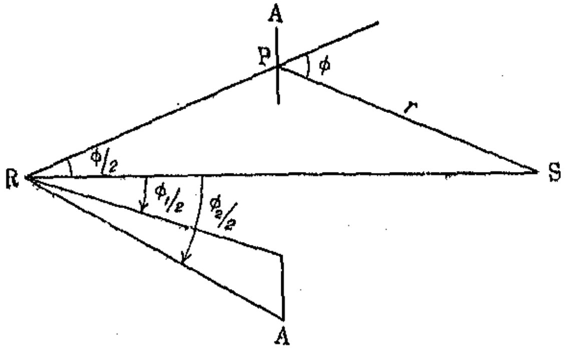

Fig. 26.

---

* Van der Broek, *Phys. Zs.*, **14**, 32, 1913.

† Chadwick, *Phil. Mag.*, **40**, 734, 1920.

counted on the same screen in the usual way. Let φ_1, and φ_2 be the solid angles subtended by the inner and the outer edges respec-

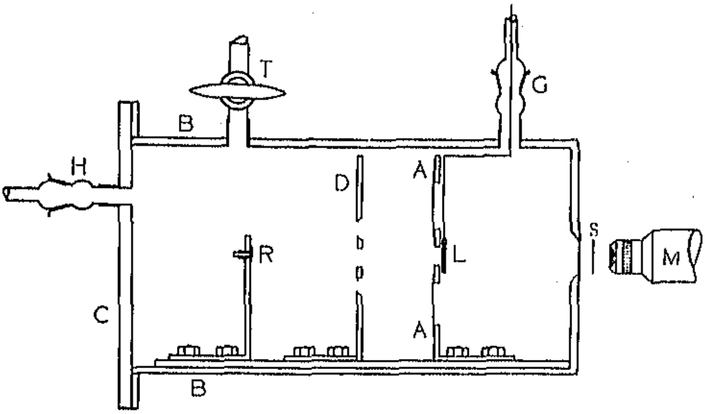

Fig. 27. Chadwick's apparatus for determining the nuclear charge.

tively of the foil to R. The solid angle subtended by an elementary annular ring at R.

$$= 2\pi \sin\frac{\varphi}{2}\, d\left(\frac{\varphi}{2}\right).$$

Assuming Q=number of α-particles emitted by the source per second the number falling on the elementary ring

$$= \frac{1}{2}Q \sin\frac{\varphi}{2}\, d\left(\frac{\varphi}{2}\right).$$

The number scattered per unit area of the screen S placed normally to RS.

$$= \frac{1}{2}Q \sin\frac{\varphi}{2}\, d\left(\frac{\varphi}{2}\right)\frac{nta^2}{4r^2}\operatorname{cosec}^4\frac{\varphi}{2}$$

Integrating this between the limits $\frac{\varphi_1}{2}$, $\frac{\varphi_2}{2}$, the total number scattered on the annular ring AA is

$$\frac{Qnta^2}{8r^2}\int_{\varphi_1/2}^{\varphi_2/2}\operatorname{cosec}^3\frac{\varphi}{2}\, d\left(\frac{\varphi}{2}\right)$$

$$= \frac{Qnta^2}{16r^2}\left[ln \tan\frac{\varphi_2}{4} - ln \tan\frac{\varphi_1}{4} + \cot\frac{\varphi_1}{2}\operatorname{cosec}\frac{\varphi_1}{2} - \cot\frac{\varphi_2}{2}\operatorname{cosec}\frac{\varphi_2}{2}\right]$$

where $a = \dfrac{2Ze^2}{m_a u^2}$

per unit area of the screen. The number falling directly per sec. per unit area on the screen is $Q/4\pi l^2$ where l=distance between the source and the screen.

Thus the quantity a, and hence Z can be calculated. Chadwick calculated the nuclear charges for copper, silver and platinum as $29{\cdot}3e$, $46{\cdot}3e$ and $77{\cdot}4e$ respectively, and claimed his results to be accurate within 1 to 2%. This proves directly that the nuclear charge of the elements is numerically equal to their atomic number.

80. Validity of the Inverse Square Law.—According to Rutherford's theory of α-ray scattering, the amount of scattering in a given direction varies inversely as the fourth power of the velocity of the α-particles, provided the law of inverse square was correct for all distances. Since it could now be assumed that Z is exactly equal to A, Chadwick showed that his experiment could be utilised to find out whether the inverse square law of force was true for all distances of approach to the nucleus. He used the apparatus employed in his nuclear charge determination. By using Pt as the scattering material and three different velocities of α-rays he found the law of inverse square to be true within a distance of approach from the nucleus $d=7\times10^{-12}$ cm.

The experiment was repeated with greater precision by Rutherford and Chadwick* (1925) using the same annular ring-method as in Chadwick's experiment. For gold, platinum, silver and copper-foils which they examined, the laws of inverse square of force was found to hold accurately within a distance $d=5\times10^{-12}$ cm.

It should however be emphasized that on account of large value of Z it is difficult, to approach with α-particles at our disposal, to a sufficiently small distance of the nucleus. For with a straight collision (φ=180°......the particles turned back in the same direction from which they were projected) we have the minimum value

$$d_0 = \frac{4Ze^2}{m_a u^2}.$$

With α-particles having $u=2\times10^9$ cm./sec. which are almost the swiftest α-particles at our disposal, we obtain the following values of d_0.

U	$Z=92$	$d_0=15{\cdot}6.$	10^{-13} cm.
Cu	29	5.	10^{-13} cm.
Mg	12	2.	10^{-13} cm.
He	2	0·34.	10^{-13} cm.

---

* Rutherford and Chadwick, *Phil. Mag.* **50**, 889, 1925,

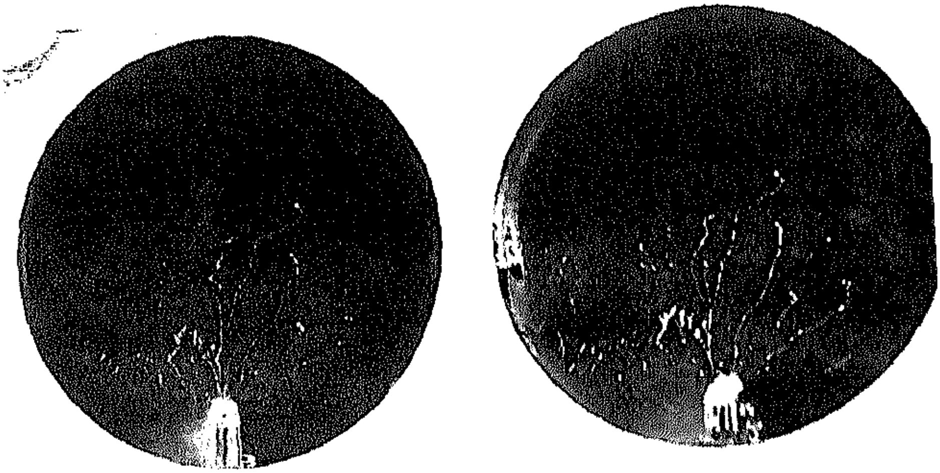

Fig. 28. Tracks of β-rays from RaD (*Petrova*).

(*p.* 163)

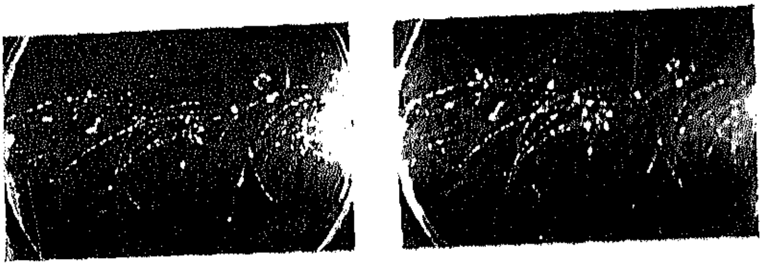

Fig. 28*a*. Tracks of γ-rays from RaC in magnetic field (*Skobeltzyn*)

(*p.* 164)

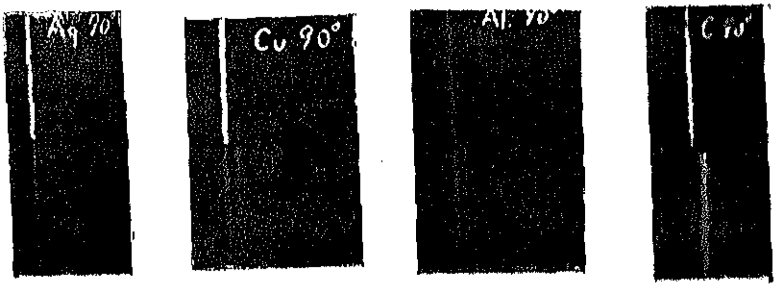

Fig. 12. Relative intensities of modified and unmodified lines in Compton Scattering phenomenon. Mark the progressive increase in the intensity of modified line from Ag, Cu, Al, to C.

(*p.* 200)

[*f. p.* 163

Hence the region near the vicinity of nuclei of heavy particles cannot be explored by α-particles. We must look to light particles like Mg, Al......where closer nuclear distance can be approached. In such cases, considerable deviation from the inverse square law has been found (see chapter on *Nuclear Physics*).

81. The Properties of β and γ-rays.—The physical nature of the β and γ-rays has already been discussed in the beginning of this chapter. The β-rays from radioactive bodies are negatively charged particles moving with very high velocity ranging between ·30*c* to ·98*c*. Their *e/m* has been determined by Kaufmann and Bucherer (II, §§ 28, 29), and they have been identified with the electrons. The β-rays can produce ionisation and are absorbed by matter, but they can penetrate a greater thickness of matter than the α-rays. Like α-rays, the β-rays also are scattered by atomic nuclei; in fact, on account of much smaller mass of the β-rays, the scattering takes place much more readily in their passage through matter, than in the case of α-rays. The quantitative investigation of absorption and scattering is however complicated by mutual interference of the two phenomena, so that it is difficult to decide whether the β-rays possess a definite range like the α-rays, or not. A typical appearance of the Wilson's cloud-chamber photograph of the β-ray tracks from Ra D in air is shown in Plate III, Fig. 28. It will be seen that the β-particle follows a zig-zag course on account of constant deflexion of its path due to scattering. It should also be noticed that the tracks are not continuous, as in the case of α-rays. This is due to the weaker ionisation produced by the β-rays. This stereoscopic pair of photographs has been obtained by Petrova[‡] a co-worker of Meitner.

Early works on the scattering of β-particles were performed by Crowther[*] and Schonland[†]. The experiment was found difficult for several reasons, such as—(1) inhomogeneity of β-rays, (2) occurrence of multiple scattering, (3) inefficiency of scintillation method of observation, and (4) the unavoidable presence of γ-rays in the source of β-rays. The theory of β-ray scattering was developed by J. J. Thomson and Rutherford. Much later works, both theoretical and experimental have since been done on the subject by Schonland[§],

---

[*] Crowther, *Proc. Roy. Soc. A*, **84**, 226, 1910.

[†] Crowther and Schonland, *Proc. Roy. Soc. A*, **100**, 526, 1922.

[‡] Petrova, *Zs. f. Phys.*, **55**, 621, 1929.

[§] Schonland, *Proc. Roy. Soc. A*, **101**, 299, 1922; **113**, 87, 1926; **119**, 673, 1928.

Geiger and Bothe,[*] Chadwick and Mercier[†], Bothe[‡], Wentzel[§], Mott[||] and others. For a summary of these works see Rutherford, Chadwick and Ellis' *Radiations from Radioactive Substances* (1930), Chap. VIII.

The γ-rays, as already has been stated, are very short electromagnetic waves, shorter than the X-ray waves. They possess the special property of ejecting β-rays from matter on which they fall. The velocity with which these secondary β-rays are emitted depend upon the wavelength of the exciting γ-rays. On this principle, the wavelengths of γ-rays have been determined from the measurement of the velocity of the secondary β-rays, and have been found to be of the order of 10^{-10} cm. The actual method will be given later in the chapter on *Nuclear Structure.*

The production of secondary β-rays by the γ-rays is remarkably shown in Fig. 28*a*, plate III, which is a Wilson cloud-chamber-photograph of γ-ray tracks from Ra C in air under a magnetic field of 1030 gauss, obtained by Skobelzyn. The curvature of the tracks is due to the magnetic field. When γ-rays pass through air, they eject electrons from the air molecules. The paths of the electrons are rendered visible by means of the ions which they produce in air.

We shall now conclude this chapter with an account of some other physical effects produced by the radioactive radiations.

82. Evolution of Heat by Radioactive Substances.—It was noticed by the early experimenters that all radioactive substances having tolerably long life go on evolving heat at a uniform rate. This continuous evolution of heat, without any provocating agent appeared to be a great puzzle, and in some quarters it was held that the phenomenon was a direct violation of the first law of thermodynamics, i.e., *energy was being created out of nothing.* Experiments however showed that the evolution of heat was due to the stoppage of α, β and γ-rays by radioactive matter, and in fact the heat evolved per second was found to be exactly equal to the energy of α, β, γ-rays stopped by matter. So it became clear that no violation of the first law was involved in this process.

---

[*] Geiger and Bothe, *Zs. f. Phys.*, **6**, 204, 1921.
[†] Chadwick and Mercier, *Phil. Mag.*, **50**, 208, 1925.
[‡] Bothe, *Zs. f. Phys.*, **13**, 365, 1923.
[§] Wentzel, *Ann. d. Phys.*, **69**, 335, 1922.
[||] Mott, *Proc. Roy. Soc. A*, **124**, 425, 1929.

The rate of evolution of heat by radioactive matter was investigated by many observers including Curie, Paschen, Precht, Poole and Dewar. But to illustrate the investigation it would suffice to describe the apparatus used by Rutherford and Barnes*.

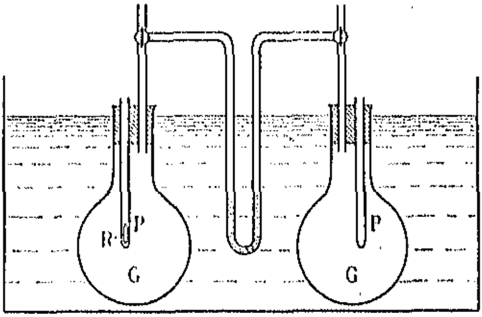

Fig. 29
Rutherford and Barnes' Differential Calorimeter.

As shown in Fig. 29, Rutherford and Barnes' apparatus was a differential calorimeter consisting of two glass-flasks G, G immersed in a water bath. The two are connected by a manometer containing xylol. Two test tubes P, P are inserted in the flasks and the radioactive preparation R is placed inside one of these. As the preparation evolves heat, the air within the walls of G expands and raises the pressure in the limb of the manometer nearest it. The rate of increase of pressure is noted, and then the radioactive preparation is taken out. Next a small heating coil is placed inside P, and is heated by means of regulated current so that the rate of increase of pressure in the manometer becomes absolutely the same as before. The heat supply to the coil may be easily obtained by measuring the current and the voltage; and this must be equivalent to the rate at which heat is evolved by the radioactive body.

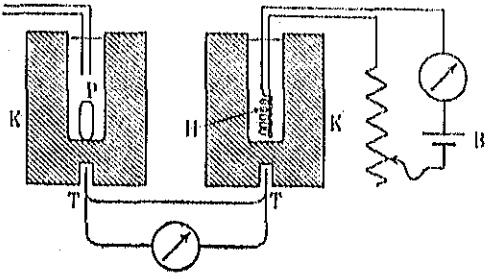

Fig. 30. Angstrom's Compensation Calorimeter.

A modification of this apparatus was devised by Ångstrom† and used by von Schweidler and Hess‡. This is shown in Fig. 30. In this the flasks were replaced by two metallic calorimeters K, K which are absolutely identical in size. The one contains the active preparation P, the other contains a heating coil H heated by regulated current from a battery B. T is a thermocouple connected to a galvanometer with each of its two junctions placed inside a hollow space in the two calorimeters. The heating is so regulated that the galvanometer shows no deflection. The heat evolved by the coil is therefore equal to the heat evolved by the radioactive body. The apparatus is however slow in action on account of the heaviness of the calorimeters.

---

* E. Rutherford and H. T. Barnes, *Phil. Mag.*, 7, 202, 1904.

† K. Ångstrom, *Phys. Zs.*, 6, 685, 1905.

‡ E. v. Schweidler and V. F. Hess, *Wiener Ber.*, 117, 879, 1908.

THE HEAT EVOLVED BY RADIUM AND ITS DECOMPOSITION PRODUCTS.

A direct measurement of the evolution of heat by radium in equilibrium with radon and shortlived products was made by Meyer and Hess*. The experimental conditions were such that the α and β rays were completely absorbed and 18% of the γ-rays were absorbed by the calorimeter (calculated from the dimensions of the calorimeter and the absorption coefficient of γ-rays). The rate of evolution of heat was found to be 132 cal. per gm. of radium in equilibrium combination with its product per hour.

This does not tell us anything about the proportions contributed by the different rays. This was first attempted by Eve,† and by Moseley and Robinson.‡ They determined the total ionisation produced by the three kinds of rays separately, and assumed these to be proportional to the energy content of the different rays. The assumption is however rather uncertain.

Ellis and Wooster§ determined separately the heat evolved by γ-rays according to a special method. They used a cylindrical calorimeter vessel of which one sector consisted of Al and the other of Pb. Both the sectors had equal outer dimensions and heat capacities, the Ra Em preparation was placed in the axis of the calorimeter surrounded by a copper tube which absorbed completely the α and β rays. The heat emitted by this tube warmed the two sectors equally so that the difference of temperature observed between the two sectors was caused by the greater absorption of γ-rays in lead. In this way it was determined that the energy of γ-rays emitted by a gm. of Ra (in equilibrium combination with its products) amounts to 8·7 cal. per hour. The amount of energy due to the rays from the different products was observed by Meyer and Hess by using Ra freed from its decomposition products, as well as from those of Ra Em in equilibrium with its shortlived products. The amount of heat evolved was determined from time to time and was found to increase steadily from 25 cal. to 114 cal. per hour after a long time. An extrapolation to $t=0$ gives the amount evolved by Ra alone. For details original papers* must be consulted. The results are shown in Table 7.

---

* St. Meyer and V. F. Hess, *Wiener Ber.*, **121**, 603, 1912.

† A. S. Eve, *Phil. Mag.*, **27**, 394, 1914.

‡ G. H. J. Moseley and H. Robinson, *Phil. Mag.*, **28**, 327, 1914.

§ C. D. Ellis, and W. A. Wooster, *Proc. Camb. Phil. Soc.*, **22**, 595, 1925; **50**, 521, 1925.

Table 7.—Heat evolution due to α, β, γ-rays in cal. per hour.

Substance	Rutherford and Robinson				Meyer and Hess		Theoretical (after Meitner)			
	α	β	γ	α+β+γ	α+β+γ		α	β prim.	β+γ sec.	α+β+γ
Ra	25·1			25·1		25·2	23·2		0·9	24·1
Ra Em	28·6			28·6		114·2	26·5			26·5
Ra A	30·5			30·5			29·0			29·0
Ra B		4·7	0·86	52·7				8·9 to 10·8	1·7	58·9 to 60·8
RaC + C′	39·4		7·7				37·7		10·6	
Sum	123·6	4·7	8·6	136·9	139·4	139·4	116·4	8·9 to 10·8	13·2	138·5 to 140·4

We shall now show that the experimental figures are in agreement with the energy of different rays theoretically calculated. When an α-particle of mass m and velocity v, is emitted by an atom of mass M and velocity V, then the back momentum imparted to the atom is given by the law

$$mv = MV,$$

so that the amount of energy which becomes free in this process is given by the formula

$$E_1 = \tfrac{1}{2}(mv^2 + MV^2) = \tfrac{1}{2}mv^2\left(1 + \frac{m}{M}\right)$$

---

* Recently a new method for measuring a very small amount of heat evolution has been given by Orthmann (*Zs. f. Phys.* **60**, 137, 1930).

Let Q = number of α-particles emitted per sec. by 1 gm. of Ra. Then the amount of heat evolved per hour is given by

$$W_1 = \frac{1800\ Qmv^2}{J}\left(1+\frac{m}{M}\right)$$

Putting the values of v in the case of Ra and its different products from Table 5, and putting $Q = 3{\cdot}5 \times 10^{10}$ we obtain the figures shown in column 8 of Table 7.

The energies obtained in this way are somewhat smaller than the observed values, and Rutherford and Robinson believed that the difference is larger than the experimental error, and that the radioactive bodies evolve heat in certain other forms still undiscovered. Hess and Lawson are of opinion that Rutherford's value of Q was too small.

The amount of energy due to the stoppage of β and γ-rays are exceedingly small compared to that of α-rays, but they have given very interesting informations regarding the number and origin of these rays. They will be treated in the chapter on *Nuclear Physics.*

83. Age of Minerals from Radioactive Data.—The origin and age of the Earth has excited speculations among philosophers in all ages. According to the nebular hypothesis of Kant and Laplace, the Earth and the other planets had separated at some distant epoch from the central nebular mass which later condensed into the Sun.* In process of time, these detached masses underwent rapid cooling and became condensed as liquid with a solid crust on the surface. According to certain indirect evidences the inside of the earth consists of a fluid *magma* mostly composed of molten iron in which the other elements either in elementary or compound form are dissolved. When the surface cooled, some of these materials separated like slags out of molten iron in the smithy, and formed the solid lithosphere to a depth which has been estimated variously at 100 to 200 kilometers. In process of time, as the surface cooled down still further, life appeared on the earth and gradually underwent the different stages of evolutions studied by the Paleontologists. It is a favourite problem with the scientists of different classes to find out the epoch at which the formation of earth's crust started. The geologists were the first in the field, attacking the problem mainly from the records of plant and animal life left on different rocks.

---

* For modern theories of the origin of the solar system, see Jeffreys, *Ergebnisse d. exakten Naturwiss,* 7, 1.

They thus divided the rocks into a number of groups in order of the age. The earliest rocks were called *azoic* as they showed no traces of life. The next sample was called *protozoic*, as life appeared in them in extremely simple form (protozoa). Then passing through the *mesozoic* age when reptiles flourished, the present age (*kainozoic*) reached when mammals and ultimately man have appeared on the earth. Each of these epochs is further subdivided into a number of sub-epochs shown in Table 8. For a complete knowledge of the groups, a standard book on geology must be consulted.

Lord Kelvin attacked the problem from a purely physical point of view. It was observed that the temperature of the Earth's interior increases with depth at the rate* of about 2°C per 100 metres. If this rate of increase continues, ultimately a depth will be reached when the temperature will be so great that all substances are in the molten state. This he assumed to be 3900°C. He next observed experimentally the mean conductivity of the rocks, that is to say, the rate at which heat is flowing by conduction from the interior to the outside. Next he pictured to himself the following mathematical problem. Let us suppose that initially the temperature of the crust was 3900°C, and it was allowed to cool by loss of heat. What time would elapse before the surface would be cooled to the present temperature and the rate of flux of heat would equal the observed rate? Solving this problem† he found a figure of about 100 million years, which was considered by the geologists to be hopelessly low.

It is now recognised that there was one great flaw in Lord Kelvin's assumptions. He believed that the only source of heat was the high temperature in the inside of the earth. But the discovery of radioactivity showed that in addition to this source, we have another, namely, the heat evolved by radioactive bodies contained in minerals as discussed in §82.

To obtain a precise estimate of this quantity, an analysis was undertaken of the amount of U and Th contained in the rocks found in the different geological epochs. It was found that if it were assumed that the core of the earth contained radioactive matters U or Th to the same extent as the rocks, the amount of heat evolved would be much larger than what was needed for compensating the energy loss by cooling. This can be seen from the following considerations.*

---

* E. Kayser, *Lehrbuch der Geologie*, p. 60.

† See *Text Book of Heat*, Saha and Srivastava, p. 381.

Let Q = the amount of heat lost per sec. by cooling, K = conductivity of earth's crust, and r = radius of the earth. Then

$$Q = 4\pi r^2 . K. \frac{d\theta}{dx},$$

where $d\theta/dx$ denotes the temperature gradient along the depth of the earth's crust. From actual observations it has been found that K = ·004 cal/cm.^{2} sec., $d\theta/dx = 3{\cdot}2 \times 10^{-4}$ grad/cm. Also $4\pi r^2 = 5{\cdot}1 \times 10^{18}$ cm^2. Hence $Q = 6.10^{12}$ cal/sec. Since the amount of heat evolved by 1 gm. of U is $2{\cdot}5 \times 10^{-8}$ cal/sec., the rate of earth's cooling can be compensated by $\frac{6.\ 10^{12}}{2{\cdot}5 \times 10^{-8}} = 2{\cdot}4 \times 10^{20}$ gm. of U. Supposing U occurs throughout the earth's volume in the same proportion as in the rocks, the total amount of U contained in the earth would be $3{\cdot}6 \times 10^{22}$ gm. which is thus 150 times greater than the amount required for compensation. Similarly the amount of Th calculated in the above way is 130 times greater than the required amount.

The belief has therefore grown that the interior of the Earth contains radioactive matter in much less proportion than the rocks and minerals forming the earth's crust.

The age of the minerals, that is the time which has elapsed since they were first deposited in the solid state from the fluid magma can be estimated in a less objectionable way, from the helium and the lead contents of the rocks. It was early noticed that many geologically old minerals rich in radioactive substances U and Th contained helium in considerable quantities. Most of these minerals were very compact in form and dense in structure and impervious to water and air. It was therefore supposed that ever since the epoch when these substances separated from the fluid magma as solid rocks, the U and Th contained in them have been disintegrating and ultimately the α-rays emitted during these disintegrations have been accumulating as helium. So an estimation of the helium-content would yield a good value for the age of the rocks.

It was shown even in the early days of radioactivity that helium was present in the gas released on heating a radium-salt or dissolving it in water. Strutt† (Lord Rayleigh II) showed how the helium content in the original rocks from which the radioactive matter has been extracted can yield us an estimate of the age of the rock. To take one example: the mineral thorianite from Ceylon from which W. Crookes first discovered thorium, was found to contain 68% of Th and 11% of U, and yielded 8·9 c.c. of helium gas at N. T. P. per gm. of the mineral. Now one gm. of U in equilibrium with its products yields $9{\cdot}7 \times 10^4$ α-particles per sec. which correspond to $1{\cdot}10\times10^{-4}$ c. mm. of He-gas per year. One gm. of Th in equilibrium with its products produces $2{\cdot}7\times10^4$ α-particles which correspond to $3{\cdot}1\times10^{-5}$ c. mm. of He per year.

---

* After O. Hahn, *Handbuch der Physik*, XXII, p. 292,

† Strutt, *Proc. Roy. Soc. A*, **84**, 379, 1911.

So 1 gm. of the mineral would produce per year $11\times{\cdot}11+3{\cdot}1\times{\cdot}68$ or $3{\cdot}3\times10^{-5}$ c.mm. of He per year. Continuing at this rate, the mineral would require $\frac{8{\cdot}9\times10^3}{3{\cdot}3\times10^{-5}}=2{\cdot}7\times10^8$ years or 270 million years to produce the quantity of helium actually found in it. Hence the lowest estimate of the time of deposit of Ceylon-thorianite is 270 million years.

Two assumptions are involved in the above calculation: (1) at the time when the mineral was formed, no helium was present throughout its volume, (2) no helium gas has escaped from the mineral during the time it has been in existence. The second assumption may be taken to be true as long as the mineral is very compact, and impervious to air and water. The first also may be taken to be correct, as the hot fluid magma from which the mineral separated is not likely to hold any gas in solution.

In the table, on the next page, the age of minerals of different geological epochs determined according to the above method is given. The table is due to Lawson*.

Another way of calculating the age of the minerals is from the estimation of their lead-contents. It has been explained in §60, 61 that the end-products of the transformation series of both U and Th are isotopes of lead. Since the amount of lead formed per year from any of these elements in equilibrium with its products can be calculated, the age of the minerals can also be calculated from their lead contents in exactly the same way as in the case of helium. This would give a more reliable estimate of the age, as it does not involve the assumptions made in the other case. The ages calculated in this way are shown in column V of the table.

Recently Lord Rayleigh II has found a considerable amount of helium to be present in some old specimens of the mineral

---

* R. W. Lawson, *Naturwissenschaften*, 5, 429, 452, 1917.

Table 8.—Age of radioactive minerals.

Geological Epoch	Mineral	Locality where found	AGE CALCULATED IN MILLION YEARS	
			From He-content	From Pb-content
1. Tertiary or Kainozoic				
Pleistocene ...	...	...	...	...
Pliocene ...	Zircon	Campbell Island, N. Z.	1·5	...
Miocene ...	Zircon	Expailly, Auvergne	5·7	...
Oligocene ...	Siderite	Rhein province	7	...
Eocene ...	Haematite	...	31	...
2. Secondary or Mesozoic				
Cretaceous ...	...	...	...	...
Jurassic ...	...	...	...	...
Triassic ...	...	...	...	...
3. Newer Palæozoic				
Permian ...	Zircon	N. E. Tasmania	38	...
Carboniferous	...	...	...	...
Devonian ...	Haematite	Caen ...	112	...
4. Protozoic and older Palæozoic				
Silurian ...	Thorianite	Ceylon (S.) ...	226	...
	Thorianite	Ceylon (G.) ...	212	
Ordovician ...	Zircon	Oslo, Norway...	...	300
Cambrian				
Upper pre-	Zircon	Ceylon ...	250	...
Middle pre-	Sphen	Arendal, Norway	330	...
	Sphen	Tweederstrand, Norway	385	...
Lower pre-	Zircon	Ontario, Canada	550	
	Sphen	Ontario, Canada	570	
Tertiary (?)	Uranite	Spruce, Pine, N. Carolina	...	380
Middle pre-	Uranite	Annerod, Norway	...	1050
	Uranite	Quebec, Ontario	...	1250
5. Archaean or Azoic	Zircon	Mozambique ...	...	1600

beryl (composition $Al_2\ Be_3\ (Si\ O_3)_6$. He analysed a large number of specimens of beryl obtained from widely distant localities and belonging to different geological epochs. He observed the largest He-content (77·6 c.mms. per gm.) in beryl from pegmatite on the Bangalore-Kankanhalli Road, Mysore, India. Geological evidences show that this particular specimen belongs to the basic archæan platform of India. In general, he found that the He-content in beryl in rocks of the same age vary within wide limits, *e.g.*, for Archæan rocks it varies from 77·6 to ·0550 c.mms. per gm. But as a rule the minerals of any particular age are richer in He-content than those belonging to the following ages. He ascribes the variation to the possibility that beryl deposited in the same age can lose He by varying amounts on account of exposures. From this it appears plausible that He is continually generated from beryl throughout geological time in a way which is not yet clearly understood. It could not have been present at any early stage in the history of any specimen. For, in that case the tertiary specimens (youngest) which have the least opportunity of losing their content should have been the richest in He compared to the others.

Books Recommended.

S. T. Meyer and E. v. Schweidler—*Radioaktivität* (1916).

E. Rutherford—*Radioactive Substances and Their Radiations* (1913).

E. Rutherford, J. Chadwick and C. D. Ellis—*Radiations from Radioactive Substances* (1930).

A. S. Russel—*The Chemistry of Radioactive Substances* (1924).

F. Soddy—*Interpretation of Radium* (1920).

G. Hevesy and F. Paneth—*A Manual of Radioactivity* (1926).
(English translation)

Handbuch der Physik, Bd. XXII, Chap. 2 C, D, and Chap. 3 A, B, C.

K. W. F. Kohlrausch—*Radioactivität* in *Handbuch der Experimental Physik*, Bd. XV, (1928).

Report of the International Radium Standards Commission, Brussels, 1930—in *Review of Modern Physics*, Vol. 3, p. 427, 1931.

CHAPTER V

THE PHYSICAL PROPERTIES OF LIGHT

84. Introduction.—It need hardly be emphasized that light is the chief agency through which impressions of the phenomenal world is conveyed to our senses. Through its interaction with matter, it gives rise to physical phenomena which fill up the largest part of Nature's canvas. It is therefore clear that if we wish to understand Nature, we must try to have a correct idea of the physical properties of light.

The task is not an easy one, as the properties of light can only be inferred from the phenomena to which it gives rise through its interaction with matter. The process of study has therefore been both deductive and inductive, and the different theories of light which have been proposed from time to time have undergone rather violent changes of fortune in course of time. But though a final theory may not be in sight even now, our knowledge of light has progressed enormously owing to the constant effort to verify, supplement or supersede the existing theories, and to extend their scope of explanation to new fields of experience. It is difficult to take the reader through the innumerable circuitous paths and sidetracks along which knowledge on this subject has developed ; we rather confine ourselves to the modest task of presenting only the salient landmarks.

85. Physical Properties of Light—Corpuscular Theory of Light.—Every student of Physics is conversant with the early controversies regarding the nature of Light. The earlier philosophers had speculated from the rectilinear propagation that light consisted in the flight of *corpuscles.* The velocity of light was found by Römer to possess the value of 3×10^{10} cm. per sec. from observations of the eclipses of Jupiter's satellites. A set of particles moving with such enormous velocity is expected to exert pressure on material bodies on which they may fall. Though at the time no experiments could be carried out to demonstrate this effect, the observation that the tails of comets were found always to be turned opposite to the sun were cited in favour of the existence of the pressure of light.

The laws of refraction seem to have been known to the Arabs, but in Europe they were first made public by Descartes who derived his knowledge from the works of Snellius, a professor in the University of Leyden. The discovery of this law gave rise to the following question : if the velocity of light in empty space be c, what is the velocity in a medium having the refractive index n? It was shown that the velocity should be cn on the corpuscular theory of light.

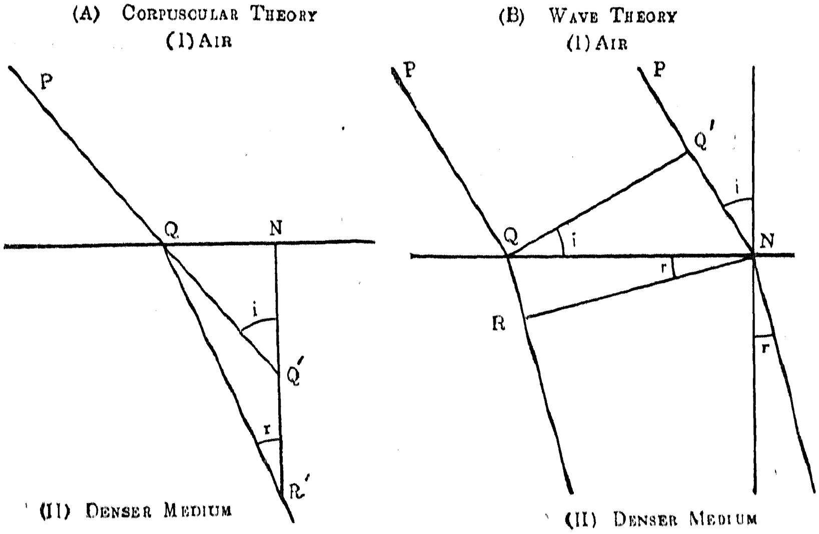

Fig 1. Refraction of light.

Diagram 1 (A) illustrates the propagation of light on the corpuscular theory : (I) is air, (II) is a denser medium. PQ indicates the ray of light in medium (I), QR′ in medium (II). If light consists of particles having momentum G, the component tangential to the dividing surface ON will have the same value. Hence the normal component must be different.

Let G_1 and G_2 be the momenta in the two media. Then putting their tangential components equal

$$G_1 \sin i = G_2 \sin r$$

Therefore,
$$\frac{G_2}{G_1} = \frac{V_2}{V_1} = \frac{\sin i}{\sin r} = n$$

or,
$$V_2 = nV_1 \text{ or } nc \quad . \quad . \quad . \quad . \quad . \quad . \quad . \quad . \quad . \quad . \qquad (1)$$

if medium (I) is vacuum.

Diagram 1 (B) illustrates the propagation of light on the wave-view. PQ is the ray, QQ′ is the wave-front in medium (I). QR is the ray in medium (II), NR is the wave-front in it. It is clear that by the time the wave-front traverses the distance Q′N in (I), it traverses the distance QR in (II). Hence if U_1, U_2, are the wave velocities in the two media,

$$\frac{U_2}{U_1} = \frac{\mathrm{QR}}{\mathrm{Q'N}} = \frac{\sin r}{\sin i} = \frac{1}{n}$$

or

$$U_2 = \frac{U_1}{n} = \frac{c}{n} \quad . \quad . \quad . \quad . \quad . \quad . \quad . \quad . \qquad (2)$$

if (I) is vacuum.

THE WAVE-THEORY OF LIGHT

The wave theory of light was first expressed in a definite form by Ch. Huygens in 1678, to account primarily for the phenomenon of double refraction. According to this theory, the velocity of light in a refractive medium is c/n and this fact is in sharp contra-distinction to the result obtained from the corpuscular theory. But as Huygens failed to account successfully for the rectilinear propagation of light, the theory was abandoned for a long time. Huygen himself discovered the phenomenon of *polarisation or two-sidedness of light*, which is impossible to explain on any form of the corpuscular theory. But even this phenomenon could not be explained on Huygens' form of the wave-theory as he thought that light consisted of waves of condensation or rarefaction in the hypothetical medium *aether*.

86. Revival of the Wave-theory.—The revival of the wave theory is, as is well known, due to Th. Young, in the early years of the nineteenth century. He showed that two beams of light, originally coming from one source, but split up into two sources by artificial means, can produce darkness (*Interference of light*) at points where they overlap. This experiment was reported to have been done by Grimaldi in 1665, who concluded from his experiments that as two beams of light can produce darkness light was not *material* at all ; but not much credence was given to his experiments. Fresnel who entered the field in 1814, was the first to suggest that light consisted of *transverse waves* in aether. By the introduction of this hypothesis, he was able to account for the phenomenon of polarisation. Further, by using the device of dividing the wave front into zones which were regarded as giving rise to secondary wavelets, and using the phenomenon of destructive interference of these wavelets, he was able to account for the rectilinear propagation of light. (This is known usually as *Huygens' Principle*, but in its present accepted form, it appears to be due to Fresnel.)

87. Heterogeneity of Light.—The numerous experiments which were performed on interference and diffraction had the effect of convincing every investigator of the essential correctness of the wave theory of light. It also led to a proper understanding of the heterogeneous nature of light, which was first demonstrated in 1665 by Newton's prismatic analysis of white light. Newton had taken a right step towards the explanation of the phenomenon by saying that white light was heterogeneous and consisted of light of different colours, and these were separated by a prism as their refractive indices in glass are different. Young showed that lights of different colours have different wavelengths, and he obtained nearly correct values of these wavelengths from a study of Newton's rings. But a precision method of measuring the wavelength was first discovered by Fraunhofer in his diffraction grating which has, to this day, remained a powerful instrument for the analysis and measurement of the wavelength of light of all kinds.

88. Extension of the Range covered by Light.—For a long time, the word 'light' was used to denote visible light beginning from red (λ=7000 Å. U.) to violet (λ=4000 Å. U.). But there is no reason why the phenomenon should be confined between these two limits. As a matter of fact, we now know that there may be no limit on either sides. The wavelengths of different kinds of light are given in the following table.

Table 1.—Electromagnetic Waves.

Radiation	Wavelength	Method of Production	Method of detection and analysis	Discoverer
Cosmic rays (Super γ-rays).	·0000001 to ·001 Å. U.	Conversion of matter into energy.	Measurement of absorption-coefficient.	Hess Kolhörster (1913), Millikan (1923), etc.
γ-rays ...	·001 to ·09 Å. U.	Radioactive disintegration.	β-ray spectrum and crystal reflection.	

Radiation	Wavelength	Method of Production	Method of detection and analysis	Discoverer
X-rays ...	·01 to 136 Å. U.	Bombardment of metal targets by electrons.	1. Crystal reflection, and photography or ionisation chamber. 2. Grating diffraction (soft X-rays).	Röntgen (1895) Laue (1912). Compton (1925) Thibaud (1926) (soft X-rays).
Extreme ultraviolet.	136 Å. U. to 1000 A. U.	Vacuum spark.	Photography with vacuum gratings, plane and concave.	Millikan (1919) Lyman (1906) Siegbahn
Middle and near ultraviolet.	1000 to 4000 Å. U.	Vacuum spark.	Photography with prisms:— Fluorite ... (1100 to 2300 A. U.) Quartz (1850 to 11000 A. U.)	Schumann (1890) Ritter (1802).
Visible light.	4000 to 7000 Å. U.	Spark, arc, flame.	Photography with quartz and glass prisms.	Newton.
Infra red ...	7000 A. U. to ·4 mm.	Heating ...	1. Wire gratings and thermo couples. 2. Residual rays:— From quartz ..... $8{\cdot}5\ \mu$ ($1\mu = 10^{-4}$cm.) From sylvine $60\ \mu$. From KI ... $96\ \mu$.	Rubens and Nichols (1898).
Short Hertzian waves.	1 to 10 mm.	Spark gap	1. Focal isolation 2. Coherer ...	Wood (1912). Nichols and Tears (1924). Bose (1902).
Hertzian waves.	1 mm. to 10^4 metres (no upper limit).	1. Spark gap 2. Triode valve oscillator.	1. Coherer. 2. Crystal rectifier. 3. Triode valve.	Hertz (1887).

89. Discovery of Spectrum Analysis.—The Spectrum analysis of light which was clearly formulated by Kirchhoff in 1859 was very far-reaching and extremely fruitful in its consequences. The atomic theory of matter had been formulated only a few decades ago by Dalton to explain the laws of chemical combination, but apart from the chemical properties, no precise physical method was known for the identification of any atom. Kirchhoff's discovery showed, for the first time, that every atom, when properly excited, emits light of *definite wavelengths* which are as characteristic of it as a voice is characteristic of a man, or a note is characteristic of a musical instrument. A rich succession of finds of new elements followed this discovery, but for the purpose of this book, it should be remembered as having established the first connection between light and atomic physics. Ever since the discovery, works on the characteristic spectra of elements and compounds are being carried on incessantly. The volume of knowledge thus gained is enormous and daily growing in size, and it has been mainly responsible for all the information we have got regarding the structure of the atom. An element like Fe emits more than 6000 lines between λ3000 to λ7000. This is sufficient to show that the atom cannot be of a simple structure like a lead bullet but must be extraordinarily complex, as has actually been found to be the case.

90. Vicissitudes of the Wave-theory of Light.—Though the wave theory of light has added so much to our stock of knowledge, its further course has not been without difficulty. If light consists of waves, the question naturally rises :—Waves in what? The earlier workers had said that light was due to waves in æther, a hypothetical element inherited from ancient times. But in spite of the best efforts to assign definite physical properties to æther, it remained largely metaphysical. Huygens thought that æther was a kind of superfine gas; but a gas is incapable of transverse vibrations ; so Fresnel thought that æther has the properties of an elastic solid. But there are grave difficulties in the acceptance of this hypothesis. For an elastic solid, when disturbed, gives rise not only to transverse waves moving with the velocity $\sqrt{\mu/\rho}$ but also to longitudinal waves possessing the velocity $\sqrt{\dfrac{\lambda+2\mu}{\rho}}$. Some physicists thought that probably gravitational action is propagated as longitudinal waves, but the suggestion could never be proved. Apart from this difficulty, if c be equal to $\sqrt{\mu/\rho}$ either the rigidity of æther is very great, or ρ is extremely small. But it is inconceivable that μ is exceedingly large, for then we are led to the strange hypothesis that planets and stars can move unhampered through a medium possessing great rigidity. If on the other hand, ρ be supposed to be extremely small, it is difficult to assign to such a medium the properties of a rigid body. Further all efforts to detect absolute motion through æther gave negative results. So by 1905, all hopes of obtaining a material picture of æther, free from contradictions, had disappeared.

91. The Electromagnetic Theory of Light.—Up to the time of Fresnel, the phenomenon of Light was regarded only as an isolated group, and no connection could be traced between this and other groups of natural phenomena such as electricity and magnetism. Though such a connection had been suspected by many, the first experimental proof was afforded by Faraday. He put a piece of glass between the poles of an electromagnet and passed a beam of polarized light through the glass parallel to the lines of force. It was found that when the magnetic field was switched on, the plane of polarisation was rotated through an angle which varied as the field. This clearly indicated that the polarisation of light can be affected by an external magnetic field.

In order to explain Faraday effect Fresnel supposed that plane-polarised light consisted of equal amounts of circularly polarised light of opposite directions (right handed and left handed), and when this is passed through an isotropic medium in a magnetic field along the direction of the lines of force, the two oppositely circular polarised components are resolved and they travel with unequal velocities through the medium.

The resultant effect is that when they recombine after traversing the magnetic field, the plane of vibration of the new plane-polarised light is rotated with respect to that of the original light.

This idea was verified by Brace* who succeeded in showing that the two components are actually decomposed in the magnetic field, and one of these is retarded, while the other is accelerated by the field.

Faraday's experiment does not appear to have been followed by any speculation regarding the connection between light and magnetism. The first useful clue was obtained in the celebrated experiment of Kohlrausch and Weber (Note 1, Appendix) who found that the ratio between the e. m. and e. s. units of electricity is just equal to the velocity of light.

---

*Brace, *Wied. Ann. d. Phys.*, **26**, 576, 1885; *Phil. Mag.*, (6), **1**, 464, 1901.

In many quarters, this result was interpreted as indicating that electrical action is propagated with the velocity of light. But these speculations for the most part remained barren until Maxwell, with clear intuition, formulated the hypothesis that light is an electromagnetic disturbance in space.

92. Maxwell's Field Equations.—Though we are in possession of all the mathematical work by which Maxwell arrived at his far-reaching theory, the mental processes which led him to the work are not quite clear. Before his time, scientists used to talk of two kinds of æther: (I) Fresnel's æther which carried the light-waves, (II) Faraday's æther which finds itself in a state of stress when subjected to electrical and magnetic forces. Maxwell thought that the two æthers cannot be different but must be the same, and hence when light passes through them, the vibrations must give rise to electric and magnetic force. This conviction, coupled with the knowledge of Kohlrausch and Weber's results, led him to a train of mathematical works regarding the magnetic action produced by an electrical current, and the electrical action produced by a varying magnetic field. They express the mutual relation subsisting between the magnetic and electrostatic fields in any dielectric medium, and will be found in any book on classical electrodynamics. From these equations, Maxwell showed that light may be supposed as consisting of propagations of an alternating electric and magnetic force at right angles to each other, and at right angles to the direction of the ray. He further showed that his equations lead exactly to the same expressions for reflection and refraction as are obtained from the elastic solid theory of æther, but in addition, he obtained a new result that $n^2 = k$, the dielectric constant of the medium.

93. Hertz.—It is to the genius of Hertz that the world is indebted for the demonstration of the fullest possibilities of Maxwell's ideas, particularly of the hypothesis that a light ray is always accompanied by an alternating electric and magnetic force. He demonstrated by mathematical investigation that every oscillatory discharge produces about it electric and magnetic forces which are at right angles to each other and move forward with the velocity of light. The most efficient form is given by the Hertzian open oscillator.

Hertz produced electromagnetic waves varying from 100 to a few metres in length and showed that these waves had all the properties of light. His experiments were taken up all over the world, and still shorter waves were produced purely by electrical means. Righi, Lebedew*, Lampa†, and Sir J. C. Bose‡ made very small oscillators and could produce waves as short as 4 mm. This is about 3 octaves lower than the longest infra-red ray. Recently this gap also has been bridged by Arcadiewa§, Nichols and Tears‖.

94. Maxwell to Lorentz.—Hertz's experiments and the short wave experiments clearly demonstrate that visible light can be produced by very minute Hertzian oscillators of atomic dimensions, in other words, when an atom is excited to emit light, it may be likened to a Hertzian oscillator having a minute self-inductance and capacity. To work out this idea more fully, we must have some model of the electrical structure of the atom. This was not forthcoming for a long time, and at first only crude models were used. But from 1880, the electrical theory of matter seems to have captured the minds of many physicists, and Lorentz in particular introduced the idea of discrete charged particles to supplement the theory of Maxwell.

This was a distinctly progressive step, for Maxwell's theory, as left by that great investigator, was confined to the treatment of light as an electromagnetic disturbance in free space (or free æther as it was then called), and it hardly made any serious effort to explain the phenomena in the interior of material bodies. The introduction of the electron rendered this possible—this became the go-between between matter and light (or æther as they put it in those days). Thus Lorentz recast the whole theory of dispersion—constructed by Sellmeyer and Helmholtz on the basis of oscillations of elastic solid particles—in the mould of Maxwell's theory. The vibrations of the electrons took the place of the vibrations of the elastic solid particles. The equivalent electric current due to motion of electrons was added to Maxwell's displacement current, and expressions were obtained for the variation of refractive index with wavelength, which proved to be of great use in subsequent investigations. But the greatest triumph lay in the successful handling of Zeemann effect, which was due simultaneously to Lorentz and Larmor (*vide* Chap. X).

---

* P. Lebedew, *Wied. Ann.*, **56**, 1, 1896.

† A. Lampa, *Wien. Ber.*, **105**, 587, 1049, 1896.

‡ J. C. Bose, *Asiatic Soc. Bengal, India*, 1895.

§ A. Arkadiewa, *Zs. f. Phys.*, **24**, 153, 1924.

‖ E. F. Nichols and J. D. Tear, *Phys. Rev.*, **21**, 587, 1923.

95. The Electron as an Oscillator.—In all these investigations, we regard the oscillations of the electron as causing the phenomena of light. The electron becomes the atomic resonator. Following an investigation by Rowland, it was indeed proved by Lorentz that an accelerated electron becomes the source of electromagnetic radiation in the way represented in the following diagram (Fig. 2).

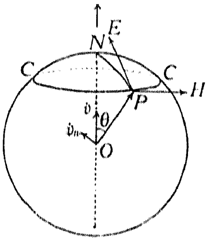

Fig. 2

Suppose O denotes the position of the vibrating electron. If it vibrates with an acceleration $\dot{v}$ in the direction ON, electromagnetic waves will spread out from O. Let OP denote the direction (θ) of one of the rays. Then the disturbance at P will consist of an electric field E in the direction PE and a magnetic field H along PH. The direction of the electric and magnetic fields will be at right angles to each other. The magnetic field is tangential to the circle CC, and the electric field lies in the meridian plane OPN.

By making use of the idea of the electron-resonator, J. J. Thompson deduced his famous formula for scattering of X-rays, which proved to be of great use in the earlier days of investigations on the nature of X-rays. This work therefore pre-supposed the essential identity of X-rays and light long before Laue's discovery of diffraction of X-rays by crystals placed it beyond all shades of doubt.

96. Revival of the Corpuscular Theory—The Quantum.—With the discovery of Hertzian wave, when the triumph of the electromagnetic wave-theory of light seemed to be complete, there rose clouds from other quarters, and in fact from an observation first made by Hertz himself. The Maxwell-Hertz theory deals more with the propagation of light in any medium, it leaves the question of generation of light, at least when atomic dimensions are concerned, very much to itself.

About the year 1890, some physicists began to study this problem from another point of view. It is well-known that when we heat a body, it begins after some time, to glow, and emit light. It just becomes visible at a temperature of 525°C and as the temperature is still further raised, shorter waves of the spectrum begin to be emitted. At 800°C the colour emitted is still dull red, at 1300° it becomes yellowish, while at about 2500°C almost all the colours appear. At the temperature of arc, the light becomes bluish white. The connection between colour and the temperature is so close that experienced people can guess the correct temperature by simply looking at the furnace. Still, the nature of colour emission to some extent depends upon the physical nature of the body. But Lummer and Wien showed that we can realise a special type of body in which the emissivity has nothing to do with the physical characteristics, but depends only on the temperature of the body. Such a body is known as a *perfectly black body,** and many experiments were performed, to find out how the intensity of light of a particular colour emitted by such a body, varies with the temperature. The results of these experiments form the basis of the theories of temperature radiation to which we now turn our attention.

In the phenomena just described heat is being converted to light. It is well-known that heat is molecular motion, so that in this process, we are disturbing the atoms, they are knocking against each other, and their "electromagnetic" constitution is being disturbed. The question arises : whether we can find out in what way the emission of light depends upon the temperature? The task is a very arduous one, for it aims at connecting two great groups of natural phenomena *viz.*, Heat and Light.

After the great success of the electromagnetic theory the path seemed to be clear enough. Let us take a black body chamber filled up with radiation, and containing some monatomic gas. Let us introduce a *via media* between radiation and the gaseous molecule. This is achieved by the introduction of Hertzian oscillaors of molecular dimensions ; these serve a double purpose: they absorb energy from the field of radiation, and transfer this energy by collision to the gaseous molecules. Planck† showed from Maxwell's theory and from the theory of Hertzian oscillators, that the following relation subsists between the energy of an oscillator and the density of radiation in the space:

---

* For a full account of the subject see Saha and Srivastava, *A Text Book of Heat*, Chap. XI.

† For the deduction of this relation see M. Planck, *Wârmestrahlung*, Chap. V, Sec. II.

$$E_\nu = \frac{3c^2 U_\nu}{8\pi\nu^2} \quad . \; . \; . \; . \; . \; . \; . \; . \; . \; . \quad (3)$$

where E_ν = energy of an oscillator.

U_ν = density of radiation of frequency ν.

The oscillator is again in equillibrium with the gaseous molecules. Hence according to the law of equipartition of energy*

$$E_\nu = 3kT \quad . \; . \; . \; . \; . \; . \; . \; . \; . \; . \; . \quad (4)$$

Hence from (3) and (4),

$$U_\nu = \frac{8\pi\nu^2}{c^3} kT \quad . \; . \; . \; . \; . \; . \; . \; . \quad (5)$$

This law, deduced in various ways and at various dates by Rayleigh, Jeans, and Lorentz is obviously wrong, as all the energy is thrown into short waves, and was experimentally found to hold good only for long waves. Planck† obtained an alternative formula which was subsequently found to be correct for all regions of wave-lengths, but for doing so he had to introduce assumptions of a very radical nature.

He assumes that the oscillators can have either a *quantum of energy* ε or some multiple of it. It cannot have any intermediate value. Thus if we have an assembly of N resonators, some of them have the energy 0, some ε, some 2ε, . . . and so on. The average energy is easily calculated to be

$$\frac{\varepsilon}{e^{\varepsilon/kT}-1} \text{ instead of } kT. \quad . \; . \; . \; . \; . \quad (6)$$

We have to make $\varepsilon = h\nu$ in order that the formula may conform to the experimental results. Planck's assumption therefore marks a radical departure. *The energy of an oscillator is supposed to be proportional to its frequency*, and it can have, at any instant, an amount of energy which is a *multiple of* $h\nu$. Since the oscillator derives its energy by absorption from the field of radiation, it follows that radiation itself is atomic in structure, *i.e.*, should occur in cells having the energy-content '$h\nu$'. At least this was the interpretation which was put by Einstein on Planck's hypothesis, and though, it was opposed to the usual concepts of light propagation, Einstein brought very strong experimental evidence in support of this view. This evidence is derived from the phenomena of *photoelectricity*, originally discovered by Hertz, and subsequently elucidated by Righi, Hallwachs and Lenard.

---

* For an account of the Principle of Equipartition of Energy see Saha and Srivastava, *Text Book of Heat*, Chap. III, §19, or any standard work on kinetic theory of gases.

† M. Planck, *Verh. d. D. Phys. Ges.*, 1900.

97. The Photoelectric Phenomena.—The subject of "Photoelectricity" arose out of an observation by Hertz* that the passage of a discharge between two electrodes connected to a source of high potential is rendered much easier when the cathode is illuminated by ultraviolet light. The phenomenon was further investigated by Righi and Hallwachs† who showed that when an insulated metallic plate is illuminated by means of ultraviolet light, it becomes positively charged. Lenard showed that the positive electrification was due to the emission of electrons from the metallic surface. He measured the ratio e/m of the charged particles and found it was identical with that for cathode particles. Ultraviolet light can therefore release electrons from a metal. The velocity of these electrons was found to be extremely small, of the order of a few volts.

Lenard‡ showed further that when the plate is illuminated by mono-chromatic light, electrons are released with all velocities, beginning with a definite maximum. The value of the *maximum energy* was found to change with frequency in a linear fashion. The time and intensity of illumination had no effect on the position of this maximum, though more electrons were released in proportion.

The nature of these results will be clearer after the study of the following description of an experiment of this class carried out with great care by Millikan§ :—

In these experiments, the metallic surface which is to be illuminated must be fresh, and free from contamination of any absorbed gas or oxide layer. As this is difficult to carry out in the open, Millikan put the whole apparatus (Fig. 3) in vacuum within a glass vessel. Three cast blocks of metallic Li, Na and K are mounted on a wheel at the centre of the vessel.

---

* H. Hertz, *Ann. d. Phys.*, **31**, 983, 1887.

† W. Hallwachs, *Ann. d. Phys.*, **33**, 301, 1888.

‡ P. Lenard, *Wien. Ber.*, **108**, 1649, 1899; *Ann. d. Phys.*, **2**, 359, 1900; *Ann. d. Phys.*, **8**, 149, 1902.

For detailed study of photoelectricity, see *Photoelectric Phenomena* by Hughes and du Bridge, 1932.

§ R. A. Millikan, *Phys. Rev.*, **7**, 362, 1916.

Any one of them can be illuminated by light coming from a monochromatic source. Photoelectrons are released and tend to pass to the collecting cylinder C which is connected to an electrometer. A retarding potential (potential which prevents the electron from passing to C) is applied between C and the alkali block, and the current between them measured. This falls gradually as the value of the retarding potential is increased, and ultimately reduces to zero value (curves in Fig. 4). The value of the potential for which this occurs is the *maximum retarding potential*. It represents the maximum energy with which electrons are released from the plate by light of frequency ν. We have

$$\tfrac{1}{2}mv^2 = \text{energy of the electron} = eV \quad . \quad . \quad . \quad . \quad (7)$$

where V= maximum retarding potential.

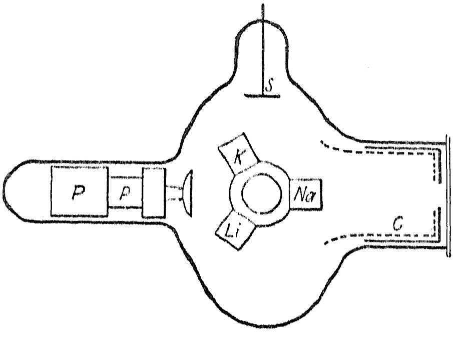

Fig. 3.
Millikan's apparatus for studying photoelectric effect.

The blocks Li, K and Na are mounted on a rotating spindle which can be set in motion by an electromagnetic arrangement from outside. P is a knife-edge. As a block comes against P, a slice is cut off, and a fresh surface can be exposed. The apparatus is kept highly evacuated. S is a copper disc which is used for compensating the contact potential difference between sodium and the collecting cylinder. The source of light was a mercury vapour quartz lamp, and it was passed through a monochromator, and rays of definite wavelengths were allowed to illuminate the alkali block. The curves in Fig. 4 (*a*) and (*b*) show how the current varies with the value of the retarding potential for different wavelengths.

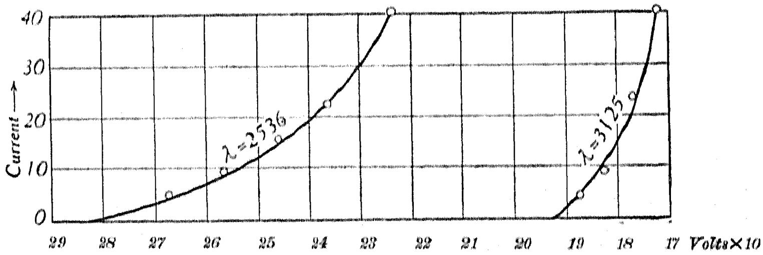

Fig. 4(*a*). Variation of photoelectric emission with retarding potential (Sodium).

Lenard and after him Millikan used the lines λ 2536, 3125, 3650, 4339, 4047 and 5461 of mercury for investigating the photoelectric emission of Na-plates. For any particular wavelength the current diminishes as the retarding potential increases, until the current falls sharply* to zero, *i.e.*, the retarding potential is just sufficient to stop the photoelectric emission. While examining the curves, the reader should bear in mind that the zero-point of voltage on the abscissa-axis has been chosen quite arbitrarily. It is due to the method of applying the voltage. A battery of high e.m.f. is shunted by a variable high resistance and one terminal is connected through the electrometer to the illuminated plate, so that different positive potentials can be imposed on it. In calculations only the difference in voltage is needed, hence the position of the zero-point is immaterial.

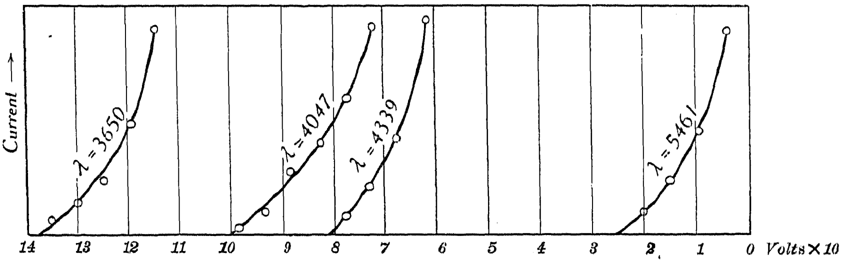

Fig. 4(b)

It was also found that the maximum retarding potential varied linearly with the frequency as shown in the above curve (Fig. 5).

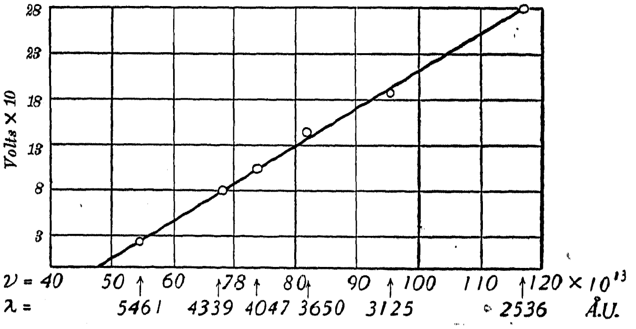

Fig. 5. Variation of retarding potential with frequency of light. (Sodium)

---

* In the recent experiments of Du Bridge, it has been found that the maximum potential is not so sharp as appears from Millikan's experiment, but changes with temperature. In fact, the sharp cut is expected only at absolute zero. This however does not interfere with our argument, as Millikan's experiment may be supposed to have been conducted at absolute zero. See however Du Bridge, *Phys. Rev.*, **32**, 961, 1928.

We obtain from the above experiments the following result, first derived by Lenard and verified by Millikan :—

$$\tfrac{1}{2}mv^2 = eV = \alpha\nu + \text{constant} \quad \ldots\ldots \quad (8)$$

The interpretation of this equation was given by Einstein* in 1905. He stated that a beam of light may be supposed to consist of corpuscles or light-cells each possessing the energy $h\nu$. When this corpuscle falls on a metal, it gives its whole energy to some electron. The electron requires certain amount of energy to be released from the atom. Let this be denoted by A. The balance will be converted to the kinetic energy of the electron. According to the law of conservation of energy, we have

$$\tfrac{1}{2}mv^2 = eV = h\nu - A \quad \ldots\ldots\ldots \quad (9)$$

or

$$eV = h(\nu - \nu_0) \quad \ldots\ldots\ldots\ldots \quad (9a)$$

If the incident light has a frequency less than ν_0, it cannot release any electrons. This is known as the "*threshold frequency*" and it has got a characteristic value for each substance. For alkalies, ν_0 corresponds to infra red light, hence they are photoelectrically sensitive to visible light up to red. A table of values of ν_0 will be found in the chapter on *Thermoions.*

The investigations on photoelectric emission therefore clearly indicate that light of frequency ν consists of corpuscles each having the energy $h\nu$. It can be easily shown that photoelectric emission is inexplicable on any other theory. For example it has been found that red light, however strong, and however prolonged the exposure may be, is incapable of releasing a single electron from an element like zinc for which ν_0 correspond to ultraviolet light. But the feeblest ultraviolet radiation of sufficiently large frequency can release the photoelectron instantaneously. The point is illustrated by the following example due to N. R. Campbell.

Suppose Q is the strength of the source. Then the light absorbed by an atom at a distance r in time t is given by

$$E = \frac{Q}{4\pi r^2} \cdot \pi a^2 t \quad \ldots\ldots\ldots\ldots \quad (10)$$

where a = radius of the atom.

We can put E slightly greater than $\tfrac{1}{2}mv^2$ the energy with which the photoelectrons are emitted, and can calculate the time t required for

---

[*] A. Einstein, *Ann. d. Phys.*, **17**, 132, 1905; **20**, 199, 1906.

absorption of this energy by a source Q. Q may be so feeble that t may be as large as 45 minutes. But experiments showed that the release of the photoelectron was instantaneous. So the law of continuous distribution of radiant energy in space implied in (10) is false. The light-corpuscles having the energy-quanta $h\nu$ cannot be further subdivided. The number of quanta passing at a distance r per unit area varies inversely as the square of r.

The photo-electric experiments can therefore be regarded as crucial tests in favour of the new corpuscular theory of light, according to which each corpuscle of light has the energy $h\nu$. 'h' is known as *Planck's universal constant.* Its value, obtained from photoelectric experiments is

$$h=6{\cdot}577\times10^{-27} \text{ ergs. sec.}$$

This can be obtained in the following way. The straight line in the figure 5 cuts the axis of ν at about $\nu\sim48.10^{13}$. Since it is of the form

$$V=\frac{h}{e}\nu+A,$$

we at once get from the figure

$$\frac{h}{e}=1{\cdot}375.\quad10^{-17}$$

Using $e=4{\cdot}774.10^{-10}$ e. s. units, we get

$$h=6{\cdot}577.\ 10^{-27}.$$

98. Further Evidences in favour of the Quantum Theory of Light.*—The view that light of frequency ν can be supposed to consist of particles having the energy content '$h\nu$' has received confirmation from many other directions, and has now become fundamental for atomic physics, as the reader will subsequently find for himself. Einstein further postulated that a light-particle of energy $h\nu$ may be supposed to possess the mass $h\nu/c^2$, and the momentum $h\nu/c$ in the direction of propagation. These results follow from his law deduced from the principle of relativity that mass and energy are equivalent, being connected by the relation $E=mc^2$. It can further be shown to give a satisfactory explanation of the ancient problem of the orientation of tails of comets.

---

* For a fuller account of the subject treated in this and the following sections of this chapter see *Astronomy*, Russell, Dugan and Stewart, II.

99. Pressure of Light.—Astronomers had from very old times observed that when a comet sweeps past the perihelion of its orbit, it develops a tail in addition to its central nucleus, but the orientation of its tail continuously changes so as always to be opposite the sun as shown in Fig. 6. These facts receive a ready explanation if we suppose that when at a distance from the sun, the comet consists of a central nucleus alone, probably composed of gaseous matter. When it nears the sun, strong light from the sun falls on the gaseous envelope, and exerts a *pressure* on the particles composing it. As a result the particles are impelled far into space in a direction opposite to the sun's rays and form the tail.

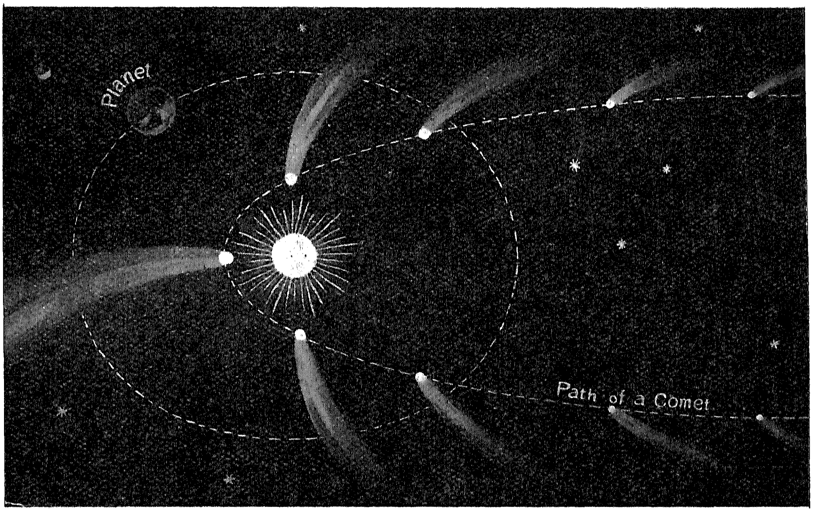

Fig. 6. The tails of a comet in different positions on its orbit.

But the hypothesis that light can exert pressure on material bodies did not receive experimental verification for a long time. The failure of the early experiments was largely due to the ignorance of the investigators about the correct magnitude of the light-pressure. Maxwell was the first to throw light on this point. He deduced from the electromagnetic theory of light, that the magnitude of the pressure should be I/c, where I=the intensity of light. The occurrence of the large quantity c in the denominator makes light pressure extremely small, for example, the pressure of sunlight is only 5×10^{-5} dynes per cm.^{2} Very fine apparatus is needed to detect such a small quantity, and still more elaborate arrangements are needed to get rid of various spurious effects. It was only in 1900 that Lebedew* first succeeded in demonstrating experimentally the pressure of light.

But Maxwell's proof of the existence of light-pressure had one limitation. It applied only to obstacles whose dimensions are larger than the wavelength of ordinary light. As atoms are much smaller than light-waves, it follows that his proof cannot be extended to atoms. The tails of comets therefore remain unexplained unless we suppose that they are formed of cosmic dust, *i.e.*, of particles of about 10^{-5} cm. in linear dimensions. But the observations of cometary spectra show that the tails are composed of gases.

100. Pressure of Light from the Quantum Theory.—This difficulty is removed by the quantum theory. For let us suppose that a light quantum $h\nu$ falls on the atom and is absorbed by it. In this process a momentum of $h\nu/c$ will be imparted to the atom in the form of a forward kick. The action may be likened to that of a bullet on a target. When the bullet gets embedded on the target, the momentum is imparted to the latter. The resultant pressure on the assembly of atoms is $\Sigma(h\nu/c) \times$ number of atoms receiving the kick × number of times each atom receives the kick per unit time, and this is I/c, where I is the amount of light absorbed by the atoms on unit surface in unit time. We thus arrive at the same result as Maxwell. If there is no absorption there can be no pressure, in agreement with Maxwell.

101. The Selective Radiation Pressure.—Thus the quantum idea of light not only removes all doubt regarding the existence of radiation pressure on atoms, but it yields us a sounder view regarding the nature of such pressure. It says that such pressure is exerted only if the atom is capable of *absorbing the radiation.* Thus if white light is incident on Na-vapour, it is only the D_1 and D_2 light (and certain other lines, see Chap. VIII) which can exert pressure on the Na-atoms. The action is therefore *Selective.*

These results have been applied with great success to explain the formation of "stellar atmospheres." We illustrate the case with reference to the sun. The sun is supposed to consist of the *photosphere*, a central condensed core which gives white light like an

---

* Lebedew, *Ann. d. Phys.*, 6, 438, 1901.

For details of these experiments, see *Treatise on Heat* by Saha and Srivastava, intensely heated solid body, surrounded by a dilute atmosphere (technically known as the *Chromosphere*) containing almost all elements known on the earth in the vapour form. The gases of the chromosphere (or the lower part of it which is called the *Reversing Layer*) gives rise to the Fraunhofer Spectrum by the *Selective absorption* of the outflowing stream of white radiation. A question which puzzled the astrophysicists before 1920 was the great height reached by some heavy atoms like Ca. For according to Maxwell's law, the number of atoms of an element like Ca at a height h is given by $n=n_0e^{-mgh/k\theta}$. As g on the sun is about 27 times g on the earth, and $\theta=6000°$K, it can be easily shown that an element like Ca cannot reach to greater heights than say 10 km. over the photosphere. But observations show that Ca rises to as great heights as 14000 km., as revealed by its chief characteristic lines H and K. This behaviour is not confined to Ca, but is shared by Sr, Fe, Na and many other elements possessing strong absorption lines.

The phenomenon is thus explained: Let us suppose that a pulse $h\nu$ corresponding to λ 3968 (H) or λ3933 (K) of Ca (rather of Ca$^+$, *vide* Chap. IX) hits a Ca$^+$-atom. The increment in upward velocity imparted to it is $h\nu/mc=2{\cdot}5$ cm./sec. But when Ca$^+$ absorbs this radiation, it is excited to higher state which is however unstable. After an interval of 10^{-8} sec. it reverts back to the original state and is ready to receive another pulse. So the acceleration imparted to the Ca$^+$-atom in a second is $\frac{h\nu}{cm}\cdot A$, where A is the number of times the Ca$^+$-atom is hit by the quantum of H and K-lines. As A is very large (nearly 10^8), the upward acceleration due to selective radiation pressure becomes very large, and probably exceeds the solar gravity. So the atoms of Ca$^+$ can reach great heights.

The idea of "Selective Radiation Pressure" is of great use in astrophysics and original sources* should be consulted to obtain a better idea of it.

102. The Compton Scattering.—The theory that light consists of discrete particles having the energy $h\nu$ and the momentum $h\nu/c$ has received a very strong experimental support from a number of elegant experiments performed by A. H. Compton† of Chicago. We have already mentioned that X-rays are a kind of light having, on the average, thousand times larger frequency than ordinary light. According to the light-atom view, they have therefore thousand times more energy than quanta of visible light. What happens when the X-ray quanta fall on free electrons? We can regard the process as one of collision between two particles. It is clear that in this process the electron will receive some energy from the photon (light quantum) and be thrown forward. Thus the photon will be deprived of a part of its stock of energy. Since according to the atomic view of light, the frequency is proportional to the energy, the frequency of the scattered photon will be diminished, or it will have a larger wavelength. Compton* and simultaneously Debye† showed that exact mathematical expressions for change of wavelength and other quantities can be obtained by applying the well-known laws of conservation of energy and of linear momentum.

---

* M. N. Saha, *Nature*, 1921. E. Milne, *Handbuch d. Astrophysik*, III (1) Chap. 2.

† A. H. Compton, *Phil. Mag.*, **21**, 715, 1923; **22**, 409, 1923; *Bull. Nat. Res.*, No. 20, 16, 1922.

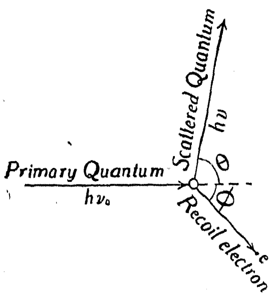

Fig 7. Scattering of light quanta by electron.

Fig. 7 illustrates Compton scattering phenomena. The primary beam consisting of photons having the energy $h\nu_0$ and momentum $h\nu_0/c$ in the direction of motion encounters an electron which is supposed to be free. Let us suppose that the electron is thrown forward with a velocity v, at an angle φ to the original direction of motion of the photon. The photon is scattered at an angle θ, with the energy $h\nu$.

Applying the principles of conservation of energy, we have

$$\left.\begin{array}{c}\text{Total energy}\\ \text{before}\\ \text{collision}\end{array}\right\} = \left.\begin{array}{c}\text{Energy of the}\\ \text{electron}\\ \text{after collision}\end{array}\right\} + \begin{array}{c}\text{Energy of}\\ \text{photon}\\ \text{after collision}\end{array}$$

$$h\nu_0 = \tfrac{1}{2}m_0v^2 + h\nu \quad . \; . \; . \quad (11)$$

Applying the law of conservation of linear momentum parallel to the original direction of flight of the quantum, as well as perpendicular to it, we have the two other equations :

$$\left.\begin{array}{c}\text{Impulse of photon}\\ \text{in the original}\\ \text{direction}\end{array}\right\} = \left.\begin{array}{c}\text{Impulse of}\\ \text{the electron}\end{array}\right\} + \begin{array}{c}\text{Impulse of photon (after}\\ \text{collision) in the original}\\ \text{direction of photon.}\end{array}$$

---

* A. H. Compton, *Phys. Rev.*, **21**, 207 and 483, 1923; *Bull. Nat. Res.*, No. 20, 19, 1922.

† P. Debye, *Phys. Zeits.*, **24**, 161, 1923.

or $$\frac{h\nu_0}{c} = m_0 v \cos\varphi + \frac{h\nu}{c}\cos\theta \quad . \quad . \quad . \quad . \quad (12)$$

Impulse normal to the original direction of flight = Impulse of the electron + Impulse of photon (after collision) perpendicular to primary rays

or $$0 = m_0 v \sin\varphi - \frac{h\nu}{c}\sin\theta \quad . \quad . \quad . \quad (13)$$

There are three equations, and four quantities to determine ν, v, θ, φ. One of these must therefore be taken as known, and others expressed in terms of it. Let θ be this quantity. Then we have on eliminating φ

$$\left(\frac{h\nu_0}{c}\right)^2 + \left(\frac{h\nu}{c}\right)^2 - 2\,\frac{h\nu_0}{c}\,.\,\frac{h\nu}{c}\cos\theta = m_0{}^2 v^2 \quad . \quad . \quad (14)$$

With the aid of (11), we obtain

$$\nu = \nu_0 - \frac{h}{m_0 c^2}\nu_0{}^2\,(1-\cos\theta)$$

$$v^2 = 2\left(\frac{h}{m_0 c}\right)^2 \nu_0{}^2\,(1-\cos\theta)$$

In deducing these expressions we have assumed that

$$h\nu_0 << m_0 c^2$$

This condition is fulfilled in the case of X-rays, but there may be cases (γ and cosmic rays) where this may not hold good.

Let $\triangle\nu$ be the change in frequency. We have

$$\triangle\nu = \frac{h\nu_0{}^2}{m_0 c^2}(1-\cos\theta) \quad . \quad . \quad . \quad . \quad . \quad . \quad . \quad . \quad . \quad (15)$$

and the energy received by the electron

$$\tfrac{1}{2} m_0 v^2 = h\,\triangle\nu = \left(\frac{h\nu_0}{c}\right)^2 \frac{1-\cos\theta}{m_0} \quad . \quad . \quad . \quad . \quad (16)$$

In actual experiments, the change in wavelength of the photon is observed. Let us have

$$\triangle\lambda = \lambda - \lambda_0$$

$$= -\frac{c}{\nu^2}\,\triangle\nu = \frac{c}{\nu_0{}^2}(\nu_0 - \nu)$$

Now $\frac{h}{m_0c}$=·0242 Å. units. Hence

$$\triangle\lambda = \frac{h}{m_0c}(1-\cos\theta) \quad . \; . \; . \; . \; . \; . \; . \; . \; . \quad (17)$$

$$= \cdot 0242\,(1-\cos\theta) . \; . \; . \; . \; . \; . \; . \; . \; . \; . \; . \quad (17a)$$

Also $$\triangle\lambda = \frac{\cdot 2h}{m_0c^2}\sin^2\frac{\cdot\theta\cdot}{2} = 2\,A\,\sin^2\frac{\theta}{2} \quad . \; . \; . \; . \quad (18)$$

where A=·0242 Å. U.

Compton showed that the relation (17) can be put to an experimental test if the wavelength of scattered X-radiation be accurately measured. An idea of scattering of X-rays has already been given. When a beam of X-rays fall on matter, they are scattered sideways. The subject was mathematically treated by J. J. Thomson (*vide* Chap. VI) who proceeded on the hypothesis that X-rays are electromagnetic waves which, falling on the electrons of atoms give them an acceleration parallel to the field. The accelerated electrons radiate energy on all sides which constitute scattered light. The scattering formula of Thomson (*vide* VI, § 112) was experimentally tested by Barkla, and led to the first rough enumeration of the number of electrons contained in an atom (*vide* Chap. VI).

In his experiments, Barkla* noticed that the scattered X-rays undergo a certain amount of softening or increase in wavelength. Compton argued that if the scattering atom be sufficiently light, then its electrons are bound to the atom with energy which may be very small compared to the energy carried by the photon; under such conditions, the electrons may be regarded as *free*, and the change of wavelength can be calculated as given in the text. He devised an ingenious apparatus to measure the change in wavelength at different angles of the modified radiation (X-ray photons modified by collision), and found that relation (17) is completely verified.

103. Experimental Verification of Compton's Theory.—The change in wavelength of the scattered radiation was verified by means of the apparatus in Fig. 8.

R ... Rontgen ray tube, A being the anticathode.
S, S ... lead slits to get a parallel beam.

---

* C. G. Barkla, *Phil. Mag.*, **7**, 550, 1904.

D ... scattering substance.

S′, S′... slits in the path of the scattered beam. By adjusting them, rays scattered at any angle θ can be spectroscopically examined. Thus in the figure $\theta = 90°$.

O ... crystal.

I ... ionisation-chamber.

E ... electrometer.

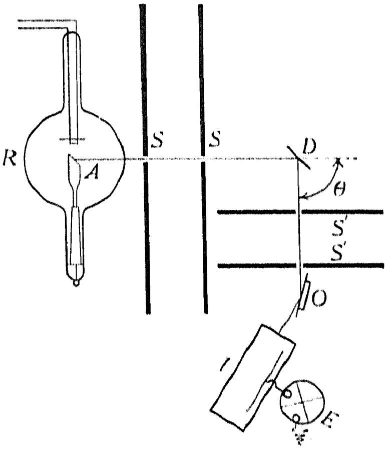

Fig 8. Apparatus for studying Compton effect.

The anticathode was of molybdenum which gave the characteristic K lines of Mo, *viz.*, K_α, K_β strongly on a continuous background.

The beam scattered from D which was a slab of graphite was analysed by the crystal and the intensities measured by the electrometer. The intensities were plotted against the glancing angles. The results are shown in curve in Fig. 9.

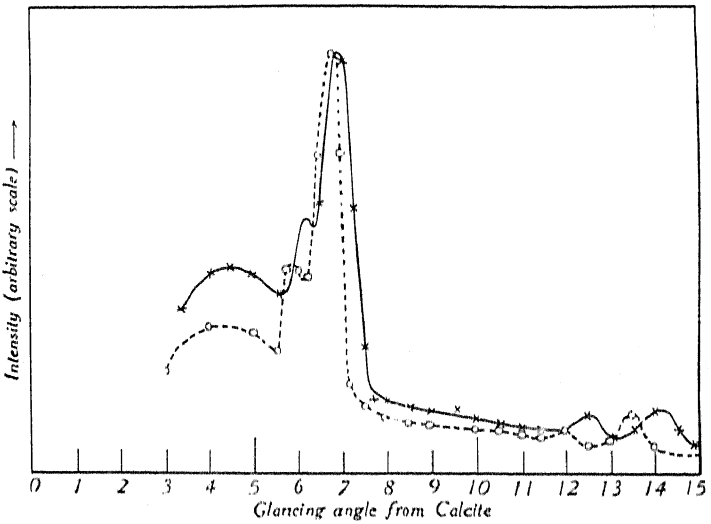

Fig. 9.

The broken line represents the intensity of the primary beam of X-rays from Mo. The first smaller maximum is due to K_β, the second and higher maximum is due to K_α (this is not resolved).

The wavelength of the K_α-line as measured from the glancing angle is $\lambda = \cdot708$ Å. units. The other parts of the curve correspond to general X-radiation with which we are not concerned. The full line represents the intensity of the beam scattered at 90°. The whole spectrum, including the maxima indicating K_α and K_β are displaced. Measurement of the glancing angle showed that the wavelength of modified $K_\alpha = \cdot730$ Å. We have therefore $\Delta\lambda = \cdot022$, while according to theory it ought to be ·024. The agreement is therefore perfectly satisfactory.

Later Compton, Kallman and Mark, Dauvillier and De Broglie and others substituted the photographic method in place of the ionisation chamber, and experimented with characteristic rays of different elements and different radiators. Their results are shown in Table 2. The photographic method is very laborious and sometimes exposures extending over 90 hours are needed.

Table 2.

Incident radiation	λ_0 (Å. U.)	$\Delta\lambda$ (Å.U.) at $\theta = 90°$	Observer
Wo K	0·203	~ ·0240	De Broglie, P. A. Ross Duane and Allison
Ag K	0·500	·0223	De Broglie, Hagen
Mo K	0·708	·0242	Compton
Au L	1·100	·0240	Dauvillier
Zn K	1·436	·0238	Kallmann and Mark
Cu K	1·541	~ ·0240	Dauvillier

Compton was not satisfied with a bare verification of his theory, but proceeded to put to test the other implications of his theory. A full account of these cannot be given here for which original sources must be consulted. A few leading results are given:

(1) *Change of Wavelength at Different Angles.*

According to (18), $\Delta\lambda$ should vary as $\sin^2 \theta/2$. This was verified* by using a Mo-tube, and a graphite radiator. For a given angle of scattering the intensity of different wavelengths in the scattered beam was measured by varying the glancing angles, and the position of the displaced K_a-line was determined from the position of the intensity maximum.

---

* A. H. Compton, *Phys. Rev.*, 22, 409, 1923.

The apparatus used is given in Fig. 10. T is the Mo-anticathode, and R the graphite radiator. The primary X-rays from T scattered at R at angles θ pass through the slits S_1 and S_2, and then to the crystal O of the Bragg Spectrometer I. In this way the wavelength scattered at an angle θ can be measured. The angle θ may be changed simply by shifting the X-ray tube, and the spectrum of primary radiation may be obtained by removing the radiator and receiving the direct beam, without disturbing the slits or the crystal. The intensity of the scattered beam for various glancing angles was thus known.

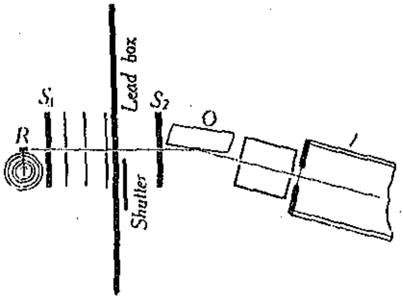

Fig. 10. The experimental arrangement.

The results obtained are shown in Fig. 11. The Kα-molybdenum line has been scattered at 45°, 90° and 135°. The upper curve A shows the spectrum of primary rays, the curves below, B, C, D that for rays scattered at 45°, 90°, 135°, respectively. It will be noticed that the primary wavelength appears in every case at exactly the same position. But in B, C and D a second wavelength occurs at a glancing angle which increases rapidly with larger angle of scattering. Calculation shows that $\Delta\lambda$ is exactly proportional to $\sin^2 \theta/2$.

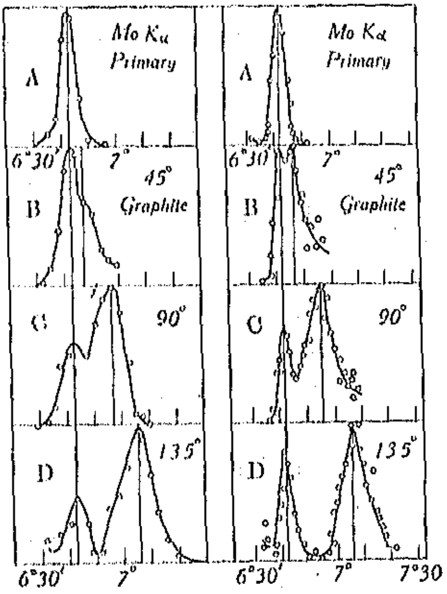

Fig. 11. Graphical representation of scattered wavelength.

(2) *Modified and Un-modified Lines.*

It has been already mentioned that the Compton scattering is due to free electrons. But in the scattering material, all electrons are bound, being attached to some atoms. They can be regarded as *free* only when the atom is light, and energy of binding of electrons is very small compared to the energy carried by the photon. But there may be atoms where this condition is only partially fulfilled, *i.e.*, the outer electrons may be regarded as free, whereas inner electrons are bound. In such cases, the inner electrons show Compton scattering without change in wavelength. So there will be two beams: (1) a *modified beam* showing increase in wavelength, (2) an *unmodified beam.* The comparative intensities of the two beams will vary from element to element. For light atoms all scattered radiation is modified; for heavy atoms, there are practically no modified rays. These inferences were verified by Ross,* and are illustrated in Plate III, Fig. (12-V). In this the scatterings for the four different elements C, Al, Cu, Ag at the same angle 90° have been compared. It will be seen that as we pass from the lighter to heavier elements along the series, the intensity of the scattered radiation remarkably diminishes, while the intensity of the primary radiation gradually increases.

A beautiful series of microphotograms of the intensity distribution of modified and unmodified lines for elements from Li to Cu has been obtained by Woo.†

λ-rays ($\lambda = 10^{-11}$ cm.) have about 100 times the frequency of medium X-rays, and hence relative to them, electrons of almost all atoms may be regarded as free. γ-rays show no unmodified lines. This was observed by Ross,‡ and also by Compton.§

(3) *Experimental Evidence regarding Recoil Electrons.*

Compton and Simon‖ proved the existence of recoil electrons by using the Wilson cloud-chamber method of photographing the track of electrons.

The distribution of recoil electrons and scattered photon in different directions is shown in Fig. 13.

The radius of the dotted semicircle denotes the energy of the primary quanta $h\nu_0$ and the arrow to the extreme left denotes the direction of incidence. The full curve in the upper half of the

---

*P. A. Ross, *Proc. Nat. Acad.*, **10**, 304, 1924.

† Y. H. Woo, *Phys. Rev.*, **27**, 122, 124, 1926. See also Compton's *X-rays*, p. 268, Fig. 110.

‡ P. A. Ross, *Science* **57**, 614, 1923.

§ A. H. Compton, *Phil. Mag.*, **41**, 760, 1921.

‖ A. H. Compton and W. Simon, *Phys. Rev.*, **25**, 306, 1925.

figure shows the distribution of energy of the scattered quanta $h\nu$, and the curve in the lower half shows that of the recoil electron. The amounts of scattering at different angles marked 1, 2, . . . 10 are indicated by the radius vectors starting from the centre of scattering, and the corresponding energies E of the recoil electrons are represented in the lower figure by radius vectors of same numbers 1, 2, . . . 10. It will be seen that in the direction $\theta=0$, $h\nu=h\nu_0$, and then as θ increases, $h\nu$ diminishes and it reaches minimum value ($\Delta\lambda=2A_0$) at $\theta=180°$. The distribution of energy of the recoil electron is complementary to that of the scattered photon.

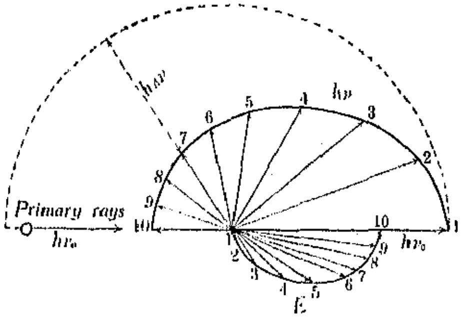

Fig. 13. Energy distribution of scattered photon and recoil electron.

Compton arrived at the idea of this experiment from an examination of the tracks of γ-rays and of hard X-rays obtained by C. T. R. Wilson* and Bothe†. The latter had sent a beam of γ-rays through a cloud chamber, and photographed the tracks. The γ-rays when they hit the atoms and molecules in the cloud chamber release electrons with considerable velocities which passing through the atoms ionise them. The track of ionisation is visible in the curved paths shooting out from the direction of the main beam. Compton observed from a scrutiny of these photographs that some paths of these secondary electrons were short, others long. The two types of tracks can be clearly seen from the photograph in Fig. 14, which

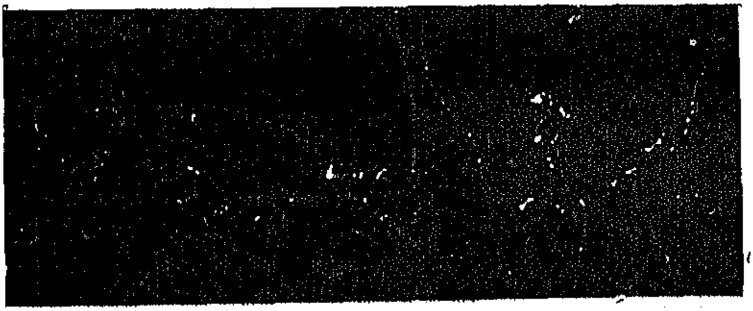

Fig. 14

---

* C. T. R. Wilson, *Proc. Roy. Soc. A.*, **104**, 1, 192, 1923.

† W. Bothe, *Zs. f. Phys.*, **16**, 319, 1923.

shows the tracks of the hard X-rays. He concluded therefore that two processes were at work. A γ-ray may release an electron either by recoil (as in Compton effect), or it may give the whole of its energy to some electron which emerges out with the velocity $\frac{1}{2}mv^2 = h(\nu - \nu_0)$, as in photoelectric effect. These may be called "Photoelectrons." The tracks of these two kinds of electrons will be characteristically different.

104. Geiger and Bothe's Experiment.—Though Compton's experiments form the most unmistakable proof that light consists of swarms of particles with the energy $h\nu$, and linear momentum $h\nu/c$ along the direction of flight of photons, and that both these quantities are retained by the photon until it encounters matter, yet the difficulty of reconciling this view with the wave theory of light is so great that attempts have been made to show that Compton's results may be deduced on alternative grounds. According to a view advocated for a time by Bohr, Kramers and Slater,* the conservation laws which were assumed by Compton were interpreted as being of statistical nature, *i.e.*, they were supposed to hold good when a large assembly of particles was concerned. For individual processes they were not supposed to be correct. But this view was negatived by the experiments of Geiger and Bothe† who showed that the laws held good for each unit mechanism and not merely for the average. This they proved by showing that the scattering of the photon and ejection of the recoil electron are simultaneous processes. This should be the case on the quantum theory, while on the statistical view of the phenomena, there should be no correlation between the two.

The principle of the apparatus is illustrated in Fig. 15.

The apparatus consists of two Geiger-point-counters P, P (*vide* I, § 13) placed opposite each other with the wires in the same line facing each other. The primary beam of X-rays is passed between the two counters, and is scattered by H_2-gas. In accordance with the theory given in § 102, the scattered quanta go to one side, the electrons to the other side as represented in Fig. 15. One counter (to the left) which is closed by a thin Pt-foil (for preventing the passage of electrons) detects only scattered photons and may be called the photon-counter. The other is exposed to the recoil electrons, as well as the photons scattered on this side. This may be called the electron-counter.

---

* N. Bohr, H. A. Kramers, J. C. Slater, *Phil. Mag.*, **47**, 785, 1924; *Zs. f. Phys.*, **24**, 69, 1924.

† W. Bothe, and H. Geiger, *Zs. f. Phys.*, **26**, 44, 1924; **32**, 639, 1925; *Naturwiss.*, **20**, 440, 1925.

Whenever a photon enters the photon-counter there is a sudden kick in the recording electrometer due to the photoelectrons emitted by it from the Pt-foil. But the kicks registered in the electron-counter are directly due to the recoil electrons. The impulses of the counters were recorded photographically on a moving film. Bothe and Geiger observed that over a total period of 5 hours, there were 66 coincidences, that is, the emissions of the electron and of the quantum were simultaneous processes. They also calculated that on the statistical theory, the probability for such a coincidence was 1 in 400,000.

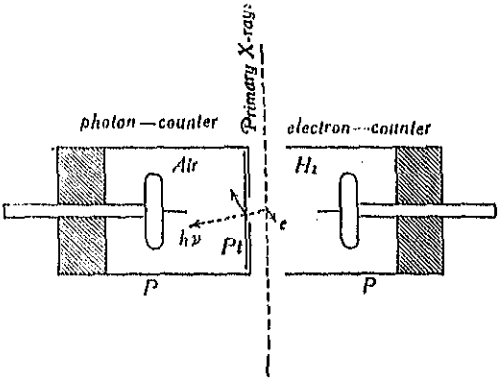

Fig. 15. Geiger and Bothe's apparatus.

Much work has been done recently on the further development of Compton effect. But we shall not elaborate the subject here and defer it to a later chapter.

Further evidences regarding the quantum view of light have been obtained from the phenomena of combination scattering (the *Raman Effect*) in which the collision of light quanta with molecules causes a modification of the quantum depending on the vibration characteristics of the molecule. This subject will be treated in detail in Chap. XXII.

The picture of light represented here is however not complete, as it fails to take account of the phenomenon of *polarisation*, and the electromagnetic aspect of light. We shall discuss this question later on.

CHAPTER VI

RÖNTGEN RAYS

105. Story of Their Discovery.—Röntgen-rays were discovered by W. K. Röntgen, professor of physics in the university of Würzberg in Bavaria in the year 1895. While working with a highly evacuated cathode ray tube, he noticed that a screen containing a deposit of barium platino-cyanide placed accidentally in the vicinity began to glow with fluorescent light. He was thus aware of the generation of a new kind of radiation whose origin was traced to the sides of the glass tube where the cathode rays impinged. The most remarkable thing about these rays was that even if a partition of wood or of other substances which are usually opaque to visible light was placed between the tube and the screen, the fluorescence continued. The rays were therefore quite different in nature from any hitherto known, as they possessed the property of passing through substances which are usually classed as opaque. It was found that the rays blackened a photographic plate even when these were wrapped in black paper.

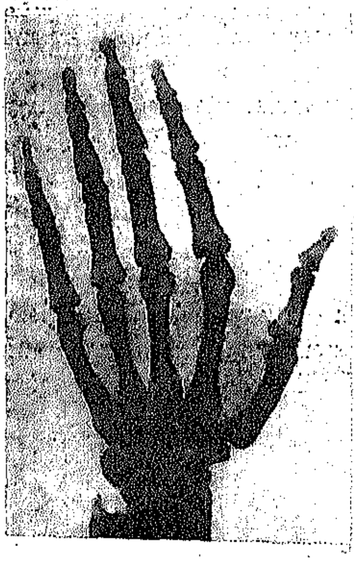

Fig. 1. A Röntgen-photograph of hand.

Röntgen was aware of the tremendous importance of these rays for surgery and medical therapy, and gave to the world the first Röntgenograph of the human hand in which the bones were marked out from the flesh (Fig. 1). In this chapter we shall deal with the physical nature of the new rays.

Röntgen found that the rays could not be deflected by a magnet. Hence they could not be corpuscular but were electromagnetic in nature like the ordinary waves of light. But he encountered great difficulty in establishing their identity with light. For all attempts to observe the usual properties associated with light, namely, reflection at a plane surface, refraction in matter, interference, diffraction and polarisation yielded only negative results. For seventeen years the nature of the rays presented great difficulties, till Laue in 1912 proved decisively that the Röntgen-rays were a kind of ultraviolet light having wavelengths of the order of 1 A.U., *i.e.*, thousand times shorter than that of ordinary ultraviolet light. The Röntgen rays were also called *X-rays* owing to their unknown nature.

106. Investigations on the Nature of X-rays between 1895 and 1912.—During all these years many important experiments were performed for elucidating the nature of X-rays. In 1896, J. J. Thomson and others observed that these rays rendered the air or gas through which they passed conducting. X-rays thus possess the property of ionising gases like cathode rays. This property is utilised for measuring their intensity and performing important experiments on absorption (*vide supra*).

It was gradually found that X-rays were produced as a result of the impact of high speed cathode particles on the metallic target (anticathode). The knowledge of this fact gave rise to the common form of X-ray tubes usually seen in the market.

107. Description of a Common X-ray Tube.*—An ordinary X-ray tube is shown in Fig. 2. It consists of a concave cathode C usually made of aluminium. Aluminium is used as it sputters least. The anticathode T is generally in the form of a circular plate inclined at

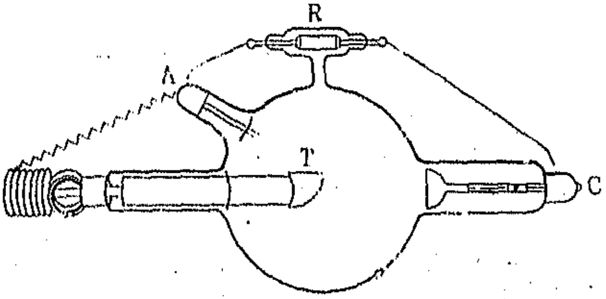

Fig. 2. A common X-ray tube.

---

* Other types of X-ray tubes used in modern investigations will be described in a later section.

an angle of 45° to the beam of cathode rays. It is usually provided with a backing of heavy copper tube which is sometimes hollow and cooled with water for carrying away the heat. The distance between the cathode and the anticathode is such that the cathode ray beam is focussed by the concave cathode as sharply as possible on the anticathode. Sometimes after continuous run the tube becomes hard, that is to say, the discharge refuses to pass. This is due to the absorption of residual gas by the walls of the glass vessel. To cope with this situation a piece of platinised asbestos is kept in a pocket at R; this when heated evolves some gas which is ionised by cathode rays and facilitates the passage of discharge. This heating is caused automatically in the following way: When the discharge refuses to pass between anticathode and cathode, it passes through the pocket R, because two wires lead out from it within short distance of anode A and cathode C. The spark jumps on to these wires and the resulting discharge heats the asbestos. The function of anode A has not been very clearly understood, but it is said that it stops the current from flowing in the reverse direction. This process is known as softening of the tube. At the present time a valve is attached in place of R through which small quantities of air may be allowed to leak in.

Stokes* and Wiechert† suggested that X-rays were electromagnetic waves which were generated due to the sudden stoppage of high velocity cathode rays on the target. A very small fraction of the energy (*vide supra*) is found to be converted to X-rays the rest of it being converted into heat. Marx‡ undertook an elaborate series of experiments to find out the velocity of propagation of X-rays. He found that it had the same value as the velocity of light. According to some critics the result was not however unambiguous.

108. Interaction of X-rays with Matter.—It appears that Röntgen himself was aware of the fact that when X-rays are incident on matter, they could give rise to secondary radiations of several kinds.

In 1900 Dorn discovered that when X-rays fall on matter, they eject cathode rays. This is analogous to the photoelectric effect. In 1905 Barkla obtained unmistakable proofs of secondary X-rays (*i.e.*, X-rays emitted by matter which are excited by the passage of a beam of primary X-rays), and concluded that the waves were transverse in nature.

---

* Stokes, *Proc. Manch. Lit. Phil. Soc.*, 1898.

† E. Wiechert, *Sitzungsber. d. Phys. Ges.*, 1894.

‡ Marx, *Ann. d. Phys.*, **20**, 677, 1906.

The result of interaction of X-rays with matter is shown in the following diagram (Fig. 3). X-rays coming from the anticathode T of an X-ray tube pass through the slits S, S and fall on the matter R. The various secondary emission phenomena which they can give rise to by interaction with R are indicated against the arrows. The arrows do not indicate the direction of emission, which on the other hand spreads more or less in all directions.

The scattering of X-rays can be easily demonstrated by putting a piece of matter, say a paraffin block in the path of the X-ray beam. It is found that if a fluorescent screen be placed anywhere in the surrounding space, it begins to glow showing that X-rays are scattered by the block on all sides. The phenomenon is analogous to the scattering of light by the atmosphere which gives rise to the blue of the sky. The phenomenon of scattering was investigated in a series of classic memoirs by Barkla,* of which an account is given in § 110.

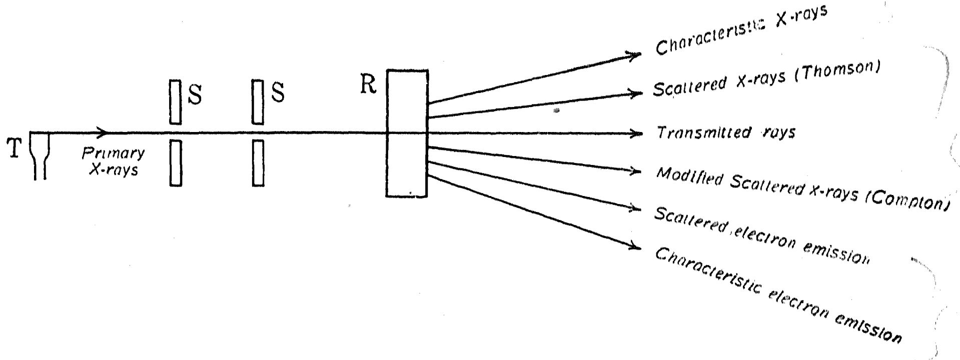
T
Primary X-rays
S
S
R
Characteristic X-rays
Scattered X-rays (Thomson)
Transmitted rays
Modified Scattered X-rays (Compton)
Scattered electron emission
Characteristic electron emission

Fig. 3. Interaction of X-rays with matter.

109. Emission of Characteristic Radiation.

—The phenomenon of fluorescence is well-known in optics. If salts of some substances in solution be exposed to sunlight and then brought in the dark, they begin to glow with light characteristic of the salts. Thus a solution of quinine sulphate is seen to glow with blue light, an alcoholic solution of chlorophyl with red light, etc. This property is shown necessary, any strong source of light would do. to be noted is the fact that the nature of the very little to do with the nature of the light imulated light is characteristic of the substance, red by Stokes that the *exciting light must* , *must have larger frequency than the light* known as *Stokes' Law of Fluorescence.* The law was not understood for a long time, but the ht makes it absolutely clear. For the law simply hat the energy of the exciting quantum must be gy of the quantum excited.

---

* C. G. Barkla, *Proc. Roy. Soc. A*, **77**, 247, 1906.

† Fluorescent screen contains a layer of barium platino-cyanide, which begins to glow (or fluoresce) as soon as X-rays fall on it. This must be distinguished from the fluorescence described in § 109 where X-rays are emitted when primary X-rays fall on matter.

analogous to this was discovered by Barkla and the region of X-rays. They found that when o a primary beam of X-rays, then in addition to which does not differ in nature from the primary diations of a quite different type are emitted by trast to scattered radiation these rays are charac- r which has been exposed to primary X-rays, and n as *characteristic radiation.* The only provision radiation must be sufficiently harder than the nerated by fluorescence. If they are softer, no tion is excited. Barkla and Sadler perceived in nalogy to Stokes' Law in the region of optical matter of fact, it is merely Stokes' Law applied

.

nena depicted in Fig. 3 due to encounter of matter characteristic electron emission, and scattered The former is analogous to photoelectric effect. s they fall on matter liberate electrons according $mv^2 = h(\nu - \nu_0)$. The phenomenon has already been V. The Compton scattering, discovered by A. H. a softening effect of the incident radiation due to t imparting a part of its energy to the electrons. s energy from the quantum, this electron appears This emission is known as scattered electron been already treated in Chapter V.

---

nd Sadler, *Phil. Mag.*, **16**, 550, 1908.

110. Study of Absorption of X-rays.—The most important feature which distinguishes X-rays from other radiations is their high penetrating power. But it was early found that X-rays of different qualities differ widely in their penetrating power. If the potential applied to the X-ray tube is small, the rays which are emitted are not very penetrating, while if the potential is made large, rays of great penetrating power can be produced. The potential can be roughly measured by placing a spark gap between two metal spheres in parallel with the X-ray tube; the length of the gap between the spheres when a spark just passes determines the potential across the X-ray tube. In radio-therapy, and metal-radiography potentials as high as 600 KV are used. Rays of great penetrating power are also necessary when heavy metal castings are examined for flaws in their structure. Penetrating rays are also called *hard rays*, and non-penetrating rays are called *soft rays*. We shall see later on that the shorter the wavelength of X-rays, the harder they are.

The absorption of X-rays can be quantitatively studied with the aid of the following apparatus (Fig. 4).

X-rays are generated at the target T. The rays are restricted to a narrow beam by means of a lead slit S and allowed to enter an ionisation chamber I. On opening a key in the circuit (not shown) discharges pass through the electrometer which shows a deflection. Two deflections are obtained, one with the absorbing material A, in the path of the beam, and the other without it. The ratio of the two deflections is taken as the ratio of the intensities of X-rays entering the ionisation chamber in the two cases; and this gives a measure of the absorbing power of the material. The procedure is repeated with X-rays of different hardness. The results are discussed in the following section.

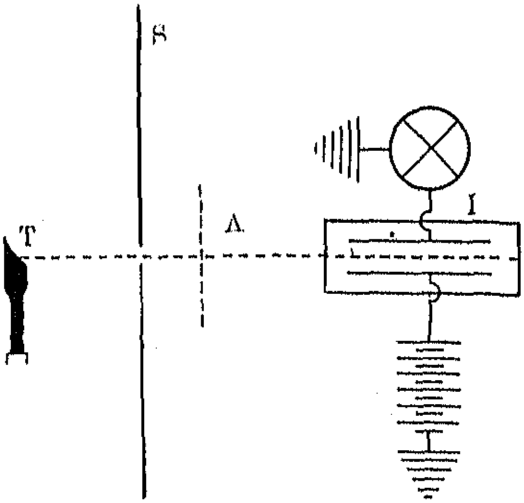

Fig. 4. Study of absorption of X-rays.

111. Results of Investigation.—Early workers found that the primary X-rays emitted by an X-ray tube do not obey the well known Beer's law in optics. The Beer's law is

$$I = I_0 \, e^{-\mu d}$$

where I_0 = the intensity of the primary beam,

I = the intensity of the primary beam after the absorber is interposed,

d = the thickness of the absorbing material,

μ = a constant known as the *absorption coefficient.*

Thus
$$ln \frac{I_0}{I} = \mu d$$

When $ln\, I_0/I$ was plotted against d, the thickness of the absorbing sheet, it was found that the graph was not a straight line. Also by increasing the voltage across the tube, the nature of the graph changed. It was supposed to be due to the fact that the primary X-rays were not homogeneous but that they consisted of rays of different penetrating powers.

Let I_0 be the intensity of total radiation, consisting of different intensity components I_1, I_2, I_3, ... I_n having absorption coefficients μ_1, μ_2, μ_3 .... μ_n for a particular substance, then the total intensity I of transmitted ray will be given by the equation

$$I = I_1 e^{-\mu d} + I_2 e^{-\mu_2 d} + I_3 e^{-\mu_3 d} + \ldots\ldots$$

Hence it is clear that Beer's law in its simple form will not hold for heterogeneous radiations.

Barkla and Sadler found that when a copper foil was irradiated by means of primary hard X-rays from the target, it emitted a *fluorescent* radiation all around, which had the remarkable property of being homogeneous and characteristic of copper. In other words when different thicknesses of aluminium were placed in the path of these secondary radiations, $ln \cdot I/I_0$ plotted against d came out to be very *nearly* a straight line. Thus this radiation was found to possess a definite penetrating power. It must be remembered, however, that the primary X-rays give rise to scattered rays when they fall on the copper foil. This scattered radiation was the cause of the slight deviation from Beer's law observed in the case of the fluorescent radiation examined by Barkla and Sadler. But for heavy elements, the effect of the scattered radiation was small compared to that of fluorescent radiation. Sadler,* however, eliminated it in an ingenious way. His arrangement is diagrammatically shown in Fig. 5. He allowed primary X-rays from the anticathode A of an X-ray tube to pass through the slits S, S and then to fall on a copper foil R_1.

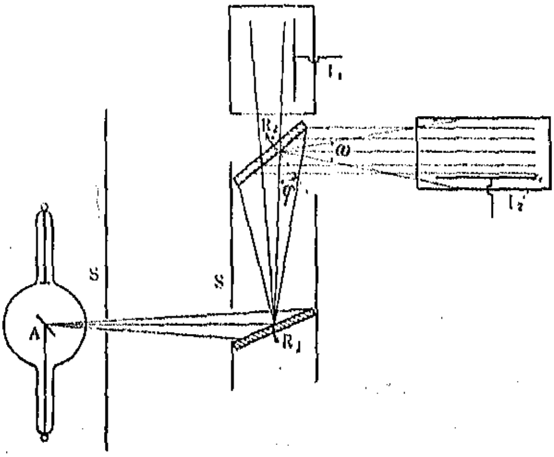

Fig. 5. Barkla and Sadler's apparatus for studying the absorption of characteristic radiation.

The foil gives rise to secondary characteristic radiations and a feeble scattered radiation. These fall on another nickel foil R_2 as shown in the figure. The nickel foil emits its characteristic radiation, the homogeneity of which can be studied by means of an ionisation chamber I_2. By this device the scattered radiation was almost totally suppressed.

It was found by Barkla and Sadler that the characteristic radiation of copper can excite characteristic radiation in all elements like Ni preceding it in the periodic classification. But the copper radiation cannot excite zinc to emit its characteristic radiation. From these crude experiments, Barkla further discovered that when comparatively heavy elements like W and Pt are irradiated with hard X-rays, two kinds of fluorescent radiations widely differing in penetrating power are emitted. This discovery was made by Barkla in the following way. The copper foil R_1 in Fig. 5 was replaced by a thin sheet of W, and the foil R_2 was permanently removed. Allowing comparatively soft primary radiations to fall on R_1, the hardness of the *fluorescent radiation* emitted was studied by observing its absorption in an Al-foil placed between R_1 and I_1. He found that for a certain range of hardness of the primary radiation, the characteristic radiation showed no increase in hardness, that is, was homogeneous. But when the hardness of the primary beam was increased to a critical value, the fluorescent rays showed a sudden rise in hardness. This was attributed by Barkla to the emission of a different characteristic radiation by W of greater penetrating power. Thus two characteristic radiations are emitted by W. The radiation of greater penetrating power was called K, and that of smaller penetrating power L radiation.

---

* C. A. Sadler, *Phil. Mag.*, 18, 107, 1909.

Measurement by modern X-ray spectroscopes has shown that the K and L radiations are, however, composite of different radiations K_α, K_β, . . . (for the K-radiation), and L_α, L_β, L_γ, ... (for L-radiation), the subgroups differing slightly in their penetrating powers. These small differences could not, however, be detected by Barkla's rough measurements. In the case of lighter elements Barkla observed the K-radiations only. For the L-radiations in these cases were very soft and were therefore absorbed by air.

It is thus clear that if we study the absorption of *primary beam* by W by changing the hardness of the former, we shall find that the absorption increases suddenly for some critical hardness of the primary rays. This is due to the emission of L-characteristic radiation by W, the energy of which is absorbed from the primary beam. If the hardness be increased still further, there will be another sudden rise in absorption corresponding to the emission of K-radiation. For these and later developments see Chapter XI.

The quantity μ in Beer's law can be written as

$$I = I_0 e^{-\frac{\mu}{\rho}\rho d}$$

where ρ is the density of the absorber. Let $\rho d = m$, where m is the mass of matter traversed by a pencil one cm.^{2} in cross-section. Hence

$$I = I_0 e^{-\frac{\mu}{\rho} m}$$

μ/ρ is known as the *mass absorption coefficient* of the substance. Sometimes, instead of μ/ρ, the quantity $\mu A/L\rho$ is taken as the measure of absorption. Here A is the atomic weight of the absorber, and L

the Avogadro number. Since $\rho L/A$ denotes the number of atoms in unit volume of the substance, we may introduce a new constant μ_{atom} and put

$$\mu_{\text{atom}} = \frac{\mu}{\rho}\ \frac{A}{L}$$

It is known as the *atomic absorption coefficient* and is denoted by μ_A. It represents absorption by an individual atom. Beer's law takes the form

$$I = I_0\ e^{-\frac{\mu}{\rho}\ \frac{A}{L}\ \frac{mL}{A}}$$

$$= I_0\ e^{-\mu_A\left(\frac{mL}{A}\right)} = I_0\ e^{-\mu_A n}$$

where n is the number of atoms traversed by X-rays per unit area.

After the development of the crystal method of analysing characteristic X-rays, the absorption coefficients of a large number of substances have been determined for a wide range of wavelengths (λ 11,000 to 80 X. U.). A table showing some of these results are given at the end of this chapter. The μ/ρ-values (mass-absorption coefficients) are given. The values for wavelengths longer than λ 2250 X. U. have been recently obtained by Jönsson. For a full review of the results special treatises (Compton's *X-rays*, p. 184 and *Handbuch der Experimental Physik*, **24**, Kirchner, pp. 230 to 237) should be consulted.

For efficient methods of production of fluorescent radiation see §145 on "Spectroscopic Methods," and for the relation of absorption coefficient with atomic constants see Chap. XI.

112. Scattering of X-rays.—The scattering of X-rays was investigated by Crowther and more in detail by Barkla between the years 1903 and 1926. They found that scattering occurred at all depths and increased in amount with the thickness of matter traversed by X-rays. It was also found that elements of lower atomic weight up to sulphur scatter very much the same, mass for mass, but for heavier elements the relations are a bit complex. Barkla introduced a coefficient of scattering σ which is similar to the absorption coefficient μ introduced in §111. The loss of intensity of the primary rays due to scattering is expressed by the law

$$I = I_0\ e^{-\sigma/\rho\ m}$$

where ρ = density of the scattering matter and m = mass of scattering matter traversed by X-rays per unit cross-section. It was shown by J. J. Thomson that

$$\frac{\sigma}{\rho} = \frac{8\pi}{3}\frac{e^4 L}{m^2 c^4}\cdot\frac{Z}{A}$$

where L = Avogadro number, A = atomic wt., and Z = atomic number. As Barkla was guided by this theory in his works on scattering, a brief account of it is given below.

113. J. J. Thomson's Theory of X-ray Scattering.—It can be proved from the electromagnetic theory of light, that when a particle of charge e moves with an acceleration $\dot{v}$, it generates an electromagnetic field in space. The value of the electric and the magnetic fields* due to this at a distance r is given by

$$E = H = \frac{e\dot{v}_n}{c^2 r} \quad . \quad . \quad . \quad . \quad (1)$$

Here $\dot{v}_n$ denotes the normal acceleration, *i.e.*, the component of acceleration in a direction normal to the line of sight of the observer. So we can express $\dot{v}_n$ as

$\dot{v}_n = \dot{v}\sin\theta$, where θ = the angle between the direction of acceleration and the line of sight.

This can be understood from Fig. 2, §95.

The energy flux, *i.e.*, the rate at which energy is radiated by the particle (the so-called *Poynting vector*) is

$$S = \frac{c}{4\pi}[E.H]$$
$$= \frac{e^2\dot{v}_n{}^2}{4\pi r^2 c^3} \quad . \quad . \quad . \quad . \quad (1a)$$

This is the fundamental equation of radiation by an accelerated charged particle.

J. J. Thomson applied this theory to the phenomenon of X-ray scattering. He supposed that the X-rays were, like light, electromagnetic waves in space accompanied by electric and magnetic fields which are at right angles to each other and to the direction of the beam. The matter through which the X-rays pass is supposed to consist of atoms each of which contains a number of electrons. These electrons are set in accelerated motion by the periodic electric field associated with the beam of X-rays. As the electrons are accelerated they begin to radiate energy on their own account. The sum total of these radiated energy forms the total scattered energy and it is at the expense of the energy of the primary beams.

---

* For a proof of this relation see Compton's *X-rays*, Chap. II, page 40.

Let us take an unpolarised beam OP of X-rays (Fig. 6) falling upon some electrons at P. We want to find the amount of energy scattered at Q. Draw two lines P1 and P2 in the plane perpendicular to OP, P1 being normal to the plane OPQ and P2 in the plane of OPQ. Then the electric vector at P can be decomposed in the directions P1 and P2. Let these components be E_{p_1} and E_{p_2}. Further since the primary beam is unpolarised, the electric vector lies in the plane perpendicular to OP at random. So we can set $E_{p_1} = E_{p_2} = E_p$.

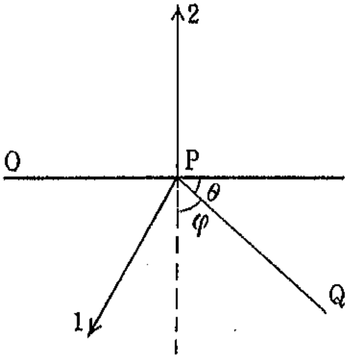

Fig. 6.

Now the electrons at P are subjected to varying e. m. f. along P1, P2. The motion of the electron along any direction can be written as

$$m\ddot{x} + fx = -eE_p \quad . \quad . \quad . \quad . \quad (2)$$

where x is the displacement-vector along either P1 or P2, and f is the force of restitution. In the general case the incident radiation is continuous. Hence it can be written as

$$E_p = \int E e^{ipt}\,dp \quad . \quad . \quad . \quad . \quad . \quad (3)$$

The motion is also quite complex and can be written as a Fourier's series

$$x = \int \xi\, e^{ipt}\,dp \quad . \quad . \quad . \quad . \quad . \quad . \quad (4)$$

Let the natural frequency of the electron be

$$p_0 = \sqrt{f/m} \quad . \quad . \quad . \quad . \quad . \quad . \quad . \quad (5)$$

Then it follows from equations (2, 3, 4 and 5) that

$$\xi\,(p_0^2 - p^2) = -\frac{e}{m}E, \qquad x = -\frac{e}{m}\int \frac{1}{p_0^2 - p^2} E e^{ipt}\,dp$$

and $$\dot{v} = \ddot{x} = \frac{e}{m}\int \frac{p^2}{p_0^2 - p^2} E e^{ipt}\,dp$$

In the visible region we assume that $p \leqslant p_0$. This assumption will give us the Rayleigh formula of scattering for the visible range. But for the X-ray region we can suppose that $p \leqslant p_0$. This gives us

$$\dot{v} = -\frac{e}{m} \cdot E_p \qquad \ldots \ldots \qquad (6)$$

where $\dot{v}$ denotes the average acceleration along the directions P1 or P2 along which the components of the electric field at P act.

Hence according to (1*a*), the energy radiation at P due to the acceleration along P1 is

$$\frac{e^2}{4\pi c^3 r^2} \cdot \left(\frac{eE_p}{m}\right)^2$$

for, $\dot{v}_n = \dot{v} \sin\,(\mathrm{P}\widehat{1\,\mathrm{P}}\mathrm{Q}) = \dot{v}$, since P1 is normal to the plane OPQ. Again the energy radiation due to the acceleration along P2 is

$$\frac{e^2}{4\pi c^3 r^2} \left(\frac{eE_p}{m}\right)^2 \cos^2\theta$$

where θ=the angle between the primary and the scattered beam. For, here $\dot{v}_n = \dot{v} \sin\,(\mathrm{P}\widehat{2\,\mathrm{P}}\mathrm{Q}) = \dot{v} \sin\varphi = \dot{v}\cos\theta$.

Hence the total energy S scattered at Q is given by

$$S = \frac{e^4}{4\pi c^3 m^2 r^2} E_p{}^2\,(1+\cos^2\theta) \qquad \ldots \ldots \qquad (7)$$

Now according to Maxwell's theory, energy density at P is

$$\frac{\Sigma E_p{}^2}{4\pi} = \frac{1}{2\pi} E_p{}^2$$

and this is equal to $\frac{I}{c}$ where I = intensity of primary radiation at P.

Hence eliminating $E_p{}^2$ we have

$$S = \frac{e^4}{2m^2 c^4 r^2} I\,(1+\cos^2\theta) \qquad \ldots \ldots \qquad (8)$$

or

$$\frac{S}{I} = \frac{e^4}{2m^2 c^4 r^2}(1+\cos^2\theta) \qquad \ldots \ldots \qquad (9)$$

The total amount of radiation scattered in space is obtained by integrating the above expression over the whole surface of the sphere of radius r about P.

We have

$$2\pi \int_0^\pi (1+\cos^2\theta)\, r^2 \sin\theta\, d\theta = 4\pi\,(1+\tfrac{1}{3})\, r^2 = \frac{16\pi}{3} r^2$$

Hence the total intensity of scattered radiation

$$S_0 = \frac{8\pi e^4}{3m^2c^4} \cdot I \quad \ldots \ldots \ldots \ldots (10)$$

Hence
$$\sigma_e = \frac{S_0}{I} = \frac{8\ \pi e^4}{3m^2c^4} \quad \ldots \ldots \ldots \ldots (11)$$

Putting the values of e, m, and c in (11), we get $S_0/I = 6{\cdot}6 \times 10^{-25}$. This gives the scattering due to one electron. Suppose now that there are n atoms per unit volume, and each atom contains Z electrons. Then the total scattering by the mass contained in unit volume is

$$\sigma = \frac{8\pi}{3} \cdot \frac{e^4}{m^2c^4} nZ \quad \ldots \ldots \ldots \ldots (12)$$

If ρ = density of the scattering substance, then the mass scattering coefficient according to the definition is σ/ρ. We have further $n = \mathrm{L}/(\mathrm{A}/\rho) = (\rho L)/A$. Hence the mass-scattering coefficient is

$$\frac{\sigma}{\rho} = \frac{8\pi}{3} \cdot \frac{e^4 L}{m^2c^4} \cdot \frac{Z}{A} \quad \ldots \ldots \ldots \ldots (13)$$

Now $\dfrac{e}{mc} = 1{\cdot}77 \times 10^7$, $\dfrac{eL}{c} = 9{\cdot}645 \times 10^3$. Hence

$$\frac{\sigma}{\rho} = {\cdot}40.\ \frac{Z}{A} \quad \ldots \ldots \ldots \ldots (14)$$

That is, the mass scattering coefficient is proportional to Z/A of the scattering substance. The simple theory sketched above applies only to amorphous solids. In case of crystals, liquids and gases the theory has to be supplemented by factors depending upon their internal structures. Much recent work has been done on this subject. For an account of this see §§ 133, 134, 155.

113a. Experimental Study of Scattering.—The phenomenon of X-ray scattering was experimentally investigated by Barkla* and later on by Hewlett.† The apparatus used by them are similar in essential features and has been shown in Fig. 7. The main purpose of these experiments was to determine the intensity of scattered X-rays for different angles of scattering, and then to find out the sum total of the intensity of the scattered radiation. The latter would be equal to S_0 in equation (10). Primary radiations from the anticathode T fall on the scatterer R. The scattered radiations are emitted and are received in the ionisation chamber I. The latter is carefully screened from the direct effect of the primary radiations. The variation of intensity of scattered radiation with θ, the angle between the primary and the scattered beams can be studied by changing the position of the ionisation chamber. Hewlett measured the variation of intensity of the scattered radiation over angles $\theta=0$ to $\theta=180°$. Then a curve was drawn in which the ordinates represented the scattered intensity S and the abscissæ the angles of scattering θ. The integration necessary to get the total scattered intensity S_0 was performed both geometrically and mechanically. Recent workers have improved their apparatus, for example, Coade[*] has designed a hemi-spherical ionisation chamber which surrounds the scatterer. In this case the integration of (S, θ) curve is not necessary, for the scattered rays from all sides enter the chamber together.

---

* C. G. Barkla, *Phil. Mag.* **21**, 648, 1911.

† C. W. Hewlett, *Phys. Rev.*, **19**, 266, 1922.

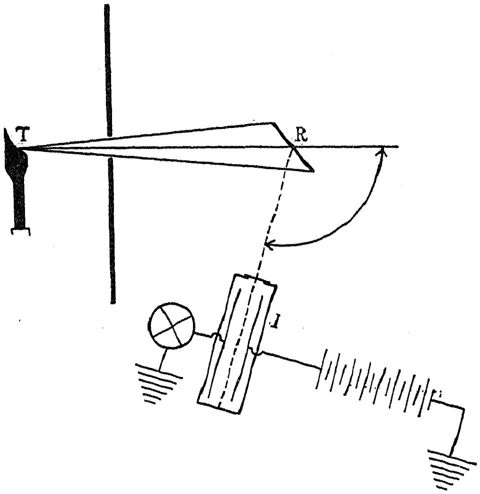

Fig 7. Apparatus to study the mass-scattering coefficient of matter.

In this way Barkla found that the mass scattering coefficient σ/ρ for light substances was very nearly ·2. We find from (14) that this can be explained if we suppose $Z/A = \frac{1}{2}$, *i.e.*, the number of electrons per atom is approximately half of the atomic weight. This result which was obtained at a time when there were wild speculations regarding the number of electrons in an atom (it was supposed sometimes that the number of electrons was equal to atomic weight multiplied by 1830) helped much to clarify our notions of atomic structure. These results were published almost simultaneously with Rutherford's estimation of nuclear charge from observations of large angle scattering of α-rays by matter.

---

[*] Coade, *Phys. Rev.*, **36**, 1109, 1930.

A typical set of results for light elements is shown in the following table due to Hewlett who used very nearly monochromatic rays (K_α of Mo) for these measurements.

Table 1.—Mass-scattering coefficients ($\lambda \approx 0{\cdot}7$ Å.U.)

Scattering Substance.		$\left(\frac{\sigma}{\rho}\right)_{\text{obs.}}$	$\frac{2Z}{A}$
Diamond	C ...	0·199	1·00
Graphite	C ...	0·201	1·00
Lithium	Li ...	0·168	0·84
Benzene	C_6H_6 ...	0·238	1·17
Mesitylene	$C_6H_3(CH_3)_3$ ...	0·244	1·20
Octane	C_8H_{18} ...	0·248	1·24

It will be seen from the equation (13) that the mass-scattering coefficient is independent of wavelength of primary X-rays; but this was found hardly to be true even in light elements like carbon. Hewlett* proved that the value of the mass-scattering coefficient of carbon approximates to the theoretical value only when the primary rays have the wavelength 0·3 Å.U. As the wavelength becomes shorter and shorter, the intensity of scattering falls below the value predicted by the theory. Many attempts were made to explain this fact on the classical theories, but were unsuccessful. The discovery of the Compton effect and the new quantum mechanics have tided over the difficulty successfully.

Thomson's theory predicted that the mass-scattering coefficient would depend on the atomic number of the scatterer. The X-ray scattering for heavy elements was investigated by Barkla and Dunlop.† They found that σ/ρ varied with Z, and for the same element it changed rapidly with wavelength.

In Fig. 8, Barkla and Dunlop's curves have been shown in which the ratio of σ/ρ of Pb, Sn, Ag, Cu, to σ/ρ for Al is plotted against the wavelength. Aluminium was selected because the scattering coefficient of this element did not vary much with increasing wavelength. It is clear from the curves that the scattering increases rapidly with wavelength in the case of heavy elements.

---

* Hewlett, *Phys. Rev.*, **19**, 286, 1921.
† Barkla and Dunlop, *Phil. Mag.*, **31**, 229, 1916.

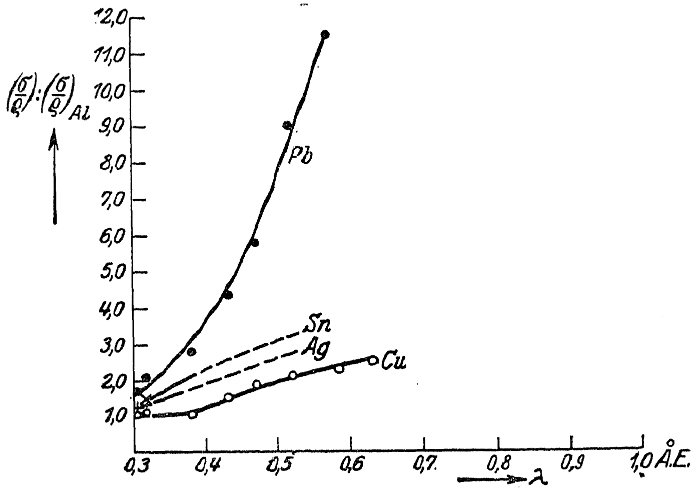

Fig. 8. Mass-scattering Coefficient of Pb, Sn, Ag, Cu.

The interpretation is that when the wavelength is long compared with the distances between the electrons in the atoms, the phases of the rays scattered from the different electrons are nearly the same, and so the total intensity increases. If the Z electrons act like a unit, the Thomson equation becomes

$$S=\frac{I\,(Ze)^4}{2(Zm)^2c^4r^2}(1+\cos^2\theta).$$

$$=\frac{IZ^2e^4}{2m^2c^4r^2}(1+\cos^2\theta)$$

$$=S_e\,Z^2 \quad . \quad . \quad . \quad . \quad . \quad . \quad . \quad . \quad . \quad . \quad . \quad . \quad (15)$$

where S_e is the scattering due to single electron.

It has been found by Allen* that actually the Z^2-law is followed in the case of heavy atoms, in which we have a large number of electrons concentrated in a small space. On the other hand, for lighter atoms the Z-law is followed, as in their case the electrons are situated at comparatively large distances apart, and may be supposed to be scattering independently.

---

* Allen, *Phys. Rev.*, **24**, 1, 1924.

114. The Polarisation of Scattered X-rays.—Barkla[*] first showed that the scattered X-rays are polarised. His apparatus has been schematically represented in Fig. 9.

X-rays from the tube R, limited by a slit, are allowed to fall on the carbon block P. The scattered X-rays fall on the second carbon block at A and are re-scattered. The first block acts as a polariser and the second block as an analyser. The ionisation chamber I is placed first in the position I_1 and then at I_2[†]. It was found that the intensity at I_1 was maximum, while at I_2 it was minimum.

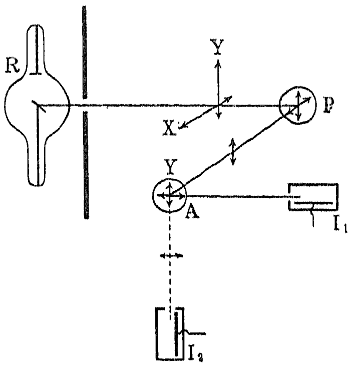

Fig 9. Barkla's apparatus.

In Thomson's theory the primary rays have been supposed to be unpolarised; but we can always resolve an unpolarised beam into two beams polarised at right angles to each other (say along X and Y directions), so that the electric vector is always perpendicular to the direction of propagation. In a direction θ, there will be two scattered beams polarised at right angles to each other and having the intensities

$$\frac{Ie^4}{2r^2m^2c^4} \text{ and } \frac{Ie^4}{2r^2m^2c^4}\cos^2\theta$$

as has been already derived in §113. In Barkla's experiment when the beam scattered at $\pi/2$ (*i.e.*, along X) was examined, the intensity of the latter component was zero. In other words the electric vector of the scattered ray PA was only along Y. If this polarised scattered radiation falls on the second scatterer, a similar argument will show that there will be no ray along AI_2, for it lies along the electric vector of the first scattered ray as well as of the second scattered ray. At I_1, however, the intensity of the re-scattered rays will be maximum for reasons which are obvious. Barkla's discovery proved conclusively that the X-rays are electromagnetic pulses or waves.

115. Diffraction of X-rays—Early Works.—In order to establish the wave-nature of X-rays, attempts were made by Röntgen himself to observe their diffraction and interference. He tried to observe whether there was any variation of intensity within the geometrical shadow of a slit illuminated by X-rays, but the result was negative. The experiment was repeated by Wind and Haga in 1901 with a V-shaped slit (it consisted of two straight jaws intersecting at one end, the other ends being a few μ wide, so that the narrow end of the wedge-shaped slit is only several μμ in width). The result obtained was that the slit image was found broadened at the narrow end. If the effect be ascribed to diffraction, the wavelength of X-rays employed could be obtained on measurement of the distribution of intensity at different points of the image of the narrow end of the slit and determination of the observed positions of the maxima on the negative. Our present knowledge of X-ray wavelengths inclines us to the belief that the effect of diffraction had actually been observed in this experiment. Some doubt was, however, thrown on the conclusion by the subsequent repetition of Haga and Wind's experiment, and careful measurement of the plates by the photometric method by Walter and Pohl* in 1908. They observed that the amount of broadening depended largely upon the time of exposure, and other minor effects produced by the photographic plate, and consequently the experiments mentioned were not regarded as conclusive.† Attempts were made to calculate the wavelength of X-rays by observing the velocity of secondary electrons ejected, on the basis of Einstein's photoelectric equation, and the value was found to be of the order 10^{-8} cm. Though both the method and the results were correct, the photoelectric equation had not acquired the prestige it has got now; so the method did not command general confidence, though it produced a general impression that X-rays were electromagnetic waves thousand times shorter than ultraviolet light.

---

[*] Barkla, *Proc. Roy. Soc.*, 77, 247, 1906.

[†] AI_1 is parallel to Z-axis, and AI_2 is parallel to Y-axis.

116. Laue's Discovery. — After a number of fruitless attempts, the X-ray diffraction was demonstrated with undreamed-of precision by Prof. Laue‡ at Munich. He directed his attention to the use of a suitable diffraction grating, as is used in optical diffraction experiments. The requisites of such a grating can be easily seen from the fundamental equation of diffraction of light of any wavelength λ. The fundamental equation is

---

* Walter and Pohl, *Ann. d. Phys.*, 29, 331, 1909.

† For diffraction pattern of X-rays obtained with slits, see § 160.

‡ Laue, Friedrich and Knipping, *Sitz. Ber. d. Bay. Akad. d. Wiss.* 303, 1912.

$$\sin\theta = \frac{n\lambda}{d} \qquad \ldots\ldots\ldots\ldots \qquad (16)$$

where θ = the angle of diffraction, and n = the integer indicating the order of the diffraction spectra and d is the grating space. This shows that in order to have a measureable value of θ in the first order, d should not be much greater than λ; for if d be $\gg \lambda$, θ will be too small for practical purposes. In other words, the grating space must not be much larger than the wavelength of the diffracting light. Thus a grating with 5500 lines to the cm. (*i.e.*, $d = 1{\cdot}8 \times 10^{-4}$ cm.) would be quite all right for light of the wavelength $\lambda = 5892 \times 10^{-8}$ cm., for $\theta = \sin^{-1}\left(\frac{5{\cdot}892}{18}\right)$, but it would be quite useless for light having $\lambda \sim 10^{-8}$ cm. Such light would require a grating having 1000 times as many lines per cm., *i.e.*, the grating space should be of the order of 10^{-8} cm., *i.e.*, of molecular dimensions.

Laue showed that though it was impossible to manufacture such gratings artificially, Nature herself had provided such gratings. These are the crystals. The crystals according to a school of crystallographers including Bravais (1829), Schönflies (1879) and von Fedorov (1892),* owe their characteristic geometrical shape to the arrangement of the constituent atoms in space according to a regular geometric pattern. To take one illustrative example :—

NaCl crystals occur in the form of a regular cube, or can be shown to consist of a number of elementary cubes placed in close juxtaposition. We can explain this formation by supposing that the sodium and the chlorine atoms are placed alternately at the corners of a cube as in Fig. 10. A structure like this forms an elementary brick in the formation of an NaCl crystal, and if we arrange a number of such bricks suitably, we shall imitate the actual process of growth of the crystals. If the "growth" be perfect, the ultimate structure would be a cube, very much like the

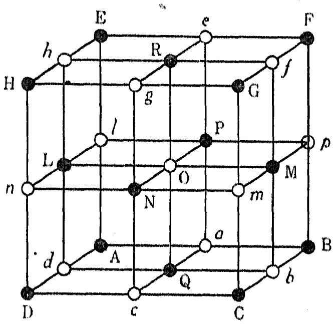

Fig. 10. The NaCl Crystal.

---

* For an account of the subject, see Sec. II, § 120.

elementary one. On this view, the crystal of NaCl consists of *space-lattices* formed by the intersection of three sets of parallel planes which are mutually at right angles, and intersect at equal intervals, the points of intersections being alternately filled by sodium and chlorine atoms. Supposing that the atoms represent opaque space, then the picture is the same as if we had taken a number of plane gratings having space of the order of molecular dimensions, and placed them one over the other, in a pile, the alternate gratings having their lines perpendicular to each other. Such a grating may be called a *space grating.*

Laue calculated the actual diffraction by such gratings in the following way :—

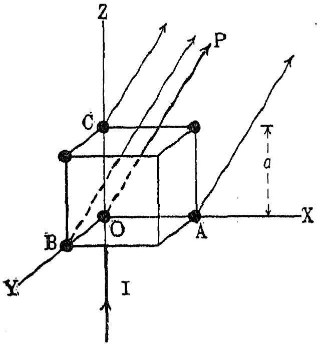

Fig. 11. Diffraction of X-rays by crystals (Laue).

The position of the atoms may be denoted with reference to a set of coordinate axes (x, y, z), the planes of reference coinciding with the principal planes of the lattice structure. In the case of cubic planes, as in Fig. 11, the axes are mutually at right angles. Let the position of an atom be denoted by *ma*, *na*, *pa*, where *m*, *n*, *p* are whole numbers. Let now a plane beam of X-rays with the direction cosines (α_0, β_0, γ_0) be incident on the atoms. Laue supposed that as the plane wave falls on an atom, the electrons composing the atom are thrown into vibration by the electric vector associated with the beam. In fact, the phenomenon is identical with that contemplated in Thomson scattering. But as the atoms are regularly arranged, there is regular phase difference amongst the waves scattered by the atoms of the lattice. For example, let O and A be two atoms and I be the incident beam. Let OA be the direction of the x-axis, and OP be the direction of the diffracted beam. Then the path-difference between the rays diffracted from O and *A* can be seen from Fig. 11*a* to be

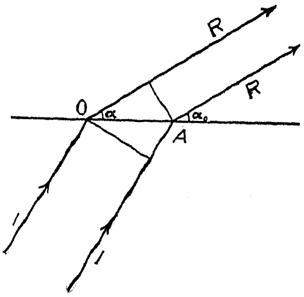

Fig. 11*a*. Diffraction at a plane grating.

$$a\,(\alpha-\alpha_0)$$

where α_0=cos AOI, α=cos AOP and a=OA.

In the general case, we have also to find out the path difference caused by the atoms placed along the y and z-axis. These are

$$a(\beta-\beta_0), \quad \text{and} \quad a(\gamma-\gamma_0) \qquad \text{respectively.}$$

It is clear that the diffracted beams will intensify each other if the following conditions are satisfied :—

$$a(\alpha-\alpha_0)=h_1\lambda, \quad a(\beta-\beta_0)=h_2\lambda, \quad a(\gamma-\gamma_0)=h_3\lambda. \quad . \quad . \quad (17)$$

where h_1, h_2, h_3 are three integers.

Though we have used the term 'diffracted beam,' it is clear that we are dealing with interference of beams scattered by the atoms. The scattering is now coherent, whereas in the case of amorphous substances (where there is no order in the arrangement of atoms), the scattering would be non-coherent.

From equation (17), we obtain

$$\left.\begin{aligned}\alpha&=\alpha_0+h_1\frac{\lambda}{a}\\ \beta&=\beta_0+h_2\frac{\lambda}{a}\\ \gamma&=\gamma_0+h_3\frac{\lambda}{a}\end{aligned}\right\} \quad . \quad . \quad . \quad . \quad . \quad . \quad . \quad . \quad (18)$$

By squaring and adding these terms, and making use of the relation $\alpha_0{}^2+\beta_0{}^2+\gamma_0{}^2=\alpha^2+\beta^2+\gamma^2=1$, we obtain,

$$\frac{\lambda^2}{a^2}(h_1{}^2+h_2{}^2+h_3{}^2)=-\frac{2\lambda}{a}(h_1\alpha_0+h_2\beta_0+h_3\gamma_0)$$

or

$$\lambda=-2a\frac{(h_1\alpha_0+h_2\beta_0+h_3\gamma_0)}{h_1{}^2+h_2{}^2+h_3{}^2} \quad . \quad . \quad . \quad . \quad (19)$$

If we suppose that the direction of the incident beam lies along the z-axis, we have

$$\alpha_0=\beta_0=0, \quad \gamma_0=-1.$$

So that

$$\lambda=+2a.\frac{h_3}{h_1{}^2+h_2{}^2+h_3{}^2} \quad . \quad . \quad . \quad . \quad . \quad . \quad . \quad (20)$$

The numbers h_1, h_2, h_3 denote the order of diffraction. We have further

$$\frac{h_1}{\alpha}=\frac{h_2}{\beta}=\frac{h_3}{\gamma+1} \quad . \quad . \quad . \quad . \quad . \quad . \quad . \quad . \quad . \quad . \quad (21)$$

So if we allow a linear beam of X-rays to pass through a crystal and allow it to fall on a photographic plate, we expect to obtain on the plate spots corresponding to maxima given by (19) arranged in a symmetrical manner, depending upon the orientation of the crystal axis with respect to the direction of incidence. This experiment was first tried by Laue, Friedrich and Knipping and is described in the next section.

It is clear from equation (19), that only one particular wavelength can be diffracted by a space grating when equation (19) is satisfied. The next wavelength to be diffracted must satisfy the equation (19) with different sets of values of (h_1, h_2, h_3). The intermediate wavelengths may not give rise to a diffraction maximum at all. Here lies the difference between a space grating and a plane grating.

The intensity of the maxima is difficult to find out, and is beyond the scope of this work. It will suffice to mention, that as this is a case of Thomson scattering, the intensity formula given in §113 must hold good here. It is

$$S = I\frac{Z^2e^4}{m^2c^4}\cdot\frac{1+\cos^2\theta}{2}$$

Here Z is the number of electrons contained in the scattering centres (atoms), $(1+\cos^2\theta)$ is the polarisation factor or the *Thomson factor.*

In the case of Laue phenomena, the intensity relation is not so simple, but the equation referred to above is to be multiplied by two factors, (1) structure factor P, (2) atom factor F. These two will be explained at the end of the chapter. The intensity relation can be written as

$$\frac{S}{I}\propto\frac{e^4}{m^2c^4}\,\frac{1+\cos^2\theta}{2}\,\Sigma P.F.$$

We shall return to this formula in a later section (§133, 134).

117. Experimental Verification of Laue's Theory.—The verification of Laue's theory was undertaken by Laue, Friedrich and Knipping in 1912. The original apparatus used by them is illustrated in Fig. 12. For this purpose, a beam of X-rays from the tube T rendered parallel by a system of lead apertures S_1, S_2, S_3 and reduced to a fine pencil by a narrow circular hole was allowed to traverse a crystal C, and then impinge on a photographic plate P. The first crystal tried was ZnS (zinc sulphide) and the results obtained were in good agreement with theory. A photographic reproduction of Laue spots with ZnS crystal is given in Fig. 13, (Plate III). In the figure S is an opening in the Laue camera at which a fluorescent screen is placed and the crystal adjusted by sighting.

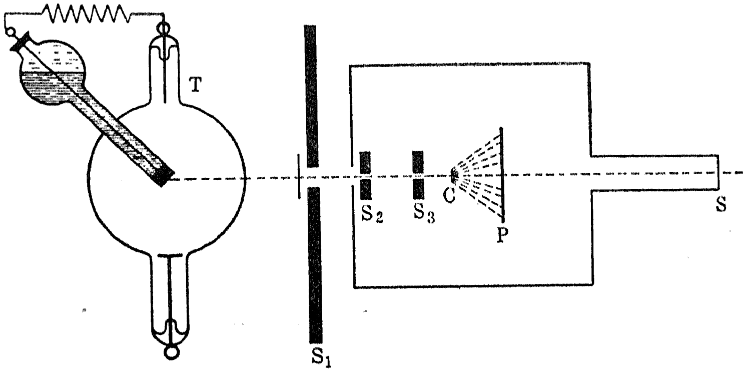

Fig. 12. Laue, Friederich and Knippings' apparatus.

In the original experiment, exposures of 20 to 60 hours were given. The source was an ordinary gas-tube with water cooled anticathodes. With modern technique, only a few minutes exposure is sufficient.

118. Results of Laue Experiment.—Laue had kept the (100) face of the crystal perpendicular to the direction of the beam. Suppose Fig. 14 illustrates a Laue pattern for such a case. Here D is the photographic plate and C is the crystal of zinc sulphide. The beam of X-rays passes through two slits S′ and S″ and falls on the crystal. Suppose for any Laue point, the direction cosines of the line joining the spot to the point where the direct beam strikes the photographic plate (central spot) are α, β, $-\gamma$.

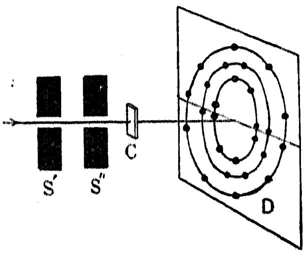

Fig. 14. Formation of Laue's spots.

Then according to Laue's theory

$$\alpha = h_1 \frac{\lambda}{a}, \quad \beta = h_2 \frac{\lambda}{a}, \quad 1+\gamma = h_3 \frac{\lambda}{a}$$

We have taken $\cos\varphi = -\gamma$.

If now the distance between the plate and the crystal be x, and the distance between the Laue spot and the central spot be r, then

$$\tan\varphi = \frac{r}{x}.$$

In Laue's original experiment* $x = 3{\cdot}56$ cm. and a Laue spot was found at a distance of 1·25 cm. from the central spot.

Therefore $$\tan\varphi = \frac{1{\cdot}25}{3{\cdot}56} = {\cdot}350 \quad\text{or}\quad \varphi = 19^\circ 20'$$

Hence $$\cos\varphi = -\gamma = {\cdot}9436 \quad\text{or}\quad 1+\gamma = {\cdot}0564$$

or $$h_3\frac{\lambda}{a} = {\cdot}0564 \quad . \;\; . \;\; . \;\; . \;\; . \;\; . \;\; . \;\; . \;\; . \;\; . \;\; . \;\; . \qquad (22)$$

taking $h_3 = 1$, we have $\lambda/a = {\cdot}0564$

Again it has been proved that

$$\frac{\lambda}{a} = \frac{2h_3}{h_1{}^2 + h_2{}^2 + h_3{}^2}$$

So taking $h_3 = 1$, we get

$$\frac{\lambda}{a} = \frac{2}{h_1{}^2 + h_2{}^2 + 1}$$

For h_1 and h_2 we may substitute 3 and 5.

Therefore, $$\frac{\lambda}{a} = \frac{2}{9+25+1} = \frac{2}{35} = {\cdot}0571 \quad . \;\; . \;\; . \qquad (23)$$

The difference between the first and the second value of λ/a can be ascribed to experimental error. It is clear from the equation that the Laue spots will be arranged in circles round the central spot. The first circle will correspond to $h_3 = 1$, and so on.

For $$r = x\tan\varphi = x.\frac{\sqrt{1-\cos^2\varphi}}{\cos\varphi}$$

$$= x.\frac{\sqrt{1-\gamma^2}}{-\gamma} = x\cdot\frac{\sqrt{h_3\frac{\lambda}{a}\left(2 - h_3\frac{\lambda}{a}\right)}}{1 - h_3\frac{\lambda}{a}}$$

For a fixed value of $\frac{h_3\lambda}{a}$, we therefore have

$$r = \text{constant} \quad . \;\; . \;\; . \;\; . \;\; . \;\; . \;\; . \;\; . \;\; . \qquad (24)$$

---

* Laue, Friedrich and Knipping, *Ann. d. Phys.*, **41**, 971, 1913.
For a better method of interpreting Laue's experiment see §130.

Hence Laue spots corresponding to h_3 λ/a lie on circles on the photographic plate. It has been found in eqn. (23) that $\lambda/a = \cdot0571$. In order to find the wavelength λ, we require the value of a.

Let us suppose that in a volume a^3, one molecule is included. Then if N is the number of atoms in a gram molecule, a^3N is the volume of a gram molecule. If m be the molecular weight and ρ the density of ZnS, then

$$a^3N = \frac{m}{\rho} \quad \text{or} \quad a = \sqrt[3]{\frac{m}{N\rho}} = \sqrt[3]{\frac{97\cdot4}{6\cdot0\times10^{23}\times4\cdot06}}$$

So for ZnS $a = 3\cdot42\times10^{-8}$ cm. From equation (23) we therefore get

$$\lambda = 3\cdot42\times10^{-8}\times\cdot0571$$

$$= \cdot195\times10^{-8} \text{ cm.}$$

Laue's method gave us the first accurate value of the wavelength of X-rays. It is to be noted here that in Laue's method diffraction is supposed to take place from atoms placed at regular intervals along three axes of reference. But this way of looking at crystals does not help us in unravelling its structure completely. In Braggs' theory given in the next section the phenomenon is viewed from a different standpoint which proves to be more fruitful.

119. Braggs' Theory of Reflexion of X-rays.

119. Braggs' Theory of Reflexion of X-rays.—It has been mentioned in the introduction that early attempts for observing the reflexion of X-rays gave no positive results. Immediately after Laue's successful demonstration of the diffraction of X-rays, Sir W. H. Bragg and W. L. Bragg* showed that X-rays can be regularly reflected from the cleavage plane of crystals. The experiment is described in the subsequent section, but here we give a brief sketch of the ideas which led the Braggs to their fruitful and fundamental discovery.

We have seen in the previous section that a crystal may be supposed to owe their form to regular arrangement of constituent atoms in space according to a geometric pattern. Crystals further possess certain characteristic cleavage faces, *i.e.*, when they are struck or subjected to a mechanical stress, they split most easily across some definite planes called cleavage planes. Anybody who has handled mica or calcite is aware of this fact. The Braggs argued that the cleavage planes owe their characteristic property to the fact that the concentration of atoms is maximum along them, and hence they can be used for demonstrating the reflexion of X-rays. The explanation will be clear from the following diagram (Fig. 15).

---

* W. H. Bragg and W. L. Bragg, *Proc. Roy. Soc.*, **88**, 428, 1913.

The Fig. 15 represents a cross-section of the NaCl crystal cut perpendicular to an axis. Here the arrangement of atoms in the plane are represented by the circular dots placed at the corners of each little square. Now consider successively the planes passing through the lines OX, OA, OD, OC and OB, and perpendicular to the plane of the paper. It is clear that the maximum concentration of atoms is along OX, and least along a line like OB, which is almost haphazardly drawn. Along OD, the number is one in a length of $\sqrt{5}$, along OA it is one in a length of $\sqrt{2}$. The planes passing through OX, or OA are cleavage planes.

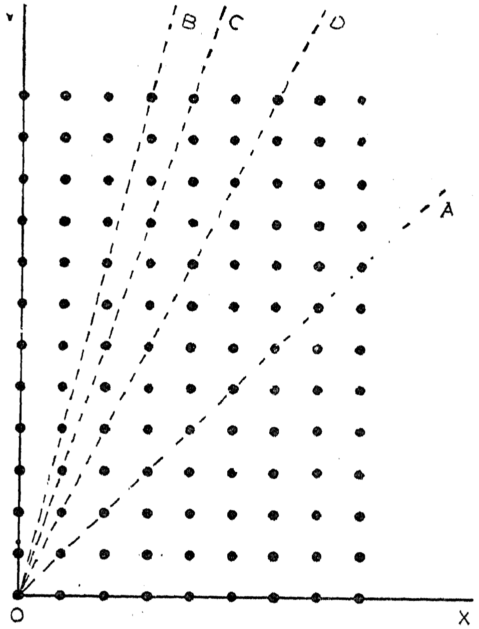

Fig. 15. The cleavage face of a crystal.

The Braggs supposed that the crystal may be supposed to consist of plane parallel lattices OXN, (ON being normal to the paper) or OAN, which are separated by the distances a (for OAX), or $a\sqrt{2}$ (for OAN). They further assumed that when X-rays fall on the crystal they are most copiously reflected from OA, because this has the maximum concentration of atoms. Moreover on account of the regular arrangement of planes, a regular phase difference exists between the rays reflected from successive planes as in the Fabry-Perot interferometer. This is illustrated in Fig. 16. For example, taking the two successive pp planes parallel to the cleavage plane OX of the previous figure, we find that the path difference between the rays reflected from these two planes is $2d\sin\theta$,

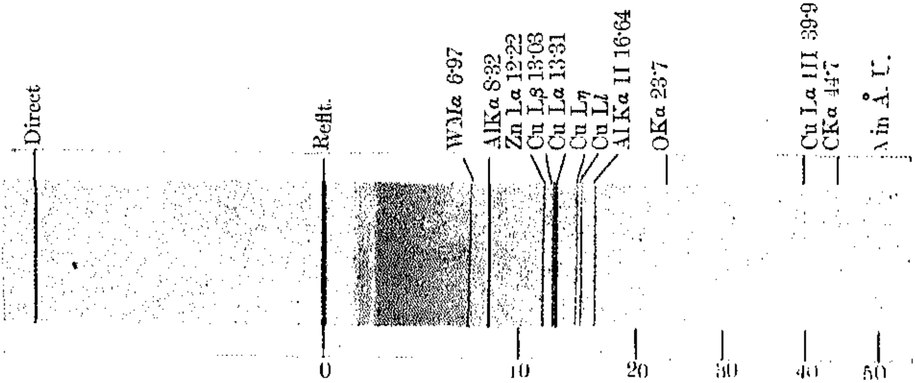

Fig. 48. Grating Diffraction Spectrum of X-rays (*Siegbahn and Magnusson*).
(*p.* 276)

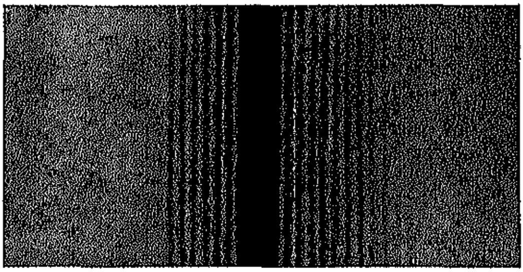

Fig. 74. Pattern of X-ray diffraction by slit (Kellström).
(*p.* 315)

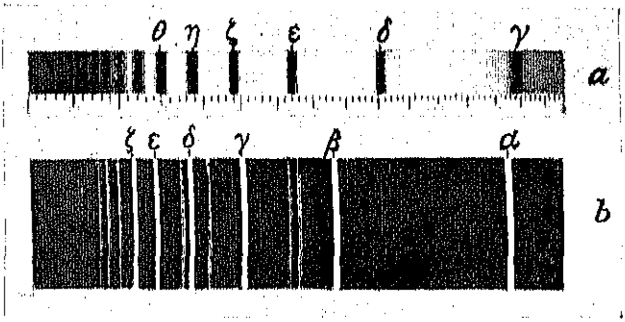

Fig. 4. The Balmer lines of hydrogen. : (*a*) Sirius, (*b*) Vacuum tube.
(*p.* 321)

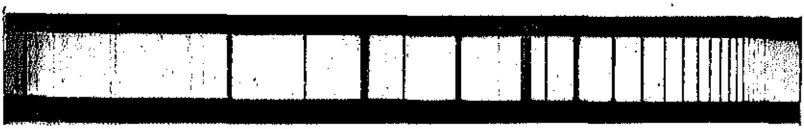

Fig. 5. Spectrum of Zeta Tauri showing Balmer lines in absorption.
(*p.* 330)

[*f. p.* 231

where θ=glancing angle, and d=the distance between the two planes.

If $$2d \sin\theta = n\lambda, \qquad . \ . \ . \ . \ . \ . \ . \ . \ (25)$$ then rays of wavelength λ will show a strong maximum in the reflected beam. In other words, if we allow a monochromatic beam of X-rays to fall on the crystal face pp, and gradually vary the glancing angle, we shall find maximum intensity in the reflected beam at angles θ given by the relation

$$\theta = \sin^{-1} \frac{n\lambda}{2d}$$

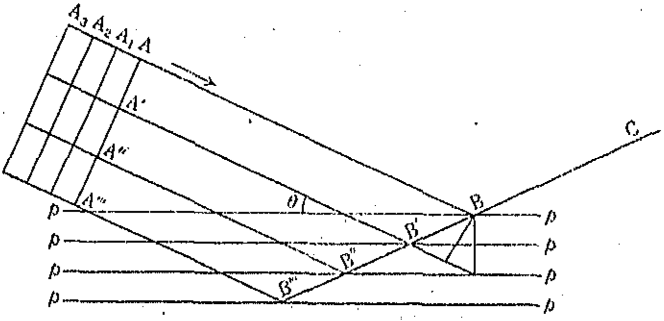

Fig. 16. Reflection of X-rays at crystal lattices (*Bragg*).

If we give to n successively the values 1, 2, 3, ... n, we get maxima in the first, second, ... nth order of reflexion.

It must be noted that in the above equation, θ is the only quantity that can be measured, while n, λ, d are unknown. But d and n can be computed by other means which will be dealt with in the next section. Hence λ can be calculated.

Braggs' law is utilised in unravelling the crystal structure from Laue photographs, powder photographs, etc. In fact it is the fundamental equation of X-ray crystallography.

We can determine the atom plane responsible for giving rise to any maxima according to Braggs' principle of crystal reflection in the following way.

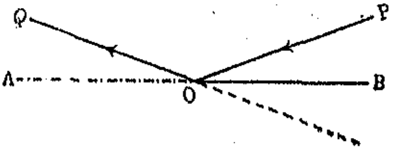

Fig. 17. The median plane.

Let a beam of X-rays PO (Fig. 17) be incident on a crystal at O and let Q be the position of a diffraction maximum. The atomic plane which gave rise to the maximum can be found from the following construction. Bisect the angle QOP, and draw a perpendicular to the bisector at O. Then this line AOB is the section of the atomic plane concerned in this case. This is known as the *median plane.* The angle θ can be calculated from the geometry of the figure. Hence the atomic plane can be completely determined.

The above results obtained by Laue, and Bragg from kinematical principles are based upon the following assumptions :—

(1) The atoms in the grating (space or plane) scatter spherical waves which are coherent, because the phase difference is maintained due to their regular arrangement.

(2) The absorption of the incident beam (primary extinction) is negligible (*vide* however §§142).

(3) The interference between the rays scattered by the electrons in the atom is neglected. It is assumed that an atom contains a charge Z concentrated at one point (*vide* however §§ 133, 134, 155).

(4) The lattice is taken to be ideal. This is however far from the truth. The lattices in practice are much distorted, so that the regularity of arrangement is not perfect. This gives rise to the secondary extinction, which means that the intensity of diffraction spectra is less than what it ought to be in the case of ideal lattice.

Many workers including Debye,* Darwin,† Ewald‡ and Waller‖ have developed a dynamical theory of X-ray diffraction which takes into account deviations from the ideal conditions as enumerated above, and many others, as for example, the heat motion of atoms and the dispersion inside the crystals. For an account of these original papers should be consulted. A discussion of these developments is also given by Ott in *Handbuch der Experimental Physik*, VII, Chaps. 2 and 3.

SECTION II

120. Classical Crystalline Theory¶.—Long before the period when the study of exact sciences was taken up, the natural crystals had been the subject of much speculation. Early observers were puzzled by the regular arrangement of facets in crystals like quartz and calcite. The word *crystal* originates from the Greek equivalent of ice, for it was supposed in the middle ages, that the natural crystals are pieces of ice which have been petrified by extreme cold.

---

* P. Debye, *Ann. d. Phys.*, **43**, 49, 1914.

† C. G. Darwin, *Phil. Mag.*, **27**, 314, 1914.

‡ P. Ewald, *Phys. Zs.*, **22**, 29, 1925.

‖ I. Waller, Dissertation, Uppsala Univ., 1925.

¶ For a good account of this subject the student may consult Tutton, *Crystallography and Practical Crystal Measurement* (1922); Hilton, *Mathematical Crystallography* (1903). See also later references.

As early as 1784, Haüy published the results of a large number of measurements of crystals. In that, he showed that even though two crystals of the same substance may have different appearance, the angles between corresponding faces are always the same.

In order to study the geometrical properties of crystals, it is necessary to refer it to three axes OX, OY, OZ inclined to each other at angles α, β, γ, placed anywhere inside the crystal (Fig. 18).

In general, the axes OA, OB, OC are chosen parallel to any three edges of a crystal, none of which are parallel to one another. Then the planes XOY, XOZ, and ZOY are parallel to some faces of the crystal.

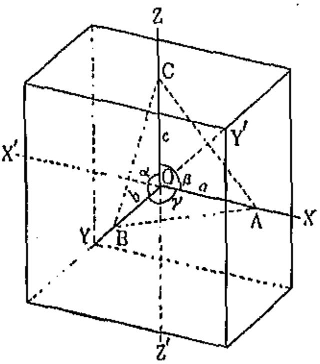

Fig. 18.
Axes of reference in a crystal.

Let ABC be a fourth face cutting the axes at A, B, C, and let OA : OB : OC = $a : b : c$.

The plane ABC is known as the *parametric face.** If there be any other face A′ B′ C′ of the crystal, making intercepts OA′, OB′, OC′ and if

$$OA' : OB' : OC' = \frac{a}{h} : \frac{b}{k} : \frac{c}{l},$$

then (h, k, l) are known as *Millerian indices* of the face A′ B′ C′ with respect to the particular parametric face chosen. The ratio $a : b : c$ is known as the *axial ratio.* b is generally put equal to unity in reference books on crystallography and so the axial ratio is given as $a : 1 : c$. The quantities (h, k, l) are inversely proportional to the intercepts which the face in question makes with the axes, and consequently they are directly proportional to direction ratios† of the normals to the face. The Millerian indices (hkl) of any face are rational numbers and are generally small integers. The law of rational indices has been found to be true experimentally, and it was on this principle, and on the law of constancy of angles in different crystals of a given substance, that the whole theory of crystal structure was based.

---

* Direction ratios become proportional to direction cosines if the axes are rectangular.

† It may be questioned that the parametric face being any arbitrary plane, there will be no uniformity in the nomenclature of the Millerian indices. But in actual practice these indices are transferred with reference to standard axes of symmetry in the crystal which brings about uniformity in the nomenclature. For details of the axes of symmetry see §121,

It will be out of place here to describe the procedure by which the axial ratios $a:b:c$ and the indices (h, k, l) of various faces are found. It will suffice to say that the angles between different faces are measured by means of an instrument known as the *goniometer*.* The calculation of the ratio $(a : b : c)$ and of (h, k, l) becomes a problem in trigonometry.

We can simply illustrate how the different planes in a crystal are referred to by their Millerian indices.

In the figure (19), OX, OY and OZ are three rectangular axes. The plane ABC makes equal intercepts $a=b=c$ on the three axes, and so its indices are (111). The plane BCEF is a (011) plane and similarly we can mark out (110), (101) and other planes.

Again suppose any plane makes intercepts 2 : 3 : 1 on the three axes. Its indices are then as $\frac{1}{2}:\frac{1}{3}:1$, so that the plane is a (326) plane.

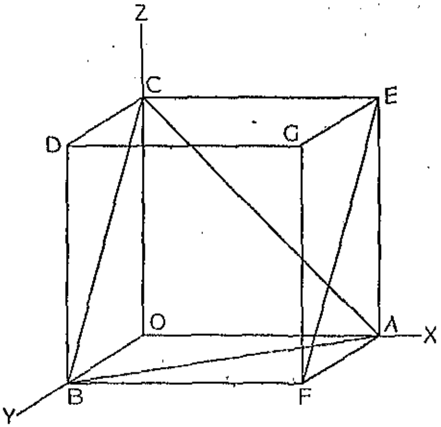

Fig. 19.

121. Crystal Classes.—The most important characteristic of crystals is their perfect *symmetry* in the position of vertices, faces, edges, etc. Crystals have been classed according to the symmetry they exhibit. The elements of symmetry are the following :—

(1) *Axis of Symmetry.*—When the crystal is such that it can be rotated about a line through an angle $2\pi/n$, where $n=2, 3, 4$ or 6, and in the new position the crystal remains *identical*, this line is called an axis of symmetry. The axis of symmetry is said to be two-fold, three-fold, four-fold or six-fold according as $n=2, 3, 4$ or 6.

Thus in Fig. 21, the line b O, b'O or b''O is an axis of four-fold symmetry, and each of the dotted lines aO, a'O, a''O or a'''O is an axis of three-fold symmetry.

(2) *Plane of Symmetry.*—A crystal is said to have a plane of symmetry if every point upon one side of the plane has a corresponding point on the opposite side of it in a mirror image relation. Thus in Fig. 24, the plane XOY is a plane of symmetry. Other planes of symmetry can be seen in Fig. 21. They will be explained later.

---

* For an account of this instrument see A. E. H. Tutton, *Crystallography and Practical Crystal Measurement*, Vol. I.

(3) *Centre of Symmetry.*—A point within a crystal is a centre of symmetry, if a line drawn to it from any point on its surface and extended beyond by an equal distance, encounters another point exactly similar to the second.

In the beginning of this section, the crystal has been referred to a system of co-ordinate axes parallel to three edges of faces of the crystal. In the case of some crystals, there are three axes of symmetry perpendicular to each other; and so it is advantageous to take the crystallographic axes of symmetry as the axes of reference. Such crystals can be divided into three classes: (1) Orthorhombic, (2) Tetragonal, (3) Cubic.

In all these three varieties the axes of reference are at right angles to each other, but the axial ratios are different. Thus, for

Orthorhombic . . . $a : b : c$ . . . all intercepts are unequal
Tetragonal . . . . . $a : a : c$ . . . two intercepts are equal
Cubic . . . . $a : a : a$ . . . all intercepts are equal.

If the axes are not at right angles, we get two more classes: (4) Monoclinic, (5) Hexagonal.

In the monoclinic crystals, $\alpha=90°$, $\gamma=90°$, but β may have any value, and a, b, c are all *unequal.* In hexagonal crystals, $\alpha=90°$, $\beta=60°$, $\gamma=90°$, but the axial ratios are $a : c : a$.

Next there are two more classes. These are: (6) Rhombohedral, and (7) Triclinic.

In the rhombohedral class $\alpha=\beta=\gamma\neq90°$ and $a=b=c$. The triclinic type is the most general type, for here we have axes inclined to each other in any possible angle and the axial lengths are all unequal.

Table 2.

Crystal	Axial angles	Characteristic ratios
Cubic ..	$\alpha=90°$, $\beta=90°$, $\gamma=90°$ ...	$a : a : a$
Tetragonal ...	$\alpha=90°$, $\beta=90°$, $\gamma=90°$ ..	$a : a : c$
Orthorhombic ...	$\alpha=90°$, $\beta=90°$, $\gamma=90°$ ...	$a : b : c$
Monoclinic ...	$\alpha=90°$, β, $\gamma=90°$ ...	$a : b : c$
Hexagonal ...	$\alpha=90°$, $\beta=60°$, $\gamma=90°$ ...	$a : c : a$
Rhombohedral ...	$\alpha=\beta=\gamma\neq90°$	$a : a : c$
Triclinic ...	$\alpha\neq\beta\neq\gamma\neq90°$	$a : b : c$

---

[*] A good account of this subject has been given in *The Structure of Crystals*, Wyckoff (1924), Chap. I. See also *Handbuch der Experimental Physik*, Bd. VII (1), Niggli.

The characteristic angles and ratios of different varieties of crystals are collected in table 2 for ready reference.

122. The Point Group.—All crystals can be placed in one of these seven classes. But these have been still subdivided into 32 classes, according to the elements of symmetry possessed by them. Each of these is called a *point group*. The elements of symmetry are, as has been already mentioned, one or more axes of polyfold symmetry combined with planes of symmetry and centres of symmetry. The point groups are thus classes of crystal symmetry. The different combinations of these symmetries have given rise to these point groups, and it can be proved analytically that they can be only 32 in number.

In the triclinic system where the axial ratios and angles are all unequal the symmetry is least, and so there are only two point groups associated with it. One of these is known as *asymmetric*, for there is no symmetry in it. In the other there is only a centre of symmetry, meaning thereby that in a triclinic crystal there can be two faces having the indices h, k, l and $-h, -k, -l$. The latter is often written as $\bar{h}, \bar{k}, \bar{l}$.

As there is no other symmetry in a triclinic crystal, there cannot be two faces having the indices h, k, l and $\bar{h}, k, l$. From a study of these indices the point group to which the crystal belongs can be found. The largest number of point groups (symmetry characteristics) occurs in the tetragonal and cubic crystals; because in these crystals there can be simultaneously planes of symmetry, centre of symmetry as well as rotational symmetry. Two such simple varieties of cubic crystals are shown in Figs. 20 and 21. The tetrahedron $AA'A''A'''$ belongs to the cubic class in which the axes of reference are the lines u, v, w joining the opposite sides of the tetrahedron and passing through the centre of

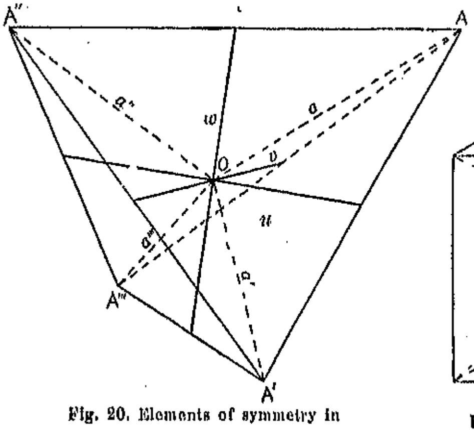

Fig. 20. Elements of symmetry in tetragonal crystal.

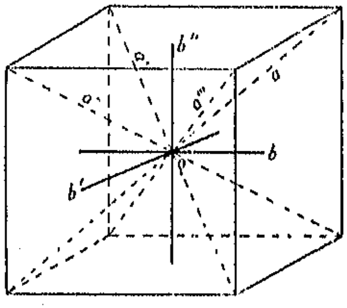

Fig. 21. Elements of symmetry in a cubic crystal.

gravity O. In this case, there are three two-fold axes *u*, *v*, *w*, and four three-fold axes AO, A′O, A″O and A‴O.

Fig. 21 also shows a cubic crystal having a different grouping of symmetry. There are three four-fold axes *b*, *b′*, *b″*, four three-fold axes *a*, *a′*, *a″*, *a‴*, also six two-fold axes (not shown) joining the middle points of parallel sides of the figure.

It is very important to find out the point-group (or one of the classes of symmetry) to which the crystal belongs. This can be done with the aid of the goniometer as has been said already; unfortunately X-ray methods do not give complete information on this question (see §130).

123. The Bravais Lattice.—We were discussing so long the outward appearance of crystals. But apart from the external appearance the crystalline nature is inherent in the substance. Any battered grain of sand is crystalline, while the most perfect model of crystal made of glass is not crystalline. It is a matter of common experience that when a rhombohedral crystal like calcite is struck gently with a hammer, it breaks up into smaller rhombohedrons. It was quite natural to suppose that calcite is made up of extremely small rhombohedral units of atomic dimensions. If these rhombohedral units are placed side by side, we get a complete crystal. The development in this direction is due to Bravais (1850). When these elementary units of crystalline structure known as *unit cells* are placed side by side, so that the structure extends continuously, we get a *Bravais lattice*. Such a lattice is shown in Fig. 22. In this the lines are drawn parallel to the three axes of reference x, y, z. The intervals at which the parallel lines are drawn are in the ratio $a : b : c$, the axial ratios of the crystal found by goniometric measurements. The lattice belongs to the triclinic type ($a \neq b \neq c$, $\alpha \neq \beta \neq \gamma \neq 90°$), and consists of a large number of unit cells OADFECG (drawn in thick line) placed side by side. If we take $a = b = c$, and $\alpha = \beta = \gamma \neq 90°$, we get a rhombohedral lattice to which the crystal of calcite belongs. If it can be

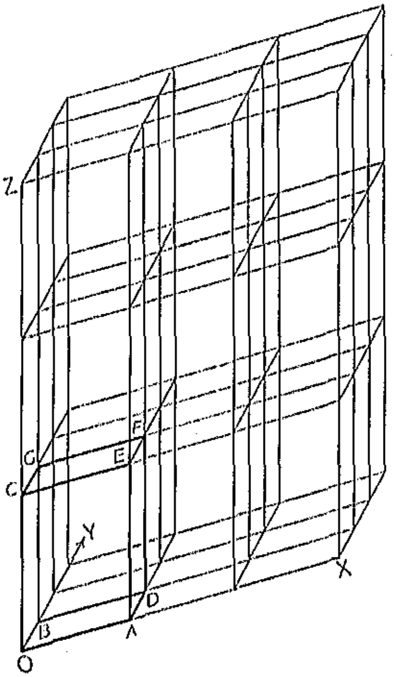

Fig. 22. The Bravais lattice.

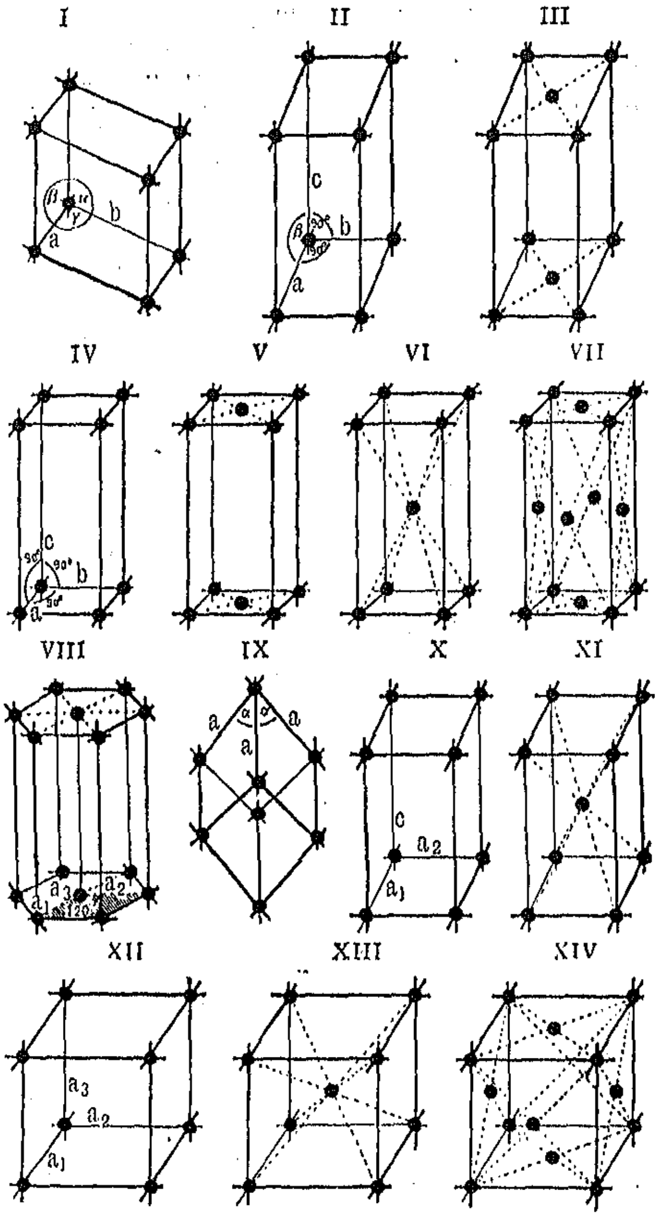

Fig. 28. The fourteen Bravais lattices.

I. Triclinic. II. Simple monoclinic. III. Base-centred monoclinic. IV. Simple orthorhombic. V. Base-centred orthorhombic. VI. Body-centred orthorhombic. VII. Face-centred orthorhombic. VIII. Hexagonal. IX. Rhombohedral. X. Simple tetragonal. XI. Body-centred tetragonal. XII. Simple cubic. XIII. Body-centred cubic. XIV. Face-centred cubic.

determined how many molecules of $CaCO_3$ are accommodated in one unit cell, we can find out the arrangement of Ca and CO_3 in it. We utilise the theory of point-groups (or classes of symmetry) for this purpose. We suppose that *the atoms are arranged at the corners of the lattice*, and must follow the symmetry valid for this class of crystal. The corners of the Bravais lattice thus become the centres of point-groups, and the elements of symmetry which were facets and edges when the complete crystal was studied, now become the molecules themselves. It can also be shown analytically that in general the molecules must arrange themselves with the same symmetry which is exhibited by the crystal as a whole.

We have seen that crystals can be divided into seven classes depending upon their axial ratios and angles. So there must be corresponding seven classes of elementary unit 'bricks' or *lattices*. But Bravais showed that the total varieties of lattices possible should be 14 instead of seven. The student can easily verify this fact from Fig. 23. For example, take the orthorhombic system (IV to VII). If at the centre of the simple orthorhombic (IV) we imagine a new atom to be situated as in (VI), we get a *body-centred* orthorhombic, which represents a *new* lattice of this system. Let us imagine a structure consisting of eight such contiguous body-centred orthorhombic lattices. If we join the eight central atoms, we see that we obtain another body-centred orthorhombic lattice. Thus we cannot build simple lattices out of body-centred lattices, and *vice versa*. Hence the latter is a fundamental kind of lattice by itself. Similarly we have two more kinds, the *base-centred* and *face-centred* orthorhombic lattices. But if we try the same procedure for the triclinic system, we find that this gives only *one* kind of lattice. For the figure formed by joining the eight central atoms is in this case another *simple* triclinic lattice. In the same way the cubic system gives three different varieties:

(i) The simple lattice,
(ii) Body-centred lattice,
(iii) Face-centred lattice.

In a simple cubic lattice, the molecules are situated at the corners of the cube; in a body-centred lattice they are placed at the corners as well as at the centre of the cube; in the case of face-centred lattice they are situated at the corners as well as in the centres of faces of the cube. These three cases can be seen in Fig. 23, XII, XIII, XIV. All the fourteen lattices are shown in Fig. 23 (I to XIV).

Seven of them are of the simple kind, while the other seven are examples of *inter-penetrating lattices*. The body-centred cubic lattice is clearly seen to be the resultant of two lattices, the origin of one being (0, 0, 0), while that of the other $a/2$, $a/2$, $a/2$.

124. Space-groups.—We have seen that Bravais postulated fourteen-space lattices in which the vertices of the unit cells are supposed to be occupied by point-groups. The position of one atom with respect to a point-group to which it is attached must be the same in every part of the crystal. In order to achieve this, the 32 kinds of point-groups are associated with the 14 lattices, and the resultant arrangement of symmetry characteristics which will be combined in all directions are known as *space-groups.*

For example, consider the structure of a calcite crystal. The unit cell of calcite must have a place for the Ca atom as well as for the CO_3 radicle. The CO_3 radicle consists of a carbon atom surrounded by three oxygen atoms. We can assign the calcium atom to one of the corners of the lattice, and the carbon atom to the next corner. The oxygen atoms must be arranged in a pattern (or point group) which is consistent with the rhombohedral characteristics to which class calcite belongs. But it has been found that there are a large number of ways in which these point-groups can be arranged at the corners of lattices satisfying these conditions, and each of these ways is known as a *space-group.* Their total number is 230 and they were studied by Sohncke and Schoenfliess at the end of the last century. It will be out of place to discuss here the nature of the space groups, but one single case may be illustrated with diagram. In Fig. 24, x, y, z are the axes of reference in a monoclinic crystal having XOY as the plane of symmetry and OZ the two-fold axis of rotation. To a point P there is a corresponding point at P_{11}, because XOY is a plane of symmetry, and another point at P_1, because OZ is a two-fold axis of rotational symmetry. This point-group is fitted in the Bravais monoclinic lattice in Fig. 25. In this lattice O is the origin and X, Y, Z are the axes, OADEFCG is the unit cell. The centre of the point-group in Fig. 24 is placed at O, A_1, A_2, . . . etc., B_1, B_2, . . . etc., C_1, C_2, . . . etc., (Fig. 25) extending in all directions, and form the special space group. It will be seen that in the space group illustrated above (Fig. 25), there are four atoms* within the unit cell. This is one of the characteristics of a

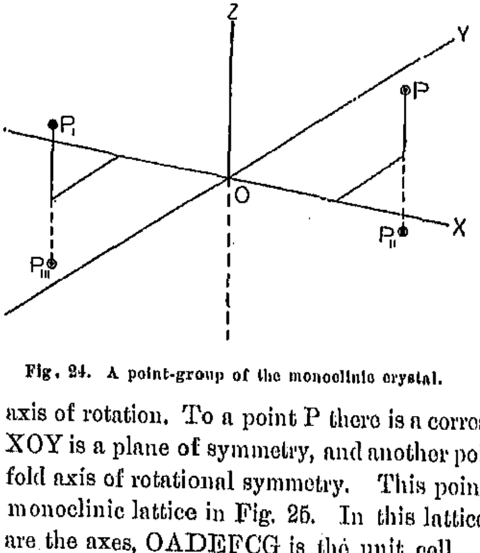

Fig. 24. A point-group of the monoclinic crystal.

---

* Some atoms apparently in the unit cell do not really come within this cell, as they are situated below or above the bounding planes. They can be easily distinguished by comparison with Fig. 24 in which P_{11} and P_{111} lie below the XOY plane, and P and P_1 above it.

monoclinic crystal. So whenever we find a crystal belonging to monoclinic system with the symmetry shown in Fig. 24 and having four atoms in its unit cell, we may at once conclude that the arrangement of the atoms (space group) in the crystal is most probably as shown in Fig. 25. The co-ordinates of any atom P in the point-group are known as its parameters.

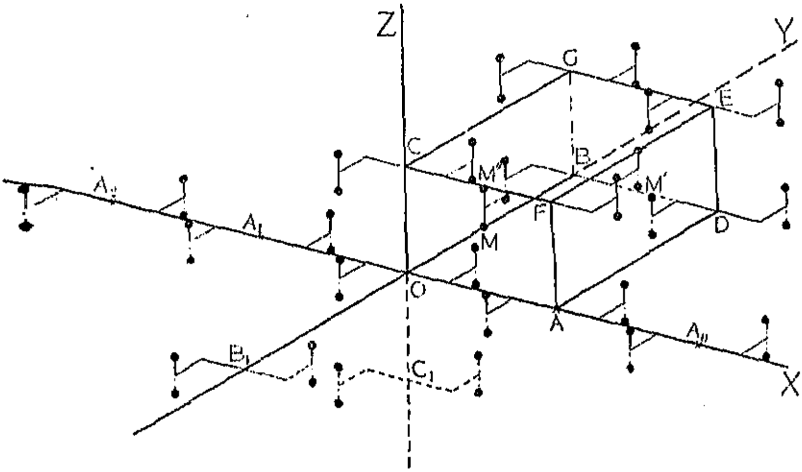

Fig 25. A space-group of the monoclinic crystal.

In order to know the structure completely it is necessary to find out to which of the space groups a crystal belongs, and to determine the parameters of the atoms in the space group. The former can be done by finding

(*i*) The dimensions of the unit cell,
(*ii*) The number of atoms in the unit cell, and
(*iii*) The symmetry characteristics (point groups).

There are four methods for determining the above factors. These are

(1) Bragg method,
(2) Powder method (Debye-Scherrer and Hull),
(3) Laue method,
(4) Rotating crystal method (Schiebold).

We shall briefly consider these methods one by one. The parameters lso can be found from the above four methods. If all the four toms in the above unit cell (Fig. 25) be alike, the parameters of P alone n Fig. 24 are sufficient; if the atoms are different, the parameters of P_I, P_{II}, P_{III}) have also to be determined.

125. Investigation of Crystal Structure by Braggs' Method*.

—It is clear from the foregoing treatments (§§116, 119) that

---

[*] For a full review of this subject see W. H. Bragg and W. L. Bragg, *X-rays and Crystal Structure*, Chap. III (1924).

both in Laue's method and the Bragg method, we have to deal with interference of X-rays scattered by the electrons composing the constituent atoms of a crystal; in Laue's method we examine the transmitted beam, in Bragg's method, we examine the beam scattered on the side of incidence. The cleavage face of the crystals behaves like a mirror in this case, and the rays which are most copiously reflected are those satisfying the Bragg relation

$$n\lambda = 2d \sin \theta$$

If the crystal be cut along any other face possessing the Millerian indices (h, k, l) Bragg's law takes the form

$$n\lambda = 2d_{hkl} \sin \theta'$$

where d_{hkl} is the least distance between two parallel consecutive planes having the indices (h, k, l), and $\theta' =$ the new glancing angle.

Bragg's method of studying the crystal structure consists in finding out d_{hkl}, the grating space or the least distance between two consecutive atomic planes having the indices (h, k, l). From a knowledge of d_{hkl}, and also from the relative intensities of reflection for different values of n (order of reflexion), the crystal structure can be deduced. For illustrating the method we take the simple case of cubic crystals like Rocksalt (NaCl), and Sylvine (KCl). Bragg's apparatus for studying the crystal structure is shown on the next page (Fig. 26). The arrangement is generally known as Braggs' X-ray Spectrometer.

A strong beam of X-rays from the anticathode A of an X-ray tube is allowed to pass through two slits S and L, and is then incident on the crystal C which is fixed on a table having a vernier attached to it, that can be rotated on a concentric graduated circle. Thus the table can be rotated about an axis through its centre; but the graduated circle is fixed to the base of the spectrometer. The angle through which the crystal (with its table) is rotated can thus be read accurately by means of the vernier. I is an arm which can rotate about the common axis of the table and the circle, though independently of the former. There is another vernier attached to this arm, so that the rotation of the latter can also be read on the graduated table. The ionisation chamber is placed on the arm I. When the glancing angle θ satisfies the Bragg's equation

$$n\lambda = 2d \sin \theta,$$

the X-rays are reflected by the crystal, in a direction making an angle 2θ with the original direction of the X-rays. Hence if the ionisation chamber is placed in that direction, the electrometer will show a strong ionisation current. For best results, the proper alignment of the focus of the anticathode, the slits and the axis of rotation of the table T is very necessary. The crystal C is placed such that the axis of rotation of the table lies on its surface. In order to prevent stray radiations from entering the ionisation chamber, a slit D is provided in front of it. The ionisation chamber is filled with methyl chloride vapour. The X-rays enter the chamber through a window covered with thin aluminium foil. The crystal is at first placed on the table so that the (100) plane is on the axis of rotation. The crystal is rotated gradually while the arm carrying the ionisation chamber is rotated through double the angle. The ionisation current observed is plotted against 2θ. The peaks show those glancing angles which satisfy the Bragg equation for the wavelength of characteristic rays of the target used. The (100) plane is then replaced by the (110) and (111) planes, and a similar procedure, as described above, is gone through. The diagram (27) shows the actual curves obtained. The anticathode used was palladium and the voltage and current in the X-ray tube was so maintained that a strong beam of Pd K_{α} radiation was available.

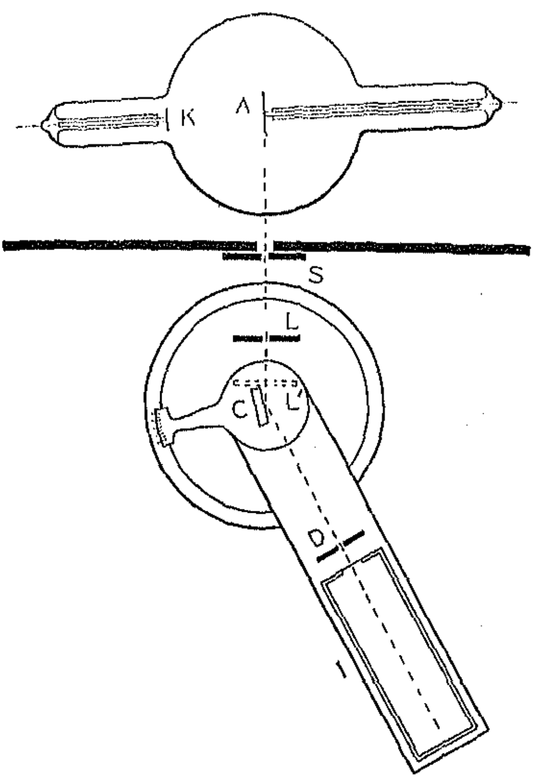

Fig. 26. Braggs' X-ray Spectrometer.

We find that the (100) face of KCl, shows peaks at the angles 10°46′, 21°38′, 32°40′. Now remembering that these are the 2θ-values, the ratio between the corresponding $\sin\theta$-values is obtained as

$$\sin 5°23' : \sin 10°49' : \sin 16°20' = 1 : 2 : 3$$

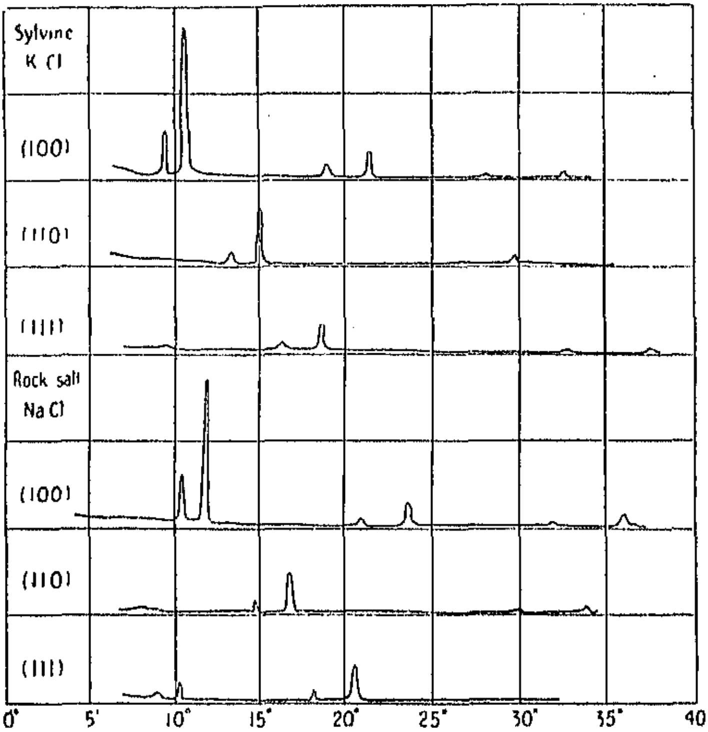

Fig. 27. Reflection of X-rays at various crystal-planes (KCl, NaCl).

We are sure that they are the first, second, and third order reflections from the (100) face. For other faces we get three reflections and the same relation holds. When the first order reflections from the three faces (100), (110) and (111) of KCl are compared, the ratio between the grating constants d_{100}, d_{110} and d_{111} are obtained. Thus for the KCl crystal

$$d_{100} : d_{110} : d_{111} = \frac{1}{\sin 5°23'} : \frac{1}{\sin 7°37'} : \frac{1}{\sin 9°25'},$$

or

$$\frac{1}{d_{100}} : \frac{1}{d_{110}} : \frac{1}{d_{111}} = 1 : \sqrt{2} : \sqrt{3}.$$

Similarly for the NaCl crystal we obtain a weak first order reflection from the (111) face at about half the corresponding angle for KCl. Considering this we obtain for NaCl

$$d_{100} : d_{110} : d_{111} = 1 : \frac{1}{\sqrt{2}} : \frac{2}{\sqrt{3}}.$$

But if we leave this weak reflexion out of our consideration, the ratio for NaCl becomes identical with that for KCl.

126. Interpretation of Results.—While explaining Bravais lattices, it was said that the lattices having cubic symmetry were three in number, the simple, face-centred and body-centred. KCl is known to have cubic symmetry, and so must belong to one of the three lattices. It is to be found which of the three types gives the ratio of $d_{100} : d_{110} : d_{111}$ as obtained from the experiment. Let us consider crystals of the three lattices one by one.

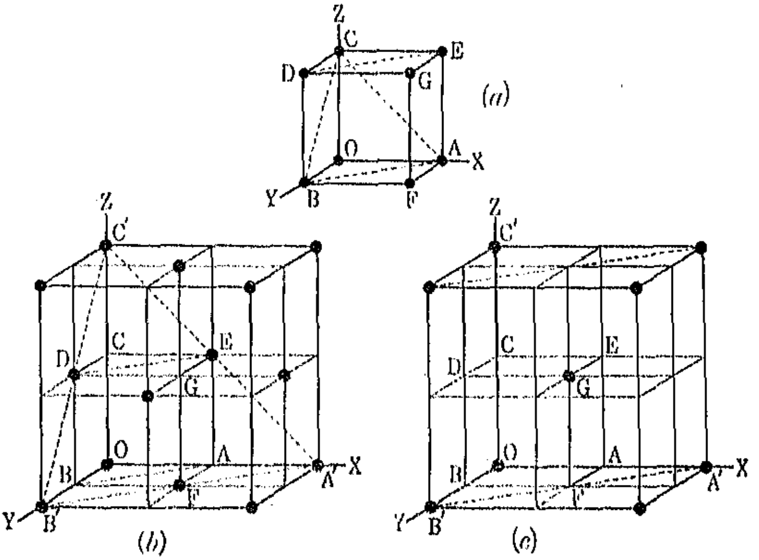

Fig. 28. The three cubic crystal lattices.

In Fig. 28,

(*a*) is a unit cell OBFAECDG of simple cubic lattice,

(*b*) consists of eight such cells of a face-centred cubic lattice,

(*c*) consists of eight such cells of a body-centred cubic lattice.

Let a be the side of the unit cell, O be the origin and OX, OY, OZ be the system of cubic axes in all the three cases. Now according to the definitions of the Millerian indices the faces parallel to OBDC will be the (100) faces, those parallel to BDEA the (110) faces, and those parallel to ABC the (111) faces.

The equation of any plane (hkl) referred to cubic axes is

$$hx+ky+lz = a$$

The distance of the plane from the origin is given by

$$d = \frac{a}{(h^2+k^2+l^2)^{\frac{1}{2}}}$$

according to the theorems of analytic geometry of three dimensions.

Hence in the case of the simple lattice (a) for the first (100) plane $d=a$, and for the next $d=2a$. Therefore d_{100}, the distance apart between two consecutive (100) planes is

$$d_{100} = a$$

Similarly,

$$d_{110} = \frac{2a}{\sqrt{2}} - \frac{a}{\sqrt{2}} = \frac{a}{\sqrt{2}}$$

$$d_{111} = \frac{2a}{\sqrt{3}} - \frac{a}{\sqrt{3}} = \frac{a}{\sqrt{3}}$$

Therefore

$$\frac{1}{d_{100}} : \frac{1}{d_{110}} : \frac{1}{d_{111}} = 1 : \sqrt{2} : \sqrt{3} \quad . \quad . \quad . \quad (26)$$

This ratio was obtained for KCl experimentally, and consequently the lattice of KCl must be of the *simple cubic* type.

For reference, it will be necessary to find similar relations between grating constants for the other two lattices. From the figures it is clear that for a face-centred cube the d_{100} and d_{110} will remain the same as those for the case of a simple cube.

For the first (111) plane the equation is

$$x+y+z = a,$$

but as no atom is situated on this plane, we shall have to take the next (111) plane

$$x+y+z = 2a$$

Similarly the next (111) plane containing any atoms is

$$x+y+z = 4a$$

Therefore

$$d_{111} = \frac{2a}{\sqrt{3}}.$$

Therefore

$$\frac{1}{d_{100}} : \frac{1}{d_{100}} : \frac{1}{d_{111}} = 1 : \sqrt{2} : \frac{\sqrt{3}}{2} \quad . \quad . \quad . \quad (27)$$

for the *face-centred cube*. For a body-centred cube, d_{100} is the same as before, but d_{110} and d_{111} are different. But the equation of the first (110) plane is

$$x+y=2a$$

for, no atom exists at a distance a, $3a$, etc., from the origin.

Hence $$d_{110}=\frac{4a}{\sqrt{2}}-\frac{2a}{\sqrt{2}}=\sqrt{2}\,.\,a.$$

Again for d_{111} plane the equation is

$$x+y+z=2a$$

The next parallel (111) plane passes through the atom G at the centre of the cube. Its equation is

$$x+y+z=k=a+a+a=3a$$

Therefore $$d_{111}=\frac{3a}{\sqrt{3}}-\frac{2a}{\sqrt{3}}=\frac{a}{\sqrt{3}}$$

For, we have to take the distance between two consecutive parallel planes having the same indices (111).

Therefore $$\frac{1}{d_{100}}:\frac{1}{d_{110}}:\frac{1}{d_{111}}=1:\frac{1}{\sqrt{2}}:\frac{\sqrt{3}}{1}\quad . \quad . \quad . \quad (28)$$

for a *body-centred lattice*.

Thus we have calculated the lattice constant d for the three faces (100), (110) and (111) of the three types of cubic lattices. We collect these values in the following table for ready reference.

Table 3.

Cube	d_{100}	d_{110}	d_{111}
Simple ..	a	$\frac{a}{\sqrt{2}}$	$\frac{a}{\sqrt{3}}$
Face-centred ...	a	$\frac{a}{\sqrt{2}}$	$\frac{2a}{\sqrt{3}}$
Body-centred ...	a	$a\sqrt{2}$	$\frac{a}{\sqrt{3}}$

For sodium chloride as depicted in the diagram of experimental curves (Fig. 27),

$$\frac{1}{d_{100}}:\frac{1}{d_{110}}:\frac{1}{d_{111}}=1:\sqrt{2}:\frac{\sqrt{3}}{2},$$

and so it is concluded that the sodium chloride lattice is *face-centred*. It has been found that out of the alkali halides, only KCl belongs to the simple cubic type, while others belong to either face-centred or body-centred lattice.

This dissimilarity between the structure of NaCl and KCl was explained by Bragg in this way. Bragg argues that in the case of KCl, the reflections from the (111) face showed a peculiarity, in that, we may suppose that the odd order of reflections were absent, so that the second order spectrum was taken for the first. If that correction is made, we shall have to double the grating constant of (111) planes. We shall get then

$$\frac{1}{d_{100}} : \frac{1}{d_{110}} : \frac{1}{d_{111}} = 1 : \sqrt{2} : \frac{\sqrt{3}}{2}.$$

So the structure of KCl also comes out to be that of the face-centred type, as depicted in Fig. 10.

Here the white circles are say, chlorine atoms, while the black ones represent potassium or sodium atoms. The sodium-chloride and potassium-chloride crystals thus come out to possess a similar structure. But it has still to be explained why odd order reflections vanish in the case of (111) face of KCl, and not in the case of NaCl. In the case of KCl, the potassium and chlorine atoms having atomic numbers 19 and 17 respectively contain almost equal number of electrons. The scattering power of an atom depends upon the number of electrons composing it. In the figure, the white circles alone form a face-centred lattice, and so do the black circles. If the scattering power of black and white circles are thus the same, the structure reduces almost to the case of a simple cubic lattice as was first found in the case of KCl. Now the (100) and (110) planes contain atoms of both the kind. But the (111) plane contains white circles or black circles alternately. The grating constant d_{111} for the white circles will be the distance between the first plane containing white circles and the next plane containing similar circles. But midway between them there is another plane containing black circles. The wave reflected from this plane will destroy the first order reflections from the planes containing white circles. It will strengthen all even order reflections, but will cut out odd order reflections. In the case of KCl the scattering powers of potassium and chlorine are almost equal, and so the odd order reflection is totally suppressed and the crystal behaves as a simple cube. In the case of sodium chloride, the atoms Na (11) and chlorine (17) have different scattering powers, so the suppression of odd order spectra is not complete. But still we find in Fig. 27 the first order reflection from (111) face for NaCl is much weaker compared to the second order reflection. The structure of NaCl and KCl crystals is thus completely explained in the light of experimental results if we assume that in both of them the Na or K, and the Cl atoms are situated alternately at the lattice points of a face-centred cube.

127. The Dimensions of the Unit Cell.—We have to find now how many molecules of NaCl are associated with a unit cell. Consider a unit cell in the structure of NaCl shown in Fig. 10. Four corners of this unit cell are occupied by four Na-atoms, and the four alternate corners by four Cl-atoms. But each of these eight atoms is being shared by eight such contiguous unit cells from all sides. So on the average one molecule of NaCl is associated with two unit cells. The volume of two unit cells is evidently equal to $2\,(d_{100})^3$. So the unit volume of the crystal contains $1/2(d_{100})^3$ molecules of NaCl.

If M is the molecular weight of the crystal and m the mass of a hydrogen atom, the weight of a molecule is Mm. Hence we get

$$\frac{Mm}{2\,(d_{100})^3}=\rho$$

where ρ is the density of the crystal. For sodium chloride

$$M=58,\quad m=1{\cdot}662\times10^{-24}\text{gms.},\quad \rho=2{\cdot}17$$

Therefore $$(d_{100})^3=\frac{Mm}{2\rho}=\frac{58\times1{\cdot}662\times10^{-24}}{2\times2{\cdot}17}=22{\cdot}21\times10^{-24}$$

Hence $$d_{100}=2{\cdot}81\times10^{-8}\text{ cm.}$$

Hence the grating space of sodium chloride is $2{\cdot}81\times10^{-8}$ cm. In order to find the wavelength of palladium K_α-rays, we see from Fig. 27, that the first order reflection occurs at 6° 0′. From Bragg's law

$$\lambda=2\times2{\cdot}81\times10^{-8}\,.\,\sin 6^\circ$$
$$={\cdot}587\times10^{-8}\text{ cm.}$$

Hence the wavelength of K_α rays of Pd is $\cdot587\times10^{-8}$ cm. or $0{\cdot}587$ Å.U.

128. Powder Spectroscopy.*—It was discovered by Debye and Scherrer† in Germany and Hull‡ in America about the year 1916 that a diffraction pattern is obtained when a thin film of powdered crystal is substituted for the single crystal in the Bragg or Laue methods. If the individual crystals of this powder are haphazardly oriented so that they make all possible angles with the incident X-rays, all orders of reflection from all possible atomic planes can be recorded at the same time. There are very few substances which grow single large crystals, and so Bragg's method can be applied only to a limited number of substances; in other cases the powder method is suitable.

The arrangement of apparatus in powder spectroscopy is shown in Fig. 29. A fine beam of *monochromatic* X-rays is allowed to fall on a paper capsule P containing the finely powdered crystal. Any minute crystal may be oriented at such an angle with respect to the incident beam that the Bragg relation is satisfied for an atomic plane $(h\ k\ l)$ in it. Thus we have

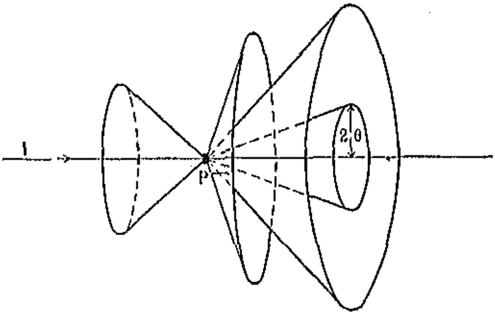

Fig. 29. Principle of powder photography.

$$n\lambda = 2d_{(hkl)} \sin \theta_n \quad \text{. . . . .} \quad (29)$$

where d_{hkl} is the grating constant for a plane $(h\ k\ l)$ and θ_n the glancing angle. As θ_n is the angle between the incident X-rays and some atomic plane, the angle between the reflected ray and the direction of the incident ray will be $2\theta_n$ (see §119). There will be other crystals in the powder in which the atomic plane $(h\ k\ l)$ is inclined at an angle θ_n but with different azimuth. It is thus obvious that all the reflected rays from the atomic plane $(h\ k\ l)$ will lie on a cone with its apex at P and semivertical angle $2\theta_n$. If a photographic plate be kept perpendicular to the direction of the incident beam, a series of circles will be recorded on it. Plate IV, Fig. 30, shows a Debye-Scherrer photograph of a crystal of wurtzite ZnS, taken with CuK-rays§. In order to record reflections with large values of θ_n a photographic film bent in the form of a circle with P as centre is substituted for the plate. Fig. 31 on the Plate IV shows a

---

* For a detailed account see Wyckoff, *The Structure of Crystals* (1924).

† P. Debye and P. Scherrer, *Phys. Zeits.*, **18**, 291, 1917.

‡ A. W. Hull, *Phys. Rev.*, **10**, 661, 1917.

§ CuK radiation consists of K_α and K_β. The latter can be almost completely removed by putting a filter of Ni. For filtering actions *vide* Chap. XI.

PLATE IV

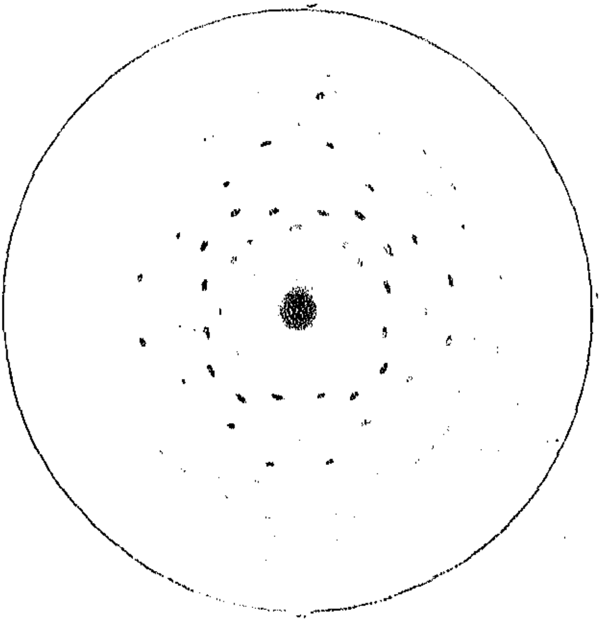

Fig. 18. Laue's spots for ZnS.
(*p.* 227)

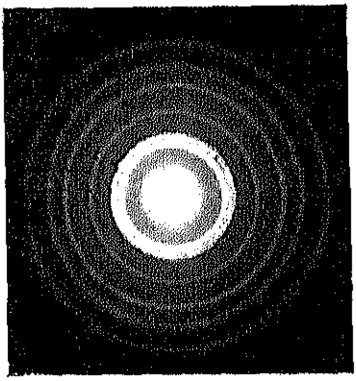

Fig. 30. X-ray diffraction pattern for powder.
(*p.* 250) (*Debye Sherrer*)

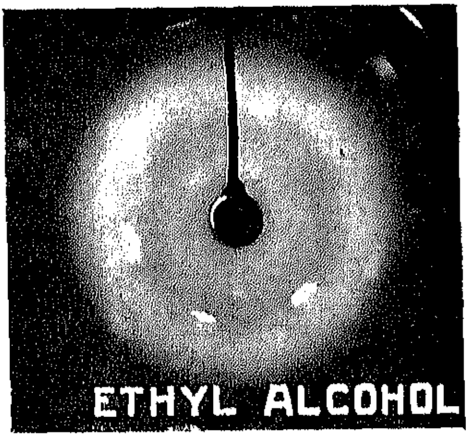

Fig. 35. Diffraction pattern for X-rays in ethyl alcohol.
(*p.* 261)

Fig. 31. X-ray diffraction pattern for powder (*Hull*).
(*p.* 250)

[*f. p.* 250

powder film photograph (due to Hull) of CSi (carborundum) taken with CuK_α rays. The central black-spot is due to the direct beam*. The lines are the intersection of cones with cylinder which forms the film in this case.

The lines which are straight in the plate have $2\theta_n = 90^\circ$, and the lines beyond it curve on the other side. It is obvious from the equation that no reflection is possible from planes for which $d_{hkl}/n < \lambda/2$.

As the reflections are taking place only from a few particles, the energy required to get a good powder photograph is greater than that in any X-ray diffraction phenomena; and so large exposures with greater current density in the X-ray tube is needed. If the crystal is not finely ground (to 250 meshes), it becomes necessary to rotate the powder when the photograph is being taken, otherwise the lines will be discontinuous and dotted. If on the other hand the powder is very finely ground then the diffraction lines will be broad and diffuse. Scherrer† gave an expression connecting the width of the lines and average size of particles. This is

$$B = 2\sqrt{\frac{\log 2}{\pi}} \cdot \frac{\lambda}{D} \cdot \frac{1}{\cos \theta/2} + b$$

where B = the deserved width of lines,
D = thickness of the crystal,
C = the constant of apparatus.

As D becomes small, B tends to become large, showing thereby that the crystal powder is nearing amorphous conditions. Thin sheets of metal are conglomerations of large number of crystals, and so behave like powders. It has been found that metal foils which have been made by heating give sharp circular patterns. On the other hand foils made by rolling processes do not give complete circles; the circles are discontinuous and marked by regularly placed patches on it. It shows that in this process the crystals tend to adjust themselves in one particular orientation. A large number of data have been obtained in this connection in recent years, and have thrown much light on the inner structure of metals and other useful substances. In many ways these researches have also helped industry‡.

The method of X-ray photography has been applied for analysing the structure of wool, human hair, fibres, rubber, celluloid, and many other organic substances. It was formerly supposed that these substances had no crystalline structure. But Astbury§ and others found that the fibrous substances mentioned above possess a pseudo-crystalline structure which changes when they are stretched or subjected to other mechanical treatments. These substances give diffuse rings interspersed with spots. From this it is concluded that the crystalline particles forming these matters are not oriented in all directions. In fact Astbury came to the conclusion that the molecules of these substances exists in long chains, the length of which is many times greater than the breadth, and lie along the length of the fibre. Similarly unstretched rubber has been found to be noncrystalline, but when stretched, it exhibits a crystalline structure.

---

* The central beam produces halation, so it is shielded by means of a lead disc. The plate is a positive and so the central spot is black.

† P. Scherrer *Phys. Zeits*, **19**, 474, 1918.

‡ See Glocker's *Materialprufüng mit Röntgenstrahlen*.

§ Astbury, *Phil. Trans. Roy. Soc. A*, **230**, 75, 1932.

129. Calculation of Spacing from Powder Photographs.—

We will take the case of cubic crystal of MgO which has been analysed by Wyckoff. It has been shown in §126 that the grating space of a plane (hkl) for a simple cubic crystal is given by the equation

$$d_{hkl} = \frac{a}{\sqrt{h^2+k^2+l^2}} \quad . \; . \; . \; . \; . \; . \; . \; . \; . \; . \quad (30)$$

where a is the dimension of the unit cell, or in other words the grating space of (100) plane. Rearranging the equation we have

$$\frac{4a^2\sin^2\theta}{\lambda^2} = (h^2+k^2+l^2)n^2 \quad . \; . \; . \; . \; . \; . \; . \; . \quad (31)$$

The expression on the right-hand side is always an integer, so the sine-squares for different lines are proportional to integers. Since θ for different lines in a powder photograph are directly known, this conclusion can be verified. In the case of MgO it was found that for the first five lines in the powder photograph, the sine-squares are in the ratio 3 : 4 : 8 : 11 : 12. In the table below the various possible values of (hkl) and the corresponding values of $(h^2+k^2+l^2)n^2$ are given.

Table 4.

$(h\,k\,l)$	n	$(h^2+k^2+l^2)n^2$
100	1	1
110	1	2
*111	1	3
*100	2	4
120	1	5
*110	2	8
100	3	9
*113	1	11
*111	2	12

We find that $(h^2+k^2+l^2)n^2$ of those planes marked with stars are in the ratio 3 : 4 : 8 : 11 : 12, and so the first five lines in the case MgO observed may be due to the reflection from these planes. In this way the indices of the planes which are effective in reflection are calculated. Again λ is known. Hence a can be calculated from the relation (31). The eqn. (30) then readily gives the spacing d_{hkl}. In the case of crystals of lesser symmetry (tetragonal, orthorhombic, etc.) the value of $(h^2+k^2+l^2)n^2$ is not an integer, and so it is not easy to determine for them the planes of reflection, for they involve the axial ratios and angles which are different for different crystals. The spacings for face-centred and body-centred cubic lattices are computed in the way shown in §126.

The only disadvantage in this method is that one diffraction line can be ascribed to a large number of planes, for example, there are 48 planes having the same $(h^2+k^2+l^2)$-value with different combinations (positive and negative values, and interchange of h, k, l, . . .) of the indices. So the determination of indices is not unique.

130. Laue Method.—In the beginning of this section we interpreted Laue photographs by considering the scattering of X-rays from atoms placed at the lattice points. But there is a still better method of interpreting them, if we imagine that the crystal is made up of a series of planes passing through the atoms parallel to any face (hkl); any Laue-spot can be regarded as due to reflection of X-rays from these planes as in the Bragg or powder methods, in accordance with the equation

$$n\lambda = 2d_{hkl} \sin \theta_n,$$

where

$$d_{hkl} = \frac{a}{\sqrt{h^2+k^2+l^2}}$$

for simple cubic crystals, a being the side of the unit cell.

In Fig. 32, the X-rays fall on the crystal (not shown) at O, K is any atomic plane in the crystal.* We suppose that the X-rays are reflected by the plane and give rise to a Laue spot at R, and O′ is the image of the central spot. The method is however not identical with the Bragg method, as in this the continuous part of the rays are effective, instead of the characteristic part as in the Bragg or powder methods. So in obtaining Laue photographs the target must be so chosen that it gives intense continuous radiation and the voltage must be considerably high.† The reason is obvious; for the characteristic radiation may not find any atomic plane oriented at an angle satisfying the equation above. In Bragg's method and powder method, suitable glancing angles of reflection for a characteristic ray is obtained by rotating the crystal or powdering it, respectively. But there is no such provision in the Laue method, and so a continuous radiation is used.

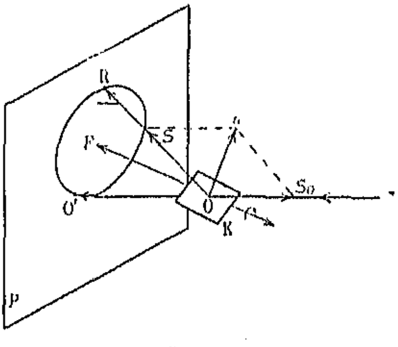

Fig. 32.

131. Symmetry in Laue-Diagrams.—Since the inclination of possible atomic planes is governed solely by symmetry, the distribution of

---

* The figure is rather exaggerated.

† For best results, the use of a tungsten target with 50 to 60 KV pressure is suggested.

Laue-spots will also depend on the symmetry of the crystal and its orientation with respect to the X-ray beam. As diffraction effects have been shown to be equivalent to internal reflections from atomic planes parallel to the (h, k, l) plane, there can be no difference between the results obtained from planes $(h\,k\,l)$ and $(\bar{h}\;\bar{k}\;\bar{l})$.* Consequently every Laue photograph will have a centre of symmetry. And it can be shown that the 32 classes of crystal symmetry reduce to only 11 classes when their symmetry with respect to the X-ray effect is considered.† This has already been remarked before.

In Plate IV, Fig. 13, we have illustrated the Laue's spots for ZnS. Here the X-ray beam was kept perpendicular to the (100) face of a cubic crystal of ZnS, or in other words it was along a fourfold axis of symmetry, and so the photograph also shows a fourfold symmetry. In the same way, in Fig. 34, the Laue spots of cubic crystal of MgO show a fourfold symmetry. Reverting to Fig. 32, OF is a line in the plane of incidence as well as in the atomic plane, and F is a point (not Laue-point) on the photographic plate. If θ be the glancing angle, $\angle FOR = \theta$. We can imagine other atomic planes containing the line FO and inclined to OO′ at an angle θ. The line FO is known as the *Zone-axis*. The atomic planes having different grating constants will reflect some wavelength λ in the continuous radiation used; and it is obvious that these reflected rays will lie on the surface of a cone with O as apex, FO as axis and the semi-vertical angle θ. The intersection of this cone with the plate will be an ellipse passing through O′. Thus Laue photograph consists of dots placed on ellipses passing through the central spot O′.

132. Interpretation of Laue-Photographs. — In Fig. 33, suppose the atomic plane EE reflects the X-ray beam at K and gives rise to a Laue spot R on the plate PP. Let O be the central spot. KN is drawn perpendicular to atomic plane K, meeting the plane of the photographic plate at N. Then N is called the *gnomonic projection* of the Laue spot R.

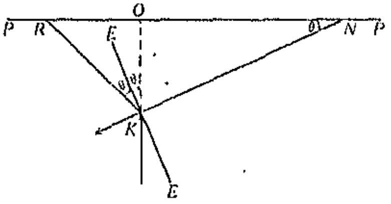

Fig. 33. The gnomonic projection.

If X-rays are initially made perpendicular to the (100) plane we can write down the indices of all planes giving rise to Laue spots from this projection. This is done as follows. Taking O to be the origin, and OK to be the z-axis, we have

$$OR = r \tan 2\theta, \text{ and } r = ON \tan \theta$$

---

* The plane $(\bar{h}\;\bar{k}\;\bar{l})$ is the same as $(-h\text{-}k\text{-}l)$. It is conventional to denote a negative index by putting a bar above it.

† *Vide* Wyckoff, *The Structure of Crystals*, p. 117.

where r is the distance OK. Since r and OR are known, the position of N is therefore known. Again the line KN is normal to the plane K, and so its direction cosines are given by

$$L : M : N = x : y : r$$

where (x, y) are the co-ordinates of the gnomonic spot N. Now the Millerian indices of the reflecting plane are proportional to these direction cosines, and so

$$h : k : l = x : y : r$$

Here r the distance between the crystal and the plate is fixed for all spots. The indices h, k, l thus are determined from the co-ordinate of the gnomonic spots. Fig. 34 shows a gnomonic projection of the Laue spots for MgO, while the inset is the corresponding Laue photograph. It will be seen that for the x-axis, we have $k=0$, and parallel to it are the ordinates having $k=1$, $2 \ldots \bar{1}, \bar{2}$, etc., and a similar argument applies for h. As the indices are whole numbers, they all lie on the intersection of $h=0$, 1, 2 . . . etc., with $k=0$, 1, 2 . . . . . Thus the indices of the reflecting planes can be readily known by constructing a gnomonic projection diagram for the spots as shown in this figure.

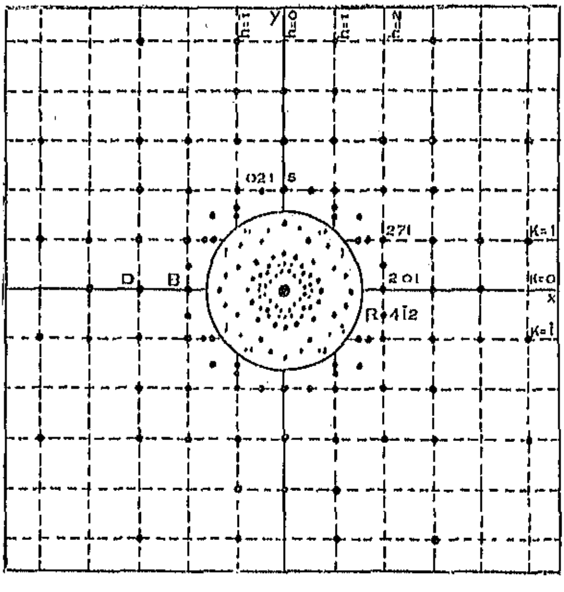

Fig. 34. The gnomonic projection for the Laue spots of MgO.

Calculation of the Spacings.—In the case of Laue spots it is difficult to calculate the spacing, for the wavelength λ giving rise to any particular spot is unknown. By decreasing the voltage across the X-ray tube, and noting which Laue spots vanish we can find the approximate λ and hence the approximate spacing. For intenser spots the wavelength can be guessed from the voltage. For a full reference of the exact experimental procedures see Wyckoff, *The Structure of Crystals*, pp. 117 to 140.

In general it is better that the Laue photograph be supplemented by spectrometric (Bragg or powder) or other methods for the determination of a. When this is done, it becomes simpler to find the spacings (*vide* eqn. 30, 31).

*Schiebold Method.**—In order to avoid the ambiguity about the wavelength, the photograph is taken in Schiebold's method by rotating a small crystal about a crystal axis, and using monochromatic X-rays. In this arrangement the spacing can be directly calculated. One disadvantage of this method is that a longer exposure is required.

133. The Complete Determination of Crystalline Structure—The Structure Factor.

—In the cubical crystal, the value of $a=d_{100}$ is found from the methods given above. The volume V of the unit cell is given by

$$V = a^3$$

If m be the mass of the chemical molecule, n the number of molecules in the unit cell, then ρ the density is related as $\rho = mn/V$ from which we at once get the value of n. In § 124 on space-groups we have emphasised the fact that knowing the crystallographic symmetry and the value of n, the interior structure can at once be known. The general methods have been described. But the problem is not so simple, for complexities arise in many ways, two of which will be discussed briefly.

(1) We have seen that in crystal analysis we find the spacing or the distance between two successive atomic planes. If in Fig. 24 we have an atom at the origin O, the spacings of (100) planes will have to be halved, while the spacings of the plane passing through P, P$_1$, O will remain the same. In the same way in the body-centred and face-centred crystals, the spacings have been halved for some planes while not for others. All these facts have to be taken into account in the structure determination.

(2) Even if the correct space-group is obtained, the structure determination is far from complete unless the parameters of the atoms in the unit cell are known. For the space-groups can only give a large number of probable atomic arrangements. The more the number of dissimilar atoms, the more difficult becomes the determination. The problem is

---

* E. Schiebold, *Zeit. f. Krystallographie*, **57**, 579, 1923. See also J. D. Bernal, *Proc. Roy. Soc. A*, **113**, 117, 1926.

approached from a study of the relative intensities of the reflections from various planes. In § 126 we have seen how Bragg arrived at the correct solution of the structure of NaCl from a study of the intensity of reflection from various planes. The intensity of reflection is the sum total of scattered intensities contributed by the atoms in the various planes. So it includes an *amplitude factor* and a *phase factor*. The phase factor arises from the fact that the reflected rays coming from the different atoms in any crystal plane have got phase differences with respect to each other, which renders the intensity of reflection from one plane different from that due to another. On the other hand the amplitude factor has its origin in the fact that in the mechanism of scattering by a particular atom, all the outer electrons in the atom take part; but there will be again a phase difference between the scattered radiations coming from the different electrons. The phase difference therefore depends upon the electron distribution in any particular atom, and is consequently different for different atoms. Hence the scattering powers of different atoms, as well as of the same kind of atoms in different configurations, will also be different. Inversely the determinations of structure factor and amplitude factors can give an idea of the possible configurations of atoms in the various planes, and of electrons in the atoms of a crystal.

The phase factor commonly goes by the name *structure factor* and depends on the relative positions of the atoms (or their parameters). It can be shown that if in any set of parallel planes (hkl) there are different atoms with co-ordinates (x_1, y_1, z_1), (x'_1, y'_1, z'_1), ... etc. with the scattering power σ_1, atoms with co-ordinates (x_2, y_2, z_2), (x'_2, y'_2, z'_2), ... etc. with the scattering power σ_2, and so on, the total intensity* is given by

$$I = A^2 + B^2$$

where $A = \sigma_1 \sum \cos 2\pi n\ (hx_1 + ky_1 + lz_1) + \sigma_2 \sum \cos 2\pi n\ (hx_2 + ky_2 + lz_2)$

$$B = \sigma_1 \sum \sin 2\pi n\ (hx_1 + ky_1 + lz_1) + \sigma_2 \sum \sin 2\pi n\ (hx_2 + ky_2 + lz_2)$$

and n denotes the order number as usual.

The study of space groups gives us choice of a large number of positions of the atoms in the unit cell; these are successively tried in the above formula and the resulting intensity is compared with the experimentally observed value. Take the example of the NaCl crystal. The student can substitute for himself the values of the co-ordinates of the sodium atoms in the unit cell in Fig. 25 as (000; $a0a$; $aa0$; $0aa$), and also those of chlorine atoms (as aaa; $a00$; $00a$; $0a0$) in the above equations. It will be found that for odd values of n and odd values of (hkl) the scatterings due to chlorine and sodium oppose each other, while for even values of n they re-inforce each other. Bragg's observations on NaCl (*vide* Fig. 27, §125) are in conformity with this theory.

---

* This is derived in the same way as vibrations with the same frequency but possessing different amplitudes and phases are compounded in Acoustics or Optics. For an account of this subject see Wyckoff, *loc. cit.*

Hence the assignment of the above co-ordinates to the Na and Cl atoms gives us the most probable structure of the NaCl crystal. The same holds for any other crystal, *i.e.*, if the intensity of reflections for any crystal is experimentally determined, then out of the manifold alternative structures suggested by the study of the space-groups of the crystal, that structure will be the *most probable* which satisfies the obtained intensity distribution.

134. Atom Factor and Atomic Structure Factor.—In the last section the structure factor (phase factor) of crystals has been taken into account. Now we shall consider the amplitude factor. This factor involves the scattering power σ in the last expression. The scattering power for amorphous substances is given by Thomson's formula (eqn. 9) as shown in § 113, and it contains the factor $(1+\cos^2 2\theta)$, θ being the glancing angle. But Bragg found that in the case of planes for which the structure factor was the same (say in those planes of NaCl in which Cl and Na atoms co-operate), the intensity falls off rapidly with θ (*vide* curves in Fig. 27). He gave the empirical relation*

$$I = C\frac{1+\cos^2 2\theta}{\sin^2\theta} \cdot e^{-B\sin^2\theta} \quad . \quad . \quad . \quad . \quad . \quad . \quad (32)$$

where C is a constant depending upon the wavelength of the primary X-rays, $e^{-B\sin^2\theta}$ is known as the *Debye factor* (B being very small, this factor is almost equal to 1) and it is due to the thermal agitation of the atoms in the crystals. Darwin† and Compton proposed a theoretical] (modified Thomson) intensity formula for crystalline substances taking into account the change in refractive index of the X-rays as they pass through the crystal (see eqn. below). In this, the factor $\sin^2\theta$ in the denominator of Bragg's empirical relation was replaced by $\sin 2\theta$, so that there remained a factor $\cot\theta$ which was to be accounted for. The discrepancy must be attributed to the amplitude factor alone. The distance of the electrons from the centre of the atoms containing them is in general comparable to the inter-atomic distances. It is well-known that in a diffraction grating if the width of the ruled lines are comparable to the distance between the successive lines of the grating, the intensity of the higher order spectra rapidly falls oft. The same principle was applied to explain the above discrepancy in the scattering formula. The 11 electrons of the Na atom are distributed in different shells round the atomic core and so they cannot be taken as one unit of 11 electrons. Their effective value must be considered. This value is known as the *atomic structure factor* or *atom factor*. It is denoted by F. Taking this into account the theoretical formula then takes the form as deduced by Compton,*

---

* W. H. Bragg, *Phil. Mag.*, **27**, 881, 1914.

† C. G. Darwin, *Phil. Mag.*, **27**, 325, 1914.

$$\frac{W\omega}{I_0} = \frac{1}{2}\,\frac{N^2\lambda^3F^2}{\mu}\cdot\frac{e^4}{m^2c^4}\,\frac{(1+\cos^2 2\theta)}{\sin 2\theta}\cdot e^{-B\sin^2\theta} \quad . \quad . \quad . \quad (33)$$

Here N is the number of electrons in unit volume, I_0 is the intensity of the primary beam, F is the atomic structure factor, and μ is the absorption coefficient of the crystal. As crystals are not perfect reflectors, in experiments on intensity determinations they are generally rocked with an angular velocity ω, and $W\omega$ is the total intensity (or the integrated intensity) for any wavelength. $W\omega/I_0$ is measured as usual, and when every thing else in the expression above is known, F can be at once calculated. For NaCl, this factor is partly due to Cl and partly to Na.

Let F_{Cl} and F_{Na} be the atomic structure factors of Cl and Na atoms, then for those planes for which n and hkl are odd, the observed atomic factor F_1 will be

$$F_1 = F_{Na} - F_{Cl}$$

and similarly for even values of n, the observed atom factor F_2 will be

$$F_2 = F_{Na} + F_{Cl}$$

Hence $\quad F_{Na} = \frac{1}{2}(F_1 + F_2), \qquad F_{Cl} = \frac{1}{2}(F_2 - F_1)$

The values of F_{Cl} and F_{Na} are very important, for they throw light on the structure of the atoms of Cl and Na. Compton showed that if $p(r)$ is the probability of an electron being found within the distances r and $r+dr$ with respect to the (hkl) plane from the centre of the atom, the atomic structure factor is given by

$$F = Z\int_{-d}^{+d} p(r)\cos\frac{4\pi r\sin\theta}{\lambda}\,dr \quad . \quad . \quad . \quad . \quad . \quad . \quad (34)$$

where d is the grating constant and Z is the atomic number. If the variation of the atomic structure factor with the glancing angle θ be known, then the distribution of electrons can be determined. This is done in the following ways:

(*a*) *By trial, i.e., by assuming a value of the probability factor* $p(r)$. Bragg, James and Bosanquet† assumed it to be equal to $1/2r$ and integrated the above expression. As electrons are distributed in various shells, F can be expressed as a summation each term of which is due to electrons in a particular shell, *i.e.*, we have

---

* See Compton's *X-rays and Electrons* (1927), p. 125.

† W. H. Bragg, R. W. James and Bosanquet, *Phil. Mag.*, **41**, 309, 1921.

$$F = \sum \frac{\sin \frac{(4\pi r \sin \theta)}{\lambda}}{4 \frac{\pi r}{\lambda} \sin \theta} \qquad (35)$$

Bragg concluded from the above considerations that in the Na atom there are

7 electrons in a shell of radius ... ... ·29 Å.U.
3 electrons in a shell of radius ... ... ·76 Å.U.

and in the Cl atom

10 electrons in a shell of radius ... ... ·25 Å.U.
5 electrons in a shell of radius ... ... ·86 Å.U.
3 electrons in a shell of radius ... ... 1·76 Å.U.

(*b*) *By expanding the expression for atomic structure factor into a Fourier series.*—This was first suggested by W. H. Bragg,* and carried on by Duane, Compton, Havighurst† and W. L. Bragg‡. They have arrived at interesting results on the distribution of electrons around atoms from this analysis.

135. The Ionic, Atomic and Molecular Crystals.—(1) *Inorganic Crystals.*—From the above analysis, we see that 10 electrons are assigned to the Na and 18 to the Cl atom. But it is well-known that the ordinary atom of Na contains 11 electrons and chlorine contains 17 electrons. Hence it is supposed that in the formation of the NaCl-crystal, the Na-atom loses one electron which passes over to chlorine, so that the crystal is made up of Na^+ and $\overline{\mathrm{Cl}}$-ions placed regularly according to the cubic lattice pattern. Such compounds are called by the chemists '*ionic.*' Most of the inorganic salts form ionic type of crystals. But there are others in which the electrons remain with the parent atom. They are supposed to be held together by *non-ionic* linkages, and here again two kinds of binding are distinguished, *viz.*, *atomic* and *molecular.*

In the atomic molecules the linkage is of nonpolar origin, but still the valency characteristics of the individual atoms are generally preserved, while in the molecular type this may not be always true. Thus diamond is an example of atomic molecule and graphite is of molecular type. It has been found that all organic crystals are of molecular type.

(2) *Organic Crystals.*—Of the two kinds of organic crystals, aliphatic and aromatic, the X-ray analysis of only the first has been carried at some

---

* W. H. Bragg, *Phil. Tran. Roy. Soc. A*, **215**, 253, 1915.
† Havighurst, *Phys. Rev.*, **28**, 869, 1926.
‡ W. L. Bragg, *Proc. Roy. Soc. A*, **123**, 537, 1929.

length. The aliphatic crystals have been shown by Bragg and Piper to consist of long chains of molecules. While among the aromatic crystals, the benzene ring constitution has been proved by K. Lonsdale* to be true in the case of hexamethyl-benzene.

136. The Structure of Liquids.—If a thin film of liquid is substituted for the powdered crystal in the Debye-Scherrer method, a diffraction halo is obtained around the central spot on the photographic plate. This discovery was made by Debye and Scherrer in 1916. In Fig. 35, Plate IV, is shown a diffraction photograph of ethyl alcohol with CuK radiations. The halo is broad and diffuse, but it still proves the existence of some sort of regular molecular arrangement inside the liquid. This arrangement has been called a *cybotactic* (tendency of molecules to arrange themselves in the form of chains) *group* by Stewart. For example, in the case of polar compounds like fatty acids and primary alcohols, two diffraction haloes are observed. Stewart† supposed that the polar molecular chains have a tendency to group themselves in end to end position, as shown below diagrammatically for ethyl alcohol liquid. Here two ethyl alcohol molecules are shown one vertically above the other, with the polar OH-groups away from each other. This arrangement goes on repeating itself as shown by the next pair.

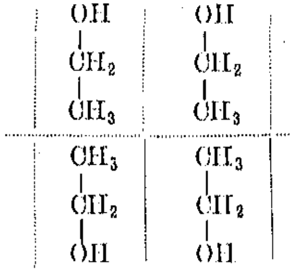

$$\begin{array}{c|c}
OH & OH \\
| & | \\
CH_2 & CH_2 \\
| & | \\
CH_3 & CH_3 \\
\hline
CH_3 & CH_3 \\
| & | \\
CH_2 & CH_2 \\
| & | \\
OH & OH
\end{array}$$

The distance between the polar (OH) groups in the same chain can be calculated from Braggs' equation $n\lambda = 2d \sin \theta$, where 4θ is the angle subtended by one of the haloes at the liquid film. The other stronger halo does not change with the length of carbon chain when different substances of the same series are studied. For this reason it is concluded that the spacing depends upon the distance between the neighbouring chains. These groups are not stable but break up as soon as they are formed, but even in the short time for which they exist, they give rise to this halo. There is some diffuse scattering at small angles which has been explained by Raman and Ramanathan‡ to be due to scattering caused by the sudden fluctuation of density in the liquid similar to the case of optical scattering by liquids dealt by Einstein and Smoluchowski. A very large number of liquids[*] were experimented upon, and the haloes obtained were interpreted on similar lines.

---

* K. Lonsdale, *Proc. Roy. Soc.*, **123**, 494, 1929.
† Stewart, *Phys. Rev.*, **30**, 232, 1927; see also **31**, 1, 1928.
‡ Raman and Ramanathan, *Proc. Indian Ass. Cult. Sc.*, **8**, 127, 1923.

137. Methods of X-ray Spectroscopy.—During the last twenty years, two methods distinct from each other have been developed in the Spectroscopy of X-rays. These are

(I) Method depending on the phenomenon of diffraction of X-rays by crystals, according to Braggs'[†] formula.

(II) The method discovered by A. H. Compton and R.L. Doan[‡] depending on the phenomenon of diffraction of X-rays by ordinary plane or concave gratings at the grazing angle of incidence (*vide* § 143). This is also known as the absolute method of determination of wavelengths.

We shall discuss briefly some of the important methods developed under each of the two heads.

I. (A) THE METHOD OF FIXED CRYSTALS

The simplest method depending on the principle of X-ray diffraction by crystals is due to Moseley. Moseley[‖] used the Bragg formula $n\lambda=2d \sin\theta$, and devised the arrangement illustrated below (Fig. 37) for finding out the wavelengths of the K and L characteristic radiations of 45 elements between Al and Au. Since d is known, the problem is to find out the glancing angle θ for different wavelengths of an element.

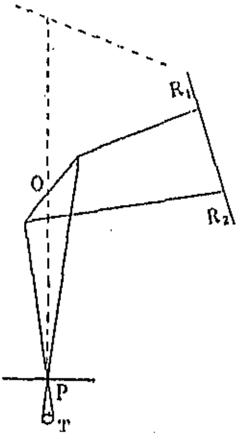

Fig. 37. Moseley's fixed crystal method.

A divergent beam of X-rays, coming from the focus T of the target of an X-ray tube, and after being limited by a slit at P falls on the fixed crystal O. If the extreme rays of the beam make glancing angles θ_1 and θ_2 with the crystal, a photographic plate placed in their path will record a spectrum $R_1 R_2$

---

[*] Drücker, *Phys. Zeits.*, **29**, 273, 1928;
For a collected account of these works see P. Krishnamurti, *Indian Jour. Phys.*, **14**, 543, 1930.

[†] W. H. and W. L. Bragg, *Proc. Roy. Soc.* A, **88**, 428, 1913.

[‡] A. H Compton and R. L. Doan, *Proc. Nat. Acad. Sci.*, **11**, 598, 1925.

[‖] Moseley, *Phil. Mag.*, **26**, 1024, 1913.

consisting of the wavelength region between $\lambda_1 = 2d\sin\theta_1$ and $\lambda_2 = 2d\sin\theta_2$ in the first order. By varying the inclination of the crystal with the line of symmetry of the beam, different parts of the spectrum can be mapped. It may be noted however that the spectrum obtained in this way is never a pure spectrum, for, a glancing angle θ does not correspond to only one wavelength λ, but also to $\lambda/2$, $\lambda/3$, ... the latter being reflected in 2nd, 3rd . . . orders. But as the intensity in higher orders falls off very rapidly, this defect matters little, and can be removed by putting appropriate filters in the path of the beam.

The method had many sources of error. The glancing angles θ_1 and θ_2 could not be measured accurately, for the simple reason that the axis of rotation of the crystal is at O. Moreover, as the crystal is rotated (say, in the clockwise direction), the wavelength λ_1, which was formerly reflected from a particular point, will be reflected now from other points lying on the crystal till the other extreme end of the beam is reached. The consequence will be that the spectral line at R_1 will not be sharp, but will be broad like a band. And if the reflecting power of the crystal in various parts of its crystallographic face is not uniform, as is generally the case, the band obtained will be irregular and ghostly in structure.

I. (B) Bragg's Focussing Method.

In order to avoid some of the uncertainties, W.H. Bragg devised the *focussing method.* In this (see Fig. 38 below) *the distance between the slit* S_1 *and the crystal is the same as the distance of the slit* S_2 of his ionisation chamber. The centre of rotation K of the crystal, the slits S_1 and S_2 lie on a circle. An ionisation chamber was used by Bragg instead of a photographic plate.

The beam entering through the slit S_1, falls on the crystal A A, when it is a tangent to the circle on which S_1, K, S_2 lie.

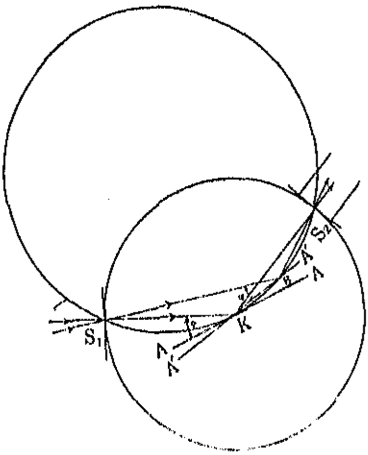

Fig. 38. The Bragg focussing method.

Let a wavelength λ_1, having glancing angle θ be reflected from K and received in the ionisation chamber through the slit S_2. If the crystal be now rotated to the position A′A′, the same wavelength will be reflected from the point B, which from the geometry of the figure, must lie on the circle passing through the slits and the centre of rotation of the crystal,

S_1 K A is the angle made by the tangent A K with the chord S_1 K, so that all angles equal to this must lie on the opposite segment. Hence B must lie on the circle, and the reflected ray from B must enter the slit S_2.

So in one setting of the ionisation chamber, only rays of one single wavelength will enter into it, and it is immaterial whether the reflection is taking place from the centre or any other part of the crystal. If 2β be the angle subtended by the arc S_1 S_2 at the centre K, the glancing angle is given by $\theta = 90^0 - \beta$.

Necessity for rocking the crystal.—If the reflecting power of the crystal is uniform in different parts of its reflecting face, the fixed crystal method may work well; but if otherwise, the crystal must be rocked within a degree. The rapidity of rocking must be adjusted according to the sensitivity of the ionisation apparatus, otherwise an illusive fine structure will be indicated, due to non-uniformity in the reflecting power of different parts of the crystal. In practice perfect crystals are so rare that it is the universal custom now to keep the crystal rotating, otherwise in the fixed crystal method false lines due to imperfection of the crystal may appear and vitiate the result.

I. (C) SIEGBAHN'S PRECISION MEASUREMENTS.*

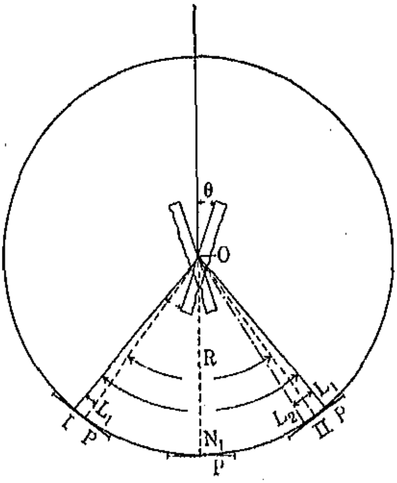

Fig. 39. Principle of Siegbahn's Spectrograph.

Siegbahn's spectrograph is almost the same in principle as that of W. H. Bragg, the only difference lies in the fact that photographic plates are used in place of ionisation chambers.

The principle of the instrument is illustrated in Fig. 39.

The crystal is set parallel, to the beam, and the axis of rotation (through O) is brought on the surface of the crystal. The photographic plate P is held tangentially, to the divided circle. It is apparent that the focussing condition does not apply rigorously to the case of a photographic plate; for the plate touches the circle at one point only. The approximate glancing angle θ is found by the ordinary methods. The plate is then brought into the position I, so that it makes an angle $2\theta_a - \beta$ with the direction of the X-ray beam (β is only a small angle chosen arbitrarily). The crystal is brought to the position I and the spectrum line is recorded at L_1. The plate is now brought to the position II, by rotating the arm carrying it through $4\theta_a - 2\beta$. The crystal is also brought to the position II. The spectrum line is recorded at L_2. From the figure

---

* For Siegbahn's methods see *Spektroskopie der Röntgenstrahlen* (1931).

$$4\theta_h = 4\theta_a - 2\beta + \delta$$

where θ_h is the correct glancing angle, δ is the angle subtended by $L_1 L_2$ at the centre. The distance $L_1 L_2$ is measured on the comparator, and if R is the distance of the plate from the centre,

$$\delta = \frac{L_1 L_2}{R}$$

in circular measure.

The small angle β is given different values, both on the positive and the negative direction. The mean θ_h gives the most accurate value of the glancing angle.

In Siegbahn's apparatus the points N_1, L_1 and L_2 are so near each other that the deviation from focussing condition does not matter much. Moreover, the radius R is kept large, the beam is narrow and the angle through which the crystal is rotated is read very accurately on a vernier scale. The crystal is selected so that its lattice planes are not distorted, and so has uniform reflecting power.

Compton and Doan's method of X-ray spectroscopy will be described later in § 143.

138. Dispersive Power of a Crystal.

—The dispersive power of a crystal is denoted by $d\lambda/d\theta$. From Braggs' equation:

$$n\lambda = 2d \sin \theta$$

we get

$$\frac{d\lambda}{d\theta} = \frac{2d \cos \theta}{n}$$

For small values of θ this becomes

$$\frac{d\lambda}{d\theta} = \frac{2d}{n} = \text{constant.} \quad . \quad . \quad . \quad . \quad . \quad (36)$$

Resolving Power.—Thus the dispersive power for any crystal for the same order of reflection is constant. On the other hand, the resolving power of any spectral instrument would depend to a large extent on the breadth of the X-ray lines, and therefore on the breadth of the slit. But due to the fact, that the X-rays enter inside the crystal, the width of the lines will not only depend on the width of the slit, but also on the thickness of the crystal traversed by the ray. The resolving power can be calculated from the diagram below (Fig. 40).

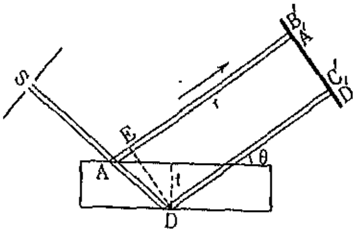

Fig. 40.

Let the source be a slit of width s at a distance a from the crystal which has the thickness t. Let us assume that the crystal is inclined to the beam SA at a glancing angle θ. Then according to Braggs' Law, a wavelength λ will be reflected, and will be recorded at B$'$A$'$. The breadth of the line B$'$A$'$ will be equal to that of the slit to a first approximation. But the incident beam will penetrate into the crystal to some depth and be reflected from the lattice planes in the interior. All these reflected beams will be recorded on the plate, so that instead of getting sharp lines on the plate we will get bands with one sharp intense edge and the intensity falling off on the other side. This fading is due to the fact that X-rays are absorbed as they enter the crystal, and the rays reflected from lower layers thus become weak.

We can now try to calculate the true resolving power. It will be seen from the geometry of the diagram that the breadth of the spectrum line is equal to $s+2t\cos\theta$ where t is the thickness of the crystal, and s the breadth of the slit.

For, $$\mathrm{AD} = \frac{\mathrm{DE}}{\sin 2\theta},$$

Also $$\mathrm{AD} = \frac{t}{\sin\theta} = \frac{\mathrm{DE}}{\sin 2\theta},$$

or $$\mathrm{DE} = 2t\cos\theta.$$

Therefore the breadth of the line $= s + \mathrm{DE} = s + 2t\cos\theta$.

In order that the images of two wavelengths are resolved, their centres must be $s+2t\cos\theta$ apart, otherwise they will overlap. If we have two wavelengths λ and $\lambda+d\lambda$ to resolve, the crystal must rotate through an angle $d\theta$ such that

$$n d\lambda = 2d\cos\theta \; d\theta$$

Since the reflected ray rotates twice as fast as the crystal, it will rotate through an angle $2d\theta$. If we keep the plate at a distance r from the crystal, then the displacement on the plate of the images of the two wavelengths is equal to $2\,r d\theta$. In order that the two wavelengths are separated

$$2r\,d\theta > s + 2t\cos\theta$$

or

$$d\lambda > \frac{d\cos\theta}{nr}(s + 2t\cos\theta)$$

$$> \frac{d\cos\theta}{nr}(s + 2t\cos\theta) \quad . \quad . \quad . \quad (37)$$

Thus in order to design an apparatus having high resolving power, we must make $d\lambda$ small. To ensure this a large value of r is taken. The crystal is so chosen that not only its grating space d should be small, but also it is advantageous to take t the thickness of the crystal, to be as small as possible. Spectroscopes have been designed to increase their resolving power taking account of the factors in the above expression.

139. Seemann's Schneiden and Loch-Kamera Spectrographs.

graphs.—Seemann drew attention to the fact that the breadth of the spectrum lines in X-rays not only depends upon slit-breadth but also on the thickness of the crystal. And in order to overcome these difficulties, he modified his apparatus in the following way.

(1) *Schneiden Method.*—In this method (Fig. 41) the slit is dispensed with, and instead, a wedge W made of lead or gold, is placed on the crystal table so that the sharp edge of the wedge touches the crystal C and lies on the axis of rotation of the latter. This has the effect of greatly reducing the breadth of the reflected beam, so that in the above equation (37) we can put the effective width of the slit to be zero. The lines obtained from this arrangement are sharp. It is interesting to note that this arrangement always satisfies focussing condition. The crystal table is rotated as usual, and the various spectrum lines are recorded on the plate. But in this method the effect due to the thickness of the crystal has not been eliminated. This is done in the next arrangement.

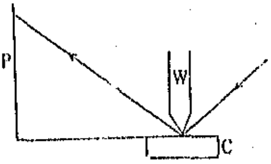

Fig. 41. The Schneiden method.

(2) *Loch-Kamera.*—In this arrangement (Fig. 42) the slit is placed not in the incident beam but in the *reflected beam*. The slit S_1 in the diagram shows its position with respect to the crystal. A broad beam of X-rays falls on the crystal K_1 and only that part of the spectrum is allowed to pass through the slit which obeys Bragg's law. As the glancing angle is fixed, the crystal cannot be rotated so as to photograph the whole spectrum; but instead of that it is simply displaced perpendicular

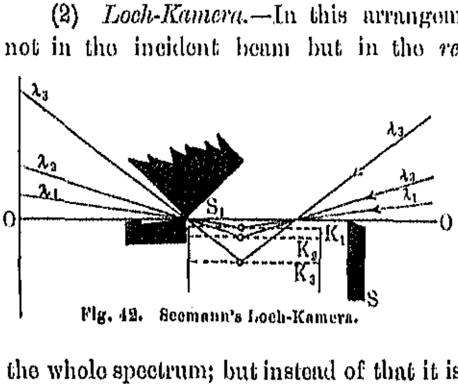

Fig. 42. Seemann's Loch-Kamera.

---

* See Siegbahn, "*Spektroskopie der Röntgenstrahlen,*" 1931.

to its face. In the positions of the crystal shown by dotted lines K_2 and K_3 the glancing angles are different, and therefore different wavelengths $\lambda_1, \lambda_2, \lambda_3$......can be photographed.

140. Spectroscopy of Hard X-rays.

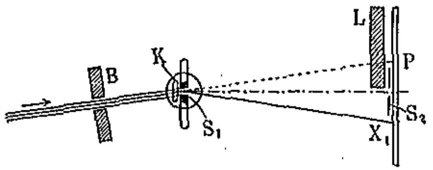

Fig. 43.
Siegbahn's apparatus for hard X-ray Spectroscopy.

140. Spectroscopy of Hard X-rays.—In the preceding part of this section, the important spectroscopic methods have been described, and it has been pointed out that in the Bragg-Siegbahn method the glancing angle should be very accurately measured. But in the case of hard X-rays (beyond ·7 Å. U.) the glancing angle becomes very small and so it is not possible to measure it very accurately. Hence in these cases, distances between spectral lines are measured instead of angles.

Siegbahn's Apparatus.—Siegbahn* designed an apparatus illustrated in Fig. 43 for measurement of the wavelength of hard X-rays (up to ·5 Å. U.).

He uses a transmission method first tried by Rutherford and Andrade† for determining the wavelength of γ-rays. The lead slit B limits the beam of incident X-rays. The rays then fall on the crystal K of calcite or rocksalt. This crystal has been cut perpendicular to the cleavage plane, and so the atomic planes which will reflect the rays, are perpendicular to the faces. A fine slit S_1 made of gold is placed next to the crystal. The crystal, the slit, and the arm carrying the photographic plate P are rigidly connected and can be rotated round an axis passing through the slit S_1. The distance between the slit S_1 and the plate P is about a meter. The plate P is adjusted parallel to this crystal by optical means, and a second slit S_2 is placed close to the plate P so that a line drawn through the slits 1 and 2 is normal to the photographic plate. First of all the arm carrying the crystal plate, and the slit 1 is rotated so that the direct beam passes through the slit 2 and produces an image on it. The arm is now rotated and brought to the position shown in the diagram so that the X-rays get reflected and are recorded at X_1. In order to cut off the direct beam, a lead block L is placed before the photographic plate. The arm is brought to a symmetric position on the other side and another photograph is taken. The distance between the two spectral lines subtends an angle 4φ at the slit, and as the distance between slit S_1 and the plate P is known, so that θ can be calculated from the formula

---

* Siegbahn, "*Spektroskopie der Röntgenstrahlen,*" 1931.
† Rutherford and Andrade, *Phil. Mag.*, **28**, 263. 1914.

$$\tan 2\theta = \frac{a}{x}$$

where θ = the glancing angle, a = half the distance between the recorded lines, and is measured by a travelling microscope. x = the distance between plate and the slit S_1.

This method is accurate for small wavelengths, but for larger wavelengths inaccuracies creep in due to the fact that the photographic plates are never true planes but are buckled and twisted. The whole apparatus is enclosed in a lead box to prevent fogging of the plates.

We describe below the spectroscopes designed for the region of extreme long wavelengths (between λ 2 to 45 Å. U.). For the intermediate region (λ 0·5 to 2 Å.U.) generally the Bragg Spectrometer can be used. Siegbahn has recently designed a more accurate 'tube' spectrometer for this region, an account of which can be found in his book *Spektroskopie der Röntgenstrahlen.*

141. Spectroscopy of Soft X-rays (beyond 2 Å. U.).—

Moseley's Vacuum Spectrograph.—In the region beyond 2 Å.U. the absorption due to air becomes very strong and so it becomes necessary to put the spectrograph inside an evacuated chamber.

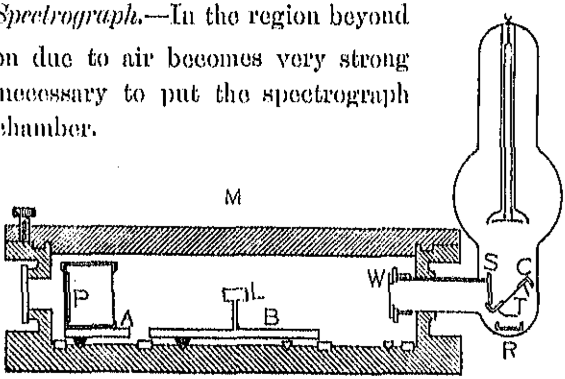

Fig. 44. Moseley's Vacuum Spectrograph.

Moseley's* original vacuum spectrograph, designed on this principle is shown in Fig. 44. The chamber M is connected to the X-ray tube R by means of a side tube W. The end of this tube is closed by means of a thin goldbeater's skin. X-rays originate from the target T and pass through the gold-beater's skin at W into the chamber M. This skin separates the high vacuum side of the X-ray tube from the comparatively low vacuum in the chamber (pressure 1 mm). P is a photographic plate chamber in the holder A. The crystal L of potassium ferricyanide is mounted on the table B. Moseley's apparatus is worked by the fixed crystal method, and so is not convenient.

Siegbahn's Vacuum Spectrographs.—In Siegbahn's vacuum spectrograph shown in Fig. 45, the crystal as well as the photographic plate can be rotated from outside. The crystal and the plate holder are connected to two vacuum-tight ground metallic cones coaxial with each other. This system of cones pass out of the bottom of the chamber which has got a corresponding ground cone to fit the above cones. With the help of a little grease the whole arrangement becomes vacuum-tight.

---

* Moseley, *Phil. Mag.*, 27, 703, 1914.

The crystal can be rotated from outside and set for any glancing angle, for the cone to which the crystal-holder is fixed has four verniers attached to its lower end where it emerges out of the chamber. This vernier slides against a circular graduated scale (15″) which is fixed to the cone carrying the plate-holder.

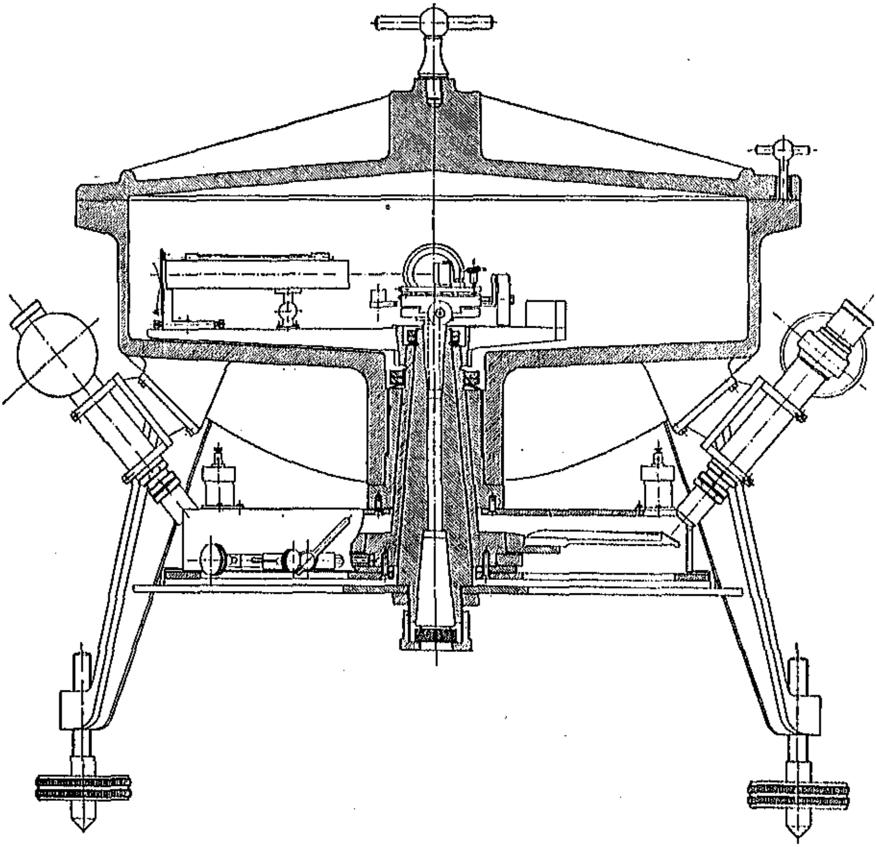

Fig. 45. Siegbahn's Vacuum Spectrograph.

Two microscopes diametrically opposite each other are rigidly fixed to the chamber, and the circular scale is read by means of it. The microscope provides the zero-position for the plate-holder and of the crystal. The crystal is rocked from outside without disturbing the vacuum. The crystal is set parallel to the beam, as well as to the axis of rotation which is made to pass through the face of the crystal. The X-ray tube is fitted up into the chamber by means of a side tube. A thin foil of aluminium is used to separate the high vacuum side of the X-ray tube from that of the low vacuum in the chamber. But when required to work near the region of λ 8 Å.U. this aluminium foil becomes a disadvantage, for it absorbs heavily, as its K-absorption limit is reached. A thin foil (5 μ) can work up to 12 to 13 Å.U. In order to overcome this difficulty high vacuum spectrographs have been devised in which the aluminium foil is removed. The X-ray tube and the spectrograph chamber have the same vacuum. Siegbahn had to take elaborate precautions to achieve this, for some air leaks into the chamber through the greased cones. A thin plate of Acheson graphite has been used in place of aluminium in this laboratory with good result.

He re-designed his apparatus* in 1926, and made the size of the chambers small and compact so that it was not difficult to maintain very high vacuum with the fast pumps at his disposal. The sensitivity of the recording apparatus was increased, by substituting a Geiger-counter for the Schumann photographic plates. Formerly, the limit to which long-wave spectroscopy had been extended was 11 Å.U., the K-series of Na. But with high vacuum spectrographs, it was extended to 73 Å. U. by Siegbahn and Dauviller in 1927. There was a further difficulty regarding the choice of crystals. For long wavelengths a crystal of large spacing is required. Gypsum (d=7·5 Å.U.) and mica (d=9·9 Å.U.) were used by previous workers. But they are not suitable for long wavelengths, for the glancing angles become very large and the spectrum lines tend to become curved. It was discovered by Müller, Shearer and Bragg† in 1924, that the crystals of fatty acids have very large spacings. For example, the palmitic acid crystal has d=35 Å.U., and the cerotic acid 72 Å.U. Thoraeus‡ in his work on the K-series of O and F used the former, and Dauvillier§ used melissic acid crystals, and mapped the spectrum region up to 73 Å.U., the wavelength of boron K-lines. Now-a-days the line grating method has replaced the crystal method of spectroscopy in these regions. It will be discussed in § 143.

142. The Double-Crystal Spectrometer.—We have seen in § 138 that the broadening of X-ray lines is due to the fact that when X-rays fall on a crystal, they penetrate inside the crystal and thus reflections take place also from lower planes. But this principle applies to hard radiations only. Generally, in the case of perfect crystals (though really speaking there are no perfect crystals), the upper layers reflect a large part of the X-rays and shield the lower layers; and therefore the lines become rather sharp. This effect was explained by Bragg who showed that the absorption at the upper layers increases when the crystal is set at an appropriate angle for reflection. It was denoted by him as *primary extinction*. In the general case therefore where the primary extinction occurs, the breadth of the X-ray lines observed must be due to some other cause.

---

* Siegbahn's *Spektroskopie der Röntgenstrahlen*, 1931.

† Müller, Shearer and Bragg, *Trans. Chem. Soc.*, **123**, 3156, 1923.

‡ Thoraeus, *Phil. Mag.*, **1**, 312, 1926.

§ Dauvillier, *Jour. de Physique*, **8**, 1, 1297.

The broadening of the X-ray lines has been investigated by many workers, as it is known from spectroscopic theory that many of the X-ray lines consist of close multiplets. In order to analyse them the photometric study of intensity distribution along the breadth of the lines has become necessary.

It has been already mentioned on p. 264 that due to the imperfection of the crystal a false broadening as well as some irregularities occur in the structure of the lines. In order to avoid this, the crystal is rocked through a small angle. The breadth still persisting is the true breadth of the line and must be ascribed to some other reason. The photometric study of the true breadth of the lines shows that the intensity distribution follows the Gaussian curve. The reason for this is that the surface of the crystal is in *the mosaic form*, that is, a natural crystal consists of minute crystals oriented in all possible directions. And so when the reflection takes place from the mosaic, the distribution of intensity across the line takes the Gaussian form.

In order to make a closer study of the broadening effect, the method of double-crystal spectrometer was devised by Davis and Stempel*, and improved by others. The chief advantage of this method is to increase the dispersion, and to make the breadth of the lines independent of the slit-breadth; but due to double reflection the intensity of the finally reflected beam is much reduced and so the photographic method cannot be applied. The method is illustrated in Fig. 46. X-rays fall on the crystal A at the point *a*. If the ray finds suitable glancing angle, it is

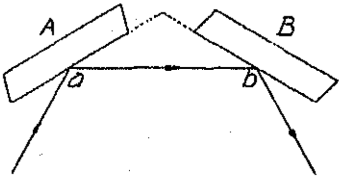

Fig. 46.
The Double-crystal Spectrometer.

---

* Davis and Stempel, *Phys. Rev.*, 17, 526, 1921.

reflected to the second crystal B. If this crystal is also placed at the appropriate glancing angle, the ray again gets reflected and is received in an ionisation chamber (not shown in the diagram). Important results concerning the satellites of X-ray lines, Compton effect, etc., have been obtained by this method. For further information the original papers* may be consulted.

Curved Crystals.—Recently Johann†, Cauchois‡ and Carlsson§ have used cylindrically curved crystals of gypsum and mica for analysing X-ray spectra. A thin slice is cut from the natural crystal, and by a suitable arrangement of screws it is bent into an arc of a circle (radius 50 cms.), so that the reflecting surfaces are curved instead of being planes. The slit, the crystal and the photographic plate are arranged in the Rowland mounting positions as in Fig. 49. The chief advantage of this method is that a broad beam can be used, and for this a large focal spot of the X-ray tube with a large current density can be employed without the risk of damaging the anticathode. On account of the curvature of the crystal, the beam is sharply focussed by reflection. Further the glancing angle of the incident rays would vary over a wide range, so that a large part of the spectrum can be photographed at a time.

143. Absolute Method of X-ray Spectroscopy.—Thibaud and Hunt, Söderman, and Siegbahn and Magnusson's Apparatus.—Compton and Doan‖ (1924) allowed a beam of X-rays from a Cu target to be reflected from a crystal of calcite set at the proper glancing angle. The reflected ray consisting of Kα-radiation was next allowed to fall on a plane and coarse metal grating (with 50 lines per mm.) at a very small incident angle. The experiment formed a sequel to the total reflexion (§159) of X-rays by glass and metal plates discovered by Compton sometime ago. In this experiment they wanted to study the same effect with the aid of gratings. It was found that not only was the beam totally reflected by the grating, but a spectrum was also present consisting of higher order diffraction images of Kα_1. This discovery gave a new method for X-ray spectroscopy.

---

* Allison, *Phys. Rev.*, **38**, 203, 1931; Spencer, *Phys. Rev.*, **38**, 618, 1931.

† Johann, *Zs. f. Phys.*, **69**, 185, 1931.

‡ Cauchois, *Comptes Rend.*, **194**, 369, 1932.

§ Carlsson, *Zs. f. Phys*, **80**, 604, 1933.

‖ Compton and Doan, *Proc. Nat. Acad. Sc.*, **11**, 598, 1925.

The usual arrangement for such experiments can be studied from the diagram given below (Fig. 47).

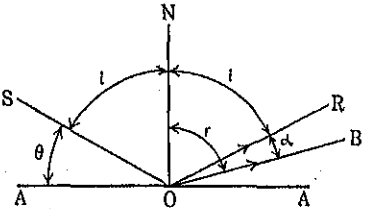

Fig. 47.

Let AA be the grating surface, and SO be a beam of X-rays incident at an angle i., R is the direction of the totally reflected ray. In a direction OB, the intensity of the diffracted beam will be a maximum if

$$n\lambda = d\,(\sin r - \sin i)$$

where r is the angle of diffraction (this is obtained from the theory of the plane gratings), d is the spacing of the grating lines. If α is the angle BOR then

$$n\lambda = d\,[\sin(\alpha + i) - \sin i]$$

If we take θ to be the glancing angle, the above equation becomes

$$\begin{aligned} n\lambda &= d\,[\cos(\theta - \alpha) - \cos\theta] \\ &= 2d \sin\frac{2\theta - \alpha}{2} \cdot \sin\frac{\alpha}{2} \\ &= \frac{d}{2}(2\theta\alpha - \alpha^2) \quad . \; . \; . \; . \; . \; . \; . \; . \; . \; . \; . \quad (38) \end{aligned}$$

for θ and α are small.

If OB is on the other side of OR, the formula takes the form

$$n\lambda = \frac{d\,(2\alpha\theta + \alpha^2)}{2} \quad . \; . \; . \; . \; . \; . \; . \; . \; . \quad (38a)$$

It has to be noted that α and θ are small angles, and consequently they have to be measured accurately. θ must be less than θ_m the critical angle of reflexion. It will be proved in the section on the optics of X-rays that

$$\sin\theta_m = \sqrt{1 - \mu},$$

where μ is the refractive index.

This method of finding wavelengths is known as *absolute*, because the value of d (spacing) is not known from any crystalline theory, but directly from the measurements of the grating space, which can be easily done with the aid of a standard optical line.

Some workers have used plane metal gratings, but generally glass gratings are preferred on account of their larger reflecting power. The grating space varies from 200 to 1100 lines per mm. according to the nature of the work.

Thibaud* and Hunt† were the first to apply this method to the spectroscopy of extremely soft X-rays, and they succeeded in photographing the K-series of B and C. Later Söderman* with improved apparatus reached the K-series of Be and Li. The latest apparatus based on this principle is due to Siegbahn and Magnusson†. This is described below (Fig. 48*a*).

---

* Thibaud, *Jour. d. Phys. et le Radium*, 8, 447, 1927.

† Hunt, *Phys. Rev.*, 30, 567, 1927.

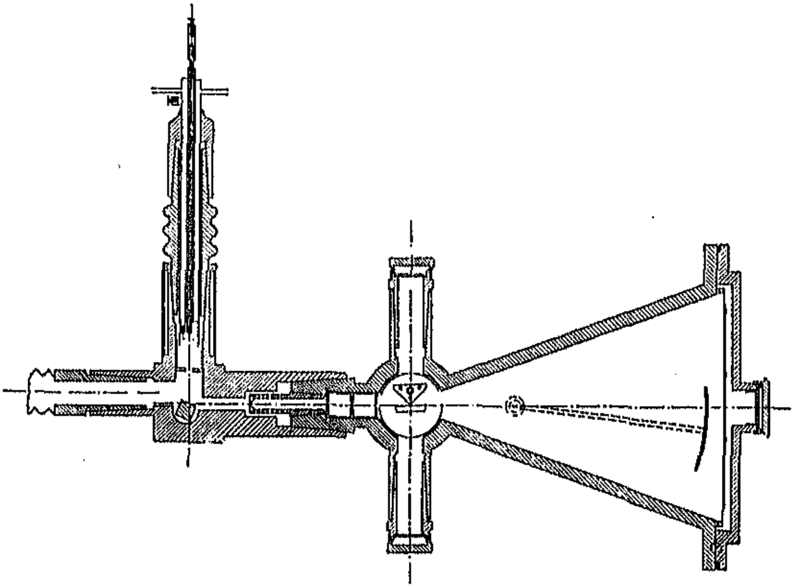

Fig. 48*a*. Siegbahn and Magnusson's Apparatus.

A chamber of triangular shape as shown in the diagram encloses the grating and the photographic plate. The grating is housed in the circular portion at the middle of the figure. The grating holder has a steel-wedge just at the axis of rotation (as in Seemann's spectrographs). The holder fits into the chamber from the top by means of ground cones. The upper portion of this grating holder has a circular head graduated to a fraction of a degree. This scale is read by means of microscopes (not shown in the diagram) fixed to the body of the chamber. The microscopes read the angles through which the grating is turned. The steel-wedge in front of the grating limits the beam (as explained in Seemann's apparatus), so that the error due to divergence of the beam is eliminated. The chamber ends on one side (to the left) in a ground cone to which fits a corresponding cone of the X-ray tube‡. The X-rays come from the target and are collimated by a series of slits shown in the diagram. The base of the triangle forming the chamber contains the plate-holder. The lid to the extreme right can be removed when loading the plate, and is easily

---

* Söderman, *Zs. f. Phys.*, 52, 795, 1929.

† Siegbahn and Magnusson, *Zs. f. Phys.*, 62, 435, 1930.

‡ The entire system to the left of the grating is the X-ray tube. For the description of this see § 145, (2).

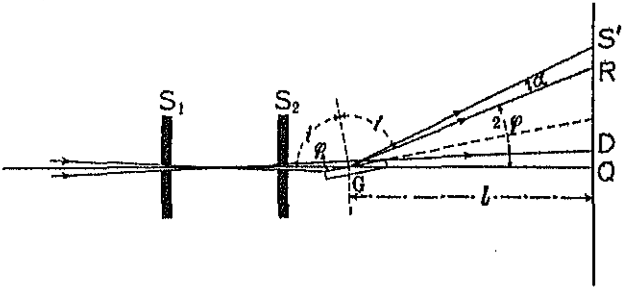

Fig. 48b. (Thibaud).

replaced. A lead sheet in the form of an arc is placed between the grating and the plate, and serves to shield from fogging the unexposed part of the plate. This shield can be operated from outside without disturbing the vacuum. The chamber and the X-ray tube are evacuated together through a side tube.

A typical spectrogram is shown in Fig. 48, Plate V. R is the reflected ray and the various order of spectra can be seen beyond it.

Measurement of wavelength can be done in the following way as illustrated in Fig. 48b. Here i=angle of incidence and ϕ=glancing angle.

If R be the reflected image at a distance x from the central spot O and l the distance between the plate and grating, then we have

$$\tan 2\phi = x/l$$

Let S′ be the image of any spectrum line. Then

$$\tan (2\phi + \alpha) = \frac{x+a}{l} \quad . \quad . \quad . \quad . \quad . \quad . \quad . \quad . \quad (39)$$

where a is the distance of the line S′ (whose wavelength is to be calculated) from the reflected image R.

From the above two equations ϕ and α are found, and substituted in the equation

$$n\lambda = \frac{d}{2}\,(2\alpha\phi + \alpha^2) \quad . \quad . \quad . \quad . \quad . \quad . \quad (40)$$

The value of λ is thus readily obtained.

Dispersion.—Differentiating the equation (40),

$$\frac{d\alpha}{d\lambda} = \frac{n}{(\phi+\alpha)\,d}$$

or $$\Delta\lambda = \frac{(\phi+\alpha)\,d}{n}\Delta\alpha = \frac{(\phi+\alpha)\,d}{n}\,\Delta(\phi+\alpha) = \frac{\psi d}{n}\,\Delta\psi$$

where $\phi+\alpha = \psi$, the divergence.

The dispersion is seen to be very small, simply because d is comparatively large; and it depends on the angle of divergence only.*

144. Concave Grating.—Osgood† applied the focal property of the concave grating to X-ray spectroscopy and reached λ166 Å. U. of Al in the region of soft X-rays.

Since then Edlen‡, Ekefors§, Arvvidsson‖ and others have constructed new apparatus for the spectroscopy of extreme ultra-violet rays using small glancing angle of incidence (about 5·6°) with concave gratings having a radius of curvature of about one metre and 1184 lines per mm. The same apparatus can be used for very soft X-rays (40 Å. U. to 150 Å. U.). Siegbahn¶ is of the opinion that the concave gratings are more suited for this range than the plane gratings.

Fig. 49 above shows a sketch of the arrangement. The concave grating G and the first slit Sp lie on the circle having its centre at O and radius equal to the radius of curvature of the grating. A thin photographic plate is bent along the arc of the circle and different wavelengths are focussed on it. C is the image of the totally reflected line.

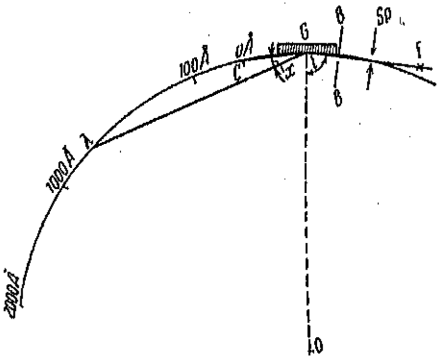

Fig. 49. The concave grating spectrograph.

Comparison of crystal and grating methods.

It has been found that there is a systematic difference between the values of any wavelength obtained by the crystal and the grating method. This has led to a controversy regarding the relative merit of the two methods, which has not yet been satisfactorily cleared up. The difference cannot be attributed to experimental error; there must be some fundamental difference in our understanding the theory of either of the methods. Bearden** is of the opinion that the grating measurements are in error, for he found agreement between the values of the same wavelength as obtained from the crystal method and the prism refraction method (§ 158). Bäcklin* and Cork do not subscribe to this opinion on reasonable grounds. They point out that the agreement between the crystal and the prism methods is due to the use of the same auxiliary constants in the calculation of wavelengths in both cases. On the other hand the grating method is direct and does not depend upon the values of the auxiliary constants.

---

* For the calculation of resolving power see A. W. Porter, *Phil. Mag.*, 5, 32, 1067, 1928.

† Osgood, *Phys. Rev.*, **30**, 567, 1927.

‡ Edlen, *Zs. f. Phys.*, **73**, 476, 1932.

§ Ekefors, *Zs. f. Phys.*, **71**, 53, 1932.

‖ Arvvidsson, *Ann. d. Phys.*, **12**, 787, 1932.

¶ Siegbahn, *Proc. Phys. Soc.*, **45**, 689, 1933.

** Bearden, *Phys. Rev.*, **39**, 1, 1932.

145. X-ray Tubes.—During the four decades that have elapsed since Röntgen's discovery, a large number of X-ray tubes of new patterns have been designed to meet the requirements of the various applications to which these rays have been put. But all of them can be classed broadly in two groups :

(1) Ion type, and (2) Electron type.

The original X-ray tube made by Röntgen was of the ion type, and a description of that apparatus has been given in the beginning of the chapter. In every X-ray tube, there must be a cathode, an anticathode or anode and an insulating material separating the two. In Röntgen's X-ray tube a glass globe separates the cathode from the anticathode. Further, the space between the cathode and the anticathode must be capable of conducting electric current at a very high voltage. There are two methods of achieving this, and each of them has given rise to the two classes of X-ray tubes mentioned above. In the first the ions act as the carriers of electricity, and in the seconds the carriers are the electrons.

(1) *The Ion-type Tubes.*—In these tubes, the space between the cathode and the anticathode is evacuated to about 10^{-2} to 10^{-3} mm. pressure. If now high voltage be applied, so that the cathode is negative and anticathode is positive, a current will pass through the tube. The magnitude of this current will depend upon the pressure of the residual gas inside. It is supposed that the electrons first originate from the cathode which ionise the residual gas and the ions are driven with great velocity by the negative electric potential of the cathode on to the anticathode. The cathode is generally a concave piece of aluminium, which is chosen because it sputters least. The anticathode is placed at a distance from the cathode equal to the radius of curvature of the latter. The high velocity electrons are focussed on the anticathode, and as they are stopped, X-rays are generated.

---

* Bäcklin, *Phys. Rev.*, 40, 112, 1932.

It has been found that the intensity of X-rays depends upon the magnitude of the current, while their penetrability depends on the voltage applied to the X-ray tube. The current depends not only on the voltage but also on the residual gas pressure. And consequently a slight change in the gas pressure will mean a change in the current passing through the tube. Ion type X-ray tubes generally have a tendency to become harder (*i.e.*, gas pressure tends to decrease, because the gas is absorbed by the walls of the tube) when a discharge is passing through them; and when this happens, the current diminishes and with it the intensity of X-rays as well. On the other hand the high tension equipment tends to no-load characteristics and so the voltage rises to some extent. The rise of voltage means the production of X-rays of greater penetrating power, and much less intensity. For these reasons unless the gas pressure is under control, it is difficult to get X-rays of uniform quality from this type of tubes. There are several devices by which the gas pressure is adjusted, but still this type of tubes is far from satisfactory. Below we give the diagram of a demountable type of ion X-ray tube which is widely used in laboratories (Fig. 50).

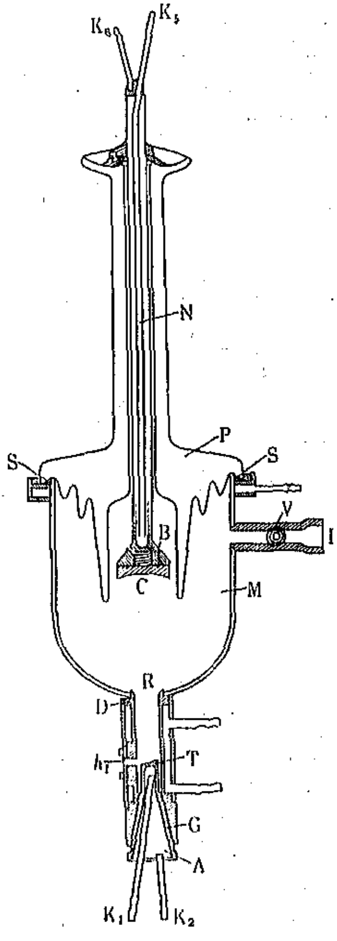

Fig. 50. The Hadding tube.

This tube was designed by A. Hadding* in 1920. C is the cathode and it has been screwed on to copper tube B with its lower end closed. This copper tube has another narrow tube N passing through it coaxially. K_5 and K_6 are inlet and outlet pipes and water is allowed to flow through them so as to cool the cathode. In these tubes there is a further disadvantage that they are not self-rectifying, and so the positive ions present inside the tube give rise to an inverse current which heats up the cathode. The cathode system is passed through a massive porcelain insulator P. This rests upon the metal body of the tube M. The space S is filled with picein or sealing-wax to make the apparatus vacuum tight. The metal body has an aperture R in its lower part just opposite to the cathode, and a metallic tube D is soldered to it so as to make a vacuum-tight joint. The lower end of this tube is ground conically so as to fit the anticathode A. The grinding must be perfect so that with a slight amount of Ramsay-vacuum grease, the joint is capable of maintaining very high vacuum. The target is fixed at T, and K_1, K_2 are the pipes for leading water to cool the anti-cathode. The body of the tube is also water-cooled by means of concentric jackets, because it also gets heated due to the bombardment by stray cathode rays, and tends to emit vapour. The plane of the target makes an angle of 45° with the direction of the cathode rays. The tube D has three holes, one of which can be seen at h_1 in the figure. The holes are just in front of the centre of the target T and they act like windows through which X-rays come out. They are covered with thin aluminium foils ('01 mm.) so that the X-rays are not much absorbed while coming out from the target. The three windows can be utilised at the same time. The aluminium foil is pressed by rubber packing and two screws, so that the vacuum is maintained. There is one side tube I which is connected to the pump, and the needle-valve V is attached to the side tube. By means of the needle valve the vacuum inside the tube can be adjusted to the required amount. It is shown diagrammatically in Fig. 51. It has a very narrow aperture closed by a needle, and this latter forms the lower end of a fine screw working in the body of the valve. When this screw is raised or lowered, the needle allows small quantities of air to leak in through the aperture. The vacuum is thus adjusted. The needle-valve is not a self-adjusting instrument. If there is a slight change in the pressure due to the evolution of gas from the walls of the tube or from the sealing material, the needle valve cannot cope with it. It has to be closed, and the high-tension current switched off; otherwise the cathode may be damaged by reverse current. But the needle-valve, as such, is always at the control of the experimenter.

---

* Hadding, *Zs. f. Phys.*, 3, 369, 1920.

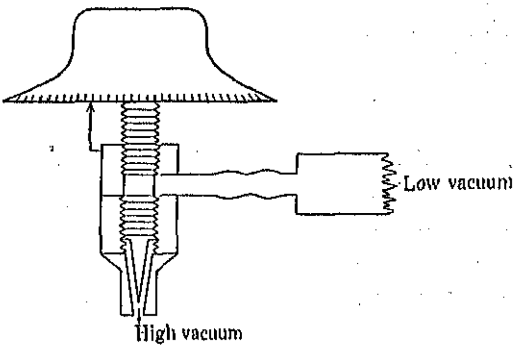

Fig. 51. The needle valve.

(2) *The Electron-type Tubes.*—W. D. Coolidge devised in 1913 a very interesting method of getting complete control over the current and voltage (*i.e.*, intensity and penetrating power of X-rays). In this method

all such erratic factors such as adjusting the gas pressure have been eliminated. The tubes of this pattern have a special kind of cathode which contains a spiral of tungsten wire at its centre. The tube is first evacuated completely so that it allows no current to pass through it when the high-tension is switched on. The tungsten filament is heated to white-heat by passing a current of few amperes through it. It then emits copious quantities of electrons. If now high tension be applied, a current of electrons begins to flow from the cathode to the anticathode. The current through the X-ray tube depends on the absolute temperature of the tungsten filament according to the Richardson formula (*vide* chapter on Thermionics).

$$i = A\,T^2\,e^{-b/T}$$

where i is the current/cm.^{2},

$$A = \frac{2\,\pi\,k^2\,me}{h^3},\ b = \frac{e\phi}{k} - \frac{3}{2}T,\ \phi = \text{thermionic potential.}$$

The absolute temperature of the filament is controlled by the heating current, so that the H. T. current passing through the tube can be easily controlled. Thus we can vary the intensity of X-rays without changing their penetrating power. If however the vacuum is not perfect, the filament rapidly oxidizes and ultimately breaks down. Generally the vacuum is disturbed by the vapour coming from the grease or sealing material between the joints. To avoid this Hevesy and Ott dispensed with the grease, and used lead or rubber packings between the joints.

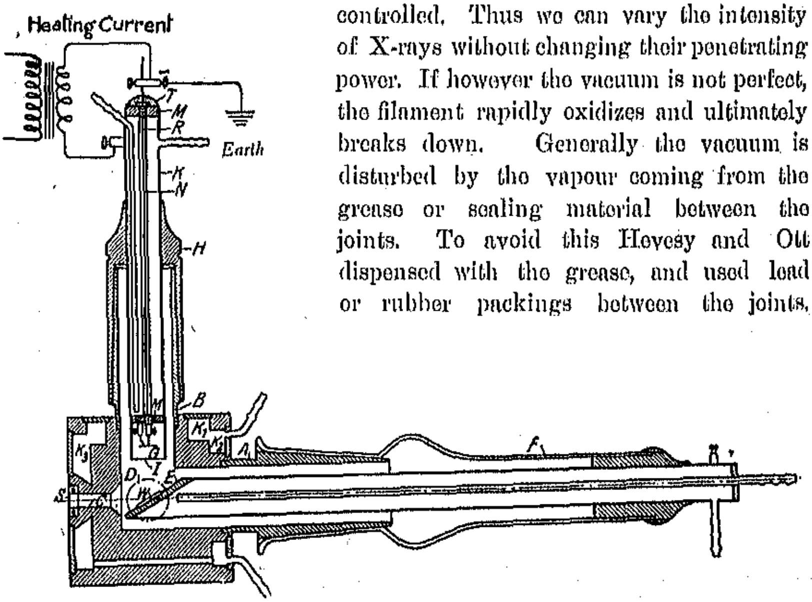

Fig. 52. Siegbahn's hot cathode metal tube.

Many workers have used thoriated tungsten or oxide coated Pt filaments instead of ordinary tungsten wires. These have the advantage that they emit copious amounts of electrons at lower temperature and so there is no risk of burning the filament. We give below the description of an electron type of tube used in spectroscopic experiments by Siegbahn (Fig. 52).

C is a metal cube bored out in two adjacent faces A and B, and ground metal cones are fixed over them. The metal cone A fits into a corresponding glass cone attached to a glass tubing F. This tubing has another cone at its upper end, and the anticathode piece E is fitted into it. The anticathode is similar in design as in the case of ion tubes. In the cone B, fits another cone H which has the cathode K soldered to it. The cathode piece is almost the same as in the case of ion tubes, the only difference being a narrow quartz tube R through which a stout copper wire N carrying the current to the filament is inserted. The upper end of the wire is sealed with sealing wax at T. The filament G is suspended from the lower end of the wire N, and the body of the cathode. If a source of potential (say a step-down transformer as shown) is connected to the upper end of the copper wire N and the body K of the cathode, a current will flow through the filament, and will heat it to the required temperature. I is a metal tube surrounding the filament, and is used to focus the thermions on the anticathode W. The aperture S acts like a window. The tube has another aperture at one of its sides, and the pump is connected through it. The strength of the insulating material will determine the voltage which can be applied to the X-ray tube. For very high voltages (200 to 400 KV), long side tubes of glass of special make are used. These tubes are made use of in the radiography of metal castings.

It has been pointed out that the intensity of X-rays depends upon the high-tension current passing through it. The current input of a tube solely depends upon the efficiency with which the anticathode is cooled. In fact, the energy expended in an X-ray tube is almost all transformed into heat, and very little into radiation. This heat will eventually melt the anticathode unless it is conducted out rapidly. For works with general radiations, it is advantageous to use a metal in the target which has large heat conductivity and high melting point. The size of the focal spot of the target has much to do with the input limit. Müller* has given the relation connecting the maximum power input W_{max}, the melting point T_m and the conductivity k of the anticathode as

$$W_{max} = 15{\cdot}8.\,\frac{(T_m - T_o)\ \delta.k}{\theta}$$

where θ is a function of the dimensions of anticathode, δ = the area of the focal spot, and T_0 = the temperature of the flowing water.

For very soft X-rays (5 to 100 Å) the electron type of tube is very suitable. But there is one objection, namely, the tungsten vaporises from the filament and deposits upon the target. From the spectroscopic point of

---

*Müller, *Proc. Roy. Soc. A.*, **117**, 30, 1927; *Proc. Roy. Soc. A.*, **125**, 507. 1929. For avoiding melting, rotating targets are used. See Müller, *loc. cit.*

view, this is a disadvantage, for the tungsten lines also appear in the spectrum. This can be avoided by interposing a thin *cellophane* foil between the cathode and the anticathode. In this way, tungsten vapour is prevented from settling on the anticathode. But then the electrons lose a part of their velocity in passing through the foil. This can be compensated for by using a little more tension.

146. X-ray Tubes designed for Chemical Analysis.—It is well known that X-rays have proved to be extremely useful to the chemical analyst. If an alloy containing several substances be put on the anti-cathode of an X-ray tube, the relative intensity of the X-ray lines from this will tell the analyst the proportion of the ingredients in the alloy. The discovery of new elements like Hafnium*, and Rhenium were made with the help of X-ray spectroscopy. The powder or the mineral to be investigated can be easily pressed into the grooves in a brass or copper anti-cathode which can be placed in any of the X-ray tubes described before. Laby† and others claim that an ingredient existing even in so small a proportion as one in 10^6 can be detected with certainty by this method. As in the usual form of X-ray tubes the sample to be analysed is subjected to bombardment by cathode rays, it either evaporates or gets dislodged from the anticathode. To prevent this, a new type of tube is used in which the sample is irradiated by X-rays of sufficient hardness to excite its characteristic fluorescent rays, and the latter can be spectroscopically studied. This method is better suited for analysis work than the other, for it gives more correct ratio of the quantity of the ingredients. The only disadvantage is that longer exposures have to be given, for the fluorescent rays are much weaker than the primary rays. In order to get a strong beam of fluorescent rays the X-ray tube has been modified by Coster‡ and Hevesy§. The cathode and the anti-cathode of the Coster's tube are shown in Fig. 53. In this the focussing cylinder of the hot-cathode C is made of the shape shown in the figure.

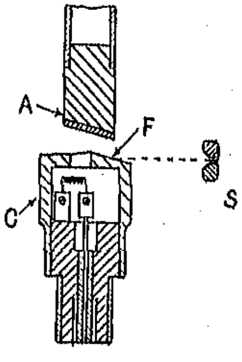

Fig. 53. Coster and Hevesy's X-ray tube.

---

* For an account of the discovery of Hafnium and Rhenium, see Hevesy, *Chemical Analysis by X-rays*, Chap. XI, p. 182.

† Laby, Turner and Eddy, *Proc. Roy. Soc. A*, 127, 20, 1930.

‡ Coster, *Zs. f. Phys.*, 40, 756, 1927.

§ Hevesy, *loc. cit.*

The sample to be examined is placed at F on the cylinder C. The primary X-rays are produced in the anti-cathode A and fall on the sample. The window S of the tube is so placed that primary rays cannot pass out of it, while fluorescent rays can easily emerge out. The sample is placed at F because it is necessary to give to it a negative potential, otherwise the X-rays produced from it will be largely (about 86%) due to the scattered electrons from the anti-cathode. It is clear that the secondary radiator must be placed inside the X-ray tube, otherwise the intensity of fluorescent radiation will be very much reduced.

147. High Tension Arrangements.—Formerly induction coils run by interrupted direct currents were used to excite X-ray tubes. But at the present time high tension transformers with rectifying accessories have replaced them. Still it is useful to say a few words about the induction coils. The induction coils have straight cores made of silicon steel having high permeability and specific resistance, and at the same time low hysteresis. The primary coils of thick copper wire are wound round the core. The primary coil and the core are enclosed in a thick micanite cylinder. The secondary coils are wound and slid over the micanite cylinder which serves the purpose of insulating the primary from the secondary. When an interrupted direct current passes through the primary, very high voltage is developed at the terminals of the secondary.

The motor-mercury-interrupters are the most well-known. This is shown in Fig. 54. Two rotating jets of mercury J, J are allowed to fall on metal sectors A, A, A, A placed in the form of arcs of the same circle but separated from each other. The jets are always in one line and so make electrical connections between the sectors placed diametrically opposite when the jets fall upon them. The jets come out from two narrow tubes, dipping in a trough of mercury. These tubes are fixed in a wooden conical block which in turn is coupled to the shaft of an electric motor. The jets and the sectors are enclosed in a metal chamber the bottom of which forms the mercury trough referred to above. This chamber is filled with coal gas to prevent arcing at the time of break. A condenser C is placed across the interruptor as shown in the diagram (Fig. 54). The capacity of this condenser, the speed of interruption and the inductances of the primary are so arranged that the secondary voltage at the time of make is far less than that at the time of break. And as the

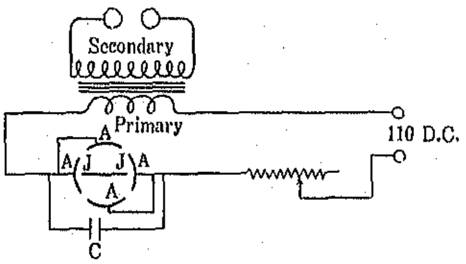

Fig. 54. The high tension induction coil.

voltages at make and break are opposite each other, the induction coils give more or less unidirectional current. But the reverse current cannot be totally eliminated unless a rectifier is used. With the ion-type of tubes, induction coils with rectifier give quite satisfactory results. If no rectifier is used the cathode gets heated and in course of time gets pitted with deep holes. Even the rectifier need not be a very efficient one, for the reverse current which we have to suppress is very feeble compared to the direct current. The rectifiers generally used are known as *valve rectifiers*, and their rectifying property is due to assymmetric electrodes in an electric bulb containing low vacuum.

The interrupters are always the source of trouble as they are not suitable for continuous work. The magnetic circuit of an induction coil is not closed, and so it is not so efficient. It is no wonder that at present they have been replaced almost completely by transformer outfits.

148. High Tension Transformers.—The transformers are similar in construction to the induction coil. But the core is closed, and the whole apparatus is kept immersed in oil for insulation as well as for cooling.

The transformer is fed with alternating current, and consequently the secondary also produces alternating current at high voltage. The rectification must be very efficient in this case. A Coolidge tube (hot-cathode or electron type) is self-rectifying. But still it is better to rectify the current before it passes through an X-ray tube, for otherwise half of each cycle will be lost. The rectification is managed in two ways:—

(1) Mechanically, (2) By Kenotrons.

In the first case (Fig. 55), a synchronous motor running at the same frequency as that of the primary alternating current, has a large disc M made of insulating materials like fibre or micanite fixed to its spindle P. This disc has two metallic sectors S_1 and S_2 attached to the rim diametrically opposite to each other. A, B, C, D are four metallic knobs placed in the position shown in the figure.

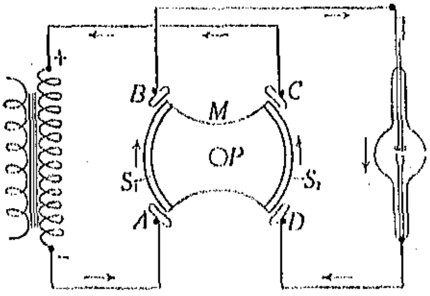

Fig. 55. The mechanical rectifier.

In this position A and B, C and D are connected by the metallic sectors, so that the electron-current flows in the direction of the arrow from A to B, then through the X-ray tube to D and finally returns through C. Half a cycle later B and C, A and D will be connected, but by that time the current also has reversed, for the synchronous motor always keeps in phase with alternations of the supply current. The result is that the current through the X-ray tube is in the same direction. (Note that the sectors do not actually touch the knobs. They pass close to them, and on account of high voltage the current sparks over.) It is easy to follow that the synchronous motor is not necessary when the A. C. generator is within easy reach of the high-tension plant; for the insulating disc can be mounted on the shaft of the generator itself. The synchronous motor rectifiers are not convenient to work with, for the rotating parts undergo wear and tear very quickly.

(1) *The Kenotron Rectifier.*—Kenotron rectifiers are just like electron X-ray tubes. They have a heated tungsten filament as cathode, and a massive metal cylinder as anode. The bulb is evacuated completely so that no high-tension current can pass through them unless the filament is heated. The focussing device used in electron X-ray tubes is absent in kenotrons, for otherwise X-rays would also be produced in them. The filament is heated strongly and the fall of potential across the kenotron is small, and very soft X-rays are produced which cannot come out of the glasswalls.

For good rectification one, two, four or six of them can be used together. In the last case three transformers having the same output are fed with three-phase alternating current. The rectified current does not consist of pulses, but is very uniform.

Below is given (Fig. 56) a four-kenotron rectifier circuit (Graëtz* circuit). The four kenotrons A, B, C, D are placed in the four arms of a wheatstone net whose diagonals are occupied by the secondary windings of the transformer, and the X-ray tube.

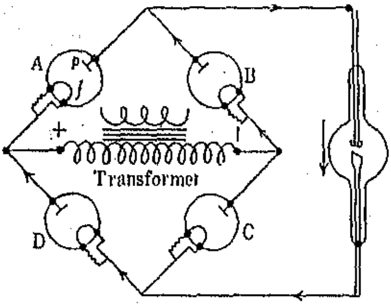

Fig. 56. Graetz's full-wave kenotron rectifier.

The position of the filaments of the kenotrons with respect to the high tension transformer must be carefully noted.

In the kenotron A, p is the plate which must be positive and f the filament must be negative, if the current is to pass. The plates of A and B are connected together, while the filaments of C and D are connected together. Also the filaments of A and B are connected to the plates of D and C respectively. The filament of the X-ray tube is joined to the plates of A and B, while the anticathode to the filaments of C and D. It is easily seen that by this arrangement only the two kenotrons on one pair of the opposite arms of the bridge become effective at a time, and the current through the X-ray tube is rectified always in the same direction.

---

* For these see *Handbuch der Experimental-physik*, Kirchner, 24, (1), 74.

The heating current for the kenotrons are obtained from four step-down insulated transformers. The arrows mark the direction of the flow of electrons.

The pulsations of current plotted against time will take the form shown in Fig. 57. The current is unidirectional but not steady. In order to smooth out these pulses, condensers are joined in parallel with the X-ray tube. These condensers are capable of withstanding high voltage. At the time of the gaps between the pulses, the charge stored in the condensers supplies the current to the X-ray tube. As a result the pulsations are smoothed out to some extent as shown by the thick lines in the figure.

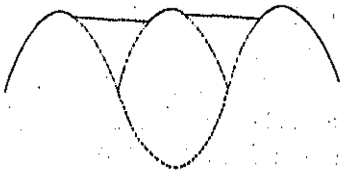

Fig. 57. The cycle after rectification.

But still the voltage applied to the X-ray tube cannot be taken to be constant. In the experiments on the excitation voltages of X-ray lines, and determination of the Duane and Hunt limit, batteries of several thousand cells have to be used for obtaining very steady voltages. We shall describe later another high-tension circuit used in many laboratories at present.

149. Continuous X-rays—The Pulse Theory.—Soon after the discovery of X-rays, Stokes* and Wiechert† put forward a theory of the production of X-rays. They said that as the rapidly moving cathode particles are suddenly brought to rest in the metallic traget of the anticathode, the energy of the particles is partially converted into an electromagnetic pulse travelling in space. The phenomenon is thus exactly the same as the emission of radiation by accelerated electrons in accordance with Hertz's theory. The intensity I_0 of this pulse in a direction making an angle θ with the direction of cathode rays is given by the formula (see § 113, eqn. (1*a*)).

$$I_0 = \frac{e^2 a^2 \sin^2\theta}{4\pi r^2 c^3} \quad . \quad . \quad . \quad . \quad . \quad . \quad . \quad . \quad (41)$$

where $a = -dv/dt$ the retardation, and other symbols have usual meanings. This expression shows that the intensity I_0 will be maximum in a direction $\theta = \pi/2$, and minimum in a direction $\theta = 0$

---

* G. Stokes, *Proc. Manchester, Lit. and Phil. Soc.*, 1898.
† E. Wiechert, *Sitz. ber. d. Phys. Ges.*, 1894 (Königsberg).

or π. The Stokes-Wiechert theory enables us to get a general idea of the space distribution of intensity of continuous X-rays.

Further the pulse should be completely plane polarised, for the electric vector of the pulse is in the direction of motion of the cathode rays. The polarisation of general X-rays was experimentally studied by Barkla (*vide* § 156) and the phenomenon was actually observed. It is however found that the X-rays are only *partially* polarised in the plane defined by the line of motion of cathode rays and the direction of the emitted rays. This can be ascribed to the fact that as the cathode rays enter the target, some of them are deflected from their original path and the direction of acceleration changes, and this gives rise to radiation in which the electric vectors lie in different directions.

Before the discovery of the crystal method of X-ray spectroscopy, the chief methods of studying the continuous X-rays were their distribution in space (§ 152), their polarisation (§ 156) and the efficiency of their production (§ 151). The experimental results obtained were in general agreement with the pulse theory of generation of X-rays. But the original theory had to be modified in order to take into account certain discrepancies discovered when accurate methods of spectroscopy were introduced. Thus the pulse theory failed completely to explain certain features of the intensity distribution of the continuous spectrum for different wavelengths. According to Stokes' theory the electro-magnetic pulse should contain all wavelengths from $\lambda=0$ to $\lambda=\infty$ and hence can be resolved into continuous spectrum. The harder radiations are produced when the cathode particles just enter the target, and as the velocity is more and more reduced by gradual penetrations into the target, the softer components of the spectrum are emitted. Duane and Hunt* studied the distribution of intensity in various parts of the continuous spectrum by the then newly discovered method of crystal spectroscopy. They showed that the continuous spectrum did not extend from $\lambda=0$ to $\lambda=\infty$, but that it had a sharp limit on the short wavelength side, and on the long wavelength side extended indefinitely, though the intensity diminished very rapidly. In Fig. 60 the intensity variation of the continuous spectrum of some of the targets are illustrated.

Further they discovered the striking fact that the frequency ν_{max} corresponding to the short wave limit λ_{min} was related to the impressed voltage V across the tube by the quantum relation

---

* Duane and Hunt, *Phys. Rev.*, 6, 166, 1915.

$$h\nu_{\max} = Ve \quad . \quad . \quad . \quad . \quad . \quad . \quad . \quad . \quad . \quad (42)$$

where e=charge on the electron, and h=Planck's constant. Hence

$$\lambda_{\min} = \frac{hc}{eV} \quad . \quad . \quad . \quad . \quad . \quad . \quad . \quad . \quad . \quad (43)$$

No interpretation of this remarkable observation could be supplied by the Stokes-Wiechert theory. On the other hand the effect becomes exceptionally clear on the quantum view of radiation. For a cathode particle falling through an electric potential V cannot acquire an energy greater than eV, and when it is suddenly stopped the whole of its energy may be converted to radiation which explains the result.

As the nature of the retardation of cathode particles was not known, the structure* of the pulse was a matter of guess. In fact it was likened to noise produced by a hail of bullets striking a tin-shed, which contains all pitches of sounds without any regularity. Many attempts were made to analyse certain assumed forms of the pulse into its Fourier components so that the intensity distribution in the spectrum might agree with the experimental results. Though some agreement was obtained with the experimental curve, the sharp stoppage at the short wavelength limit was unintelligible till explanation was forthcoming from the quantum theory as mentioned above. The fact that X-rays show the phenomena of interference and of diffraction by crystals point out that they must consist of long trains of waves. On the other hand the pulse assumed in Stokes' theory are finite and irregular. In order to reconcile these facts, Kramers† gave a theory of the continuous X-rays based on a combination of classical and quantum theory.

150. Duane and Hunt's Experiments.—The above relation (43) was subjected to an accurate experimental test by Duane and Hunt. Their arrangement is illustrated in the diagram (Fig. 59) below. The radiation from the target T falls through the slits S, S on the crystal C. The diffracted rays are received in the ionisation chamber I. The wavelength of diffracted ray is given by the Bragg law $\lambda = 2d \sin \theta$.

---

[*] E. H. Kennard, *Phys. Zeits.*, **24**, 372, 1923; see also Compton's *X-rays*, Chap. II.

[†] H. A. Kramers, *Phil. Mag.*, **46**, 869, 1923.

The glancing angle is slowly increased from 0, while the ionisation chamber is rotated through twice the angle. As there is no wavelength between 0 and λ_{min}, for the corresponding glancing angles the electrometer showed no current. But as soon as $\theta = \sin^{-1}(\lambda_{min}/2d)$ is reached, the electrometer indicates a current. λ_{min} is calculated from this value of θ in Bragg's equation.

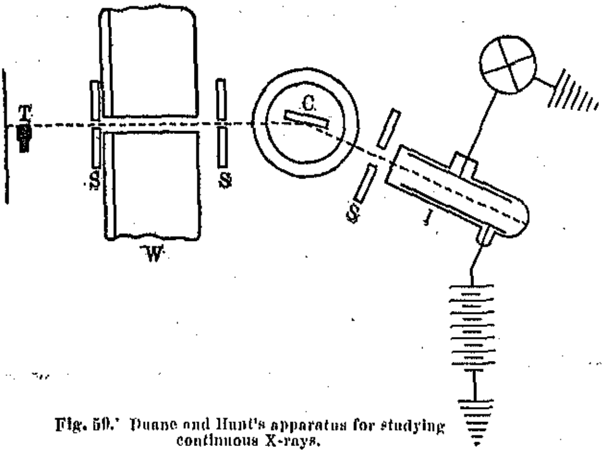

Fig. 59. Duane and Hunt's apparatus for studying continuous X-rays.

Duane and Hunt used 20000 small storage cells, so that the potential across the tube could be accurately varied by small amounts. The potential V was very accurately measured by an electrostatic voltmeter.

This method enabled them to make an accurate determination of the Planck's constant h. If V be the applied potential in volts, the relation (43) can be written as

$$h = \frac{eV\lambda_{min}}{300\,c} \quad \ldots\ldots\ldots\ldots \quad (44)$$

Since V and λ_{min} was accurately determined, h could be calculated. Thus using V=40 KV for tungsten anticathode, λ_{min} was obtained as 0·310 Å.U. (from a calcite crystal). This gives $h = 6{\cdot}58 \times 10^{-27}$ erg. sec. Duane and Hunt used different potentials between 25 to 40 KV and obtained a mean value of $h = 6{\cdot}50 \times 10^{-27}$ erg. sec. The experiment was repeated by Webster*, Ulrey†, Müller‡, Blake and Duane§, and Wagner‖, and they obtained very consistent values of h.

---

* Webster, *Phys. Rev.*, **18**, 155, 1921.
† Ulrey, *Phys. Rev.*, **11**, 401, 1918.
‡ Müller, *Phys. Zeits*, **19**, 489, 1918.
§ Blake and Duane, *Phys. Rev.*, **10**, 624, 1917.
Wagner, *Ann. d. Phys.*, **57**, 401, 1918.

151. Distribution of Energy in the Spectrum.—The study of distribution of energy in the continuous spectrum has been made by many workers (*loc. cit.*). The apparatus used is similar to Duane and Hunt's* arrangement shown in the preceding section. The curves obtained by plotting the intensity at different wavelengths against wavelengths for a constant potential are known as *isotherms*. On the other hand when the intensity of one particular wavelength was plotted against potential across the tube as abscissa, the resulting curve was denoted by the term *isochromat*.

It was also found that the intensity of a particular wavelength for the same potential varied directly as the atomic number of the material of the target used in the X-ray tube. In the curves reproduced below (Fig. 60), we have the isotherms for different targets Pt, Sn, Ag, Cu, Co, Al for the same potential 10470 volts. The intensity of any wavelength is maximum for platinum and minimum for aluminium, but one thing is notable, that the short-wave limit is independent of the material of the target and depends only on the potential of the tube.

This is shown by the fact that all curves meet at one point on the wavelength axis.

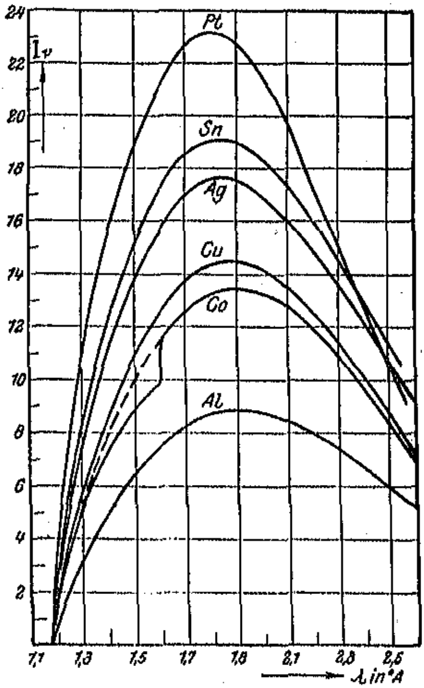

Fig. 60. The intensity distribution of continuous X-rays. (Pt, Sn, Ag, Cu, Co, Al).

From a detailed study of these curves, Kulenkampff† came to the conclusion that the intensity I_ν for the frequency region between ν and $\nu+d\nu$ can be denoted by the formula

$$I_\nu = C\{Z(\nu_0-\nu)+bZ^2\} \quad . \quad . \quad . \quad . \quad . \quad . \quad . \quad . \quad (45)$$

---

* Duane and Hunt, *loc. cit.*

† Kulenkampff, *Ann. d. Phys.*, **69**, 548, 1922.

where b is a very small constant*, Z is the atomic number of the material of the target, C is a constant, and ν_0 is the maximum frequency limit. Now $\lambda = c/\nu$ or $d\lambda = -c/\nu^2.d\nu$. Hence

$$I_\lambda = C\frac{c^2}{\lambda^2}\left\{Z\left(\frac{1}{\lambda_{min}} - \frac{1}{\lambda}\right) + \frac{b}{c}Z^2\right\} \quad . \quad . \quad . \quad . \quad . \quad (46)$$

This equation when plotted with I as ordinate and λ as abscissa represents in general the curve known as the *Isothermal Curve* or simply the *Isotherm*. Again

$$I_\nu = C\left\{Z\left(\frac{eV}{h} - \nu\right) + bZ^2\right\} \quad . \quad . \quad . \quad . \quad . \quad . \quad (47)$$

So that the intensity for a frequency ν, increases linearly with the potential across the tube. The straight line represented by the eqn. (47) taking I as ordinate and V as abscissa is known as the *Isochromatic Curve.* Differentiating (46) for finding the wavelength for maximum intensity, we get

$$\frac{dI_\lambda}{d\lambda} = -\frac{2}{\lambda_{min}} + \frac{2}{\lambda} - \frac{2b}{c}Z + \frac{1}{\lambda}$$

and putting $dI_\lambda/d\lambda = 0$ for the maximum intensity, we get

$$\frac{3}{\lambda} = \frac{2}{\lambda_{min}} + \frac{2b}{c}Z$$

or

$$\lambda_{max} = \frac{3}{2}\cdot\frac{\lambda_{min}}{1 + \frac{b}{c}Z.\lambda_{min}} \quad . \quad . \quad . \quad . \quad . \quad . \quad . \quad . \quad (48)$$

where λ_{max} is that wavelength for which the intensity is a maximum. In equation (48), b is a very small quantity. Hence we have approximately

$$\lambda_{max} = \tfrac{3}{2}\lambda_{min}$$

That is, for a fixed voltage, the wavelength of maximum intensity is $\frac{3}{2}$ times the short wave limit for all targets. This conclusion is of great practical importance in selecting the voltage to be applied across

---

* Strictly speaking b is not a constant, but a function of ν. It has been found experimentally that it can be represented by the relation

$$b \propto \nu_0\left[1 - e^{+16(\nu-\nu_0)/\nu}\right]$$

which shows that at $\nu = \nu_0$, $b = 0$; but when ν is much below ν_0, b is nearly a constant. See W. W. Nicholas, *Bur. Stand. Journ. Res.*, 5, 843, 1930.

the tube to study any part of the spectrum. If the voltage be so chosen that $eV = \frac{3}{2} . ch/\lambda$, then the wavelength λ would correspond to that of the maximum intensity of the spectrum.

The results discussed above are true only for thick targets. The difference between the thin targets and thick targets must be clearly understood. In case of the thick targets the cathode rays get easily deflected and their velocity is reduced, and so the intensity of the softer components of the spectrum is cut down. Kulenkampff's above experiments were done with thick targets. In the case of thin targets these disturbing effects are not present. Webster* and Nicholas† found that the intensity of continuous radiations from thin foils of Al and Au ('0826μ) were distributed almost equally in various wavelengths, and also the discontinuity at λ_{min} was definite, *i.e.*, not preceded by gradual fall as in Fig. 60.

Efficiency of X-ray Production (*Continuous*).—The efficiency of X-ray production may be defined as the ratio of the *total intensity* of X-rays produced to the power supplied to the tube. We have

$$\varepsilon = \frac{I}{E} = \frac{I}{Vi} = \frac{\Sigma I_1}{\Sigma \frac{1}{2} mv^2}$$

where I = total intensity, V = voltage, i = current through the tube, I_1 the intensity produced by the stoppage of a single electron, and $\frac{1}{2} mv^2$ is the kinetic energy of the electron.

The efficiency of X-ray production is extremely small, most of the energy being converted to heat. The quantity was experimentally determined by Beatty and others by measuring the total intensity I by an ionisation method. They found that only a small part of the energy, about 1 part in 10^4 is converted to X-rays. Later, calorimetric methods were introduced by Wien, Rump and others. The beam of X-rays was allowed to fall on a block of lead which was thick enough to absorb all the X-rays. The total heat produced, which is equivalent to the energy of the X-rays, was then obtained from measurement of the rise of temperature in the lead block. The result of these experiments can be expressed as follows

$$\varepsilon = C. V. Z.$$

where V = potential in KV's, and Z is the atomic number of the anticathode material. C is a constant of the order of 10^{-6}. The formula was tested by Rump up to 150 KV's. It is found that the efficiency is directly proportional to the atomic number, so that heavy elements give more continuous radiation than light elements.

---

* Webster and others, *Proc. Nat. Acad. Sci.*, **14**, 679, 1928.

† Nicholas, *Bureau of Stand. Jour. Res.*, **2**, 837, 1929.

See Rump, *Zs. f. Phys.*, **43**, 278, 1927; also Kirchner, *H. d. Exp. Physik*, **24/1**, 101—114, where all references would be found.

152. Space-Distribution of Continuous X-rays.—According to the pulse theory, the direction of maximum emission of continuous X-rays lies at right angles to the direction of motion of the cathode rays, and that of the minimum in the direction of motion. It was shown by Sommerfeld that as the cathode rays are moving with a velocity comparable to that of light the Stokes equation should be replaced by the equation

$$I_\theta = \frac{a^2 e^2}{4\pi r^2 c^3} \frac{\sin^2\theta}{(1-\beta\cos\theta)^6} \quad . \quad . \quad . \quad . \quad . \quad . \quad . \quad (49)$$

where $\beta = v/c$. The new factor in the denominator was obtained by the introduction of relativity correction.* Further in the case of thick targets, the velocity of the cathode rays range from $v_{\max}$ to 0, and so the intensity is to be summed up for all these values of v. If the total intensity be S, then we have

$$S = {}_0\int^t I_\theta \, dt = \frac{ae^2}{16\pi r^2 c^3} \frac{\sin^2\theta}{\cos\theta} \left\{ \frac{1}{(1-\beta\cos\theta)^4} - 1 \right\} \quad . \quad . \quad . \quad (50)$$

Here t is the time taken by the cathode ray to form the pulse. One direct conclusion from the modified distribution formula (50) is that the intensity distribution depends both upon θ as well as β. In fact it can be shown† that according to this relation when β is very small, the intensity maximum corresponds to $\theta = \pi/2$, but as β increases from 0·1 to 1, the maximum shifts progressively from $\theta = \pi/2$ to almost to $\theta = 0$. The minimum of intensity corresponds to $\theta = 0$ for all values of β.

The above conclusions have been experimentally verified by the works of Stark and Löbe‡. Their results were in general agreement with the theory, but the intensity maxima obtained were not found to be very pronounced. It was pointed out by Sommerfeld that the experimental results on space-distribution may be vitiated by various disturbing factors. Firstly the finite thickness of the target modifies the distribution considerably in several ways. For example, in the above calculations, it is assumed that the path of the cathode ray is rectilinear inside the target; but in practice this is far from truth. It is well-known that a part of the cathode rays are completely deflected in random directions from their original path and they strike the walls of the tube giving rise to the brilliant fluorescence observed on the sides of the X-ray tubes. Then again as the X-rays come out from various depths of the target, they are absorbed. This absorption is different in different directions according to the thickness of the target traversed by the rays. Further the characteristic radiation of the anticathode presents another difficulty, as they are emitted in all directions with equal intensity. To avoid these difficulties, Stark* and Löbe made use of anticathodes of carbon blocks, for which the absorption of X-rays is very small and the characteristic radiations emitted are also too soft to be detected. Stark observed that the absorption coefficient of X-rays for Al was less in the forward direction than in the backward. This means that for small values of θ, the proportion of harder rays in the continuous beam was greater than that for the larger angles. This was ascribed to the Döppler effect of the radiating electrons, on account of which the proportion of hard rays will be different in different directions of observation, increasing uniformly between $\theta=\pi$ to $\theta=0$.

---

* For a proof of this relation see Sommerfeld, *Atomic Structure and Spectral Lines* (1923), p. 33, 533.

† A. Sommerfeld, *Phys. Zeits.*, **10**, 969, 1909.

‡ W. Löbe, *Ann. d. Phys.*, **44**, 1033, 1914.

Thus on the whole these results supported the pulse theory. But fresh objections were raised from other quarters. Wagner† studied the distribution of intensity in various wavelengths in the continuous spectrum for the *same direction* ($\theta=90°$) of observation and obtained a (S_λ, λ) distribution curve. Repeating the experiment for another angle ($\theta=150°$), he found that the two (S_λ, λ) curves converged precisely to the *same maximum frequency limit*. It meant that the emission of maximum frequency was not affected by the Döppler effect, though the velocity of the emitting electrons must have been greatest in this case. This result was very tantalising and led to a great deal of controversy regarding the constitution of the electron itself.

153. Kulenkampff's Experiment.

153. Kulenkampff's Experiment.—In order to make a thorough test of these anomalies, Kulenkampff‡ set up the following apparatus (Fig. 61) for an accurate investigation on the space distribution of continuous radiations. He used a thin target of low atomic weight, so that the disturbing effects mentioned above are minimised.

---

* Stark, *Phys. Zeits.*, **10**, 902, 1909.

† Wagner, *Phys. Zeits.*, **21**, 621, 1920.

‡ Kulenkampff, *Ann. d. Phys.*, **87**, 597, 1928.

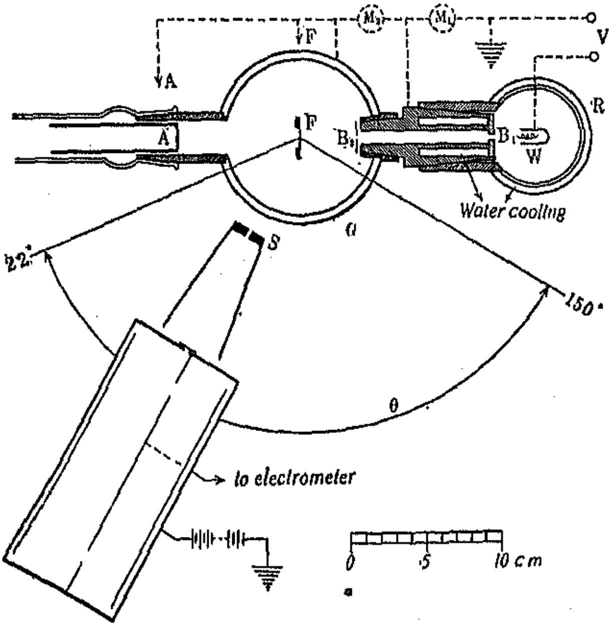

Fig. 61. Kulenkampff's apparatus.

A thin metal target F of Al (0·6 μ in thickness) is placed in the centre of the brass cylinder G. R is a metal X-ray tube whose cathode W is just seen in front of the slit system B$_1$ and B$_2$. The hot-cathode W has been inserted from above and insulated from R by means of a glass tube (not shown). The potential is applied between W the cathode and A the anode. The foil F is also connected electrically with A. The cathode rays are limited by the slits B$_1$ and B$_2$ and fall on the foil F. The emitted X-rays are allowed to pass out through a slit 7 mm. in width cut in the side of the brass cylinder G and covered with a thin aluminium foil. The X-rays are received in the ionisation chamber after being limited by a slit S. M$_2$ and M$_3$ are two milliamperemeters to measure the high tension current. The cathode ray beam was controlled so that only a fraction of a milliampere was allowed to flow between A and F, because a larger current density might rupture the foil. The ionisation chamber could be rotated about F as centre so that the intensity distribution in various directions could be studied. As shown in Fig. 61, the range of angles extended between 22° and 135°. The different wavelengths whose distribution in space was studied in the continuous spectrum were separated by means of suitable filters (*vide* Chapter XI).

The results of investigation are illustrated by the three curves 1, 2, 3 in Fig. 62. Each of the curves shows the distribution of intensity (represented by radius vectors) with angle θ for the same voltage 31 KV* across the X-ray tube. The three curves 1, 2, 3 correspond to three separate wavelengths 0·43 Å.U., 0·53 Å.U. and 0·73 Å.U. respectively. In the case of the curve (1) the filter was an aluminium sheet 8 mm. in thickness, while for (2) and (3) thin sheets of Ag and Zr were used. The curves show maxima at 55°, 52° and 48° respectively. Thus it is to be noticed that the position of intensity maximum shifts towards larger angles as the radiation increases in hardness. These results with thin target are at variance with those of Stark and Löbe's experiments with thick targets of C. The Döppler effect cannot be the cause of this variation. Sommerfeld explained these results with the aid of wave-mechanics.

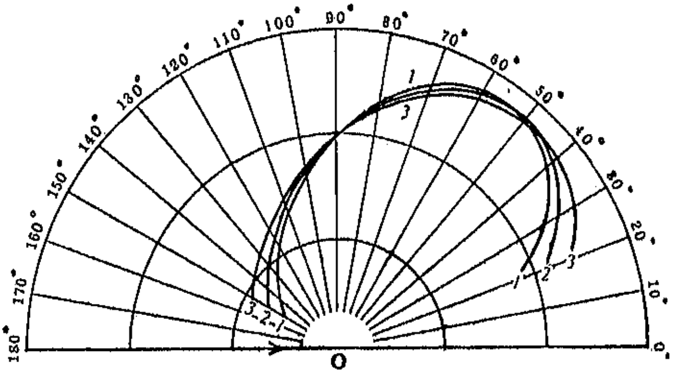

Fig. 62. Space distribution of continuous X-rays (*Kulenkampff*).

Sommerfeld regarded the incident cathode ray beam as an electron wave falling on the atomic nuclei and getting modified by scattering. An emergent electron may thus be regarded as a wave having an energy smaller than that associated with it before incidence. If the electron be in this way slowed down from a velocity v_1 to a velocity v_2, the difference in energy will be given out as a radiation of frequency ν, which according to De Broglie's fundamental assumption is given by

$$\nu = \frac{m}{2h}\left(v_1^2 - v_2^2\right) \quad . \; . \; . \; . \; . \; . \; . \; . \; . \quad (51)$$

Sommerfeld suggested that in eqn. (49) v is to be replaced by the mean velocity $(v_1+v_2)/2$. Then we should obtain the correct position of the intensity maximum for any wavelength in the spatial distribution. This is done as follows.

---

*This corresponds to the short wave limit 0·39 Å. U.

Differentiating eqn. (50) and putting $dS/d\lambda=0$, we get

$$\frac{2\sin\theta}{(1-\beta\cos\theta)^6}\left\{\cos\theta-\beta\cos^2\theta-3\beta\sin^2\theta\right\}=0$$

The value of θ satisfying this equation corresponds to the maximum of intensity. Let this be $\theta_{\max}$. Putting $\cos\theta_{\max}=x$, we have

$$2\beta x^2+x-3\beta=0$$

or

$$x=\frac{1}{4\beta}\left\{\sqrt{1+\tfrac{3}{2}(4\beta)^2}-1\right\} \quad \ldots\ldots \quad (52)$$

For $\beta=0$, we get from this equation $\theta_{\max}=\pi/2$ as in the classical case.

Now let V_1 be the potential corresponding to the incident velocity v_1 of the electron, and V_2 the potential corresponding to its emergent velocity v_2. Then

$$\tfrac{1}{2}mv_1{}^2=eV_1 \text{ and } \tfrac{1}{2}mv_2{}^2=eV_2$$

and

$$\beta=\frac{v_1+v_2}{2c}=\sqrt{\frac{2e}{mc^2}}\cdot\frac{\sqrt{V_1}+\sqrt{V_2}}{2} \quad \ldots\ldots \quad (53)$$

Also from (51) $\quad h\nu=e(V_1-V_2)$ and $h\nu_{\max}=eV_1$

Hence

$$\frac{\lambda_{\min}}{\lambda}=\frac{V_1-V_2}{V_1}$$

Therefore

$$V_2=V_1\left(1-\frac{\lambda_{\min}}{\lambda}\right) \quad \ldots\ldots \quad (54)$$

In Kulenkampff's experiment $V_1=31$ KV., $\lambda_{\min}=0{\cdot}39$ Å.U., and $\lambda=0{\cdot}43$, $0{\cdot}53$ and $0{\cdot}73$ Å.U. The value of V_2 corresponding to any of the three values of λ can be calculated from (54), and substituting this value of V_2 in (53) we get the corresponding β. If in eqn. (52) we now use the above calculated value of β, we at once get $\cos\theta_{\max}$, and hence $\theta_{\max}$ the angle corresponding to the intensity maximum. The result of this computation is shown below.

Calculated $\theta_{\max}$	56·6°	53·1°	50·2°
Observed $\theta_{\max}$	55°	52°	48°

The agreement between the calculated and the observed values is quite satisfactory.

SECTION III

154. Optics of X-rays.—Throughout the whole of the first decade after the discovery of X-rays, a controversy centred around the question whether the newly discovered rays were corpuscular or undulatory in nature. We have already described how Barkla* showed in 1905 that the X-rays scattered from graphite were polarised, but it was not before 1912 that all controversies were finally set at rest by the discovery of Laue of the diffraction of X-rays through crystals. Since Laue's discovery, all the phenomena which come under physical optics have also been observed in the case of X-rays. These phenomena are: Scattering, Polarisation, Refraction, Total Reflexion, Dispersion and Anomalous Dispersion, Diffraction on passage through three-dimensional gratings (crystal diffraction), Diffraction by line gratings, Diffraction by straight edges and slits, and Interference phenomenon as in the case of Lloyd and Fresnel's mirrors.

Some of these phenomena have been already mentioned in the earlier sections. We shall take up them here in more detail, and also treat the other phenomena, *viz.*, diffraction by slits and interferences by mirrors in outline.

155. Space Distribution of Scattered Intensity.—The general theory of X-ray scattering has already been given in § 113. We shall now consider the nature of distribution of the scattered rays in space. Experiments by Hewlett, Debye and others have shown that the simple theory of scattering given by Thomson is inadequate in explaining all the results obtained. They proceeded on the assumption that deviations from Thomson's formula are mainly due to the interference of the rays scattered from different scattering centres. The effect can further be distinguished in three ways, *viz.*, (1) when the interference is between the rays coming from different molecules, (2) when it is between those from different electrons in the same atom, and (3) when it is between those from the atoms in the same molecule. These cases have already been dealt with for crystals.

Case (1) was investigated by Hewlett† and others. He observed the intensity of X-rays scattered by liquid mesitylene [$C_6H_3(CH_3)_3$] for different angles of scattering θ, and plotted a curve with the intensity as ordinates and θ as abscissæ. Hewlett's curve for $\lambda = 0{\cdot}7$ Å.U. (K_α of Mo) between $\theta = 0$ to $180°$ is shown (in broken line) in Fig. 63. According to Thomson's theory, the space distribution of intensity should follow the $(1+\cos^2\theta)$-law. The intensity calculated according to this law is shown by the full curve in Fig. 68. It will be noticed that between 180° and 40° the theory agrees well with the results of experiment. But between 0° and 40° there is a marked departure. The experimental curve shows an intensity peak at $\theta = 10°$ which is not predicted by the theory. Barkla and Ayers* had also observed that the amorphous substances showed an excess scattering in the forward direction, which increased markedly when shorter wavelengths were used. The intensity peak seems to have an important bearing on the structure of the liquids and amorphous substances†. In the case of liquids, the molecules have a tendency to form into a crystalline array, but the formation breaks up very soon. On account of this transitory nature of the array, the phase difference between the scattered rays coming from two neighbouring molecules remains constant, and they give rise to the intensity peak by reinforcement of the rays scattered from them. The extreme case of the molecular reinforcement of the scattered rays is met with in crystals where the molecules are arranged according to a regular pattern. We have already described how this had been utilised by Laue in his brilliant discovery of the crystal grating.

---

* Barkla, *loc. cit.*

† Hewlett, *Phys. Rev.*, **20**, 688, 1928.

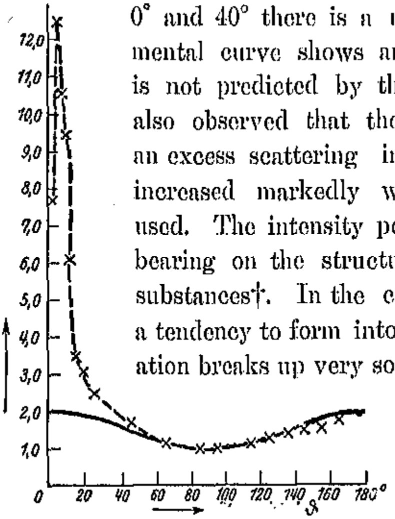

Fig. 68. Hewlett's scattering curve for mesitylene.

Let us now consider the effect of interference of the rays scattered by intra-atomic electrons. Striking results have been obtained on this subject in the recent investigation of scattering by gases and vapours. As in these cases the molecules are free to move in perfect chaos, there can be no phase relation between the rays scattered by different molecules, and interference can take place only between those from electrons in the same atom. Debye‡, Thomson and others corrected the original Thomson equation of scattering by taking into account this interference effect. The calculation is complicated and we shall not enter into details of it. Debye has shown that in the simple case of a system consisting of two electrons lying at a distance r from each other, the Thomson formula should be replaced by

---

* Barkla and Ayers, *Phil. Mag.*, **21**, 275, 1911. † See §136.

‡ Debye, *Ann. d. Phys.*, **46**, 809, 1915.

$$S = 2\,S_e\left(1+\frac{\sin x}{x}\right) \quad . \quad . \quad . \quad . \quad (55)$$

where

$$S_e = \frac{I\,e^4}{2\,r^2\,m^2\,c^4}\,(1+\cos^2\theta) \quad . \quad . \quad . \quad (56)$$

which represents the scattering due to a single electron, and

$$x = \frac{4\,\pi\,r}{\lambda}\sin\frac{\theta}{2}$$

This leads to an intensity distribution curve in which the intensity would rise and fall periodically. But this is not experimentally observed. It was suggested by Compton* that in the case of scattering by individual atoms, the modified scattering phenomenon (Compton effect) will play an important part. From this consideration he obtained the expression

$$S = ZS_e\left[\frac{f^2}{Z}+1-\frac{f^2}{Z^2}\right] \quad . \quad . \quad . \quad . \quad . \quad . \quad (57)$$

where

$$f = Z\int_0^\infty u(r)\,\frac{\sin kr}{kr}\,dr \quad \text{and} \quad k=\frac{2\pi}{\lambda}$$

The factor f^2/Z^2 is due to classical scattering, and $1-f^2/Z^2$ due to modified scattering. f is known as the *structure factor* of the atom, and it tells us in what way the Z moving electrons behave, if their probability of lying at a distance between r and $r+dr$ from the centre of the atom is $u(r)$. The term $u(r)$ evidently depends upon the nature of the electron distribution round the atomic core. This distribution has been worked out by Hartree and others from considerations based upon New Quantum Mechanics. Wollan†, Herzog‡ and Barret§ have applied these results to calculate the intensity distribution of scattered radiations by monatomic gases, with the aid of eqn. (57), and have obtained results in general agreement with experimental observations.

Finally we come to the case of interference occurring between the scattered rays coming from the atoms in the same molecule. In recent years Debye* and his co-workers have taken up this kind of investigation with polyatomic molecules†. Their arrangement is very simple. A box containing two windows covered by thin Al-foils is filled with the vapour to be investigated. CuKα radiations (λ 1·537Å.U.) are allowed to enter the box through one window, and the scattering is observed through another. A photographic film bent into the form of a circle receives the scattered rays. In the typical case of CCl_4-vapour, three intensity peaks were observed at $\theta=36°$, 65° and 110°.

---

* Compton, *Phys. Rev.*, **35**, 925, 1930.

† Wollan, *Phys. Rev.*, **37**, 862, 1931.

‡ Herzog, *Zs. f. Phys.*, **69**, 207, 1931; **70**, 583, 590, 1931.

§ Barret, *Phys. Rev.*, **32**, 22, 1928.

For an account of these works see *Review of Modern Physics.*, **4**, p. 205, article by E. O. Wollan.

According to Van't Hoff and Le Bel the four Cl-atoms in CCl_4 are arranged at the corners of a regular tetrahedron, while the C-atom is situated at the centre of gravity. Debye assumed the distance between any two Cl-atoms to be the same, say l, and calculated the intensity distribution of the rays scattered by such a system. He obtained the expression

$$S=\frac{1+\cos^2\theta}{2}\,4\,\psi^2\left[1+\frac{3\sin x}{x}\right] \quad . \quad . \quad . \quad . \qquad (58)$$

where

$$x=\frac{4\pi l}{\lambda}\sin\frac{\theta}{2} \quad . \quad . \quad . \quad . \quad . \quad . \quad . \quad . \quad . \qquad (59)$$

and ψ contains the Thomson equation as well as the structure factor of atoms consisting of 17 electrons. But neglecting the latter we can write

$$\psi=\frac{Ie^4}{2r^2m^2c^4}\,Z \quad . \quad . \quad . \quad . \quad . \quad . \quad . \quad . \qquad (60)$$

The expression (58) is thus found to be similar to (55) which was obtained by Debye for the case of scattering by two electrons separated by a fixed distance r. In Fig. 64 the theoretical distribution according to (58) is shown graphically in which the scattered

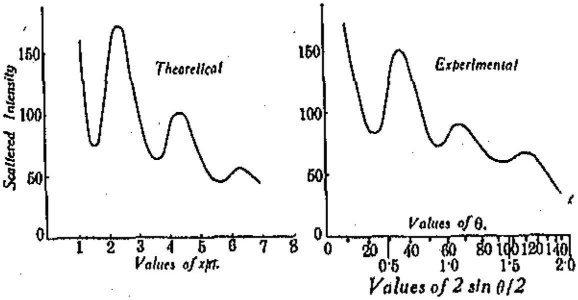

Fig. 64. Debye's scattering curve for CCl_4.

---

* Debye, *Proc. Phys. Soc.*, 42, 340, 1930; *Phys. Zeits.*, 21, 419, 1930.

† See also report by F. Kirchner, *Ergebnisse der Exakten Naturwisenscheften*, 11, 64, 1932.

intensity is plotted along the ordinates and the x/π-values as the abscissæ. The curve shows intensity maxima at $x=5\pi/2$, $9\pi/2$ and $13\pi/2$ approximately. The experimental curve has also been shown in the same figure for comparison.

Taking the first maximum at $x=5\pi/2$, we have from eqn. (60)

$$\sin\frac{\theta}{2}=\frac{5}{8}\,\frac{\lambda}{l}\quad\ldots\ldots\ldots\ldots\quad(61)$$

As has been mentioned, the first intensity peak was obtained experimentally at $\theta=36°$. Substituting this value of θ in eqn. (61), we get $l=3{\cdot}1$ Å.U. Similar calculations for the second and the third maxima give $l=3{\cdot}01$ Å. U. and $2{\cdot}96$ Å. U. (approx.). The three values of l do not differ much from each other, which shows that the intensity law given by eqn. (58) is fairly correct. This result supports also in a general way the regular tetrahedral structure of CCl_4-vapour assumed in the theory.

The scattering due to the C-atom has been neglected in the above deductions, as this is much smaller compared to that of Cl-atoms. All other Cl derivatives of methane have also been studied, and the results found to agree with the theory. Debye showed in this way that in the case of optically active isomers of dichloromethane ($C_2H_2Cl_2$), the distances between two Cl-atoms were different for its different isomers. Thus for the cis.-position he found $l=3{\cdot}6$ Å. U. and for the trans.-position $l=4{\cdot}1$ Å. U. as shown below

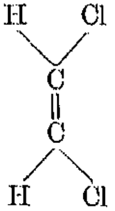

cis., $l=3{\cdot}6$ Å. U.

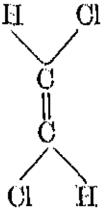

trans., $l=4{\cdot}1$ Å. U.

by the chemical formulæ for the two isomers.

156. Polarisation of General X-rays.—Although in Thomson's theory (§ 113) of X-ray scattering it has been assumed that the primary beam is unpolarised, actually a partial polarisation of the primary beam of general X-rays is observed. This was first demonstrated by Barkla* from the following experiment (Fig. 65).

---

* Barkla, *Phil. Trans. Roy. Soc. A.*, **204**, 467, 1905.

X-rays from the anticathode of an X-ray tube pass through a lead slit and fall on a scatterer. The beam scattered at $\pi/2$ is observed in two mutually perpendicular directions (in the plane perpendicular to the direction of the primary beam) by means of two ionisation chambers shown in the figure. Barkla found that the intensity of the scattered beam was *maximum* along the direction perpendicular to the line of motion of the cathode rays, and the intensity was *minimum* along the direction parallel to that of the motion of the cathode rays (but though never equal to zero). The corresponding position of ionisation chamber have been marked in the figure as maximum and minimum respectively.

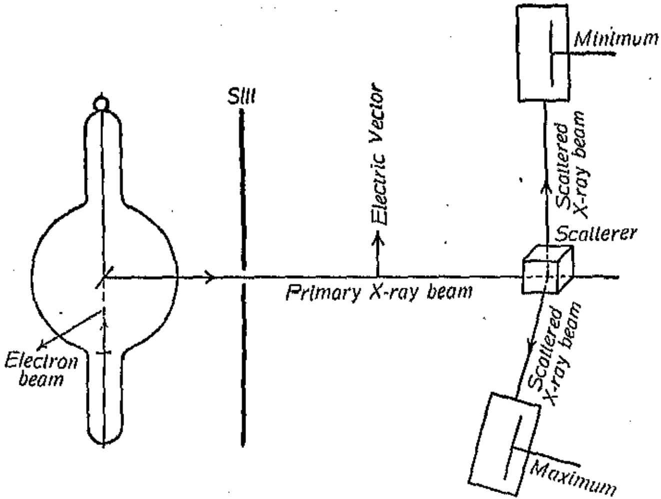

Fig. 65. Barkla's apparatus.

Barkla interpreted his results as follows. The line joining the cathode and the anticathode shows the direction of motion of the cathode rays. Since the rays are stopped in this direction, the resulting electromagnetic radiation will have its electric vector along this direction (shown by the vertical arrow, in the figure), and will, therefore, be *polarised*. When it falls on the scatterer, the electrons in it are accelerated only along this direction. According to Hertz's theorem, there is no radiation along the direction of motion of an accelerated electron, but radiation is maximum in a perpendicular direction.

These remarks do not however strictly apply to the whole of the radiation generated, but a part of it being *unpolarised*, its electric vector lies at random in a plane perpendicular to the direction of propagation of the primary beam. The intensity of the scattered radiation due to these unpolarised rays will never show fluctuation for any definite angle of scattering.

If I_1 and I_2 be the intensities in the two directions (maximum and minimum), the percentage polarisation may be defined as

$$P = \frac{I_1 - I_2}{I_1 + I_2} \cdot 100$$

If $I_2 = 0$, the rays are completely polarised. The experiment was repeated by Bassler* who found that the polarisation of the general radiation decreases with the voltage across the tube.

157. Quantitative Estimation of X-ray Polarisation.—Barkla's experiments on polarisation described in §156 relate to total X-radiation emitted by an anticathode. Many experiments have since been performed to find out how the percentage of polarisation varies in the different wavelengths of the continuous spectrum. The apparatus used by P. A. Ross† in such experiments is described below (Fig. 66).

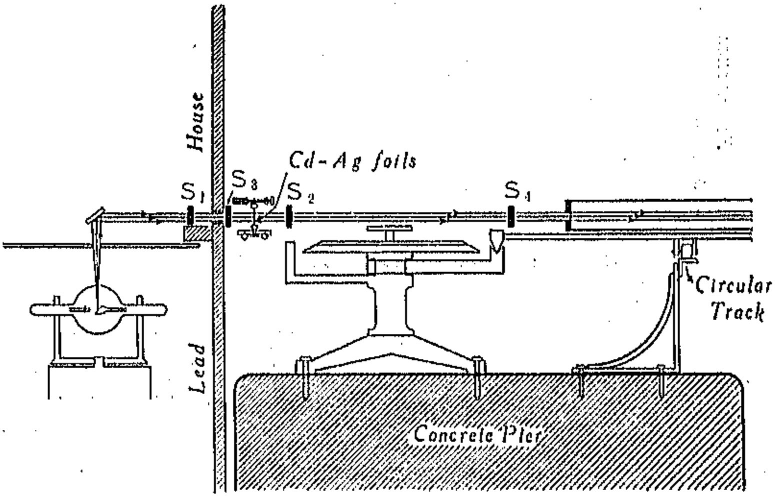

Fig. 66. Ross' apparatus for studying polarisation of X-rays.

X-rays coming from the tungsten target of a tube fall on the scatterer which was in this case a block of graphite. The scattered rays are observed in a direction at right angles to the direction of the primary beam of X-rays. Two foils of Ag and Cd are allowed to come alternately in the path of the scattered rays by means of an electromagnetic shutter. After passing through the foils the scattered rays limited by slits S_2, S_4 enter the ionisation chamber, and their intensities are measured. Foils of Ag and Cd are chosen because these occupy successive positions in the periodic table. (See Chap. XI).

---

* E. Bassler, *Ann. d. Phys.*, **28**, 860, 1909.

† Ross, *Jour. Opt. Soc. Am.*, **16**, 375, 433, 1928.

All other frequencies are absorbed by the foils, only the frequency region lying between K-limits of Ag and Cd are transmitted. At first the tube is so oriented that the cathode rays are perpendicular to the plane of the paper, so that the electric vector of X-rays is perpendicular to the plane of the paper. Then the X-ray tube is rotated through a right angle and placed in the position shown in the figure, so that the observation may be taken in a direction parallel to the electric vector.

By using different pairs of filters, different frequency bands can be examined for their state of polarisation. The curve in Fig. 67 shows the result of the experiment. The state of polarisation of the wavelength band in the continuous spectrum between the K-absorptions of Cd and Ag (λ·4632 and ·4850 Å.U.) has been plotted against the applied potential.

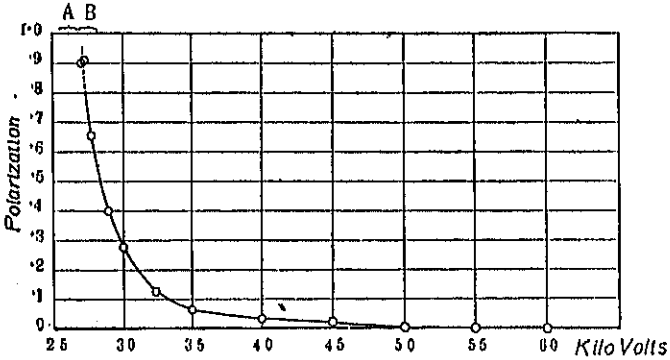

Fig. 67. Percentage polarisation for different wavelengths.

At the short wave limit (Duane-Hunt limit), the polarisation is complete. As the voltage increases, polarisation for this wavelength diminishes. It has been found that the characteristic radiations produced by cathode ray bombardment are very feebly polarised irrespective of the voltage applied to excite them. The fluorescent rays are not at all polarised (Compton*).

158. The Refraction of X-rays.—The failure to detect refraction of X-rays in the early days was a matter of some perplexity to the early investigators. Röntgen himself tried to observe the refraction of X-rays, but failed. As we now know, the failure was due to lack of proper knowledge regarding the value of the refractive index in the region of X-rays. Guidance can be obtained on this point by extending the usual Sellmeier dispersion formula for the X-ray region. According to this formula

$$\mu^2 = 1 + \frac{e^2}{\pi m} \sum \frac{n_s}{(\nu_s^2 - \nu^2)} \quad . \quad . \quad . \quad . \quad . \quad (62)$$

---

* Compton, *Phil. Mag.*, 8, 961, 1929.

where ν_s is a natural frequency of the medium, n_s is the number of electrons per unit volume of the substance possessing this frequency, e and m are charge and mass of the electron. For deduction of this formula, see any text-book on Optics, or Compton's *X-rays*, p. 208.

Now when we are considering X-rays, the characteristic frequency ν_s which is in the optical region, is very small compared to ν, the frequency of X-radiation, and can be neglected. We have therefore

$$\mu = 1 - \frac{e^2}{2\pi m} \frac{\Sigma n_s}{\nu^2} = 1 - \frac{e^2 N}{2\pi m \nu^2} \quad . \quad . \quad . \quad (63)$$

where N is the total number of absorption electrons per unit volume. These conditions hold good for substances like glass, rock-salt, etc. for which the natural frequencies are much smaller than X-ray frequencies.

There are two points to be noticed about (63). First μ is <1, *i.e.*, the X-ray waves travel with velocity $>c$ within the medium. But a velocity $>c$ is an impossibility. A little reflection however shows that really no mistake is being made. For the relativity proposition that all velocities should be $<c$ applies to group velocity U. This is the velocity with which energy is propagated. This is different from the wave-velocity v which in this case is $>c$. We have, in fact, according to a well-known theorem due to Lord Rayleigh I

$$U = v + \nu \cdot \frac{\partial v}{\partial \nu} = c\left(1 - \frac{\alpha}{\nu^2}\right) \quad . \quad . \quad . \quad . \quad (64)$$

which is less than c.

The second point is the magnitude of α/ν^2. It can be shown that it is a small quantity of the order of 10^{-6}. Let us take glass; and find its refractive index for $\lambda = 1{\cdot}279$ Å. U. Taking $N = 10^{23}$, we obtain from (63) $\alpha/\nu^2 = 5{\cdot}2 \times 10^{-6}$.

These preliminary ideas show why the early experiments were unsuccessful. Since $\mu < 1$, we have to set the prism in the position of *maximum deviation* if we want to demonstrate refraction. But under the influence of optical analogy, the early experimenters always tried the minimum deviation position.

Refraction is now studied by any of the following methods:—

(*a*) Deviation from Bragg's Law; (*b*) By the prism*, (*c*) From total reflection. Of these (*a*) is historically older.

---

* Siegbahn, Larsson and Waller, *Naturwiss*, **52**, 1212, 1924.

(*a*) *Deviation from Braggs' Law.*

It was independently pointed out by Darwin* and Ewald† that Braggs' Law of reflexion was only approximately correct, for when X-rays pass into matter, and penetrate one or two atomic layers of the crystals, they come under the influence of the internal electric field of the electrons composing the crystal; or as we should say now the wavelength inside the crystal changes from λ to $\mu\lambda$. For these internal rays, the Bragg angle $\theta = \sin^{-1}(n\lambda/2d)$ therefore changes, but as the effect is extremely small, it could not be detected for a very long time. In 1920, Stenström‡ photographed the first five order spectrum of Ca K_β (3·083 Å. U.) with a crystal of gypsum and plotted a curve of $\log(\sin\phi_n/n)$ against n, where n and ϕ_n are the orders of reflection, and the corresponding angle of reflexion. Had Braggs' law continued to hold, $\log(\sin\phi_n/n)$ would have been independent of n, and the graph would be a straight line parallel to the abscissa-axis which represents n. But Stenström found that the graph was hyperbolic as shown in Fig. 68, for the reflexion of K_β of potassium with gypsum. It can be shown that the curve can be represented by a formula of type

$$\ln\frac{\sin\phi_n}{n} = A + \frac{B}{n^2}, \qquad . \quad . \quad . \quad . \quad (65)$$

it is further evident that Braggs' law is only true for high order reflexions, and the greatest deviation from it comes in the first order reflexion. In other words, the wavelength found by Braggs' law from first order reflections will be slightly greater.

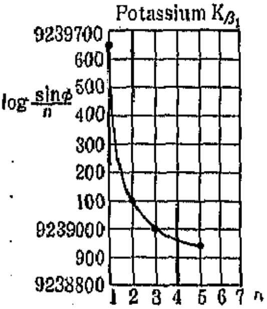

Fig. 68.

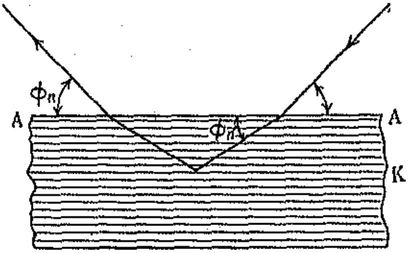

Fig. 69. Refraction of X-rays at a crystal plane.

The calculation of the refractive index from these curves can be carried out as follows (Stenström) with the help of Fig. 69 which illustrates the refraction of X-rays by crystal planes.

---

* Darwin, *Phil. Mag.*, 27, 315, 1914.
† Ewald, *Phys. Zeits.*, 21, 617, 1920.
‡ Stenström, *Dissertation*, Lund, 1919.

In Fig. 69, K represents the crystal, and AA the section of a cleavage plane. Let λ and ϕ_n be the wavelength and glancing angle of X-rays in air, and λ' and ϕ'_n the corresponding quantities inside the crystal. We have now the following equations:

$$n\lambda' = 2d \sin \phi'_n \quad \ldots \ldots \ldots \ldots \quad (66)$$

and

$$\mu = \cos \phi_n \,/\, \cos \phi'_n = \lambda/\lambda' \quad \ldots \ldots \quad (67)$$

Out of these equations, we have to eliminate the dashed quantities, and find a relation between λ and $\sin \phi_n$. We have

$$n\lambda' = \frac{n\lambda}{\mu} = 2d \sin \phi'_n$$

$$= 2d\,(1-\cos^2 \phi'_n)^{\frac{1}{2}}$$

$$= 2d\left[\,1 - \frac{1-\sin^2\phi_n}{\mu^2}\,\right]^{\frac{1}{2}} \quad \ldots \ldots \quad (68)$$

from which after a little work, and remembering that μ is nearly unity, we obtain:

$$n\lambda = 2d \sin \phi_n \left[\,1 - \frac{1-\mu}{\sin^2 \phi_n}\,\right] \quad \ldots \ldots \quad (69)$$

The equation can be further simplified by putting $\sin^2 \phi_n$ within the brackets equal to $n^2\lambda^2/4d^2$, and $1-\mu=\delta$. We then obtain:

$$n\lambda = 2d \sin \phi_n \left[1 - \frac{4d^2}{n^2}\,\frac{\delta}{\lambda^2}\right] \quad \ldots \ldots \quad (70)$$

It is easy to verify that

$$ln\,\frac{\sin \phi_n}{n} = ln\,\frac{\lambda}{2d} + \frac{2d^2}{n^2}\,\frac{\delta}{\lambda^2}$$

$$= A + \frac{B}{n^2} \quad \ldots \ldots \ldots \ldots \quad (71)$$

where

$$A = ln\,\frac{\lambda}{2d}, \quad B = \frac{2d^2}{\lambda^2}\,\delta \quad \ldots \ldots \quad (71')$$

This explains the curve given in Fig. 68.

It is obvious from the last equation (71) why Bragg's equation is correct for larger values of n. In order to find δ for any particular wavelength λ for a crystal, we find the glancing angles φ_1 and φ_2 for the n_1 and n_2 orders of reflexion. Then from the above equations, we have

$$n_1\lambda = 2d\left[\,1 - \frac{\delta}{\sin^2\varphi_1}\,\right] \sin \varphi_1$$

$$n_2\lambda = 2d\left[\,1 - \frac{\delta}{\sin^2\varphi_2}\,\right] \sin \varphi_2$$

By eliminating λ, we obtain

$$\delta = 1 - \mu = \frac{\dfrac{\sin\varphi_1}{n_1} - \dfrac{\sin\varphi_2}{n_2}}{\dfrac{1}{n_1 \sin\varphi_1} - \dfrac{1}{n_2 \sin\varphi_2}} \quad \ldots \ldots \quad (72)$$

In the table below are given the refractive indices of the mica crystal for Cu Kα radiation.

Table 5.

λ	Order n	Glancing angle	$\delta\times10^{+6}$
Cu $K\alpha_1$ 1537 X.U.	1	4° 26′ 27″·2	8·74
	2	8° 53′ 56″·1	9·44
	3	13° 24′ 53″·7	8·62
	5	22° 44′ 29″·2	8·97
	7	32° 46′ 0″	9·19
	9	44° 5′ 35″	8·94
		Mean	$\delta=8{\cdot}94\times10^{-6}$

The deviation detected in Bragg's law amounts to 1 in 10,000, and it was very creditable to the experimenters that they could at all detect such a small quantity. In the actual experiments, great precaution was taken to eliminate errors due to the temperature effect on the grating space of crystals.

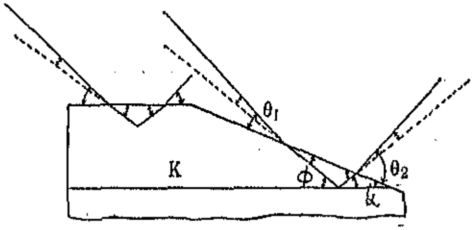

Fig. 70. Refraction at a cut crystal surface.

A modification of the above method was suggested by B. Davis*, which gave more correct values of refractive index. It is briefly described below.

In Fig. 70, K is a crystal of calcite a part of whose surface has been cut at a small angle with the natural surface. A beam of X-rays is allowed to fall on this face at a small angle θ_1. The ray gets refracted as it enters, and is then reflected from the atomic planes if the glancing angle φ satisfies the Bragg-equation. If θ_1 and θ_2 are the angles between the incident and refracted rays at the cut surface of the crystal, we have

$$1-\delta=\frac{\cos\theta_1}{\cos(\phi-\alpha)}=\frac{\cos\theta_2}{\cos(\varphi+\alpha)} \quad \ldots\ldots \quad (73)$$

where α is the inclination of the cut surface of the crystal to the natural face.

From the above equations φ can be eliminated, and δ can be calculated. The errors of measurements are minimised, for the difference between θ_1 and φ can be artificially made large.

---

* B. Davis and H. M. Terril, *Proc. Nat. Acad. Sc.*, 8, 357, 1922.

It may amount to 3″. In the first method, the difference between φ and φ' was small, and so greater accuracy was not possible.

(*b*) *The Prism Method*

The principle of the prism method is illustrated in Fig. 71 *a*, *b*.

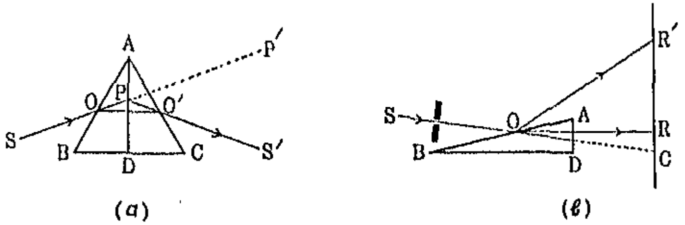

(*a*) (*b*)

Fig. 71. Refraction by prism.

(*a*) represents the method of finding out the refractive index by means of a prism. SO is the incident beam, O′S′ is the refracted beam. We have $\mu = \sin\frac{1}{2}(A+\delta)/\sin\frac{1}{2}A$ where $\delta = S'PP'$. Instead of using the full-prism, we can use the half-prism ABD, so that the beam SO, on entering the prism, takes the path OO′, and emerges normal to the face AD. We have then $\mu = \sin i/\sin r = \sin(\frac{1}{2}A+\varepsilon)/\sin\frac{1}{2}A$ where $A/2$ = angle of the prism, ε = deviation $= \delta/2$.

This principle is utilized for measuring the refractive index of X-rays by the prism and is illustrated in (*b*).

Here ABD is the prism, A is the refracting angle, and the face AD is perpendicular to the emergent beam. R′RC is a photographic plate which receives the rays. SO is the X-ray beam which gets totally reflected at O and the reflected beam falls on the screen* at R′. SOC is the direct beam, and OR is the *refracted* beam. Note that the angle of refraction is now larger than the angle of incidence. We have

$$\mu = \frac{\cos(\text{glancing angle SOB})}{\cos(\text{AOR})}$$

$$= \frac{\cos\alpha}{\cos(\alpha-\beta)} \quad \ldots\ldots\ldots\ldots\ldots \quad (74)$$

where $\beta = ROC = RC/OR = b/r$ and $2\alpha = R'OC = R'C/OR = a/r$. The angles α and β are very small, as the photographic plate is kept at a large distance of about a meter from the prism. Expanding (74) we obtain

---

* The figure is rather exaggerated. In actual practice the distance OR is much greater than the size of the prism.

$$1-\mu=\delta=\beta\left(\alpha-\frac{\beta}{2}\right). \qquad (74')$$

$$=\frac{b\,(a-b)}{2r^2} \qquad (75)$$

159. Total Reflexion of X-rays.—Stenström's work on deviation from Bragg's law gave the scientific world an idea of the order of value of refractive index for X-rays of crystals commonly used for X-ray spectroscopy. The value of μ was found to be slightly less than unity. From this fact Compton* put forward the view in 1922 that the phenomena of total reflexion can be observed in the case of X-rays if the glancing angle is made very small. In collaboration with his students he was able to demonstrate the effect experimentally within a short time. Their arrangement is illustrated in the Fig. 48*b* on page 276. Instead of a grating G shown in this figure, they substituted a plane glass mirror. When the glancing angle was small, the beam of X-rays was totally reflected and recorded on the photographic plate P.

As the refractive index of matter for X-rays is less than unity, there will be a maximum glancing† angle beyond which no refraction will take place. According to the laws of physical optics we have

$$\cos\psi=\mu$$

where ψ is the critical angle of glancing for total reflection, and μ is the refractive index. For total reflexion, the glancing angle must always be less than the critical angle ψ. This phenomenon has been utilised to determine the absolute value of wavelength by means of ruled gratings (see § 143).

The above equation reduces to

$$\sin\psi=\sqrt{1-\mu^2}=\sqrt{2\delta}.$$

The intensity of reflected X-rays do not obey rigorously Fresnel's law of intensity of reflexion. Recently Thibaud‡ modified Fresnel's law taking into consideration the high frequency of X-rays. The results are in good agreement with his theory. Some values of refractive indices found out by this method are given below.

---

* Compton, *Phil. Mag.*, **45**, 1121, 1923.

† The maximum is however not very sharp.

‡ Thibaud, *Jour. de Physique*, **1**, 37, 1930.

Table 6.*

	λ Å. E.	ψ_0	$\delta \times 10^6$
Glass ...	1·279	10′	4·2
Silver ...	1·279	22′·5	21·5

159a. Dispersion of X-rays.—According to formula (63), we have

$$\delta = 1 - \mu = \frac{e^2}{2\pi m} \frac{N}{\nu^2} \quad . \quad . \quad . \quad . \quad . \quad . \quad . \quad . \quad (63')$$

or

$$\delta/\lambda^2 = Ne^2/2\pi mc^2 \quad . \quad . \quad . \quad . \quad . \quad . \quad . \quad . \quad (76)$$

If the theory be correct, δ/λ^2 should be a constant. This deduction was tested by Larsson† whose results are reproduced in Fig. 73.

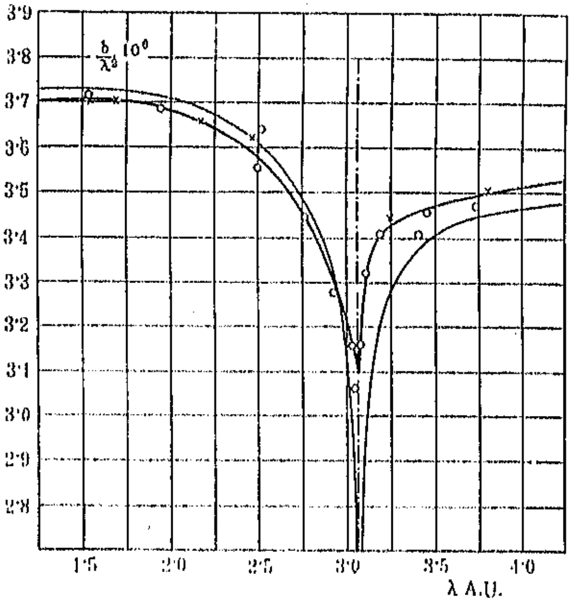

Fig. 73. Anomalous dispersion of X-rays (Larsson).

The curve represents the dispersion of calcite from $\lambda = 1{\cdot}25$ Å.U. to $\lambda = 4{\cdot}25$ Å.U. The value of μ was determined from deviations from Bragg's Law. The ordinate represents δ/λ^2, and the abscissa λ. We find that the curve is straight between 1·25 Å.U. to 2 Å.U.

---

* For more details see Nähring, *Phys. Zeits.*, **31**, 799, 1930.

† Larsson, *Dissertation*, Uppsala Univ., 1929.

For this region at least, the theory holds good, and it enables us to determine N and compare it with its value obtained by direct methods. We have $N=(A\rho Z)/M$ where A=Avogadro number, ρ=density, Z=total number of electrons in the molecule and M=molecular weight.

Substituting the values for $CaCO_3$ ($Z=50$, $\rho=2{\cdot}71$, $M=100$), we find that $N={\cdot}81\times10^{24}$. Also putting $e=4{\cdot}77\times10^{-10}$ e.s.u., $m=9{\cdot}02\times10^{-28}$ gm. and $c=3\times10^{10}$ cm/sec. in eqn. (76), we obtain $\delta/\lambda^2=3{\cdot}83\times10^{-6}$ (Å. U.)$^{-2}$. Hence $\delta=1{\cdot}91\times10^{-6}$ for $\lambda={\cdot}707$ Å. U. (Kα of Mo).

It has been found experimentally that δ/λ^2 for calcite is $3{\cdot}68\times10^{-6}$ for Mo Kα. The agreement is quite satisfactory. Hence the Lorentz theory holds good at least for this region of wavelength.

In the same way as we have found the total number of electrons per unit volume, we can also find the number of K-electrons per unit volume. Using the Drude-Lorentz equation we have

$$\delta=\frac{e^2}{2\pi m}\sum_{1}^{N}\frac{n_s}{\nu^2-\nu_s^2}\,.$$

$$=\frac{e^2}{2\pi m}\left[\frac{N_k}{\nu^2-\nu_k^2}+\frac{N-N_k}{\nu^2}\right]$$

where N_k = number of K-electrons per unit volume and ν_k = the K-absorption frequency. If $\nu^2-\nu_k^2$ be small, the first part of the expression becomes larger than the second part. In this way N_k can be determined. Nardroff* showed from this experiment that there are two electrons in the K-shell.

Anomalous Dispersion.

A glance at the curve in (Fig. 73) shows that the (δ/λ^2), λ curve is straight only up to 2Å.U. After this the value of δ/λ^2 rapidly diminishes and reaches a minimum value at 3·083 Å.U. Beyond this point it rises again.

This feature is exactly analogous to anomalous dispersion in optical region. As is well-known, anomalous dispersion occurs in the neighbourhood of an absorption line of the substance. In the X-ray region, there are no absorption lines, but only absorption edges, *i.e.*, at one point the absorption suddenly increases owing to the photoelectric ejection of an electron from some shell. For calcium the absorption edge has been found to start from 3·083 Å.U., and near about this point we get anomalous dispersion. Evidently μ has the maximum value at this point.

---

* Nardroff, *Phys. Rev.*, **24**, 149, 1923.

Kallman and Mark* worked out a formula for dispersion in the neighbourhood of an absorption edge on the analogy of the corresponding phenomenon in the optical region. They obtained the formula

$$\frac{\delta}{\lambda^2} = \frac{e^2 N}{2\pi c^2 m} - \frac{e^2 N_k}{2\pi c^2 m}\left(\frac{\lambda}{\lambda_k}\right)^2 \log\left[1-\left(\frac{\lambda_k}{\lambda}\right)^2\right] \quad . \quad . \quad (77)$$

where N_k is the number of K-electrons per unit volume. This equation holds only in the neighbourhood of the absorption edge, as the damping factor was neglected in its deduction. At the absorption edge itself, it ceases to hold. Prins† took into account the damping factor and gave a formula for the absorption edge itself.

160. Diffraction of X-rays by Slits.—As pointed out already, though the diffraction of X-rays by slits was long sought for, but the conclusions were never free from doubt. Sommerfeld had microphotographed plates taken by Koch‡ in 1909, and the tentative values of the wavelength of X-rays found by him from these data were, as we now know, fairly correct. In recent times, this technique has been much further developed as can be seen from the photograph (Fig. 74, Plate V). This is reproduced from a paper by Kellström§. The wavelength used for this photograph is large, [Al Kα (8Å.U.)] The slits were ·006mm. in width, which were first roughly measured by means of a comparator. The actual arrangement is simple, and is similar to those usually given in text-books on physical optics for observing diffraction of optical rays. The distance between the plate and the slit in Kellström's experiment was 41 cm. The plate shown is a copy of the original magnified 30 times. An exposure of 2 to 3 hours with 15 m. A. current and 8 to 10 KV. in the X-ray tube is sufficient. The whole apparatus was enclosed in a vacuum chamber.

---

* Kallman and Mark, *Ann. d. Phys.*, **82**, 385, 1927.
† Prins, *Zs. f. Phys.*, **47**, 479, 1928.
‡ Koch, *Ann. d. Phys.*, **38**, 507, 1912.
§ Kellström, *Uppsala Dissertation,* 1932.

For the position of the minimum, the usual Fraunhofer diffraction formula for a slit was used. We have

$$n\lambda = s.\frac{d_n}{b} \quad . \; . \; . \; . \; . \; . \; . \; . \; . \; . \; . \quad (78)$$

where $n=1$, 2, 3, etc., s=the slit width d_n = the distance of nth minimum from the centre and b=the distance from the slit to the plate.

The table below gives some results obtained from Kellström's experiment.

Table 7.—Diffraction by slits with Al Kα (8 Å. U.)

	Order n	d_n in mm.	s in mm.
Minima	1	·0525	·006601
	2	·1044	·006639
	.3	·1564	·006596
		Mean	·00659

By assuming the value of the wavelength of Al Kα (8·3 Å. U.) the value of s (the slit width) is found rigorously from equation (78). It is about 10% larger than the value found by measurement with a comparator. The same slit was used in the experiment with CKα and the value of its wavelength was found out to be correct within ·5% of the known spectroscopic value.

161. Interference of X-rays (Lloyd's mirror method).—The arrangement known as Lloyd's mirror in optics is a very direct method for observing the interference of light from a direct source and a virtual source. The virtual source is produced by means of reflection from one single mirror. Recently Kellström has extended this method to the case of X-rays. A beam of X-rays is allowed to pass through a very narrow slit (width ·0015 mm.) and then fall on a glass plate at a grazing angle of incidence. A photographic plate kept at a distance of about 50 mm. records the interference pattern due to the direct beam from the slit and the reflected beam. The usual formula gives

$$n\lambda = \frac{c}{a+b}\, d_n$$

where c=the distance between real and the virtual sources, a= the horizontal distance of the slit and the glass plate and b=the distance between glass plate and the photographic plate.

In an experiment of this kind Kellström used Kα radiations of Aluminium, and from the value of its wavelength the distance between the real and the virtual sources was found. It agreed with the value, measured experimentally. If now any other radiation is used with the same arrangement, then its wavelength can be computed from the value of c. The value of λ for CKα line was found to agree with known values within ·5%. It must be realised that this method as well as the previous one are only comparison methods*.

Books Recommended.

1. A. H. Compton, *X-rays and Electrons* (1927).
2. M. Siegbahn, *Spektroskopie der Röntgenstrahlen* (1931).
3. F. Kirchner, *Handbuch der Experimentalphysik*, 24 (2), *Allgemeine Physik der Röntgenstrahlen* (1930).
4. A. E. H. Tutton, *Crystallography and Practical Crystal Measurements* (1922).
5. H. Hilton, *Mathematical Crystallography* (1903).
6. R. W. G. Wyckoff, *The Structure of Crystals* (1931).
7. W. L. and W. H., Bragg, *X-rays and Crystal Structure* (1924). (New edition entitled *The Crystalline State* published in 3 vols., 1933).
8. H. Ott, *Handbuch der Experimentalphysik*, 7 (2), *Strukturbestimmung mit Röntgeninterferenzen* (1928).
9. Hevesy, *Chemical Analysis by X-rays* (1932).
10. Glocker, *Materialprüfung mit Röntgenstrahlen* (1929).

---

* For the above methods see Kellström, *Dissertation*, 1932.

*Table 1.—Mass-absorption coefficient** (μ/ρ) *of Elements.*

λ X. U. / Element		100	200	300	400	500	600	700	800	9003	1000	1100	1320	1400	1760	2250	3026	4146	6973	8320	11880
1	H		·40	·42	·45	·45	·44	·51	·57	·6											
3	Li			·172	·208	·245	·306	·403													
6	C	·146	·170	·197	240	·310	·412	·540	·72	1·00	1·30	2·1	3·5	4·0	7·8	15					
7	N		·177	·224																	
8	O		·183	·240	·338	·498	·746	1·10	1·55	2·12	2·87										
12	Mg		·232	·430	·875	1·56						16		35	63	126					
13	Al	·164	·269	·531	1·05	1·91	3·18	5·00	7·50	10·3	1·38	20·0	31·5	38	74	140	320	771	2800	344	767
16	S	·190	·42	·93	1·78		5·9	9·5													
26	Fe	·265	1·07	3·18	7·17	14·3	23·3	36·3	51·7	69·6	95	126	220	270	60	104					
27	Co		1·17	3·52																	
28	Ni	·328	1·40	4·10		18	30	45		82	118	159	253	288	69	135					
29	Cu	·323	1·53	4·47	10·1	18·8	31·6	49·2		97	133	181	265	40	75	143	321	621	2·120	3450	7550
30	Zn	·38	1·77	5·10	11·6	22·2	37·2	57		107	152	188	40	48	91	170					
42	Mo		4·02	12·7	26 7	48 6	80·7	18·8	27·2	37 5	51										
47	Ag	1·13	5·75	18	38·4	11	18·7	25·6		57	75	92	155	176	320	590	1330	461	1260	1770	
50	Sn	1·16	6·30			13·1	21·6	31		65	87	115	198	223	400	725					
74	W	3·4	3·20	8·60	19·8	38	65						113	141							
78	Pt	3·69	4·16	11·5	24·5	45·5	75·5	112		158	165	92	145	161	282	520	939	1290	1190	1530	
79	Au	3·64	4·28			51	77	116		154	110	98	148	173	300	500					
82	Pb	3·78	4 62	13·9	32·7	59·3	91	133		140	77	100	166	185	340						
83	Bi	3 78	5·10	14·8																	
90	Th	3·88	5·47																		

---

* These values are taken from Compton's *X-rays*, p. 184, table VI-5. The values for long wavelengths λ 3026 to 11880 X. U. are due to Jönsson (*Dissert.*, Uppsala University, 1928).

CHAPTER VII

BOHR'S THEORY OF THE SPECTRUM OF HYDROGEN

162. Experimental Study of Spectra of Elements.—During the whole of the last century, the belief was almost universal that the atom was a non-divisible particle of mass with certain combining powers. In the foregoing chapters, we have seen how this belief has been completely shattered owing to the discovery of the proton and the electron, and recognition of the fact that all elements are made up of these two, which may be regarded as the two primordial elements. We have now to explain the chemical and physical properties of elements in terms of their electrical structure. Kirchhoff's discovery has shown that the most characteristic property of the atom is its spectrum. As was already remarked we can compare the atom to a musical instrument, each spectral line then becomes a characteristic note of this instrument. But even the most casual acquaintance with spectral data shows that the analogy must not be stressed too far. Even hydrogen, the simplest of elements does not give a single line, but apparently an infinite number. An element like iron gives in the visible range not less than 6000 lines of different wavelengths. This fact led Rowland to remark that the atom is more complicated than even the grand piano.

The very vastness of spectroscopic data (witness—the eight thick volumes of Kayser and Runge's and Kayser and Konen's Handbuch der Spektroskopie—even these are not sufficient to report all the results), combined with their complexity repelled even the greatest physicists of the last century against making any serious attempt in understanding them.

In 1912, Niels Bohr of Copenhagen succeeded in obtaining the first clues to a successful explanation of the spectra of elements by he combined application of the nuclear theory of the atom, and the quantum theory of light. Before describing Bohr's theory, we shall give a brief account of the work of systematisation which preceded this work.

163. Work of Systematisation—Balmer's Discovery.—The work of systematisation was started by Balmer*, a teacher in a gymnasium at Basle, Switzerland, 1885. Hydrogen†, when excited in the discharge tube, gives a multitude of lines of which four stand out prominently from amongst the rest. These four lines are known as

$H\alpha$ . . .	λ 6562·79 Å. U. . .	Red
$H\beta$ . . .	λ 4861·327	Green
$H\gamma$ . . .	λ 4340·47	Blue
$H\delta$ . . .	λ 4101·74	Violet

Balmer showed that the wavelengths of these four lines can be represented by the simple mathematical formula :—

$$\lambda = 3645{\cdot}98 \quad \frac{m^2}{m^2-4} \quad . \; . \; . \; . \; . \; . \; . \; . \qquad (1)$$

m is an integral number > 2, $m=3, 4, 5, 6$ for $H\alpha$, $H\beta$, $H\gamma$, $H\delta$, respectively. About this time, Hartley showed that it is more convenient to use reciprocals of wavelengths or wave-numbers, instead of wavelengths‡.

If now Balmer's law is expressed in wave-numbers, it appears that the hydrogen lines can be represented by the formula

$$\nu = R\left(\frac{1}{2^2} - \frac{1}{m^2}\right) \quad . \; . \; . \; . \; . \; . \; . \; . \qquad (1')$$

where $R = 109690 \text{ cm}^{-1}$

If the law be correct, there is no reason why the series should stop at $m=6$. In fact observation shows that there is a line corresponding to every integral value of m. The astronomer Huggins discovered about 9 lines in the spectrum of the star Sirius, and 35 lines represented by the above formula have been discovered in the spectrum of the solar chromosphere. With improved technique, about 21 lines have been photographed in a Geissler tube discharge by

---

* Balmer, *Wied.-Ann.*, 25, 80, 1885.

† Apart from the Balmer lines, a large number of fainter lines appear when the discharge tube is run on low voltage. They are said to form the secondary spectrum of hydrogen. The secondary spectrum has now been shown to be due to the H_2-molecule, while the primary (Balmer) spectrum is due to the H-atom.

‡ This point will be discussed in greater length when the spectra of alkalies is taken up. It is important to remember

Frequency . . . . . . $\nu = c/\lambda_{\text{vac}}$ (sec^{-1})
Wave-number . . . . . . $\nu = 1/\lambda_{\text{vac}}$ (cm^{-1})

R. W. Wood.* A spectrum of Hydrogen lines has been reproduced in Fig. 1, Plate V.

The lines shown in this photograph are of the Balmer series, as obtained in the spectra of Sirius (a), Vacuum tube (b).

According to formula (1′), the distance between the successive Balmer lines ought to diminish with increasing m, and the series ought to terminate at

$$\nu = R/2^2, \qquad \lambda = 3645{\cdot}81 \quad . \; . \; . \; . \; . \; . \; . \quad (1'')$$

This point is known as the **convergence limit** of the series. A list of Balmer-lines with their wavelengths and wave-numbers is given in Table 1. It will be seen that the table contains a number of other series in addition to Balmer's, and the whole series of lines are attributed to the hydrogen atom. The full significance of the different series will be clear from the next section.

164. Bohr's Elementary Theory of the Hydrogen Spectra.—We shall now give an account of Bohr's elementary theory of the H-spectra. This is the fundamental work which has been the basis of all subsequent investigations connected with the atom.

Bohr† set to himself the task of explaining the remarkable regularities in the spectrum of H which have been just discussed. The first necessity was a model of the H-atom. In this he was guided by Rutherford's discovery that the positive electricity occupied a very minute space at the centre of the atom. He compared the atom to a planetary system as already suggested by Nagaoka‡ in 1904. The nucleus of positive electricity with its large mass plays the rôle of the sun. The electron with its small mass plays the role of the planet. As in the case of the planets, the electron is attracted towards the nucleus according to the inverse square law (the law is not however gravitational, but electrical, and the force is due to attraction of electrical charges of opposite signs). The electron is prevented from falling into the nucleus by its constant motion as in the case of planets. Bohr showed that the whole theory of planetary motion can be applied with certain modifications to the problem of motion of the electron round the nucleus.

---

* R. W. Wood, *Proc. Roy. Soc. A*, **97**, 455, 1920.

† Niels Bohr, On the Constitution of Atoms and Molecules, *Phil. Mag.*, **26**, 1, 476, 857, 1913.

‡ H. Nagaoka, *Phil. Mag.*, **7**, (6), 445, 1904.

Table 1.—Series Spectra of Hydrogen.

Observer		n	Lyman Series $\nu = R_H\left(\frac{1}{1^2}-\frac{1}{n^2}\right)$				
			λ_{vac} (obs.)	λ_{vac} (cal)	ν (cal.)		
Millikan*		2	1215·7	1215·68	82258·31		
Lyman		3	1026·0	1025·73	97491·36		
		4	972·7	972·54	102822·94	Term values	
Observer		n	Balmer Series $\nu = R_H\left(\frac{1}{2^2}-\frac{1}{n^2}\right)$			n	$T_{(n)}$
			λ_{air} (obs.)	$\lambda_{(air)}$ (cal.)	ν (cal.)	1 2	109677·82 27419·512
Houston†	Hα	3	6562·8473 6562·7110	6562·793	15233·216	3	12186·458
	Hβ	4	4861·3578 4861·2800	4861·327	20564·793	4	6854·881
	Hγ	5	4340·497 4340·429	4340·466	23032·543	5	4387·131
Values of Paschen, Curtis and Ruark	Hδ	6	4101·7346	4101·738	24373·055	6	3046·619
	Hε	7	3970·0740	3970·075	25181·343	7	2238·331
	Hζ	8	3889·0575	3889·052	25705·957	8	1713·717
Ruark‡	Hη	9	3835·397	3835·387	26065·61	9	1354·06
	Hθ	10	3797·910	3797·900	26322·90	10	1096·77
	Hι	11	3770·634	3770·633	26513·24	11	906·43
	Hκ	12	3750·152	3750·154	26658·03	12	761·64
	Hλ	13	3734·372	3734·371	26770·68	13	648·99
	Hμ	14	3721·948	3721·948	26860·09	14	559·58
Wood§	Hν	15	3711·980	3711·973	26932·21	15	487·46
	Hξ	16	3703·861	3703·855	26991·24	16	428·43
	Hο	17	3697·159	3697·154	27040·16	17	379·51
	Hπ	18	3691·553	369·557	27081·16	18	338·51
	Hρ	19	3686·833	3686·834	27115·85	19	303·82
	Hσ	20	3682·825	3682·810	27145·47	20	274·20
	Hτ	21	3679·372	3679·355	27170·96	21	248·71
	Hυ	22	3676·378	3676·354	27193·07	22	220·60

---

* Millikan, *Astrophys. Jour.*, **52**, 47, 286, 1920; **53**, 150, 1921.
† Houston, *Astrophys. Jour.*, **64**, 81, 1926.
‡ Ruark, *Astrophys. Jour.*, **58**, 46, 1923.
§ Wood *Phil. Mag.*, **42**, 729, 1921.

Observer	n	Balmer Series $\nu = R_H\left(\frac{1}{2^2} - \frac{1}{n^2}\right)$			Term values	
		λ_{air} (obs.)	λ_{air} (cal.)	ν (cal.)	n	T_{cal}
Davidson and Stratton* H_{23}	23	3673.76	3673.761	27212.36	23	207.33
H_{24}	24	3671.43	3671.478	27229.06	24	190.41
H_{25}	25	3669.50	3669.466	27244.10	25	175.48
H_{26}	26	3667.68	3667.681	27257.42	26	162.25
H_{27}	27	3666.10	3666.097	27269.24	27	150.44
H_{28}	28	3664.66	3664.679	27279.78	28	139.90
H_{29}	29	3663.42	3663.405	27289.34	29	130.41
H_{30}	30	3662.24	3662.258	27297.81	30	121.86
H_{31}	31	3661.24	3661.221	27305.54	31	114.13
H_{32}	32	3660.31	3660.280	27312.55	32	107.11
H_{33}	33	3659.38	3659.424	27319.04	33	100.71
H_{34}	34	3658.61	3658.641	27324.79	34	94.88
H_{35}	35	3658.10	3657.926	27330.14	35	89.53
H_{36}	36	3657.25	3657.269	27335.05	36	84.62
	37		3656.666	27339.55	37	80.12
	∞		3645.981	27419.674	∞	

Observer	n	Ritz-Paschen Series $\nu = R_H\left(\frac{1}{3^2} - \frac{1}{n^2}\right)$			Term values
		λ_{air} (observed)	λ_{air} (calculated)	ν (calculated)	
Paschen	4	18751.3	18751.1	5331.58	
	5	12817.6	12818.1	7799.31	
Brackett	6	1.09μ	10938.1	9139.81	
	7	10049.8	10049.4	9948.14	
Poetker†	8	9546.2	9546.0	10472.24	
	9	9229.7	9229.1	10832.40	
	10	9015.3	9014.9	11089.62	
	11	8863.4	8862.79	11280.03	

Observer	n	Brackett Series $\nu = R\left(\frac{1}{4^2} - \frac{1}{n^2}\right)$		
		λ_{air} (obs.)	λ_{air} (cal.)	ν (cal.)
Brackett	5	4.05μ	40510.4	2467.75
	6	2.63μ	26251.78	3808.26

Observer	n	Pfund Series $\nu = R_H\left(\frac{1}{5^2} - \frac{1}{n^2}\right)$		
		λ_{air} (obs.)	λ_{air} (cal.)	ν (cal.)
Pfund	6	7.40μ	74578.0	1340.512

This table has been collected from *Handbuch der Astrophysik*, 3, (2), p. 460, article by W. Grotrian.

---

* Davidson and Stratton, *Mem. R. A. S.*, 64, 105, 1927.

† Poetker, *Phys Rev.*, 30, 418, 1927.

In the case of the H-atom, at first he supposed it to consist of a central stationary nucleus which has got the same mass as the hydrogen atom and a charge of $+e$, with one electron revolving round it in an orbit. The matter was further simplified by the assumption that the orbit is circular. The equation of motion can now be written as:—

$$ma\omega^2=\frac{Ee}{a^2} \quad . \quad . \quad . \quad . \quad . \quad . \quad . \quad . \quad . \quad . \quad (2)$$

where a=radius of the circular orbit, ω=angular velocity of the electron. The total energy W of the system is equal to potential energy plus kinetic energy. Thus

$$W=-\frac{eE}{a}+\tfrac{1}{2}\,ma^2\omega^2=-\frac{eE}{2a} \quad . \quad . \quad . \quad . \quad . \quad . \quad . \quad (3)$$

Potential energy is taken as negative, because the force is attractive.

We have got two quantities to determine, *viz.*, a and ω, whereas we have only one equation. Hence a further equation between a and ω must be found. In the case of planetary motion, a second equation is given by the law of rate of description of areas (Kepler's second law)

$$m\alpha^2\omega = \text{constant} \quad . \quad . \quad . \quad . \quad . \quad . \quad . \quad . \quad (4')$$

The value of this constant which is essential for the solution of the problem is obtained from a knowledge of the initial conditions of projection, namely the velocity with which the planet is projected at a definite instant, and the distance of the point of projection. Now if these are u and a, the constant=mua for circular orbits. But in the case of motion of the electron in the atom it is not possible to obtain the initial condition. Hence some other method must be used for finding out the value of the angular momentum $ma^2\omega$ which is constant. Nicholson* had formerly observed that Planck's quantum h had the same dimensions as the angular momentum. With characteristic intuition, Bohr put

$$ma^2\omega = n.h/2\pi \quad . \quad . \quad . \quad . \quad . \quad . \quad . \quad . \quad . \quad (4)$$

With this second condition, we can completely solve the equation of motion. We get

$$W_n=-\frac{2\pi^2e^2E^2m}{h^2}\cdot\frac{1}{n^2} \quad . \quad . \quad . \quad . \quad . \quad . \quad . \quad (5)$$

$$a=\frac{h^2}{4\pi^2e^2m}\cdot n^2$$

---

* Nicholson, *Monthly Not. Roy. Astr. Soc.*, **72**, 679, 1912.

Thus the quantum condition (4) puts a restriction to the number of possible stable orbits. Only such orbits (or energy states) are possible which are distinguished by an integral quantum number n. They have the energy W_n and radius an^2 as given by formulæ (4) and (5).

A glance at this formula shows that the energy of the system when the electron is at infinite distance from the nucleus is taken to be zero. As we take orbits possessing decreasing values of n, the energies become more and more negative and varies as $1/n^2$. The orbit with the lowest energy corresponds to $n=1$. According to general principles in dynamics, this should be the most stable state of the H-atom. Compared to this, the other states are all unstable.

The phenomena occurring in a hydrogen tube, through which a discharge is passed may be pictured as follows: by means of a discharge, we convert a fraction of the H_2-molecules which compose the gaseous mass into H-atoms, some of the atoms are in state (1), a smaller number are in state (2) . . . and so on in the various energy states as described above. It is clear that the atom with higher energy values (larger values of n) will always tend to revert to states of lower energy value (smaller values of n). What happens to the difference of energy when such a process takes place? Bohr postulates that the balance of energy is emitted in space as radiation. If the frequency of this radiation is ν, then in accordance with Planck's fundamental postulate its energy should be $h\nu$. Bohr put

$$h\nu = W_i - W_f \quad . \quad . \quad . \quad . \quad . \quad . \quad . \quad . \quad . \quad (6)$$

where the subscript f denotes a final orbit, i denotes the initial orbit. This is known as *Bohr's Second Postulate*. This gives us the frequency ν in terms of the energy difference of the states of the H-atom. We have

$$\nu = \frac{2\pi^2 e^4 m}{h^3}\left(\frac{1}{n_f^2} - \frac{1}{n_i^2}\right) \quad . \quad . \quad . \quad . \quad . \quad . \quad . \quad . \quad (7)$$

If we put $n_f=2$, and allow n_i to take all integral values 3, 4, 5, ... etc., we get a formula for the frequency ν which is quite similar to the formula discovered by Balmer for the visible lines of the H-atom.

Bohr shows that the formula agrees not only in form, but also in absolute value with Balmer's formula. The Rydberg Constant

$$R = \frac{2\pi^2 e^4 m}{h^3} \quad . \quad . \quad . \quad . \quad . \quad . \quad . \quad . \quad . \quad . \quad (8)$$

Taking the known values of e and h Bohr found that R should be theoretically 109723, while from spectroscopic data R was found to have the value 109676. The agreement was thus found to be excellent. But Bohr's theory predicted more than what it proved. If the theory be correct, there should be further series of lines to be represented by the formulæ

$$\nu=R\left[\frac{1}{1^2}-\frac{1}{n^2}\right] \qquad \text{Lyman-series} \quad . \quad . \quad (9)$$

where $n=2, 3, \ldots$

and

$$\nu=R\left[\frac{1}{3^2}-\frac{1}{n^2}\right] \qquad \text{Paschen-series} \quad . \quad . \quad (9')$$

where $n=4, 5, 6, \ldots$ Of these series the first is the most important, but calculation shows that the wavelength of the first line of this series should be about 1216 Å.U. This is in the Schumann region. This explains why previous investigators, working with glass or quartz apparatus were unable to obtain it. But shortly before Bohr's theory was published, Prof. Lyman* of Harvard was able to photograph the entire series in his vacuum spectrograph. It is therefore known as the *Lyman series.*

The other series corresponding to $n_f=3$ was observed by Paschen† before the advent of Bohr's theory, and the second series corresponding to $n_f=4$ was discovered by Brackett‡. Both of them are in the infrared. A similar series corresponding to $n_f=5$ was observed by Pfund§ in the extreme infrared. The wavelengths of the lines of the different series of the H-spectra are shown in Table 1.

Let us now see whether the radius of the electronic orbit as given by Bohr's theory agrees with previous estimates of the radius of the H-atom. According to (5) we have $a_n=an^2$, where $a=h^2/4\pi^2e^2m$. Substitution of these values shows that $a=\cdot 538\times 10^{-8}$ cms. It is in agreement, as far as the order of dimensions, with the values obtainable from the kinetic theory. The radius of the nth orbit is an^2.

165. Mechanism of Emission and Absorption.—The mechanism of emission is represented by Fig. 2. Here we have represented the different possible orbits by circles denoted by 1, 2, 3 . . . etc. and the transitions giving rise to different series are represented by radial lines.

---

* Lyman, *Astrophys, Jour.*, 23, 181, 1906 ; 43, 89, 1916.

† Paschen, *Ann. d. Phys.*, 27, 537, 1908.

‡ Brackett, *Astrophys. Jour.*, 56, 154, 1922.

§ Pfund, *Jour. Opt. Soc. Am.*, 9, 193, 1924.

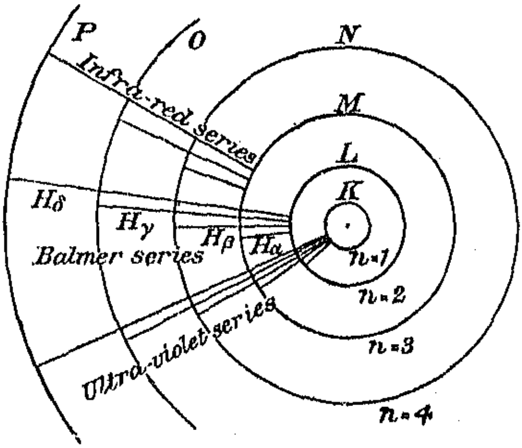

Fig. 2. Emission and absorption of H-Spectra.

Let us consider hydrogen gas in a discharge tube; then when no discharge is passed the gas consists only of molecules. When discharge is passed a fraction of molecules are broken up into atoms and some of the atoms are excited to higher levels. The lines are produced owing to the innate tendency of the electrons in the excited states to fall to lower levels as described previously. The intensity of the lines emitted depends upon the *probability* that an electron will return from a higher level to a lower level. The excited states are maintained by discharge; and if it were stopped, they would return to normal states in no time and the gas will be rendered non-luminous.

Absorption.—In absorption the opposite process takes place. When light falls on the atoms, it is absorbed by the electron which therefore receives an increment in its energy just as in a photo-electric process, and shifts to a higher level. But absorption is clearly possible only when the energy of the incident photon is equal to the energy difference between two stationary states. Hence only the characteristic lines can be absorbed out of a continuous spectrum.

When continuous light is passed through a column of H_2-vapour, it is found to be perfectly transparent to the lines of the Balmer series. This does not contradict Bohr's theory because in the normal states hydrogen exists in the molecular stage. It is incapable of absorbing Balmer lines, and can do so only when the molecules split up into H-atoms with their electrons in the second quantum states. That this is possible was first shown by Ladenburg and Loria* who obtained absorption of H_α and H_β by passing continuous light through a hydrogen tube in which H_2 was subjected to a continuous electrical discharge. The Balmer lines now occur in absorption because on account of the discharge, the molecules are more or less broken up into atoms, and some of them occur in the 2-quantum state, and are rendered capable for absorbing the Balmer lines. A sketch of Ladenburg's apparatus is given below (Fig. 3).

---

* Ladenburg and Loria, *Ann. d. Phys.*, **38**, 249, 1913.

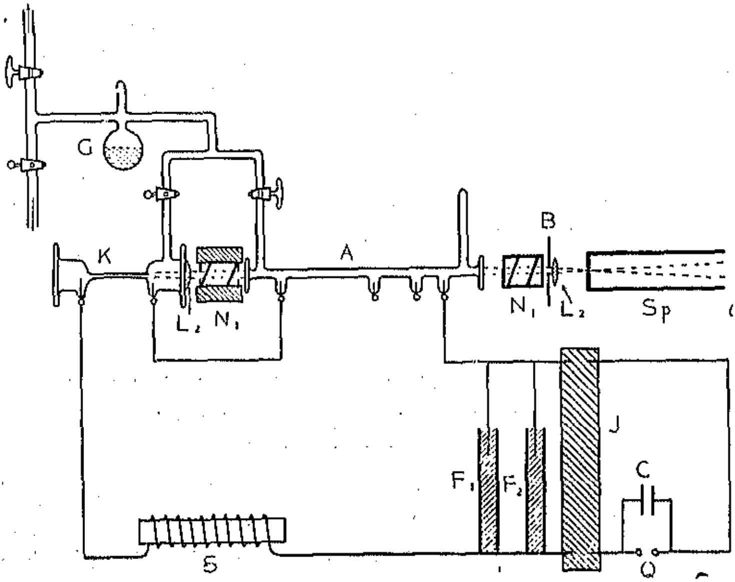

Fig. 3. Ladenburg's apparatus.

K . . .	is the source of continuous light. It is a discharge-tube of very small diameter and contains the H-gas at a high pressure.
A . . .	is a hydrogen discharge-tube containing H_2 at one mm.
N_1, N_2. .	is a pair of Nicol's prism.
Sp. . . .	is the spectrograph.
S . . .	is the secondary of an induction coil with a spark gap Q in the circuit.
$L_1 L_2$ . .	are lenses for focussing light.

The discharge tubes K and A are filled with pure dry hydrogen by means of the arrangement at the top. On starting, the two nicols are crossed, so that light from the source K cannot pass through the spectrograph. Only the bright emission lines of Hydrogen from the tube A are seen. On turning the nicol, the nature of the spectrum at once changes. The spectrum is found to consist of a continuous background due to the source K, together with the Hα and Hβ emission lines of Hydrogen; further two dark lines appear on the edges of Hα and Hβ where they cut across the continuous background. This is shown in Fig. 4 (*a*) which is a reproduction of Ladenburg's result. If the nicols are turned still further, the dark lines broaden until the bright line in between them is obliterated.

Using the gas in the absorption tube at 25 mm. pressure; the dark line appears at the centre of the bright line (Fig. 4 *b*). On gradually turning the nicols, the dark line again broadens, until finally the bright line is entirely cut off.

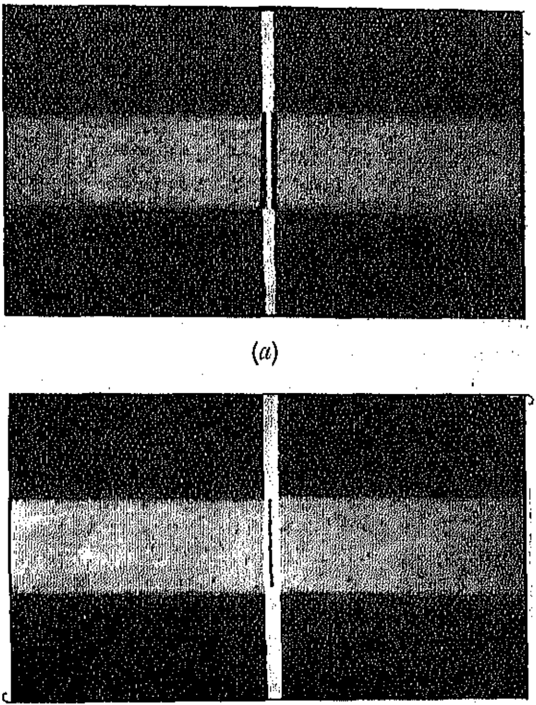
(*a*)

(*b*)

Fig. 4. Absorption of Balmer lines.

The interpretation of the above results is as follows. On account of electric discharge, some of the molecules of hydrogen in the absorption tube A are broken up into H-atoms, a few of which are excited to the 2-quantum state and are capable of absorbing Hα and Hβ lines from the continuous radiation passing through it. We thus get two dark absorption lines at the edges of the emission line Hα and Hβ.

166. The Higher States of the H-atom.—According to Bohr's theory, the radius of the *n*th orbit of the atom is given by

$$a_n = an^2 = \cdot538\times10^{-8}\ n^2$$

For the line H35 (observed in the Chromosphere)

$$a = 7{\cdot}5\times10^{-6}\ \text{cm.},$$

when the pressure in the tube is very large, the mean distance between atoms may be less than the radius of the higher orbits. Hence these orbits can be developed only in regions of extreme tenuity. This probably explains why in an ordinary vacuum tube only a few lines are observed. If the pressure be progressively diminished as in Wood's experiment (*vide infra*) more lines come out. The same phenomenon is illustrated in the spectra of stars, and in the Fraunhoffer spectrum of the sun which is a dwarf star (*i.e.* star with a rather dense atmosphere). In the sun we get only five Balmer lines in absorption. In the spectrum of Sirius, which is a dwarf A-star but with a less tenuous atmosphere, we get about 10 lines in absorption. In the spectrum of α-Cygni (a giant star with extremely tenuous atmosphere) not less than 24 lines of the Balmer series are observed in absorption. This has been illustrated by Fig. 5, Plate V, which is a photograph of the hydrogen lines in absorption as obtained in the spectrum of Zeta Tauri, another giant star.

167. Continuous Spectrum of Hydrogen.—During the total solar eclipse of 1905, J. Evershed photographed the spectrum of solar chromosphere and obtained no less than 35 Balmer lines in emission.

He reached nearly the convergence limit of Balmer series and further observed that this was followed by a continuous emission spectrum which just started at the convergence limit λ 3645·81 and extended for some distance into the ultraviolet. Afterwards, this continuous spectrum has also been observed in the laboratory in emission as well as in absorption (for alkali elements). Bohr showed that this continuous spectrum is due to the combination of a free electron with the bare hydrogen nucleus. In the stars as well as in the vacuum tube) a large percentage of H-atoms may be completely ionised and may contain a large proportion of free electrons. If a free electron possessing the kinetic energy $\frac{1}{2}mv^2$ approaches an H^+ particle, it may be captured in any one of the quantum orbits. If it is captured in the second orbit, the diminution of energy of the system (proton + free electron) is given by

$$W = \tfrac{1}{2}\, mv^2 + Rh/2^2 \quad . \quad . \quad . \quad . \quad . \quad (10)$$

for $Rh/2^2$ is the energy of the combined system in the 2-quantum state. To this the energy of free electron must be added (we suppose the proton to be at rest). We may suppose that the whole amount of the energy liberated in a capture is given out in radiation. The frequency ν is given by

$$\nu = \frac{R}{2^2} + \frac{1}{2}\cdot\frac{mv^2}{h} \quad . \quad . \quad . \quad . \quad . \quad (11)$$

Since $\frac{1}{2}mv^2$ can have all values from 0 to ∞, formula (11) represents a continuous spectrum starting from the end of Balmer series and extending to the ultraviolet. The intensity in different parts of the spectrum will depend upon the number of free electrons with the requisite amount of energy and their chances of capture in the second quantum orbit. It is quite clear that not only the Balmer series, but other characteristic series will also be attended by similar continuous spectra starting from the series limit and extending indefinitely to the ultraviolet. The continuous spectra are sometimes known as the *recombination spectra.*

168. Bohr's elementary theory is not sufficient.—Bohr's theory was thus successful in explaining many old facts and predicting new ones. But it could not be regarded as final or sufficient, as it left a number of questions unanswered, and gave rise to difficulties of a peculiar nature. First of all, according to this theory the spectral lines should be single, while actual observations showed that every one of the Balmer lines has a *complex structure* and contains at least *two close components.* Secondly, Bohr's ideas are in flagrant contradiction to the mechanical conception of Nature. On Bohr's model, the electron exists in a number of quantised states characterised by integral numbers. Suppose at any time, the electron is in orbit number 5; experience tells us, that it cannot remain long there, but will jump back to some lower orbit. To which particular one will it fall? Is it the 4th or the 3rd or the 2nd? This question cannot be decided on dynamical grounds. Hence we have to introduce an element of probability. We say that the electron possesses a certain definite probability for passing from the nth state to a lower state m. Einstein[*] denotes this probability in the general case of any atom by the symbol A_{nm}. If we have N_n atoms in the nth quantum state, then in time dt, the number which returns to the lower state m is given by

$$N_n \, . \, A_{nm} \, . \, dt \qquad . \quad . \quad . \quad . \quad . \qquad (12)$$

But in making this picture, we are sacrificing the law of causality which demands that the whole future course of a dynamical system should be determined by the laws of motion and by the initial or boundary conditions, just as in the case of planetary motion. But we have seen that such conditions cannot be found for motion of the electron round the nucleus. We have to introduce the quantum conditions rather arbitrarily, and then we have to endow the electron with a certain amount of will power of its own, which enables it to determine its own *Destiny*. This conception is contrary to all the canons that philosophers have established since the days of Galileo.

---

[*] A. Einstein, *Phys. Zeits.*, **18**, 121, 1917. See *A Text Book of Heat*, Saha and Srivastava, Chap. XI, p. 546.

Bohr was conscious of this difficulty in his theory and in collaboration with his students has been trying to improve it by continued efforts. An account of these efforts as well as the attempts made by other workers which successively led to the Correspondence Principle, Matrix Mechanics, and Wave-Mechanics, will be found in suitable volumes. The problem at issue became clearer when attempt was made to extend Bohr's theory to the explanation of the spectra of other elements as well as to allied phenomena like Zeemann effect, X-ray spectra and Stark effect.

169. General Explanation of Spectra of Elements.—Bohr showed that in the general case the atom consists of a central positive charge Ze with Z electrons revolving round it. These Z electrons may be supposed to be arranged in different layers. But it may be supposed that the light vibrations are due to only one, namely, the outermost electron. The equation of motion of this electron may be formulated in the same way, as in the case of hydrogen. The electrical field in which this electron moves is due to a nuclear charge $+Ze$ which is compensated by that due $Z-1$ electrons distributed round the nucleus in an unknown way. Roughly the field is due to a net charge of unity in the centre. Hence it is probable that the frequencies of lines of elements should be represented in the same way as those of the H-lines, with the same Rydberg constant. As a matter of fact, detailed analysis of the spectra of other elements (see § 183) by Rydberg, Ritz and others showed that the frequency of a spectral line in the general case can be represented by formulæ of the following type

$$\frac{\nu}{R}=\frac{1}{[\varphi(n)]^2}-\frac{1}{[\varphi'(m)]^2} \quad . \quad . \quad . \quad . \quad . \quad . \quad (13)$$

where φ and φ' are functions of integral numbers n and m of the type

$$\varphi(n)=n+\alpha+\frac{\beta}{n}+\frac{\gamma}{n^2}+\ldots \quad . \quad . \quad . \quad . \quad . \quad . \quad . \quad (14)$$

Now before taking the general case of spectra let us see whether there are other spectra which present a greater similarity to the spectrum of Hydrogen.

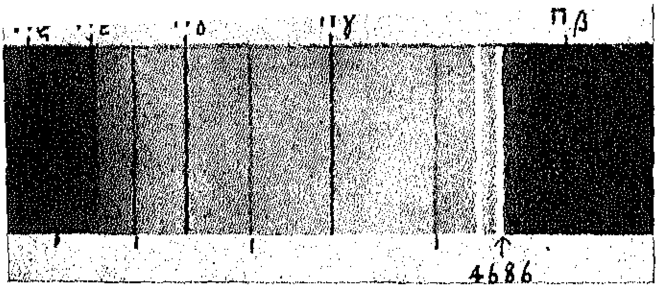

Fig. 5r. Spectrum of ζ-Puppis showing lines (Pickering Series) of ionised helium between successive H-lines.

p. 333

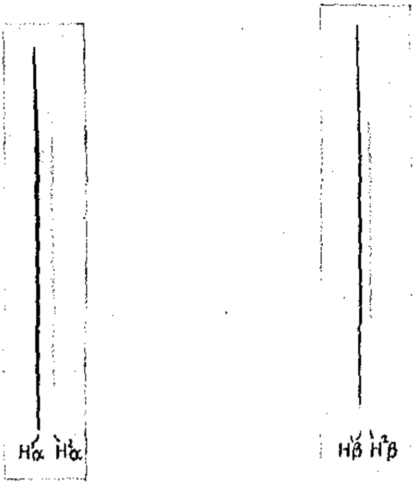

Fig. 6. Balmer lines of ordinary H, compared to those of H².

p. 337

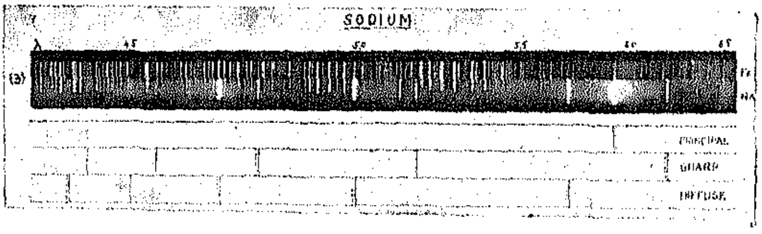

Fig. 1. Emission lines of Na-*s*, *p*, *d* series (*A. Fowler*).

p. 361

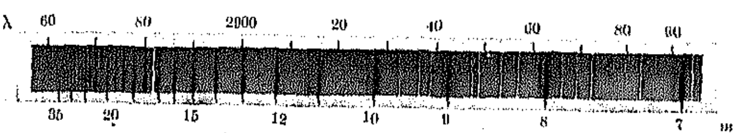

Fig. 4. Absorption spectrum of Na (*Datta*).

p. 368

[*f. p.* 333

170. Lines of Ionised Helium.—Prof. Pickering of Harvard discovered in 1898 a series of lines in the spectrum of ξ-Puppis, which are distributed midway between the Balmer lines as shown in Fig. 5*a*, Plate VI.

He found that these lines could be represented by the formula.

$$\nu = R\left[\frac{1}{2^2} - \frac{1}{(n+\frac{1}{2})^2}\right] \quad . \quad . \quad . \quad . \quad . \quad . \quad . \quad . \quad (15)$$

The wavelengths of the lines corresponding to $n = 3, 4, 5, 6$ . . . are λ 5412, 4541, 4199, ...

Somewhat later, G. E. Hale showed that if in Pickering's formula, we give to n the value 1, and reverse the terms we obtain a line having the frequency

$$\nu = R\left[\frac{1}{(1+\frac{1}{2})^2} - \frac{1}{2^2}\right] \quad . \quad . \quad . \quad . \quad . \quad . \quad . \quad (15')$$

with the theoretical wavelength λ 4688. A bright line of this description occurs in the spectra of many nebulæ and of very hot stars, though its actual wavelength was found to be somewhat shorter, namely 4686 Å.U. Owing to the similarity of the series formula of these lines to the Balmer formula, they were ascribed to a form of hydrogen (cosmic hydrogen) existing in the hotter stars. They were first observed by A. Fowler* in the laboratory in 1912, when a condensed discharge was passed through a mixture of H and He. Later, they were obtained in discharge through pure He, showing that they are due to helium pure and simple.

171. Lines of Cosmic Hydrogen are due to Ionised Helium.—Bohr showed that the lines of cosmic hydrogen form really the *enhanced* spectrum of He. Helium is the element next to H, it has got a nucleus having the charge $2e$, mass $4\,m_H$, with two electrons revolving in orbits about the nucleus. The spectrum of He proper consists of a large number of lines which were systematised in six series by Runge and Paschen (see *infra* Chap. XII) We are not concerned with their explanation at this stage, nor is it possible with simple mechanics, partly because we are here dealing with the problem of three bodies. But if He loses one electron, the problem of its spectral radiation becomes mathematically soluble. We can write out the equation exactly as in §164, only the central charge is now $E=2e$. We then obtain

---

* A. Fowler, *Monthly Notices*, **73**, 62, 1912; *Proc. Roy. Soc. A.*, **90**, 426, 1914.

$$\nu = \frac{2\pi^2 e^2 E^2 m}{h^3}\left[\frac{1}{n^2} - \frac{1}{n'^2}\right] \quad . \quad . \quad . \quad . \quad . \quad . \qquad (7')$$

$$= RZ^2\left[\frac{1}{n^2} - \frac{1}{n'^2}\right]$$

in the general case, where $E=Ze$. For the H-atom $Z=1$, but for He^+, $Z=2$, so that $R_{He}=4R_H$. The lines of He^+ are therefore given by

$$\nu = 4R\left[\frac{1}{n^2} - \frac{1}{n'^2}\right] \quad . \quad . \quad . \quad . \quad . \quad . \quad . \quad . \qquad (7'')$$

$$= R\left[\frac{1}{(n/2)^2} - \frac{1}{(n'/2)^2}\right]$$

A table of wavelengths of lines due to He^+ are given in the next page. It will be noticed that the wavelengths of He^+-lines possessing the same mathematical formula as lines of Balmer series have considerably smaller values. Thus the He^+-line

$$4\,R\left(\frac{1}{4^2} - \frac{1}{6^2}\right) = R\,\left(\frac{1}{2^2} - \frac{1}{3^2}\right)$$

has not the wavelength λ6562 but λ6560·13. Compare the wavelengths of Hβ, Hγ, etc. in Table 2. The cause of this discrepancy is explained in the next section.

172. Motion of the Nucleus—Variation in the Value of the Rydberg Constant.—According to the elementary form of Bohr's theory, the Rydberg constant ought to be invariable. But A. Fowler pointed out that this was not so. He showed that for the Balmer lines of hydrogen

$$R_H = 109678$$

while for the Pickering lines and other lines of He^+, it was found that both from steller as well as laboratory data.

$$R_{He} = 109723$$

This variation in the value of R in the case of He explains why the wavelength of the line $4\,R\,(1/3^2 - 1/4^2)$ is 4686 and not 4688.

The objection, instead of proving to be any serious obstacle to Bohr's theory, led to one of its most conspicuous triumphs. Bohr[*] pointed out that in the elementary theory, the nucleus has been supposed to be at rest.

---

[*] N. Bohr, *Zs. f. Phys.*, 2, 423, 1920; *Astrophys. Jour.*, 71, 228, 1928.

But this is not strictly true. According to dynamical principles, it is the centre of gravity of the system consisting of the nucleus and the electron which is at rest. Though in the preliminary treatment, the nucleus was supposed to be at rest, the error was not much, for the proton is 2000 times heavier than the electron, and the centre of gravity of the system proton-plus electron very nearly coincides with the centre of gravity of the proton. But we can easily work out the rigorous theory (*vide* Appendix, note 3). We have then merely to substitute the reduced mass $mM/(m+M) = m(1-m/M)$ in place of m throughout the treatment in § 164(M is the mass of the nucleus). Hence we obtain that for

Table 2.—Wavelengths of He$^+$*-lines.*

Observer	Series	n	$\lambda_{\text{vac.}}$ (obs.) ÅU.	$\lambda_{\text{vac.}}$(cal.) Å. U.	ν (cal.).
Edlen*	$\nu = 4R_{\text{He}}\left(\frac{1}{1^2} - \frac{1}{n^2}\right)$	2	303·6	303·79	329166
		3	256·3	256·33	390123
Lyman†	$\nu = 4R_{\text{He}}\left(\frac{1}{2^2} - \frac{1}{n^2}\right)$	3	1640·4	1640·49	60957·35
		4	1215·2 (?)	1215·18	82292·42
		5	1085·2	1084·98	92167·51
Fowler‡	$\nu = 4R_{\text{He}}\left(\frac{1}{3^2} - \frac{1}{n^2}\right)$	4	4685·760	4685·760	21335·31
		5	3203·138	3203·145	31210·33
		6	2733·326	2733·334	36574·55
		7	2511·233	2511·238	39809·01
		8	2385·427	2385·435	41908·29
		9	2306·215	2306·227	43347·50
Paschen‖		10	2252·810	...	...
Evans¶	$\nu = 4R_{\text{He}}\left(\frac{1}{4^2} - \frac{1}{n^2}\right)$	5	...	10123·72	9875·09
	(Pickering series)	6	6560·130	6560·168	15239·31
		7	5411·551	5411·57	18473·80
		8	4859·342	4859·36	20573·10
		9	4541·612	4541·63	22012·37
		10	4338·694	4338·71	23041·87
		11	4199·857	4199·87	23803·59
		12	4100·409	4100·08	24382·93

$$\left.\begin{aligned} &\text{Hydrogen,} \quad R = \frac{2\pi^2 e^4 m}{h^3}\left(1 - \frac{m}{M}\right) = R\left(1 - \frac{m}{M}\right) \\ &\text{Helium,} \quad R_{\text{He}} = \frac{2\pi^2 e^4 m}{h^3}\left(1 - \frac{m}{4M}\right) = R\left(1 - \frac{m}{4M}\right) \end{aligned}\right\} \quad . \; . \; . \; . \quad (16)$$

---

* Edlen and Ericson, *Zs. f. Phys.*, **59**, 656, 1929.

† Lyman, *Astrophys. Jour.*, **60**, 1, 1924.

‡ Fowler, *loc. cit.*

‖ Paschen, *Ann. d. Phys.*, **50**, 901, 1916.

¶ Evans, *Phil. Mag.*, **29** (6), 284, 1915.

where $$R = 109737{\cdot}2$$

R is the Rydberg constant when M tends to infinity.

From the difference in the value of the Rydberg constant, it is easy to calculate the important ratio m/M. We have from (16)

$$\frac{m}{M} = \frac{4}{3}\,\frac{R_{\mathrm{He}} - R_{\mathrm{H}}}{R} = \frac{1}{1836}$$

This is the most accurate value of m/M so far determined.

Spectrum of the Heavy Isotope of Hydrogen (Deuton)

We have seen in Chapter III, §39, that atoms of most elements in the periodic table consist of isotopes, that is, particles having the same number of electrons in the outer shell, but differing slightly in atomic weight. The nature of the spectrum emitted by the different isotopes is absolutely identical, as this depends only on the constitution of the outer shell, but the lines are found to possess slightly different wavelengths. This is partly due to the action of the mass of the nucleus, which makes the Rydberg constant somewhat different. According to (16), taking the motion of the nucleus into consideration, we have

$$R = \frac{2\pi^2 e^4 m}{h^3}\left(1 - \frac{m}{M}\right) = R_\infty\left(1 - \frac{m}{M}\right) \quad . \quad . \quad . \quad . \quad (17)$$

where 'M' is the mass of the nucleus. If two isotopes possess the masses M and M', the frequencies ν and ν' of the corresponding lines are connected by the relation

$$\frac{\nu'}{\nu} = \frac{1 - m/M'}{1 - m/M} \text{ or } \frac{\delta\nu}{\nu} = m\,\frac{\delta M}{MM'} \quad . \quad . \quad . \quad . \quad (18)$$

where $$\delta M = M' - M.$$

The change in frequency is generally very slight in the case of heavy elements, but recently Urey, Brickwedde and Murphy have succeeded by this method in discovering a heavy isotope of hydrogen in which the mass is 2. It consists of a proton and a neutron, and is denoted by H^2. The lines of this hydrogen isotope (called *Diplogen* by Lord Rutherford, *Deuton* by the American investigators) are expected to show very considerable shift. In fact

$$\frac{\delta\nu}{\nu} = \frac{m}{2M} = \frac{1}{2\times1836} = -\frac{\delta\lambda}{\lambda}, \text{ or } \delta\lambda = -\frac{\lambda}{2\times1836} \quad . \quad . \quad . \quad . \quad (19)$$

The wavelengths of the characteristic lines of H^2 calculated according to the above formula and the observed values are given in Table 3.

Table 3.—Isotope shift of the spectral lines of heavy hydrogen.

	H_α	H_β	H_γ	H_δ
λ in Å. U. ..	6562·85	4861·3	4340·49	4101·73
δλ (Calculated) ...	1·793	1·326	1·185	1·119
δλ (Observed)				
Ordinary H	...	1·346	1·206	1·145
Sample I	...	1·330	1·199	1·103
Sample II & III	1·791	1·313	1·176	1·088

Urey, Brickwedde and Murphy* have actually been able to observe the effect in the second order spectrum of a 21 ft. concave grating with a dispersion of 1·31 Å. U. per mm. They took a sample of ordinary dry hydrogen in a discharge tube. On passing discharge under 4000 volts and 1 ampere current, and increasing the exposure by 4000 times of that required for photographing the ordinary Balmer lines (generally 2 sec. in this arrangement), they observed a faint companion of the main H^1_β, H^1_γ and H^1_δ lines in the spectrum. The faint components were supposed to be the H^2_β, H^2_γ and H^2_δ- lines respectively, and they appeared at the expected positions (between 1 and 2 Å. U. from the main lines towards the shorter wavelength side) as can be readily seen from table 3.

A photograph showing the H^2 components of the $H\alpha$ and $H\beta$ lines is reproduced in Fig. 6, Plate VI from a photograph given in Aston's Isotopes (1933 edition). In order to make sure that the faint lines were not ghosts or due to some impurity, they used three different samples of hydrogen all obtained from the evaporation of liquid hydrogen, the first at atmospheric pressure, and the other two near the triple point. It was found that on account of greater concentrations attained in the samples II and III, the H^2 lines obtained with them were more intense than in the first case.

From the relative increase of the exposure so that the H^2 line just appeared on the photographic plate, the relative abundance of H^2 in the first sample was approximately calculated as 1 in 4000.

173. Fine Structure of Balmer Lines.—So far we have been regarding the Balmer lines as if they are simple geometrical lines, possessing a mathematically definite wavelength. But a little acquaintance with spectroscopy shows that every spectral line has some small though finite breadth extending in exceptional circumstances over several Ångstrom units. The breadth is due to a variety of causes: (1) Döppler motion of radiant centres which changes the wavelength from λ to $\lambda\,(1 \pm v/c)$, where v is the velocity of the radiant atom, (2) pressure effect, etc. The broadening can be reduced by working at low temperatures and at very low pressures. But still a finite breadth persists which has been ascribed to natural damping of the atomic resonator.

---

* Urey, Brickwedde and Murphy, *Phys. Rev.*, **40**, 1, 1932.

Michelson was the first to show that even when extreme care is taken to reduce broadening, the Balmer lines show a structure, as if they are composed of at least two, and probably of more close components. Michelson found the distance between the two components of Hα to be ·13Å. units approximately.

On account of the great theoretical interest of the problem, the fine structure of Balmer-lines and of the helium-lines λ 4686, and of the other members of the series $\nu = 4R_{\text{He}}\,(1/3^2 - 1/n^2)$ have been attacked by a large number of investigators with the aid of interference spectroscopes of high resolving power (like the Michelson or the Lummer-Gehrecke plate interferometer). The subject is too technical to be described here and reference may be made to the original sources.* The usual method is to photograph the lines, and then to take a micro-photometric record of the distribution of intensity along the breadth of a spectral line. Each individual component of a line is theoretically expected to give a curve similar to that in Fig. 7,

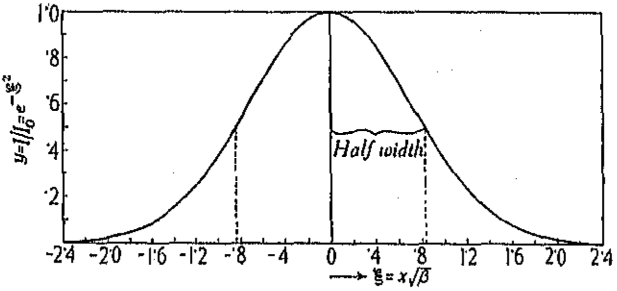

Fig. 7. Intensity distribution along the breadth of the spectral line.

---

* See for a critical account, Lau, *Phys. Zeits.*, 25, 60, 1924; Hansen, *Ann. d. Physik* (5), 78, 558, 1925; Keussler, *Ann. d. Physik* (6), 7, 225, 1930. For works on He⁺-lines, see Paschen, *Ann. d. Physik* (5), 82, 689, 1927. A very good account is given in Sommerfeld's *Atombau und Spektrallinien* (1924), Chap. VI.

which is a probability curve.* This is due to the fact that the radiant centres are moving towards or away from the observer with the velocity ± v where v varies from 0 to ∞. The wavelength is therefore changed from λ_0 to $\lambda_0\,(1+v/c)$, *i.e.*, by $\Delta\lambda=\lambda_0 v/c$. The intensity at a distance $\Delta\lambda$ from the centre is proportional to the number of radiant centres possessing the velocity v, and according to Maxwell's law, this is proportional to $e^{-\frac{1}{2}mv^2/kT}$ *i.e.*, $e^{-a\,(\Delta\lambda)^2}$. Thus the distribution of intensity follows the e^{-ax^2} law, where $x = \Delta\lambda$.

The half-width of the line is given by the distance from the centre to where the intensity reduces to half its value; the half-width can be shown to be equal to

$$b = \frac{\lambda_0}{c}\,\sqrt{(2ln2)\,R}\,\sqrt{\frac{T}{A}},$$

where T = temperature, A = atomic weight of the radiant centre and R=gas-constant.

The total area included between the curve and abscissa represents the intensity of the line. The height may be taken to be a fair measure of the intensity.

When there are several components of different intensities very close to each other, the curves may overlap if the half widths of each line are comparable to the separation. We may thus get a distorted curve, and it becomes very difficult to recognise the individual components in such cases, particularly when the components are of unequal intensity.

Fig. 8 represents the intensity curve of Hα-line as measured and corrected by Hanson when the pressure of the discharge tube was ·2 – ·015 mm., and the current through the tube was ·2 to ·04 amp/cm.², and some oxygen was added to the tube.

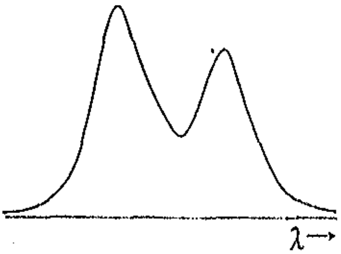

Fig. 8. Intensity distribution of Hα (*Hansen*).

The reason for mentioning these details is that the form of the curve is found to vary rather widely with experimental conditions. The broadening depends, besides Döppler-motion, on pressure, presence of electrical fields, presence of foreign gases, etc..., which produce sometimes assymmetry of a puzzling nature. Very careful work is needed to eliminate all these disturbing elements.

---

* See *Text-Book of Heat*, by Saha and Srivastava, p. 719.

From the curve given above and others, it can be easily seen that in H_α, two components separated by a distance $\Delta\lambda = {\cdot}132$ Å. U. can be clearly recognised. The separation is calculated from the distances between the two peaks which may be taken to represent the centres of the two components. But the curves for the two overlap, and both the violet and the red components appear to be assymmetric on one side. This is explained by assuming that there are other fainter components, as shown in Fig. 9, which is taken from Hansen's paper. Here the experimental curve is shown as composed of three component curves of which the middle one is almost completely overlapped by the other two.

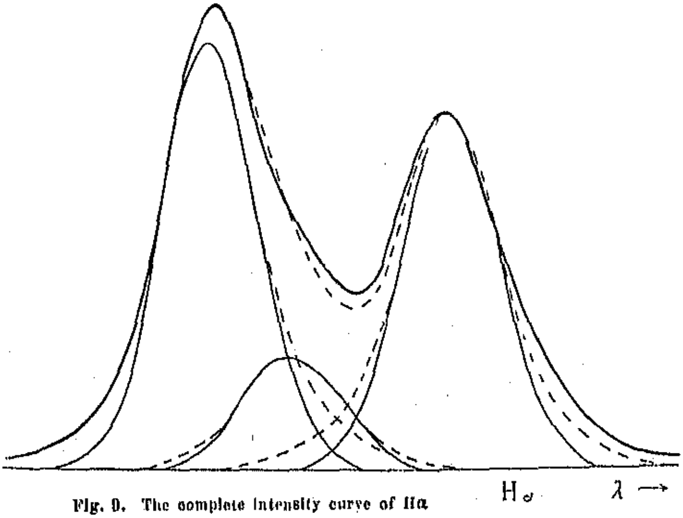

Fig. 9. The complete intensity curve of Hα

Further discussion is postponed till we consider the theoretical explanation of the doubling.

174. Explanation of Fine Structure of Balmer Lines.—The first explanation of the fine structure of Balmer lines was given by A. Sommerfeld.* Though this explanation has been modified in very essential respects, it is important as marking a fresh landmark in the history of atomic physics, as this theory gave the first clue towards the explanation of the complex features of alkali spectra. A brief sketch of the theory is given below, though for a complete exposition the notes at the end of the present chapter should be consulted.

---

* A Sommerfeld, *Atombau und Spektrallinien* (1924), Chap. II, p. 122.

SOMMERFELD'S GENERALISATION OF BOHR'S ELEMENTARY THEORY.

The orbits of planets round the sun are generally elliptical; only in very rare cases are they circular. In assuming that the orbit of the electron round the nucleus is circular, Bohr at first put a restriction on the possible modes of motion of the electron. Sommerfeld showed that this restriction was unnecessary. We can formulate the motion more generally and take both r and θ as variable. Since the force is central, the orbit in this case is generally elliptic as proved in §74; the full particulars of motion can be worked out as follows:—

Let the nucleus be taken as the origin (Fig. 10) and r, θ denote the position of the electron at any instant. Then we have

$$\left.\begin{aligned} &\text{Kinetic energy} = T = \tfrac{1}{2}\, mv^2 = \tfrac{1}{2}\, m\,(\dot{r}^2+r^2\dot{\theta}^2) \\ &\text{Potential energy} = -\frac{e^2}{r} = V \\ &T = \tfrac{1}{2}\, m\,(\dot{r}^2+r^2\dot{\theta}^2) = \frac{1}{2m}\left(p_r^2+\frac{p_\theta^2}{r^2}\right) \end{aligned}\right\} \quad \ldots\ldots \quad (20)$$

We have
$$p_r = \frac{\partial T}{\partial \dot{r}} = m\dot{r}, \quad p_\theta = \frac{\partial T}{\partial \dot{\theta}} = mr^2\dot{\theta}, \quad \ldots\ldots\ldots \quad (20')$$

where p_r and p_θ are known as generalised momenta.

The equations of motion are

$$\frac{d}{dt}\left[\frac{\partial(T-V)}{\partial \dot{r}}\right] - \frac{\partial T}{\partial r} = 0$$

$$\frac{d}{dt}\left[\frac{\partial(T-V)}{\partial \dot{\theta}}\right] - \frac{\partial T}{\partial \theta} = 0$$

These reduce to

$$m(\ddot{r}-r\dot{\theta}^2) = -\frac{e^2}{r^2}, \quad \frac{d}{dt}(mr^2\dot{\theta}) = 0. \quad \ldots\ldots \quad (21)$$

As proved on p. 150, it can be shown that the orbit is the conic

$$r = \frac{l}{1+\varepsilon\cos\theta} \quad \ldots \quad (21')$$

where the values of l and ε have to be obtained from the initial conditions. In the present case, the initial conditions cannot be obtained, for reasons mentioned on p. 324, their place is taken by the *quantum conditions*. For the case of motion in a circle, Bohr assumed the quantum condition to be

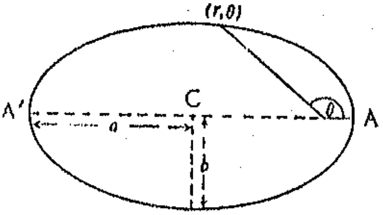

Fig. 10. The elliptic orbit.

$$p_\theta = mr^2\dot{\theta} = \frac{nh}{2\pi} \quad \ldots\ldots\ldots\ldots \quad (22)$$

Sommerfeld, and W. Wilson* thought that this was only a special case of the more general quantum condition

$$\oint\oint dp.\, dq = nh \quad . \quad . \quad . \quad . \quad . \quad . \quad . \quad . \quad . \quad . \quad . \qquad (22')$$

where q is the positional coordinate and p the corresponding momentum coordinate, n is an integral number.

The integration extends over the whole orbit. When $q=\theta$, $p=p$, (22′) reduces to Bohr's condition

$$\oint\oint dp_\theta\, d\theta = 2\pi p_\theta = kh, \quad . \quad . \quad . \quad . \quad . \quad . \quad . \qquad (22a)$$

because from equation (22), p_θ is constant and θ varies from 0 to 2π. Thus Bohr's assumption is seen to be a special case of the Sommerfeld-Wilson condition (22a). The second quantum condition is

$$\oint p_r\, dr = \oint m\dot{r}\, dr = n'h \quad . \quad . \quad . \quad . \quad . \quad . \quad . \qquad (22b)$$

With the aid of equations (20′), (21′) and (22), this integral reduces to the form

$$\frac{kh}{2\pi}\varepsilon^2 \oint \frac{\sin^2\theta\, d\theta}{(1+\varepsilon\cos\theta)^2} = n'h \quad . \quad . \quad . \quad . \quad . \quad . \quad . \qquad (22c)$$

This integral can be shown to have the value $\frac{2\pi}{\varepsilon^2}\left[\frac{1}{\sqrt{1-\varepsilon^2}}-1\right]$

Hence we obtain $\quad \frac{1}{\sqrt{1-\varepsilon^2}}-1=\frac{n'}{k}$

or

$$\varepsilon^2 = 1-\frac{k^2}{(n'+k)^2} \quad . \quad . \quad . \quad . \quad . \quad . \quad . \quad . \quad . \qquad (23)$$

Thus the eccentricity of the orbit is expressed in terms of the two quantum numbers n' and k.

Further from the theory of central orbits, we have

$$A=2\text{ (rate of description of areas)}=\sqrt{\mu l},$$

where μ = force on unit mass at unit distance $=e^2/m$, and l = latus rectum of the orbit. Also $A=r^2\dot{\theta}$.

Here $\quad r^2\,\dot{\theta}=\frac{kh}{2\pi m}$, $\qquad$ hence $\left(\frac{kh}{2\pi m}\right)^2=\frac{e^2}{m}\,l. \quad . \quad . \quad . \quad . \qquad (24)$

The ellipse can now be completely determined if we can obtain the value of a, the semi major-axis. This can be obtained from the formula (24), and the relation $a=l/(1-\varepsilon^2)=l\,(n'+k)^2/k^2$.

We have then

$$\left.\begin{aligned} l &= \frac{h^2}{4\pi^2e^2m}\;k^2 \\ a &= \frac{h^2}{4\pi^2e^2m}(n'+k)^2 \end{aligned}\right\} \quad . \quad . \quad . \quad . \quad . \quad . \quad . \qquad (25)$$

---

* W. Wilson, *Phil. Mag.*, **31**, 161, 1916.

i.e., a has the same value as in Bohr's elementary theory.

$$\text{The total energy} = \tfrac{1}{2}\left(m\dot{r}^2 + mr^2\dot{\theta}^2\right) - \frac{e^2}{r}$$

$$= -\frac{e^2}{2a} = -\frac{2\pi^2 e^4 m}{h^2}\cdot\frac{1}{(n'+k)^2} \quad \ldots\ldots \quad (25')$$

with the aid of (25). Thus if we put $n = n' + k$, the expression for energy retains the same form as in Bohr's theory.

175. Summary of the Results.—The main results are :—

$$\left.\begin{aligned} \varepsilon^2 &= 1 - \frac{k^2}{(n'+k)^2} \\ E &= -\frac{2\pi^2 e^4 m}{h^2}\cdot\frac{1}{(n'+k)^2} \\ a &= \frac{h^2}{4\pi^2 e^2 m}(n'+k)^2 \\ b &= \frac{h^2}{4\pi^2 e^2 m}\cdot k^2 \end{aligned}\right\} \quad \ldots\ldots \quad (24')$$

If we put $n = n' + k$, the total energy of the states has the same value as in Bohr's elementary theory, but the mechanical interpretation of the states becomes different. A state (n) with the energy $-Rh/n^2$ may be due to the motion of the electron in a number n of different orbits in which n remains the same, k may vary from n, $n-1$, ... to 1.

For example, when $n=2$, we have two orbits

$$\begin{aligned} k &= 2, \quad n' = 0, \quad \varepsilon = 0 \\ k &= 1, \quad n' = 1, \quad \varepsilon = \sqrt{3}/2 \quad \ldots\ldots\ldots \quad (26) \end{aligned}$$

the first of which is a circle and the other an ellipse. The orbit corresponding to $k=0$ is not possible, for the orbit then becomes parabolic.

For $n=3$, we have three orbits

$$\left.\begin{aligned} k &= 3, \quad n' = 0, \quad \varepsilon = 0 \\ k &= 2, \quad n' = 1, \quad \varepsilon = \sqrt{5}/3 \\ k &= 1, \quad n' = 2, \quad \varepsilon = \sqrt{8}/3 \end{aligned}\right\} \quad \ldots\ldots \quad (26')$$

An orbit which has the *total quantum number n, and the azimuthal quantum number k, is denoted by n_k*. Orbits for $n = 1, 2, 3, 4, \ldots$ are shown in the following diagram (Fig. 11).

A line like Hα is now seen to be due to the transition of the electron from any one of the three 3_k orbits to any two of the two 2_k orbits, and the same holds for other lines of the Balmer series.

Every Balmer line is thus seen to be composite, consisting of a number of lines possessing equal energies. Thus Hα should consist of 6 superposed lines, but Sommerfeld showed that transitions between all kinds of orbits are not allowed, but they are restricted by a *principle of selection.* The allowed transitions are those for which

$$\Delta k = \pm 1.$$

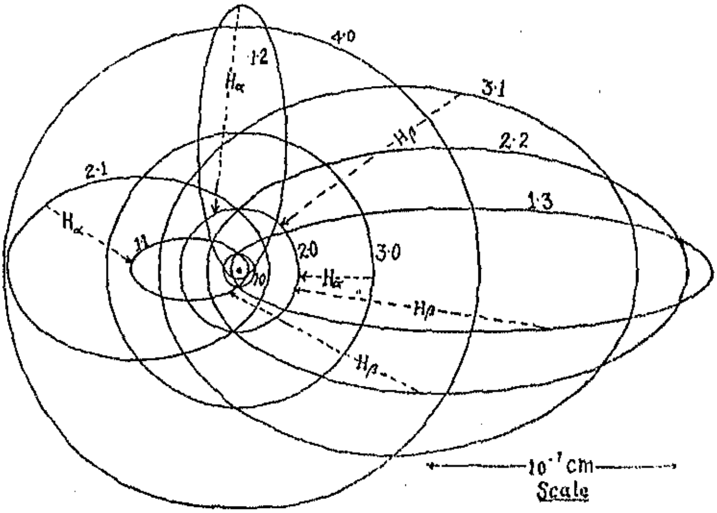

Fig. 11. The different n_k quantised orbits.

Transitions Δk=0, 2, 3, . . . are not allowed. This is the selection principle for azimuthal quantum number, which was first introduced empirically, but is explained by the Correspondence Principle, as well as by Matrix and Wave Mechanics.

The Balmer-lines, according to this hypothesis, should consist of three superposed components Ia, IIb, IIIa as shown below.

$$\begin{tikzcd}
 & n=2 & n=3 & \\
a & 2_2 & 3_3 \arrow[l] & \mathrm{I} \\
b & 2_1 & 3_2 \arrow[l] & \mathrm{II} \\
 & & 3_1 \arrow[uul] & \mathrm{III}
\end{tikzcd}$$

But the components are not actually coincident, for reason, stated in the next paragraph.

176. Correction due to Relativity.—But Sommerfeld* showed that the energy-values of the different orbits possessing the same total quantum number are equal only to a first approximation, as long as we can take the kinetic energy to be $\frac{1}{2}mv^2$. But Einstein has taught us, in his special theory of Relativity, that the exact expression for the kinetic energy of a particle is given by

$$\text{K.E.} = m_0c^2\left[\frac{1}{\sqrt{1-v^2/c^2}} - 1\right]$$

Using this expression for the kinetic energy, Sommerfeld showed that the energy of electron in the n_k -orbit is given by

$$\frac{W}{m_0c^2} = \left\{1 + \frac{\alpha^2Z^2}{(n'+\sqrt{k^2-\alpha^2Z^2})^2}\right\}^{-\frac{1}{2}} - 1 \quad . \quad . \quad . \quad . \quad (27)$$

where α is the constant quantity $2\pi e^2/ch$, and Ze is the nuclear charge.

It is easily seen, substituting the value of e, c and h, that

$$\alpha = (7{\cdot}295 \pm {\cdot}005)\,10^{-3} = \frac{1}{137} \text{ nearly.}$$

Since α is a small quantity, we can put, as a first approximation

$$n'+\sqrt{k^2-\alpha^2Z^2} = n'+k = n$$

Then we get

$$W = -\tfrac{1}{2}m\,\frac{(\alpha Z)^2c^2}{n^2} = -\frac{2\pi^2e^4Z^2m}{h^2n^2} \quad . \quad . \quad . \quad . \quad . \quad . \quad (27')$$

which is Bohr's expression for energy in the nth orbit. But if we carry out the second approximation, *vide* p. 357. we obtain after some work

$$-\nu_{nk} = \frac{RZ^2}{n^2} + \frac{R\alpha^2Z^4}{n^4}\left(\frac{n}{k} - \frac{3}{4}\right) + \ldots \text{higher terms} \quad . \quad . \quad . \quad . \quad (28)$$

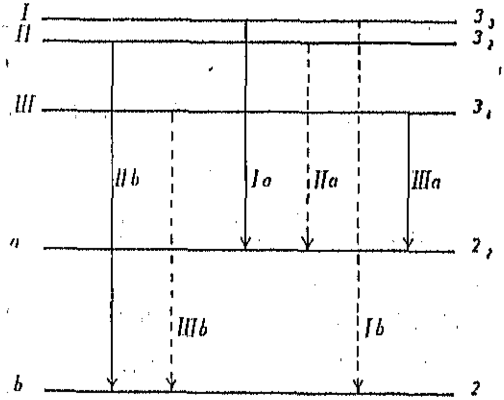

Fig. 12.

---

* A. Sommerfeld, *Ann. d. Phys.*, 51, 1, 1916. See also *Atombau*, Chap. 6.

The first term is the usual Balmer term. The second is the correction to be applied.

The quantity α is known as *Sommerfeld's Fine Structure Constant.* On account of the smallness of the value of α (it is about 1/137), the correction to be applied to Bohr's value of ν_{nk} is extremely small. But even this small value suffices to give a partial explanation of the fine structure as shown below.

Let $\Delta\nu$ denote the departure of ν_{nk} from the Bohr-value as given by (28). The value of $\Delta\nu/R\alpha^2$ for the different orbits which give rise to $H\alpha$ are shown in the following scheme, in which *a*, *b* represent the two n_k levels arising from $n=2$, and I, II, III represent the three $n_{k'}$ levels of $n=3$. A line arising from the transition I to *a* has been called I*a*, and so on for other lines. The scheme of transitions has been shown diagrammatically in Fig. 12. in which the dotted lines I *b*, III *b* . . represent the transitions orbidden according to the selection principle.

Table 4.

	$\dfrac{\Delta\nu_{nk}}{R\alpha^2}$	$n=2$		$n=3$	$\dfrac{\Delta\nu_{nk}}{R\alpha^2}$	
a	$\dfrac{1}{2^4}\cdot\dfrac{1}{4}$	2_2	$\longleftarrow$	3_3	$\dfrac{1}{3^4}\cdot\dfrac{1}{4}$	I
b	$\dfrac{1}{2^4}\cdot\dfrac{5}{4}$	2_1	$\longleftarrow\ \nwarrow$	3_2	$\dfrac{1}{3^4}\cdot\dfrac{3}{4}$	II
				3_1	$\dfrac{1}{3^4}\cdot\dfrac{9}{4}$	III

We have now the following $\Delta\nu_{nk}$-values for the components.

Table 5.

Component	$\Delta\nu_{n_k}$	$\Delta\lambda_{nk}$ (calcul.) Å.U.	Remarks
I *a*	$R\alpha^2.(\cdot 0125)$	$-0\cdot0314$	Very strong
II *b*	$R\alpha^2.(\cdot 0688)$	$-0\cdot173$	Strong
III *a*	$-R\alpha^2.(\cdot 0121)$	$+0\cdot0304$	Weak

The $\Delta\lambda_{nk}$-values in the third column are calculated from the relation $\Delta\lambda = -\lambda^2 . \Delta\nu$. The first two values are negative and the third positive. We thus hope to get three components, two of which are towards the violet, and the other towards the red side of the spectrum. But the latter will be very weak. So neglecting this there remains two components, one of which is more violet than the other.

Let us now compare these figures with the experimental results. Referring back to the curve in Fig. 9, we can easily identify the violet component with II *b*, and the red component with I *a*. The distance between them was found to be $\Delta\lambda = {\cdot}142$ Å. units. From this, we can calculate the value of α, and compare it with the value obtained by directly substituting the values of *e*, *c* and *h*. We have

$$\Delta\nu = R\alpha^2\,({\cdot}0563) = -\frac{\Delta\lambda}{\lambda^2}$$

$$\text{Hence }\ \alpha^2 = \frac{\Delta\lambda}{\lambda^2 . R \times {\cdot}0563} = \frac{{\cdot}142}{(6563)^2 \times {\cdot}0563 \times 109674} = 5{\cdot}32 \times 10^{-5}$$

$$\text{or} \qquad \alpha = 7{\cdot}290 \times 10^{-3} \text{ or } \frac{1}{137} \text{ approximately} \quad . \quad . \quad . \quad . \quad (29)$$

The value obtained by substituting the values of *e*, *c*, *h* is

$$\alpha = 7{\cdot}295 \times 10^{-3}.$$

The agreement appears to be excellent. For the sake of convenience the different components obtained from experimental results are shown separately in Fig. 13, in which the intensities of the components are represented approximately as proportional to their lengths. The corresponding $\Delta\lambda$-values are shown below each component.

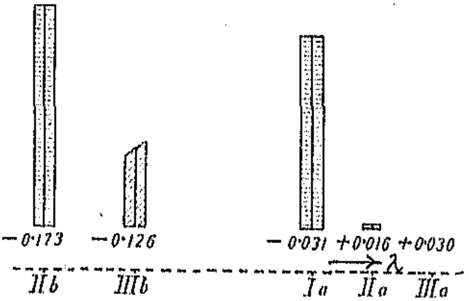

Fig. 13. Hα-components as obtained from Hansen's analysis.

But this figure shows a rather strong component on the red side of the violet component II *b*. Calculation shows that this exactly corresponds to III *b* which corresponds to the transition $3_1 \rightarrow 2_1$ and is forbidden according to selection principles. But III *b* is a rather strong line. The red component is also assymmetric (see curve), but this is probably due to III *a*. Further, according to theory, the red component I*a* should be stronger than the violet II *b*, but this is not seen to be the case.

177. Fine Structure of He⁺ Lines.—He⁺-lines possess the Rydberg number $4R$ corresponding to $Z=2$ in formula (7′). Hence the separation ought to be $2^4=16$ times larger than in the case of corresponding hydrogen lines. Hence for testing Sommerfeld's theory of fine structure, Paschen chose the line

$$\lambda\, 4686 = 4\, R_{\mathrm{He}} \left(\frac{1}{3^2}-\frac{1}{4^2}\right) \quad . \quad . \quad . \quad . \quad . \quad . \quad . \quad (30)$$

Actually the separation is not so large, as the denominator is 3^2 in place of 2^2 in the series formula. In this case also it was found that though Sommerfeld's theory is to certain extent supported, certain extra lines occur which are forbidden by the selection principle as in the case of hydrogen. The components of He⁺ according to Sommerfeld's theory are shown in the following scheme.

Table 6.

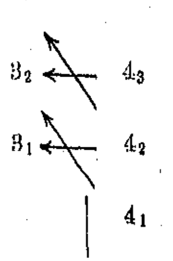

	$\frac{\Delta\nu_{nk}}{R\alpha^2}$	$n=3$	$n=4$	$\frac{\Delta\nu_{nk}}{R\alpha^2}$	
I	$\frac{2^4}{3^4}\cdot\frac{1}{4}$	3_3	4_4	$\frac{2^4}{4^4}\cdot\frac{1}{4}$	*a*
II	$\frac{2^4}{3^4}\cdot\frac{3}{4}$	3_2	4_3	$\frac{2^4}{4^4}\cdot\frac{7}{12}$	*b*
III	$\frac{2^4}{3^4}\cdot\frac{9}{4}$	3_1	4_2	$\frac{2^4}{4^4}\cdot\frac{5}{4}$	*c*
			4_1	$\frac{2^4}{4^4}\cdot\frac{13}{4}$	*d*

We have then the following $\Delta\nu_{nk}$ values for the allowed transitions.

Table 7.

Component	$\Delta\nu_{nk}$	$\Delta\lambda_{nk}$ Å. U. (calc.)	Remark
a I	$R\alpha^2$ (·0337)	−0·04321	Strong
b II	$R\alpha^2$ (·1116)	−0·1430	Strong
c III	$R\alpha^2$ (·3663)	−0·1696	Strong
c I	− $R\alpha^2$ (·0287)	+0·0368	Weak
d II	− $R\alpha^2$ (·0549)	+0·07038	Weak

These deductions may be compared with following microphotometric records (Fig. 14) of the components of λ 4686 obtained by Paschen and his co-workers. In this case the investigators found that there was good deal of difference in the appearance and relative intensities of the lines according as the discharge tube is run by a transformer or by D.C. current. The D.C. discharge gave the best results. The figure shows a number of peaks in the intensity distribution in the line 4686. The peaks stand for the components. The x-axis represents measurements on the comparator. The dispersion being known, λ for any component is known.

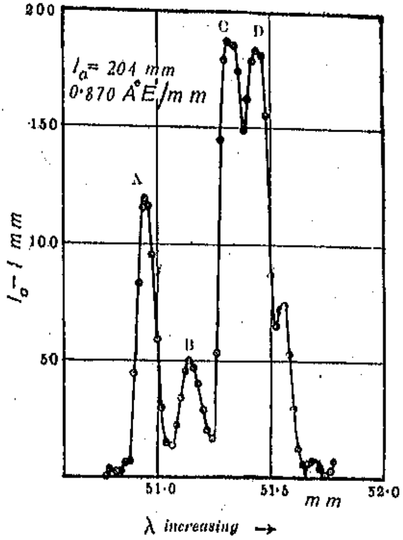

Fig. 14. Paschen's microphotogram of He$^+$ line (λ4685·8 to 4685·9).

The results are analysed in the following table.

Table 8.

	λ observed	λ calculated	Line		Intensity cal.	Intensity obs.
		5·023	II*d*	9+8	·575	———
		·890	I*e*	3	·225	
		·844	II*e*	7+6	·875	
		·837	I*b*	2	1	
D	5·809	·810	I*a*	1	20	7
C	·711	·710	II*b*	4+5	21·66	7·5
B	·553	·544	III*d*	12+13	1·33	1
A	·388	·384	III*e*	10+11	6·50	3

The letters A, B, ... in the first column denote the peaks in curve, reckoned from the left. The wavelength of the zero line has been taken to be λ 4685·8532. The wavelength of I*a* should be $\lambda_0 - \cdot 0432 = 4685 \cdot 810$ according to table 7. We obtain from table 8 $\lambda_{obs.}$ of I*a* = 4685·809. We find that I*a*, II*b*, III*e* come out strongly as expected, *but IIId which is fairly strong, should not, according to the Selection Principle,* occur at all. Further we get two faint companions to the red side of I*a* which will be further discussed.

The observed intensities are given on column 6. The figures in columns 4 and 5 will be explained later.

178. These anomalous results in the fine structure of the lines of H and He^+ were first satisfactorily explained by Goudsmit and Uhlenbeck* on the hypothesis of "rotating electron". Their treatment can be understood only after the reader is familiar with the technicalities of the alkali spectrum to be described in chapter VIII, and with the vector representation of atoms as represented in chapter X. But for the sake of continuity, the treatment is included here; it should be read only after chapters VIII and X are read.

Goudsmit and Uhlenbeck showed that the families of terms in the hydrogen spectrum is just like that of the alkalies, *i.e.*, they consist of

a doublet *s*-sequence $1s,\ 2s,\ 3s,\ 4s \ldots$ with $j=\frac{1}{2}$
a doublet *p*-sequence $2p,\ 3p,\ 4p \ldots$ with $j=\frac{1}{2}$ and $\frac{3}{2}$
a doublet *d*-sequence $3d,\ 4d \ldots$ with $j=\frac{3}{2}$ and $\frac{5}{2}$
a doublet *f*-sequence $4f \ldots$ with $j=\frac{5}{2}$ and $\frac{7}{2}$.

and the energy values of terms having identical n and j, but different k, are the same and given by Sommerfeld's expression for the energy value of the n_k orbit.

Thus we have†

$$2S_{\frac{1}{2}} = 2P_{\frac{1}{2}} = 2_1$$
$$3P_{\frac{3}{2}} = 3D_{\frac{3}{2}} = 3_2.$$

So the diagram showing the transitions should be replaced by the following :

Table 9.

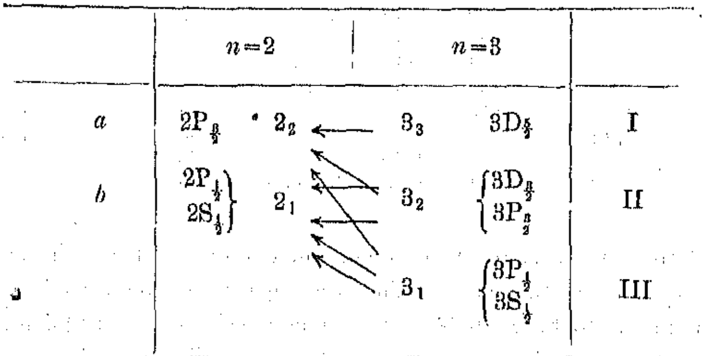

---

* Goudsmit and Uhlenbeck, *Nature*, **117**, 264, 1926 ; *Physica*, **5**, 266, 1925.

† In representing the terms, we are following here the Russell-Saunders' notation. $^2S_{\frac{1}{2}}$ stands for $3^2S_{\frac{1}{2}}$, where the superscript 2 to the left of S denotes that it is a doublet. This has been omitted as it is common to all terms. The number 3 to the left denotes total quantum number.

The actual number of components expected is indicated schematically in Table 10 and Fig. 15. An approximate idea of intensity of the lines can also be formed from the nature of the transitions giving rise to them, remembering that transitions for which $\triangle k = -1$ give strong lines, and $\triangle k = +1$ give weak lines.

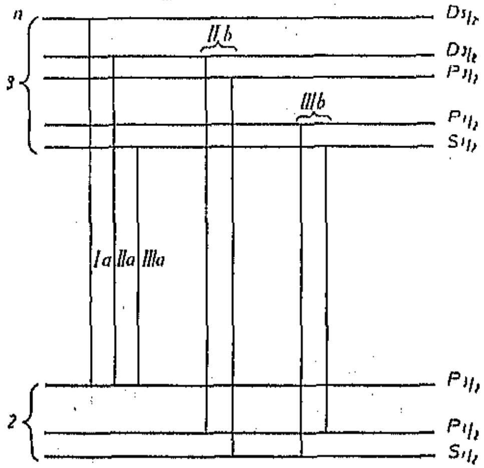

Fig. 15. The components of Hα according to the Spin-theory.

Table 10.—Fine structure components of Hα

lines . . . . . . components	$\triangle\lambda_{nk}$ Å. U.		Intensity	
	Calcul.	Observed	Calcul.	Observed
I*a* . . . $2P_{3/2} - 3D_{5/2}$	−0·03314	−0·031	9	9
II*b* . . . $(2P_{1/2} - 3D_{3/2}) + (2S_{1/2} - 3P_{3/2})$	−0·173	−0·173	7·08	8·4
II*a* . . . $2P_{3/2} - 3D_{3/2}$	. . .	+0·016	1	
III*b* . . . $(2P_{1/2} - 3S_{1/2}) + (2S_{1/2} - 3P_{1/2})$	. . .	−0·126	1·18	
III*a* . . . $2P_{3/2} - 3S_{1/2}$	+0·0304	+0·030	·18	

We thus see that according to the Theory of Goudsmit and Uhlenbeck there ought to be as many as seven components in Hα, but a few overlap, leaving us 5 independent components. Of these, the last one is due to transition having $\triangle k = +1$ and is therefore rather faint. On account of great breadth of all H-lines, it is not found possible to separate the components unambiguously, but the presence of III*b* is unmistakable. The calculated and observed values of $\triangle\lambda_{nk}$ and intensities are shown in columns 2 and 3 of the last scheme (Table 10). From these results the explanation given by Goudsmit and Uhlenbeck is found to be corroborated beyond doubt.

We can explain in a similar way the occurrence of extra components of λ 4686 of He^+ in Paschen's microphotograph. We find now that the real scheme is :—

Table 11.

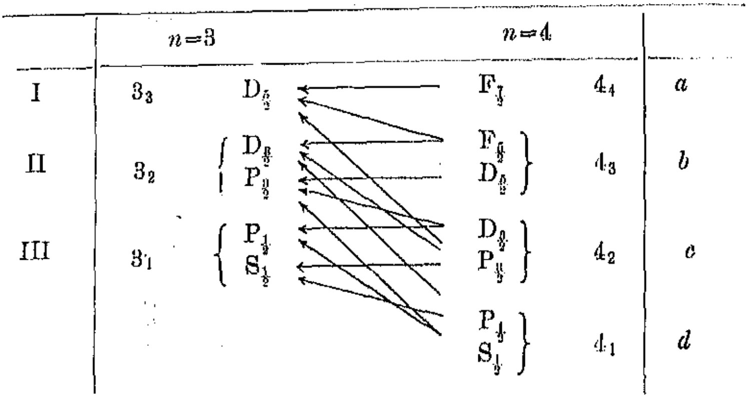

instead of table 6 on p. 348, so that the number of components are 13.

Table 12.—Fine structure components of He^+4686.

Identification	$\triangle\lambda_{nk}$ (Å. U.)		Intensity	
	Calculated	Observed	Calculated	Observed
a I...$D_{\frac{5}{2}} - F_{\frac{7}{2}}$	−·0432	−·0442	20	7
b II...$(D_{\frac{3}{2}} - F_{\frac{5}{2}})+(P_{\frac{3}{2}} - D_{\frac{5}{2}})$	−·1430	−·1422	21·66	7·5
c III...$(P_{\frac{1}{2}} - D_{\frac{3}{2}})+(S_{\frac{1}{2}} - P_{\frac{3}{2}})$	−·4696	−·4652	6·48	8
b I...$D_{\frac{5}{2}} - F_{\frac{5}{2}}$	+·016		1	...
c I...$D_{\frac{5}{2}} - P_{\frac{3}{2}}$	+·0368	+·0488	·22	2
c II...$(D_{\frac{3}{2}} - P_{\frac{3}{2}})+(P_{\frac{3}{2}} - D_{\frac{3}{2}})$	−·009		·875	...
d II...$(D_{\frac{3}{2}} - P_{\frac{1}{2}})+(P_{\frac{3}{2}} - S_{\frac{1}{2}})$	+·07038		·57	0
d III...$(P_{\frac{1}{2}} - S_{\frac{1}{2}})+(S_{\frac{1}{2}} - P_{\frac{1}{2}})$	−·309	−·300	1·335	1

These components are diagrammatically shown in Fig. 16.

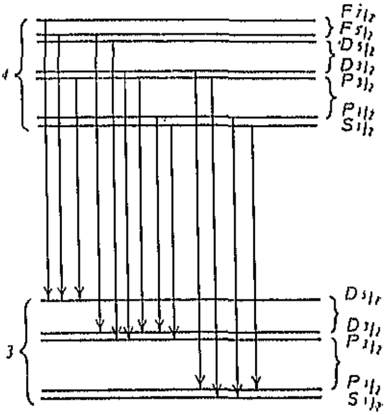

Fig 16. The components of He^+4686 according to the spin-theory.

Thus theoretically, as many as 13 components may exist of which a few overlap. Six components are distinctly observed. The calculated and observed values of wavelengths $\Delta\lambda_{nk}$, and intensities are given in columns 2, 3 and 4, 5 of table 12.

The agreement is again quite satisfactory, inasmuch as the theory accounts for all the observed lines both with respect to their wavelengths as well as their intensities.

179. Intensity of the Components.—The treatment of the problem becomes incomplete without a discussion of the relative intensities of the components.* The subject of intensity will be taken in a later chapter, but a brief resume may be given here. The Hα-line consists of components which can be shown in the following multiplet form.

3 2	$^2S_{\frac{1}{2}}$	^2P	$^2P_{\frac{3}{2}}$	$^2D_{\frac{3}{2}}$	$^2D_{\frac{5}{2}}$
$S_{\frac{1}{2}}$		6 1	5 2		
$P_{\frac{1}{2}}$	7 1			4 5	
$P_{\frac{3}{2}}$	2			2 1	1 9

Thus of the 7- theoretical components of Hα those marked

1, 2, 4 form a *pd*- multiplet
5, 6 ... *sp*- ...
3, 7 ... *ps*- ...

---

* Saha and Banerjee, *Zs. f. Phys.*, **68**, 704, 1931.

The relative intensities in *any* multiplet are given by the numbers within each small square. Thus for the three *pd*-lines

$$P_{\frac{3}{2}} - D_{\frac{5}{2}} : P_{\frac{3}{2}} - D_{\frac{3}{2}} : P_{\frac{1}{2}} - D_{\frac{3}{2}} = 9 : 1 : 5.$$

according to the Ornstein-Dorgelo* rule (*vide infra*).

But we cannot form any precise estimate of the intensity of any line unless the relative values of the intensities of each multiplet are known. These have been calculated in recent years with the aid of quantum mechanics. The units of intensities in the three multiplets are to each other as

$$\begin{array}{ccccc} 2p-3d & : & 2s-3p & : & 2p-3s \\ 1 & : & 1{\cdot}04 & : & {\cdot}09 \end{array}$$

This enables us to calculate the relative intensities of the various separable components as shown in the table below.

Table 13.

	Line.	Line in multiplet.	Intensity.	
Chief red component	I*a*	1	9×1	= 9
Chief violet component.	II*b*	4+5	5+2 (1·04)	= 7·08
	III*b*	6+7	1 (1·04)+1×·09	= 1·13
	II*a*	2	1	= 1
	III*a*	3	·2×·09	= ·18

Most investigators, contrary to the above calculations, have found the violet component of Hα to be stronger than the red component. Otherwise the presence and intensity of III*b* is well-accounted for. II*a* and III*a* are too close to each other to be distinguished.

Recently this problem was investigated by Keussler in absorption. He finds that the red component is more strongly absorbed than the violet component, and the ratio between the absorption coefficients is ·76, whereas theory requires 7·06/9=·78. The apparent weakening of the red component in emission appears to be due to self-absorption.

---

* Ornstein and Lindeman, *Zs. f. Phys.*, **67**, 1, 1931.

The He⁺ - line λ 4686.—We shall now discuss the intensities of the components of the He⁺ line λ 4686. These form five multiplets as sketched in the following diagram, and their relative intensities are shown below.

Table 14.—Intensity of He⁺ λ 4686.

		d		*c*		*b*		*a*
		$S_{\frac{1}{2}}$	$P_{\frac{1}{2}}$	$P_{\frac{3}{2}}$	$D_{\frac{3}{2}}$	$D_{\frac{5}{2}}$	$F_{\frac{5}{2}}$	$F_{\frac{7}{2}}$
III	$S_{\frac{1}{2}}$		1 $\boxed{12}$	2 $\boxed{11}$				
	$P_{\frac{1}{2}}$	1 $\boxed{13}$			5 $\boxed{10}$			
II	$P_{\frac{3}{2}}$	2 $\boxed{8}$			1 $\boxed{6}$	9 $\boxed{5}$		
	$D_{\frac{3}{2}}$		5 $\boxed{9}$	1 $\boxed{7}$			14 $\boxed{4}$	
I	$D_{\frac{5}{2}}$			9 $\boxed{3}$			1 $\boxed{2}$	20 $\boxed{1}$

The units of intensities in the different multiplets are :

$$\begin{array}{ccccccccc} 3d-4f & : & 3p-4d & : & 3s-4p & : & 3d-4p & : & 3p-4s \\ 1 & : & \cdot 85 & : & 1\cdot 11 & : & \cdot 025 & : & \cdot 225 \end{array}$$

So the intensities of the components are as follows:

I *a* . . . . . 1 × 20 = 20
II *b* . . . . . 1 × 14 + ·85 × 9 = 21·65
III *c* . . . . . ·85 × 5 + 1·11 × 2 = 6·48
I *b* . . . . = 1
I *c* . . . . . 9 × ·025 = ·225
II *c* . . . . . 1 × ·025 + 1 × ·85 = ·875
II *d* . . . . . 5 × ·025 + 2 × ·225 = ·575
III *d* . . . . . 1 × ·225 + 1·11 = 1·335

These calculations are given in column 4, 5 of Table 8. The results are in very good agreement with observed values.

180. The Fine Structure of Hydrogen Lines.—According to the special theory of relativity, the kinetic energy of a particle is given by

$$T = m_0c^2\left[\frac{1}{\sqrt{1-\beta^2}} - 1\right], \text{ where } \beta = \frac{v}{c} \quad . \quad . \quad . \quad . \quad . \quad . \quad (31)$$

Hence the total energy W of the electron is

$$W = T + V = m_0c^2\left[\frac{1}{\sqrt{1-\beta^2}} - 1\right] - \frac{e^2Z}{r} \quad . \quad . \quad . \quad (32)$$

For simplification, let us use $E = W + m_0c^2$. Then

$$E = \frac{m_0c^2}{\sqrt{1-\beta^2}} - \frac{e^2Z}{r} \quad . \quad . \quad . \quad . \quad . \quad . \quad . \quad . \quad . \quad . \quad (32')$$

whence

$$\frac{1}{\sqrt{1-\beta^2}} = \frac{E + e^2Z/r}{m_0c^2} \quad . \quad . \quad . \quad . \quad . \quad . \quad . \quad . \quad . \quad . \quad (33)$$

Again, we have

$$p_r = m\dot{r}, \; p_\theta = mr^2\dot{\theta} \quad . \quad . \quad . \quad . \quad . \quad . \quad . \quad . \quad (34)$$

Hence

$$v^2 = \dot{r}^2 + r^2\dot{\theta}^2 = \left(\frac{p_r}{m}\right)^2 + \left(\frac{p_\theta}{mr}\right)^2$$

or

$$\beta^2 = \frac{v^2}{c^2} = \frac{1}{m^2c^2}\left[p_r^2 + \frac{p_\theta^2}{r^2}\right] \quad . \quad . \quad . \quad (35)$$

The quantity m in this formula is the relativity mass $= m_0/1\sqrt{-\beta^2}$. Hence we have from (35)

$$\frac{1}{1-\beta^2} = 1 + \frac{1}{m_0^2c^2}\left(p_r^2 + \frac{p_\theta^2}{r^2}\right)$$

From (32′), and the last expression, we obtain

$$\frac{1}{m_0^2c^4}\left(E + \frac{e^2Z}{r}\right)^2 = 1 + \frac{1}{m_0^2c^2}\left(p_r^2 + \frac{p_\theta^2}{r^2}\right)$$

or

$$p_r^2 + \frac{p_\theta^2}{r^2} = \frac{\left(E + \frac{e^2Z}{r}\right)^2}{c^2} - m_0^2c^2 \quad . \quad . \quad . \quad . \quad (36)$$

Let us now introduce the quantum conditions

$$\oint p_\theta\, d\theta = kh, \qquad \oint p_r\, d_r = n'h \quad . \quad . \quad . \quad . \quad (37)$$

The first reduces to $p_\theta = kh/2\pi$. Substituting this value of p_θ in (36), we obtain

$$p_r^2 = A + \frac{2B}{r} + \frac{C}{r^2} \quad . \quad . \quad . \quad . \quad . \quad . \quad . \quad . \quad . \quad . \quad . \quad (38)$$

where $A = \frac{E^2}{c^2} - m_0^2c^2$, $B = e^2Z\frac{E}{c^2}$, $C = -\frac{h^2}{4\pi^2}(k^2 - \alpha^2Z^2)$ (39)

where α is the constant $2\pi e^2/ch$ (Sommerfeld's fine-structure constant). From the second quantum condition, we have

$$\oint p_r\, dr = n'h$$

i.e.
$$\oint \sqrt{A + \frac{2B}{r} + \frac{C}{r^2}} = n'h$$

The integration can be effected by the method of residues. We obtain :

$$n'h = -2\pi i\left\{\sqrt{C} - \frac{B}{\sqrt{A}}\right\}$$

Substituting the values of A, B, C, we obtain

$$\frac{E}{\sqrt{m_0{}^2c^4 - E^2}} = \frac{1}{\alpha Z}\left(n' - \sqrt{k^2 - \alpha^2Z^2}\right) \quad \ldots\ldots \quad (40)$$

From this, we obtain, after some work,

$$E = m_0c^2\ \left\{1 + \frac{\alpha^2Z^2}{(n' + \sqrt{k^2 - \alpha^2Z^2})^2}\right\}^{-\frac{1}{2}}$$

or
$$W = m_0c^2\left[\left\{1 + \frac{\alpha^2\ Z^2}{(n' + \sqrt{k^2 - \alpha^2Z^2})^2}\right\}^{-\frac{1}{2}} - 1\right]. \quad \ldots \quad (41)$$

We find, as a first approximation, that

$$W = -\tfrac{1}{2}\ \frac{m_0c^2\alpha^2Z^2}{(n'+k)^2} = -\frac{2\pi^2m_0e^4Z^2}{(n'+k)^2h^2} \quad \ldots\ldots \quad (41')$$

as obtained in the simple theory.

Let us now carry out the second approximation. We notice that

$$n' + \sqrt{k^2 - \alpha^2Z^2} = (n' + k)\left(1 - \frac{\alpha^2Z^2}{2kn}\right)$$

and
$$\left(n' + \sqrt{k^2 - \alpha^2Z^2}\right)^{-2} = \frac{1}{n^2}\left(1 + \frac{\alpha^2Z^2}{kn}\right)$$

and
$$E = m_0\, c^2\left\{1 + \frac{\alpha^2Z^2}{n^2} + \frac{\alpha^4Z^4}{kn^3}\right\}^{-\frac{1}{2}} \quad \ldots\ldots \quad (42)$$

This is of the form $(1+\beta+\gamma)^{-\frac{1}{2}}$, where β, is of the first order, γ is of the second order. We have then

$$(1+\beta+\gamma)^{-\frac{1}{2}} = 1 - \tfrac{1}{2}\beta + \tfrac{3}{8}\beta^2 - \tfrac{1}{2}\gamma$$

$-\frac{1}{2}\beta m_0c^2$ gives us the expression (41′).
The second order term is

$$\tfrac{3}{8}\beta^2 - \tfrac{1}{2}\gamma = -\frac{Rh\alpha^2Z^4}{n^4}\left(\frac{n}{k} - \frac{3}{4}\right)$$

which is the second order term in (28).

Hence we have

$$W = -\frac{2\pi^2 m_0 e^4 Z^2}{h^2(n'+k)^2} - \frac{Rh\alpha^2 Z^4}{n^4}\left(\frac{n}{k} - \frac{3}{4}\right) \quad . \quad . \quad . \quad . \quad (27a)$$

This expression has been quoted on page 345 and is suitable for practical use, as shown in §176.

181. Orientation of the Kepler-Orbits.*—In §174, it was supposed that the motion of the electron was confined to one particular plane (r, θ). This condition is unnecessary. We can suppose that the co-ordinates of the electron are (r, θ, φ) as shown in Fig. 17. AKA′ is the orbit of the electron, OP the external axis. Q denotes the position of the electron in the orbit at any time. It has the declination angle $\pi/2 - \theta$, and the right ascension φ. ON is the normal to the orbit of the electron, $\angle PON = \alpha$ is the tilt of the orbit to the equatorial plane E′KE. Then we have

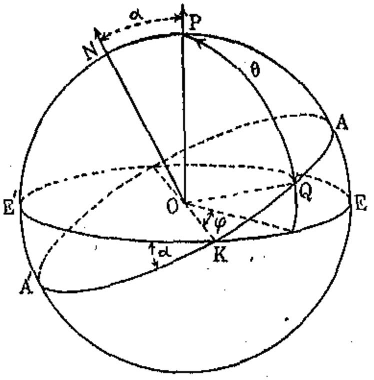

Fig. 17. Position of an electron in the $(r, \theta, \phi,)$ diagram.

$$\left.\begin{array}{l} T = \frac{1}{2} m\,(\dot{r}^2 + r^2\dot{\theta}^2 + r^2 \sin^2\theta\,\dot{\varphi}^2), \qquad V = -\frac{e^2}{r} \\ p_r = m\dot{r}, \quad p_\theta = mr^2\dot{\theta}, \quad p_\phi = mr^2 \sin^2\theta\,\dot{\varphi} \end{array}\right\} \quad . \quad . \quad . \quad (28)$$

T can also be written in terms of the p's as

$$T = \frac{1}{2m}\left[p_r^2 + \frac{p_\theta^2}{r^2} + \frac{p_\phi^2}{r^2 \sin^2\theta}\right] \quad . \quad . \quad . \quad . \quad . \quad (29)$$

It is also clear that

$$T = \tfrac{1}{2}\,[p_r\,\dot{r} + p_\theta\,\dot{\theta} + p_\phi\,\dot{\varphi}] \quad . \quad . \quad . \quad . \quad . \quad . \quad . \quad (30)$$

The quantum-conditions are

$$\oint p_r\,dr = n'h, \quad \oint p_\theta\,d\theta = k_1 h, \quad \oint p_\phi\,d\varphi = k_2 h,$$

The limits are for r from . . . $r_{\min}$ to $r_{\max}$ and back,
φ from . . . 0 to 2π
θ from . . . $\theta_{\min}$ (PA) to $\theta_{\max}$ (PA′) and back,

---

* See A. Sommerfeld, *Atombau und Spektrallinien* (1924), Chap. 2, p. 139.

We thus see that in place of k, we have k_1 and k_2. It can be shown that

$$k = k_1 + k_2 \quad . \quad . \quad . \quad . \quad . \quad . \quad . \quad . \quad . \quad . \quad (31)$$

To see this, let us suppose that the actual orbit is in the plane OA which makes an angle of α with the equatorial plane. Then we can refer the motion of the electron to r and ψ, where ψ represents the angle described by the radius vector in the plane OAA$'$. Now we have

$$\oint p_\psi \, d\psi = kh \quad . \quad . \quad . \quad . \quad . \quad . \quad . \quad . \quad . \quad . \quad (32)$$

Now since $T = \frac{1}{2} (p_r \dot{r} + p_\theta \dot{\theta} + p_\phi \dot{\varphi}) = \frac{1}{2} (p_r \dot{r} + p_\psi \dot{\psi})$,

we can put
$$\left.\begin{array}{l} p_\psi \dot{\psi} = p_\theta \dot{\theta} + p_\phi \dot{\varphi} \\ \oint p_\psi \, \delta\psi = \oint p_\theta \, d\theta + \oint p_\phi \, d\varphi \end{array}\right\} \quad . \quad . \quad . \quad . \quad . \quad (33)$$
and

the limits being defined as before.

Now p_ψ is the whole momentum in the orbital plane, and p_ϕ its component in the equatorial plane. Their vectors are perpendicular to ON and OP respectively. We have therefore:

$$p_\phi = p_\psi \cos \alpha, \qquad \angle \alpha = \text{PON}$$

or from (33),
$$k = k_1 + k_2, \qquad k_2 = k \cos \alpha$$

Thus
$$\cos \alpha = \frac{k_2}{k_1 + k_2}, \qquad k_1 + k_2 = k \quad . \quad . \quad . \quad . \quad . \quad . \quad (34)$$

These mathematical considerations show that the orbits cannot be orientated at random, but only at definite angles given by $\cos^{-1} k_2/(k_1+k_2)$ to the external axis. When k is given, k_2 can have all integral values below k, *i.e.*, $k, k-1, \ldots 0 \ldots . -k$. Hence α is given by

$$\cos^{-1} 1 = 0, \quad \cos^{-1} \frac{k-1}{k}, \ldots \quad \cos^{-1} 0 = \frac{\pi}{2}, \ldots \cos^{-1} (-1) = \pi$$

as shown in Fig. 17a for $k = 1$, $k = 2$ and $k = 3$.

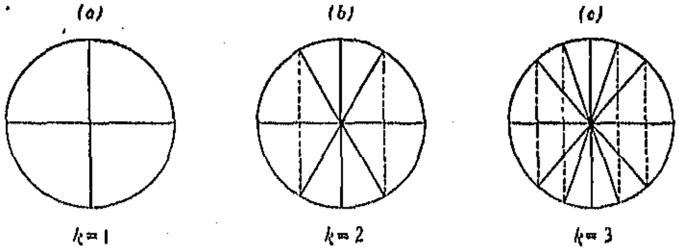

Fig. 17a. The orientation of Kepler-orbits.

The energy of the orbit of course remains unchanged. Strictly speaking the orbits AKA$'$ and EKE$'$ in Fig. 17, and the others shown in Fig. 17a

should be confocal ellipses with the external orbit passing through their common focus. But this does not alter our arguments given above.

Books Recommended.

1. A. Fowler's *Report on Series in Line Spectra* (1922).
2. A. Sommerfeld, *Atombau und Spectrallinien* (1924) (English Translation, 1923).
3. W. Grotrian, *Handbuch der Astrophysik*, III/2, (1930).
4. R. C. Gibbs, *Review of Modern Physics*, 4, 278 (1932),
5. L. Pauling and S. Goudsmit, *Structure of the Line Spectrum* (1930).
6. F. Hund, *Linien Spektren und Periodisches System der Elemente* (1927).
7. A. Smekal, *Quanten* (1933), Kap. 3.
8. P. Foote and F. Mohler, *The Origin of Spectra* (1922).
9. N. Bohr, *Theory of Spectra and Atomic Constitution* (1922).
10. M. Born, *Problems of Atomic Dynamics* (1926).
11. W. Pauli, *Quantentheorie* in *H. d. Phys.*, 23, Kap. 1, 1926.
12. A. Ruark and H. Urey, *Atoms, Molecules and Quanta* (1930).

CHAPTER VIII

SPECTRA OF THE ALKALI METALS—THE DOUBLET SPECTRUM

182. General Description.—Next to hydrogen, the spectra of the alkali atoms are the simplest in structure. It has been found that amongst themselves they show a strong *family likeness*. Hence it will suffice to describe only the spectrum of sodium whose structure will be clear from the photograph shown in Fig. 1, Plate VI.

An examination of the photograph shows that a large number of lines in this spectrum occurs in *pairs*. Hartley showed in 1890 that the wave-number difference between the two lines of a doublet is constant, *viz*., 17 in the case of Na. This is also a characteristic feature of the other alkali metals and of many other elements; generally this constant frequency difference increases roughly as the square of the atomic number.

Further scrutiny of the spectrum of sodium shows that the doublets are alternately *sharp* and *diffuse*. They can therefore be separated into two groups as shown in Fig. 1 under the heading *sharp* and *diffuse*. As a first step towards the analysis of the spectrum, Rydberg separated the two groups, sharp and diffuse, as shown in Table 1 on the next page.

Next, the frequencies of the longer member of each pair in the two sets were plotted against successive integral numbers, beginning from $n=2$, as shown in Fig. 2. It was found that both the sharp and diffuse sets tend to come to the same limit.

From the form of the curve, Rydberg suggested that the lines of the sharp series may be represented roughly by a modified Balmer formula

$$\nu_1 = A_1 - \frac{R}{(n+s)^2}, \quad \nu_2 = A_2 - \frac{R}{(n+s)^2} \quad . \quad . \quad . \quad . \quad . \quad (1)$$

where n is the running integral number, *viz*., 3, 4,......, and s is a fraction which was found to be roughly 0·643 for sodium, and the constants were found to have the values

$$A_1 = 24475{\cdot}65,\ A_2 = 24492{\cdot}83,\ A_2 - A_1 = 17{\cdot}18.$$

Table 1.—Sharp and Diffuse Lines of Sodium.

n	ν Sharp Series	$\Delta\nu$	ν Diffuse series	$\Delta\nu$
2	8766·3 8783·1	16·8	12199·5 216·6	17·1
3	16227·4 16244·5	17·1	17575·3 592·5	17·2
4	19398·3 19415·5	17·2	20063·2 20080·3	17·1
5	21038·4 21055·6	17·2	21413·7 21430·9	17·2
6	21995·0 22012·2	17·2	22227·1 22244·2	17·1
7	22601·2 22618·4	17·2	22754·8 22771·9	17·1
8	23009·6 23027·1	17·5	23118·7 23135·3	16·6
9	23300·3 23317·1	16·8	23377·0 23394·0	17·0

This formula may be regarded as a generalization of Balmer's formula for hydrogen. Rydberg showed that R has approximately the same value in both cases, *viz.*, 109678 cm.$^{-1}$

The lines of the diffuse series are represented by an analogous formula :—

$$\nu_1 = A_1 - \frac{R}{(n+d)^2}, \quad \nu_2 = A_2 - \frac{R}{(n+d)^2} \quad . \quad . \quad . \quad (2)$$

where A_1, A_2 *have the same values as in the case of sharp series*, d is another fraction whose value is 0·998 for sodium.

These two series include most of the lines, but a group of strong lines including the strongest lines D_1, D_2 and the lines λ 3303, 2852 are found *not* to be included in the above formulæ as shown in Fig. 1 though the frequency difference of the two D-lines is just 17. For the other lines, $\Delta\nu$ progressively diminishes. These lines are taken in a later section.

The Rydberg-Schuster Law.—For every other alkaline element, the characteristic lines can be grouped into sharp and diffuse series

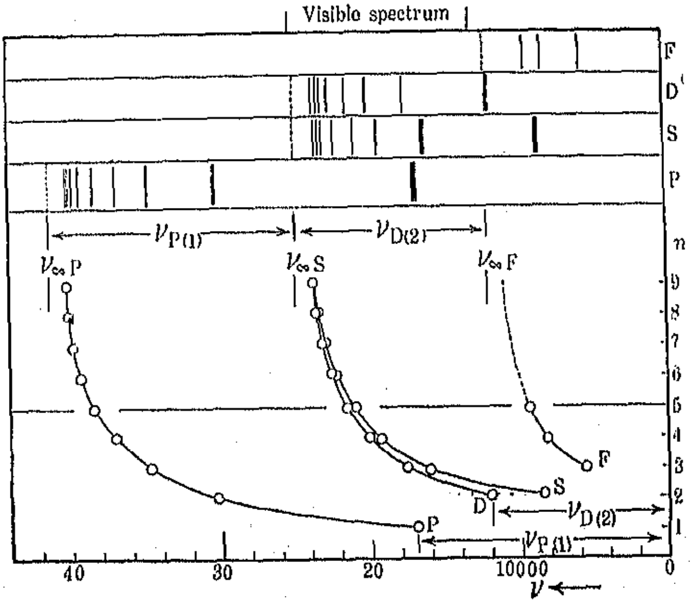

Fig. 2. The (ν-n) diagram for sodium.

as in the case of Na, but Δν increases with the atomic number. We have in fact for

	Li	Na	K	Rb	Cs
Δν =	3	17·3	57·7	237·5	554·0

For lithium Δν is so small that the lines appear single unless high resolving power be used. In lithium also, we have, besides the series of sharp and diffuse lines, a strong group of lines including the strongest line λ 6708 which could not be classified. But Rydberg and Schuster observed that if in the formula for sharp series* for Li

$$\nu = A_1 - \frac{R}{(n+s)^2} = 28601{\cdot}1 - \frac{109721{\cdot}6}{(n+{\cdot}5951)^2}\ , n = 2, 3\ ..$$

we give to n the value 1, we get a frequency

$$\nu = A_1 - \frac{R}{(1+s)^2} = 28601{\cdot}1 - 43380 = -\ 14779 \quad . \quad . \ (3)$$

The inverse of this frequency is

$$\lambda = \frac{10^8}{14779}\ \text{Å} = 6766\ \text{Å}.$$

---

* For Li $A = 28601{\cdot}1$, $s = {\cdot}5951$, $d = {\cdot}9974$.

Allowing for the roughness of the formula used, Rydberg and Schuster felt convinced that the principal line of lithium λ 6708 formed the *negative member of the sharp series*,

i.e.
$$-\frac{1}{\lambda 6708} = A - \frac{R}{(1+s)^2} \quad . \; . \; . \; . \; . \; . \; . \; . \quad (3')$$

We may now invert the formula, and regard λ 6708 as the leading member of a new series

$$\nu = \frac{R}{(1+s)^2} - \frac{R}{(n+p)^2}, \quad . \; . \; . \; . \; . \; . \; . \; . \quad (4)$$

where p is so chosen that $R/(2+p)^2 = 28601$, the convergence limit of the sharp and diffuse series, p is found to have the value $-\cdot 0424$. The other members of this series are obtained if we give to n the values 3, 4, 5, 6, ... They give us approximately the lines which are not included in the sharp or diffuse series, *viz.*, λ 3232, λ 2741 ......, which form a new series. This is known as the *Principal Series* for reasons stated later.

183. The Families of Terms in the Alkali Spectrum.—Summarising the result in the case of lithium, we find that the oscillation number of each line can be regarded as in the case of hydrogen as the difference between two terms

$$\nu = T_1 - T_2 \quad . \; . \; . \; . \; . \; . \; . \; . \; . \quad (5)$$

The terms can be represented approximately by the general type of formula

$$T = R/(n+\varphi)^2$$

where R is the Rydberg number, φ is a fraction characteristic of the series and the element, and n is the running integral number, which starts with 1, 2 or 3 and can take up all successive integral values. For an alkali element, we have a number of characteristic values of φ, giving us different families of terms. For Lithium, we have the families

$$\left.\begin{aligned} ns &= \frac{R}{(n+s)^2} = \frac{R}{(n+\cdot 5951)^2}, \quad n=1, 2, 3, .. \\ np &= \frac{R}{(n+p)^2} = \frac{R}{(n-\cdot 0404)^2}, \quad n=2, 3, 4, .. \\ nd &= \frac{R}{(n+d)^2} = \frac{R}{(n-\cdot 0026)^2}, \quad n=3, 4, 5 .. \end{aligned}\right\} \quad . \; . \; . \quad (6)$$

The formulæ are only approximate. For better representation, a Hicks or Ritz type of formula (*vide infra*) involving more constants is preferable.

Following Paschen, it is usual to denote a term by the symbol nx. Thus $4p$ denotes the fourth member of the p-series which is approximately represented by $R/(4+p)^2$.

It is clear that in the case of alkalies $1s$ is the biggest term. The principal series is represented for lithium by

$$\nu = 1s - np = \frac{R}{(1+s)^2} - \frac{R}{(n+p)^2}, \quad n = 2, 3, \quad . \quad . \quad (7)$$

where $s = \cdot5951$, $p = -\cdot0404$

The sharp series is represented by

$$\nu = 2p - ns = \frac{R}{(2+p)^2} - \frac{R}{(n+s)^2}, \quad n = 2, 3, \quad . \quad . \quad (8)$$

The diffuse series is represented by

$$\nu = 2p - nd = \frac{R}{(2+p)^2} - \frac{R}{(n+d)^2}, \quad n = 3, 4, \quad . \quad . \quad (9)$$

In the case of the other alkali elements the same laws hold good, only the p-terms are double, *i.e.*, we have two close sets of terms

$$\frac{R}{(n+p_1)^2}, \frac{R}{(n+p_2)^2}$$

which are represented by the symbols np_1, np_2. It is the difference

$$\triangle\nu = R\left[\frac{1}{(2+p_1)^2} - \frac{1}{(2+p_2)^2}\right] \quad . \quad . \quad . \quad . \quad . \quad . \quad . \quad (10)$$

which give the spectra their characteristic doublet appearance. Lithium is also no exception, the p-terms are double, but $\triangle\nu$ is very small being equal to 3. Hence it was neglected in the preliminary discussions. Closer investigations showed that the d-terms are also double, but the difference is small except in the case of the heaviest elements. For Cs, $3d' - 3d = 98$, for Rb it is 8·0 (for $4d' - 4d$), and for K, the difference is 2·74.

It has already been mentioned that the formula used for representing a family of terms, say $ns = R/(n+s)^2$ . . . is only approximate. For accurate representation, many other types of formulæ involving a larger number of constants are used.

Before the reader can fully grasp this point, he should have a good acquaintance with the methods used for calculating the absolute values of terms. For details, A. Fowler's *Report on Series in Line Spectra* (Chapter V) should be consulted, but some rough ideas of the procedure may be given here.

It is clear from the series representations, that if we can fix up the value of *any single term* of the atomic spectrum accurately, the correct values of the other terms can be easily found. For example, in the Sharp Series we have

$$\nu \text{ for a line} = 2p_1 - ns \text{ or } 2p_2 - ns.$$

So if we know either $2p_1$ or $2p_2$ correctly, we obtain

$$ns = 2p_{1,2} - \nu$$

Hence from the value of the wavelengths of the members of the sharp series, the absolute value of all ns terms can be calculated. Similarly, if we can trace the successive members of the diffuse series, the nd-terms also can be obtained.

Convergence Frequency.—Let us now see how the absolute values of $2p_1$ or $2p_2$ or any other term can be accurately calculated. It is easy to see that *this can be done the more accurately, the larger is the number of series lines known.* Suppose, we can trace the $2p-ns$ series up of Na to the 10th line. Then we have for

$$\nu = 2p_1 - 12s = 23797\,; \quad 2p_1 = \nu + 12s$$

$$12s = \frac{R}{(12+s)^2} = \frac{109678}{(12+\cdot 65)^2} = 679$$

Hence $$2p_1 = 23797 + 679 = 24476.$$

A slight error in the value of s does not change the value of $12s$ materially, as it is added to a large integral number. Hence the value of $12s$ as given above may be taken to be nearly correct. 's' is obtained from a preliminary Rydberg representation, and may be improved by successive approximations.

In most of the alkali elements the term-values were calculated with the greatest accuracy by S. Datta who measured the wavelengths of the sharp and diffuse series to a large number of members. But this is not possible in most other elements. In such cases the absolute values of terms are to be calculated from a few sequences, and are liable to large errors.

Representation of Terms.—We have mentioned that the Rydberg formula represents the terms of a family only roughly. We give below a few of the numerous other more accurate formulæ used.

(*a*) Ritz used formulæ of type

$$T = \frac{R}{\left(n+\alpha+\frac{\beta}{n^2}\right)} \quad \ldots \ldots \ldots \quad (11)$$

and certain other variants of this formula.

(*b*) Hicks-Mogendorff:

$$T = \frac{R}{\left(n+\alpha+\dfrac{\beta}{n^2}\right)^2} \qquad \ldots\ldots\ldots \qquad (12)$$

(*c*) Fowler and Reynolds:

$$T = \frac{R}{\left(n+\alpha+\dfrac{\beta}{n}+\dfrac{\gamma}{n^2}\right)^2} \qquad \ldots\ldots\ldots \qquad (13)$$

‡A complete account will be found in Fowler's *Report on Series in Line Spectra*, Chap. V.

184. The Bohr-diagram of Optical Levels of Alkali Elements.

184. The Bohr-diagram of Optical Levels of Alkali Elements.—Bohr represented the levels of alkali atoms by a diagram which has become indispensable for a proper understanding of the quantum theories of spectral lines. This is shown below in Fig. 3.

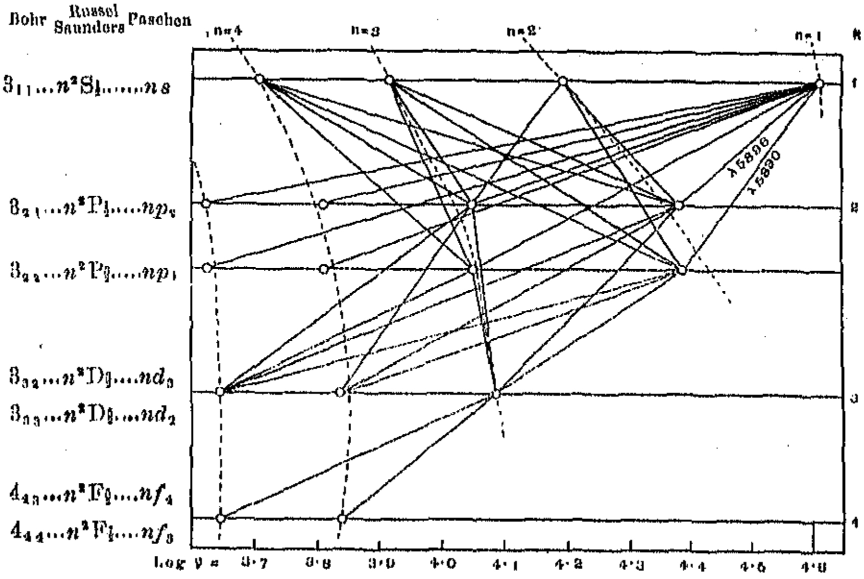
Bohr
Russel Saunders
Paschen
$3_{11} \ldots n^2S_{\frac{1}{2}} \ldots ns$
$3_{21} \ldots n^2P_{\frac{1}{2}} \ldots np_2$
$3_{22} \ldots n^2P_{\frac{3}{2}} \ldots np_1$
$3_{32} \ldots n^2D_{\frac{3}{2}} \ldots nd_3$
$3_{33} \ldots n^2D_{\frac{5}{2}} \ldots nd_2$
$4_{43} \ldots n^2F_{\frac{5}{2}} \ldots nf_4$
$4_{44} \ldots n^2F_{\frac{7}{2}} \ldots nf_3$
n=4
n=3
n=2
n=1
k
1
2
3
4
λ5896
λ5890
Log ν =
3·7
3·8
3·9
4·0
4·1
4·2
4·3
4·4
4·5
4·6

Fig. 3. Bohr-diagram for sodium.

NOTE.—The uppermost horizontal line contains the family of *s*-terms, beginning with $n=1$. The next two contain the families of two *p*-terms. Here *n* . . . begins with 2. The fourth horizontal line contains the *d*-terms beginning with $n=3$. This ought to be shown double. The lowest line contains a fresh set of terms, called *fundamental terms.* There is however nothing fundamental about them and the notation is a misnomer. These terms were inferred from the existence of a set of lines in the infrared discovered by Runge and Bergmann in the spectra of alkali elements ; they can be represented by the series formula

$$\nu = \frac{R}{(3+d)^2} - \frac{R}{(4+f)^2} \text{ or } 3d-4f$$

where f is a very small fraction.

The symbols to the left of the figure are due to Paschen, Russell-Saunders, and Bohr. Paschen's notation has been already explained. The other symbols will be explained in due course.

The abscissa represent log ν and has been drawn to represent the levels of sodium. The diagonal lines represent observed combinations. It should be noted that s-terms combine with p-terms, but not with another s or d-terms . . . . , p-terms combine with s or d-terms, but not with p or f-terms.

185. Importance of the Principal Series.—The lines forming the principal series are not only more intense than lines belonging to the sharp and diffuse groups, but they possess another characteristic property which distinguishes them from the lines of other groups. When an absorption spectrum is taken through the vapour of the element, it is only the lines belonging to the principal series which come out as absorption lines. No lines belonging to the sharp or diffuse series occur in absorption.

This was demonstrated in a large number of experiments carried out by R. W. Wood*, Bevan†, and S. Datta‡ and others.

In these experiments, the metal is contained in a steel tube of about a meter in length which is closed at the two ends by quartz plates. The ends are watercooled, and the body of the tube is heated electrically by wires wrapped round it on asbestos sheets. The pressure is maintained at a few mms. of mercury, and can be varied at will by varying the temperature of the heating coils. A source of continuous light (*e.g.*, an arc fed with boron oxide, or uranium oxide, or a water spark) is rendered parallel by means of a lens and allowed to traverse the column of vapour and received on the slit of a quartz-spectrograph. The resulting spectrum appears as shown in Fig. 4, Plate VI.

Only the principal lines are absorbed, but none of the sharp or diffuse lines.

---

* R. W. Wood, *Astr. Jour.*, **29**, 97, 1909 ; R. W. Wood and R. Fortrat, *ibid.* **43**, 73, 1916.

† Bevan, *Proc. Roy. Soc. A*, **85**, 58, 1911.

‡ S. Datta, *Proc. Roy. Soc. A*, **101**, 542, 1922.

186. Explanation of the Ionisation Potential of Alkali Elements.—Bohr had shown how to interpret these results with the aid of quantum mechanics. An alkali element like Na comes after an inert gas, Neon in this case. These elements further possess the valency unity, and can easily lose one electron and acquire a net positive charge. From these features, it is supposed that the electrons are distributed about the nucleus as shown in the following diagrams (Fig. 5).

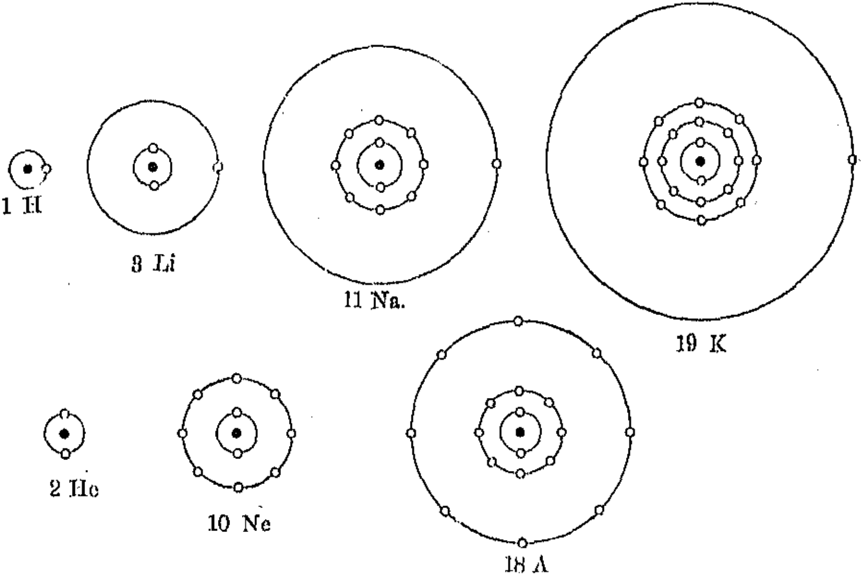

Fig. 5. Distribution of electron in atoms.

Thus the core of Na consists of a nucleus of charge 11, surrounded by two shells of electrons consisting of 2 and 8 electrons respectively. The eleventh electron is at an outer orbit, at a much greater distance. This electron, by its motion is supposed to give rise to the families of terms discussed in §183.

It is clear that the dynamical problem of working out the motion of this electron in the field of the core is an extremely difficult task, and it has not yet been rigorously solved. But the diagram gives us a picture of the various stationary states. It is clear that $-h$ (1*s*) is the energy of the electron in its innermost possible orbit, when the atom is unexcited, just as $-h.R/1^2$ is found to be the energy of the normal H-atom. When the electron is excited, it passes to the higher families of orbits sketched in Fig. 5.

We can find out as in Chap. XIII, the ionisation-potential of the normal sodium atom. We have

$$1s = 41449 = 5{\cdot}12 \text{ volts}$$

i.e., if to the valency electron of the sodium atom, we can add an amount of energy corresponding to 5·12 electron-volts, the electron will pass to infinity, *i.e.*, the atom will be ionised.

The ionisation of sodium can be effected either by electron bombardment (*vide* chap. XIII) or by light when photons possessing an energy content $h\nu$ where $\nu >$ convergence frequency of the p-series is allowed to pass through the vapour. The quanta of light release the valency electron by photoelectric action. We get

$$\text{Na} + h\nu = \overset{+}{\text{Na}} + e \quad . \quad . \quad . \quad . \quad . \quad . \quad . \quad . \quad . \quad (14)$$

The electron is released with the energy $h\,(\nu - \nu_0)$.

This gives rise to continuous absorption beginning at the end of the p-series, and was obtained by several investigators. The absorption is maximum at $\nu = \nu_0$ and gradually becomes fainter.

It is clear that normally all sodium atoms are in the $1s$-state ; when the temperature is raised, some will pass to the higher states, their proportion is given by the Maxwell-formula

$$N = \frac{g_1}{g_0} N_0\, e^{-\epsilon/kT} \quad . \quad . \quad . \quad . \quad . \quad . \quad . \quad . \quad (15)$$

where ϵ = energy-difference between the two states, g_1 and g_0 are weight factors (*vide infra*). We have $g_0 = 2$ for the normal orbit $^2S_{\frac{1}{2}}$. For $^2P_{\frac{1}{2}}$ $(2p_2)$ $g_1 = 2$, for $^2P_{\frac{3}{2}}$ $(2p_1)$ $g_1 = 4$.

For the $2p_1$-state of Na, $\epsilon = -h\,(2p_1)$, so that for the excitation from normal to $2p_1$-state, $\epsilon = h\,[(1s)-(2p_1)]$, *i.e.*, corresponds to λ 5890 = 2·095 volts = 48·33 k. cal. Also $g_0 = g_1 = 2$.

Hence $$ln \frac{N}{N_0} = -\frac{48{\cdot}33 \times 10^3}{1{\cdot}985 \times T} = -\frac{24{\cdot}34 \times 10^3}{T}$$

Therefore, at a temperature of 600°, only $e^{-40{\cdot}6}$ or $2{\cdot}3 \times 10^{-18}$ fraction of Na-atom is in the $2p$-state.

Hence when continuous light passes through Na-vapour, only such pulses are absorbed which can raise the electron from the $1s$ to any allowed higher orbit. Hence only $1s - np$ lines, or lines forming the principal series are absorbed. As the number of atoms in the $2p$-state is negligible, no $2p-ns$, or $2p-nd$ lines are absorbed. But if T be sufficiently raised, say to 2000°K, $N/N_0=5{\cdot}2.10^{-6}$ and we can expect absorption of $2p-ns$ and $2p-nd$ lines. The absorption of $2p-nd$-lines of sodium was first observed by N. K. Sur and R. N. Ghosh.*

We shall now discuss how the motion of the electron gives rise to different families of terms. The explanation was first given by Sommerfeld.

187. Sommerfeld's Interpretation of Families of Terms.—We have seen in Chap. VII that the motion of the electron is characterised in the case of hydrogen by two quantum numbers n and k. Sommerfeld showed that terms belonging to a certain family are characterised by the same value of k.

Thus for the s - family , $k=1$
... p - ... , $k=2$
... d - ... , $k=3$
... f - ... , $k=4$ . . . etc.

e.g., the term $5p$ gives the energy of the 5_2-orbit, $7d$ gives the energy of the 7_3-orbit, etc. . . . . .

Selection Principle.—To explain the observed combinations and absence of other possible combinations Sommerfeld proposed the rule, that *when once the electron is in an excited orbit, it can pass by emission of radiation only to such orbits for which $\Delta k=\pm 1$, or the aximuthal quantum number changes by unity. Changes corresponding to $\Delta k=0, \pm 2$ are forbidden.* Thus for the

principal series $1s-np$, $\Delta k=-1$, ($k=2$ to $k=1$)
diffuse ... $2p-nd$, $\Delta k=-1$, ($k=3$ to $k=2$)
sharp ... $2p-ns$, $\Delta k=+1$, ($k=1$ to $k=2$)

Generally the lines arising from the transition $\Delta k=-1$ are stronger than those arising from $\Delta k=1$.

The principle explains the absence of combinations like $1s-ns$ or $1s-nd$. In the first case $\Delta k=0$, in the second case $\Delta k=2$.

Forbidden Lines.—It is however found that lines corresponding to $\Delta k=0$ or ± 2 occur feebly under special circumstances, *e.g.*, when the emitting centres are in a strong c. s. field. One example of occurrence of $1s-nd$ lines may be found in S. Datta's absorption-experiments. Such lines are said to be due to *forbidden transitions*.

---

* N. K. Sur and R. N. Ghosh, *Phil. Mag.*, **49**, 60, 1925.

Though the selection principle was introduced as an empirical measure to explain observed facts, it later on received theoretical justification from the correspondence principle (*vide infra*).

188. The Doubling of the Levels.—Though Sommerfeld's theory successfully accounts for the occurrence of different families of terms, it gives no explanation of the doubling of the p-levels which imparts to alkali spectra their chief characteristic feature. As mentioned before $\Delta p = 2p_1 - 2p_2$ increases with the atomic weight as can be seen from curve in Fig. 7, in which $\Delta\nu$-values are plotted as the ordinates and the corresponding atomic numbers along the abscissæ. The appearance of the principal lines $1s-2p_1$, $1s-2p_2$ in absorption for alkali elements Li, Na, K, Rb, Cs is shown in the photograph in Fig. 8, Plate VII. The black lines are the absorption lines, while the bright lines are due to the source. It will be noticed that the separation between two absorption lines of each element strikingly increases as we pass from Li to Cs, *i.e.*, with increasing atomic weight.

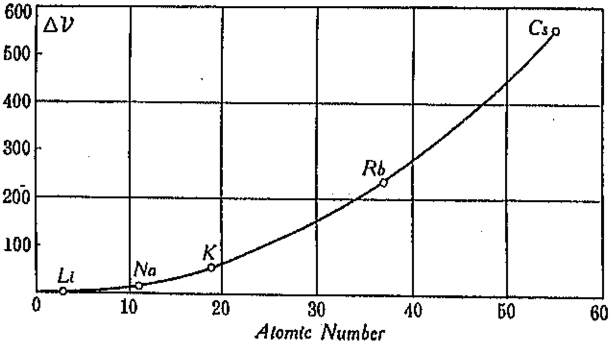

Fig. 7. Variation of doublet separation with atomic number.

The other p-terms are also double, but the difference

$$\Delta\nu = R\left[\frac{1}{(n+p_1)^2} - \frac{1}{(n+p_2)^2}\right]$$

goes on decreasing on account of increasing values of n. For the second member λ 3303 of the p-series of Na, $\Delta\nu = 5{\cdot}49$, for the third member λ 2852, $\Delta\nu = 2{\cdot}49$.

Similarly, it has been found that the *d* and *f*-levels are also double, but the separations $\triangle d$, $\triangle f$ are extremely small, and become apparent only in the case of Rb and Cs. For Cs, $\triangle d = 97·9$. But the combinations between the *p* and *d*-terms are somewhat peculiar. We do not get four lines, but three, as shown below for Cs. An explanation of this fact will be given in Chap. X.

Table 2.

	$2p_1$ 19672·3	$2p_2$ 20226·3
$3d$ 16807·1	2865·2	×
$3d'$ 16905·0	2767·3	3321·3

Summarising, we may say that terms of every family excepting the *s* is double, and this feature has not yet been accounted for (*vide* Chap. X). It is usual to distinguish the two terms by attaching numerical subscripts to them as in p_1, p_2 $(p_1 < p_2)$. This is the old notation followed by Fowler and Paschen. Similar notation is also used to distinguish between the two components of the *d* and *f*-series of terms. When we consider spectra of more complex elements, we shall see that the splitting of terms still further increases. Thus in calcium and other two-valence elements, each *p*, *d* and *f*-level is triple and is denoted by (p_1, p_2, p_3), (d_1, d_2, d_3), etc. . . . . . (*vide* further Chap. IX).

The doubling of the *p*, *d*, *f*-levels in alkali spectra is sometimes known as the *Duplicity Phenomenon.*

189. Spectra of other Elements.—We have seen that the alkali metals which are similar in their chemical properties possess similar spectra. This correspondence between chemical properties, and spectra is found to be general. Elements belonging to the same group in the periodic classification possess similar spectra. Thus Be, Mg, Zn, Cd and Hg and to a certain extent Ca, Sr and Ba which are all *divalent* and possess similar properties are found to possess very similar spectra, as described in Chap. IX. Similarly elements of the third group, comprising B, Al, Ga and In which are *trivalent,* show quite similar spectra.

ELEMENTS POSSESSING ALKALI-LIKE SPECTRA—ENHANCED SPECTRA OF ALKALINE EARTH ELEMENTS

Before taking the general case of spectra of elements, we shall give a brief description of certain spectra which are remarkably similar to the spectra of alkali metals. These are the "*Enhanced Spectra*" of alkaline earth elements which were first intensively studied by the astronomer Sir Norman Lockyer.

Long before the discovery of the electron, Lockyer, guided by his experience of the spectra of different classes of stars, had put forward a hypothesis that *the nature of the spectrum of an element was not invariable, but varied with the stimulus.* To make matters clear, let us take the spectrum of calcium in the flame, the arc, and the spark as shown in Fig. 9, Plate VII. In the flame, the excitation is lowest, in the arc it may be said to be average and it is highest in the spark. The excitation may be rendered still higher by putting a number of condensers in parallel with the spark (method of condensed discharge) which enables more electrons to pass through the gas and break it up thoroughly. Lockyer found that certain lines of calcium are peculiarly sensitive to excitation. In the flame the strongest line is the *g*-line of Fraunhofer λ 4227, while two other characteristic lines, *viz.* — the H, λ 3968 and the K, λ 3934 are rather faint. With increase of stimulus, the H and K line are *relatively* more intensified than the *g*. In the arc, they are almost equal in strength, while in the spark the H and the K are much more intense than the *g*-line. The lines of calcium can be divided into two groups —one set of lines showing a behaviour similar to that of the *g*-line; they are known as the *arc lines.* The second set gets intensified along with the H, K-lines, and are known as *enhanced lines or spark lines.* The phenomenon is quite general and is shown by all elements without exception.

190. Systematisation of Enhanced Spectra.—Lockyer observed that the enhanced lines of elements become progressively more intensified in the hotter stars, which were supposed to be earlier in evolution, and he thought that they were due to some primordial form of the element (protoelements). Thus the *g*-line was ascribed to ordinary calcium while the H, K were ascribed to *proto-calcium.* The hypothesis about these proto-elements was naturally rather vague.

A similar behaviour is shown by all divalent elements. The real clue to the change in the character of the spectrum was obtained by the systematisation of the enhanced spectrum, particularly that of magnesium which was carried out by A. Fowler very thoroughly. He showed that the enhanced spectrum of magnesium is exactly similar to that of Na, *i.e.*, consists of doublets which can be referred to families

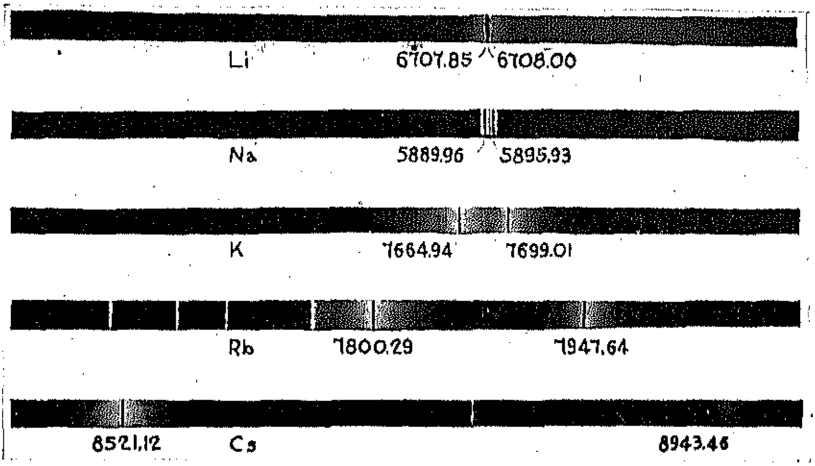

Fig. 8. Absorption of principal lines of the alkali metals.
(*p.* 372)

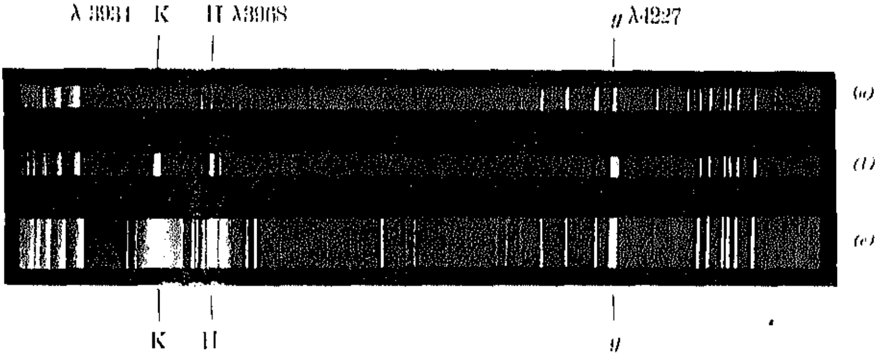

Fig. 9. (*a*) Furnace, (*b*) Arc, (*c*) Spark Spectra of Ca, showing the relative intensities of H, K, *g* lines.
(*p.* 374)

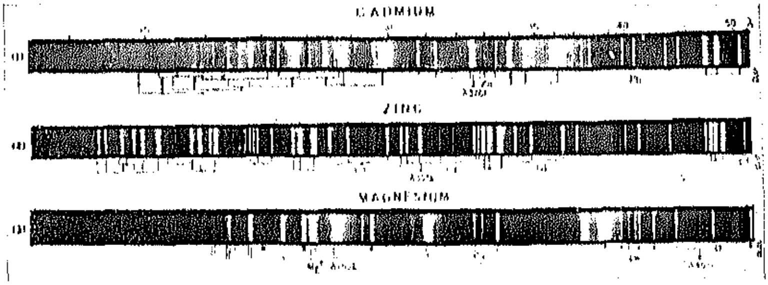

Fig. 2. Spectra of Zn, Cd, Mg.
(*p.* 381)

[*f. p.* 374

of single *s*-terms, double *p*-terms, double *d*-and *f*-terms possessing transitions absolutely identical with Na. The values are shown below.

Table 3.—The term-values of Mg^+.

n	ns	np		nd		nf	ng
1	121267·4	...	$\Delta\nu$	.	$\Delta\nu$	...	
2	51462·2	85506·44 85597·99	91·55	...		...	
3	28481·2	40616·1 40646·6	30·5	49777·0 49776·0	−1·0	...	
4	18069·3	23798·4 23812·5	14·1	27955·3		27467·4	
5	12482·7	15636·7 15644·3	7·6	17846·3		17577·2	--
6	9137·6	...		12366·5		12204·8	12194·6
7	6975·2	...		9069·4		8965·6	8957·6

He further found that the sets of terms can be represented by a Rydberg series, but the Rydberg number is now $4R$ instead of R, as shown below. This is a general feature of the enhanced spectra of all other divalent elements.

$$ns = \frac{4R}{(n + \cdot 919)^2}\,; \qquad nf = \frac{4R}{\left(n + \cdot 0994112 \pm \frac{\cdot 00719}{n}\right)^2}\;. \qquad (16)$$

This last fact afforded the clue to the explanation of enhanced spectra. They are not due to an element in the ordinary neutral state, *but due to the element which has lost one electron.* Thus magnesium possesses usually 12 electrons of which two are valence electrons. If owing to the passage of a strong discharge, one electron is entirely lost, it will be left with 11 electrons of which 2+8 electrons are strongly bound, and only one electron is left free. The structure becomes similar to that of Na with the difference that the light-electron now moves in a field which is due to a central charge of 12 shielded by 10 electrons. The net charge is therefore 2. Hence the Rydberg number is $4R$ as in the case of ionised helium.

191. Sommerfeld and Kossel's Displacement Law.—

Sommerfeld and Kossel* generalised this observation. They stated that if an element be deprived by an electric discharge of a number of its outer electrons, its spectra would in general be similar to that of the element preceding it in the periodic table by a number of steps equal to the number of electrons removed. The Rydberg number would however be Z^2R, where Z is the net nuclear charge.

---

* Sommerfeld, *Atombau und Spektrallinien*, Chap. VIII., (1924); A. Fowler, *Proc. Roy. Soc. A.*, **103**, 413, 1923.

Thus if we take the successive elements Al, Si, P and S, and pass such a strong discharge through them that Al is deprived of two electrons, Si of three electrons, P of five and S of six, we obtain

$$Al^{++},\quad Si^{+++},\quad P^{+IV},\quad S^{+V}$$

These should possess doublet spectra like the alkali elements with the Rydberg numbers

$$3^2R,\quad 4^2R,\quad 5^2R,\quad 6^2R,\quad \text{etc.}\ldots$$

Similarly $\quad Al^{+},\quad Si^{++},\quad P^{+++},\quad S^{+IV},\ldots$

should possess spectra similar to that of Mg. These deductions have all been verified, as will be apparent as we proceed further with the subject. The different groups of ionised elements which thus gives similar series spectra as the alkali elements are shown in the following table.

Table 4.

Li I	Be II	B III	C IV	N V	O VI	
Na I	Mg II	Al III	Si IV	P V	S VI	Cl VII
K I	Ca II					
Rb I	Sr II					
Cs I	Ba II					
Cu I	Zn II	Ga III	(Ge IV)	As V	Se VI	
Ag I	Cd II	In III	Sn IV	Sb V	Te VI	
Au I	Hg II	Tl III	Pb IV			

The nomenclature used here to denote the state of ionisation of an atom is due to Paschen. A neutral element of Na is represented as Na I, *i.e.*, with the number I following it. Similarly the singly ionised atom of Na would be denoted on this scheme as Na II, the doubly, trebly, fourfold . . . ionised atoms as NaIII, NaIV . . . . etc., and so on for other atoms.

A collection of literature on the important works of analysis of the alkali-like spectra up to the year 1931 will be found in *Review of Modern Physics*, 4, 317, 1932 in an article by R. C. Gibbs.

192. Resonance Lines, Ionisation and Resonance Potentials of Alkali Metals.

—The principal lines $1s-2p_1$ and $1s-2p_2$

of the alkalies are known as the Resonance lines, because these are the first lines to be excited in an electron bombardment of the atoms, and they come out in absorption at ordinary temperatures of the metal vapours. The two D-lines λ5890 and λ5896 of Na belong to this class. They can be so easily excited in emission or in absorption, because they correspond to the transition of the optical electron from its normal $1s$ orbit to the next higher orbit $2p_{1,2}$. But as has been mentioned before, $2p$ is a double orbit consisting of $2p_1$ and $2p_2$, and transitions from $1s$ to both these levels are allowed by selection principles. We therefore should get a pair of lines $1s-2p_{1,2}$ in each case. The energy in volts required to excite the optical electron from the $1s$ to the $2p_{1,2}$ states is called the *Resonance potential* of the element. Corresponding to the two lines we ought to get two resonance potentials, but as the energy difference $2p_1—2p_2$ is generally very small, we get experimentally only one resonance potential, which corresponds to the lower one of the two.

If the optical electron is given an amount of energy equal to that of the $1s$-state, the electron leaves the atomic system, and the atom is ionised. The energy necessary for this can be calculated from the value of $1s$-term with the aid of the relation $eV=h\nu$ where ν = frequency of $1s$-state. This is known as the *Ionisation potential*.

Table 5.

Element	$1s-2p_{1,2}$			$1s$	V
	λ	ν	V (volts)	ν	Ionisation Potential
3 Li	6707·8	14903·8	1·84	43486·3	5·368 volts
11 Na	5890 5895·93	16973·3 956·2	2·094 2·092	41449·0	5·11
19 K	7665 7699	13042·8 12985·1	1·609 1·602	35006	4·32
37 Rb	7800·3 7947·6	12816·5 579	1·58 1·55	33689	4·15
55 Cs	8521·1 8943·5	11732·3 178·3	1·45 1·38	31404·6	3·87
29 Cu	3247·5 74	30783·6 535	3·8	62308	7·692
47 Ag	3280·7 3383	30473 29552·3	3·762	61096	7·542
79 Au	2428	41174	5·1	70000 ?	8 to 9 ?

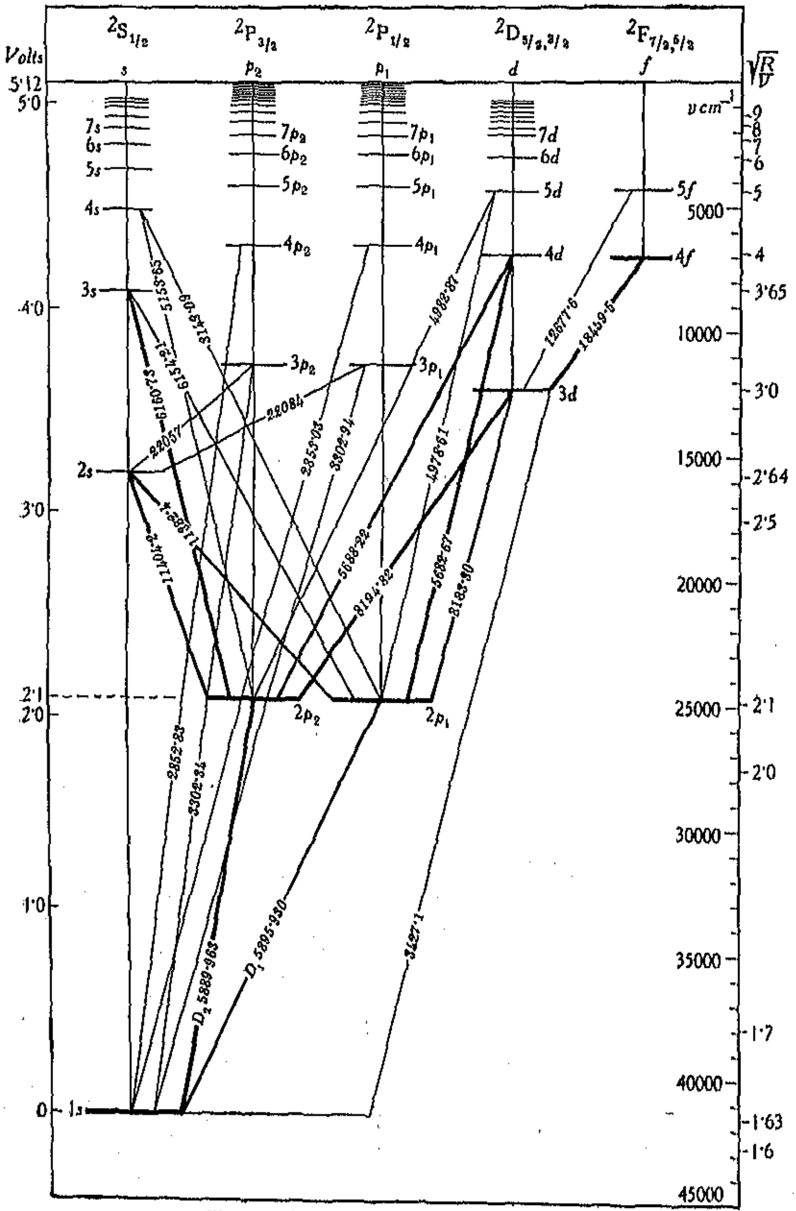

Fig. 10.—The complete Bohr diagram for Na.

The value of the ionisation potential V in volts can be easily calculated from the relation $eV = h\nu$. The student can verify

$$1 \text{ volt} = 8110 \text{ cm}^{-1} = 12340 \text{ Å. units,}$$

and the I.P. in volts $= \dfrac{\text{convergence frequency}}{8110} = \dfrac{12340}{\text{Limiting wavelength}}$

Thus the I. P. of H = 109765/8110 = 13·54 volts.

The resonance and ionisation potentials and the resonance lines of alkali metals are shown above. The mono-valent elements Cu, Ag and Au have spectra similar to those of the alkalies. Their resonance lines and excitation potentials are also given in the same table 5.

193. Bohr-diagram for Sodium.—The complete Bohr diagram for a typical element (sodium) of the first group is shown on p. 378 in Fig. 10. It gives the important series lines of Na showing the transitions which give rise to them.

The terms of the alkali spectra form a doublet *s*, *p*, *d*, *f*.....system, *i.e.*, we have *s*, p_1, p_2, d_1, d_2,........terms. These are shown on the topmost horizontal line. Separation between d_1 and d_2 terms being very small, *d* is shown as single in the diagram. The terms in Russel-Saunders' new notations are shown just above the corresponding old notations. The scale frequency is given on the vertical line to the extreme right. Energy increases from bottom to top of this line. The frequencies of a family of terms belonging to a particular series (*e.g.* 1*s*, 2*s*, 3*s*........of *s*-series, $2p_1$, $3p_1$, $4p_1$...of doublet p_1 series,...) are shown by the positions of short horizontal lines along the vertical line below each term. Thus we see the *ns*-family of terms begin with $n=1$, $np_{1,2}$ terms with $n=2$, and so on. The diagonal lines represent the various transitions, the corresponding wavelengths being indicated on them. The lines of the sharp, diffuse and principal series, can be clearly distinguished. For, all the lines starting from *ns*-system and terminating in $2p_1$ or $2p_2$-level belong to the sharp series, lines starting from *nd*-levels and terminating in $2p_1$ or $2p_2$ fall in the diffuse series, others starting from np_1 or np_2-levels and terminating in 1*s*-level belong to the principal series, while lines terminating in 3*d*-level belong to the fundamental series.

The excitation potential of lines are shown on the vertical scale to the extreme left. The $\sqrt{R/\nu}$ values shown in the extreme right give directly the total *effective* quantum number *n* for the orbits. Their significance will be clear later on.

Books Recommended.

See the books mentioned at the end of Chap. VII.

See also *Seriengesetze der Linienspektren* by F. Paschen and R. Götze (1922).

CHAPTER IX

SPECTRA OF ELEMENTS OF GROUP II

Two-valence Elements

194. Elements of Group II.—A glance at the Periodic Table shows that group II contains elements of which the following

Be	Mg	Zn	Cd	Hg
4	12	30	48	80

form the odd group, and the four elements

Ca	Sr	Ba	Ra
20	38	56	88

are said to form the even-group.

These elements are generally bivalent and on electrolysis, the atoms are found to carry two positive charges. It is therefore supposed that they possess two easily detachable electrons, as is represented in the following diagrams (Fig. 1).

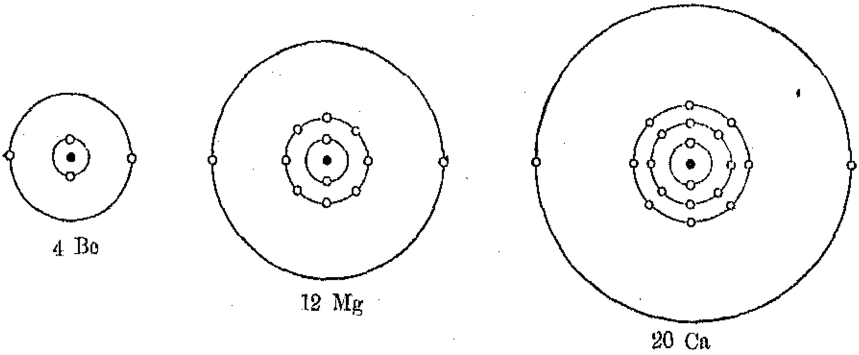

Fig. 1. Electron distribution in two-valence elements.

The inner electrons form an inert-gas shell, and the optical spectrum may be supposed to be due to the vibration of the two outer electrons. When one electron is knocked off, the elements become ionised, and then they emit a spectrum entirely due to one electron, like alkalies as already discussed in Chap. VIII. We shall not discuss this spectrum (spark) in this chapter.

The ionised spectra of the succeeding elements B, Al, Ga, In, Tl are exactly similar in structure to the spectra which are going to be discussed here, in accordance with Sommerfeld and Kossel's rule.

195. General Features of the Spectra.—In the spectra of all two-valence elements, the number of lines are more numerous than in the alkalies, but the most distinctive feature is the occurrence of lines in groups of three forming *triplets*. A representative picture is reproduced in Fig. 2, Plate VII.

Besides the triplet lines, there are other lines like the line λ 4227 of Ca which occur rather detached. These lines also belong to the arc-spectrum (neutral element). They are known as forming the "Singlet" spectrum.

196. The Triplet Spectrum of Magnesium.—In Table 1, the frequencies of lines forming the sharp and diffuse series of magnesium are shown. It will be apparent from an inspection of these tables that the two series come to the same limit, as in the analogous case of the sharp and diffuse series of alkali metals.

Fowler showed that the lines forming the sharp series which are denoted by the symbols

$$2p_1 - ns\,; \quad 2p_2 - ns\,; \quad 2p_3 - ns$$

can be represented as follows:

$$\left.\begin{aligned} 2p_1 &= 39760{\cdot}5\,; \qquad 2p_2 = 39801{\cdot}4\,; \qquad 2p_3 = 39821{\cdot}3 \\ ns &= R\,/\,(n + 0{\cdot}375125 - 0{\cdot}058307/n - 0{\cdot}002355/n^2)^2 \end{aligned}\right\} \quad . \quad . \quad (1)$$

where n has all integral values from 2 onwards.

Similarly the diffuse series can be represented by

$$\nu_1 = 2p_1 - nd\,; \quad \nu_2 = 2p_2 - nd\,; \quad \nu_3 = 2p_3 - nd$$

where $2p_1$, $2p_2$, $2p_3$ have the same values as in the case of the sharp series and nd is given by a Ritz-formula *

$$nd = \frac{R}{\left(n + 0{\cdot}825371 + \dfrac{0{\cdot}023416}{n} - \dfrac{0{\cdot}036780}{n^2}\right)^2} \quad . \quad . \quad . \quad (2)$$

In the case of Ca, Sr, Ba, n apparently begins with 2 for the d-series, while for the elements of the odd series, n begins with 3. These large d-terms are the distinctive features of the even-group.

---

* A. Fowler and W. H. Reynolds, *Proc. Roy. Soc. A*, **89**, 137, 1913.

Table 1.

n	Sharp Series	$\Delta\nu$	Diffuse Series	$\Delta\nu$
2	19286·0 19326·9 19346·8	40·9 19·9		
3	29961·2 30002·1 30021·9	40·9 19·8	26045·9 26086·6 26106·7	40·7 20·1
4	33979·4 34020·2 34039·8	40·8 19·6	32280·9 32322·0 32341·8	41·1 19·8
5	35943·6 35984·3 36004·2	40·7 19·9	35057·1 35096·7 35117·2	39·6 20·5
6	37051·7 37092·3 37112·0	40·6 19·7	36531·9 36571·8 36591·6	40·0 19·8

197. Failure of the Rydberg-Schuster Law.—The first ns-term for Mg has the value

$$2s = 20474{\cdot}5, \qquad \text{with } n=2,$$

and this holds for all elements. It is much smaller than $2p$.

We have seen in the case of the alkali metals that by putting $n=1$ in the formula for the sharp series, we obtain the term $1s$ and $1s-2p$ gives the most important line of the element (the *Resonance Line*). It was only natural that the same procedure should be tried in the present case. If we put $n=1$ in the formula (1), we obtain

$$1s = 85570, \text{ and } 1s - 2p_2 = 45780.$$

Search was made for a line in this region for magnesium, and at the corresponding regions for other elements. But in no case was any trace of such a line found. It became clear that it is definitely absent in the case of two-valence elements. A closer investigation of this fact led Pauli to his famous *Exclusion Principle* which has furnished the most powerful key for the understanding of atomic physics.

198. The Diffuse Triplet in the Other Elements.—So far we have been considering Mg as a typical representative of two-valence elements. The other elements of this group certainly show an analogous sp-series, *i.e.*, lines belonging to the sharp series can be expressed as the difference between three $2p$-terms minus a set of ns-terms forming Rydberg sequence. The only point of departure is that the constant differences $2p_1-2p_2$, $2p_2-2p_3$ go on increasing with the weight of the element, as the following table 2 shows. It is found that $\Delta\nu_1 : \Delta\nu_2 = 1:2$ approximately.

The diffuse series of magnesium is apparently explained by assuming the existence of a single nd-sequence, but as in the case of the alkali elements the d-term has been found to be *not* single, but triple. The apparent singleness in the case of Mg is due to small separation between the components. If larger resolving power be used these d-levels are also found to be triple. In the case of heavier elements, the multiplicity of the d-level is apparent from the appearance of the diffuse lines, which do not consist of three lines, but shows a more complex pattern, as shown in the typical photograph for calcium (Fig. 3, Plate VIII).

Table 2.

At. Wt.	Element	$\Delta\nu_1$ $2p_1-2p_2$	$\Delta\nu_2$ $2p_2-2p_3$	Ratio $\Delta\nu_1/\Delta\nu_2$
24·32	Mg	40·9	19·9	2·164
40·07	Ca	105·9	52·3	2·025
87·63	Sr	394·2	186·8	2·11
137·37	Ba	878·2	370·5	2·37
65·38	Zn	388·9	189·8	2·054
112·4	Cd	1171·1	541·9	2·161
200·4	Hg	4630·6	1767·3	2·62

For Ca, there are three chief lines, in this group ν 22441, 22542 and 22590. The first ν 22441 is accompanied by two faint satellites ν 22436 and 22432, the second line ν 22542 is accompanied by a satellite ν 22538, the third has no satellite.

In the above diagram, note that the constant frequency difference occurs in a characteristic way, not between the chief lines, but *between a line and a satellite.*

The combination between the p and d terms can be represented in the following tabular form :—

Table 3.

	$2p_3$ 34146·9	$2p_2$ 34094·6	$2p_1$ 33988·7
$3d''$ 11556·4	(9) 22590·4	(5) 22538·3	(3) 22432·4
(3·7)			
$3d'$ 11552·6		(9) 22542·0	(5) 22436·1
(5·6)			
$3d$ 11547·0			(9) 22441·7

A triplet pd-multiplet

It can be easily verified that any line is the difference between the $2p$ in the same column and $3d$ in the same row, thus for the first satellite of the strongest line, the frequency is

$$22436{\cdot}1 = 33988{\cdot}7 - 11552{\cdot}6$$
$$= 2p_1 - 3d'$$

The existence of the triplet nature of the "d – terms" is thus quite well established. The differences $3d'' - 3d'$, $3d' - 3d$ increases with the atomic number as shown for Ca, Sr and Ba below.

Besides the series above mentioned, series analogous to Bergmann series were found in these spectra. They are due to $3d-mf$ combinations, and the number of f-terms has been found to be triple. Thus the triplet spectrum is found to be characterised by one single sequence of s-terms and sequences of triple p, d and f-terms.

Table 4.

	$3d''$		$3d'$		$3d$
Ca	11556·3	3·7	11552·6	5·6	11547·0
Sr	10918·2	14·9	10903·0	23·0	10880·0
Ba	11334·1	55·1	11279·0	67·4	11211·6

199. The Inner Quantum Number.—We have now to explain why six lines are obtained in the scheme given in Table 3 instead of nine which are possible. It is clear that some selection principle is needed to explain the absence of three lines p_3d, p_3d', p_2d. For doing this, Sommerfeld introduced the idea of "*inner quantum numbers*".

It is unnecessary to give a historical retrospective of these works, it will suffice to give the final result. Suppose we describe the three p-terms

$$p_3 \qquad p_2 \qquad p_1$$

by the new notation

$$p_0 \qquad p_1 \qquad p_2, \qquad (p_0 > p_1 > p_2)$$

and the three terms

$$d'' \qquad d' \qquad d$$

by

$$d_1 \qquad d_2 \qquad d_3 \qquad (d_1 > d_2 > d_3)$$

Then the table can be rewritten as :—

Table 5.

	$2p_0$ 34146·7	$2p_1$ 34094·6	$2p_2$ 33988·7
$3d_1$ 11556·4	(9)	(5)	(3)
$3d_2$ 11552·6		(9)	(5)
$3d_3$ 11547			(9)

The subscripts stand for the *inner quantum number* j. Then the observed combinations are explained by the rule :—

$$\begin{tikzcd}[row sep=small] & j+1 \\ j \arrow[ur] \arrow[r] \arrow[dr] & j \\ & j-1 \end{tikzcd}$$

that is j can change by ±1 or 0. $\Delta j = \pm 2, \pm 3, \ldots\ldots$ are forbidden.

The reader will naturally ask, how have these numbers been arrived at, and what is their theoretical significance? These points will become clear when we consider Zeeman Effect (Chap. X). For the present, it will be useful to remember that

$$p_0 > p_1 > p_2$$

i.e., a term possessing a higher j is less in value than its companion with a lower j.

From a scrutiny of observed combinations we can find out the inner quantum numbers of belonging to other families. Thus for s, $j = 1$, for f, $j = 2, 3, 4$ ..... etc. A typical d-f-set of lines of Ba is shown opposite.

Table 6.

	d_1 32995·6	181	d_2 32814·1	381	d_3 32432·7
f_2 4634	28361		28179		27798
24					
f_3 4610			28203		27822·7
105					
f_4 4505					27927·7

It can be easily verified that the observed lines satisfy the j-selection principle given above.

INNER QUANTUM NUMBER FOR TERMS OF ALKALI ELEMENTS.

In Chap. VIII, §188, we referred to the duplicity phenomenon in alkali spectra. The two associated p, d and f-terms, in this case can be distinguished from each other by inner quantum numbers. We may describe the terms as

$$\begin{array}{llllllll} s_1 & p_1 & p_2 & d_2 & d_3 & f_3 & f_4 & \text{etc} \ldots \\ & p_1 & > p_2 & d_2 & > d_3 & f_3 & > f_4 & \text{etc} \ldots \end{array}$$

This assignment of the inner quantum number explains the observed combinations, *e.g.*, in the spectrum of caesium we obtain only three lines in a p-d combination instead of four, as shown in table 7.

Table 7.

	$2p_1$ 20226	554	$2p_2$ 19672
$4d_2$ 5356	(10) 14870		(5) 14315
21			
$4d_3$ 5395			(10) 14336

There is no line corresponding to $2p_1 - 4d_3$ because $\Delta j = 2$.

The above assignment of inner quantum numbers for one valence elements is however not final, for, a study of Zeeman-effect has shown, that these j-values should be uniformly decreased by half as follows:

$$S_{\frac{1}{2}}\ ,\quad \overbrace{P_{\frac{1}{2}}\ ,\quad P_{\frac{3}{2}}}\ ,\quad \overbrace{D_{\frac{3}{2}}\quad D_{\frac{5}{2}}}\ ,\quad \overbrace{F_{\frac{5}{2}}\quad F_{\frac{7}{2}}}\ \ldots \text{etc.}$$

It is apparent that this change does not alter the arguments given above regarding combinations.

The idea of inner quantum number thus introduced *ad hoc* to explain observed facts, has been found to be indispensable for the understanding of the mysteries of intra-atomic motion, as will be discussed in the next chapter.

200. The Singlet Spectrum.—The singlet spectrum is very difficult to investigate as the lines stand rather isolated, and there is no clue like constant differences which can enable one to group related lines. The classification of singlet lines therefore was an arduous affair. But it was shown that the spectrum consists of

(*a*) A principal series of lines which can be represented by the formula

$$1\mathrm{S} - n\mathrm{P}$$

where $n = 2, 3, 4 \ldots .$ The capital letters were used for *singlets*, and small letters for *triplets*.

*n*P *is given by a formula of the Ritz-type, e.g.*, for magnesium, the principal series is given by

$$1\mathrm{S} - n\mathrm{P} = 61672 - \frac{R}{(n+p)^2}, \quad n = 2, 3, 4, \quad . \quad . \quad . \quad . \quad . \quad (3)$$

The first member is λ 2852 and the following ones are λ 2026, 1828, etc. . . . .

The singlet 1S-term has been found to be the largest term in the spectra of two-valence elements. The normal unexcited state of the atom is therefore characterised by 1S. This conclusion is further corroborated by the fact that if the absorption spectra of two-valence elements be studied in the same way as for alkalies, it is only the lines of the principal series of the singlet spectrum (*e. g.*, the *g*-line λ 4227 for Ca) which occur in absorption, *besides a few others to be presently described.* No other line belonging to the singlet spectrum, and no line belonging to the triplet spectrum is absorbed. A photograph of the absorption spectra of calcium vapour is reproduced in Fig 4, Plate VIII. The strong absorption line seen in this spectrum is the *g*-line of Ca, the other absorption lines belonging to the 1S−*n*P-series are beyond the range Ca.

(*b*) Besides the *p*-series the singlet spectrum consists of lines which form sharp and diffuse series :

Sharp series : $2\mathrm{P} - n\mathrm{S}$, $n = 2, 3, \ldots .$
Diffuse series : $2\mathrm{P} - n\mathrm{D}$, $n = 3, 4, \ldots .$
F-series : $3\mathrm{D} - n\mathrm{F}$, $n = 4, 5, \ldots .$
etc. . . .

Zeeman Effect.—All singlet lines show normal Zeeman pattern, while the splitting of triplet lines is more complex (*vide* Chap. X).

201. The Inter-Combination Lines.

—Besides the triplet and singlet lines, there are found in the spectra of all two-valence elements certain feeble lines which do not seem to belong to either group. They have been traced to inter-combination between the singlet and the triplet terms.

The most important of these lines belong to the combination $1S_0-2p_1$. A list of such lines is given in Table 8 (2nd column). That they arise from the 1S-state is proved by the fact that they can be obtained in absorption. Thus the mercury λ 2536 easily comes out reversed in all absorption experiments. It is remarkable that we do not get any line corresponding to the combinations

$1S_0-2p_0$	$1S_0-2p_2$	$1S_0$ .... 84178·5 cm^{-1}
for Hg, $\nu=37642·3$	$\nu=44040·2$	$2p_0$ .... 46536·2
$\lambda=2656·6$	$\lambda=2270·8$	$2p_2$ .... 40138·3

except under very special conditions.

The absence of this possible combination is explained by assigning to the 1S-term of the j-value 0, and adding a supplement to the selection rule for the j-quantum number

$$j=0 \rightarrow j=0$$

is forbidden. The inner quantum numbers of the singlet terms can then be shown to be as follows:

$$S_0, \quad P_1, \quad D_2, \quad F_3 \ldots.$$

The correctness of these assignments is justified by the occurrence of lines belonging to the following combination for Mg:—

$$2p_1-5D_2=36152,\ \lambda\ 2765·34; \qquad 2p_2-5D_2=36112,\ \lambda\ 2768·5$$

We have no line corresponding to $2p_0-5D_2$. This shows that, the j for the singlet d-term is 2.

The complete Bohr-diagram for a typical two-valence elements, *viz.*, Mg is shown in Fig. 5, p. 388.

202. Resonance Lines, Ionisation Potentials, etc., of Two-Valence Elements.

—The lines $1S-2P$ and $1S-2p_2$ ... are known as the resonance lines of two-valence elements, because they are the first lines to be excited in an electron bombardment, and they are obtained in absorption even when the temperature of the vapour is only barely sufficient to give appreciable vapour pressure.

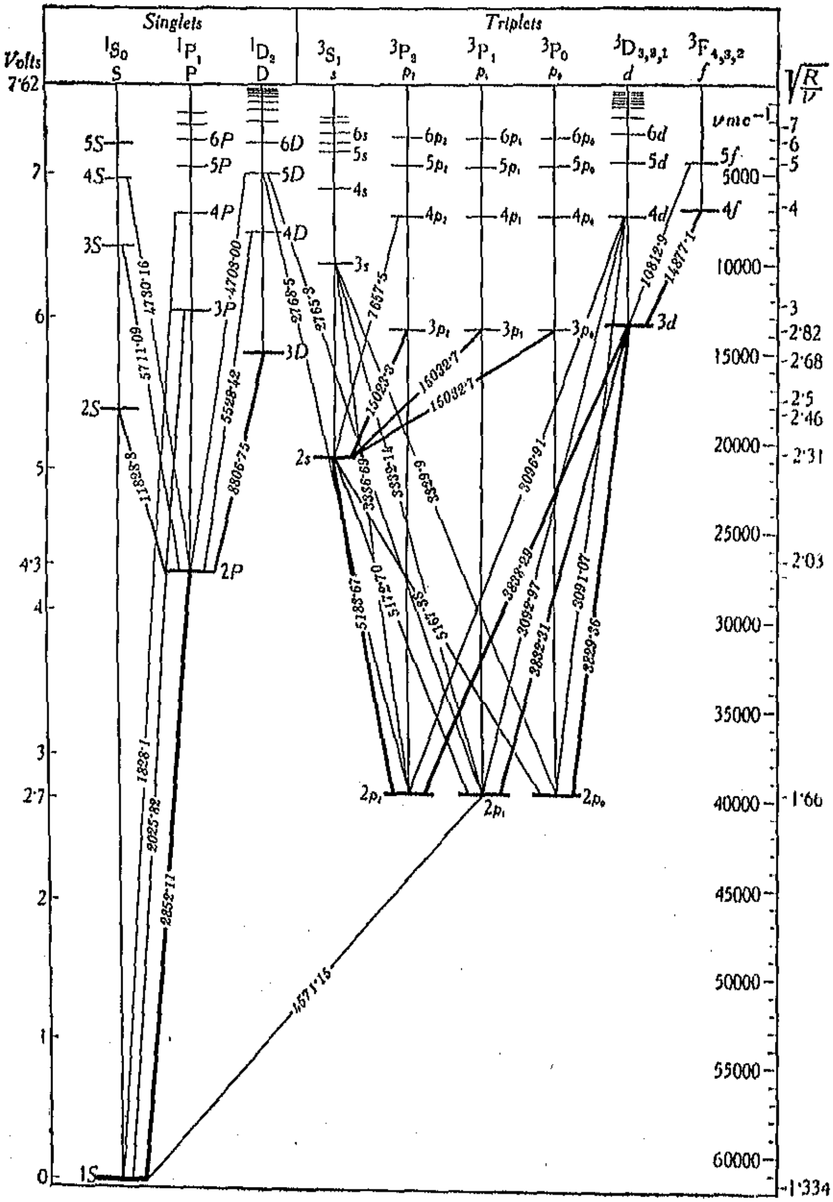

Fig. 5. The complete energy level scheme for Mg.

The ionisation-potential can be calculated from the value of 1S-term with the aid of formula on page 378. The resonance lines, the resonance potentials and the ionisation potentials of the two-valence elements are shown in the following table :

Table 8.

Element	$1S_0-2p_1$		$1S_0-2P$		$1S_0$ ν (cm^{-1})	V (Ionisation potential in volts)
	λ in Å.U.	V in volts	λ in Å.U.	V in volts		
4. Be	4547·9	2·71	(50) 2348·7	5·25	75194·3[*]	9·281
12. Mg	4571·2	2·70	2852·1	4·33	61672	7·61
30. Zn	3075·9	4·01	2138·6	5·77	75766·8	9·35
48. Cd	3261·0	3·78	2288·0	5·39	72538·8	8·95
80 Hg	2536·5	4·86	1849·5	6·67	84178·5	10·39
20 Ca	6572·8	1·88	4226·7	2·02	49304·8	6·09
38 Sr	6892·6	1·79	4607·3	2·68	45936·5	5·67
56 Ba	7911·3	1·56	5535·5	2·23	42029	5·19
88 Ra		1·5 ?		2·6		5 to 5·5

The inter-combination lines $1S_0-2p_2$ are faint in the case of elements of low atomic weight, and become stronger as we take the heavier elements as was first pointed out by De Krönig.

DESCRIPTION OF FIG. 5.

The sharp, principal and diffuse terms are classified into two systems, *viz.*, (1) the singlet S, P, D-terms, and (2) the triplet $s, p_{0,1,2}, d_{1,2,3}, f_{2,3,4}$......terms. These are shown on the topmost horizontal line. The Russel-Saunders' new notations are shown just above the corresponding old notations of terms. The scale of frequency is given on the vertical line to the extreme right. Energy increases from bottom to top of this line. The frequencies of a family of terms belonging to a particular series (*e.g.* 1S, 2S, 3S . . . . . of the singlet S-series, $2p_1$, $3p_1$, $4p_1$ . . . . of triplet p_1-series . . .) are shown by the positions of short horizontal lines along the vertical line below each term. Thus we see that the family of ns terms begin with $n=1$, $np_{0,1,2}$-terms begin with $n=2$, and so on for other terms. The diagonal lines represent the different possible transitions, and the wavelength corresponding to each transition is indicated on it. Besides the lines belonging to the sharp, principal, diffuse and fundamental series the inter-combination lines of Mg, λ 4571, 2768·5, 2765 are clearly seen.

---

[*] F. Paschen and P. G. Kruger, *Ann. d. Phys.*, 8, 1010, 1931.

The excitation potentials of the lines are shown on the vertical scale to the extreme left.

203. Alkaline Earth-like Spectra.—According to the displacement law of Sommerfeld and Kossel, as explained in § 190, there will be other elements in the periodic table, which would emit the same kind of series spectra in their singly or multiply ionised states as the neutral alkaline earth atoms. These elements are shown in Table 9 below. A list of important works done on the analysis of their spectra will be found in *Reviews of Modern Physics*, **4**, 317, 1932.

Table 9.

Be I	B II	C III	N IV	O V	Zn I	Ga II	Ge III	As IV	Se V
Mg I	Al II	Si III	P IV	S V	Cd I	In II	Sn III	Sb IV	Te V
Ca I	—	—	—	—	Hg I	Tl II	Pb III		
Sr I	—	—	—						
Ba I	—								

CHAPTER X

ZEEMAN EFFECT

204. Connection between Phenomena of Light and Magnetism.—As stated in Chapter V it was first shown by Faraday in 1845 that an intimate connection exists between the phenomena of light and magnetism. He found that a beam of polarised light, on passing through a plate of glass placed between the poles of an electromagnet parallel to the field, has its plane of polarisation turned through an angle proportional to the field (Faraday Effect). Though this experiment clearly established that light and magnetism are closely related phenomena, a further attempt was made by him to demonstrate the connection by a still more direct experiment, *viz.*, by putting a source of light within a magnetic field, and observing whether the nature of emission could be varied. But no positive results were obtained. The same experiment was performed by Zeeman in 1896 with marked success.

205. Lorentz and Larmor's Theory of Zeeman Effect.—The success of Zeeman's experiments was largely due to the fact that he was guided in his experiments along a definite route laid down by H. A. Lorentz who, almost simultaneously with J. Larmor, worked out on the classical electron theory how light vibrations are affected by a magnetic field. A sketch of their theories is given below:

The model of the luminous atom or oscillator was an electron which executed a simple harmonic motion about a fixed centre of force. The frequency of vibration of the electron was taken to be identical with the frequency of light emitted. It was supposed that such an electron constituted a miniature Hertzian oscillator, and the state of polarisation of the light emitted could be obtained by extending to this case the results deduced in the case of the Hertzian oscillator.

Lorentz* and Larmor proved that the nature of oscillations undergoes a radical change when it is placed in a magnetic field.

Let the equation of motion of the undisturbed oscillator be

$$m\frac{d^2x}{dt^2} = -\mu x,\ m\frac{d^2y}{dt^2} = -\mu y,\ m\frac{d^2z}{dt^2} = -\mu z\ \ .\ \ .\ \ .\ \ (1)$$

Then we have $(x, y, z) = A\cos(2\pi\nu t + \alpha, \beta, \gamma)$, where $4\pi^2\nu^2 = \mu/m$. Suppose now a uniform magnetic field of strength H in the direction of the z-axis is superposed on this system. The equations of motion of the electron are now:

$$m\frac{d^2x}{dt^2} = -\mu x + \frac{eH}{c}\frac{dy}{dt}\ \ .\ \ .\ \ .\ \ .\ \ .\ \ .\ \ (2a)$$

$$m\frac{d^2y}{dt^2} = -\mu y - \frac{eH}{c}\frac{dx}{dt}\ \ .\ \ .\ \ .\ \ .\ \ .\ \ .\ \ (2b)$$

$$m\frac{d^2z}{dt^2} = -\mu z\ \ .\ \ .\ \ .\ \ .\ \ .\ \ .\ \ .\ \ .\ \ .\ \ .\ \ .\ \ (2c)$$

Lorentz showed that this equation can be solved if we introduce two new variables

$$\xi = x + iy, \qquad \eta = x - iy\ \ .\ \ .\ \ .\ \ (3)$$

They satisfy the two equations :—

$$\left.\begin{aligned} m\frac{d^2\xi}{dt^2} + \mu\xi + i\frac{eH}{c}\frac{d\xi}{dt} &= 0 \\ m\frac{d^2\eta}{dt^2} + \mu\eta - i\frac{eH}{c}\frac{d\eta}{dt} &= 0 \end{aligned}\right\}\ \ .\ \ .\ \ .\ \ .\ \ .\ \ .\ \ (4)$$

Now put $\qquad \xi = Fe^{2\pi i\nu_1 t},\ \ \eta = Fe^{2\pi i\nu_2 t}$

Then ν_1 and ν_2 satisfy the equations

$$\left.\begin{aligned} \nu_1^2 - \nu^2 + \frac{eH}{2\pi cm}\nu_1 &= 0 \\ \nu_2^2 - \nu^2 - \frac{eH}{2\pi cm}\nu_2 &= 0 \end{aligned}\right\}\ \ .\ \ .\ \ .\ \ .\ \ .\ \ .\ \ (5)$$

From this we obtain, since $eH/2\pi cm$ is a small quantity

$$\nu_1 = \nu - \frac{eH}{4\pi cm},\ \nu_2 = \nu + \frac{eH}{4\pi cm}$$

---

* For an account of Lorentz' theory see Lorentz, *Theory of the Electron*, Chap. III.

The new vibrations are therefore

$$\left.\begin{array}{lll} x+iy=Fe^{2\pi i\nu_1 t} & \ldots & \nu_1=\nu-\dfrac{eH}{4\pi cm} \\ x-iy=Fe^{2\pi i\nu_2 t} & \ldots & \nu_2=\nu+\dfrac{eH}{4\pi cm} \\ x \quad\; =Fe^{2\pi i\nu t} & & \end{array}\right\} \quad \ldots \quad (6)$$

Interpretation of the Results.—Suppose the observation is made along the z-axis. Then according to (6), the z-component would not be visible (see Fig. 1*a*).

$x+iy=Fe^{2\pi i\nu_1 t}$. . . represents a vibration in which we have $x=F\cos 2\pi\nu_1 t$, $y=F\sin 2\pi\nu_1 t$. It represents circular motion of the electron in the anticlockwise direction. The light vibrations emitted from such an oscillator are circularly polarised in the anticlockwise direction.

Similarly, $x-iy=Fe^{2\pi i\nu_2 t}$ represents circular motion of the electron in the clockwise direction. The light vibrations are circularly polarized in the clockwise direction. Thus when viewed parallel to the field, a single line splits up into two lines on opposite sides of the original position of the line with the frequency difference

$$\triangle\nu=\frac{eH}{4\pi cm} \quad \ldots\ldots\ldots\ldots \quad (7)$$

They are circularly polarised in opposite directions.

It is found that $\nu_1>\nu_2$ hence $eH/4\pi cm$ is negative, or the sign of e is negative. Also the value of e/cm can be obtained from the observed value of $d\nu$ or $d\lambda$.

Since $$d\nu=d\left(\frac{c}{\lambda}\right)=-c\frac{d\lambda}{\lambda^2}=\frac{eH}{4\pi cm},$$

we have $$\frac{e}{cm}=\frac{4\pi c}{H}\frac{d\lambda}{\lambda^2} \quad \ldots\ldots\ldots\ldots \quad (8)$$

From actual measurements of $d\lambda/H$, e/cm was found* to be 1·77 × 10⁷. Hence the vibrating electrical charge is identical with the *electron*.

Transverse View.—When the emitted light is viewed perpendicular to the field, say along the y-axis, there should appear three lines :

(1) a line corresponding to $x=Fe^{2\pi i\nu t}$. This is in the position

---

* *Vide*, Babcock, *Contr. Mt. Wilson Observatory*, 12, 109, 1922.

For an account of determination of e/mc from Zeeman effect see Note 2, Appendix.

of the original line, but is polarised with vibration parallel to the field (π-component).

(2) of the vibration $x+iy = F\,e^{2\pi i\nu_1 t}$, we observe only $x = F\cos 2\pi\nu_1 t$, as the line of view is along the y-axis. This is polarized with vibration perpendicular to the field, and the line is separated from the central one by the frequency difference $\Delta\nu = eH/4\pi cm$ (σ-component).

(3) similarly of the vibration $x-iy = F\,e^{2\pi i\nu_2 t}$, only the component $x = F\cos 2\pi\nu_2 t$ is effective in giving rise to a line at a distance $\Delta\nu = -eH/4\pi cm$, and with vibration perpendicular to the field (σ-components).

The deductions are graphically represented in the diagram (Fig. 1) below.

In this the single line at the top represents the position of the original wavelength of frequency ν. The longitudinal and transverse views of the effect are represented below in (*a*) and (*b*) respectively. The arrow at the top shows the direction of the magnetic field *H*. When viewed along this, as in (*a*) only two components are seen at a distance of $+\Delta\nu$ and $-\Delta\nu$ respectively from the original line. They are circularly polarised and their senses of polarisation are shown by the two circular arrows. When viewed at right angles to the direction of *H* as in (*b*), three lines are visible. One is in the position of the original line ν, and the other two separated from this by an interval $+\Delta\nu$ and $-\Delta\nu$ respectively. The components polarised parallel to the direction of the magnetic field are denoted by the sign ‖, and those polarised perpendicular to the direction by ⊥. They are generally referred to as π- and σ-components respectively. Each σ-component is half as intense as the π-component.

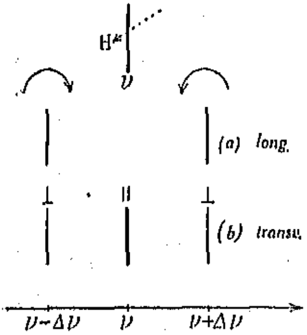

Fig. 1. Graphical sketch showing normal Zeeman Effect.

It will be noticed that except the direction of polarisation, the features of longitudinal effect are included in those of the transverse effect which represents the general phenomenon. Hence in future, only the transverse effect will be considered.

The quantity $\Delta\nu = eH/4\pi cm$ will be denoted by '*a*' throughout this chapter.

206. Experimental Verification.[*]—In his earliest experiments, Zeeman used a Na-flame which was placed within the pole-pieces of a strong electromagnet. He observed the D-lines with an ordinary spectrograph, and the polarisation was tested with a Nicol prism. On account of the small resolving power used, the Zeeman components were not separated but the lines were found to be broadened, and the edges were found to be polarised in accordance with Lorentz's theory.

In later investigations carried out at Tübingen by Paschen and Back, the experimental methods were enormously improved. The improvements consisted in :—

(*a*) *The use of spectrographs of high resolving power.*—For this purpose, either interference spectroscopes (Fabry-Perot or Lummer-Gehrake or Echelon grating[†]) or concave gratings are used. In the experiments of Runge and Paschen, continued by Back at Tübingen, a concave grating of 6·32 m. radius of curvature, and with 110,000 lines was used sometimes up to the sixth order. The resolving power is $n \times 110{,}000$, where n=order number, so that for λ 4400 Å, we can resolve rays separated by ·01 Å.U. in the fourth order. This resolving power can be exceeded in interference spectroscopes, but then the interpretation of the result becomes somewhat difficult.

The polarisation of the components was examined in the usual way by placing a quarterwave plate and a nicol between the spectral apparatus and the electromagnet. In the case of transverse effect where the lines are linearly polarised, only the nicol was used.

(*b*) *Source of Light.*—The source of light should be such that it would give lines of extreme fineness with sufficient intensity. An intermittent vacuum spark of special design was used in most Tübingen experiments.[‡]

In this the metal under investigation forms one electrode of the arc, and a strip of tungsten held at the end of a brass rod forms the other electrode. The two are enclosed vacuum-tight in a brass cylinder and the whole is placed between the pole pieces of the electromagnet. The first electrode is kept fixed and the W-electrode is rotated about its central axis, so that during each revolution the two electrodes come in contact only once. At each contact an arc is formed which breaks after a short interval. The vacuum may be obtained by using suitable pumps.

---

[*] For details, see *Handbuch der Experimental physik*, Bd. XXII, pp. 31—68; Baly's *Spectroscopy*, **3**, Chap. II, p. 401.

[†] See Wood's *Physical Optics* (1914), Chap. VIII, p. 265, Chap. XVIII, p. 503; *Hd. Exp. Phys.*, *loc. cit.*, p. 45.

[‡] Back, *Ann. d. Phys.*, 70, 333, 1923; **76**, 317, 1925. See also Landé and Backs' book *Zeemaneffect und Multipletstruktur der Spektrallinien* (1925), Chap. VII, p. 128.

The ordinary methods of producing spectral lines used in the laboratory are either the vacuum tube discharge or the vacuum spark with an air gap in parallel. The former cannot be used in this case as the discharge is affected by the magnetic field, while in the latter the lines obtained are not so intense. These disadvantages have been removed in the vacuum arc method. Further, by this arrangement the gaseous substances may also be investigated by introducing the gases in the brass cylinder and using pure carbon electrodes.

Magnetic Fields.—Magnetic fields of 21,000 gausses are ordinarily used, and under special circumstances, fields as high as 50,000 gausses have been used. This required very expensive electromagnets of special construction. For observing *Paschen-Back Effect* (see *infra*) even fields of several hundred thousand gausses are needed. Methods for producing extremely large fields for a very short interval of time have been devised by Kapitza and Skinner* in the Cavendish Laboratory.

A few typical photographs taken in the Tübingen apparatus are reproduced in Fig. 2, Plate VIII. These have been five times enlarged. Wavelength increases towards the right.

Description of photographs.

(1) Normal triplet.—Zeeman pattern for lines of singlet spectrum.

The line is Cd λ 6438·71, 2P − 3D (singlet). The π-components are above and σ-components below. Note that the π-component is doubly more intense than each σ-component.

Anomalous Zeeman Pattern.

(2) Zeeman effect of doublet spectra.

Below—without magnetic field, *Above*—under the field.

Left — D_2 of Sodium, λ 5890·19, $^2S - {}^2P_{\frac{3}{2}}$,

Right—D_1 .... λ 5895·16, $^2S - {}^2P_{\frac{1}{2}}$.

Observe that D_1 is split into 4 components and D_2 into 6 components.

Zeeman effect of triplet spectrum.—The lines were $^3P_{0,1,2} - {}^3S_1$, λ 4680·38, 4722·34, 4810·71 of Zn. Looking from left to right observe that

---

* Kapitza and Skinner, *Proc. Roy. Soc. A*, **105**, 619, 1924; **106**, 602, 1924; **100**, 224, 1925.

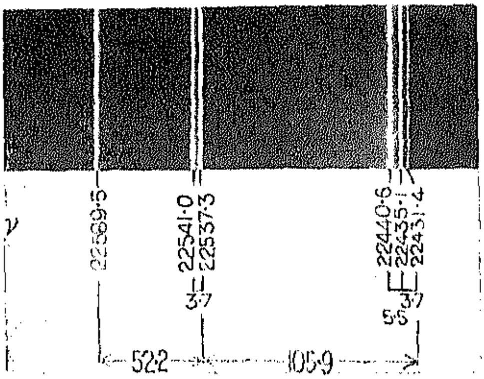

Fig. 3. The diffuse triplet of Ca.
(*p.* 383)

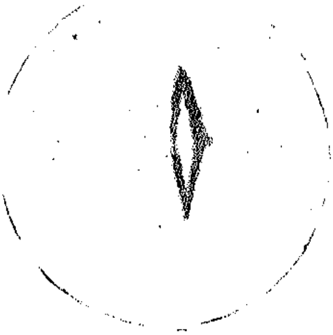

Fig. 9. Stern-Gerlachs' photograph for Ag rays.
(*p.* 410)

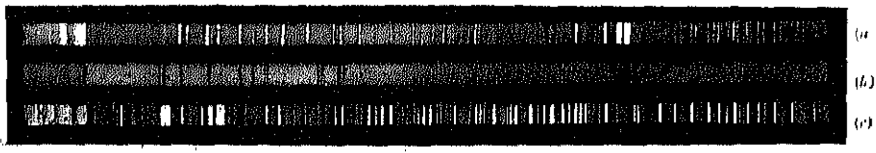

Fig. 4. Absorption Spectrum of Ca vapour.
(*a*) *g*-line reversed. (*b*) *g*-line in absorption. (*c*) Comparison.
(*p.* 386)

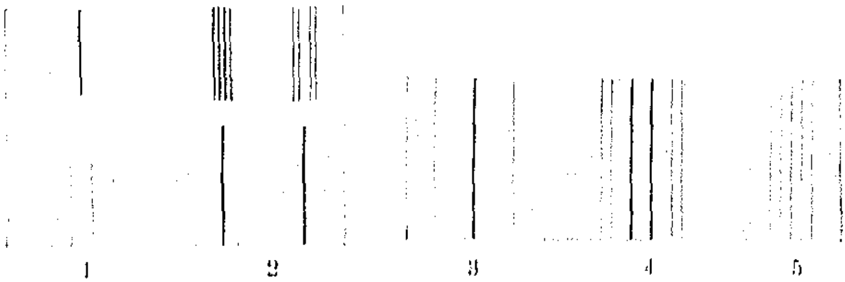

Fig. 2. Zeeman effect for singlet, doublet and triplet spectra.

(1) Normal triplet for Cd λ6438·71
(2) D_2 λ 5890 of Na (*left*)
(3) D_1 λ 5896 of Na (*right*)
(3) Zn λ 4680.
(4) Zn λ 4722.
(5) Zn λ 4810.

(*p.* 396)

(3) λ 4680·38 .... $^3P_0 - {}^3S_1$ gives 3 components
(4) λ 4722·34 .... $^3P_1 - {}^3S_1$ ... 6 ...
(5) λ 4810·71 .... $^3P_2 - {}^3S_1$ ... 9 ...

The extreme left and right components of λ 4810·71 are very faint, and cannot be clearly distinguished in the reproduction.

It will be observed that the Zeeman pattern becomes more and more complex, as the inner quantum numbers of the terms producing the lines increase. We proceed to a discussion of the complex type of Zeeman effect in §208.

207. Larmor's Treatment.—Larmor's treatment of normal Zeeman Effect was different though the result was the same. He showed that the effect of a uniform magnetic field on the motion of an electron moving in any orbit is to impress on the whole system a uniform precession about an axis parallel to the field with the angular velocity

$$\omega = \frac{eH}{2mc}$$

For proving the theorem, we observe that equations (1) can be written in the form

$$\left.\begin{aligned} m(\ddot{x} - 2\omega_H \dot{y}) &= -\mu x \\ m(\ddot{y} + 2\omega_H \dot{x}) &= -\mu y \\ m\ddot{z} &= -\mu z \end{aligned}\right\} \quad \ldots\ldots \quad (9)$$

where
$$\omega_H = \frac{eH}{2cm}$$

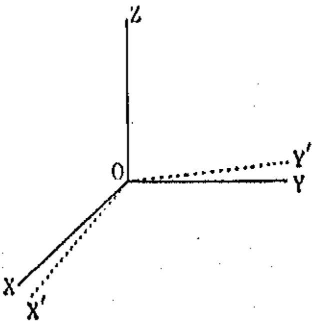

Fig. 3. The rotating axes.

This equation can be given an interesting dynamical interpretation. Let us suppose that the electron is moving in the plane of x, y and the velocities in the plane are $\dot{x}$ and $\dot{y}$. Let the plane now rotate uniformly with the angular velocity ω about the z-axis (Fig. 3). Then if U and V are the velocities* referred to axes fixed in space but instantaneously coincident with the moving axes OX and OY, we have

$$U = \dot{x} - y\omega, \quad V = \dot{y} + x\omega,$$

for, to the ordinary velocity, we must add the velocity due to the revolution of the plane OXY. The components of the rotational velocity are $-y\omega$, $x\omega$. In a similar way the accelerations f and g referred to the same fixed axes can be shown to be given by

---

* See Webster, *The Dynamics of Particles and of Rigid, Elastic and Fluid Bodies* (1912), Chap. VII, § 103 where the general case is treated.

$$\left.\begin{aligned} f &= U - V\omega & g &= V + U\omega \\ &= \ddot{x} - 2\dot{y}\omega - x\omega^2 & &= \dot{y} + 2\dot{x}\omega - y\omega^2 \\ &= \ddot{x} - 2\dot{y}\omega & &= \ddot{y} + 2\dot{x}\omega \end{aligned}\right\} \quad . \quad . \quad . \quad (11)$$

for when ω is small, ω^2 can be neglected. Then the equations of motion become

$$\left.\begin{aligned} m\,(\ddot{x} - 2\omega\dot{y}) &= F_x \\ m\,(\ddot{y} + 2\omega\dot{x}) &= F_y \end{aligned}\right\} \quad . \quad . \quad . \quad . \quad . \quad . \quad . \quad . \quad (12)$$

Hence comparing (9) and (12), we find that if $\omega = \omega_H$, the two sets of equations become identical, *i.e.*, the effect of the magnetic field is simply to impart to the orbit of the electron a precession with the angular velocity $\omega = eH/2mc$ round the axis of the external field, as depicted in Fig. 4.

The orbit of the electron is represented by the ellipses AP. The magnetic field is represented by H. The paths described by the aphelion and the perihelion during precession are represented by upper and lower circles respectively.

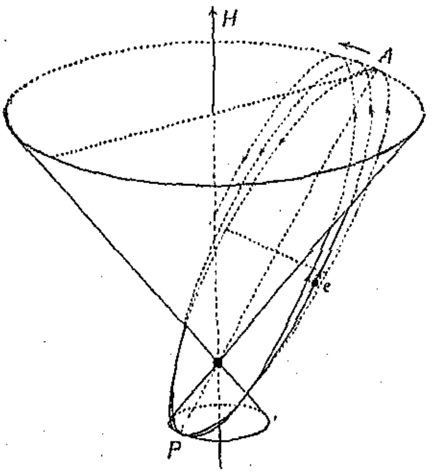

Fig. 4. Precession of orbit in a magnetic field.

Larmor's treatment can be adapted to quantum mechanics. The effect of this precessional motion is to increase the energy of the system by the amount

$$\triangle W = h\,\frac{k\cos\alpha}{2\pi}\,\omega \quad . \quad . \quad . \quad . \quad . \quad . \quad . \quad . \quad (13)$$

where α is the angle between the orbit-axis and the axis of the magnetic field and k is the azimuthal quantum number. This can be shown by referring to Fig. 17 on page 358.

There it was shown that the K. E. in three dimensions is given by

$$T = \tfrac{1}{2}\,m\,(\dot{r}^2 + r^2\theta^2 + r^2\sin^2\theta\,\dot{\varphi}^2)\,, \quad . \quad . \quad . \quad . \quad (14)$$

Let now the axis of the field be denoted by OP. Then on account of the imposition of the field, the orbit processes round OP with the velocity ω_H. To take account of this precessional effect, it will suffice if we write in (14) ψ in place of φ, where $\psi = \varphi + \omega_H t$. It is clear that ψ is the longitude referred to axes fixed in space. Then we obtain $T' = \frac{1}{2} m\,(\dot{r}^2 + r^2\dot{\theta}^2 + r^2 \sin^2\theta\, \overline{\dot{\phi}+\omega_H}^2)$

or $$T' = T + mr^2 \sin^2\theta . \dot{\varphi} . \omega_H = T + p_\phi . \omega_H \quad . \quad . \quad (15)$$

But $$p_\phi = p_\psi \cos\alpha \quad \text{and} \quad p_\psi = kh/2\pi$$

Hence $$T' = T + p_\psi \omega_H \cos\alpha \quad . \quad . \quad . \quad . \quad . \quad . \quad . \quad . \quad . \quad (15')$$

Hence $$\Delta W = \frac{hk \cos\alpha}{2\pi}\, \omega_H \quad . \quad . \quad . \quad . \quad . \quad . \quad . \quad (16)$$

We have therefore $$\Delta\nu = \frac{\Delta\omega}{h} = \frac{eH}{4\pi e m}\, k \cos\alpha$$

$$= ak \cos\alpha \quad . \quad . \quad . \quad . \quad . \quad . \quad . \quad . \quad . \quad . \quad (17)$$

Hence we have the Zeeman-separations of the H-atom given by

$$\Delta\nu = a\,(k \cos\alpha - k' \cos\alpha') = a\,(k_1 - k_1') \quad . \quad . \quad . \quad . \quad (18)$$

where k', α' refer to the initial orbit. Both $k \cos\alpha = k_1$ and $k' \cos\alpha' = k_1'$ are integral. We therefore find that (17) explains the observed normal effect if we suppose that

$\Delta k_1 = \pm 1, 0$ only,

and $\Delta k_1 = \pm 1$, give us components with circular polarisation,

$\Delta k_1 = 0$ gives us components polarized parallel to the field.

This result was arrived at simultaneously by A. Sommerfeld* and P. Debye†.

208. Anomalous Zeeman Effect.—On account of the great potential importance of Zeeman-effect in throwing light on the structure of the atom, an intense interest was created throughout scientific world, and many famous investigators including Michelson, Paschen, Runge and Preston joined in systematic investigations of Zeeman-effect of spectral lines. Soon after the investigations were commenced it became however apparent that the simplicity presented by Lorentz's model of the atom was rather illusory. As shown in the reproductions of the patterns (Fig. 2, Plate VIII) only a few lines were found to split according to Lorentz's model, most lines were found to split in much more complicated patterns, though it was evident from the nature of the results, that some regularity ran through the mass of apparently complex results.

---

* A. Sommerfeld, *Phys. Zeits.*, 17, 491, 1916.

† P. Debye, *Göttinger Nachr.*, 1916.

In the following diagrams, some of these complex Zeeman patterns (shown in Plate VIII, Fig. 2) are represented graphically.

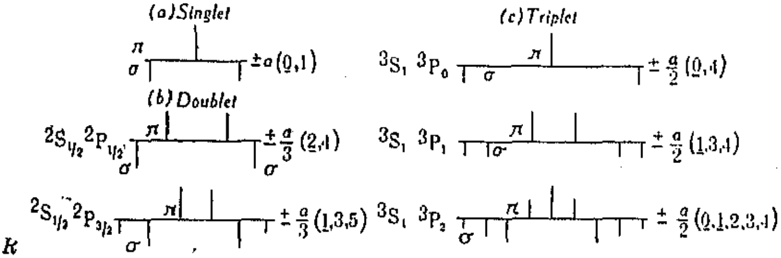
(a) Singlet
π
σ
±a (0,1)
(b) Doublet
$^2S_{1/2}\ ^2P_{1/2}$
π
σ
σ
$\pm\frac{a}{3}(\underline{2},4)$
$^2S_{1/2}\ ^2P_{3/2}$
π
σ
$\pm\frac{a}{3}(\underline{1},3,5)$
K
(c) Triplet
$^3S_1\ ^3P_0$
π
σ
$\pm\frac{a}{2}(\underline{0},4)$
$^3S_1\ ^3P_1$
π
σ
$\pm\frac{a}{2}(\underline{1},3,4)$
$^3S_1\ ^3P_2$
π
σ
$\pm\frac{a}{2}(\underline{0},\underline{1},2,3,4)$

Fig. 5. Graphical sketch of anomalous Zeeman effect.

The first pattern (*a*) represents the normal Zeeman splitting for singlets. The second pattern (*b*) shows the splitting of the D_1 and D_2-lines of sodium. The D_1 splits up into four components of which the two outer are σ-components. The displacements of these on the frequency scale are given by $\pm 4a/3$; these for the inner two which are the π-components are $\pm 2a/3$, where a is $eH/4\pi cm$. The D_2-line λ 5890 is split up into six components, the two inner $\pm a/3$ are π-components, the four outer $\pm 3a/3$, $\pm 5a/3$ are σ-components. These facts may be symbolically represented by

$$1s-2p_1 \quad . \quad . \quad . \quad D_1 \quad . \quad . \quad . \quad . \quad . \quad . \quad \pm\frac{a}{3}(\underline{\mathbf{2}},\ \mathbf{4})$$

$$1s-2p_2 \quad . \quad . \quad . \quad D_2 \quad . \quad . \quad . \quad . \quad . \quad . \quad \pm\frac{a}{3}(\underline{\mathbf{1}},\ \mathbf{3},\ 5)$$

where the short line below a number denotes π-components.

Similarly the lines of divalent elements (*e.g.*, Zn green triplet) forming the *ps*-triplet are separated according to the pattern (*c*). These can be represented as follows :

$$2p_0-2s \quad . \quad . \quad . \quad . \quad \pm\frac{a}{2}(\underline{\mathbf{0}},\ \mathbf{4})$$

$$2p_1-2s \quad . \quad . \quad . \quad . \quad \pm\frac{a}{2}(\underline{\mathbf{1}},\ 3,\ 4)$$

$$2p_2-2s \quad . \quad . \quad . \quad . \quad \pm\frac{a}{2}(\underline{\mathbf{0}},\ \underline{1},\ \mathbf{2},\ 3,\ 4)$$

209. Discovery of Regularities in Complex Zeeman Patterns.—An intensive study of these Zeeman patterns showed that the splitting is governed by very significant rules. These were discovered by Preston and Runge.

Preston's Rule.—Preston showed that all lines belonging to the same type of spectral classification show the same type of Zeeman splitting, *e.g.*, we have seen that all the alkalies Cu, Ag, Au, and the ionised elements Be^+, Mg^+, Ca^+, Sr^+, Ba^+ . . . . . show the same type of spectra, *i.e.*, they have all got *doublet* lines belonging to principal, sharp, and diffuse series. Preston found that all lines of these elements given by the formula

$$\nu = R'\left[\frac{1}{(1+s)^2} - \frac{1}{(n+p_1)^2}\right]$$

where $R' = R$, $4R$, or $9R$ are split like the D_1-line of Na, no matter what the value of n. Such lines are

$$Ca^+\ \lambda\ 3968\ \ldots\ Sr^+\ \lambda\ 4215\ \ldots\ Ba^+\ \lambda\ 4934$$

belonging to $1s-2p_1$ combination. The companion line represented by

$$\nu = R\left[\frac{1}{(1+s)^2} - \frac{1}{(m+p_2)^2}\right]$$

is split into 6 components like the D_2-line of Na. This rule holds not only for the D_1 and D_2, but for all lines of the sharp and to a certain extent of the principle series (for exceptions, see Paschen-Back effect). For the *pd*-lines of trivalent elements like Al, the Zeeman patterns are

$$\left.\begin{aligned}
2\,p_2 - 3\,d_3\ \ldots\ &\pm \tfrac{a}{15}\,(\underline{\mathbf{1}},\ \underline{3},\ \mathbf{15},\ 17,\ 19,\ 21)\\
2\,p_2 - 3\,d_2\ \ldots\ &\pm \tfrac{a}{15}\,(\underline{\mathbf{4}},\ 8,\ \mathbf{1\underline{2}},\ \mathbf{16},\ 24)\\
2\,p_1 - 3\,d_2\ \ldots\ &\pm \tfrac{a}{15}\,(\underline{\mathbf{1}},\ 11,\ \mathbf{13})
\end{aligned}\right\}$$

The rule was found to be of great importance in determining the series characteristic of lines and was very largely used by spectroscopists in the early days of empirical classification.

Runge's Rule.—Runge found that the separations are integral multiples of small aliquot parts of the normal separation a. The rule is illustrated in the description of the Zeeman effect of D_1, D_2 and of the *pd*-group. The common denominator of the aliquot part for the same group of lines is called the Runge denominator. Thus for the D_1, D_2 lines, the Runge denominator is 3, for the *ps*-triplet it is 2 for the doublet *pd*-group it is 15 and so on. These aliquot parts were found to be characteristic of the series characteristics of the terms.

210. Sommerfeld's Generalisations.—After the rise of the quantum theory of line spectra, Sommerfeld* showed that these rules required a new interpretation. For according to the principle of combination, the frequency of each line is the difference of two numbers, each of which multiplied by h represents the energy of a particular quantum state of the atom. The Zeeman splittings have therefore to be further referred to the component terms. For illustration we take the D_2 line of sodium *viz.*,-$1s - 2p_2$. $A-h\,(1s)$ is the energy of the light-electron of Na in the $1s$-state, $A-h\,(2p)$ is the energy in the $2p$-state. When the atom is placed in a magnetic field, then on account of the interaction between the magnetic field and the light-electron, the energy will be different from the undisturbed value by $h\Delta\nu_i$ or $h\Delta\nu_f$ in the initial or final state respectively. We have therefore

$$\Delta\nu = \Delta\nu_i - \Delta\nu_f$$

and the problem is now reduced to finding out the value of $\Delta\nu$ *for each kind of spectral terms which we come across in spectral classification.* The systematisation was pushed through by Sommerfeld and his pupils who first assumed that $\Delta\nu$ for every kind of orbit can be represented by ap/q, where p and q are some numbers characteristic of each kind of orbit, depending on the values k, r, j but not on n.

211. The Atom as a Magnet—The Bohr-magneton.—As the original Bohr-Sommerfeld model did not hold out any hope of explaining the anomalous effect, the more general assumption was made that *each atom, in any quantum state, may be regarded as an elementary magnet with a definite axis and a definite magnetic moment* μ.

Let us see how this conclusion was arrived at.

We shall discuss in chapter XVI the detailed theories of magnetism. The intimate relation between magnetism and electricity was first discovered by Oersted who discovered that a wire carrying a current

---

*A. Sommerfeld, *Atombau und Spektrallinien* (1924), Chap. 8, §8, p. 612.

produces a magnetic field about it. Following these studies, Ampere showed that if a current i passes through a wire enclosing a plane area S, the magnetic action of the area is equal to that of a normally polarised magnetised shell occupying the same area, and having the total moment iS. This theorem is the foundation of current electricity; but here we are concerned with the attempt of Ampere to explain natural magnetism in terms of small currents of molecular dimensions existing within magnetic bodies. In chapter XVI, we have described how this theory has received complete verification, and how at the present time, all the phenomena of magnetism are explained in terms of different kinds of motion of the electron.

It is clear that on this view, Bohr's hydrogen orbits possess definite magnetic moments. Taking a circular orbit, we find that the magnetic moment of the orbit

$$\mu = iS$$

where S = area, i = equivalent current in e.m. units.

Now $S = \pi r^2$, and $i = e/cT$, where T is the periodic time, and c in the denominator converts it to e.m. units. Hence we have

$$\mu = \frac{e\pi r^2}{cT} = \frac{e\omega r^2}{2c} \quad . \; . \; . \; . \; . \; . \; . \; . \; . \quad (19)$$

According to Bohr's theory $\quad mr^2\omega = \dfrac{kh}{2\pi}$

Hence $\quad \mu = k\dfrac{eh}{4\pi cm}$

Thus the magnetic moment of the electron in the k^{th} orbit is an integral multiple of the elementary quantity $eh/4\pi cm$.

To the quantity $eh/4\pi cm$ the name of *Bohr-magneton* has been given. Even if the orbit be elliptic, the magnetic moment is given by

$$k\frac{eh}{4\pi cm} \quad . \; . \; . \; . \; . \; . \; . \; . \; . \; . \; . \; . \quad (20)$$

where k is the azimuthal quantum number. The axis of the magnet is along the normal to the orbit.

212. The Atom in a Magnetic Field.—The results of anomalous Zeeman effect show that the magnetic moment of the general atom is more complex than that of the H-atom, for otherwise the Zeeman splitting would be always normal. Let us suppose that it is given by $\mu\alpha$, where $\mu = eh/4\pi cm$, and α is a function of quantum numbers which is to be determined.

When such a magnet is placed in the magnetic field H with its axis inclined at an angle θ to the field, the atom has the additional energy

$$h\triangle\nu_i = H\mu_i \cos\theta_i$$

where μ_i = magnetic moment of the initial state.

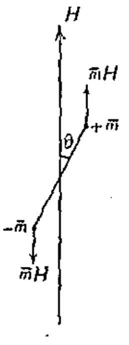

Fig. 6

This can be easily deduced with the help of Fig. 6 where $\bar{m}$ denotes the pole strength of the elementary magnet.

If the atom now passes to another quantum state with the magnetic moment μ_f, and angle of inclination θ_f, the additional energy due to the field is

$$h\triangle\nu_f = H\mu_f \cos\theta_f$$

Hence the Zeeman separation is given by

$$\triangle\nu = \frac{H}{h}(\mu_i \cos\theta_i - \mu_f \cos\theta_f)$$

We have therefore

$$\triangle\nu = \frac{eH}{4\pi cm}(\alpha_i \cos\theta_i - \alpha_i \cos\theta_f)$$

$$= a(\alpha_i \cos\theta_i - \alpha_f \cos\theta_f)$$

Using this expression we have now to find out the value of α for the general type of atom, from an analysis of the data on Zeeman effect.

From a scrutiny of these results, it was deduced by several investigators (Sommerfeld*, Bohr, and Pauli) that α in the first instance is dependent on the "*inner quantum" number and not on the azimuthal quantum number.* To understand how this conclusion was arrived at, acquaintance with original work is necessary, but some idea may be formed from a reference to the anomalous Zeeman patterns of sodium. Sodium D_1 and D_2 lines have the same k for initial and final orbits, namely 2 and 1, but their Zeeman patterns are different. Hence α cannot be dependent on k alone. A better example is the Zeeman pattern of the three lines forming the triplet *ps* group of two-valence elements, which are widely different, though k for the initial and final orbits are the same in all cases. First as a tentative measure, α was taken proportional to j, which for $2p_0$ was taken to be 0, for $2p_1$ to be 1, for $2p_2$ . . . 2, and this supposition, after some modification proved to be thoroughly successful. We now put the magnetic moment of an atom

---

* For details see A. Sommerfeld, *loc. cit.*

$$\alpha\,\mu = \mu\, g\, j \quad . \quad . \quad . \quad . \quad . \quad . \quad . \quad . \quad . \quad . \quad (21)$$

where j= inner quantum number, 'g' is a factor to be determined. It was first correctly determined by Landé, and has received the name of *Landé-factor.*

The change in energy of an atom-magnet measured in frequency is given by

$$\Delta\nu = a\; g\; j \cos\theta = a\; g.\; m \quad . \quad . \quad . \quad . \quad . \quad . \quad . \quad (22)$$

where $m = j\cos\theta$; m is known as the *magnetic quantum number.* The possible values of m are

$$j,\;\; j-1,\;\; j-2,\;\; \ldots\; -j$$

i.e., for a term having the inner quantum number j, there are $2j+1$ magnetic quantum numbers.

Thus the m's are projections of j on the external magnetic axis, as shown in Fig. 7.

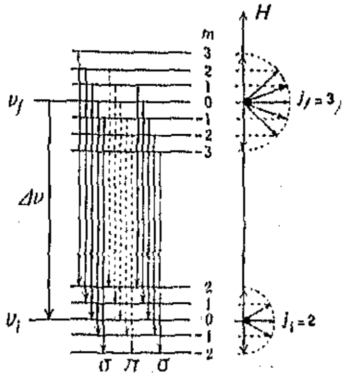

Fig. 7—The magnetic quantum number.

H represents the direction of the external magnetic field. $j_f = 3$ is the j-vector of the final quantum orbit. This is represented by the radius vector of the upper dotted semicircle. The corresponding m-values are shown by the projections of the radii in different directions on the magnetic field axis. It is easy to see that $m=3$ along the direction of H, then it diminishes successively by 1, and finally $m=-3$ in a direction opposite to that of H. m thus takes the *seven* values $+3$, 2, 1, 0, -1, -2 and -3, and the corresponding quantum sublevels are shown against the projections. Similarly the j-vector of the initial orbit is $j_i = 2$ (radius of the lower dotted circle), and the corresponding quantum sublevels have $m=2, 1, 0, -1$ and -2. The three sets of lines corresponding to the transitions $\Delta m = \pm 1$ and 0 are shown by the three systems of arrows.

We have then for any transition from initial to final orbit

$$\frac{\triangle\nu}{a} = g_i m_i - g_f m_f \quad . \quad . \quad . \quad . \quad . \quad . \quad . \qquad (23)$$

which gives the Zeeman separation of any spectral line.

213. Correlation of Formula to Experimental results.—With the aid of this formula, it is possible to get all the Zeeman components. Correct values of the g's and m's were obtained after repeated trials. We give here a few chief results; the full results will be given later.

(1) It was found that for terms of even multiplet, all the j's must be half numbered.

(2) For terms of odd multiplets, j's have integral values.

All the g values were at first obtained by trial, and theoretical interpretation came later. But at the present time it is possible to write out g and j values from a few simple rules which will be explained later.

There must be a selection principle for m, and this is the same as that for j. Allowed transitions are

$$m \rightarrow m \qquad \ldots \text{ giving } \pi\text{-components}$$

$$m \begin{array}{l} \nearrow m+1 \\ \searrow m-1 \end{array} \qquad \ldots \text{ giving } \sigma\text{-components}$$

The transition $m=0 \rightarrow m=0$ is allowed. The justification for these rules was given by the correspondence principle and later by Wave-mechanics (*vide infra*).

The methods of writing out the Zeeman separations on this basis are illustrated in the following tables.

Take for example the D_1 line of sodium. It arises out of the doublet sp_1 combination or a transition ${}^2P_{\frac{1}{2}} \rightarrow {}^2S_{\frac{1}{2}}$. The g-values of the initial and the final terms are 2 and 2/3 respectively. These are shown in the first three columns of the table. Again for each of the two terms, $j=\frac{1}{2}$, hence $m = +\frac{1}{2}$ or $-\frac{1}{2}$, and the corresponding mg-values are $-1, +1$ for ${}^2S_{\frac{1}{2}}$, and $-\frac{1}{3}, +\frac{1}{3}$ for ${}^2P_{\frac{1}{2}}$. These are shown in column 4. The allowed transitions are $(-1 \rightarrow -\frac{1}{3})$, $(1 \rightarrow \frac{1}{3})$, $(-1 \rightarrow \frac{1}{3})$ and $(1 \rightarrow -\frac{1}{3})$ as marked by arrows. We thus get altogether 4 components having the separations $\Delta\nu/a = \pm\frac{1}{3}$ (2, 4) as represented in the last column. The two components having

$\Delta\nu/a = \pm 2/3$ arise out of transitions $\Delta m = 0$, and they are π-components, and the other two ($\Delta m = \pm 1$) are σ-components.

Table I.

Combination	Term	m g	$-3/2$	$-1/2$	$1/2$	$3/2$	$\frac{\Delta\nu}{a}$
	$^2S_{\frac{1}{2}}$	2		-1	1		
$D_1 \ldots s\, p_1$				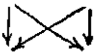			$\pm \frac{1}{3}(\underline{2}, 4)$
	$^2P_{\frac{1}{2}}$	$2/3$		$-1/3$	$1/3$		
	$^2S_{\frac{1}{2}}$	2		-1	1		
$D_2 \ldots s\, p_2$			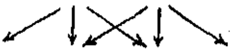				$\pm \frac{1}{3}(\underline{1}, 3, 5)$
	$^2P_{\frac{3}{2}}$	$2/3$	$-6/3$	$-2/3$	$2/3$	$6/3$	

		m g	-2	-1	0	1	2	
	$^3S_1$	2		-2	0	2		
$p_0\ s$				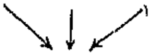				$\pm \frac{1}{2}(\underline{0}, 4)$
	$^3P_0$	0			0			
	$^3S_1$	2		-2	0	2		
$p_1\ s$				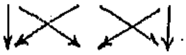				$\pm \frac{1}{2}(\underline{1}, 3, 4)$
	$^3P_1$	$3/2$		$-3/2$	0	$3/2$		
	$^3S_1$	2		-2	0	2		
$p_2\ s$			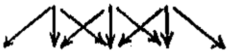					$\pm \frac{1}{2}(\underline{0}, \underline{1}, 2, 3, 4)$
	$^3P_2$	$3/2$	$-6/2$	$-3/2$	0	$3/2$	$6/2$	

Similar analyses show that the D_2-line would split up into 6 components; while for the ps-triplet, we would get 3 components from $s\,p_0$-combination, 6 from $s\,p_1$ and 9 from $s\,p_2$.

These results agree with the experimental results quoted in Fig. 5, p. 400.

Proceeding on this basis of analysis of Zeeman-separation, Back and Landé, worked out in detail the theoretical Zeeman patterns for a large number of multiplet spectral lines. For a comprehensive list, see the tables published in *Bureau of Standard Journal of Research*, by Kiess and Meggers, **1**, 641, 1928, or p. 198 to 203 of Back and Landé's book (*loc. cit.*).

As a result of extensive studies of the intensities of the Zeeman components, certain general rules regarding their relative intensities have been arrived at. It is found that when the Zeeman components arise from transitions between orbits which have the same number of magnetic levels, as in the doublet sp_1, and triplet p_1s-combinations in the last table, the π-components corresponding to the *extreme* (vertical) arrows in the scheme are the strongest, while the σ-components corresponding to the *middle* (slanting) arrows in the scheme are the strongest. But when the Zeeman components arise from transitions between orbits which possess unequal number of magnetic levels as in doublet sp_2 and triplet p_0s, p_2s combinations, the rules are reversed. Thus for the triplet p_1s, the π-components $\Delta\nu/a = \pm\frac{1}{2}$ are the strongest and σ-components $\Delta\nu/a = \pm 3/2, 4/2$ are almost equally strong, while for the triplet p_2s, the π-components $\Delta\nu/a = 0$, and σ-components $\Delta\nu/a = \pm 2/2$ are the strongest. The intense components are denoted in thick types in the last column of the table.

214. Experimental Test of Directional Quantisation of Atoms : Stern and Gerlach Experiment.—The above theory of Zeeman effect involved many assumptions which were only gradually verified. One of the chief assumptions is that if an atom magnet be placed in a magnetic field, the equilibrium position is not given by the classical theory of magnetism, for in that case, the magnet would always align itself parallel to the lines of force. Neither is the axis oriented at random, but is inclined at definite angles

$$\theta = \cos^{-1}\frac{1}{j}\,(j, j-1 \quad . \quad . \quad . \quad -j)\, . \quad . \quad . \quad . \quad . \qquad (24)$$

to an arbitrarily fixed external axis, as shown in Fig. 7, p. 405.

The deduction is rather surprising, for it signifies that the atom-axis can point only to certain privileged directions as indicated by arrows in Fig. 7, any haphazard direction is not allowed.

Though the entire explanation of Zeeman effect is based on this hypothesis, the phenomenon affords no direct proof of this, as we are here concerned only with the difference of the term values arising out of the oriented states. Stern and Gerlach* however devised an ingenious method for experimental verification of this paradoxical hypothesis. Their experimental arrangement is shown in Fig. 8.

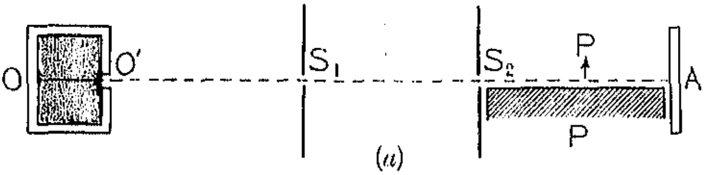

Fig. 8. Arrangements of Stern-Gerlach Experiment.

A beam of silver atom produced by heating silver in a small oven O, and rendered parallel by a number of fine slits S_1, S_2 is allowed to pass through a *non-homogeneous* magnetic field PP, and is received on a photographic plate A. The inhomogeneous field is produced between two pole-pieces of an electromagnet, shaped as shown separately in Fig. 8 (*b*). On developing the plate no trace is obtained of the direct beam, but two traces are obtained equidistant from, and on either side of what would have been the trace of the direct beam. The direct beam has evidently been split up into two beams by the influence of the magnetic field. The interpretation of this result is as follows.

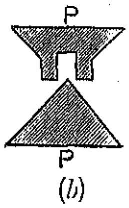

Fig. 8.

The energy of an atom-magnet whose axis is inclined at an angle $\theta = \cos^{-1}(m/j)$ to a magnetic field H is

$$-mg.\frac{eh}{4\pi m_0 c}H \quad \ldots\ldots\ldots \quad (25)$$

as proved in §212. The components of its magnetic moment along the direction of H is equal to $mg.\,eh/4\pi m_0 c$, that is to say, mg-Bohr magnetons. Now according to the assumption involved in equ. (24), m can assume $(2j+1)$ values between $+j$ and $-j$. When a stream of such atoms is sent through a *non-homogeneous* magnetic field of gradient dH/ds, each atom would be subjected to a force

$$mg.\frac{eh}{4\pi m_0 c}.\frac{\partial H}{\partial S} \quad \ldots\ldots\ldots \quad (26)$$

---

* O. Stern and W. Gerlach, *Ann. d. Phys.*, 74, 673, 1924; W. Gerlach, *Ann d. Phys.*, 76, 163, 1925.

This force would split up the atom-beam into $(2j+1)$ separate streams corresponding to the $(2j+1)$ different values of the magnetic moment. Further, the deviation of any stream from its original course would be proportional to the factor mg. We can obtain an expression for the deviation in the following way.

Suppose v=the velocity of the silver atoms corresponding to the oven temperature T (in absolute scale), and l=the length of the wedge-shaped pole-piece. Then the atom is subjected to the magnetic field for a time l/v. Since it possesses an acceleration $f=\partial H/\partial s.\ (mg.\ eh/4\pi m_0c)/m_0$, the atom is deflected on coming *just outside* the field, by an amount

$$s=\tfrac{1}{2}ft^2=\frac{1}{2m_0}\cdot\frac{\partial H}{\partial s}\cdot\left(\frac{l}{v}\right)^2\cdot\frac{eh}{4\pi m_0c}mg$$

But $$\tfrac{1}{2}m_0v^2=\tfrac{3}{2}kT^*$$

for atoms in equilibrium, where k=Boltzmann's constant.

Hence $$s=\frac{l^2}{6kT}\cdot\frac{\partial H}{\partial s}\cdot\frac{eh}{4\pi m_0c}\cdot mg \quad . \quad . \quad . \quad . \quad (27)$$

This would be the deflection of the trace on photographic plate if the latter is placed just outside the pole-pieces. But in actual practice the plate is situated some distance apart. If a=distance between the plate and the end of pole-pieces, the additional deflection is $f.\ la/v^2$, so that the total deflection

$$s=\frac{1}{6kT}\cdot\frac{\partial H}{\partial s}\cdot\frac{eh}{4\pi m_0c}\cdot mg.\ l^2\left(1+\frac{2a}{l}\right). \quad . \quad . \quad (28)$$

as proved on p. 83, Chap. III.

For silver atoms, as already mentioned, two traces were obtained. This can be seen from an actual photograph reproduced in Plate VIII, Fig. 9 from the original due to Gerlach. On measuring the deflections, it was found with the aid of relation (28) that these corresponded to $mg=\pm1$. It leads to the conclusion that *the Ag-atoms orient themselves in the magnetic field in such a way that their resolved magnetic moment along the field direction is ±1 Bohr magnetons.*

---

[*] Stern found, however, from direct measurements that the mean velocity of the silver atoms issuing through the slit is given by the expression $\frac{1}{2}mv^2=3{\cdot}5\ kT/2$.

This is exactly what is to be expected from the spectroscopic theory. For, the normal state of Ag-atom is $^2S_{\frac{1}{2}}$, which gives only two values of $m = +\frac{1}{2}$ and $-\frac{1}{2}$; and $g=2$. So we get $mg = +1$ and -1.

The results expected for other spectroscopic states of normal atoms can be predicted in a similar way. A number of cases is shown in the following table, the expected pattern being graphically shown in column 5 of the table (the scale is arbitrarily chosen).

Experiments have been performed by Phipps and Taylor*, and Wrede† on hydrogen, Leu‡ on K, Na and Tl, Taylor§ on Li and other investigators on different elements in the periodic table to test the predictions given in Table 2. Except in the cases of Bi, Sb, Ni and Fe, they have obtained patterns in good agreement with theoretical predictions. In other cases, on account of experimental difficulties, the results are in general inconclusive. Taylor's results on Li have also been found to be anomalous.

Table 2.—Theoretical Stern-Gerlach Pattern of Elements.

Elements	Norm. state	g	mg	Stern-Gerlach Pattern
H, Li, Na, K; Cu, Ag, Au	$^2S_{\frac{1}{2}}$	2	$-1 \quad +1$	│ │
Zn, Cd, Hg ...	$^1S_0$	0	0	│
Sn, Pb ...	$^3P_0$	0	0	│
Tl (81) ...	$^2P_{\frac{1}{2}}$	2/3	$-1/3 \quad +1/3$	││
	$^2P_{\frac{1}{2}}$	4/3	$-6/3 \quad -2/3 \quad +2/3 \quad +6/3$	│ │ │ │
	$^3P_1$	3/2	$-3/2 \quad 0 \quad +3/2$	│ │ │
	$^3P_2$	3/2	$-6/2 \quad -3/2 \quad 0 \quad +3/2 \quad +6/2$	│ │ │ │ │
P, N ...	^4S	2	$-3 \quad -1 \quad +1 \quad +3$	│ │ │ │

---

* E. Phipps and J. B. Taylor, *Phys. Rev.*, **29**, 309, 1927.
† E Wrede, *Zs., f. Phys.*, **41**, 569, 1927.
‡ A. Leu, *Zs., f. Phys.*, **41**, 551, 1927; **49**, 498, 1928.
§ R. G. J. Fraser, *Proc. Roy. Soc. A*, **114**, 212, 1927
‖ J. B. Taylor, *Zs., f. Phys.*, **52**, 846, 1929.

215. Landé's Tables of Inner Quantum Numbers and g-Values.—The inner quantum numbers and g-values for the families of terms in an alkali spectra (doublet) are shown below in table 3. Landé was able to arrive at these values empirically from an analysis of the great mass of data on the Zeeman splitting of multiplets collected by the long and painstaking experiments of Back carried out at Tübingen.

For the doublet ($s=1/2$) sharp-series $j=1/2$, for the principal series $j=1/2$, $3/2$, and so on. The g-values are 2 for the s-series, $2/3$, $4/3$ for the p-series corresponding to $j=1/2$, $3/2$ respectively, and so on for other family of terms.

Table 3.—Doublet Terms ($s=1/2$).

	j				
$k=1$, s	$\frac{1}{2}$				
$k=2$, p	$\frac{1}{2}$	$\frac{3}{2}$			
$k=3$, d		$\frac{3}{2}$	$\frac{5}{2}$		
$k=4$, f			$\frac{5}{2}$	$\frac{7}{2}$	
$k=5$, g				$\frac{7}{2}$	$\frac{9}{2}$

$l \backslash j$	$\frac{1}{2}$	$\frac{3}{2}$	$\frac{5}{2}$	$\frac{7}{2}$	$\frac{9}{2}$
0	$\frac{2}{1}$				
1	$\frac{2}{3}$	$\frac{4}{3}$			
2		$\frac{4}{5}$	$\frac{6}{5}$		
3			$\frac{6}{7}$	$\frac{8}{7}$	
4				$\frac{8}{9}$	$\frac{10}{9}$
	g-values				

For the singlet terms, the Zeeman effect has been found to be normal. Their inner quantum numbers and g-values are shown below.

Tabe 4.—Singlet Terms ($s=0$).

	j				
$k=1$ s	0				
2 p		1			
3 d			2		
4 f				3	
5 g					4

$l \backslash j$	0	1	2	3	4
0	0				
1		1			
2			1		
3				1	
4					1
	g-values				

For the triplet ($s=1$) terms, the j- and g-values are shown below.

Table 5.—*Triplet terms* ($s=1$).

	j					
$k=1$, s		1				
$k=2$, p	0	1	2			
$k=3$, d		1	2	3		
$k=4$, f			2	3	4	
$k=5$, g				3	4	5

l \ j	0	1	2	3	4	
0		$\frac{2}{1}$				
1	0	$\frac{3}{2}$	$\frac{3}{2}$			
2		$\frac{1}{2}$	$\frac{7}{6}$	$\frac{4}{3}$		
3			$\frac{2}{3}$	$\frac{13}{12}$	$\frac{5}{4}$	
4				$\frac{3}{4}$	$\frac{21}{20}$	$\frac{6}{5}$
	g-values					

For quartet ($s=\frac{3}{2}$) terms, the values are as follows.

Table 6.—*Quartet terms* ($s=\frac{3}{2}$).

	j					
$k=1$, s		$\frac{3}{2}$				
$k=2$, p	$\frac{1}{2}$	$\frac{3}{2}$	$\frac{5}{2}$			
$k=3$, d	$\frac{1}{2}$	$\frac{3}{2}$	$\frac{5}{2}$	$\frac{7}{2}$		
$k=4$, f		$\frac{3}{2}$	$\frac{5}{2}$	$\frac{7}{2}$	$\frac{9}{2}$	
$k=5$, g			$\frac{5}{2}$	$\frac{7}{2}$	$\frac{9}{2}$	$\frac{11}{2}$

l \ j	$\frac{1}{2}$	$\frac{3}{2}$	$\frac{5}{2}$	$\frac{7}{2}$	$\frac{9}{2}$	$\frac{11}{2}$
0		$\frac{2}{1}$				
1	$\frac{8}{3}$	$\frac{26}{15}$	$\frac{8}{5}$			
2	0	$\frac{6}{5}$	$\frac{48}{35}$	$\frac{10}{7}$		
3		$\frac{2}{5}$	$\frac{36}{35}$	$\frac{78}{63}$	$\frac{4}{3}$	
4			$\frac{4}{7}$	$\frac{62}{63}$	$\frac{116}{99}$	$\frac{14}{11}$
	g-values					

216. Mechanical Interpretation of Inner Quantum Number.

—From the above tables, we find that the inner quantum number j can be represented as the *vector sum* of two numbers, l, which is $(k-1)$, and s which is obtained from the multiplicity by the rule $s=(r-1)/2$.

We shall now explain what is meant by vector sum. If we have two vectors a and b, their resultant c is given by

$$c^2 = a^2+b^2-2ab\cos\theta$$

and according to the value of θ, $a+b$ can have all values between $a+b$ and $a-b$. Let us now assign to c, in accordance with the general trend of the quantum theory, only such values which differ from $a+b$ by integral numbers, *i.e.*,

$$e = a+b,\ a+b-1,\ a+b-2 \quad . \quad . \quad . \quad . \quad . \quad (a-b) \text{ or } (b-a)$$

whichever is positive.

Then e is said to be the quantum vector sum of the vectors a and b.

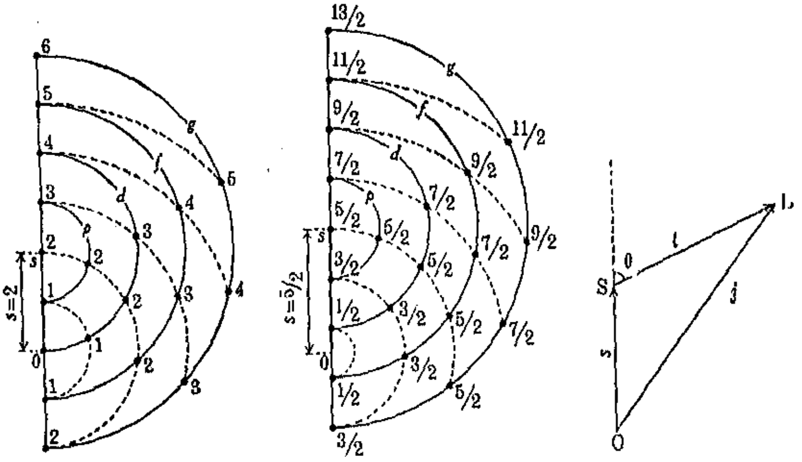

(*a*) (*b*) (*c*)

Fig. 9. The vector model of l, s, j-moments.

With this definition of e, we find that for the doublets the j-values are given by

$$|j| = |\overline{k-1}+\tfrac{1}{2}|$$

For singlets, $|j| = |\overline{k-1}+0|$, for triplets $j = |k-1+1|$. Thus the j=values for ${}^3\mathrm{P}$ are given by

$$|1+1| = 0, 1, 2$$

Hence we see that in general

$$j = |l+s| \quad . \quad . \quad . \quad . \quad . \quad . \quad . \quad . \quad . \quad . \quad (29)$$

where $l=k-1$, and $s=0,\ \tfrac{1}{2},\ \tfrac{2}{2} \ldots$ for singlets, doublets and triplets.

This rule is quite general, and has been found to be correct for spectra of higher multiplicities. We have, in general

$$s = \frac{r-1}{2} = 0,\ \tfrac{1}{2},\ \tfrac{2}{2},\ \tfrac{3}{2} \quad . \quad . \quad . \quad . \quad . \quad . \quad . \quad . \quad (30)$$

for singlets, doublets, triplets, quartets, etc. . . . , where r=multiplicity number.

The geometrical construction for obtaining the vector sum of two vectors $\boldsymbol{l}$ and $\boldsymbol{s}$ with a given angle θ between them is known as the *triangle of vectors* and is shown in Fig. 9(*c*). The method is as follows: draw a vector $\boldsymbol{s}=OS$, and from S draw the vector $\boldsymbol{l}=SL$ on the same scale and making angle θ with it. Then OL is the vector sum $\boldsymbol{j}$ of $\boldsymbol{s}$ and $\boldsymbol{l}$.

Sommerfeld utilised this method for obtaining l, $\boldsymbol{s}$, $\boldsymbol{j}$-schemes for odd and even multiplets of s, p, d, f, g-terms, as illustrated in Figs. 9 (*a*) and (*b*) for quintet and sextet respectively. For odd multiplicities we know $s=0$, 1, 2, 3 . . . for singlet, triplet, quintet, septet . . . . Further, $l=0$, 1, 2, 3, 4, 5 for s, p, d, f, g-terms. From the origin $s=0$, the successive dotted circles $s=1$, 2, 3, 4 . . . are drawn. For quintet $s=2$; this is represented by the arrow O2. With the upper end 2 of this arrow as centre successive circles in full line are drawn having radii of 0, 1, 2, 3, 4, 5 units. These represent the l-vectors for s, p, d, f, g series respectively as marked on them. The points at which any of the $\boldsymbol{s}$-circles cut the s, p, d, f . . . circles are marked with the same value of $\boldsymbol{s}$. Then the figures on any series-circle give at once all the j-values for the quintet terms of that series.

Thus from Fig. 9 (*a*), we have for quintet p-terms $j=3$, 2, 1; for quintet d-terms $j=4$, 3, 2, 1, 0 and so on. The method may be extended for even multiplicity, only here we have to use half-quantum numbers $s=\frac{1}{2}$, 3/2, 5/2 . . . . for doublet, quartet, sextet . . . The last case is illustrated in Fig. 9 (*b*).

The j-values for singlet, doublet, triplet and quartet s, p, d, f, g-terms have been given on page 413 and those for the higher multiplicities are given below, and they will be found useful later, when complex spectra are discussed.

Table 7.

l	Quintet, $s=2$							l	Sextet, $s=\frac{5}{2}$						
0			2					0			$\frac{5}{2}$				
1		1	2	3				1		$\frac{3}{2}$	$\frac{5}{2}$	$\frac{7}{2}$			
2	0	1	2	3	4			2	$\frac{1}{2}$	$\frac{3}{2}$	$\frac{5}{2}$	$\frac{7}{2}$	$\frac{9}{2}$		
3		1	2	3	4	5		3	$\frac{1}{2}$	$\frac{3}{2}$	$\frac{5}{2}$	$\frac{7}{2}$	$\frac{9}{2}$	$\frac{11}{2}$	
4			2	3	4	5	6	4		$\frac{3}{2}$	$\frac{5}{2}$	$\frac{7}{2}$	$\frac{9}{2}$	$\frac{11}{2}$	$\frac{13}{2}$

217. The Vector Model of the Atom.—Let us now consider the mechanical interpretation of this most interesting result. Since $\mu g j$ represents the magnetic moment of the atom, and $j = | k-1+s |$ we are led to the conclusion that magnetism of atoms arises from two entirely different causes. In the final result, these are vectorially added. These causes are:

(1) The motion which gives us the k-quantum number.

The k-quantum number has been identified with orbital motion, and it was remarked a little while ago (see equation 20) that the magnetic moment of an electron moving in an orbit with the azimuthal quantum number k is

$$k.\frac{eh}{4\pi cm}$$

But the present analysis shows that this is not quite right. The magnetic moment corresponding to the k-quantum number is

$$(k-1)\frac{eh}{4\pi cm} \text{ or } l\frac{eh}{4\pi cm} \quad . \quad . \quad . \quad . \quad . \quad (31)$$

This result therefore required a thorough revision of the Bohr-Sommerfeld theory, and was later justified by Wave-mechanics.

(2) The second part of magnetism arises from the multiplicity quantum number s. It is $s.eh/4\pi cm$.

We have now to consider the mechanical interpretation of the s-quantum number.

218. The Spin-Quantum Number.—A scrutiny of the spectral data shows that s increases with the complexity of the atom. Thus we have the following multiplicity for elements of successive groups:

I.	II.	III.	IV.	V.	VI.	VII.
Na	Mg	Al	Si	P	S	Cl
Doublets	Singlets	Doublet	Singlet	Doublet	Singlet	Doublet
	Triplets	Quartet	Triplet	Quartet	Triplet	Quartet
					Quintet	

We ascribe the lines to the motions of a simple electron, modified by the presence of other electrons in the incomplete shells. Hence the complexity observed is due to the action of the remaining electrons in the incomplete shell.

Thus in accordance with the considerations given on page 369 we suppose that sodium (11) has a completed Ne-like structure, and one valency electron. The lines observed are due to the motion of the valency electron. Elements like Mg are sometimes called two-valence elements. Though most of the arc lines are due primarily to the vibration of one electron, the presence of the other electron profoundly modifies its motion, and converts the spectrum into a singlet and triplet system of lines.

Pauli brought conclusive evidence to prove that the increasing multiplicity observed when there are more than one electron in the incomplete shell, must be due to a superposition of the individual effects due to each of the valency electrons. *Further, a single electron moving in a radically symmetrical field does not give us a singlet spectrum, for which $s=0$, but a doublet spectrum $s=1/2$, as is exemplified in the case of the alkali elements.*

According to Pauli, the motion of each electron is characterized by four quantum numbers n, l, s and m. He further discovered the remarkable fact that s has a fixed value, and is equal to $\frac{1}{2}$ *for each electron.* This causes some difficulty when we wish to interpret the results from the point of view of mechanics. For a particle, as we understand it, can have only 3-independent degrees of freedom, and hence the number of independent quantum numbers should not exceed three. This is exemplified in the Bohr model of the H-atom. Here we have three quantum numbers n, k and m. 'n' represents total energy, k the angular momentum and $m=k\cos\theta$ represents tilt of the axis of the orbit to some axis fixed in space. Now we find that we must ascribe a fourth quantum number to the electron. We are therefore endowing it with more degrees of freedom than a conventional geometrical particle is capable of possessing.

219. The Rotating Electron.—Goudsmit and Uhlenbeck[*] suggested that the difficulty can be got over by supposing that the electron is not to be conceived as a geometrical particle, but as a sphere with definite extensions, and rotating about an axis fixed in itself. The conception is not new, for a theory of rotating electrons was developed by Abraham[†] to account for magnetism from classical electromagnetism. He showed that if a spherical charge e having the radius a is made to rotate with the angular velocity ω about an axis fixed in itself, it possesses definite mechanical and magnetic moments. These are :

---

[*] Goudsmit and Uhlenbeck, *Naturwiss*, **13**, 953, 1925; *Nature*, **117**, 264, 1926.

[†] Abraham, *Electricity and Magnetism*.

$$\left.\begin{array}{ll}\text{Mechanical Moment} & \Omega = \frac{2}{9}\cdot\frac{ae^2}{c^2}\,\omega = \frac{1}{3}\,ma^2\omega \\[2ex] \text{Magnetic Moment} & \mu = \frac{a^2e}{3c}\,\omega \\[2ex] \text{Ratio} \;\ldots\ldots & \frac{\mu}{\Omega} = \frac{e}{mc}\end{array}\right\}\quad \ldots (32)$$

It may be observed that the ratio between μ and Ω for orbital motion is just half this, *viz.*, $e/2mc$.

Goudsmit and Uhlenbeck postulated that the electron inside the atom is rotating with such velocity that its mechanical moment

$$\Omega = s\,\frac{h}{2\pi} = \frac{1}{2}\,\frac{h}{2\pi}$$

This enables us to calculate ω. It can be easily verified that

$$\frac{a\omega}{c} = \left(\frac{3}{2}\right)^2 \frac{1}{\alpha} \quad \ldots\ldots\ldots\ (33)$$

where α = Sommerfeld's constant.

The linear velocity at the periphery of the electron thus comes out to about 308 times the velocity of light, a deduction which has still remained incomprehensible.

In spite of the difficulty that the surface has to rotate with a speed which is about 308 times the velocity of light, the rotating electron has got some very recommendatory features. The ratio of the magnetic moment to the mechanical moment comes out to be e/mc which is more in accord with the results of the gyromagnetic experiments on the ratio between the two moments.* It also removes a mechanical difficulty. According to the orientation hypothesis, the atom-magnet can be in equilibrium, at any tilt to an external axis given by $\theta = \cos^{-1}(m/j)$. But according to classical dynamical principles, only the position $\theta = 0$ (the atom-axis parallel to the magnetic field) is one of stable equilibrium. The position $\theta = \pi$ (atom-axis anti-parallel to the field) is one of unstable equilibrium. The others are not positions of equilibrium at all. But if we suppose the electron to rotate rapidly round an axis, it behaves more or less like a gyroscope, and hence the orientation of the electron-axis at any angle does not present an insuperable mechanical difficulty.

---

* See Chap. XVI on Magnetism.

If magnetism arises from the orbital and spinning motions of the electron, the question arises whether it is possible to observe directly the magnetism due to an individual electron. Many attempts have been made to observe this without success. Bohr has given from the uncertainty principle a very simple argument to show that it is not possible to observe this phenomenon.

Suppose observation is made on a single electron by means of a magnetometer placed at a distance R from it. The electron has a magnetic moment $\mu = eh/4\pi cm$ and it produces a magnetic field at a distance R given by

$$H \sim \frac{\mu}{R^3} \quad . \quad . \quad . \quad . \quad . \quad . \quad (34)$$

or

$$\Delta H \sim \frac{\mu}{R^4} \Delta R \quad . \quad . \quad . \quad . \quad . \quad (34')$$

If H can be measured, μ can be determined. For the success of the experiment, the error in the determination of H must be less than H itself, or

$$\Delta H < H \quad . \quad . \quad . \quad . \quad . \quad . \quad (35)$$

or from (34), (34′)

$$\frac{\mu}{R^4} \Delta R < \frac{\mu}{R^3}$$

i.e.,

$$\Delta R < R \quad . \quad . \quad . \quad . \quad . \quad . \quad (36)$$

Now if v = velocity of the moving electron, the magnetic field due to it is

$$H_i \sim \frac{ev}{cR^2}$$

or

$$\Delta H_i \,|\!\sim \frac{e}{cR^2} \Delta v \quad . \quad . \quad . \quad . \quad . \quad (37)$$

According to *Heisenburg's uncertainty Principle*,* whenever an observation is made on any system, there arises an uncertainty in the measurement given by

$$\Delta p \, \Delta q \geqq h/2\pi$$

In our present experiment the uncertainty is

$$\Delta v \, \Delta R \geqq h/2\pi m$$

or from (87)

$$\Delta H_i \geqq \frac{e}{cR^2} \frac{h}{2\pi m} \frac{1}{\Delta R}$$

---

* *Vide* Condon and Morse, *Quantum Mechanics*, Secs. 6 and 62.

Hence
$$\frac{e}{cR^2}\,\frac{h}{2\pi m}\,\frac{1}{\Delta R} \leqslant \frac{\mu}{R^3} \quad \ldots\ldots\ldots \quad \text{from (35)}$$
$$\leqslant \frac{eh}{4\pi mc}\cdot\frac{1}{R^3}$$

or
$$\frac{1}{\Delta R} \leqslant \frac{1}{2R} \quad \text{or} \quad \Delta R \geqslant R \quad \ldots\ldots\ldots \quad (38)$$

This condition is contrary to the condition (36), which proves the impossibility of the proposition.

The idea of the rotating electron provides a very suggestive picture of mechanical processes involved in the production of series lines. If it is correct, the elementary spectrum, *i.e.*, *the spectrum produced by the motion of an electron round a bare nucleus* (as in H-atom) *should be a doublet spectrum, as in alkalies. In other words, the hydrogen spectrum should be exactly analogous to the spectrum of sodium.* Goudsmit and Uhlenbeck* proved that this was exactly the case, and calculated the energy-values of the H-atom on the new basis, and was able to explain completely the fine structure† of the Balmer lines and of the He$^+$ line λ 4686. These calculations are given in the following section.

220. The Rotating Electron in the Field of the Nucleus.‡—The calculations given here are rather too complex and are of the nature of patch work, but unfortunately no simpler method of arriving at the final results for this fundamental problem has yet been found. In the following we give only the barest steps, bringing out only the physical points. Many steps will appear to be rather arbitrary and certain assumptions not quite obvious will have also to be made.

A method of deducing the results from Matrix Mechanics was given by Heisenberg‖ and Jordan. Dirac¶ has given another method which makes use of the principle of relativity and his form of quantum mechanics. None of these methods is, however, easy to grasp and physically "*anschaulich*" though they may be logically more sound provided the reader has mastered the foundations of these logics. In the following the method of Goudsmit and Uhlenbeck is followed.

---

* See Pauling and Goudsmit, *Structure of Line Spectra*, Chap IV, p. 58.

† This subject has already been discussed in Chap. VII, § 178.

‡ For detailed account see *H. d. Astrophysik*, **8**, (1), 410, article by S. Rosseland.

‖ W. Heisenburg, and P. Jordan, *Zs. f. Phys.*, **37**, 256, 1926.

¶ P. Dirac, *Proc. Roy. Soc. A*, **117**, 610, 1928; **118**, 351, 1928.
W. Pauli, *Zs. f Phys.*, **36**, 266, 1926.

According to classical electromagnetism, an electric field $\boldsymbol{F}$ moving with the velocity $\boldsymbol{v}$ produces the magnetic field $\boldsymbol{H}$, given by

$$\boldsymbol{H}=\frac{1}{c}[\boldsymbol{F}\,\boldsymbol{v}] \quad . \quad . \quad . \quad . \quad . \quad . \quad . \quad . \quad . \quad (39)$$

If an electron, moves in the field of the nucleus of charge Ze, at a distance r, we have

$$F=\frac{Ze}{r^3}\,\boldsymbol{r}$$

Hence we have

$$\boldsymbol{H}=\frac{1}{c}\,\frac{Ze}{r^3}[\boldsymbol{r}.\,\boldsymbol{v}].$$

Now we have from the quantum conditions:

$$m\,[\boldsymbol{r}.\boldsymbol{v}]=l.\frac{h}{2\pi}$$

Hence

$$\boldsymbol{H}=l.\,\frac{h}{2\pi mc}\,\frac{Ze}{r^3} \quad . \quad . \quad . \quad . \quad . \quad . \quad . \quad (40)$$

Now the electron possesses an intrinsic magnetic moment $(\boldsymbol{s}\;h/2\pi)\;e/mc$ due to, as we say, its rotation about an axis. Hence in the magnetic field $\boldsymbol{H}$, it will undergo a precession with the angular velocity

$$\omega_H=\frac{e}{2mc}\boldsymbol{H}=\frac{Ze^2}{2m^2c^2}\;\frac{1}{r^3}.\;l\,\frac{h}{2\pi} \quad . \quad . \quad . \quad . \quad (41)$$

The extra energy due to this precessional motion is given by

$$\triangle W=\omega_H.\,s.\,\frac{h}{2\pi}.\;\;\cos\,(l.\,s)$$

$$=\frac{1}{2}.\;\frac{Ze^2h^2}{(2\pi mc)^2}.\;\;\frac{1}{r^3}\;sl.\cos\,(sl). \quad . \quad . \quad . \quad . \quad (42)$$

It was found however that this gave double the increment required. Thomas* showed that the precession treated here is that observable in a co-ordinate system in which the electron is at rest. What we want, however, is the precession in a system in which the nucleus is at rest and the electron moves with the velocity

---

* Thomas, *Nature*, **117**, 514, 1926; *Phil. Mag.*, **7** (3), 1, 1927.

ω_H. This is known as the *Thomas precession.* It reduces the angular velocity of precession to half its value (*vide* Note 4, Appendix), we have therefore

$$\triangle W = \frac{1}{4}\frac{Ze^2h^2}{(2\pi mc)^2}\cdot\frac{1}{r^3}\cdot sl.\cos(l\,s). \quad . \quad . \quad . \quad . \quad . \quad . \quad (43)$$

Again r is not a constant in the general case of orbit, so we have to take its mean value. We have (*vide* Chap. XVIII on Wave Mechanics)

$$\left(\frac{1}{r^3}\right)=\left(\frac{Z}{a_0n^2}\right)^3\cdot\frac{n^3}{l(l+\frac{1}{2})(l+1)}=\frac{Z^3}{a_0{}^3}\cdot\frac{1}{n^3\,l(l+\frac{1}{2})(l+1)}.$$

'a_0' is the normal radius of the H-atom. The nuclear charge 'Ze', it should be noticed, occurs because the radius of the electron moving round a nucleus with a multiple charge Ze is a_0/Z.

Putting this value in (43), we obtain after some work

$$\triangle W=Rhc\alpha^2Z^4\cdot\frac{1}{n^3l(l+1)(l+\frac{1}{2})}\cdot sl.\cos\hat{sl} \quad . \quad . \quad . \quad (44)$$

Ordinarily $$\cos\hat{sl}=\frac{s^2+l^2-j^2}{2sl},$$

because j is the resultant of s and l, but in quantum mechanics, we have the general rule that if 'a' is a quantum number

$$a^2 = a(a+1).$$

Hence $$sl.\cos sl = \tfrac{1}{2}\,[s(s+1)+l(l+1)-j(j+1)] \quad . \quad . \quad . \quad (45)$$

We have to add to (44) the Sommerfeld Relativity Correction

$$\Delta\nu = \frac{R\alpha^2Z^4}{n^3}\left(\frac{3}{4n}-\frac{1}{k}\right). \quad . \quad . \quad . \quad . \quad . \quad . \quad . \quad (46)$$

It was shown that for k we should substitute $l+\frac{1}{2}$. Hence we have, for the state (n, l, j)

$$\Delta\nu = R\alpha^2Z^4\cdot\frac{1}{n^3}\left[\frac{j(j+1)-l(l+1)-s(s+1)}{2l(l+\frac{1}{2})(l+1)}+\frac{3}{4n}-\frac{1}{l+\frac{1}{2}}\right]. \quad (47)$$

For the term $T(n, l, j=l+\frac{1}{2})$, we find putting $s=\frac{1}{2}$, $j=l+\frac{1}{2}$

$$\Delta\nu=\frac{R\alpha^2Z^4}{n^3}\left(\frac{3}{4n}-\frac{1}{l+1}\right) \quad . \quad . \quad . \quad . \quad . \quad . \quad . \quad (47')$$

For the term $T(n, l, j=l-\frac{1}{2})$, we have putting $s=\frac{1}{2}$, $j=l-\frac{1}{2}$

$$\Delta\nu=\frac{R\alpha^2Z^4}{n^3}\left(\frac{3}{4n}-\frac{1}{l}\right) \quad . \quad . \quad . \quad . \quad . \quad . \quad . \quad (47'')$$

Hence we find that for hydrogen and hydrogen-like ions

$$^n\mathrm{S}_{\frac{1}{2}} = {}^n\mathrm{P}_{\frac{1}{2}},\quad {}^n\mathrm{P}_{\frac{3}{2}} = {}^n\mathrm{D}_{\frac{3}{2}},\quad {}^n\mathrm{D}_{\frac{5}{2}} = {}^n\mathrm{F}_{\frac{5}{2}}$$

as stated in § 178.

The investigation shows that the hydrogen spectrum is exactly similar in nature to the alkali spectrum with the conditions just given. The student can now read the discussion on Fine-Structure given in § 178, Chap. VII.

221. Doubling of Levels in Alkali Spectra.—We mentioned in § 188, about the doubling of terms in alkali spectrum, *viz.*, all terms excepting the S-family are double. In the present chapter, we have seen that the doubling is due to the interaction of the spin of the valence-electron with its orbital moment due to *ls*-coupling. If we assume the core of alkali atoms to behave like a charge $(Z-s_o)\,e$ where s_o is the screening due to the outer shell, then we can easily obtain a quantitative expression for the doubling. We have only to substitute $Z-s_o$ for Z in formulæ 47′, 47″. We thus obtain that for a term $T(n, l, j=l+\frac{1}{2})$ we have

$$\nu = \frac{R(Z-\sigma)^2}{n^2} - \frac{R\alpha^2(Z-s_o)^4}{n^3}\left(\frac{3}{4n} - \frac{1}{l+1}\right) \quad . \quad . \quad . \quad (48)$$

and for the companion-term $T(n, l, j=l-\frac{1}{2})$ we have

$$\nu = \frac{R(Z-\sigma)^2}{n^2} - \frac{R\alpha^2(Z-s_o)^4}{n^3}\left(\frac{3}{4n} - \frac{1}{l}\right) \quad . \quad . \quad . \quad (49)$$

Thus we have

$$n^2T_{l-\frac{1}{2}} - n^2T_{l+\frac{1}{2}} = \frac{R\alpha^2(Z-s_o)^4}{n^3} \cdot \frac{1}{l(l+1)}$$

$$= 5{\cdot}82 \, . \, \frac{(Z-s_o)^4}{n^3} \cdot \frac{1}{l(l+1)}\ \mathrm{cm}^{-1} \quad . \ (50)$$

where we use
$$R\alpha^2 = \frac{109765}{(137)^2} = 5{\cdot}82\ \mathrm{cm}^{-1}$$

But though this formula gives a general explanation of the doubling, it cannot be used in this simple form to give us the value of σ, *i.e.*, we cannot identify σ and s_0. It is very difficult to calculate the screening due to the completed shells. It is largely affected by the nature of the orbit described by the valency electron, so that σ varies for different families of terms. This subject will be more rigorously treated in a later section.

The vaules of s_o obtained for the *p*-separations, as calculated with the aid of (50), are given below for the Li- and Na-groups.

Table 8. $\Delta\nu = 2^2P_{\frac{1}{2}} - 2^2P_{\frac{3}{2}}$ of the Li-group.

Spectrum	Li	Be^{+}	B^{++}	C^{+3}	N^{+4}	O^{+5}	F^{+6}
$\Delta\nu$ (cm^{-1})	·338	6·61	34·1	107·4	259·1	533·8	
s_0	2·02	1·94	1·88	1·86	1·84	1·82	

Table 9. $\Delta\nu = 3^2P_{\frac{1}{2}} - 3^2P_{\frac{3}{2}}$ of the Na-group.

Spectrum	Na	Mg^{+}	Al^{++}	Si^{+3}	P^{+4}	S^{+5}	Cl^{+6}
$\Delta\nu$ (cm^{-1})	17·2	91·6	234	461·8	794·8	1267·1	1889·5
s_0	7·45	6·606	6·180	5·916	5·741	5·696	5·504

222. Interpretation of the Landé g-factor.—The hypothesis of 'rotating electron' enables us to obtain an insight into the explanation of the Landé g-factor for which the correct expression was deduced by Landé from empirical data as mentioned in § 215. The mathematical treatment* is given below and it further illustrates the coupling relation existing between the l-, and s-vectors which define the mechanical moments associated with the light-electron.

Let us proceed as in the simple case, and place the atom in a magnetic field H, and let us consider the change in the energy of the atom. The atom is now complex, having two types of motion given by l and s (see Fig. 10). Let OZ represent the direction of the field, and let us draw a sphere of unit radius round O. Let us draw the vectors OJ, OL and OS to represent the vectors j, l, s and cutting the sphere at the points J, L and S.

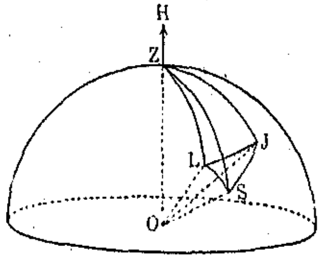

Fig. 10. The l, s, j-vector model.

Then we have empirically, according to Landé

$$\Delta\nu = g\left(\frac{eH}{2mc}\right). j \cos (j. H) \quad . \; . \; . \; . \; . \qquad (51)$$

---

* See E. Back and A. Landé, *Zeemaneffect und Multiplettstruktur*, Chap. 2, p. 39.

But the increase of energy can also be calculated in the following way. The atom, or rather the electrons composing the atom, possess two types of motion, (*a*) one which endows the atom with the mechanical moment $l.\, h/2\pi$, (*b*) the other which gives to it the mechanical moment $s.h/2\pi$. When the atom is placed in the magnetic field, it will execute a precessional motion round OZ, and there will be increase in energy due to each of the two motions. According to (13), the increase in energy due to the l-motion is

$$\triangle\nu_1 = \frac{e}{4\pi mc} \cdot H.l.\cos(\overline{l.H})$$

and increase due to s-motion is

$$\triangle\nu_2 = \frac{e}{2\pi mc} \cdot H.\, s \ \cos(\overline{s.H}).$$

But from the Fig. 10, $(\overline{lH})$ = ZL, and $(\overline{sH})$=ZS. Hence we have

$$\triangle\nu = \triangle\nu_1 + \triangle\nu_2 = \frac{eH}{4\pi mc}[l.\cos \mathrm{ZL} + 2s.\cos \mathrm{ZS}].$$

We have now to take the average values of the angles cosZL and cos ZS as the atom-magnet with its axis, precesses round OZ. We find from Fig. 10 with the aid of spherical trigonometry that

$$\cos \mathrm{ZL} = \cos \mathrm{JL}.\cos \mathrm{ZJ} - \sin \mathrm{JL}.\sin \mathrm{ZJ}.\cos \mathrm{ZJL}$$

and the average value of

$$\overline{\cos \mathrm{ZL}} = \overline{\cos \mathrm{JL}}.\ \overline{\cos \mathrm{JZ}}$$

Similarly,

$$\overline{\cos \mathrm{ZS}} = \overline{\cos \mathrm{JS}}.\ \overline{\cos \mathrm{JZ}}.$$

Hence we have

$$\triangle\nu = \cos \mathrm{ZJ}.\ \frac{eH}{4\pi mc}[\, l.\cos \mathrm{JL} + 2s.\cos \mathrm{SJ}].$$

Comparing this with (51), we obtain that

$$jg = [l.\cos \mathrm{JL} + 2s \cos \mathrm{JS}]. \quad \ldots\ldots \quad (52)$$

Now according to ordinary mechanics,

$$\cos \mathrm{JL} = \frac{j^2 + l^2 - s^2}{2jl} \quad \ldots\ldots\ldots \quad (53)$$

But in the new quantum mechanics, the square of vector $a = |\, a\,|^2 = a(a+1)$. Hence we have

$$\cos \mathrm{JL} = \frac{j(j+1) + l(l+1) - s(s+1)}{2\,jl}, \quad \cos \mathrm{JS} = \frac{j(j+1) + s(s+1) - l(l+1)}{2js}$$

Applying these values to (52), and writing $j(j+1)$ for j^2 we obtain

$$g = 1 + \frac{j(j+1) + s(s+1) - l(l+1)}{2\,j(j+1)} \quad \ldots\ldots \quad (54)$$

which is Landé's expression for g.

In deducing this expression, we have made use of the assumption that l and s are strongly coupled to each other, giving a definite j, and that the external magnetic field is unable to break this coupling. But the field may be so great that the coupling is more or less broken. This phenomenon was discovered by Paschen and Back in 1912, and is known as the *Paschen-Back Effect.* A short account is given in the following section.

223. The Paschen-Back Effect.—In 1912, while observing the Zeeman effect of the resonance line of lithium, *viz.*, $\lambda\,6708{\cdot}2$, Paschen and Back* found that the results obtained by them were in flagrant contradiction with Preston's rule.

The line $\lambda\,6708{\cdot}2$, like all resonance lines of the alkali elements consists of a close doublet $1s-2p_1$ and $1s-2p_2$ . . . which corresponds to D_1 and D_2 of Sodium. The actual wavelengths are $\lambda=6707{\cdot}85$, 6708, $\Delta\lambda={\cdot}15$, $\Delta\nu={\cdot}34\text{cm}^{-1}$. According to Preston's rule, these lines should split up into complex patterns, the longer member splitting into four components like D_1, and the shorter into six components like D_2. But the natural separation between the lines is so small, that even with a field of 10,000 Gauss, the normal Zeeman separation is $\Delta\nu = eH/4\pi mc = {\cdot}47\text{cm}^{-1}$ and exceeds the natural distance between the components of the line $\lambda\,6708$. Paschen and Back used a field which was about 3·2 times larger. They found that the two lines appeared to merge into a single line which gave a normal Lorentz-triplet with its π-component at $\lambda = 6707{\cdot}9$, *i.e.*, at a distance of $\frac{2}{3}\,\Delta\nu_{\text{natural}}$ from the original longer component towards shorter λ, and the σ-components at the theoretical distances $eH/4\pi cm$ on each side of the central component.

Similar anomalous results were obtained for Hα, the second pair of lines of the principal series of sodium, *viz.*, $1s-3p_1$, $\lambda\,3302{\cdot}94$ and $1s-3p_2$, $\lambda = 3302{\cdot}34$, $\Delta\nu = 5{\cdot}49\text{cm}^{-1}$, as well as for the third pair $1s-4p_1$, $\lambda\,2853{\cdot}031$ and $1s-4p_2$, $\lambda\,2852{\cdot}83$, $\Delta\nu = 2{\cdot}49\text{cm}^{-1}$, and also for the oxygen triplet given below :—

$$\begin{array}{lll} 2p^3\ 3s\ {}^5S_2 - 2p^3\ 3p\ {}^5P_3 \ldots\ldots \lambda\,3947{\cdot}438 & & \\ \qquad\qquad\qquad\qquad\quad {}^5P_2 \ldots\ldots \lambda\,3947{\cdot}628 & \Delta\nu = 1{\cdot}205\ \text{cm}^{-1} \\ \qquad\qquad\qquad\qquad\quad {}^5P_1 \ldots\ldots \lambda\,3947{\cdot}781 & \Delta\nu = {\cdot}676\ \text{cm}^{-1} \end{array}$$

and many other narrow multiplet lines having organic connection with

---

* F. Paschen and E. Back, *Ann. d. Phys.*, **39**, 929, 1912. For details see *H. d. Expt. Phys.*, 22, Chap. IV, pp. 124—70.

Description :

(*a*) No field.

(*b*) 2800 Gauss ; broadening of three lines.

(*c*) 6187 Gauss ; in spite of broadening not separated.

(*d*) 7738 Gauss ; right edge of the left lines strengthened.

(*e*) 10930 Gauss The middle π-component of the normal Zeeman triplet, which is ultimately to predominate, appears here for the first time, and gradually strengthens. The second line disappears.

(*f*) 12770 Gauss
(*g*) 21830 „
(*h*) 27880 „

Further splitting of broadened lines on the left and of the components on the right. New components in the broadened parts on the left. Diffuse broadening on the right in (*g*) and (*h*).

(*i*) 31900 Gauss. Components disappear, broadenings become fainter, and separate on both sides of the middle component. The π-component is fully formed, the side components (σ) are still being formed.

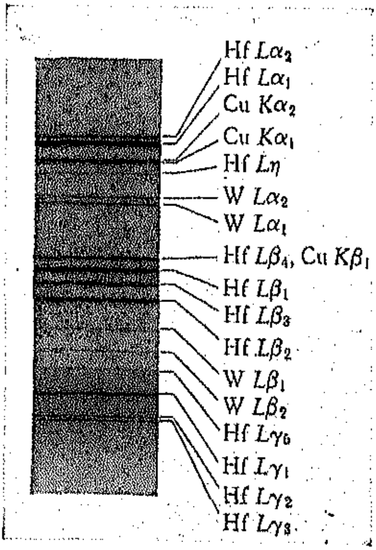

Fig. 10. X-ray spectrum of Hf.

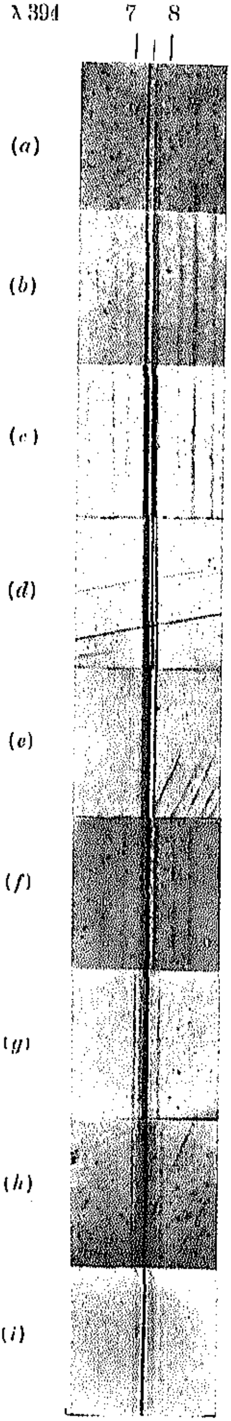

Fig. 11a. Zeeman effect for the oxygen triplet λ 3947·4, 3947·08, 3947·79 Å. units. Transition from weak to strong field. (*Paschen and Back*)

(*p.* 427)

each other. Lines which are not organically connected did not show this result, though their wavelengths may be very close to each other.

Paschen and Back concluded from their experiments that the departure from Preston's rule is observable only when $\Delta\nu_{\text{Lorentz}}$ is comparable to $\Delta\nu_{\text{natural}}$. When the magnetic field is so strong that this actually happens it is said to be *strong.* It is, therefore, apparent that the term "strong," is only a relative one, for a field of 32,000 Gauss which is considered strong for Li emitting λ 6708, is weak for the Na-atom emitting the D_1, D_2 lines, for now $\Delta\nu_{\text{mag.}}/\Delta\nu_{\text{nat.}} = 1{\cdot}6/17 = {\cdot}1$ only. Hence to observe the Paschen-Back effect of Na emitting D_1 and D_2, a field at least five times as great, *i.e.*, a field of 160,000 Gauss is necessary.

Fig. 11, taken from a paper by Paschen and Back shows how complex Zeeman patterns gradually transform, when we pass from a weak to a strong field, into a Lorentz triplet.

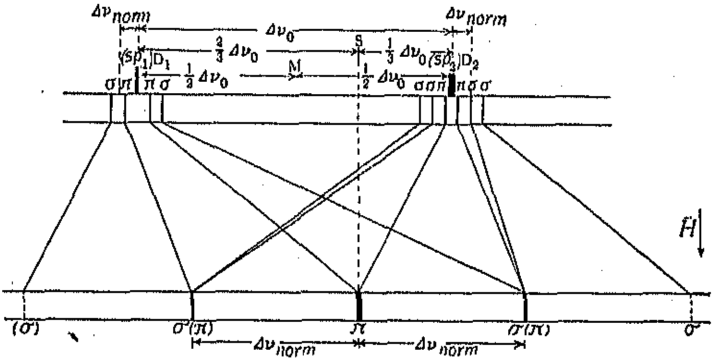

Fig. 11. The Paschen-Back effect for Sodium.

The Zeeman patterns of the oxygen lines mentioned on page 426 as the field is gradually increased so as to become strong, are shown in Fig. 11*a*, Plate X reproduced from an original due to Back.

224. Explanation of Paschen-Back Effect.—In §220, we have seen that in the case of a single electron moving in the field of an atom core with completed shells (as in the case of alkali metals, or for aluminium-like elements), the energy level becomes split up into two levels, on account of the coupling between the *s*, and *l*-vectors. The amount of this splitting in frequency units is

$$\left.\begin{aligned} \Delta\nu &= A\, s.\, l.\, \cos sl \\ \text{where} \qquad A &= \frac{R\alpha^2 (Z-\sigma)^4}{n^3\, l(l+\frac{1}{2})(l+1)} \end{aligned}\right\} \quad \ldots\ldots \quad (55)$$

Let the atom be placed in a magnetic field. The total increment in energy is now

$$\Delta\nu = \frac{eH}{4\pi cm}(l.\cos\overline{lH} + 2s.\cos\overline{sH}) + A.\,sl.\cos(\overline{sl})$$

or

$$\frac{\Delta\nu}{eH/4\pi cm} = l\cos\overline{lH} + 2s\cos\overline{sH} + \beta\,\overline{ls}.\cos\overline{sl} \quad \ldots\ldots \quad (56)$$

where

$$\beta = A\Big/\frac{eH}{4\pi cm}$$

We have seen in §222, that when the coupling between s and l is strong, they unite to form a 'j' vector. The value of s for a single electron is $=\frac{1}{2}$; and $j=l+\frac{1}{2}$ and $l-\frac{1}{2}$. Corresponding to the two values of j, the orbit splits up in two with the energy difference equal to that in (50). The additional splitting of each orbit, due to the magnetic field, in such cases, can be calculated as described in §212, as was first shown by Landé.*

But when H is very large, β is small, the coupling between s and l is broken and the inner quantum number j ceases to have any meaning. In such cases, the s and l-axes precess independently round H, and we can put

$$s\cos(\overline{sH}) = m_s\,,\ \text{where } m_s = s, s-1, \ldots -s$$

$$l\cos(\overline{lH}) = m_l\,,\ \text{where } m_l = l, l-1, \ldots -l$$

and

$$\cos(\overline{sl}) = \cos(\overline{sH})\cos(\overline{lH})$$

from spherical trigonometry, and $sl\cos(\overline{sl}) = m_s m_l$. Hence we have

$$\Delta\nu = m_l + 2m_s + \beta m_s m_l\,,$$

where β is a small fraction.

Let us now apply these formulæ to the doublet terms in the alkali spectra. First, we have to find out the term values without the field. This is obtained from the formula (55)

$$\nu = \nu_0 + A.\,sl.\cos(\overline{sl}) \quad \ldots\ldots\ldots \quad (57)$$

Now the two terms correspond to $j=l+\frac{1}{2}$, $j=l-\frac{1}{2}$, and we have

$$\cos\overline{(sl)} = \frac{j(j+1)-s(s+1)-l(l+1)}{2sl}.$$

---

* A. Landé, *Zs. f. Phys.*, **8**, 273, 1922.

Hence we have $j = l+\frac{1}{2}, \quad \nu = \nu_0 + Al/2$

$j = l-\frac{1}{2}, \quad \nu = \nu_0 - A(l+1)/2$

or $\Delta\nu = A(2l+1)/2$

For $P_{\frac{1}{2}}$ . . . . . $\nu = \nu_0 - A$, $\quad P_{\frac{3}{2}}$ . . . . . . $\nu = \nu_0 + A/2$

We have $\nu_0 = \frac{1}{3}(2P_{\frac{3}{2}} + P_{\frac{1}{2}})$ . . . . (58)

i.e., the neutral frequency ν_0 is obtained by attaching the weight 2 to $P_{\frac{3}{2}}$ and the weight 1 to $P_{\frac{1}{2}}$ and finding out the centre of gravity. The c.g. is equal to ν_0.

For $D_{\frac{5}{2}}$ $\quad \nu = \nu_0 + A$, $\quad D_{\frac{3}{2}}$ $\quad \nu = \nu_0 \;\; 3A/2$

$\nu = \frac{1}{5}(3D_{\frac{5}{2}} + 2D_{\frac{3}{2}})$ . . . . (59)

i.e., the weights of $D_{\frac{5}{2}} : D_{\frac{3}{2}}$ are as 3 : 2.

The Zeeman splitting for strong fields and transition from weak to strong fields in the case of the *sp*-doublet of sodium is shown in the following diagram (Fig. 12).

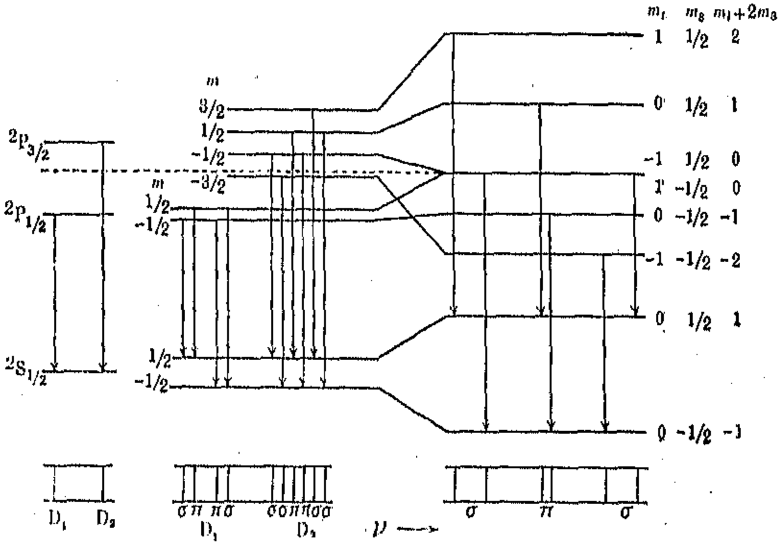

Fig. 12.—The complete Zeeman effect for D_1, D_2 lines of sodium Transition from weak to strong field.

This figure gives a complete symbolic representation of Paschen-Back effect. $S_{\frac{1}{2}}$ is the lower orbit, $P_{\frac{3}{2}}$, $P_{\frac{1}{2}}$ are the higher orbits. $P_{\frac{3}{2}} = \nu_0 + A/2$, $P_{\frac{1}{2}} = \nu_0 - A$, so that ν_0 is at the c.g. of the two levels, because the weight of $P_{\frac{3}{2}}$ is 4, while that of $P_{\frac{1}{2}}$ is 2.

In a weak field, $P_{\frac{3}{2}}$ breaks up into 4 magnetic levels having $m = \frac{3}{2}, \frac{1}{2}, -\frac{1}{2}, -\frac{3}{2}$, and $P_{\frac{1}{2}}$ into two levels having $m = \pm\frac{1}{2}$. The lower orbit $S_{\frac{1}{2}}$ also splits into two m-levels $m = \pm\frac{1}{2}$. Transitions take place according to the selection rule $\Delta m = \pm 1$ or 0, so that we get 4 components for D_1, $S_{\frac{1}{2}} - P_{\frac{1}{2}}$ and 6 components for D_2, $S_{\frac{1}{2}} - P_{\frac{3}{2}}$ as shown by the central arrow scheme. The π- and σ-components are also indicated. The behaviour of the level system in a strong field is shown by the scheme to the right. Here the l, s-coupling is broken, and we have to quantise m_l and m_s separately. For ${}^2P_{\frac{3}{2},\frac{1}{2}}$, $l = 1$, $s = \frac{1}{2}$, so that we have $m_l = 1, 0, -1$ and $m_s = \frac{1}{2}, -\frac{1}{2}$, and by their combination we get 6 levels $(1, \frac{1}{2})$, $(0, \frac{1}{2})$, $(-1, \frac{1}{2})$, $(1, -\frac{1}{2})$, $(0, -\frac{1}{2})$ and $(-1, -\frac{1}{2})$. The corresponding $(m_l + 2m_s)$-values are 2, 1, 0, 0, −1, −2. The two 0 levels combine in the position of the common c.g. of the level system, so that we finally get 5 levels. Similarly ${}^2S_{\frac{1}{2}}$ gives us two magnetic levels $(m_l + 2m_s) = \pm 1$. Transitions now occur according to the rule $\Delta(m_l + 2m_s) = 0, \pm 1$, giving respectively one pair of π-components and two pairs of σ-components. If the interaction between ls-vectors be very small, the separation between the two components of the same pair is very small, and the lines reduce to normal Zeeman pattern.

The position of the central line is given by $\nu D_1 + \frac{2}{3}\Delta\nu_0$ or $\nu D_2 - \frac{1}{3}\Delta\nu_0$, where $\Delta\nu_0$, denotes the natural separation between D_1 and D_2. The two σ-components for strong fields are situated symmetrically from it at a distance of $\Delta\nu_{\text{Lorentz}}$.

Books Recommended.

1. E. Back and A. Landé, *Zeemaneffect und Multiplettstruktur der Spektrallinien* (1925).
2. E. Back and G. Joos, *Handbuch der Experimentalphysik*, **22**, (1932).
3. A. Sommerfeld, *Atombau und Spektrallinien* (1931).
4. E. Baly, *Spectroscopy*, 3, (1927).
5. L. Pauling and S. Goudsmit, *Structure of Line Spectra* (1930).
6. G. Birtwistle, *The Quantum Theory of the Atom* (1926).
7. G. Birtwistle, *The New Quantum Mechanics* (1928).
8. A. Smekal, *Quanten*, (1933).
9. A. Landé, *Zeemaneffect, H. d. Physik*, **21** (1929).

CHAPTER XI

THE X-RAY SPECTRA OF ELEMENTS

225. Introduction.—In Chapter VI, we have given a preliminary account of the discovery of characteristic X-rays of elements, and of Moseley's measurement of their wavelengths. In this chapter, we shall make a detailed study of these spectra, since they are indispensable for affording knowledge of the structure of atoms. The pioneering work of Moseley on the K-spectrum extended from Ca to Zn. After the premature death of Moseley in the Great World War, the work was chiefly carried out by Siegbahn in his laboratory at the universities of Lund and Upsala in Sweden. At the present time, the data are completely known up to U 92; for U, $\lambda K\alpha = \cdot 154$ Å units. For lighter elements, data are now available up to Li. Work at both extremes requires special apparatus. The references to these works will be found in table 2, compiled chiefly from Lindh's *Handbuch d. experimentalphysik*, 24/2 and Siegbahn's *Spektroskopie der Röntgenstrahlen* (1931).

226. Survey of Experimental Data.—In the case of elements Ca to Zn, Moseley found that the spectrum consists of two close doublets $K\alpha_1$, $K\alpha_2$, and another line on the short wavelength side called by him $K\beta$. When elements of higher atomic weight were examined, a larger number of lines were obtained which were designated by the symbols $K\beta_2$, $K\gamma$ . . etc. . . . . . Besides these, a number of faint lines are found to appear, on the short wavelength side of the main lines, when long exposures are given. They are known as *satellites* to the main lines. A diagrammatic sketch of the chief lines and of their satellites is given in Fig. 1.

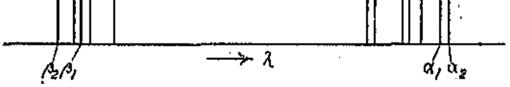

Fig. 1. The structure of K-spectrum.

Moseley's photograph of the K-spectrum, reproduced in Fig. 2, showed clearly that the characteristic lines of elements were not arranged haphazardly as in optical spectra, but followed some regular laws. Moseley found that

$$\sqrt{\frac{\nu}{\frac{3}{4}R}} = Z-1 \text{ (approximately)}$$

where ν=frequency of any of the Kα-lines. The agreement of this empirical rule with experimental data is shown in table 1 where ν_0 stands for the Rydberg constant R.

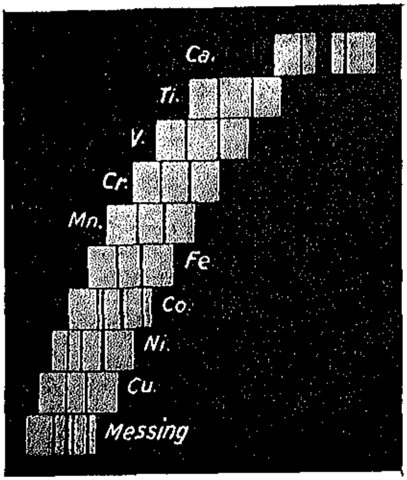

Fig. 2.—Moseley's photograph of K-spectra of elements.

Table 1. Showing $Z \propto \sqrt{\nu/\frac{3}{4}\nu_0}$ *for K-series of Elements from* Ca *to* Zn.

At. Nr.	Element	λ in Å. U.	$\sqrt{\nu/\frac{3}{4}\nu_0}$	At. Nr.	Element	λ in Å. U.	$\sqrt{\nu/\frac{3}{4}\nu_0}$
20	Ca	α...3·357 β...3·085	19·00	26	Fe	α...1·945 β...1·765	24·99
21	Sc	...		27	Co	α...1·794 β...1·635	26·00
22	Ti	α...2·766 β...2·528	20·99	28	Ni	α...1·664 β...1·504	27·04
23	Va	α...2·521 β...2·302	21·96	29	Cu	α...1·548 β...1·408	28·01
24	Cr	α ..2·295 β... 2·088	22·98	30	Zn	α...1·446 β ...	29·01
25	Mn	α ..2·117 β 1·923	23·99				

It has been the practice to represent $\sqrt{\frac{\nu}{R}}$ against atomic number graphically. These curves are known as *Moseley Curves* for the lines. Such curves for $K\alpha_1$, $K\alpha_2$, $K\beta_1$, $K\beta_2$,—due to Siegbahn for elements Zn to Pt are shown in Fig. 3.

It will be seen that the curves are very nearly straight lines, of which the two for α_1, α_2 and those for β_1, β_2 are very close, and they approach each other continually as we proceed towards lighter elements. In fact the α_1, α_2-curves coincide beyond Zn and the β_1, β_2 lines beyond Sc. Further, these curves make our ideas regarding the origin of X-ray spectra and their relation with the natural system of elements particularly clear. It is seen that in respect of emission of characteristic X-ray lines, there is not a trace of periodicity. So the outer electrons of atoms which determine their periodic properties have nothing to do with X-ray spectra. Moreover, we observe that the hardness of the rays increases uniformly with the increase of the nuclear charge. The conclusion therefore is that X-ray

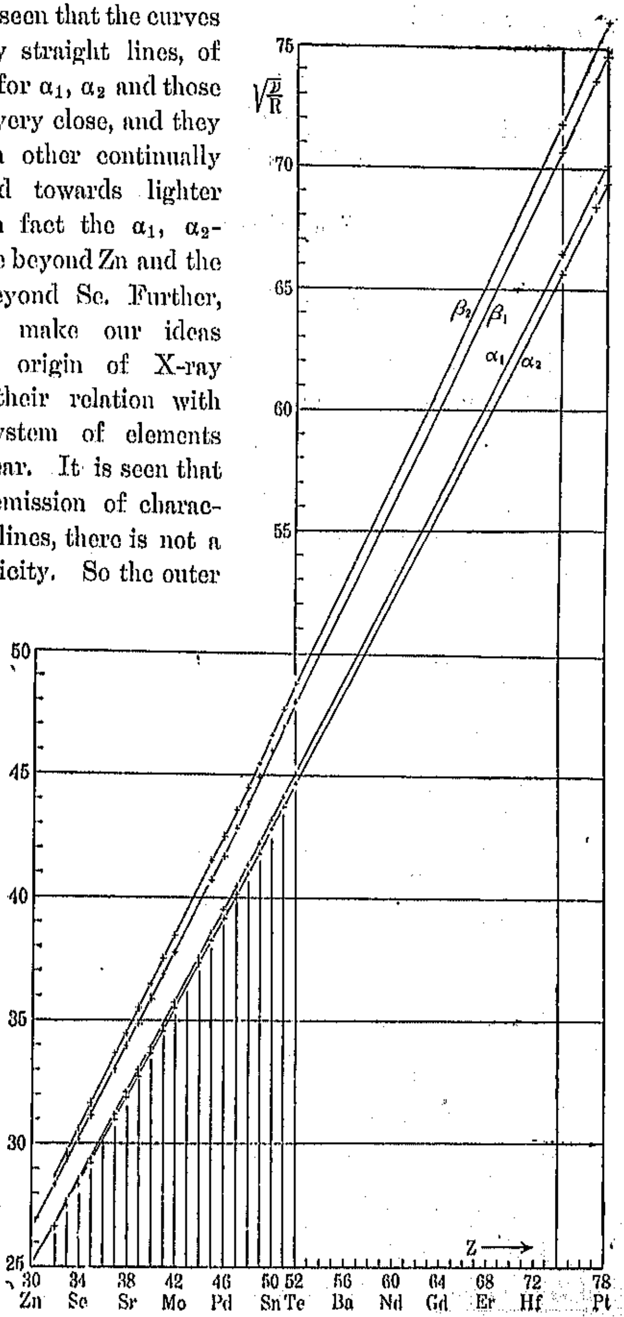

Fig 3.—Moseley curves for K-series of elements.

spectra must be associated with the electrons very close to the nucleus. We shall return to this question later on.

It was found from the nature of these curves that generally

$$\sqrt{\nu/R} = A(Z-s)$$

where $A = \sqrt{3}/2$ for Kα, $2\sqrt{2}/3$ for Kβ, s is a fraction very nearly equal to unity. From this empirical relation, it follows that

$$\nu_{K\alpha} = R(Z-s)^2\left[\frac{1}{1^2} - \frac{1}{2^2}\right]$$

$$\nu_{K\beta} = R(Z-s')^2\left[\frac{1}{1^2} - \frac{1}{3^2}\right]$$

It should be remembered that these rules are empirical, and not exact as in optical spectra.

227. Origin of Characteristic Lines.—These formulæ at once suggested the following explanation : The Kα-line is due to the quantum jumps of an electron moving in the field of a central charge of $(Z-s)e$ units, from an orbit in which $n = 2$ to one in which $n = 1$. But how is this process rendered possible in an atom? It is clear that the electron whose jump gives rise to the Kα_1, α_2 line must be an inner electron, so that to work out the idea more precisely we must have a working hypothesis of the electron structure of the atom. The experiments of Rutherford on large angle scattering of α-rays show that the atom consists of a central positive charge Ze surrounded by Z electrons. From the very beginning, it has been assumed that these electrons are arranged in different layers or shells, each shell containing a *definite number* of electrons. At first attempts were made to find out the number of electrons required to fill up a shell from classical dynamical conditions of stability of rings of electrons,* but ultimately empirical methods based on physical considerations were found to be more suitable. Rydberg found that the atomic numbers of the inert gases satisfy the following remarkable relation

	2	10	18	36	54	86
	He	Ne	A	Kr	Xe	Rn

$$Z = 2(1^2 + 2^2 + 2^2 + 3^2 + 3^2 + 4^2)$$

From this observation, it was concluded that a layer consisting of 2, 8, 8, 18, 18, 32 electrons forms a stable system. The innermost layer was supposed to consist of 2, the next of 8, the next one of 18 electrons. . . . . The picture of the constitution of inert gases according to this view is given on page 369 (Fig. 5).

---

* *Vide* A. H. Compton. X-rays and Electrons, 30.

The alkali metals are formed when there is one excess electron added to the closed layers.

With this model, let us now consider the motion of an electron in the innermost shell of any, say the Argon atom.

This electron moves in the field due to the central charge which is counterbalanced by the forces of repulsion due to the other electrons. As most of the electrons excepting those which are in its own shell are external to it, and are distributed almost symmetrically in the space about it, the forces of repulsion very nearly cancel each other. The net force may be represented by $-(Z-\sigma)e^2/r^2$ where σ is known as the *screening constant* for the innermost electron, $\sigma e^2/r^2$ represents the sum total of the repulsive forces due to the electrons. If now the total quantum number n of the orbit be taken as unity, the energy of the electron, according to the Bohr theory $= -\frac{(Z-\sigma)^2}{1^2}hR$. Next consider an electron in the next level. For this electron the screening constant σ' is much larger, for the electrons in the first shell all repel it. The screening is augmented further by the electrons in its own shell. We can neglect the effect of electrons which are in the outer shells. The net effect is that the electron may be supposed to revolve under a central force of $(Z-\sigma')e^2/r^2$ where σ' is different from σ and is larger. If now the total quantum number of the orbit is 2, its energy, according to Bohr's theory is $-\frac{(Z-\sigma')^2Rh}{2^2}$.

Hence if an electron jumps from the shell (2) to the shell (1), the energy radiated will have the frequency

$$\frac{\nu}{R}=\frac{(Z-\sigma)^2}{1^2}-\frac{(Z-\sigma')^2}{2^2} \quad . \ . \ . \ . \ . \ . \ . \ . \ . \quad (1)$$

If we put $\sigma=\sigma'$, it reduces to Moseley's form. But Moseley's form was only a first approximation as is apparent from table 1, and must be discarded now for more precise formulations. Further, it is also apparent that the above explanation is only partially correct, for it does not explain why there are two K-lines, *viz.*, Kα_1 and Kα_2 both being due to the jump of the electron from the second to the first shell. But it tells us definitely that for the motion of electrons in the innermost shell, the total quantum number *n must be assumed to be 1, for the electrons in the next shell, n must have the value 2,* and similar considerations of the origin of the K_β-lines show that it is due to the jump of an electron from a shell in which $n = 3$.

The discovery of this fact enables us to give mathematical precision to the hitherto hypothetical shells of electrons. The innermost shell, which is composed of electrons for which $n = 1$ may be called the K-shell. The next one having $n = 2$ is known as the L-shell, and so on. We can designate the shells having $n = 3, 4, 5,$ .... by the successive letters of the alphabet M, N, O, P .... The $K\alpha$-lines are due to the transition of the electron from L→K, the K_β from M→K as illustrated in Fig. 4.

One difficulty in the above explanation might have suggested itself to the reader. As the number of electrons in an atom is limited, *the number of electrons in each shell also must be limited,* otherwise there can be no stability. Hence *the transition of an electron from L to K is possible only when the K-level has already lost one electron.* These views are supported by the work on the excitation potentials of characteristic X-rays (§231) and on the absorption-spectra of X-rays (§229). In the figure above the dotted circle represents the level at infinite distance. In order that the K-spectra be emitted, an electron must first pass from K-level to this dotted level, as shown by the fourth arrow.

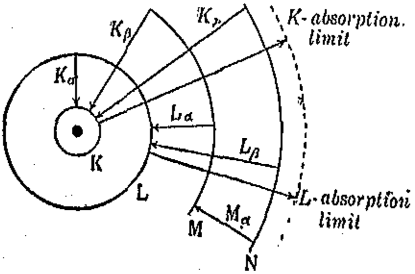

Fig. 4.—The origin of characteristic X-ray lines.

228. The L-Spectrum of Elements.—Moseley found only a few lines in the L-spectrum of elements, but Siegbahn who made it the special subject of his study in his laboratory found no less than 13 lines in the spectra of 48 elements from 30 Zn to 92 U. The number is found still further to increase when exposures are of longer duration. The figures given below show actual photographs (Fig. 5), and diagrammatic representation of the L-lines of certain elements (Fig. 5*a*).

The strongest line is the α_1, which is followed by a weak satellite α_2 on the longer wavelength side. 'l' is the longest line; both l and are rather faint and were discovered by Siegbahn.

The β-group consists of a number of lines of which the strongest is denoted by β_1. Similarly the strongest in the γ-group is denoted by γ_1. The nomenclature has undergone rather rapid changes, but is more or less fixed now (see Chart on p. 447).

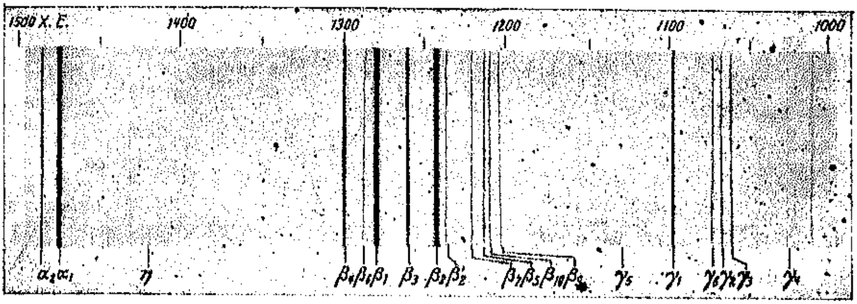

Fig. 5.—The L-spectrum of W. (*Siegbahn*).

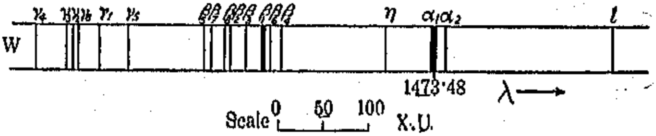

Fig. 5a

It is needless to dwell on the regularities in the L-spectrum at this place, as the discussion will be rendered easier after we have considered the absorption X-ray spectra of elements. Moseley who got only a few strong lines found that their frequencies could be roughly represented by the formula

$$\frac{\nu}{R} = (Z-b)^2 \left[\frac{1}{2^2} - \frac{1}{3^2}\right] \quad . \quad . \quad . \quad . \quad . \quad . \quad . \qquad (2)$$

according to which the wavelength of any line in the same series should increase inversely as the square of the atomic number of elements. The approximate correctness of this formula is very clearly exhibited by the schematic representation in Fig. 6. In this the relative positions of lines of the elements from 92 U to 11 Na in the K, L, M, N series have been shown on the wavelength scale. The lines belonging to the same series branch out in a parabolic curve.

The explanation which is suggested by this formula (2) is quite obvious. The L-lines are due to the transition of an electron from the M and N-levels to the L-level. But except for this broad fact, no further conclusion can be derived from (2). The multiplicity of lines in the L-spectrum shows that both M and N-levels are capable of being divided further into *sub-levels*.

A table of wavelengths of the L-series is given at the end of this chapter, where the references to the sources are given.

The M and N-series were discovered in the case of the heaviest elements by Siegbahn, and his pupils. They are respectively due to transitions (3←4) and (4←5) of n-values. For details, see Lindh or Siegbahn, *loc. cit.*

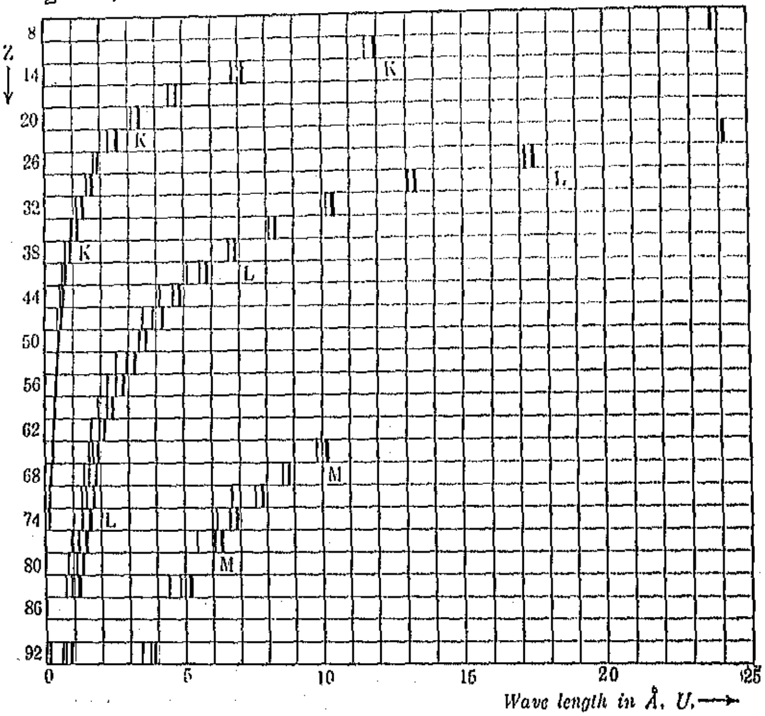

Fig. 6.—Schematic representation of X-ray lines for elements U to Na.

229. Absorption-Spectra of X-rays.—Though the absorption of X-rays was extensively studied by Barkla by the ionisation method, the study of the absorption spectra of X-rays with the newly discovered methods of X-ray spectroscopy was first made by Wagner* and De Broglie.† The experiments are quite analogous to the corresponding optical experiments. A beam of continuous X-rays (or white X-rays) is allowed to pass through a film of the substance whose absorption spectra is to be examined and the transmitted X-rays are analysed in a spectrometer. The spectrometer used is of the Seemann (Wedge) type, so that photograph of a wide region can be taken on the same plate at one exposure.

---

* Wagner, *Ann. d. Phys.*, **46**, 868, 1915.

† De Broglie, *Comp. Rend.*, **163**, 87, 1916.

Discussion of results. The nature of absorption X-ray spectra is found to be quite different from what is obtained in the optical region. *There is no trace of monochromatic absorption corresponding to the emission lines* $K\alpha_1,\alpha_2$ or $K\beta$, but an absorption edge appears in the position of the limit of the K-series, *viz.*, at the wavelength corresponding to $\nu = (Z-\sigma)^2 R/1^2$. This is illustrated in Fig. 7 which is reproduced from a photograph taken by Wagner.

Explanation of the Photographs.—The photographs are original negatives. In these experiments, three thin parallel strips of Cd (48), Ag (47) and Pd (46) which are three successive elements in the periodic classification were kept before the photographic plate at a small distance from it, with some space between the strips. The parts covered by the strips are indicated by Cd, Ag, Pd written against them. We find that *there is no line absorption but sharp discontinuities occur in the intensity of the transmitted beam at certain points.* These are known *as absorption discontinuities or absorption edges.* Beginning from Pd, we recognise the sharp absorption edge at the bounding lines between black to the right and white to the left. The black parts denote that the X-rays corresponding to these wavelengths are transmitted copiously, but as we come to the discontinuity, absorption suddenly sets in and very little X-rays of this and shorter wavelengths are transmitted, so no blackening is produced; but after some distance, X-rays again begin to be transmitted through the plates. The same feature is repeated with Ag and Cd-plates, but now the absorption edge is shifted towards the *left* (*short wavelength side*). In the parts which are freely transmitted for Pd, discontinuity coincident in position with the Ag-edge is noticed. This is due to the silver in the photographic plate. As X-rays to the left of the absorption edge are more intensely absorbed (by Cd), the blackening is more intense on this side. The slight contrast is due to over-exposure.

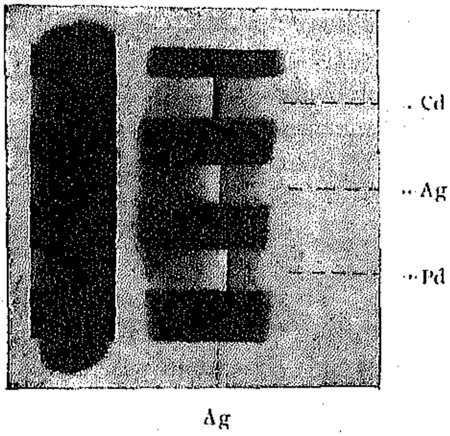

Fig. 7.—K-Absorption edges for Pd, Ag, Cd.

230. Explanation of the Absorption Edge.—The absorption edge observed in X-rays is quite similar to the absorption edge appearing at the limit of the principal series of sodium and other alkali elements (*vide* § 182). We have seen that the absorption edge in the optical spectrum of sodium denotes a physical process in which the valency electron is split off from the sodium atom under the influence of incident quanta, *i.e.*, when light of frequency ν_o falls on the atom and is absorbed, the electron acquires energy and is split off from the atom. The process may be symbolically written as follows :—

$$\mathrm{Na} + h\nu_o = \mathrm{Na}^+ + e$$

When $\nu > \nu_o$, the electron is split off with the kinetic energy $\frac{1}{2}mv^2 = h(\nu - \nu_o)$. The absorption edge thus indicates the beginning of photo-ionisation of the atoms due to the ejection of the valency electron under the influence of light of suitable wavelength.

The absorption edge observed in X-rays is also similarly explained. *It corresponds to the photoelectric ejection of an electron from the K-shell.* The process can be written as :—

$$\mathrm{Na} + h\nu_K = \mathrm{Na}^+ (\mathrm{K}) + e$$

Na^+ (K) indicates that the ionisation is in the K-shell or one K-electron has been ejected by the incident quantum, ν_K is the frequency of the absorption edge.

The minimum frequency at which this process can occur must correspond to the energy with which an electron is bound in the K-shell *viz.*, to $-E/Rh = (Z-\sigma)^2/1^2$. Hence we have

$$\frac{\nu_K}{R} = \frac{(Z-\sigma)^2}{1^2} \quad \text{or} \quad \sqrt{\nu_K/R} = Z - \sigma$$

Why there is no line absorption of X-rays? Let us now see why we do not obtain any line absorption corresponding to the characteristic K-emission lines, as in optical spectra. In the emission of Kα an electron falls from the L-shell to the K-shell. Absorption of Kα would be possible only if an electron from the K-shell could pass, as a result of increase of energy due to absorption, to the L-shell. As experiments have not yet revealed any such absorption line, we are led to infer that in the ordinary atom, the K-electron is prevented by certain unforeseen circumstances, even when its energy is increased by an appropriate amount, to pass to the *L* or any other higher shell. But what can these circumstances be? The answer is that *each shell has got assigned to it a definite quota of electrons, and as the shells are ordinarily full, they cannot receive any further electron.* Hence no absorption of any characteristic line is possible. The continuous absorption beginning at the K-limit shows that the K-electron, as a result of absorption of light, passes to infinity where the shells no longer exist. Absorption beyond the edge indicates that the K-electron passes to infinity with the energy given by Einstein's photo-electric equation

$$\tfrac{1}{2}mv^2 = h(\nu - \nu_K)$$

It is further to be noted that each element gives only one K-absorption edge. This leads to the conclusion that the K-levels are absolutely single.

231. Mechanism of Emission—Excitation Potential of Characteristic X-ray Lines.—The idea that *each shell can contain a definite number of electrons and cannot accommodate more than this number* is very fundamental for atomic physics, and clears up many other points regarding emission as well. The $K\alpha$-line is due to the jump of an electron from the L-shell to the K-shell, but this is clearly impossible *unless the K-shell has already lost one electron.* If the K-shell retained its full quota of electrons, there would be no emission of characteristic K-lines. In other words, if we want to obtain the characteristic K-lines in emission, *a necessary condition is that a K-electron must be ejected first.* That this is actually the case was first proved experimentally by Webster, and later verified by Wooten,* Jönson† and others.

In Webster's‡ experiment, the experimental tube was of the Coolidge pattern, provided with a Rhodium anticathode. The electrons were accelerated from a battery of 20160 lead accumulators so that the voltage could be varied accurately in small steps. The apparatus used was a Bragg-ionisation spectrometer with a Calcspar crystal, and set to the $K\alpha$-line of Rh. It was found, as the voltage was varied, that this ray was not obtained even when the potential was raised to the value corresponding to the emission frequency of $K\alpha$ as given by the Einstein equation

$$V = \frac{h\nu}{e} \text{ or } \qquad V = \frac{12{\cdot}340}{\lambda \text{ in Å.U.}} \text{ Kilovolts} \quad . \quad . \quad . \quad . \quad (8)$$

Since Rh $K\alpha$ $\lambda = 612$, X. Units, $V = 21$ kilovolts nearly.

---

* Wooten, *Phys. Rev.*, **13**, 71, 1919.
† Jönson, *Zs. f. Phys.*, **43**, 845, 1925.
‡ Webster, *Phys. Rev.*, **9**, 220, 1917.

The intensity obtained at lower potentials was wholly due to the continuous radiation. If the voltage be now gradually raised over this value, then the intensity of the line rises *linearly* with the voltage, as shown in Fig. 8.

But when a value of 23·3 Kvs is reached, the curve is suddenly found to jump upwards, as shown in Fig. 8. The cause of this sudden increase is the emission of the characteristic line in addition to the general radiation of the same wavelength already present there.

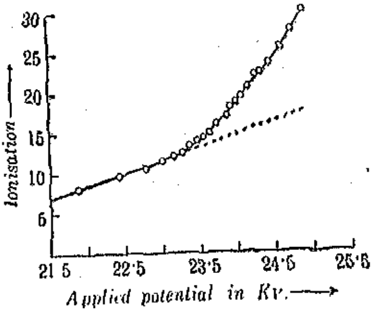

Fig. 8.—Excitation of K-radiation (Rh).

We can now plot the intensity of the characteristic $K\alpha_1\alpha_2$ doublet against the impressed voltage. This is shown in Fig. 9.

For this purpose, the voltage is taken as abscissa, and the difference between the ordinate values of the curved part (the actual curve) and the straight part (obtained by prolonging the earlier part of the curve indicated by dots in Fig. 8.) as ordinate. This represents the *actual intensity of the characteristic line.* Curve A_1 obtained in this way gives us the intensity of $K\alpha_1, \alpha_2$. Curve A_2 shows the variation of intensity of the $K\beta$-line obtained by the same procedure. It is seen that the two curves meet the abscissa at a point which is about 23·3 kV and this corresponds, as application of equ. (3) shows, to the wavelength $\lambda = {\cdot}533$Å.U. which is the absorption edge of the K-spectrum of rhodium. From this experiment the following conclusions can be drawn :—

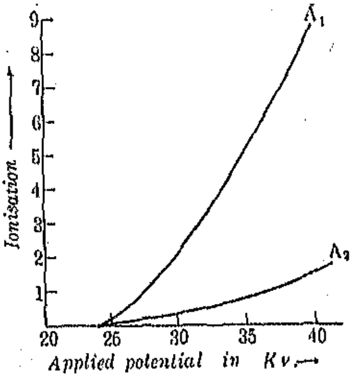

Fig. 9.—Intensity variation of Kα, Kβ lines with excitation voltage. (Curve $A_1 = K\alpha$, $A_2 = K\beta$).

(1) The $K\alpha_1\alpha_2$ and $K\beta$ lines in the K-spectrum are emitted at one and the same characteristic voltage.

(2) The value of this voltage corresponds to the absorption edge of the K-spectrum.

These experiments therefore prove that an electron must be removed from the K-shell, before the Kα-line or any other characteristic line can be emitted. When this is done, all the lines of the K-spectrum appear simultaneously.

232. The L-absorption Spectrum.—When the X-ray absorption spectrum of an element is taken in its L-region, it is found as in the K-spectrum, that there is no absorption corresponding to the L-emission lines, but now *three absorption edges*, are found. They are denoted by L_1, L_2, L_3 in the order of their ν-values. Their positions with respect to the L-lines are shown in the following diagram (Fig. 11) and an actual photograph* due to Sandstrom of the L-absorption edges of Tl is reproduced in Fig. 10.

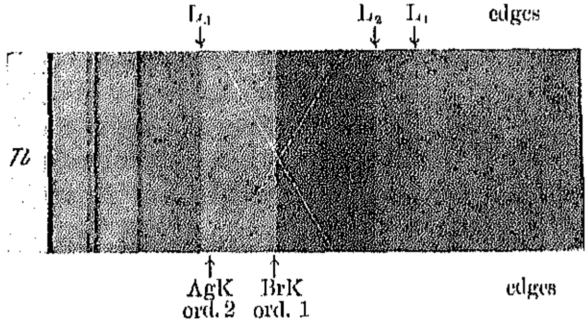

Fig. 10.—L-absorption edges of Tl.

It is found that the absorption edges ν_1, ν_2, ν_3 of the elements can be represented by formulæ of the type:—

$$\sqrt{\nu_{L_1}/R} = Z-\sigma_{L_1}/2,\ \sqrt{\nu_{L_2}/R} = Z-\sigma_{L_2}/2,\ \sqrt{\nu_{L_3}/R} = Z-\sigma_{L_3}/2$$

Here σ_{L_1}, σ_{L_2}, σ_{L_3} are known as the screening constants for the L_1, L_2, L_3 sublevels.

These L-absorption edges can be interpreted in the same way as the K-edge. They indicate the photo-electric ejection of the electron from the L-shell, for which $n=2$. But the experiment shows that when $n=2$, the ejection can take place in 3 different ways, or another alternative view is that the L-shell is capable of further subdivision into three sublevels as shown in Fig. 11.

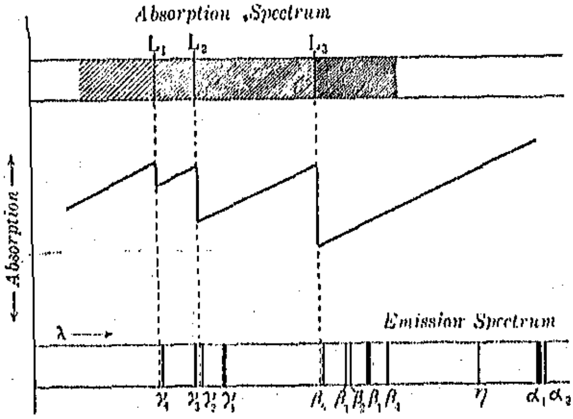

Fig. 11.—Schematic representation of L-absorption edges and L-lines.

---

* Sandstrom, *Zs. f. Phys.*, 65, 632, 1930.

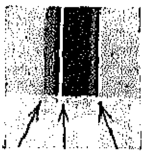

Fig. 12.
M-absorption edge of U.

Similarly, the M-absorption spectrum has been also studied for U and found to consist of five different edges which were at first denoted by M_1, M_2, M_3, M_4, M_5 in the decreasing order of their ν-values. Fig. 12 shows a photograph of M-absorption edge for U reproduced from that due to Coster.*

Tables of L and M-absorption edges, in wavelength and frequency units are given in the appendix.

233. Absorption Levels and Origin of Lines.—The insufficiency of Moseley's explanation of the origin of characteristic X-ray lines was first pointed out by Kossel,* who concluded from Moseley's measurements, that though the frequencies of lines should be regarded as difference between term values, as Rydberg had shown for optical lines, these term values are not always represented by equations of the Moseley type. He observed that the frequency of the $K\beta$ line can be expressed as the sum of the frequencies of $K\alpha$ and $L\alpha$-lines, that is

$$\nu_{K\beta} = \nu_{K\alpha} + \nu_{L\alpha}$$

exactly, and from this fact, he concluded that generally

$$\nu_{K\alpha} = \nu_K - \nu_L,\ \nu_{K\beta} = \nu_K - \nu_M,\ \ \nu_{K\gamma} = \nu_K - \nu_N, \text{ etc.} \ldots$$

where $h\,\nu_K$ denotes the energy required to remove an electron from the K-shell to infinity, and ν_L, ν_M have similar meaning.

After the discovery of the absorption edges, the values of ν_K's and ν_L's could be obtained directly from experiments.

It was found that the ν's of $K\alpha_1$ and $K\alpha_2$ were respectively equal to $\nu_K - \nu_{L_3}$ and $\nu_K - \nu_{L_2}$. *There is no line having the frequency* $\nu_K - \nu_{L_1}$. These facts are represented in the following diagram (Fig. 13).

Similarly, $K\beta$ which for heavy elements was found to be a close doublet arises from transition from M_3 and M_2 to K. No lines corresponding to transition from (M_1, M_4, M_5) to K were found. $K\beta_1$ was found single on account of the small difference in the value of M_3 and M_2, but when greater resolving power is used it is found to be double.

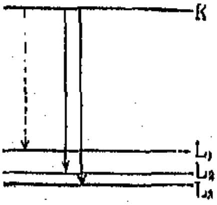

Fig 13.—The forbidden $(K - L_1)$ transition.

---

* Coster, *Phys. Rev.*, 19, 20, 1922.

Origin of the L-spectrum. Some of the stronger L-lines are certainly due to transitions from the M-levels to the L-levels. If all transitions were available, there would be altogether 15 lines, while only 7 lines were found. The origin of the 7 lines according to the energy level diagrams is shown below (Fig. 14).

234. Explanation of the Origin of X-ray Lines.—The fact that there are no lines corresponding to $L_1 \rightarrow K_1$, etc. . . . . . shows that there is some selection principle which limits the possible transitions. The full explanation is due to Pauli. He showed that the transitions

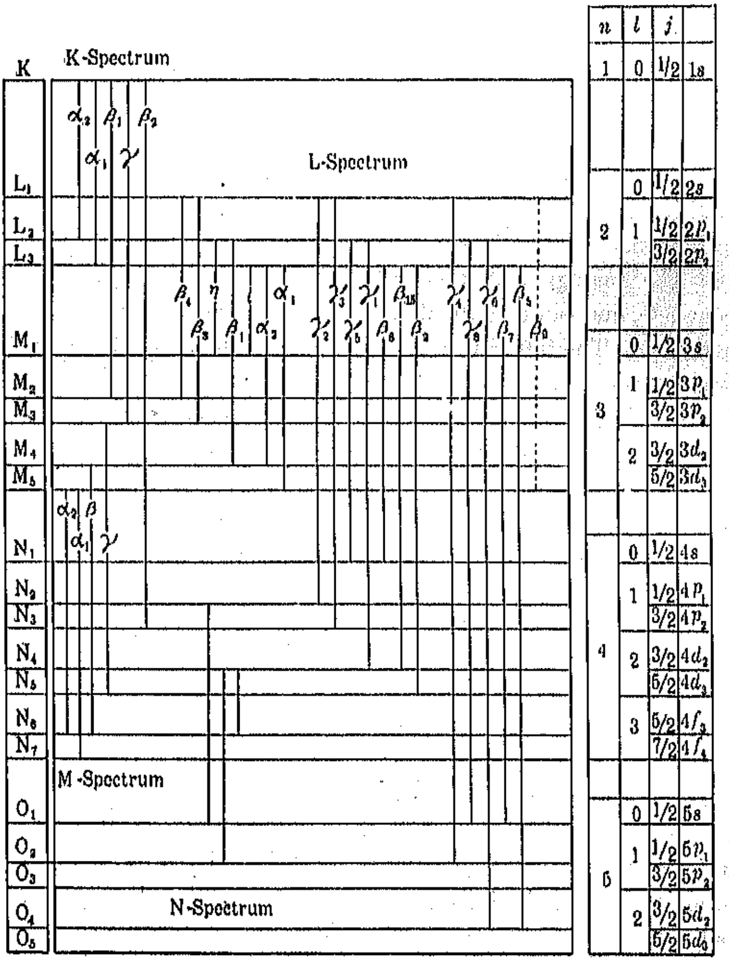

n	l	j	
1	0	1/2	1s
2	0	1/2	2s
	1	1/2	$2p_1$
		3/2	$2p_2$
3	0	1/2	3s
	1	1/2	$3p_1$
		3/2	$3p_2$
	2	3/2	$3d_2$
		5/2	$3d_3$
4	0	1/2	4s
	1	1/2	$4p_1$
		3/2	$4p_2$
	2	3/2	$4d_2$
		5/2	$4d_3$
	3	5/2	$4f_3$
		7/2	$4f_4$
5	0	1/2	5s
	1	1/2	$5p_1$
		3/2	$5p_2$
	2	3/2	$5d_2$
		5/2	$5d_3$

Fig. 14. – Chart showing the origin of K, L, M, N, X-ray lines.

are fully explained if it be supposed that to the sub-levels we ascribe the same quantum characteristics as to the optical levels of alkali elements (*vide* p. 379). This is illustrated in columns 2, 3 and 4 to the right of Fig. 14.

Thus K is denoted by 1*s*. This means that for $n=1$, $k=1$, $j=\frac{1}{2}$. This is also otherwise evident, for if $n=1$, k must be 1 according to Sommerfeld's theory.

L_1 is denoted by 2*s*. This explains why there are no lines corresponding to $L_1 \rightarrow K_1$. This is forbidden by the selection principle that Δk must be equal to ± 1. L_2 and L_3 are represented by $2p_1$ and $2p_2$, $k=2, j=\frac{1}{2}, \frac{3}{2}$ respectively for L_2 and L_3.

In a similar way, M_1 may be denoted by 3*s*, M_2 and M_3 by $3p_1$, $3p_2$; M_4, M_5 by $3d_2$, $3d_3$. The L-group of lines can thus be divided into three multiplets as shown. Here we have to add the additional rule that $\Delta j = \pm 1$, or 0; $\Delta j = \pm 2, \pm 3 \ldots$, etc., are forbidden.

The analogy with the levels of the alkali elements is therefore complete, and can be extended to M and N-levels wherever these are complete. The full scheme of X-ray lines (diagrammatic) with their present commonly accepted notation of terms for Tungsten is shown in the above diagram (Fig. 14). The corresponding key diagram for notations is represented in Fig. 15. It is customary to denote the various lines belonging to a particular series by the Greek letters, $\alpha_1, \alpha_2, \ldots, \beta_1, \beta_2 \ldots, \gamma_1, \gamma_2, \ldots, \eta, l \ldots$ where the subscripts of increasing values denote gradually weaker components.

235. Survey of the Term-values. The Regular and Irregular Doublet Laws.—We have referred in §226 to the preliminary work of Moseley who showed that $\sqrt{\nu/R}$ for the characteristic lines is a function of the atomic number Z. This has been illustrated in Fig. 8. Since the frequency of a line is the difference between energy-values in two states of the atom, the term-values are important for all problems of atomic physics and it is necessary to take a survey of them. These term-values can in most cases be obtained from the values of the absorption edges, but it has been found that in many cases the absorption edges have complex structure (fine structure, see *infra*). Hence it has now become customary to calculate the values of the edges from the wavelength of the characteristic lines with the aid of the principle of combination, but the value of one or two absorption edges at

		K_1	L_1	L_2	L_3	M_1	M_2	M_3	M_4	M_5	
		$1s$	$2s_1$	$2p_1$	$2p_2$	$3s$	$3p_1$	$3p_2$	$3d_1$	$3d_2$	
$1s$	K_1										
		K-Spectrum									
$2s$	L_1										
$2p_1$	L_2	α_2									
$2p_2$	L_3	α_1									
			L-Spectrum								
$3s$	M_1			η	l						
$3p_1$	M_2	β_3	β_4		t						
$3p_2$	M_3	β_1	β_3		s						
$3d_1$	M_4		β_{10}	β_1	α_2						
$3d_2$	M_5		β_9		α_1						
						M-Spectrum					
$4s$	N_1			γ_5	β_6						
$4p_1$	N_2		γ								
$4p_2$	N_3	β_2	γ_3								
$4d_2$	N_4			γ_1	β_{15}		δ	γ_2			
$4d_1$	N_5		γ_{11}		β_2			γ_1			
$4f_2$	N_6								β	α_2	
$4f_1$	N_7									α_1	
$5s$	O_1			γ_8	β_7						
$5p_1$	O_2		γ_{13}								
$5p_2$	O_3		γ_4								
$5d_2$	O_4			γ_6	β_5						
$5d_1$	O_5										
$5f_3$	O_6										
$5f_4$	O_7										

Fig. 15.—The key diagram of notations of X-ray lines.

Each pair of lines arising from transitions between the same initial level, and two different final levels having the same n, l, but different j, or *vice versa* are known as the *relativity doublet*. The pairs of such lines are enclosed in separate rectangles. Those in dotted rectangles are due to forbidden transitions.

least must be accurately known. Generally the K-absorption edge is taken, but in the case of heavy elements, the L_3-edge is also taken as the starting point.

We illustrate the calculation by taking the case of U. Here start was made with the value of the L_3-level, which was obtained from measurement of the absorption edge. We thus have $L_3=1264{\cdot}2$. Again $\nu_{K\alpha_1}=K-L_3$ and $\nu_{K\alpha_2}=K-L_2$. Hence $L_2-L_3=\nu_{K\alpha_1}-\nu_{K\alpha_2}=278.{\cdot}5$ from the known frequency interval between the $K\alpha_1$, $K\alpha_2$ lines. Therefore $L_2=1264{\cdot}2+278{\cdot}5=1542{\cdot}7$. Further L_1 is experimentally determined from the absorption limit as 1602·6. The three L-levels L_1, L_2, L_3 are thus determined. Now taking these values and with the aid of different L-lines which arise due to M→L transitions, we can calculate the term-values for various M-levels. The successive steps are shown below:—

$L_3 = 1264{\cdot}2$ ... absorption limit experimentally determined.

$L_2-L_3 = 278{\cdot}5$ ... $\Delta\nu=\nu_{K\alpha_1}-\nu_{K\alpha_3}$, experimentally determined.

$L_2=1264{\cdot}2+278{\cdot}5 = 1542{\cdot}7$ ... can be determined experimentally as well.

$L_1 = 1602{\cdot}6$ ... absorption limit experimentally determined.

$M_1=L_2-\eta=1542{\cdot}7-1134{\cdot}2 = 408{\cdot}5$ ... ν_η ... exp. determined.
$\quad =L_3-l=1264{\cdot}2-855{\cdot}7 = 408{\cdot}5$ ... ν_l ... " "
$M_2=L_1-\beta_4=1602{\cdot}6-1220{\cdot}8 = 381{\cdot}8$ ... ν_{β_4} ... " "
$M_3=L_1-\beta_3=1602{\cdot}6-1285{\cdot}7 = 316{\cdot}9$ ... ν_{β_3} ... " "
$M_4=L_2-\beta_1=1542{\cdot}7-1268{\cdot}3 = 274{\cdot}4$ ... ν_{β_1} ... " "
$\quad =L_3-\alpha_2=1264{\cdot}2-989{\cdot}9 = 274{\cdot}3$ ... ν_{α_2} ... " "
$M_5=L_3-\alpha_1=1264{\cdot}2-1002{\cdot}8 = 261{\cdot}4$ ... ν_{α_1} ... " "

The values can further be checked by testing them with other combinations.

The values of N-levels can be obtained by taking either the M-values as starting points, and utilizing the frequencies of M-lines, or taking the L-levels, and utilizing the frequencies of L←N lines. Similarly we can also calculate the values of the O-levels. Some of these calculations are illustrated below:—

$N_1=L_2-\gamma_5=1542{\cdot}7-1436{\cdot}8=105{\cdot}9$ ... ν_{γ_5} ... exp. determined
$\quad =L_3-\beta_6=1264{\cdot}2-1158{\cdot}2=106{\cdot}0$ ... ν_{β_6} ... " "
$N_2=L_1-\gamma_2=1602{\cdot}6-1509{\cdot}1=93{\cdot}5$ ... ν_{γ_2} ... " "

$N_3 = L_1 - \gamma_3 = 1602{\cdot}6 - 1526{\cdot}2 = 76{\cdot}4 \ldots \nu_{\gamma_3} \ldots$ exp. determined
$N_4 = L_2 - \gamma_1 = 1542{\cdot}7 - 1485{\cdot}2 = 57{\cdot}5 \ldots \nu_{\gamma_1} \ldots$ " "
$N_5 = L_3 - \beta_2 = 1264{\cdot}2 - 1210{\cdot}1 = 54{\cdot}1 \ldots \nu_{\beta_2} \ldots$ " "
$O_1 = L_2 - \gamma_8 = 1542{\cdot}7 - 1519{\cdot}5 = 23{\cdot}2 \ldots \nu_{\gamma_8} \ldots$ " "
$O_3 = L_1 - \gamma_4 = 1602{\cdot}6 - 1588{\cdot}7 = 13{\cdot}9 \ldots \nu_{\gamma_4} \ldots$ " "

A comprehensive list of the term-values for K, L_1, L_2, L_3 and M_1 M_2, M_3, M_4, M_5-levels of elements from 92U to 4Be have been collected in table 2, where the sources are mentioned. In case of lighter elements only a few data are available, as in their case absorption edges and emission lines have not been generally determined except for a few, as they occur in very soft region. Recently some works have been done on light elements by Thibaud, Södermann, M. Siegbahn, Magnusson, Holweck and others. Some of their data have been included in table 2.

The first survey of term-values was made by Bohr and Coster* in 1923, who represented them in the form of curves with Z as abscissae, and $\sqrt{\nu/R}$ as ordinate. The curves (Fig. 16) reproduced here have been adopted from the original Bohr-coster diagram.

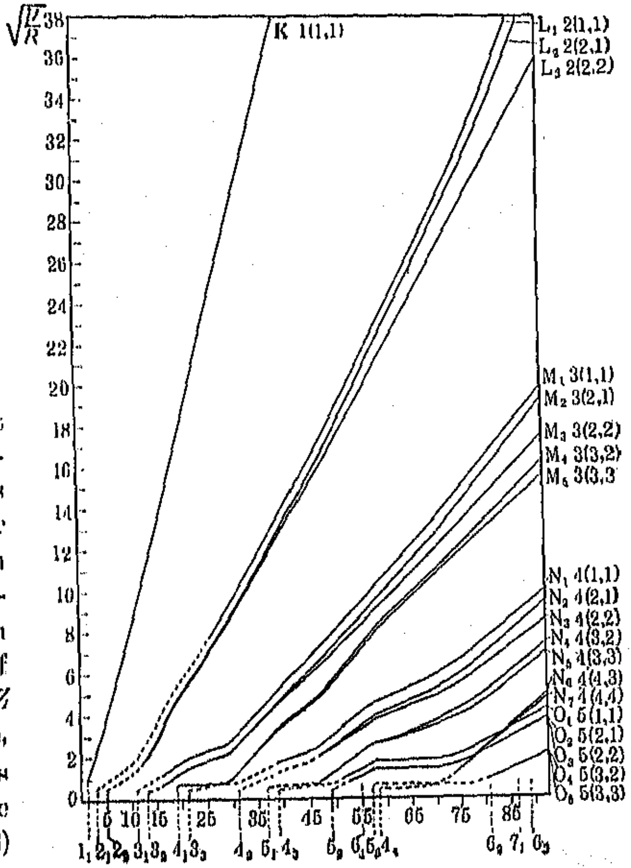

Fig. 16. The Bohr-Coster diagram.

---

* N. Bohr and D. Coster, *Zs. f. Phys.*, 13, 342, 1923.

Table 2.—Level values of Elements.

$[a = \nu/R, \quad b = \sqrt{\nu/R}]$

Atomic number	Element		K		L$_1$		L$_2$		L$_3$	
92	U	*a* *b*	8474	92·05	1602·6	40·03	1542·7 *·75*	39·28	1264·2	35·56
90	Th	*a* *b*	8087	89·93	1506·5	38·81	1449·1 *·74*	38·07	1199·0	34·63
83	Bi	*a* *b*	6669	81·66	1207·0	34·74	1157·1 *·72*	34·02	988·3	31·44
82	Pb	*a* *b*	6478	80·49	1168·3	34·18	1119·6 *·72*	33·46	960·0	30·98
81	Tl	*a* *b*	6299	79·37	1130·2	33·62	1082·4 *·72*	32·90	932·0	30·53
80	Hg	*a* *b*	6119	78·22	1092·4	33·05	1046·4 *·70*	32·35	904·5	30·07
79	Au	*a* *b*	5942	77·08	1057·1	32·51	1011·4 *·71*	31·80	897·7	29·63
78	Pt	*a* *b*	5771	75·97	1021·3	31·96	976·7 *·71*	31·25	850·9	29·17
77	Ir	*a* *b*	5606	74·87	987·9	31·43	944·2 *·70*	30·73	825·6	28·73
74	W	*a* *b*	5120	71·55	890·8	29·85	849·9 *·70*	29·15	751·3	27·41
73	Ta	*a* *b*	4969	70·49	860·7	29·34	820·6 *·69*	28·65	728·0	26·98
72	Hf	*a* *b*	4815	69·39	831·1	28·83	791·8 *·69*	28·14	704·7	26·55
71	Cp	*a* *b*	4664	68·34	800·9	28·30	762·5 *·69*	27·61	681·2	26·10
70	Ad	*a* *b*	4516	67·20	772·9	27·80	735·5 *·68*	27·12	659·2	25·67
68	Er	*a* *b*	4233	65·06	718·5	26·80	682·8 *·67*	26·13	615·9	24·82
67	Ho	*a* *b*	4096	64·00	692·0	26·31	656·9 *·68*	25·63	594·7	24·39

Figures in italics are the differences $\Delta\sqrt{\nu/R}$ *between two adjacent* $\sqrt{\nu/R}$*-values*

Table 2.—Level values of Elements—(continued).

$[\,a = \nu/R, \quad b = \sqrt{\nu/R}\,]$

M₁		M₂			M₃		M₄			M₅	
408·5	20·21	381·5	*·68*	19·53	316·8	17·80	274·2	*1·24*	16·56	261·2	16·16
380·3	19·50	354·3	*·68*	18·82	296·5	17·22	255·5	*1·24*	15·98	243·8	15·61
294·6	17·16	272·2	*·66*	16·50	234·0	15·30	198·0	*1·23*	14·07	189·9	13·74
283·7	16·84	262·1	*·65*	16·19	225·9	15·03	190·3	*1·24*	13·79	182·8	13·52
272·6	16·51	251·4	*·65*	15·86	217·4	14·74	182·7	*1·22*	13·52	175·6	13·25
261·0*	16·22	239·11*	*·69*	15·53	208·07*	14·45	*175·64	*1·18*	13·27	*168·79	13·00
252·2	15·88	231·8	*·66*	15·22	201·9	14·21	168·6	*1·23*	12·98	162·2	12·74
242·0	15·56	221·9	*·66*	14·90	193·9	13·92	161·2	*1·22*	12·70	155·3	12·46
233·2	15·27	213·7	*·66*	14·62	187·4	13·69	155·3.	*1·23*	12·46	149·8	12·24
207·3	14·40	189·3	*·64*	13·76	167·5	12·94	137·5	*1·21*	11·73	132·9	11·53
199·8	14·14	182·1	*·65*	13·40	162·0	12·73	132·4	*1·22*	11·51	128·1	11·32
192·1	13·86	175·2	*·62*	13·24	155·8	12·48	127·0	*1·21*	11·27	122·9	11·09
183·6	13·55	166·8	*·63*	12·92	149·4	12·22	121·0	*1·22*	11·00	117·4	10·84
176·0	13·30	160·6	*6·3*	12·67	144·2	12·01	116·5	*1·22*	10·70	112·9	10·63
163·6	12·79	147·7	*·64*	12·15	133·6	11·56	107·3	*1·20*	10·36	104·1	10·20
156·9	12·53	141·5	*·63*	11·90	128·1	11·32	102·6	*1·19*	10·13	99·7	9·98

* Calculated from L-absorption edge and L-emission lines.

Table 2.—Level values of Elements—(continued).

[$a = \nu/R, \quad b = \sqrt{\nu/R}$]

Atomic Number.	Element.		K		L₁		L₂		L₃	
66	Dy	*a* *b*	3961	62·94	666·8	25·82	632·5 *·67*	25·15	574·2	23·96
65	Tb	*a* *b*	3830	61·89	641·8	25·33	608·3 *·67*	24·66	553·9	23·53
64	Gd	*a* *b*	3700	60·83	617·5	24·84	585·0 *·65*	24·19	534·1	23·11
63	Eu	*a* *b*	3573	59·77	593·6	24·36	561·6 *·66*	23·70	514·4	22·68
62	Sm	*a* *b*	3451	58·75	570·3	23·88	538·9 *·67*	23·21	495·0	22·25
60	Nd	*a* *b*	3209	56·65	525·5	22·93	495·6 *·66*	22·26	457·8	21·40
59	Pr	*a* *b*	3093	55·61	503·6	22·44	474·8 *·65*	21·79	439·6	20·98
58	Ce	*a* *b*	2978	54·57	482·9	21·98	454·4 *·66*	21·32	421·9	20·54
57	La	*a* *b*	2867·0	53·54	461·4	21·48	434·7 *·63*	20·85	404·4	20·11
56	Ba	*a* *b*	2757·2	52·51	441·6	21·01	414·6 *·65*	20·36	386·7	19·66
55	Cs	*a* *b*	2649·8	51·48	420·3	20·50	394·8 *·63*	19·87	369·3	19·22
53	I	*a* *b*	2442·8	49·42	382·1	19·55	357·6 *·64*	18·91	335·8	18·32
52	Te	*a* *b*	2343·6	48·41	364·8	19·10	340·4 *·65*	18·45	320·2	17·89
51	Sb	*a* *b*	2246·4	47·41	346·8	18·62	323·4 *·64*	17·98	304·7	17·45
50	Sn	*a* *b*	2149·5	46·36	327·4	18·09	304·9 *·63*	17·46	288·1	16·97
49	In	*a* *b*	2057·2	45·36	311·3	17·64	289·4 *·63*	17·01	274·9	16·58

Table 2.—Level values of Elements—(continued).

$[\,a = \nu/R,\ \ b = \sqrt{\nu/R}\,]$

M₁		M₂			M₃		M₄			M₅	
150·0	12·25	136·0	*·59*	11·66	123·7	11·12	98·6	*1·19*	9·93	95·8	9·79
145·1	12·05	130·2	*·64*	11·41	118·8	10·90	94·2	*1·19*	9·71	91·7	9·58
139·1	11·79	124·7	*·62*	11·17	114·2	10·69	90·3	*1·19*	9·50	87·7	9·36
133·2	11·54	119·5	*·61*	10·93	109·6	10·47	86·1	*1·19*	9·28	83·8	9·15
127·2	11·28	113·8	*·61*	10·67	104·9	10·24	81·8	*1·20*	9·04	79·8	8·93
116·6	10·80	104·1	*·60*	10·20	96·1	9·80	74·2	*1·29*	8·61	72·5	8·51
111·5	10·56	98·6	*·63*	9·93	91·7	9·58	70·4	*1·19*	8·39	68·8	8·29
106·0	10·30	94·2	*·59*	9·71	87·7	9·36	66·7	*1·19*	8·17	65·4	8·09
101·0	10·05	88·5	*·64*	9·41	82·5	9·08	63·1	*1·14*	7·94	61·8	7·86
95·5	9·77	84·2	*·59*	9·18	78·7	8·87	58·9	*1·20*	7·67	57·7	7·60
89·5	9·46	77·8	*·64*	8·82	72·9	8·54	54·6	*1·15*	7·39	53·6	7·32
79·1	8·89	68·5	*·61*	8·28	64·4	8·02	46·7	*1·19*	6·83	45·7	6·76
74·6	8·64	65·0	*·58*	8·06	61·2	7·82	43·5	*1·22*	6·60	42·5	6·52
70·0	8·37	60·6	*·59*	7·78	57·1	7·47	40·0	*1·15*	6·32	39·2	6·26
63·9	7·99	54·4	*·61*	7·38	51·2	7·16	35·1	*1·24*	5·92	34·4	5·87
60·6	7·78	50·9	*·65*	7·13	48·1	6·94	32·9	*1·20*	5·74	32·8	5·73

Table 2.—Level values of Elements—(continued)
$[\, a = \nu/R, \quad b = \sqrt{\nu/R}\,]$

Atomic Number	Element		K		L_1		L_2		L_3	
48	Cd	*a* *b*	1967·6	44·36	296·0	17·20	274·8 *·62*	16.58	260·8	16·15
47	Ag	*a* *b*	1880·9	43·67	282·0	16·79	261·3 *·63*	16·16	248·6	15·77
46	Pd	*a* *b*	1794·0	42·36	266·2	16·32	245·9 *·64*	15·68	234·3	15·31
45	Rh	*a* *b*	1709·6	41·35	250·7	15·83	231·2 *·62*	15·21	220·6	14·85
44	Ru	*a* *b*	1629·1	40·36	237·7	15·42	218·6 *·63*	14·79	209·1	14·46
42	Mo	*a* *b*	1473·4	38·38	211·3	14·54	193·7 *·62*	13·92	186·0	13·64
41	Nb	*a* *b*	1398·5	37·40	198·9	14·10	181·7 *·62*	13·48	174·7	13·22
40	Zr	*a* *b*	1325·7	36.41	186·6	13·66	170·0 *·62*	13·01	163·8	12·80
39	Y	*a* *b*	1256·1	35·44	175·8	13·26	159·0 *·61*	12·65	154·4	12·43
38	Sr	*a* *b*	1186·0	34·44	162·9	12·76	147·6 *·61*	12·15	142·7	11·95
37	Rb	*a* *b*	1119·4	33·46	152·0	12·33	137·2 *·62*	11·71	132·8	11·52
35	Br	*a* *b*	902·6	31·61			117·8	10·85	114·3	10·69
34	Se	*a* *b*	932·0	30·53			108·4	10·41	105·4	10·27
33	As	*a* *b*	874·0	29·56	112·6	10·61	100·0 *·61*	10·00	97·4	0·87
32	Ge	*a* *b*	817·6	28·59			91·6	9·57	89·3	9·45

Table 2.—Level values of Elements—(continued).
$[\, a = \nu/R, \quad b = \sqrt{\nu/R} \,]$

M_1		M_2			M_3		M_4			M_5	
57·1	7·56	48·0	*·63*	6·93	45·4	6·74	30·5	*1·22*	5·52	30·0	5·48
54·7	7·40	44·57	*·72*	6·68	42·21	6·52	27·73	*1·25*	5·27	27·17	5·22
49·0	7·06	41·9	*·59*	6·47	39·8	6·31	25·6		5·46	25·2	5·02
45·6	6·76	37·8	*·61*	6·15	36·0	6·00	22·4	*1·27*	4·73	22·0	4·69
43·0	6·56	35·7	*·59*	5·97	34·1	5·84	21·0	*1·26*	4·58	20·7	4·55
37·5	6·12	30·5	*·60*	5·52	29·2	5·40	17·3	*1·24*	4·16	17·1	4·14
34·7	5·89	28·1	*·59*	5·30	26·9	5·19	15·4	*1·27*	3·92	15·2	3·92
31·8	5·64	25·4	*·60*	5·04	24·4	4·94	13·5	*1·27*	3·67	13·3	3·65
30·3	5·50	24·2	*·58*	4·92	23·3	4·83	13·0	*1·22*	3·61		
26·2	5·12	20·4	*·60*	4·52	19·6	4·43	9·7	*1·22*	3·11		
24·11*	4·92*	18·46	*·62*	4·30	17·80*	4·23	8·8		2·91	8·3	2·88
19·48	4·41	13·60*		3·69	13·21*	3·64	5·27		2·3	5·13*	2·26
16·7	4·09	11·6	*·68*	3·41			3·9		1·97		
14·9	3·86	10·3	*·66*	3·20			3·0		1·73		
12·0	3·59	8·8	*·61*	2·97			1·8		1·34		

---

* Values due to Ingelstam and Ray, *Zs. f. Phys.*, **88**, 218, 1934.

Table 2.—Level values of Elements—(continued).

[$a = \nu/R$, $b = \sqrt{\nu/R}$]

Atomic Number	Element		K		L$_1$		L$_2$		L$_3$	
31	Ga	a b	765·6	27·67	…	…	86·0 …	9·27	84·1	9·17
30	Zn	a b	711·7	26·68	88·4	9·40	77·1 ·62	8·78	75·4	8·68
29	Cu	a b	661·6	25·72	81·0	9·00	70·3 ·62	8·38	68·9	8·30
28	Ni	a b	614·1	24·78	74·8	8·65	64·6 ·61	8·04	63·2	7·95
27	Co	a b	568·1	23·83	…	…	58·8 …	7·66	57·7	7·60
26	Fe	a b	523·0	22·89	62·5	7·91	53·2 ·62	7·29	52·2	7·22
25	Mn	a b	481·9	21·95	…	…	48·3	6·95	47·4	6·88
24	Cr	a b	441·1	21·00	…	…	43·0	6·56	42·3	6·50
23	Va	a b	402·7	20·07		…	38·5	6·20	37·9	6·16
22	Ti	a b	365·8	19·13	…	…	34·0	5·83	33·6	5·80
21	Sc	a b	331·2	18·20	…	…	30·3	5·50	30·0	5·48
20	Ca	a b	297·4	17·25	…	…	25·8	5·08	25·5	5·05
19	K	a b	265·6	16·30	…	…	21·7	4·66	21·5	4·64
18	A	a b	235·7	15·35	…	…	…	18·21		4·266
17	Cl	a b	207·9	14·42	…	…	14·9	3·86	14·8	3·85
16	S	a b	181·9	13·49	…	…	12·72	3·566	12·63	3·555

Table 2.—Level values of Elements—(continued).

[$a = \nu/R$. $b = \sqrt{\nu/R}$]

M₁		M₂	M₃		M₄	M₅	
13·4	3·66	*·58*	9·5	3·08		3·2	1·79
10·1	3·18	*·59*	6·7	2·59		0·9	0·95
8·9	2·98	*·59*	5·7	2·39		0·4	0·63
8·2	2·86	*·54*	5·4	2·32		0·7	0·84
7·6	2·76	*·59*	4·7	2·17		0·5	0·71
6·9	2·63	*·61*	4·1	2·02		0·4	0·63
…	…		3·8	1·95		0·6	0·39
…	…		3·1	1·76		0·2	0·45
…	…		3·0	1·73		0·5	0·71
…	…		2·6	1·61		0·4	0·63
…	…		2·7	1·64		0·8	0·89
…	…		1·7	1·38		0·4	0·63
2·4	…		1·2	1·10		0·3	0·55
…	…		…	…		…	…
1·41†	1·188		0·5	0·71		…	…
1·23†	1·11		0·4	0·63		…	…

Table 2.—Level-values of Elements—(continued).

$[a = \nu/R, \quad b = \sqrt{\nu/R}]$

Atomic Number	Element		K		L₁		L₂		L₃	
15	P	a b	157·8	12·56	...	...	9·4	3·07		
14	Si	a b	135·4	11·64	...	...	...	...	7·261†	2·695
13	Al	a b	114·8	10·71	...	...	5·364†	2·316	5·346†	2·312
12	Mg	a b	96·0	9·80	...	...	...	...	3·642	1·91
11	Na	a b	76·67†	8·75	...	...	...	...	...	...
9	F	a b	50·5*	7·1	...	...	...	...	...	...
8	O	a b	39·0*	6·245	...	...	...	...	...	...
7	N	a b	29·3*	5·41	...	...	...	...	...	...
6	C	a b	20·6*	4·54	...	...	...	...	...	...
5	B	a b	14·2*	3·77	...	...	...	..	...	...
4	Be	a b	11·27	3·36	...	...	...	...	...	...

Sources:

(1) Siegbahn, *Spektroskopie der Röntgenstrahlen* (1931).

(2) Lindh, *H. d. Exp. physik*, **24**, (1928).

†(3) Södermann, *Phil. Mag.*, **10**, 600, 1930: Data for sodium by grating method.

*(4) Holweck, (Siegbahn, *loc. cit.*, p. 429); Data for F, O, N, C, B by absorption method.

‡(5) Siegbahn and Magnusson, *Zs. f. Phys.*, **87**, 291, 1934: Data for L_2, L_3, M_1-levels of Cl, S, Si, Al, Mg—by the method of curved grating.

(6) Ingelstan and Ray, *loc. cit.*: Data for Rb, Br M-levels.

Table 2.—Level-values of Elements—(continued).

$[a = \nu/R, \quad b = \sqrt{\nu/R}]$

M_1	M_2	M_3	M_4	M_5
…	0·5			…
	…	0·71	…	
…	0·5			…
	…	0·71	…	
…	0·4			…
	…	0·63	…	
…	0·5			…
	…	0·71	…	

On account of recent works the lower parts of the curves have been considerably modified. For these see Fig. 31, §241.

A glance at these curves shows that each of them can be divided into two sections—one part in which the course of the curve is regular, a second part in which it begins to be irregular. Confining ourselves to the regular part, we find

$$\sqrt{\nu/R} = aZ + b \text{ nearly}$$

or

$$\nu/R = \frac{(Z-\sigma)^2}{n^2}$$

where n is the total quantum number, σ = the screening constant which is a function of n, l and j.

The Irregular Doublet Law.—We further observe that the L_1- and L_2-curves are nearly parallel, whereas the L_2, L_3-curves more and more diverge from each other with increasing values of Z. G. Hertz* first showed that

$$\sqrt{\nu_{L_1}/R} - \sqrt{\nu_{L_2}/R} = {}^{\cdot}63 \text{ (nearly constant)}$$

The approximate correctness of this law is illustrated in table 2, column 8, under L_2 in italics. The value of the difference varies from ·75 in U to ·62 in Fe.

---

* G. Hertz, *Zs. f. Phys.*, 3, 19, 1920.

Similarly, if we take the curves for $\sqrt{\nu/R}$-values, for M_1 and M_2, M_3 and M_4, N_1 and N_2 ..... N_3 and N_4 ..... they are found to run more or less parallel. We have in fact

$$\sqrt{\nu_{M_1}/R} - \sqrt{\nu_{M_2}/R} = \text{·68 for U to ·59 for Co}$$

$$\sqrt{\nu_{M_3}/R} - \sqrt{\nu_{M_4}/R} = \text{1·24 for U to 1·22 for Sr}$$

$$\sqrt{\nu_{N_1}/R} - \sqrt{\nu_{N_2}/R} = \text{·63 for U to ·64 for Cs}$$

as can be verified from the table 2.

These empirical relations are known as the *Irregular Doublet Law*.

The Regular Doublet Law.—The early investigators on X-ray spectroscopy observed that a characteristic frequency difference exists between certain pairs of lines in the X-ray spectra. This is now known to arise from the difference $L_2 - L_3$, and it occurs between lines which can be easily found from an inspection of chart 14 on p. 445. As illustration we take the difference in frequency as experimentally determined of the following characteristic lines of W.

L-lines :	η 642·60	β_1 712·39	γ_5 806·57	γ_6 849·98
	l 544·05	α_2 613·90	β_6 708·06	β_5 751·32
	98·55	98·49	98·51	98·66
K-lines :	α_1 4368·2	L-absorption limits :		L_2 850·28
	α_2 4269·3			L_3 751·30
	98·9			98·98

We have already explained that the characteristic difference $L_2 - L_3$ increases very rapidly with atomic number, as is clear from an inspection of the curves in Fig. 16 and from comparison of the figures on columns 8 and 10 of the table 2. These differences are however independently shown in table 3. They are taken from Siegbahn's *Spektroskopie der Röntgenstrahlen* (1931).

Sommerfeld* deduced from certain theoretical deductions (which have however undergone considerable changes) that

$$\Delta(\nu/R) = \frac{\alpha^2 (Z-d)^4}{2^4}$$

where α = the Sommerfeld fine structure constant, and d was found to have very nearly the value 3·5. The validity of this law can be

---

* A. Sommerfeld, *Atombau und Spektrallinien* (1924), Chap. 6, §4.

Table 3.—Values of d for L_2, L_3-levels.

Z	$\Delta\nu_L/R$	$Z-d$	d	Z	$\Delta\nu_L/R$	$Z-d$	d
41 Nb	6·89	37·50	3·50	63 Eu	47·19	59·48	3·52
42 Mo	7·70	38·53	3·47	64 Gd	50·66	60·48	3·52
44 Ru	9·49	40·54	3·46	65 Tb	54·38	61·49	3·51
45 Rh	10·48	41·53	3·47	66 Dy	58·30	62·49	3·51
46 Pd	11·56	42·52	3·48	67 Ho	62·46	63·50	3·50
47 Ag	12·69	43·59	3·51	68 Er	66·85	64·50	3·50
48 Cd	13·97	44·52	3·48	70 Yb	76·1	66·5	3·50
49 In	15·29	45·50	3·50	71 Cp	82·5	67·6	3·30
50 Sn	16·73	46·50	3·50	73 Ta	92·70	69·52	3·48
51 Sb	18·29	47·50	3·50	74 W	98·54	70·49	3·51
52 Te	19·94	48·50	3·50	76 Os	111·08	72·51	3·49
53 I	21·71	49·49	3·54	77 Ir	118·64	73·50	3·50
55 Cs	25·30	51·48	3·52	78 Pt	125·92	74·49	3·51
56 Ba	27·70	52·46	3·54	79 Au	133·80	75·51	3·49
57 La	30·01	53·46	3·54	81 Tl	150·49	77·50	3·50
58 Ce	32·38	54·44	3·56	82 Pb	160·02	78·56	3·44
59 Pr	35·03	55·46	3·54	83 Bi	169·73	79·58	3·42
60 Nd	37·86	56·59	3·51	90 Th	250·86	86·57	3·43
62 Sm	43·95	58·50	3·50	92 U	278·71	88·51	3·49

Mean $d = 3·492$,

seen from columns 4 and 8 of table 3. The doublet levels L_2, L_3 were formerly known as *Relativity Doublets.* But now they are called *Spin Doublets*, because the two levels have got the same k, *viz.* 2, but differ in their j-values which are $\frac{1}{2}$ and $\frac{3}{2}$ respectively. We shall come to the theoretical treatment presently. The differences between M_2 and M_3 ($n = 3$, $k = 2$, $j = \frac{1}{2}$, $\frac{3}{2}$), M_4 and M_5 ($n = 3$, $k = 3$, $j = \frac{3}{2}$, $\frac{5}{2}$) follow laws similar to $\Delta\nu = L_2 - L_3$, and will be treated later on.

236. Theoretical Explanation of X-ray Spectra of Elements.—We shall now attempt to give a theoretical treatment of the facts discussed in the previous sections regarding the origin of characteristic X-ray spectra. The fact that the X-ray lines can be explained by assuming that inner shells of electrons possess states which have the same quantum characteristics as the states assumed by the valency electron in alkali spectra, gave rise in the early stages to the widespread belief, that the X-ray term values and their differences can be calculated in the same way as term-values of hydrogen (§164) or alkalies (Chap. XII), by introducing suitable screening constants. But this belief is rather misleading. Characteristic X-rays are produced when one electron is removed from any completed inner shell, and a fresh electron from some outer shell jumps to take its position. The apparent similarity to alkali spectra is due to the operation of Pauli's Principle according to which defect of one electron from a closed shell produces the same kind of terms as are possessed by a single electron lying outside the closed shells.

For a proper understanding of the origin of the X-ray lines, it is necessary to have a complete knowledge of the electron-composition of atoms. This is described in Chap. XII. The following account should be read after the reader has some knowledge of the subject-matter of that chapter.

The origin of the K-spectrum.—There are normally two electrons in the K-shell of each element. When one of these is removed either by electron bombardment as in X-ray tubes or by photo-ionisation (Fluorescence method, *vide* §245), and an electron jumps from some higher shell to take its position, the K-lines are emitted. The transition for $K\alpha_1\alpha_2$ may be denoted graphically as follows :—

$$\begin{array}{ccc} 1s^2.2p^5 & \leftarrow & 1s.2p^6 \\ {}^2P_{\frac{1}{2}},\ {}^2P_{\frac{3}{2}} & \leftarrow & {}^2S_{\frac{1}{2}} \\ L_2 \quad L_3 & \leftarrow & K \end{array}$$

The normal constitution of the atom is $1s^2.2s^2.2p^6\ldots$ etc. and $1s.2p^6$ denotes that one electron is ejected from the $1s^2$ or K-shell, leaving to it only one electron. The energy relation can be written as

$$1s^2 + h\nu_K = 1s + e$$

For avoiding cumbrousness, the other electron shells are not written.

Since this state is unstable, one electron jumps from the $2p^6$-shell to $1s$ forming the structure $1s^2.2p^5\ldots$ Now according to Pauli's principle $2p^5$ gives us either ${}^2P_{\frac{1}{2}}$ (L_2) or ${}^2P_{\frac{3}{2}}$ (L_3) owing to two different dispositions of the spins and the orbital l momenta of the five electrons.

The final configuration is $1s^2\ 2p^5$, *i.e.*, one electron is lost from the $2p$-shell, the other shells remaining complete. The energy which should be given to the completed atom for getting this configuration, *i.e.*, for ejecting an electron from the $2p^6$-shell is $h\nu_{L_2}$ or $h\nu_{L_3}$ according to the relation :—

$$2p^6 + h\nu_{L_2} = 2p^5\ {}^2P_{\frac{1}{2}} + e$$
$$2p^6 + h\nu_{L_3} = 2p^5\ {}^2P_{\frac{3}{2}} + e$$

The energy radiated as the electron jumps from $2p^6$ to $1s$ is given by

$$\nu = \nu_i - \nu_f = \nu_K - \nu_{L_2}, \nu_{L_3}$$

It should be added that there is some difference between the treatments of energy relations in this case and in optical cases. In the latter case, the state of zero energy is taken to be that composed of the ionised atom and the electron at infinity. So the variable part of the energy term comes out negative. Thus the energy of the H-atom when the electron is in third orbit is taken to be $H(3) = -Rh/3^2$, that of the second orbit $H(2) = -Rh/2^2$, and

$$\nu = \nu_i - \nu_f = (-R/3^2) - (-R/2^2)$$
$$= R\left[\frac{1}{2^2} - \frac{1}{3^2}\right]$$

In the present case, it is inconvenient to follow the precedent in optical spectra and take as our standard zero state the system ionised atom plus the electron, as ionisation is due to the ejection of the electron from different shells in the different cases of X-ray spectra, and not from the outermost layer as in optical spectra. Hence only the normal non-ionised atom is taken to be the standard zero state. We can adopt this procedure also for optical spectra. If we adopt this procedure for hydrogen, the energy of the initial state of H_β (orbit 3) is $Rh\ (1/1^2 - 1/3^2)$, energy of the final state (orbit 2) is $Rh\,(1/1^2 - 1/2^2)$. The emitted frequency

$$\nu = \nu_i - \nu_f = R\left(\frac{1}{1^2} - \frac{1}{3^2}\right) - R\left(\frac{1}{1^2} - \frac{1}{2^2}\right)$$
$$= R\left(\frac{1}{2^2} - \frac{1}{3^2}\right)$$

The two treatments, therefore, give identical results.

The difference $\Delta\nu = \nu_{L_2} - \nu_{L_3}$ is, however, halogen-like and not alkali-like. For example, if we take a Cu-atom ionised in the L_2-level, it may be replaced by a F-like core with an outer shell of electrons as shown below :—

Cu ionised in L_2-shell . . . (29) $1s^2\ 2s^2\ 2p^5 \mid 3s^2\ 3p^6\ 3d^{10}\ 4s$
F (normal) . . (9) . . $1s^2\ 2s^2\ 2p^5$ . . . ${}^2P_{\frac{1}{2}} - {}^2P_{\frac{3}{2}} = 410\ \text{cm}^{-1}$ $\Delta\nu/R = \cdot 00374$
Ne^{+} (9) . . $1s^2\ 2s^2\ 2p^5$ . . . $= 782\ \text{cm}^{-1}$ $= \cdot 00712$
Na^{++} (9) . . $1s^2\ 2s^2\ 2p^5$ . . . $= 1364$ $= \cdot 0124$
Mg^{+3} (9) . . $1s^2\ 2s^2\ 2p^5$ . . . $= 2226$ $= \cdot 0202$
Al^{+4} (9) . . $1s^2\ 2s^2\ 2p^5$ . . . $= 3440$ $= \cdot 0323$

In F, $2p^5\ {}^2P_{\frac{1}{2}} > 2p^5\ {}^2P_{\frac{3}{2}}$, $\Delta\nu = 410\ \text{cm}^{-1}$. This difference* increases with atomic number, *i.e.*, with, the central charge. For the X-ray region, $\Delta\nu$ is much larger, because the central charge is so large.

---

* These data are due to Söderqvist, *Zs. f. Phys.*, **76**, 317, 759, 1932.

The above considerations enable us to fix up the theoretical methods for finding the X-ray term-values for any atom. Let us, first of all, take the problem of calculation of ν_K, *i.e.*, the energy required to eject one electron from the K-level. This electron normally moves in a field which may be supposed to be composed of three fields: (1) that due to the central charge (+ *Ze*), (2) the field due to the companion electron, (3) and the field due to the shell of electrons outside of the K-shell. If the force due to the outer electrons could be neglected, the problem is reduced to the helium problem (*vide* Chap. XII). We have two electrons in the shell with $n = 1$, $k = 1$, moving round a nucleus with the charge (+*Ze*). The companion electron in the K-shell should be treated separately, as this being in the same quantum orbit, produces the phenomenon of *exchange resonance* as in the case of helium. These considerations receive support when we survey the σ_K-values, σ_K being defined as in §235, p. 459, for all elements from U 92 downwards up to 2 He. This is shown in column 2, 6 of the following table 4, and the accompanying curve in Fig. 17.

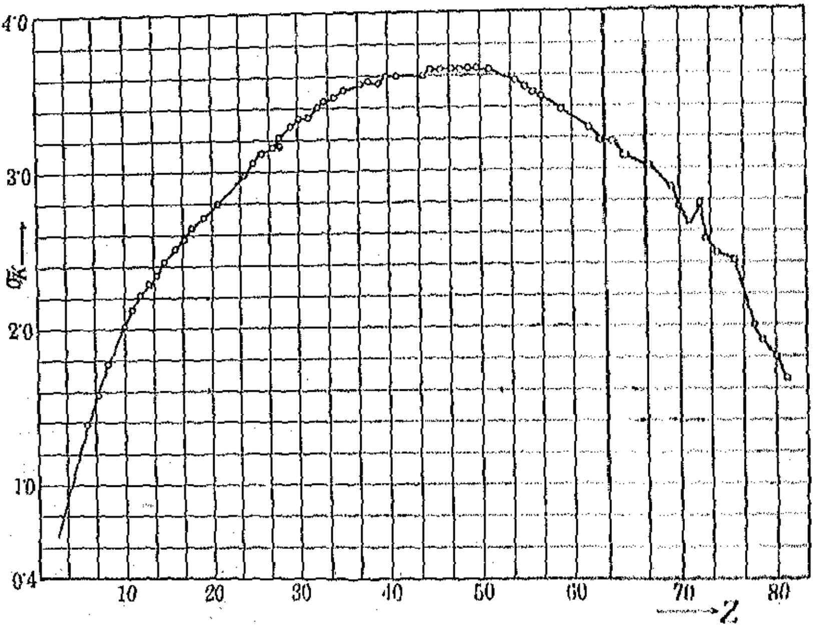

Fig. 17. Variation of screening constants for K-level of elements with atomic number.

NOTES: Strictly speaking the regular K-spectrum of elements stops with Ne, as below Ne the L-shells are not complete. However

Table 4.—σ-Values of K and L-levels.

Element	σ_K	σ_{L_1}	σ_{L_2}	Element	σ_K	σ_{L_1}	σ_{L_2}
92 U	−0·05	11·94	13·44	40 Zr	3·59	12·68	13·92
90 Th	+0·07	12·38	13·86	39 Y	3·56	12·48	13·70
83 Bi	1·34	13·52	14·96	38 Sr	3·56	12·48	13·70
82 Pb	1·51	13·64	15·08	37 Rb	3·54	12·34	13·58
81 Tl	1·63	13·76	15·20	35 Br	3·49	...	...
79 Au	1·92	13·98	15·40	34 Se	3·47	...	...
78 Pt	2·03	14·08	15·50	33 As	3·44	11·78	13·00
77 Ir	2·13	14·14	15·54	32 Ge	3·41	...	...
74 W	2·45	14·30	15·70	31 Ga	3·33	...	...
73 Ta	2·51	14·32	15·70	30 Zn	3·32	11·20	12·44
72 Hf	2·61	14·34	15·72	29 Cu	3·28	11·00	12·24
71 Cp	2·66	14·40	15·78	28 Ni	3·22	10·70	11·94
70 Ad	2·80	14·40	15·76	27 Co	3·17	...	...
68 Er	2·94	14·40	15·74	26 Fe	3·11	10·18	11·42
67 Ho	3·00	14·38	15·74	25 Mn	3·05	...	11·10
66 Dy	3·06	14·36	15·70	24 Cr	3·00	...	10·88
65 Tb	3·11	14·34	15·68	23 Va	2·93	...	10·60
64 Gd	3·17	14·32	15·62	22 Ti	2·87	...	10·34
63 Eu	3·23	14·28	15·60	21 Sc	2·80	...	10·00
62 Sm	3·25	14·24	15·58	20 Ca	2·75	...	9·84
60 Nd	3·35	14·16	15·48	19 K	2·70	...	9·68
59 Pr	3·39	14·12	15·42	18 A	2·65	...	...
58 Ce	3·43	14·04	15·36	17 Cl	2·58	...	9·38
57 La	3·46	14·04	15·30	16 S	2·51	...	9·08
56 Ba	3·49	13·98	15·28	15 P	2·44	...	8·86
55 Cs	3·52	14·00	15·26	14 Si	2·36	.	8·61
53 I	3·58	13·90	15·18,	13 Al	2·29	...	8·368
52 Te	3·59	13·80	15·10	12 Mg	2·20	...	8·08
51 Sb	3·59	13·76	15·04	11 Na	2·25	...	...
50 Sn	3·64	13·82	15·08	10 Ne	...	...	...
49 In	3·64	13·72	14·98	9 F	1·804	4·68 *	...
48 Cd	3·64	13·62	14·86	8 O	1·76	4·16	...
47 Ag	3·33	13·42	14·68	7 N	1·60	...	...
46 Pd	3·64	13·36	14·64	6 C	1·46	2·78	...
45 Rh	3·65	13·24	14·48	5 B	1·116	2·30	...
44 Ru	3·64	13·16	14·42	4 Be	1·048 *	...	...
42 Mo	3·62	12·92	14·16	3 Li	0·853	...	...
41 Nb	3·60	12·80	14·04	2 He	0·657	...	...

by using X-ray methods, a number of semi-optical lines have been obtained for lower elements in positions predicted for Kα-lines. They do not show the doublet structure and become increasingly diffuse as we take lower elements. In the case of Be the breadth of the lines is about 15 Å. units as can be seen from Siegbahn's microphotogram reproduced in Fig. 19. The nature of the line also varies considerably with the physical states as well as its states of chemical combination. But it is clear that the radiation is due to the ejection of an electron from the K-shell, and the subsequent filling of this level by a semi-optical electron. We are therefore justified in talking of K-radiations of these elements. This subject will be fully discussed later in § 240 in connection with the spectroscopy of soft X-rays.

---

* The σ_K-values for Be, Li, He and σ_{L_1}-values for 9 F to 5 B are from electron bombardment experiments (see tables 5 and 7). The other data are computed from table 2. The σ_{L_1}-values for Ni, Cu and As are from Thoræu's measurement of $K\beta_3$ (*vide* § 239).

It is also clear that the element He may be supposed to be the first giving the K-spectrum, as it is the first element to have its K-shell complete. Hence ν_K for He may be taken to correspond to the ionisation potential of He, *viz.*, 24·45 volts. The curve for σ_K shows that it is continuous up to He. This is in support of the method proposed for calculating ν_K -limits theoretically from atomic models.

From an inspection of the (σ_K, Z) diagram it is found that the curve is parabolic, with kinks at places where a shell is beginning to be completed and a new shell is beginning to be formed. As for example for 20 Ca, $\sigma = 2{\cdot}78$, while for 21 Sc, $\sigma = 2{\cdot}80$. In Sc the $3d$ shell is beginning to be formed. It is quite probable that some of these values require revision.

The value of σ becomes approximately constant for 37 Rb to 56 Ba (within 3·54 to 3·64) and this gave rise formally to the belief that σ_K is constant for all elements. The belief was strengthened from a calculation of σ by Sommerfeld from entirely different considerations (§238)which gave almost the same result. But beyond Ba, σ_K begins to diminish, and for 92U, σ_K actually becomes negative, *i.e.*, there is negative screening. No explanation has yet been forthcoming for this paradoxical result. σ can be roughly represented by the formulae

$$\sigma_K = {\cdot}895 + {\cdot}124\,Z - {\cdot}0014\,Z^2 \;\ldots\ldots\ldots\; \text{up to } Z = 20$$
$$\sigma_K = {\cdot}895 + {\cdot}124\,(Z-1) - {\cdot}0014\,(Z-1)^2 \;\ldots\; \text{between } Z = 20 \text{ to } 92.$$

237. Calculation of ν_K.—According to the ideas developed, ν_K should be calculated from the wave-mechanical equation :

$$\nabla_1^2\psi + \nabla_2^2\psi + \frac{8\pi^2 m}{h^2}\left[W + \frac{Ze^2}{r_1} + \frac{Ze^2}{r_2} - \frac{e^2}{r_{12}} + V\right]\psi = 0.$$

where $\nabla_1^2 = \left(\frac{\partial^2}{\partial x_1^2} + \frac{\partial^2}{\partial y_1^2} + \frac{\partial^2}{\partial z_1^2}\right)$, and $(x_1\ y_1\ z_1)$

are the coordinates of one K-electron, ∇_2^2 is the same operator for the second K-electron, r_1, r_2 are the distances of the electrons from the nucleus, W = total energy, r_{12} = mutual distance between the electrons, V = potential due to the outer shells.

If $V = 0$, the equation reduces to the He-problem which was first formulated by Heisenberg,* and numerical formulae for calculation of W were given by Hylleras and Kellner.† The value of V may be represented by formulae of the type

$$V = \sum \frac{e^2}{r_{L_1}} + \sum \frac{e^2}{r_{L_2}}$$

where the summation extends over electrons composing the shells L_1, L_2 .... and r_{L_1}, r_{L_2} ... are the radii of the shells.

The value of V has not yet been calculated, but it can be shown, that it contributes substantially to the 'screening.' For if we omit V in the wave-mechanical equation we get the value of W by using the formula for He-like ions given by Hylleras:

$$E_1/Rh = Z^2 - [Z + \cdot 31488 - \cdot 01752/Z + \cdot 00548/z^2]$$

$$E_2/Rh = (Z + 1)^2 \quad . \quad . \quad . \quad . \quad . \quad . \quad . \quad . \quad . \quad . \quad . \quad . \quad . \quad (4)$$

where E_1 = energy of the first electron, and E_2 = that of the second electron.

This formula (4) is in agreement with values of I. P.'s of atoms stripped to the He-core as recently determined by Edlén‡ (*vide* columns 2 and 3 of table 5).

In this table the figures in the 2nd column give us the ionisation potentials of elements stripped to the He-core as experimentally determined by Edlén, the 3rd column gives us the values calculated from (4), the 4th column gives the corresponding ν/R values. σ is obtained from the relation $\nu/R = (Z - \sigma)^2$. It is seen that σ tends to take the limiting value ·655. So the contribution of the companion electron in the K-shell to screening may be taken to be ·655. The remaining part of screening is certainly due to the outer shells of electrons. The 6th and 7th columns show the ν_K / R

---

* Heisenberg, *Zs. f. Phys.*, 39, 499, 1926.
† Hylleras and Kellner, *Zs. f. Phys.*, 54, 737, 1929 ; 65, 209, 1931.
‡ Edlén, *Zs. f. Phys.*, 84, 746, 1933.
§ ν/R-values are calculated on the basis of R = 13·54 volts.

Table 5.—σ-values for atoms stripped to He-core.

Element	I. P. of Stripped atom (volts)		ν/R (Equ. 4)	σ	ν_K/R	σ_K
	Exp. (Edlén)	Theor. (Equ. 4)				
2 He	24·465	24·45	1·81	·655	1·8 [*]	0·657
3 Li+	75·256	75·272	5·56	·642	4·61	0·853
4 Be+2	153·108	153·09	11·30	·637	8·71	1·048
5 B+3	258·028	258·0	19·05	·634	14·2 [†]	1·116
6 C+4	390·018	390·0	28·81	·632	20·6	1·46
7 N+5	549·081				29·3	1·60
8 O+6	735·218				39·0	1·76
9 F+7					50·5	1·894
10 Ne+8						

and σ_K values taken from table 2, and we find that the energy of ejection has now fallen down considerably. Taking C we find that $\nu_K/R = 20·6$, whereas ν/R for the stripped atom is 28·81, and $\sigma_K - \sigma = ·828$, *i.e.*, the four electrons which in the gaseous state has the combination $2s^2\ 2p^2$ now produce the screening ·828. As the outer shells become filled up, $\sigma_K - \sigma$ rapidly increases as expected, and ultimately reaches a steady value, after which σ_K diminishes rapidly, and actually reaches a negative value for U. The physical cause of this negative screening is yet unknown.

238. The Regular Doublet Law.—The explanation of the empirical relation known as the regular doublet law was first attempted by Sommerfeld,[‡] and is merely an adoptation of the methods evolved for explaining the doublet separation in the spectrum of H or better the spectra of alkali elements (*vide* Chap. X).

---

[*] Skinner's data from critical potential: K-excitation potential of He, Li, Be are 24·37, 62·5 and 118 volts respectively. Skinner, Be: *Proc. Roy. Soc. A*, **140**, 277, 1933; Li: *ibid.* **135**, 84, 1932; He: *Nature*, Feb. 6, 1932.

[†] Holweck's data (from absorption).

[‡] A. Sommerfeld, *Atombau und Spektrallinien* (1924), Kap. 6, p. 442.

But the explanation is theoretically not satisfactory, because though in the $L_2 - L_3$ difference we have to deal with a doublet p-difference, the terms arise not from the presence of one electron outside the closed shells as in the case of the alkali elements, but from the defect of one electron to a completed $2p$-shell. The X-ray doublet difference should therefore be linked with the $2p^5 \ldots ({}^2P_{\frac{3}{2}} - {}^2P_{\frac{1}{2}})$ difference of fluorine-like atoms. But this problem has not yet been theoretically solved. In the absence of such treatments we give an outline of Sommerfeld's theory.

According to this, the doublet separation for two terms having same n, l but having their $j = l + \frac{1}{2}$ and $l - \frac{1}{2}$ is given by

$$\Delta\nu/R = \frac{\alpha^2 (Z-\sigma_2)^4}{n^3} \cdot \frac{2l+1}{2l\,(l+\frac{1}{2})\,(l+1)}$$

Here we are assuming that the screening is σ_2. When $l=1$ and $n = 2$, the above formula reduces to

$$\Delta\nu/R = \frac{\alpha^2\ (Z-\sigma_2)^4}{2^4}$$

Sommerfeld first assumed a value of 3·5 uniformly for σ_2. If this were correct we should obtain a consistent value of $\alpha^2/2^4$ from the observed doublet difference, and this should equal $\cdot 332 \times 10^{-5}$ as obtained in §176. But this was found to be far from being the case, as table 6 shows. We find that the value of the constant differs from $\cdot 35 \times 10^{-5}$ for Ca to $\cdot 446 \times 10^{-5}$ for Th. It has been explained by several investigators by taking the second order terms in α^2. But in view of the fact that the theoretical basis is unsatisfactory an account of these works are not given. The reader may consult p. 325 of Siegbahn's *X-rays*. The problem of calculation of energy values of electrons in different shells is

Table 6.

Element.	$\Delta \frac{\nu_L}{R}$	$\frac{\alpha^2}{2^4} = \Delta \frac{\nu_L}{R} \frac{1}{(Z-3\cdot5)^4} . 10^5$
20 Ca	0·26	0·35
25 Mn	0·82	0·38
30 Zn	1·70	0·345
35 Br	3·30	0·344
40 Zr	6·11	0·344
45 Rh	10·53	0·355
50 Sn	16·83	0·360
55 Cs	25·69	0·365
60 Nd	37·93	0·372
65 Tb	54·27	0·379
70 Ad	76·07	0·389
75 Re	104·97	0·402
80 Hg	141·18	0·412
90 Th	249·03	0·446

therefore an open one, and may be attempted in years to come with the aid of the methods developed by Hartree and Fermi* (method self-consistent fields).

239. The Term Values of L_1 and L_2-levels.—*The* ν_{L_1}-*values.* The values of the L -levels from absorption are known up to 37 Rb. The corresponding σ_{L_1}-values are calculated from the relation $\sqrt{\nu_{L_1}/R} = (Z-\sigma_{L_1})/2$ and shown in column 6 of table 7. For other elements, the absorption limit has not yet been obtained, but we can determine ν_{L_1} from the relation

$$\nu_{L_1} = \nu_{\beta_3} + \nu_K - \nu_{K\beta}$$

In this way ν_L has been calculated for 26 Fe, 28 Ni, 29 Cu, and 33 As from Thoræus' measurement of $L\beta_3$. The σ_{L_1}-values thus obtained are shown in column 7, table 4. The σ_{L_1}'s are plotted against the atomic number in the lower curve of Fig. 18. A few other ν_{L_1}-values for elements below 26 Fe may be calculated roughly by a number of indirect methods, *e.g.*, from the empirical relation given by Hertz and Sommerfeld

$$\sqrt{L_1} - \sqrt{L_2} = \text{const.} = {\cdot}64$$

as has been done by Stoner,† or by the method of electron bombardment. Data for 9 F to 5 B in column 6 of table 7 are obtained by the latter method.

As ν_{L_1} measures the energy of ejection of the electron from the L_1-shell, the problem of determining ν_{L_1} may be started from that of Beryllium-like atoms which have the structure $1s^2\ 2s^2$. We have therefore added in table 7 the experimentally determined values of the I. P.'s of atoms stripped to the Be-shell, *viz.*, of Be, B^+, C^{+2} . . . . The corresponding screening constants are shown in column 4. It can be seen that σ_L-values in column 6 tend in the limit to σ for Be. It is found that the I. P. of atoms stripped to the Be-core can be represented by the empirical formula

$$E = (Z-2{\cdot}34)^2 + {\cdot}427 - \frac{2{\cdot}61}{(Z-2{\cdot}34)} + \frac{3{\cdot}25}{(Z-2{\cdot}34)^2}$$

---

* Fermi., *Zs. f. Phys.*, **48**, 72, 1928 ; **49**, 550, 1928.

† Stoner, *Phil. Mag.*, **2**, 97, 1926.

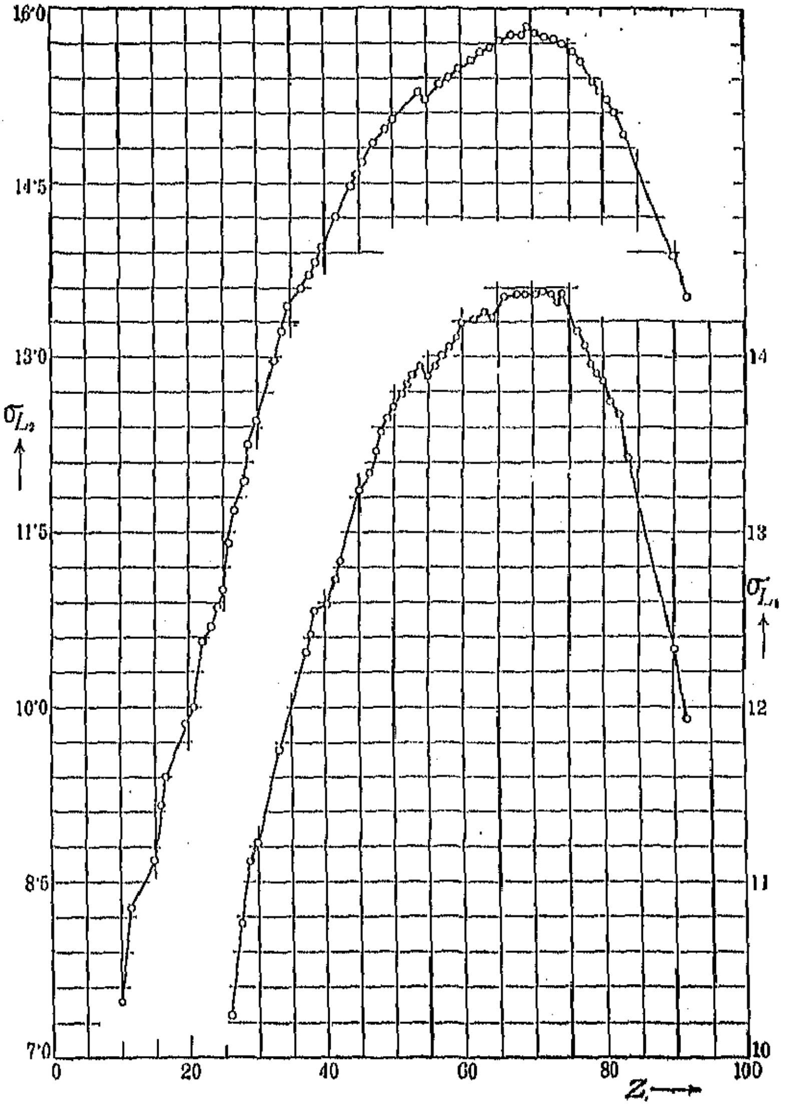

Fig. 18. ($\sigma - Z$) curves for L_1 and L_2-levels.

The values of σ_{L_2}, calculated according to the formula

$$\sqrt{\nu_{L_2}/R} = (Z - \sigma_{L_2})/2$$

are shown in columns 4 and 8 of table 4, and the variation of σ_{L_2} values with atomic number is shown in the upper curve of Fig. 18.

Table 7.

Element	I. P. (volts) of stripped atom	ν/R	σ	ν_{L_1}/R	σ_{L_1}
4 Be	9·276	·685	2·345	...	...
5 B+	24·998	1·846	2·28	1·82 *	2·30
6 C++	47·637	3·518	2·248	2·6	2·78
7 N^{+3}	77·038	5·69	2·229	...	
8 O^{+4}	113·298	8·367	2·215	3·69	4·16

The σ_{L_1}*-levels.* The L_2 and L_3-absorption levels have been given in Table 2 up to 12 Mg, and a few of them are also shown in column 5 of table 8.

Table 8.

Element	I. P. of stripped atom	ν/R	σ	ν_{L_2}/R	σ_{L_2}
10 Ne	21·49	1·59	7·48	...	...
11 Na+	46·78	3·455	7·28	...	...
12 Mg++	80·91	5·976	7·112	3·642	8·08
13 Al^{+3}	121·77	8·993	7·018	5·364	8·368
14 Si^{+4}	168·72	12·473	6·940	7·261	8·61
15 P^{+5}	221·9	16·38	6·978	9·4	8·86

As ν_{L_2}, ν_{L_3} indicate the energy of ejecting an electron from the $2p^6$-shell, the starting point for the calculation of the σ_{L_2}-values should be the neon-like atom. This has not yet been attempted. In table 8 we have given the I. P. of atoms ionised to the Ne-like core as far as known, and the calculated values of screening constants are shown in column 4. It is seen at once that σ_{L_2}-values in column 6 tend in the limit to σ for Ne. The σ_{L_2}-values are roughly represented by the empirical formula

$$\sigma = 7{\cdot}728 + {\cdot}277\,(Z-10) - {\cdot}00231\,(Z-10)^2 - {\cdot}000001\,(Z-10)^3$$

The I. P. of atoms stripped to the Ne-core can be represented by the empirical formula

$$E = (Z-6{\cdot}746)^2 + 1{\cdot}917 - \frac{42{\cdot}8}{(Z-6{\cdot}745)} + \frac{70{\cdot}165}{(Z-6{\cdot}745)^2}$$

---

* Data from electron bombardment method.

240. Soft X-Rays.—A few years ago practically nothing was known about the region between 10 Å. U. and 500 Å. U. This was almost entirely due to the lack of proper technique. The rays are too long for crystals and too short for optical gratings as usually used. Further the rays are completely absorbed by air. In fact before 1924, the softest X-rays photographed were the Lα-line of Cu (13·3 Å. U.) and Kα of Na (11·88 Å. U.). On the optical side, Lyman* and Fricke had carried the measurement of He-lines to Ca λ 500 Å. U. though this was rapidly surpassed by Millikan and Bowen† who, in their investigation, reached as low a wavelength as 40 Å. U.

In 1924, Thoraeus‡ and Dauvillier§ used crystals of palmitic and melissic acids, having the grating constants $d = 27$ Å. U. and 73 Å. U. and photographed the L-series of Va (24·2 Å. U.), and K-series of O (23·28 Å. U.). As the crystals were rather imperfect, the lines obtained were broad and diffuse.

Great advance in technique was however made by Thibaud‖ in 1927 who used plane gratings at a grazing angle of incidence, and he succeeded in recording the Kα-line of B (68 Å. U.). At this stage, the investigation was taken up by many workers, including Siegbahn and his pupils a description of whose apparatus has been given in §§143 and 144.

241. Survey of Results.—Our knowledge of spectra of elements in this region is at present growing very rapidly. Roughly speaking, investigations in this region give us the data for those parts of the Bohr-Coster curves where they begin to get irregular, *e.g.*, for the K-spectrum below Na, or the L-spectrum below Ca . . . etc.

THE K-SPECTRUM FROM 11 NA TO 3 LI

As mentioned on page 464, the K-spectrum is regular only up to 11 Na; for elements of lower atomic weight, the $2p$-shell is not complete, and the lines are not sharp. The lines are therefore increasingly diffuse, and the wavelength depends also on the state of chemical combination. The older results may be taken to have been superseded by those of Siegbahn* and his pupils who used the concave grating as described on page 277 and got much sharper lines. As a typical example we take the Kα-line of Be. The line is about 15 Å. units wide, has a sharp beginning on the short wavelength side at 110·95 Å. U., and a microphotometer curve shows a number of subsidiary peaks as represented in Fig. 10. The analysis of the peaks is shown in the figure, as well as in the scheme below. Similar peaks have also been found in the microphotogram of the Kα-line of C by Prins.† He takes these peaks to be satellites to the main line C Kα at λ 44·31Å.U. and their positions are given below :—

---

* Lyman, *Astr. Jour.*, **60**, 1, 1924.
† Millikan and Bowen, *Phys. Rev.*, **23**, 1, 1923.
‡ Thoraeus, *Phil. Mag.*, **1**, 312, 1926; **2**, 1007, 1927.
§ Dauvillier, *Journ. de Physique*, **8**, 1, 1927.
‖ Thibaud, *Phys. Zeit.*, **29**, 9, 241, 1927.

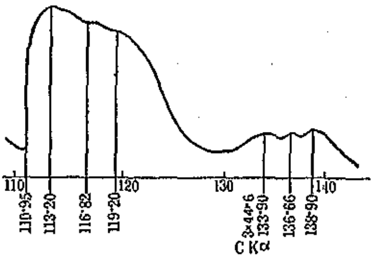

Fig. 10. Microphotogram of Be Kα-line.

	Kα	Kα′	Kα″		Observer
6 C . . .	44·31	43·67	43·28	Å. Units	Prins

	edge	Max. 1	Max. 2	Max. 3		
4 Be . .	110·95	113·2	116·8	119·2	Å. U.	Siegbahn

The K-lines increasingly become sharper as elements of higher atomic weights are taken.

The K-absorption edges of C, N, and O were first obtained by Thibaud‡ in 1927. Recently Siegbahn§ has devised a new method in which a copper arc is used as the source of continuous radiation. The copper arc does not actually give a continuous spectrum, but is so rich in lines that it can be regarded as giving continuous light. On using a foil of Al as an absorber, a sharp cut was obtained at λ170·5 Å. U. This corresponds to the L_2-absorption edge of Al. The method is very promising and further results are awaited with interest.

Very recently O'Bryan and Skinner‖ have investigated the K-emission spectrum of Li, Be, B, C, and L-emission spectrum of

---

* Siegbahn, *Zs. f. Phys.*, **87**, 1934.
† Prins, *Zs. f. Phys.*, **81**, 507, 1933.
‡ Thibaud, *loc. cit.*
§ Siegbahn, *Proc. Phys. Soc.*, 1933.
‖ H. M. O'Bryan, H. W. Skinner, *Phys. Rev.*, **45**, 370, 1934.

Na, Mg, Al, Si by using a 2-metre curved grating, and have obtained results (band heads and peaks) similar to those of Siegbahn. Their results for Li, and those for other light elements due to Siegbahn and Magnusson are quoted in the table below:

Table 9.—K-emission lines and edges for light elements.

Element	λ (Å. U.)	ν/R	$\sqrt{\nu/R}$	Remarks
11 Na	11·88	76·91	8·76	λ corresponds to line
9 F	18·27	50·0	7·07	
8 O	23·61	38·55	6·20	
7 N	31·59	28·90	5·38	
6 C	43·74			λ corresponds to band head
5 B	66·2	13·79	3·71	
4 Be	110·95	8·21	2·86	
3 Li	225·3	4·04	2·01	

THE L-SERIES LINES

In the L-region Siegbahn and Thoraeus obtained the L-series lines up to vanadium (23). In the case of iron β_6 ($L_1 \leftarrow M_{2,3}$), η($L_2 \leftarrow M_1$), β_1 ($L_2 \leftarrow M_4$), l ($L_3 \leftarrow M_1$), $\alpha_{1,2}$ ($L_3 \leftarrow M_{4,5}$) have been observed. In the case of vanadium only the α and β lines could be detected. With the advent of grating spectroscopy Kellström* and Howe† pushed the results up to Ca (20).‡ The $L\beta$ line has not been observed after Mn, and $L\alpha$-lines after Ca. The reason is that these lines are due to transitions ($L_{2,3} \rightarrow M_{4,5}$) and the ($M_4$, M_5)-group disappears after calcium and so no transition can take place. The l and η lines persist up to phosphorus (15) as proved by Siegbahn and Magnusson after which the L-spectrum becomes a band with a structure depending on the chemical combination of the element.

A list of the L-series lines for elements Cu to S is given in tables at the end of the chapter. When sulphur as a sulphate was used, the l and η lines could be resolved, but with pure sulphur they could not be resolved. *l*, η lines could be resolved up to Fe, but in recent researches by Siegbahn they appear separated up to S.

---

* Kellström, *Zs. f. Phys.*, 58, 511, 1929.

† Howe, *Phys. Rev.*, 35, 717, 1930.

‡ It is doubtful whether the $L\alpha$-line of Ca is at all obtained, for Howe does not report it, but Kellström's results show a fairly strong line.

With phosphorus the *l*-line becomes a band with a sharp edge at 91·15 Å. U. and two maxima at 96·3 and 97·9 Å. U. In the case of Si, Al, Mg the L-series lines are very interesting. The line group forms a band with a sharp limit on the short wave side. It has been suggested by Siegbahn that the sharp edge is due to transition from a conduction electron level. In order to test this point he took two photograms, in one of which metallic aluminium was taken and in the other alumina. Aluminium is a good conductor, while alumina is not. The spectrograms were found to be entirely different. The alumina spectrum was more or less similar to P, containing two maxima, at 184·0 Å. U. and 198·60 Å. U. In Fig. 20 the dotted line is the microphotograph of alumina spectrum, while the continuous line is that due to aluminium. In the latter the maxima are not evident, but there is a sharp edge at 170·49 Å. In this case transitions are taking place between the vacated K-shell and conduction

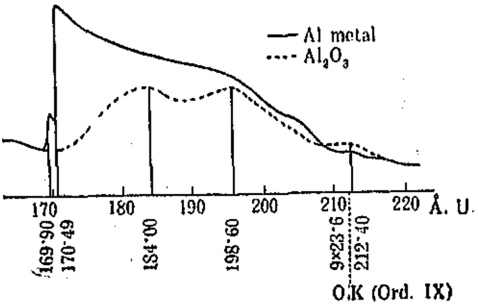

Fig. 20. Microphotograms of the L-lines of Al. [—— From Aluminium, - - - From alumina.]

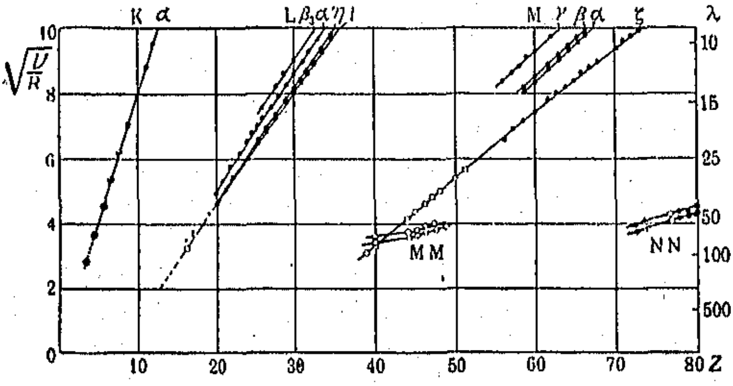

Fig. 21. Moseley diagram for K, L, M, N-series lines of elements.

The dotted extension of K and L η*l*-lines corresponds to band emission. ● K-series: Thibaud, Söderman; L-series: Kellström; M-series: Lindberg N-series Magnusson. ○Prins and Takens. × Siegbahn.

(Sommerfeld-Fermi) electron levels, and consequently the regular L-emission is masked. In the case of alumina there are few of these electrons and so it has a different structure. The Moseley curves of the $L\alpha$ and Ll, η lines have been shown in Fig. 31 due to Prins and Takens. The level value of M_1-shell can be obtained from the energy of the l, η lines and those of $L_{2,3}$-shells. These values have been incorporated in table 2.

THE L-ABSORPTION SPECTRUM.

The L-absorption spectrum has been obtained by the crystal method up to 37 Rb (L_1 = 5·985 Å. U.) by Coster and Mulder.[*] Prins and Takens[†] have worked with Cu, Ti, and Ca and their values are given in table 10 for $L_{2,3}$ shells.

Table 10.—L_2, L_3-absorption limits.

Element	λ	ν/R	$\sqrt{\nu/R}$
29 Cu	12·9	70·7	8·41
22 Ti	27·29	33·41	5·78
20 Ca	33·63	25·59	5·09

The absorption edge depends upon the chemical state of the absorber, but still these values are in good accord with the values of $L_{2,3}$ shells found from K-absorption and K-series lines. Siegbahn has introduced a new method of studying the absorption spectrum which has already been described. His results are illustrated in the table 11.

Table 11.—$L_{2,3}$-absorption edge of Si, Ag, Mg.

Element	λ	ν/R	$\sqrt{\nu/R}$
14 Si ... L_3	125·5	7·26	2·69
13 Al ... L_2	169·90	5·364	2·316
L_3	170·47	5·346	2·312
12 Mg ... L_3	250·20	3·642	1·91

THE M SERIES.

Using the crystal method, Lindberg[‡] extended the M-series to Ce (58). But he found that only γ ($M_3 \leftarrow N_5$), β ($M_4 \leftarrow N_{6,7}$), α_1($M_5 \leftarrow N_{6,7}$) continue up to that element using the line grating. Thibaud[§] found that the $M\gamma$, $M\zeta$ ($M_{4,5} \leftarrow N_{2,3}$) persist up to Mo. Prins and Takens[‖] have obtained the $M\zeta$ lines of elements Y(39) to Sb (51). The tables at the end of the chapter give his results.

---

[*] Coster and Mulder, *Zs. f. Phys.*, **38**, 264, 1926.

[†] Prins and Takens, *Zs. f. Phys.*, **84**, 65, 1933.

[‡] Lindberg, *Dissertation, Uppsala University*, 1931.

[§] Thibaud, *loc. cit.*

[‖] Prins and Takens, *Zs. f. Phys.*, **75**, 741, 1932; **77**, 705, 1932.

In a recent paper Siegbahn and Magnusson* have considerably extended the results, and have found Mηl lines corresponding to ($M_{3,3} \leftarrow N_1$) transitions for the elements 35 Br to 47 Ag. The Mζ ($M_{4,5} \leftarrow N_{2,3}$) lines were separated into their components for 35 Br to 37 Rb. Between 37 Rb—40 Zr, the ($M_{4,5} \leftarrow N_{2,3}$) lines merge into one, and after that all the three lines become single as reported by Prins and Takens.†

The strongest line is due to Mζ ($M_{4,5} \leftarrow N_{2,3}$) and M$\eta l$-lines persist from 35 Br to 48 Pd after which it has not been found. The most important feature of the M-series lines from the theoretical point of view are the *lines which originate from the transitions within M-levels themselves.* We shall discuss them under the N-series, because there also similar lines have been obtained. The MM-lines obtained by Prins and Takens and by Siegbahn and Magnusson are listed in Table 12.

Table 12.—MM-lines for elements 35 Br to 50 Sn (λ in Å. U.)

Element	$M_2 \leftarrow M_4$	$M_3 \leftarrow M_{4,5}$	Element	$M_2 \leftarrow M_4$	$M_3 \leftarrow M_{4,5}$
35 Br	109·41	113·8	44 Ru	62·21	68·34
37 Rb	91·51	96·71	45 Rh	59·3	65·6
38 Sr	85·93	91·38	46 Pd	56·38	62·83
39 Y	81·5	86·5	47 Ag	54·1	60·6
40 Zr	76·6	81·71	48 Cd	...	58·8
41 Nb	72·13	78·21	50 Sn	47·3	54·15
42 Mo	68·8	74·7			

	$M_1 \leftarrow M_3$	$M_1 \leftarrow M_2$
35 Br	144·41	156·1
37 Rb	144·41	...

The transitions $M_1 \leftarrow M_3$, $M_1 \leftarrow M_2$ have been obtained only for 35 Br and 37 Rb. In Fig. 31 the Moseley curve for the M-lines including MM transition-lines has been shown.

As is usual in the case of very soft X-rays, the structure of the lines depends on the state of the target, and its crystalline structure. In the case of some elements Siegbahn and Magnusson‡ have obtained bands with sharp edge on the short-wave side, and with a maximum. They ascribe these bands to transition from conduction electron levels, and denoted them as Y_1 and Y_2. The positions of the maximum (λ in Å. U.) are shown in table 13.

---

* Siegbahn and Magnusson, *Zs. f. Phys.*, 88, 589, 1934.

† Prins and Takens, *loc. cit.*

‡ Siegbahn and Magnusson, *loc. cit.*

Table 13.—M-emission bands.

Element	$M_{4,5}-Y_1$	$M_{4,5}-Y_2$
38 Sr	96·37	
40 Zr	75·0	70·4
41 Nb	67·81	61·76
42 Mo	59·81	55·3
44 Ru	48·95	44·76
45 Rh		40·78
46 Pd	40·44	37·35
47 Ag	36·83	

THE N-SERIES.

The N-series lines were first discovered by Doljsek* in 1922, but the results were in doubt, till Thibaud's work confirmed them. He showed that in the N-series mostly the inter-level transitions ($N_{4,5} \leftarrow N_{6,7}$) are obtained. This has been verified by various workers† for elements of higher atomic number, 73 Ta to 81 Tl. Siegbahn and Magnusson (*loc. cit.*) have extended these measurements for 71 Cp to 55 Co.

In Cs and Ba there are three regular N-lines close together, the energy of which corresponds to transitions ($N_{4,5} \leftarrow O_{2,3}$). In the spectrogram the lines are resolved. It is likely that these lines do not come out after I, for in the plate containing Cs spectrum there is no line due to I, although CsI was taken as the target. The O_2, O_3-levels just begin to be filled up at I (53). There is no evidence of inter-level transitions for these elements.

In the table at the end of the chapter, the wavelength of all these regular N-lines for Cs 55 to Bi 83 are given.

For the rare earths from 57 La to 71 Cp, the N-lines have an interesting structure. They are in the form of bands having peaks. The peaks have been identified to be due to ($N_{4,5} \leftarrow O_{2,3}$)-transitions, and also the inter-level transitions ($N_{4,5} \leftarrow N_{6,7}$).

The Moseley diagram is shown in Fig. 31.

Siegbahn and Magnusson (*loc. cit.*) have also experimented upon 81 Tl, 82 Pb, 83 Bi, 90 Th and 92 U, and they find that ($N_{6,7} \leftarrow O_{4,5}$) have been resolved, and have sufficient intensity; but the lines ($N_{4,5} \leftarrow O_{2,3}$) are not present.

---

* Doljsek, *Zs. f. Phys.*, **10**, 129, 1922.

† Thibaud, del Rosario, Prins and Takens, Magnusson, *Zs. f. Phys.*, **79**, 161, 1932; Chalklin, *Phil. Mag.*, **16**, 363, 1933.

In tables at the end of the chapter all the N-lines are shown. For full Moseley diagrams of M, MN, N and NN-lines see Siegbahn and Magnusson's latest paper (*loc. cit.*).

In the N-spectra of heavy elements, the lines $N_4 \leftarrow N_6$ and $N_5 \leftarrow N_{6,7}$ have been obtained by a number of workers. The transition in these cases also takes place in the levels with the same total quantum number. In table 14 Magnusson's results supplemented by other data are given.

Such lines in which $\Delta n = 0$ are very common in optical spectra and it is surprising that they are not so common in X-ray region.

Table 14.—Lines due to NN-transitions (λ in A. U.)

Element	$N_4 \leftarrow N_6$	$N_5 \leftarrow N_{6,7}$	Element	$N_4 \leftarrow N_6$	$N_5 \leftarrow N_{6,7}$
59 Pr	109·34	113·27	74 W	55·8	58·50
60 Nd	102·67	108·7	76 Os	51·8	54·6
62 Sa	95·7	98·4	77 Ir	50·1	52·8
63 Eu	...	...	78 Pt	48·0	50·9
65 Tb	...	86·76	79 Au	46·8	49·4
66 Dy	...	83·34	80 Hg	43·6	61·4*
68 Er	72·7	76·3	81 Tl	...	46·35
70 Ad	65·1	69·4	82 Pb	42·25	44·95
71 Cp	62·99	65·70	83 Bi		
73 Ta	58·1	61·0			

241-a. Probability of Inter-transition in the L-shells.—Coster†, Saha and Mukherjee‡ tried to observe the $L_1 - L_3$ transition in the case of heavy elements like W. In this case although the excitation voltage corresponds to that of the L_1-shell, yet the wavelength of the $L_1 - L_3$ transition will be long, about 6·8 Å. units for W. It was suggested that the energy of the $L_1 - L_3$ transitions is just greater than some of the outer M-shells, and so it is internally absorbed. Take the example of W. For this element we have

	L_1	L_3	$L_1 - L_3$	M_1	M_2	M_3	M_4	
74W	890·8	751·3	139·5	207·3	189·3	167·5	137·5	. . (ν/R)

---

* Rosario, *Phys. Rev.*, **41**, 136, 1932. Values for Tl and Pb are from Siegbahn and Magnusson's latest paper (*loc. cit.*). The other data are due to Magnusson.

† Coster, *Phil. Mag.*, **43**, 1070, 1922.

‡ Saha and Mukherjee, *Nature*, **133**, 377, 1934.

Thus $L_1 - L_3$ difference just exceeds the value of M_4. This state of affairs stops at about 68 Er. For this element we have

	L_1	L_3	$L_1 - L_3$	M_1	M_2	M_3	M_4	M_5	
68 Er	718·5	615·9	102·6	163·6	147·7	133·6	107·3	104·4	. . (ν/R)

We thus see that here $L_1 - L_3$ is smaller than any of the M-levels. So it was suggested that for this and other similar elements, $L_1 - L_3$ lines should be observed. But this has not yet been experimentally verified. O'Bryan and Skinner (*loc. cit.*) recently reports that in the L-bands of Si, Al, Mg, the $L_1 - L_3$ transitions are very likely present. But they are not definite, for the transitions of conduction electrons mask them. These lines fall in the optical region. For the MM- and NN-transitions the energy of the rays is less than that of the outer N and O shells. So they are not absorbed.

O-series.—Siegbahn and Magnusson find a broad band for thorium at λ 174·2 Å. U. which may be due to transition from conduction electron levels. One of the peaks inside this band corresponds to the transition to O levels, and the value of the $O_{4,5}$ level thus found agrees well with the values found from N-series data. The earlier results of Thibaud are doubtful.

242. Investigation of the Inner Energy Levels of Atoms by means of Magnetic Spectra of Secondary Electrons.—Mention was made on page 206 of Sagnac and Dorn's discovery that when a metal plate is irradiated by X-rays, secondary electrons possessing large velocities are emitted in addition to characteristic and scattered X-radiation. Many methods were tried to measure accurately the energy of these secondary electrons. The following may be noted :—

1. By subjecting the electrons to a known magnetic field, and measuring the curvature of the orbits. This method generally known as the *magnetic spectrum method* was first tried by Dorn.

2. By finding out the retarding potential which would stop the emission of electrons. This was tried by Laub.*

3. By measuring the absorption coefficient of electrons in known gases.

Of these methods, the first alone has survived. The apparatus of Dorn was successively improved by De Broglie,†

---

* Laub, *Ann. d. Phys.*, **26**, 712, 1908.

† De Broglie, *Jour de Physique*, **2**, 265, 1921.

Whiddington,* Rutherford and Robinson.† In this chapter, we shall describe the apparatus used by Robinson (Fig. 19).

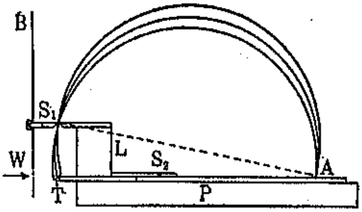

Fig. 22. Robinson's Apparatus.

The apparatus‡ is a modification of De Broglie's original design and differs from it in certain details which aim at reduction of the time of exposure, and sharpening of the spectral lines. It is enclosed completely in a brass box B having an aluminium window W through which X-rays are admitted. L is an L-shaped piece of lead carrying two fine slits (of lead) S_1 and S_2. The target T is so placed that its middle point is vertically below the slit S_1, and in the same horizontal line with the second slit S_2 as shown in Fig. 22. It may be oriented at any angle to the incident beam of X-ray. De Broglie puts it perpendicular to the beam. The photographic plate P is put on L so that it just projects under the slit S_2, which gives us a fiducial point on the plate. When everything is in position, the chamber is evacuated to as high a vacuum as possible, and X-rays passing through W are allowed to fall on T. A uniform magnetic field is applied by means of a pair of Helmholtz-Gaugain coils perpendicular to the plane of the paper. As the magnetic field disturbs the cathode rays of the X-ray tube, Robinson used compensating magnetic fields to nullify the deflection.

The target T must be thin, otherwise the photo-electrons lose part of their velocity in coming through the layer of matter in the target, so that the spectral lines lose their sharpness. In the case of salts, or substances in the form of powder, a thin layer is spread uniformly over a piece of paper.

The photoelectrons are emitted in all possible directions and those possessing the same energy describe a circular path having approximately the same radius and are recorded on the plate P at a certain point A. Since S_1TA is a right angle, it is evident that S_1A is a diameter of the circle. Electrons emitted from either side of T and passing through S_1, but possessing the same energy will hit the plate on either side of A, so that the line will have a finite breadth, depending on the dimensions of that part of T which has been irradiated by X-rays, and the distance S_1 T.

---

* Whiddington, *Phil. Mag.*, **43**, 1116, 1922.

† Robinson and Rawlinson, *Phil. Mag.*, **28**, 277, 1914.

‡ Robinson, *Proc. Roy. Soc. A*, **104**, 455, 1923.

243. Calculation of the Energy of the Electrons.

—By adjusting these dimensions the lines can be made fairly sharp. The velocity v of those electrons which have been recorded at A can be found from the relation

$$v = \frac{e}{mc} H. R. \quad . \quad . \quad . \quad . \quad . \quad . \quad . \quad . \quad . \quad . \quad (5)$$

where R is the radius of the path described by the electrons having the same energy, and H is the strength of the field in absolute units. H is measured by the ordinary electrical means of search coil and flux-meter. The radius of curvature R is obtained from the geometry of the apparatus in the following way.

After the exposure for recording electrons is finished, a fine beam of light is focussed on the slit S_2 through a system of lenses fixed to the chamber B vertically above S_2. This fine beam of light leaves a fiducial mark on the photographic plate, so that its position with respect to the apparatus is known. It is evident from the figure that S_1A is the diameter of the circle TS_1A, hence

$$S_1A = 2R$$

In the right-angled triangle S_1TA, the distance TA is

$$TA = TS_2 + S_2A \quad . \quad . \quad . \quad . \quad . \quad . \quad . \quad . \quad . \quad (6)$$

The distance S_2A is the distance of a spectrum line at A from the fiducial point S_2 and is measured on a comparator. TS_2 is the horizontal distance between S_1 and S_2 and is measured by a travelling microscope. Denoting these lengths by x and c, we have

$$4R^2 = a^2 + (c+x)^2 \quad . \quad . \quad . \quad . \quad . \quad . \quad . \quad . \quad (7)$$

where $a = TS_1$, or the vertical distance between S_1 and S_2. The measurement of the plate is made from the centre of the spectrum line.

From (5) and (7) the value of v is at once obtained.

244. Experimental Results.

—It was observed by Laub* and Dorn that the maximum velocity of the secondary electrons was independent of the intensity of the rays, but depended on their hardness. But the mechanism of emission was first clearly elucidated by the experiments of M. De Broglie (*loc. cit.*).

---

* Laub, *loc. cit.*

De Broglie illuminated a Ag-plate with tungsten K-radiation and obtained the magnetic spectrum of secondary electrons in an apparatus which differs from the one described here in only non-essential details. Fig. 23 shows his results.

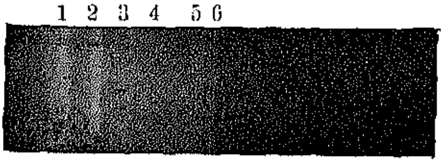

Fig. 23. Magnetic Spectra of Ag ... (*De Broglie*).

It is clear from the photograph that the magnetic spectrum does not consist of a continuous band which would indicate electrons having all velocities from $v = 0$ to $v_{\max}$, but of discrete lines. This shows that a very large proportion of electrons corresponding to any particular line have definite and identical velocities. For example—the energies ε_4, ε_5, ε_6 of the electrons giving rise to lines 4, 5 and 6 as determined by the formula in §243, was found to satisfy exactly the following relation :—

4. $\varepsilon_4 = h\nu_{K\alpha_2} - h\nu_K$ of Ag.
5. $\varepsilon_5 = h\nu_{K\alpha_1} - h\nu_K$ of Ag.
6. $\varepsilon_6 = h\nu_{K\beta} - h\nu_K$ of Ag.

These relations at once give us the mechanism of secondary emission. The monochromatic X-radiations, $K\alpha_1$ and $K\alpha_2$ of tungsten falling on Ag-atoms cause the ejection of electrons from the K-shell of Ag in accordance with Einstein's photoelectric equation, *i.e.*, as a photon of energy $h\nu_{K\alpha_1}$ or $h\nu_{K\alpha_2}$ falls on any of the K-electron in Ag-atom, the latter absorbs the whole energy; a part $h\nu_K$ is spent in releasing the electron from the K-shell, the remainder is converted to the kinetic energy of the electron.

It is clear that the magnetic spectrum apparatus provides us with an independent method for determining the energy-levels of electrons in all atoms. When a photon of sufficient energy (the $K\alpha$-line of some element) is allowed to traverse an atom, it will release electrons from all levels, and we should have lines in the magnetic spectrum having frequencies

$$\nu-\nu_K,\ \nu-\nu_{L},\ \nu-\nu_{L_2},\quad \nu-\nu_{L_3},\ \ldots\ldots,\ \nu-M\ \ldots\ \text{etc.}$$

These deductions have been verified in the extensive experiments of Robinson* and his co-workers. If the frequency of the exciting radiation be too soft for any energy-level, no electron will be ejected from that level, but electrons may be ejected from outer levels. Thus Ag Kα, $\nu/R = 1632{\cdot}7$ cannot eject any electron from U K-shell (ν_K/R of U = 8477), but it can release electrons from the L_1 ($\nu_{L_1}/R = 1603$) and all outer shells.

245. Fluorescent Emission.—In addition to lines which can be interpreted as due to photoelectric effect in the inner layers, De Broglie† got other lines for which a different origin had to be found. They are shown as 1, 2 and 3 in Fig. 23. De Broglie observed that

1. $\varepsilon_1 = \nu/R$ of Ag $K\alpha_1$ − ν/R of Ag L-level.
2. $\varepsilon_2 = \nu/R$ of Ag $K\beta_1$ − ν/R of Ag L-level.
3. $\varepsilon_3 = \nu/R$ of Ag $K\beta$ − ν/R of Ag M-level.

These relations afford the key to the origin of the lines. They are due to the ejection of electrons from L-levels of the Ag-atom by the K-radiation of Ag. This K-radiation of Ag is however only secondary, and it owes its origin to the fact that as the primary W $K\alpha,\alpha'$ releases an electron from the K-shell of Ag, another electron falls immediately from the $L_{2,3}$ or some higher level to the K-level, and thus gives rise to fluorescent K-radiation of Ag. But this K-radiation, in coming out of the atom, may hit electrons in any of the outer L or M-shells, and release them giving rise to a secondary group of electrons. This phenomenon is known as *internal conversion.*

246. Investigation of Internal Conversion in Wilson-Chamber (Auger-effect).—The internal conversion of fluorescent radiation was studied by Auger‡ in the Wilson chamber and therefore it is sometimes known after him (*Auger effect*). The Wilson chamber was filled with krypton strongly diluted with hydrogen. Monochromatic X-rays possessing energy equal to 14, 20, 28 and 60 KV were successively passed through the chamber. The photographs of the secondary electrons released from krypton atoms were taken in the usual way. The fluorescent Kα-line of krypton has an energy equal to 14 KV and the electron in the L_2-shell has the energy 2 KV, so that when the fluorescent Kα-line of krypton, produced by the primary X-radiation releases an electron from the L_2-shell by internal conversion, the electron will have the energy 12 KV. This corresponds to a length of the track equal to 12 mm on the original plate and 24 mm. in the reproduction. In Fig. 24 (*a*), we observe the tracks of these electrons alone, because the electron released from the K-shell of krypton by the incident radiation has very little energy. In the next photograph (*b*) corresponding to 20 kilovolts we observe the same fluorescent electron tracks of same length, but in addition we also observe shorter tracks due to release of an electron from the K-shell directly (energy=6 KV). Further the two tracks sometimes diverge from the same point as we should expect from the mechanism. The same pair of tracks are observed in the Figs. 24(*c*) and (*d*) for 28 and 60 kilovolts respectively. They start from the same point and one has the length characteristic of the electron produced by internal conversion, while the other track due to the electron

---

* Robinson and Young, *Proc. Roy. Soc. A.*, **128**, 92, 1930.

† De Broglie, *loc. cit.*

‡ P. Auger. *Ann. de Physique*, **6**, 234, 1926.

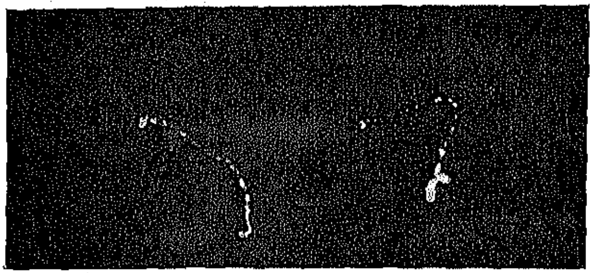
14 K. volts

Fig. 24 (*a*). Auger effect in krypton.

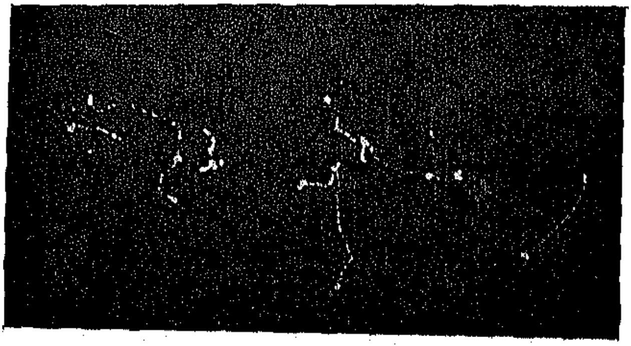
20 K. volts

Fig. 24 (*b*)

released from the K-shell by the primary ray seems to be much longer.

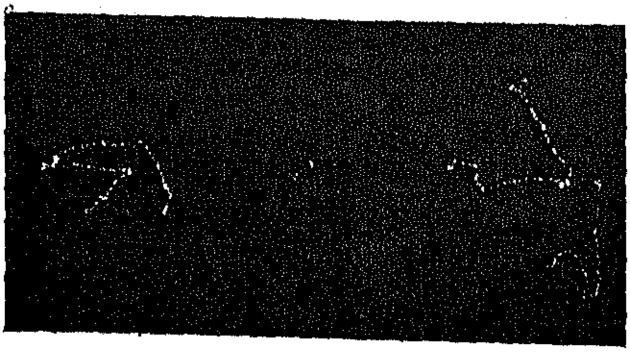

28 K. volts

Fig. 24(c)

246a. Calculation of Energy Levels from β-ray Spectrum.— It was however found that values of the energy levels obtained from the magnetic spectrum of these fluorescent electrons are somewhat different from the values as determined by the methods of X-ray spectroscopy. This point is illustrated in the following example due to Robinson and Cassie.* Mo Kα-line (ν/R=1287·8) was allowed to fall on a Cu-target, and the magnetic spectrum of the secondary electrons was obtained in the usual way. A number of lines shown in table 15 could be interpreted as being due to internal conversion of fluorescent Cu K-radiation excited by molybdenum Kα-line, but the energy values of the Cu-levels (column 3) are found to be sensibly different from the values obtained by spectroscopic methods (*vide* column 4).

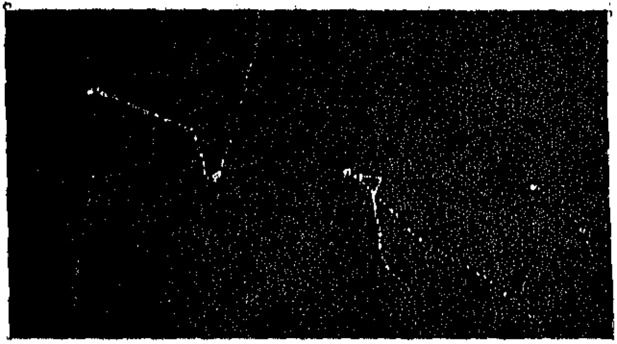

60 K. volts

Fig. 24 (d)

---

* Robinson and Cassie, *Proc. Roy. Soc. A.*, 113, 282, 1927.

Table 15.—$L_{1,2}$-levels of Cu calculated from internal conversion.

Line ν/R	Interpretation	Energy level (calculated)	Actual value
506·9	592·8 (ν/R of Cu $K\alpha_1$) − 85·9	L_1 = 85·9	L = 80·5
519·3	" " −73·5	L_2 = 73·5	$L_{2,3}$ = 68·8
572·4	655·9 (ν/R of Cu $K\beta$) − 83·5	L_1 − 83·5	L_1 = 80·5

Thus when the fluorescent $K\alpha$-radiation of Cu in passing through the extra nuclear electrons releases an electron from the L_1-level, it requires the energy ν/R=85·9 which is near to, but somewhat greater than, the value 80·5 obtained for the L_1-level of copper from direct absorption experiments. When the fluorescent $K\beta$ of Cu in passing through electron shells releases the same electron, the energy required is found to be ν/R=83·5. Similar anomaly is observed in the case of electrons released from the L_2 and L_3-levels.

But the same authors showed that when the Cu K-radiations from an X-ray tube are directly used to irradiate a Cu-plate, the energy required to release the electrons from the various shells are found to have quite normal values, as shown in the following table :

Table 16.

Line ν/R	Interpretation	Energy level	Actual value
512·3	592·8 (ν/R of Cu $K\alpha_1$) − 80·5	L_1 = 80·5	L_1 = 80·5
524·3	" " −68·5	$L_{2,3}$ = 68·5	$L_{2,3}$ = 68·8

These results were explained by Robinson and Cassie in the following way. When a photon of suitable energy is allowed to traverse a normal atom, the energy spent for releasing an electron from any shell is of course equal to the normal energy of binding of the electron in the shell. But the case is different when a fluorescent line, say $K\alpha$ traverses the shells of extra-nuclear electrons. Now the atom is not normal but ionised, as it has already lost one electron from the L_2-shell. Hence the energy of binding in the L_1 or the L_2-shell is increased, because now the external screening due to the

L_2-shell diminishes. This explains the results in a general way, but a quantitative treatment of the results is still awaited.

The nature of secondary electron emission being understood in a general way, the activity at the present time in this line has turned on quantitative experiments. Before giving a description of these works, we describe the results of one typical experiment due to Robinson on secondary emission from gold when illuminated by Ag K-radiation.

The silver radiation consists of the following lines:—

Ag $K\alpha_1$ . . . . $\nu/R = 1632{\cdot}3$,
Ag $K\alpha_2$ . . . . $\nu/R = 1619{\cdot}6$,
Ag $K\beta_1$ . . . . $\nu/R = 1837{\cdot}2$,
Ag $K\beta_2$ . . . . $\nu/R = 1875{\cdot}0$,

In the following table is shown the energy of photo-electrons ejected by these rays from a gold-plate, and the interpretation of the results.

Table 17.—Primary β-ray spectrum of gold irradiated by Ag K-radiation.

Incident radiation / Energy absorbed	Ag $K\alpha_1$ 1632·3	Ag $K\alpha_2$ 1619·6	Ag $K\beta_1$ 1837·2	Ag $K\beta_2$ 1875·0
$L_1 = 1060{\cdot}2$	*572·1* 577·5	*559·4* 564·1	*777·0* 782·8	
$L_2 = 1014{\cdot}4$	*617·9* 622·5	*605·2* 619·0	*822·8* 827·9	*860·6* 862·1
$L_3 = 878{\cdot}5$	*753·8* 755·4	*741·1* 743·6	*958·7* 961·8	*996·5* 1000·5
$M_1 = 252{\cdot}9$	*1379·4* 1386·0	*1366·7* 1372·0		
$M_2 = 235{\cdot}1$	*1397·2* 1404·2			
$M_3 = 202{\cdot}8$	*1429·5* 1434·2	*1416·8* 1421·9	*1634·4* 1637·2	*1707·0* 1714·0
$M_4 = 169{\cdot}3$	*1463·0* 1472·8		*1667·9* 1676·2	

The figures in italics are the actual values of the energy of the electrons as calculated from spectroscopic data, *e.g.*, Ag $K\alpha_1 - L_1 =$

1632·3 − 1060·2 = 572·1. The other value (577·5) is the observed value. The difference between the two values is small, and can be ascribed to breadth of the lines and other experimental errors.

The relative intensity of lines in the β-ray spectrum has been studied by Robinson. For this see his original paper (*loc. cit.*).

247. Space Distribution of Photo-electrons.—Early workers on the phenomena of photo-electricity discovered that when a thin metal foil is irradiated by means of ultra-violet light, the photo-electrons are emitted in all possible directions, but there was a great preponderance of them in the forward than in the backward direction with respect to the incident rays. Similar observation was made by Cooksey[*] in the case of photo-electrons emitted by matter irradiated by X-rays.

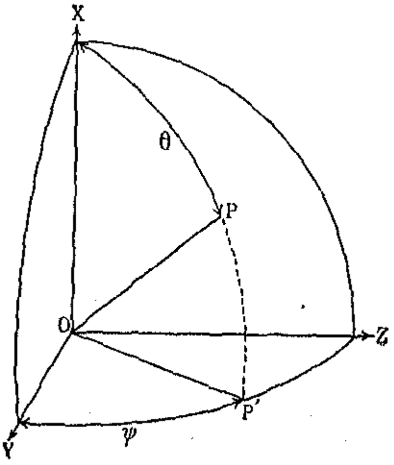

Fig. 25.

It was found that the space distribution of photo-electrons depended on the nature of the secondary target, the frequency of the primary rays and their state of polarisation. According to classical theory, the ejected electrons should lie in the plane perpendicular to the direction of the rays, because the electric vector may be anywhere in this plane when the rays are unpolarised. For polarised rays, the electrons should be ejected parallel to the electric vector. These rules are generally true, but still it has to be explained why the photo-electrons are emitted in other directions at all. The space distribution has been chiefly studied by the following three methods :—

(1) Geiger Counter method (Bothe).

(2) Wilson Cloud Chamber (Kirchner, Bubb, Auger & Perrin, and William, Nuttall and Barlow).

(3) By the β-ray spectrum method (Watson and Akker).

---

[*] Cooksey, *Phil. Mag.*, 24, 37, 1912.

Out of the above workers, Kirchner and Bubb used polarised X-rays, *i.e.*, X-rays scattered by a paraffin block. In the case of polarised X-rays, the lateral distribution is studied, while for unpolarised rays longitudinal distribution is studied. In Fig. 25, OX is the direction of the incident beam, OY is its electric vector. If any photo-electron is driven in the direction OP, then ψ is the *lateral* angle and θ the *longitudinal* angle.

248. Experiments and Results.—(1) *Longitudinal distribution: Bothe's* Method.* The principle of this method is illustrated in Fig. 26. The rays are allowed to pass into a chamber K filled with a gas whose photo-electric emission is studied. The lower half of the chamber contains the Geiger counter Z, which can be moved on a semicircle around the centre F. The photo-electrons enter through the slit M and are received in the counter. By changing the angle θ, the emission in different directions can be studied. The curve (Fig. 27) below shows his results with $CHCl_3$ in polar co-ordinates. There is a marked assymmetry in the position of the direction of maximum emission. It does not lie in the direction of the electric vector. The reason will be explained in the next section, but a brief idea may be given. The quantum of X-rays gives the electron a forward impulse equal to $h\nu/c$. The space distribution follows the $\sin^2\theta$-law but with a forward component. William and Nuttall† repeated the same observation by using a cloud chamber. They obtained results similar to Bothe's and are illustrated in curve Fig. 28. It has been found that the value of this forward component depends upon the hardness of incident X-rays and the absorption frequency of the shell from which the electron is ejected.

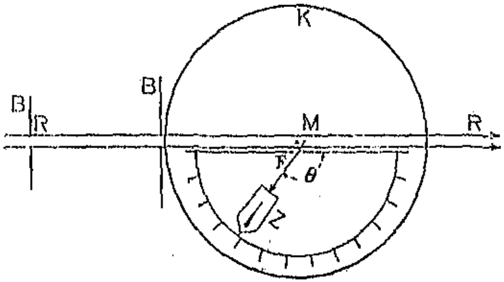

Fig. 26. Bothe's apparatus.

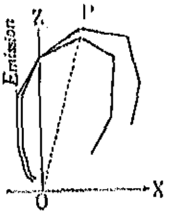

Fig. 27. Assymmetric distribution of photo-electrons in space (*Bothe*).

---

* Bothe, *Zs. f. Phys.*, 26, 59, 1924.

† William and Nuttall, *Proc. Roy. Soc. A*, 121, 611, 1928.

(2) *Lateral distribution.*—The lateral distribution of photoelectrons was investigated by Kirchner* and Bubb† by the cloud chamber method using polarised X-rays. In the lateral distribution no assymmetry has been detected. The distribution more or less follows $\cos^2\psi$-law, and it is independent of the hardness of primary rays as shown in Fig. 29. The maximum emission lies in the plane of polarisation. B is the theoretical distribution ($\cos^2\psi$-law curve) and A is the experimental curve due to Bubb.

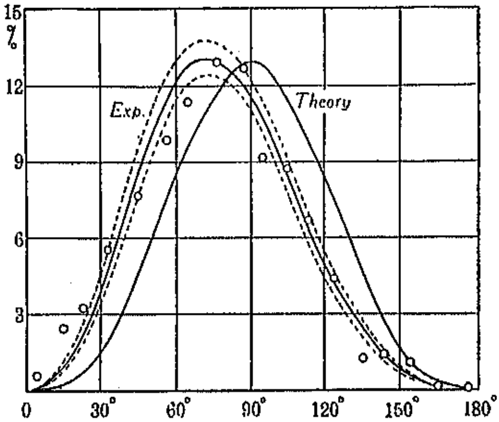

Fig. 28. William and Nuttall's curve. The single curve in thick line is theoretical $\sin^2\theta$-distribution law, and the dotted curve is the experimental curve. It will be seen that the maximum of the experimental curve does not lie at $\theta=90°$, otherwise it is very similar to the theoretical curve.

249. Theoretical Explanation. Auger and Perrin's Theory.

249. Theoretical Explanation. Auger and Perrin's Theory.—Auger and Perrin‡ suggested that when the electrons come out from the levels, their direction of ejection remains the same as the original direction of motion round the nuclei at that instant but the probability of the emission is proportional to $\cos^2\zeta$, where ζ=POY in Fig. 25 is the angle made by the direction of ejection with the electric vectors of the primary rays. In Fig. 25, OP is the direction of ejection and if OP be of unit length it is clear the probability P_ζ of

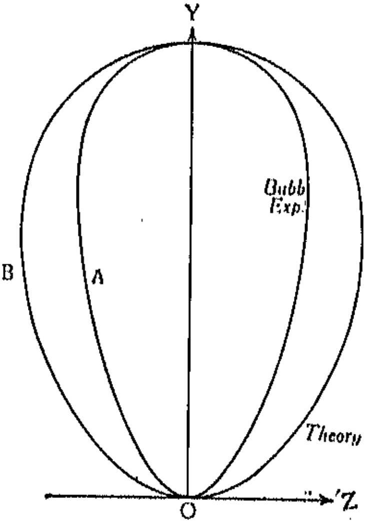

Fig. 29. Lateral distribution of Photoelectrons.

---

* Kirchner, *Phys. Zeits.*, 27, 385, 1926; *Ann. d. Phys.*, 83, 521, 1927.
† Bubb, *Phys. Rev.*, 23, 137, 1924.
‡ Auger and Perrin, *Jour. de. Physique*, 8, 93, 1927.

emission is given by

$$P_\zeta \, d\omega = \cos^2 \zeta \, d\omega,$$

where $d\omega$ is the area of element perpendicular to OP.

But $\cos^2 \zeta = \sin^2 \theta \cos^2 \psi$, $d\omega = \sin \theta \, d\theta \, d\psi$, for ψ is the projection of OP on the plane ZOY, and

$$P_\theta \, d\theta = \frac{\sin^3 \theta \, d\theta \int_0^{2\pi} \cos^2 \psi \, d\psi}{\int_0^{\pi} \sin^3 \theta \, d\theta \int_0^{2\pi} \cos^2 \psi \, d\psi} = \tfrac{3}{4} \sin^3 \theta \, d\theta \quad . \, (8a)$$

and
$$P\psi d\psi = \frac{\cos^2 \psi \, d\psi \int_0^{\pi} \sin^3 \theta \, d\theta}{\int_0^{2\pi} \cos^2 \psi \, d\psi \int_0^{\pi} \sin^3 \theta \, d\theta} = \frac{1}{\pi} \cos^2 \psi \, d\psi \quad . \, (8b)$$

Hence longitudinal space distribution follows the $\sin^3 \theta$-law, while the azimuthal or lateral distribution follows the $\cos^2 \psi$-law according to Auger and Perrin's theory. Generally the $\cos^2 \psi$-law is more or less true in the case of polarised ray as can be seen from Fig. 29, in which A is the experimental curve of Bubb, B is that calculated from the equation (8*b*).

In the case of longitudinal distribution (Fig. 28), there is a marked difference between the experimental and theoretical curves. There is a forward component which cannot be explained by Auger's theory. Sommerfeld and his co-workers worked out the problem on wave-mechanical principles and obtained formulae for distribution similar to those of Auger and Perrin. Mention may be made of Bubb* and Watson's† theory in this connection. In order to explain the spreading of the photo-electrons, Bubb supposed that the electron gets an impulse in the direction of the electric vector, as a forward impulse due to the pressure of radiation $h\nu/c$ which is imposed on the momentum due to the motion of the electron round the nucleus at the time of ejection. His theory however did not fit in with experimental results.

Watson on the other hand refuses to admit that the initial momentum of the electron has anything to do with the space distribution. According to him, the electrons are ejected according to the classical theory as explained in §247, but due to the scattering by the nucleus of the parent atom, the distribution is changed. He applied Rutherford's theory of nuclear scattering of β-particles to this case, and derived expression for the longitudinal as well as for lateral distribution; these agreed with the experimental results.

---

* Watson, *Phys. Rev.*, 34, 547, 1929.
† Bubb, *Phil. Mag.*, 49, 824, 1925.

He came to this conclusion from his work on the distribution of photo-electrons ejected from solids by the β-ray spectrum method, as will be described presently. He found that in the case of a thick target there was uniform distribution. As the target was thinned the selective emission began to take place, as found by other workers.

Early in 1912, Richardson* suggested that the forward component was due to the fact that the quantum imparted not only its energy $h\nu$ but also its momentum $h\nu/c$ on the electron in its direction of motion. If θ_o be angle made by the direction of maximum emission with the direction of X-rays

$$\cos\theta_o = \frac{h\nu}{c}\Big/ mv.$$

where v is the velocity of the emitted electron. Thus the forward component should depend on the frequency of the primary rays as well as on velocity of the emitted electron, which amounts to a dependence on the absorption frequency of the level from which the electron was ejected. This was found actually to be the case.

But it was also found that the forward component as given by Richardson was smaller than that found experimentally, when the frequency of the X-rays was very much larger than absorption frequency of the level of the ejected electron. Sommerfeld† suggested from wave-mechanical principles, that

$$\cos\theta_o = \frac{2v}{c} = 2\beta.$$

while according to Richardson

$$\cos\theta_o = \frac{h\nu}{c}\Big/ mv = \frac{1}{2}\,\frac{mv^2}{c}\,\frac{1}{mv} = \frac{\beta}{2}$$

neglecting the binding energy of the photoelectron.

---

* Richardson, *Phil. Mag.*, 46, 721, 1912.

† *Vide* Sommerfeld, *Wave Mechanics* (1930), Chap. 2, p. 184. Sommerfeld's theory gives for the K-electron a distribution

$$I_{(\theta\psi)} \sim \left[\,1 + \frac{16\pi}{\lambda}\,\frac{k\cos\theta}{k^2 + \dfrac{Z^2}{a^2}}\,\right]\sin^2\theta\,\cos^2\psi$$

where $k = \dfrac{2\pi m}{h}v$, and $a = \dfrac{h^2}{4\pi^2 m e^2}$

William and Nuttall's* values seem to strengthen Sommerfeld's theory.

Watson and Akker utilised the magnetic spectrum method of De Broglie-Robinson to find out the emission in different directions of electrons of various velocities. In their first apparatus,† they used photographic recording, but as it could not give an accurate ratio of the number of electrons of different velocities, they used the Geiger-counter instead. Their final apparatus‡ is briefly described below (Fig. 30).

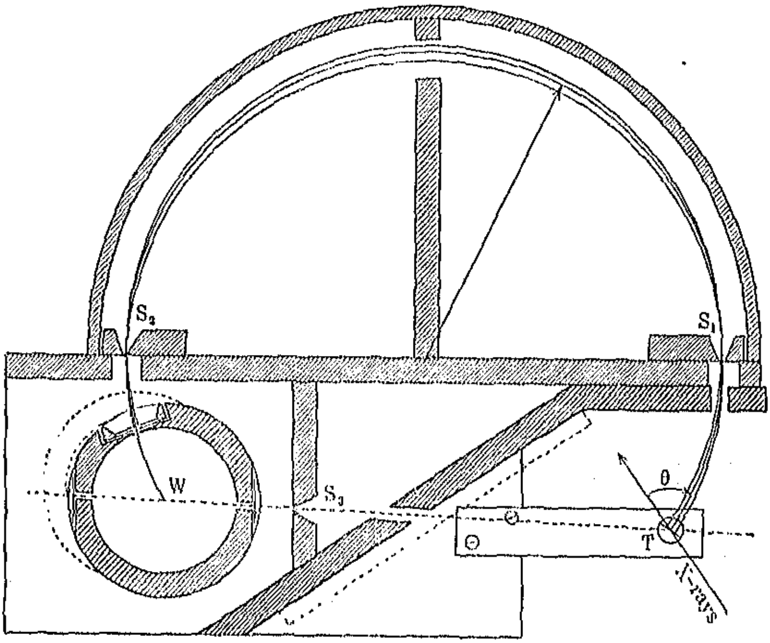

Fig. 30. Watson and Akker's apparatus.

The target T sends out electrons when it is irradiated by X-rays as

---

The maximum is found by differentiating the above distribution. We thus get

$$\theta_{\max} = \frac{\pi}{2} - \frac{8\pi}{\lambda} \cdot \frac{k}{k^2 + \dfrac{Z^2}{a^2}}$$

Hence the maximum will shift towards forward direction as the wavelength decreases. From the above relation after some work we can arrive at the form $\cos\theta_0 = 2\beta$.

* William and Nuttall, *loc. cit.*

† Watson and Akker, *Phys. Rev.*, **30**, 479, 1927; *Proc. Roy. Soc. A*, **126**, 138, 1929.

‡ Watson and Akker, *Phys. Rev.*, **37**, 1637, 1931.

shown in Fig. 30. The electrons ejected normally from the target are made to pass through slits S_1 and S_2 by means of a magnetic field, and are received in the Geiger-counter W. The slit S_3 is for setting the counter by direct photoelectrons from the target. The whole apparatus can be rotated about T, so that θ can be varied. The target is an exceedingly thin piece of celluloid over which the substance is deposited by sputtering. For further details see original papers. By altering the magnetic field electrons of different velocities can be recorded by the counter.

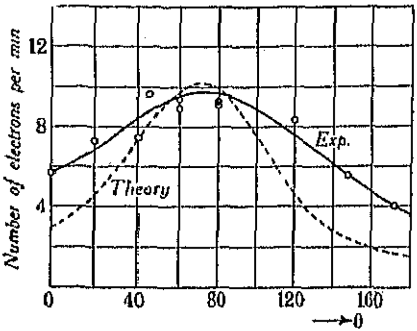

Fig. 31. Curve showing the longitudinal distribution of photoelectrons (*Watson and Akker*).

Watson and Akker used gold as the source of electrons and Mo Kα as primary rays. The distribution of L_3-electrons with the longitude θ is shown here in Fig. 31.

The maximum is a little forward of $\theta = 90°$, the same as observed by others. The dotted line is theoretical curve due to the wave-mechanical theory of Sommerfeld and Schur*

$$N_\theta = \left[1 + \frac{4\, I_L}{h\nu} \sin^2\theta + \frac{2v}{c} \cos\theta \left\{ 1 + \left(1 + \frac{11\, I_L}{h\nu} \right) \sin^2\theta \right\} \right]$$

where I_L is the mean energy of binding of $L_{2,3}$ electrons. The agreement is marked near the maxima while at other places there is variance.

With their earlier apparatus they found the following facts:

(1) L_2 and L_3 electrons are emitted more or less uniformly than those from the K and L_1 shells.

(2) The angle of maximum emission is smaller in the case of the L_2 and L_3 electrons than in the case of K and L_1. In other words the average forward momentum of L_2 and L_3 electrons is greater than that of K and L_1 electrons.

(3) The distribution of K and L_1 electrons are the same as those of M_1, and that of M_2 and M_3 the same as L_2 and L_3 respectively.

These results are in conformity with wave-mechanical theory.

---

* Sommerfeld and Schur, *Ann. d. Phys.*, 4, 409, 1930.

250. Absorption of X-rays: Experimental Methods.*— The method of measuring the absorption coefficient of the general X-rays has already been given in Chap. VI. It was mentioned there that absorption coefficient of X-rays for matter varies rapidly with wavelength and so the absorption coefficient of general X-rays tell us very little about the mechanism of absorption. For this purpose it is necessary to know the laws governing the absorption of monochromatic rays by matter.

Bragg and Pierce† were the first to make a systematic study of the absorption coefficient of monochromatic X-rays with different substances. A sketch of their apparatus is shown below (Fig. 32).

X-rays from target T are limited by the slits S_1, S_2 and then allowed to fall on the spectrograph (whose crystal C is only shown). After reflexion the rays enter the ionisation chamber I, so that their intensity is measured when the crystal is set at the proper angle. The crystal allows only monochromatic rays to enter the ionisation chamber. The absorbing material is inserted at A, and the intensity is again measured. The experiment is repeated by keeping the screen at B (in the path of the ray after reflexion). The mean of the intensities with screen at A and at B positions gives us a measure of the absorption. The mass absorption coefficient is calculated from the equation

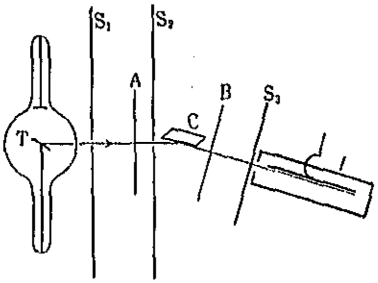

Fig. 32. Bragg and Pierce's apparatus.

$$I = I_0 e^{-\mu d}, \quad \mu_\lambda = \frac{1}{d} \ln \frac{I_0}{I}$$

where I_0 and I have the usual meanings and d is the thickness of the screen.

The intensity of X-rays must not vary during the time of exposure. The thickness of the screen must be uniform. (For other details see Kirchner's *Handbuch der Exp. physik*, **24**, p. 219). The rays entering the ionisation chamber may contain fluorescent and scattered X-rays from the absorber, as well as scattered rays from the crystal. Further, the absorption coefficient of the crystal is different for different wavelengths. Some of these disturbing factors can be eliminated by placing the absorber in different positions and using narrow slits. Siegbahn and Wingardh's* arrangement may be consulted for these details.

---

* A good survey of the experimental work on this subject will be found in Kirchner, *H. d. Exp. physik*, 24/1, Chap. 5, 1930.

† Bragg and Pierce, *Phil. Mag.*, 28, 626, 1914.

The *mass absorption coefficient* is not however the true photo-electric absorption. It includes the *photo-electric absorption coefficient* τ, as well as *absorption due to scattering* σ. Thus

$$\mu/\rho = \tau/\rho + \sigma/\rho$$

σ/ρ is the mass scattering coefficient, as found out in Chap. VI, § 113. σ is generally small compared to τ in the case of rays of long wavelengths and elements of larger atomic number Z, and so in such cases it is generally neglected. In the case of hard X-rays however this cannot be done, for τ and σ are now of the same order of dimensions.

251. Study of Absorption in Long Wave-length Region.—Jönsson† worked in the region from ·7Å to 11Å and obtained very interesting results. His apparatus was of the usual Siegbahn type, and so he used photographic recording. The apparatus was enclosed in a vacuum chamber, and the crystal was rocked by a motor housed inside the chamber. The X-ray tube was of special design which enabled him to use the characteristic lines of many different substances as primary rays.

His original paper may be consulted for these details. For ·7Å, he used Mo Kα-rays. For works in the long wavelength region he used Na Kα (λ 11·8Å). For the intermediate wavelengths he used about 21 substances one after the other in his anticathode. The design of his apparatus was such as to allow him do all these operations quickly.

The reflected beam was allowed to fall on the photographic plate in such a way that its upper part passed through the absorber while the lower part did not. Consequently in a single exposure the intensity of the spectrum line could be recorded, both with and without the absorber in the path. The photographic plate was then microphotographed, and I/I_0 was very easily calculated. The rest of the procedure is as usual.

---

* Siegbahn and Wingardh, *Phys. Zeits.*, 21, 83, 1920; Wingardh, *Diss. Lund.*, 1923.

† Jönsson, *Diss. Uppsala*, 1928.

It must be noted that the blackening of a photographic plate depends not only upon the intensity of rays, but also on the time of exposure. Schwarzschild gave the following relation connecting the blackening, intensity and time of exposure :

$$S = f(I\,t^p)$$

where S is the measured blackening, I is the intensity of X-rays, t the time of exposure and p is a constant which depends upon the particular variety of plate used.

In order to measure the intensity more correctly, Jönsson* devised an arrangement of sectors which allowed the unabsorbed rays to be recorded on the plate for different lengths of time. A B C D is the photographic plate. The arrangement of sectors is shown in Fig. 33. On account of the peculiar forms of the sectors, as they rotate, different parts of the spectral line are exposed for different lengths of time. *a b c d* is the spectrum line, in which *e* is the part not absorbed by the absorber, *d* the part which has passed through the absorber, *a*, *b*, *c* are those parts of the spectrum line which have been exposed for various durations by the sectors.

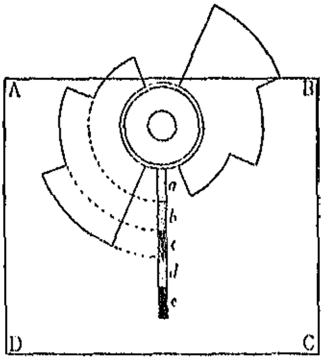

Fig. 33. Jönsson's apparatus.

From a study of the blackening with different lengths of time, the blackening due to intensity alone can be estimated.

252. Review of Experimental Results.—We shall now make a general survey of the experimental results. We shall first discuss how for a definite substance, the absorption coefficient varies with the wavelength. We take the case of Pt. The absorption coefficients of Pt from λ = ·08 Å. units to 9·8 Å. units are shown in the following table. When we plot μ_A and μ/ρ against λ, we get the curves shown in Fig. 34.

---

[*] Jönsson, *Diss. Uppsala*, p. 12, 1928.

Table 18.—Absorption coefficient for Pt.

Pt. Z = 78.

λ	0·081	0·09	0·10	0·15	0·20	0·30	0·40	0·50	0·60	0·631	0·70	0·709	0·80
μ	2·50	2·95	3·7	7·8	4·2	11·5	24·5	45·5	75·2	87·0	107	119	150
					K								L

λ	0·90	1·0	1·09	1·104	1·17	1·293	1·389	1·433	1·529	1·656	1·752	1·787	1·934
μ	169	164	87	81	110	135	152	173	206	228	280	291	354
	L_1	L_2	L_3										

λ	2·00	2·50	2·74	3·02	3·35	3·59	4·14	5·39	6·973	8·319	9·868
μ	408	596	756	939	1120	1370	1290	1640	1190	1530	2440
							M_1				

The curve shows that μ is very small for very hard rays, and gradually rises as the wavelength is increased. A peak value is reached at the point K after which absorption drops to a fraction of the peak-value. This absorption discontinuity occurs at λ = 0·15 A. units, and this is the same as the K-absorption edge of Pt mentioned on p. 439. For when general X-rays pass through Pt and fall on a photographic plate, the rays on the shorter wavelength side of the K-edge will be strongly absorbed, whereas those on the longer side will be

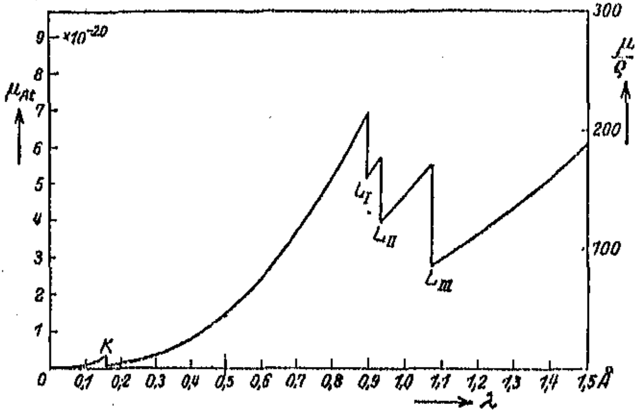

Fig. 84. Absorption coefficient of Pt for different wavelengths.

transmitted more copiously, giving rise on the photographic plate to a discontinuity explained on p. 439.

After we pass the K-discontinuity, μ gradually rises till we come to three further discontinuities lying close together. These are the L_1, L_2 and L_3-absorption edges.

253. Variation of μ with Wavelength λ, and Atomic Number *Z* of the Absorber.

—The act of absorption consists in the photo-electric ejection of the electrons composing the atoms, when the frequency of incident rays is sufficiently large. If $\nu > \nu^K$, X-rays can release electrons from all levels from the K downwards. But when the frequency of X-rays falls just below ν_K, the K-electrons can no longer be ejected. The act of photo-electric ejection is now confined to the outer shells. Hence there is a sudden jump in the value of the absorption coefficient at the K-limit, as shown in Fig. 34.

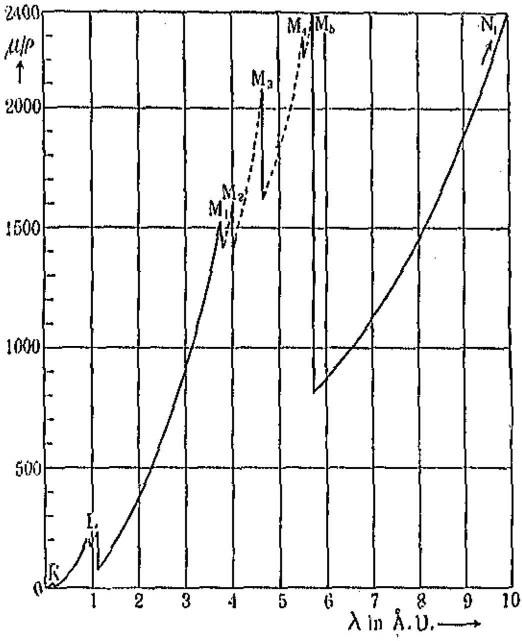

Fig. 35. The M-absorption discontinuities of Pt.

The frequency corresponding to the K-discontinuity is known as the K-absorption frequency, and the potential obtained from the equation $eV = h\nu_K$ is known as the K-ionisation potential.

The L_1, L_2, L_3 and other further discontinuities can be explained in the same way.

Fig. 35 shows the absorption curve of Pt up to 10 Å units. The five M-absorption discontinuities can be easily distinguished in it. These curves give some idea of the variation of τ/ρ with λ. We have besides to find how μ varies with *Z*, the atomic number of the absorber.

For obtaining information on this point we consider the curve in Fig. 36 which shows the variation of μ with Z for a wavelength of 1 Å unit.

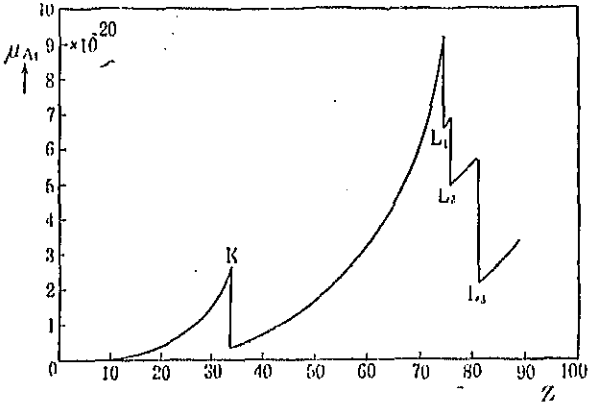

Fig. 36. Absorption coefficient for different elements (λ = 1 Å. U.).

We observe that there is a strong K-absorption up to $Z=34$, after which the pulse of wavelength 1 Å. unit becomes too soft to eject any electron from the K-shell. It should further be noticed that the (λ, μ)-curve is less steeper than the (Z, μ)-curve.

254. Absorption Filters.—It was early recognised that if a beam of X-rays is passed through thin sheets of matter (say aluminium) then not only was the beam absorbed but its spectral composition also changed. In other words, the transmitted beam contained more of harder rays. The reason, of course, is quite clear from the foregoing sections. The absorption coefficient varies as the third power of the wavelength (not near the absorption edge), and so the softer components are absorbed to a much greater extent than the harder ones. This fact has been utilised in separating harder components from softer components in a beam of general X-rays, in short as a method for monochromatising the rays to some extent. The absorbing sheet of matter is known as the *absorption filter.*

There are two methods for studying the phenomenon :—

(1) in which the softer rays are cut down ;
(2) in which the harder rays are cut down.

The first method has already been given in outline, and the second method depends upon the fact that at the absorption discontinuity of a substance the absorption coefficient suddenly increases.

THE FIRST METHOD

In the table below, the half-value thickness in mm. are given for different wavelengths of some substances. Half-value thickness means that thickness of the absorber which will cut down the intensity of the primary rays to half their value. If μ_λ is the absorption coefficient of a substance for a wavelength λ, then the half-value thickness

$$d = \frac{1}{\mu_\lambda} \ln \frac{I_0}{I} = \frac{\ln 2}{\mu_\lambda} \quad . \; . \; . \; . \; . \; . \; . \; . \quad (9)$$

Table 19.—Half-value thickness in mm.*

λ (Å. U.)	0·1	0·2	0·4	0·6	0·8	1·0	1·5	2·0
Air ..	...	...	...	7200	3500	1950	690	330
Water ...	40	33	19·2	9·6	4·8	2·5	0·79	0·34
CO_2 ...	21	17·5	12·5	7·6	4·3	2·4	·82	0·36
Al ...	15	9·8	2·4	0·79	0·35	0·18	0·056	0·024
Cu ...	...	0·51	0·078	0·025	0·011	0·0055	...	...

An inspection of the table will show that for Al the half-value thickness for a wavelength ·4 Å units is 2·4 mm. while for ·6 Å. units it is ·79 mm. So if a filter of aluminium 2·4 mm. in thickness is used, it will cut down the intensity of the ·4 Å unit rays to one-half of their value, but that of ·6 Å units rays to ⅛th. For this can be calculated readily as shown below.

$$x = \frac{1}{\mu} \ln I_0/I = d\,\frac{\ln I_0/I}{\ln 2} \quad . \; . \; . \; . \; . \; . \quad (10)$$

Putting $x = 2{\cdot}4$ mm., $d = 0{\cdot}79$, I_0/I comes out to be 8. By maintaining the voltage across the X-ray tube to a value such that the short wave limit is near ·3 Å. units, an aluminium filter of 2·4 mm. thickness will allow the spectral region between ·3 to ·4 Å.

---

* Adopted from Siegbahn's *Spektroskopie der Röntgenstrahlen*, p. 469.

units to pass, and the softer parts will be mostly absorbed, only a negligible quantity of them will be present in the beam.

The same purpose will be served by using smaller thickness of heavier metals, but aluminium is generally chosen because of its advantageous mechanical properties, and because it does not give rise to fluorescent rays in the harder regions, nor does it contain any absorption discontinuities.

THE SECOND METHOD (SELECTIVE FILTERING)

In many applications of X-rays it becomes necessary to remove harder lines of characteristic rays. For example, in powder photography, out of the $K\alpha$ and $K\beta$ of the primary rays, the $K\beta$ rays have to be removed. If we select a substance whose K-discontinuity occurs somewhere between $K\alpha$ and $K\beta$, then a filter of that substance of suitable thickness will absorb $K\beta$ completely, and $K\alpha$ only slightly. In the table below, selective filters for separating the $K\alpha$ and $K\beta$ lines of various substances are given.

Table 20.—Selective filters for cutting out $K\beta$ and separating $K\alpha$-rays.

Element	Cr	Mn	Fe	Ni	Cu	Zn	Mo	Rh	Pd	Ag	W	Pt
$\lambda K\alpha$ in Å. units	2·29	2·10	1·93	1-66	1·54	1·43	0·709	0·614	0·586	0·560	0·211	0·188
Selective Filter	V	Cr	Mn	CO	Ni	Cu	Zr	Ru	Ru Rh	Rh Pd	Yb Hf	W Os

The selective filter is of the material whose atomic number is one less than that of the element whose $K\beta$ rays are to be filtered out. Similar tables can be made for the L-absorption discontinuities. The thickness of the filter is adjusted by experience. If the filter exists in the powder form it is pressed against a paper by means of gum.*

255. Mathematical Relationship between Absorption Coefficient, Wavelength and Atomic Number (τ, λ, Z).—We shall now deal with the quantitative relation between the absorption

---

*For better methods of filtering see Ross., *Journ. Opt. Soc.*, **16**, 433, 1928; Küstner, *Zs. f. Phys.*, **71**, 324, 1931.

coefficient, the wavelength and the atomic number of the absorber, with the aid of data obtained as a result of the experiments described in the previous section. Early workers gave various empirical mathematical formulæ for expressing the true absorption τ/ρ as a function of Z and λ. Most of these formulæ are of the type

$$\tau/\rho = CZ^n \lambda^m \quad . \quad . \quad . \quad . \quad . \quad . \quad . \quad . \quad . \quad (11)$$

where C is a constant. n was generally taken to lie between 3 and 4, and m between 2·5 and 3. But all these formulæ had only limited applicability. A few of these formulæ are described below:

Bragg and Pierce* . . . . . . $\mu_{At} = CZ^4 \lambda^{5/2}$

for $Z = 13$ to 79, $\lambda = {\cdot}49$ to ${\cdot}61$ Å. units.

Hull and Rice† . . . . $\mu/\rho = C\lambda^3$

where $C = 430$ for Pb, 150 for Cu, 14·9 for Al.

Glocker‡ . . . . $\mu = {\cdot}0004\ Z^{3\cdot14} \lambda^{2\cdot8}$, for $\lambda > \lambda_K$

$= {\cdot}0195\ Z^{2\cdot58} \lambda^{2\cdot8}$, for $\lambda < \lambda_K$

Richtmeyer ‖ . . . . $\tau/\rho = {\cdot}0136.\dfrac{Z^4}{A}\lambda^3$, for $\lambda < \lambda_K$

$\tau/\rho = {\cdot}000529\ \dfrac{Z^{4\cdot3}}{A}\lambda^3$, for $\lambda > \lambda_K$

Attention should be drawn to the point that τ denotes the *real photoelectric absorption*, and is equal to $\mu - \sigma$, where μ is the *absorption coefficient* and σ is the *scattering coefficient.*

From theoretical considerations we find that the total absorption will be a composite quantity made up of the absorption values corresponding to the ejection of photoelectrons from different shells. We can therefore write

$$\tau = \tau_K + \tau_{L_1} + \tau_{L_2} + \tau_{L_3} + \quad . \quad . \quad . \quad . \quad . \quad . \quad . \quad (12)$$

---

* W. H. Bragg and S. E. Pierce, *Phil. Mag.*, **28**, 626, 1914.

† A. W. Hull and M. Rice, *Phys. Rev.*, **8**, 326, 1916.

‡ Glocker, *Phys. Zeits.*, **19**, 66, 1918.

‖ F. K. Richtmyer, *Phys. Rev.*, **18**, 13; 1921, **27**, 1, 1926; **30**, 760, 1927.

For other empirical formulæ proposed by Siegbahn, Kossel, Owen, Hewlett, Duane and Mazumder, Wingardh, Allen (*Phys. Rev.*, **28**, 907, 1926) and others see Kirchner, *loc. cit.*, pp. 238—243.

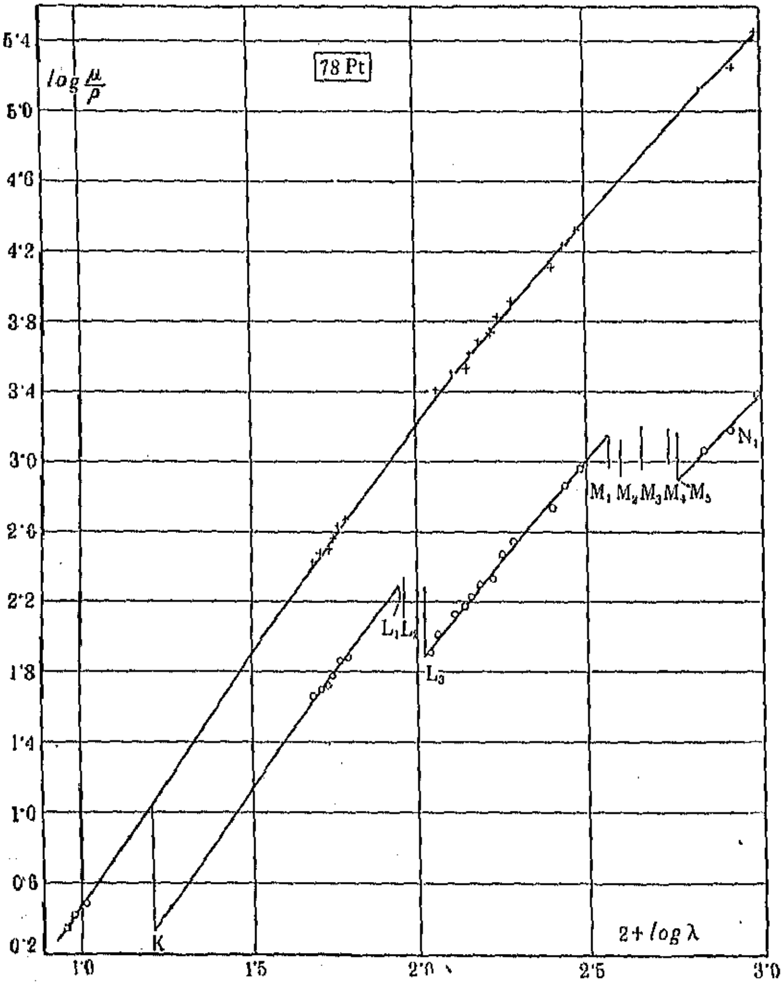

Fig. 87. Variation of mass-absorption coefficient for Pt with wavelength.

where τ_K, τ_{L_1}, τ_{L_2} ..... are absorption coefficients due to ejection of photoelectrons from K, L_1, L_2 and other levels. Now we can write

$$\tau_K/\rho = C_K\lambda^m \;.....\; \text{for } \lambda = 0 \text{ to } \lambda = \lambda_K$$

$$= 0 \;..........\; \text{for } \lambda > \lambda_K$$

$$\tau_{L_1}/\rho = C_{L_1}\lambda^{m'} \;....\; \text{for } \lambda = 0 \text{ to } \lambda = \lambda_{L_1}$$

$$= 0 \;..........\; \text{for } \lambda > \lambda_{L_2}$$

and so on for τ_{L_2}/ρ, τ_{L_3}/ρ, τ_{M_1}/ρ, ... etc., with m'', m''', ... etc., as the powers of λ.

So that the equation (12) can now be written as

$$\tau/\rho = C_K \lambda^{m} + C_{L_1} \lambda^{m'} + \quad . \; . \; . \; . \; . \; . \; . \; . \; . \; . \qquad (13)$$

The equation holds good from $\lambda = 0$ to $\lambda = \lambda_K$. For wavelengths $> \lambda_K$ but $< \lambda_{L_1}$, the first term is to be omitted.

Regarding the power of λ for different levels, Jönsson[†] obtained results of great value which show that this index is almost the same for all the levels. For illustrating this point we show the curve which represents relation between $\log \tau/\rho$ and $\log \lambda$ in Fig. 37.

We find that the curve consists of a set of parallel straight lines limited between the discontinuities ($\lambda_{K_1}, \lambda_{L_1} \ldots .$). Since experiment proves that the straight lines are strictly parallel to each other, it is clear that the index has got the same value for each part of the curve. Jönsson found it equal to 3 in all cases, which is also in accord with the quantum theories of absorption treated later. We can therefore put

$$\left.\begin{aligned} &\tau/\rho = (C_K + C_{L_1} + C_{L_2} + \ldots . .)\lambda^3 \text{ for } 0 < \lambda < \lambda_K \\ \text{and} \quad &\tau/\rho = (C_{L_1} + C_{L_2} + C_{L_3} + \ldots . .)\lambda^3 \text{ for } \lambda_K < \lambda < \lambda_{L_1} \end{aligned}\right\} (14)$$

and so on.

256. The Absorption Jumps.—The value of the ratio between absorption coefficients immediately preceding and following any absorption discontinuity may be denoted by the term *absorption jump* δ. To make the designation more definite we may add suitable subscripts to it, *e.g.*, δ_{KL_1}, $\delta_{L_1L_2}$ .... etc. Thus it has been found for Pt that $\delta_{KL_1} = 6{\cdot}0$, $\delta_{L_1L_2} = 1{\cdot}4$. When the values of these absorption jumps are known, they enable us to determine the relation between the constants *C's* in formula (14). Thus we have

$$\delta_{KL_1} = \frac{(C_K + C_{L_1} + C_{L_2} + \ldots . .)\,\lambda_K^3}{(C_{L_1} + C_{L_2} + \ldots . .)\,\lambda_K^3} = \frac{C_K + C_{L_1} + \ldots .}{C_{L_1} + C_{L_2} + \ldots .} \qquad (15)$$

---

[*] We are neglecting the probability of the simultaneous ejection of two electrons from the same or different orbits by the same quantum. Probability for such transitions, if they exist at all, is extremely small compared to that of the ejection of a single electron.

[†] Jönsson, *Diss. Uppsala* p, 72, 1928.

Similarly

$$\left.\begin{aligned}\delta_{L_1L_2} &= \frac{C_{L_1}+C_{L_2}+C_{L_3}\;\ldots\ldots}{C_{L_2}+C_{L_3}+\ldots.}\\ \delta_{L_2L_3} &= \frac{C_{L_2}+C_{L_3}+C_{M_1}+\ldots}{C_{L_3}\pm C_{M_1}+\ldots.}\\ \delta_{L_3M_1} &= \frac{C_{L_3}+C_{M_1}+C_{M_2}+\ldots}{C_{M_1}+C_{M_2}+\ldots.}\end{aligned}\right\}\quad \ldots\ldots \quad (16)$$

It is to be seen that the absorption jumps δ's are independent of the wavelength λ. It has been found (*vide* table 21) that δ_K is large for light elements and gradually drops to smaller value for heavy elements. As for example, for Al $\delta_{KL_1} = 13{\cdot}3$, and falls to the value 5·4 for Pb. A full set of values is given in table 21.

From expression (16) we further obtain that

$$\delta_{KL_1} - 1 = \frac{C_K}{C_{L_1}+C_{L_2}+C_{L_3}+} \quad \ldots\ldots \quad (17)$$

The absorption equations can now be written in the forms :

$$\tau/\rho = \frac{\delta_{KL_1}}{\delta_{KL_1}-1}\,C_K\,\lambda^3 \quad \text{for } 0 < \lambda < \lambda_K \quad \ldots \quad (18)$$

$$\tau/\rho = \frac{1}{\delta_{KL_1}-1}\,C_K\,\lambda^3 \quad \text{for } \lambda_K < \lambda < \lambda_{L_1}\ldots \quad (19)$$

Thus the coefficient of λ^3 in the first case is δ times that in the second case. Similar results can be obtained for the other discontinuities. This point is well illustrated in Fig. 37. For if we take logarithm of formulæ (18) and (19) we obtain

$$\log\frac{\tau}{\rho} = \log\frac{C_K}{\delta_{KL_1}-1} + \log\delta_{KL_1} + 3\log\lambda \; (0 < \lambda < \lambda_K)$$

$$\log\frac{\tau}{\rho} = \log\frac{C_K}{\delta_{KL_1}-1} + 3\log\lambda \qquad (\lambda_K < \lambda < \lambda_{L_1})$$

Thus the vertical distance between the successive parallel steps in Fig. 37 is equal to $\log\delta_{KL_1}$. As the δ's are independent of λ and only depend on C's, we can find the total L-discontinuity $\delta_{L_1M_1}$. This is given by

$$\delta_{L_1M_1} = \delta_{L_1L_2}\cdot\delta_{L_2L_3}\cdot\delta_{L_3M_1}$$

In the case of Ag, $\delta_{L_1M_1} = 1{\cdot}25 \times 1{\cdot}47 \times 3{\cdot}17 = 5{\cdot}8$

257. Jönsson's Universal Absorption Curve.—Jönsson showed that if the ordinates of the KL_1-branch of the absorption curve be multiplied by δ_{KL_1}, the new curve will be a continuation of the absorption curve for $0<\lambda<\lambda_K$. In the same way if the ordinates of the L_1L_2-branch of the absorption curve be multiplied by $\delta_{L_1L_2}$, we get a continuation of the curve in the region $\lambda_{L_2L_1}$. In this way he obtained what is known as the *universal absorption curve*, for a particular element.

This result is illustrated by the straight extension of the KL_1 branch of the curve in Fig. 37.

258. The Value of Absorption Jumps.—Jönsson further showed that the absorption jump at the K-limit is approximately given by

$$\delta_{KL_1} = \nu_K/\nu_{L_1}$$

where ν_K and ν_L represent the K and L-absorption frequencies. The truth of this empirical law is illustrated in the following table, in which the δ-values are shown for different elements.

Table 21.—Values of δ for different elements.*

Element	δ_{KL_1}	ν_K/ν_{L_1}	$\frac{\delta-1}{\delta}$	Element	δ_{KL_1}	ν_K/ν_{L_1}	$(\delta-1)/\delta$
13 Al	12·6	13·3	·92	47 Ag	6·65 §	6·7	·85
26 Fe	9·2	8·5	·89	50 Sn	6·56 §	6·5	·85
28 Ni	8·3	8·3	·88	54 Xe	5·6 †	6·3	·84
29 Cu	8·2	8·2	·88	74 W	5·65 §	5·7	·83
30 Zn	7·5	8·2	·88	78 Pt	6·0 ‖	5·6	·82
36 Kr	6·1 †	7·6	·87	79 Au	5·65 §	5·6	·82
42 Mo	7·0	6·9	·86	82 Pb	5·4 §	5·5	·82
46 Pd	6·8	6·8	·85				

We have $$\delta_{KL_1} = \frac{\nu_K}{\nu_{L_1}} = \frac{4\,(Z-s_1)^2}{(Z-s_2)^2} = A + \frac{B}{Z} + \frac{C}{Z^2}. \quad . \quad . \quad (20)$$

---

* Adopted from Kichner, *loc. cit.*, p. 256.

† P. Auger, *Ann. de Phys.*, 6, 224, 1926.

‡ E. C. Stoner and L. A. Martin, *Proc. Roy. Soc. A*, **107**, 312, 1925.

§ F. K. Richtmyer, *loc. cit.*

‖ S. J. M. Allen, *loc. cit.* The other data in table 21 are due to Jönsson.

so that the smaller the Z, the larger will be the value of δ. This explains why δ_{KL_1} has a large value for light elements and gradually diminishes for heavy elements. For the other discontinuities similar results, though not very satisfactory, have been obtained. In the case of L-discontinuities, Backhurst* showed that

$$\delta_{L_1L_2} = \frac{1}{\sqrt{2}} \cdot \frac{\nu_{L_1}}{\nu}$$

and so on. The δ-values for L-discontinuities are given in the table below.

Table 22.

Elements	$\delta_{L_1L_2}$	$\delta_{L_2L_3}$	$\delta_{L_3M_1}$	$\delta_{L_1M_1}$	$(\delta_{L_1} - 1)/\delta_{L_1}$
47 Ag	1·25	1·47	3·17	5·8	·20
78 Pt	1·4	1·8	2·8	7·1	·29
79 Au	1·2	1·4	2·5	4·2	·17

As true absorption is due to emission of photoelectrons, a knowledge of the true absorption coefficient τ gives us immediate information regarding the number of photoelectrons emitted by the passage of X-rays through matter. The number n of photoelectrons which are emitted per atom by the passage of rays of unit intensity through a distance of 1 cm. is given by

$$n = \frac{\tau_{At}}{h\nu} \quad . \quad . \quad . \quad . \quad . \quad . \quad . \quad . \quad . \quad . \qquad (21)$$

In this expression, we are considering the total true absorption and therefore total photo-emission from all the levels. But we can now separate the total absorption into individual part absorptions, and find out a relation between absorption jumps and the number of photoelectrons emitted from each level. It can be shown that (21) can be rewritten as

$$\left.\begin{aligned} \tau_K + \tau_{L_1} + \tau_{L_2} + \ldots &= n\ h\nu = (n_K + n_{L_1} + n_{L_2} \ldots) h\nu \\ &\qquad \text{for } \lambda \text{ just} < \lambda_K \\ \text{and } \tau_{L_1} + \tau_{L_2} + \ \ldots\ldots &= n' h\nu = (n_{L_1} + n_{L_2} + \ldots) \, h\nu \\ &\qquad \text{for } \lambda \text{ just} > \lambda_K \end{aligned}\right\} (22)$$

---

* Backhurst, *Phil. Mag.*, 7, 353, 1929.

where n_K is the number of photoelectrons released from the K-level, n_{L_1} the number released from the L_1 level etc. . . . Hence we have with the aid of (22)

$$\frac{\delta_{KL}-1}{\delta_{KL}} = \frac{n_K}{n_K+n_{L_1}+n_{L_2}+\ldots} = \frac{\nu_K-\nu_L}{\nu_K} \quad . \quad . \quad . \quad (23)$$

The last terms form Jönsson's empirical law, and we have similar relations for other discontinuities. These relations enable us to find out the relative number of electrons ejected from the different shells of any element. In the table below we illustrate the case of Pt.

Table 23.—Relative number of electrons in different shells. (*Pt 74*).

$\frac{\nu_K}{\nu_{L_1}} = \delta_{KL}$	$\frac{n_K}{n_K+n_L+n_M+\cdots}$	$\frac{\nu_{L_1}}{\nu_M} = \delta_L$	$\frac{n_L}{n_L+n_M+n_O}$	δ_M	$\frac{n_M}{n_M+n_N+n_O}$
5·6	·82	4·22	·76	4·6	·78

Thus of the total number of ejected electrons

82 %	are K-electrons
(100 – 82)×·76 = 14 %	are L- „
(100 – 82 – 14) ×·78 = 3 %	are M- „
(100 – 82 – 14 – 3) = 1 %	are N+0 „

Hence $n_K : n_L : n_M : n_{(N+O)} = 82 : 14 : 3 : 1$

In an atom of Pt (Z=78), we know that there are

2...K, 8.. L, 18...M, 50... (N+O) electrons.

So the relative ionisability of the electrons (or the probability of emission) are

$$n'_K : n'_L : n'_M : n'_{(N+O)} = 2000 : 88 : 8 : 1$$

259. Dependence of τ/ρ upon Z.—It has already been mentioned that C the constant in the equation (14) involves some power of Z. Early workers put

$$C = C_1 Z^4,$$

but later it was found that the fourth power law did not represent the observed facts correctly. Some of these laws have been given already on p. 505. These empirical laws involving fractional powers of Z, do not probably represent any great advance. In fact Jönsson showed that if the quantity

$$\left(\log \frac{\tau}{\rho} \cdot \frac{\nu_K}{\nu_L} \quad \frac{A}{Z}\right)$$

be plotted against log $(Z\lambda)$, where A = atomic weight and L = Loschmidt number, the curve is a *straight line*, from which he deduced, as can be easily verified, that

$$C = C_1 \quad Z^4$$

This is known as *Jönsson's universal absorption curve* and is illustrated in Fig. 38. With its aid the true absorption τ/ρ for any element Z corresponding to any wavelength λ can be at once read out.

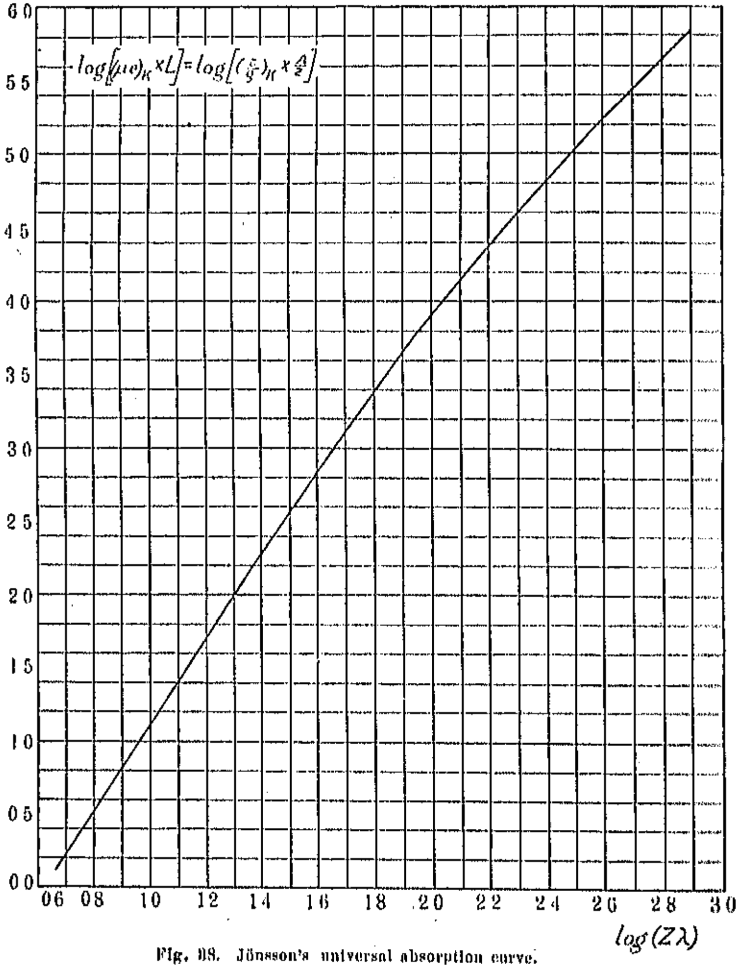

Fig. 38. Jönsson's universal absorption curve.

260. Theories of Absorption.—Though a rigorous theoretical treatment of the problem of absorption is outside the scope of this book, we shall give a short account of the preliminary work of J. J. Thomson [*] and L. De Broglie [†] which may serve as an introduction to the more detailed works of Kramers who used the orbital theory, or to the more recent works of Sommerfeld, Wentzel and Stobbe who used wave-mechanics.

Before considering these theories the reader should see that the atomic absorption coefficient (*i.e.*, absorption per atom) is

$$\tau_{\mathrm{At}} = \frac{\mu A}{\rho L}$$

It has the dimensions of an 'area', for the dimension of μ is $[\mathrm{L}]^{-1}$, μx being a fraction, and A/ρ = volume = $[\mathrm{L}]^3$. L, the Loschmidt-Avogadro number is dimensionless.

J. J. THOMSON'S THEORY.

We give a short account of J. J. Thomson's classical theory which was the starting point of later works. This theory may be read in conjunction with his theory of X-ray scattering (§113) with which it has many points in common.

When a beam of X-rays, or radiation of any kind passes over matter, then according to the electromagnetic theory, an alternating e. m. f., acts on it for a short time, and sets the electrons in motion. The work so done may be said to be abstracted from the energy of the primary radiation. The process can be mathematically treated as follows.

The acceleration f imparted to the electron is Ee/m where E = e. m. f. due to the light.

The total displacement of the electron

$$x = \frac{Ee}{m}\left(\frac{d}{c}\right)^2$$

where d = length of the pulse.

---

[*] J. J. Thomson, *Conduction of Electricity through Gases* (ed. 2), p. 326.

[†] L. De Broglie, *Ann. d. Physique*, **3**, 33, 1922.

For an account of pre-wave-mechanics theories, see Compton's *X-rays and Electrons*, Chapter XII and original papers of Kramers, (*Phil. Mag.*, **46**, 836, 1923.)

For wave-mechanical theories, see Bethe, *H. d. Phys.*, **24**, 475-85, or the original papers amongst which the following may be selected: Stobbe, *Ann. d. Phys.*, **7**, 661, 1930; Wentzel, *Zs. f. Phys.*, **38**, 518, 1926.

Let us suppose that the restoring force is

$$F = -4\pi^2 m \nu_0^2 x$$

Hence the work done $= -\int_0^x F . \, dx = \dfrac{e^2}{mc^2} \cdot \dfrac{2\pi^2 d'}{\lambda_0^2} \cdot E^2$

This is equal to $\tau_{\varepsilon} . \, \varepsilon$, where ε is the total energy of the incident pulse, and τ_e is the fraction absorbed by a single electron.

Now the quantity E^2 can be expressed in terms of energy density of the pulse from the relation that the total energy of the pulse

$$\varepsilon = \frac{1}{8\pi}(E^2 + H^2)\, 2d = \frac{E^2}{4\pi}\, 2d$$

Hence τ_e the coefficient of absorption due to a single electron is

$$\tau_e = \frac{e^2}{mc^2} \cdot \frac{4\pi^3 d^3}{\lambda_0^2} \quad . \; . \; . \; . \; . \; . \; . \; . \quad (24)$$

Here we have introduced a hypothetical quantity d, the length of the pulse. If we take $2d = \lambda$, we obtain

$$\tau_e = \frac{e^2}{mc^2} \cdot \frac{\pi^3 \lambda^3}{2\lambda_0^2} \quad . \; . \; . \; . \; . \; . \; . \; . \quad (25)$$

Hence absorption in the K-shell is given by

$$\tau_K = \frac{e^2}{mc^2} \cdot \frac{\pi^3 \lambda^3}{2\lambda_K^2} N_K \quad . \; . \; . \; . \; . \; . \; . \quad (26)$$

where N_K is the number of electrons in the K-shell.

It is easy to see that τ_K has the dimensions of area, because $\dfrac{2}{3}\dfrac{e^2}{mc^2}$ = the classical radius of the electron $= 1{\cdot}9 \times 10^{-13}$ cm.

so that $\dfrac{e^2}{mc^2} = 2{\cdot}8 \times 10^{-13}$ cms.

and $\pi^3 \lambda^3 N_K / 2\lambda_K^2$ has the dimension of length.

In order to express τ_K in terms of Z the atomic number of the absorber, we use the usual Bohr-Mosely form of frequency of the K-electrons

$$\nu_K = \frac{2\pi^2 e^4 m Z^2}{h^3 c} \cdot \frac{1}{n_K^2}$$

in (26). This gives us

$$\tau_K = C_K \,.\, Z^4 \,\lambda^3 \quad . \quad . \quad . \quad . \quad . \quad . \quad . \quad . \quad . \quad (27)$$

where
$$C_K = \frac{2\pi^7 e^{10} m}{h^6 c^4 n_K^4} \,.\, N_K$$

Substituting $N_K = 2$ and $n_K = 1$, we get $C_K \sim 2 \times 10^{-2}$. Eqn. (27) is of the form obtained experimentally.

L. De Broglie* obtained formulæ in substantial agreement with the above, though his methods were different. His formula was

$$\tau = \frac{\pi e^2}{mc^2} \lambda^3 \left\{ \left(\frac{N_K}{\lambda_K^2} \eta_K \right) + \left(\frac{N_L}{\lambda_L^2} \eta_L \right) + \quad . \quad . \quad \right\} \quad . \quad . \quad . \quad (28)$$

Here τ represents the total photo-electric absorption by K, L, . . . electrons, and, the factors η represent the connection between the hypothetical quantity which is called the length of the pulse, and the wavelength.

261. Fluorescent X-rays.—The discovery of the phenomenon of fluorescence in X-rays by Barkla has already been mentioned in § 109. It was early found that the fluorescent rays are characteristic of their radiated matter, and in order to excite them, the exciting radiation must be of a higher frequency than the fluorescent radiation. The emission of fluorescent radiation is in fact closely related to absorption of X-rays. When a beam of primary X-rays of energy just greater than the K-absorption energy of an element falls on it, the K-electron of the atom is ejected by photoelectric absorption, and an electron from some higher shell falls back to the vacant K-shell, and K-fluorescent radiation is emitted. This method of fluorescent excitation was largely used to obtain the characteristic X-rays before the development of crystal spectroscopy. But its chief use at present consists in obtaining a strong beam of monochromatic X-rays (Küstner†), and also in chemical analysis (§146).

From the theories of X-ray absorption described in the previous section it is clear that for every quantum of radiation absorbed by matter, there should be emitted a corresponding quantum of fluorescent radiation. But in reality, an exact proportionality is never found. The total intensity of fluorescent radiation is always found to be less than that of the exciting radiation. This is certainly due to the internal absorption of fluorescent rays (Auger processes) which is rather strong in the case of light elements. We thus come to the interesting question of *efficiency* of the production of fluorescent radiation. This may be defined as

---

* De Broglie, *loc. cit.*

† Küstner, *Zs. f. Phys.*, 70, 324, 1931.

$$\alpha_K = N_K/n_K$$

for the K-emission, where N_K = the number of K-quanta emitted as fluorescent radiation and n_K = the number of K-quanta absorbed by the radiator. N_K can be determined experimentally by measuring the intensity of fluorescent radiation, and n_K from absorption experiments with the aid of relation (23) on p. 511.

Two methods are employed for determining the efficiency of fluorescence. In the first, the cloud-chamber method of studying the photoelectric absorption (§246) is used and the number of single and double tracks are counted. If s = the number of single tracks, then s corresponds to the number of processes in which fluorescent rays have been emitted without being internally absorbed. If again e = the number of double tracks, it denotes that the total number of photoelectrons emitted is $s+e$. Hence we have

$$\alpha_K = \frac{s}{s+e}$$

This method has been developed by Auger, and later on by Locher and applied in cases of Xe, Ne, O and Kr. Their results are shown in the table on the next page.

In the second method the intensity of the fluorescent radiation is directly measured with the aid of an ionisation chamber. It can be shown* that if I, A, μ, τ_K, λ denote respectively the intensity, cross-section, total absorption coefficient, K-photoelectric absorption coefficient and wavelength of the primary beam of X-rays, and I', μ', λ' are the corresponding quantities for the fluorescent beam, then

$$\alpha_K = \frac{4\pi r^2}{A} \cdot \frac{\mu+\mu'}{\tau_K} \cdot \frac{\lambda'}{\lambda} \cdot \frac{I'}{I}$$

where r is the distance of the aperture of the ionisation chamber from the radiator. I'/I is equal to the ratio of the ionisation currents due to the fluorescent rays and the primary rays. This being measured, α_K, can be calculated. This method was used by Compton and Martin. Various corrections are however necessary on account of the non-homogeneity of the fluorescent radiation, and the photo-electric absorptions taking place in the ionisation chamber. For details see original papers.*

---

* For the proof of this relation see Compton's paper (*supra*).

The results of the experiments of Locher, Auger, Compton, Martin and others are shown in the following table in which the

Table 24.—Efficiency of production of K-fluorescent radiation of elements.

Element	Observer	Method	K-efficiency in %
8 O	Locher	Cloud chamber	8·2
10 Ne	,,	,,	8·3
18 A	,,	,,	14·9
18 A	Auger	,,	7 (?)
26 Fe	Harms	Ionisation	28·2
26 Fe	,,	,,	29
27 Co	Berkey	,,	38
28 Ni	Martin	,,	37
28 Ni	Compton	,,	35
29 Cu	Harms	,,	37·8
29 Cu	Martin	,,	40
30 Zn	Harms	,,	40·3
30 Zn	Martin	,,	46
33 As	Berkey	,,	53
34 Se	Compton	,,	54
34 Se	Harms	,,	51·7
34 Se	Martin	,,	59
35 Br	Compton	,,	56
35 Br	Martin	,,	59
36 Kr	Auger	,,	50
38 Sr	Harms	,,	61·5
42 Mo	Compton	,,	68
47 Ag	Berkey	,,	72
48 Cd	,,	,,	70
50 Sn	,,	,,	66
51 Sb	,,	,,	64
52 Te	,,	,,	59
53 I	Martin	,,	75
54 Xe	Auger	Cloud chamber	71

---

* The following works may be consulted:—

Auger, *Comp. Rend.*, **182**, 1215, 1926; Locher, *Phys. Rev.*, **40**, 482, 1932; Compton, *Phil. Mag.*, **8**, 961, 1929; Martin, *Proc. Roy. Soc. A*, **115**, 420, 1927; Stephenson, *Phys. Rev.*, **43**, 527, 1933; Harms, *Ann. d. Phys.*, **82**, 87, 1926; Berkey, *Phys. Rev.*, **54**, 437, 1934.

fourth column gives the efficiency of K-fluorescent emission. It will be seen that generally the efficiency increases with atomic number of the radiator, and for the lighter elements like Al it is even non-existent. This is attributed to Auger processes taking place as explained already. Recent experiment of Berkey however shows that for elements heavier than 42 Mo the K-fluorescent yield decreases. The reason for this is not understood, as there is no satisfactory theory of this phenomenon at present. An wave mechanical theory of fluorescence has been given by Wentzel.* But it does not account for the above discrepancy. All the experiments however verify the remarkable fact that the efficiency is independent of wavelength of the primary rays, provided that it is shorter than the corresponding absorption limit.

Books Recommended.

1. M. Siegbahn, *Spektroskopie der Röntgenstrahlen* (1931).
2. A. Lindh, *H. d. Experimental physik* (1930).
3. F. Kirchner, *H. d. Experimental physik*, 24/1, 1, 1930.
4. A. H. Compton, *X-rays and Electrons* (1924).
5. G. Hevesy, *Chemical Analysis by X-rays* (1932).
6. A. Sommerfeld, *Atombau*, 5th edition (1933).

---

* G. Wentzel, *Zs. f. Phys.*, **43**, 524, 1927.

Table 25.—Wavelengths of K and L-series emission lines of elements.
(λ in X. units: 1 X. U. = 10^{-11} cm)

Elements	K-Series			L-Series								
λ in X. U.	α_2	α_1	β_1	l	α_2	α_1	η	β_2	β_4	β_1	β_3	γ_1
92 U	130·95	126·40	111·87*	1064·9	920·62	908·74	803·5	753·07	746·4	718·51	708·79	613·59
91 Pa	...	...	...	1088·5	942·7	930·9	827·8	772·1	768·3	740·7	730·7	632·5
90 Th	136·8	132·3	116·9*	1112·8	965·85	954·05	852·8	791·92	791·92	763·56	753·24	651·76
83 Bi	165·25	160·41	142·05*	1313·7	1153·01	1141·50	1056·5	953·24	975·01	950·02	936·66	811·43
82 Pb	170·04	165·16	146·06*	1347·4	1184·08	1172·58	1090·0	980·83	1005·63	980·83	967·21	838·01
81 Tl	174·66	169·80	150·11*	1381·9	1216·26	1204·93	1125·4	1008·22	1036·99	1012·99	998·50	865·71
80 Hg	..	...	...	1418·41	1249·51	1238·63	1161·6	.037·70	1069·2	1046·52	1030·46	894·6
79 Au	184·83	179·96	159·02*	1456·9	1285·02	1273·77	1200·3	1068·01	1104·22	1081·28	1065·50	924·61
78 Pt	190·04	182·23	163·70*	1496·4	1321·55	1310·33	1240·3	1099·74	1139·86	1117·58	1101·65	955·99
77 Ir	195·50	190·65	168·50*	...	1359·8	1348·47	1281·7	1132·97	1177·15	1155·40	1138·47	988·76
76 Os	201·31	196·45	173·61*	...	1398·66	1388·59	...	1168·84	...	1194·90	...	1022·96
75 Re	...	...	...	1627·3	1441·0	1429·97	1370·6	1204·1	1256·3	1236·03	1217·6	1058·7
74 W	213·45	208·62	184·22*	1675·0	1484·38	1473·36	1418·1	1242·03	1298·73	1279·17	1259·92	1096·30
73 Ta	219·73	214·88	189·91*	1724·9	1529·78	1518·85	1467·9	1281·90	1343·07	1324·23	1304·09	1135·58
72 Hf	226·53	221·73	195·15	1777·4	1577·04	1566·07	1519·7	1323·5	1389·3	1371·1	1349·7	1176·5
71 Cp	213·58	228·82	201·71	1831·8	1626·36	1615·51	1573·8	1367·2	1437·2	1420·7	1398·2	1220·3
70 Ad	240·98	236·28	208·34	1890·	1678·9	1667·8	1631·	1412·8	1488·2	1472·5	1449·4	1264·8
69 Tm	248·61	243·87	214·87	1951·1	1733·9	1722·8	1692·3	1460·2	1541·2	1526·8	1502·3	1312·7
68 Er	256·64	251·97	222·15	2015·1	1791·4	1780·4	1754·8	1510·6	1596·4	1583·4	1557·9	1362·3
67 Ho	264·99	260·30	...	2082·1	1852·1	1841·0	1822·0	1565·7	1655·3	1643·5	1616·0	1414·2
66 Dy	273·75	269·03	237·10	2154·0	1915·6	1904·6	1892·2	1619·8	1716·7	1706·6	1677·7	1469·7
65 Tb	282·86	278·20	245·51	2229·0	1982·3	1971·5	...	1679·0	1781·4	1772·7	1742·5	1526·6

* The $K\beta_1$ lines for elements 92 U to 73 Ta are in reality $\beta_{1,3}$ values combined.

Table 25.—Wavelengths of K and L-series emission lines of elements.—(*Continued*)
[λ in X. units: 1 X. U. = 10^{-11} cm.]

Elements	K-Series			L-Series								
λ in X. U.	α_2	α_1	β_1	l	α_2	α_1	η	β_2	β_4	β_1	β_3	γ_1
64 Gd	292·61	287·82	253·94	2307·1	2052·6	2041·9	...	1741·9	1849·3	1842·5	1810·9	1588·6
63 Eu	302·65	297·92	263·07	2390·2	2127·3	2116·3	...	1808·2	1922·1	1916·3	1882·7	1654·3
62 Sa	313·02	308·33	272·50	2477	2205·7	2195·0	2214	1878·1	1996·4	1993·6	1958·0	1723·1
60 Nd	335·95	331·25	292·75	2670·3	2375·6	2365·3	2404·2	2031·4	2162·2	2162·2	2122·2	1873·8
59 Pv	348·05	343·40	303·60	2778·1	2467·6	2457·7	2500	2114·8	2250·1	2253·9	2212·4	1956·8
58 Ce	361·10	356·47	305·01	2885·7	2565·1	2556·0	2614·7	2204·1	2344·2	2351·0	2305·9	2044·3
57 La	374·66	370·04	327·26	3000	2668·9	2659·7	2734	2298·0	2443·8	2453·3	2405·3	2137·2
56 Ba	388·99	384·43	340·22	3128·7	2779·0	2769·6	2857·1	2399·3	2549·8	2562·2	2511·0	2236·6
55 Cs	404·11	399·59	353·62	3259·6	2895·6	2886·1	2983·3	2506·4	2660·5	2677·8	2622·9	2342·5
53 I	437·03	432·49	383·15	3549·7	3150·9	3141·7	...	2746·1	2905·9	2930·9	2868·2	2577·5
52 Te	454·91	450·37	...	3710·1	3291·0	3282·0	...	2876·1	3040·0	3070·0	3001·3	2706·5
51 Sb	473·87	469·31	...	3880·3	3440·8	3431·8	3599·6	3016·6	3184·3	3218·4	3145·1	2845·1
50 Sn	494·02	489·57	434·30	4063·3	3601·1	3592·2	3781·8	3167·9	3336·3	3377·9	3298·9	2994·9
49 In	515·48	511·06	453·58	4259·3	3772·4	3763·7	3976·1	3331·2	3499·0	3547·8	3461·9	3155·3
48 Cd	538·32	533·90	474·08	4471·3	3956·4	3947·8	4187·5	3506·4	3674·3	3730·1	3636·4	3328·0
47 Ag	562·67	558·28	496·01	4697·6	4153·8	4145·6	4410·1	3693·8	3861·1	3926·6	3824·5	3514·9
46 Pd	588·63	584·27	519·47	4939·6	4366·6	4358·5	4650·2	3900·7	4062·3	4137·3	4025·7	3716·4
45 Rh	616·37	612·02	544·49	5207·0	4595·6	4587·8	4911·2	4122·1	4280·2	4364·0	4244·7	3935·7
44 Ru	646·06	641·74	571·31	5486·4	4843·7	4835·7	...	4361·9	4512·6	4611·0	4476·4	4172·8
43 Ma	...	...	...	...	...	...	...	...	...	...	...	...
42 Mo	712·805	707·831	630·978	...	5401	5395·0	5836	4910·0	5041·0	5166·5	5004·7	...
41 Nb	748·89	744·65	664·38	6510	5718	5712·0	6196	5226·0	5330·6	5480·3	5297·1	5024·8
40 Zr	788·51	784·30	700·28	6899	6056·7		6593·9	5574·2	5651·7	5823·6	5618·6	5373·8
39 Y	831·32	827·12	739·19	...	6435·7		7031·0	...	6007·7	6203·9	5974·1	...
38 Sr	877·61	873·45	781·30	7822	6848·6		7506	...	6391·8	6610·0	6358·2	...
37 Rb	927·76	923·64	826·96	...	...		...	...	6800·9	...	6769·4	...

35 Br	1041·66	1037·59	930·87	9564	8358	9235	...	...	8109	
34 Se	1106·52	1102·48	990·13	10272	8972	9939	...	...	8718	
33 As	1177·43	1173·44	1055·10	11048	9652	10711	...	8912	9395	
32 Ge	1255·21	1251·30	1126·71	11922	10415	11587	...	...	10153	
31 Ga	1340·87	1337·15	1205·20	12890	11270	12560	...	.	11010	
								β₄	β₃	β₁
30 Zn	1436·03	1432·17	1292·55	13950	12230	13610	...	11160		11960
29 Cu	1541·23	1537·395	1389·35	15260	13306	14830	...	12100		13030
28 Ni	1658·35	1654·50	1497·05	16730	14530	16170	...	13140		14280
27 Co	1789·19	1785·29	1617·44	18280	15940	17770	...	...		15640
26 Fe	1936·012	1932·076	1753·013	20150	17580	19650	...	15610		17290
25 Mn	2101·49	2097·51	1906·20	22340	19390	...	...	...		19170
24 Cr	2288·91	2285·03	2080·6	24730	21530	...	...	...		21190
23 Va	2502·13	2498·35	2279·7	27700	24200	...				
22 Ti	2746·81	2743·17	2509·0	31330	27370	...				
21 Sc	3028·40	3025·03	2773·9	35710	31370	...				
20 Ca	3354·95	3351·69	3083·4	40900	36270	...				
19 K	3737·07	3733·68	3446·8	47730	...	47230				
17 Cl	4721·2	4718·2	4394·2	67900	...	67330				
16 S	5363·7	5361·3	5021·1	79980	...	79290				
15 P	6142·5		5792·1							
14 Si	7111·06		6754·5							
13 Al	8320·5		6965							
12 Mg	9869·0		9539							
11 Na	11880									
9 F	18270									
8 O	23610									
7 N	31590									
6 C	43740	band								
5 B	66200	heads.								
4 Be	110950	See								
3 Li	225300	§241.								

The table has been adopted from Siegbahn's *Spektroskopie der Röntgenstrahlen* (1931), pp. 183 to 186 and 236 to 240. For sources of wavelengths for light elements see §241.

Table 26.—Wavelength of M-emission lines of elements (λ in X. U.).

Element	α_2	α_1	β	γ	Element	α_2	α_1	β	γ
92 U	3916	3902	3708	3473	66 Dy	9555	9524	9345	8127
90 Th	4143	4130	3934	3672	65 Tb	9946	9917	9772	8468
83 Bi	5119	5108	4899	4522	64 Gd	10428	10394	10233	8826
82 Pb	5288	5274	5065	4665	63 Eu	11003	10932	10723	9192
81 Tl	5461	5450	5239	4815	62 Sm	11475	11406	11238	9580
79 Au	5842	5828	5612	5135	60 Nd	...	12650	12375	10483
78 Pt	6045	6034	5816	5309	59 Pr	...	...	...	10975
77 Ir	6262	6249	6025	5490	58 Co	..	14030	13755	11511
76 Os	...	6477	6254	5670					
75 Re	...	6715	6491	5875					
74 W	. .	6969	6743	6076					
73 Ta	...	7237	7008	6299					
72 Hf	...	7524	7289	6530					
71 Cp	...	7824	7585	6748					
70 Yb	8138	8122	7893	7009					
68 Er	8794	8783	8576	7530					
67 Ho	9165	9143	8947	7849					

Table 27.—M-lines for elements 35 Br to 51 Sb (λ in Å. U.)

<table>
<tr><th>Element</th><th>$M_2 \leftarrow N_1$</th><th>$M_3 \leftarrow N_1$</th><th>$M_1 \leftarrow N_3$</th><th>$M_4 \leftarrow N_2$</th><th>$M_5 \leftarrow N_3$</th></tr>
<tr><td>35 Br</td><td>76·86</td><td>79·76</td><td>186·07</td><td>191·04</td><td>192·57</td></tr>
<tr><td>37 Rb</td><td>57·04</td><td>59·48</td><td>126·71</td><td>127·84</td><td>128·66</td></tr>
<tr><td>38 Sr</td><td>51·32</td><td>53·61</td><td colspan="2">108·06</td><td>108·70</td></tr>
<tr><td>39 Y</td><td>48·5</td><td>...</td><td colspan="2">92·3</td><td>93·6</td></tr>
<tr><td>40 Zr</td><td>...</td><td>...</td><td colspan="2">80·34</td><td>81·71</td></tr>
<tr><td>41 Nb</td><td>40·7</td><td>..</td><td colspan="3">72·13</td></tr>
<tr><td>42 Mo</td><td>37·3</td><td>...</td><td colspan="3">64·35</td></tr>
<tr><td>44 Ru</td><td>28·21</td><td>...</td><td colspan="3">52·32</td></tr>
<tr><td>45 Rh</td><td>27·95</td><td>29·79</td><td colspan="3">47·59</td></tr>
<tr><td>46 Pd</td><td>27·8</td><td>...</td><td colspan="3">43·48</td></tr>
<tr><td>47 Ag</td><td>...</td><td>..</td><td colspan="3">39·79</td></tr>
<tr><td>48 Cd }*</td><td></td><td>...</td><td colspan="3">36·75</td></tr>
<tr><td>50 Sn }</td><td></td><td></td><td colspan="3">31·26</td></tr>
<tr><td>51 Sb }</td><td></td><td></td><td colspan="3">28·76</td></tr>
</table>

* These values are due to Prins and Takens *loc. cit.* The other values are due to Siegbahn, *loc. cit.*

Table 28.—N-lines for light elements (λ in Å. U.).

Element	$N_4 \leftarrow O_3$	$N_4 \leftarrow O_2$	$N_5 \leftarrow O_3$
55 Cs	183·8	188·6	190·3
56 Ba	159·06	163·25	164·6
57 La	150·75		152·62
58 Ce	140·2		144·4
59 Pr	136·5		
60 Nd	128·9		
62 Sa	116·66		118·12
63 Eu	112·0		
65 Tb	100·77		102·23
66 Dy	97·2		
	$N_6 \leftarrow O_5$	$N_6 \leftarrow O_4$	$N_7 \leftarrow O_5$
81 Tl	113·03	115·34	117·74
82 Pb	100·21	102·38	104·34
83 Bi	91·6		93·16

Values of Tl, Pb, Bi are due to Siegbahn and Magnusson, *Zs. f. Phys.*, 88, 559, 1934.

CHAPTER XII

THE PERIODIC CLASSIFICATION AND PRINCIPLES OF ATOM-STRUCTURE

262. General Statement of the Problem of Atom-Structure.—In the foregoing chapters a general description has been given of the experiments by which it was established that the atom consists of a central nucleus of positive electricity occupying a minute volume, and surrounded by a swarm of electrons which revolve round it in orbits determined by quantum mechanics. From the experiments on large angle scattering of α-rays, it has been established that the net nuclear charge on the nucleus is Ze where Z is the *ordinal number* expressing the position of the atom in the periodic classification. A rough measure of the number of electrons in an atom was first determined by Barkla's experiment on scattering of X-rays, and it is now admitted that the number is equal to Z, so that the atom as a whole is neutral. In the present chapter, the arrangement of the electrons, and their motion will be studied. The mechanics of the electron has been studied only in the simple case of hydrogen, which shows that it is very much different from classical dynamics. The electron has also been found to be a more complex entity than a mere point charge of electricity. We have now to generalise these conceptions in the case of any atom. To achieve this purpose, Bohr began with a review of the chemical and the physical properties of the atoms known at the time. The chemical properties are summarized, in what is known as the *Law of Periodic Classification*, while the physical evidences were drawn from optical and X-ray spectra. Bohr put to himself this question: suppose we start with a central nucleus having the charge Ze, and bring to it the Z electrons one after another, till the neutral atom be formed. What are the quantum-specifications of the motion of these electrons, how will they be arranged in different shells, and how do these arrangements account for chemical properties and for the spectra of the elements?

Table 1.—The Periodic Classification of Elements.

Period	I	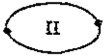 II	III	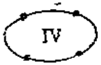 IV	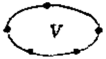 V	VI	VII	VIII			
I	1 **H** 1·0078										2 **He** 4·002
II	3 **Li** 6·940	4 **Be** 9·02	5 **B** 10·826	6 **C** 12·000	7 **N** 14·008	8 **O** 16·000	9 **F** 19·00				10 **Ne** 20·183
III	11 **Na** 22·997	12 **Mg** 24·32	13 **Al** 26·97	14 **Si** 28·06	15 **P** 31·02	16 **S** 32·06	17 **Cl** 35·457				18 **A** 39·944
IV	19 **K** 39·100	20 **Ca** 40·08	21 **Sc** 45·10	22 **Ti** 47 90	23 **V** 50·95	24 **Cr** 52·01	25 **Mn** 54·93	26 **Fe** 55·84	27 **Co** 58·94	28 **Ni** 58·69	
	29 **Cu** 63·57	30 **Zn** 65·38	31 **Ga** 69·72	32 **Ge** 72·60	33 **As** 74·93	34 **Se** 79·2	35 **Br** 79·916				36 **Kr** 83·7
V	37 **Rb** 85·44	38 **Sr** 87·63	39 **Y** 88·92	40 **Zr** 91·22	41 **Cb** 93·3	42 **Mo** 96·0	43 **Ma** 97·8	44 **Ru** 101·7	45 **Rh** 102·91	46 **Pd** 106·7	
	47 **Ag** 107·880	48 **Cd** 112·41	49 **In** 114·8	50 **Sn** 118·70	51 **Sb** 121·77	52 **Te** 127·5	35 **I** 126·932				54 **Xe** 131·3
VI	55 **Cs** 132·81	56 **Ba** 137·37	57 **La** * 138·92	72 **Hf** 178 6	73 **Ta** 181·5	74 **W** 184·0	75 **Re** 186·31	76 **Os** 190·8	77 **Ir** 193·1	78 **Pt** 195·23	
	79 **Au** 197·2	80 **Hg** 200·61	81 **Tl** 204·39	82 **Pb** 207·22	83 **Bi** 209·00	84 **Po** 209·99	85 212?				86 **Rn** 222
VII	87 223·?	88 **Ra** 225·97	89 **Ac** 227	90 **Th** 232·12	91 **Pa** 231·04	92 **U** 238·14					

* 58-71 Rare Earths		58 **Ce** 140·13	59 **Pr** 140·92	60 **Nd** 144·27	61 **Il** 146·0 ?	62 **Sm** 150·43	63 **Eu** 152·0
64 **Gd** 157·3	65 **Tb** 159·2	66 **Dy** 162·46	67 **Ho** 163·5	68 **Er** 167·64	69 **Tm** 169·4	70 **Yb** 173·5	71 **Lu** 175·0

263. The Periodic Classification.—We shall now review in a short compass the periodic properties of the atoms on which a large amount of subsequent discussions are based. The periodic properties of atoms were discussed in the last century by Lothar Meyer and Mendeléeff, and illustrated by the atomic volume curves and the Periodic Table (table 1). As the explanation of these curves and tables are quite well known, we shall not stop to discuss them.

Bohr in his survey of Atom-structure made use of a modified scheme of the Periodic Classification given by Julius Thomsen of Copenhagen which not only contained all the points contained in the previous discussions, but brought out new features not included in these schemes. This scheme is reproduced in Fig. 1.

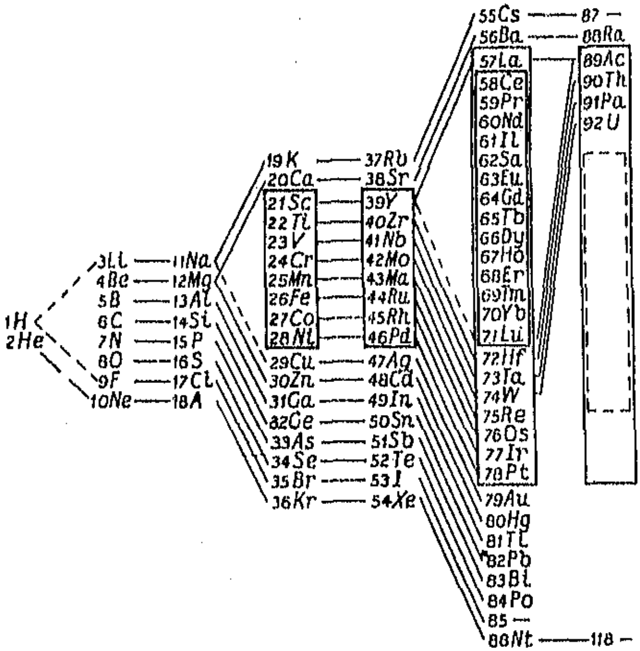

Fig. 1. Julius Thomsen's Periodic Table.

In this scheme, each vertical column represents a horizontal row in the usual Mendeléeff Table. The first column, consisting of hydrogen and helium, stands apart, and constitutes the first period. The second and third short periods are constituted by the groups :—

(3) Li to (10) Ne and (11) Na to (18) A respectively.

Each of these groups contains eight elements: elements similar in properties being opposite each other, *e.g.*, (Li—Na), (Be—Mg), (B—Al) ... etc ... The first pair Li or Na is monovalent, the second pair is divalent, ... and the valency goes on increasing by one, till we come to the end of each period, where we meet with the inert gases (10 Ne—18 A) which possess no valency. The fourth and fifth periods (19 K to 36 Kr) and (37 Rb to 54 Xe) are the long periods and each contains 18 elements, and though they are closed by inert gases, they contain a group of corresponding elements possessing entirely new properties. These are (21 Sc to 28 Ni) in group IV and (39 Y to 46 Pd) in group V. They are shown separately being included within vertical oblongs, and the elements with corresponding properties are connected by long strokes, *e.g.*, 11 Na with 19 K, and 37 Rb; 13 Al with 31 Ga and 49 In etc .... Those connected with upward or downward long strokes constitute respectively the even and the odd sub-groups of Mandeléeff's classification. We need not consider the further periods at this stage.

264. Idea of Closed Shells.—Bohr connected this phenomenon of periodicity of chemical properties with the idea of shells of electrons introduced in Chap. VII. It was at first thought that the electrons are arranged not haphazardly but in distinct shells consisting of 2, 8, 8, 18, 18, 32 .... electrons respectively, as represented in Fig. 5 on p. 369.

When the shells are complete, we get inert gases. Thus helium consists of a shell of two electrons, Ne of an inner shell of 2 and an outer one of 8, argon of three shells consisting of 2, 8 and 8 electrons. These shells are saturated, and possess no valency. When we add one further electron, we get the alkalies Li, Na, K, Rb, Cs and the element number 87 (still undiscovered). These elements are monovalent, and they can easily lose *one electron*, and acquire a net positive charge of unity as in electrolysis. It is supposed that the extra electron determines the chemical valency, and such elements are said to possess a unit positive electro-valency. In a compound formation like NaF, it is supposed that the loosely bound

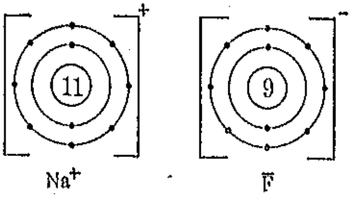

Fig. 2. Formation of NaF molecule.

electron in Na passes on to F, so that the molecule really consists of Na^+ and F^- ions held together by forces of electrostatic origin, as illustrated in the diagram (Fig. 2).

When Na loses one electron, it possesses a Ne-like structure and the ion is magnetically neutral. Fluorine on the other hand has only 5 electrons in the outer shell, and can complete its shell if an extra electron be added to it. As the inert gas structure is more stable, this process of acquisition of an electron can easily be brought about. Fluorine is thus said to possess an *affinity* for electrons, and a *negative electro-valency* of unity. Similarly all halogen atoms possess an electron affinity.

These views were justified by later works. The first electron in Na requires an energy of only 5·12 electron-volts for detaching it completely from the atom, while for detaching the second, an energy of 46·78 electron-volts are necessary. This shows that the second electron is very firmly attached to the nucleus and cannot be easily split off from the atom. If on the other hand an electron be added to F, it gives out energy corresponding to about 6 electron-volts. The fluorine atom thus possesses an innate capacity for absorbing an electron, and thus acquiring the inert gas structure.

265. Electron-Composition and Valency.—If we now bring 2 electrons to the inert gas shells, we obtain the elements Be (4), Mg (12), Sr (38), Ba (56) and Ra (88) which are all divalent. This is explained on the assumption that both the electrons freshly brought are loosely bound and can be easily lost. Thus in the formation of MgF_2 it is supposed that Mg loses two electrons, which go over to fluorine forming two F^- ions. Thus the constitution of the complex is supposed to be (F^-, Mg^{++}, F^-), the constituents being held together by forces of electrostatic origin, as shown in the

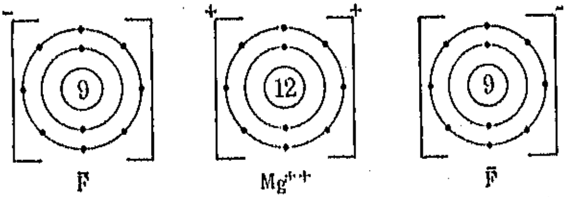

Fig 3. Formation of magnesium fluoride molecule.

diagram (Fig. 3). This hypothesis is supported by the values of the I.P.'s of Mg. It has been found that the

1st I. P. of Mg = 7·61 Volts,
2nd ... = 14·97 Volts,
3rd ... ∼ 80 Volts.

Thus it is seen that it is easy to remove two electrons from Mg, but the removal of the third electron requires a disproportionate expenditure of energy. This is ascribed to the fact that Mg^{++} has a neon-like closed structure.

We can explain in a similar way the formation of compounds like $MgCl_2$, MgO or MgS which may be supposed to consist of Mg^{++} and Cl^- Cl^-, or O^{--}, or S^{--}. Thus oxygen or sulphur is supposed to possess a negative electrovalency of two, *i.e.*, they possess the innate capacity of acquiring two electrons, and pass on to an inert gas structure as illustrated in Fig. 4.

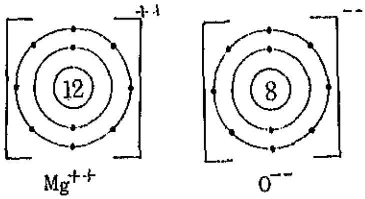

Fig 4. Formation of MgO-Molecule.

Higher-Valence Elements.—If we bring a further electron to the inert gas shells, we get B (5), Al (13), Sc (21), Y (39), La (57), Ac (89). Now boron and aluminium are trivalent, forming compounds like BCl_3, and Al Cl_3 which show that all the three electrons are loosely bound. These elements are therefore called *three-valence* elements. Similarly C and Si, N and P, O and S, F and Cl, possessing respectively 4, 5, 6 and 7 electrons outside the closed helium, and neon shells are respectively known as 4, 5, 6 and 7-valence elements.

266. Periodicity of Spectra.—It has been found that not only the chemical properties, but the spectra of elements are repeated in the groups. This has been illustrated in Chaps. VII and IX, in the case of one and two-valence elements. It is not possible at this stage to discuss the spectra of other elements, but it was known from early studies that the spectra increases in complexity with the number of electrons outside the closed shells, and elements possessing similar properties like C and Si possess similar spectra. A rough idea of the increasing complexity of spectra shown by these elements is indicated in the scheme on page 416 which shows that complexity of spectra increases with the number of electrons in the incomplete shell.

267. Bohr's Theory of Electron-Composition of Atoms.—Before we proceed further with the properties of the remaining groups in the periodic table, we shall discuss how Bohr* sought to explain the results just discussed from his theory of atom structure and succeeded in giving a precise mathematical formulation to the vague ideas prevailing before his time. He pictured to himself a nucleus possessing a net charge Ze to which electrons are brought one after another, till the quota is full. The Z-electrons must be arranged in the different levels which have been brought to light as a result of X-ray analysis (*vide* Chap. XI). We have seen that these levels are denoted by the letters K, L, M, N, O . . . corresponding to the total quantum numbers $n=1, 2, 3, 4$ . . . etc. respectively. The question arises : how many electrons are required to fill up each of these levels completely ? Then again each of the levels L, M has been found to be multiple as a result of the experiments of Wagner and De Broglie on the absorption spectra of X-rays. How many electrons are needed to fill up each of these sub-levels ?

If we bring an electron to a bare nucleus Ze, it is clear that this is caught in a K-level, for n must be one, and $k=1$ and $E=-RhZ^2/1^2$. If we now bring a second electron, what will be its quantum characteristics ? An answer to this question is furnished from a study of the chemical and spectral properties of the element He which has a central charge $+2e$, and has two electrons. If we take He^+, we know that the normal level of the electron corresponds to $n=1$, $k=1$, and the energy is $-Rh. 2^2/1^2$. If now a second electron be brought to the He^+-ion, so as to complete the He-atom, what will be the quantum number of the normal state of this electron ? The electron now revolves in the field due to combined action of the nucleus and the first electron, and gives rise to the terms which are known from a study of the He-spectrum. The first ionisation potential of He has been found to be 24·5 volts, so that n must be 1. If n were 2, the I. P. would have been too small. The electron is therefore in the $1s$ or K-shell, and since He is an inert gas, it is supposed that the two electrons in the $1s$-shell form a closed group, *i.e.*, complete the shell. (For a description of the He-spectrum, see § 278).

When we turn to the next element Li, we find that it has three electrons. It is reasonable to suppose that the two inner electrons form a closed group, but the third electron is in a new shell L having $n=2$. This hypothesis is supported by the facts that the I. P. of Li is quite small, *viz.*, 5·37 volts, and the element is strongly monovalent, and electropositive in character, An analysis of the optical spectrum of Li tells us that the lowest orbit is $2^2S_{\frac{1}{2}}$, *i.e.*, the third electron is in the $2s$-shell.

---

* N. Bohr, *Zs. f. Phys.*, 9, 1, 1922; 13, 117, 1923; *Ann. d. Phys.*, 71, 228, 1923.

Bohr next made use of the idea that *similarity in chemical and spectral properties arises from similarity in the constitution of the incomplete electron-shell outside the closed levels.* The element next to Li which is similar to it in its properties is Na (11) and hence we have to postulate that for Na, there is only one loose electron, and this has the same quantum characteristics as the valency electron in Li. This is also supported from an examination of the optical spectrum of Na. The fundamental term is $3^2S_{\frac{1}{2}}$, and the electron must be in a new shell. Hence with Na, the M shell begins.

This shows that we must accommodate the electrons which are necessary to build up the intermediate elements from 4 Be to 10 Ne in the L-shell ($n=2$). The total number of electrons required to fill up completely the L-shell, *i.e.*, its sublevels L_1, L_2, L_3, *i.e.*, $2s$, $2p_1$ $2p_2$ is 8; and similarly the total number required to fill up the M_1, M_2, M_3, *i.e.*, $3s$, $3p_1$ $3p_2$ levels must also be 8. In this way the periodicity of properties of the second and third periods are explained.

268. Assignment of Proper Quota of Electrons to Sublevels: (Mainsmith-Stoner.)—But how are these 8 electrons distributed amongst the sublevels L_1, L_2, L_3 or $2s$, $2p_1$, $2p_2$? The correct assignment was given by Stoner* and Mainsmith†, and are shown below :—

L_1	L_2	L_3
$2S_{\frac{1}{2}}$	$2P_{\frac{1}{2}}$	$2P_{\frac{3}{2}}$
2	2	4

Two electrons are needed to fill up L_1, two to fill up L_2 and four to fill up L_3. The case of L_1 can be easily grasped, for it has the same k and j-values as K, and hence it can be saturated by the same number of electrons as K. This leaves 6 electrons for L_2,

---

* E. C. Stoner, *Phil. Mag.*, 48, 719, 1924.

† J. D. Mainsmith, *Jour. Soc. Chem. Ind.*, 44, 944, 1925.

L_3 combined. Stoner assigned 2 to L_2 and 4 to L_3, *but it is more in keeping with facts to combine the two levels and assign 6 electrons to 2p*. According to these conceptions, the constitutions of the elements from H to Ne are as follows :—

1. H. $1s$.

2 He	$\boxed{1s^2}$		
3 Li	$\boxed{1s^2}\,2s.$	11 Na	$\boxed{1s^2\ 2s^2\ 2p^6}\,3s$
4 Be	$\boxed{1s^2.}\,2s^2.$	12 Mg	$\boxed{1s^2\ 2s^2\ 2p^6}\,3s^2$
5 B	$\boxed{1s^2}\,2s^2,\ 2p.$	13 Al	$\boxed{1s^2\ 2s^2\ 2p^6}\,3s^2\ 3p$
6 C	$\boxed{1s^2}\,2s^2,\ 2p^2.$	14 Si	$\boxed{1s^2\ 2s^2\ 2p^6}\,3s^2\ 3p^2$
7 N	$\boxed{1s^2}\,2s^2,\ 2p^3.$	15 P	$\boxed{1s^2\ 2s^2\ 2p^6}\,3s^2\ 3p^3$
8 O	$\boxed{1s^2}\,2s^2,\ 2p^4$	16 S	$\boxed{1s^2\ 2s^2\ 2p^6}\,3s^2\ 3p^4$
9 F	$\boxed{1s^2}\,2s^2,\ 2p.^5$	17 Cl	$\boxed{1s^2\ 2s^2\ 2p^6}\,3s^2\ 3p^5$
10 Ne	$\boxed{1s^2 \mid 2s^2,\ 2p^6}$	18 A	$\boxed{1s^2\ 2s^2\ 2p^6\ 3s^2\ 3p^6}$

In this scheme $1s$ stands for K, $2s$ for L_1, $2p$ for L_2 and L_3 combined, for X-ray levels have been found to have the same characteristics as the alkali levels. $1s^2 \ldots$ denotes that there are 2 electrons in the $1s$ or K-shell. $2p^5 \ldots$ denotes that there are 5 electrons in the $2p$-shell. The $2p$-shell is filled completely when 6 electrons are brought to it. Then we get an inert gas Ne. The inert gas structure is enclosed within a cartouche. When the $2p$-levels have been filled a fresh period begins. This is shown in the second column.

269. Spectra of Alkali Elements.—The above hypothesis regarding the electron composition of atoms not only explains the periodic properties, but along with a few other principles, gives a complete qualitative explanation of the spectra of all elements, optical as well as X-ray.

We shall first discuss the spectra of alkali elements as prelude to the general study of spectra of elements.

The electron composition of the alkali-metals are shown below :—

3 Li	$\boxed{1s^2}2s$	$Be^+, B^{++}, C^{+3}, N^{+4} \ldots$
11 Na	$\boxed{1s^2 2s^2 2p^6}3s$	$Mg^+, Al^{++}, Si^{+3}, P^{+4} \ldots$
19 K	$\boxed{1s^2 2s^2 2p^6 3s^2 3p^6}4s$	Ca^+, Sc^{++}
37 Rb	$\boxed{1s^2 2s^2 2p^6 3s^2 3p^6 3d^{10} 4s^2 4p^6}5s$	Sr^+
55 Cs	$\boxed{1s^2 2s^2 2p^6 3s^2 3p^6 3d^{10} 4s^2 4p^6 4d^{10} 5s^2 5p^6}6s$	Ba^+

We see from the above scheme that for each alkali element, as well as for such ionised elements which are reduced by electrical discharge to the alkali stage (*vide* elements to the right of each in the above representation), we have normally one single electron in the *ns*-shell, outside the closed atomic core. This electron imparts to the elements not only their common chemical properties, but also account for the similarity of their spectra. The quantum mechanical state of the electron in the normal state may be completely represented according to a new system of notation introduced by Russell and Saunders by the symbol :

$$n^2S_{\frac{1}{2}}$$

where n . . . denotes total quantum number ; it is 2 for Li-group, 3 for Na-group, etc. . .

S . . . it denotes that the l-quantum number $=0$, so that the magnetism of Na-atoms in Stern and Gerlach's experiment arises from the spin of the valency electron alone.

$\frac{1}{2}$ . . . inner quantum number of the electron in the *s*-state. For

$$j = |\,l+s\,| = |\,0+\tfrac{1}{2}\,| = \tfrac{1}{2}.$$

i.e., we have to deal with a spinning electron possessing the rotational moment of inertia $\frac{1}{2}\,\frac{h}{2\pi}$, moving in the field of the atomic core.

The problem of the motion of the electron in such a case, *e.g.*, in Na-like atoms may be treated in the same way as the problem of the spinning electron round the bare nucleus, provided the field due to the atom core can be properly taken account of. For the general case of Na-like atoms, the nuclear charge is Ze, surrounded by a K-shell of two electrons, and L-shell of eight electrons. The action of these shells may be supposed to be represented by a charge $-\sigma e$, concentrated at the centre. 'σ' is known as the *screening constant*. We have then

$$-n^2S_{\frac{1}{2}} = \frac{R(Z-\sigma)^2}{n^2}$$

But in Chap. VIII, the energy of the *normal* term was empirically represented by

$$1s = \frac{RZ^2}{(1+s)^2}$$

where Ze = net nuclear charge. In this case, the total quantum number was taken to be 1, whereas now it is taken to be $n=2$ for Li, 3 for Na . . . etc . . . The two representations appear to be contradictory to each other.

But it will be shown later that the present assignment is the only theoretically sound one possible. The representations used by spectroscopists were only empirical and must now be revised.

The Excited States of Alkali Elements.

The further excited states of alkali elements are obtained by increasing successively the quantum numbers of the valency electron. For sodium-like atoms, they are graphically represented in the following diagram (Fig. 5). Normally the optical electron is at $3s$ which gives the normal term $^2S_{\frac{1}{2}}$. The next transitions are shown by the symbol (1). We get

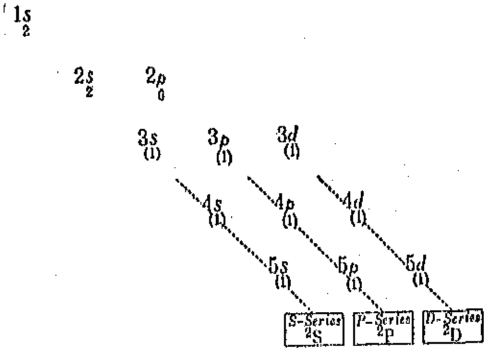

Fig. 5. Structure diagram of Na.

successively ²P, ²D-terms. All terms arising from a diagonal displacement form the successive members of a Rydberg sequence.

From the above Fig. 5, we find that after the normal $3s$ orbit, the next orbit of the electron is $3p$, yielding the pair of terms:

$$3\ {}^2\mathrm{P}_{\frac{1}{2}} \ \ldots\ 2p_1 \text{ of Paschen} = 24489{\cdot}31 \text{ cm}^{-1}$$

$$3\ {}^2\mathrm{P}_{\frac{3}{2}} \ \ldots\ 2p_2 \ \ldots\ldots = 24472{\cdot}10 \text{ cm}^{-1}$$

We are again using the Russell-Saunders notation. 'P' denotes that l of the orbit equals 1. The state has two possible energy values according as the vectors l and s are in the same or opposite directions, *i.e.*, according as the spin-moment is parallel or anti-parallel to the orbit moment of the electron.

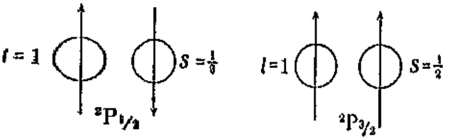

Fig. 6. The formation of p-terms.

The calculation of this separation has already been given in § 221.

We shall confine our attention to the main energy term of the electron moving in the p-orbit. We may represent the energy as being given by

$$3\ {}^2\mathrm{P} = -\frac{Rh\,(Z-\pi)^2}{3^2}$$

where π = screening factor due to the $2s^2\ 2p^6$ - electrons, when the valency electron is in the $3p$-orbit. 'π' is different from 'σ', since the electron now affects the inner shell in a different way (*vide* §239).

The origin of the other terms, and of the Rydberg sequences is represented graphically in Fig. 5. Each term excepting those forming the S-family has a double value on account of the interaction between s and l. The origin of the Rydberg sequence is also clearly indicated in the diagram.

270. The Irregular Doublet Law.—The correctness of the above assignment of *total quantum* numbers is supported by an empirical law due to Millikan and Bowen which aimed at correctly locating the resonance lines $n^2\mathrm{S}$—$n^2\mathrm{P}$ of each group of elements stripped by electrical discharge of its outer electrons so as to be reduced to an alkali-like structure. We illustrate the case by taking the Na-group.

The energy-value of the normal term is

$$3\ {}^2\mathrm{S} = \frac{Rh\,(Z-\sigma)^2}{3^2}$$

The energy-value of the p-terms, disregarding the spin interaction is

$$3^2P = -\frac{Rh\,(Z-\pi)^2}{3^2}$$

We have therefore

$$\nu = {}^2S - {}^2P = \frac{(Z-\pi)^2}{3^2} - \frac{(Z-\sigma)^2}{3^2} = AZ + B$$

where $A = \frac{2(\sigma-\pi)}{9}$, $B = -\frac{\sigma^2 - \pi^2}{9}$

Now supposing that σ and π, the screening factors of $1s^2\ 2s^2\ 2p^6$ shells due to the valency electron in the $3s$ and $3p$ orbits, do not vary as the nuclear charge is varied, the following conclusion can be easily drawn :

The frequencies of the resonance lines of the Na-like elements, *i.e.*, elements which are reduced by electrical discharge to 11 electrons like Na, *e.g.*, Mg^+, Al^{++}, Si^{+++} and for a similar reason of the other groups of alkali-like elements, will form to a first approximation, an arithmetic progression. This was found to be actually the fact as illustrated in the following table.

Table 2.—Illustration of the irregular doublet law.

Element	11 Na	12 Mg^+	13 Al^{+2}	14 Si^{+3}	15 P^{+4}	16 S^{+5}	17 Cl^{+6}	18 A^{+7}
${}^2S_1 - {}^2P_1$ $3s - 3p$	16961	35669	53680	71280	88649	105866	123001	
		18713	*18011*	*17600*	*17369*	*17217*	*17135*	
${}^2P_2 - {}^2D_2$ $3p - 3d$	12199	35730	62037	88672	114755	140313		
		23531	*26307*	*26635*	*26083*	*25558*		
${}^2D_3 - {}^2F_3$ $3d - 4f$	5415	22308	51658	93782	148386	215206		
		16893	*29350*	*42124*	*54604*	*66820*		
${}^2D_2 - {}^2F_2$ $3d - 4f$	5492	20354	41351	66640				
		14862	*20997*	*25289*				
${}^2S_1$ cm^{-1}	41449	121267	229548	364177	524491	709560	920160	
I.P. in volts	5·12	14·97	28·32	44·95	64·7	87·6	113·6	

Note.—This conclusion was first drawn by Millikan and Bowen* from a study of the curves given by G. Hertz† about the values of the X-ray energy levels of L_1, L_2 (*vide* p. 449). As stated in §235 Hertz showed that

$$\sqrt{\nu_{L_1}}-\sqrt{\nu_{L_2}} = \text{constant} \quad . \quad . \quad . \quad . \quad . \qquad (2)$$

The law is explained if we assume that for the L-shell

$$\sqrt{\frac{\nu_{L_1}}{R}}=\frac{Z-\sigma}{2},\ \sqrt{\frac{\nu_{L_2}}{R}}=\frac{Z-\pi}{2},$$

i.e., the screening constants in the two levels do not vary as the nuclear charge is increased. Millikan and Bowen extended this rule to the optical region in the way mentioned above, though the two cases are not exactly parallel.

It is apparent that the above deduction of the irregular doublet law is of the roughest nature possible, and cannot stand closer scrutiny. Yet in the hands of Millikan and Bowen, it served as a valuable clue for identifying the resonance lines of elements reduced by an exceptionally strong electrical discharge to the one-valence state (stripped atoms). This was done by passing a spark between the electrodes under very high vacuum (the method of hot sparks). Under such conditions, no spark usually passes between the electrodes (no discharge state), but when these are very close, electrons are pulled out by the large electrical field, and these ionise the atoms to such an extent that they lose most of their outer electrons. For example if we take Si, we can get by these methods, the spectra of Si, Si+, Si++, Si+++ and possibly of higher stages of ionisation all mixed together. How can one, from such a medley of experimental data, pick out the lines of the element in any particular stage of ionisation ?

Millikan and Bowen showed that for the alkali-like elements, the pair of resonance lines can be easily picked out with the aid of the semi-empirical rule, as illustrated in table 2.

It is clear that the rule should hold only for all transitions for which the total quantum number does not change. If $\Delta n \neq 0$, the rule should not hold, as shown in the $3d$-$4f$-series. For these and other extensions, various papers* which have appeared on the subject may be consulted.

271. Calculation of Term Values : Penetrating and Non-Penetrating Orbits.

271. Calculation of Term Values : Penetrating and Non-Penetrating Orbits.—We shall now consider the general problem of calculation of the term-values for the alkali elements from the atomic model. The general alkali element may be taken to consist of a nucleus, round which we have a number of electrons forming closed shells as in an inert gas. This structure is what is known as the *atom core.* The valency electron revolves round the core in orbits whose n and k are given. A rough idea of the dimensions of the core can be obtained from indirect evidences such as intensity of X-ray reflection in crystals.* The values for the alkali elements are shown below, where r stands for the radius of the atom core, a_0 that of the normal hydrogen orbit, and ζ=ratio of the dimension of atom core and that of H-orbit.

---

* Millikan and Bowen, *Phys. Rev*., **24**, 209, 1924; **25**, 295, 1925. M. N. Saha and P. K. Kichlu, *Indian Journal of Physics*, **2**, 319, 1928.

† G. Hertz, *Zs. f. Phys*., **3**, 19, 19.

Table 3.—Radius of the atom core.

Ion	Li+	Na+	K+	Rb+	Cs+	
r	·28	·41	·82	1·20	1·48	Å. Units
$\zeta=r/a_0$	·53	·77	1·54	2·26	2·80	

If the core continued to remain undisturbed during the motion of the valency electron, the compensating field which it produced might be put equal to that of concentrated charge $Z_a e$ at the centre, where Z_a is the number of electrons in the core. In this case, the screening constant would be simply Z_a, and the energy value would be $-Rh(Z-Z_a)^2/n^2$, where n = total quantum number of the orbit. For Na, this would mean that the energy of the electron in the $3p$, $3d$ or $3s$ orbits would be the same, *viz.*, $-Rh/3^2$. But a glance at the term-values shows that this is far from being the case.

For illustration, we represent the term values by effective total quantum number in table 4. We put

$$T = R/n_e^2 \text{ or } n_e = \sqrt{R/T} \quad . \quad . \quad . \quad . \quad (3)$$

n_e may be called the *effective total quantum number.* This can be easily calculated when the term-value is known. Thus for Na $3s\ {}^2S_{\frac{1}{2}}$, $T = 41449·0$, and n_e can be easily shown to be 1·63. For $3p\ {}^2P_{\frac{1}{2}}$, $n_e = 2·12$ . . . , etc.

---

* *Vide* Chap. VI, § 134.

Table 4.—Term-values for Na-spectrum and the effective quantum number n_e.

$n =$	3	4	5	6
s $l=0$	41,449·0 1·63	15,709·5 2·64	8,248·3 3·65	5,077·3 4·65
p $l=1$	24,475·7 2·12	11,176·1 3·14	6,406·3 4·14	4,151·3 5·14
d $l=2$	12,276·2 2·99	6,900·4 3·99	4,412·5 4·99	3,061·9 5·99
f $l=3$		6,860·4 4·00	4,390·4 5·00	3,043·0 6·00

A glance at this table shows that n_e for the d and f-terms are very nearly equal to the total quantum number, while for the s and p terms, n_e strongly deviates from n. Thus for the $3s$-orbit, $n = 3$, but $n_e = 1·63$; the same is true for the other s-orbits. For the $3p$-orbits, $n = 3$, but $n_e = 2·12$ . . . etc. . . . In fact we can classify the orbits into two classes* (1) *non-hydrogenic* orbits, *e.g.*, the s and p orbits in the case of Na where n_e strongly deviates from n, (2) *hydrogenic orbits, e.g., d, f* orbits for Na where n_e is very nearly n.

The physical argument for the existence of the two different classes of orbits was first given by Schrödinger.† He showed that the non-hydrogenic orbits are those which, on Sommerfeld's orbital theory, are strongly eccentric; *e.g.*, for the ns-orbits of Na, we have $\varepsilon = (1-k^2/n^2)^{\frac{1}{2}}$ and for $3s$, $\varepsilon = ·943$, for $4s$, $\varepsilon = ·968$, for $3p$, $\varepsilon = ·745$. Those for which the eccentricity is zero or small continue to be hydrogenic; thus for both $3d$ and $4f$, $\varepsilon = 0$.

The correctness of this explanation is readily seen if we review the term-values and values of the effective total quantum number for the other alkalies. This is calculated in table 5 and shown graphically in Fig. 6. It is seen there that for Li only s-orbits are non-hydrogenic, the p-orbits are hydrogenic. This is apparent from the fact that for Li, the first p-orbit is $2p$, $n = 2$, $k = 2$, $\varepsilon = 0$, while

---

* Good accounts of this subject will be found in Sommerfeld's *Atombau* . . . (4th Edition), §4 ; W. Grotrian, *H. d. Astrophysik*, 3/2, Chap. 5.

† E. Schrödinger, *Zs. f. Phys.*, 4, 347, 1921.

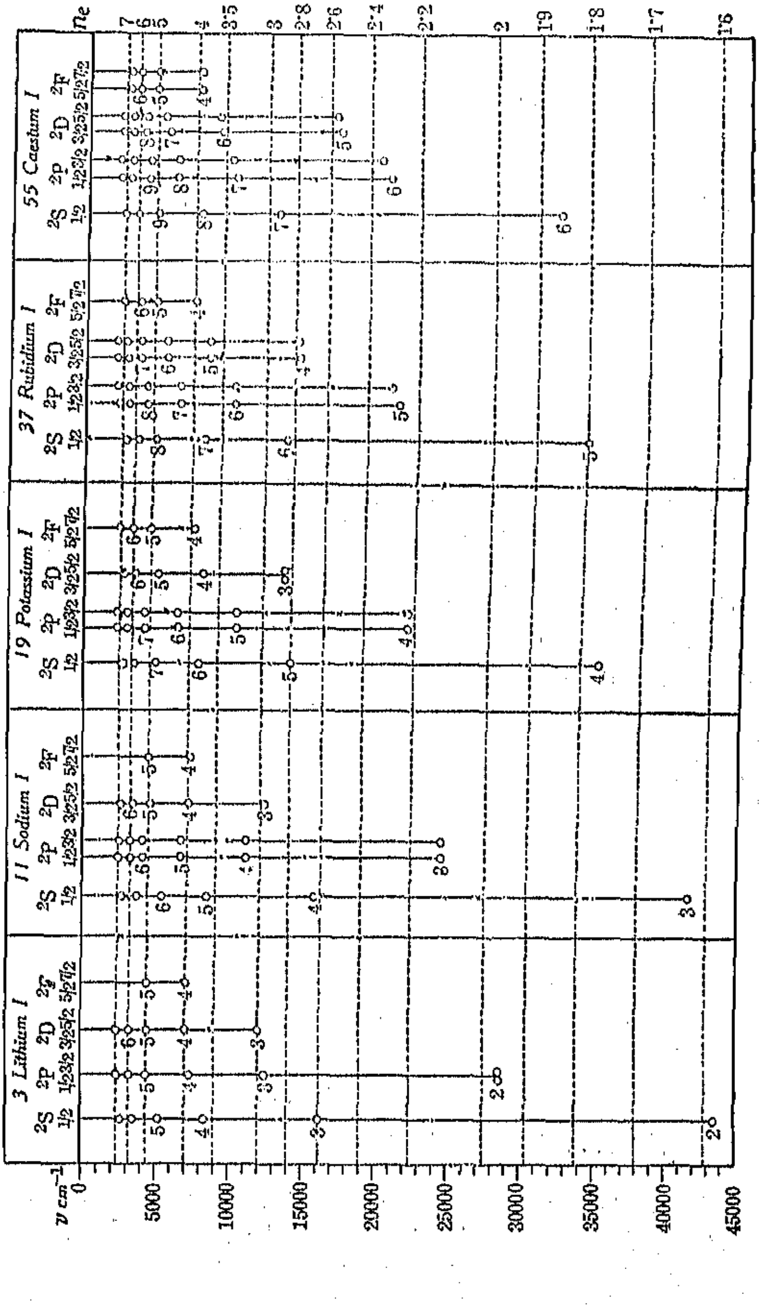

Fig. 6. The hydrogenic and non-hydrogenic terms of alkali elements Li, Na, K, Rb, Cs.

for Na the case is otherwise, for Rb even the *d*-orbit is non-hydrogenic, for $4d$ is the first *d*-term and

$$\varepsilon = (1-3^2/4^2)^{\frac{1}{2}} = \sqrt{7}/4 = \cdot 65$$

Let us now see why in strongly eccentric orbits, the term-values become non-hydrogenic. The argument first given by Schrödinger is as follows :—

Table 5.—The effective quantum number for the S, P, D-terms of alkali elements.

Total Quantum number n	Lithium			Sodium			Potassium			Rubidium			Ceasium		
	S	P	D	S	P	D	S	P	D	S	P	D	S	P	D
2	1·59	1·96													
3	2·596	2·956	2·998	1·627	2·117	2·991	...	...	2·854	...	...	2·767	...	...	2·548
4	3·598	3·954	3·998	2·643	3·133	3·988	1·771	2·232	3·80	...	...	3·736	...	..	3·528
5	4·60	4·955	5·0	3·647	4·138	4·987	2·80	3·263	4·770	1·811	2·280	4·698	...	...	4·525
6	5·60	5·950	6·0	4·640	5·141	5·987	3·761	4·270	5·758	2·845	3·317	5·677	1·870	2·33	5·524

It has been shown in §174, that an n_k-orbit in the hydrogen atom possesses the eccentricity

$$\varepsilon = (1-k^2/n^2)^{\frac{1}{2}}$$

and the distance of nearest approach of the electron to the nucleus is

$$d = a\,(1-\sqrt{1-k^2/n^2})$$

$$= \frac{a_0 n^2}{Z}\,(1-\sqrt{1-k^2/n^2})$$

It is clear that when $k \ll n$, the orbit is too much eccentric, and the valency electron may approach very close to the inner shell particularly in the case of the *s*-orbits, as shown below :—

	$1s$	$2s$	$3s$	$4s$ ....
d/a_0	1	·536	·522	

When we take the one-valence elements and ions, *e.g.*, the Na-like atoms, the normal orbit is $3s$ and the radius of the normal Na-atom has been estimated to be ·77 Å. units. Supposing the calculations for hydrogen apply to this case, the distance of nearest approach of the valency electron to the nucleus is ·40Å units. But the radius of the Na$^+$-core has been estimated from measurements of intensity of X-ray reflection to be ·41Å units. Hence we find that the electron in the 3s and other higher 4s-states approach very close to the core. Schrödinger supposed that in these and similar cases when the electron approaches too close to the inner core, it penetrates the latter. What will be its subsequent motion? It is clear that now the electric field will be greatly enhanced, as the screening due to outer electrons is partly removed, and hence the electron will describe an eccentric orbit of smaller dimensions. After describing this orbit, it may be expected to come out, and describe the remaining part of the outer orbit. The supposed path is represented in the following Fig. 7.

For such penetrating orbits, calculation of term-values is somewhat complex, and this is carried out in the next section. But it can be inferred even without these calculations that the energy values of these terms will diverge greatly from the hydrogenic values, *i.e.*, from RZ^2/n^2.

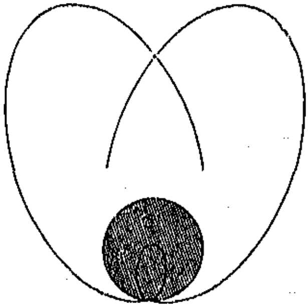

Fig. 7. The penetrating orbit.

272. Term-values for Penetrating Orbits.*

—Starting from Schrödinger's ideas, Van Urk† gave an approximate calculation of the energy value of the electron for a penetrating orbit of alkali-like elements. The atom is supposed to consist of the inert-gas-like core round which the valency electron moves in the n_k -orbit The core is assumed to have the radius ζa_0. Beyond the distance ζa_0, the valency electron moves in a field which is due to an effective charge z which is 1 for a neutral atom like Na, 2 for a singly ionised atom (Mg$^+$) 3 for a doubly ionised atom (*e.g.*, Al^{++}), etc. The charge on the outermost layer of the core is taken to be z_s (*e.g.*, for Na, it is $2s^2$ $2p^6$ $z_s = 8$), so that when the valency electron penetrates this outer shell, the effective nuclear charge under which it moves becomes

---

* The treatment given here has been adapted from that given in Pauling and Goudsmit's "*Structure of Line Spectra,*" Chap. III, where all the references will be found.

† Th. Van Urk, *Zs. f. Phys.*, **13**, 268, 1923.

$\varkappa_s + \varkappa$. The expressions for the potential energy are now respectively

$$V(r) = -\frac{\varkappa e^2}{r} \ldots \text{for } r > \zeta a_0 \ldots\ldots \text{(outside the core)} \quad . \quad . \quad (4)$$

$$= -\frac{(\varkappa_s + \varkappa)e^2}{r} + \frac{\varkappa_s e^2}{\zeta a_0} \ldots \text{for } r < \zeta a_0 \ldots \text{(inside the core)}. \; (4')$$

$\varkappa_s e^2/\zeta a_0 \ldots$ is the constant potential of the outer shell of the core inside itself.

It is clear, from Fig. 7, that the complete orbit consists of two parts, (1) a part lying outside the core which is segment of one ellipse which may be called the *outer*, and (2) a part lying inside the shell which is segment of another ellipse which may be called the *inner*. The inner ellipse is much smaller than the outer. The dimensions of these ellipses may be calculated in the usual way.

The Hamiltonian for the motion of the electron is

$$H = \frac{1}{2m}(p_r^2 + p_\theta^2/r^2) + V(r) = W \quad . \quad . \quad . \quad . \quad (5)$$

where W the energy constant. Now $p_\theta = kh/2\pi$ and this is common to both the ellipses.

The value of n_r is given by the integral

$$n_r h = \int \sqrt{2m\left(W + \frac{\varkappa e^2}{r}\right) - \frac{k^2 h^2}{4\pi^2 r^2}}\, dr$$

$$+ \int \sqrt{2m\left[W + \frac{(\varkappa + \varkappa_s)e^2}{r} - \frac{\varkappa_s e^2}{\zeta a_0}\right] - \frac{k^2 h^2}{4\pi^2 r^2}}\, dr.$$

The integration is to extend over the whole orbit. It is not possible to carry out the integration unless the form of the orbit is known. When the form is known, W can be expressed as a function of (k, n_r), but on account of the introduction of unknown quantities like $\varkappa_s$, ζa_0 which should be as far as possible eliminated, W is no longer simply $-R\varkappa^2/(n_r + k)^2$ as in the case of hydrogen. Van Urk gives an approximate solution in the following way. The part of the orbit external to the core, being too much eccentric, may be supposed to be almost a complete ellipse. We may put for the external region

$$(a) \qquad W = -\frac{\varkappa^2 e^2}{2a_0 n_a^2} = -\frac{R^2 \varkappa^2}{n_a^2}$$

where n_a is the outer effective quantum number.

The semi-major axis $= a_0\, n_a^2/\varkappa$ and we may be put $n_a = k + n_{ra}$ where

$$n_{ra}\, h = \oint \sqrt{2m\left(W + \frac{\varkappa e^2}{r}\right) - \frac{k^2\, h^2}{4\pi^2\, r^2}}\; dr.$$

It is clear that n_{ra} may be fractional, as the outer part of the orbit is alone considered. It can now be shown that the part of the orbit inside the core is also a complete orbit which passes out into the outer orbit (*a*) somewhat as shown in Fig. 7. For this region, we have

$$(b) \quad W = -\frac{(\varkappa + \varkappa_s)^2 e^2}{2a_0\, n_b^2} + \frac{\varkappa_s\, e^2}{\zeta a_0} = -\frac{R\,(\varkappa + \varkappa_s)^2}{n_b^2} + \frac{2R\varkappa_s}{\zeta} \quad . . (6)$$

where n_b is the inner total quantum number and $n_b = k + n_{rb}$, where

$$n_r\;\; h = \oint \sqrt{2m_0\left[W + \frac{(\varkappa + \varkappa_s)\, e^2}{r} - \frac{\varkappa_s\, e^2}{\zeta a_0}\right] - \frac{k^2 h^2}{4\pi^2\, r^2}}\;.\;\; dr$$

over the inner ellipse, and semi-major axis $= a_0\; n_b^2/\,(\varkappa + \varkappa_s)$

Let us see if (*b*) is consistent with our picture. The energy must be the same for both orbits, hence we have

$$\frac{\varkappa^2}{n_a^2} = \frac{(\varkappa + \varkappa_s)^2}{n_b^2} - \frac{2\varkappa_s}{\zeta}$$

Now $(\varkappa + \varkappa_s) \gg \varkappa$, but $n_a \cong n_b$, hence we have

$$\frac{(\varkappa + \varkappa_s)^2}{n_b^2} \cong \frac{2\varkappa_s}{\zeta}$$

or

$$\frac{2a_0\; n_b^2}{\varkappa + \varkappa_s} \cong \zeta a_0\; \frac{\varkappa + \varkappa_s}{\varkappa_s} \cong \zeta a_0$$

Now $2a_0 n_b{}^2/(\varkappa + \varkappa_s)$ is the major axis of the inner orbit and it is less than ζa_0, the radius of the core. Hence the valency electron, on penetrating into the core describes a complete ellipse. We have seen that the path outside the core may be taken to be an almost complete ellipse. But there must be a steady and continuous passage from the outer orbit to the inner. Hence we may take that the complete path is as depicted in Fig. 7, consisting of a big outer ellipse and a small inner ellipse, which pass continuously from the one to the other. A minimum value for n_e the effective total quantum number for which this assumption can hold good may be obtained from the observation that the aphelion distance of the electron in the inner orbit must be at least equal to ζa_0, otherwise the electron will never come out of the core. This gives us the condition

---

* See also M. Born, *Vorlesungen über Atom mechanik*, Chap. 3, p. 194.

$$\frac{a_0\, n_b^2}{z + z_s}\,(1 + \varepsilon) = \zeta a_0$$

where $$\varepsilon = \sqrt{1 - k^2/n_b^2}$$

From these two equations, we obtain after some work

$$n_b = \frac{\zeta(z + z_s)}{\sqrt{2\zeta(z + z_s) - k^2}} \quad . \; . \; . \; . \; . \; . \; . \quad (7)$$

From what has been just said it is clear that $n_r = n_{ra} + n_{rb}$

But $$n_b = n_{rb} + k = n - n_{ra}$$

Hence $$n_{rb} = \frac{\zeta(z + z_s)}{\sqrt{2\zeta(z + z_s) - k^2}} - k \quad . \; . \; . \; . \; . \; . \; . \; . \quad (8)$$

Now $$\triangle = n - n_a = n_b - k$$

gives us the value of *quantum defect*.* According to wavemechanics, we can replace k^2 by $l\,(l + 1)$ and k by $(l + \frac{1}{2})$. Then from (8) we obtain

$$n_{rb} = \triangle = \frac{\zeta(z + z_s)}{\sqrt{2\,\zeta(z + z_s) - l\,(l + 1)}} - (l + \tfrac{1}{2}) \quad . \; . \quad (8a)$$

This formula shows that the quantum defect is independent of the total quantum number n, and thus is approximately the case as is clear from Fig. 6 and Table 5.

Further the value of ζ for the ions of the alkali elements can be obtained from X-ray data, and $\triangle$ may be actually calculated by taking $z_s = 2$ for Li and 8 for Na and other alkalies. The agreement between calculated and observed values is shown in Table 6.

273. The Term-values for Hydrogenic Orbits : Polarisation of the Atomic Core.—Even the term-values of the orbits which are not eccentric like the $3d$-term of Na is not exactly equal to R/n^2, but differ slightly from it. The defect is of the order of ·01 in the total quantum number. Born and Heisenberg† suggested that

---

* It will be noticed that n_a is the same as n_e defined by eqn. (3).

† Born and Heisenberg, *Zs. f. Phys.*, 4, 347, 1921.

Table 6.—Observed and calculated values of Rydberg correction Δ for the alkali elements.

	S		P		D	
Element	Observed	Calculated	Observed	Calculated	Observed	Calculated
Li	0·40	0·39	0·04	...	0·00	...
Na	1·35	8·36	0·85	0·51	0·01	...
K	2·19	2·14	1·71	1·23	0·25	0·47
Rb	3·13	2·70	2·66	1·78	1·34	0·96
Cs	4·06	3·05	3·59	2·13	2·46	1·28

this might be due to the polarisation of the core in the field of the valency electron, the effect of which is to add a small term to the expression for force due to the point-nucleus.

It is proved, in treatises on Classical Electricity and Magnetism (*vide* Jeans, *Electricity and Magnetism* p. 130) that when a small spherical metallic conductor is placed in an electrical field F the conductor becomes polarized, *i.e.*, positive electricity accumulates on one side, and negative electricity on the other. The electric moment of the induced dipole is αF, where α is called the polarizability of the ion and this is equal to a^3, where a is the radius of the sphere. The energy of polarisation is equal to $-\frac{1}{2}\, a^3 F^2$.

Now since in an alkali atom, $F = -e/r^2$, we have the polarisation energy equal to $-a^3 e^2/(2r^4)$. This is to be added to the usual energy $-e^2 Z/r$, and its value is small compared to the Coulombian energy $-e^2 Z/r$. The polarisation energy can therefore be treated as a perturbation term and its average value can be calculated with the aid of wavemechanics. The expression for energy for such an orbit now becomes

$$W = -\frac{RZ^2}{(n-\delta)^2} = -\frac{Z^2 e^2}{2a_0\, n^2} - \frac{a^3 e^2}{2}\left(\overline{\frac{1}{r^4}}\right) \quad . \quad . \quad . \quad . \quad (9)$$

Expanding in powers of δ/n, and remembering that δ is a small quantity, we have

$$\delta = \frac{n^3 a_0\, a^3}{2Z^2}\left(\overline{\frac{1}{r^4}}\right)$$

The value of $\left(\overline{\frac{1}{r^4}}\right)$ can be obtained from wavemechanics (*vide* Smekal, *Quanten*, p. 286). We have then*

$$\delta = \frac{3\,a^3 Z^4 \left\{ 1 - \dfrac{l\,(l+1)}{3n^2} \right\}}{4a_0{}^3\,(l-\frac{1}{2})\,(l+\frac{1}{2})\,(l+1)\,(l+3/2)} \quad . \quad . \quad . \quad . \quad . \quad (10)$$

The values of δ calculated for the *d*-series of Na with the aid of (10) are shown in table 6*a*.

Table 6a.—The quantum defect δ *for the d-terms of Na.*

$n =$	3	4	5	6	7	8	∞
δ observed	0·010	0·0112	0·0126	0·0124	0·0125	0·0110	...
δ calculated	0·009	0·0102	0·0107	0·0110	0·0111	0·0112	0·0116

The value of a in eqn. (10) necessary for the above computation has been calculated for a number of ions (including alkali and alkaline earth) by Pauling† theoretically by introducing suitable screening constants in the wave-mechanical expression for the polarizability of hydrogen-like orbits. He obtains for Na⁺ $a = 0{\cdot}18 \times 10^{-24}$. For details of this calculation see his original paper. The values of polarization or atomic refraction have also been experimentally obtained by Fajans and Joos‡, Heydweiller§, and Wasastjerna‖ from measurements of refraction of their salt-solutions. From these data a can be easily calculated¶.

274. The Modified Regular Doublet Formula (Landé).—

According to § 221, the doublet separation for the terms of one-valence elements is given by

$$\Delta\nu = 5{\cdot}82\,\frac{(Z-\sigma)^4}{n^3\,l\,(l+1)}\ \text{cm}^{-1} \quad . \quad . \quad . \quad . \quad . \quad (11)$$

---

* I. Waller, *Zs. f. Phys.*, **38**, 635, 1926.

† L. Pauling, *Proc. Roy. Soc. A*, **114**, 181, 1927.

‡ K. Fajans and G Joos, *Zs f. Phys.*, **23**, 1, 1924. See also Born and Heisenberg's discussion, *Zs. f. Phys.*, **23**, 388, 1924.

§ A. Heydweiller, *Phys. Zeits.*, **26**, 526, 1925.

‖ I. A. Wasastjerna, *Comm. Phys. Math. Soc. Sc. Fennicae*, **1**, 38, 1921.

¶ This calculation depends upon the relation $R = \frac{4}{3}\pi N\alpha$, where R denotes the atomic refraction defined by $R = V\,(n^2-1)/(n^2+2)$, where V = gm. atomic volume, n = refractive index and N = Avagadro number. For details see Debye, *Polar Molecules* (1929), p. 12, 61.

This expression should hold only for hydrogenic orbits. For penetrating orbits it is clear that the formula has to be modified, and an approximate value was given by Landé.* It is needless to repeat the calculations for which the original paper may be consulted. The final formula may be quoted. This is

$$\triangle\nu = 5{\cdot}82\ \frac{(z+z_s)^2\ z^2}{n_e{}^3\ l\,(l+1)}\ \mathrm{cm}^{-1}\quad .\ .\ .\ .\ .\ .\ (12)$$

Comparing with formula (11), we find that the difference consists in substituting

$$(z + z_s\ )^2\ z^2 \text{ for } (Z-\sigma)^4,$$

and n_e the effective quantum number, for n the theoretical total quantum number.

275. Spectra of Two-valence Elements.—A general description of the spectra of two-valence elements has been given in Chapter IX. In this section, we shall deal with their theoretical explanation. In the spectra of alkali elements we had to deal with the motion of one single electron in the field of a magnetically neutral core. But here besides the core we have to deal with two electrons, which influence each other by their electric and magnetic interactions. This case therefore brings out new features and principles, a thorough grasp of which is essential to the understanding of spectra of atoms in general.

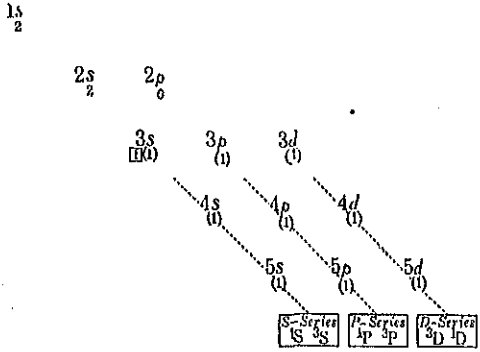

Fig. 9. Structure diagram of Mg.

As typical of this class, we take Mg possessing normally the structure

$$12\ \mathrm{Mg}\ \ldots\ \boxed{1s^2\ 2s^2\ 2p^6.}\,3s^2$$

The normal structure is $3s^2$ and the excited states are obtained by keeping one electron in the lowest level $3s$ and increasing the quantum number of the other in successive steps, *i.e.*, by putting it in the orbits $3p$, $3d$, $4s$, $4p$ .... as shown graphically in Fig. 9.

---

* Landé, *Zs. f. Phys.*, 25, 46, 1924.

The above diagram represents the fact that excited states are obtained by keeping one electron in $3s$, and allowing the other to run through higher levels. The correlation between electron-composition and the observed optical terms are shown in the following table.

Table 7.—Term values of MgI (12).

S-terms		P-terms		D-terms	
Electron structure	Terms	Electron structure	Terms	Electron structure	Terms
$3s^2$	$^1S_0 = 61672{\cdot}1$	$3s\ 3p$	$^1P_1 = 26620{\cdot}7$ $^3P_0 = 39821{\cdot}3$ $^3P_1 = 39801{\cdot}4$ $^3P_2 = 39760{\cdot}5$	$3s\ 3d$	$^1D_2 = 15268{\cdot}9$ $\left.\begin{array}{l}{}^3D_1\\{}^3D_2\\{}^3D_3\end{array}\right\} = 13714{\cdot}7$
$3s\ 4s$	$^1S_0 = 18160$ $^3S_1 = 20474$	$3s\ 4p$	$^1P_1 = 12325{\cdot}5$ $^3P_0 = 13824{\cdot}1$ $^3P_1 = 13824{\cdot}1$ $^3P_2 = 13820$	$3s\ 4d$	$^1D_2 = 8537{\cdot}4$ $\left.\begin{array}{l}{}^3D_1\\{}^3D_2\\{}^3D_3\end{array}\right\} = 7479{\cdot}5$
	↓ *s*-sequence		↓ *p*-sequence		↓ *d*-sequence

276. The Russell-Saunders' Notation.—Here in describing the terms, we have introduced the Russell-Saunders' notation which can be fully explained now. We write

$$\begin{array}{lcccccccc} & S, & P, & D, & F, & G, & H, & I, & J\ldots\ldots \\ \text{for} & l=0, & 1, & 2, & 3, & 4, & 5, & 6, & 7\ldots\ldots \end{array}$$

The multiplicity is indicated by the corresponding integral number, added as a superscript to the left of these capital letters. Thus ^3P denotes triplet p-terms. ^5D denotes a quintet d-term. The inner quantum number is denoted by the corresponding number added as a subscript as in $^3P_0$, $^3P_1$, $^3P_2$ .... An integral number placed before the symbol denotes the total quantum number. Thus

$5\,^4P_{\frac{3}{2}}$ .... denotes a quartet p-term, having $j = \frac{3}{2}$,

the total quantum number being 5. The total quantum number is very often omitted.

Sometimes for purposes of further elucidation, the electron-structure giving rise to the term is added before. Thus we may write

$$\text{Mg} \ldots \boxed{1s^2\ 2s^2\ 2p^6}\ 3s.\, 3d\ {}^3\text{D}_2$$

For the sake of shortness the closed shells may be omitted. We may write simply

$$\text{Mg.} \ldots 3s\ 3d\ {}^3\text{D}_2$$

276a. The Russell-Saunders' Coupling.—Let us now see how the observed terms can be explained from the electron composition. The basic ideas have been already foreshadowed, but it is better to collect them here. These are as follow:

(*a*) It is only the electrons outside the closed shells which determine the nature of the spectrum. The inner closed shells may, for the present, be left out of account except for calculations of energy.

(*b*) The quantum-characteristics of each electron is of the *doublet* type and is determined by the shell which it happens to occupy.

This simply means that the electron must also be regarded as a unit magnetic dipole having a definite magnetic moment, and has its motion defined by n, l, s and m. 'l' denotes orbital momentum, s . . . . denotes the spin and is equal to $\frac{1}{2}$. They combine to form j, and the magnetic quantum number

$$m = j,\ j-1,\ \ldots\ldots,\ -j.$$

Thus for an electron in the $5d$-shell, $n = 5$, $l = 2$, $s = \frac{1}{2}$, and j has the values $\frac{3}{2}$, $\frac{5}{2}$, and

$$\text{for} \qquad \left.\begin{aligned} j &= \tfrac{3}{2},\ m = \tfrac{3}{2},\ \tfrac{1}{2}, -\tfrac{1}{2}, -\tfrac{3}{2} \\ &= \tfrac{5}{2},\ m = \tfrac{5}{2},\ \tfrac{3}{2},\ \ \tfrac{1}{2}, -\tfrac{1}{2}, -\tfrac{3}{2} - \tfrac{5}{2} \end{aligned}\right\}$$

(*c*) When there are more than one electron outside the closed shells, the observed spectral terms are obtained by considering the mutual interaction of the outer electrons with each other. The general case of interaction is rather difficult to treat, but the most important case (*Russell-Saunders' Coupling*) can be illustrated with the aid of the Mg-spectrum.

Here we find that the inner electron is in the $3s$-level. It has $n = 3$, $s_1 = \frac{1}{2}$, $l_1 = 0$. Let us first take an excited state of the other electron, say $3p$ then this electron has $n = 3$, $s_2 = \frac{1}{2}$, $l_2 = 1$. For calculating interactions, n may be left out of account altogether.

It is found that in most cases, the electrons interact through each vector separately, *i.e.*, s_1 and s_2 interact as if the l's are not present at all, and the l's interact as if the s's are not present. The case is similar to that of Paschen-Back effect described in § 224. In that case, it was found that when external field H is weak, the coupling between the l and s-vectors of the electron is not broken. They continue to combine, the terms retaining their individual j-value. When, however, H is strong the s- and l-vectors precess individually round the axis of H, and the coupling between them is broken.

In the present case, we suppose that in the presence of s_1 (l_1 being zero may be neglected altogether), the coupling between s_2 and l_2 is broken and s_2 combines with s_1. The resultant is

$$|s_1+s_2| = |\tfrac{1}{2}+\tfrac{1}{2}| = 1, \text{ or } 0$$

i.e., the electrons have their spins either in the same direction or in opposite directions. When they are in the opposite directions, the resultant $S = 0$, we get singlets; when they are in the same direction, $S = 1$, we get the triplet spectrum. The two schemes are represented in Fig. 9*a*.

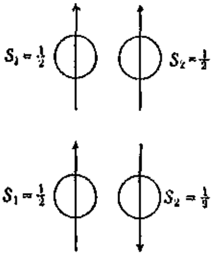

Fig. 9*a*. The origin of singlet and triplet terms.

We have to consider the interaction of l_2 with S. l_2 combines with each of these S-values separately. We have for singlets, $j=|S+l_2|=l_2$, *i.e.*, we get $j = 0, 1, 2, 3, \ldots$ for ^{1}S, ^{1}P, ^{1}D. . . terms, as illustrated in table 7 which were originally obtained from considerations of Zeeman effect.

For triplets, $j = |S+l_2| = |1+l_2|$
When $l_2 = 0, j = 1$, *i.e.*, $^3S_1$-term.
When $l_2 = 1, j = |l_2+1| = l_2, l_2 \pm 1$.

Thus we get ^{3}P-terms with $j = 0, 1, 2$, ^{3}D-terms with $j = 1, 2, 3$. The final result is that we find

$3s. ns$ . . . gives a sequence $^1S_0$, $^3S_1$-terms.
$3s. np$ „ „ $^1P_1$, $^3P_{0,1,2}$-terms.
$3s. nd$ „ „ $^1D_2$, $^3D_{1,2,3}$-terms.

The principal series is due to the transition

$$\begin{array}{ccc} 3s^2 & \leftarrow & 3s\ np. \\ ^1S_0 & \leftarrow & ^1P_1,\ ^3P_{0,1,2} \\ 3s & \leftarrow & np \end{array}$$

In the above representation the first line represents the transition from the initial $3s.\,np$ to the final $3s^2$-configuration of the outer electron shells. The second line represents the terms. The third line shows that the transition really consists in the np-electron jumping to the $3s$-shell, the other electron remaining stationary in the $3s$-level. We get only ${}^1S_0 - {}^1P_1$, ${}^1S_0 - {}^3P_1$ lines. The others are barred by the selection principle for the j-quantum number.

The line ${}^1S_0 - {}^1P_1$ is stronger than the inter-combination line, as the electron has not to change its direction of spin. But ${}^1S_0 - {}^3P_1$, the inter-combination line is weak as the jumping electron has to reverse its direction of spin.

All excited terms and lines are thus explained. But $3s^2 \ldots$, *i.e.*, when both electrons are in the $3s$-level, gives only an ${}^1S_0$-term, no ${}^3S_1$-term arises from this combination, as will be explained in Chap. XIV. This fact first led Pauli to the enunciation of the *Exclusion Principle*:

"*No two electrons in the atom can have all their quantum numbers identical.*"

Thus when both electrons are in the $3s$-orbit, they have both $n=3$, $s=\frac{1}{2}$, $l=0$. Hence they must have their m-values different. If $m_1=\frac{1}{2}$, m_2 must be $-\frac{1}{2}$, and $\Sigma m = 0$, *i.e.*, the spins must be anti-parallel. $3s^2 \ldots$ can therefore give us only ${}^1S_0$-term as actually observed. But if we take the combination $3s.ns$, the electrons have different values of n. Hence m_1 and m_2 can have the values $\pm\frac{1}{2}$. Thus we get ${}^1S_0$ as well as ${}^3S_1$-terms. Further application of Pauli's Principle will be given later.

We have thus been able to explain all the optical terms of two-valence elements discussed in Chap. IX. In addition to these terms, certain others have been found which are due to the simultaneous passage of both electrons to higher states, as is represented by the following typical example:

$$3s\,.\,3p \leftarrow 3p^2$$

The nature of these terms will be considered later on.

N. B.—It should be noted that in spite of a general similarity, there are certain differences between the spectra of elements of the odd group and the even group. They will be discussed later.

277. Term Intervals in the Spectra of Two-valence Elements.—We shall now give a short discussion on the term-values of the two-valence elements. It is observed, at least, in the case of light elements like Mg, that the singlet-triplet separation is very large, and is of a higher order than the separation observed amongst the component lines of a triplet set. In fact it is of the same order as the term values themselves.

The triplet intervals follow striking regularities. As shown on p. 383, we have

$$
\begin{aligned}
{}^3P_0 - {}^3P_1 : {}^3P_1 - {}^3P_2 &= 1 : 2 \\
{}^3D_1 - {}^3D_2 : {}^3D_2 - {}^3D_3 &= 2 : 3
\end{aligned}
$$

For heavy elements, the interval ratio departs considerably from ideal values (see the case of Hg on p. 383).

A theoretical explanation of these regularities can be given by extending the method given for the alkali elements. It was shown that the energy of an electron may be represented by

$$W = W_0 + W_r + W(sl)$$

where W_0 is the energy calculated according to the Bohr-Sommerfeld theory, W_r is the relativity correction, and $W(sl)$ is the energy of interaction between the spin and orbital momentum vectors of the electron. Both W_r and $W(ls)$ involve α^2, where α is the Sommerfeld fine-structure constant. (W_r is given by formula (46), $W(ls)$ by formula (44) of p. 422). In the case of two-valence elements, the energy of the system consisting of the two electrons may be written as follows :—

$$
\begin{aligned}
W = W(e_1) + W(e_2) + W(e_1 e_2) + \Sigma W_r + W(s_1 s_2) + W(s_1 l_1) \\
+ W(s_1 l_2) + W(s_2 l_1) + W(s_2 l_2) + W(l_1 l_2)
\end{aligned}
$$

where $W(e_1)$, $W(e_2)$ are the energies of the electrons number 1 and 2 supposed to be non-magnetic, calculated on the Bohr-Sommerfeld theory, after introducing suitable screening constants. $W(e_1 e_2)$ is the interaction energy due to electrostatic interaction between the two electrons.

$W(r)$	Relativity correction.
$W(s_1 s_2)$	Interaction energy between the spin vectors of the two electrons.
$W(s_1 l_1)$	Interaction energy between the spin and l-vectors of the first electron.
$W(s_1 l_2)$	Interaction energy between the spin of the first, and l-vector of the second electron, etc.

All terms of the above expression excepting $W(e_1)$, $W(e_2)$, $W(e_1e_2)$ involve Ra^2.

Heisenberg* showed from an application of Pauli's principle that the electrostatic interaction energy term has to be taken with opposite signs when *par*-(spins in opposite directions) and *ortho*-terms (spins in the same direction) are involved. As a proper understanding of the subject involves a knowledge of wave-mechanics, we do not pursue the subject any further at this place. Thus though the singlet and triplet levels are due to antiparallel and parallel orientations of two spins respectively, the large separation is but an indirect consequence of the configuration.

Let us now consider the separations amongst the component levels of a triplet group. For the particular case in view, we have $l_1 = 0$, hence the relevant energy terms take the simple form

$$\triangle W = W(s_1s_2) + W_1(s_1l_2) + W(s_2l_2)$$

Heisenberg showed that $W(s_1s_2)$ and $W(s_1l_2)$ can both be neglected in comparison to $W(s_2l_2)$ when the effective nuclear charge $(Z-s)e$ is large. For $W(s_1l_2)$ varies as $(Z-s')^3$ whereas $W(s_2l_2)$ varies as $(Z-s)^4$. The entire triplet separation is therefore given by

$$\triangle W = W(s_2l_2)$$

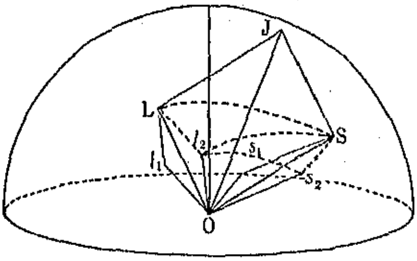

Fig. 9*b*. The vector model of two-electron system.

According to (44) on p. 422, $W(s_2l_2) = a\, s_2\, l_2 \cos(s_2l_2)$

The coupling between s_1, s_2, l_1, l_2, S, L . . . is shown in Fig. 9*b* in which the radii of the unit sphere Os_1 represents s_1, Ol_1 represents l_1 . . . . . and so on. In this case, the coupling between s_2 and l_2 is broken and they individually precess about the *j*-axis of the resultant term, which is due to the combination of resultant S and L. We have from Fig. 9*b*, taking the spherical triangle $S\, s_2\, l_2$

$$\overline{\cos(s_2l_2)} = \overline{\cos(Ss_2)}\cos(Sl_2)$$

Then from the spherical triangle $S\, L\, l_2$ we have

$$\overline{\cos(S\, l_2)} = \overline{\cos(S\, L)}\ \overline{\cos(L\, l_2)}$$

---

* See Heisenberg's work under helium problem, § 279.

Hence we have dropping the dashes for the sake of convenience

$$\cos\,(s_2\, l_2) = \cos\,(S\, L).\, \cos\,(S\, s_2).\, \cos\,(L\, l_2)$$

We have therefore

$$\begin{aligned}\triangle\nu &= a l_2 s_2 \cos\,(S\, L).\, \cos\,(S\, s_2).\, \cos\,(L\, l_2)\\ &= a\, LS \cos SL\left[\frac{s_2}{S}\cos\,(Ss_2).\, \frac{l_2}{L}\cos\,(Ll_2)\right]\\ &= A\, L\, S\, \cos\,(SL) \quad . \; . \; . \; . \; . \; . \; . \; . \; . \; . \; . \; . \qquad (16)\end{aligned}$$

where $$A = a\left[\frac{s_2}{S}\cos\,(Ss_2).\, \frac{l_2}{L}\cos\,(Ll_2)\right]$$

It is easily seen for all the three terms of a triplet group, arising out of coupling of any $(s_2 l_2)$ electron with the $3s$-electron, A has got the same value. We have therefore using the value

$$-\cos\,(SL) = [S\,(S+1) + L\,(L+1) - J\,(J+1)]/2SL,$$

for $^3\mathrm{P}_0$ . . . . $J = 0,$ $\quad S = 1,\ L = 1$ . . . $-\triangle\nu = 2A$

$^3\mathrm{P}_1$ . . . . $J = 1,$ . . . . $-\triangle\nu = A$

$^3\mathrm{P}_2$ . . . . $J = 2,$ . . . . $-\triangle\nu = -A$

Hence $^3\mathrm{P}_0 = \nu_0 + 2A,$ $\qquad ^3\mathrm{P}_1 = \nu_0 + A,$ $\qquad ^3\mathrm{P}_2 = \nu_0 - A$

$$\nu_0,\ \text{the c. g. of the terms} = \frac{^3\mathrm{P}_0 + 3.\ ^3\mathrm{P}_1 + 5.\ ^3\mathrm{P}_2}{1+3+5}$$

i.e., we assign the weights 1, 3, 5, to the $^3\mathrm{P}_0$, $^3\mathrm{P}_1$, $^3\mathrm{P}_2$ terms in accordance with the rule that $g = 2j + 1$.

We have further $$\frac{^3\mathrm{P}_1 - {}^3\mathrm{P}_2}{^3\mathrm{P}_0 - {}^3\mathrm{P}_1} = \frac{2}{1}$$

The value of A can easily be calculated in terms of a. We have

$$\begin{aligned}A &= a\left[\frac{s_2}{S}\cos\overline{Ss_2}.\ \frac{l_2}{L}\cos\overline{Ll_2}\right]\\ &= a\left[\frac{s_2\,(s_2+1) + S\,(S+1) - s_1\,(s_1+1)}{2\,S\,(S+1)}\right.\\ &\qquad\left.\times\frac{l_2\,(l_2+1) + L\,(L+1) - l_1(l_1+1)}{2L\,(L+1)}\right]\end{aligned}$$

We have $S = 1,\ s_2 = s_1 = \frac{1}{2},\ l_1 = 0,\ l_2 = L.$ Hence it follows that

$$A = \tfrac{1}{2}a = \frac{1}{2}\ \frac{R\alpha^2\,(Z-S_0)^4}{n^3\ l_2\,(l_2+\frac{1}{2})\,(l_2+1)}$$

For the ^{3}P-difference, we put $l_2 = 1$, then we have

$$A = \frac{1}{2}\,\frac{R\alpha^2\,(Z-S_0)^4}{3n^3} \quad . \; . \; . \; . \; . \; . \; . \; . \; . \; . \qquad (17)$$

A is known from experimental data, hence with the aid of (17), $(Z-S_0)$ can be easily calculated. For a few two-valence elements and ions, the value of S_0 . . . . . the screening constant, as calculated from the above formula is shown in the following tables.

Table 8.—$\Delta\nu = 2\,({}^3\mathrm{P}_0 - {}^3\mathrm{P}_2)$

Spectrum	Be	B^{+}	C^{++}	N^{+3}	O^{+4}
$\Delta\nu$	3·02	22·8	79·1	204·1	459·5
S_0	2·30	2·19	*2·16*	2·14	

Table 9.—$\Delta\nu = 3\,({}^3\mathrm{P}_0 - {}^3\mathrm{P}_2)$

Spectrum	Mg	Al^{+}	Si^{++}	P^{+3}	Si^{+4}	Cl^{+5}
$\Delta\nu$	60·8	187·3	39·4	696	1128	1720
S_0	7·13	6·55	6·23	6·04	5·89	5·77

From this calculation, we find that two $1s$-electrons and one $2s$-electron produce the screening 2·30 in Be, . . . and it decreases to the value 2 in Be-like ions of high nuclear charge. For Mg, the $1s^2.2s^2 2p^6.3s$ . . . *i.e.*, 11 electrons produce the screening 7·13 which steadily decreases in the Mg-like stripped ions.*

278. The Helium-Spectrum—General Description.

—In this connection, we may consider the arc-spectrum of helium. This element has the normal electron structure $1s^2$ and the excited states arise from the structure $1snx$. The constitution is the same as that of the alkaline earth elements, and the helium spectrum should have the same general features as two-valence elements have. But no indication of such a structure was found in the early studies of its spectrum.

Helium was, as is well-known, first discovered in the sun by the astronomer Sir Norman Lockyer in 1868 while observing the flash-spectrum of the sun during the total Solar Eclipse at Guntur in India. He observed a prominent yellow line λ 5875 besides the yellow pair of sodium lines. As this line could not be obtained from any terrestrial element, it was ascribed to a new element, till then undiscovered, which was named *Helium* (after *Helios*, the Greek name for the sun-god). Thirty years later, helium was obtained by Sir W. Ramsay in the Norweigian mineral clevite. The spectrum of helium was studied in great detail by Kayser and Runge for the visible, near infrared and near ultraviolet regions. They thought that as helium was the element next to hydrogen in the periodic classification, its spectrum would show great simplicity. This expectation, however, was not fulfilled. They found that the observed spectral lines of He were more complex than the hydrogen lines, in fact it could be classified into two distinct sets, each consisting of a sharp, diffuse, and principal series as in the case of alkali elements. The terms of each set and the prominent lines are shown in table 9 and in Fig. 10. The terms of first set were in those days never found to combine with the terms of the second set, and hence it was supposed that ordinary Helium was a mixture of two different elementary gases to which the names *Parhelium* and *Orthohelium* were given. But all attempts to separate the two supposed constituents failed and the hypothesis of two separate elements has now been definitely disproved, though the nomenclature remains. It was further shown that the parhelium lines are all *single*, while the orthohelium lines are *double*.

---

* The present discussion is based on a paper by S. Goudsmit and C. J. Humphreys, *Phys. Rev.*, **31**, 960, 1928.

It was clear that the lines included in the series of Kayser and Runge did not represent all the lines due to He. Helium gas was found to be perfectly transparent to light from extreme ultraviolet to infrared, including all its emission lines. Hence none of the lines observed by Kayser and Runge represented the resonance line of helium. These were found by Lyman to lie in the region of vacuum spectroscopy and is shown in table 10. The resonance line is λ 584·4, $^1S_0 - {}^1P_1$, where $^1S_0$ is the normal term of parhelium from $1s^2$, and the next are λ 537·7, 522·2, 515·6 forming a Rydberg sequence. A diagrammatic view of the origin of helium lines, and term values is given in Figs. 10 and 11.

It will be seen that while the parhelium terms are all single, the orthohelium terms have been represented as *triplets* in the Russell Saunders' notation, instead of as doublets. The separations of triplet terms must be however very small, as can be seen from table 9, where the orthohelium terms are represented as doublets as in the alkali elements. We shall return to their explanation in §279

Table 10.—The arc lines of HeI: Wavelengths in Å. units.

	Parhelium (*singlet*)				Orthohelium (*triplet*)		
n	$1S-nP$ $1S=198307{\cdot}9$	$2S-nP$ $2S=32032{\cdot}51$	$2P-nS$ $2P=27175{\cdot}17$	$2P-nD$ $2P=27175{\cdot}17$	$2s-np_{1,2}$ $2s=38454{\cdot}7$	$2p_{1,2}-ns$ $2p_1=29223{\cdot}9$ $2p_2=29222{\cdot}8$	$2p_{1,2}-nd$
2	584·4 $2P=27175{\cdot}17$	λ 20582·04			λ 10830·30 λ 10829·09 $2p_1=29223{\cdot}92$ $2p_2=29222{\cdot}85$		
3	λ537·1 $3P=12100{\cdot}56$	λ 5015·67	λ 7281·35 $3S=13445{\cdot}23$	λ 6678·15 $3D=12205{\cdot}09$	λ 3888·646 ·603 $3p_1=12746{\cdot}08$ $3p_2=12745{\cdot}99$	λ 7065·185 ·707 $3s=15073{\cdot}87$	λ 5875·618 ·960 $3d=12209{\cdot}10$
4	λ 522·2 $4P=6817{\cdot}21$	λ 3964·73	λ 5047·74 $4S=7369{\cdot}82$	λ 4921·93 $4D=6863{\cdot}40$	λ 3187·743 $4p=7093{\cdot}59$	λ 4713·143 ·375 $4s=8012{\cdot}53$	λ 447·477 ·689 $4d=6866{\cdot}16$
5	λ 515·6 $5P=4367{\cdot}45$	λ 3613·64	λ 4437·55 $5S=4646{\cdot}52$	λ 4387·93 $5D=4391{\cdot}76$	λ 2945·104 $5p=4509{\cdot}96$	λ 4120·812 ·981 $5s=4963{\cdot}63$	λ 4026·189 ·358 $5d=4393{\cdot}49$
6	λ 512·1 $6P=3035{\cdot}05$	λ 3447·59	λ 4168·97 $6S=3195{\cdot}17$	λ 4143·77 $6D=3049{\cdot}33$	λ 2829·06 $6p=3117{\cdot}66$	λ 3867·46 ·62 $6s=3374{\cdot}42$	λ 3819·606 ·753 $6d=3050{\cdot}57$
7	λ 510·1 $7P=2230{\cdot}52$	λ 3354·52	λ 4023·99 $7S=2331{\cdot}21$	λ 4009·27 $7D=2240{\cdot}00$	λ 2763·80 $7p=2283{\cdot}31$	λ 3732·85 ·99 $7s=2442{\cdot}29$	λ 3705·003 ·139 $7d=2241{\cdot}00$
8	λ 508·6 $8P=1708{\cdot}40$	λ 3296·76	λ 3935·91 $8S=1775{\cdot}25$	λ 3926·53 $8D=1714{\cdot}58$	λ 2723·18 $8p=1743{\cdot}79$	λ 3652·00 ·12 $8s=1849{\cdot}40$	λ 3634·24 ·37 $8d=1715{\cdot}62$

(*Par*) $1\,{}^1S_0$ −(*Ortho*) $2\,{}^3P_1$ = λ 591·6 . . . . Inter-combination Line.

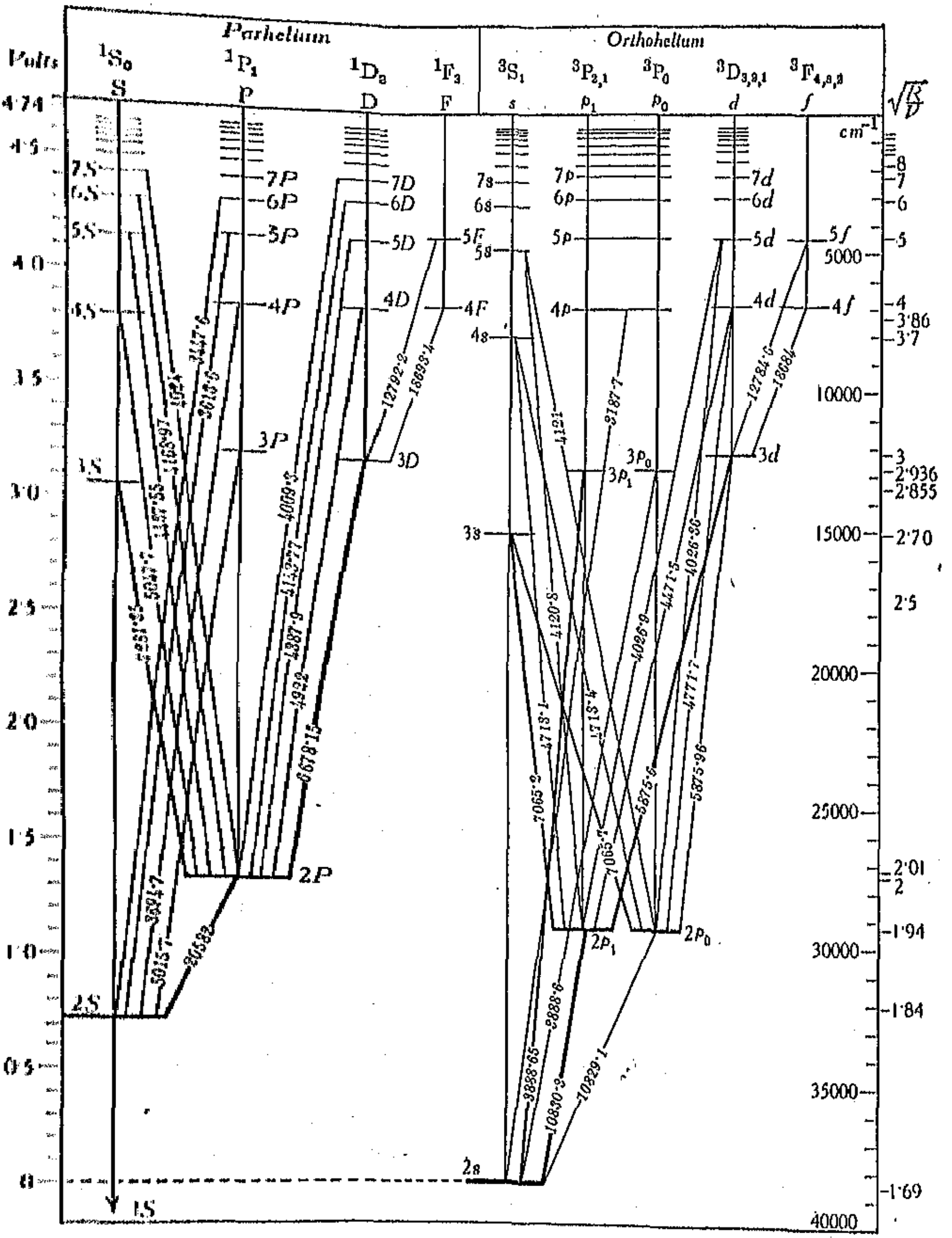

Fig. 10. Bohr-diagram for HeI.

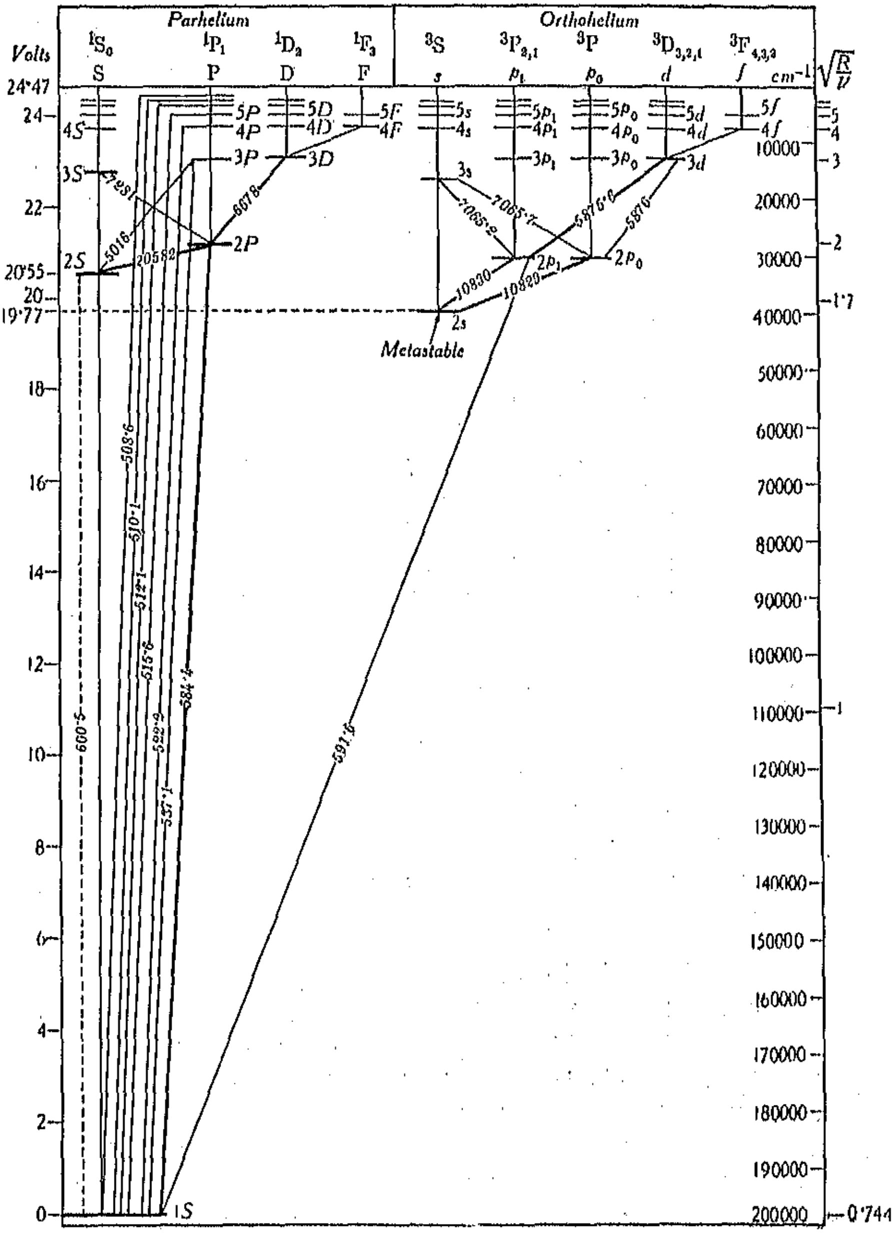

Fig. 11. Bohr-diagram for HeI, showing the resonance line λ584·4 Å. U.

The line λ 5875·6, the original one which heralded the discovery of helium is $1s\,2p\ {}^3P - 1s\,3d\ {}^3D$. One of the most interesting lines in the helium spectrum is the intercombination line λ 591·6, $1^1S_0 - 2^3P$, where ${}^1S_0$ is the fundamental (parhelium) term and ${}^3P$ is an ortholielium term. ${}^1S_0 = 198307{\cdot}9\ \text{cm}^{-1}$ corresponds to an ionisation potential of 24·476 volts; the resonance potential is 20·8 volts. These results have been verified by the electron bombardment method. Besides the lines given in table 10 there are many forbidden lines due to parhelium and ortholielium. The more intense of these lines with their transitions are indicated in the table given below.

Table 11.—Forbidden lines in HeI spectrum.

Transition	Wavelength	Ortho or Parhelium
$2^1S_0 - 6^1S_0$	3466·7	Par
$2^1P_1 - 3^1P_1$	6631·8	„
$2^1S_0 - 3^1D_2$	5042·2	„
$2^3S_1 - 5^3S_1$	2985	Ortho.
$2^3P_2 - 3^3P_2$	6067·1	„
$2^3S_1 - 3^3D_{3,2,1}$	3809·05	„

Besides showing the terms and transitions in the par and ortholielium spectrum, Fig. 11 shows also the effective quantum number for the various terms calculated from the formula $n_0 = \sqrt{R/\nu}$. These at once show that all singlet and triplet d and f-terms of He are almost perfectly hydrogenic. The p-terms of parhelium are also hydrogenic, but the p-terms of ortholielium are slightly non-hydrogenic. The s-terms of both par and ortholielium are strongly non-hydrogenic.

279. Theoretical Explanation of the Spectrum of Helium.—Theoretical attempts to explain the arc spectrum of helium have primarily been directed into two channels: first, a good number of attempts were made in the early days of quantum mechanics to deduce theoretically the ionisation potential of helium from purely mathematical considerations. In this case, we have to deal with the motion of two particles round a nucleus, the problem therefore reduces to a special case of the celebrated dynamical problem of three bodies which had remained unsolved since the days of Newton. Attempts were made by Bohr, Kramers and others to solve the problem by assuming special models, *e.g.*, by assuming that the electrons are at the opposite ends of a diameter, or their orbits were tilted at 90° or 120° to each other. These attempts gave, as a rule, results at variance with the actual value of the I. P., showing that something fundamental was lacking in the assumptions or in the mathematical formulation of the problem.

The second set of difficulties was about the multiplicity of the lines. The electron structure of the atom is $1s.nx$, and if Russell-Saunders' coupling holds, helium should give us singlet and triplet terms and the singlets should contain the fundamental level $1s^2\ {}^1S_0$ as in the case of two-valence elements. In fact the spectrum of helium should show the same structure as that of magnesium. The parhelium terms can be at once identified with the singlet terms, but a difficulty arises in the case of the orthohelium terms which instead of being triplets, are found to be doublets. Further no intercombination was found to occur between the two sets of terms in the visible range.

These peculiar features of the He-spectrum were completely explained by Heisenberg.* He showed that the orthohelium terms are really triplets, and the large separations between the corresponding members of ortho and para-series (triplet-singlet separation) arise from the different signs of the electrostatic interaction energy-terms between the two electrons as mentioned on p. 555. As regards the remaining terms, we have as in § 277

$$\triangle W = W(s_1 s_2) + W(s_1 l_2) + W(s_2\ l_2)$$

But $W(s_1\ s_2)$ and $W(s_1\ l_2)$ can no longer be neglected in comparison to $W(s_2\ l_2)$ as in §277, as here the nuclear charge is small. A rigorous calculation of $W\ (s_1 s_2)$ and $W\ (s_1 l_2)$ from wave-mechanics up to certain amount of approximation is to be found in an article by Bethe.† For $Z = 2$, the signs of $W(s_1\ s_2)$ and $W(s_1\ l_2)$ are found to be opposite to that of $W(s_2\ l_2)$ and of the same order, hence we no longer find ${}^3P_0 > {}^3P_1 > {}^3P_2$.

It was suspected from these considerations that probably the doublet terms are really triplets as in the case of other two-valence elements, only the separation between two terms was extremely small and anomalous. This hypothesis was put to experimental test for the lines

λ 5876 (D_3, $2^3P - 3^3D$), λ 4471 ($2^3P - 4^3D$), λ 7066 ($2^3P - 3^3S$)

---

* Heisenberg, *Zs. f. Phys.*, **39**, 499, 1926.

† *Vide* Smekal's *Quanten*, p. 377

by Hansen and Houston.* They used double interferometers of Fabry-Perot pattern, possessing large resolving power, and were able to show that the ortho-helium P-terms were really triple, as shown below in Fig. 12 for λ 7066.

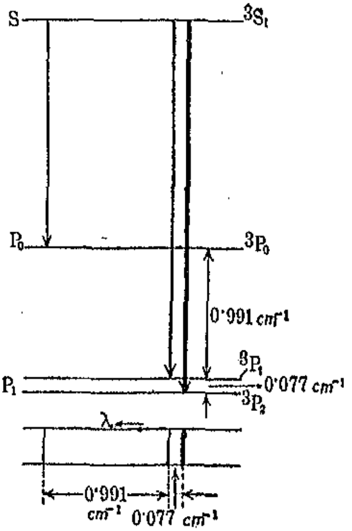

Fig. 12.

In addition to its triplet character, the components show several very interesting points of departure from the corresponding ^3P-terms of alkaline earths. We have in the alkaline earths :—

$$^3P_0 > {}^3P_1 > {}^3P_2 \ldots \text{ and}$$

$$\frac{^3P_0 - {}^3P_1}{^3P_1 - {}^3P_2} = \frac{1}{2} \text{ approximately}$$

But in helium

$$^3P_0 < {}^3P_1 < {}^3P_2 \ldots \text{ and}$$

$$^3P_0 - {}^3P_1 : {}^3P_1 - {}^3P_2 = 12 : 1$$

for $^3P_0 = 29222{\cdot}85$, $^3P_1 = 29223{\cdot}84$, $^3P_2 = 29223{\cdot}93$

The *d*-term is also expected to be triple, but the separations seem to be extremely small and different workers do not agree in their values of the separations. The observation shows that the ^3P-term is inverted, and $^3P_2$, $^3P_1$ are so very close that they can be regarded as one term. This also explains the anomaly in the intensity of the components of λ 5876 observed by Ornstein and Burger.†

They found that the intensity ratio

$$\lambda\, 5875{\cdot}62 : \lambda\, 5875{\cdot}96 = {}^3P_{21} - {}^3D : {}^3P_0 - {}^3D = 8 : 1$$

This ratio does not agree with that for a doublet structure, but for a triplet structure, as shown in the following scheme :

	$^2P_{\frac{1}{2}}$	$^2P_{\frac{3}{2}}$
$^2D_{\frac{3}{2}}$	5	1
$^2D_{\frac{5}{2}}$		9

	$^3P_0$	$^3P_1$	$^3P_2$
$^3D_1$	15	$12-u$	u
D_2		$33+u$	$12-u$
D_3			63

---

* Hansen and Houston, *Nat. Acad. Sci.*, 13, 91, 1927; *Astr. Jour.*, 68, 246, 1928.

† Ornstein and Burger, *Zs. f. Phys.*, 26, 57, 1924; 33, 437, 1926.

We have to suppose that the ^{3}D's are merged into one level. Then we have, in case the terms are doublets, the following ratio for intensities :—

$$^2P_{\frac{1}{2}} - {}^2D : {}^2P_{\frac{3}{2}} - {}^2D = 5 : 1+9 = 1 : 2.$$

But if we assume that the P-terms are triplet, we can suppose that since now $^3P_{1,2}$ merge into almost one level, hence the ratio of the intensities is

$$^3P_0 - {}^3D : {}^3P_{1,2} - {}^3D = 15 : 45+75 = 1 : 8 \text{ as observed.}$$

The Ionisation Potential of Helium and Helium-like Ions.—Hylleras and Kellner* obtained from wave-mechanics the value of I. P. of He and He-like ions. Hylleras showed† that E_1, the I. P., is given by the following formula :—

$$E_1/Rh = [Z^2 - \tfrac{5}{4}\,Z + {\cdot}31488 - {\cdot}01752/Z + {\cdot}00548/Z^2]$$

The spectrum of Li^+ † is exactly similar to that of He and has been investigated by Schüler‡ and Werner,§ and the resonance lines $^1S - {}^1P$ were obtained by Erickson‖ and found to lie at λ199·263 Å.U. The same investigators have also obtained the spectrum of Be^{++} which is also He-like, and got the resonance line at λ 100·250. The I. P's of Li^+ and Be^{++} are found to obey the formula given by Hylleras.

After He, the other inert gases forming the zero group in the periodic table are Ne, A, Xe, Kr and Rn. They all form closed-shell structures with the outer configuration $2p^6$ for Ne, $3p^6$ for A, etc...... These structures are borne out by their high ionisation potentials and extremely complicated nature of their spectra. We shall treat the subject fully in Chap. XIV.

280. Spectra of Three-Valence Elements.—According to the periodic classification the following elements possess the valency three :—

5.B . . . . 13.Al . . . 31.Ga . . . . 49.In . . . . 81.Th.

---

[*] Hylleras and Kellner, *loc. cit.*
[†] Hylleras, *loc. cit.*
[‡] Schüler, *Zs. f. Phys.*, 42, 487, 1927.
[§] Werner, *Nature*, **115**, 191, 1924; **116**, 574, 1925.
[‖] Erickson and Edlén, *Zs. f. Phys.*, **59**, 656, 1930.

Let us now consider their spectra. Their electron-structure is shown below.

5 B	$\boxed{1s^2}\ 2s^2\ 2p$	C$^+$, N^{++}, . . .
13 Al	$\boxed{1s^2\ 2s^2\ 2p^6}\ 3s^2\ 3p$	Si$^+$, P^{++}, . . .
31 Ga	$\boxed{1s^2\ 2s^2\ 2p^6\ 3s^2\ 3p^6}\ 3d^{10}\ 4s^2\ 4p$	Ge$^+$, As^{++}, . .
49 In	$\boxed{1s^2\ 2s^2\ 2p^6\ 3s^2\ 3p^6\ 3d^{10}\ 4s^2\ 4p^6}\ 4d^{10}\ 5s^2\ 5p$	Sn$^+$, Sb^{++} . . .

In all these elements, there is only one electron outside the closed shells, and it is in the np-state. The fundamental level is therefore given by the terms :—

$$n\,^2\mathrm{P}_{\frac{1}{2}},\quad n\,^2\mathrm{P}_{\frac{3}{2}}$$

The duplicity is due, as in the case of the p-terms of the alkali elements, to the interaction of the l-moment with the spin of the valency electron. Let us take 13 Al as the representative of this group of elements. The structure diagram of Al is shown below in Fig. 13, which shows that in the normal atom the valency electron is in the $3p$-orbit.

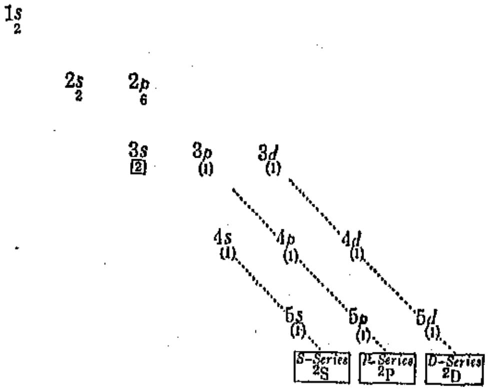

Fig. 13. The structure diagram of Al.

The excited states are obtained by increasing the quantum number of the light electron successively. They are shown in the accompanying diagram. Here the two electrons in the 3s-shell remain undisturbed while the diagonal displacement of the other electron gives rise to a doublet sequence of terms, as shown enclosed in rectangles.

The term-values of Al are shown in the following table.

Table 12.—The term values of Al I.

n	nS terms	nP terms	$\Delta\nu$	nD terms	$\Delta\nu$
3		$^2P_{3/2}$ 48168·87 $^2P_{1/2}$ 48280·88	112·01	$^2D_{5/2}$ 15844·15 $^2D_{3/2}$ 15845·49	1·34
4	22933·27	$^2P_{3/2}$ 15316·48 $^2P_{1/2}$ 15331·70	15·22	$^2D_{5/2}$ 9347·22 $^2D_{3/2}$ 9351·71	4·49
5	10591·58	$^2P_{3/2}$ 8003·24 $^2P_{1/2}$ 8009·19	5·95	$^2D_{5/2}$ 6043·31 $^2D_{3/2}$ 6047·37	4·06
6	6136·76	$2P_{3/2}$ 4943·19 $^2P_{1/2}$ 4946·01	2·82	$^2D_{5/2}$ 4112·09 $^2D_{3/2}$ 4114·33	2·24
7	4007·67	$^2P_{3/2}$ 3350·6 $^2P_{1/2}$ 3352·6	2·0		

The resonance lines are due to transitions $3p \leftarrow 3d$ and $3p \leftarrow 4s$ as shown in the following scheme for aluminium. The figures within brackets denote intensities of the corresponding lines. These lines have been obtained in absorption.

Table 13.—Resonance lines of Aluminium.

	4 $^2S_{1/2}$ 22933·27	3 $^2D_{3/2}$ 15845·49	3 $^2D_{5/2}$ 15844·15
3 $^2P_{1/2}$ 48280·88	(10 R) λ 3944·03 ν 23347·61	(10 *R*) λ 3082·16 ν 32435·39	
3 $^2P_{3/2}$ 48168·87	(10 R) 3961·54 ν 25235·60	(6 R) λ 3092·84 ν 32323·38	(10) R λ 3092·72 ν 32324·72

The important lines (with their intensities) in the spectrum of Al as well as their origins are schematically represented in the following diagram (Fig. 14).

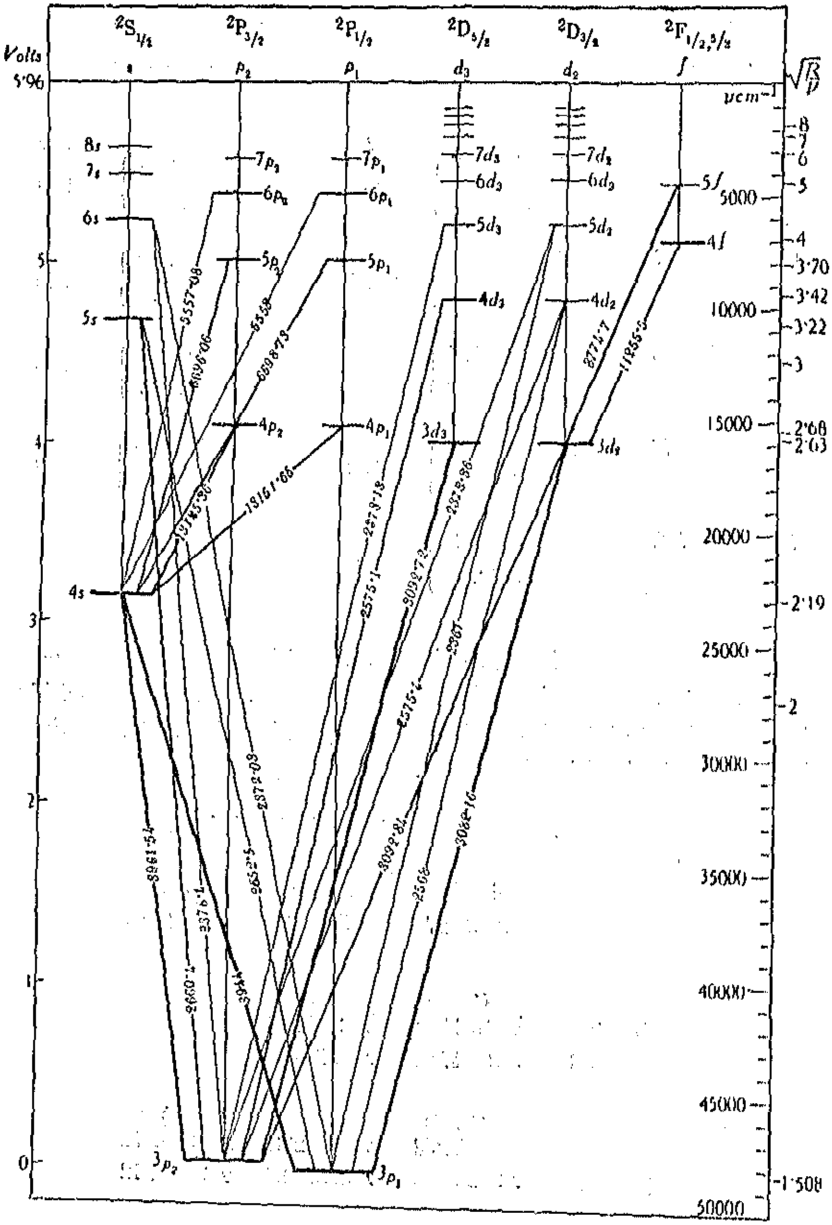

Fig. 14. The Bohr-Grotrian diagram of Al I.

The ionisation and resonance potentials of this group of elements can be easily calculated from spectral data and have been verified by electron-bombardment experiments. These are shown in table 14.

Table 14.—The resonance and ionisation potentials of B, Al, Ga, In, Tl.

Element	$2\ {}^2P_{\frac{1}{2}, \frac{3}{2}}$ -terms		${}^2S_{\frac{1}{2}}$ -term	Resonance lines ${}^2P_{\frac{1}{2}, \frac{3}{2}} - {}^2S$	R. P. in volts $({}^2P_{\frac{1}{2}} - {}^2S_{\frac{1}{2}})$	I. P. in volts $({}^2P_{\frac{1}{2}})$
5 B*	67544·6 67529·1	$\Delta\nu$ 15·5	27504·6	λ 2496·86 ν 40040 λ 2497·82 ν 40024·5	4·942	8·33
13 Al	48280·88 48168·9	112·0	22933	λ 3944·16 ν 25346·94 λ 3961·68 ν 25234·87	3·128	5·957
31 Ga	48379·8 47553·8	826	23591	λ 4033·2 ν 24787·5 λ 4172·2 ν 23961·4	3·059	5·970
49 In	46667·9 44455·3	2212·6	22294·8	λ 4102 ν 24372·4 λ 4511·4 ν 22160	3·008	5·759
81 Tl	49264·2 41471·5	7792·7	22786	λ 3776 ν 26476·7 λ 5350·6 ν 18684·2	3·267	6·076

That the p-terms are the fundamental levels can easily be proved by absorption experiments. Only the lines possessing the p-levels as final orbits appear in absorption, as shown in the analysis of the absorption spectrum of aluminium in table 13.

---

* R. A. Sawyer, *Phys. Rev.*, **29**, 357, 1927; Bowen, *ibid.*, **29**, 231, 1927. R. A. Millikan and J. S. Bowen, *Phys. Rev.*, **26**, 310, 1926.

Of the two fundamental states, $P_{\frac{1}{2}} > P_{\frac{3}{2}}$, hence according to Maxwell's law, the proportion of the atoms in the two states at the temperature T is $(g_2/g_1)e^{-h\Delta\nu/kT}$, where g_1, g_2 are the weights of the $P_{\frac{1}{2}}$ and $P_{\frac{3}{2}}$ - states; they are as $2:4=1:2$; $\Delta\nu = {}^2P_{\frac{1}{2}} - {}^2P_{\frac{3}{2}}$. This difference gradually increases with the atomic weight as shown in column 2 of table 14, and for Tl it reaches the large value of about ·96 volts nearly. Hence for such elements, only the lines ending in ${}^2P_{\frac{1}{2}}$ are expected to appear in absorption. The lines having ${}^2P_{\frac{3}{2}}$ as their final orbits appear in absorption only when the temperature is sufficiently high to produce a sufficient number of atoms in the ${}^2P_{\frac{3}{2}}$ - state.

281. Application of the Regular and Irregular Doublet Laws.—The doublet difference ${}^2P_{\frac{1}{2}} - {}^2P_{\frac{3}{2}}$ can be explained in the same way as in the case of the alkali elements.

We have, in this case, as in §221

$$\Delta\nu = \frac{R\,\alpha^2\,(Z-\sigma)^4}{n^3 l\,(l+1)} \quad . \quad . \quad . \quad . \quad . \quad . \quad . \quad . \quad (18)$$

The value of $Z-\sigma$ can be calculated when $\Delta\nu$ is known, *e.g.*, for Al, $\Delta\nu = 112·07$.

Hence, putting $n=3$, $l=1$ in (18), we have

$$Z-\sigma = 5·674, \qquad \sigma = 7·326$$

The values of σ calculated in this way for a certain number of three-valence elements and ions are given below :—

Table 15.—$\Delta\nu = 2\,{}^2P_{\frac{1}{2}} - 2\,{}^2P_{\frac{3}{2}}$

Spectrum	B	C+	N++	O^{+3}	F^{+4}	Ne^{+5}	Na^{+6}
$\Delta\nu$	15·5	66·76	179·3	398·4			
σ	2·45	2·332	2·292	2·252			

The spectra of three-valence elements are thus seen to be extremely simple in their constitution. Some doubt may be expressed regarding the use of the term three-valence, for the constitution is $ns^2\,np$, there is only one electron outside the closed shell ns^2. But the shell ns^2 is not so solidly formed as np^6 owing to the smallness

Table 15a.—$\Delta\nu = 3^2P_{\frac{1}{2}} - 3^2P_{\frac{3}{2}}$

Spectrum	Al	Si+	P++	S^{+3}	Cl^{+4}	A^{+5}	K^{+6}
$\Delta\nu$	112·07	287	559·5	950·2	1500		
σ	7·326	6·82	6·519	6·318	6·147		

of the number of electrons and of large interaction of the np-electron with the ns^2-shell, as both have the same total quantum number. In the case of alkali elements the interaction of the s-electron on the p-shell is small. Thus the s-electrons in three-valence elements can easily be made to pass from the inner to the outer shell, producing the constitution $ns.\ np^2$ and giving rise to a complex system of lines given by the scheme

$$ns^2\ np \leftarrow ns.\ np^2$$
$$^2P \leftarrow {}^4P,\ {}^2PDS$$

transition $\qquad ns \leftarrow np.$

The calculation of terms arising out of $ns.\ np^2$-combination really falls under complex spectra (Chap. XIV). Such lines have actually been observed for Al. Such transitions may be called *inner transitions* (*vide* §340).

In addition to these transitions, the second s-electron is also found to pass to the p-level

$$ns.\ np^2 \leftarrow np^3$$
$$^4P,\ {}^2PDS \leftarrow {}^4S,\ {}^2DP$$

transition $\qquad ns \leftarrow np$

The existence of these transitions justifies the use of the term *three-valence spectra.*

The ionised elements Si^+, P^{++}, S^{+3}, Cl^{+4} have also been found to possess spectra similar to that of Al. These have been investigated by Fowler, Millikan and Bowen and others,* and their resonance potentials corresponding to $^2P_{\frac{1}{2}} - {}^2S_{\frac{1}{2}}$ have been found to be 8'08, 14'54, 22'38 volts respectively.

---

* Si+:

A. Fowler, *Proc. Roy. Soc. A*, **103**, 413, 1923; *Phil. Trans. A*, **225**, 1, 1926. P. K. Kichlu, *Jour. Opt. Soc. Am.*, **14**, 455, 1927.

P++, S^{+4}, Cl^{+4}; J. S. Bowen and R. A. Millikan, *Phys. Rev.*, **26**, 0, 282, 1925; **31**, 34, 1928.

282. The Exclusion-Principle of Pauli.—The Exclusion Principle which was first enunciated by Pauli to explain the non-existence of a triplet term in an ns^2-combination as described in §276*a* was further extended by him to include the *p*, *d* and *f*-shells of electrons, and afforded an explanation of the fact first suggested correctly by Mainsmith and Stoner that to fill a definite sub-level, a definite number of electrons is necessary, 2 for *s*, 2 for $p_{\frac{1}{2}}$, 4 for $p_{\frac{3}{2}}$ etc. The principle has since proved to be fundamental in Atomic Physics. We shall now discuss it in detail.

The principle has been enunciated as follows :—

"*No two electrons in an atom can have all their quantum numbers identical.*"

As we have seen in Chap. X the motion of every electron is characterized by four quantum numbers n, l, s, and m. The significance of these quantum numbers, though already discussed, may again be pointed out. n is the total quantum number; $l=k-1$ . . . represents orbital motion, the mechanical moment of the orbit being $lh/2\pi$ and the magnetic moment due to this motion is $l.\ eh/4\pi cm$; s represents the spin quantum number and it is always $\frac{1}{2}$ for a single electron and the mechanical moment due to this motion is $\frac{1}{2}.\ h/2\pi$ and the magnetic moment is $\frac{1}{2}\ h/2\pi.\ e/mc$. The inner quantum number j is the vector sum of l and s and has therefore the values $l+\frac{1}{2}$ and $l-\frac{1}{2}$ for an one-valance element. The magnetic quantum number m is equal to $j \cos \theta$, and has the values

$$m = j, j-1 \ldots\ldots -j.$$

Hence m represents a new degree of motion, *viz.*, the tilt of the magnetic axis to any external field. The four quantum numbers represent the four degrees of freedom possessed by an electron.

Let us now find out how many electrons will be required to fill up an *s*-orbit, say the K (1*s*), L_1 (2*s*) or M_1 (3*s*), etc. . . . Now n, l, s are the same for the electrons, hence according to Pauli's principle, they must differ in their m-values, *i.e.*, the total number required to fill up any *s*-level is equal to the number of possible m-values in this level. For an *s*-level, $j=\frac{1}{2}$, and the possible m-values are $\frac{1}{2}$ and $-\frac{1}{2}$, hence two electrons are necessary to fill up an *s*-level.
Similarly for the *p*-level, we have the sub-levels

for $j=\frac{1}{2}, \ldots P_{\frac{1}{2}}$ or $L_2 \ldots m = \frac{1}{2}, -\frac{1}{2}$

$j=\frac{3}{2}, \ldots P_{\frac{3}{2}}$ or $L_3 \ldots m = \frac{3}{2}, \frac{1}{2}, -\frac{1}{2}, -\frac{3}{2}$

Hence there are six different magnetic levels for a p-electron. Therefore the total number of electrons required to fill up completely a p-level is *six* as we obtain in the elements B to Ne whose electron structure has been shown on p. 533.

Boron has the structure $2s^2$ $2p$, and gives a simple doublet spectrum discussed in § 280. But occasionally by means of electric discharge the states $2s$ $2p^2$, $2p^3$ may also be produced. The spectrum given by carbon whose normal constitution is $2s^2$ $2p^2$, and of subsequent elements is more complex, and cannot be discussed in this chapter. But in all these elements the structures $2s$ $2p^{x+1}$, and $2p^{x+2}$ can be produced by electrical discharge showing that the $2s^2$-shell is not so solidly formed. Thus the use of such terms as four-valence or five-valence elements for C, N, O .... is justified.

When we reach Ne, the p-shell is completed, we get $\Sigma m=0$, hence the resultant term is ${}^1S_0$, *i.e.*, Ne is magnetically neutral. But all the intervening elements will show a complex set of spectral terms which are discussed in Chap. XIV.

It is clear that after the Neon-shell is completed, the formation of $3s$ and $3p$-shells will begin, taking us up to Argon $3s^2 . 3p^6$ as shown on p. 533.

After Argon the formation of $3d$-shells begins.

When an electron is in the d-shell, we have

$$s=\tfrac{1}{2},\ \ l=2, \qquad j=\tfrac{3}{2}, \text{ or } \tfrac{5}{2}$$

For $\quad D_{\frac{3}{2}}\ , m=\frac{3}{2}, \frac{1}{2}, -\frac{1}{2}, -\frac{3}{2}, \qquad D_{\frac{5}{2}}\ , m=\frac{5}{2}, \frac{3}{2}, \frac{1}{2} -\frac{1}{2} -\frac{3}{2}, -\frac{5}{2}.$

Hence altogether, the d-electron can assume 10 different magnetic levels. Therefore according to Pauli's principle, the number of electrons required to fill up a d-level is 10. Similarly the number required to fill up an f-shell is 14. For when an electron is in the f-shell, we get the terms $F_{\frac{5}{2}}$, $F_{\frac{7}{2}}$, corresponding to which we obtain $6+8=14$ magnetic levels.

283. Magnetic Quantum Numbers for Strong Fields.—In order to illustrate the operation of Pauli's Principle, it is sometimes more convenient to make use of magnetic quantum numbers for strong fields, m_s and m_l, which were introduced in §224, for explaining Paschen-Back effect. The use of these numbers is also justified by the fact that in the majority of cases so far observed, the interaction between the electrons is of the Russell-Saunders type, *i.e.*, the s-vectors of the electrons interact as if the l-vector is not present, the l-vectors interact as if the s-vector is not present.

We have for an s-electron, $l=0$, $s=\frac{1}{2}$, $m_l = 0$, $m_s = \frac{1}{2}, -\frac{1}{2}$.

Hence the number of different levels (m_s, m_l) are $(\frac{1}{2}, 0)$ and $(-\frac{1}{2}, 0)$. The maximum number of electrons in the s-shell is 2.

For a p-electron

$$s=\tfrac{1}{2},\ m_s = \tfrac{1}{2}, -\tfrac{1}{2}$$

$$l=1,\ m_l = 1, \quad 0, -1$$

Hence m_s and m_l can be combined in $2\times3 = 6$ different ways, and corresponding to these 6 magnetic levels, 6 electrons are necessary to fill up a p-shell completely.

For a d-electron

$$s = \tfrac{1}{2}, \quad m_s = \tfrac{1}{2}, -\tfrac{1}{2}$$

$$l = 2, m_l = 2, \quad 1,\ 0,\ -1,\ -2.$$

So m_s, and m_l . . can be combined in $2 \times 5 = 10$ ways, and 10 electrons are needed to fill up the d-shell completely.

284. Formation of Elements after Argon.—After Argon, which has the constitution $\boxed{1s^2.\ 2s^2.\ 2p^6.\ 3s^2.\ 3p^6}$, the fourth period begins. The next level is $3d$ and for the next element K, the nineteenth electron should find itself in the $3d$-shell, and K should show properties considerably different from those of Na. But we know, as a matter of experience, that K has very nearly the same chemical and spectral properties as Na, hence the electron must be normally in the $4s$-orbit and not in $3d$, though the latter has a smaller total quantum number. The energy-value of $4s$ is actually found to be *larger* than that of $3d$. This is explained by the idea of penetrating orbits. The $4s$-orbit, as explained on p. 540, is strongly eccentric. Hence the electron penetrates the shell, and the energy value is much increased. The $3d$ orbit is hydrogenic and hence its energy-value is very nearly equal to $Rh/3^2$. Actually it is 13470, which is slightly larger on account of the strong polarisation of inner orbits by $3d$. Even the $4p$-orbit of K is larger than $3d$, for this is also strongly eccentric. For the next element Ca, the constitution should be $4s^2$, otherwise the similarity of its chemical and spectral properties to Mg which has the constitution $3s^2$ cannot be explained. But the next element Scandium cannot have the constitution $4s^2 . 4p$, for then it would have the same chemical properties as Al.

This is far from being the fact, as a glance at the Periodic Classification on p. 526 shows. In fact Sc has chemical properties which are rather widely different from those of Al. The spectrum of scandium is also found to be more complex than the very simple spectrum of aluminium discussed in §279. From these facts, it is concluded that Sc has not got the aluminium-like constitution $4s^2$, $4p$, but the entirely new constitution

$$21 \text{ Sc} \quad . \; . \; . \; . \qquad \left.\begin{matrix} . \; . \; . \; . \; 3d \; 4s^2 \\ . \; . \; . \; . \; 3d^2 \; 4s \end{matrix}\right\}$$

The possibility of these new constitutions can be seen from the following arguments. Sc^{+++} has just the same constitution as Argon, *viz.*, $\boxed{1s^2 . 2s^2 . 2p^6 . 3s^2 . 3p^6}$. When we bring a fresh electron to form Sc^{++}, the electron may be either in $3d$ or $4s$-shell giving rise to the alternative structures :—

$$Sc^{++} \quad . \; . \; . \; 3p^6 . 3d \text{ or } 3p^6 . 4s.$$

Which of them has the less energy-value? In K and Ca^+, which have got the same number of electrons as Sc^{++}, evidence of spectra tells us that $3p^6 . 4s$ has the lesser energy, and is more fundamental, but even in these atoms, the d-terms are somewhat abnormally large as shown in the following table.

Table 16.

Element	$4s$	$4p$	$3d$
K	35006	22020·8 21963	13467 13471
Ca^+	95719·2	70528·7 70305·7	82008 82069·5
Sc^{++}	174156	137590·8 137117·1	199693
Ti^{+++}	268439	220905·3 220086·9	348817

Thus in Ca$^+$, the 3*d*-terms very nearly approach the 4*s*-term in value, and are larger than the 4*p*-terms. Bohr postulated that in Sc^{++} and subsequent elements like Ti^{+++}, ,V^{+4} Cr^{+5},. the 3*d*-terms will be actually larger than the 4*s*-terms, and will constitute the normal terms. These predictions have actually been verified, as is seen from the following Moseley curves. In the case of Sc^{++} though the 4*s*-orbit is eccentric, yet it can be proved that on account of the high value of the central charge its energy value is less than that of the 3*d*-term. Hence Bohr's conclusions are justified.

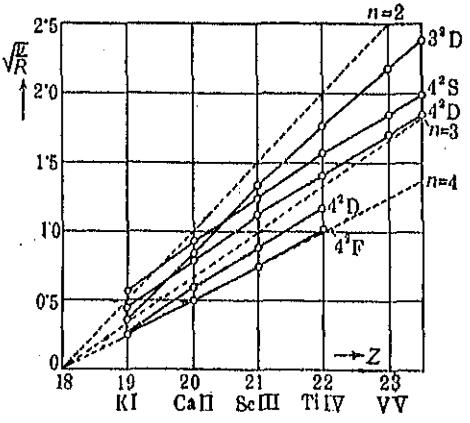

Fig. 15. The Bohr-diagram for K, Ca$^+$, Sc^{++}, Ti^{+3}, V^{+4}.

As the normal constitution of Sc^{++} is $3p^6 3d$ the constitution of Sc$^+$ will be

$$\boxed{1s^2\ 2s^2\ 2p^6\ 3s^2\ 3p^6}\ 3d^2$$

Sc$^+$ . . . .

$$\boxed{1s^2\ 2s^2\ 2p^6\ 3s^2\ 3p^6}\ 3d\,.\,4s$$

the 20th electron may be caught in 3*d* or 4*s*-shell. There is a competition between the two levels 3*d* and 4*s* for capture of the electron. But for calcium, the normal constitution is different

Ca . . . . $\boxed{1s^2\ 2s^2\ 2p^6\ 3s^2\ 3p^6}\ 4s^2 \ldots {}^1S_0 = 49305$

The configuration $\boxed{1s^2\ 2s^2\ 2p^6\ 3s^2\ 3p^6}\ 4s\,.\,3d$ gives the terms

$$^3D_{1,2,3},=28969,\ 28955,\ 28933, \qquad {}^1D_2=27455$$

Since for Ca$^+$ . . . $3\,p^6\ 4s$. has the lesser energy value, the $3p^6$. $4s.3d$-structure gives rise to the large D-terms in Ca (for a similar reason in Sr and Ba) as explained earlier, which differentiate them in some measure from the group Mg, Zn, Cd, Hg. They are also found to behave somewhat differently in their chemical behaviour and are therefore placed in the odd-group. There is thus a difference in the electron-structure of Ca and Sc$^+$ though both have the same number of electrons. There are other fundamental differences between the Ca and the Mg groups to which we shall return later in the chapter on *Complex Spectra.*

285. Formation of Transitional Group of Elements.—When a fresh electron is brought to the Sc$^+$-shell it may be caught either in the $4s$ or the $3d$-shell. The constitution therefore becomes :—

$$\mathrm{Sc}^+ \begin{cases} \boxed{1s^2\ 2s^2\ 2p^6\ 3s^2\ 3p^6}\ 3d^2 \\ \boxed{1s^2\ 2s^2\ 2p^6\ 3s^2\ 3p^6}\ 3d.4s \end{cases} \qquad \mathrm{Sc} \begin{cases} \boxed{1s^2\ 2s^2\ 2p^6\ 3s^2\ 3p^6}\ 3d^2\,.\,4s \\ \boxed{1s^2\ 2s^2\ 2p^6\ 3s^2\ 3p^6}\ 3d\,.\,4s^2 \end{cases}$$

The structure $3p^6\ 3d^3$ though possible, is not actually found. These structures have been completely confirmed by spectroscopic analysis which will be discussed in Chap. XIV. When we take the elements after Sc we expect that the fresh electrons will continue to fill up the $3d$-shell till it is saturated. For Ti, the structure is

$$22\ \mathrm{Ti}\ \ldots\ldots \quad \begin{matrix} \boxed{1s^2\ 2s^2\ 2p^6\ 3s^2\ 3p^6}\ 3d^3\,.\,4s \\ \boxed{1s^2\ 2s^2\ 2p^6\ 3s^2\ 3p^6}\ 3d^2\ 4s^2 \end{matrix}$$

and generally for the elements coming after Ti the structure is

$$3p^6\,.\quad 3d^x\,4s$$

or

$$3p^6\,.\quad 3d^{x-1}\,.4s^2.$$

This state of affairs will continue till the d-shell is completely filled up. According to Pauli's principle, the d-shell is completed only when $x=10$. The group therefore closes when we reach the 29th element copper, which has the constitution :—

$$29\ \mathrm{Cu} \quad \begin{matrix} \boxed{1s^2\ 2s^2\ 2p^6\ 3s^2\ 3p^6}\ 3d^{10}\ 4s\ \ {}^2\mathrm{S}_{\frac{1}{2}} & = & 62308{\cdot}00 \\ \boxed{1s^2\ 2s^2\ 2p^6\ 3s^2\ 3p^6}\ 3d^9\ 4s^2\ \ {}^2\mathrm{D}_{\frac{5}{2},\frac{3}{2}} & = & 51105{\cdot}3,\ 49062{\cdot}6. \end{matrix}$$

Thus the group of elements 21 Sc to 28 Ni possesses the outer structure $3d^x\,.\,4s$ or $3d^{x-1}.4s^2$ and hence they are unlike any other preceding elements. They constitute a group with entirely new chemical properties. They have got variable valency of two or three, their salts are always strongly coloured, and most of them are strongly paramagnetic, and Fe, Ni and Co are ferromagnetic in the solid state. On account of these strongly marked characteristic properties, Thomsen put them in an entirely new group enclosed within a vertical oblong in Fig. 1, and called them the *First Transitional Group*. This classification has been completely justified by considerations of electron structure, as described above.

On account of their peculiar electron-structure, the spectra of these elements are extremely complex, consisting of thousands of lines, the origin of most of which has however been explained from Pauli's Principle as will be discussed in Chapter XIV. We shall now proceed with consideration of formation of the remaining elements, after devoting a few remarks to copper.

CHEMICAL AND PHYSICAL PROPERTIES OF COPPER.

When the transitional group is closed, we come to copper which has got the normal constitution $3d^{10}4s$. The $3d^{10}$-level gives us a $^1S_0$-term and hence the Cu^+ -core * is magnetically neutral like an inert gas. The electron in the $4s$-level gives us a doublet $^2S_{\frac{1}{2}}$ -term as the fundamental level (62308 cm^{-1}). The constitution of the excited atom is obtained by increasing the quantum numbers successively and forming the structures $3d^{10}\,4p$, $3d^{10}\,4d$, $3d^{10}\,5s$. It is apparent that these structures give rise to alkali-like terms, and consequently copper is, in certain respects, exactly similar to the alkali elements in its chemical properties, and in its spectra. This is verified by the existence of monovalent compounds like Cu_2Cl_2, Cu_2O as well as by the existence of doublet lines which can be grouped in a fundamental doublet spectrum like the alkali lines. It has been found from the analysis of the copper spectrum that the resonance lines arise as in table 17.

Table 17.

$4s$ \ $4p$	31773 $^2P_{\frac{1}{2}}$	31524 $^2P_{\frac{3}{2}}$
$^2S_{\frac{1}{2}}$ 62308	λ 3273·97	λ 3247·5

But besides these doublet lines, the arc spectrum of copper shows a large number of other lines which cannot be explained on the above basis. These include the strong green line which impart to flames sprinkled with copper salts their characteristic green coloration. That these lines are connected with the arc-spectrum can be seen from the fact that they arise from the $3d^{10}4p$-levels referred to above, and can be arranged as shown in table 18.

Table 18.

	31773 $^2P_{\frac{1}{2}}$	31524 $^2P_{\frac{3}{2}}$
$^2D_{\frac{3}{2}}$ 49062·6	λ 5782·13	λ 5700·25
$^2D_{\frac{5}{2}}$ 51105·5		λ 5105·68

---

* Spectrum of Cu^+: A. G. Shenstone, *Phys. Rev.*, **29**, 380, 1927.

This analysis * shows that copper possesses besides the fundamental $3d^{10}.4s\ {}^2S_{\frac{1}{2}}$ -level, two large metastable ${}^2D$ levels possessing the values ${}^2D_{\frac{5}{2}} = 51105{\cdot}5$ and ${}^2D_{\frac{3}{2}} = 49062{\cdot}6$ cm.$^{-1}$.

These levels have been ascribed to the electron-structure

$$3d^9.\ 4s^2$$

i.e., in copper we have 11 electrons outside the $3p^6$-shell, but we can put ten of them in $3d$ and one in $4s$, or nine in $3d$, two in $4s$. The structure $3d^9$ gives inverted ${}^2D$-terms, and $4s^2$ gives us an ${}^1S_0$-term. Thus we get the metastable ${}^2D$-levels.

It is supposed that the $3d^9.\ 4s^2$-structure gives to copper some of the properties of the transitional group, enabling it to form divalent compounds like $CuCl_2$, CuO, etc., . . . while the normal Cu-atom forms monovalent compounds.

When copper is excited, one electron may be shifted from $4s$ to orbits like $4p$, $4d$, ... giving rise to structures like

$$3d^9.\ 4s.\ 4p,\quad 4d^9.\ 4s.\ 4d,\ .\ .\ .\ .\ .\ .\ .\ .$$

which give us the quartet and doublet type of optical terms, and thus account for the complexity of the arc spectrum of copper.

These terms can be treated only under *Complex Spectra.*

286. Formation of Elements after Copper.—After copper, we get zinc which possesses the structure

$$30.\ Zn\ .\ .\ .\ .\ 1s^2.\ 2s^2\ 2p^6.\ 3s^2\ 3p^6\ 3d^{10}.\ 4s^2.$$

No other alternative structure is possible. Thus zinc possesses strongly bivalent properties like Mg and possesses the same type of singlet and triplet spectrum. The elements after zinc are formed by bringing electrons to the $4p$-shells as shown below :—

31. Ga $\boxed{1s^2\ 2s^2\ 2p^6\ 3s^2\ 3p^6}\ 3d^{10}\ 4s^2.\ 4p$ . . . . Ge^+, As^{++}

32. Ge $\boxed{1s^2\ 2s^2\ 2p^6\ 3s^2\ 3p^6}\ 3d^{10}\ 4s^2\ 4p^2$

33. As $\boxed{1s^2\ 2s^2\ 2p^6\ 3s^2\ 3p^6}\ 3d^{10}\ 4s^2\ 4p^3$

34. Se $\boxed{1s^2\ 2s^2\ 2p^6\ 3s^2\ 3p^6}\ 3d^{10}\ 4s^2\ 4p^4$

35. Br $\boxed{1s^2\ 2s^2\ 2p^6\ 3s^2\ 3p^6}\ 3d^{10}\ 4s^2\ 4s^5$

36. Kr $\boxed{1s^2\ 2s^2\ 2p^6\ 3s^2\ 3p^6\ 3d^{10}\ 4s^2\ 4p^6}$

---

* A. G. Shenstone, *Phys. Rev.*, **28**, 449, 1926. P. K. Kichlu, *Ind. Journ. Phys.*, **1**, 401, 1926.

Thus in these elements, the properties of the regular group are repeated as shown in Fig. 1 with the aid of inclined strokes joining corresponding elements. The spectra of these corresponding elements have identical structure.

287. Formation of the Fifth Period.—After the completion of the fourth period the formation of the fifth period from 37 Rb to 54 Xe begins. The story of its formation is exactly similar to that of the fourth period, and it can be divided into three sections :—

$$(a) \qquad 37\ \text{Rb}\ \boxed{1s^2\ 2s^2\ 2p^6\ 3s^2\ 3p^6\ 3d^{10}\ 4s^2.\ 4p^6}\ 5s$$

$$38\ \text{Sr}\ \boxed{1s^2\ 2s^2\ 2p^6\ 3s^2\ 3p^6\ 3d^{10}.\ 4s^2\ 4p^6}\ 5s^2.$$

The 37th electron does not pass to the $4d$-shell but to the $5s$-shell as in K. Similarly for Sr.

(*b*) The elements after Sr ... 39 Y to 46 Pd ... are constituted in the same way as 21 Sc to 28 Ni and form the *second transitional group.*

These elements, however, possess more alternate structures for their ground states than the elements of the first transitional group. Their structures are shown below :—

$$\text{Common core: } \boxed{1s^2\ 2s^2\ 2p^6\ 3s^2\ 3p^6\ 3d^{10}\ 4s^2\ 4p^6}$$

39Y	40Zr	41Nb	42Mo	43Ma	44Ru	45Rh	46Pd
$4d\ 5s^2$	$4d^2\ 5s^2$	$4d^4\ 5s$	$4d^5\ 5s$		$4d^7\ 5s$	$4d^8\ 5s$	$4d^{10}$
$4d^2\ 5s$	$4d^3\ 5s$	$4d^3\ 5s^2$	$4d^4\ 5s^2$	—	$4d^8$	$4d^9$	$4d^9\ 5s$
$4d^3$	$4d^4$	$4d^5$	$4d^6$		$4d^6\ 5s^2$	$4d^7\ 5s^2$	$4d^8\ 5s^2$

These states have actually been verified, and they account for the very great complexity of their spectra.

The 47th element Ag has the constitution $\boxed{4\ d^{10}}$ $5s$ and like copper, it possesses an alkali-like doublet spectrum, and forms monovalent salts like AgCl, Ag_2O. It does not however seem to possess a strong $4d^9.\ 5s^2$-structure like copper.

(*c*) The elements after silver are formed in the same way as the group 29 Cu to 36 Kr by the filling up of the $5s$. $5p$-levels by fresh electrons as shown below :—

$$\text{Common core: } \boxed{1s^2\ 2s^2\ 2p^6\ 3s^2\ 3p^6\ 3d^{10}\ 4s^2\ 4p^6}\ 4d^{10}\ 5s^2$$

48 Cd	49 I	50 Sn	51 Sb	52 Te	53 I	54 Xe
... $5s^2$	$5s^2\ 5p$	$5p^2$	$5p^3$	$5p^4$	$5p^5$	$5p^6$

We may add to these Cs and Ba belonging to the 6th period. The constitutions of these two elements are:

$$55\ \mathrm{Cs}\ldots\boxed{1s^2\ 2s^2\ldots\ldots}\ldots 5p^6\ 6s.\quad 56\ \mathrm{Ba}\ldots\boxed{1s^2\ 2s^2\ \ldots}\ 5p^6\ 6s^2$$

These elements show the same characteristics as the pairs K and Ca, Rb and Sr; only the metastable *d*-terms are comparatively much larger as shown below.

Table 19.

Element	$6s$	$5d_{\frac{3}{2}>\frac{5}{2}}$	$6p_{\frac{1}{2}>\frac{3}{2}}$	$4f_{\frac{3}{2}>\frac{5}{2}}$
Cs	31404·6	16905 807	20226 19672	6932·6
Ba^+	80655	75781·7 74980	63394 68703	32397 32172

For barium, the term-values are

$$\begin{array}{lll}
6\,s^2\ \ldots\ldots & {}^1S_0 = 42029 & 6s\,6p\ \ldots\ldots\quad {}^1P_1 = 23969\\
6s\,5d\ \ldots & {}^1D_2 = 30634 & \left.\begin{array}{l}{}^3P_0 = 29763\\ {}^3P_1 = 29393\\ {}^3P_2 = 28515\end{array}\right\}\\
 & \left.\begin{array}{l}{}^3D_1 = 32995\\ {}^3D_2 = \quad 814\\ {}^3D_3 = \quad 433\end{array}\right\} &
\end{array}$$

The above figures illustrate the abnormally large metastable 5*d*-terms quite clearly. We shall return to detailed considerations of these terms in Chap. XIV.

288. The Rare Earths.—We shall now consider the elements after barium. A glance at the Periodic Table on p. 527 shows that we now come across a new group of elements (from 57 La to 71 Lu) with entirely new properties not shown by any group of elements occurring before. Most of these elements were discovered in the Scandinavian peninsula, (which is one of the oldest land masses on the surface of the Earth), amongst eruptive deposits, and were at first thought to occur in extremely small quantities. They were subsequently traced in similar geological formations in other parts of the world and have been found not to be so rare as at first thought. Almost all show strong trivalency, forming oxides having the formula M_2O_3 or chloride MCl_3, though a few, at the head of the group, form other oxides (*e.g.*, 58 Ce forms stable CeO_2, Ce_2O_3 being unstable). On account of the extreme similarity in the properties of these elements their separation from each other by methods at the disposal of the chemists was found to be an extremely difficult task. Life studies of these interesting elements were made by Urbain, Auer von Welsbach and others, and special treatises in chemistry should be consulted for more detailed information on them.

On the physical side, it was found that most of the compounds containing these elements were strongly paramagnetic. The spectra were found to be extraordinarily rich in lines surpassing even elements of the iron group.

Great controversies had taken place in the past concerning the identification of these elements or priority in discovery by independent investigators, for which the curious reader may consult special treatises on the subject. But the investigation of the characteristic X-ray spectra of these elements settled once for all the identity of the elements, and their sequence in the Periodic Classification. Before 1921, only two elements in the group, *viz.*, No. 61 and No. 72 had remained undiscovered.

It was at this stage that Bohr considered these elements from his theory of atom-structure or electron-composition of atoms. His views may best be illustrated with the aid of a chart (table 20) given on p. 583, which illustrates in a picturesque way, the formation of successive shells of electrons, as well as the spectra of elements. By glancing at the chart, the reader can at once find out how with its aid, the discussions given in the previous paragraphs regarding the formation of various groups, and the electron composition of the elements are clearly visualised.

In this diagram, we have written the levels with the same k diagonally ($1s$, $2s$, $3s$ . . . . . . ; $2p$, $3p$, $4p$, ...). Again the sub-levels $p_{\frac{1}{2}}$, $p_{\frac{3}{2}}$, $d_{\frac{3}{2}}$, $d_{\frac{5}{2}}$, ... have been combined, as the record of complex spectra shows that the splitting of the n_K-levels is rather artificial. The number of electrons filling any k-level is given by

$$N_K = 2\,(2k-1)$$

according to Pauli's exclusion principle as explained in §282. With the aid of this and the evidence of optical spectra as guide, the entire scheme of electronic composition of atoms has been built up. The chart visualises the composition very clearly. Thus let us take the elements O and S. They have the compositions :

8 O . . . $1s^2\ 2s^2\ 2p^4$
16 S . . . $1s^2\ 2s^2\ 2p^6\ 3s^2\ 3p^4$

Table 20.—Electron-Composition of Atoms.

		Transitional Group I	Transitional Group II	Transitional Group III and Rare Earths	
H . . $1s$ **He** . $1s^2$	$1s$ 2	21 Sc . . $3d\ 4s^2$ $3d^2\ 4s$ 22 Ti . . $3d^2\ 4s^2$ $3d^3\ 4s$ 23 V . . $3d^3\ 4s^2$ $3d^4\ 4s$ 24 Cr . . $3d^4\ 4s^2$ $3d^5\ 4s$ 25 Mn . $3d^5\ 4s^2$ $3d^6\ 4s$ 26 Fe . . $3d^6\ 4s^2$ $3d^7\ 4s$ 27 Co . . $3d^7\ 4s^2$ $3d^8\ 4s$ 28 Ni . . $3d^8\ 4s$ $3d^9\ 4s^2$	39 Y . . $4d\ 5s^2$ $4d^2\ 5s$ 40 Zr . . $4d^2\ 5s^2$ $4d^3\ 5s$ 41 Nb . . $4d^3\ 5s^2$ $4d^4\ 5s$ 42 Mo . . $4d^4\ 5s^2$ $4d^5\ 5s$ 43 Ma . . $4d^5\ 5s^2$ $4d^6\ 5s$ 44 Ru . . $4d^7\ 5s$ $4d^8$ 45 Rh . . $4d^8\ 5s^2$ $4d^9$ 46 Pd . . $4d^{10}$ $4d^9\ 5s$	$4d^{10}\ 5s^2\ 5p^6$ 57 La . . . . . . $5d\ 6s^2$ 58 Ce . . $4f$ . . $5d\ 6s^2$ 59 Pr . . $4f^2$ . . . . . $6s^2$ 60 Nd . . $4f^3$ . . . . . $6s^2$ 61 Il . . $4f^4$ . . . . . $6s^2$ 62 Sm . . $4f^5$ . . . . . $6s^2$ 63 Eu . . $4f^6$ . . . . . $6s^2$ 64 Gd . . $4f^7$ . . . . . $6s^2$ 65 Tb . . $4f^8$ . . . . . $6s^2$ 66 Dy . . $4f^9$ . . . . . $6s^2$ 67 Ho . . $4f^{10}$ . . . . $6s^2$ 68 Er . . $4f^{11}$ . . . . $6s^2$ 69 Tm . $4f^{12}$ . . . . $6s^2$ 70 Yb . . $4f^{13}$ . . . . $6s^2$ 71 Lu . . $4f^{14}$. $5d\ 6s^2$ 72 Hf . . $4f^{14}$. $5d^2\ 6s^2$ 73 Ta . . $4f^{14}$. $5d^3\ 6s^2$ 74 W . . $4f^{14}$. $5d^4\ 6s^2$ 75 Re . . $4f^{14}$. $5d^5\ 6s^2$ 76 Os . . $4f^{14}$. $5d^6\ 6s^2$ 77 Ir . . $4f^{14}$. $5d^7\ 6s^2$ 78 Pt . . $4f^{14}$. $5d^9\ 6s^2$	$5s^2\ 5p^6\ 5d^{10}$, 89 Ac . . . . $6d$ 90 Th . $5f$. $6d$ $6d^2$ 91 Pa . $5f^2$. $6d$ $6d^3$ 92 U . $5f^3$. $6d$ $6d$
Li . . . . $2s$ Be . . . . $2s^2$ B . . $2s^2\ 2p$ C . . . . . $2p^2$ N . . . . $2p^3$ O . . . . $2p^4$ F . . . . $2p^5$ **Ne** . . . $2p^6$	$2s$ $2p$ 2 6				
Na . . $3s$ Mg . $3s^2$ Al . . $3s^2\ 3p$ Si . . . . $3p^2$ P . . . . $3p^3$ S . . . . $3p^4$ Cl . . . . $3p^5$ **A** . . . . $3p^6$	$3s$ $3p$ 2 6	$3d$ 10			
Cu $3d^{10}4s$ Zn . $4s^2$ Ga . $4s^2\ 4p$ Ge . . . $4p^2$ As . . . $4p^3$ Se . . . $4p^4$ Br . . . $4p^5$ **Kr** . . . $4p^6$	$4s$ 2 19 K . . $4s$ 20 Ca . $4s^2$	$4p$ 6	$4d$ 10	$4f$ 14	
Ag $4d^{10}5s$ Cd . . $5s^2$ In . . $5s^2 5p$ Sn . . . $5p^2$ Sb . . . $5p^3$ Te . . . $5p^4$ I . . . . $5p^5$ **Xe** . . . $5p^6$	37 Rb . $5s$ 38 Sr . $5s^2$	$5s$ 2	$5p$ 6	$5d$ 10	$5f$ 14
Au $5d^{10}6s$ Hg . . $6s^2$ 1 Tl . . $6s^2\ 6p$ 2 Pb . . . . $6p^2$ 3 Bi . . . $6p^3$ 4 Po . . . $6p^4$ 5 — . . . $6p^5$ 6 **Rn** . . . $6p^6$	55 Cs . $6s$ 56 Ba . $6s^2$		$6s$ 2	$6p$ 6	$6d$ 10
	87 — . $7s$ 88 Ra . $7s^2$			$7s$ 2	$7p$ 6

The inert gases end in closed shells xp^6, where $x=2$ for Ne, 3 for A, ... The composition of regular groups is shown on the sides, and that of the transitional groups at the top with indications (by dotted lines) of their proper places in the scheme.

We have considered up to Ba which we found has the composition

$$\begin{array}{lr|l} 56\ \text{Ba}\ \ldots\ \boxed{1s^2\ 2s^2\ 2p^6\ 3s^2\ 3p^6\ 3d^{10}} & 4s^2\ 4p^6\ 4d^{10} & 4f \\ & 5s^2\ 5p^6 & 5d \\ & 6s^2 & 6p \end{array}$$

What will be the state of the electrons which are next brought to form the elements with higher nuclear charge?

We find that there are various possibilities. The electron may be in the $4f$, $5d$ or $6p$ shell. In fact, even when the elements 47 Ag to 56 Ba were being formed, there was just the probability that the $4f$-shell should be occupied. But actual experience shows that this does not take place, and it can be explained from the idea of penetrating orbits. For the $4f$-shell corresponds to a circular orbit, as $k=4$, $n_r=0$, hence the energy of a $4f$-electron in Ag is expected to be $-R/4^2=12352$ cm.$^{-1}$ approximately. But the $5s$ and $5p$ shells are very strongly eccentric and hence the energy of binding is much larger. In fact $5s\ {}^2S_{\frac{1}{2}}$ for Ag is 61096 cm.$^{-1}$, and $5p\ {}^2P_{\frac{1}{2}} = 31543{\cdot}6.$ cm.$^{-1}$ Hence the $5s$ and $5p$ shells are filled by preference giving rise to elements Ag to Xe ($5p^6$) and after that to Cs and Ba. But in Ba, as mentioned before, the $6s\ 5d$ combination is nearly as strong as $6s^2$. What happens afterwards?

Bohr concluded from general considerations that the further electrons brought in will not pass to $6p$, but either to $4f$ or $5d$. Thus the next elements will probably have the outer shell composed as follows:

$$4f^{x}\ 5d^2\ 6s, \qquad 4f^{x}\ 5d\ 6s^2$$

i.e., the electrons will be distributed amongst the $4f$, $5d$ and $6s$-shells. $6s$ cannot contain more than two, and later work has shown that $5d$ contains at most one or two. In fact the structures giving rise to the lowest term in La have been found to be

$$57\ \text{La}\ \ldots\ldots,\ 5p^6 5d^2 6s,\ \ 5p^6 5d\ 6s^2$$

As more electrons are brought they are accommodated in the $4f$-shell, In fact, a discussion of the paramagnetic properties of the compounds of these elements shows that the trebly ionised atom has the constitution $4f^x$.

Composition of trebly ionised rare-earths.

Common core: $[1s^2\,2s^2\,2p^6\,3s^2\,3p^6\,3d^{10}\,4s^2\,4p^6\,4d^{10}\,5s^2\,5p^6]$

Element	(58Ce	Pr	Nd	Il	Sm	Eu	Gd	Tb	Dy	Ho	Er	Tm	Yb	Lu)+++
Electrons in *f*-shell	1	2	3	4	5	6	7	8	9	10	11	12	13	14

According to Pauli's Principle, the *f*-shell can accommodate 14 electrons, hence correspondingly we get the fourteen elements from 57 La to 71 Lu.[*] The trebly-ionised atom has the constitution $4f^x$. When fresh electrons are brought, they are distributed over $5d$ and $6s$ according to energy relations. The exact composition of the outer shells of the neutral elements, at the time when Bohr gave out his hypothesis, could not be predicted.

289. The Discovery of Hafnium[†].—But it is clear that according to the above hypothesis, the composition of the elements at two limits, (57 La and 58 Ce at the beginning of the rare earth group, and of 70 Yb and 71 Lu at the end) is somewhat problematic. This agrees also with some characteristic deviation of the properties of these elements from the rest of the rare earth group. In fact, some chemists prefer to exclude La from the rare-earth group. In its chemical properties, La is strikingly similar to 39Y. We may suppose that it has the composition .... $5d^2\ 6s$, or $5d\ 6s^2$ rather than $4f\ 5d\ 6s$. But after La, the $4f$-shell begins to be completed. So 58 Ce will have the composition $4f\ 5d^2\ 6s$ or $4f\ 5d\ 6s^2$, and it falls under the rare-earth group.

Let us next consider what will be the composition of elements 71 and 72? We have the alternatives

$$71.\ \ \text{Lu}\quad 4f^{14}\left.\begin{array}{l}5d^2\ 6s\\ 5d\ \ 6s^2\end{array}\right\}\qquad\qquad 72.\ \ \text{Hf}\quad 4f^{14}\left.\begin{array}{l}5d^2\ 6s^2\\ 5d^3\ 6s\end{array}\right\}$$

---

[*] Element 71 is called Lutecium by the French workers after *Lutetia*, classical name for Paris, but was named Cassiopeium by *Auer von Welsbach*, and is so called by the German writers.

[†] An excellent account of the discovery of Hf will be found in the article by F. Paneth, *Ergebnisse der exakten Naturwissenschaften*, 2, 163, 1923. See also Gr. Hevesy, *Chemical Analysis by X-rays*, Chaps. XI—XIV.

At the time these speculations were being made, element 72 was still undiscovered, though a claim had been made for it by Urbain who called it Celtium. Urbain thought that Celtium was trivalent and had properties similar to those of the rare earths. But Bohr's investigations showed that for 72, the $4f$-shell was complete, and the four extra electrons formed the combination $5d^2\ 6s^2$, exactly like 22Ti ($3d^2\ 4s^2$) or 40 Zr ($4d^2\ 4s^2$). Hence Bohr thought that 72 was not a rare earth at all, but must be similar in properties to Ti and Zr.

These expectations were fulfilled. As elements similar in chemical properties are generally found associated in the same geological specimens, Bohr directed Hevesy and Coster[*] to look for the "new element" in some Zircon minerals (Norweigian Zircon). These investigators attacked the problem röntgenographically, and were rewarded in their first attempts. The L-lines of the element 72 appeared in their calculated positions, with such intensity as to convince the investigators that the element was contained in the sample in fair proportion. The X-ray spectra of Hf are shown in photograph (Fig. 16, Plate IX) reproduced from the original due to Hevesy.[†]

In fact all commercial salts of Zircon contain about 5% Hafnium, and it occurs in the earth's crust in the proportion of $1 : 10^{-5}$. It is thus only five times less plentiful than nickel.

To the new element, the name *Hafnium* was given in honour of Bohr's native city 'Copenhagen' which is the English rendering of the Danish name '*Havn*' meaning port.

The optical lines of Hafnium were afterwards photographed by Hansen[‡]; they have also been classified and it has been shown that normal electron-composition is $5d^2\ 6s^2$. It was found that the stronger lines of Hf were recorded by Eder and Valenta in the spectrum of Zr much earlier and were ascribed to impurities.

290. Discovery of Elements of Atomic Numbers 43, 61, 75.—Besides Hafnium, a number of other elements in the periodic table remained undiscovered up to 1927. These are number 43, 61, 75, 85 and 87 in the Periodic Table. Of these, 43 and

---

[*] D. Coster and G. De Hevesy, *Nature*, **111**, 79, 1923.

[†] Hevesy, *Chemical Analysis by X-rays*, p. 226.

[‡] Hansen, and Werner, *Nature*, **112**, 618, 900, 1923; *Naturwiss*, **12**, 528, 1924.

75 were predicted by Mendéleeff to be analogous to Manganese in their chemical properties (*vide* Periodic Table 1, p. 526), and were called by him *Eka* and *Dwi-manganese* respectively (*Eka* is a Sanskrit word meaning one, *Dwi* means two). 61 is a rare-earth, 85 should belong to the halogen group (*Eka-iodine*), and 87 should be an alkali-element, like caesium (*Eka-caesium*).

In 1925, 43 and 75 were discovered by Noddack and Tacke* and were called Masurium and Rhenium. They expected these two elements to occur together on account of general similarity in their chemical properties, and looked for them in the mineral colombite $Fe(NbO_3)_2$ and in the ore called Platinum earth which were known to contain large number of neighbouring elements, *viz.*, 24 to 29 ; 44 to 47 ; 76 to 79. Colombite was the source mainly tried, the other not being available. The source was subjected to suitable chemical processes to concentrate the proportion of elements having the predicted properties of Eka and Dwi-manganese. When a concentration of about 1% was supposed to be attained, the source was subjected to X-ray analysis by Berg and Tacke†. To obtain standard lines for comparison it was mixed with some niobium compound. By this method they were able to identify lines of 43 Masurium‡ and 75 Rhenium.§ Re is now available in the market, but Ma is not.

Element 61 has been claimed to be discovered by Harris, Yntema and Hopkins‖ (1926) in the University of Illinois, U.S.A., and called Illinium by them, and by Rolla¶ in Italy, and called Florentium.

The elements Eka-iodine, and Eka-caesium have not yet been discovered.

291. Elements after Hafnium.—The elements 73 to 78 form the 3rd transitional group having the compositions $4f^{14}\ 5d^{x}\ 6s^2$, or $5d^{x+1}\ 6s$. The last element is Pt whose electron composition is . . .

---

* W Noddack, I Tacke and O. Berg, *Naturwiss.*, 13, 567, 1925.

† An excellent account of the discovery, analysis and properties of Re will be found in an article by W. Noddack, *Ergebnisse der Exakten Naturwissenschaften*, 6, 333, 1927.

‡ Masurium—so called after the Masurian lakes in East Prussia where in 1914, during the Great World War, the invading Russian army was routed by the Germans.

§ Rhenium—named after the Rhineland province in Germany.

‖ J. H. Harris, L. F. Yntema and B. S. Hopkins, *Nature*, 117, 792, 1926.

¶ Rolla and Fernandes, *Zs. f. Anorg. Chem.*, 157, 371, 1926.

$5d^9\ 6s$, or $5d^{10}$. After this we come again to the regular group 79 Au to 86 Rn having the compositions shown below.

Composition of 79 Au to 88 Ra.

Common Core: $[1s^2\ 2s^2 \ldots\ 4s^2\ 4p^6\ 4d^{10}\ 4f^{14}\ 5s^2\ 5p^6\ 5d^{10}]$

Element ...	79 Au	80 Hg	81 Tl	82 Pb	83 Bi
Composition ...	$6s$	$6s^2$	$6s^2 6p$	$6s^2 6p^2$	$6s^2 6p^3$
Element ...	84 Po	85 —	86 Rn	87 —	88 Ra
Composition ...	$6s^2 6p^4$	$6s^2 6p^5$	$6s^2 6p^6$	$\left.\begin{matrix}6s^2 6p^6\\ 7s\end{matrix}\right\}$	$\left.\begin{matrix}6s^2 6p^6\\ 7s^2\end{matrix}\right\}$

Of these 87 is still unknown, and 88 Ra has chemical properties similar to Ca, Sr, Ba.

ELEMENTS AFTER RADIUM.

Only four elements are known after radium, and they are all radioactive. 89 Ac is generally separated with La in chemical analysis, and 90 Th has properties analogous to Ce. Elements 91 (sometimes called Brevium) is obtained only in minute quantities as a result of the β-ray disintegration of UX_1, and is identical with Protactinium.

The electron composition of these elements is only conjectural and the chart on p. 583 may be consulted. There is competition now between $5f$, $6d$ and $7s$-shells. The following structures are provisionally given:

89 Ac...$6d\ 7s^2$ 90 Th... $6d^2\ 7s^2$ 91 Pa ? 92U...$5f^3\ 6d^2\ 7s$
$5f\ 6d\ 7s^2$ $6d\ 7s^2$
$5f\ 6d^2\ 7s$ $5f^2\ 6d^3\ 7s$

The composition for Ac is suggested by its analogy with La, and that of Th with Ce. But it is not clear whether U is a rare-earth or a transitional element. It seems to partake of the characters of both.

No element has yet been discovered after U and frequent attempts have been made to show that there is a limit to the number of atoms which can occur. According to (41) on p. 357, the energy of a single electron moving round a nuclear charge $+Ze$ is given by

$$W = mc^2\left[\left\{\frac{\alpha^2\ Z^2}{[n+\sqrt{k^2-\alpha^2 Z^2}]^2}+1\right\}^{-\frac{1}{2}}-1\right]$$

where α = Sommerfeld-constant, the expression within root-sign becomes negative and the energy becomes complex if $Z > k/\alpha$, *i.e.*, for $Z > 137$. According to this view, there cannot be any element having $Z > 137$, *i.e.*, there can be altogether 137 elements. According to Flint and Richardson*, the number should be $1/\alpha\sqrt{2}$, *i.e.*, about 98, and still another view limits it to 92. But the reasonings behind these arguments are not very convincing.

As a matter of fact, a determined search for elements having $Z > 92$ does not seem to have yet been made. On account of some mysterious reasons, the screening constant for the K-electrons in U becomes negative (*vide* p. 465) and this fact, which is yet unexplained, may be connected in some way with the failure to detect such elements. If they are found to occur at all, they are expected to form, according to one view, Rare Earths of Group II, and according to another view transitional elements of group IV. The rare-earth hypothesis may explain why so far it has been found impossible to chemically separate the elements.

In a recent announcement Fermi† claims that when *neutrons* are allowed to bombard a U-atom, radioactivity is induced on it, and it gives out β-rays. The product of this radioactive disintegration would be element number 93. But the element 93 or any higher element has not yet been discovered in any mineral occurring within the earth's crust. Just at the time of final proof reading, it is announced in Nature that element 93 has been discovered at Prague in pitchblende, and its properties are stated to be analogous to 43 Ma and 75 Re. If the announcement be found to stand criticism, then elements after 89 form transitional group IV, having the composition $6d^x\ 7s^2$, there being no electron in $5f$.

Books Recommended.

1. N. V. Sidgwick, *The Electronic Theory of Valency*, 1932.
2. L. Pauling and S. Goudsmit, *The Structure of Line Spectra*, 1930.
3. N. Bohr, *Atomic Theory and the Description of Nature* (Four Essays with an Introductory Survey), 1934.
4. M. Born, *Vorlesungen über Atommechanik*, 1, 1925.
5. W. Grotrian, *Handbuch der Astrophysik*, 3 (1), 1930.
6. F. Hund, *Linien spektren und periodisches System der Elemente*, 1927.
7. W. Noddack, *Ergebnisse der exakten Naturwissenschaften*, 6, 1927.
8. F. Paneth, *Ergebnisse der exakten Naturwissenschaften*, 2, 1923.
9. G. Hevesy, *Chemical Analysis by X-rays*, 1932.
10. R. F. Bacher and S. Goudsmit, *Atomic Energy States*, 1932.

---

* Flint and Richardson, *Proc. Roy. Soc. A*, **117**, 637, 1928.

† Fermi, *Nature*, **133**, 757, 898, 1934.

CHAPTER XIII

CRITICAL POTENTIALS OF ELEMENTS

The subject treated in this chapter is of vast dimensions, and cannot be adequately described in a single chapter of a Text Book. Only leading ideas are given, and a few representative experiments are described. For complete study, reference must be made to the bibliography given at the end of the chapter.

292. Introduction: Lenard's Experiment.—Shortly after the discovery and isolation of the electron, Lenard took the first steps for studying the phenomena connected with the passage of electrons through gases. He was followed by Ramsauer, Mayer, etc., and Franck and Hertz in Germany, and by Townsend in England. But the greatest impetus to these studies was given after Bohr's theory of spectra had obtained general recognition, and provided the physicists with a working model of the structure of the atom which approximated to facts.

Lenard* showed that if a parallel beam of electron-rays be passed through a gas, two changes are observed when the length of the gas column traversed is gradually increased. First a decrease, in the intensity, *i.e.*, the number of rays reaching the target decreases secondly an increasing diffuseness in the shape of the cross-section of the bundle. The apparatus with which he worked is now of historical interest, but it served as the model for future experiments and is described below (Fig. 1) in the improved form given to it later by H. F. Mayer.†

G. . . . . A heated Tungsten filament which is used as source of electrons.

B_1, B_2 . Slits. A potential difference is applied between B_1 and B_2 which endows the electron with the requisite velocity. They then emerge through a third slit into the space H_2. The latter is covered with metal, and hence there is no field in H_2.

---

* P. Lenard, *Ann. d. Phys.*, **2**, 359, 1900; **12**, 449, 714, 1903.

† H. F. Mayer, *Ann. d. Phys.*, **64**, 451, 1921.

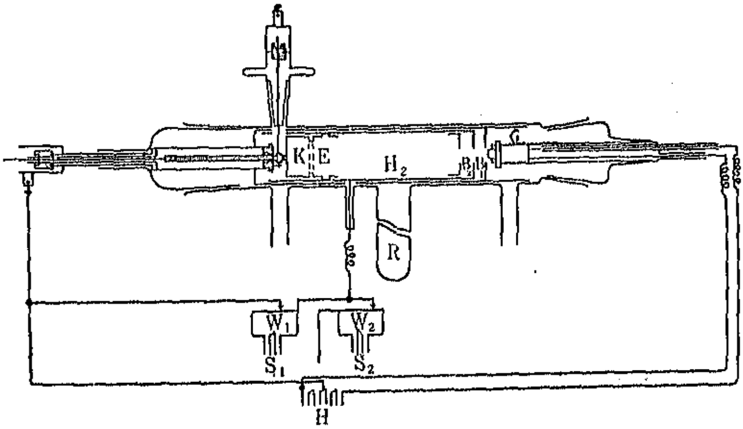

Fig 1. Modified Lenard's apparatus (*Mayer*).

E. . . . . A wire-gauze.

K. . . . A second parallel wire-gauze covering the receiver (Faraday Cylinder).

An opposite e. m. f. of such dimension is applied between E and K, that only such electrons which possess the original velocity as acquired in passing between B_1 and B_2 can pass into K. The receiver is connected to a quadrant electrometer which measures the charge.

All these parts are contained within a glass vessel which can be exhausted to any vacuum, and then filled with any gas at a desired pressure. The receiver K can be shifted parallel to itself so that the distance traversed by the electrons can be varied.

It was found that the current decreases as the length is increased. Lenard sought to explain the decrease on the hypothesis of elastic collisions. As the electrons pass through the gas, they come into collision with the gas molecules, and are turned back without suffering any diminution in velocity. According to the kinetic theory of gases, the number n which succeeds in passing a distance x without being turned back by collisions is given by

$$n = n_0 \, e^{-x/\lambda}$$

where n_0 = initial number, λ = mean free path.

Here we suppose that the electron is a rigid sphere, and it collides with the molecule, which is another rigid sphere having a much larger mass. It can be shown from dynamics that in such encounters the electron suffers no diminution in its kinetic energy, *i.e.*, the collision is elastic. We have then

$$\lambda = \frac{1}{x} \log_e n_0/n = \frac{1}{x} \log_e I_0/I,$$

because n is proportional to I, the current due to the electron beam.

What is the mean free path of the electron? According to the kinetic theory if we have a mixture of gases A, B, C, ... S etc., the mean free path of A is given by

$$\frac{1}{\pi\lambda_A} = \sum_{X=A}^{X=S} n_X \sqrt{1+m_A/m_X} \cdot \left(r_A + r_X\right)^2$$

where r_A, r_B .... are radii, n_A, n_B .... are concentrations and m_A, m_B. . . . are masses of the molecules A, B. . . . . S.

We suppose that in the present case we have only two types of particles with which the vessel is filled up, the molecules and the electrons. Let the gas molecules have the radius r and let us suppose that the electrons have vanishing radius and concentration. Then

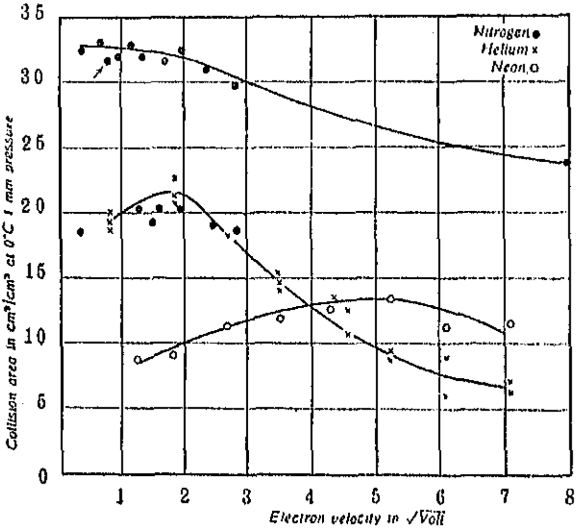

Fig. 2*a*

$$\lambda = \frac{1}{4\sqrt{2}\pi n r^2} = (\log_e I_0/I)/x$$

is the mean free path of the molecules.*

---

* Vide *A Text Book of Heat*, Saha and Srivastava, p. 123. See also Loeb's *Kinetic Theory of Gases*, (1934).

So this experiment enables us to calculate the collision radius of the atoms or molecules with which the vessel is filled up. The collision radius of gases calculated according to this method was found to be of the same order of dimensions as obtained from gas-kinetic theories, but they were found to vary with the velocity of the primary electrons in an unexpected manner as shown in curves, Figs. 2*a* and 2*b* for N_2, He, Ne, Kr, Xe, A and H_2.

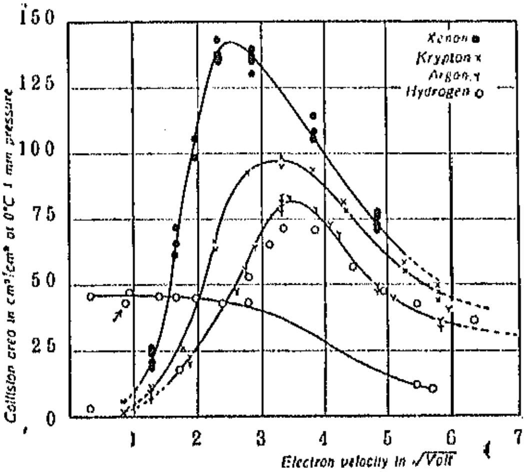

Fig. 2*b*. Variation of collision radius of gas molecules with velocity of the electrons (*Ramsauer*)

These experiments have been continued by Ramsauer and others using improved methods which will be described later.

293. Inelastic Collisions.—Further experiments showed that the encounter of an electron with an atom or molecule gives rise to more complex phenomena than those described in the preceding section.

It was known quite early, from the study of cathode rays, and β-particles (which are only fast electrons) that the electrons can ionise the gas through which they pass (see for example the track of a β-ray photographed by the cloud-chamber method of C. T. R. Wilson, Plate III, Fig. 28, where the presence of these secondary ions are shown by small tracks). Collision in such cases cannot be elastic; the electron imparts a part of its energy to the colliding gas-molecule which is broken up by the impact into a positive part (positive ion) and a negative electron. The collision is therefore *inelastic*.

From several lines of argument, various physicists came to the conclusion that an electron acquires the capacity to produce ions by collision only when they possess a minimum amount of energy; and that this minimum energy depends upon the nature of the gas through which the electrons pass. The subject was thus investigated by Lenard* (1902) by means of the arrangement shown in Fig. 3.

F. . . . Glowing filament which is the source of electrons.

G. . . . Grid.

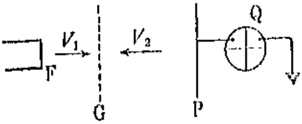

Fig. 3. Lenard's apparatus for studying inelastic collisions.

P . . . collecting plate.

Q . . . electrometer.

V_1 . . Accelerating potential applied between F and G.

V_2 . . Retarding potential applied between G and P.

$V_2 > V_1$ and the pressure is so chosen that $\lambda \gg FG$, but $< GP$, so that the electrons emerge into the space GP with full velocity, acquired by free fall between F and G.

Under ordinary conditions no electron will be able to reach the collecting plate, because the retarding potential V_2 is much larger than the accelerating potential V_1. The plate will therefore show no accumulation of charge. However there are two possible circumstances under which P may show a positive charge :—

(*a*) The electron may after passing through the grid collide with a gas molecule and ionise it, the positive ion so formed will be immediately drawn to the plate P under the influence of the potential V_2. P will therefore be positively charged.

(*b*) Instead of ionising, the electron may excite the atom to a higher state and cause it to radiate; and if the wavelength of the emitted radiation is short enough to eject photo-electrons from the plate, the plate will evidently be positively charged.

It should here be mentioned that only the first possibility was considered by Lenard, the second was pointed out several years later by Bohr and van der Bijl† from considerations of Bohr's theory of atomic structure.

Lenard's original experimental methods would be considered rather crude in these days and the results cannot be regarded as quantitative, but he established quite definitely one piece of experimental result, that, when the velocity of the electrons are varied (by varying V_1), it is found that at certain definite values of V_1 the rate of charging of P shows abrupt changes. This leads us to the conclusion that the gas-molecule is ionised by collision only when the electron has got certain definite amounts of energy. Experimenting with hydrogen, oxygen and CO_2, Lenard found the value of V_1 to be about 11 volts.

---

* P. Lenard, *Ann. d. Phys.*, **8**, 149, 1902.

† H. Van der Bijl, *Phys. Rev.*, **10**, 546, 1917.

This conclusion is now known to be inaccurate. What Lenard was observing was the ionisation potential of mercury vapour which was always present in his experimental vessels, as an impurity from the pump he was using.

294. Franck and Hertz's Experiments on the Critical Potentials.

—A great impetus to these studies was given by Franck and Hertz* who showed that the results obtained by Lenard and his pupils receive a ready explanation in terms of Bohr's picture of the atom. As most of these early works were performed with Hg vapour, the reader should make himself thoroughly familiar with the energy levels of the Hg atom which is similar to that of Mg described in §202.

It would have been much simpler if the experiments could have been done with the H-atom, because it is very easy to describe the different quantum states of the H-atom (see p. 327). But hydrogen occurs usually in the form of molecules which complicates the matter. It is easiest to work with Hg-vapour. An Hg-atom contains two valency electrons, and the structure of its spectra is similar to those of Mg, Zn, Cd and to a certain extent to those of Ca, Sr, Ba. Spectroscopic analysis showed that the fundamental state is $^1S_0$. The next states are $^3P_0$, $^3P_1$, $^3P_2$ and $^1P_1$. If the Hg-atoms are bombarded by electrons, then provided the energy of the bombarding electrons is sufficiently large, some of the Hg-atoms will have one of their valency electron raised to those higher levels $^3P_{0,1,2}$ and $^1P_1$. But these states are unstable, hence after an interval of time (10^{-7} to 10^{-9} sec.) the electron will fall back to the $^1S_0$ state. In this process radiation

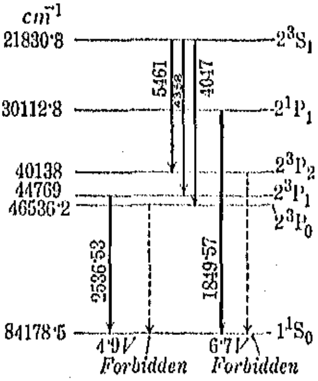

Fig. 4. Energy levels of Hg atom.

---

* Franck and G. Hertz, *Zs. f. Phys.*, 17, 409, 1916.

will be emitted. According to the selection-principle, however, transition from $^3P_0$, $^3P_2$ to $^1S_0$ is forbidden, hence, we have only emissions of the lines λ 2536·52 and λ 1849·5 corresponding to transitions from $^3P_1$, $^1P_1$ to $^1S_0$. These transitions are shown in Fig. 4.

According to this scheme, inelastic collision of electrons with Hg-atoms should commence, when the energy of the bombarding electrons is increased to 4·9 electron-volts. Further, at this voltage, the Hg-vapour would radiate only the line λ 2536, and none else.

These conclusions were experimentally verified by Franck and Hertz as follows.

EXPERIMENT OF FRANCK AND HERTZ.

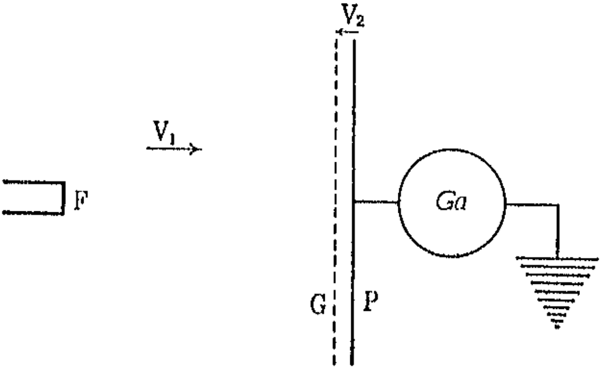

Fig. 5. Franck and Hertz's apparatus.

This apparatus requires little explanation. F is the filament, G is the grid which is now placed close to the collecting plate P. A sensitive galvanometer replaces the electrometer of Lenard's apparatus. $V_1 \gg V_2$ and $\lambda \ll FG$, so that the electrons suffer many collisions in passing from F to G.

In the actual apparatus, the plate and grid were in the form of coaxial cylinders mounted within a glass tube, and the filament was mounted centrally. The glass vessel could be evacuated and filled with the gas to be investigated.

Since $V_1 \gg V_2$ the latter will not be able to prevent the primary electrons from reaching P. The galvanometer therefore shows a small current which was found to vary as $(V - V_0)^{\frac{3}{2}}$ in accordance with the Child-Langmuir relationship (*vide infra*). When however V_1 exceeds 4·9 volts, the electrons can communicate the whole of their energy by collision to Hg-atoms and can be prevented from reaching P by V_2. Hence there is a sudden drop in the current. This is illustrated in Fig. 6, which represents the result of Franck and Hertz for Hg-vapours. As V_1 is further increased the current again goes on increasing. At 6·7 volts, there is a second drop due to the excitation of the $^1P_1$-level.

The method described above is however open to several sources of error. These are :—

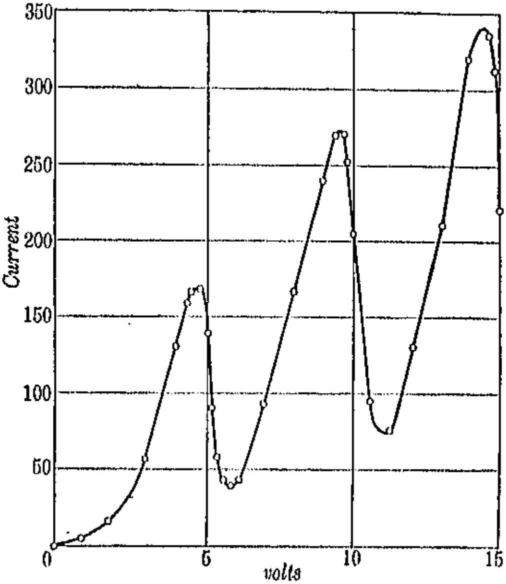

Fig. 6. Franck and Hertz's curve for mercury vapour.

(*a*) *Maxwellian Distribution of Velocity.*—We assume that the primary electrons come out of the filament with zero velocity and the K.E. possessed by them in collision space is only due to the applied accelerating potential. This assumption, however, is not justified, because the electrons as they emerge from the filament possess a Maxwellian distribution of velocity.

Table 1.—Velocity distribution of electrons emitted from a heated filament.

Percentage of electron emission	Energy in volts (Fil. temp. 2400°C)
90 %	0·022 volts
75 %	0·059
50 %	0·143
25 %	0·29
10 %	0·48
1 %	0·95
0·1 %	1·42
0·0001 %	2·85

This error may be corrected for by finding the velocity-distribution approximately, which is done by varying the retarding potential applied between the filament and the collecting plate and drawing a curve between the plate current and the applied retarding voltage. The results obtained from such a curve are shown in table 1.

(*b*) *Potential Drop along the Filament.*—Our next assumption is that all the electrons fall through the same accelerating potential. But owing to its high resistance the potential drop along the filament is considerable. Therefore electrons coming from different parts of the filament fall through different potentials.

The above defects have been remedied to a large extent by improving the source of electrons. In choosing a satisfactory source several factors have to be taken into consideration, *e.g.*, the effect of the gas under investigation on the filament, the possibility of dissociation of the gas at the filament surface, the length of time the filament retains its properties under the conditions of the experiment, etc. However for most purposes the following source is found to be satisfactory. A small nickel body is fused at the middle of a tungsten filament. Owing to the high conductivity the potential drop across it is very small, and the wire applying the accelerating potential is attached to this body. The error is thus practically eliminated.

To reduce the error due to Maxwellian velocity distribution among the electrons, this nickel body is covered with a layer of alkaline earth oxide. The work function (*vide infra*) of alkaline earth-oxides being very low, electrons are copiously emitted at comparatively low temperatures and so have low initial velocity and a narrow velocity distribution.

The method of magnetic resolution to separate a beam of electrons with a sharp maximum velocity limit from an inhomogeneous beam has also been used.

(*c*) Since the collisions can take place anywhere between the filament and the grid, the velocities of the bombarding electrons range between zero and the maximum (corresponding to the potential applied). This deprives the apparatus of much of its sensitiveness, *i.e.*, the maxima are not very sharp. This is corrected by putting an auxiliary grid very close to the filament and applying the accelerating potential between the two.

(*d*) *Contact Potential.*—Besides the accelerating potential applied, another source of potential exists between the filament and the grid. This is the contact e. m. f. which always exists between two dissimilar metal surfaces. The value of this may be previously determined and allowed for, or the apparatus may be calibrated with a gas possessing known critical potentials.

Franck*, Einsporn† and Knipping‡ have used Franck and Hertz's method in accurately determining the critical potentials of Hg-atoms. Einsporn adjusted the pressure of the Hg-vapour (·01 to 6 mm.) in the apparatus, so that the number of collisions is fairly large and he increased the accelerating voltage by steps of 0·1 volt. Further he put a grid just in front of the filament, as in Fig. 8, so that $FG_1 < \lambda$, and the full accelerating potential is applied between F and G_2. Between G_1, G_2 there is very little field, and $G_1 G_2 \gg \lambda$, so that many collisions can take place in the space $G_1 G_2$. This arrangement increases the sensitiveness of measurement considerably. One of his curves is given below (Fig. 7). It will be observed that the first maximum occurs at 3·8 volts instead of at 4·9 volts. This is due to contact potential and other sources of error. To get the accurate value of the resonance potential the difference between the first two maxima ought to be taken. As has been pointed out by Einsporn himself, most of the maxima of the curve can be interpreted as various combinations of different resonance potentials as shown in the table 2 on p. 600.

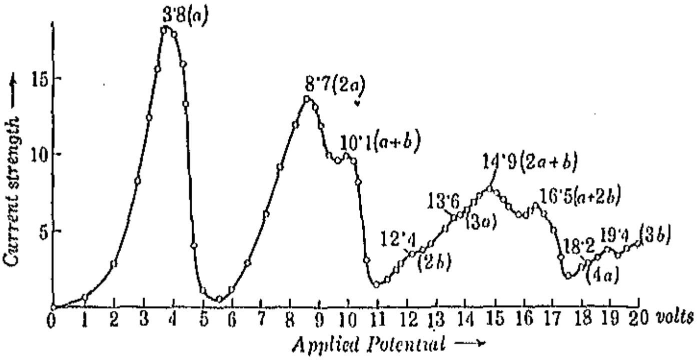

Fig. 7. Einsporn's curve for critical potentials of mercury.

295. Distinguishing Ionisation Potential from Resonance Potential – Experiment of Bergen Davis and Goucher.—Though Franck and Hertz's experiment described in the preceding section afforded a straightforward experimental verification of Bohr's theory, it failed to distinguish between the resonance and ionisation

---

* J. Franck and P. Knipping, *Zs. f. Phys.*, 1, 320, 1920.

† J. Franck and E. Einsporn, *Zs. f. Phys.*, 2, 18, 1920.

‡ E. Einsporn, *Zs. f. Phys.*, 5, 208, 1921.

Table 2.—Critical potentials of Hg.

Observed voltages		Combinations of $a = 4{\cdot}9$ volts and $b = 6{\cdot}7$ volts.	Diff. bet. calculated and observed values
From Curve	Corrected		
3·8	4·9	$a = 4{\cdot}9$	0
		$b = 6{\cdot}7$	
8·7	9·8	$2a = 9{\cdot}8$	0
10·1	11·2	$a+b = 11{\cdot}6$	−0·4
12·4	13·5	$2b = 13{\cdot}4$	+0·1
13·6	14·7	$3a = 14{\cdot}7$	0
14·9	16·0	$2a+b = 16{\cdot}5$	−0·5
16·5	17·6	$a+2b = 18{\cdot}3$	−0·7
18·2	19·3	$4a = 19{\cdot}6$	−0·3
19·4	20·5	$3b = 20{\cdot}1$	+0·4
20·1	21·2	$3a+b = 21{\cdot}4$	−0·2

potentials. Bergen Davis and Goucher* devised the following modification by which the two potentials can be distinguished from each other. Two grids G_1 and G_2 were used between the filament and the plate, and three suitable potentials V_1, V_2 and V_3 were applied.

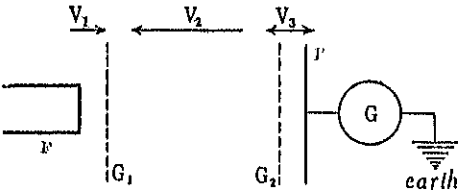

Fig. 8. Davis and Goucher's apparatus.

$$V_2 > V_1 > V_3$$

V_1 ..... accelerating potential which can be varied as usual.
V_2 ..... retarding potential $> V_1$.
V_3 ..... small constant potential whose direction can be reversed.

Further,

$$\lambda > FG_1 \text{ but } < G_1\,G_2.$$

Beginning from zero, the value of V_1 is gradually raised and for each value of V_1 two values of plate current are read corresponding to the two directions (direct and reversed) of V_3.

Davis and Goucher obtained the following curves in Fig. 9 with Hg-vapour :

+ current denotes that the current flows from the plate to the earth, – current denotes that the flow is in the opposite direction. We consider this curve in detail and examine it part by part.

---

[*] B. Davis and F. S. Goucher, *Phys. Rev.*, **10**, 101, 1917.

(1) O R . . . . . The electrons enter the collision space G_1 G_2 with the full velocity corresponding to V_1. As long as $V_1 <$ resonance potential, the collisions are elastic. The primary electrons cannot reach the plate because $V_2 > V_1$, whatever may be the direction of V_3. Hence the current is zero.

(2) RI . . . . . As soon as V_1 reaches the value 4·9 (the first resonance potential of Hg), the electrons in the space G_1G_2 suffer inelastic collision with Hg-atoms, and excite them to the $^3P_1$-orbit. These excited atoms radiate the light λ 2536 in about 10^{-7} seconds, and return to the normal state $^1S_0$. This radiation falling on P and G_2, releases photoelectrons. If V_3 is from $P \rightarrow G_2$, the electrons released from P cannot leave it while those from G_2 are assisted in passing to P. A negative current is therefore obtained. If V_3 is now reversed ($G_2 \rightarrow P$), the photoelectrons from P are enabled to leave it while those from G_2 are held up. Hence P shows a positive current over the part RI . . . . . in Fig. 9.

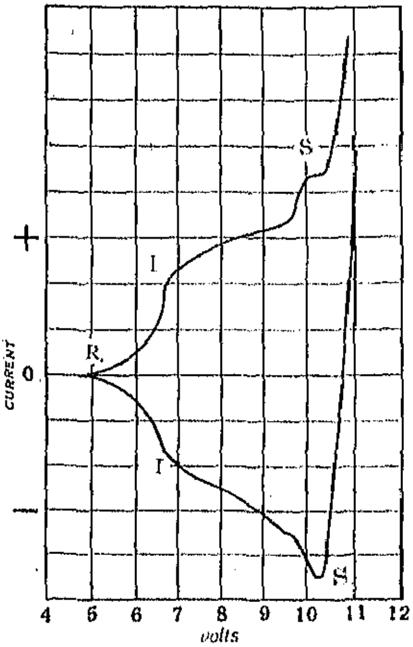

Fig. 9. Davis and Goucher's experimental curve for mercury.

When V_1 is further increased, inelastic collisions become more frequent, and radiation of λ 2536 becomes stronger. Hence the galvanometer current (both positive and negative) goes on increasing. At 6·7 volts, the currents show a further discontinuous rise. This is due to a fresh process just starting, *viz.*, the excitation of Hg-atom to the $^1P_1$-state, attended with the emission of λ 1849. This can be interpreted as the second resonance potential of Hg.

(3) The points S, S and beyond.

The next abrupt rise in the rate of increase of the current dI/dV_1 occurs at points S, S which correspond to about 10·4 volts. The most remarkable thing about this point is that for both the directions of V_3, the current is +ve. This is explained by taking 10·4 volts as the *ionisation potential* of Hg. The electrons from the filament F are accelerated by V_1 volts and when they pass beyond G_1, they possess sufficient energy to ionise the Hg atom against which they impinge. These primary electrons together with those which they have knocked out of the neutral atoms, fall back to the left side of G_1, under the influence of large retarding potential V_2. The positive Hg-ions formed by these collisions are however accelerated towards P by V_2. The galvanometer therefore shows a large +ve current. Since $V_3 \leqslant V_1$, its direction has very little influence on these positive ions.

296. Hertz's Methods of Determining the Resonance and Ionising Potentials.—The double grid methods described above have been further improved in several ways by Hertz*. He developed two distinct methods, one for the measurement of ionisation potential, and another for the measurement of resonance potentials based on two distinct principles, and in a third method he combines the two together. We describe the methods one by one.

(1) METHOD OF SPACE CHARGE (IONISATION POTENTIAL).

In Fig. 10, F_1 is a filament emitting electrons. F_2 is a second filament heated to very high temperature and enclosed in a cylindrical box R with a grid side towards F_1. Electrons emitted from F_1 are drawn by an accelerating potential V_1 into the box where collisions with gas molecules take place. A retarding potential V_2, less than the critical potential of the gas under examination, is applied to F_2 to keep the electrons away from it. A galvanometer Ga is connected between F_2 and R.

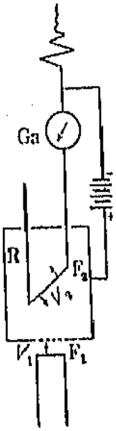

Fig. 10. Hertz's apparatus.

As the temperature of F_2 is raised the electron emission from F_2 increases, and the galvanometer indicates an increasing electron-current. But very soon the space inside the box acquires a high electron-density, and it exerts a strong repulsive force on the negatively charged filament F_2 and prevents any further electron emission from it (*space charge effect*). This puts a limit to the maximum electron current between F_2 and R. The limiting current is practically uninfluenced by any resonance radiation due to inelastic collisions taking place in the box.

---

* Hertz, *Zs. f. Phys.*, **18**, 311, 1923.

On the other hand if V_1 is large enough to cause ionisation of molecules by the impact of electrons from F_1, the positive ions are readily attracted to F_2, thereby neutralising a part of the charge on it. This allows further electron emission from F_2, and the galvanometer shows a sudden increase of current.

A typical result obtained by this method for neon is illustrated in the curve I of Fig. 14. It is clearly seen that the ionisation potential is nearly 21 volts.

The method is however open to the error due to distribution of electron velocities.

(2) METHOD OF RESIDUAL CURRENT (RESONANCE POTENTIAL).

An objectionable feature common to most of the preceding methods is that they measure the effect of inelastic collisions as superposed on the effects of all types of impact taking place at a lower potential. In order to avoid this uncertainty Hertz* devised the apparatus shown in Fig. 11.

F is the heated filament from which electrons are accelerated by means of a potential V_1 into the cylindrical space R having grid sides. It is surrounded by another coaxial cylinder P. The space in R is perfectly field-free. A small retarding potential V_2 (about 0·1 volts) $\ll V_1$ is applied between the grid and P.

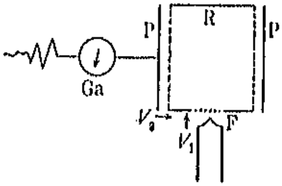

Fig. 11. Hertz's apparatus for resonance potential experiment.

With a particular value of V_1, we give a small value to V_2, say 0·1 volts, and then put it equal to zero. The electrometer current is noted in the two cases. In the first case, only those electrons which possess energy greater than 0·1 volts will reach P, while in the second case, nearly all the electrons will travel to P. The difference in the two currents gives therefore the number of electrons having energy less than 0·1 volts after any inelastic collision has occurred in the space. V_1 is now increased in steps and every time the two operations (with V_2) are repeated. As long as no inelastic collision takes place, the current remains steady. But at, say, the first resonance impact, the electrons give their whole energy to the molecules and are brought to rest, so a very few of these electrons can travel to P against the retarding potential V_2. But if the potential be

---

* G. Hertz, *Zs. f. Phys.*, 18, 307, 1923.

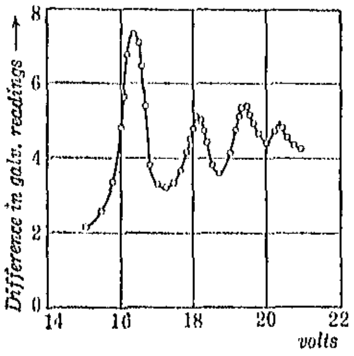

Fig. 12. Ionisation potential curve for Ne.

accelerating, they can travel to P. So at an inelastic collision, due to excitation of the molecule to resonance, there is a sudden increase in the difference between the currents with or without the retarding potential V_2 as shown in the curve in Fig. 12, for Ne. Complete ionisation of atoms, however, has no effect on the result.

In the curve shown opposite the first excitation potential of Ne at 16·65 volts, and the second at 18·45 volts are clearly distinguished. In order to make corrections for distribution of velocities, amongst the bombarding electrons, Ne is mixed with He in the collision chamber; the He-excitation potentials obtained (on the same curve) are corrected by comparison with their standard spectroscopic values, and the same corrections are applied to Ne.

The method has been employed to Kr by Hertz and Kloppers,* who have obtained the I. P. = 13·3 volts. The spectroscopic value is 13·94 volts.

(3) HERTZ'S METHOD FOR RESONANCE AND IONISATION POTENTIALS.

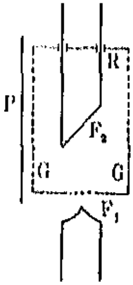

Fig. 13. Hertz's apparatus for resonance and ionisation potentials.

By a slight modification of the apparatus of method (1) Hertz has combined the above two methods, so that both resonance and ionisation potentials can be measured by the same apparatus. The apparatus is shown in Fig. 13 which, as can be easily seen, is a combination of the arrangements used in methods (1) and (2).

To get the ionisation potential, P is connected to the grid G, and then the same procedure is adopted as in method (1). To obtain the potentials corresponding to resonance the heating current from F_2 is withdrawn, and it is connected to R, and then we proceed as in method (2).

The result of experiment for Ne is illustrated in Fig. 14, where the curve I gives the ionisation potential V_i and the curve R gives the first resonance potential

---

* G. Hertz and R. K. Kloppers, *Zs. f. Phys.*, **31**, 463, 1925.

V_r. V_r is corrected by comparison with standard He curve as explained in method (2), and the same correction is then applied to V_i. A little uncertainty however remains, because we do not know which point on the curve R corresponds to the point i, which is obtained by the intersection of the horizontal part of the curve with the sloping part. This error is minimised by using a small retarding potential and confining the velocity-distribution of electrons from F_1 within a narrow limit.

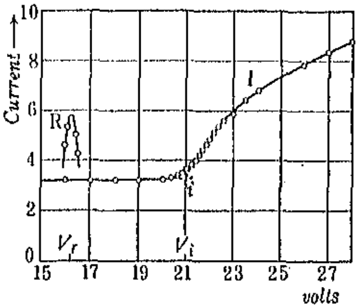

Fig. 14. Critical potentials of neon.

297. Controlled Excitation of Spectra.—Franck showed that when Hg atoms are bombarded by electrons having an energy of 4·9 electron-volts, the atoms are just excited to the higher state immediately next to the normal. This state is unstable and the atom returns in about 10^{-8} sec. to the normal state $^1S_0$, after emission of the line λ 2536. Now λ 2536 has according to the quantum theory the same energy as an electron falling through a potential difference of 4·9 volts, hence the experiment affords a proof of Bohr's theory of spectra of atoms.

These investigations were continued by many workers. We shall describe the experiments on the controlled excitation of spectra of Mg by Foote, Meggers and Mohler.* They developed a method in which the atoms were excited by bombardment with electrons whose velocity could be regulated. Fig. 15 shows an improved form of their apparatus due to Ruark.†

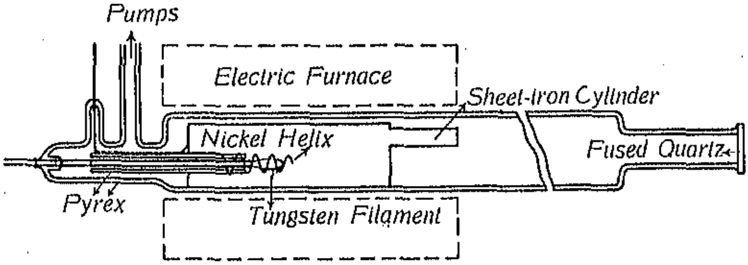

Fig. 15. The apparatus for controlled excitation of spectra. (*Ruark*)

---

* P.D. Foote, W.F. Meggers and F.L. Mohler, *Phil. Mag.*, **42**, 1002, 1921.
† A. E. Ruark, *J. Op. Soc. Am.*, **11**, 199, 1925.

The apparatus consists of a pyrex glass tube and is closed by a transparent plate of fused quartz which is open to the spectroscope. The vessel is placed within an electric furnace, which vaporises the substance placed within the vessel. Electrons are provided by a heated tungsten filament. The grid is in the form of a nickel helix surrounding the heated filament. An iron sheath encloses a field-free collision space between the filament and the grid.

By observing the minimum potentials at which the different lines of the spectrum are excited, a direct determination may be made of the amount of energy necessary for their production. The values so obtained in all cases confirm the deductions from the quantum theory, *i.e.*, the equation $eV=h\nu$ has been thoroughly tested. Another interesting point about this method is that higher series lines are readily photographed.

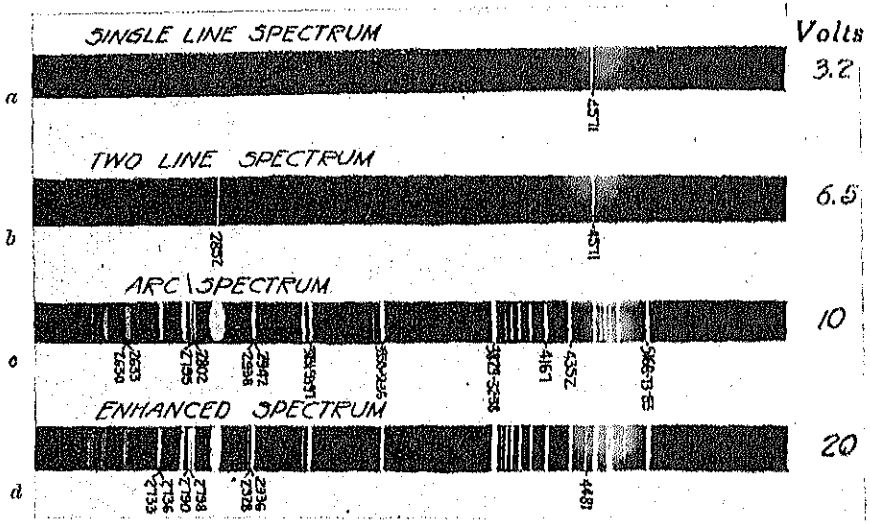

Fig. 10. Controlled excitation of the spectra of Mg.

Let us consider the case of Mg in some detail. Mg was subjected to a thorough investigation by Foote, Meggers and Mohler. As mentioned already the spectrum of Mg is similar to that of Hg and its energy levels are shown in Fig. 5, p. 388.

The following were the results for four successive ranges of potentials between 0 to 20 volts:

(1) 0—2·7 volts: When the energy of the bombarding electrons is less than 2·7 volts which is the first resonance potential of Mg, the collisions are elastic and no radiation is observed.

(2) 2·7 − 4·33 volts: The three levels $^3P_2$, $^3P_1$, $^3P_0$ are very close together in the case of Mg and are not distinguishable by this method. So when bombarding electrons have an energy of 2·7 volts or more, the normal Mg atom is excited to any of these $^3P_{0,1,2}$ states. But a return to normal state from all of these excited states is not possible. Only one transition $^3P_1 \rightarrow {}^1S_0$ is allowed by the selection principle for inner quantum numbers. Therefore the radiation will consist of one line only, *viz.*, λ 4571. This was found to be the case (*vide* Fig. 16*a*). Incidentally the equation $eV = h\nu$ is also verified, because according to the above equation λ 4571 should correspond to 2·7 volts.

(3) 4·33 − 7·61 volts: The second resonance potential of Mg is 4·33 volts, and the bombarding electrons with this amount of energy will be able to excite the atom to 2 $^1P_1$ state. According to Bohr's selection principle for the azimuthal quantum number, no transition can take place from this level to any of the next three $^3P_{2,1,0}$ levels. Therefore only one transition, *viz.*, 2 $^1P_1 \rightarrow {}^1S_0$ which corresponds to λ 2853 is possible. So at this stage of excitation the Mg spectrum consists of two lines only, λ 4571 and λ 2852 (see Fig. 16*b*). It ought to be noted that if the transition $2\,^1P_1 \rightarrow 2\,^3P_1$ were possible, the line λ 7587 would have appeared in the spectrum, but using dicyanin stained plates which are highly sensitive at this wavelength, no trace of the line could be found. This is a very interesting verification of Bohr's selection principle.

(4) At 7·61 volts and beyond: At 7·61 volts the bombarding electrons completely ejects one electron from the Mg atom. This electron returns to the ground level $^1S_0$ by successive inter-orbital transitions. As there are numerous atoms approaching equilibrium by the various different combinations of transitions possible, we get in the radiation the complete arc spectrum of Mg (Fig. 16*c*). The spectrum *c* corresponding to an excitation potential of 10 volts shows an enhanced doublet besides the arc spectrum. This is due to the fact that, a Mg$^+$ atom requires an energy of 4·4 volts to excite it from its ground level ($^2S_1$) to the next higher energy level which is a doublet ($^2P_{\frac{1}{2},\frac{3}{2}}$). A normal Mg atom may be brought to this state by two successive collisions with 10-volt electrons, as shown in Fig. 16A.

As this excited Mg^+ atom returns to the normal state, an enhanced doublet λ 2803, 2795 (corresponding to transition $^2P_{1,2} \rightarrow {}^2S_1$) is emitted. When the electronic current at which the experiment is performed is low, the chance of two successive collisions is small and these lines are weak, but at high currents they are quite strong. Beyond 12·01 volts (7·61+4·4) one impact is sufficient to ionise a Mg atom and to bring it to $^2P_{\frac{1}{2},\frac{3}{2}}$ state; so this doublet is quite distinct even with very low currents.

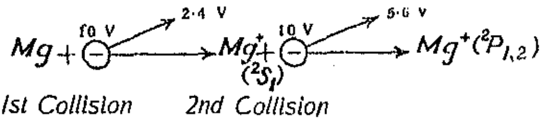

Fig. 16A. Inelastic collision of Mg with 10V electrons.

To remove a second electron from a Mg^+ atom, 14·97 volts are necessary. At higher currents this double ionisation is achieved by two successive collisions and the complete first spark spectrum is obtained just beyond this voltage (*vide* Fig. 16*d*). If however the current is low a voltage of 22·58 (14·97+7·61) is necessary to excite the spark spectrum. Ruark has succeeded in this with such low current densities as 0·1 to 0·2 milliamperes per cm^2.

At 46·9 and 1299 volts the L and K radiations appear. Though at this stage the second spark spectrum of Mg is expected to appear, but it does not do so. This is probably due to the small chance of three successive collisions that would be necessary.

The above is a brief account of the work of Foote, Meggers and Mohler with Mg. The full table is given on p. 609.

The theoretical critical potentials of He, Ne and Hg have been confirmed by this method by Hertz. In some cases, *e.g.*, Ne where the first appearance of certain lines cannot be distinguished with sufficient accuracy, photometric measurements of line intensities are taken and an intensity-voltage curve plotted. The curves were usually found to cut the axis at considerable angles and so gave quite definite values of the critical potentials.

298. Critical Potentials for Soft X-ray Emission as Determined by the Method of Electron Bombardment.—Methods of controlled electron bombardment have been employed by Richardson, Compton, Thomas, Kurth, Hamer and Singh and others for the investigation of critical potential of elements for soft X-ray emission. Electrons of controlled velocity from a filament are allowed to bom-

Table 3.—Controlled excitation of the spectrum of Mg.

Series Notation	Wavelength or wave number	Energy in volts	Types of Collision	Type of Spectrum
$1\,^1S_0-2\,^3P_1$	λ 4571 Å.U. ν 21871 cm^{-1}	2·70	Inelastic collision at the first resonance potential of Mg I (Mg $^1S_0 \rightarrow$ Mg $^3P_{2,1,0}$)	Singlet spectrum
$1\,^1S_0-2\,^1P_1$	λ 2853 ν 35051	4·33	Inelastic collision at the second resonance potential of Mg I. (Mg $^1S_0 \rightarrow$ Mg $^1P_1$)	„
$^2S_{\frac{1}{2}}$	ν 61672	7·61	Inelastic collision at first R. P. (Mg $^1S_0 \rightarrow$ Mg$^+$ $^2S_{\frac{1}{2}}$)	Complete arc spectrum, singlet and triplet.
$^2S_{\frac{1}{2}}-{}^2P_{\frac{1}{2},\frac{3}{2}}$	λ 2803 ν 35669 λ 2795 ν 35761	4·4	Inelastic collision at first R. P. of Mg$^+$ (Mg$^+$ $^2S_{\frac{1}{2}} \rightarrow$ Mg$^+$ $^2P_{\frac{1}{2},\frac{3}{2}}$)	Enhanced doublet spectrum.
$^1S_0$	ν 121267	14·97	Inelastic collision at the second I. P. (Mg$^+$$^2S_{\frac{1}{2}} \rightarrow$ Mg^{++} $^1S_0$)	Complete enhanced spectrum.
$^2S_{\frac{1}{2}}+{}^1S_0$	ν 182939	22·58	Inelastic collision with ejection of both valence electrons (Mg $^1S_0 \rightarrow$ Mg^{++} $^1S_0$)	Complete enhanced and arc spectra.
L $\alpha_{1,2}$ ...	λ ν 380000	46·9	Inelastic collision with ejection of an L-electron from Mg I.	L-Radiation
Kα ...	λ 9·869 ν/R 92·4	1299	Inelastic collision with ejection of a K-electron from Mg I.	K-radiation

bard a target of the material to be examined enclosed in a vacuum chamber. At critical potentials soft X-rays generated by the bombardment cause photo-electric emission from a metal plate enclosed in the same chamber, and this can be detected by an electrometer. A number of auxiliary plates are used to eliminate secondary effects due to the residual gas in the chamber.

Experiments of this type however reveal a large number of critical potentials. Thus Fe, Co, Ni, Cu each shows as many as 48 critical potentials, and similar results are shown by many other elements. Their significance in many cases is not clear. A full account of these works will be found in Lindh's *H. d. Expt. physik*, **24/2**, p. 364—391, or reference may be made to original papers.*

299. Critical Potential of Molecules†—Introduction.—As far as the problem of electronic impacts with atoms or monatomic molecules is concerned, the methods of investigation described above are quite satisfactory. But as soon as we come to the electronic impacts with polyatomic (including diatomic) molecules, the whole problem becomes complicated and the methods described above are found to be entirely inadequate for the purpose. The main point of difference between the two problems is that in the case of atoms, the inelastic collision results in the excitation of the atom to one of the higher energy levels or in its ionisation; whereas in the case of a polyatomic molecule, this may either be ionised without dissociation or may be dissociated in a variety of ways. For example in the case of iodine, at least the three following changes occur :—

$$\begin{aligned} &(1) \quad I_2 \rightarrow I_2^+ + e \\ &(2) \quad I_2 \rightarrow I^+ + I + e \\ &(3) \quad I_2 + e \rightarrow I^- + I. \end{aligned}$$

Therefore in the case of molecules the indication of the nature of the ions produced is as important as the measurement of the energy necessary for an inelastic impact.

---

* The following papers may be consulted :

Richardson and Chalklin, *Proc. Roy. Soc. A*, **119**, 60, 1928; **110**, 247, 1926.
Compton and Thomas, *Phys. Rev.*, **28**, 601, 1926.
Hamer and Singh, *Phys. Rev.*, **29**, 608, 1927.
Kurth, *Phys. Rev.*, **18**, 461, 1921.
Thomas, *Phys. Rev.*, **25**, 322, 1925.

† A very excellent account of this subject has been given by H. D. Smyth in *Reviews of Modern Physics*, **3**, 347, 1931. We have freely drawn from it.

The nature of gaseous ions has been extensively studied by the methods of positive-ray analysis as developed by Thomson, Wien and Dempster. But the early results are mostly useless from the point of view of molecular critical potentials, because the production of ions was not a controlled process. Some work done by Thomson* and Dempster† with H_2 molecules is however worthy of note. Thomson found that in a hydrogen discharge H_3^+, H_2^+ and H^+ ions are formed. Dempster using a thermoionic source of electrons studied the effect of pressure on the relative proportion of these ions keeping the accelerating voltage constant. He found that at low pressures the proportion of H_2^+ preponderates, while at comparatively higher pressures, all the three are almost equal in proportion. From this he concluded that the primary result of the electronic collision is to ionise the hydrogen molecule without dissociating it, *i.e.*, to produce H_2^+ ions. The dissociation of the gas and the consequent production of H^+ and the complex H_3^+ is the result of the collisions of H_2^+ ions with neutral gas molecules.

300. Modern Experimental Arrangements.—All modern investigations on the subject have been undertaken with the object of studying the effects of collisions of electrons with gas molecules as a function of the energy of the impinging electrons, more specially to find the energy required by an electron to produce, single, double or multiple ionisation or to cause ionisation of varying degree to be accompanied by dissociation. Therefore all the experimental arrangements are essentially combination of an electronic source of controllable velocity and an ion-analyser. In any good apparatus, the following requirements have to be met as far as possible :

(*i*) A source of electrons whose energy can be controlled.

(*ii*) Great intensity, so that the apparatus may immediately detect an inelastic collision.

(*iii*) No collision in the analyser, so that the primary result of the impact may not be complicated by spurious effects.

---

* J. J. Thomson, *Rays of Positive Electricity*, p. 116, 1913.

(*iv*) High resolving power, so that even the ions whose e/m are only slightly different *i.e.*, N^+, NH^+, NH_2^+, NH_3^+ may be distinguished.

(*v*) No thermal dissociation on the filament.

The problem of attaining these requisites can be best stated by quoting the words of Smyth. "The difficulties involved in satisfying the requirement (*i*) are the same as those arise in ordinary ionisation potential experiments. They are best met by calibrating the apparatus with a gas whose ionisation potential is known. This is not particularly difficult though always subject to criticism. It is the last four requirements that are mutually conflicting. Thus to get great intensity of ionisation, there must be many collisions, *i.e.*, high gas density in the ionisation chamber, and large slits in the mass spectograph. But these conditions endanger requirements (*iii*) and (*iv*). Or if we try to increase the number of electrons by using a powerful electron source, we have to use a large hot filament endangering requirement (*v*)" (Smyth).

We shall now describe some of the methods developed by utilising these principles.

Smyth's Apparatus.—Since the requirements (*ii*) and (*iii*) demand that pressure in the collision space should be higher than the pressure in the analysing space, Smyth* utilised the *method of differential pumping*, (originally developed by Thomson for his positive ray analysis) in his apparatus for maintaining this difference of pressure. The apparatus is illustrated in Fig. 17 and described on p. 613.

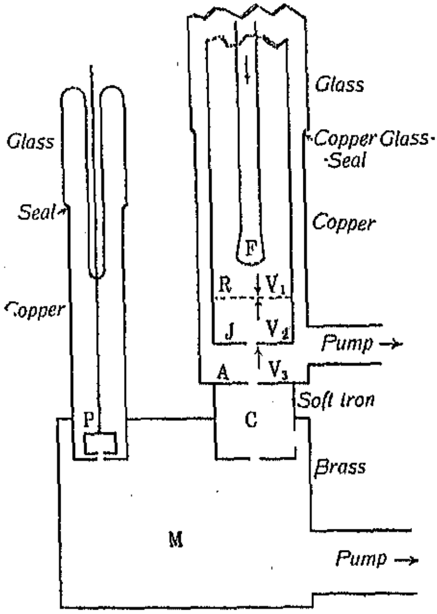

Fig. 17. Smyth's apparatus.

---

* H. D. Smyth, *Proc. Roy. Soc. A*, **102**, 283, 1922; **104**, 121, 1923, and later papers.

F . . . Source of electrons.

R . . . Grid. A variable potential difference V_1 is applied between F and R to accelerate the electrons with the proper energy.

J . . . A glass cylinder one end of which is closed with a metal plate provided with a slit. The space between R and J is the collision space. V_2 is a small reverse potential to draw the positive ions from R to J.

C . . . Collimating space provided with two slits which are collinear with the first slit. It is made of soft iron sides so that the space inside is free from external magnetic field.

V_3 . . . A large potential applied between J and A. It accelerates positive ions from J into the space C.

The positive ions are collimated by the system of slits and they enter the mass spectrograph M with high velocity. The magnetic field is at right angle to the plane of the paper. The paths are now circles and the particles after describing the full semi-circle enter through a slit into the Faraday cylinder P. The current is measured by an electrometer.

There are two high vacuum pumps, one working on the space between A and J, and the other on the space M. Gas is continuously allowed to flow into the space R J. So the pressure at J is kept pretty high. But since the spaces R J and M are separated by a fine orifice, the vacuum at M continues to remain fairly high. The ratio between the pressures in M and R J may be varied from 1 : 10 to 1 : 1000.

When any gas has to be investigated it is allowed to flow steadily into the collision space R J. The first step now is to determine the nature of the ions formed. For this purpose the electron speed and the pressure are kept fixed, say, at 30 volts and ·05 mm. respectively. (These values are chosen after some preliminary experiment.) V_2 is varied in steps and a curve is plotted with electrometer current against the accelerating field. For a given value of the latter, the e/me of the ion entering P is given by

$$me/e = \rho^2 H^2 / 2Ve$$

where $V =$ the total accelerating potential, and $H =$ magnetic field. Fig. 18 represents such a curve for hydrogen and it clearly shows that H^+, H_2^+, H_3^+ ions have been produced. The areas contained by the different peaks give the relative number or intensities of the different kinds of ions (neglecting for the present the H^+_{3-1}, H^+_{3-1} peaks).

The next step is to distinguish between the primary ions (*i.e.*, ions produced directly as a result of electronic impact) and the secondary ions (produced as a result of some secondary collision, probably of the gas molecule with the primary ion). For this a series of experiments are performed at various pressures and a curve is plotted with pressure as the abscissa and the relative intensities of different ions as *ordinates*. Fig. 18*a* shows that the proportion of H_2^+ decreases with increase of pressure, while that of H^+ and H_3^+ increases. This suggests that H_2^+ is the primary product. The conclusion is further confirmed by the fact that the curves for both H^+ and H_3^+ when extrapolated pass through the origin. These ions are therefore evidently produced entirely by secondary effects.

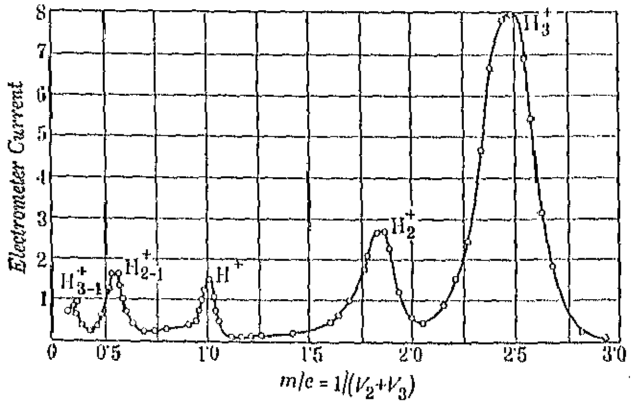

Fig. 18. Curve showing the critical potentials of hydrogen.

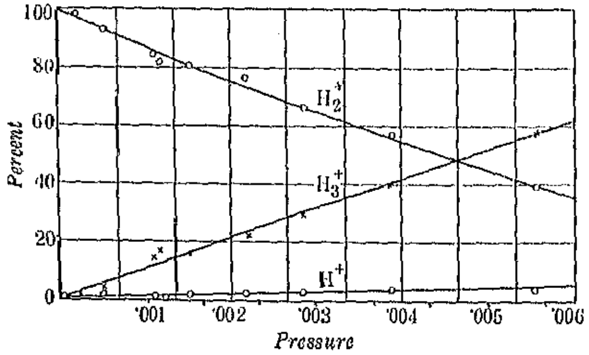

Fig. 18 *a*. The intensity-pressure curve for different ions.

To find the potential at which the ions appear, the intensities of all the types of ions are plotted against the voltage V_1 accelerating the electrons. The pressure is kept fixed but reasonably high, otherwise the secondary ions may not form at all. The voltage at which the curve (extrapolated if necessary) for any ion cuts the axis of V_1 gives the appearance-potential for that ion. In the case of hydrogen all the three curves cut the axis at the same point, indicating that they are the result of the same primary process, *i.e.*, the production of H_2^+ ions.

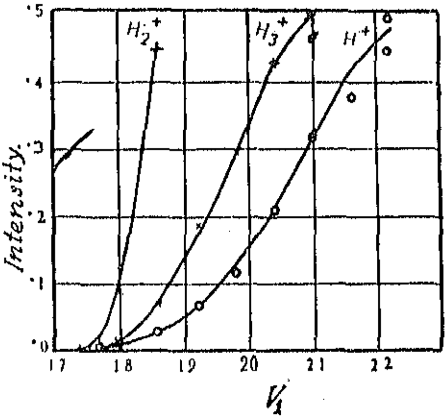

Fig. 10. The intensity-voltage curves for H_2^+, H_3^+, H^+ ions.

The peaks H^+_{2-1} and H^+_{3-1} have been explained by Smyth, who is the pioneer worker in this field, as due to the ions which exist as H_2^+ or H_3^+ in the collision space but break up subsequently into H^+-ions.

Smyth's apparatus has undergone several modifications* at the hands of later workers, Smyth, Hogness and Lunn, Kallmann, Bleakney and others to suit their special purposes.

Secondary effects.—From the above discussion of Smyth's work on hydrogen we conclude that H_2^+ is the primary result of the electron impact with the hydrogen molecule, but there is every possibility that the H^+-ion may directly be produced at higher potentials and some H_2^+-ions may be the result of secondary effects. It is evident that Smyth's apparatus is unsuitable for detecting these effects.

The collision of the second kind also plays an important part in secondary effects. Harnwell† working with a mixture of He and Ne in equal proportions found that the ratio of intensities of two ions,

---

* The following papers may be consulted:—

Hogness and Lunn, *Phys. Rev.*, **26**, 44, 1925.
Smyth and Stueckelberg, *Phys. Rev.*, **36**, 472, 1930.
Smyth, *Jour. Frank. Inst.*, **198**, 795, 1924; *Phys. Rev.*, **25**, 452, 1925.

† Harnwell, *Phys. Rev.*, **29**, 683, 1927.

i.e., He^+/Ne^+ decreases with increase of pressure. This indicates a collision of the following type:

$$He^+ + Ne = He + Ne^+$$

whereby the neurtal atom with lower ionisation potential is ionised by an ion of higher ionisation potential, and the latter itself is converted into a neutral molecule.

In general, therefore, following types of collisions will occur;

$$A^+ + B = A + B^+$$

where $I_A > I_B$. It has been further found by the same worker that the probability of such collisions resulting in an electron transfer is inversely proportional to $I_A - I_B$. Such collisions have an important bearing on the problem of distinguishing between primary and secondary ions by the effect of variation of pressure. Suppose electron impact with a gas molecule AB results in the production of two primary ions A^+ and B^+. The following collisions are then likely to occur:

$$A^+ + AB \rightarrow AB^+ + A$$
$$\text{and} \quad B^+ + AB \rightarrow AB^+ + B.$$

And if the probability of the first reaction is greater than the second, it is evident that an increase of pressure would tend to increase the ratio of the intensities B^+/A^+ and it would appear that B^+ is a secondary ion. Among other secondary effects affecting the relative intensities of the ions produced may be mentioned the angular scattering of the ions in the analysing space and the space charge effect in the collision space. But these two factors are usually too small to be of any practical importance.

301. Bleakney's Apparatus.—The differential pumping method of Smyth described above suffers from one great drawback, namely, the gas pressure in the collision space being very high, secondary collision phenomena take place very readily, and they may actually mask some of the less prominent primary effects. Bleakney* devised an apparatus in which a low uniform pressure was maintained throughout the apparatus (both in the collision space and in the analysing chamber), and the disturbing effects due to secondary collision were completely overcome. The pressure is so low that the m. f. path of the ions is greater than the dimension of the analyser, hence no collision takes place in the analyser space. The analyser used is also of a different type. Bleakney's apparatus is described in Fig. 20(*a*) (side view) and 20(*b*) (end-view).

---

* Bleakney, *Phys. Rev.*, **34**, 157, 1929; **35**, 1180, 1930.

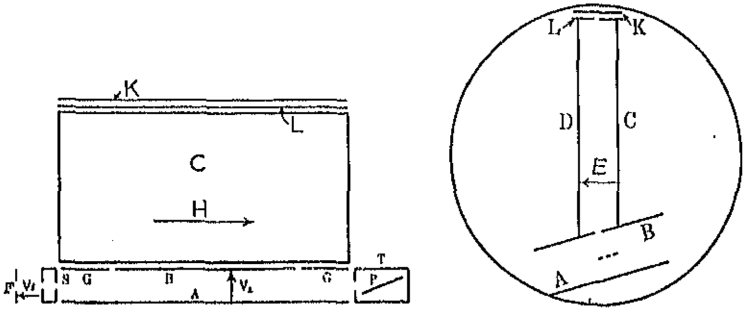

(*a*) (*b*)

Fig. 20. Bleakney's apparatus: (a) side-view, (b) end-view.

Electrons from a source F are accelerated by means of a potential V_1 through a long slit S into the collision chamber AB. A long solenoid encircles the whole apparatus, and the magnetic field due to it keeps the electrons in AB confined to a narrow line from S to P. By means of a second accelerating potential V_2, positive ions formed in AB are drawn through slits in B into the analysing chamber C. Here they pass between two condenser plates C, D (*vide* Fig. 20*b*) and are subjected to the joint action of an electric field E and a magnetic field H, the respective displacements due to which balance each other. For one set of values of V_2, E and H, the ions that can reach the plate K are characterized by having

$$m/e = VH^2/E^2c^2$$

where V = the fraction of V_2 effective in accelerating the ions, and the current due to this ion is noted as usual.

The great merit of the method is that the gas pressure being very low, the probability of secondary collisions is almost absent. Bleakney noted that the formation of H_2^+ from neutral H_2 begins at 15·4 volts. This value, however, differs slightly from Smyth's value of 15·9 volts. He observed a second ionisation occurring at 18·0 volts. This corresponded to the formation of the H^+-ion by primary collision of electrons with H_2-molecules. His most important resultant in this connection was the observation of fast H^+-ions appearing at 26±1 volts. No indication of this was obtained in earlier methods as it was evidently masked by secondary collisions. The peak in the potential curve corresponding to the formation of these ions is, however, very diffuse, but they have been confirmed by the careful investigations of Lozier.[*]

The long slits necessitates the use of long solenoids and this fact puts, however, a limitation to Bleakney's method. Further, the collision frequency being very small the intensity of the ions is not sufficient and the resolving power of the analyser is low. In the case of H_2 the following primary processes were observed.

Table 4.—Critical Potentials of H_2.

Gas	Ions	Appearance Potential	Probable Process
H_2	H_2^+	15·9 volts	$H_2 \rightarrow H_2^+$
	H^+	18·0	$H_2 \rightarrow H^+ + H$ (dissociation and ionisation)
	H^+ (fast)	26·0	$H_2 \rightarrow H^+ + H + K.E.$
	H^+ (fast)	46	$H_2 \rightarrow H^+ + H^+ + K.E.$

Theoretical interpretation of the results obtained by Smyth, Bleakney and others are not unambiguous in all cases, and have been found to be accompanied with the excitation of different states of rotations and vibrations of the molecule, as well as their electronic excitation. This can be taken up only after the student is acquainted with the interpretation of Molecular Spectra. In a few cases the results can however be easily interpreted. Thus, the process corresponding to 18·0 volts most probably indicates the dissociation of H_2-molecule into H-atoms, and ionisation of an H-atom. The heat of dissociation of H_2 is 4·5 volts and the I. P. of the H-atom is 13·5 volts which together amount to 18·0 volts. Similarly, the critical potential corresponding to 15·9 volts agrees with the theoretical ionisation potential of H_2 calculated[†] from the ground state of H_2^+.

Similar results have also been obtained for N_2, O_2, NO, H_2O, I_2, HCl, CH_4 and other gases. We shall discuss these results in the chapter on *Molecular Spectra.*

The probability of the three primary processes of ionisations of H_2 (H_2^+, H^+ and H^+ fast) has been studied by Bleakney, and is illustrated in Fig. 21 due to him.

---

[*] Lozier, *Phys. Rev.*, 36, 1285, 1930.

[†] Burrau, *Danske Vid. Selsk. m. phys. meddel*, 7, No. 14, 1927. See also Smekal, *Quanten theorie*, p. 639.

In these the percentage of total current contributed by each of the three kinds of ions is plotted against different electron velocities. The uppermost curve corresponds to H_2^+ the-ions,

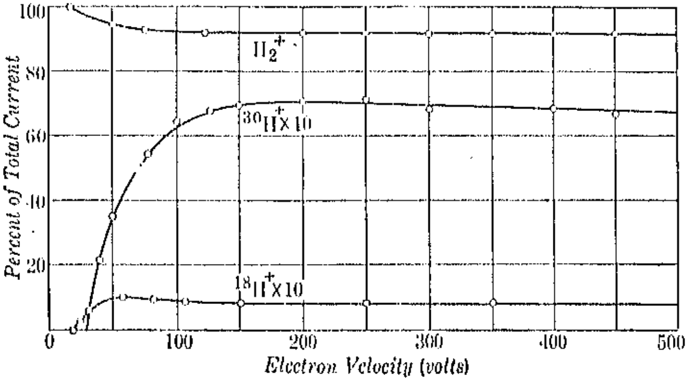

Fig. 21. Curves illustrating the probability of different modes of ionisation of H_2.

middle curve to fast H^+-ions with ordinates ten times magnified, and the lowest curve to H^+-ions also having the ordinates multiplied by 10. The probability of secondary processes of ionisation in Smyth's method has, however, been found to be much greater compared to that of the formation of H^+ and H^+ (fast) by primary collisions mentioned above.

302. Einstein's A and B Coefficients.—In section 168, we briefly indicated that Einstein introduced a factor A_{nm} which determines the probability that an atom which has been excited to a level denoted by the symbol n can spontaneously pass to a lower level denoted by m, thereby giving rise to the radiation

$$h\nu_{mn} = E_n - E_m \quad . \quad . \quad . \quad . \quad . \quad . \quad . \quad . \quad (1)$$

where E_n and E_m denote energies in the higher and lower levels. The factor A_{nm} determines the intensity of the line. If we have N_n exceited atoms at any time the amount of energy radiated per second by the atoms is given by

$$N_n \ A_{nm} \, h\nu_{mn}$$

Let us now consider the inverse process, that is, excitation of an atom from the lower state m to the upper state n by absorption of radiation $h\nu_{mn}$. For this purpose we assume that the N_m atoms are placed in a field of radiation in which the energy density corresponding to the radiation of frequency ν_{mn} is denoted by U_{mn}. It is clear that all the radiation quanta of energy $h\nu_{mn}$ which fall on the N_m atoms cannot be absorbed. There is a definite probability factor. Let this be denoted by B_{mn}. Then the total absorption of the energy of frequency ν_{mn} is given by the expression

$$N_m \; U_{mn} \; B_{mn} \, h\nu_{mn}$$

Einstein showed that it is possible to find out a relation between the A and B coefficients by considering the equilibrium of radiation in a blackbody chamber of temperature T in which exchange of energy takes place due to emission and absorption of radiation by the atoms. In the equilibrium state we must have the emitted energy equal to the absorbed energy. We have, therefore,

$$N_m \; U_{mn} \; B_{mn} = N_n \; A_{nm}$$

$$U_{mn} = A_{nm} \,/\, B_{mn} . \; N_n \,/\, N_m \; . \quad . \quad . \quad . \; (2)$$

According to the law of distribution of energy

$$N_n = \frac{g_n}{g_m} \; N_m \; \text{exp.} \left(- \frac{E_n - E_m}{kT} \right)$$

where g_m and g_n are the weight factors (equal to $2j+1$) of the states m and n respectively. Therefore,

$$U_{mn} = \frac{A_{nm}}{B_{mn}} \frac{g_n}{g_m} \text{exp.} \left(- \frac{E_n - E_m}{T} \right) . \quad . \quad . \quad . \; (3)$$

Comparing this expression with Wien's displacement law we have

$$U_{mn} = \alpha \, \nu^3{}_{mn} \, f \, (\nu_{mn} \,/\, T)$$

Further it follows $E_n - E_m = h\nu$, since the A's and B's do not depend on the temperature. This is exactly the frequency condition assumed by Bohr in his theory of hydrogen spectrum, *viz.*, the difference of energy in the two states is emitted as radiation, and is proportional to the frequency of the radiation.

But this expression leads to Wien's distribution law. Since in equilibrium, the radiation density is found experimentally to obey Planck's law, we must have neglected in the above treatment of energy-balance an additional process of compensation. Einstein traces this in the influence of the radiation of frequency ν_{mn} on the excited atoms N_n. He postulates that an excited atom may be stimulated to emission under the influence of radiation, and this may be put equal to

$$N_n \; U_{mn} \; B_{nm}$$

where B_{nm} is the probability factor of stimulated emission.

In place of (2) we have now

$$N_n A_{nm} + N_n B_{nm} U_{mn} = N_m B_{mn} U_{mn}$$

Hence
$$U_{mn} = \frac{N_n A_{nm}}{N_m B_{mn} - N_n B_{nm}}$$

$$= \frac{g_n A_{nm}}{g_m e^{(E_n - E_m)/kT} B_{mn} - g_n B_{nm}} \quad . \quad . \quad . \quad . \quad (4)$$

Now $U_{mn} = \infty$ when $T = \infty$, therefore, $g_m B_{mn} = g_n B_{nm}$

and we get
$$U_{mn} = \frac{A_{nm} / B_{nm}}{e^{h\nu/kT} - 1}$$

On comparing this expression with Planck's Law (eqn. 6, p. 185) we get

$$A_{nm} / B_{nm} = \frac{8\pi h\nu^3}{c^3}$$

Though in this treatment *the existence of stimulated emission* or *negative absorption* has been proved on the assumption of Planck's Law, the argument may be reversed, *i.e.*, by assuming the existence of stimulated emission, we can deduce Planck's Law.

The ideas introduced by Einstein in the previous treatment have been the starting point of many fruitful investigations in physical science, and we shall therefore add some experimental proofs in support of these ideas.

303. Life of the Atom in the Excited State.—In the first place, we assumed that an excited atom left to itself will emit radiation and return to the normal state. Let N_{n_0} be the number of excited atoms to start with. Let dN_n be the number of atoms which return to the normal state in time dt. Then we have

$$dN_n = - N_n A_{nm} \, dt$$

or
$$dN_n / N_n = - A_{nm} \, dt$$

Integrating, we have

$$N_n = N_{n_0} e^{-A_{nm} t} \quad . \quad . \quad . \quad . \quad . \quad . \quad . \quad . \quad (5)$$

where N_{n_0} is the number of atoms which would have zero energy having unit quantum weight. The process is exactly analogous to a radioactive decay, and we can speak of the *average life* of an excited atom in the same sense as in radioactivity. When there are only two states, the average life of the atom in the excited state is given by

$$\tau = 1/A_{nm}$$

Wien has determined the life of excited atoms experimentally. Before proceeding to a discussion of his experiments we shall try to give an idea of the value of the life from classical electrodynamics.

It is only very recently that the newer developments in Quantum Mechanics have enabled us to calculate τ. This cannot be taken here, but we shall give the value of τ for the Planck dipole.

According to classical electrodynamics the model resonator is an electrical dipole as mentioned on p. 183. The rate at which energy* is radiated by the dipole having the total energy content E is given by

$$-\frac{dE}{dt} = \frac{8\pi^2\nu^2}{3c^3} \cdot \frac{e^2}{m} E$$

from which it follows that $E = E_0\, e^{-\gamma t}$, where $\gamma = \frac{8\pi^2 e^2 \nu^2}{3c^3 m}$. . . (5a)

Comparing (5a) with (5), we have

$$\tau = \frac{1}{A_{nm}} = \frac{3mc^3}{8\pi^2\nu^2 e^2} \sim 10^{-8} \text{ seconds} \quad . \quad . \quad . \quad . \quad (6)$$

WIEN'S EXPERIMENT.

Wien† made a direct determination of the mean life of Hg-atoms by means of the apparatus shown in Fig. 22. It is a positive ray tube in which the anode is situated beyond R, and K is the perforated cathode through which positive ions may pass into the chamber B. These are gas molecules or atoms which have lost an electron each in the space R, but catch one while passing into B in some higher state of excitation. On account of the voltage applied across the tube, the ions are endowed with high velocity which persists even when they enter B as excited atoms. But here as they pass to lower states, a streak of light is produced with increasing faintness at the lower ends. These streaks of light can be spectrophotographed. On taking microphotogram of the spectral lines along their length, it is found that the intensity of the streak of light falls off according to exponential law

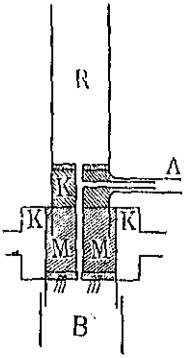

Fig. 22.
Wien's apparatus.

$$I = I_0\, e^{-\gamma x}$$

---

* See Pauli's *Quantentheorie* in *H. d. Phys.*, 23, 50, 1926.

† W. Wien, *Ann. d. Phys.*, 73, 483, 1924.

If the ions have travelled for t sec. between two points on the spectrum separated by a distance x, we have then $x = vt$. Hence

$$I = I_0 e^{-\gamma vt}$$

By analogy with equation (5) this gives us the mean life $\tau = 1/\gamma v$. He deduced from such experiments $\tau \cong 0{\cdot}98 \times 10^{-7}$ secs. This result however cannot be taken to be very accurate, for it is uncertain at which moment a particular process of excitation began and when it ended. Further, abnormally long life of atoms excited to metastable levels may considerably affect the mean life of ordinarily excited atoms.

Wien's experiment thus gives us merely a qualitative test of the life of atoms. Many quantitative experiments have since been done to determine the life accurately. We give below an account of one of these experiments.

WEBB AND MESSENGER'S EXPERIMENT

Webb and Messenger* employed an indirect method for the determination of the mean life of $^3P_1$-Hg-atoms. These atoms were excited by the electron bombardment method to the state $^3P_1$ and then the persistence of the radiation was measured after excitation was stopped. For large vapour pressures of mercury in the excitation chamber the persistence was found to be large on account of diffusion of radiation by repeated absorption and remission†. But at a very small concentration the persistence approached a limiting value of about 10^{-7} sec. which is the mean life of the excitation process.

Their apparatus is shown in Fig. 23 and described below.

F	an oxide coated hot cathode.
G, H . .	two grids of nickel gauze.
P	photoelectric plate connected to a Compton electrometer E.
Q	Quartz window which separates the excitation and detecting systems, permitting only radiation to pass and preventing metastable Hg-atoms from reaching P.
S	shielding electrode.

---

* H. W. Webb and H. A. Messenger, *Phys. Rev.*, 33, 319, 1929.

† A detailed theory for this has been worked out by E. Milne, *Journ. London Math. Soc.*, No. 1, 1926. Webb and Messenger's results however do not agree with Milne's law of variation of τ with pressure.

T. . . . tube enclosing the whole system. One end of T is a little tapered so that liquid mercury may collect in it. It is enclosed by a water bath which can be kept at any steady temperatures between 80° to −20° C. By heating the chamber to different temperatures, different vapour pressures of mercury can be obtained.

M . . . . the point where a diffusion pump is attached. It operates continuously and prevents accumulation of vapour in any part.

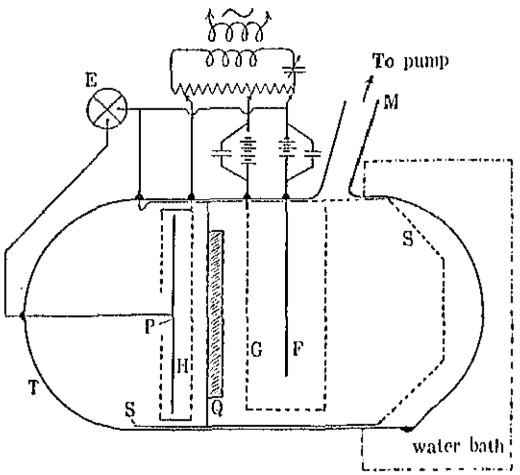

Fig. 23. Webb and Messenger's experiment.

Electrons from F are accelerated by an alternating voltage acting between G and F. Electrical connections are so arranged that Hg-atoms are excited by electron bombardment only during the positive half of the cycle. Radiation emitted from excited atoms ejects photo-electrons from P, between which and H an alternating voltage of the same frequency and phase is applied as between G and F. By this arrangement a positive photoelectric current is made to exist during the positive half cycle of e.m.f., but there is no current to or from the plate during the negative half cycle. By applying a suitable voltage between F and G (6 volts) and regulating the vapour pressure of mercury, it is ensured that only λ 2537 is emitted.

For very low frequencies (below 60 cycles per second called the "*zero frequency*") emission of radiation is practically complete during positive half cycle in which a maximum photoelectric current exists. But as the frequency is gradually increased, on account of the persistence of the excited state in the negative cycle, more and more photoelectrons are ejected from H and travel to P during the negative cycle. This reduces the electrometer current by some extent. But at very high frequency (*infinite frequency*) the current approaches a limiting value which is nearly half of the current at zero frequency (see Fig. 24).

The frequency of the A. C. voltage is varied between 60 cycles per second to about 10^7 cycles per sec. (radio frequency). The source of A. C. voltage supply* was a valve oscillator circuit with suitable condensers and inductances.

To calculate τ from these data, an *R/frequency* curve is drawn in which the frequency ν of the applied voltage is plotted as abscissæ and R the ratio of the current at any frequency to that at zero frequency as ordinates. This curve is shown in Fig. 24.

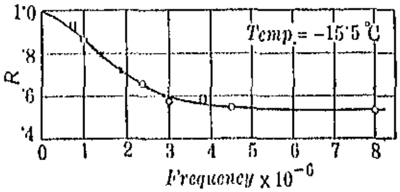

Fig. 24. The *R*/frequency curve.

If, as is generally the case, the time-excitation process follows a sine curve during the positive half cycle, and the photoelectric characteristic of the plate system is such that the current changes from saturation value to zero as soon as the voltage is reversed, it can be shown (*loc. cit.*) that

$$\frac{1}{\tau} = 2\pi \nu_{\frac{1}{2}} \quad . \; . \; . \; . \; . \; . \; . \; . \; . \; . \; . \qquad (7)$$

This formula is deduced on the supposition that the radiation decays according to the exponential law

$$I = I_0 \, e^{-t/\tau}$$

and $\nu_{\frac{1}{2}}$ represents the frequency at which the current falls by half the difference between the currents at zero and infinite frequencies. Generally the above simplifying conditions are found approximately to hold good. So τ can be easily calculated from the *R*/frequency curve. In cases where these conditions are not satisfied, calculation of τ can be made from the forms of the time-excitation curve, voltage-current curve and working out the area enlosed by the *R*/frequency curve by integration. For details the original paper should be consulted. τ is calculated for different concentrations of mercury atoms obtained by varying the temperature over a wide range, and a graph is plotted with $1/\tau$ as ordinates and concentration as abscissæ. This is shown in Fig. 25. At very low concentration the phenomenon of repeated absorption and remission of radiation by Hg-atoms is practically absent, and τ gives the mean life corresponding to a single process of excitation and emission. A value of $\tau = 10^{-7}$ sec. was obtained for the mean life of $^3P_1$-state of mercury atom.

---

* Webb, *Phys. Rev.*, **23**, 311, 1924.

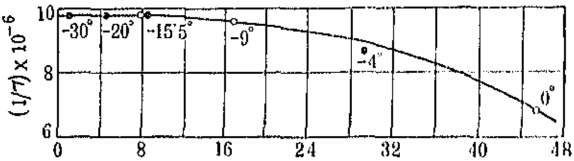

Fig. 25. Curve illustrating the relation between concentration and life of the atom.

It is very necessary however that only the $^1S_0 - {}^3P_1$ λ 2537 line and no other radiation should be excited during the process. This condition is evidently satisfied, because the radiations which may follow due to further excitation of $^3P_1$-state are

$$\lambda\,2655\ 2^3P_1 - 4^1D_2 \qquad \text{and} \qquad \lambda\,4358\ 2^3P_1 - 2^3S_1$$

The mean lives of these two radiations are evidently much smaller. The presence of such atoms with widely different lives would make the R/frequency curve very irregular. But this is not found to be actually the case. Further it is found that R does not change much with change of the peak value of the voltage between 6 to 2·5 volts. This supports the above view.

Recently Garrett[*] repeated Webb and Messenger's experiment with greater precision and obtained $\tau = 1{\cdot}08 \times 10^{-7}$ sec. for 2^3P_1-state, and $\tau = 2{\cdot}9 \times 10^{-10}$ sec. for 2^1P_1-state of Hg. The curves in Figs. 24 and 25 are due to Garrett.

304. Measurement of Life of Metastable Atoms.

The life of metastable atoms is of a different order of magnitude than that of excited atoms and can be measured with simpler arrangements. It will be described in Chap. XIV that $2p^5\,3s\ {}^3P_{0,2}$ states of Neon are metastable, as atoms once excited to this state cannot pass to the *fundamental* $2p^6\ {}^1S_0$ state on account of the selection principle that $\Delta j \neq 2$ or $(0 \rightarrow 0)$. Meissner, Dorgelo and Graffunder[†] found experimentally that the life of the $^3P_2$-state was of the order of 1/240 and that of $^3P_0$ of the order of 1/2000 of a sec. We describe below a modification of the same experiment due to Matuyama.[‡]

---

[*] P. H. Garrett, *Phys. Rev.*, 40, 779, 1932.

[†] Meissner and Graffunder, *Ann. d. Phys.*, 84, 1009, 1927.

[‡] Matuyama and Meissner, *ibid.*, 76, 124, 1925; Dorgelo, *Zs. f. Phys.*, 34, 766, 1925.

E .... source of steady light excited by a D. C. generator.

L_1, L_2, L_3, L_4 ...... lenses for condensing the light and rendering the beam parallel.

A .... Absorption tube containing neon which is excited by joining the electrodes B and C to the secondary terminals of a high frequency oscillator.

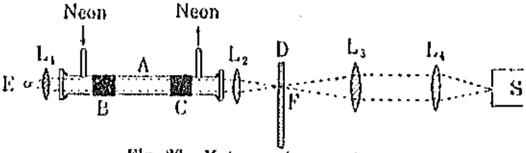

Fig. 26. Matuyama's apparatus.

D .... Rotating disc of bakelite having its rim lined with copper for a length of 6 cm. When this comes into contact with a brush placed below, a flash is sent through the neon tube A. For the remaining part of the revolution the tube is cut off from the source of excitation. One revolution takes nearly ·04 sec. but the time for which the neon tube is excited is ·002 sec. The disc D contains a light-hole F which is placed at a variable distance from the contact piece so that the light from E after traversing the absorption tube can pass into the spectroscope S only at a definite interval after the excitation is cut off.

When a discharge passes through A, a number of Ne atoms are excited to the $^3P_2$-state. When the excitation is cut off they persist for some time and may be assumed to decay according to the exponential law :

$$N = N_0 e^{-t/\gamma}$$

Now unexcited neon is completely transparent to all light in the visible region, but when it is excited to the $^3P_2$-state it would be able to absorb a number of lines in the red of which the line λ 6402 ($2p^5\, 3s\ {}^3P_2 — 2p^5\, 3p\ {}^3D_3$) may be utilised for quantitative measurements. If neon is not excited, this line would pass through the tube in full strength and be recorded on the photographic plate. If, however, the gas is excited it will be considerably enfeebled on account of absorption by the $^3P_2$-atoms. The amount of absorption may be taken to be proportional to the number of $^3P_2$-atoms present. If the light hole is very close to the copper contact piece, the absorption will be maximum. But if it is placed at varying distances the absorption will be gradually enfeebled. A curve may be drawn showing the logarithm of absorption against the time which has elapsed between the excitation of the Neon tube and the passage of light λ 6402 through the light hole into the spectroscope. If the conditions were so simple as described, this would be a straight line and from the slope τ can be calculated, but in actual practice a straight line is never obtained on account of the decay of the excited atoms through collisions of the second kind and other factors. For further details regarding the measurement of absorption the original papers may be consulted.

305. Thermal Excitation of Gases—Introduction.—So long we have been considering cases in which the ionisation or excitation of atoms and molecules are brought about either by means of electronic impacts or by the impact of light quanta. But there are agents other than electronic impacts and light impacts which can stimulate atoms and molecules to different excited states or even to single, double, or higher stages of ionisation. One of these agents is heat. The general effect of heat on matter may be described as a gradual loosening of its component parts. At the lowest temperature, all substances exist in the solid state; when more heat is added, they pass to the liquid state (*Fusion*); at still higher temperatures the liquid becomes a vapour consisting of discrete molecules (*Vaporisation*). When the vapour is further heated, the molecules break up into component atoms. What happens next when the atoms are further heated? We can suppose that the atoms collide so violently against each other that electrons (at least the outer ones) are knocked off, and the atoms get *ionised*.

The disruption of an electron by thermal excitation is not however an abrupt process. Before the stimulus reaches the stage of ionisation, heat may be sufficiently great to excite the valence electron to second, third or higher levels of excitation. But these states being unstable, the electron will at once fall back to its normal orbit, emitting as a consequence the various series of optical spectra characteristic of the atom. Thus the ionisation of an element due to heat is always preceded by the emission of its spectral lines. If the gas consists of di- or poly-atomic molecules, the effect of heat, in the first instance, is to cause dissociation of the molecules; but preceding that, the molecules will emit band spectra corresponding to the vibration and rotational excitation of their component parts, or change in the electronic states of the molecules as a whole.

The temperature at which the complete ionisation of molecules takes place is generally very high. Take for example the case of water. The various stages leading to the thermal ionisation of its component atoms are shown below:

Table 5.

State	Process	Temperature
1. Solid to liquid ...	Fusion	0°C
2. Liquid to gas ...	Vaporisation	100°C
3. Molecules (gas) to atoms	Band emission $H_2O \rightarrow 2H + O$	3500°C
4. Atoms excited ..	Emission of arc lines of O	...
5. First ionisation ...	$O \rightarrow O^+ + e$	$O^+ \begin{pmatrix} B_5\text{-stars} \\ 15000°K \end{pmatrix}$
6. Excited states of ionised atoms.	Emission of spark lines	...
7. Second ionisation ...	$O^+ \rightarrow O^{++} + e$	$O^{++} \begin{pmatrix} O_5\text{-stars} \\ 35000°K \end{pmatrix}$

We thus see that the first ionisation of the oxygen atom formed by the dissociation of H_2O molecules takes place at a temperature of about 15000°K, and second ionisation at as high a temperature as 35000°K. Such high temperatures are almost impossible to attain in the laboratory, the maximum available being not greater than 4000°K. From this it becomes evident that the processes of thermal excitation are rather difficult for laboratory study, but not quite impossible. In fact before a clear theory of thermal ionisation was given by the senior author of this book, A. S. King had demonstrated that by simply heating an element in a high temperature furnace, the atoms can be excited to luminescence. He also found that groups of lines are very sensitive to temperature-excitation. Some come out easily at low temperatures (class I), others come out only at very high temperatures (classes III and IV). The right materials for investigations on thermal excitations are however the stars, for in them the surface temperature may reach to any value as high as 10^5°K. In fact even towards the end of the nineteenth century when nothing was known about the structure of the atom, Sir Norman Lockyer had concluded from his extensive studies of the spectra of the stars that elements exist in them in different and more primitive form than those existing in our laboratories. He elaborated a hypothesis of proto-atoms and evolution of elements. But as the senior author had shown his results can be best explained by the hypothesis that in stars atoms are excited to higher states and ionised to successive degrees by thermal excitation.

306. Thermal Ionisation as a Case of Reversible Chemical Reaction.—We shall now consider the process of thermal ionisation a little more closely. Let us suppose that the effect of heat on an atom of Ca is to knock off one electron and ionise it. For simplifying the situation, we shall neglect excited states of the unionised atom. Then we can represent the process of ionisation by the chemical symbols:

$$Ca \rightleftarrows Ca^{+} + e \quad . \quad . \quad . \quad . \quad . \quad . \quad . \quad . \quad . \quad (8)$$

The process may be likened to a reversible chemical reaction, just like the dissociation of NH_4Cl into NH_3 and HCl. For such reactions we have, according to the laws of thermodynamics, the total change in the thermodynamical potential of the system equal to zero, that is

$$\delta\Phi = 0$$

where Φ stands for the thermodynamical potential for the whole system and is equal to $U + pV - TS$, $U =$ internal energy, $p =$ pressure, $V =$ volume, $T =$ absolute temperature and $S =$ entropy of the system. In the present case we have

$$\Phi_{Ca^+} + \Phi_e - \Phi_{Ca} = 0 \quad . \quad . \quad . \quad . \quad . \quad . \quad . \quad (9)$$

Instead of using the function Φ we shall use the associated function $\Psi = -\frac{\Phi}{T} = S - \frac{U+pV}{T}$. Then

$$\Psi_{Ca^+} + \Psi_e - \Psi_{Ca} = 0 \; . \quad . \quad . \quad . \quad . \quad . \quad . \quad . \quad (10)$$

Using the thermodynamical expression for Ψ we have for one molecule of calcium vapour

$$\Psi_{Ca} = C_{p_{Ca}}\, lnT - R\, ln\, p_{Ca} + R\, ln \frac{(2\pi m)^{\frac{3}{2}} k^{\frac{5}{2}}\, g}{h^3} - \frac{U_{Ca}}{T} \quad . \quad . \quad (11)$$

Here the subscript Ca denotes that the quantities concerned refer to the calcium atom. Thus g is the weight factor of neutral calcium, $C_{p_{Ca}}$ its molecular specific heat, and U_{Ca} its energy at the A.N. (absolute null-point of temperature), m=mass of Ca-atom, h = Planck's const., k = Boltzmann constant and R = gas constant. If now the pressure p_{Ca} be expressed in atmospheres, R and C_p in calories per degree and we convert the logarithms to the base 10, we get

$$\frac{\Psi_{Ca}}{2{\cdot}30\,R} = \frac{5}{2}\log T - \log p + C_{Ca} - \frac{U_{Ca}}{2{\cdot}3\,RT} \quad . \quad . \quad . \quad (12)$$

Here C_{Ca} is the chemical constant for Ca-gas and is given by

$$C_{Ca} = -1{\cdot}587 + \tfrac{3}{2}\log M + \log g.$$

We have now to calculate the Ψ-function for Ca$^+$ and electrons. We suppose that they are monatomic gases, and their Ψ is given by formula similar to (11), only in the case of the electron $m = 1/1849$. The equation (10) reduces to

$$ln\frac{p_{Ca^+}\,p_e}{p_{Ca}} = -\frac{U}{RT} + \frac{5}{2}\; ln\, T + ln\left(I.\frac{g_e\,g^+}{g}\right) \quad . \quad . \quad (13)$$

where g_e = weight factor* of the electron, and g, g^+ those of normal and ionised Ca. Expressing p in atmospheres we have

$$\log\frac{p_{Ca^+}\,p_e}{p_{Ca}} = -\frac{U}{2{\cdot}30\,RT} + \frac{5}{2}\log T - 6{\cdot}49 + \log\frac{g_e\,g^+}{g} \;. \quad (14)$$

where $U = (U_{Ca^+} + U_e - U_{Ca})$ = heat of ionisation of Ca At the A.N. The chemical constants of Ca and Ca$^+$ cancel out provided we neglect g, and 6·49 is the value of the chemical constant of the electron, *i.e.*, $-6{\cdot}49 = -1{\cdot}587 + \tfrac{3}{2}\log(1/1849)$.

If we start only with Ca, and go on heating it, then all Ca$^+$ and electrons will be the decomposition products of the original amount of Ca. Suppose we have n gram molecules of Ca per unit volume to start with. Let a fraction 'x' be ionised. Then we have

$$p_i = p_e = nxkT, \quad p_a = n(1-x)kT$$

Hence p = total pressure $= p_i + p_e + p_a = n(1+x)\,kT$

We have finally

$$p_i = p_e = \frac{x}{1+x}\,p, \quad p_a = \frac{1-x}{1+x}\,p$$

Then equation (14) reduces to

$$\log\frac{x^2}{1-x^2}\,p = -\frac{U}{4{\cdot}573T} + \frac{5}{2}\log T - 6{\cdot}49 + \log\frac{g_e\,g_i}{g_a} \;. \; (15)$$

---

* The weight factor $g = 2j+1$, where j is the inner quantum number of the ground term. It comes in the expression for entropy as an extra summation term. The reason for this is the fact that an atom when placed in a magnetic field can take only $2j+1$ positions of orientations, and this increases the entropy of the system.

This equation was first given in 1920 by the senior author*, and applied widely by him to explain the spectrum of the Sun and other heavenly bodies.

J. Eggert was the first to show that the chemical constant of the electron may be calculated from the Sackur formula $C = -1{\cdot}587 + \frac{3}{2}\log M$. He applied the law of reaction isobar to calculate the ionisation in the interior of stars as postulated in Eddington's theories of stellar structure, but his values of U, the heat of ionisation, were rather hypothetical. Lindemann deduced the ionisation formula for hydrogen, but did not make any practical application of it.

For calculating the percentage of ionisation of any element according to the above formula under varying temperature and pressure, we require a knowledge of the heat of ionisation. The corresponding quantity in chemical reactions (*e.g.*, in the reaction $NH_4Cl \rightleftharpoons NH_3 + HCl - U$) is called the heat of reaction and is obtained from calorimetric experiments. But in the present case U can be obtained indirectly from spectroscopic data (from the limit of convergence of the principal series of the element), or from the direct determinations of the ionisation potential by Franck, Hertz and others. We have

$$U \text{ in cal.} = I \times 23050 = \nu_0 \times 2{\cdot}844$$

where I = ionisation potential in volts, ν_0 = convergence frequency of the principal series in wave numbers. Thus for Na, it has been found that $\nu_0 = 41000$ whence $I = 5{\cdot}12$ volts; we have $U =$ 117 k cal.; *i.e.*, 117 k cal. of heat are evolved when one gram atom of Na^+ combines with one gram atom of electrons to form one gram atom of neutral Na-gas. The reaction can be represented by the chemical symbol

$$Na = Na^+ + e - U$$

It is found that the alkali elements have the least I.P., inert gases have the largest I. P. (*vide* Table, at the end of this chapter).

Formula (15) is derived on the assumption that all electrons arise from the decomposition of the original mass of Ca. In other words, we assume the system to be *unicomponent*. But the electron can also arise from the decomposition of other elements. Hence it is useful to consider

---

*M. N. Saha, *Phil. Mag.*, 40, 472, 809, 1920; *Proc. Roy. Soc. A*, 99, 135, 1921.

the modification of formula (15) when the system is a *bicomponent* one, *i.e.*, the electron density is arbitrary. We have then

$$ln \frac{p_i\ p_e}{p_a} = -\frac{U}{RT} + \frac{5}{2} ln\ T + ln\ (I g_i\ g_e / g_a) \quad . \quad . \quad . \quad . \quad . \quad (16)$$

or $$\log \frac{x}{1-x} \cdot \frac{f}{1+f} \cdot p = -\frac{U}{4{\cdot}573T} + \frac{5}{2} \log T - 6{\cdot}49 + \log \frac{g_i\ g_e}{g_a}. \quad (17)$$

where x is the percentage of metal ionised and f = proportion of free electrons to the original number of undecomposed atoms. This modification was given by Prof. H. N. Russell.*

307. Calculation of the Percentage Ionisation of Elements.

—With the aid of (15), we can calculate the ionisation for any element whose I. P. is known under varying T and p. We give opposite a table showing percentage ionisation of Ca under varying temperature and pressure.

Table 6.—Percentage Ionisation of Calcium.

Pressure / Temp.	1 atmos.	10^{-2} atmos.	10^{-4} atmos.
2000°K	...	...	$1{\cdot}4 \times 10^{-3}$
3000	...	..	1
4000	...	2·8	26
5000	2	20	90
6000	8	64	99
7000	23	91	100
8000	46	98·5	"
9000	70	100	"
10000	85	"	"
11000	93	"	"
12000	96·5	"	"
13000	98	"	"

It is seen that ionisation becomes perceptible only when the temperature is sufficiently high, much higher than the temperatures which we can command in the laboratories. Such temperatures are obtainable only in the Sun and the stars which have surface temperatures varying from 3000°K to 30000°K.

The above calculations of ionisation have been made after neglecting the weight factor. The inclusion of weight factors causes the calculations to be somewhat revised. Thus in the case of calcium, we have

$$g_e = 2, \quad g_i = 2, \quad g_a = 1$$

g_e is henceforth always taken to be 2 owing to the fact that the electron has spin. $g_a = 1$, as the constitution of Ca is $4s^2\ {}^1S_0$, it is magnetically neutral and hence may be regarded as spherically symmetrical. Ca^+ is just like K, having the electron constitution $4s\ {}^2S_{\frac{1}{2}}$, hence $g_i = 2$.

---

* H. N. Russell, *Astro. Phys. Journ.*, 55, 119, 1922.

The ionisation formula for Ca is therefore

$$ln\ \frac{x}{1-x} p_e = -\frac{U_{Ca}}{RT} + \frac{5}{2}\ ln\ T + ln\ I + ln\ 4 \quad . \quad . \quad . \quad (18)$$

where $$I = (2\pi m)^{\frac{3}{2}}\ k^{\frac{5}{2}}\ / h^3.$$

But in the case of Na, we have $g_a = 2$, $g_i = 1$, as Na^+ has the constitution $2p^6\ {}^1S_0$ and is magnetically neutral.

We have therefore $$ln\ \frac{g_i\ g_e}{g_a} = ln\ 1 = 0.$$

The ionisation of Na is given by

$$ln\ \frac{x}{1-x} p_e = -\frac{U_{Na}}{RT} + \frac{5}{2}\ ln\ T + ln\ I$$

Equation (18) can also be written in the form

$$ln\ \frac{x}{1-x} p_e = -\frac{(U_{Ca} - RT\ ln\ 4)}{RT} + \frac{5}{2}\ ln\ T + ln\ I \quad . \quad . \quad . \quad (19)$$

Thus compared to Na, the effective I. P. of Ca or any other similar atom is reduced by $(ln 4)/23000$ volts. At $T=6500°$ (temperature of the Sun), this amounts to 17 k cal. or ·74 volts. The I. P. of Ca is reduced to 5·3 volts, *i.e.*, calcium shows almost the same percentage of ionisation as sodium. The I. P. of barium which has normally the same value as that of sodium, is reduced to 4·44 volts, slightly higher than that for potassium, *i.e.*, Ba is almost completely ionised in the Sun.

We therefore see that the percentage ionisation of an atom depends to a large extent on its ionisation potentials. A full table of such data as determined by experiments described in earlier sections or from spectroscopic data is given at the end of this chapter.

We are thus in a position to calculate percentage ionisation of elements in stars under varying temperature and pressure by using equations (15, 18, 19), from a knowledge of ionisation potential, and other spectroscopic data for these elements. It is now necessary that we should be able to detect experimentally the degree of ionisation of different elements in any star. The chief method for this depends upon the analysis and classification of spectral lines emitted by a star and comparison of their intensities. Suppose the spectrum of a certain star shows a very strong K-line, but a faint *g*-line of Ca. Since the *g*-line is due to neutral Ca atom, and

H, K-lines, due to Ca^+, our conclusion will be that in this particular star most of the calcium atoms must be in a completely ionised state, *i.e.*, as Ca^+, and a relatively very small proportion in the neutral state. Further the ratio of intensities of the K and g-lines would give roughly the proportion of Ca^+-atoms. This then enables us to make a rough estimate of the temperature of the star with the aid of (19), provided the values of ionisation potential are known and an approximate idea of pressure of its atmosphere can be formed from other evidences. Formula (19) coupled with suitable spectroscopic data is therefore expected to yield most valuable information regarding the physical conditions of stellar bodies.

308. Darwin and Fowler's Modification of the Ionisation Formula.—The ionisation formula (15) is however incomplete as it does not take into account the excited states. In the deduction of (15) the assumption has been made that when a mass of Ca atoms is heated, the products of decomposition are Ca^+ and electrons. As already mentioned this is not quite true. At sufficiently high temperature a substantial percentage of normal Ca-atoms exists in excited states, so that there will always be found besides normal and ionised atoms and electrons a number of neutral Ca-atoms excited to higher states.

We shall illustrate the method of taking into account the excited states in the simplest case of hydrogen.

Let p_i = be the partial pressure of the ionised atom
p_e = ... electrons.
p_n = ... atoms in the
n th quantum state.

Let us now consider the equilibrium between the atoms in the nth quantum state, H^+ and electrons. We have

$$ln\,K_n = ln\,\frac{p_i\;p_e}{p_n} = -\frac{\chi_n}{kT} + \frac{5}{2}ln\,T + ln\,(I.\,g_i\;g_e/g_n)\quad .\quad .\quad (20)$$

g_i, g_e, g_n denote the weight facts of H^+, the electrons, and the H-atoms in the nth quantum state. As a special case, for $n = 1$, we have

$$ln\,K_1 = ln\,\frac{p_i\,p_e}{p_1} = -\frac{\chi_1}{kT} + \frac{5}{2}\,lnT + ln\,(I.\,g_e\,g_i\,/g_1)\quad .\quad .\quad .\quad (21)$$

Hence subtracting, we have

$$ln\,(p_n\,/\,p_1) = -\frac{\chi_1 - \chi_n}{kT} + ln\,(g_n\,/\,g_1)\quad .\quad .\quad .\quad .\quad .\quad .\quad (22)$$

which is just the thermodynamical equation for equilibrium between two allotropic modifications of the same substance. We have

$$p_1 : p_2 : \ldots . : p_n = g_1 e^{\chi_1 / kT} : g_2 e^{\chi_2/kT} \quad \ldots : g_n e^{\chi_n / kT} \quad . \; . \; (23)$$

To find out an expression for ionisation, we observe that

$$\frac{p_n}{p_i p_e} = T^{-\frac{5}{2}} e^{\chi_n / kT} . (g_n / I g_i g_e) \quad . \; . \; . \; . \; . \; . \quad (24)$$

Adding up for all values of p_n and putting $p = \Sigma p_n$, we obtain

$$\frac{p}{p_i p_e} = \frac{T^{-\frac{5}{2}} e^{\chi_1/kT} b(T)}{I g_i g_e}$$

where $b(T) = g_1 + g_2 e^{-(\chi_1 - \chi_2)/kT} + \ldots + g_n e^{-(\chi_1 - \chi_n)/kT} \quad \ldots . (25)$

Hence we have the final formula

$$ln \frac{p_i p_e}{p} = -\frac{\chi_1}{kT} + \frac{5}{2} ln T + ln (I g_i g_e) - ln b(T) \quad . \; . \; . \quad (26)$$

If the ionised atom be such that it possesses easily excitable metastable or higher levels, as is the case with Ca+ (and also with Sr+ and Ba+) which have a normal $4s$-level, and a metastable $3d$-level, then on ionisation it may pass not only to the normal level, but also to some of these higher levels, *e.g.*, in the case of calcium, we have $\Delta \nu (4s - 3d) = 13650$ cm^{-1} and also easily excitable higher levels ($\Delta \nu (4s - 4p) = 25414, 25191$ cm^{-1} frequencies of H and K-lines). The great strength of the H and K-lines in stellar spectra and of the presence of subordinate lines of Ca+ in these show that the excitation to these levels is quite considerable. For taking account of these facts, we have to introduce a further summation $b'(T)$ for the ionised atom:—

$$b'(T) = g_{i,1} + g_{i,2} e^{-(\chi_1 - \chi_2)/kT} + \ldots + g_{i,n} e^{-(\chi_1 - \chi_n)/kT} . \quad (27)$$

where $g_{i,n}$ = weight factor, χ_n the relative energy of any metastable or higher orbit. The χ's now refer to the ionised atom.

Then the ionisation formula becomes, if we put $g_e = 2$,

$$ln \frac{p_i p_e}{p} = \frac{\chi_1}{kT} + \frac{5}{2} ln T + ln 2I - ln b(T) + ln b'(T) \quad . \; . \; . \quad (28)$$

If we suppose that both $b(T)$ and $b'(T)$ are confined to single terms, $b(T) = g_a$, $b'(T) = g_i$, and formula (28) reduces to (13).

This expression differs from the expression (13) in having the extra terms $b(T)$ and $b'(T)$. It was first derived by Darwin and Fowler* by their special method of calculating statistical averages by means of complex integration.

---

* Darwin and Fowler, *Phil. Mag.*, 45, 1, 1923.

For the case of hydrogen, we have

$$g_n = 2 + 2.3 + 2.5 \quad . \quad . \quad . \quad . \quad . \quad . \quad = 2n^2$$

Hence $b(T) = 2 + 2.2^2\, e^{-\frac{Rh}{kT}\left(\frac{1}{1^2}-\frac{1}{2^2}\right)} \; . \; . \; . \; . \; . \; + 2n^2\, e^{-\frac{Rh}{kT}\left(\frac{1}{1^2}-\frac{1}{n^2}\right)} + \; . \; .$

The series is easily seen to be divergent. Darwin and Fowler are of opinion that this is not a serious difficulty as the conditions postulated for the development of the higher orbits cannot hold in any actual case. The radius of the nth orbit is $a_o\, n^2$, and if the pressure be finite, such large orbits cannot be developed. The series will therefore terminate, or the higher terms will have to be multiplied by some factor which will make them vanishingly small. Such corrections have been introduced by Urey and Fermi.*

For more complex type of atoms, the ionisation formulae will naturally be more complex.

MULTIPLE IONISATION

In certain cases, as we shall see presently, an atom may suffer double or treble ionisation. A notable example is silicon which is obtained in the stellar range in three successive stages of ionisation, as Si, Si^+, Si^{++}, Si^{+++}.

For such cases, we are called upon to find out formulae for the calculation of ionisation in the different stages. This can be done by an extension of the methods already given. Only the final results are given here.

Let x_0 be the fraction of atoms in the normal state, and x_1, x_2, ... x_n be the fractions of atoms in the first, second, ... nth stages of ionisation. Then we have

$$1 = x_0 + x_1 + x_2 + \; . \; . \; . \; + x_n$$

Let f be the proportion of free electrons to the original number of neutral atoms and K_n be given by the equation

$$ln\, K_n = ln\,(p_{n+1}\, p_e \,/\, p_n) = -\frac{\chi_n}{kT} + \frac{5}{2}\, ln\, T + ln\, 2I - ln\, b_n\,(T) + ln\, b_{n+1}\,(T)$$

where χ_n = energy of ionisation from M^{+n} to $M^{+(n+1)}$ stage.

Then we have

$$\left.\begin{aligned} ln\;\; \frac{x_1}{x_0}\;\; \frac{f}{1+f}\;\; p &= ln\, K_0 \\ ln\;\; \frac{x_2}{x_1}\;\; \frac{f}{1+f}\;\; p &= ln\, K_1 \\ . \;\; . \;\; . \;\; . \;\; . \;\; . \;\; . \;\; . \;\; &. \;\; . \;\; . \\ ln\; \frac{x_n}{x_{n-1}}\;\; \frac{f}{1+f}\;\; p &= ln\, K_n \end{aligned}\right\} \; . \; . \; . \; . \; . \; . \; . \; . \; . \; (29)$$

---

* Urey, *Astro. Phys. Jour.*, 59, 1, 1914; Fermi, *Zs. f. Phys.*, 26, 54, 1924.

We illustrate the use of formula (29) by a special case.

It is found that the first I. P. of Ca is 6·09 volts, the second I. P. is 11·82 volts. Ca++ has argon-like structure, hence its I. P. is very high; actually it is found to be nearly 51 volts. In the stellar range, we therefore expect to get Ca, Ca+, and Ca++. Let the fraction of Ca+ and Ca++ be x and y respectively. Then (29) reduces to

$$\log \frac{x}{1-x-y} \cdot \frac{f}{1+f} \cdot p_e = -\frac{U_1}{2{\cdot}3\,RT} + \frac{5}{2}\log T - 6{\cdot}49$$

[Put $x_0 = 1 - x - y$, $x_1 = x$ in the first equation of (29)]

$$\log \frac{y}{x} \cdot \frac{f}{1+f} \cdot p_e = -\frac{U_2}{2{\cdot}3\,RT} + \frac{5}{2}\log T - 6{\cdot}49 \quad . \quad . \quad . \quad (29')$$

We have neglected the extra factors $b\,(T)$, $b'(T)$ in these deductions.

Subtracting one from the other, we have

$$\log \frac{x^2}{(1-x-y)\,y} = \frac{U_2 - U_1}{2{\cdot}3\,RT} \quad . \quad . \quad . \quad . \quad . \quad . \quad . \quad . \quad (30)$$

309. Application of the Ionisation Formulae towards a Physical Explanation of the Spectra of Stars.—From the application of the laws of radiation it has been found that the surface temperatures of stars are found to vary from 3000°K for red stars to over 20000°K for white stars. The surfaces of stars therefore present the best material for the application of the ionisation formulæ. As light is the only material reaching us from these distant universes, all that we can hope to know about them must be from the analysis of their light. But before any theory was known, the astronomer Sir Norman Lockyer undertook a systematic investigation of the spectra of stars. He discovered the remarkable fact that inspite of their large numbers, the spectra of stars can be classified into about five or six well defined groups, which show signs of a continuous transition from one stage to the other. The work was then continued at the Harvard College Observatory by Prof. E. C. Pickering and Dr. (Miss) A. J. Cannon, who photographed, before 1914, the spectra of not less than one hundred thousand stars. The result was in the main a confirmation of Lockyer's result, and can be described in the following words of Prof. H. N. Russell :—

> "The spectra of the stars show remarkably few radical differences in type. More than 99 per cent of them fall into one or the other of the six great groups which during the classic work of the Harvard College Observatory were recognised as of fundamental importance, and received as designations, by the process of the survival of the fittest, the rather arbitrary

letters B, A, F, G, K, M. That there should be so few types is noteworthy, but much more remarkable is the fact that they form a continuous series. Every degree of gradation between the typical spectra denoted by B and A may be found in different stars, and the same is true to the end of the series, a fact recognised in the familiar decimal classification, in which B_5A, for example, denotes a spectrum half way between the typical examples B and A. The series is not merely continuous, it is linear. There exists slight difference between the spectra of different stars of the same spectral class, such as A, but these relate to minor details. Almost all the stars of the small outstanding minority fall into three other classes (or rather four), denoted by the letters P, O, N, R. Of these, O undoubtedly precedes B at the head of the series, while R and N which grade one into the other, come probably at its end, though in this case the transition stages are not clearly worked out."

Since the above was written, much further work has been done particularly by Prof. Plaskett at the Dominion Observatory, Victoria, Canada, on the O-type of stars,[*] and by the Harvard workers on the M-stars[†]. The result has been the extension on the upper side of the decimal notation to spectra of O-class and on the lower side up to the M-class. The temperature range varies from 3000°K to 35000°K. Besides these regular types, other low temperature types (generally very small in number) have been discovered and denoted by the letters R, S, N [‡].

General Features of Variation.—A general idea of the variation of stellar spectra can be gathered from Fig. 27 which is a modification of one originally due to Lockyer, and subsequently modified by Milne, and the analysis of the results is summed up in Table 7.

EXPLANATION OF THE TABLE

The first column contains the name of the elements, the second column the particular characteristic line by which it is detected. The third column gives the spectral designation of the line in the notation at present adopted (Russell, Saunders and Shenstone), column 4 gives the excitation energy in electron volts for raising the neutral atom from the normal state to the particular state in which it can absorb the line. Thus for the Si^{++}line λ 4552, etc., the excitation voltage is calculated as follows. We start with normal Si. The first I. P. is 8·12 volts, the second I. P. is

---

[*] H. S. Plaskett, *Publ. Dominion Astr. Observatory, Victoria, Canada,* **1**, 375, 1921; **4**, No. 17.

[†] Menzel, *Harvard Circular*, **158**, 1924.

[‡] Merril, *Astro. Journ.*, **61**, 13, 1926.

*Table 7.—Stellar Lines of Astrophysical Importance.**

Element.	Line λ in Å.U.	Spectral Description.	Excitation Potential.	Appearance.	Maximum.	Disappearance.
H	4861 (Balmer series)	$2p-4d$ $-4s$	10·16		A_0	
He	4471	$1s\,2p-1s\,4d$ $^3P-{}^3D$	20·85	A_0	B_0	O_5
He+	4686	$3d-4f$	72·62	B_0	O_7	O_1
C	...	...	...	...	...	...
C+	4267	$2s^2\,3d-2s^2\,4f$ $^2D-{}^2F$	32·07	B_8	$B_{2,3}$	O_9
C++	4648, etc. (Triplet)	$2s\,3s-2s\,3p$ $^3S-{}^3P$	63·8	B_2	$O_{8,9}$	O_7
N	...	...	...	...	...	...
N+	3995	$2p\,3s-2p\,3p$ $^1P-{}^1P$	32·88	A_0	B_5	B_0
N++	4097	$2s^2\,3s-2s^2\,3p$ $^2S-{}^2P$	74·30	B_0	O_7	O_5
O	...	...	...	...	...	...
O+	4417	$2p^2\,3s-2p^2\,3p$ $^2P-{}^2D$	39·73	B_6	B_1	O_7
O++	3760	$2p\,3s-2p\,3p$ $^3P-{}^3D$	84·64	B_0	O_9	O_5
Na	5896	$3s-3p$ $^2S-{}^2P$	0	Lowest	Lowest	B_9
Mg	4352	$3s\,4p-3s\,4d$ $^1P-{}^1D$	4·3	Lowest	$K_{2,5}$	A_0
Mg+	4481	$3d-3f$ $^2D-{}^2F$	16·46	G_0	A_2	O_7
Al	3944	$3p-4s$ $^2P-{}^2S$	0	Lowest	Lowest	A_0
Al+	3900·7	$3s\,4p-3s\,4d$ $^1P-{}^1D$	13·35			

* For a fuller list, see Russell, *Astro. Journ.*, **61**, 223, 1925.

Table 7.—(continued)

Element.	Line λ in Å.U.	Spectral Description.	Excitation Potential	Appearance.	Maximum.	Disappearance.
Si	3905	$3p^2 - 3p\ 4s$ $^1S_0 - {}^1P$	1·90	Lowest	G_0	A_2
Si+	4131	$3d - 4f$ $^2D - {}^2F$	18·32	F_0	A_0	B_0
Si++	4552	$3s\ 4s - 3s\ 4p$ $^3S - {}^3P$	43·2	B_5	B_2	O_0
Si+++	4088	$4s - 4p$	81·6	B_2	O_9	O_0
P						
P+						
S						
S+	4162	$3p^2\ 4p - 3p^2\ 4d$ $^4D - {}^4F$	30·3		B_8	
S++	4253	$3p\ 4s - 3p\ 4p$ $^3P - {}^3D$	51·8		B_1	O_8!
Ca	4227	$4s^2 - 4s\ 4p$ $^1S_0 - {}^1P$	0	Lowest	Lowest	B_9
	4455	$4s\ 4p - 4s\ 4d$ $^3P - {}^3D$	1·92		K_2	F_0
Ca+	3933 (K) 3968 (H)	$4s - 4p$ $^2S - {}^2P$	6·1	Lowest	K_0	O_0
Sr	4607	$5s^2 - 5s\ 5p$ $^1S_0 - {}^2P$	0	Lowest	Lowest	F_0
Sr+	4077 4215	$5s - 5p$ $^2S - {}^2P$	5·67	...	K_2	A_0
Ba	5535		0			
Ba+	4904 4554	$6s - 6p$ $^2S - {}^2P$	5·18	...	M	A_3

16·26 volts. The normal state of Si++ is $1s^2\ 2s^2\ 2p^6\ 3s^2$. But in this state Si++ can absorb the line $3s^2\ {}^1S_0 - 3s\ 3p\ {}^1P_1$ which is in the Schumann region.

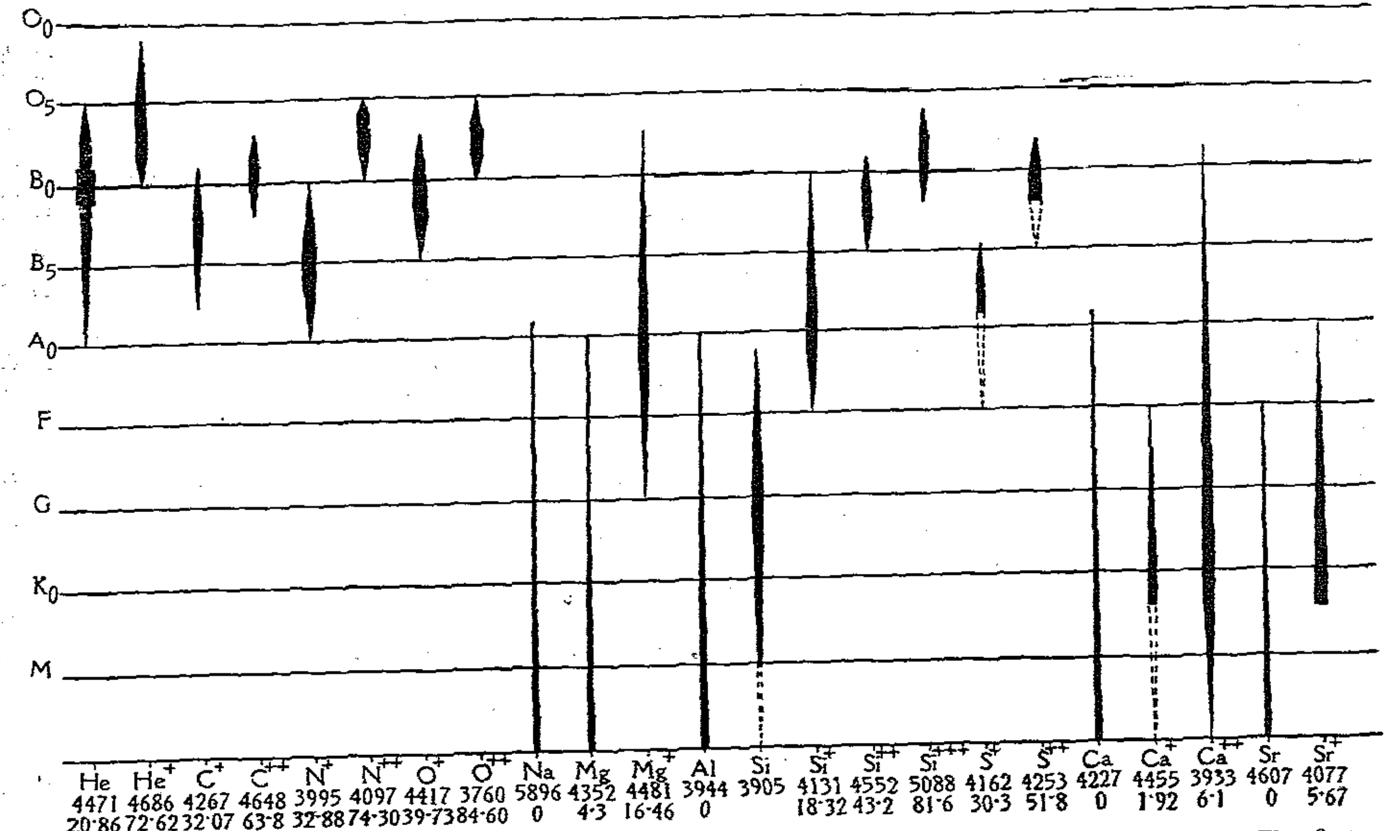

Fig. 27.—Lockyer's diagram illustrating variation of intensity of spectral lines in stellar sequence. The first row gives the name of the element, the second the wavelength of the characteristic line, the third gives the excitation potential. See also table 7.

The particular group of astrophysical lines λ 4552, etc., is due to the transition $3s\ 4s \leftarrow 3s\ 4p$. Hence we must add an amount of energy which can raise the electron in Si++ from the $3s^2$-stage to the $3s4s$ stage. According to A. Fowler,* this energy is equivalent to 18·9 volts. Hence the excitation potential of the line is $8{\cdot}12+16{\cdot}26+18{\cdot}9=43{\cdot}3$ volts. Lines like λ 4227, which are the resonance lines of normal atoms, require no preliminary excitation. Their I.P. is put equal to zero.

In the fifth column, the particular stellar class at which a line just appears is given. The principal lines of normal atoms appear in stars with the lowest temperature, but the subordinate lines or enhanced lines appear only at a certain higher stage depending upon the excitation required. The temperature of this stage is generally higher, the higher the excitation potential, *e.g.,* compare He λ 4471 for which the I. P. is 20·86 volts, and which appears at a stellar surface having the temperature 10000°K. In the sixth column the stage at which the intensity of the line is maximum is given. The maximum is generally flat. The maximum enables us to calculate the electron pressure as first pointed out by Fowler and Milne (*vide* p. 644).

The seventh column gives us the stage at which the line disappears. If it is a principal line like the Ca *g*-line, the disappearance means that the element is about 99% ionised. If the line belongs to a subordinate series, the percentage ionisation may not be so complete. The temperatures under each class, and the electron pressures are calculated from the application of the ionisation theory.

The table as well as Fig. 27 show that the lines of an element just appear at a certain stage, rise to a maximum and disappear at the other end. Thus the helium line λ 4471 just appears at the A_0-class, rises to a maximum intensity at the B_0-class (indicated by maximum thickness of the line representing He λ 4471 in Fig. 27) and disappears at the O_5-class. Or take particularly the case of silicon. We find that it is present in three successive stages of ionisation, which succeed and partly overlap each other in the stellar range.

The explanation of these facts is at once suggested by the ionisation theory. Thus the disappearance of the silicon line λ 3905 at A_2 denotes that Si is completely ionised at this temperature. The appearance of the Si^+ line λ 4131 at the F-stage indicates that silicon is considerably ionised at this stage, and further excited to the level of *3d* in which it can absorb the line λ 4131.

---

* A. Fowler, *Phil. Trans.*, 225, 1, 1926.

For the sake of numerical illustration, we take the g-line of Ca. This has maximum intensity in stars with the lowest temperature and disappears at A_0. The presence of maximum at the lowest temperature is easily understood, for the g-line is a principal line and can be absorbed by Ca-atoms in their normal state. The concentration of normal calcium atoms is maximum at the lowest temperature, since at higher temperatures, their proportion is diminished by excitation to higher levels and by ionisation. The disappearance at the B_9-stage is due to complete ionisation of calcium. A glance at Table 7 shows that if we calculate according to the simple ionisation formula, the ionisation of calcium becomes complete at $T = 13000°K$, $p = 1$ atmos., or at $T = 9000$, $p = 10^{-2}$ atmos. We cannot find out the exact temperature of the A-class unless we make some assumption regarding the value of the pressure on stellar atmospheres. In the early investigations, pressure was assumed to vary from 1 atmos. to 10^{-2} atmos. In this way, the following results were compiled :—

Appearance of K (λ 3933) M	Ionisation of Ca begins at	4000°K
Disappearance of g (λ 4227) B_8	Ca completely ionised at	13000°
Appearance of Mg+ (λ 4481) G_0	Mg considerably ,, ,,	7000°
Disappearance of K (λ 3933) O_9	Ca+ completely ,, ,,	20000°
Disappearance of Mg+ (λ 4481) O_7	Mg+ completely ,, ,,	23000°

The method is however uncertain owing to a number of reasons. First of all, the pressure is chosen arbitrarily. Secondly only a qualitative account is taken of the fact that the different lines require different amounts of material for their production. A well-known example is that of sodium D-lines. It is found that the smallest amount of sodium (10^{-7} gm/cm^3) in a flame will bring out the principal lines very strongly, while much larger amounts are required to bring out the subordinate lines in the same region. Thus the formula cannot be applied for any quantitative purpose unless the amount of matter required for the marginal appearance of a line be known.

ELECTRON PRESSURE FROM MAXIMUM INTENSITY OF SUBORDINATE SERIES LINES AND ENHANCED LINES.

(Fowler and Milne)

A very elegant method for determining the electron pressure was discovered by Fowler and Milne. They observed that there is a remarkable difference in the variation of intensity of the principal lines of neutral elements and of their subordinate lines in the stellar sequence. The principal lines of neutral elements are most intense at the lowest temperatures and gradually die out with increase of temperature (*vide* the behaviour of Ca *g* in Fig. 27). But the subordinate line or lines of an ionised element appear at a stage depending on its excitation potential ; they are at first very faint, gradually rise to a maximum at some intermediate stage and then again fall off to zero intensity as shown in the following figures.

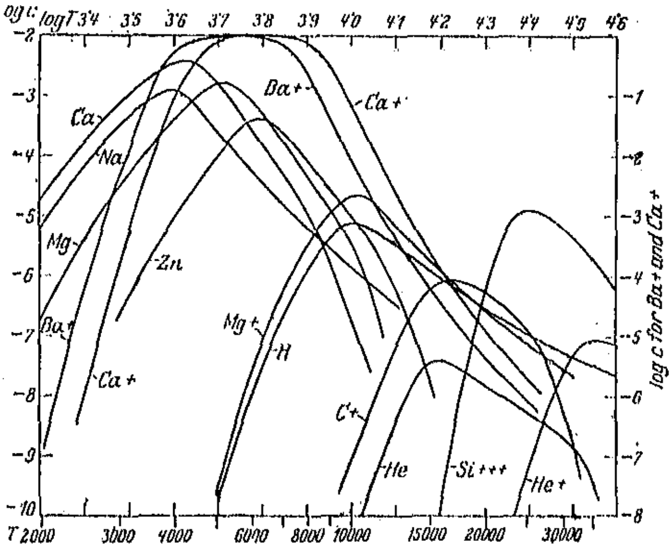

Fig. 28. Variation of intensity of lines of subordinate series and enhanced lines of elements with temperature. The abscissae represent temperatures, the ordinates concentrations of excited atoms.

Fowler and Milne explain the phenomenon in the following way: At the lowest temperature all atoms are in the normal state, there are none in the higher states. With increase of temperature, the higher states begin to come out. When the temperature still further rises, the atoms begin to get ionised, and the proportion of atoms in the excited states begins to fall off. A maximum must have been reached in the interval.

When the above ideas are translated into mathematical language, and conditions for maximum concentration of excited levels applied, we get a relation connecting the electron pressure in the reversing layer, and the temperature at which maximum intensity is reached. From eqn. (28), we have

$$\frac{x}{1-x}\, p_e = e^{-\chi/kT}\ T^{\frac{5}{2}}\ .\ 2I.\ \frac{b'(T)}{b(T)}, \text{ where } b = \Sigma g_r\ e^{-(\chi-\chi_r)/kT}$$

Applying the condition for maxima, we get

$$p_e = \frac{\chi_r + \frac{5}{2}kT}{\chi-\chi_r}\, e^{-\chi/kT}\, T^{\frac{5}{2}}\ .\ 2I\,\frac{b'(T)}{b(T)}\,; \qquad \frac{x}{1-x} = \frac{\chi_r - \frac{5}{2}kT}{\chi-\chi_r}\ . \quad (31)$$

As an example of the application of Fowler and Milne's formula, we take the case of the zinc triplet $^3P - {}^3S$, λ 4810, 4722, 4680 (*vide* Fig. 28). They attain the maximum intensity at the G_0-stage where the temperature may be supposed to lie between 5000° and 7000°; we have in this case $V_0 = 9{\cdot}34$ volts, $V_r = 5{\cdot}33$ volts, $b'(T) = 2$, $b\,(T) = 1$. Substituting proper values in (31) we obtain

for $T = 5000°$, $p_e = 1{\cdot}38 \times 10^{-6}$ atmos., $x = {\cdot}61$
6000°, $= 8{\cdot}0 \times 10^{-6}$ „ $= {\cdot}62$
7000°, $= 1{\cdot}6 \times 10^{-8}$ „ $= {\cdot}63$

where x is the fraction ionised.

These pressures are very much smaller than the pressure of one to 10^{-2} atmospheres formerly chosen. To obtain consistent values of T and p_e for stars of different types, all available data should be discussed and sifted. This has been done by Fowler and Milne, by Cecelia H. Payne and Pannekoek, and the reader may be referred to the original papers.* The final results do not appear to be concordant.

310. The Fraunhofer Spectrum of the Sun.—As the sun is so much nearer to us than the other stars, its spectrum can be studied in much greater detail and is suitable for a more extensive application of the ionisation formula. The spectrum of the Sun was studied in a monumental work by H. A. Rowland about 40 years ago. This has been revised in recent years by a committee of the Mount Wilson Solar Observatory. The revised catalogue† contains 20,027 Fraunhofer lines with wavelengths given up to the third place of decimal in the Rowland region (λ 2725 to λ 7314) and of 1,808 lines in the infra red (λ 7333 to λ 10195). Of these lines 12,502 or about 59 per cent have been accounted for, *i.e.*, either identified with known lines of elements or of compounds or as telluric lines (lines due to absorption of sunlight in the atmosphere of the earth). In this way about 57 terrestrial elements have been found in the sun.

---

* For details of this calculation, see Fowler and Milne, *Month. Not. Roy. Astr. Soc.*, **83**, 401, 1923; **84**, 499, 1924; Pannekoek, *H. d. Astrophysik*, III/1, 323; R. H. Fowler, *Statistical Mechanics*, Chap. XV; also H. N. Russell and J. Q. Stewart, *Astro. Journ.*, **59**, 197, 1914.

† *Revision of Rowland's Preliminary Table of Solar Wavelengths* (with an extension to the present limit of infra red), by C. E. St. John, D. E. Moore, L. M. Ware, E. F. Adams, and H. D. Babcock, published by the Carnegie Institution of Washington, 1928.

According to the theory of evolution, the earth was originally a tiny fragment of the sun, hence the sun (and probably the other stars as well) should be composed of the very same elements which have been found on the earth. The crust of the earth is composed of 92 elements. The occurrence of the elements in the sun is shown in the following Table.

*Table 8.—Elements in the Sun**

I	II	III	IV	V	VI	VII	VIII
1H							2He
(3Li)	4Be	5B	6C	7N	8O	(9F)	(10Ne)
11 Na	12Mg	13Al	14Si	(15P)	16S	(17Cl)	(18A)
19K	20Ca	21Sc	22Ti	23V	24Cr	25Mn	26Fe 27Co 28Ni
29Cu	30Zn	31Ga	32Ge	(33As)	(34Se)	(35Br)	(36Kr)
(37 Rb)	38Sr	39Yt	40Zr	41Cb ?	42Mo	(43Ma)	44Ru 45Rh 46Pd
47Ag	48Cd	49In	50Sn ?	51Sb	(52Te)	(53I)	(54Xe)
(55Cs)	56Ba	57La†	72Hf	(73Ta)	74W	(75Re)	(76Os) (77Ir) 78Pt
79Au	(80Hg)	81Tl ?	82Pb	(83Bi)	(84Po)	85	(86Rn)
87—	(88Ra)	(89Ac)	(90Th)	(91Pa)	(92U)		

† *Rare Earths*

58 Ce (65 Tb)	59 Pr 66 Dy	60 Nd (67 Ho)	(61 Il) 68 Er ?	62 Sa (69 Tu)	63 Eu 70 Yb ?	64 Gd (71 Lu)

( ) denotes absence ; ? presence doubtful. Of the other elements shown as present He occurs only in the chromospheric spectrum. The most notable absentees are :

---

* Taken from a paper by Ch. St. John, *Mount Wilson Contributions*, No. 385.

(1) The halogens, (2) The inert gases, (3) Elements of the fifth group excepting nitrogen, (4) The radioactive elements.

The explanation of these facts is very interesting, but can be touched here only in outline. Taking the alkali elements we find that the Na-lines D_1 and D_2 are very strong, the resonance lines of K (λ 7699, 7665) are very feeble, while Li (λ 6708), Rb (λ 7947 and 7800), Cs (λ 8943, 8521) lines are found to be entirely absent. The absence of Rb and Cs and the extreme feebleness of K are completely explained as being due to the almost complete ionisation of these elements in the sun as their I.P.'s have very low values. These are shown in Table 9.

Table 9.—Percentage ionisation of elements of groups I and II in the Sun and spots.

Alkali Elements	I. P.	Percentage of neutral atoms		Line (λ in Å.U.)	Intensity		Alkaline Earth	I. P.	Percentage of neutral atoms		Line (λ in Å.U.)	Intensity	
		4000°	6000°		Sun	Spot			4000°	6000°		Sun	Spot
Li	5·37	90·3	15	6708	0	5	B	9·5	100	96·9			
Na	5·11	81·5	9·6	5896 5890	20 30	60 90	Mg	7·6	99·7	80·8	5184	30	30
K	4·32	30·9	2·2	7699 7665	5 6	12 15	Ca	6 1	97·4	53·8	4227	20	40
Rb	4·16	21·9	1·7	7948 7800	ab. ...	0 1	Sn	5·67	95·1	14·0	4607	1	4
Cs	3·81	9·3	·9	8943 8521	ab. ...	ab. ...	Ba	5·18	70	11	5535	ab.	ab.

The percentage ionisation of the elements has been calculated from equation (15) on the supposition that $p_e = 10^{-2}$ atmos. and neglecting weight factors and presence of metastable states as mentioned on pp. 634 and 635. The tables do not explain why Na and Ca, K and Sr, Rb and Ba, in spite of their great difference in I.P. (about 1 volt in each case) are almost equally ionised in the sun. This is explained on the next page.

The principal lines of the ionised elements Rb^+, Cs^+ are in the Millikan region, hence they cannot be traced in the Fraunhofer spectrum. But if any part of the solar surface undergoes a local cooling, Rb and Cs may partly return to the neutral state. This is exactly what happens in the spots, for A. Fowler had proved that the spectra of spots is similar to that of K-type of stars and hence the temperature in them cannot far exceed 4000°C.

It was predicted from such arguments as above that Rb and Cs may occur in the spot in the neutral state. The verification of this prediction by Prof. H. N. Russell, who discovered the infra red pair of Rb λ 7911, 7800 (resonance lines) in some spot spectra taken by Dr. Brackett of Mount Wilson Observatory, constitutes one of the earliest triumphs of the ionisation theory. The intensities of the lines of neutral K and Na are increased in the spot spectra as shown in Table 9 in accordance with the predictions of the ionisation theory.

For more detailed comparison between the spot spectrum and the Fraunhofer spectrum see a paper by H. N. Russell in the *Astrophysical Journal*, **55**, 119, 1922.

SOME APPARENT DIFFICULTIES IN THE IONISATION THEORY.

We shall now explain the apparently higher ionisation of the alkaline earths in the sun. A glance at Table 9 shows that while Na and Ba have almost identical I. P.'s, *viz.*, 5·12 volts and 5·18 volts, respectively, still, while the arc lines of Na are very strong in the Fraunhofer spectrum, the resonance line of Ba λ 5534 is found to be entirely absent. Thus Ba seems to be completely ionised in the sun. A partial explanation of this fact has already been given in §307, where it was shown that owing to the extra term in the ionisation formula containing the weight factors, the effective I. P. of Ba is reduced by about ·74 volts on the sun and this becomes 4·38 volts, *i.e.*, has almost the same value as that of K. A complete explanation is afforded by (28) which takes into account the metastable states. Owing to the existence of a metastable $3d$-level of Ba^+ which differs little in energy from the lowest $4s$-level, the I. P. is reduced by about $(RT\ ln\ 8)/23000$ volts instead of by $(RT\ ln\ 4)/23000$ volts, *i.e.*, by about 1·08 volts. The effective I. P. becomes 4·10 volts, almost the same as that of Rb. Hence Ba is found to be completely ionised in the sun.

The calculation is as follows:—From a comparison of formulae (18) and (28) we find that the extra terms in the ionisation of barium over that of sodium are $\log 2 + \log b'(T) - \log b(T)$. Now $b\ (T)$ is very nearly unity, as the fundamental state of Ba is $6s^2\ {}^1S_0$, and the next states are

$6s\,5d\;{}^3D$, ${}^1D$ and $6s\,6p\;{}^3P$, ${}^1P$. These are so much removed from the fundamental state in energy value that they do not sensibly contribute to the value of $b(T)$. As a matter of fact, exact calculation shows that $b(T)=1{\cdot}25$.

But such is not the case with ionised barium. The fundamental state is $6s\;{}^2S_{\frac{1}{2}}$; but the two next metastable states ${}^2D_{\frac{3}{2},\frac{5}{2}}$ are very close to it ($\Delta\nu = 4875$ and 5675) (*vide* Paschen and Götze, *Seriengesetze der Linien-spektren*, p. 97). The weight factors for $D_{\frac{3}{2}}$ and $D_{\frac{5}{2}}$ are 4 and 6 respectively, and an exact calculation shows that at $T=6000°$, $b'(T)$ is very nearly 5. Hence the extra term in barium is $\log 2 + \log 5 - \log 1{\cdot}25 = \log 8$ as mentioned already.

Broadly speaking, the abnormal ionisation of barium is to be ascribed to the fact that though it can exist in its normal state in only one way, *viz.*, $6s^2\;{}^1S_0$, it can be ionised to a large number of possible states of closely lying energy values, *viz.*, to $6s\;{}^2S_{\frac{1}{2}}$ and $5d\;{}^2D_{\frac{3}{2},\frac{5}{2}}$ the latter with large weight factors. Thus the barium anomaly is no longer an outstanding difficulty (*vide* Pannekoek, *loc. cit.*, pp. 306—309, where this explanation seems to have been missed).

As regards other missing elements, we sometimes come across difficulties of a nature peculiar to each element. Take, for example, the element oxygen. This is the most plentiful element in the crust of earth, and it was naturally expected that it would show very prominently in the Sun. But for a long time, no trace of any line of oxygen could be found in the Fraunhofer spectrum. It was only in 1914, forty-five years after Kirchhoff's discovery, that Runge observed a triplet in the extreme red which he proved to be identical with an oxygen triplet. But why did this triplet of oxygen occur so faintly in the Fraunhofer spectrum? The answer is provided from an analysis of the spectrum of oxygen. Hopfield* has shown that the principal lines of oxygen, *viz.*, $2p^4\;{}^3P - 2p^3 3s\;{}^5S$ are in the Schumann region, and hence they are entirely cut off. The lines of oxygen which can be used for identification belong to minor combinations, *viz.*, to $2p^3 3s\;{}^5S - 2p^3 3p\;{}^5P$ and require very high stimulus, about 10 volts, for their production. Hence the prospect of getting O-lines in the Sun is very small, though the element may be more plentiful than calcium, the lines of which are so prominent in the Sun.

---

* Hopfield, *Astr. Journ.*, **59**, 114, 1924.

In fact the ionisation theory coupled with a knowledge of the constitution of the spectra of elements leads us to a complete justification of the saying of Rowland— "If the earth were suddenly heated to the temperature of the Sun, its spectrum would probably be the same as that of the Sun."

Spectra of Faculae.—Just as spots are regions of local cooling the faculae are regions where the temperature has been increased over that of the general photosphere. Hence it was predicted that the spectrum of the faculae would be similar to that of F-class of stars. This prediction was verified by Dr. St. John of the Mount Wilson Solar Observatory who took simultaneous photographs of the spectra of the Sun and the faculae, and found that the lines of Ti^+ were considerably enhanced in the faculae.

311. Influence of Pressure on Ionisation and Spectrum of the Solar Chromosphere.—If we refer back to formula (15), we find that besides temperature pressure has an appreciable influence on ionisation. A reduction in pressure is always accompanied by an increase in the percentage ionisation. Fig. 29 shows how the percentage ionisation of helium and ionised helium increases with decreasing pressure.

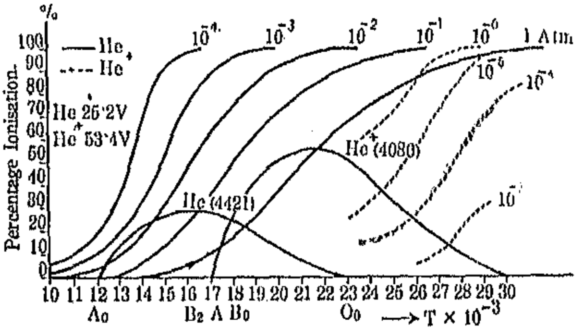

Fig. 29. Increase of percentage ionisation with decrease of pressure.

The ordinates represent ionisation, the abscissæ temperatures. Helium has an I. P. of 24·45 volts, hence very high temperatures are required to ionise helium completely. Thus at 1 atmos. pressure, ionisation reaches 90 % at a temperature of nearly 27000°. But if the pressure be diminished to 10^{-4} atmos., then ionisation becomes complete at about 15000° (*vide* Fig. 29).

This simple fact provides us with a qualitative explanation of the important difference between the Fraunhofer spectrum and the spectrum of the Solar Chromosphere. Lockyer was the first to find out that the two are not the exact reversal of each other as an application of Kirchhoff's law would lead us to expect. Generally speaking, the enhanced lines (lines due to ionised elements) are more prominent in the chromospheric spectrum than the arc lines. Thus taking calcium, we find that the *g*-line due to Ca can scarcely be noted in the higher layers of the solar atmosphere, while the H and K lines due to Ca^+ continue to be very strong. This is due to the fact that as we rise higher up, the pressure diminishes so fast that in spite of the fall in temperature, the ionisation rapidly increases, and at greater heights (about 5000 km.) calcium is completely ionised. In fact the spectrum of the upper chromosphere is largely made up of enhanced lines and is more like the reversal of the Fraunhofer spectrum of a star with the higher temperature of 10000°K and having very much less pressure (*e.g.*, α-Cygni which is a super giant).

Another noteworthy effect is the appearance of helium lines in the chromosphere. Helium is an element with the largest I.P., *viz.*, 25·4 volts, and its radiation potential is also extremely high, about 20·5 volts. Hence in stars up to the A-class, it is not even stimulated to any higher excited orbits. It is only in B-stars having temperatures ranging from 13000°K to 25000°K that we get He-lines. In the Fraunhofer spectrum of the sun which comes from the reversing layer, there is no trace of any helium line. But in the chromosphere, where the pressure has been reduced hundred or about thousand times, the helium lines come out very prominently.

Fowler and Payne* had actually obtained in 1903 experimental evidence to the effect that a reduction of pressure causes increased stimulus. They showed that while the Mg-arc in air shows no trace of the line λ 4481, which is due to Mg^+, the arc in vacuum (under reduced pressure) emits this line very strongly (see Fig. 30).

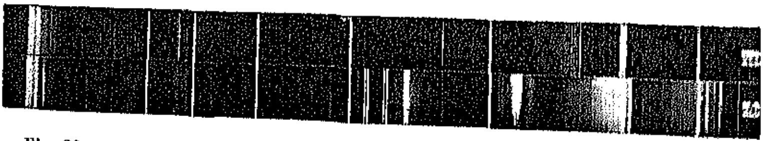

Fig. 30. Development of the lines of ionised Mg in the vacuum arc (Fowler and Payne).

The upper figure is the spectrum of Mg in open arc, the lower in vacuum arc. Notice the appearance of λ 4481 of Mg^+ in the lower.

---

* Fowler and Payne, *Proc. Roy. Soc. A.*, 72, 253, 1904.

312. Experimental Verification of the Ionisation Theory.—According to the ionisation theory, all atoms at high temperatures would lose electrons. At low temperatures, gases consist of uncharged atoms or molecules, hence they do not conduct electricity at all. But since at high temperatures electrons are given off, a considerable amount of electrical conductivity may be expected in the vapour.

A large number of experiments was done in the early years of this century to find out whether a gas can be made electrically conducting by heat alone. Mercury was the gas generally used in these experiments. But the choice was rather unfortunate, as mercury has a high I. P. (about 10·45 volts), and calculation with the aid of (15) shows that at least a temperature of 6000°K is needed to produce appreciable ionisation. Such a temperature cannot be realised in the laboratory, hence for experimental verification, we must choose a substance which possesses very low ionisation potential. We have seen that elements belonging to the alkali group have the lowest I.P., *viz.*, Cs. . . 3·88, Rb. . . . 4·16, K. . . 4·38, Na . . . 5·12 volts, and calculation shows that even at 2000°K, they would be considerably ionised. When these elements were tried,* it was found that they showed very considerable conductivity at 2000°K approximately, and in the case of Cs at much lower temperatures.

The apparatus by means of which these experiments were carried out is shown in Fig. 31.

The apparatus consists of a vacuum graphite furnace, first used by A. S. King of the Mount Wilson Solar Observatory, in which the elements at a definite pressure are heated to high temperatures. F is a tube made of Acheson graphite. It is held by two tightly fitting iron blocks which are carried by two water cooled stout brass tubes SS. The brass tubes stand out from a water cooled brass base but are insulated from the latter by rubber washers. The whole is enclosed by a cubical cast iron mantle provided with two windows of quartz facing the graphite tube, and a side tube (not shown in the figure) which is also provided with a quartz window, and is used for measurement of temperature with the aid of a Wanner pyrometer. The graphite tube is heated to temperatures of 2000°K—3000°K by the passage of a current of the order of 1000 amperes from a low tension transformer (used for welding) through the leads S,S. *f* is a second smaller furnace which is heated by a smaller subsidiary current not shown in the diagram; T is a thermocouple passing through a rubber tube at the bottom

---

*Saha, Sur, and Mazumdar, *Zs. f. Phys.*, 40, 648, 1927.

of the brass plate. The substance, say Na, is placed in *f* and heated to the desired temperature, which is given by T. From this we can find out the saturated vapour pressure. The vapour then passes out into the

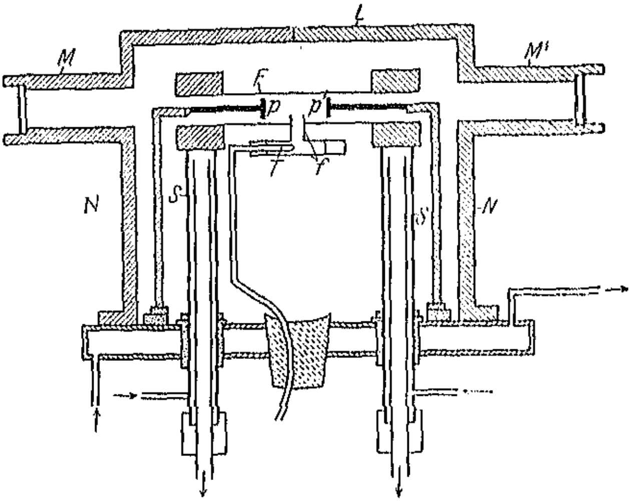

Fig. 81. Apparatus for showing electrical conductivity of heated vapours.

furnace F, which has a much higher temperature. Here the vapour is ionised. *p,p* are two Acheson carbon discs, mounted on molybdenum holders which are carried by the iron stands between S and N. These stands are carefully insulated from the brass discs and connected by means of wires passing through the rubber cork to a source of e. m. f. In series we have a micro or milliammeter (not shown in the diagram). The whole apparatus is highly evacuated. Ordinarily no current passes between *p,p*. Suppose we start with Na in *f* at a temperature of 500°C. This gives a vapour pressure of 3 to 4 mm. of mercury. We keep *f* always at this temperature. The temperature of F is now varied from 1000°K to 2000°K in steps. The voltage across *p, p* is only 1 volt. It is found that the current in the measuring instrument rapidly increases with increase of temperature in F. With Hg, Zn, Cd which have I. P.'s varying from 9 to 10·5 volts, no current measurable with a microammeter was obtained even at the highest temperatures. Mg which has an I. P. of 7·61 volts gave only a small current at the highest temperatures. Na and K on the other hand gave appreciable currents even at 1000°K, and at the highest temperature, *viz.*, 2000°K the conductivity was so great that the current could be measured only by a milliammeter. When no vapour was introduced in F, there was absolutely no conductivity even at the highest temperature.

These experiments prove in a qualitative way that vapours consisting of atoms can be made electrically conducting by heat alone, and the conductivities increase as elements with lower ionisation potentials are taken. Quantitative experiments are much more difficult to carry out.*

313. Ionisation in a Mixture of Gases.—It is proved in treatise on thermodynamics† that if a substance like NH_4Cl dissociates into two components, NH_3 and HCl, and then one of the products of decomposition, say HCl be added in excess, the degree of dissociation of NH_4Cl is considerably suppressed. The analogous phenomenon in ionisation was discovered by A. S. King, and follows from a direct application of Russell's formula (17), p. 633. Ca was taken in a vacuum graphite tube, and heated to 2000°K. The H and K lines indicating the presence of Ca^+ were obtained in emission. Now some Cs was introduced into the furnace, and it was found that the H, K-lines had completely disappeared, or the ionisation of calcium has been almost completely suppressed. As caesium has a very low I. P., it introduces a very large excess of electrons in the reaction space, hence ionisation of Ca is suppressed in accordance with equation (17).

A numerical calculation will make the point clear. The ionisation formula may be written in the form

$$\frac{n_e\, n_i}{n_a} = \left(\frac{2\pi mk}{h^2}\right)^{\frac{3}{2}} T^{\frac{3}{2}} e^{-\chi/kT} \left(g_e\, g_i/g_a\right).$$

Substituting proper values of constants, we have at 2000°K, for calcium $n_e\, n_i\, /\, n_a = 5 \times 10^5 = n_e\, x/(1-x)$, where x is the fraction of calcium atoms ionised ; for caesium, $n_e\ n_i\, /\, n_a = n_e\, x'\, /(1-x') = 4{\cdot}8 \times 10^{10}$, where x' is the fraction of caesium atoms ionised.

The actual number of electrons per c.c. will differ according as we have pure calcium in the furnace or introduce caesium. If we have at first only calcium, and suppose it exerts a pressure of 1 atmos., we obtain since pressure is $n\ (1+x)\ kT$, (n = number of calcium atoms per c. c. to start with), $n = 3{\cdot}7 \times 10^{18}$. Now x is given by the relation $nx^2/(1-x^2) = nx^2$ (since x is small) $= 5 \times 10^5$, from which $x = 4 \times 10^{-7}$, and the number of Ca^+ atoms as well as of free electrons per c.c. is equal to $1{\cdot}5 \times 10^{12}$. Now if we introduce caesium, and it also exerts a pressure of 1 atmos., we get $x' = 1{\cdot}14 \times 10^{-4}$, $n_e = 4{\cdot}2 \times 10^{14}$. The number of free electrons is now nearly 300 ($= 4{\cdot}2 \times 10^4/1{\cdot}5 \times 10^{12}$) times increased. Since $n_e\, n_i$ = constant, the proportion of Ca^+ atoms will be about 300 times diminished, *i.e.*, the H, K-lines will now disappear. This was actually found to be the case.

---

* Langmuir and Kingdon (*Proc. Roy. Soc. A*, **107**, 61, 1925) have shown that the thermal ionisation of Cs-vapour can be found from measurements of positive and negative emission from a tungsten filament in a vapour of Cs. For further works see Mayer, *Ann. d. Phys.*, **4**, 367, 1930.

† See, for example, *A Text Book of Heat* by Saha and Srivastava, p. 45.

This also explains the phenomenon observed by Paschen that if an element under some condition of excitation gives a spectrum in which neutral lines and enhanced lines are freely mixed together, the enhanced lines can be almost entirely suppressed if some more easily excitable element is introduced into the reaction space.

The method is now extensively used in the Mount Wilson Solar Observatory for separating lines due to the successive stages of ionisation of an element. For example, let us take the rare earths. They have I. P.'s varying from 5 to 6 volts, and in the vacuum furnace, even at the lowest temperatures, the arc lines and the spark lines appear mixed up. In such cases King introduces some Cs-vapour. The ionisation of the rare earths is suppressed and we get only the arc lines.

314. Stark Effect.—Shortly after the discovery of Zeeman Effect in 1896 attempts were made by Zeeman himself and others to find out whether there exists an analogous electrical effect, that is to say, whether spectral lines are decomposed into components when the source is placed in a strong electrostatic field. For a long time the electrical analogue of Zeeman effect could not be discovered. It was only in 1913 that J. Stark * succeeded in proving that Balmer lines emitted by the H-atom in strong electrostatic fields are split up into several components.

Reviewing the causes of failure of earlier investigators, we find that they were due to (i) absence of proper technique, (ii) to the choice of elements other than hydrogen for experimentation. A strong electrical field must be used, but it is difficult in the ordinary discharge tube to seal any subsidiary electrodes between which any strong field can be applied because the space is too conducting and short circuiting takes place between the electrodes. Stark overcame these difficulties by utilising his knowledge of the technique of the canal-ray tube. In this, discharge takes place between the anode and perforated cathode, in a space where the pressure is not very low. The positive particles stream through the orifices in the cathode and the space is filled with characteristic radiation of the gas. Stark used a cathode with fine bores so that a difference

---

*J. Stark, *Ann. d. Phys.*, 43, 965 783, 1914.

of pressure, could be maintained between the positive ray space and discharge space. The pressure in the first was about 10^{-2} mm., while in the second it was about 10^{-6} mm. (no discharge state). He found that under this condition a third electrode can be sealed behind the perforated cathode and a high field can be applied between the cathode and this electrode. His arrangements for viewing the emission of light parallel and perpendicular to the direction of the field is shown in the accompanying diagrams (Fig. 32). The third electrode F being within the cathode dark space, no discharge takes place between F and C. Positive ions accelerated through C pick up an electron on their way in the space between F and C and then they revert to the normal state after emitting light in that space.

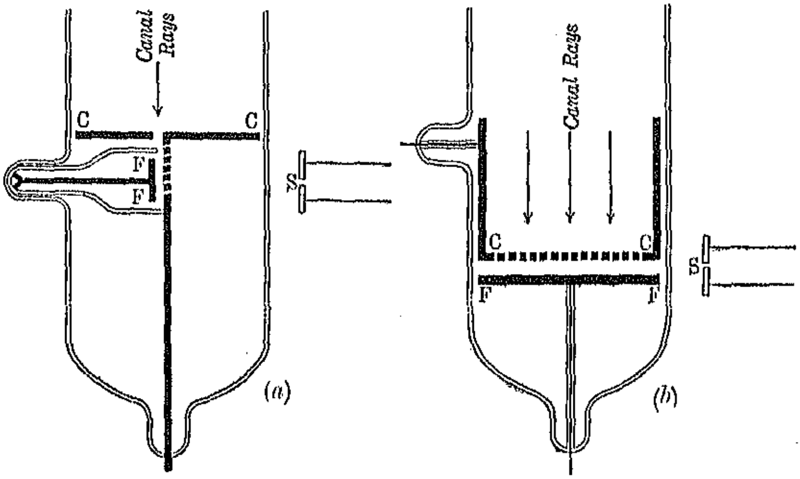

Fig. 32. Arrangement for observing (a) Longitudinal and (b) Transverse Stark effects.

Photographs of Stark-effect-splitting of H_α, H_β, H_γ-lines obtained by Mark and Wierl * are reproduced in Fig. 33, Plate X. The results obtained by Stark and others for Hydrogen can be summarised as follows :—

(1) Every Balmer line is decomposed into a number of components and this number increases with the series number of the line.

(2) When viewed in a transverse direction, the lines are found to be polarised, some parallel to the direction of the field (π-components), some perpendicular (σ-components).

---

* Mark and Wierl, *Zs. f. Phys.*, **53**, 526, 1929; **55**, 156, 1929; **57**, 494, 1929.

(3) When observation is in a direction parallel to the field, the π-components are invisible and the σ-components are found to be un-polarised.

(4) Generally the strong π-components lie outside and strong σ-components lie inside.

(5) In the case of hydrogen the splitting and polarisation is generally symmetrical about the original line, but for lines of other elements they are generally un-symmetrical.

(6) The distances of the components of hydrogen lines from the centre measured in frequency units are integral multiples of a certain unit which is proportional to the field strength and is the same for all lines of the Balmer series.

A little after the announcement of his discovery by Stark, Lo Surdo * found that the same effect can be observed in the faint light emitted in the cathode dark space. A glance at Fig. 3, p. 45, shows that in the region of cathodic glow, the potential changes very rapidly. The electrical field is therefore very great. Lo Surdo found that if the pressure be so chosen that the length of the cathode dark space is between 1 and 10 mm. and if the potential difference and current are sufficiently large, the light emitted shows Stark splitting. In this method only transverse observation can be made and as the fall of potential is not uniform throughout the space, the separation is not the same at all points. The spectrophotograph of Hα-line taken by Foster† using a modified Lo-Surdo tube is reproduced in Fig. 34, Plate X.

315. Theories of Stark Effect.—Unlike Zeeman Effect, Stark Effect cannot be explained by classical theories. Shortly after Stark's discovery Schwarzschild‡ and Epstein§ showed almost simultaneously that all the observational results could be almost completely explained from Sommerfeld's orbital theory. This was naturally regarded as a great triumph for the Quantum Theory. An account of this theory is given below. But a very rough and preliminary calculation may be given which enables us to make a rough guess about the magnitude of the effect to be expected.

---

* Lo Surdo, *Phys. Zeits.*, **15**, 122, 1914; *Lincei Rend.*, **23**, 117, 1914; *N. Cim.*, **7**, 335, 1917.

† Foster, *Proc. Roy. Soc. A.*, **123**, 108, 1929.

‡ Schwarzschild, *Ber. d. Preuss. Akad.*, 548, 1916.

§ Epstein, *Ann. d. Phys.*, **50**, 489, 1916.

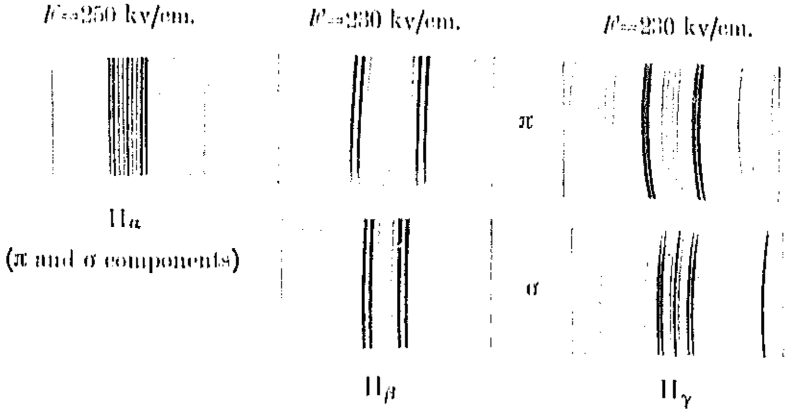

Fig. 88. Stark effect components (π and σ) for Balmer lines (*Mark and Wierl*).

(*p.* 657).

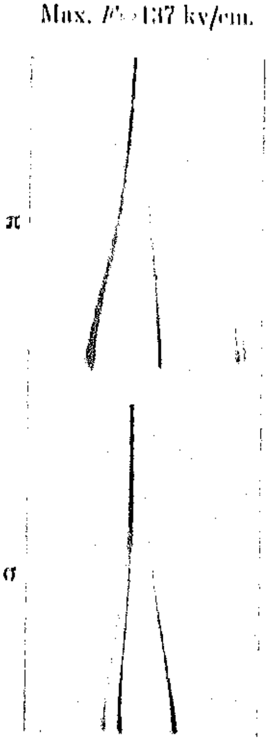

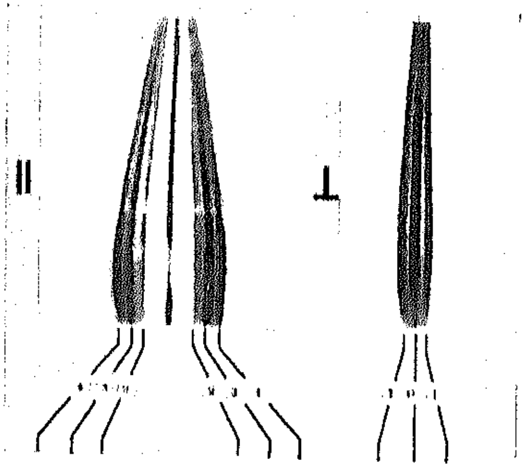

Fig. 91. Lo Surdo photograph of Stark effect for Hα (*Foster*).

(*p.* 658).

Fig. 92. Stark effect for He line 2^1P-4^1D (*Foster*).

(*p.* 672).

We have seen that the negative energy of the electron moving under central charge Ze is given by $-e^2Z/2a$, where a is the radius of the orbit. his may be put as

$$E = -\tfrac{1}{2}\, ea\, eZ/a^2 = -\tfrac{1}{2}\, eaF, \text{ where } F = eZ/a^2$$

the radial field in which the electron moves. We may suppose that hen an external field F_z is introduced, the change in energy is

$$\Delta E = -\tfrac{1}{2}\, \alpha\, ea\, F_z\,, \quad \text{or} \quad \Delta\nu = -\tfrac{1}{2}\, \alpha/h\,.\, ea\, F_z$$

here α is a numerical constant to be determined.

Now we have $a = h^2\, n^2/4\pi^2\, e^2mZ$. Hence we have

$$\Delta\nu = \alpha \frac{h}{8\pi^2 emZ} F_z\,.\, n^2.$$

We shall see presently that the actual expression is very similar in pearance to the above. The natural field strength due to the nucleus a distance a is given by ($a = a_0n^2$, a_0 = radius of the normal H-atom).

$$F = \frac{eZ}{a^2} = Z.\frac{4{\cdot}77 \times 10^{-10}}{({\cdot}538 \times 10^{-8})^2}\,.\,\frac{1}{n^4} = \frac{Z}{n^4}\, 5{\cdot}13 \times 10^9 \text{ volts/cm.}$$

The highest field used in the laboratory is of the order 10^5 volts/cm. o $\Delta\nu$ due to the field is of the order 10^{-3} times the ν of the line. The tark Effect splitting under a field 10^5 volts/cm. is of the order of 10 cm^{-1}, nce it is of a larger order of dimension than the Zeeman splitting tained with the usual fields.

The earlier theoretical investigations of Stark Effect on Quanm Theory as carried out by Epstein were on Sommerfeld's lines*. e have seen that the success of this method depends upon the oper choice of the coordinate system which can lead to separation variables. Epstein showed that this can be done by the use parabolic coordinates. But though the results obtained are und to explain the observations correctly, the physical points e not so clearly brought out. For this, we may turn to the ternative method of Bohr who uses the method of perturbations. e give short accounts of both theories.

A. Method of Epstein.

Let the nucleus be the origin of coordinates and let the direcn of the field be chosen to represent the z-axis. Then with ference to this axis and a plane of reference passing through the axis a point P may be denoted by cylindrical coordinates, z, ρ, ϕ such that

---

* Simultaneously with Epstein, Schwarzschild deduced the same result the use of angle variables (*Berl. Sitzungsberichte,* 1916).

$$r^2 = z^2 + \rho^2, \quad ds^2 = dz^2 + d\rho^2 + \rho^2 d\phi^2 \quad . \quad . \quad . \quad (32)$$

Let us now take any $(z\rho)$-plane, and replace z and ρ by the parabolic coordinates ξ and η. This can be done by putting

$$z + i\rho = \tfrac{1}{2}(\sqrt{\xi} + i\sqrt{\eta})^2 \quad . \quad . \quad . \quad . \quad . \quad . \quad . \quad (33)$$

Equating real and imaginary parts of equation (33), we get

$$z = \tfrac{1}{2}(\xi - \eta), \quad \rho = \sqrt{\xi\eta} \quad . \quad . \quad . \quad . \quad . \quad . \quad . \quad . \quad (34)$$

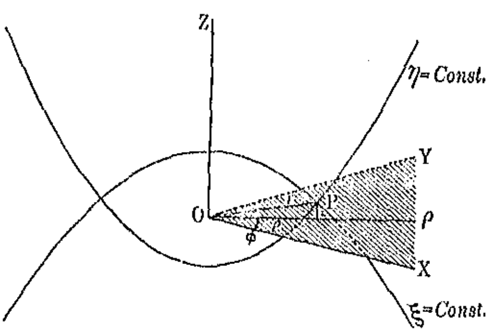

Fig. 35

Expressing ρ in terms of ξ alone and η alone we get

$$\rho^2 = -2\xi(z - \xi/2) \quad . \quad (35)$$

$$\rho^2 = 2\eta(z + \eta/2) \quad . \quad (36)$$

Equation (35) represents a set of parabolas with their axis along the negative z-direction and latus rectum$=2\xi$ and equation (36) indicates a set of parabolas with their axis along the positive z and latus rectum$=2\eta$. The focus is common. It is thus clear that (ξ, η) define two symmetrically situated points in $(z\rho)$-plane. Thus a system of values ξ, η, ϕ may be used to represent all points in space.

The potential energy of the electron moving under a central Coulombian force and in a space which is traversed by a constant electrical field F along the z-axis is given by

$$E_{\text{pot}} = -\frac{Ze^2}{r} + Fez \quad . \quad . \quad . \quad . \quad . \quad . \quad . \quad . \quad (37)$$

$$E_{\text{kin}} = \tfrac{1}{2} m[\dot{z}^2 + \dot{\rho}^2 + \rho^2\dot{\phi}^2] \quad . \quad . \quad . \quad . \quad . \quad . \quad (38)$$

Hence the total energy W is given by

$$W = \tfrac{1}{2}m[\dot{z}^2 + \dot{\rho}^2 + \rho^2\dot{\phi}^2] - \frac{Ze^2}{r} + Fez$$

Expressing W in terms of ξ and η we get

$$W = \tfrac{1}{8}m[\dot{\xi}^2(1+\eta/\xi) + \dot{\eta}^2(1+\xi/\eta) + 4\xi\eta\dot{\phi}^2] - \frac{2Ze^2}{\xi+\eta} + \tfrac{1}{2}eF(\xi - \eta) \quad (39)$$

We have now

$$p_\xi = \frac{\partial T}{\partial \xi} = \frac{m}{4}\left(1+\frac{\eta}{\xi}\right)\dot{\xi}\,;\; p_\eta = \frac{\partial T}{\partial \eta} = \frac{m}{4}\left(1+\frac{\xi}{\eta}\right)\dot{\eta}\,;\; p_\phi = m\,\xi\,\eta\,\dot{\phi}$$

Substituting the values of p_ξ, p_η and p_ϕ, we can give to equation (39) the Hamiltonian form :

$$\begin{aligned} W &= \frac{1}{2m}\left[\frac{4p_\xi{}^2}{(1+\eta/\xi)} + \frac{4p_\eta{}^2}{(1+\xi/\eta)} + \frac{p_\phi{}^2}{\xi\eta}\right] - \frac{2e^2Z}{(\xi+\eta)} + \tfrac{1}{2}eF(\xi-\eta) \\ &= \frac{1}{2m(\xi+\eta)}\left[4\xi\,p_\xi{}^2 + 4\eta\,p_\eta{}^2 + \left(\frac{1}{\xi}+\frac{1}{\eta}\right)p_\phi{}^2 \right. \\ &\qquad\qquad \left. - 4e^2mZ + me\,F(\xi^2-\eta^2)\right] \quad . \quad (40) \end{aligned}$$

We have to use now, Sommerfeld's quantum conditions :

$$\oint p_\xi\,d\xi = n_1h\,;\quad \oint p_\eta\,d\eta = n_2h\,;\quad \oint p_\phi\,d\phi = \lambda\,h \quad . \quad . \quad (41)$$

Since W does not contain ϕ explicitly, it is a cyclic coordinate, so that

$$p_\phi = \frac{\lambda h}{2\pi} \quad . \quad . \quad . \quad . \quad . \quad (42)$$

Hence equation (40) becomes

$$\begin{aligned} W = \frac{1}{2m(\xi+\eta)}\Bigg[\,4\xi\,p_\xi{}^2 + 4\eta\,p_\eta{}^2 + \left(\frac{1}{\xi}+\frac{1}{\eta}\right)\frac{\lambda^2h^2}{4\pi^2} - 4e^2mZ + \\ meF\left(\xi^2-\eta^2\right)\Bigg]. \quad . \quad . \quad . \quad . \quad . \quad . \quad . \quad . \quad (40') \end{aligned}$$

Now the variables can be separated. We have

$$\begin{aligned} 4\xi\,p_\xi{}^2 - 2m\xi W - 2me^2Z + meF\xi^2 + \frac{1}{\xi}\,\frac{\lambda^2h^2}{4\pi} = -\,4\eta\,p_\eta{}^2 \\ +\,2\,m\eta W + 2\,me^2Z + meF\eta^2 - \frac{1}{\eta}\,\frac{\lambda^2h^2}{4\pi} = \text{constant} = 2\alpha \quad . \quad (43) \end{aligned}$$

So that

$$\left.\begin{aligned} p_\xi{}^2 &= A_1 + 2\,\frac{B_1}{\xi} + \frac{C_1}{\xi^2} + D_1\xi \\ \text{and} \qquad p_\eta{}^2 &= A_2 + 2\,\frac{B_2}{\xi} + \frac{C_2}{\xi^2} + D_2\xi \end{aligned}\right\} \quad . \quad . \quad (44)$$

$$\left.\begin{aligned} &\text{where } A = A_1 = A_2 = \tfrac{1}{2}\,mW,\; C = C_1 = C_2 = -\,\frac{1}{4}\left(\frac{\lambda^2h^2}{4\pi^2}\right) \\ &D_1 = -\,\frac{meF}{4},\; D_2 = \frac{meF}{4},\; B_1 = \tfrac{1}{4}(me^2Z+\alpha),\; B_2 = \tfrac{1}{4}(me^2Z-\alpha) \end{aligned}\right\} . \quad (45)$$

The first and second quantum conditions given in equation (41) take the general form

$$\oint \sqrt{A + 2\,B/\xi + C/\xi^2 + D\xi}\,.\,d\xi = nh \quad . \quad . \quad . \quad (46)$$

The above elliptical integral yields (see Sommerfeld *Atombau*, 4th ed., p. 779).

$$-\,2\pi i \left\{ C^{\frac{1}{2}} - \frac{B}{A^{\frac{1}{2}}} \;-\; \frac{D}{4A^{\frac{3}{2}}}\Big(\frac{3B^2}{A} - C\Big)\Big) \right\} = nh.$$

$$\text{Hence} \quad B = A^{\frac{1}{2}}\left(C^{\frac{1}{2}} - \frac{inh}{2\pi}\right) + \frac{D}{4A}\left(C - \frac{3B^2}{A}\right). \quad . \quad . \quad (47)$$

Since the term in D is small, we can neglect it to find the value of B^2/A to the first approximation. The equation (47) then reduces to

$$B = A^{\frac{1}{2}}\left(C^{\frac{1}{2}} - \frac{nhi}{2\pi}\right) + \frac{D}{4A}\left(\frac{3n^2h^2}{4\pi^2} + \frac{3nhi}{\pi}\,C^{\frac{1}{2}} - 2C\right) \quad . \quad . \quad (48)$$

Substituting now the values of B and D from equation (45) and adding the two equations thus obtained, we get

$$me^2Z = A^{\frac{1}{2}}\left[4C^{\frac{1}{2}} - \frac{(n_1+n_2)\,ih}{\pi}\right] + \frac{meF}{4A}\left[\frac{3}{8}\,\frac{(n_2{}^2 - n_1{}^2)h^2}{\pi^2} + \frac{3}{2}\,\frac{(n_2 - n_1)\,ihC^{\frac{1}{2}}}{\pi}\right] \quad . \quad . \quad . \quad . \quad . \quad . \quad (49)$$

To the first approximation the correction term involving F may be neglected, so that

$$A = -\,\frac{m^2e^4Z^2\pi^2}{h^2(n_1 + n_2 + \lambda)}.$$

From this, it is clear that $n_1 + n_2 + \lambda = n$, the total quantum number.

Substituting the value of A in the second expression on the right hand side of equation (49), we get

$$A = \frac{1}{2}\,mW = -\,\frac{\pi^2m^2e^4Z^2}{h^2n^2} - \frac{3h^2}{16\pi^2eZ}\,.\,(n_2 - n_1)\,n$$

$$\text{Hence} \quad W = -\,\frac{2\pi^2me^4Z^2}{h^2n^2} - \frac{3h^2}{8\pi^2meZ}\,.\,(n_2 - n_1)\,n \quad . \quad . \quad . \quad (50)$$

There are many points in the above treatment which have not received adequate explanations such are, for example, the shape of the orbits and the limits of integration, etc. For these, the original papers may be consulted. We see that the original elliptic orbit may be inclined at any angle to the axis of the external field as shown in Fig 40. Hence $\lambda = k \sin \beta$, where k is the azimuthal quantum number and β is the angle between the axis of the field and the orbit. It is thus clear that λ can have all values from k, $k-1$, ... , $-k$. If we use wave mechanics it can have all

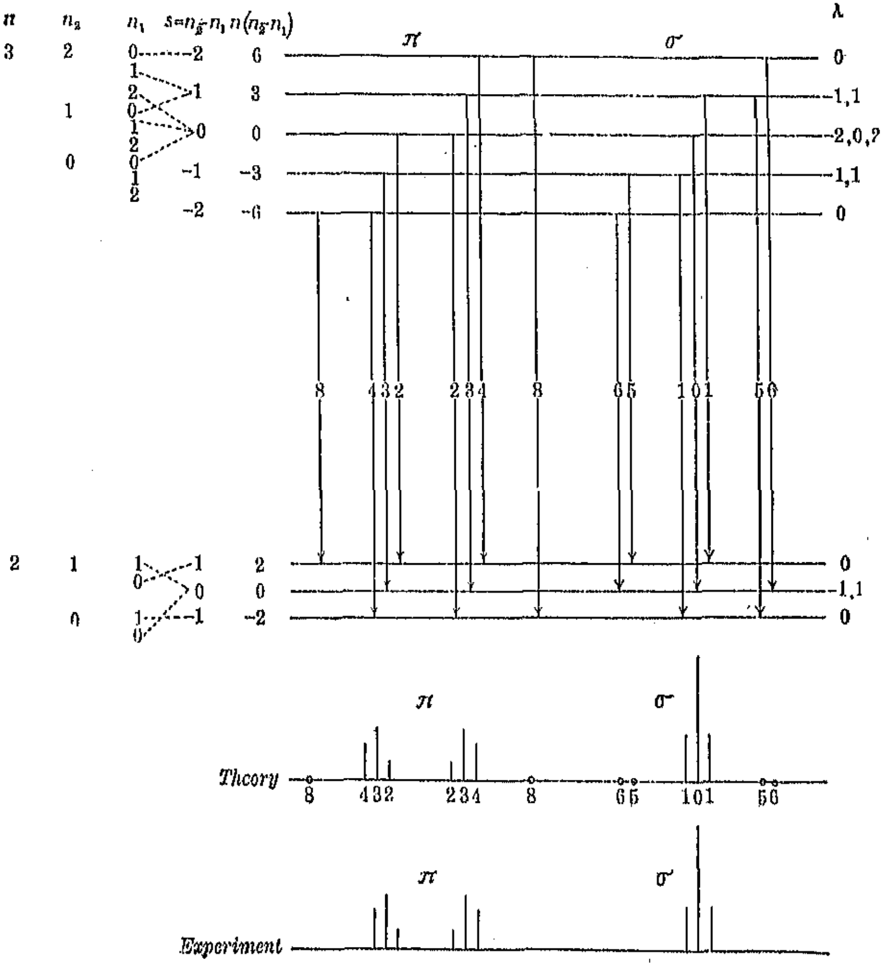

Fig. 86. The transition diagram showing the origin of Stark-effect components for Hα.

values from l, $l-1$, ... to $-l$. λ is therefore the component of the l-quantum number resolved along the electric axis. Since the total quantum number $n=n_1+n_2+\lambda$, we find that n_1 and n_2 should always be less than $n-1$. An application of the Correspondence Principle shows that there would be a selection principle given by $\Delta\lambda = \pm 1, 0$. Thus though λ does not appear in W in equation (50) it controls the transitions and therefore limits the number of components and determines their polarisation. $\Delta\lambda = 0$ gives us spectral lines linearly polarised parallel to the field.

$\Delta\lambda = \pm 1$ gives two lines circularly polarised in the plane normal to the field. The origin of the components calculated according to formula (50), and the selection principle just discussed is shown in the accompanying diagram (Fig. 36).

Explanation of the Diagram.—From formula (50) we see that every level n is decomposed into sub-levels given by all possible values of $n_2 - n_1 = s$, which may be called the *Stark Effect quantum number.* The values of n_2 are given in the second column. Thus for $n=3$ the n_2-values are 2, 1, 0. The values of n_1 for each of the different values of n_2 are 2, 1, 0. The possible values of $n_2 - n_1$ are shown in the fourth column; for any value of $n-1$, they range from $n-1$ to $-(n-1)$. It is seen that any sub-level given by a particular value of $n_2 - n_1 = s$ may arise from different combinations of n_1 and n_2. Thus $s=2$ arises only in one way, $s=1$ in two ways, $s=0$ in three ways and so forth as indicated in the diagram by the dotted lines. The fifth column gives the separations in terms of the unit $3Fh/8\pi^2me$. The figures under λ on the right hand side show the values of λ calculated from the formula $\lambda = n-(n_1+n_2+1)$. It is seen that if a particular sublevel arises in a number of ways, there are an equal number of values of λ, and corresponding to any positive value of λ, there is always a negative value. The transitions for π and σ-components and the separations are shown by the vertical strokes. We find that for every $\Delta\lambda = +m$ there is a transition for which $\Delta\lambda = -m$. Hence when the effect is observed *longitudinally* we get two sets of oppositely polarised waves of the same frequency emitted by a large number of excited atoms, so the resulting radiation appears to be *unpolarised.* This is in contradistinction to the case of Zeeman Effect where the frequencies of the right handed

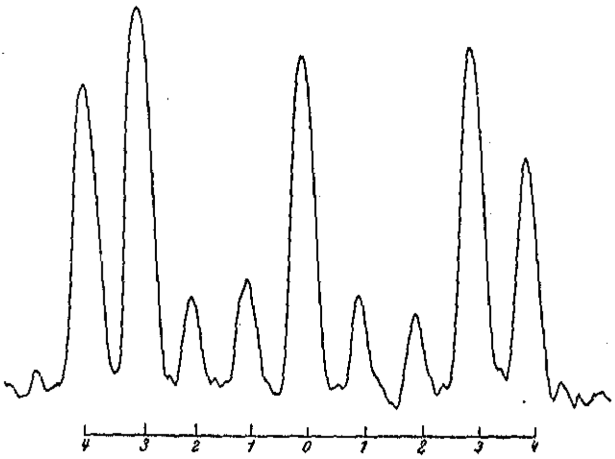

Fig. 37. Microphotogram of Stark effect components of H_α.

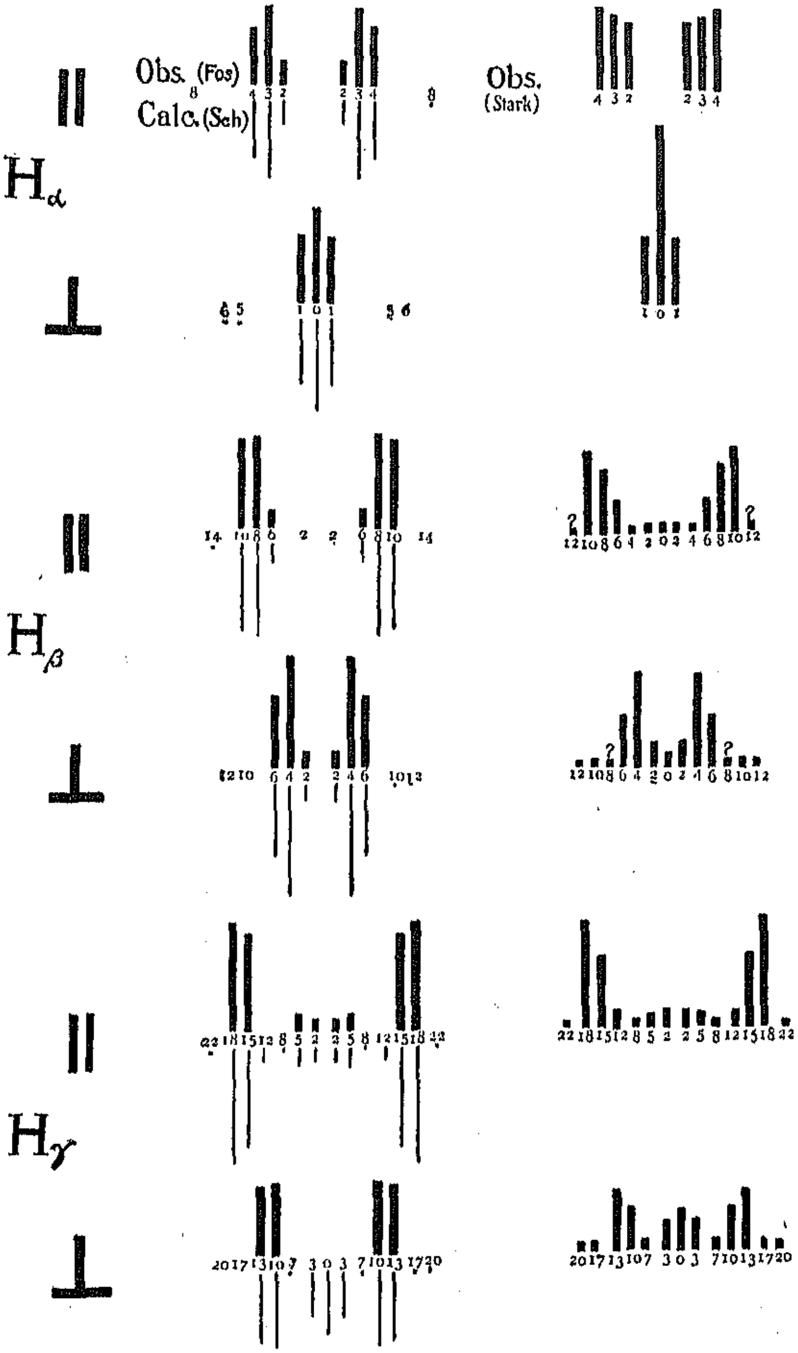

Fig. 88. Calculated and observed intensity-distribution of the Stark effect components of $H\alpha$, $H\beta$, $H\gamma$-lines.

and left handed components are different and therefore they can be distinguished from each other. A microphotograph of the Hα line taken under a field of 250 kv/cm. by Mark and Wierl is shown in Fig. 37.

As far as the Balmer lines are concerned the experimental results were found to be in complete accord with the theory. This is shown in Fig. 38 where the calculated and observed intensities of the components are given. But in the above calculation the relativity effect as well as the spin-interaction energy have been neglected. This is justified because the field used is so great, that the Stark separations are many times larger than the fine-structure separations.

Thus the natural distance between the red and violet components of Hα is ·365 cm^{-1}, while the unit of separation for Stark effect under a field of 10^5 volt/cm is 2·82 cm^{-1}. The extreme separation for the components of Hα may be $16 \times 2{\cdot}82 = 44{\cdot}8$ cm^{-1}. The Stark effect separations are less than natural separation, only for fields of strength 1000 volts/cm or less, but under such low fields the splitting follows more complicated laws (§316).

B. Bohr's Method

We now propose to give an alternative treatment of Stark effect due to Bohr which brings out the physical picture of the process more vividly. Bohr showed that the first-order Stark effect energy may be considered as the energy of a permanent electric dipole in the electric field. Our electrical system in the case of the hydrogen atom consists of a nucleus and the electron. It is clear that as long as the electron revolves in a circle the field energy (the energy of the system on account of its being placed in a uniform field) of the system (electron and proton) will vanish, but this is no longer the case when the orbit is an ellipse. In this case it can be shown that the field energy is $\Delta W = \frac{3}{2} a\varepsilon eF \sin\beta$, where a and ε are respectively the major axis and eccentricity of the orbit and β is the angle between the axis of the field and the axis of the orbit. This can be proved as follows:

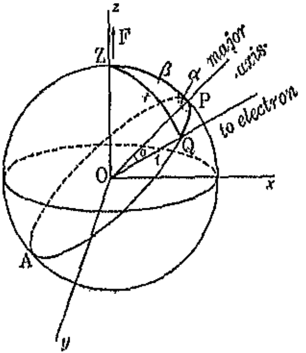

Fig. 39

Let O be the nucleus and OZ be the direction in which the electric field F is applied. With O as centre draw a unit sphere. Let QPA be the section in which the plane of the orbit cuts the unit sphere. The polar coordinates r and θ of the electron in its orbit and the angles χ, β and α are as shown in Fig. 39. Let OP be the line joining the nucleus and the electron whose coordinates at any instant are (x_0, y_0, z_0).

The potential energy of the system when the electron is on the line OQ is given by

$$\psi = Fe\, z_0 = Fe\, r \cos \chi$$

From the spherical $\triangle$ZQP, we have

$$\cos \chi = \cos \theta . \cos \beta + \sin \theta . \sin \beta \cos \alpha$$

Therefore $\quad \psi = Fe\, r\, [\cos \theta . \cos\beta + \sin \theta . \sin\beta \cos\alpha]$

$$= Fe\, [\xi \cos \beta + \eta \sin \beta \cos \alpha]$$

Average potential energy $\overline{\psi}$ of the system is

$$\overline{\psi} = Fe\, [\overline{\xi} \cos \beta + \overline{\eta} \sin \beta \cos \alpha] \quad . \quad . \quad . \quad . \quad . \quad . \quad . \quad (51)$$

where

$$\overline{\xi} = \frac{1}{T}\int_0^T \xi\, dt, \quad \overline{\eta} = \frac{1}{T}\int_0^T \overline{\eta}\, dt . \quad . \quad . \quad . \quad . \quad . \quad . \quad (52)$$

The point $(\overline{\xi}, \overline{\eta})$ in the plane of the orbit is called the *electrical centre.* According to the geometry of the ellipse if $u = \angle$PCN = eccentric anomaly, and mean anomaly $= m = 2\pi t/T$ we have the following relations from Fig. 40.

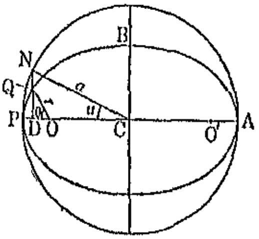

Fig. 40

$$\xi = r \cos\theta = \text{DO}$$

$$= \text{CD} - \text{CO} = a\,(\cos u - \varepsilon),$$

$$\eta = r \sin\theta = \text{QD} = b \sin u,$$

$$m = nt = u - \varepsilon \sin u.$$

where $n = 2\pi/T$, T being the period.

$$\text{Hence } \overline{\xi} = \frac{1}{2\pi}\int_0^{2\pi} a\,(\cos u - \varepsilon)(1 - \varepsilon \cos u)\, du = -\frac{3a\,\varepsilon}{2}$$

$$\overline{\eta} = \frac{1}{2\pi}\int_0^{2\pi} b \sin u\,(1 - \varepsilon \cos u)\, du = 0$$

That $\overline{\eta} = 0$ is otherwise evident from symmetry. Thus the electric centre is a point on the major axis midway between the centre and the empty focus. Hence the average energy due to the field is given by

$$\overline{\psi} = \overline{\xi}\, eF \cos \beta = -\tfrac{3}{2}\, a\varepsilon e\, F \cos \beta \quad . \quad . \quad . \quad . \quad . \quad . \quad (53)$$

In Bohr's perturbation theory, it is shown that the average potential energy of a system subject to any periodic secular perturbation does not vary with time (See Birturistle, *Quantum Theory*, § 133, from which this treatment is adopted). Therefore we get

$$-\tfrac{3}{2}\, a\varepsilon\, \cos\beta = \frac{\bar{\psi}}{eF} = \text{const.} \quad . \quad . \quad . \quad . \quad . \quad . \quad . \qquad (54)$$

The above equation shows that the projection of the electric centre on the OZ-axis is a fixed point, so that the electric centre would move in a plane $z = \frac{3}{2}\, a\varepsilon \cos\beta$ normal to the direction of F. Although $\bar{\psi}$ = const., *i.e.*, $\varepsilon \cos\beta$ is constant, the values of ε and β are not constant. To obtain the final solution, we proceed in the following manner:

We shall find out the frequency of the motion of the electric centre due to the perturbing electric force F and also the geometrical shape of its orbit which will lead us to the solution of the problem.

Let the coordinates of the electric centre be (x, y, z). Then

$$\left(\frac{3a\varepsilon}{2}\right)^2 = x^2 + y^2 + z^2 . \quad . \quad . \quad . \quad . \quad . \quad . \quad . \quad . \qquad (55)$$

The angular momentum of the electron $mr^2\dot{\theta} = mA$

It has been shown on p. 150 that $A = \sqrt{\mu l}$

where μ is the force per unit mass and l = latus rectum $= a\,(1-\varepsilon^2)$.

$$\text{Hence the angular momentum} = m\sqrt{\frac{e^2}{m}\, a\,(1-\varepsilon^2)} \quad . \quad . \quad . \quad . \qquad (56)$$

If λ, μ, ν are the components of the angular momentum

$$\lambda^2 + \mu^2 + \nu^2 = e^2\, ma\,(1-\varepsilon^2) \quad . \quad . \quad . \quad . \quad . \quad . \quad . \qquad (57)$$

Substituting the value of ε^2 from (57) in (55) we get

$$x^2 + y^2 + z^2 = \frac{9a^2}{4}\left\{1 - \frac{\lambda^2 + \mu^2 + \nu^2}{e^2\, ma}\right\}. \quad . \quad . \quad . \quad . \qquad (58)$$

Since the resultant angular momentum is perpendicular to the plane of the orbit, we get

$$x\lambda + y\mu + z\nu = 0 \quad . \quad . \quad . \quad . \quad . \quad . \quad . \quad . \qquad (59)$$

Now, we have $\qquad [\dot{\lambda}, \dot{\mu}, \dot{\nu}] = \dfrac{d}{dt}\,[r.\, mv] = [r.\, F]$

Therefore, $\qquad \dot{\lambda} = eFy_0\, ; \quad \dot{\mu} = -\, eFx_0\, ; \ \dot{\nu} = 0.$

Now let the average values of the differentials of the components of angular momentum be denoted by λ', μ', ν' so that we have

$$\lambda' = eF\bar{y}_e = eFy \ \text{ and } \ \mu' = -eF\bar{x}_e = -eFx. \quad . \quad . \quad . \qquad (60)$$

Differentiating (59) and averaging over λ and μ we get

$$\lambda\dot{x} + \mu\dot{y} = -(x\lambda' + y\mu') = 0. \quad . \quad . \quad . \quad . \quad . \quad . \quad . \quad . \qquad (59')$$

Differentiating (58) and substituting the value of λ', μ' from (60)

$$x\dot{x} + y\dot{y} = -\frac{9aF}{4me}(\lambda y - \mu x) \quad . \quad . \quad . \quad . \quad . \quad . \quad . \qquad (61)$$

Equations (59′) and (61) yield

$$\dot{x} = \frac{9aF}{4me}\mu \text{ and } \dot{y} = -\frac{9aF}{4me}\lambda$$

Therefore, $$\ddot{x} = \frac{9aF}{4me}\mu' \text{ and } \ddot{y} = -\frac{9aF}{4me}\lambda' \quad . \quad . \quad . \quad . \quad . \quad . \qquad (62)$$

Solving the differential equations (62) we get

$$x = A\cos(2\pi\,\omega_F t + \alpha),\ y = B\cos(2\pi\omega_F t + \beta) \quad . \quad . \qquad (63)$$

where $$\omega_F^2 = \frac{9F^2}{16\,\pi^2 m}$$

According to equation (5), p. 324, $a = n^2h^2/4\pi^2e^2m$

Hence $$\omega_F = \frac{3F.\,nh}{8\pi^2 me}$$

It is clear from equation (63) that the path of the electric centre E is an ellipse with its centre on the z-axis as shown in Fig. 41. The period of the secular change introduced by the field F is considerably smaller than the period of motion of the electron in its orbit and therefore Bohr uses his Perturbation theory with complete success for determining the energy change in this doubly periodic system possessing frequencies ω and ω_F.

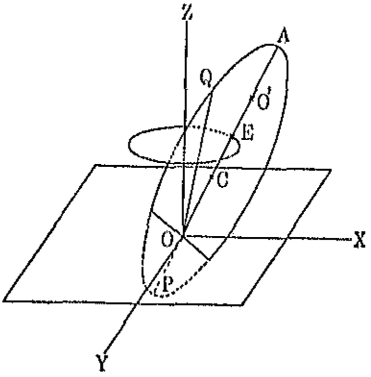

Fig. 41

According to Bohr's theory (*vide* chapter on *Light and Matter*)

$$\triangle W = \omega\,\delta J + \omega_F\,\delta J_F$$

where $$\delta J = nh \text{ and } \delta J_F = n_F\,h.$$

Since $$\omega = \frac{4\pi^2e^4m}{n^3h^3}, \quad \text{we get}$$

$$\triangle W = \frac{4\pi^2e^4m}{n^3h^3}.\,nh + \frac{3\,Fnh\,n_F h.}{8\pi^2 me}$$

$$= \frac{4\pi^2me^4}{n^2h^2} + \frac{3Fh^2}{8\pi^2me}\,n\,n_F$$

Since $n_F/n = \varepsilon \cos \beta$ we see that the maximum value of n_F/n is equal to 1 and this happens when $\varepsilon = 1$, $\beta = 0$, *i.e.*, the orbit is a parabola or a line passing through the nucleus. Such orbits are however not possible, as already discussed in §175. Hence the maximum value of n_F is equal to $n-1$ and on account of $\cos \beta$, it can take all values $0, \pm 1, \pm 2, \ldots, \pm(n-1)$.

316. Further Work on Stark Effect.—STARK EFFECT OF H-LINES FOR WEAK FIELD. The reader might have noticed certain peculiar features in the treatment of Stark Effect of H-lines. As was shown in § 178, any level in the H-atom distinguished by the total quantum number n consists of a number of sub-levels having characteristic values of l and j. In the present treatment no account has been taken of l and j, but new quantum numbers have been introduced whose interpretation is entirely different. The quantum number λ is in fact equal to $l\cos\theta$, and it is therefore equal to the projection of l on the axis of the electric field.

As has been already mentioned the treatment is not justified at field strengths below 5000 volts/cm. This case is, however, only of theoretical interest as the Stark splitting under these circumstances can hardly be observed. Kramers* proceeding from Sommerfeld's theory of fine-structure of H-lines showed that in this case the formula for energy change is given by

$$\triangle E \cong hf.\ \frac{f}{R}.\ \frac{1}{\alpha^2 Z}$$

where $f = 3\,hF/8\pi^2 Zem_0$, the unit splitting in linear Stark Effect, α = fine structure constant. The exact expression is

$$\triangle E = h\left(\frac{3h}{8\pi^2 Zem_0}\right)^2 \lambda$$

A long discussion of the deduction of this formula is to be found in *H. d. Physik*, **23**, §28. The reason for the absence of a term proportional to F is easily explained. When the field is strong, ω_F is much larger than the relativity precession and the electrical centre of gravity lies always on one side of the plane (Fig. 41) through the nucleus and perpendicular to the field. When, however, ω_F is very small compared to relativity precession, the electrical centre is carried by the latter first on one side and then on the other side of the plane so that the first order term is once positive and then negative, and the time average is zero. The Kramers-treatment is, however, only of mathematical interest, as the assumption on which it was based (relativistic interpretation of fine-structure), have been found to be insufficient. Schlapp* and Rojansky† have given treatments of the case from Dirac's relativistic theory of fine structure of H-lines. For this original papers may be consulted.

---

* Kramers, *Zs. f. Phys.*, 3, 199, 1920.

It is found that after the fine-structure limit is passed the splitting is up to certain range proportional to F as discussed in § 314 and § 315. But if the field is further increased the splitting is no longer represented by the formula (50). Takamine and Kokubu‡ showed in their investigation of the Stark effect of the H_γ lines that the central σ-component now becomes unsymmetrical relative to the unshifted line. Sommerfeld§ showed that these results are approximately explained by the second order terms in F derived by Epstein ‖ from the old Quantum Theory. Later a number of workers¶ showed from Wave-Mechanics that the energy W of an atom in an electric field may be expressed by

$$W = W_0 + W_1 F + W_2 F^2 + W_3 F^3 + \ldots\ldots$$

where W_0 represents the energy of the atom in the absence of the field. $W_1 F$ may be called the energy of the first order effect, $W_2 F^2$ of the second order effect and so on. The expression for W_1 has been already given. We have

$$W_2 = -\frac{h^6}{16\,(2\pi)^6 m_0{}^3 e^6 Z^4} \cdot n^4 \{17\, n^2 - 3\,(n_2 - n_1)^2 - 9\,\lambda^2 + 19\}$$

This expression can easily be shown to be equal to

$$W_2 = -\left(\frac{h^2}{4\pi^2 e^2 m_0 Z}\right)^3 \cdot \frac{1}{16} \cdot n^4 \{17\, n^2 - 3\,(n_2 - n_1)^2 - 9\,\lambda^2 + 19\}$$

$$= -(a_0 n^2)^3 \frac{1}{16\,Z} \{17\, n^2 - 3\,(n_2 - n_1)^2 - 9\,\lambda^2 + 19\} \quad . \quad . \quad (64)$$

The second order Stark Effect can be considered as the field energy due to the polarisation of the atom when placed in an electric field. In §273, we mentioned that this energy is $W = -\frac{1}{2}\, a^3\, F^2$. Expression (64) may be considered as the quantum mechanical average value of W_2 for the H-atom.

---

* Schlapp, *Proc. Roy. Soc. A.*, **119**, 313, 1928.

† Rojansky, *Phy. Rev.*, **33**, 1, 1929.

‡ Takamine and N. Kokubu, *Proc. Tokyo-Math. Soc.*, **9**, 394, 105, 1918.

§ Sommerfeld, *Ann. d. Phys.*, **65**, 36, 1921.

‖ Epstein, *Ann. d. Phys.*, **51**, 184, 1916.

¶ G. Wentzel, *Zs. f. Phys.*, **38**, 518, 1926. I. Waller, *Zs. f. Phys.*, **38**, 635, 1926. P. S. Epstein, *Phys. Rev.*, **28**, 695, 1926.

STARK EFFECT FOR NON-HYDROGENIC ATOMS.

It was known from the early experiments of Stark himself that almost all atomic lines show Stark Effect, but generally the splitting varies not as the first power of F but as the second power of F. Foster* showed that in non-hydrogenic atoms, the first order effect begins to become prominent at comparatively large fields. The results, perplexing as they may appear, admit of a simple physical explanation. We have seen that in the case of elements other than hydrogen, the orbits can be broadly divided into two classes (i) penetrating orbits, (ii) non-penetrating orbits. It is clear from §271 that for penetrating orbits the first order Stark Effect would be entirely absent because for the outer part of the orbit the electrical centre is on one side of the nucleus and for the inner part of the orbit it is on the opposite side. The potential energy due to the dipole moment therefore vanishes when time average is taken over the whole orbit. If the field be sufficiently great, the outer part of the orbit may be so distorted that the additional energy may be greater than the energy contributed by the inner orbit. In this case the first order effect would begin to appear even for penetrating orbits. For non-penetrating orbits like $4d$ or $5d$ of helium there should be a first order effect even with comparatively low fields.

Foster† has made very extensive investigations on the Stark Effect of helium lines in a modified Lo Surdo arrangement. His results on the Stark Effect of $^2P-{}^4D$ line is illustrated in Fig. 42, plate X. The reader will mark that the field goes on increasing gradually from 0 at the origin to 45·5 k.volts at the bottom. It is to be observed that at higher fields the separations increase less slowly showing the preponderance of the first order effect. Besides a number of fresh lines appears which are due to forbidden transitions like $^2P-{}^4P$ and $^2P-{}^4F$, $\Delta k=\pm 0, 2$. The selection principle is apparently violated but in reality there is no violation as in strong fields l no longer exists, but we have the quantum number $\lambda=l\cos\theta$ and the selection rules are $\Delta\lambda=\pm 1, 0$. For further information special treatises‡ and original papers on the subject may be consulted.

---

* Foster, *Proc. Roy. Soc. A*, **114**, 47, 1927; **117**, 137, 1928.

† J. S. Foster, *Proc. Roy. Soc. A*, **117**, 137, 1928; **123**, 112, 1929.

‡ See, for example, Smekal, *Quantentheorie* (1933), Kap. 3, pp. 403-428, article by H. Bethe; J. Stark, *H. d. Exp. physik*, **21**, 400, 1927.

Books Recommended

1. J. Franck and P. Jordan, *Anregung von Quantensprüngen durch Stösse*, 1926.

2. P. D. Foote and F. L. Mohler, *The Origin of Spectra*, 1922.

3. K. T. Compton and F. L. Mohler, *Report of the National Research Council on Ionisation Potentials and Related Subjects*, 1924.

4. G. Joos, *H. d. Experimental physik*, **22**, 1929. (*Ergebnisse und Anwendungen der Spektroskopie*).

5. H. D. Smyth, *Reviews of Modern Physics*, **3**, 1931.

6. A. Pannekoek, *H. d. Astrophysik*, **3/1**, Chapter 3.

7. R. H. Fowler, *Statistical Mechanics*, 1925.

8. C. H. Payne, *Stellar Atmosphere*, 1925.

9. Freundlich, *H. d. Physik*, **11**, 1925.

10. A. S. Mitchell, *Solar Eclipses*, 1923.

11. A. S. Eddington, *Internal Constitution of Stars*, 1926.

12. J. H. Jeans, *Astronomy and Cosmogony*, 1929.

13. J. Stark, *Handbuch der Exp. physik*, **21**, 1927.

14. G. Birtwistle, *The Quantum Theory of the Atom*, 1926.

15. Andrade, *The Structure of the Atom*, 3rd ed., 1927.

16. Baly, *Spectroscopy*, **3**, 1929.

17. Minkowski, *Stark effect*, in *H. d. Physik*, **21**, 1929.

18. Pauling and Goudsmit, *The Structure of Line Spectra*, 1930.

19. A. Smekal, *Quanten theorie*, article by Bethe, 1932.

20. For more recent works on Stark Effect see Condon, *Phys. Rev.*, **43**, 648, 1934.

APPENDIX TO CHAPTER XIII.

*Table.—Ionisation Potentials of Elements.**

Element		I	II	III	IV	V	VI
1	H	13·530					
2	He	24·465	54·144				
3	Li	5·364	75·256	121·840			
4	Be	9·276	18·119	153·108	216·628		
5	B	8·245	24·998	37·740	258·028	338·525	
6	C	11·203	24·260	47·637	64·169	390·018	487·550
7	N	14·460	29·443	47·201	77·038	97·397	549·081
8	O	13·549	34·941	54·625	77·026	113·298	137·424
9	F	17·4	34·81	62·35	87·34	156·369	184·261
10	Ne	21·49	40·96	63·2	...	...	...
11	Na	5·113	47·065	71·307	98·409	137·638	171·374
12	Mg	7·608	14·959	79·736	108·774	140·466	185·566
13	Al	5·956	18·733	28·306	119·386	153·109	189·347
14	Si	8·077	16·261	33·329	44·915	165·660	203·835
15	P	11·11	19·78	30·04	42·8	64·7	
16	S	10·31	23·3	34·9 ± ·4	47·08	63	
17	Cl	12·96	23·15	39·7	53·20	67·48	
18	A	15·69	27·72	40·7	...	...	
19	K	4·32	31·68	47	...		
20	Ca	6·09	11·82	51·0	69·9		
21	Sc	6·57	12·84	24·3	...		
22	Ti	6·81	13·60	27·6	43·67		
23	V	6·76	14·1	26·4	48	64	
24	Cr	6·67	16·64	...	50·4	73	
25	Mn	7·40	15·72				
26	Fe	7·82	16·19				
27	Co	8·5	16·9-17·3				
28	Ni	7·606	18·13				
29	Cu	7·69	20·19	29·5 (?)			
30	Zn	9·34	17·89	40 (?)			
31	Ga	5·97	20·43	30·6	63·9		
32	Ge	8·09	15·88	34·07	45·5	90	
33	As	10·5	20·1	28·19	49·9	62·4	
34	Se	9·70	21·59	33·9	42·72	72·80	81·4
35	Br	11·80	22·6	25·7	50·0		
36	Kr	13·94	24·4	31·23			

---

* The values are in volts, calculated on the basis of $R = 13{\cdot}54$ volts.

The values for elements of rare earth and transitional groups are the *principal ionisation potentials, i.e.*, those corresponding to the energy required for the change from the lowest energy state of the atom in one degree of ionisation to the lowest energy state of the next. For other ionisation potentials corresponding to changes between various metastable energy states of the atoms and the ions see § 343, table 44, of Chap. XIV.

Table.—Ionisation Potentials of Elements—(contd).

Element	I	II	III	IV	V	VI
37 Rb	4·16	27·3	...			
38 Sr	5·67	10·98	...			
39 Y	65	12·3	20·6	33·83		
40 Zr	6·92	13·97	24·00	36·1		
41 Cb	...	...	24·2			
42 Mo	7·35					
43 Ma	...					
44 Ru	7·7					
45 Rh	7·7					
46 Pd	8·3	19·8				
47 Ag	7·53	21·9				
48 Cd	8·95	16·84	35			
49 In	5·76	18·79	27·91	40·57		
50 Sn	7·3	14·5	30·5	44·0	58	
51 Sb	8·5	1	24·7	37·71	...	
52 Te	8·96	...	29·5	...	60	72·0
53 I	...	...	...			
54 Xe	12·078	21·1	27·1			
55 Cs	3·88	23·4				
56 Ba	5·18	9·96				
57 La	5·59	11·38	19·10			

Element.	58 Ce	59 Pr	60 Nd	62 Sm	64 Gd	65 Tb	66 Dy	70 Yb
1st I. P.	6·59	5·76	6·31	6·55	6·65	6·74	6·82	7·06

Element.	75 Re	76 Os	79 Au	80 Hg	81 Tl	82 Pb	83 Bi	88 Ra
1st I. P.	7·85	8·7	9·25	10·39	6·47	7·95	8·0	5·176
2nd I. P.				18·67	20·30	15·0		
3rd I. P.					29·7	31·5		

SOURCES :

(1) H—O : B. Edlén, *Zs. f. Phys.*, **84**, 746, 1933. (2) F+ , F++, F^{+3} : I. S. Bowen, *Phys. Rev.*, **45**, 82, 1934. (3) F^{+4}, F^{+5} : B. Edlén, *Zs. f. Phys.*, **89**, 179, 1934. (4) Na—Si : J. Söderqvist, *Nova Acta Reg. Soc. Sc., Upsala*, Sr. IV, **9**, No. 7, 1934. (5) Cl^{+2}, Cl^{+3}, Cl^{+4} : I. S. Bowen, *Phys. Rev.*, **45**, 401, 1934. (6) Rare earths and transitional elements: Rolla and Piccardi, *Phil. Mag.*, 7, 296, 1929. (7) Br^{+3} : A. S. Rao, Krishnamurti, *Proc. Phys. Soc.*, **46**, 531, 1934. (8) Se+ : K. R. Rao and S. G. Krishnamurti (*unpublished*). (9) Cb^{+2}, Cb^{+3} : Gibbs and White, *Phys. Rev.*, **31**, 50, 1928. (10) Os : Albertson ; *Phys. Rev.*, **45**, 304, 1934. (11) Ra : Rasmussen, *Zs. f. Phys.*, **87**, 607, 1934. (12) Ra+ : *ibid*, **86**, 24, 1933.

CHAPTER XIV

COMPLEX SPECTRA

317. Definition of Complex Spectra.—The simple types of spectra have been described in Chapters VIII and IX. The term *complex spectra* denotes those which consist of a large number of lines amongst which it is difficult, at the first sight, to detect any regularity. A typical example of complex spectra is afforded by that of iron shown in Fig. 1, Plate XII, reproduced from the photographs of Fabry and Buisson. It consists at the first sight of an innumerable number of lines crowded in a small space and not affording any guiding features such as groups showing constant frequency differences. As a matter of fact over 6000 lines have been measured between the regions λ 6000 to λ 2000, and with a few exceptions (these belong to Fe^+) most belong to the Fe-atom itself. At first sight, such a complex case seemed to baffle all solutions; but at the present time, thanks to the light thrown by successive advancements in the quantum theory, the origin of majority of the lines is understood.

318. History and Methods of Classification of Lines.—The methods which have been used for the classification of the lines of complex spectra are generalisations of the methods already described. The first requisite for the classification of lines forming complex spectra is a list of lines which should be as complete as possible; such lists are provided partly by Kayser, Runge and Konen's *Handbuch der Spektroskopie*, but in many cases, particularly for the ultraviolet and infrared regions, they have to be supplemented by newer data, which are scattered over numerous journals. Then the wavelengths are reduced to frequencies on the international scale, and the characteristics of each line as far as known are noted. These characteristics include data on intensity, behaviour in flame, in arc and spark, the type of Zeeman splitting, and data on absorption. These are collected and properly utilized. A comparative study of the behaviours of lines in the flame, arc or spark, enable the workers to separate the lines due to the neutral element from those due to the same element ionised to different degrees. Data on Zeeman effect, wherever they could be properly interpreted were found useful for fixing up the type of multiplicity (*vide* §215).

Whenever a certain group of lines could be obtained in absorption, it was almost certain that they arose from fundamental levels.

Earlier workers like Rydberg and Paulson * confined their attention to finding out groups of lines possessing *common frequency differences*. From the analogy of alkali and alkaline earth elements, it was natural to expect that such lines were organically connected. The work of Paschen on the classification of lines of neon was a great landmark in the progress of the subject. The spectrum of neon consists of about 800 lines between λ 10,000 and λ 2,000. Paschen showed that the lines could be arranged into series which he called $s \leftarrow p$ and $p \leftarrow d$ series. He discovered 4*s*-terms, 10*p*-terms and 12*d*-terms, each set being composed of Rydberg sequences up to the 7th or the 8th member. Such a work is almost unparalleled for the brilliancy of its execution, because it was done at a time when most of the principles which lie at the basis of classification of complex spectra were unknown.

319. Catalan's Classification of Manganese Lines.—The work which gave the most powerful stimulus to the classification of lines of complex spectra is due to Catalan on the analysis of the spectrum of manganese.† Catalan showed that in this spectrum, groups of associated lines occur which show the same features as the *pd*-groups of two-valence elements (*vide* p. 383). As explained already, this group is due to the transition between three *p*-terms and three *d*-terms giving rise to 6 lines instead of 9, the remaining 3 being excluded by the selection principle for the inner quantum number. Catalan found that in the case of Mn, there were groups of lines which were evidently connected in a similar manner, but the number in each group was much larger. A typical group of such lines discovered by Catalan is given opposite.

Table A.—Lines in the manganese-multiplet $3d^6\,4s\,{}^6D - 3d^6\,4p\,{}^6D$ (Catalan).

S. No.	Wave-length λ	ν (cm⁻¹)	Intensity.
1	4018·1	24880·3	8
2	4035·7	24771·7	5
3	4041·3	24737·1	10
4	4048·7	24691·9	4
5	4055·5	24650·6	8
6	4058·0	24630·0	2
7	4063·5	24602·2	4
8	4068·0	24575·0	2
9	4070·3	24561·4	2
10	4079·2	24507·4	6
11	4079·4	24506·3	6
12	4082·9	24485·2	6
13	4083·6	24481·0	6

---

* For details see Fowler's *Report on Series Spectra* (1922), p. 10.

† The work was done at the laboratory of Prof. A. Fowler, Imperial College of Science and Technology, London. See M. A. Catalan, *Phil. Trans. A.*, No. 223, 127, 1922.

The wavelengths, frequencies and intensities of the group of lines shown in the above picture are given below.

Catalan showed that the lines can be represented as follows :

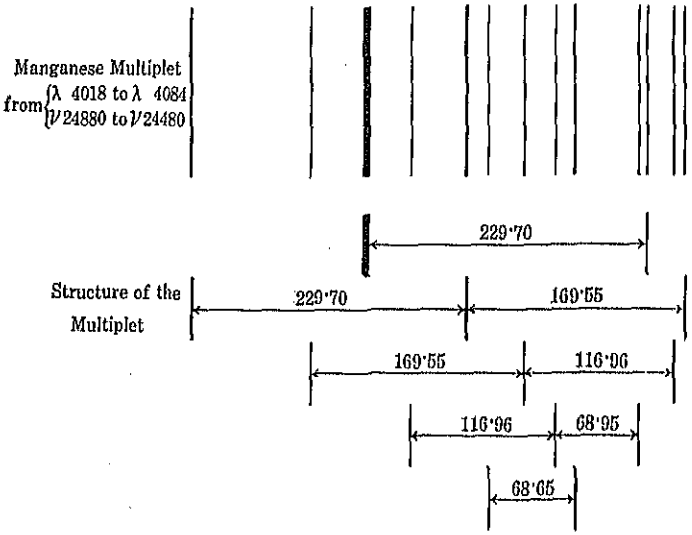

Fig. 2. Catalan's Systematisation of a group of lines in Mn-Spectrum.

It is better to represent this group of lines in a tabular form as shown on the next page. In table 2, three multiplets are given of which the middle one corresponds to the lines shown in Fig. 2.

As is clear from the table, the thirteen lines arise from differences between two groups of term, one group shown on the horizontal row consisting of five terms with the differences 68·6, 117·2, 169·6, 229·9 and the other group consisting of six other terms shown in a vertical column. From Zeeman effect, it was later shown by Back that the five horizontal terms are sextet *d*-terms, with the inner quantum numbers

$\frac{1}{2}, \frac{3}{2}, \frac{5}{2}, \frac{7}{2}, \frac{9}{2} = \mid \frac{5}{2}+2 \mid = \mid s+l \mid$, $s=\frac{5}{2}$ (sextet), $l=2$ (*d*-term).

There are many other similar groups of lines which are due to combination between these five *d*-terms, and other new terms. Two of these are shown, one above, the other below the multiplet treated here. The topmost multiplet is $^6\text{D} - {}^6\text{F}$ the lowest is $^6\text{D} - {}^6\text{P}$.

It was later shown that the three multiplets are due to the transitions

$$3d^6 4s\ {}^6\text{D} - 3d^6 4p\ {}^6\text{FDP}$$

Table 2.—Catalan's Multiplets for Mn

$3d^6 4s$ / $3d^6 4p$	$^6D_{\frac{1}{2}}$	68·6 $D_{\frac{3}{2}}$	117·2 $D_{\frac{5}{2}}$	169·6 $D_{\frac{7}{2}}$	229·9 $D_{\frac{9}{2}}$
$^6F_{\frac{1}{2}}$	4 26035·8	2 26104·7			
28·5 $F_{\frac{3}{2}}$	4 26007·3	6 26075·9	2 26192·9		
48·9 $F_{\frac{5}{2}}$	...	5 26027·00	5 26143·9	2 26319·5	
71·4 $F_{\frac{7}{2}}$	..	...	8 26072·8	6 26242·1	1 26471·8
95·42 $F_{\frac{9}{2}}$	...	...	...	9 26146·6	3 26376·3
115·3 $F_{\frac{11}{2}}$	...	...	...	...	10 2626·0
$D_{\frac{1}{2}}$	6 24561·4	2 24360·1			
55·1 $D_{\frac{3}{2}}$	6 24506·3	2 24575·0	4 24692·0		
89·8 $D_{\frac{5}{2}}$		6 24485·2	4 24602·2	5 24771·7	
121·1 $D_{\frac{7}{2}}$			6 24481·1	8 24650·6	8 24880·3
143·2 $D_{\frac{9}{2}}$				6 24507·4	10 24737·1
$^6P_{\frac{3}{2}}$	4 27622·0	4 27690·7	3 27807·6		
103·1 $P_{\frac{5}{2}}$		4 27587·6	6 27704·6	4 27874·1	
162·2 $P_{\frac{7}{2}}$			3 27542·4	6 27711·9	6 27941·6

The term *multiplet* is given to a group of lines which can be arranged as shown in the above diagram. The number of associated terms may be 3, 4, 5, 6, 7 or even more: terms associated in the above way form a family. The spectrum of manganese was found by Catalan to be resolvable into families of terms, consisting of sextets (families consisting of a maximum of six terms) and quartets, and octets.

320. The Inner Quantum Number.—At this point Sommerfeld* became acquainted with Catalan's work, and with his usual insight recognised in this work the key to the riddle of complex spectra. He had already introduced the azimuthal quantum number k which specified the s, p, d, f-terms. But some of these families of terms may be double as we have seen for alkali elements, or treble as in the case of p, d, f-terms of alkaline earths.

Catalan's work on the Mn-spectrum showed that terms may possess even higher multiplicity, *e.g.*, in the multiplet given on p. 6¯9, the number of d-terms is 5, and the number of f-terms is 6. As more complex spectra began now to be classified, it was found necessary to coin a notation which will correctly represent the characteristics of these terms.

At one time, the following notation was used to denote the characteristics of a term:

n^r_{kj} . . . . here n is the total quantum number, r is the multiplicity ($r=1$ for singlets, 2 for doublets, 3 for triplets), $k=$Sommerfeld azimuthal quantum number, $j=$inner quantum number.

The successive terms of a family were distinguished from each other by putting the inner quantum number, represented by successive integral number, as subscripts to p, d, ... etc. Thus the three p-terms of a triplet spectrum are distinguished from each other as p_0, p_1, p_2.

But these numbers were at first introduced only tentatively, and they have been fixed only after a good deal of trial. All terms of even multiplicity were found to be half-integral, and terms of odd multiplicity to be integral. The model of Catalan's multiplets served as a great stimulus, between 1921-27, for the classification of spectra. All that was needed to be done was to hunt out a number of constant frequency differences, and then classify the lines into multiplets. As a fine example, may be mentioned Laporte's classification of the spectrum of Fe (*Zs. f. Phys.*, **23**, 135, 1924; **26**, 1, 1924).

The significance of the inner quantum number was, however, first made clear from the study of Zeeman effect of lines of alkali and alkaline earth elements. We showed there how it has been proved that j is the vector sum of s and l where l is the reduced azimuthal quantum number, and s is the spin quantum number which has always the value $\frac{1}{2}$ for a single electron.

The mechanical moment of a single electron due to spin$=\frac{1}{2}\,h/2\pi$.

The mechanical moment of a single electron due to orbital motion$=l\,h/2\pi$.

---

* A. Sommerfeld, *Atombau*, 4th. ed., Chap. 8.

Hence the resultant moment $= |l+s|.\ h/2\pi = (l+\frac{1}{2}).\ h/2\pi$ or $(l-\frac{1}{2}).\ h/2\pi$.

But though the angular moment of the atom as a whole is obtained by the simple vectorial addition of l and s, the calculation of magnetic moment, and of the energy present great difficulties. We have already illustrated in §221, how these motions are coupled in the case of a single electron, and how the interaction between the two vectors can be mathematically worked out.

321. Two Electron Problems.—The problem becomes more difficult when two electrons or more are involved, but one such case (alkaline earth elements) has already been worked out in §277.

Let us analyse the work given in §277 more closely. There it was proved that the nature of the spectrum is completely explained if we suppose that the s-vectors of the two electrons are vectorially added to give a resultant S as if the l's are not present, and the l-vectors are vectorially added, as if the s's are not present, to give a resultant L. The resultant S, and L then combine to give the inner quantum number J. Thus for two electrons

$$S = |s_1+s_2| = |\tfrac{1}{2}+\tfrac{1}{2}| = 0, 1 \ldots \text{Singlets, Triplets}$$

$$L = |l_1+l_2| = (l_1+l_2), \ldots\ldots\ldots (l_1-l_2) \text{ or } (l_2-l_1)$$

and $$J = |S+L|$$

Thus for triplet P,

$$J = |1+1| = 0, 1, 2.$$

In table 8 we have indicated the method of adding l-vectors of two electrons occupying different shells. The middle column of the table denotes the vector sum L of l_1 and l_2 for a given value of l_1 when l_2 takes values 0, 1, 2, 3 and 4 successively. The resultant L-values are denoted by the terms S, P, D, ... to which they give rise. Thus from the table it becomes at once evident how we can obtain the quantised vector sum of l, s over several electrons.

Now we can give in a tabular form the addition of s-vectors of two different electrons. Here we have to remember, as mentioned in §218, that in going from one atom to the next having its valency higher by unity, the multiplicity splits up into two values, one being a unit higher, the other a unit lower. This has its explanation in the fact that the spin of the new electron adds itself either parallel or antiparallel to that of the previous other electrons, and the resultant spin of the atom is greater or less by half than that of the previous atom and consequently the multiplicity is greater or less by unity. It is a natural inference from this that all the s's making up S are either parallel or antiparallel to S. Thus the results are as indicated in table 4.

The tables for the resultant j-values obtained on the addition of L and S are given in the chapter on Zeeman Effect.

Table 3.—The vector summation of l_1, l_2 vectors.

l_2	L							l_2
	0	1	2	3	4	5	6	
s 0	S					$\boxed{l_1=0\ldots S}$		0 *s*
p 1		P						1 *p*
d 2			D					2 *d*
f 3				F				3 *f*
g 4					G			4 *g*
s 0		P				$\boxed{l_1=1\ldots P}$		0 *s*
p 1	S	P	D					1 *p*
d 2		P	D	F				2 *d*
f 3			D	F	G			3 *f*
g 4				F	G	H		4 *g*
s 0			D			$\boxed{l_1=2\ldots D}$		0 *s*
p 1		P	D	F				1 *p*
d 2	S	P	D	F	G			2 *d*
f 3		P	D	F	G	H		3 *f*
g 4			D	F	G	H		4 *g*

THE ENERGY RELATIONS FOR TWO ELECTRON-SYSTEMS.

The calculation of the term values in the case of two-valence elements has already been given in §277. But it should be pointed out that the method of calculation used there does not generally apply to all cases. It applies only to the cases where the RS-coupling holds, that is to say, the interaction is such that the coupling between the l and s vectors of individual electrons are broken so that s_1 and s_2 combine to form a resultant S, and l_1 and l_2 combine to form a resultant L, and L and S combine to give J-values equal to $|L+S|$. For this kind of coupling, the Landé interval rule is followed, but there are many two-valence elements and ions for which the rule is not followed, as for example, that of Ba given below :

$$56\ \mathrm{Ba}\ 6s6p\ldots\ {}^1\mathrm{P}_1=23969,\ {}^3\mathrm{P}_0=29763{\cdot}3,\ {}^3\mathrm{P}_1=29392{\cdot}8,\ {}^3\mathrm{P}_2=28514{\cdot}8$$

$$^3\mathrm{P}_0-{}^3\mathrm{P}_1=370{\cdot}5,\ {}^3\mathrm{P}_1-{}^3\mathrm{P}_2=878{\cdot}0$$

Here $^3\mathrm{P}_1-{}^3\mathrm{P}_2 : {}^3\mathrm{P}_0-{}^3\mathrm{P}_1=2{\cdot}37 : 1$ and not $2 : 1$. The deviation from Landé interval rule may be taken to be a measure of the departure of the case from that of ideal RS-coupling.

322. The jj-coupling.—Another kind of coupling is illustrated in the following case. Let us take the elements C, Si, Ge, Sn, Pb. Their normal constitution, as a glance at table 20 on p. 583 shows, is np^2. We do not consider this state for the present. The next state is $np.\ \overline{n+1}\ s$; *i.e.*, in C it is $2p.3s$, in Si $3p.4s$, etc . . . If Russell-Saunders' coupling held in these cases, we should have the following terms:

Table 4.—The vector summation of s_1, s_2-vectors.

S / s_1	0 Singl.	$\frac{1}{2}$ Doubl.	1 Trip.	$\frac{3}{2}$ Quar.	2 Quin.	$\frac{5}{2}$ Sext.	3 Sept.	S / s_1
						$s_2 = 0$		
0	0							0
$\frac{1}{2}$		$\frac{1}{2}$						$\frac{1}{2}$
1			1					1
$\frac{3}{2}$				$\frac{3}{2}$				$\frac{3}{2}$
2					2			2
						$s_2 = \frac{1}{2}$		
0		$\frac{1}{2}$						0
$\frac{1}{2}$	0		1					$\frac{1}{2}$
1		$\frac{1}{2}$		$\frac{3}{2}$				1
$\frac{3}{2}$			1		2			$\frac{3}{2}$
2				$\frac{3}{2}$		$\frac{5}{2}$		2
						$s_2 = \frac{3}{2}$		
0			1					0
$\frac{1}{2}$		$\frac{1}{2}$		$\frac{3}{2}$				$\frac{1}{2}$
1			1		2			1
$\frac{3}{2}$				$\frac{3}{2}$		$\frac{5}{2}$		$\frac{3}{2}$
2					2		3	2

$$S = |\, s_1 + s_2 \,| = |\, \tfrac{1}{2} + \tfrac{1}{2} \,| = 0, 1 \ \ldots \text{ singlets, triplets,}$$
$$L = |\, l_1 + l_2 \,| = |\, 1 + 0 \,| = 1 \ \ldots\ldots \text{ P-terms,}$$
and $$J = |\, S + L \,| = |\, 0 + 1 \,|,\ |\, 1 + 1 \,| \ \ldots\ {}^1\mathrm{P}_1,\ {}^3\mathrm{P}_{0,1,2}.$$

Thus $np.\ \overline{n+1}\ s$ should give us four terms, ${}^1\mathrm{P}_1$ and ${}^3\mathrm{P}_{0,1,2}$.

On analysis of the spectra, four terms were obtained, with the j-values 1, 0, 1, 2, the smallest of which can be regarded as a singlet term, and the other three as triplet terms; but these do not usually satisfy the Landé rule, as table 5 shows.

*Table 5.—Triplet P separations for C, Si, Ge, Sn, Pb.**

Elem.	Config.	${}^3\mathrm{P}_0 - {}^3\mathrm{P}_1$	${}^3\mathrm{P}_1 - {}^3\mathrm{P}_2$	${}^3\mathrm{P}_3 - {}^1\mathrm{P}_1$	$\dfrac{{}^3\mathrm{P}_1 - {}^3\mathrm{P}_2}{{}^3\mathrm{P}_0 - {}^3\mathrm{P}_1}$	Ion	${}^2\mathrm{P}_{\frac{1}{2}} - {}^2\mathrm{P}_{\frac{3}{2}}$
C	$2p\ 3s$	20	40	1100	2	C+	63·8 (1)
Si	$3p\ 4s$	77	194	1037	2·5	Si+	287 (2)
Ge	$4p\ 5s$	250	1415	903	5·6	Ge+	1764 (3)
Sn	$5p\ 6s$	274	3714	628	13·5	Sn+	4253 (4)
Pb	$6p\ 7s$	327	12902	1251	39·4	Pb+	14070 (5)

---

* From *H. d. Astr.*, 3/2, p. 616; and *Atomic Energy States*, Goudsmit and Bacher.

A glance at this table shows that for C, $^3P_1 - {}^3P_2 : {}^3P_0 - {}^3P_1 = 2 : 1$, but for Si and other elements, the relation no longer holds. For Pb, the ratio is 39·4. In fact as the atomic number increases, the four terms split up into two sets: set 1 consisting of $(^3P_{0,1})$, set 2 of $(^3P_2, {}^1P_1)$ and the difference between the two sets approaches the $^2P_{\frac{1}{2}} - {}^2P_{\frac{3}{2}}$ separation of the corresponding ion. Compare columns 4 and 8 of the table. The Zeeman splitting in these cases is *not given by the Landé formula* given in §222.

Let us see how the separations can be calculated. Let us first suppose that the RS-coupling holds. Then we have, since $l_2 = 0$,

$$\triangle W = W(s_1\ s_2) + W(s_1\ l_1) + W\ (s_2\ l_1).$$

$W(s_1 s_2)$ . . . . accounts for the singlet-triplet separation though in an indirect way (*vide* §277). This is now comparatively small, as the total quantum numbers are different. We can neglect $W(s_2\ l_1)$. $W(s_1\ l_1)$ can be calculated exactly in the same way as in §220. We have

$$\triangle \nu = Als\ \cos(l\ s). \quad . \quad . \quad . \quad . \quad . \quad . \quad . \quad . \qquad (4)$$

where $$A = a\left[\frac{s_1}{s}\cos(S\ s_1).\ \frac{l_1}{l}\cos\ (Ll_1)\right] = \frac{1}{2}\,\frac{R\alpha^2}{3n^3}(Z-\sigma)^4$$

and for $^3P_0 \ldots \nu = \nu_0 + 2A$, $^3P_1 \ldots \nu = \nu_0 + A$, $^3P_2 \ldots \nu = \nu_0 - A$.

Table 5 shows that the interval rule is followed only for the C-atom. Even for N^+; $^3P_1 - {}^3P_2 : {}^3P_0 - {}^3P_1 = 84 : 50$, the rule is not followed.

The failure of this relation for large Z shows that $\triangle W$ can no longer be represented by (4), *i.e.*, we can no longer suppose that the coupling between the l_1, s_1-vectors of the inner np-electron is broken by the $\overline{n+1}$ s-electron for heavier elements, *i.e.*, the magnetic field of the external electron is too weak to break the coupling between the ls-vectors of the inner electron. In fact in the case of the heaviest elements (Sn and Pb) we may suppose that the inner electron retains the coupling between its l and s-vectors.

The situation may be symbolically expressed as follows:

$$\triangle W = \{(s_1 l_1)(s_2 l_2)\} = (j_1)(s_2 l_2) = j_1 s_2 \ldots \text{since } l_2 = 0 \quad . \quad . \ (5)$$

This denotes that the coupling between s_1 and l_1 persists. The Russell-Saunders-coupling is represented in the same notations as follows:

$$\triangle W = \{(s_1 l_1)\ (s_2 l_2)\} = (s_1 s_2)\ (l_1 l_2) = (S)\ (L) = J \quad . \quad . \quad . \quad (5')$$

What will now be the nature of terms due to the coupling scheme in (5)? We illustrate it with the case of $np\ n+1.\ s$-states. The starting point is the singly ionised atom having the states ${}^2P_{\frac{1}{2}}$, ${}^2P_{\frac{3}{2}}$ of Pb^+. The coupling is shown in Fig. 3.

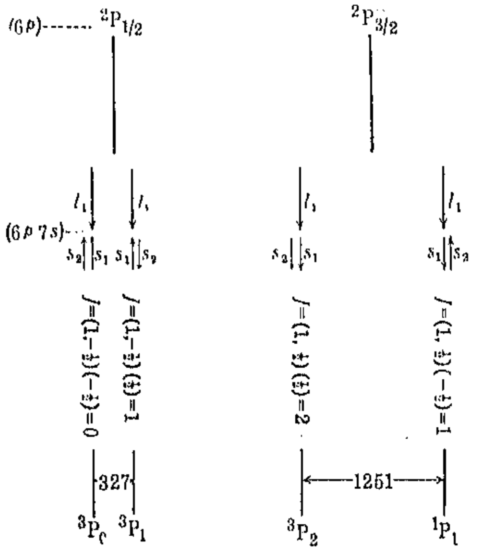

Fig. 3. jj-Coupling Scheme for $np\ (n+1).\ s$ configuration.

Thus when the Pb^+-ion is in the ${}^2P_{\frac{1}{2}}$-state, and a $7s$-electron is brought, the inner quantum number* $j = |j_1 + s_2| = |\frac{1}{2}+\frac{1}{2}|=0$ and 1, we get two terms with $j=0$, $j=1$, $T_0 > T_1$. But when the Pb^+-ion is in the ${}^2P_{\frac{3}{2}}$-state, and a $7s$-electron is brought to it, the inner quantum number of the term$=|\frac{3}{2}+\frac{1}{2}|=2, 1$. The two groups of terms have roughly the distance ${}^2P_{\frac{1}{2}} - {}^2P_{\frac{3}{2}}$ of the corresponding ion.

323. Zeeman-Effect for jj-Coupling.

—In §222, we have given a deduction of the Landé $g(j)$-factor from the hypothesis of rotating electrons for states of any multiplicity. In this deduction the assumption was made, though it was not explicitly stated there, that the coupling was of the RS-type, *i.e.*, the spins of the component electrons can be supposed to combine into a resultant S, and the l-vectors into a resultant L-vector. In cases where the RS-coupling does not hold, the Landé formula for Zeeman separation fails to hold.

Even before the present ideas took a finite shape, it was known that in many cases, the Zeeman separations did not follow any well-defined scheme as we obtained in the case of two-valence elements. The best known examples were obtained in the case of neon from

---

* Both J and j have been used throughout without distinction for the resultant inner quantum number.

Table 6. Calculated and observed Landé factor on RS, and (jj)-couplings.

Term	g-values on RS-Scheme	g-values observed			g-values on (JJ)-Scheme
		Ne	Sn	Pb	
$^3P_1$	1·50	1·50	1·500	1·501	1·50
$^3P_1$	1·50	1·46	1·375	1·35	1·33
$^1P_2$	1·00	1·03	1·125	1·150	1·17

the works of Paschen[*] and Back.[†] We do not give an account of these works here, as the spectrum of neon will be explained later. But Landé recognised that in these, we had to deal with a class of spectra which stood outside his scheme, and he called this "Second Stage Spectra." This is identical with the spectra resulting out of *jj*-type of coupling, which we are now discussing.

The abnormal values of the Landé factor in such cases is illustrated in table 6.

Let us now see how we can obtain an expression for the $g(j)$-factor in an ideal *jj*-type of coupling, involving only two electrons, as for example, in the $np. \overline{n+1}$ s-combination just treated. In such cases, the j-vectors of the electrons combine to form a resultant J, and when a magnetic field is imposed, the J-axis will precess about the axis of the external field. The component j's will individually precess about the resultant J. The total effect is therefore obtained by adding up the effects due to each electron and then averaging suitably.

Following this idea, the value of $g(J)$ can be at once put down as follows:

$$\begin{aligned} Jg(J) = \{&l_1 \cos(l_1\, J) + 2\, s_1 \cos(s_1\, J)\} \\ &+ \{l_2 \cos(l_2\, J) + 2\, s_2 \cos(s_2\, J)\}\ . \qquad . \qquad . \quad (6) \end{aligned}$$

[*vide* eqn. (52), p. 425]. But we have

$$\cos(l_1\, J) = \cos(l_1\, j_1)\cos(j_1\, J),\quad \cos(l_2\, J) = \cos(l_2\, j_2)\cos(j_2\, J).$$

Hence we have

$$\begin{aligned} J\,g(J) = &j_1 \cos(j_1\, J)\left\{\frac{l_1 \cos(l_1\, j_1) + 2\, s_1 \cos(s_1\, j_1)}{j_1}\right\} \\ &+ j_2 \cos(j_2\, J)\left\{\frac{l_2 \cos(l_2\, j_2) + 2 s_2 \cos(s_2\, j_2)}{j_2}\right\} \end{aligned}$$

---

[*] F. Paschen, *Ann. d. Phys.*, 60, 405, 1919; 63, 201, 1920.

[†] E. Back, *ibid.*, 76, 317, 1925.

Now we have $g(j_1) = \dfrac{[l_1 \cos(l_1\, j_1) + 2\, s_1 \cos(s_1\, j_1)]}{j_1}$

and a similar expression for $g(j_2)$.

Therefore, $$J\, g(J) = j_1\, g(j_1) \cos(j_1\, J) + j_2\, g(j_2) \cos(j_2\, J)\,. \quad . \quad (6a)$$

or $$g(J) = g(j_1)\frac{j_1^{\,2} + J^2 - j_2^{\,2}}{2J^2} + g(j_2)\frac{j_2^{\,2} + J^2 - j_1^{\,2}}{2\,J^2} \quad . \quad . \,(6b)$$

or $$g(J) = g(j_1)\frac{j_1\,(j_1+1) + J\,(J+1) - j_2\,(j_2+1)}{2\,J\,(J+1)}$$

$$+\, g\,(j_2)\frac{j_2\,(j_2+1) + J\,(J+1) - j_1\,(j_1+1)}{2\,J\,(J+1)} \quad . \quad . \,(7)$$

Equation (7) represents Landé g-formula for two-electron system on (jj)-coupling scheme.* Here $g(j_1)$ and $g(j_2)$ are the g-factors for the first and the second electron alone and can be calculated from equation (54), Chap. X.

Let us now apply this formula to the case of terms arising out of $np\ \overline{n+1}\,.\,s$-combination. We calculate the g (s) according to (7). These are given in the last column of table 6.

(a) $np\ {}^2\mathrm{P}_{\frac{3}{2}}\,.\,\overline{n+1}\ s$

Here $$g\,(j_1) = 4/3,\ g\,(j_2) = 2,\ J = 2.$$

$$g\,(J) = \frac{4}{3}\ \frac{\frac{3}{2}\,.\,\frac{5}{2} + 2.3 - \frac{1}{2}\,.\,\frac{3}{2}}{2.2.3} + 2.\ \frac{\frac{1}{2}\,.\,\frac{3}{2} + 2.3 - \frac{3}{2}\,.\,\frac{5}{2}}{2.2.3.} = 1 + \tfrac{1}{2} = 1{\cdot}50.$$

(b) $np\ {}^2\mathrm{P}_{\frac{3}{2}}\ \overline{n+1}.\ s\ .\ .\ .\ .\ .\ J = 1.$

Now $$g(J) = \frac{4}{3}\ \frac{\frac{3}{2}\,.\,\frac{5}{2} + 1.2 - \frac{1}{2}\,.\,\frac{3}{2}}{2.1.2} + 2.\ \frac{\frac{1}{2}\,.\,\frac{3}{2} + 1.2 - \frac{3}{2}\,.\,\frac{5}{2}}{2.1.2} = \tfrac{5}{3} - \tfrac{1}{2} = 1{\cdot}166.$$

(c) $np\ {}^2\mathrm{P}_{\frac{1}{2}}\ \overline{n+1}.\ s\ .\ .\ .\ .\ J = 1.$

Here $$g\,(j_1) = \tfrac{2}{3},\ g\,(j_2) = 2.$$

$$g(J) = \frac{2}{3}\,.\,\frac{\frac{1}{2}\,.\,\frac{3}{2} + 1.2 - \frac{1}{2}\,.\,\frac{3}{2}}{2.1.2} + 2.\ \frac{\frac{1}{2}\,.\,\frac{3}{2} + 1.2 - \frac{1}{2}\,.\,\frac{3}{2}}{2.1.2} = \tfrac{1}{3} + 1 = 1{\cdot}33.$$

A glance at table 6 shows that the coupling of $6p.\ 7s$ in Pb is completely of the jj-type. For Sn, the conversion to the jj-type is not complete.

For further illustration we take the g-values of a pd-configuration for an ideal jj-coupling. The J-values of the resultant terms as given by the RS-coupling, and the jj-coupling may be contrasted.

---

* This deduction was first given by Goudsmit and Uhlenbeck, *Zs. f. Phys.*, 35, 618, 1925.

For the RS-coupling

$$S = \left| \tfrac{1}{2} + \tfrac{1}{2} \right| = 0, 1 \quad . \quad . \quad . \quad \text{singlets, triplets.}$$
$$L = \left| 1 + 2 \right| = 3, 2, 1 \quad . \quad . \quad \text{F, D, P-terms.}$$

Hence we obtain

$$(pd) = \left. \begin{array}{lll} {}^3\mathrm{F}_{2,3,4} & {}^3\mathrm{D}_{1,2,3} & {}^3\mathrm{P}_{0,1,2} \\ {}^1\mathrm{F}_3 & {}^1\mathrm{D}_2 & {}^1\mathrm{P}_1 \end{array} \right\}$$

i.e., altogether 12 terms, of which one term has $j=4$, three have $j = 3$, four have $j = 2$, three have $j = 1$ and one has $j = 0$.

In the *jj*-coupling, we have the terms shown in the Scheme I below:

Scheme I.

$\mathrm{P}_{\frac{1}{2}}\ \mathrm{D}_{\frac{3}{2}}$	$j = 1, 2$
$\mathrm{P}_{\frac{1}{2}}\ \mathrm{D}_{\frac{5}{2}}$	$j = 2, 3$
$\mathrm{P}_{\frac{3}{2}}\ \mathrm{D}_{\frac{3}{2}}$	$j = 0,1,2,3$
$\mathrm{P}_{\frac{3}{2}}\ \mathrm{D}_{\frac{5}{2}}$	$j = 1,2,3,4$

Thus we get 12-terms with the same distribution of inner quantum numbers amongst the terms.

The $g(J)$-values of terms for an RS-coupling can be easily calculated from Landé formula. For the *jj*-coupling we can carry out the calculations by using formula (7). These are shown in table 6.

Table 7.—Landé g-values for a p d-combination.

Russell-Saunders' Coupling

J	4	3	2	1	0	
^{3}F	$\frac{5}{4}$	$\frac{13}{12}$	$\frac{2}{3}$			
^{3}D		$\frac{4}{3}$	$\frac{7}{6}$	$\frac{1}{2}$		
^{3}P			$\frac{3}{2}$	$\frac{3}{2}$	$\frac{0}{0}$	
^{1}F		1				
^{1}D			1			
^{1}P				1		
Σg	$\frac{5}{4}$	$\frac{41}{12}$	$\frac{13}{3}$	3	$\frac{0}{0}$	

(*JJ*)-Coupling.

J / j_1	4	3	2	1	0	J / j_2
$\frac{3}{2}$	$\frac{5}{4}$	$\frac{223}{180}$	$\frac{109}{90}$	$\frac{11}{10}$	...	$\frac{5}{2}$
$\frac{3}{2}$	...	$\frac{16}{15}$	$\frac{16}{15}$	$\frac{16}{15}$	$\frac{0}{0}$	$\frac{3}{2}$
$\frac{1}{2}$	...	$\frac{10}{9}$	$\frac{58}{45}$	...	...	$\frac{5}{2}$
$\frac{1}{2}$	...	...	$\frac{23}{30}$	$\frac{5}{6}$	...	$\frac{3}{2}$
Σg	$\frac{5}{4}$	$\frac{41}{12}$	$\frac{13}{3}$	3	$\frac{0}{0}$	

324. The g-sum Rule and g-Permanence Rule.—

(A)*g*-Sum Rule.:* From the above table we easily perceive the truth of a

---

*For an account of the subjects treated in §§324, 330, 331, 332, 332a, 333, see Pauling and Goudsmit, *The Structure of Line Spectra*, Chaps. VII and IX; *Handbuch der Astrophysik*, III/2, Chap. 6.

well-known rule known as *g*-sum rule which is often employed in the interpretation of spectra This runs as follows :

For the different terms which arise out of a given electron configuration, the sum of the *g*-values for those terms which have the same j is independent of the coupling scheme as well as of the field strength. From Table 7 we only see that the sum rule is independent of the coupling scheme. For illustration, we observe from the table that the sum of *g*-values for $j=3$ for $^3F_3$, $^3D_3$, $^1F_3$-terms on Russell-Saunders' scheme of coupling is $4\frac{1}{4}$ and the sum of *g*-values for the terms with $j=3$ arising out of *jj*-coupling is the same, *viz.*, $4\frac{1}{4}$. This is true for other j-values as well.

Table 8.—m and g-values for a pd-combination.

d \ p	m_{s_1}	$\frac{1}{2}$	$\frac{1}{2}$	$\frac{1}{2}$	$-\frac{1}{2}$	$-\frac{1}{2}$	$-\frac{1}{2}$
	m_{l_1}	1	0	-1	1	0	-1
m_{s_2}	m_{l_2}						
$\frac{1}{2}$	2	4 $\frac{5}{4}$	3 $\frac{4}{3}$	2 $\frac{3}{2}$	3 1	2 1	1 1
$\frac{1}{2}$	1	3 $\frac{4}{3}$	2 $\frac{3}{2}$	1 2	2 1	1 1	0 ...
$\frac{1}{2}$	0	2 $\frac{3}{2}$	1 2	0 ...	1 1	0 ...	-1 1
$\frac{1}{2}$	-1	1 2	0 ...	-1 0	0 ...	-1 1	-2 1
$\frac{1}{2}$	-2	0 ...	-1 0	-2 $\frac{1}{2}$	-1 1	-2 1	-3 1
$-\frac{1}{2}$	2	3 1	2 1	1 1	2 $\frac{1}{2}$	1 0	0 ...
$-\frac{1}{2}$	1	2 1	1 1	0 ...	1 0	0 ...	-1 2
$-\frac{1}{2}$	0	1 1	0 ...	-1 1	0 ...	-1 2	-2 $\frac{3}{2}$
$-\frac{1}{2}$	-1	0 ...	-1 1	-2 1	-1 2	-2 $\frac{3}{2}$	-3 $\frac{4}{3}$
$-\frac{1}{2}$	-2	-1 1	-2 1	-3 1	-2 $\frac{3}{2}$	-3 $\frac{4}{3}$	-4 $\frac{5}{4}$

Before showing that the sum rule holds good whether we employ a weak or a strong field, we shall give a formula for calculating the *g*-values for very strong fields where the coupling between the l and s vectors is broken. The *g*-formula for weak fields is given by equation (54), §222. In order to calculate *g*-values for strong fields, we should remember that the Landé *g*-factor can be defined as the ratio of the magnetic to the mechanical moment when the two moments are expressed in units of the Bohr magneton and $h/2\pi$ respectively (see Chap. XVI). In a strong field j ceases to exist and the ratio is taken between the components of moments parallel to the field. Thus for a single electron.

$$g_{\text{strong}} = \frac{m_l + 2\,m_s}{m} = \frac{m_l + 2m_s}{m_l + m_s} = 1 + \frac{m_s}{m} = 2 - \frac{m_l}{} \qquad (8)$$

Table 9.—Illustration of the g-sum rule for a p-d combination.

$m =$	4	3	2	1	0	-1	-2	-3	-4	
	$\frac{5}{4}$	$\frac{4}{3}$ 1 $\frac{4}{3}$ 1	$\frac{3}{2}$ 1 $\frac{3}{2}$ 1 $\frac{3}{2}$ 1 $\frac{1}{2}$ 1	1 2 1 2 1 2 1 0 1 0 1	... ...	1 0 1 0 1 2 1 2 1 2 1	1 $\frac{1}{2}$ 1 $\frac{3}{2}$ 1 $\frac{3}{2}$ 1 $\frac{3}{2}$	1 $\frac{4}{3}$ 1 $\frac{4}{3}$	$\frac{5}{4}$	STRONG FIELD
Σg	$\frac{5}{4}$	$\frac{14}{3}$	9	12	(12)	12	9	$\frac{14}{3}$	$\frac{5}{4}$	
$^3F_4$	$\frac{5}{4}$	$\frac{5}{4}$	$\frac{5}{4}$	$\frac{5}{4}$	$\frac{5}{4}$	$\frac{5}{4}$	$\frac{5}{4}$	$\frac{5}{4}$	$\frac{5}{4}$	WEAK FIELD
$^3F_3$		$\frac{13}{12}$	$\frac{13}{12}$	$\frac{13}{12}$	$\frac{13}{12}$	$\frac{13}{12}$	$\frac{13}{12}$	$\frac{13}{12}$		
$^3D_3$		$\frac{4}{3}$	$\frac{4}{3}$	$\frac{4}{3}$	$\frac{4}{3}$	$\frac{4}{3}$	$\frac{4}{3}$	$\frac{4}{3}$		
$^1F_3$		1	1	1	1	1	1	1		
$^3F_2$			$\frac{2}{3}$	$\frac{2}{3}$	$\frac{2}{3}$	$\frac{2}{3}$	$\frac{2}{3}$			
$^3D_2$			$\frac{7}{6}$	$\frac{7}{6}$	$\frac{7}{6}$	$\frac{7}{6}$	$\frac{7}{6}$			
$^3P_2$			$\frac{3}{2}$	$\frac{3}{2}$	$\frac{3}{2}$	$\frac{3}{2}$	$\frac{3}{2}$			
$^1D_2$			1	1	1	1	1			
$^3D_1$				$\frac{1}{2}$	$\frac{1}{2}$	$\frac{1}{2}$				
$^3P_1$				$\frac{3}{2}$	$\frac{3}{2}$	$\frac{3}{2}$				
$^1P_1$				1	1	1				
$^3P_0$					$\frac{0}{0}$					

In the case of several electrons possessing their individual values of m_l and m_s which differ, Pauli puts down the value of g_{strong} as follows:

$$g_{\text{strong}} = \frac{\Sigma\,(m_{li} + 2\,m_{si})}{\Sigma\,(m_{li} + m_{si})} \quad . \quad . \quad . \quad . \quad . \quad . \quad . \quad . \quad . \quad . \quad (9)$$

In Table 8 we arrange m_s and m_l values for p-electrons in the uppermost row and for d-electrons in the first column, side by side. Since six and ten electrons are required to fill the p and the d-shells respectively, we get 6 columns and 10 rows in which the corresponding m and g-values are shown as calculated from equation (9).

With the help of Table 8, we arrange in a column all the g-values arising out of this pd-configuration for a given m-value, as shown in the upper portion of Table 9.

In the lower part of the table, the g-values for a weak field are arranged. It is easy to see that the sum of the g-values for a particular

m-value is the same whether we consider them for strong or weak field.

(B) *g*-PERMANENCE RULE.

Pauli gave another similar rule known as the *g-permanence* rule which though not of very great importance may however be used in the interpretation of spectra. It may be stated as follows:

In a multiplet level characterised by definite l and s values, the sum of all the g-values for those magnetic levels which have the same m-values (but may belong to different levels) is independent of the field strength. For a weak field where j exists, we have to take the sum of g-values for magnetic levels having the same m-value but belonging to different terms. In a strong field where j no longer exists, we have to take the sum over different sets of m_s or m_l values corresponding to a particular m-value. The two sums are equal.

Symbolically we write

$$\sum_{m_s \text{ or } m_l} g_{\text{strong}} = \sum_{j} g_{\text{weak}} . \quad . \quad . \quad . \quad . \qquad (10)$$

for given m, l and s.

The g_{strong} values for a given multiplet are calculated from equation (9). In Table 9a the g-values for strong and weak fields for a triplet D-multiplet are shown.

Table 9a.—Illustration of the g-permanence rule for ^3D.

m-values	3	2	1	0	-1	-2	-3	
$j=3$	$\frac{4}{3}$	$\frac{4}{3}$	$\frac{4}{3}$	$\frac{4}{3}$	$\frac{4}{3}$	$\frac{4}{3}$	$\frac{4}{3}$	WEAK FIELD
$j=2$		$\frac{7}{6}$	$\frac{7}{6}$	$\frac{7}{6}$	$\frac{7}{6}$	$\frac{7}{6}$		
$j=1$			$\frac{1}{2}$	$\frac{1}{2}$	$\frac{1}{2}$			
Σg	$\frac{4}{3}$	$\frac{5}{2}$	3	(3)	3	$\frac{5}{2}$	$\frac{4}{3}$	
$m_s=1$	$\frac{4}{3}$	$\frac{3}{2}$	2	. . .	0	. . .	. . .	STRONG FIELD
$m_s=0$		1	1	. . .	1	1		
$m_s=-1$			0	. . .	2	$\frac{3}{2}$	$\frac{4}{3}$	

The exactness of Pauli's rule is evident from the Table 9a. With the help of the g-permanence rule we can obtain an expression for the Landé g-factor in its exact form without the use of quantum-mechanics. This fact leads us to the conclusion that g-permanence rule is a fundamental principle, quite in accordance with the new Quantum Mechanics.

325. Calculation of Optical Levels due to any Electron-Composition.—With the aid of the principles sketched in the foregoing sections, we shall now describe how the optical levels due to any electron composition can be calculated.* For the sake of simplicity, we shall suppose that the Russell-Saunders' coupling holds. This class comprises by far the majority of spectra so far classified, though in many important cases, other types of coupling hold good. RS-coupling is chosen because the mathematical working is here the simplest. As the s-vectors of the individual electrons combine to form a resultant S, and the l-vectors form a resultant L, the problem is simplified almost to the case of a single electron possessing the spin-value S, and the orbital momentum value L. The interaction energy may be calculated by applying methods which are generalisations of the method described in §277.

As a general rule the normal electron structure of the atom or the ion should be first written out. Thus taking the elements carbon to neon, we find that their normal and excited electron-structures can be written as follows:

$$[1s^2\ 2s^2]\ 2p^x, \ldots\ 2p^{x-1}\ 3s, \ldots\ 2p^{x-1}\ 3p, \ldots\ 2p^{x-1}\ 3d$$

where $x = 1, 2, 3, 4, 5, 6$ for C^+, C, N, O, F, Ne respectively. The first denotes the normal structure, and the others are excited configurations.

We have therefore first to find out optical terms arising out of the combination $2p^x$ where x varies from 1 to 6. These will give us the normal states for elements from C to Ne as well as for ions belonging to a similar group. The excited states are obtained by successively increasing the quantum numbers of one of the electrons, leaving the others in their original positions.

The cases due to the combinations $2s.\,np$, $2p.\,ns$ have already been worked out. We now consider the next combinations.

THE $2p\ np$-COMBINATION.

We have $S = \left| \frac{1}{2} + \frac{1}{2} \right| = 0, 1 \ldots$ singlets, triplets

$L = | 1 + 1 | = 2, 1, 0$ D, P, S-terms.

The j-values can be found in the usual manner, so that the terms are:

---

* The sequence of multiplets expected in the spectra of various elements was first given by F. Hund, *Zs. f. Phys.*, **33**, 345, 1925.

$$(2p\,np) = \left\{ \begin{matrix} {}^3D_{1,\,2,\,3} & {}^3P_{0,\,1,\,2} & {}^3S_1 \\ {}^1D_2 & {}^1P_1 & {}^1S_0 \end{matrix} \right\}$$

Total number of magnetic levels possessed by these terms are:

$$\left. \begin{matrix} 3+5+7 & + & 1+3+5 & + & 3 \\ 5 & + & 3 & + & 1 \end{matrix} \right\} = 36$$

Since an electron in a p-orbit possesses 6 magnetic levels and there are two such electrons, the total number of magnetic levels would be $6 \times 6 = 36$.

Proceeding as before the terms due to $2p\,nd$ combination are

$$\left. \begin{matrix} {}^3F_{2,\,3,\,4} & {}^3D_{1,\,2,\,3} & {}^3P_{0,\,1,\,2} \\ {}^1F_3 & {}^1D_2 & {}^1P_1 \end{matrix} \right\}$$

The actual numbers of magnetic levels are:

$$\left. \begin{matrix} 5+7+9 & & 3+5+7 & & 1+3+5 \\ 7 & + & 5 & + & 3 \end{matrix} \right\} = 60$$

Since an electron in a d-orbit can have 10 magnetic levels and an electron in a p-orbit can have 6 magnetic levels, the predicted number of magnetic levels would be $10 \times 6 = 60$ which is verified. For illustrating the principles just described, we take the case of doubly ionised oxygen* having the constitution $1s^2\,2s^2\,2p^2$. Its term-values are shown in Table 10.

326. Equivalent Electrons.—We shall now take up the case of equivalent electrons, *i.e.*, electrons placed in the same s, p or d-orbit. In such cases some of the states obtained in the usual manner are ruled out, for they correspond to an atom having two or more electrons with all their quantum numbers identical which means violation of Pauli's Principle. The problem has been already introduced by taking the case of two equivalent s-electrons, where an application of Pauli's Principle showed that ns^2 should give us only an ${}^1S_0$-term and no ${}^3S_1$-term. Let us now calculate the terms due to np^2. For this purpose, it is more convenient to use magnetic quantum numbers for strong fields, *i.e.*, m_s, m_l in place of j and s.

This is justified in most cases, because as the electrons are in the same level, they strongly influence each other and the coupling between the l and s-vectors of individual electrons is broken as happens when a strong magnetic field is introduced (Paschen-Back

---

* A. Fowler, *Proc. Roy. Soc. A*, **117**, 317, 1928.

Table 10.—Normal and excited terms of O^{++}-ion.

Term	Term-value (ν in cm^{-1})	$\Delta\nu$	Term	Term-value (ν in cm^{-1})	$\Delta\nu$
$2p^2 \ldots \, ^3P_0$	444661	*116*	$2p\,3d \ldots \, ^1F_3$	120132·09	
$^3P_1$	444545	*103*	$^3F_2$	120131·04	*195·79*
$^3P_2$	444352		$^3F_3$	119935·25	*178·16*
$^1D_2$	424385		$^3F_4$	119757 09	
$^1S_0$	401472		$^1P_1$	119859·28	
$2p\,3s \ldots \, ^3P_0$	177336·21	*118·36*	$^3D_1$	117365·56	*49·24*
$^3P_1$	177217 85	*256·94*	$^3D_2$	117316·32	*73·72*
$^3P_2$	176960 91		$^3D_3$	117242·60	
$^1P_1$	171513·43		$^3P_0$	115125·52	*—114·00*
$2p\,3p \ldots \, ^1D_2$	153636·88		$^3P_1$	115011·52	*— 61·45*
$^3D_1$	150728 24	*136·34*	$^3P_2$	114950 07	
$^3D_2$	150591·90	*220 05*	$^1D_2$	111816·4	
$^3D_3$	150371·85				
$^3S_1$	147036·00				
$^1S_0$	146278·09				
$^3P_0$	144365·29	*82·10*			
$^3P_1$	144283·19	*130·54*			
$^3P_2$	144152·65				
$^1P_1$	130792·43				

effect). So we are justified in using magnetic quantum numbers for strong fields, for representing magnetic levels.

Pauli's Principle requires that the terms arising out of the np^2-combination should be such that their total number of magnetic levels should not be $6\times6=36$, but ${}^6C_2=15$. So a few of the terms obtained from a $np \, . \, mp$ combination (see Table 10) have to be ruled out.

Table 11.

	a	*b*	*c*	*d*	*e*	*f*
m_s	$\frac{1}{2}$	$\frac{1}{2}$	$\frac{1}{2}$	$-\frac{1}{2}$	$-\frac{1}{2}$	$-\frac{1}{2}$
m_l	1	0	-1	1	0	-1

Let us see how this can be done. For a single p-electron, the pairs of (m_s, m_l) values are six in number as shown in Table 11.

Here the state a denotes one with $m_s = \frac{1}{2}$, $m_l = 1$, b with $m = \frac{1}{2}$, $m_l = 0$, . . . and so on.

The 15 combinations which are to be chosen so that the Pauli Principle is obeyed are shown in

Table 12.

	ab	*ac*	*ad*	*ae*	*af*	*bc*	*bd*	*be*	*bf*	*cd*	*ce*	*cf*	*de*	*df*	*ef*
M_S'	1	1	0	0	0	1	0	0	0	0	0	0	-1	-1	-1
M_L	1	0	2	1	0	-1	1	0	-1	0	-1	-2	1	0	-1
M	2	1	2	1	0	0	1	0	-1	0	-1	-2	0	-1	-2
Γ	$\frac{1}{4}a$	0	0	$\frac{1}{4}a$	$\frac{1}{4}a$	$-\frac{1}{2}a$	$-\frac{1}{4}a$	0	$\frac{1}{4}a$	$-\frac{1}{2}a$	$-\frac{1}{2}a$	0	$-\frac{1}{2}a$	0	$\frac{1}{4}a$

Table 12. Our next task is to choose pairs of M_S M_L-values in such a way, that we can at once read out the resultant terms from them. We observe that the highest M_L is 2, coupled with $M_S = 0$ (*ad*). This must be a magnetic level of ${}^1D_2$-term. Then we have the next highest $M_L = 1$ with $M_S = 1$ (*ab*). This should represent the magnetic level of a ${}^3P_2$-term, and ${}^3P_1$, ${}^3P_0$-terms come by association. We thus obtain the following regrouping of (M_S, M_L)-values :

$$(2, 0 \quad 1, 0 \quad 0, 0 \quad -1, 0 \quad -2, 0) \ldots {}^1D_2$$

$$\left(\begin{array}{lll} 1, +1 & 0, +1 & -1, +1 \\ 1, 0 & 0, 0 & -1, 0 \\ 1, -1 & 0, -1 & -1, -1 \end{array}\right) \ldots {}^3P_{0,\,1,\,2}$$

$$(0, 0) \ldots {}^1S_0$$

There is a certain amount of uncertainty in this selection, *e.g.*, the pair (0, 0) rises from the three combinations *af*, *be*, *cd* and it is not clear to which of these ${}^1S_0$-term corresponds. Disregarding this uncertainty, we obtain the following :

$$np^2 \ldots {}^3P_{0,\,1,\,2}\,, \quad {}^1D_2, \quad {}^1S_0$$

Experience has shown that the terms with the highest multiplicity and larger l-vector have the largest value. Thus ${}^3P_{0,\,1,\,2} > {}^1D_2 > {}^1S_0$. A theoretical explanation of this fact is given later.

THE np^3-COMBINATION.

The optical terms arising out of np^3-configuration should possess, according to Pauli's Principle, ${}^6C_3 = 20$ magnetic levels. Hund was the first to show that the levels which satisfy these criteria are

$$np^3 \ldots {}^4S_{\frac{3}{2}}, \quad {}^2D_{\frac{3}{2},\,\frac{5}{2}}, \; {}^2P_{\frac{1}{2},\,\frac{3}{2}}$$

The origin of these terms is illustrated in Table 13. We do not show all the combinations, but only those giving terms with the highest j. The other combinations may be written and verified easily.

Table 13.

Electron \ m_l, m_s	(1)	(2)	(3)	Σ	Term	Number of magnetic levels
(*abc*) m_s	$\frac{1}{2}$	$\frac{1}{2}$	$\frac{1}{2}$	$\frac{3}{2}$	$^4S_{\frac{3}{2}}$	4
m_l	1	0	-1	0		
(*abd*) m_s	$\frac{1}{2}$	$\frac{1}{2}$	$-\frac{1}{2}$	$\frac{1}{2}$	$^2D_{\frac{5}{2},\frac{3}{2}}$	10
m_l	1	0	1	2		
(*abe*) m_s	$\frac{1}{2}$	$\frac{1}{2}$	$-\frac{1}{2}$	$\frac{1}{2}$	$^2P_{\frac{3}{2},\frac{1}{2}}$	6
m_l	1	0	0	1		
						Total 20 levels

THE np^4-COMBINATION.

The optical terms arising out of the np^4-combination should possess $^6C_4=15$ magnetic levels like np^2 and calculation in accordance with Pauli's Principle shows that in this case we get the same terms as in the case of the np^2-shell. This is partly a consequence of the theorem that $^nC_r = {}^nC_{n-r}$. Thus the terms due to this combination are

$$np^4 \ \ldots \ ^3P_{2,1,0}, \quad ^1D_2, \quad ^1S_0$$

Inverted Terms.—There is, however, one important difference between the terms of np^4 and np^2 in spite of their similarity. The ^3P-terms in np^4 are *inverted*, *i.e.*, $^3P_2 > {}^3P_1 > {}^3P_0$.

In the cases so far studied, we have always found that of a set of associated terms, those with smaller values of j have higher numerical values than those with larger values of j. Thus in the spectra of alkaline earth elements,

$$^3P_0 > {}^3P_1 > {}^3P_2 \,;\ {}^3D_1 > {}^3D_2 > {}^3D_3.$$

But now we shall come across cases in which the reverse law holds. Such terms are known as *inverted* (*verkehrte*) terms. We shall find examples of inverted terms later on.

THE np^5-COMBINATION.

The optical terms of the np^5-combination will be identical with the optical levels of the np-configuration, because $^6C_5={}^6C_1=6$. Here also the terms are inverted, *i.e.*, $^3P_{\frac{3}{2}} > {}^2P_{\frac{1}{2}}$. Generally when the number of electrons is larger than half that are required to fill the given shell, the terms become inverted. A proof of this will be given later.

THE np^6-COMBINATION.

The case of the np^6-combination is identical with that of ns^2-combination because both of them represent a completed subgroup. As a general rule, it must be remembered that in such a saturated shell, for every electron with a given m_s and m_l-values, there is always another electron with m_s and m_l values of opposite sign. Further since the number of electrons required to fill a subshell is always even, $\Sigma m_s = 0$ and $\Sigma m_l = 0$, the resultant state is always $^1S_0$, *i.e.*, it is non-magnetic. It is as a result of this important property that in determining the optical terms of a particular configuration, the completed shells or subshells are altogether neglected.

Table 14.—Equivalent p-electrons.

Configuration	Terms					
p		^{2}P				
p^2	^{1}S		^{1}D		^{3}P	
p^3		^{2}P		^{2}D		^{4}S
p^4	^{1}S		^{1}D		^{3}P	
p^5		^{2}P				
p^6	^{1}S					

We have thus traced all the optical terms due to np^x-combination. The optical terms due to nd^x and nf^x combinations can also be obtained by the methods already employed in the foregoing pages. In Tables 14, 15, and 16, terms arising from np^x, nd^x, nf^x configurations are given.*

Table 15.—Equivalent d-electrons.

Configuration	Terms					
d^1	^{2}(D)					
d^2	^{1}(SDG)	^{3}(PF)				
d^3	^{2}(D)	^{2}(PDFGH)	^{4}(PF)			
d^4	^{1}(SDG)	^{3}(PF)	^{1}(SDFGI)	^{3}(PDFGH)	^{5}(D)	
d^5	^{2}(D)	^{2}(PDFGH)	^{4}(PF)	^{2}(SDFGI)	^{4}(DG)	^{6}(S)
d^6	^{1}(SDG)	^{3}(PF)	^{1}(SDFGI)	^{3}(PDFGH)	^{5}(D)	
d^7	^{2}(D)	^{2}(PDFGH)	^{4}(PF)			
d^8	^{1}(SDG)	^{3}(PF)				
d^9	^{2}(D)					
d^{10}	^{1}S					

Table 16.—Equivalent f-electrons.

Config.	Terms				
f^1	^{2}(F)				
f^2	^{1}(SDGI)	^{3}(PFH)			
f^3	^{2}(PDFGHIKL)	^{4}(SDFGI)			
f^4	^{1}(SDFGHIKLN)	^{3}(PDFGHIKLM)	^{5}(SDFGI)		
f^5	^{2}(PDFGHIKLMNO)	^{4}(SPDFGHIKLM)	^{6}(PFH)		
f^6	^{1}(SPDFGHIKLMNQ)	^{3}(PDFGHIKLMNO)	^{5}(SPDFGHIKL)	^{7}(F)	
f^7	^{2}(SPDFGHIKLMNOQ)	^{4}(SPDFGHIKLMN)	^{6}(PDFGHI)		^{8}(S)
f^8	^{1}(SPDFGHIKLMNQ)	^{3}(PDFGHIKLMNO)	^{5}(SPDFGHIKL)	^{7}(F)	
f^9	^{2}(PDFGHIKLMNO)	^{4}(SPDFGHIKLM)	^{6}(PFH)		
f^{10}	^{1}(SDFGHIKLN)	^{3}(PDFGHIKLM)	^{5}(SDFGI)		
f^{11}	^{2}(PDFGHIKL)	^{4}(SDFGI)			
f^{12}	^{1}(SDGI)	^{3}(PFH)			
f^{13}	^{2}(F)				
f^{14}	^{1}(S)				

---

* These tables have been adopted from those given by R. C. Gibbs, D. T. Wilber, H. E. White, *Phys. Rev.*, 29, 790, 1927.

327. Slater's Diagrammatic Method.—Slater* has illustrated the above results by a graphical method which we now proceed to explain. In this, the m_s-values in units of $\frac{1}{2}$ are plotted along the abscissa, the m_l-values in units of 1 are plotted along the ordinate. A point (m_s, m_l) in the configuration space denotes a particular magnetic state. The magnetic states for singlet, doublet and triplet terms are illustrated in the following diagrams:

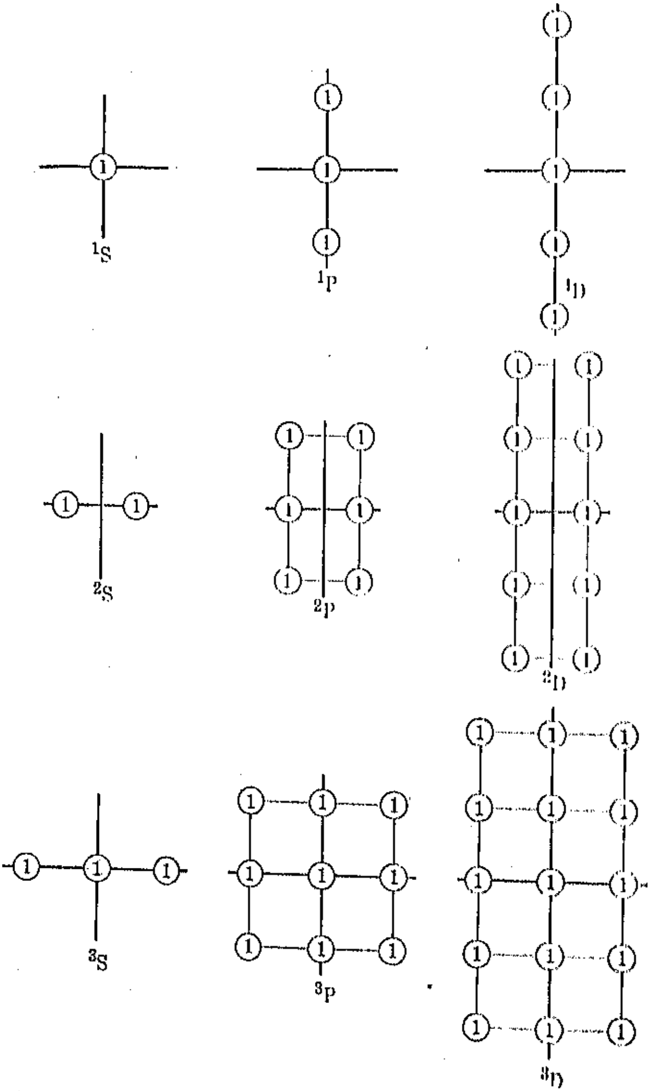

Fig. 4. Slater's representation of the magnetic states for ^{123}(SPD)-terms.

---

*J. C. Slater, *Phys. Rev.*, 34, 1293, 1929.

The magnetic states due to a single electron are represented by the doublet levels. When we want to calculate the terms due to any combination of electrons in any two states we have to take one magnetic level from each electron and find out Σm_s, Σm_l and plot them in the configuration space. Let us, for example, combine two s-levels in this way, the magnetic states for the two electrons are as shown in Table 17.

Table 17.

First s-level			Second s-level		
	a_1	b_1		a_2	b_2
m_s	$\frac{1}{2}$	$-\frac{1}{2}$	m_s	$\frac{1}{2}$	$-\frac{1}{2}$
m_l	0	0	m_l	0	0

The combinations are

$a_1\,a_2$,	$a_1\,b_2$	$b_1\,a_2$	$b_1\,b_2$
(1, 0)	(0, 0)	(0, 0)	(−1, 0)

Graphically the results can be represented as follows :—

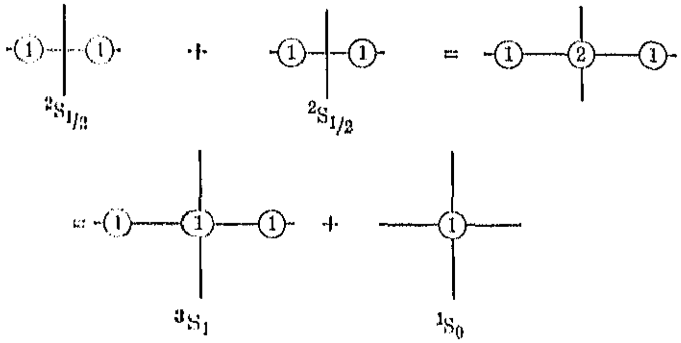

Fig. 5. Slater's diagram for ss-combination.

The magnetic state (0, 0) occurs in the two combinations $a_1\,b_2$ and $b_1\,a_2$. This is indicated by placing the number 2 inside the circle corresponding to the point (0, 0). Other figures within small circles similarly denote the number of times the particular point (M_s, M_l) occurs in the combination. It is easily seen that the resultant figure is resolvable into two figures, one corresponding to $^3S_1$-term and the other corresponding to $^1S_0$-term. If we take two equivalent s-electrons, the only possible combination is ab(0, 0) which occurs only once and gives $^1S_0$-alone as a consequence of Pauli's Principle as mentioned in §282.

We may now take an sp-combination. The magnetic levels can be represented as follows :

$a_1(\frac{1}{2}, 0)$ $b_1(-\frac{1}{2}, 0)$ for s-electron.

$a_2(\frac{1}{2}, 1)$, $b_2(\frac{1}{2}, 0)$, $c_2(\frac{1}{2}, -1)$, $d_2(-\frac{1}{2}, 1)$, $e_2(-\frac{1}{2}, 0)$, $f_2(-\frac{1}{2}, -1)$ for p-electrons.

The combinations are:

$a_1\,a_2$	$a_1\,b_2$	$a_1\,c_2$	$a_1\,d_2$	$a_1\,e_2$	$a_1\,f_2$
(1, 1)	(1, 0)	(1, −1)	(0, 1)	(0, 0)	(0, −1)
$b_1\,a_2$	$b_1\,b_2$	$b_1\,c_2$	$b_1\,d_2$	$b_1 e_2$	$b_1\,f_2$
(0, 1)	(0, 0)	(0, −1)	(−1, 1)	(−1, 0)	(−1, −1)

To indicate the results we have the following figures (Fig. 6).

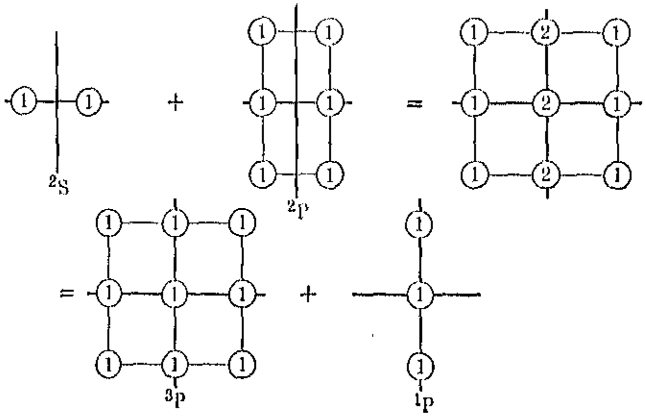

Fig. 6. Slater's diagram for *sp*-combination.

We see that the resultant figure is due to the superposition of ^{3}P and ^{1}P-states.

When we consider the case of two non-equivalent *p*-electrons we get 36 combinations which can be plotted in the configuration space as shown in Fig. 7. The magnetic state (0, 0) occurs six times and (1, 0) thrice; for others this can be easily verified by actually writing down all possible Σm_s and Σm_l values for various combinations. The figure is clearly a superposition of figures due to ^{3}D, ^{3}P, ^{3}S, ^{1}D, ^{1}P, ^{1}S-terms.

When there are two equivalent *p*-electrons the six magnetic states $a\ (\frac{1}{2},1)$, $b\ (\frac{1}{2},0)$, $c\ (\frac{1}{2},-1)$, $d\ (-\frac{1}{2},1)$, $e\ (-\frac{1}{2},0)$, and $f\ (-\frac{1}{2},-1)$ can be combined in fifteen possible ways as mentioned in §326. From Table 12 it is seen that the state (0, 0) occurs thrice, (0, 1) and (0, −1) occur twice each, and rest of the states occur only once. A Slater-diagram of all these combinations can be drawn as in Fig. 8.

Thus Pauli's Principle when applied to the 2 equivalent *p*-electrons, excludes ^{3}D, ^{3}S, ^{1}P-terms, which appear when two *p*-levels of non-equivalent electrons are vectorially added. One can clearly see this by comparing figures 7 and 8. From the principles mentioned in this section

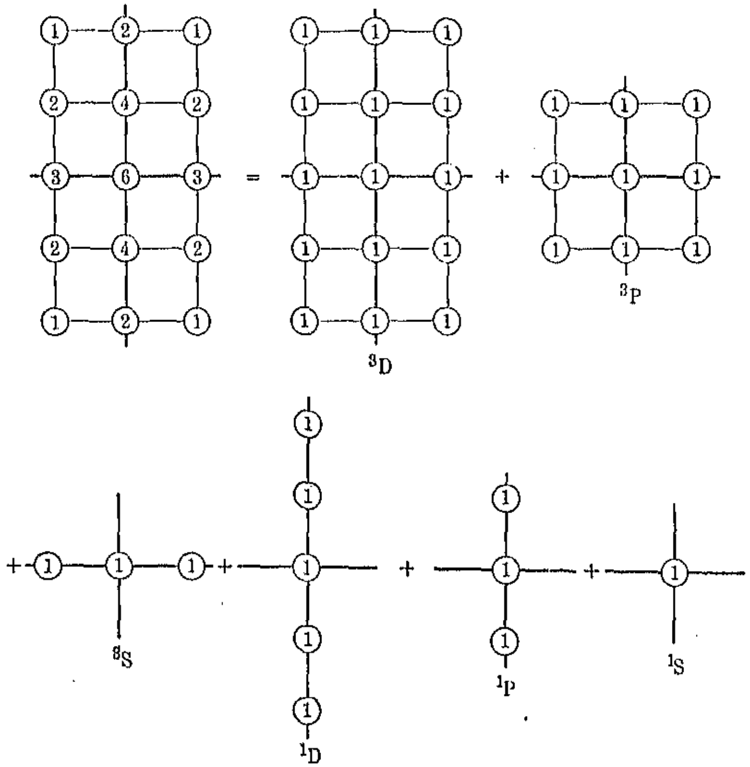

Fig. 7. Slater's diagram for two non-equivalent p-electrons.

Slater-diagram of any combination can be drawn and the terms arising therefrom can be obtained. Further, in the case of equivalent electrons $\Sigma\, m_s$ and $\Sigma\, m_l$ plotted in accordance with Pauli's Principle always lead to the correct terms. In this connection the interesting point to note is that

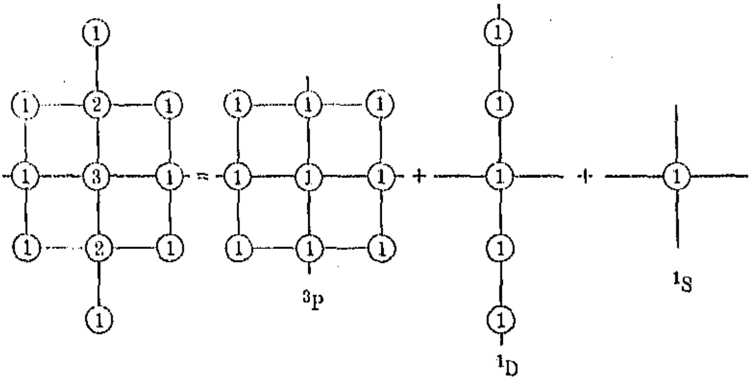

Fig. 8. Slater's diagram for two equivalent p-electron-combination.

it is the symmetrical nature of these diagrams which makes them a very handy method of calculating optical terms for various configurations.

328. Calculation of Terms of Highest and Lowest Multiplicity with Largest l-Values.—The calculation of terms for any electron configuration was first given by Hund* and Slater† who also laid down empirically certain general rules for the comparative values of the terms. These rules are:

(i) Of the terms arising from a given electron structure, the terms possessing the highest multiplicity are numerically the largest.

(ii) Of the terms belonging to the same multiplicity, those possessing the highest l are numerically the largest.

(iii) Terms arising out of a p^x, d^x, or f^x combination are regular if $x<(2l+1)$ and inverted when $x>(2l+1)$. For $x=2l+1$, we get an S-term.

For example we obtain in

$$d^2 \ldots\ldots {}^3F \; {}^3P \; {}^1G \; {}^1D \; {}^1S.$$

According to the above rules

$$ {}^3F > {}^3P > {}^1G > {}^1D > {}^1S \text{; and } {}^3F_2 > {}^3F_3 > {}^3F_4.$$

But, if we take

$$d^8 \ldots\ldots {}^3F \; {}^3P \; {}^1G \; {}^1D \; {}^1S$$

we have $\quad {}^3F > {}^3P > {}^1G > {}^1D > {}^1S.$

But $\quad {}^3F_2 < {}^3F_3 < {}^3F_4.$

These rules were subsequently deduced from theoretical considerations (*vide infra*).

We shall now give a simple method of writing down the highest terms and the terms with lowest multiplicity and highest l-value resulting from any equivalent electron structure.

Let us suppose that there are x-electrons in a given shell such that $x<(2l+1)$. Now the m_l and m_s values of these electrons can be arranged in the following manner:

m_l -values	m_s -values	
(1) $l,\ l-1, \ldots\ldots\ l-\nu+1, \ldots\ldots -l+1, -l.$	$\frac{1}{2}$	$-\frac{1}{2}$
(2) $l,\ l-1, \ldots\ldots\ l-\nu+1, \ldots\ldots -l+1, -l$	$\frac{1}{2}$	$-\frac{1}{2}$
(3) $l,\ l-1, \ldots\ldots\ l-\nu+1, \ldots\ldots -l+1, -l$	$\frac{1}{2}$	$-\frac{1}{2}$
. . . .	.	.
. . . .	.	.
. . . .	.	.
. . . .	.	.
. . . .	.	.
. . . .	.	.
(x) $l,\ l-1, \ldots\ldots\ l-\nu+1, \ldots\ldots -l+1, -l.$	$\frac{1}{2}$	$-\frac{1}{2}$

---

* F. Hund, *Zs. f. Phys.*, 33, 345, 1925.

† J. C. Slater, *Phys. Rev.*, 28, 291, 1926; 34, 1293, 1929.

Evidently, the highest m_s-value will be obtained for the zth electron when all $+\frac{1}{2}$ values are added together, *i.e.*, $\frac{1}{2}z$ will be the maximum m_s-value for resulting terms. In order to get the highest m_l-value for these z-electrons without violating Pauli's Principle we have to take the sum of all the m_l-values beginning from the top left-hand corner of the above arrangement. Thus, for the highest term:

$$\Sigma m_s = z/2 \text{ and } \Sigma m_l = \sum_{\nu=1}^{\nu=z} (l-\nu+1) = (l+1)\,z - \frac{z(z+1)}{2} \quad \ldots\ldots \quad (11)$$

The rule for obtaining the lowest multiplicity term with the highest l-value would be to take m_s-values alternately $+\frac{1}{2}$ and $-\frac{1}{2}$. Thus m_s-values would be alternately 0 and $\frac{1}{2}$ according as z is even or odd. The maximum m_l-values would be given by following equations:

$$\left.\begin{aligned} &\Sigma m_l = lz - \frac{z}{2}\,(z/2-1)\ \ldots\ z \text{ even} \\ \text{and}\quad &\Sigma m_l = lz - \left(\frac{z-1}{2}\right)^2 \ \ldots\ldots\ z \text{ odd} \end{aligned}\right\} \quad \ldots\ldots \quad (12)$$

In the following table we give the highest and lowest multiplicity terms with the largest l-value for p, d and f equivalent electron configurations.

Table 18.

Term	p-shell			d-shell					f-shell						
	1	2	3	1	2	3	4	5	1	2	3	4	5	6	7
Max. Multiplicity	${}^2P$	${}^3P$	${}^4S$	${}^2D$	${}^3F$	${}^4F$	${}^5D$	${}^6S$	${}^2F$	${}^3H$	${}^4I$	${}^5I$	${}^6H$	${}^7F$	${}^8S$
Min. Multiplicity	${}^2P$	${}^1D$	${}^2D$	${}^2D$	${}^1G$	${}^2H$	${}^1I$	${}^2I$	${}^2F$	${}^1I$	${}^2L$	${}^1N$	${}^2O$	${}^1Q$	${}^2Q$

Without the use of the above formulae we may obtain the highest terms by a scheme which is exactly equivalent to the process involved in their derivation. It runs as follows:

Write down against the m_l-values successively $l, l-1, \ldots\ldots$, and for the m_s-values $+\frac{1}{2}$ as far as consistent with Pauli's Principle. Then obtain Σm_s and Σm_l. For d and f electrons the formation of highest terms is illustrated in the Tables 19 and 19*a*. To obtain the highest term corresponding to any particular number of equivalent electrons, start from left and add up all the m_s-values in the successive vertical columns to the right until the column corresponding to the particular value of z is reached. The result is Σm_s. Similarly, find Σm_l. The Σm_s and Σm_l-values give respectively the s and l values for the highest term corresponding to this configuration. Thus for d^3, $\Sigma m_s = \frac{3}{2}$, $\Sigma m_l = 3$, which give ^{4}F as the highest term.

Table 19.—The highest term for d^x-configuration.

$x \rightarrow$	1	2	3	4	5	6	7	8	9	10
m_s =	$\frac{1}{2}$	$\frac{1}{2}$	$\frac{1}{2}$	$\frac{1}{2}$	$\frac{1}{2}$	$-\frac{1}{2}$	$-\frac{1}{2}$	$-\frac{1}{2}$	$-\frac{1}{2}$	$-\frac{1}{2}$
m_l =	2	1	0	-1	-2	2	1	0	-1	-2
	^{2}D	^{3}F	^{4}F	^{5}D	^{6}S	^{5}D	^{4}F	^{3}F	^{2}D	$^1S_0$

Table 19a.—The highest term for f^x-configuration.

$x \rightarrow$	1	2	3	4	5	6	7	8	9	10	11	12	13	14
m_s=	$\frac{1}{2}$	$\frac{1}{2}$	$\frac{1}{2}$	$\frac{1}{2}$	$\frac{1}{2}$	$\frac{1}{2}$	$\frac{1}{2}$	$-\frac{1}{2}$	$-\frac{1}{2}$	$-\frac{1}{2}$	$-\frac{1}{2}$	$-\frac{1}{2}$	$-\frac{1}{2}$	$-\frac{1}{2}$
m_l=	3	2	1	0	-1	-2	-3	3	2	1	0	-1	-2	-3
	^{2}F	^{3}H	^{4}I	^{5}I	^{6}H	^{7}F	^{8}S	^{7}F	^{6}H	^{5}I	^{4}I	^{3}H	^{2}F	$^1S_0$

Similarly, to obtain the terms for f^4, we start from the left and add m_l-values till we reach the vertical column with the number 4. We obtain $\Sigma m_s = 2$, $\Sigma m_l = 6$. Hence f^4 has ^{5}I as the highest term. When $x = 2l+1$, $\Sigma m_l = 0$, and we get S-term; when $x > (2l+1)$, we have to put $m_s = -\frac{1}{2}$, and the terms reverse.

329. Equivalent Electrons in *jj*-Coupling.—We shall now show that even when the extreme type of non RS-coupling, *i.e.*, the *jj*-coupling holds, we obtain from any electron-configuration the same number of terms as in RS-coupling with the same distribution of inner quantum number amongst them. We illustrate it with respect to the np^2-combination. We can no longer use the strong field magnetic quantum numbers m_s, m_l but should use j and m. The six-states of a p-electron are now given by

$$\begin{array}{rcccccc} & \multicolumn{2}{c}{\overbrace{\hspace{3em}}^{j=\frac{1}{2}}} & \multicolumn{4}{c}{\overbrace{\hspace{14em}}^{j=\frac{3}{2}}} \\ & a & b & c & d & e & f \\ m = & \frac{1}{2} & -\frac{1}{2} & \frac{3}{2} & \frac{1}{2} & -\frac{1}{2} & -\frac{3}{2} \end{array}$$

We may now apply Pauli's Principle in the following way:

(1) $j_1 = \frac{1}{2}, j_2 = \frac{1}{2}$; in such a case, since both j's are the same, we must have the m's different. Hence the only possible combination is

$$ab \;\ldots\; M = 0 \;\ldots\; \text{we have a term } X_0.$$

(2) $j_1 = \frac{1}{2}, j_2 = \frac{3}{2}$; in this case, since the j's are different, the m's can have any value. The combinations are

$$\left.\begin{array}{llrllr} ac \ldots & M = & 2 & bc \ldots & M = & 1 \\ ad \ldots & = & 1 & bd \ldots & = & 0 \\ ae \ldots & = & 0 & be \ldots & = & -1 \\ af \ldots & = & -1 & bf \ldots & = & -2 \end{array}\right\} J = 2, 1.$$

(3) $j_1 = \frac{3}{2}, j_2 = \frac{3}{2}$; here again Pauli's Principle would be operative. We have the following combinations:—

$$\begin{array}{rcccccc} & cd & ce & cf & de & df & ef \\ M = & 2 & 1 & 0 & 0 & -1 & -2 \end{array}$$

Hence $J = 0, 2$.

We thus obtain the following terms:

$$\begin{array}{lcl} (p_{\frac{1}{2}}\, p_{\frac{1}{2}}) & \ldots & 0 \\ (p_{\frac{1}{2}}\, p_{\frac{3}{2}}) & \ldots & 1, 2 \\ (p_{\frac{3}{2}}\, p_{\frac{3}{2}}) & \ldots & 0, 2 \end{array}$$

We thus obtain, as in RS-coupling, 5-terms with the same distribution of J, but we can no longer talk of singlets or triplets, and the relation ${}^3P_0 - {}^3P_1 : {}^3P_1 - {}^3P_2 = 1 : 2$ is no longer fulfilled.

We pass from RS-coupling to *jj*-coupling in a np^2-combination, as the charge increases, as is shown in Table 20. Here the singlet and triplet S, P, D terms and their separations are given for elements in the periodic table having electronic configurations np^2, where $n=2, 3, 4, 5$ and 6. It will be seen that as n increases, the deviation from the ideal rule of triplet separation gradually increases. This indicates that the coupling is passing more and more to the (jj)-type. The figures in italics denote differences between preceding and following terms.

Table 20.—The S, P, D -terms for elements having np^2 -configuration.*

n	RS-np^2 Element	$^3P_0$		$^3P_1$		$^3P_2$		$^1D_1$		$^1S_0$
2	C	90878·3	*14·8*	90863·5	*27·5*	90836	*10150*	80686	*11455*	69231
3	Si	65765·0	*77·06*	65687·94	*146·08*	65541·86	*6075·53*	59466·33	*9095·43*	50370·9
4	Ge	65558	*557*	65001	*853*	64148	*5715*	58433	*9242*	49191
5	Sn	59192·0	*1692*	57500	*1736*	55764	*5185·5*	50578·5	*8549·5*	42029·0
6	Pb	59821	*7817*	52004	*2831*	49173	*10808*	38365	*8000*	30365
2	N+	238849	*50*	238799	*83*	238716	*15185*	223531		[147118]
3	O++	444661	*116*	444545	*193*	444352	*19967*	424385	*22913*	401472

330. Quantitative Term Formulae.

—In the foregoing sections, we have only dealt with the laws which define the existence and quantum characteristics of spectral terms arising out of any electron configuration. In the present sections we shall discuss how the term-values, multiplet-intervals, distances between different multiplets etc., can be calculated when the electron-structure of the atom is given.

On the basis of the orbital theory the problem of calculating term-values could be solved exactly only in the case of the H-atom.

---

* Data for C, Si, Sn and Pb are taken from Goudsmit and Bacher *Atomic Energy States* (1932).

With certain assumptions, the orbital theory was in a position to throw some light on the characteristics of spectra of alkali elements as described in Chap. VIII. But this seemed to be the limit of the capacity of the orbit-theory, which failed to elucidate even the next simplest problem, *viz.*, that of He as described in §279.

This failure is partly to be ascribed to the earlier conception that the electron is merely a small sphere of electricity. But the situation changed completely with the hypothesis of the magnetic electron. With the aid of this hypothesis it was possible to explain the phenomenon of duplicity as well as the general features of complex spectra. But a new era in atomic physics was introduced with the rise of quantum mechanics and its successive phases of development, *i.e.*, matrix mechanics of Heisenberg, wave-mechanics of De Broglie and Schrödinger, and Dirac's relativity quantum mechanics. Though it is felt that problems of atomic physics require a new formulation of mechanics and though with the recent developments, some progress has been made, it is even now doubtful whether the system has yet received a final form. A detailed treatment of the problems of atomic physics on the basis of new mechanics* is outside the scope of the present work. In the present section, we confine ourselves only to general treatment based on the picture of the 'magnetic electron.'

The General Energy formula and Γ-Factors.

The energy of an atom can be written in the form (see p. 554):

$$\frac{-E}{Rhc} = \frac{T}{R} = \sum \frac{\left(Z-\sigma_1'\right)^2}{n_i^2} + \sum \frac{\alpha^2\left(Z-\sigma_2'\right)^2}{n_i^3}\left(\frac{1}{l+\frac{1}{2}} - \frac{3}{4n_i}\right)$$
$$+ \Sigma W(l_i s_i) + \Sigma W(s_i s_k) + \Sigma W(l_i l_k) + \Sigma W(s_i l_k) \qquad . (13)$$

The expression can be analysed as follows:—The first term represents the sum of the energies of the electrons regarded as point charges moving under a charge Ze, which is partly compensated by the screening σ' due to the shells of electrons both internal and external to the i^{th} electron. The i^{th} electron occupies a shell having the total quantum number $n = n_i$. The second term is due to relativity correction. It is to be noted that the two screening constants are not put equal. The third term represents interaction energy between the spin and l-vector of the i^{th} electron. The fourth term represents the spin interaction between the i^{th} electron and other electrons (h) of the system. The fifth term represents l-interaction energy of the i^{th} electron and other electrons (h) of the system. The last term represents interaction energy between the spin of the i^{th} electron and l-vectors of others (h). The summation is to be extended over all the electrons of the system. $W(s_i\, l_h)$ the interaction energy between the spin of the i^{th} and l-vector of the h^{th} electron can be neglected in certain cases as it varies as $(Z-s)^3$ as mentioned on p. 555. The value of σ^i depends on the inner electrons forming the closed shell, as well as on the electrons in the outer incomplete shell. On the other hand, closed shells do not contribute to $W(l_i\, s_i)$ or other interaction energies as for them $\Sigma\, s_h = 0$, $\Sigma\, l_h = 0$ and the resultant $J = 0$. These energies depend entirely on the electrons in the incomplete shells.

---

* For a comprehensive account of the treatment of problems of atomic physics on Quantum Mechanics, the following books may be consulted: Smekal, *Quanten theorie*, articles by Bethe, Hund and Mott; *Wave Mechanics* by Frenkel, **1**, **2**, and **3** (Oxford University Press). Dirac, *Principles of Quantum Mechanics*, 1930.

For a single electron (alkali elements), it has been shown that

$$W(l_i\, s_i) = a\, l_i\, s_i \cos(l_i\, s_i) \quad . \quad . \quad . \quad . \quad . \quad . \quad (14)$$

or since $h = 0$, the subscript i can be dropped, the total interaction energy becomes

$$W = a\, ls \cos(ls), \quad \text{where } a = \frac{Rhc\, \alpha^2\ (Z-\sigma_2)^4}{n^3\ l\,(l+\frac{1}{2})\,(l+1)} \quad . \quad . \quad (15)$$

as already given.

For the case of a single electron it has been proved that we get doublet levels. The doublet separation is just equal to this interaction energy and if it be denoted by γ, we have

$$\gamma = a\, l\, s \cos(ls) \quad . \quad . \quad . \quad . \quad . \quad . \quad . \quad . \quad (16)$$

However when the external field is sufficiently strong to break the coupling between l and s vectors, γ can no longer be represented by the equation (16). In this case the cosine of the angle between l and s is given by

$$\cos(s\, l) = \cos(s\, H).\ \cos(l\, H) = \frac{m_l\, m_s}{l\, s}$$

Hence

$$\gamma = a\, m_s\, m_l \quad . \quad . \quad . \quad . \quad . \quad . \quad . \quad . \quad . \quad (17)$$

For the two electron case, the interaction energies and term values have been calculated in § 277. The γ-factors for this case can be obtained from the general formula for several electrons. We now turn our attention to many electron systems.

331. Many Electron Problems.—In this case, interaction energy terms between the l and s vectors of the same electron, *viz.*, $\Sigma W(s_i\, l_i)$ can be written out by a generalisation of the formula (14). When we have many electrons, a large number of terms will result with different multiplicities as explained in §326, but for terms belonging to one particular multiplicity the other interaction energy expressions in equation (13) except $\Sigma W\,(l_i\, s_i)$ will be common for all the terms of the given multiplet. Hence for finding the intervals in any multiplet we have to calculate $\Sigma W\,(l_i\, s_i)$. This is done as follows. We have

$$\Sigma\, W(l_i\, s_i) = \Sigma\, a_i\, l_i\, s_i \cos\,(l_i\, s_i) \quad . \quad . \quad . \quad . \quad . \quad (18)$$

where the summation is to be carried over all electrons forming incomplete shells.

Now as already explained we have in the case of RS-coupling,

$$S = \Sigma s_i, \;\; L = \Sigma l_i$$

and $\cos\,(l_i\, s_i) = \cos\,(l_i\, L).\, \cos\,(s_i\, S).\, \cos\,(L\, S).$

Hence $\Sigma W(l_i\, s_i) = A\; L\; S.\, \cos\,(L\, S)$

where $A = \Sigma a_i \dfrac{l_i}{L}.\;\; \dfrac{s_i}{S}.\, \cos\,(l_i\, L) \cos\,(s_i\, S) \quad . \quad . \quad . \quad (19)$

Here as in the case of a single electron we set

$$\Gamma = \Sigma W\;(l_i\, s_i) = ALS \cos\,(LS) \quad . \quad . \quad . \quad . \quad . \quad (20)$$

Since $\cos\,(LS) = \dfrac{J(J+1) - L(L+1) - S(S+1)}{2LS}$

we have $\Gamma = \frac{1}{2}\, A\, [J(J+1) - L(L+1) - S(S+1)] \quad . \quad . \quad . \quad . \quad (21)$

There will be as many Γ's as the number of component terms, and this again is equal to the number of J-values. Here the Γ-value denotes the separation of the various levels of a given multiplet from a hypothetical centre, which is obtained when we neglect the interaction energy between l and s vectors of each electron.

We shall now find an expression for the strong field Γ-values. In the former case, we put

$$\cos\,(l_i\, s_i) = \cos\,(l_i\, L).\, \cos\,(s_i\, S).\, \cos\,(LS)$$

In the case of strong fields the coupling between S and L is broken and each of them precesses independently about the external magnetic field-axis H, so that we have

$$\cos\,(LS) = \cos\,(SH) \cos\,(LH).$$

Now from (20), we have

$$\Gamma = ALS \cos (LS) = ALS \frac{M_S}{S} . \frac{M_L}{L} = AM_S \; M_L \quad . \quad . \quad (22)$$

INTERVAL RULE

Let Γ_J denote the Γ-value for a term with a given J-value, which is equal to $| S+L |$. Then it is easy to see that

$$\sum_{J_{min}}^{J_{max}} (2J+1) \, \Gamma_J = 0 \; . \; . \; . \; . \; . \; . \; . \; . \quad (23)$$

i.e., if we assign to the term with the inner quantum number J the weight $2J+1$, then we obtain for the C. G. of the terms $\Gamma = 0$. Hence Γ denotes the distance of the term from the C. G. of the multiplet.

Again from (21), we have

$$\Gamma_{(J+1)} - \Gamma_{(J)} = A(J+1) \quad . \; . \; . \; . \; . \; . \; . \quad (24)$$

i.e., the interval between two successive terms is proportional to the larger J-value.

This is Landé's interval rule and the extent to which it holds can be taken as a criterion of the validity of the RS-coupling. A few examples of the interval rule are given in the following table. Here the symbols (01), (12), (23) ...... denote multiplet intervals between terms having $j = 0$ and 1, $j = 1$ and 2, $j = 2$ and 3 .... The observed intervals are given in different columns and interval ratios calculated from them are shown in the last column.

Table 21.—Interval ratios for triplet P, D, F, G, H terms.

Spectrum	Term	0 1	1 2	2 3	3 4	4 5	5 6	Ratio
V II	$3d^24s$ ^{3}P or $3d^3$ ^{3}P	219·4	393·5					1 : 1·79
Sc II	$3d\,4s$ ^{3}D	...	67·7	110·0				2 : 3·25
Fe I	$3d^74s$ ^{3}F			407·6	584·7			3 : 4·30
Fe I	$3d^74p$ ^{3}G				311·8	388·4		4 : 4·98
Ti I	$3d^34p$ ^{3}H					36·15	46·25	5 : 6·3
Cr I	$3d^44s4p$ ^{5}P		163·8	240·2				2 : 2·93
Fe I	$3d^64s^2$ ^{5}D	90·0	184·2	288·2	416·0			1 : 2·04 : 3·20 : 4·62
Fe I	$3d^74s$ ^{5}F		168·9	257·7	351·3	448·5		2 : 3·05 : 4·16 : 5·31
Ti I	$3d^24s.4p$ ^{5}G			98·4	130·5	161·4	191·2	3 : 3·97 : 4·92 : 5·82
Cr I	$3d^54p$ ^{7}P			81·4	112·5			3 : 4·15
Fe I	$3d^64s.5s$ ^{7}D		130·4	198·9	271·3	347·5		2 : 3·05 : 4·16 : 5·32
Cr I	$3d^44s.4p$ ^{7}F	39·6	78·5	116·8	153·6	189·0	229·9	1 : 1·98 : 2·94 : 3·87 4·77 : 5·62

332. Permanence of Γ-Values and Γ-Sum Rule.—Let us now arrange the Γ-values for a ³D-term in the following table for weak and strong fields, the Γ-values for weak field have been calculated from equation (21) and those for strong fields from equation (22). It is seen that the sum of Γ-values corresponding to a given value of m is the same for a strong as well as for a weak field, as was first pointed out by Landé. It is analogous to the g-Permanence rule given in §324 and is known as Γ-*Permanence Rule.*

Table 22.—Γ-values for a ³D-term.

m	-3	-2	-1	0	1	2	3	
$j = 3$	$2A$	$2A$	$2A$	$2A$	$2A$	$2A$	$2A$	WEAK FIELD
$j = 2$		$-A$	$-A$	$-A$	$-A$	$-A$		
$j = 1$			$-3A$	$-3A$	$-3A$			
$\Sigma\Gamma$	$2A$	A	$-2A$	$-2A$	$-2A$	A	$2A$	
$m_s = -1$	$2A$	A	0	$-A$	$-2A$			STRONG FIELD
$= 0$		0	0	0	0	0		
$= 1$			$-2A$	$-A$	0	A	$2A$	

The Γ-sum Rule

Goudsmit formulated another rule for Γ-values analogous to the g-sum rule mentioned on p. 689, which states that for a number of optical levels resulting from *a given electron configuration* the sum of Γ-values for the same m-value is independent of the field strength. The Γ-sum is also independent of the coupling scheme provided we take the sum for different terms arising out of a given configuration over the same j-value. This can be illustrated by table 23 in case of a p^2-configuration. The Γ-values for (jj)-coupling can be very easily calculated in the present case. The j-values are either $\frac{3}{2}$ or $\frac{1}{2}$ giving γ_l equal to $\frac{1}{2}a$ or $-a$ respectively. The $\Sigma\gamma_l$ values for the different combinations of j_1 and j_2 are shown in the middle columns. For Russell-Saunders' scheme of coupling the Γ-values for the entire configuration in terms of Γ-values for individual electrons are not so easy to be calculated. Only in the case of two electrons we can do it successfully, for the mean value of cosines occurring in equation (19) are known and given by

$$\frac{s_1}{s}\cos(s_1\,s)=\frac{s_1(s_1+1)+s(s+1)-s_2(s_2+1)}{2\,s(s+1)}$$

and

$$\frac{l_1}{l}\cos(l_1\,l)=\frac{l_1(l_1+1)+l(l+1)-l_2(l_2+1)}{2\,l\,(l+1)}$$

With the help of these cosine values we can calculate the factor A in terms of a. The results are shown in the lower part of Table 23.

Table 23.—Γ-values for a p^2-configuration.

j_1 \ J	2	1	0	j_2 \ J	
$\frac{3}{2}$	a		a	$\frac{3}{2}$	jj-Coupling.
$\frac{3}{2}$	$-\frac{1}{2}a$	$-\frac{1}{2}a$		$\frac{1}{2}$	
$\frac{1}{2}$			$-2a$	$\frac{1}{2}$	
$\Sigma\Gamma$	$\frac{1}{2}a$	$-\frac{1}{2}a$	$-a$		
$^3P_2$	$\frac{1}{2}a$			R. S. Coupling.	
$^3P_1$		$-\frac{1}{2}a$			
$^3P_0$			$-a$		
$^1S_0$			0		
$^1D_2$	0				

333. Applications of Γ-sum Rule and Γ-Permanence Rule.— (A) Γ-VALUE FOR MORE THAN TWO ELECTRONS. — As pointed above the Γ-values for the case of Russell-Saunders coupling cannot be calculated directly for more than two electrons. Indirectly, however, we can find out the value of for Γ such cases with the aid of the above rules. Let us take for example the p^3-configuration. The terms are

$$^2P_{\frac{1}{2},\,\frac{3}{2}}\qquad\qquad ^2D_{\frac{3}{2},\,\frac{5}{2}}\qquad\qquad ^4S_{\frac{3}{2}}$$

i.e., we have 1 level with $j=\frac{5}{2}$, 3 levels with $j=\frac{3}{2}$, 1 level with $j=\frac{1}{2}$.

We have therefore to find out five quantities out of which the one for the S-term is zero, because it is single. Let

$$x=\Gamma(^2D_{\frac{5}{2}}),\ y=\Gamma(^2D_{\frac{3}{2}}),\ \text{and}\ p=\Gamma(^2P_{\frac{3}{2}}),\ q=\Gamma(^2P_{\frac{1}{2}}).$$

Table 24.

Comb.	m_s	m_l	γ
a	$\frac{1}{2}$	1	$\frac{1}{2}a$
b	$\frac{1}{2}$	0	0
c	$\frac{1}{2}$	-1	$-\frac{1}{2}a$
d	$-\frac{1}{2}$	1	$-\frac{1}{2}a$
e	$-\frac{1}{2}$	0	0
f	$-\frac{1}{2}$	-1	$\frac{1}{2}a$

Here $\Gamma(^2D_{\frac{5}{2}})$ denotes the Γ-values for the ^2D-term having $j=\frac{5}{2}$. The other symbols have similar meanings. The magnetic states and the γ-values for a single p-electron are given in table 24. We have to take $^6C_3=20$ combinations of each of these states $a, b, c, \ldots\ldots$ taking three at a time and find out the Γ-values for each combination. These are shown in the last column of table 24a. In this table we have also collected together M_S, M_L and M values. With the help of table 24a we now write down in table 25 the strong field Γ-values for the same M-values in the same column and put the corresponding unknown Γ-factors for weak fields below the M's. The use of the Γ-sum rule will give us a set of equations

$$x=0,\ \ x+y+p=0,\ \ x+y+p+q=0$$

Ultimately we are left with the equation $y+p=0$.

Thus the problem cannot be completely solved as the number of equations is insufficient for determining all the variables. We have $y+p=0$, but no second equation connecting y and p. But it has been found experimentally that y as well as $p=0$. Actually small separations are obtained in p^3 $^2D_{\frac{3}{2},\frac{5}{2}}$ and in p^3 $^2P_{\frac{1}{2},\frac{3}{2}}$ and they are due to other coupling factors.

The best example of the calculation of Γ-values from these rules is afforded in the case of d^x shells. (For d^3, see Goudsmit, *Phys. Rev.*, **13**, 946, 1928.)

Table 24a.

Combination	M_S	M_L	M	Γ
1. *abc*	$\frac{3}{2}$	0	$\frac{3}{2}$	0
2. *abd*	$\frac{1}{2}$	2	$\frac{5}{2}$	0
3. *abe*	$\frac{1}{2}$	1	$\frac{3}{2}$	$\frac{1}{2}a$
4. *abf*	$\frac{1}{2}$	0	$\frac{1}{2}$	a
5. *bcd*	$\frac{1}{2}$	0	$\frac{1}{2}$	$-a$
6. *bce*	$\frac{1}{2}$	-1	$-\frac{1}{2}$	$-\frac{1}{2}a$
7. *bcf*	$\frac{1}{2}$	-2	$-\frac{3}{2}$	0
8. *cde*	$-\frac{1}{2}$	0	$-\frac{1}{2}$	$-a$
9. *cdf*	$-\frac{1}{2}$	-1	$-\frac{3}{2}$	$-\frac{1}{2}a$
10. *def*	$-\frac{3}{2}$	0	$-\frac{3}{2}$	0
11. *acd*	$\frac{1}{2}$	1	$\frac{3}{2}$	$-\frac{1}{2}a$
12. *ace*	$-\frac{1}{2}$	0	$-\frac{1}{2}$	0
13. *acf*	$\frac{1}{2}$	-1	$-\frac{1}{2}$	$\frac{1}{2}a$
14. *ade*	$-\frac{1}{2}$	2	$\frac{3}{2}$	0
15. *adf*	$-\frac{1}{2}$	1	$\frac{1}{2}$	$\frac{1}{2}a$
16. *bde*	$-\frac{1}{2}$	1	$\frac{1}{2}$	$-\frac{1}{2}a$
17. *bdf*	$-\frac{1}{2}$	0	$-\frac{1}{2}$	0
18. *cef*	$-\frac{1}{2}$	-2	$-\frac{5}{2}$	0
19. *aef*	$-\frac{1}{2}$	0	$-\frac{1}{2}$	a
20. *bef*	$-\frac{1}{2}$	-1	$-\frac{3}{2}$	$\frac{1}{2}a$

Table 25.

M / M_s	$\frac{5}{2}$	$\frac{3}{2}$	$\frac{1}{2}$	$-\frac{1}{2}$	$-\frac{3}{2}$	$-\frac{5}{2}$	
$\frac{3}{2}$ $-\frac{3}{2}$ $\frac{1}{2}$ $\frac{1}{2}$ $-\frac{1}{2}$ $-\frac{1}{2}$ $-\frac{1}{2}$ $-\frac{1}{2}$	0	0 $\frac{1}{2}a$ $-\frac{1}{2}a$ 0	a $-a$ $-\frac{1}{2}a$ $\frac{1}{2}a$	$-\frac{1}{2}a$ $\frac{1}{2}a$ $-a$ 0 0 a	0 0 $-\frac{1}{2}a$ $\frac{1}{2}a$	0	STRONG FIELD
ΣΓ	0	0	0	0	0	0	
$j=\frac{5}{2}$ $\frac{3}{2}$ $\frac{3}{2}$ $\frac{1}{2}$	x	x y p	x y p q	x y p q	x y p	x	WEAK FIELD

(B) PROOF OF INTERVAL RULE.

Table 26.

M_s \ M	2	1	0	−1	−2	
1	$\frac{1}{2}a$	0	$-\frac{1}{2}a$	$\frac{1}{2}a$		STRONG FIELD
0	0	$\frac{1}{2}a$	$\frac{1}{2}a$	$-\frac{1}{2}a$	0	
0		$-\frac{1}{2}a$	0			
0			$-\frac{1}{2}a$	0		
−1			$-\frac{1}{2}a$		$\frac{1}{2}a$	
$\Sigma\Gamma$	$\frac{1}{2}a$	0	$-a$	0	$+\frac{1}{2}a$	
$j=2$	z	z	z	z	z	WEAK FIELD
$j=1$		y	y	y		
$j=0$			x			

We shall now show that in the case of p^2 ^{3}P-terms the Interval Rule of Landé can be deduced with the aid of the above rules. We need only find out the absolute values of the term intervals in terms of the factor 'a'. Let $\Gamma(^3P_0)=x$, $\Gamma(^3P_1)=y$, $\Gamma(^3P_2)=z$ denote the Γ-values of the ^{3}P-terms. In the present case we have to take $^6C_2=15$ combinations of the magnetic states and Γ-values given in Table 24. Such combinations of two states are shown in Table 12. The final arrangement of Γ-values for strong and weak fields are given in Table 26.

Hence by applying these rules, we obtain from the above table the following three equations:

$$z=a/2,\ y+z=0,\ x+y+z=-a$$

and we have $\Gamma(^3P_0)=-a$, $\Gamma(^3P_1)=y=-a/2$ and $\Gamma(^3P_2)=z=a/2$

$$\nu(^3P_0)=\nu_0+a,\ \nu(^3P_1)=\nu_0+\tfrac{1}{2}a,\ \nu(^3P_2)=\nu_0-\tfrac{1}{2}a$$

We have further $\nu_0=\dfrac{5(\nu_0-a/2)+3(\nu_0+a/2)+(\nu_0+a)}{5+3+1}$

i.e., the C. G. of the terms is ν_0. Hence the total

$$\Delta\nu=\Gamma(^3P_2)-\Gamma(^3P_0)=3a/2$$

Plotting the values of $\Gamma(^3P_2)$, $\Gamma(^3P_1)$ and $\Gamma(^3P_0)$ as in Fig. 9, we get

$$\Gamma(^3P_1)-\Gamma(^3P_0)=\tfrac{1}{2}a$$
$$\Gamma(^3P_2)-\Gamma(^3P_1)=a$$

which gives the interval ratio

$$\Delta\,^3P_{21}:\Delta\,^3P_{10}=2:1$$

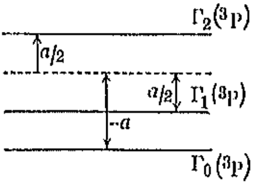

Fig. 9

(C) OCCURRENCE OF INVERTED TERMS

With the aid of these rules we can prove why terms in a p^5-configuration are inverted, *i.e.*, $P_{\frac{3}{2}}>P_{\frac{1}{2}}$. We have from § 224

$$\text{for } p \ldots\ldots\ ^2P_{\frac{1}{2}},\ \nu=\nu_0+a;\ ^2P_{\frac{3}{2}},\ \nu=\nu_0-a/2 \qquad \ldots\ldots\ (25)$$

When we take a p^5-configuration, the combinations as well as m and γ values can be easily calculated with the aid of the principles just mentioned. The working is shown in Table 27.

Table 27.

Combination	M_s	M_l	M	Γ
$a\ b\ c\ d\ e\ \ (-f)$	$\frac{1}{2}$	1	$\frac{3}{2}$	$-\frac{1}{2}a$
$a\ b\ c\ d\ f\ \ (-e)$	$\frac{1}{2}$	0	$\frac{1}{2}$	0
$a\ b\ c\ e\ f\ \ (-d)$	$\frac{1}{2}$	-1	$-\frac{1}{2}$	$\frac{1}{2}a$
$a\ b\ d\ e\ f\ \ (-c)$	$-\frac{1}{2}$	1	$\frac{1}{2}$	$\frac{1}{2}a$
$a\ c\ d\ e\ f\ \ (-b)$	$-\frac{1}{2}$	0	$-\frac{1}{2}$	0
$b\ c\ d\ e\ f\ \ (-a)$	$-\frac{1}{2}$	-1	$-\frac{3}{2}$	$-\frac{1}{2}a$

$a\ b\ c\ d\ e$ denotes the addition values Σm_s, Σm_l as given for the states a, b, c, d, e in Table 24. $(-f)$ denotes that the summation gives the same value for M_s, M and Γ as for f with the signs reversed. The reader can easily compare. Now the Γ-values can be displayed as in Table 28.

Table 28.

M_s \ M	$\frac{3}{2}$	$\frac{1}{2}$	$-\frac{1}{2}$	$-\frac{3}{2}$	
$M_s = \frac{1}{2}$	$-\frac{1}{2}a$	0	$\frac{1}{2}a$		STRONG FIELD
$M_s = -\frac{1}{2}$		$\frac{1}{2}a$	0	$-\frac{1}{2}a$	
$\Sigma\Gamma$	$-\frac{1}{2}a$	$\frac{1}{2}a$	$\frac{1}{2}a$	$-\frac{1}{2}a$	
$j = \frac{3}{2}$	$\Gamma(^2P_{\frac{3}{2}})$	$\Gamma(^2P_{\frac{3}{2}})$	$\Gamma(^2P_{\frac{3}{2}})$	$(\Gamma^2P_{\frac{3}{2}})$	WEAK FIELD
$= \frac{1}{2}$		$\Gamma(^2P_{\frac{1}{2}})$	$\Gamma(^2P_{\frac{1}{2}})$		

Using Γ-permanence rule we got from the above table

$$\Gamma(^2P_{\frac{3}{2}}) = -a/2\,;\, \Gamma(^2P_{\frac{1}{2}}) + \Gamma(^2P_{\frac{3}{2}}) = a/2$$

Therefore $$\Gamma(^2P_{\frac{1}{2}}) = a$$

Hence $$^2P_{\frac{1}{2}} = \nu_0 - a \text{ and } {}^2P_{\frac{3}{2}} = \nu_0 + a/2 \quad . \quad . \quad . \quad . \quad . \quad (26)$$

Comparison of (26) with (25) shows that now the terms are inverted.

(D) CALCULATION OF SCREENING CONSTANTS.

The absolute value of the total separations as calculated with the aid of the above rules help us to evaluate the screening constants for hydrogenic orbits provided we know the observed value of the total separations. Of course, as usual the RS-coupling should hold good. Such total separations can be obtained readily from spectral term data of the element under consideration. The calculations may be performed as already indicated for two-valence elements in § 277 and § 280. In Table 29 we give the value of 'a' and the screening constant σ for elements having a p^x-configuration.

Table 29.—σ-values for elements with p^x-configuration.

Configuration	Element	Term	Absolute Total Separation	Observed Total Separation	a	σ
p	5B	^2P	$\frac{3}{2}a$	15·9	10·6	2·432
p^2	6C	^3P	$\frac{3}{2}a$	42·3	28·2	2·720
p^3	7N	^2D	0	—	—	—
p^4	8O	^3P	$\frac{3}{2}a$	226	150·6	3·812
p^5	9F	^2P	$\frac{3}{2}a$	410	273·3	3·214
p^6	10 Ne	^1S	0	—	—	—

(E) CALCULATION OF MULTIPLET SEPARATION.

We give now one more illustration of the use to which these Γ-rules can be put. If Russell-Saunders' scheme of coupling is valid we can calculate theoretically the separations between multiplet terms. The method adopted is to obtain weak field Γ-values for component terms of different multiplets. These Γ-values can be obtained in terms of a_l for a single electron which can be numerically found out with the help of formula (15). The difference between the Γ-values for different terms of the multiplet corresponds to the required multiplet term separation, which can be easily calculated.

Table 30.—Multiplet Separations for d^3-configurations.

Term	Ti+ d^3-Configuration Multiplet—Separations				Obs. *Cal.*	
^4F	Not obs.	128·37 *133·2*	103·41 *103·6*	75·84 *74·1*	32·05 *44·4*	
^4P				122·29 *74·1*		
^2H	97·82 (*97·8*)					
^2G		120·46 *120·0*				
^2F				−59·89 *−51·8*		
j	$\frac{11}{2}$	$\frac{9}{2}$	$\frac{7}{2}$	$\frac{5}{2}$	$\frac{3}{2}$	$\frac{1}{2}$

Spectrum of Ti^+ has been thoroughly worked out by H. N. Russell* and affords an excellent example to show an agreement between observed and calculated multiplet term separations. The observed and calculated separation are tabulated in Table 30.

334. The Separation Factor A.—The factor A defined by equation (19) is called the separation factor. It is of a fundamental importance. From a knowledge of it we can easily find out Γ-values and *vice versa*. For convenience of calculation it is better to express it in terms of a_i. We will now give ready methods of evaluating this important factor in terms of a_i. The methods of obtaining A can be divided for three types of term: (i) Highest term *for* equivalent electrons, (ii) Any equivalent electron term, (iii) Non-equivalent electron terms. We will take them one by one.

(i) *Highest term for equivalent electrons.*—According to the Pauli-Principle $2(2l+1)$ electrons are required to fill up an l-shell completely. But if there are only x-electrons such that $x < (2\ l+1)$ in the l-shell, their $m_{li}\ .\ m_{si}$ values can be displayed by the following scheme :

$$\begin{array}{lllllll}
(1) & \tfrac{1}{2}\, l, & \tfrac{1}{2}\,(l-1), & \tfrac{1}{2}\,(l-2)\ldots\ldots & \tfrac{1}{2}\,(l-\nu+1)\ldots\ldots & -\tfrac{1}{2}\,(l-1), & -\tfrac{1}{2}\, l \\
(2) & \tfrac{1}{2}\, l, & \tfrac{1}{2}\,(l-1), & \tfrac{1}{2}\,(l-2)\ldots\ldots & \tfrac{1}{2}\,(l-\nu+1)\ldots\ldots & -\tfrac{1}{2}\,(l-1), & -\tfrac{1}{2}\, l \\
\vdots & \vdots & \vdots & \vdots & \vdots & \vdots & \\
(x) & \tfrac{1}{2}\, l, & \tfrac{1}{2}\,(l-1), & \tfrac{1}{2}\,(l-2)\ldots\ldots & \tfrac{1}{2}\,(l-\nu+1)\ldots\ldots & -\tfrac{1}{2}\,(l-1), & -\tfrac{1}{2}\, l
\end{array}$$

$$\Gamma = \Sigma\, \gamma_i = \Sigma\, a_i\ m_{li}\ m_{si}$$

$$= \sum_{\nu=1}^{\nu=x} \tfrac{1}{2}a\,(l-\nu+1) = \frac{ax}{2}\left(l - \frac{x-1}{2}\right). \qquad \ldots\ldots \quad (27)$$

Further $$\Gamma = A.\, M_S\ M_L$$

where $M_S = \Sigma\, m_s = x/2$; $M_L = \Sigma\, m_l = x\left(l - \frac{x-1}{2}\right)$

These M_S and M_L values are for maximum multiplicity as shown in §328.

Hence $$\Gamma = Ax.\,\frac{x}{2}\left(l - \frac{x-1}{2}\right) \qquad \ldots\ldots\ldots\ldots \quad (28)$$

Comparing (27) and (28) we get

$$A\,x = a,\ \ A = \frac{a}{x}. \qquad \ldots\ldots\ldots\ldots \quad (28')$$

It is to be noted that equation (28′) gives the separation factor for the highest term in the case of equivalent electrons alone.

---

* H. N. Russell, *Astr. Jour.*, 66, 283, 192.

(ii) *Equivalent Electrons.*—In § 333 we gave a method of obtaining Γ-values for terms due to any equivalent electron configuration in terms of the quantity a, and emphasised their importance subsequently. It will be our aim now to show that the determination of Γ-values for different terms amounts to the determination of the separation factor A. It was shown before that

$$\Gamma_{(j)}-\Gamma_{(j-1)}=A.j$$

We see from the above equation that if we divide out calculated multiplet separation obtained in terms of a by j, we will obtain the value of A. Thus, in a p^2-configuration, it was found that

$$\Gamma(^3P_2)=\tfrac{1}{2}a,\quad \Gamma(^3P_1)=-\tfrac{1}{2}a$$
$$(^3P_0)=-a$$

Therefore $\Gamma(^3P_2)-\Gamma(^3P_1)$ $=a=2A$. Hence $A=\frac{1}{2}a$

Again, $\Gamma(^3P_1)-\Gamma(^3P_0)=\frac{1}{2}a$, Hence $A=\frac{1}{2}a$.

The separation factor A may also be calculated from the total separation by dividing it by the sum of all the j-values for a given multiplet except the lowest. Thus for a p^2-configuration the total separation for a ^3P term is $\frac{3}{2}a$

Table 31.

Configuration	Terms	Total separation	A
$p, -p^5$	^2P	$\frac{3}{2}a$	a
$p^2, -p^4$	^3P	$\frac{3}{2}a$	$\frac{1}{2}a$
$\pm p^3$	^2D, ^2P	0	0
$d, -d^9$	^2D	$\frac{5}{2}a$	a
$d^2, -d^8$	^3F	$\frac{7}{2}a$	$\frac{1}{2}a$
	^3P	$\frac{3}{2}a$	$\frac{1}{2}a$
$d^3, -d^7$	^4F	$\frac{7}{2}a$	$\frac{1}{3}a$
	^4P	$\frac{4}{3}a$	$\frac{1}{3}a$
	^2H	$\frac{11}{10}a$	$\frac{1}{5}a$
	^2G	$\frac{27}{20}a$	$\frac{3}{10}a$
	^2F	$-\frac{7}{12}a$	$-\frac{1}{6}a$
	^2D } ^2D }	$\frac{5}{6}a$	$\frac{1}{3}a$
	^2P	a	$\frac{2}{3}a$
$d^4, -d^6$	^5D	$\frac{5}{2}a$	$\frac{1}{4}a$
	^3H	$\frac{11}{10}a$	$\frac{1}{10}a$
	^3G	$\frac{27}{20}a$	$\frac{3}{20}a$
	^3F } ^3F }	$\frac{7}{12}a$	$\frac{1}{12}a$
	^3D	$-\frac{5}{12}a$	$-\frac{1}{12}a$
	^3P } ^3P }	$\frac{3}{4}a$	$\frac{1}{4}a$
$\pm d^5$	All	0	0

Hence $(2+1)\,A=\frac{3}{2}a,\ \ A=\frac{1}{2}a$

In this way we can find out the separation factors A from the individual and total multiplet separations for any group of equivalent electrons. In Table 31 the total separation as well as the factor A for equivalent p and d electrons are arranged. Their values have been obtained in the manner indicated above.

(iii) *Non-equivalent Electrons.*—Our next attempt would be to calculate the separation factor A in the case of non-equivalent electrons. This is an easy affair for two electrons, but for more than two electrons the problem cannot be solved because the value of the cosines involved are not known. It is, however, possible to find out the separation factor in the case when the electron is added to a group of electrons for which the separation factor and the spin and orbital vectors are known. This is, as a matter of fact, equivalent to two-electron problem.

Now, let us suppose that the separation factor, l and s vectors for one electron are a_1, l_1 and s_1 respectively, and for the other electron or a group of electrons these quantities are a_2, l_2 and s_2. The value of A is shown to be

$$A = \sum a_i \frac{l_i\, s_i}{LS} \cos\,(l_i\; L).\cos\,(s_i\; S).$$

The quantum cosines occurring in this formula have to be taken constants in time.

The determination of A requires the evaluation of $\cos\,(l_i\; L)$ and $\cos\,(s_i\; S)$ which can only be done provided we know the way in which the quantum vectors combine with each other. For this reason we will suppose in our present derivation that the Russell-Saunders' scheme holds good so that the component terms of a given multiplet are normal and obey the interval rule closely. Thus l_1 and l_2 combine to give L, and s_1 and s_2 combine to give S which then combine to give us $J = \mid L+S \mid$.

Under such coupling scheme

$$A = a_1 \frac{l_1}{L}.\cos\,(l_1 L)\ \frac{s_1}{S}.\cos\,(s_1 S)$$

$$+ a_2 \frac{l_2}{L}.\cos\,(l_2 L)\ \frac{s_2}{S}.\cos\,(s_2 S). \quad . \quad . \quad . \quad . \quad . \qquad (29)$$

The four cosines occurring in the above formula can be calculated as usual, so that

$$A = a_1 \frac{L(L+1)+l_1(l_1+1)-l_2(l_2+1)}{2L(L+1)}.\frac{S(S+1)+s_1(s_1+1)-s_2(s_2+1)}{2S(S+1)}$$

$$+ a_2 \frac{L(L+1)-l_1(l_1+1)+l_2(l_2+1)}{2L(L+1)}.\frac{S(S+1)-s_1(s_1+1)+s_2(s_2+1)}{2S(S+1)} . \qquad (30)$$

In the case of two electrons $s_1 = s_2 = \frac{1}{2}$ and the above formula reduces to

$$A = \tfrac{1}{2}\, a_1 \frac{L(L+1)+l_1(l_1+1)-l_2(l_2+1)}{2L(L+1)}$$

$$+ \tfrac{1}{2}\, a_2 \frac{L(L+1)+l_2(l_2+1)-l_1(l_1+1)}{2L(L+1)} \quad . \quad . \quad . \quad . \quad . \qquad (31)$$

In general when a electron is coupled to a configuration of equivalent electrons as in the formation of some of the neutral elements from their ions the separation factor can be easily calculated from formula (30). As an illustration of the method we can consider a spark term characterised by definite values of l and s to which an s-electron is coupled. In this case . . . $l_2 = 0$, $s_2 = \frac{1}{2}$; $L = l_1$, $S = s_1 \pm \frac{1}{2}$.

For $\quad S = s_1 + \frac{1}{2}, \qquad A = a_1 \dfrac{s_1}{s_1+\frac{1}{2}}$

For $\quad S = s - \frac{1}{2}, \qquad A = a_1 \dfrac{s_1+1}{s_1+\frac{1}{2}}$

Similarly, for other configurations the A factors can be calculated in terms of known quantities. We will now illustrate the truth of the formula for separation factors by taking a concrete example of the spectra of iron (Table 32).

*Table 32**.

Configuration	Calculated A.	Observed A		The value for a_1
		From Adjacent levels	From Total Separation	
Fe III d^6	$^5\text{D}\ A = a_1$			exp. >120
Fe II $d^6\ s$	$^6\text{D}\ A = \frac{4a_1}{5}$	$A = 86, 81, 78, 76$	82	102
	$^4\text{D}\ A = \frac{6a_1}{5}$	$= 125, 115, 111$	119	99
Fe I $d^6\ s^2$	$^5\text{D}\ A = a_1$	$A = 104, 96, 92, 90$	98	98
$d^6\ s, s; \ldots\ ^6\text{D}+s$	$^7\text{D}\ A = \frac{2a_1}{3}$	$A = 69, 68, 66, 65$	68	102
	$^5\text{D}\ A = \frac{14a_1}{15}$	$= 93, 91, 88, 86$	92	99
$^4\text{D}+s$	$^5\text{D}\ A = \frac{9a_1}{10}$	$= 105, 93, 82, 43$	(91)	(101)
	$^3\text{D}\ A = \frac{3a_1}{2}$	$= 106, 160$	(128)	(86)

To start with we will take the simplest spectrum of Fe^{++}. The normal configuration is d^6 which gives rise to ^5D term. We call the A-value for this configuration a_1. When an s-electron is added to d^6 we get the spectrum of Fe^{+} and the terms obtained are ^6D and ^4D for which A-values have been calculated with the aid of formula (31). In the third and fourth columns the A-values from adjacent and total separation have been put down. The values of a_1 in the last column have been obtained by substituting the A-values of column 4 in the corresponding expressions of column 2. Similarly for Fe I the various A-values have been arranged. It is significant to note that the ratio of calculated A factors for the multiplets of a given configuration is very nearly equal to the ratio of observed A-values for the same multiplet. For example $^6\text{D}\ (A) : {}^4\text{D}\ (A) :: 2 : 3$ and $82 : 119 :: 2 : 2{\cdot}9$. Thus the validity of our formula is established. It will be seen from the last column that the values of a_1 calculated from different A-values is not constant. This is due to the screening produced by the added electron. This might also be ascribed to the deviation from the interval rule, otherwise the agreement is fairly good.

---

* Goudsmit, *Phys. Rev.*, 31, 960, 1928.

335. Spectra of Elements belonging to Individual Periods.—In the foregoing sections the laws of formation of terms out of any electron structure have been described without any particular reference to any atom or ion. We shall now give a brief description of these spectra, choosing only a few representative examples. A full description will occupy a big volume, and for the knowledge of spectra of individual atoms or ions, original papers must be consulted.

Spectra of Atoms and Ions with *p*-shells.

It is clear that spectra can be classified according as the light electrons in the normal state form *s*, *p*, *d* or *f*-shells. Some information of the spectra of elements and ions normally with their light electrons in *s*-shells has been already given (alkali and alkaline earth elements). We therefore take the elements and ions with their light electrons in the *p*-shell. These are shown in Table 33.

Table 33.—Normal atoms and ions with np^x-configurations.

x n	1	2	3	4	5	6
2	5 B 6 C^+ 7 N^{++}	6 C 7 N^+ 8 O^{++}	7 N 8 O^+ 9 F^{++}	8 O 9 F^+ 10 Ne^{++}	9 F 10 Ne^+ 11 Na^{++}	10 Ne 11 Na^+ 12 Ca^{++}
3	13 Al 14 Si^+ 15 P^{++}	14 Si 15 P^+ 16 S^{++}	15 P 16 S^+ 17 Cl^{++}	16 S 17 Cl^+ 18 A^{++}	17 Cl 18 A^+ 19 K^{++}	18 A 19 K^+ 20 Ca^{++}
4	31 Ga 32 Ge^+ 33 As^{++}	32 Ge 33 As^+ 34 Se^{++}	33 As 34 Se^+ 35 Br^{++}	34 Se 35 Br^+ 36 Kr^{++}	35 Br 36 Kr^+ 37 Rb^{++}	36 Kr 37 Rb^+ 38 Sr^{++}
5	49 In 50 Sn^+ 51 Sb^{++}	50 Sn 51 Sb^+ 52 Te^{++}	51 Sb 52 Te^+ 53 I^{++}	52 Te^+ 53 I^+ 54 Xe^{++}	53 I 54 Xe^+ 55 Cs^{++}	54 Xe 55 Cs^+ 56 Ba^{++}
6	81 Tl 82 Pb^+ 83 Bi^{++}	82 Pb 83 Bi^+ 84 Po^{++}	83 Bi 84 Po^+ 85 —	84 Po 85 — 86 Rn^{++}	85 — 86 Rn^+ 87 —	86 Rn 87 — 88 Ra^{++}

The fundamental terms arise from np^x, $x=1$ to 6, and the excited levels arise from $np^{x-1}\,mz$, where $m \geqq n$, and z may be *s*, *p*, *d* or *f* as detailed on p. 722. The terms expected in any atom or ions of this group are shown in Table 34.

Table 34.—Terms arising from the np^x-configuration.

	ION		ATOM		EXCITED ATOM		
x	Configuration of ground state np^{x-1}	Terms	Configuration of ground state np^x	Terms	$[np^{x-1}]$ $(n+1, 2, 3, 4 \ldots)s$	$[np^{x-1}]$ $(n+1, 2, 3, 4, \ldots)p$	$[np^{x-1}]$ $(n+0, 1, 2, 3, 4, \ldots)d$
1	ns^2	${}^1S$	$ns^2\ np$	${}^2P$	${}^2S$	${}^2P$	${}^2D$
2	$ns^2\ np$	${}^2P$	$ns^2\ np^2$	${}^3P{}^1D{}^1S$	${}^{3,1}P$	${}^{3,1}(SPD)$	${}^{3,1}(PDF)$
3	$ns^2\ np^2$	${}^3P$ ${}^1D$ ${}^1S$	$ns^2\ np^3$	${}^4S$ ${}^2D$ ${}^2P$	${}^{4,2}P$ ${}^2D$ ${}^2S$	${}^{4,2}(SPD)$ ${}^2(PDF)$ ${}^2P$	${}^{4,2}(PDF)$ ${}^2(SPDFG)$ ${}^2D$
4	$ns^2\ np^3$	${}^4S$ ${}^2D$ ${}^2P$	$ns^2\ np^4$	${}^3P$ ${}^1D$ ${}^1S$	${}^{5,3}S$ ${}^{3,1}D$ ${}^{3,1}P$	${}^{5,3}P$ ${}^{3,1}(PDF)$ ${}^{3,1}(SPD)$	${}^{5,3}D$ ${}^{3,1}(SPDFG)$ ${}^{3,1}(PDF)$
5	$ns^2\ np^4$	${}^3P$ ${}^1D$ ${}^1D$	$ns^2\ np^5$	${}^2P$	${}^{4,2}P$ ${}^2D$ ${}^2S$	${}^{4,2}(SPD)$ ${}^2(PDF)$ ${}^2P$	${}^{4,2}(PDF)$ ${}^2(SPDFG)$ ${}^2D$
6	$ns^2\ np^5$	${}^2P$	$ns^2\ np^6$	${}^1S_0$	${}^{3,1}P$	${}^{3,1}(SPD)$	${}^{3,1}(PDF)$

RULES OF TRANSITIONS.

The general transition rule is that *the light electron should change its shell* so that the l value for the shell should change by $\Delta l = \pm 1, \pm 3, \pm 5$.

$$\Delta l = 0,\ \Delta l = \pm 2, \text{ etc.} \ldots \text{ are forbidden.}$$

Thus terms of column 6 or 8 can combine with terms of column 5, for in the first case the electron jumps from an s-shell to a p-shell ($\Delta l = +1$), in the second case from a d-shell to a p-shell ($\Delta l = -1$). But terms of column 7, cannot combine with terms of column 5 for it reduces to the jumping of an electron from one p-shell to another p-shell ($\Delta l = 0$) which is forbidden. For the terms themselves ΔL may now be ± 1, ± 2, 0, etc., where $L = l$-quantum number of a term. In addition, the Selection Principle for the j-quantum number must be obeyed *for the terms.*

From a knowledge of the terms and the rules of transitions we can always predict a large number of lines, but all the predicted lines of a spectrum have been obtained in very few cases. The lines * due to O^{++} are given below in a tabular form for illustration.

---

* A. Fowler, *Proc. Roy. Soc. A.*, **117**, 317, 1928.

These lines correspond to the transition of the light electron $2p^2 \leftarrow 2p\ 3s$ and $2p\ 3s \leftarrow 2p\ 3p$.

Table 35.—Lines of O^{++} (ν in cm^{-1}).

$2p\ 3s$	$^3P_0$ 177336	$^3P_1$ 177218	$^3P_2$ 176961	$^1P_1$ 171513
$2p^2$				
$^3P_0$ 444661	×	267443	×	273148
$^3P_1$ 444545	267209	267327	267584	273148
$^3P_2$ 444352	×	267134	267391	272839
$^1D_2$ 424385	×	247167	247424	252872
$^1S_0$ 401472	×	224254	×	229959
$2p.3p$				
$^1D_2$ 153637	×	23581	23324	17876
$^3D_1$ 150728	26608	26490	26233	20785
$^3D_2$ 150592	×	26626	26369	20921
$^3D_3$ 150372	×	×	26589	×
$^3S_1$ 147036	30300	30182	29925	24477
$^1S_0$ 146278	×	30940	×	25235
$^3P_0$ 144365	×	32853	×	27148
$^3P_1$ 144283	33053	32935	32678	27230
$^3P_2$ 144152	×	32066	32809	27361

Primed and unprimed terms.—It is clear from the above rules, that when a number of different multiplets arises from any electron structure, they all have the same combining powers. Thus every one of the terms belonging to *pp* ^{3}DPS can combine with every one of the terms of *pd* ^{3}FDP in so far as the rules for the inner quantum number do not stand in the way, for $\Delta l=-1$. Thus *pp* ^{3}P can combine with *pd* ^{3}P giving very strong lines and this is apparently a violation of the selection principle $\Delta L=0$. But the violation is only apparent, as the selection principle for the l-quantum number applies to shells and electron jumps, and not to terms. Formerly when the ideas were not very clear, one such term used to be marked with a dash and the other left undashed. Thus the terms arising out of *pp* would be written *pp* $^3\mathrm{D}\bar{\mathrm{P}}\mathrm{S}$, and those out of *pd* would be written as $^3\mathrm{F}\bar{\mathrm{D}}\mathrm{P}$. The selection principle was modified: For combination between dashed and undashed terms, the selection principle is $\Delta L=0, \pm 2$, $\Delta L=\pm 1, 3$ forbidden. For combination between dashed and dashed terms, or undashed and undashed terms, $\Delta L=\pm 1$ allowed, $\Delta L=\pm 2$ forbidden. But there is no longer any need for thus making the symbolism unnecessarily complex.

The Doublet-Separation for Halogens.—The fundamental terms of the halogens are np^5 $^2\mathrm{P}_{\frac{3}{2}}$ and $^2\mathrm{P}_{\frac{1}{2}}$, where $^2\mathrm{P}_{\frac{3}{2}} > {}^2\mathrm{P}_{\frac{1}{2}}$. The differences $^2\mathrm{P}_{\frac{3}{2}} - {}^2\mathrm{P}_{\frac{1}{2}}$ are of considerable interest from the point of view of Franck's theory (*vide* chapter on *Molecular Spectra*) of formation of alkali chlorides, and were first obtained by spectroscopic methods by L. Turner.* They are given below:

Element	F	Cl	Br	I
Δν	409	881	3685	7600 cm^{-1}

The Spectrum of inert gases.—The ground state of the inert gases are np^6 $^1\mathrm{S}_0$, and so all inert gases are diamagnetic. The next states are *b*, *c*, *d* . . . as in Table 36.

Table 36.

Configuration	Terms	Number of terms	Paschen
(*b*) np^5 $(n+1, 2, \ldots .)s$	$^3\mathrm{P}_{0,1,2}$ $^1\mathrm{P}_1$	4	*s*-terms
(*c*) np^5 $(n+1, 2, \ldots .)p.$	^{3,1}DPS. . .	10	*p*-terms
(*d*) np^5 $(n+0, 1, \ldots .)d.$	^{3,1}FDP . . .	12	*d*-terms

Paschen† was the first to obtain terms *b*, *c*, *d*, . . . in the spectrum of Ne with their Rydberg sequences up to $n=11$ or 12. His notation is given in the last column. The fundamental lines of Ne arise from the transition $2p^6\ {}^1S_0 - 2p^5 3s\ {}^{3,1}P$, since $\triangle j = \pm 1, 0$, we actually get only two lines $\lambda 735{\cdot}7 = {}^1S_0 - {}^1P_1$, $\lambda\ 743{\cdot}5 = {}^1S_0 - {}^3P_1$. These were first obtained by Hertz for the case of Ne by means of his vacuum spectrograph.

---

* Turner, *Phys. Rev.*, **27**, 397, 1926.

† Paschen, *Ann. d. Phys.*, **60**, 405, 1919 ; **63**, 204, 210, 1920.

Metastable states.—If a discharge be passed through Ne and it is excited to $2p^5 . 3s\ {}^3P_2$, ${}^3P_0$-states, there is no possibility of the electron jumping to the lowest state as it is forbidden by the selection rule for the inner quantum number ($\triangle j = 0 \rightarrow 0$ or $0 \rightarrow 2$). Such an atom of neon will have fairly long life of the order of 10^{-2} sec. while the ordinary excited states have the life of 10^{-8} sec. (*vide* §304). The atom is also highly loaded with energy. In fact the energy contained is about 15 volts. Such an excited atom with fairly long life is highly reactive, for when it comes into contact with other types of atoms it can communicate its energy by collision to the latter and thereby can break them or excite them to higher state.

SERIES-CONVERGENCE.

Paschen* further noted that Rydberg sequence of the terms arising out of $2p^5$ *ns*-combination shows a very peculiar behaviour. The terms s_4, s_5 can be represented by a regular Rydberg formula, but the higher terms of s_2 and s_3 become too small and can form Rydberg sequences only when we increase their values by a number which is very nearly 782 cm^{-1}. It can be explained as shown on the scheme opposite.

The Ne⁺ ion has two states ${}^2P_{\frac{3}{2}}$ and ${}^2P_{\frac{1}{2}}$. When an electron is brought to it and when particularly the n-value is high, the coupling between l and s of the ${}^2P_{\frac{1}{2}}$ or ${}^2P_{\frac{3}{2}}$ states is not broken. Ultimately s_2, s_3 terms become equal to s_4, $s_5 - 782$ ($= {}^2P_{\frac{3}{2}} - {}^2P_{\frac{1}{2}}$ of Ne⁺). It is a case of ($j\,j$)-coupling similar to the example given in §322.

Scheme II.

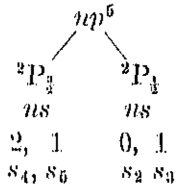

The coupling in neon in the formation of $2p^5$ (3, 4, . . .)*s*-shells is thus partly of the $j\,j$-type and the interval rule is no longer obeyed. The g-values for the terms are given in Table 6. Note their divergence from Landé g-values. The same holds for other inert gases and for the spectra of such inert gas like ions as Na⁺, Mg⁺⁺. . . . . . etc.

---

* F. Paschen, *loc. cit.*

336. Spectra of Atoms and Ions with *d*-Shells.—As we have mentioned in §285 the *d*-shell begins to be formed from Sc and it reaches the saturation value in Ni thus giving rise to the first transitional group of elements. Similarly as a glance at the chart on p. 583 shows, we have the elements of the 2nd and 3rd transitional groups due to the filling of $4d$ and $5d$-shells. In §284 we have mentioned that in the formation of the normal atom there seems to be a sort of competition between the $3d$ and $4s$-levels for the capture of the electron. But the normal states of the trebly or doubly ionised atom is always formed of only *d*-shell electrons. It is therefore convenient to start with discussion of the spectra of trebly ionised atoms. As a typical example we begin with the spectrum of Ti in various stages of ionisation which has been completely worked out by H. N. Russell.*

Table 37.—States of neutral and ionised Titanium.

Spectrum	A	B $\bar{\text{B}}$	C $\bar{\text{C}}$	D
Ti^{+3}	$3d$ .... (G_1) ^2D	$(4, 5, ...)s$ (G_2) ^2S	$(4, 5, ...)p$ ^2P	$(4, 5, ...)d$ ^2D
Ti^{+2}	$3d^2$ .... (G_1) $^3(FP)$ $^1(GDS)$	$3d\ (4, 5 .....)s$ (G_2) $^{3,1}(D)$	$3d\ (4, 5, ...)p$ $^{3,1}(FDP)$	$3d\ (4, 5, ...)d$ $^{3,1}(GFDPS)$
Ti^{+}	$3d^3$ .... (G_1) $^4(PF)$ $^2(PDF)$ $^2(GDH)$	$3d^2(4, 5, ...)s$ (G_2) $^4(PF)$ $^2(SPDFG)$ $3d\ (4, 5, ...)s^2$ (G_3) ^2D	$3d^2(4, 5, ...)p$ $^4(SPD)$ $^2(SPD)$ $^4(DFG)$ $^2(DFG)$ ^2P $^2(PDF)$ $^2(FGH)$	$3d^2(4, 5, ...)d$ $^4(PDF)$ $^2(PDF)$ $^4(PDFGH)$ $^2(PDFGH)$ ^2D $^2(SPDFG)$ $^2(DFGH)$
Ti	$3d^4$ .... (G_1) ^5D $^3(PF)$ $^3(PDFGH)$ $^1(SDG)$ $^1(SDFGI)$	$3d^3\ (4, 5, ...)s$ (G_2) $^5(FP)$ $^3(FP)$ $^3(PD)$ $^1(PD)$ $^3(FGH)$ $^1(FGH)$ ^3D ^1D $3d^2\ 4s^2$ $^3(PF)$ $^1(SDG)$ $3d^2\ 4s,5s$ $^5(PF)$ $^3(PF)$ $(SPDFG)$ $^1(SPDFG)$	$3d^2\ 4s\ 4p$ $^5(DFG)$ etc. $3d^2\ 4p^2$ $^5(DFG)$ $^3(DFG)$ $^1(DFG)$	$3d^2\ 4s\ 4d$ $^5(PDFGH)$ $^3(PDFGH)$ $^3(PDFGH)$ $^1(PDFGH)$ $3d^3\ 4d$ .... $^5(PDFGH)$

In the above table, the possible electron transitions are given. (G) denotes ground state, (G_1) denotes the lowest ground state, G_2 the next . . . and so on.

TREBLY IONISED TITANIUM: Ti^{+3}

The spectrum of Ti^{+3} is quite simple. The fundamental level is $3d\ ^2D$, the next metastable state is $4s\ ^2S$ and we get lines† due to $3d\ ^2D - 4p\ ^2P$. Sc^{++} has the same structure, but Ca^{+} has $4s\ ^2S > 3d\ ^2D$ as discussed in § 284.

---

* H. N. Russell, *Astr. Phys. Jour.*, 66, 13, 1927.

† Also the existence of a strong pair of lines due to the transition $^2D - ^2F$ has been observed. It has been found that all the series follow a Rydberg sequence nearly. Hence the absolute values could be determined in the case of Ti^{+3} spectrum.

DOUBLY IONISED TITANIUM: Ti^{+2}

Here Russell traced the lines

$$(A, B) - (C), \quad C - (\bar{A}, \bar{B}).$$

where $\bar{B}$ denotes higher Rydberg sequence terms to B. Thus B is $3d\,4s$, and $\bar{B}$ denotes $3d\,(5s, 6s, 7s, \ldots .)$. The fundamental lines are due to $(A, B)-(C)$.

A comprises 9 terms, B, 4 terms, and C, 12 terms. All these terms have been found by Russell. Here Russell counted term-values upwards from the lowest known level, *viz.*, $3d^2\ {}^3F$, for the complexity of the spectrum made the observation of a Rydberg sequence difficult. The next higher in energy, but considerably lower in term-value is the level $3d\,4s\ {}^3D$. Thus we have $3d^2\ {}^3F = 0{\cdot}0$ and ${}^3D = 38063{\cdot}50$. Hence $3d^2 > 3d\,4s$, and both of these may be called ground levels (or $3d\,4s$ is a metastable ground level). All the other terms predicted in the spectrum Ti^{++} according to the theory of Hund have been identified.

IONISED TITANIUM: Ti^{+}

This ion gives an enormous number of lines which have been traced to the transition $(AB)-C$. A gives 19 terms, B gives 17 terms, and C gives 45 terms.

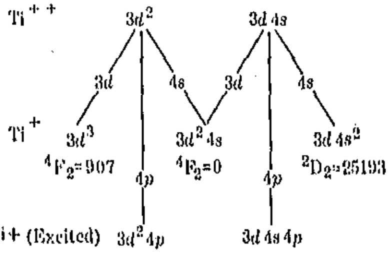

Fig. 10.

Ground States.—The formation of the ground state now becomes interesting on account of the competition between the $3d$ and $4s$-levels. The process can be thus illustrated by Fig. 10. Ti^{++} in the ground state has two levels $3d^2$ and $3d\,4s$ both of which are probable and have actually been found. When we come to Ti^{+} we can get the ground state by adding one more electron to either of the two states of Ti^{++}. Here again the added electron can be either $3d$ or $4s$ so that we will get three probable ground states, *viz.*, $3d^3$, $3d^2 4s$, $3d\,4s^2$. Now $3d^2 4s$ gives ${}^4(FP)$ and $3d^3$ also gives ${}^4(FP)$. As a matter of fact two sets of low ${}^4F$ and ${}^4P$ terms are observed. For one set the values are

$${}^4F = 0,\ 93{\cdot}94,\ 225{\cdot}47,\ 393{\cdot}22\ \text{cm}^{-1}.$$

For the other

$${}^4F = 907{\cdot}96,\ 983{\cdot}80,\ 1087{\cdot}21,\ 1215{\cdot}58\ \text{cm}^{-1}$$

It is difficult to say which of these two sets arise from $3d^3$, and which from $3d^2 4s$. Similar difficulties are very frequent in complex spectra and a good deal of ingenuity has been displayed in finding the proper electron structure for any term. The reader may refer to Russell's original paper.

NEUTRAL Ti.

The neutral atom Ti also gives an enormous number of lines which have been traced to the transition (B – C), A is no longer observed.

Ground State.—The formation of normal levels can be illustrated now as before in the case of Ti (Fig. 11).

Here also we get three ground levels which are due to $3d^3 4s$, $3d^2 4s^2$-combinations.

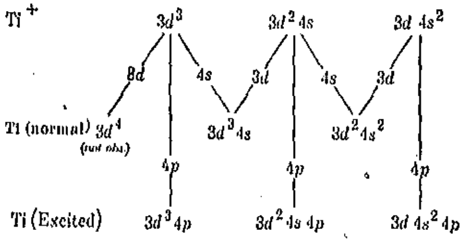

Fig. 11

337. Spectra of Other Elements of the Transitional Group.—

The above brief description of the spectrum of titanium is typical of the spectra of all elements from Sc to Ni as well as with certain modifications of elements belonging to the II and III transition series. We have simply to change the index of d in table 37 suitably and we get the electron structure of any atom or ion. Thus suppose we want to study the spectrum of Fe in different states of ionisation. We have simply to write out a table identical with 37, and increase the index of d by 4 as Fe is the fifth element from Ti. We thus get the above picture (Fig. 12) of the formation of normal states of Fe in the different stages of ionisation.

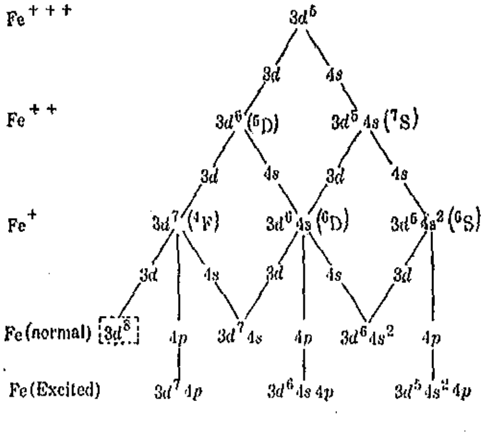

Fig. 12

The excited states can be written as explained under titanium.

338. Transitional Elements of Groups II and III.—The formation of spectra of elements belonging to transitional groups II (39 Y to 46 Pd) and III (71 Lu to 78 Pt) is exactly similar to those of the first group, except in non-essential details. For example, if in Table 37 giving the terms of Ti in different stages of ionisation, we increase the quantum numbers by unity, we obtain the terms of Zr in different stages of ionisation; if the total quantum numbers be increased by two throughout, we should obtain the terms of Hf in different stages of ionisation. But the term separations increase owing to the larger nuclear charge.

In group II, it is generally found that of the terms arising from the compositions $4d^{x}\ 5s^2$, $4d^{x+1}\ 5s$, those due to $4d^{x+1}\ 5s$ are usually lower. The reverse is the case for group I, except for 24 Cr; in group II, terms due to $4d^{x+2}$ have also been identified, and sometimes they form the lowest terms, e.g., in 46 Pd, $4d^{10}\ {}^1S_0, \ldots$ gives us the lowest term.

339. Spectra of Rare Earths.—We have previously described that the formation of the rare earths may be explained as being due to the filling up of the $4f$-shell, with three electrons distributed among $5d$ and $6s$-shells. The electron structure of the trebly ionised elements can be confidently taken to be $4f^x$ where x varies from zero in La to 14 in Lu. The general structure of the neutral atom is expected to be $4f^x\ 5d^2\ 6s$ or $4f^x\ 5d\ 6s^2$. An application of Pauli's Principle shows that atoms and ions of this type will have for each electron-structure a very large number of levels giving rise to innumerable lines. As a matter of fact, the spectra of all rare earth elements show thousands of lines and it is very difficult to separate the lines due to elements in different stages of ionisation though some very valuable work in this line has been done by King.* Nobody has yet mustered sufficient courage to undertake the classification of the lines of any of these elements in the successive stages of ionisation. A good beginning has been made by Meggers† and Russell‡ for

---

* A. S. King, various papers in *Astr. Jour.*, **68**, 194, 1928; **72**, 221, 1930, etc.

† F. Meggers, *Bur. Stand. Journ. Res.*, **5**, 73, 1930; **9**, 239, 625, 1932.

‡ H. N. Russell, *ibid.*, **9**, 625, 1932.

La, La^{+}, La^{++} and Lu, Lu^{+}, Lu^{++} (partially). A few other elements have also been tackled by other workers.* But anything like a complete classification for any element seems to be far distant, though from the experience already gained some general observations may be made.

In the case of transitional elements we have spoken of competition between the $3d$ and $4s$-shells. In the case of rare earths, there is competition between the $4f$, $5d$, $6s$-shells. The $5d$ and $6s$-shells may be taken to be equivalent, but the $4f$-shell is not so, *i.e.*, there can be no lines due to the transition of the electron from $5d$ to $6s$ but, there may be lines corresponding to the transition from $4f$ to $5d$ or to $6s$, all other electrons remaining in their position. This introduces a further complexity, since it is equivalent to the existence of allowed transitions even amongst levels arising from the fundamental electron structures. Thus fundamental lines are scattered all over the spectral region and the lines of elements in different stages of ionisation are all mixed up. We illustrate these remarks with the following examples taken from Russell and Megger's† analysis of the spectrum of La in the different stages of ionisation. Lanthanum may be considered to present the simplest case as normally the formation of $4f$-shell just begins in La.

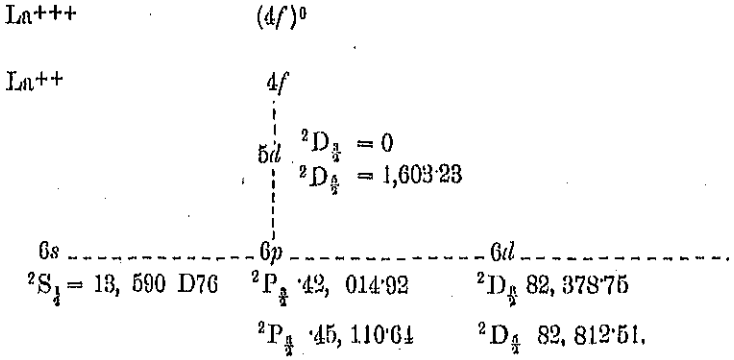
La+++
$(4f)^0$
La++
$4f$
$5d$
$^2D_{\frac{3}{2}} = 0$
$^2D_{\frac{5}{2}} = 1{,}603{\cdot}23$
$6s$
$6p$
$6d$
$^2S_{\frac{1}{2}} = 13{,}\ 590$ D76
$^2P_{\frac{1}{2}}$ ·42, 014·92
$^2P_{\frac{3}{2}}$ ·45, 110·64
$^2D_{\frac{3}{2}}$ 82, 378·75
$^2D_{\frac{5}{2}}$ 82, 812·51.

The spectrum of La^{++} is seen to be quite simple. The lowest levels are given by $5d$, and $6s$ is metastable to it. Let us now take La^{+}.

---

* For reference see *Reviews of Modern Physics*, 4, 417, to 420, 1932.

† Russell and Meggers, *loc. cit.*

SPECTRUM OF La⁺

La++−5*d*-core	La++−4*f*-core	La++−6 *s*-core
$5d4f$	$4f^2$	$4f6s$
$5d^2$	$4f5d$	$6s5d$
$5d6s$---$5d6p$---$5d6d$	$4f6s$----$4f6d$---$4f6d$	$6s^2$-----$6s6p$-----$6s6d$
$5d^2$ $^3F_2 = 00{\cdot}0$ $^3F_3 = 1016{\cdot}10$ $^3F_4 = 1970{\cdot}70$ etc. etc.	$4f5d$ $^1G_4 = 16599{\cdot}17$ etc. etc.	$6s^2$ $^1S_0 = 7394{\cdot}57$
$5d6s$ $^1D_2 = 1394{\cdot}46$ $^3D_2 = 2591{\cdot}60$ $^3D_3 = 3250{\cdot}35$ etc. etc.	$4f6s$ $^1F_3 = 15773{\cdot}77$ $^3F_2 = 14147{\cdot}98$ $^3F_3 = 14375{\cdot}17$ $^3F_4 = 15698{\cdot}74$	$4f^2$ $^3H_4 = 55107{\cdot}25$ $^3H_5 = 55982{\cdot}09$ $^3H_6 = 56837{\cdot}94$ etc. etc.

SPECTRUM OF La

La+−5*d*²-core	La+−5*d* 6*s*-core	La+−6*s*²-core
$5d^2 4f$	$5d6s4f$	$6s^2 4f$
$5d^3$	$5d^2 6s$	$6s^2 5d$—$6s^2 6p$
$5d^2 6s$-----$5d^2 6p$------	$5d6s^2$----$5d6s6p$--------	

The structures giving rise to the lowest terms are $5d^2 6s$, ... and $5d\,6s^2$.

SPECTRUM OF CERIUM.

Let us see what will be the spectrum of Ce in different stages of ionisation. We have simply to add $4f$ to the figures of La and work out the levels according to Pauli's Principle.

There can be other possibilities which we may work out as in the case of La.

Thus Ce⁺⁺⁺ $4f$

Ce⁺⁺ $4f^2$

$4f.5d$

$4f.6s$———$4f.6p$ . . . . . .

Ce⁺ $4f^3$

$4f^2.5d$

$4f^2.6s$———$4f^2.6p$ . . . . . . etc.

Ce $4f^4$

$4f^3.6d$

$4f^3.6s$———$4f^3.6p$ . . . . . . etc.

The spectrum of Ce has been partly classified by Karlson* and he found that the fundamental levels are obtained from the following electron structures:

$$\left.\begin{array}{l} 4f\,5d\;\;6s^2 \\ 4f\,5d^2\;6s \end{array}\right\}$$

340. Double Electron Transition.—It might have been noticed that in certain cases, two electrons may be simultaneously involved in a given transition. Thus take the following transition in Ti^+:

$3d^3 \leftarrow 3d\;4s\;4p$ which consists of the two transitions $(3d \leftarrow 4p) + (3d \leftarrow 4s)$. In this case, the $4s$ and $4p$ electrons from the excited state $3d\;4s\;4p$ both pass to $3d$ forming the $3d^3$-state. One transition $(3d \leftarrow 4p)$ is allowed, the other $(3d \leftarrow 4s)$ is not allowed. Such transitions generally give rise to lines which are less intense than those observed in one electron transitions.

The rule of transition may be easily formulated (Laporte):

$$\Sigma\,\Delta l_i = \pm 1, 3, \ldots \text{ etc.} \qquad (32)$$

Here l_i denotes the l-quantum number of the electrons involved in the transition.

The case of two electron transitions is probably best illustrated in the spectrum of Ca, Sr and Ba. We gave a description of the spectra of these elements in § 275 and § 284. But besides the lines described there, which were shown to belong to singlet and triplet spectra, a group of strong lines remained outside the scheme of classification. But yet there could not be the slightest doubt that they were connected with the arc spectra of these elements, as some of them could be classified under the *ns np* ^3P-levels. One such set of lines for Ca is shown opposite.

Table 38.

$4s\,4p$ / $3d^2$	$^3P_0$ 34146·0	*52*	$^3P_1$ 34096·6	*105*	$^3P_2$ 33988·7
$^3\overline{P}_0$ 10887·1			23207·5		
$^3\overline{P}_1$ 10839·8	23306·9		23254		23148·9
$^3\overline{P}_2$ 10753·0			23341·5		23235·7

The $^3\overline{P}_{0,\,1,\,2}$ terms (10753·0, 10839·8 and 10887·1 cm^{-1}) involved in the production of these lines could not be identified with any known triplet terms of calcium. Russell and Saunders* undertook an extensive investigation of these and other lines of Ca, Sr and Ba, and arrived at conclusions of fundamental importance for spectroscopy which led ultimately to a clear conception of the rules of formation of complex spectra and of Russell-Saunders coupling. As these conceptions have been introduced earlier, the results of Russell and Saunders can be easily stated. Ca^+, Sr^+, Ba^+ have the normal levels ns ($n=4, 5, 6, \ldots$ respectively) but the $(n-1)d$ ^2D levels are also fairly large, and may be called metastable, as the total quantum number of d is smaller. We can now conceive of processes as shown in Fig. 13 illustrating formation of the states of the neutral atom out of the normal ($4s$) and metastable $3d$ states of the ions.

---

* Karlson, *Zs. f. Phys.*, 85, 482, 1933.

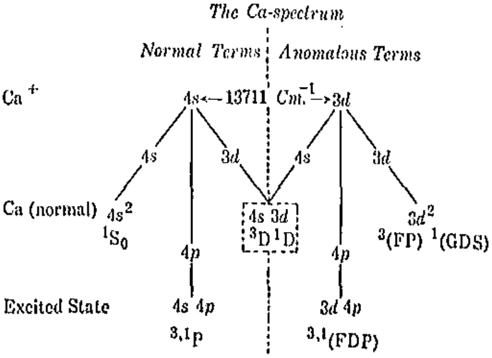

Fig. 13

Terms lying to the left of the dotted dividing line give rise to the regular singlet-triplet spectra described on p. 388. The terms to the right, which are analogous to the terms of the complex spectra are the *anomalous ones* of which an example has been cited just now. The large d-terms due to $4s.3d$ $^{3,1}D$ = 28963, 27455 cm^{-1} may be said to be common to both systems of terms.

Table 39.—$n^3\overline{P}_{0,1,2}$-values of Ca

$3d^2$ $^3P_{0,1,2}$	$3d.4d$ $^3\overline{P}$	$3d.5d$ $^3\overline{P}$	$3d.6d$ $^3\overline{P}$	$3d.7d$ $^3\overline{P}$
10753·0	741·1	−4999·8	−8333·6	−10086
10839·8	767·1	−4983·6	−8313·1	−10063
10887·1	780·6	−4977·5	−8300·4	

n^3D_1-values

n^3D_1	$3d.4s$	$3d.5s$	$3d.6s$	$3d.7s$
	28955·2	11552·4	6559·7	4254·0

The $^3\overline{P}_{0,1,2}$ terms just now cited were conclusively proved to be due to the $3d^2$-combination in the following way.

The arc spectra of these elements were further investigated for very faint lines* which can be regarded as forming higher

---

* Russell and Saunders, *Astr. Jour.*, **16**, 88, 1925.

Rydberg sequences of the multiplet $n^3P-\bar{P}^3$. A number of such multiplet $^3\bar{P}_{0,\,1,\,2}$-terms were found which combined with $4s.\,4p$ $^3P_{0,\,1,\,2}$ of Ca. Their values are given in Table 39.

The most remarkable thing about these terms is that they become negative after $n=4$. Russell and Saunders proved[*] that these terms follow a Rydberg sequence only if a number equal to *ca* 13700 be added to them, when their values approximate to the $4s.\,nd$ $^3D_2$ values as shown in Table 39. Now the difference between Ca$^+$ $4s$ $^2S_{\frac{1}{2}}$ and $3d$ $^2D_{\frac{3}{2}}$ is 13711.

The case is analogous to that of Ne and the example proves that the series of $^3\bar{P}$ terms arise when the Ca$^+$ ion is in the $3d$-^2D state, and a fresh electron is brought to any higher quantum state to form the neutral atom.

With this clue, a large number of terms belonging to such electron structures as $3d\ np$, $3d\ nd$, ... etc.... were identified. Such lines are more prominent in the spectrum of Ba as the $5d$ ^2D term of Ba$^+$ is almost equal to the $6s$ ^2S-term ($\triangle\nu = {}^2S_{\frac{1}{2}}$ 80664·9 − $^2D_{\frac{3}{2}}$ 75781·7 = 4883·2 cm^{-1}).

Terms arising out of such structures as $3d\,5d$, $3d\,5p$ for Ca become negative with respect to the normal term $4s^2\cdot{}^1S_0$. The interpretation is now apparent. These structures are produced when both the valency electrons are displaced, say in the production of $3d\,5d$, the first from $4s$ to $3d$ and the second from $4s$ to $5d$. The total energy required to cause this displacement is much larger than the energy of ionisation of the atom. Thus though the atom is neutral it has got added to it more energy than needed for ionisation.

341. The $P\bar{P}$-multiplets of Magnesium-like Elements and Ions.—Multiplets of the kind described in the foregoing section, which are due to an electron configuration in which two electrons are displaced are not confined to Ca, Sr, Ba, but are quite common in other elements. For example, in Mg, the normal constitution is $3s^2$, and the excited levels are obtained when we leave one electron in $3s$, and allow the other electron to pass to the higher

Table 40.—The ^{3}PP-*triplet of* Mg.

$3s\,3p$ $^3p^2$	$^3P_0$ 39813	*20*	$^3P_1$ 39793	*41*	$^3P_2$ 39752
$^3P_0$ 3852			35941		
$^3P_1$ 3831	35981		35962		35921
$^3P_2$ 3790					35962

---

[*] The suggestion was put forward almost simultaneously by Böhr and Wentzel, *Phys. Zeits.*, 24, 106, 1923; 25, 182, 1924.

states $3p$, $3d$, ... etc. This is the mechanism of production of the usual singlet and triplet level, but like Ca, Mg and other iso-electronic elements (Al+, Si++, . . .) show lines which cannot be fitted in the above scheme. Millikan and Bowen showed that they arise from the transition

$$3s\,3p \leftarrow 3p^2$$
$$^1P,\ ^3P \leftarrow {}^3\overline{P}_{0,1,2},\ ({}^1\overline{D}_2,\ {}^1\overline{S}_0)$$

i.e., in the production of these lines, both electrons of Mg are raised from the $3s$ to the $3p$-configuration, giving rise to the levels $^3P_{0,1,2}$, $^1D_2$, $^1S_0$, and when one falls back to $3s$, the lines forming a $P\overline{P}$-multiplet are emitted. This is illustrated for Mg in Table 40. Millikan and Bowen[*] found that the lines are strong and for ions iso-electronic with Mg they follow the law of arithmetic progression as shown in the opposite table.

The value of the $3p^2\ {}^3P_{0,1,2}$-terms is extremely small, and probably the $3p$. $4p$-terms would become negative. The reason is obvious. In the normal condition, both electrons are in the level $3s$. In the $3p^2$-state, they are both transferred to $3p$. The energy required is almost equal to the ionisation potential of Mg, for the electron has to go from $3s$ to $3p$ twice, for which the energy is more than double of that required for transition from $3s$ to $3p$.

Table 41.—$P\overline{P}$-group of lines[†] in the two-valence electron systems. Mg I to Cl VI.

Element	λ in Å.U.	ν
Mg I	2777·503	36003·56
	2779·084	35983·08
	2780·639	35962·96
	2782·226	35942·44
	2783·782	35922·35
		25727·94
Al II	1760·12	56814·3
	1761·96	56755·0
	1763·95	56690·9
	1765·81	56631·2
	1767·75	56569·1
		20295·5
Si III	1294·52	77248·7
	1296·73	77118·1
	1298·93	76936·4
	1301·13	76855·3
	1303·34	76726·0
		20050·7
P IV	1025·58	97506·0
	1028·13	97264·2
	1030·53	97037·1
	1033·14	96792·4
	1035·54	96567·9
		19948·5
S V	849·25	117751·1
	852·19	117345·0
	854·81	116985·6
	857·83	116573·3
	860·46	116216·9
		19942·6
Cl VI	724·13	138096·8
	727·54	137449·5
	730·31	136928·2
	733·89	136260·2
	736·76	135729·4

342. Inner Transition.

—In cases where the normal constitution is $ns^2\ np^x$, lines are obtained corresponding to the transition.

$$ns^2\ np^x \leftarrow ns\ np^{x+1}$$
$$ns\ \ np^{x+1} \leftarrow np^{x+2}$$

---

[*] Millikan and Bowen, *Phys. Rev.*, 25, 600, 1925.

[†] Taken from Millikan and Bowen, *Phys. Rev.*, 26, 150, 1925. The ^1DS-terms have not been identified.

A number of such lines was discovered by Millikan, Bowen* and other workers. As is obvious from the above scheme, the outermost electrons are not disturbed in the discharge, as is usual in ordinary spectra, but one or more electrons are lifted from the inner s-shell to the p-shell. The lines owe their origin to the reversion of the excited electrons to the s-shell and therefore such transitions may be called *inner*. One multiplet of this type is shown below in Table 41*a*.

Table 41a.—Inner Transition for Al.

$3s^2\ 3p$ \ $3s\ 3p^2$	$2P_{\frac{1}{2}}$ 48280·96	$2P_{\frac{3}{2}}$ 48168·9
$2P_{\frac{1}{2}}$ −8362	... ...	λ 1768·95 ν 56530·9
$2P_{\frac{3}{2}}$ −8446	ν56728·3 λ1762·79	ν 56615·2 γ 1766·31

When we take an iso-electronic system of atoms and ions whose nuclear charge increases successively by one, the multiplets are found to obey the law of arithmetic progression (irregular doublet law), as in the case of Mg-triplets of $P\bar{P}$ systems.

SPECTRAL LINES DUE TO REMOVAL OF ELECTRONS FROM INNER SHELLS.

It appears that the phenomena described above are quite general, and wherever technique has been successfully developed, lines are obtained which are due to removal of electrons from some inner shell into outer valency shells beyond the outermost shell of the normal atom. Thus in the case of Al (normal constitution $3s^2\ 3p$), Paschen† obtained lines due to inter-combination between levels arising from the structures:

$$3s\,3p\,ns\quad,\quad 3s\,3p\,np\quad,\quad 3s\,3p\,nd$$

In such cases, the transitions are governed by the Laporte rule

$$\Sigma\Delta l_i = \pm 1,\ \pm 3,\ \ldots \text{etc.}$$

where l_i denotes the l-quantum number of the electron involved in the transition.

343. Absorption Spectra due to Excitation of Inner Electrons.—The phenomenon is not only confined to emission, but extends to absorption as well, as has been demonstrated by Beutler‡ in the case of Zn, Cd, Hg, Cs and probably will be found for all elements. We illustrate the case with respect to Hg.

---

* Millikan and Bowen, *Phys. Rev.*, **26**, 160, 1925; see also Paschen (*infra*).

† F. Paschen, *Ann. d. Phys.*, **12**, 509, 1932.

‡ Beutler, *Zs. f. Phys.*, **86**, 495, 710, 1933; **87**, 19, 176, 188, 1934.

The Hg-atom has got the normal structure $6s^2\ {}^1S_0$ and all the lines of normal Hg-spectrum are explained by assuming that the Hg^+-ion has the configuration $5d^{10}6s$ and the further excited states arise from the coupling of an electron to $Hg^+\ 5d^{10}6s$-core in any level higher than $6s$. These terms are all positive. The absorption spectrum of normal Hg-vapour consists of a sequence of lines which corresponds to the transition of the electron from the normal $6s^2$ to the $6s\ mp$-states, the lines being λ 2536 ($6s^2\ {}^1S_0 - 6s\ 6p\ {}^3P_1$), λ1849 ($6s^2\ {}^1S_0 - 6s\ 6p\ {}^1P_1$), etc., forming the principal series which converge at the limit λ 1188; this corresponds to the ionisation potential of 10·38 volts. This is followed by a feeble continuous absorption corresponding to the photoionisation of the Hg-atom. But Beutler carried the absorption experiments further in the Schumann region and found a number of sharp absorption lines below λ1188 one group of which apparently formed a Rydberg series as shown below:

Table 42.—Absorption series in Hg due to the excitation of the 5d-electron.

Transitions: $5d^{10}\ 6s^2\ {}^1S_0 \rightarrow 5d^9\ 6s^2\ mp\ {}^1P_1$.

Series limit: $Hg^+\ 5d^9\ 6s^2\ {}^2D_{\frac{5}{2}} = 119692\ cm^{-1}$.

n	Absorption line λ in Å.U.	ν in cm⁻¹	nx Term value referred to $^1S_0 = 84178$ cm⁻¹	$ny = nx + 35514$	n_e
6	1301·00	76864	7314	42828	1·601
7	944·45	105881	−21703	13811	2·819
8	890·69	112272	−28094	7420	3·846
9	869·30	115035	−30857	4657	4·854
10	858·38	116498	−32320	3194	5·862
11	852·12	117355	−33177	2337	6·852
12	848·07	117915	−33737	1777	7·858
13	845·26	118307	−34129	1385	8·901
14	843·42	118565	−34387	1127	9·860
15	842·02	118762	−34584	930	10·86
16	840·97	118912	−34734	780	11·86
17	840·13	119029	−34851	663	12·86
18	839·50	119119	−34941	573	13·84

The origin of the series was traced as follows. Since the lines are due to absorption by normal Hg-vapour, they must be represented by the formula $6s^2\ {}^1S_0 - nx$. We have now to find out the electron composition yielding the sequences nx. Their values are given in column 4. It is seen that they become negative after the first term, and hence cannot be due to any electron structure in which the Hg$^+$-ion is in the normal state $5d^{10}6s$. The next metastable states of Hg$^+$-ion are $5d^9 6s^2$ $^2D_{\frac{5}{2}}$, $^2D_{\frac{3}{2}}$ and the values of these terms referred to the Hg$^+5d^{10}6s$ $^2S_{\frac{1}{2}}$ -term were obtained by Paschen* from an analysis of the spectrum of Hg$^+$. These values are given below:

$$\text{Hg}^+5d^{10}6s\ ^2S_{\frac{1}{2}} = 0 \text{ cm}^{-1}.$$

$$5d^9 6s^2\ ^2D_{\frac{5}{2}} = 35514,\ ^2D_{\frac{3}{2}} = 50554 \text{ cm}^{-1}.$$

A reference to Table 42 shows that the nx-terms tend to a limit which is very nearly equal to 35514 cm^{-1}, *i.e.*, to $5d^{10}6s$ $^2S_{\frac{1}{2}} - 5d^9 6s^2$ $^2D_{\frac{5}{2}}$. Hence nx must be identified with a system of level-values arising from the configuration $5d^9 6s^2$ np. This is further confirmed by the fact that if nx-values be increased by $\delta = 35514$ cm^{-1}, the term-values so obtained form a Rydberg sequence having the series limit 119692 cm^{-1}. The $ny = (nx + \delta)$-values are shown in column 5, and the n_e-values given by $n_e = \sqrt{R/\nu}$ are to be found in column 6. It can be shown that the ny-values may be represented by the formula

$$ny = \frac{R}{(n_e + \alpha + \beta/n^2)^2}.$$

The state $5d^9$ $6s^2$ np gives us ^{3,1}(FDP), and only one of the sets n^1P_1 has been traced. Beutler found another set of absorption lines having the series limit 134732 cm^{-1}. This is due to the transition

$^1S_0 - {}^3P$ of combination $(5d^9 6s^2\ ^2D_{\frac{3}{2}})$ np, $n = 6, 7, 8, \ldots.$

and this arises from the Hg$^+$-ion $5d^9$ $6s^2$ $^2D_{\frac{3}{2}}$. The coupling is of the jj-type but we have used the notations suitable for RS-coupling for the sake of convenience of description. The result of these investigations can now be summarised as follows. When light of proper wavelength falls on the atom, they can, if the frequency be suitable, act upon the inner electrons and throw them to any one of the outer allowed levels. In the present case the act of absorption consists in the ejection of the electron from the inner $5d$-level to the external np-levels. In a way it may be regarded as an extension of the idea of inner transitions described earlier. Similar absorption lines have been obtained in the case of Zn, Cd and Cs and probably will be found in all elements.

---

* F. Paschen, *Berl. Ber.*, 1928, p. 536; J. C. McLennan, A. B. McLay M. F. Crawford, *Proc. Roy. Soc. A*, **134**, 41, 1932.

ULTRA IONISATION.

It is seen from Table 42 that the amount of energy required for the transference of the electron from the $5d$-level to the $6p$-level falls short of the I.P. of Hg by a very small amount and in the case of transference to any one of the higher np-levels the energy actually exceeds the I.P. Though in such a process the atoms do not lose any electron, *i.e.*, remain normal, its energy content is much larger than that required to ionise the atom. A similar phenomenon is known in the case of molecular spectra where sometimes the combined energy of the electronic excitation, vibration and rotation may be larger than the energy required to dissociate the molecule. When such is the case the band lines become diffuse and give rise to a phenomenon called *Pre-dissociation.*

In the case of Hg-vapour, Lawrence*, by the electron bombardment method found a number of critical potentials which are higher than the I.P. of Hg, but less than the energy required for the double ionisation. A few such values† are

10·63, 10·88, 11·53, 13·85 Volts . . . . etc.

A few of these critical potentials have been identified with the process of transference of the $5d$-electron to any one of the outer valency levels. It appears that the phenomenon is very general and Shenstone† has suggested the name *Ultra-ionisation* for it. For details of this subject original papers may be consulted.

344. Calculation of Term-values, and Ionisation Potentials.—DEFINITION OF TERM-VALUES: The determination of the absolute values of the terms in the case of complex spectra presents a problem of some ambiguity. In the case of alkalies, the value of a term represents the energy required to take the electron to infinity when the atom is in a state which gives rise to this term. Thus when we say that

$$3s\,^2S_{\frac{1}{2}} \text{ of Na} = 41448{\cdot}6 \text{ cm}^{-1},$$

---

* E. O. Lawrence, *Phys. Rev.*, **28**, 947, 1926.

† A. G. Shenstone, *Phys. Rev.*, **29**, 380, 1927; P. T. Smith, *ibid.* **37**, 308, 1931; R. G. Loyarte and M. H. de Bose, *Phys. Zeits.*, **34**, 598, 1933.

the understanding is (41448·6) *ch*-ergs or 5·368 electron-volts of energy are required to remove the electron which is in $3s\ {}^2S_{\frac{1}{2}}$ -level to infinity, or if we write symbolically :

$$\text{Na } 3s\ {}^2P_{\frac{1}{2}} + 5{\cdot}368 \text{ volts} = \text{Na}^+ + e.$$

But applied to complex spectra, this definition of term-values becomes ambiguous, unless the state at which the ionised atom is left is clearly defined. Thus for Ne when we put the values of Ne $2p^5\ 3s\ {}^3P_2 = 39887{\cdot}61\ \text{cm}^{-1}$, we make the tacit assumption that the reference state is $\text{Ne}^+\ 2p^5\ {}^2P_{\frac{3}{2}}$ and not $\text{Ne}^+ 2p^5\ {}^2P_{\frac{1}{2}}$,

$$\textit{i.e.}, \text{ Ne } 2p^5\ 3s\ {}^3P_2 + hc\,(39887{\cdot}6 \text{ cm}^{-1}) = \text{Ne}^+ 2p^5\ {}^2P_{\frac{3}{2}} + e.$$

But if the reference state were $\text{Ne}^+ 2p^5\ {}^2P_{\frac{1}{2}}$ the value of Ne $2p^5\ 3s\ {}^3P_2$ would be $39887{\cdot}6 + 782\ \text{cm}^{-1}$, as $\text{Ne}^+\ 2p^5\ ({}^2P_{\frac{3}{2}} - {}^2P_{\frac{1}{2}}) = 782\ \text{cm}^{-1}$.

In the case of Na, there is no ambiguity, as $\text{Na}^+\ 2p^6$ possesses only one stable state, *viz.*, ${}^1S_0$.

The ambiguity, wherever it may exist, may be removed by taking the lowest state of the ionised atom as the reference state as we have explained in the case of Ne just now. But this leads to the difficulty that the values of the terms arising from the metastable state of the ionised atom when referred to this standard state no longer satisfy a Rydberg sequence formula. This has already been illustrated for Ne, and for Ca, Sr, Ba and this feature is very common in complex spectra.

N.B.—Refer to p. 725 for Ne, where it has been shown that the s_2, s_3-sequence of terms follows Rydberg sequence when $782\ \text{cm}^{-1} = \text{Ne}^+ 2p^5 ({}^2P_{\frac{3}{2}} - {}^2P_{\frac{1}{2}})$ is added to these. See also the case of anomalous terms in Ca, Sr, Ba § 340.

CALCULATION OF ABSOLUTE VALUES OF TERMS.

It has been explained in §83, that the absolute values of all terms in any spectra can be determined if only the value of one term can be obtained with precision. But this again depends upon the possibility of tracing a sufficient number of terms forming a Rydberg sequence. But this is possible only in simpler types of spectra, for complex spectra where hundreds of terms are involved, it is very difficult to trace terms which follow a Rydberg sequence. In fact in the first transitional group, only the term values in the spectra of Cr may be said to have been determined with precision by Catalan* and Gieseler.†

---

* Catalan, *Phil. Trans.*, 223, 127, 1922.

† Gieseler, *Zs. f. Phys.*, 23, 228, 1924.

This was rendered possible because Cr occupies the middle position in the group, and possesses a number of septet terms which could be easily picked out as shown below :

Table 43.—Rydberg sequence in chromium spectrum (Gieseler).

Config.	Terms	Config.	Terms				
$3d^5 4s$	$^7S_3$ 54541·26	$3d^5 4p$	$^7P_4$ 31043·24	$^7P_3$ 31155·67	$^7P_2$ 31237·09		
$3d^5 5s$	$^7S_3$ 17646·90	$3d^5 4d$	$^7D_5$ 12281·33	$^7D_4$ 12284·08	$^7D_3$ 12286·27	$^7D_2$ 12287·94	$^7D_1$ 12289·12
$3d^5 6s$	$^7S_3$ 8899·22	$3d^5 5d$	$^7D_5$ 6833·04	$^7D_4$ 6837·49	$^7D_3$ 6840·31	$^7D_2$ 6842·21	$^7D_1$ 6843·51

Unlike other atoms of this group, $3d^5\,4s\ ^7S$ and not $3d^4\,3s^2$ gives the most stable state. Catalan picked out with ease the sequence $3d^5\,4p\ ^7P$, $3d^5\ ns\ ^7S$ . . . . . up to a large number of members, and could find out their values with precision by using a Rydberg formula.

For the other elements only one or two Rydberg sequences have been traced and that also sometimes not quite unambiguously. The term-values obtained from such operations are therefore subject to a good deal of uncertainty. Thus Russell obtained from two sequences

$$\text{Fe}\ 3d^6\ 4s^2\ ^5D + 63400\ \text{cm}^{-1} = \text{Fe}^+\ 3d^6 4s\ ^6D + e.$$

As $3d^6 4s\ ^6D$ is the lowest state of Fe^+, the I.P. of Fe may be said to be 63400 cm^{-1}. But this may be uncertain to the extent of ± 1000 cm^{-1}.

ALTERNATIVE WAY OF DESIGNATING TERM VALUES.

On account of these difficulties in fixing up accurately the term-values, an alternative method is used to indicate the values of the terms. The value of the lowest term is taken to be zero, and the energy required to excite the atom from the lowest state to the state represented by the term is taken to indicate the value of the term. Thus the value of Na $3p\ ^2P_{\frac{1}{2}}$ would be under this convention equal to the wave number of D_1-line of Na, that of Na $3d\ ^2D_{\frac{3}{2}}$ would be ν of $D_1 + (^2P_{\frac{1}{2}} - {}^2D_{\frac{3}{2}})$ of Na, etc.

If ν' be the energy value defined in such a way, the absolute ν-value of the term would be given by $\nu = A - \nu'$, where A=absolute value of the lowest term in cm^{-1}.

IONISATION POTENTIALS OF THE ELEMENTS AND IONS OF THE TRANSITIONAL GROUPS.

It is clear from the foregoing discussion that in defining the ionisation potentials of atoms of complex structure, the normal states of the atom and the ion involved should be clearly stated, that is to say, we should mention the state of the normal atom from which the electron is removed, as well as the state of the ion at which it is left after the removal of the electron. This is necessary because both the neutral and the ionised atoms can normally possess more than one alternative electronic configurations and each of these configurations may give rise to a number of closely lying metastable energy levels. We illustrate our remarks by the elements of the first transitional group which were very thoroughly discussed by Russell.* A glance at the chart 20 on p. 583 shows that any of the neutral atoms forming this group may have two alternative structures in its unexcited states, *viz.*, $3d^{n-2}\,4s^2$ and $3d^{n-1}\,4s$, where n varies from 1 to 10 for K to Ni. Similarly, the corresponding ionised elements have the alternative structures $3d^{n-2}\,4s$ and $3d^{n-1}$. We now define four different ionisation potentials of any such element as follows:

(A) $X\ 3d^{n-2}\,4s^2 - X^+\ 3d^{n-2}\,4s$ . . . higher multiplicities
(B) $X\ 3d^{n-2}\,4s^2 - X^+\ 3d^{n-2}\,4s$ . . . lower multiplicities
(C) $X\ 3d^{n-1}\,4s\ - X^+\ 3d^{n-1}$ . . . higher multiplicities
(D) $X\ 3d^{n-1}\,4s\ - X^+\ 3d^{n-1}$ . . . lower multiplicities

where X stands for the element.

(A) corresponds to the removal of a $4s$-electron from $X\ 3d^{n-2}\,4s^2$ and conversion of the atom to the ion $X^+\ 3d^{n-2}\,4s$. But $X\ 3d^{n-2}\,4s^2$ as well as $X^+\ 3d^{n-2}\,4s$ possess a large number of levels. It is understood that those with the lowest energy-values (therefore possessing the *highest multiplicity* and highest l) are involved in both cases. Thus in Sc, we have corresponding to (A) Sc $3d\ 4s^2\ {}^2D_{\frac{3}{2}}$ − Sc$^+$ $3d\,4s\ {}^3D_3$ = 6·57 volts.

(B) corresponds to the removal of the $4s$-electron from $X\ 3d^{n-2}\,4s^2$ and conversion to $X^+\ 3d^{n-2}\,4s$, when both X and X$^+$ are energy states of *lower multiplicities* arising out of the two configurations respectively; *e.g.*, for Sc, we have corresponding to (B) Sc $3d\ 4s^2\ {}^2D \rightarrow$ Sc$^+$ $3d\ 4s\ {}^1D$ = 6·88 volts.

(C) and (D) correspond to similar processes between terms of higher and lower multiplicities respectively for the alternative structure $X\ 3d^{n-1}\,4s$ to $X^+\ 3d^{n-1}$. For Sc they can be represented as (C) Sc $3d^2\ 4s\ {}^4F$ − Sc$^+$ $3d^2\ {}^3F$ = 5·74 volts, and (D) Sc $3d^2 4s\ {}^2F$ − Sc$^+ 3d^2\ {}^3F$ = 5·33 volts.

The values of I.P. corresponding to the four processes (A), (B), (C), (D) for different neutral elements are shown in Table 44, columns 3, 4, 5, 6.

---

* H. N. Russell, *Astr. Journ.*, 66, 249, 1927.

Table 44.—Ionisation Potentials of elements of the first transitional group.

		NEUTRAL ATOM					IONISED ATOM			
Config.→		$3d^{n-2}4s^2 - 3d^{n-2}4s$		$3d^{n-1}4s - 3d^{n-1}$		Principal I.P.	$3d^{n-2}4s - 3d^{n-2}$		$3d^{n-1} - 3d^{n-2}$	Principal I.P.
Elem.	n	States . . . I.P. A	States . . . I.P. B	States . . . I.P. C	States . . . I.P. D		States . . . I.P. C	States . . . I.P. D	States . . . I.P. E	
19 K	1	...	...	^{2}S – ^{1}S...4·30	...	4·32	...	...	...	
20 Ca	2	^{1}S—^{2}S.. 6·21	...	^{3}D—^{2}D...5·39	^{1}D—^{2}D ..5·22	6·09	^{2}S – ^{1}S...11·83	...	^{2}D – ^{1}S...10·13	11·82
21 Sc	3	^{2}D—^{3}D.. 6·57	^{2}D—^{1}D...6·88	^{4}F – ^{3}F...5·74	^{2}F – ^{3}F...5·33	**6·57**	^{3}D – ^{2}D...12·80	^{1}D – ^{2}D...12·49	^{3}F – ^{2}D...12·19	12·84
22 Ti	4	^{3}F—^{4}F...6·79	^{3}F – ^{2}F...7·39	^{5}F – ^{4}F...6·10	^{3}F – ^{4}F...5·48	6·81	^{4}F – ^{3}F...13·60	^{2}F – ^{3}F...12·99	^{4}F – ^{3}F.. 13·45	**13·60**
23 V	5	^{4}F—^{5}F...7·04	^{4}F – ^{3}F...7·84	^{6}D – ^{5}D...6·46	^{4}D – ^{5}D...5·68	6·76	^{5}F – ^{4}F...14·4	^{3}F – ^{4}F...13·5	^{5}D – ^{4}F...14·7	14·1
24 Cr	6	^{5}D—^{6}D...7·28	^{5}D – ^{4}D.. 8·21	^{7}S – ^{6}S...6·70	^{5}S – ^{6}S...5·76	6·67	^{6}D – ^{3}F...15·1	^{4}D – ^{3}F.. 14·1	^{6}S – ^{3}F...16·6	**16·64**
25 Mn	7	^{6}S—^{7}S...7·38	^{6}S – ^{5}S...8·55	^{6}D – ^{5}D...7·06	^{4}D – ^{5}D...6·28	7·40	^{7}S – ^{6}S...15·70	^{5}S – ^{6}S...14·52	^{5}D – ^{6}S...13·80	15·72
26 Fe	8	^{5}D—^{6}D...7·83	^{5}D – ^{4}D...8·81	^{5}F – ^{4}F...7·20	^{3}F – ^{4}F...6·58	**7·83**	^{6}D – ^{5}D...16·5	^{4}D – ^{5}D...15·4	^{4}F – ^{5}D...16·3	16·19
27 Co	9	^{4}F—^{5}F...8·25	^{4}F – ^{3}F...9·0	^{4}F – ^{3}F...7·38	^{2}F – ^{3}F.. 6·90	8·5	^{5}F – ^{4}F...16·8	^{3}F – ^{4}F...16·0	^{3}F – ^{4}F...17·2	**17·3**
28 Ni	10	^{3}F—^{4}F. 8·65	^{3}F – ^{2}F.. 9·30	^{3}D – ^{2}D...7·62	^{1}D – ^{2}D.. 7·22	7·606	^{4}F – ^{3}F ..17·15	^{2}F – ^{3}F...16·50	^{2}D – ^{3}F...18·2	**18·2**

Column 7 gives the *principal ionisation potentials* of the elements, that is, the energy required to remove an electron from the lowest energy state of the neutral atom to the lowest energy state of the atom in the first stage of ionisation. For Ca, Sc, Ti, Mn and Fe this corresponds to the process of the type (A) as the lowest energy-terms for their normal and ionised atoms arise from the configurations $3d^{n-2}\,4s^2$ and $3d^{n-1}\,4s$. For K and Cr it corresponds to the type (C) as in these cases the lowest energy-terms come from the alternate structures $3d^{n-1}\,4s$ and $3d^{n-1}$ respectively for their atoms and ions. In both these cases the process involves the removal of an 4*s*-electron. For V and Co however the principal I. P. corresponds to the process X $3d^{n-2}\,4s^2$ — X$^+$ $3d^{n-1}$, which involves the removal of an 4*s*-electron and simultaneous shift of another electron from 4*s* to 3*d*. But a glance at the table shows that except in a few cases (indicated in thick figures) the values of principal I.P.'s in column 7 do not exactly agree with the values in columns 3 or 5 corresponding to (A) or (C) even in the cases they are expected to agree. In such cases, the values in column 7 should, however, be regarded as more accurate than the others, as these have been calculated from a long Rydberg sequence of lines, while those in the other columns were generally derived from the wavelengths of only first two members of the series (*vide* § 182, p. 363).

In the same way we get three sets of I. P.'s also for the ionised elements (shown in the columns 8, 9, 10 of the table). They can be explained similarly. Here the processes involved are:—

(C) X$^+$ $3d^{n-2}\,4s$ — X^{++} $3d^{n-2}$......Higher multiplicities

(D) X$^+$ $3d^{n-2}\,4s$ — X^{++} $3d^{n-2}$......Lower multiplicities

(E) X$^+$ $3d^{n-1}$ — X^{++} $3d^{n-2}$

The principal I.P.'s for Ca$^+$, Sc$^+$, Ti$^+$, Mn$^+$ and Fe$^+$ involve the removal of an *s*-electron, those for V$^+$, Cr$^+$, Co$^+$ and Ni$^+$ of a *d*-electron. The values are given in the last column.

345. The Horizontal Comparison Method.

—In § 270, we gave a short account of the irregular doublet law and pointed out how it could be utilized as a useful guide for the location of the spectral lines of iso-electronic elements or ions. Another empirical principle may now be described which has also been successful in locating such spectra. This new method has been styled as the method of *Horizontal Comparison*.[*]

We start with Table 45 to explain the way in which the spectra of certain iso-electronic elements can be located.

---

[*] M. N. Saha and K. Mazumdar, *Ind. Jour. Phys.*, 2, 67, 1928. See also Gibbs and White, *Phys. Rev.*, 29, 426, 1927.

Table 45.—Showing the regularity in $2p^{x-1}$ $(3s \leftarrow 3p)$-transitions.

$x-1$	0	1	2	3	4	5	6
(1)	...	${}^3P_2 - {}^3D_3$	${}^4P_{\frac{5}{2}} - {}^4D_{\frac{7}{2}}$	...	${}^4P_{\frac{3}{2}} - {}^4\overline{P}_{\frac{3}{2}}$	${}^3P_1 - {}^3S_1$	
(2)	${}^2S_{\frac{1}{2}} - {}^2P_{\frac{3}{2}}$	${}^3P_2 - {}^3S_1$	${}^4P_{\frac{3}{2}} - {}^4\overline{P}_{\frac{3}{2}}$	${}^5S_2 - {}^5P_2$	${}^4P_{\frac{5}{2}} - {}^4D_{\frac{7}{2}}$	${}^3P_2 - {}^3D_3$	${}^2S_{\frac{1}{2}} - {}^2P_{\frac{3}{2}}$
(3)	...	${}^3P_2 - {}^3\overline{P}_2$	${}^4P_{\frac{3}{2}} - {}^4S_{\frac{3}{2}}$	...	${}^4P_{\frac{3}{2}} - {}^4S_{\frac{3}{2}}$	${}^3P_1 - {}^3P_2$	
I	B	C	N	O	F	Ne	Na
(1) (2) (3)	... [16000] ...	9352 10348 10993 Fowler[1]	11475 12175 13433 Ingram[2]	... 12860 ... Fowler[1a]	13360 14582 15747 Dingle[3]	13798 15615 16399 Saha[4]	... 16973 ... Fowler[1b]
II	C^+	N^+	O^+	F^+	Ne^+	Na^+	Mg^+
(1) (2) (3)	... 15198 ... Fowler[1c]	17602 19816 21590 Fowler[1d]	21446 23052 26821 Fowler[1e]	... 25067 ... Jog[5]	26767 29977 33004 Kichlu[6]	27530 32323 34411 Mazumdar[7]	... 35761 ... Fowler[1f]
III	N^{++}	O^{++}	F^{++}	Ne^{++}	Na^{++}	Mg^{++}	Al^{++}
(1) (2) (3)	... 24399 ... Bowen[8]	26589 29926 32808 Fowler[1g]	31897 34410 40558 Dingle[3a]	... 38545 ... Jog[5]	39509 44822 50364 [10]	30510 48413 51970 [10]	... 53918 ... Paschen[9]
IV	O^{+++}	F^{+++}	Ne^{+++}	Na^{+++}	Mg^{+++}	Al^{+++}	Si^{+++}
(1) (2) (3)	... 32683 [10]	... [39000] ...	... [45500] ...	... [52000] ...	51921 59416 67096 [10]	53158 64216 69357 [10]	... 71740 ... ...

In the row marked I we have the elements B, C, ... Na whose normal electron structure up to Ne is $2p^x$, where x varies from 1 to 6, and for Na it is $2p^6\ 3s$. In the excited states one of the p electrons in elements up to Ne will pass on successively to higher orbits while in the case of sodium the $3s$-electron will be excited. In this way the number of p-electrons in the excited states of the elements of row I will vary from 0 to 6. The frequencies of the lines arising from the transitions between highest multiplicity levels when the electronic transition corresponds to $2p^{x-1}$ $(3s \leftarrow 3p)$ are shown under each element. The number of such transitions are denoted by (1), (2), and (3) which are shown at the top of the table and frequencies of corresponding lines are indicated similarly. If these frequencies be plotted as ordinates against $n = x - 1$ ($n = 0$ for B to 6 for Na), and a curve be drawn through the strongest of these lines, we obtain approximately a straight line, about which the other multiplets are arranged as shown in Fig. 14. It is clear from the diagram that the frequencies of the lines increase regularly for the elements or the ions of the same row as the atomic number increases.

---

[1] Fowler, *Proc. Roy. Soc. A*, **118**, 42, 1928. [1a] *Fowler's Report*, p. 168. [1b] *Fowler's Report*, p. 99. [1c] Fowler, *Proc. Roy. Soc. A*, **105**, 306, 1924. [1d] Fowler and Freeman, *ibid.* **114**, 665, 1927. [1e] Fowler, *ibid.* **110**, 484, 1926. [1f] *Fowler's Report*, p. 120. [1g] Fowler, *Proc. Roy. Soc. A*, **117**, 325, 1928.
[2] Ingram, *Phys. Rev.*, **34**, 421, 1929; Kiess, *Jour. Opt. Soc. Am.*, **11**, **4**, 1925.
[3] Dingle, *Proc. Roy. Soc. A*, **113**, 326, 1927. [3a] *ibid.* **122**, 144, 1929.
[4] Saha, *Phil. Mag.*, **4**, 326, 1927. [5] Jog, *Ind. Jour. Phys.*, **2**, 344, 1928.
[6] Kichlu, *Proc. Phys. Soc.*, **39**, 424, 1927. [7] Mazumdar, *Ind. Jour. Phys.*, **2**, 353, 1928. [8] Bowen, *Phys. Rev.*, **29**, 234, 1927. [9] Paschen, *Ann. d. Phys.*, **71**, 151, 1923. [10] Söderqvist, *Nova Acta Soc. Sc. Upsala*, IV, **96**, 1934.

The row marked II shows lines due to singly charged ions C^+ to Mg^+, having the same electronic structure as elements above them in row I, and for them the corresponding frequencies are plotted in the same manner. They also lie approximately on a straight line thus showing a linear relation between the frequency of the line and the number of electrons in the p-shell. It may also be noted that the relative positions of the lines belonging to any ion are the same in the two curves. Thus comparing the positions of the multiplets of Ne and Na^+, it will be found that ${}^3P_2 - {}^3D_3$ is just on the line, while ${}^3P_1 - {}^3P_2$ is above and ${}^3P_1 - {}^3S_1$ is below it. The lines of row III behave in a similar manner.

It is expected that the unidentified lines of F^{+++}, Ne^{+++} and Na^{+++} due to the transition $2p^{x-1}$ $(3s \leftarrow 3p)$ and of higher ionised groups of iso-electronic elements would behave similarly. The rule can, therefore, be successfully used for the location of the spectra of ionised elements in various stages of their ionisation in the following way. Take the two end-ions of row IV which give simple doublet lines 32633 and 71740 cm^{-1} as observed by Söderqvist and Fowler. We can join these lines and proceed to locate the lines of the intervening ions. The lines due to Mg^{+++} and Al^{+++} are found to lie on the same straight line; but the lines due to F^{+++}, Ne^{+++} and Na^{+++} can be located at 39000, 45500, and 52000 respectively. This can be easily verified when lists of such lines are available.

It has been shown that this rule may be utilised to locate lines due to transition $2p^{x-1}$ $(3p \leftarrow 3d)$ as well as of the higher groups Al to K and other transitions.

346. Metastable Levels and Forbidden Lines.

—So far we have used the term metastable level in a vague way without giving any serious consideration to the meaning attached to it. In the present section we describe metastable levels under two heads: (i) If an atom or ion in some excited state gives rise to certain levels such that transition from these to the levels of the ground state is barred by some selection principle, then the excited

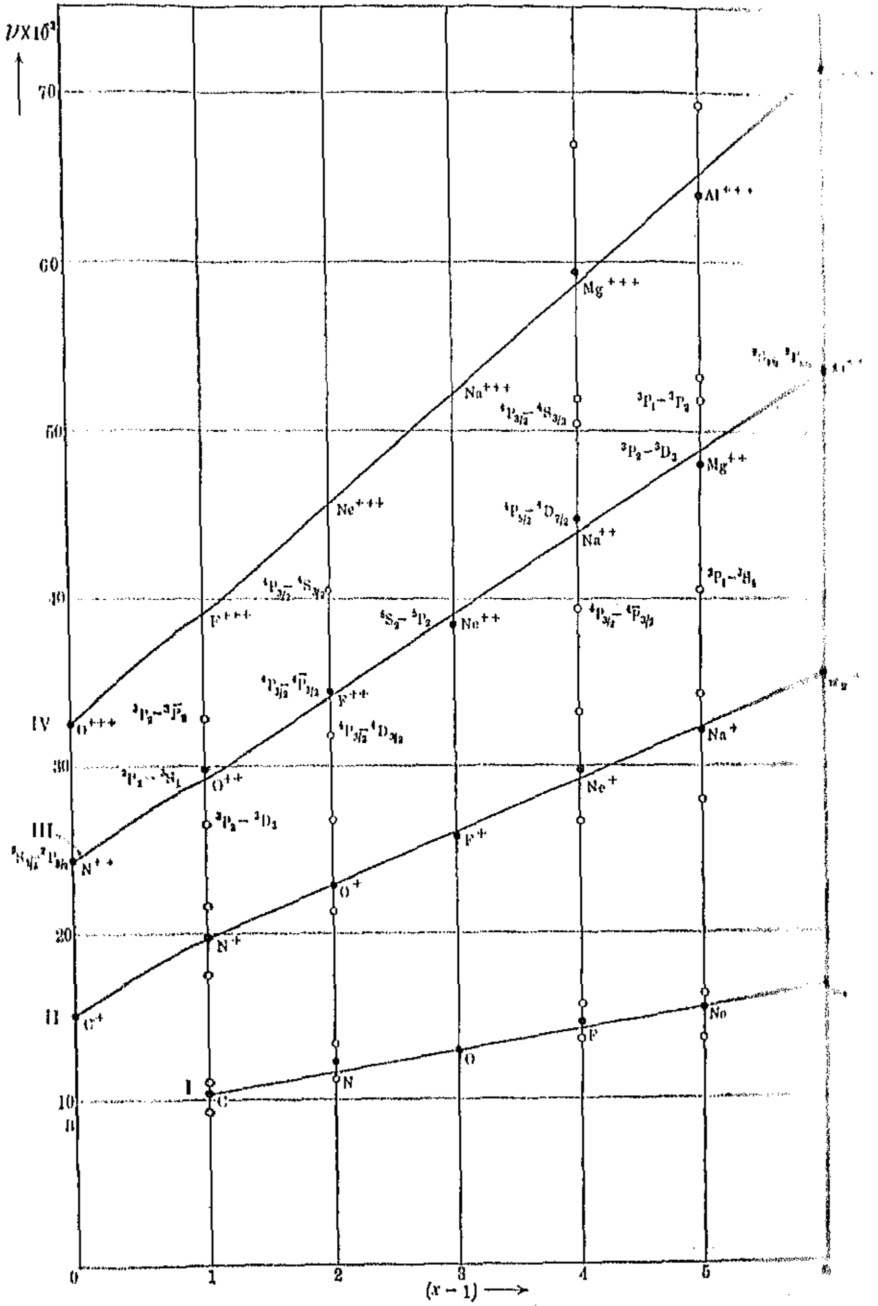

Fig. 14. Horizontal comparison of frequencies of lines due to isoelectronic systems.

levels may be said to be *metastable.* Such a case has already been mentioned in Ne $2p^5\ 3s\ ^3P_{2,\ 0}$ which cannot revert to the normal state $2p^6\ \ ^1S_0$. Plenty of other examples may be picked up in the transitional group of elements. (ii) When we take the fundamental electron configuration of an atom, we have seen that it gives rise generally to a number of levels. The atom in the unexcited condition is mostly in the lowest of these levels, but if it be excited to any of the higher levels arising from the same fundamental electron configuration, it cannot revert back to the lowest level as $\Delta l_i=0$ the electron configuration being the same. Hence the higher levels are said to be *metastable.* Thus in Oxygen, the fundamental electron configuration $2p^4$ gives rise to $^3P_{2,1,0}$, $^1D_2$, $^1S_0$. Here $^3P_2$ is the normal level. $^3P_{1,0}$, $^1D_2$, $^1S_0$ are the metastable levels.

The difference in energy between the stable and metastable levels of type (ii) in most cases is generally small, but sometimes as in O ($^3P_2-{}^1D_2$), it may be considerable. The question arises, if in such cases we may not sometimes get a weak line corresponding to such *forbidden transitions.*

The first observation of this kind in the laboratory was made by N. K. Sur* who, while measuring the arc spectrum of Pb observed two lines, which he interpreted as follows :

$$\lambda\ 7330{\cdot}3=6p^2\ ^3P_1-{}^1D_2\ ;\ \lambda\ 4618{\cdot}21=6p^2\ ^3P_1-{}^1S_0$$

They occur faintly in the arc, but more strongly when heavy currents are passed. Similar lines were observed by Sur in the arc spectrum of Bi. But in lighter elements possessing similar structure such transitions were not observed in any laboratory.

A new chapter in this direction was opened by Bowen† who proved conclusively that a number of lines which are found in the spectra of planetary nebulae and Wolf-Rayet stars (which are ancient nebulae), and whose origin was a matter of mystery for a long time could definitely be assigned to the forbidden transitions of the second type just mentioned. The most famous of these lines are λ 5006·84 and λ 4958·91 which invariably occur in the spectra of nebulae as shown in Fig. 15, Plate XI.

These lines could not be identified with the lines of any known element on earth and it was thought that they belonged to a hypothetical element called Nebulium. But no place can be found

---

* N. K. Sur, *Phil. Mag.*, 51, 633, 1926.

† Bowen, *Phys. Rev.*, 29, 231, 1927; *Astr. Journ.*, 67, 1, 1928.

PLATE XI

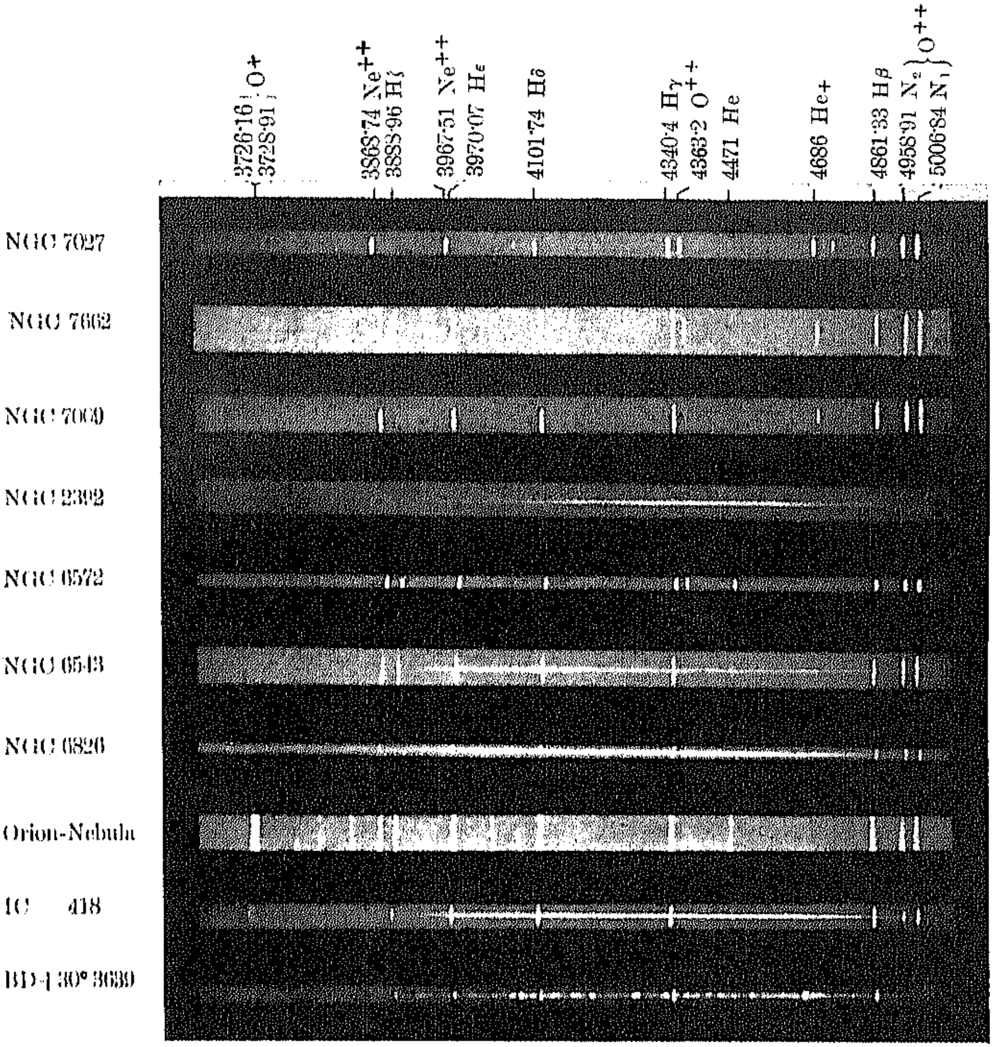

Fig. 15.—Spectra of galactic nebula (*Wright, Lick observatory Bulletin*).

(*p.* 748).

NGC 7027—denotes no 7027 in the New General Catalogue.
IC—International Catalogue.
BD—Bonnsche Durchmusterung.

[*f. p.* 748

for an element *Nebulium* in the Periodic Table. To any body who had experience of handling astrophysical data, it was apparent that the N_1 and N_2 lines were organically connected and must be due to some light element in a highly ionised state. Now Bowen found that the frequency difference between these two lines was $\Delta\nu = 193\ (=20160-19967)\text{cm}^{-1}$ and he remembered that 193 was also the difference between the fundamental terms $2s^2\,2p^2\ (^3P_1-{}^3P_2)$ of O^{++} as found by himself and Millikan in the vacuum spectrograph. It was also discovered by them that the fundamental lines of O^{++} due to the transition $(2p^2-2p3s)$ were all in the Schumann region. Hence he argued that the lines in question can only be due to the O^{++}-metastable transition $2s^2 2p^2\ {}^3P_{1,2} - 2s^2 2p^2\ {}^1D_2$ as shown in Fig. 16.

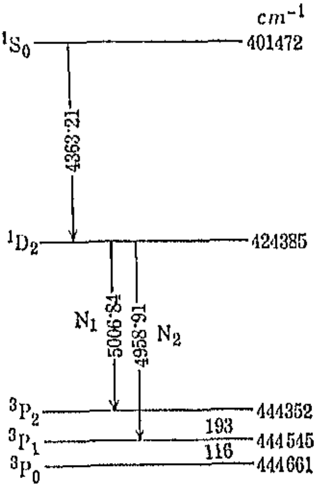

Fig. 16. Origin of nebular lines λ5006·84 and λ4958·91.

Once a clue was obtained, it was merely a matter of time before the origin of many other lines obtained in Nebulae were traced to their source. A list of such forbidden lines is given in Table 46.

Very few of these lines have been observed in the laboratory. The fact that these lines are obtained only in Nebulae led Bowen to the conclusion that it is probably the extremely low density of matter in nebulae which provides an extraordinary condition favourable for the occurrence of metastable transitions. Under ordinary laboratory conditions the time between two successive collisions can only be 10^{-8} sec., under extreme cases. Hence the atom would pass to the lowest state by collisions of the second kind before it can emit radiation. But in nebulae the density is so low that the time between two collisions is 10^4 to 10^7 secs., so that once the atom is in the metastable state, there is nothing left to it except to revert to the normal level as it has no opportunity of colliding with other atoms. While this explanation of the origin of nebular lines may be true, many attempts ever since made to observe these nebular lines in the laboratory are still without success.

Lines due to transitions in metastable levels of the second type described above were observed for the Fe^+ ion by Merrill* in

---

* Merrill, *Astr. Journ.*, 67, 391, 1928.

Table 46.—List of Forbidden lines in Astrophysical Sources.[*]

Element	Line	Transition	Occurrence
CI	4621·5	$2s^2 2p^2\ {}^3P_1 - 2s^2 2p^2\ {}^1S_0$	Nova.
NII	5754·8	$2s^2 2p^2\ {}^1D_2 - 2s^2 2p^2\ {}^1S_0$	Nova, Nebulae.
	6547·0	$2s^2 2p^2\ {}^3P_1 - 2s^2 2p^2\ {}^1D_2$	Nova, Nebulae
	6583·3	$2s^2 2p^2\ {}^3P_2 - 2s^2 2p^2\ {}^1S_2$	Nebulae, Nova.
OI	6300·3	$2s^2 2p^4\ {}^3P_2 - 2s^2 2p^4\ {}^1D_2$	Night Sky, Nova, Nebulae.
	6363·7	$2s^2 2p^4\ {}^3P_1 - 2s^2 2p^4\ {}^1D_2$	Night Sky, Nova, Nebulae.
	5577·3	$2s^2 2p^4\ {}^1D_2 - 2s^2 2p^4\ {}^1S_0$	Aurora, Nova.
OII	7321	$2s^2 2p^3\ {}^2D_{\frac{5}{2}} - 2s^2 2p^3\ {}^2P_{\frac{3}{2}}$	Nebulae.
	7324	$2s^2 2p^3\ {}^2D_{\frac{5}{2}} - 2s^2 2p^3\ {}^2P_{\frac{1}{2}}$	Nebulae.
	7332	$2s^2 2p^2\ {}^2D_{\frac{3}{2}} - 2s^2 2p^3\ {}^2P_{\frac{3}{2}}$	Nebulae.
	7334	$2s^2 2p^3\ {}^2D_{\frac{3}{2}} - 2s^2 2p^3\ {}^2P_{\frac{1}{2}}$	Nebulae.
	3726·1	$2s^2 2p^3\ {}^4S_{\frac{3}{2}} - 2s^2 2p^3\ {}^2D_{\frac{3}{2}}$	Nebulae, Nova.
	3727·8	$2s^2 2p^3\ {}^4S_{\frac{3}{2}} - 2s^2 2p^3\ {}^2D_{\frac{5}{2}}$	Nebulae, Nova.
OIII	4363·1	$2s^2 2p^2\ {}^1D_2 - 2s^2 2p^2\ {}^1S_0$	Nova, Nebulae.
	4958·9	$2s^2 2p^2\ {}^3P_1 - 2s^2 2p^2\ {}^1D_2$	Nova, Nebulae.
	5007·1	$2s^2 2p^2\ {}^3P_2 - 2s^2 2p^2\ {}^1D_2$	Nova, Nebulae.
NeIII	3342	$2s^2 2p^4\ {}^1D_2 - 2s^2 2p^4\ {}^1S_0$	Nova, Nebulae.
	3868	$2s^2 2p^4\ {}^3P_2 - 2s^2 2p^4\ {}^1D_2$	Nova, Nebulae.
	3967	$2s^2 2p^4\ {}^3P_1 - 2s^2 2p^4\ {}^1D_2$	Nova, Nebulae.
SI	5365	$3s^2 3p^4\ {}^3P_1 - 3s^2 3p^4\ {}^1S_0$	Nova.
SII	6717	$3s^2 3p^3\ {}^4S_{\frac{3}{2}} - 3s^2 3p^3\ {}^2D_{\frac{5}{2}}$	Nova.
	6731	$3s^2 3p^3\ {}^4S_{\frac{3}{2}} - 3s^2 3p^3\ {}^2D_{\frac{3}{2}}$	Nebulae.
	4068	$3s^2 3p^3\ {}^4S_{\frac{3}{2}} - 3s^2 3p^3\ {}^2P_{\frac{3}{2}}$	Nova, Nebulae.
	4076	$3s^2 3p^3\ {}^4S_{\frac{3}{2}} - 3s^2 3p^3\ {}^2P_{\frac{1}{2}}$	Nova, Nebulae.

the spectrum of η-Carinae. He observed lines due to transitions

$$3d^6 4s\ {}^6D - 3d^5\ 4s^2\ {}^4P,\ {}^4F$$

$$3d^7\ {}^4F - 3d^5\ 4s^2\ {}^4F,\ {}^4G$$

Later on Merrill discovered a number of such forbidden lines in other stellar spectra.[†]

---

[*] A good account of this subject will be found in *Ergebnisse der exakten Naturwiss*, 7, 8, 1928, article by Becker and Grotrian; see also *Proc. Nat. Acad. Sci.*, 1934

[†] Merrill, *Mt. Wil. Obs. Cont.*, Nos., **354, 381, 444.**

THE GREEN AURORAL LINE.

In the polar regions of the earth when there is a continuous night for several days or even months depending upon the latitude during the winter, the sky is sometimes found illuminated by luminous electric discharges of various forms and colour S to which the name *Aurora* is given. In the Northern Hemisphere it is designated as *Aurora Borealis* and in the Southern it is called *Aurora Austrealis.* The auroral displays are generally accompanied by magnetic storms. It has been observed that during an auroral discharge, wireless signals are greatly disturbed. Aurora is supposed to be due to the bombardment of the upper regions of the atmosphere by high-speed electrons ejected by the sun and deflected towards the magnetic poles of the earth by the earth's field. They are always found to occur above certain heights. The spectra of these auroral displays were first studied by Ångstrom in 1869 and ever since they have been objects of searching studies in the hands of Vegard,* McLennan and many others.

The spectra of auroral displays are mostly found to consist of bands due to N_2 but the most prominent feature of the spectrum is an intense green line. The green auroral line could not be traced to any element on the earth and it was supposed to be due to some hypothetical element called Geocoronium present in the higher regions of the atmosphere. Long before its identification, its wavelength was measured by Babcock† by means of a Fabry Perot Interferometer and found to be λ 5577·35 ± 0·005 Å. U. Before this determination, its wavelength was uncertain by ±20Å. U.

The auroral green line λ 5577 was first obtained by McLennan‡ in the laboratory from condensed discharge in oxygen which was mixed with an inert gas, preferably argon. Later it was obtained in pure oxygen. Then McLennan showed from the Zeeman effect of the line that it was due to the forbidden transition ${}^1D_2 - {}^1S_0$ between the metastable levels of neutral oxygen.

RED FORBIDDEN LINES OF OXYGEN.

Paschen, Hopfield, and Frerichs‖ found in the laboratory lines which they identify with the forbidden lines of oxygen as follows:

$$\lambda\ 6300 = 2p^4\ {}^3P_2 - 2p^4\ {}^1D_2 \text{ and } \lambda\ 6363 = 2p^4\ {}^3P_1 - 2p^4\ {}^1D_2.$$

---

* Vegard, *Zs. f. Phys.*, **78**, 574, 1932. Paschen, *Zs. f. Phys.*, **65**, 1, 1930.

† Babcock, *Astr. Journ.*, **57**, 209, 1923.

‡ McLennan, *Proc. Roy. Soc. A*, **114**, 1, 1927.

‖ Frerichs, *Phys. Rev.*, **36**, 39, 1930.

L. A. Sommer* thinks that these two lines occur also in the spectrum of night sky as well as in the aurora, but they are mixed up with contiguous lines of the band spectra of O_2 and N_2. The identification is open to certain amount of uncertainty. The red auroral lines, but not the green, have been detected by Bowen in the spectra of certain nebulae (*Phys. Rev.*, **36**, 600, 1930.)

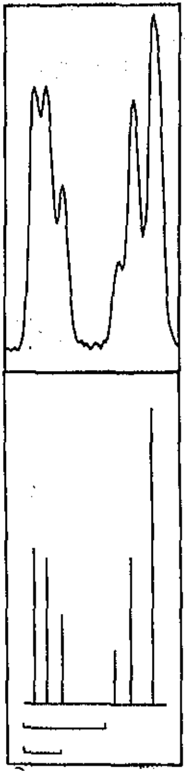

Fig. 18. Microphotogram showing the hfs- of Bi λ4722.

347. Hyperfine Structure of Spectral Lines.—We shall now close this chapter after giving a short account of the hyperfine structure of spectral lines, a subject which was discovered by A. Michelson in the year 1881, while he was looking for a source of strictly monochromatic light which can serve as a fundamental standard for wavelength measurements. He found, that many lines which were previously regarded as monochromatic when instruments of moderate resolving power were used, were found to consist of numerous close components when they were examined by his interferometer. In fact, of the many lines which he examined only one was found free from such fine structure. This was the red line of Cd λ6438 which was adopted as the primary standard in all measurements of the unit of length.

As a typical example of the hyperfine structure of spectral lines, we may take the strong line λ4722 of the Bismuth arc spectrum, photographed by Zeeman, Back and Goudsmit.† The photograph is shown in plate XII, Fig. 17, and its microphotogram is shown above (Fig. 18). The line is found to consist of six closely lying components whose wavelengths and intensities are given in Table 47.

Table 47

λ in Å.U.	Int.	ν in cm^{-1}
4722·652	5·5	21168·640
·618	5	68·792
·574	3·5	68 989
·433	2	69·620
·389	5	69·816
·332	10	70·074

---

* Sommer, *Zs. f. Phys.*, 80, 273, 1933; **77**, 374, 1932.

† Zeeman, Back and Goudsmit, *Zs. f. Phys.* **66**, 1, 13, 31, 1930 ; **70**, 1, 1931. In this subject we have followed the excellent treatment given by Pauling and Goudsmit in their book *The Structure of Line Spectra.*

PLATE XII

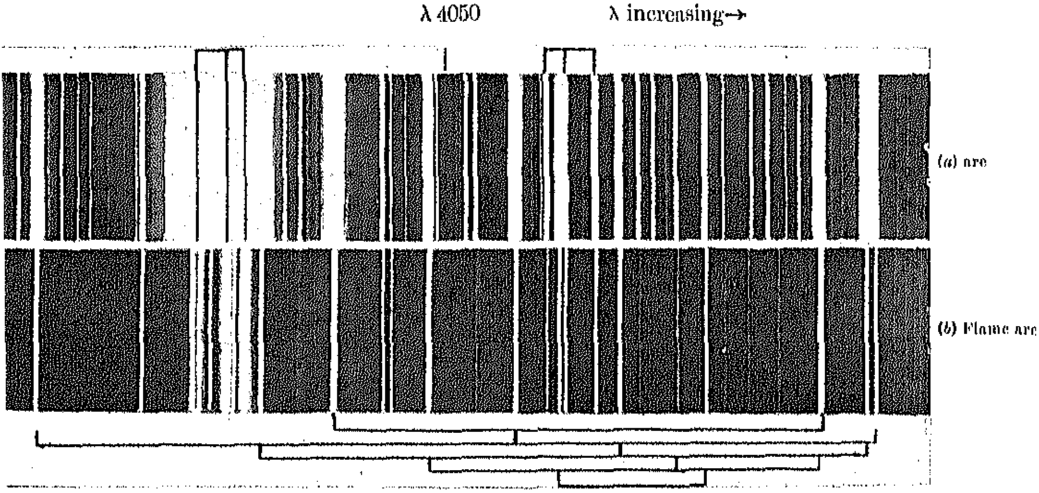

Fig. 2a.—Spectra of Mn $({}^6F-{}^6D)$-multiplet (*Catalan*).
(*p.* 677).

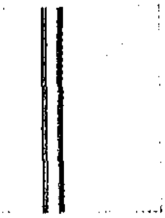

Fig. 17.
perfine Structure of
l line λ4722 (IV ord.).
oudsmit and Back)
(*p.* 752).

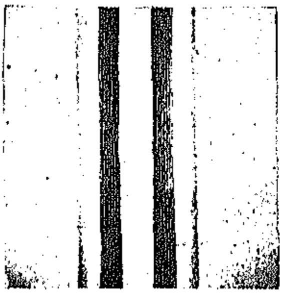

Fig. 20.
Zeeman effect in the hyperfine structure
of Bi λ 4722 (IV ord. magnified 5 times).
(*Goudsmit and Back*)
(*p.* 763).

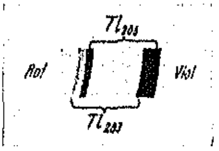

Fig. 22.
Hyperfine structure of
Tl λ 5351 (*Schüler*)
(*p.* 764).

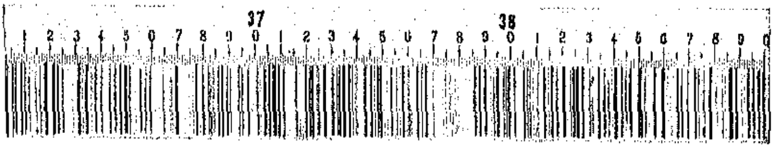

Fig. 1.—Spectrum of Fe between λ3600–λ3900 (Fabry any Buisson).
(*p.* 676).

[*f. p.* 752

PHYSICAL NATURE AND IMPORTANCE OF THE PHENOMENA.

The separations are extremely small, about 10^{-4} to 10^{-3} times the multiplet separations discussed in this chapter. Thus for Bi the multiplet separations are of the order of $\Delta\nu \simeq 15000$ cm^{-1}. But the *hf*-separations vary from 10^{-1} to 1 cm^{-1}. For a long time the origin of these separations was shrouded in mystery, as the theories of multiplet formation offered no possibility of their explanation, though suggestions were made from time to time that the *hfs*-complexity might partly be of isotopic origin, that is to say, as most elements are mixtures of isotopes having different masses, the spectral lines would possess slightly different frequencies owing to the mass-effect as given on p. 334. But though isotopes account to some extent for the *hfs*-complexity, their origin must be due to some other important factor, as there are elements like Bi which possess no isotopes, but still show clear *hfs*-complexity. At this stage Pauli came forward with the helpful suggestion that the nucleus, which is regarded in theories of multiplet structure as a spherical point of electricity, may possess, like the electron, a definite angular momentum, and a definite magnetic moment; and the *hfs*-splitting is probably due to the interaction of the nuclear magnet with the extra-nuclear electrons. This suggestion proved extremely helpful and opened a new field for exploring the structure of the nucleus with the aid of spectroscopic data as the following short account will show.

EXPERIMENTAL METHODS.

For precision works on the *hf*-structure of spectral lines the following points must be attended to: (*a*) The spectroscopic apparatus used must have extremely high-resolving power, so that frequency differences of the order of 10^{-2} cm^{-1} can be dealt with. (*b*) The source of light should be such that the lines are extremely sharp. (*c*) In the choice of the source of light, all processes like self-reversal, selective excitation which can falsify the distribution of intensity in the *hf*-structure of the spectral lines should be avoided.

The spectroscopic apparatus used in practice are mostly interference spectroscopes of the Fabry-Perot or Lummer-Gehrcke pattern. For these apparatus, see an article by G. Hansen, in the *H. d. Physik, Optik, II.* For the use of the Lummer-Gehrcke plate, the reader may consult the following papers: Gehrcke and Lau, *Multiplet Interval in Spectroscopy, Phys. Zeits.*, **31**, 973, 1930; Lau, *Zs. f. Phys.*,

63, 313, 1931. The echelon grating has also been used for this purpose with success. See E. W. Williams, *Applications of Interferometry*. The resolving power used in these apparatus is about 10^6.

The source of light now generally used in these investigations is the Schüler lamp, for a description of which the student may consult Schüler, *Zs. f. Phys.* **59,** 149, 1930; Ritschl, *ibid.* **79**, 1, 1932.

348. Hyperfine Structure of Bismuth Lines.—For getting a complete idea of the experimental and theoretical work on this subject it is advisable that the reader has a fair knowledge of the classification of the arc lines of Bismuth, because most of the earlier precision works of Back, Goudsmit and Zeeman which are now leading to the elucidation of the subject were done on Bi-lines. Bismuth was chosen because being a heavy element, its spectral lines are extremely fine; secondly, according to Aston, it has no isotopes

Table 48.—Classification of the spectral lines of Bi.*

$6p^3 \to$	$^4S_{3/2}$	$D_{3/2}$	$^2D_{5/2}$	$^2P_{1/2}$	$^2P_{3/2}$	Term value
$6p^2\ 7s$ A $(^3P_0)\ ^2S_{1/2} \to {}^4P_{1/2}$	32587·9 3067·73 (10 R)	21170·7 21169·1 21167·8 4722·12 4722·54 4722·80 (10) (10) (10)	...	(10927)	...	25975
$6p^2\ 6d$ B $(^3P_0)\ ^2D_{3/2}$ $\frac{3}{2}$	43912·2 2276·57 (10 R)	32493·0 3076·66 (2 R)	28474·2 3510·90 (6 u)	22253·0 22250·8 4492·61 (1) 4493·07 (1)	(10745)	14650
$6p^2\ 6d$ C $(^3P_0)\ ^2D_{5/2}$ $\frac{5}{2}$	44816·4 2230·64 (10 R u)	33397·5 2993·36 (6 R)	29379·2 ? 3402·80 (8)	...	11652·2 8579·74 (1)	13746
$6p^2\ 7s$ D $(^3P_1)\ ^2S_{1/2}\ \ ^4P_{3/2}$	44864·6 2228·23 (10 R)	33445·8 2989·05 (7 R)	29426·8 3397·20 (5 R)	23205·3 23203·0 4308·17 (4) 4308·58 (4)	11700·3 8544·74 (3)	13698
$6p^2\ 7s$ E $(^3P_1)\ ^2S_{1/2}\ \ ^2P_{1/2}$	45915·7 2177·22 (4 R)	34496·0 2897·99 (9 R)	...	24256·1 24254·3 4121·52 (5) 4121·81 (5)	12751·4 7840·33 (2)	12647
$6p^2\ 8s$ F $\frac{1}{2}$	47371·8 2110·31 (10 R)	35953·0 2780·52 (8 R)	...	25713·3 25711·4 3887·94 (2) 3888·23 (2)	14206·4 7036·15 (2)	11190
$6p^2\ 7s$ G $(^3P_2)\ ^2S_{1/2}\ \ ^4P_{5/2}$	48488·1 2061·70 (10 R)	37070·5 2696·76 (6 R)	33052·0 3024·67 (7 R)	...	(15320)	10074
$6p^2\ 7s$ H $(^3P_2)\ ^2S_{1/2}\ \ ^2P_{3/2}$	49459·8 2021·21 (6 R)	38041·6 2627·92 (8 R)	34023·1 2938·32 (9 R)	27799·0 3596·12 (8 R)	16295·8 6134·80 (3)	9102
$6p^2\ 6d$ I $(^3P_1)\ ^2D_{3/2}$ $\frac{3}{2}$	51017·8 1959·48 (8 R)	39599·5 2524·53 (9 R)	35581·4 2809·64 (6 R)	29354·7 ? 3405·60 (7 u)	17851·1 5599·41 (3)	7544
$6p^2\ 6d$ J $(^3P_1)\ ^2D_{5/2}$ $\frac{5}{2}$	51163·2 1953·89 (8 R)	39738·7 2515·68 (9 R)	35710·8 2799·74 (6 u)	...	(17998)	7405

* Lines investigated for *hf*-structure are underlined.

except an extremely rare radioactive one which does not count; thirdly, the lines were almost completely classified by Thorsen* and Toshniwal,† from whose analysis, the *j*-values of the terms are accurately known. This classification is given in Table 48, as a reference to this is necessary for the study of the works of Goudsmit and Back mentioned before.

According to this classification, the line λ 4722 should be single, being due to the transition $6p^3\ {}^2D_{\frac{3}{2}} - 6p^2 7s\ {}^4P_{\frac{1}{2}}$. (It should be mentioned here that the coupling is of the *jj*-type). But as mentioned above, it consists of six components (Table 47). Moreover these six components can be arranged in the form of a multiplet as shown in Table 49.

Table 49.—Multiplet structure of λ 4722.

	3		4		5		6
		·152		*·197*		*·255*	
4	21168·64		21168·792		21168·989		
·829							
5			21169·621		21169·819		21170·074

Almost every bismuth line is found on investigation to consist of components which can be arranged, as in the case of λ 4722, into *hfs*-multiplets, and the splitting was found to be characteristic of the levels. This is shown from an examination of the *hf*-structure of λ 2898 which, as a glance at Table 48 shows, is due to the transition $6p^3\ {}^2D_{\frac{3}{2}} - 6p^2\ 7s\ {}^2P_{\frac{1}{2}}$. It has therefore the same final level as λ 4722, *viz.*, $6p^3\ {}^2D_{\frac{3}{2}}$. The components of λ 2898 are shown in the form of *hf*-multiplet in Table 50, from which we find that the level $6p^3\ {}^2D_{\frac{3}{2}}$ has approximately the same splitting as in λ 4722. These intervals are easily seen to follow the Landé interval rule, for we have

Table 50.

	3		4		5		6
		·145		*·213*		*·253*	
4	34496·546		96·692		96·905		
·710							
5			95·984		96·177		96·430

$$\frac{\cdot 152}{4} = \cdot 038\ ;\quad \frac{\cdot 197}{5} = \cdot 039\ ;\quad \frac{\cdot 255}{6} = \cdot 042. \qquad . \quad . \quad . \quad (33)$$

So the separations are approximately as 4 : 5 : 6. The figures at the top row of Table 50 denote *hyperfine-structure quantum numbers f* (see §343).

---

* V. Thorsen, *Zs. f. Phys.*, 40, 642, 1926.

† G. R. Toshniwal, *Phil. Mag.*, 4, 774, 1927.

Every spectroscopic level of bismuth is thus found to be split up into a number of sublevels, and some of these splittings are shown in Table 51. In cases where total separation has been given, the *hf*-splitting was too small for the resolving power used, and therefore merely total separation has been surmised.

Table 51.

Term	f \ g	2	3	4	5	6	7	B
$6p^2$ $^2S_{\frac{3}{2}}$				Total Sep. – ·08				–·005
$^2D_{\frac{3}{2}}$	1·225		–·*152*	–·*198*	–·*256*			–·0403
$^2D_{\frac{5}{2}}$	1·20	·*254*	·*310*	·*400*	·*495*	·*571*		·0812
$^2P_{\frac{1}{2}}$	·667			1·875				·*775*
$6p^2$ $7s$ $A_{\frac{1}{2}}$	2·088			0·830				
$5d$ $B_{\frac{3}{2}}$	0·79			Total Sep. 0·1				·166
$5d$ $C_{\frac{5}{2}}$	1·20			Total Sep. 0·1				·01
$7s$. $D_{\frac{3}{2}}$	1·676			Total Sep. 0				–·01
$7s$ $E_{\frac{1}{2}}$	1·30			–0·708				·142
$7s$ $F_{\frac{1}{2}}$				0·20				·04
$7s$ $G_{\frac{1}{2}}$	1·41	0·380	·506	·633	·760	·887		·127
$7s$ $H_{\frac{3}{2}}$	0·98		·379	·473	·563			·0943

f = *hf*-quantum number, g = Landé factor; for B see eqn. (38) p. 758.

EXPLANATION OF THE RESULTS.

It is rather remarkable that though a good deal of painstaking experimental work on this line was done by Nagaoka,[*] Hansen, Wali Mohammed and others, not much progress in the subject was made till a theoretical explanation was forthcoming. Ruark[†] and Sommerfeld suggested in 1925 that the introduction of a fifth quantum number f, which they called the *hyperfine structure quantum number*, is necessary for explaining the results. This explains the Landé interval rule observed in *hf*-structure. Thus we shall see presently that the four levels into which Bismuth $6p^3$ $^2D_{\frac{3}{2}}$ are split up are characterised by the f-quantum numbers 3, 4, 5 and 6.

Greater precision was given to the idea by Pauli.[‡] He suggested that the nucleus might be regarded as possessing the mechanical moment $ih/2\pi$, where i may be called the *nuclear quantum number*. The same factor which gives rise to the mechanical moment also endows the nucleus with definite magnetic moment which, by its interaction with the valency-electrons, splits up each optical level into a number of hyperfine sublevels, possessing small differences of energy.

---

[*] H. Nagaoka, and T. Mishima, *Proc. Imp. Acad.*, 2, 249, 1926.
[†] Ruark, *Phil. Mag.*, 50, 937, 1925.
[‡] Pauli, *Naturwiss.*, 12, 741, 1924.

On account of the large mass of the nucleus, the magnetic moment is however extremely small compared to that of the electron. In order to obtain an idea of its magnitude, we may consider the simplest nucleus, *viz.*, the proton. If we suppose that this also is spinning like the electron and its mechanical and magnetic moments are entirely due to spin, the ratio between the two is expected to be given, as in the case of the electron, by the relation

$$\mu_p / \mathfrak{s}_p = e/Mc \quad . \quad . \quad . \quad . \quad . \quad (34)$$

If we suppose that $\mathfrak{s}_p = \frac{1}{2}h/2\pi, \ \ \mu_p = eh/4\pi Mc.$

Thus the protonic magnetic moment μ_p is 1846 times smaller than that of the electron.

This surmise has however not been verified. The nuclear moment of the proton from band spectra has been found to be indeed half, but the magnetic moment has not been found to be equal to μ_p. Stern and Eastermann* found from deflections of H_2-molecules in a non-homogeneous magnetic field, that the magnetic moment of the proton is $\frac{5}{2}\mu_p$. This shows that magnetism of the proton is more complex than hitherto imagined.

As the nucleus is supposed to consist of a number of protons and other particles which may be supposed to be describing spin as well as orbital motions, the resultant mechanical moment may be expected to equal the vector sum of those for the individual particles (of protons as well as of other particles). But the magnetic moments of the individual components will compound in a more complex way owing to coupling relations—as in the case of the resultant magnetic moments of the incomplete electron-shells. Following the analogy of extranuclear electrons, we may introduce a Landé factor $g(i)$. Then the magnetic moment is given by $\mu_p g(i) i$.

It is clear from the above preliminary account that a study of the hyperfine structure of spectral lines enables us to find the nuclear moment and thus throws light on the problem of its composition.

---

* Stern and Eastermann, *Zs. f. Phys.*, 85, 4, 7, 1933.

Hence in recent years a good deal of activity has been manifested in this direction. We shall now explain, taking bismuth lines for illustration, how the nuclear quantum number i can be obtained from the *hf*-structure of lines. In the two following sections, we follow the treatment given by Goudsmit.*

349. The Interaction of the Magnetic Nucleus with the Extranuclear Electrons.—If the mechanical moment vector of the nucleus be denoted by i and the total mechanical moment vector of the extranuclear electrons by j as usual, then i and j may be supposed to combine to form a new quantum number f, *the hyperfine structure quantum number* which has got all the values given by $f = |i+j|$. Therefore an optical level with a fixed value of j is split up into the f-values:

(*a*) $i+j,\ i+j-1, \ldots\ i-j \ldots$ altogether $2j+1 \ldots$ when $i > j$
(*b*) $i+j,\ i+j-1, \ldots\ j-i \ldots$ " $2i+1 \ldots$ " $j > i$.

The *hf*-separation can be worked out by considering the interaction between the nuclear magnet having the moment μ_k and the field at the nucleus due to the extranuclear electrons. Let this field be H_k. It may be mentioned here that the completed shells do not contribute anything towards the production of H_k which is due entirely to the electrons in the incomplete shell; *e.g.*, for the $(6p^3\ {}^2\mathrm{D})_{\frac{3}{2}}$ level of Bi the field is produced by the three electrons in the $6p$-shell. The energy of interaction may be written in the same way as in the case of multiplet separations. We have

$$\triangle W = \mu H_k \cos (ij) \quad . \quad . \quad . \quad . \quad . \quad . \quad . \quad . \quad (35)$$

where

$$\cos (ij) = \frac{f(f+1) - i(i+1) - j(j+1)}{2ij} \quad . \quad . \quad . \quad . \quad (36)$$

The separation between two levels having the quantum number f and f' can now be easily calculated:

$$W_f - W_{f'} = \frac{\mu H_k}{2ij}[f(f+1) - f'(f'+1)] = \frac{B}{2}(f-f')(f+f'+1). \quad (37)$$

where $B = \mu H_k / ij$. If $f' = f-1$, we have

$$\triangle W_f = Bf \quad . \quad . \quad . \quad . \quad . \quad . \quad . \quad . \quad . \quad . \quad (38)$$

i.e., $\triangle W$ is proportional to the larger f-number.

In the case of the $6p^3\ {}^2\mathrm{D}_{\frac{3}{2}}$-level of Bi, we have seen that the successive separations are as 4 : 5 : 6. From Table 49 we find that we should put $f=3, 4, 5, 6$ respectively for the sublevels into which the level $p^3\,{}^2D_{\frac{3}{2}}$ is split up. This is explained if for the Bi-nucleus 'i' is assumed to have the value $\frac{9}{2}$, for we have then

---

* Goudsmit, *loc. cit.*

$$f= |\,i+j\,| = |\,\tfrac{9}{2}+\tfrac{3}{2}\,| = 3, 4, 5, 6.$$

Goudsmit and Bacher* showed from investigations of a large number of Bi-lines that the value $\frac{9}{2}$ for the nuclear quantum number completely explains the observed splitting for all levels of Bi. This can be verified by referring back to Table 51. In Tables 49 and 50, the f-values of the upper states are obtained from the selection rule for f (see infra).

Note on Negative and Positive Values of Intervals.—In analogy with optical terms, we have to fix up a convention regarding hyperfine structure terms. If $T_f < T_{f-1} < T_{f-2}\ldots$ we say the terms are *direct;* otherwise they may be called *inverted;* thus we find that in Bi for $2p^3\ {}^2D_{\frac{3}{2}}$, $T_3 < T_4 < T_5 < T_6\ldots$, hence the terms are inverted and $T_3 - T_4$ is negative as shown in Table 51. In $2p^3\ {}^2D_{\frac{5}{2}}\ldots T_2 > T_3$; the intervals are positive.

Selection Principle and Intensity Law in the hf-multiplets.—It has been found that the quantum number f obeys the same selection principle as the inner quantum number j, *viz.*, $\Delta f=0, \pm 1$ allowed; $\Delta f=0\rightarrow 0$ forbidden.

The intensity rules for the *hfs*-components are exactly similar to those of ordinary multiplets and will be treated later.

350. Zeeman Effect of Lines possessing *hf*-Structure.

—The value of nuclear quantum number 'i' determined in the above way can further be supported from other directions. One of the methods which is applicable for Bi depends upon investigations of the Zeeman effect of its spectral lines. We shall describe the investigation for the line λ 4722 which is typical of the whole set of bismuth lines for very strong fields. For weak and intermediate fields, see Pauling and Goudsmit, *Structure of Line Spectra*, p. 219.

In bismuth, the coupling tends to the *jj*-type. Hence the Zeeman effect cannot be calculated using the Landé formula. Thus the line λ 4722 is given by the combination $6p^3\ {}^2D\ - 6p^2\,7s\ {}^4P_{\frac{1}{2}}$. Here ${}^2D_{\frac{3}{2}}$ and ${}^4P_{\frac{1}{2}}$ have been written to describe the terms for want of a better designation, but really they have not the usual meaning except that they give the inner quantum number correctly. For if ${}^2D_{\frac{3}{2}}$ were normal, its g-value would be $\frac{4}{5}$, and for ${}^4P_{\frac{1}{2}}$, g would be $\frac{8}{3}$. But Back found that g for $6p^3\ {}^2D_{\frac{3}{2}}$ is 1·225, for ${}^4P_{\frac{1}{2}}$, $g = 2·088$. So the

---

* Goudsmit and Bacher, *Zs. f. Phys.*, 66, 13, 1930.

Zeeman pattern for λ 4722 is as given in the following scheme (Table 52).

Table 52.—Zeeman components for Bi $6p^3\ {}^2D_{\frac{3}{2}} - 6p^2\ 7s\ {}^4P_{\frac{1}{2}}$
λ 4722 *supposing hf-structure to be absent.*

Term	m g	$\frac{3}{2}$	$\frac{1}{2}$	$-\frac{1}{2}$	$-\frac{3}{2}$	$\Delta\nu/a$
$^2D_{\frac{3}{2}}$	1·2227	1·836	·612	−·612	−1·838	± ·432 . . . π-comp.
		↘	↓ ↘	↙ ↓	↙	
$^4P_{\frac{1}{2}}$	2·088		1·044	−1·044		·793 1·652 } . . . σ-comp.

The line λ 4722 would thus decompose into 6 components. But as the original line itself consists of *hfs*-components, the Zeeman resolution becomes somewhat different when high fields are applied. We give below a theory of this effect which is due to Goudsmit.

When an external field H is applied, such that it is sufficiently strong to break the coupling between j and i, we can calculate the extra energy in the way as in the case of Paschen-Back effect. We have

$$\Delta W = m_j\ g(j)\ \frac{eh}{4\pi mc}\ H + m_i\ g(i)\ \frac{eh}{4\pi Mc}\ H + Bij\cos(ij). \quad (39)$$

The first term is the ordinary Zeeman effect term if the *hf*-structure were absent, $g(j)$ is the ordinary Landé factor due to extranuclear electrons, m_j is the component of the inner quantum number The second term represents the action of the field on the nuclear magnet. Its magnetic moment is $(eh/4\pi Mc)\ i\ g(i)$ and m_i is the projection of 'i' on the external field. $Bij\cos(ij)$ is the term due to interaction of 'i' and 'j', which has been already discussed and which gives us the *hf*-structure of the line. In the deduction of the expression, we suppose that the coupling between i and j is broken. Since f no longer exists, we have

$$\cos ij = m_i\, m_j/ji \quad . \quad . \quad . \quad . \quad . \quad . \quad . \quad . \quad (40)$$

as in the case of Paschen-Back effect (§224).

Now the first term is nearly 2000 times larger than the second, which can therefore be neglected. The first and third terms are of equal magnitude if H be chosen to be sufficiently large, and the expression can therefore be written as :

$$\Delta W = m\ \ g(j)\ \frac{eh}{4\pi mc}\ H + B\, m_i m_j \quad . \quad . \quad . \quad . \quad . \quad (41)$$

The Zeeman components are therefore given by

$$\triangle \nu = \frac{eH}{4\pi m_0 c}\Big[m_j \; g(j) - m_j' \; g(j') \Big] + (B\, m_j - B' m_j')\frac{m_i}{h} \quad . \quad (42)$$

The first term gives us the Zeeman components which are expected if the *hf*-structure were absent. For a field of 53700 gauss there would be, as Table 52 shows, a pair of π-components at $\triangle\nu = \pm{\cdot}432 \times 2{\cdot}526 = \pm 1{\cdot}090$ cm⁻¹, and a pair of σ-components at $\triangle\nu = \pm{\cdot}793 \times 2{\cdot}526 = \pm 2{\cdot}000$ cm⁻¹, and another pair of σ-components at $\triangle\nu = \pm 1{\cdot}652 \times 2{\cdot}526 = \pm 4{\cdot}170$ cm⁻¹. But on account of the second term in (42), each of these levels would be split up into 10 components, corresponding to the total number of m_i values ($=2i+1$). We have $B = -{\cdot}0403$, $B' = {\cdot}166$ from Table 51. The values of $(Bm_j - B'm_j')$ for the Zeeman components are shown above in Table 53.

Table 53.

$m_j \leftarrow$	$\frac{3}{2}$	$\frac{1}{2}$	$-\frac{1}{2}$	$-\frac{3}{2}$	$Bm_j - B'm_j' = \delta\nu/m_i$
$B = -{\cdot}0403$	$-{\cdot}0604$	$-{\cdot}0202$	${\cdot}0202$	${\cdot}0604$	·1030 . . . π-comp.
$B' = {\cdot}1660$		${\cdot}083$	$-{\cdot}083$		·1435 ·0628 } · · σ-comp.

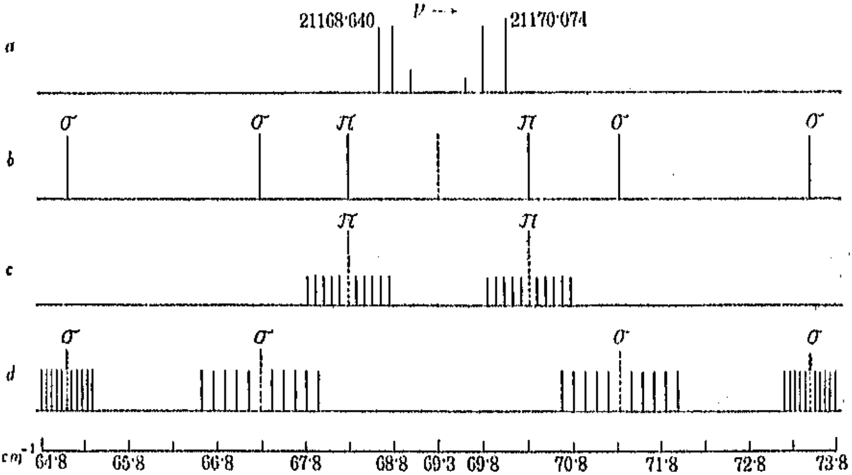

Fig. 19. Scheme showing the *hf*-splitting of Zeeman components for Bi λ 4722.

Thus the separation of the *hf*-subcomponents of the π-components are given by

$$\pm 1{\cdot}090 + {\cdot}1030\, m_i, \qquad m_i = \tfrac{9}{2}, \tfrac{7}{2} \ldots\ldots -\tfrac{9}{2}.$$

The separations of the *hf*-subcomponents of σ-components are given by

$$\pm 2{\cdot}000 + {\cdot}1435\, m_i, \qquad m_i = \tfrac{9}{2}, \tfrac{7}{2}, \ldots\ldots -\tfrac{9}{2}$$

$$\pm 4{\cdot}170 + {\cdot}0628\, m_i, \qquad m_i = \tfrac{9}{2}, \tfrac{7}{2}, \ldots\ldots -\tfrac{9}{2}$$

The scheme of these *hf*-splitting of the Zeeman components are shown in Fig. 19.

(*a*) shows the *hf*-component without field, (*b*) the position of the π and σ-component without *hf*-structure, (*c*) the π-component with *hf*-splitting, (*d*) the σ-components with *hf*-splitting. They are drawn to scale for a field of 53700 gauss.

The value of i can be inferred directly from the number of subcomponents which is $2i + 1$.

351. Comparison with Experiments.—The Zeeman effect of the Bi-line λ 4722 was very thoroughly investigated by Back and Wulff[*] in the Tübingen Laboratory, and Goudsmit and Bacher[†].

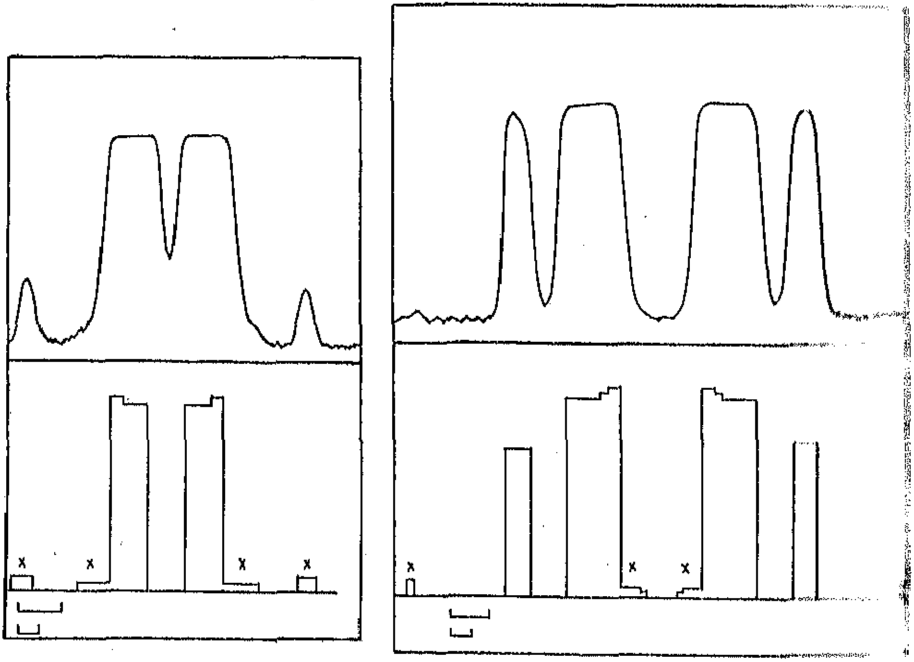

(*a*) (*b*)

Fig. 21. Microphotogram of Zeeman components of the *hfs* of λ4722: (*a*) π-components, (*b*) σ-components.

---

[*] Back and Wulff, *Zs. f. Phys.*, 66, 31, 1930.

[†] Goudsmit and Bacher, *Zs. f. Phys.*, 47, 174, 1928.

showed that the results were in complete accord with their theory. Fig. 20, Plate XII, is a reproduction of the photograph of the σ-components in the 4th order (5 times magnified) taken by Back and Wulff. The inner components show quite clearly the 10 *hfs*-subcomponents. The original photographs of the π and the outer σ-Zeeman components also showed clearly the ten *hfs*-subcomponents. The microphotograms are shown in Fig. 21 (*a*) and (*b*). The plate was overexposed, hence the *hf*-structure is not to be found in the microphotogram, but the breadth due to the totality of the *hf*-components is clearly visible. The breadths were found to be:

0·882cm^{-1} for the π-component: theoretical 9×·103 = ·927cm^{-1},
1·269 ... inner σ- „ „ 9×·1435 = 1·292,
0·520 ... outer σ- „ „ 9×·0628 = ·565.

The crosses denote the existence of lines not predicted by theory. They are due to the violation of the selection principle $\Delta f = \pm 1, 0$, ... just as in the case of optical components.

352. *Hf*-Structure of Elements Possessing more than one Isotope (Tl).

—We have so far described two methods for finding out the nuclear moment *i* of bismuth: (1) from the *hf*-separations, (2) from the *hf*-structure of the Zeeman components of the lines under strong field. A large number of lines of Bi, Bi^+, Bi^{++} have been investigated in this way, and they have all yielded the same result for the nuclear quantum number, *viz.*, $\frac{9}{2}$. This is as it should be, for '*i*' is characteristic of the nucleus, and should therefore be independent of the state of ionisation of the atom, or its particular quantum state. Besides these two methods, there is a third one for determining *i*. It consists in the study of the relative intensities of the alternate band lines of the diatomic molecules of the substance, but this subject can be taken only under *Molecular Spectra*.

It has been found that almost all the elements in the periodic table, excepting a few like He_2, C_{12}, O_{16} . . . show *hf*-structure of spectral lines. But in these cases, precision studies are complicated by the presence of isotopes.

A glance at the table given on p. 102 shows that almost all elements consist of mixtures in varying proportion of a number of isotopes having identical chemical and physical properties.

---

* See McLennan, McLay, Crawford, *Proc. Roy. Soc. A*, **129**, 579, 1931.

As the spectrum depends entirely upon the electronic composition which is the same for all isotopes, it is expected that the spectrum of different isotopes will not be different. But it has been shown in §172 that on account of the difference in mass, the Rydberg number of two isotopes are slightly different, giving rise to a displacement of frequency, which according to the theory should be

$$\Delta\nu/\nu = \frac{1}{1846}\cdot\frac{A'-A}{AA'} \quad . \quad . \quad . \quad . \quad . \quad . \quad . \quad . \qquad (43)$$

where A, A' are the mass numbers of the two isotopes.

This relation has given correct results in the case of the Deuton, and He, but in the case of heavy elements the value calculated according to (43) is found to be extremely small. Thus taking 81 Tl, which consists of 30% of Tl 203, and 70% of Tl 205, we should have

$$\Delta\nu/\nu = 2/(203\times205\times1836) = 5\times10^{-4}\ \text{cm}^{-1}\,.$$

For the line λ 5351 $6p\ ^2\text{P}_{\frac{1}{2}} - 7s\ ^2\text{S}_{\frac{1}{2}}$, we should have $\Delta\nu = 0{\cdot}0005$ cm^{-1}. This separation is of a lower order than the *hfs*-separations, but the actual results, of isotopic separation as obtained in the careful investigations of Schüler and Keyston* were found to be nearly 100 times larger.

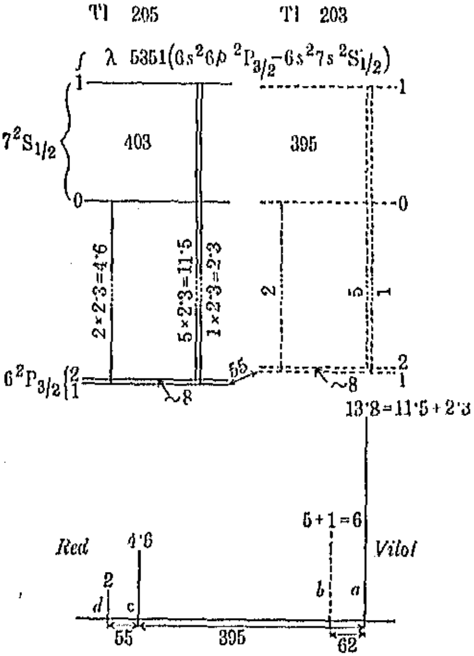
Tl 205
Tl 203
λ 5351($6s^2 6p\ ^2P_{3/2} - 6s^2 7s\ ^2S_{1/2}$)
$7^2S_{1/2}$
1
0
403
395
1
0
$2\times2{\cdot}3=4{\cdot}6$
$5\times2{\cdot}3=11{\cdot}5$
$1\times2{\cdot}3=2{\cdot}3$
2
5
1
$6^2P_{3/2}$ 2 1
~8
55
~8
2
1
$13{\cdot}8=11{\cdot}5+2{\cdot}3$
5+1=6
Red
4·6
Vilot
2
d
c
b
a
55
395
62

Fig. 23. Level scheme showing the origin of the *hf*-structure of Tl λ5351.

A picture of the *hf*-structure of Tl λ5351 is shown in Fig. 22, Plate XII, and the origin of the *hfs*-components is schematically shown opposite (Fig. 23). Four components are obtained and denoted by *a*, *b*, *c*, *d*. It was

---

[*] Schüler and Keyston, *Zs. f. Phys.*, 70, 1, 1931. A good account of the hyperfine-structure of Tl by Kallmann and Schüler will be found in *Ergebnisse der exakten Naturwissenschaften*, 11, 1932.

observed that the intensities of these components bear to each other the ratios

$$a/b = c/d = 2{\cdot}3\,;\quad a/c = b/d = 3.$$

As the proportion of the isotopes are $30:70 = 1:2{\cdot}3$, it was concluded that a and c are due to Tl_{205}, b and d to Tl_{203}. The isotopic separation thus comes out to be $\Delta\nu = {\cdot}062$ cm^{-1} which is nearly 120 times larger than the value given by the formula (43). Thus it is a general phenomenon, that the isotopic separations for heavy elements are found to be much larger than the theoretical values, and sometimes their sign is reversed. No explanation of this remarkable fact is yet forthcoming. Only the case for the isotopes of Li has been explained. For this see *Quantentheorie* by Smekal and others, p. 388.

The *hf*-components are explained by assuming that for both isotopes of Tl, $i = \frac{1}{2}$, and the optical levels are split up as shown in Fig. 23. There should be three components with the theoretical intensity ratios 5 : 1 : 2, but the splitting of $^2P_{\frac{3}{2}}$-term is very small, hence the first two appear as a single component with the intensity $5+1=6$. So the ratio $a/b = \frac{6}{2} = \frac{3}{1}$, as is actually observed.

The case of Tl is however not quite representative, because here accidentally the nuclear and magnetic moments are the same for the two isotopes. But in general the moments of the two isotopes may be widely different; in such cases, some ingenuity has to be applied before the mass-effect and *hfs*-effect can be separated.

353. Theoretical Calculations of Hyperfine Structure-Separations.

—We have shown in a general way that the *hf*-constant $B = \mu_K H_K/ij$, where μ_K is the magnetic moment of the nucleus, and H_K is the field at the nucleus produced by the extra-nuclear electrons. Of these quantities, μ_K being characteristic of the nucleus, should be independent of the state of ionisation of the atom, or the particular state of excitation of the extra-nuclear electrons; H_K, on the other hand, depends on these states. Hence if we can evaluate H_K properly, we should obtain a unique value of μ_K from the *hf*-structures of all lines of the neutral or ionised atom (only one isotope being considered at one time).

A glance at Table 51 shows the extreme difficulty of the task. The values of B for the different levels of Bi vary enormously, being sometimes positive, and sometimes negative. A theory of interaction energy between extra-nuclear electrons, and the nucleus which can give unique values of μ_K would be indeed a great triumph for the theoretical physicist. The solution of the problem does not appear to be in sight, but a brief account of the attempts chiefly due to Goudsmit and his collaborators may be given.

Interaction Energy between a Single Electron and the Nucleus (regarded as a Magnet).

The interaction energy between a single electron possessing the quantum numbers l and s, and the nuclear magnet is calculated in a way which is partly analogous to the procedure followed in §220. Let μ_K denote the magnetic moment-vector of the nucleus. Then it can be easily shown that the extra energy due to the interaction between the l-motion of the electron, and the nuclear magnet is given by

$$\triangle W_1 = \frac{e}{mc}\,\frac{1}{r^3}\,\mu_K\,.\,l\,\frac{h}{2\pi} \quad . \quad . \quad . \quad . \quad . \quad . \quad . \qquad (44)$$

This can be calculated in the same way as in §220, for the expression (42) on p. 421 can be written as

$$\triangle W = \frac{e}{mc}\,\frac{1}{r^3}\,\left(\frac{eh}{2\pi mc}\,.\,s\,.\,l\,\frac{h}{2\pi}\right) = \frac{e}{mc}\,.\,\frac{1}{r^3}\,\left(\mu_S\,l\,\frac{h}{2\pi}\right) \quad . \quad . \quad . \qquad (45)$$

where μ_S = magnetic moment-vector of the electron due to spin $= s.\,eh/2\pi mc$. Expression (44) is obtained by substituting μ_K for μ_S in (45).

To this, we have to add a second part $\triangle W_2$ due to the interaction between the spin-magnetism of the electron, and the nuclear magnet.

This is obtained by proceeding from the classical expression for the mutual energy of two magnetic dipoles having the moments μ and μ' (see Jeans, *Electricity and Magnetism*, p. 379). We have

$$-\ W_2 = \frac{\mu\mu'}{r^3}\,[\,\cos(\mu\mu') - 3\cos(\mu r)\cos(\mu' r)\,] \quad . \quad . \quad . \qquad (46)$$

Here r is the radius vector from the nucleus to the origin. Now putting $\mu = \mu_S$, $\mu' = \mu_K$, we have

$$-\triangle W_2 = \frac{\mu_S\,\mu_K}{r^3}\,[\cos(i\,s) - 3\cos(i\,r)\cos(s\,r)\,] \quad . \quad . \quad . \qquad (47)$$

because the direction of μ_S is denoted by the s-vector, that of μ_K by the i-vector.

So we have, adding (44) and (47),

$$\triangle W = \frac{e}{mc}\,\frac{1}{r^3}\left(\mu_K\,.\,\frac{lh}{2\pi}\right)\cos(il) - \frac{\mu_K\,\mu_S}{r^3}\cos(i\,s)$$

$$+\frac{3\mu_K\,\mu_S}{r^3}\cos(ir)\cos(sr)$$

We put, as already discussed in §220,

$$\mu_K = \mu_P\; i\; g(i) = \frac{m}{M}\,\frac{eh}{4\pi cm}\; i\; g(i)$$

Hence we have

$$\triangle W = 2\,q\,[il\cos(il) - is\cos(is) + 3is\cos(ir)\cos(sr)]. \quad . \quad (48)$$

where $$q = \frac{m}{M}\left(\frac{eh}{4\pi mc}\right)^2\frac{1}{r^3}\,g\,(i) = \frac{m}{M}\,g\,(i)\,\frac{Rhc\,\alpha^2\;Z^3}{2n^3\;l\,(l+\frac{1}{2})\,(l+1)}$$

as in §220.

It can now be shown that the factor

$$[il\cos(il) - is\cos(is) + 3\;is\cos(ir)\cos(sr)]$$

is proportional to cos (ij).

Since the coupling between i and l is not broken we have, applying the Landé rule for quantum-cosines

$$\cos(il) = \cos(ij)\cos(jl)$$

$$\cos(is) = \cos(ij)\cos(js).$$

It is a little more difficult to evaluate cos (ir). cos (sr). Let the direction-cosines of any of these vectors be denoted by α, β, γ followed by the proper subscript. Then we have

$$\cos(ir)\;\cos(sr) = (\alpha_i\;\alpha_r + \beta_i\;\beta_r + \gamma_i\;\gamma_r)\;(\alpha_s\;\alpha_r + \beta_s\;\beta_r + \gamma_s\,\gamma_r)$$

$$= \alpha_i\,\alpha_s\;\;\alpha_r^2\,. + \ldots. + \alpha_r\,\alpha_i\;\;\beta_r\;\beta_s\; + \ldots\ldots\ldots$$

Now the vector 'r', the unit vector to the electron, precesses in the plane of the l-motion of the electron, and therefore round the l-axis, which may be taken as the z-axis. Taking average values, we have

$$\overline{\alpha_r^2} = \overline{\beta_r^2} = \tfrac{1}{2},\;\;\overline{\gamma_r^2} = 0,\;\;\overline{\alpha_r\;\beta_r} = 0$$

Hence we have

$$\cos(ir)\cos(sr) = \tfrac{1}{2}\,(\alpha_i\;\alpha_s + \beta_i\;\beta_s)$$

$$= \tfrac{1}{2}\cos(is) - \tfrac{1}{2}\,\gamma_i\;\gamma_S$$

$$= \tfrac{1}{2}\cos(is) - \tfrac{1}{2}\cos(il).\cos(sl).$$

We have therefore

$$\triangle W = 2qij \cos ij \left[\frac{l}{j}\cos (lj) + \frac{s}{2j}\cos sj - \frac{3s}{2j}\cos (jl) \cos (sl)\right]$$
$$= \mu H_K \cos (ij)$$

Goudsmit[*] has shown that the expression within the bracket is equal to $l(l+1)/j(j+1)$, so we have finally the *hf*-separation-factor (for one electron system; *cf.* eqn. 37)

$$b = \frac{\mu H_K}{ij} = \frac{R\,\alpha^2\,Z^3}{n^3\,(l+\frac{1}{2})\,j\,(j+1)}\,g\,(i)\,\frac{m}{M} \quad . \quad . \quad . \quad . \quad . \quad (49)$$

We may compare the unit of *hfs*-separation with the unit of ordinary multiplet separation for doublet spectra. We have

$$\triangle \nu = \frac{R\alpha^2 Z^4}{n^3}\,\frac{1}{l(l+1)}$$

Hence we have $\quad \dfrac{b}{\triangle \nu} = \dfrac{l(l+1)}{Z(l+\frac{1}{2})\,j\,(j+1)}\,\dfrac{g(i)}{1838}\,\mathrm{cm}^{-1}.$

Thus the order of *hf*-splitting is Z. 1838 times smaller than that of multiplet splitting for the doublet terms. The quantity is generally too small for observation.

But this expression does not give us the *hf*-splitting of the S-term. For a glance at equation (48) shows that our expression for $\triangle W$ ceases to hold for the S-term, as for this $r=0$ and $\triangle W$ becomes infinite. We can otherwise understand, on purely physical grounds, that the *hf*-splitting would be largest for *s*-electrons and *p*-electrons of very heavy elements, as their orbits are penetrating and the electrons approach very close to the nucleus. Hence energy values of *s*-electrons would be subjected to the maximum *hf*-splitting. Experiments have also shown that the *hf*-splitting in the case of alkali elements is entirely due to *s*-terms. Thus for sodium, an element which has been very thoroughly investigated,[†] it has been found that for the $3s\ {}^2S_{\frac{1}{2}}$-term $\triangle \nu = {}^{\cdot}061\ \mathrm{cm}^{-1}$, while for the P-terms the splitting is negligible.

The investigation of the *hf*-splitting of *s*-levels cannot be undertaken by the classical methods. This must be attempted with the aid of wave-mechanical methods. This was first attempted by Casimir.[‡] According to a report by Goudsmit, Casimir is said to have proved that

$$W = qis \cos (is), \quad f = i+\tfrac{1}{2},\ i-\tfrac{1}{2}.$$

---

[*] Goudsmit, *Phys. Rev.*, 37, 663, 1931; *ibid.*, 43, 636, 1933.

[†] Schüler and Brück, *Zs. f. Phys.*, 58, 735, 1925; Granath, *Phys. Rev.*, **44**, 935, 1933.

[‡] Casimir, see Pauling and Goudsmit's *The Structure of the Line Spectra*, p. 208.

Later the problem was attacked by Hargreaves,[*] and Fermi[†] using Dirac's form of relativity wave-mechanics. A discussion of these methods cannot be attempted at this place, and the results as given by different authors, are also not concordant. For further information, the reader can refer to original sources.

For most elements, which have been investigated for their *hf*-structure, the spectra are due to more than one electron. Goudsmit has shown in a general discussion that appreciable values of *hf*-splitting are obtained only when an *s*-electron participates in the production of the optical level. He has also initiated general methods for calculating the energy due to the simultaneous interaction of two or more electrons with the nuclear magnet.

The result of all these investigations is rather disappointing. The values of μ_k calculated from different arc and spark lines of elements generally yield quite different values, hence it is probable that the mode of interaction of extra-nuclear electrons with the nucleus may be quite different from that hitherto assumed in such investigations. Probably the nature of the individual components of the nucleus has to be taken into consideration. We shall return to this subject in the chapter on *Nuclear Physics.*

Books Recommended

1. O. Laporte *Handbuch der Astrophysik*, 3/2, 1930, article on 'Theorie der Multiplett spektren.'

2. Pauling and Goudsmit, *The Structure of Line Spectra*, 1930.

3. Becker and Grotrian, *ergebnisse der exakten Naturwissenschaften*, **7**, 1928.

4. Goudsmit and Bacher, *Atomic energy States*, 1932.

5. Kallmann and Schüler, *Ergebnisse der exakten Naturwissenschaften*, **11**, 1932.

---

[*] Hargreaves, *Proc. Roy. Soc. A.*, **124**, 568, 1929.
[†] Fermi, *Zs. f. Phys.*, **60**, 320, 1928; **82**, 729, 1933.

CHAPTER XV

MAGNETISM AND ITS THEORIES

354. Historical Introduction.—Up to the year 1819, nobody seems to have suspected that there was any connection between the phenomena of electricity, and those of magnetism. Each group of phenomena was studied by itself. In this year, Oersted discovered that a wire carrying an electric current produces a magnetic field around it. This discovery marks a great landmark in the history of science, because it showed for the first time that an intimate connection exists between these two great groups of nature-phenomena.

The exact laws of production of magnetic field by a current were discovered by Ampère and Weber, and are now well-known to every student of science. Ampère showed, by a series of carefully planned experiments, and by careful mathematical analysis of the results, which according to Maxwell, are "perfect in form, and unassailable in accuracy," that the magnetic field produced by a closed coil carrying a current was the same as that of a magnetic shell occupying the area covered by the coil and filled with small elementary magnets placed normally to the plane of the coil, with similar poles pointing in the same direction (normally polarised shells). The magnetic moment per unit area of the equivalent shell was taken as equivalent to the current, and in fact this definition forms the basis of the electromagnetic system of units.

EXPLANATION OF NATURAL MAGNETISM.

Ampère suggested that natural magnetism which we observe in iron and other ferromagnetic bodies, or magnetism which can be produced in them by a magnetising field may be explained by assuming that the substance contains within itself *small closed currents of molecular dimensions.* These currents were supposed in those days

---

[*] For a history of these experiments, see Maxwell, *Electricity and Magnetism*, 11, 138-194.

to be due to the motion of small electrified particles which were present in all material bodies, particularly in good conductors of electricity. These closed currents were supposed to form elementary magnets and Weber supposed that in every magnetic substance these elementary magnets are usually orientated at random in the unmagnetised state as shown in Fig. 1. When a magnetising field is applied, each of these elementary magnets is subjected to a directive couple which tends to set them parallel to the field. But this tendency is opposed by the heat motion of the particles, so that the alignment is only partial. When the magnetising field is sufficiently large, the chaotic tendency due to heat motion can be completely overcome, and we get the phenomenon of magnetic saturation. Some of the features of Weber's theory have been incorporated in the later theory of Langevin (see *infra* § 361).

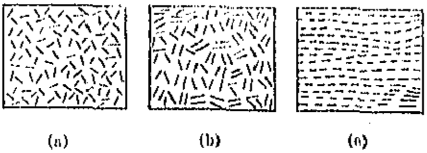

Fig. 1. Weber's Elementary Magnets.
(*a*) Without field, (*b*) Weak field, (*c*) Strong field (saturation).

DISCOVERY OF UNIVERSALITY OF MAGNETIC PROPERTIES.

Up to 1850, magnetic properties were supposed to be confined to a few substances like iron, nickel and cobalt. In 1845, Faraday proved that this was by no means the case. By suspending rods of different substances between the poles of a strong electromagnet, he found that most substances set themselves parallel to the magnetic field, if the field of the electromagnet be sufficiently large; a few elements like bismuth set themselves at right angles to the field*. Faraday showed that for the first class of substances the magnetic susceptibility χ can be proved to be greater than zero. For the latter class (*viz.*, bismuth, etc.) the susceptibility is negative (*vide infra* p. 776). To the first class, he gave the name "*paramagnetics*" and the second class was called "*diamagnetics.*" Substances like Fe possess a value of χ which is much larger than that for the usual paramagnetic bodies, and hence are put in a class by themselves and called "*ferromagnetics.*" It is however found that above a certain temperature (called the *temperature of recalescence*), the susceptibility of iron suddenly diminishes to the value for paramagnetic bodies. A further characteristic property of the ferromagnetic bodies is that they show the phenomenon of hysteresis.

---

* The repulsion of bismuth by a magnet had also been observed by Bruygmans in 1778.

Extensive investigations of the magnetic properties of all elements and their compounds have now shown that the phenomena of dia, para, and ferromagnetism are very fundamental. All material substances belong to one or the other of the three classes. Of these the ferromagnetic substances are rather few in number and consist of the three elements Fe, Co, Ni; most of their alloys having a sufficient concentration of the metals; some of their compounds, *e.g.*, the oxide and sulphide of iron; the Heussler alloys (composition: Al 10%, Mn 20%, Cu 70% approximately); as also some compounds of manganese and some ferrites of the type MeO, Me_2O_3, where Me is a metal of the iron group. The Heussler alloys, first discovered by Heussler in 1903 are remarkable that out of three constituents, which are all merely paramagnetic, a compound is formed possessing strong ferromagnetic properties. According to some authorities, they are definite chemical compounds with formulae of the type ... $[Al(Mn, Cu)_3]_x$.

Paramagnetic substances are much larger in number and consist of many metallic elements, some gases and most of the salts and oxides of elements belonging to the different transitional series, *i.e.*, from Sc (21) to Cu (29), from Y (39) to Pd (46), and the rare-earths Ce (58) to Yb (70), as also of elements belonging to Pt and U-families. These elements themselves are also paramagnetic.

All other substances are diamagnetic, and we shall see later that dia-magnetism is a universal phenomenon and underlies para as well as ferromagnetism.

355. A Review of more Recent Developments.—Since 1900, the subject of magnetism has received serious attention from both theorists and experimentalists. In 1895, P. Curie undertook with the aid of his magnetic balance (see p. 775) an extensive series of experiments for finding out the susceptibility of a large number of paramagnetic and diamagnetic bodies and their variation with temperature. These studies culminated in the discovery of two fundamental laws known after Curie;

(1) *The diamagnetic susceptibility is independent of T*

(2) *The paramagnetic susceptibility is inversely proportional to the absolute temperature,* ($\chi T = C$).

These laws were explained by Langevin on the basis of electrical theories of matter which were in vogue before 1912, and his explanation, with certain modifications, still holds the ground though it does not explain all the results. The studies of Curie and Langevin were extended to ferromagnetics by P. Weiss who introduced the idea of molecular magnetising fields, and showed that from the theoretical stand-point the ferromagnetics are to be differentiated from the paramagnetics by the existence in the former of elementary regions which are spontaneously magnetised to a saturation value characteristic of the temperature even in the absence of the external magnetic field. At the temperature of recalescence this property suddenly disappears. He further showed that his experiments pointed to the existence of atomicity in magnetism (The *Weiss-magneton*).

The subsequent progress of magnetism has been largely inspired by the quantum mechanical theories of the structure of the atom, and will be discussed in due course. We shall finish this introduction by relating briefly how the Ampère-Weber hypothesis that magnetism is due to molecular currents caused by the motion of small charged particles received experimental confirmation.

THE GYROMAGNETIC EFFECT.

It was Maxwell who first pointed out that the assumptions underlying the Ampère-Weber theory can be subjected to an experimental test. The small electrified particles revolving perpetually in closed orbits to which the ferro or paramagnetic bodies are supposed to owe their magnetism may be compared to small elementary gyroscopes. When a magnetising field is applied to the body, these elementary gyroscopes begin to execute a precessional motion round the direction of the external field as axis. This will give rise to a mechanical moment which should be capable of detection.

It does not appear that Maxwell had any idea of the magnitude of this mechanical moment. The great difficulty in his days was the absence of any definite knowledge regarding the small electrified particles which, by their motion, cause magnetism. After the discovery of the electron, it was natural to identify it with these particles. Einstein proved in 1917 that if magnetism be supposed to be due to the motion of the electrons in closed orbits, the mechanical moment Ω should be $(2mc/e)$ × magnetic moment. Since $e/mc =$ $1{\cdot}773 \times 10^7$ e.m.u., we should have $\Omega = 1{\cdot}13 \times 10^{-7}$ M, where M is the total magnetic moment of the sample. Thus the expected mechanical moment is so small, that unless very sensitive arrangements are used, the effect cannot be demonstrated. The difficulties were overcome by Einstein and de Haas in 1918 by the application of a very ingenious method (described towards the end of this chapter), and the ratio was found to have the expected value. But later and more careful experiments by Beck showed that the ratio was not $1{\cdot}13 \times 10^{-7}$, but nearly half this amount, in other words $\cdot 58 \times 10^{-7}$. This result showed that Einstein's theory required some profound modification.*

At the present time, the magnetism of the elementary magnets is no longer ascribed to the revolution of electrons in an orbit alone, but also to the *rotation of electrons* about an axis fixed in themselves. The hypothesis of the "Spinning Electrons" has been already given in connection with spectroscopy. It has been equally fruitful in explaining the magnetic phenomena, as we shall presently see.

356. Experimental Studies in Magnetism.—The usual methods which are used in the laboratory for finding out the susceptibility of ferromagnetic substances, such as the magnetometric and ballistic methods, are also applicable to para and diamagnetic substances. Thus Townsend (1896) employed the solenoid method for the investigation of the susceptibilities of a number of strongly paramagnetic solutions of iron salts. But in general, on account of the feebleness of the effect, the sensitivity of these apparatus must be greatly enhanced before the results can be accepted as reliable. Though sometimes such procedure has been adopted, it has not been very successful.

FARADAY'S METHOD

This called for new methods of experiment for dia and paramagnetic substances. One particular method which has been extensively used is due to Faraday, and was first used by him in his classical researches on magnetism. It was based upon the measurement of the force experienced by a specimen of the substance when suspended in a *nonhomogeneous magnetic field.* A mathematical expression for this force can thus be worked out. Let the substance possess the permeability μ and let the medium in which it is suspended possess the permeability μ_0. The comparative energy of this system (the work done in bringing the substance into the medium) is

---

* This experiment was first suggested by O. W. Richardson, 1904, but the first successful experiment demonstrating the relation between mechanical motion and magnetisation was performed by S. J. Barnett in 1914, (*vide infra*).

$$E = \frac{\mu - \mu_0}{8\pi} \int H^2 \, dv, \quad . \quad . \quad . \quad . \quad . \quad . \quad . \quad . \quad (1)$$

where the integration extends over the whole volume occupied by the substance. Since the force acting on the substance is $F = -\text{grad } E$, we have

$$F = -\frac{\mu - \mu_0}{8\pi} \int \text{grad } H^2 \, dv,$$

where H represents the applied magnetic field and dv an element of volume of the substance. From the relations $B = \mu H = H + 4\pi I$ and $I = kH$, where k = the magnetic susceptibility per unit volume, we get

$$F_x = (k - k_0)\, v H_y \frac{\partial H_y}{\partial x} \quad . \quad . \quad . \quad . \quad . \quad . \quad . \quad . \quad (2)$$

in the direction of x-axis, assuming the magnetic field is along the y-axis and has a gradient along the x-axis. Thus when a substance is placed in an inhomogeneous magnetic field having a gradient along the x-axis, it will experience a force along this axis and a measurement of this force gives us the relative volume susceptibility of the substance.

Using this method, the first determinations of magnetic susceptibilities for air, water, H_2, O_2 . . . were made by Faraday. He gave k-values relative to air. After Faraday, the earliest absolute determination of k was probably due to Rowland and Jacques. They gave for Bi, $k = -12{\cdot}55 \times 10^{-6}$. The negative sign denotes dia and the positive sign paramagnetism.

CURIE'S MAGNETIC BALANCE

Faraday's apparatus has now only historical interest, but the method was subsequently used by Curie,* in his classical researches, so that it sometimes goes by his name; we proceed to a description of his well-known magnetic balance.

---

* P. Curie, *Ann. de Chim. et Phys.*, 7, 289, 1895. For a critical account of experimental methods see also Sève, *ibid.* 27, 189, 425, 1912.

Curie examined the magnetic susceptibility of a large number of substances over a wide range of temperature (20° to 1370°) and for the first time definitely ascertained the fundamental distinction between, dia, para and ferromagnetism. For the production of the inhomogeneous magnetic field he used an electromagnet with inclined pole-pieces as shown in Fig. 2.

The actual balance in work is shown in Fig. 3.

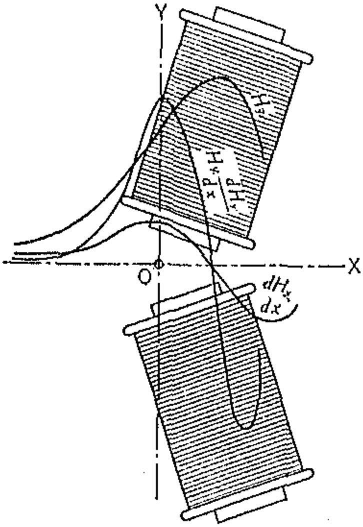

Fig. 2. Curie's magnets.

The specimen whether solid, liquid or gas was enclosed in a U-tube of a complicated form. This was attached to the torsion rod R which included a platform Q for placing small weights to maintain equilibrium, a

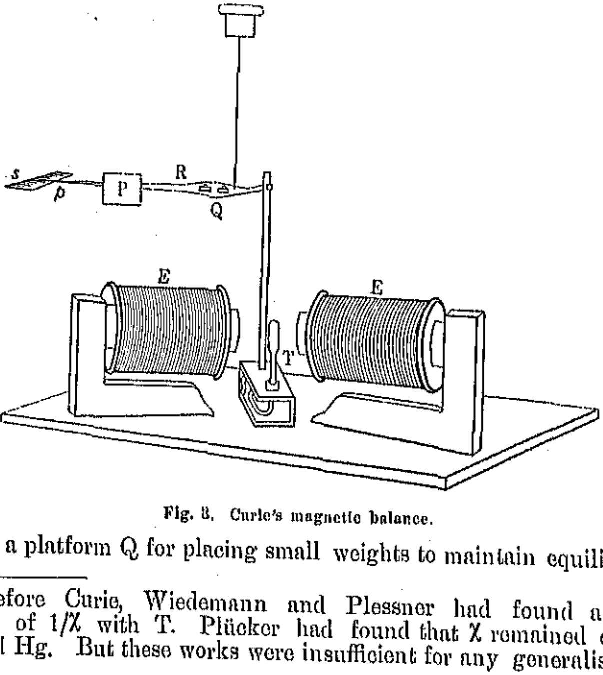

Fig. 3. Curie's magnetic balance.

---

[*] Before Curie, Wiedemann and Plessner had found a limited variation of $1/\chi$ with T. Plücker had found that χ remained constant for S and Hg. But these works were insufficient for any generalisation.

plate P which worked as a damper, and a pointer p moving on a small scale s. On applying the magnetic field, the displacement of the specimen tube was calculated directly from the movements of the pointer on the scale. A special heating oven was used to heat the tube, and the temperature was measured by a thermopile.

The main difficulty in this method was the accurate determination of H and $\partial H/\partial x$ at the point in the non-homogeneous magnetic field occupied by the moving system.

From Fig. 2, it is clear that along the axis of x, $H_x = 0$, and H_y is finite. H_y was determined by a search coil of very small dimensions, by the use of the well-known ballistic method. $\partial H_y / \partial x$ was not determined, but its equivalent $\partial H_x / \partial y$ along the axis of y, for we have $\partial H_y / \partial x = \partial H_x / \partial y$.

The search coil was moved along OY and the value of H found, from which the value of $\partial H_x / \partial y$ can be calculated. H_y, $\partial H_y / \partial x$ and $H_y \, \partial H_y / \partial x$ are then plotted in curves against the distance along the x-axis. The form of these curves is shown in Fig. 2.

The sample is generally placed at the point O, where $H_y \, \partial H_y / \partial x$ is maximum. This minimises the error due to the setting of the tube.

According to Curie's observations, for all dia-magnetics investigated, the specific susceptibility χ was found to be independent of temperature. Only Bi was found to behave in a different way. Its diamagnetic susceptibility decreased linearly with temperature up to its melting point (273°C), when the value fell abruptly, but remained constant for the liquid state over a considerable range of temperature. This is shown in Fig. 4. Amongst the paramagnetics, O_2 was subjected to a wide range of investigation, and the result obtained can be expressed by the relation

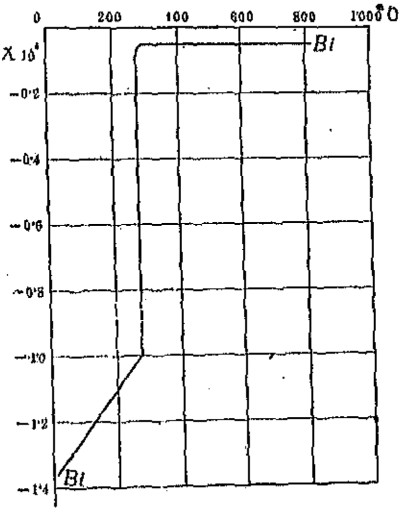

Fig. 4. Temperature variation of χ for Bi (*Honda*)

$$10^6 \, \chi_T = \frac{33,700}{T}$$

where T represents the absolute temperature. He found that in general the relation $\chi_T = A/T$ held good for all paramagnetic elements. Only the constant A was different for different elements. The law was verified also for paramagnetic salt-solutions of Fe^{++}

Fe^{+++}, Ni^{++}, Co^{++} and for palladium salts. This generalisation is usually known as *Curie's law.* It marks out the fundamental property by which the paramagnetics are to be differentiated from the diamagnetics.

The specific susceptibility of soft-iron (ferromagnetic) was found to vary with the magnetic field as well as with the temperature.

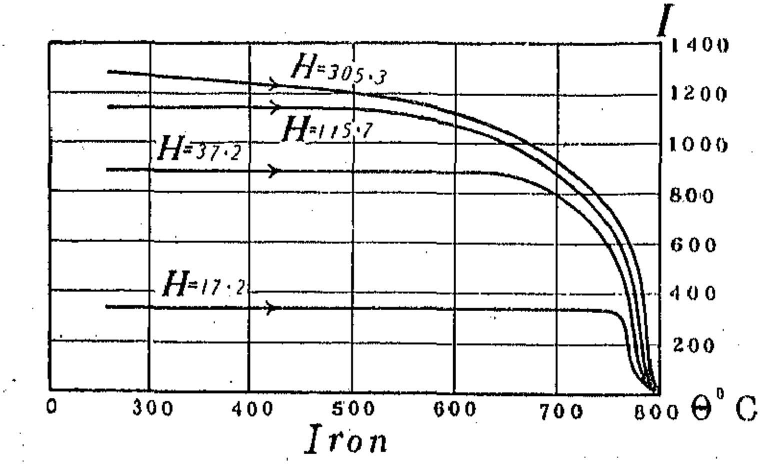

Fig. 5. Variation of magnetisation of soft iron with temperature.

Within the range of 10° to 600°C magnetisation does not show much variation with temperature (Fig. 5), but above this temperature it diminishes rapidly, and falls almost to zero at 790° under all constant fields. The magnetic susceptibility was investigated at still higher temperatures. To a first approximation it varied inversely as the absolute temperature upto 1375°C (Fig. 6). The various irregularities in χ-values seen in the curve are believed to mark the conversion of the sample of soft iron to various allotropic modifications. These results show that for the ferromagnetics χ drops abruptly at a critical temperature (Curie point), above which they behave practically as paramagnetics. For soft iron the critical temperature is 790°C, and those for Ni and Co are 360°C and 1115°C respectively.

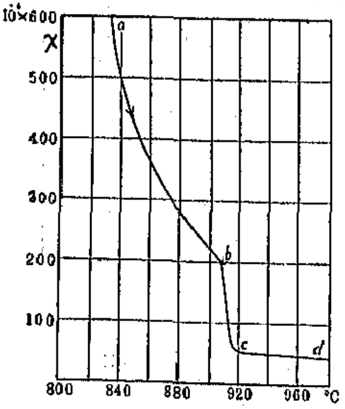

Fig. 6. Temperature-variation of the magnetic susceptibility of soft iron.

OTHER MODIFICATIONS OF THE FARADAY METHOD.

Faraday's original method was modified into different forms by various subsequent workers. Thus Théodoridés[*] and Foëx[†] investigated the magnetic susceptibility of a number of salts by a method, in which the principle of Faraday's method was used, but the deflection was measured by a null method in which the pointer was replaced by the moving coil of an electrodynamometer, and the force tending to move it was balanced by the force between this coil and a fixed one carrying a variable electric current. The extensive researches of Honda, and Owen,[‡] Honda and Ishiwara[‖] were carried out by means of a Curie balance in which many substantial modifications were effected.

Recently Prof. S. S. Bhatnagar[§] has modified the Curie Balance (Fig. 7) in such a way that observations can be taken very rapidly.

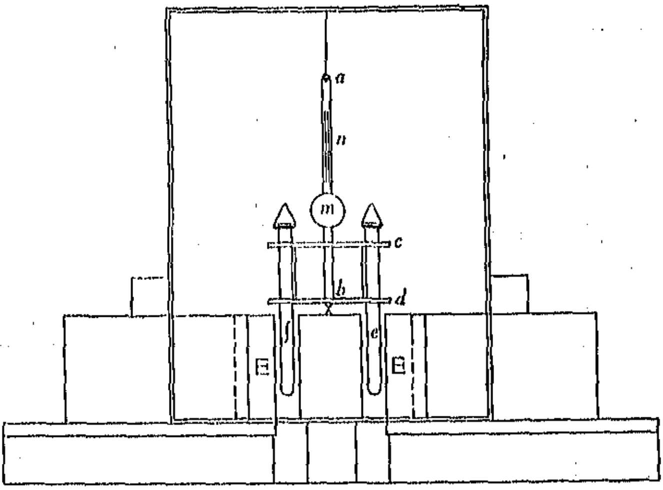

Fig. 7. Bhatnagar's magnetic balance.

Two identical glass tubes e, f are taken, and filled with identical amounts of the substance under investigation. The tubes are carried in holes on the opposite ends of a pair of horizontal aluminium strips c, d. Through the centres of these passes an aluminium beam *a b* rigidly fixed to the strips and carrying a small mirror *m* and a damping vane *n*. The entire thing is suspended from the upper end of the beam along its axis by means of a torsion fibre, so that the lower halves of the two tubes lie between the poles of an electromagnet E E (shown separately in Fig. 8). The pole-pieces of the latter are specially constructed so that the field-gradients over the spaces occupied by *e* and *f* are parallel, but oppositely directed. This special arrangement would give rise to equal and opposite forces on the two tubes thus forming a couple. When the magnet was excited, it produced a ballistic couple which was measured from the momentary deflection of the spot of light. With this apparatus, Bhatnagar and his pupils have measured the susceptibilities of a large number of salts in solution.

---

[*] Théodoridés, *Journ. de. Phys.*, 7, 3, 1922.

[†] Foëx, *Ann. de Phys.*, 16, 174, 1921.

[‡] See for example K. Honda, *Ann. d. Phys.*, 32, 1027, 1910; *Sci. Rep.*, 1, 1, 1912; M. Owen, *Ann. d. Phys.*, 37, 657, 1912.

[‖] T. Ishiwara, *Sci. Rep.*, 3, 303, 1914; Honda and Ishiwara, *Sci. Rep.*, 4, 215, 1915. For details see Honda's book *Magnetic Properties of Matter*, 1928.

[§] Bhatnagar and Mathur, *Doctorate Dissertation of K. N. Mathur.*

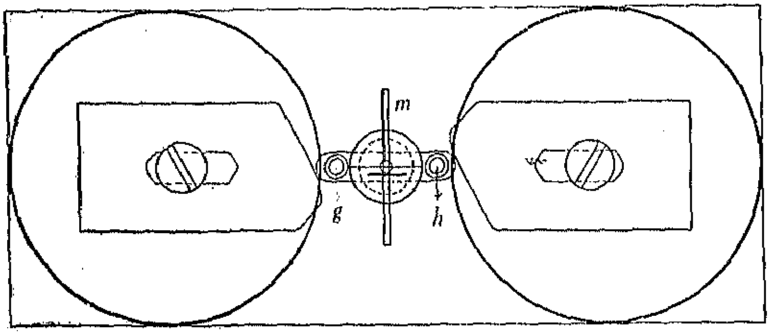

Fig. 8. The pole-pieces in Bhatnagar's magnet which produce equal and opposite field gradients at *g* and *h* the points occupied by the specimens.

356a. Gouy's Homogeneous Field Method.—Another interesting method is due to Gouy.* In this the substance in the form of a uniform cylinder of cross-section *S* is so suspended vertically in a homogeneous magnetic field between two pole pieces of an electromagnet that one end of it is inside the field and the other outside. The force experienced by the second end is negligible, and that by the first end is seen easily to be

$$F = \frac{\mu-\mu_0}{8\pi}\int_0^l \frac{\partial H^2}{\partial x}\cdot Sdx = \tfrac{1}{2}(k-k_0)H^2S \quad . \quad . \quad . \quad (3)$$

The cylinder A is suspended vertically (Fig. 9) along its axis from one arm of a balance, and as the force acts along the vertical axis, it can be counterpoised directly by adding weights to the other pan. The magnetic field being fairly uniform, *H* can be measured by means of a search coil. The method is specially suitable for absolute determination of susceptibilities of solids.

---

* For details of these and other experimental methods see Stoner, *Magnetism and Atomic Structure*, 1926, Chap. VI, III; Honda, *loc. cit.*

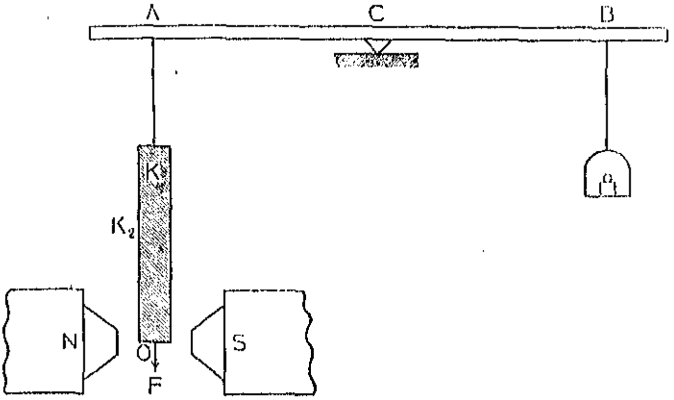

Fig. 9. Gouy's homogeneous field method.

Among the earlier workers Von Ettinghausen used the Gouy method. Wills also used (1896) the same method for experiments on Bi with magnetic fields varying from 1,600, to 10,000 gauss. His results showed that within this range *k* is independent of field strength, a result which we obtain in ferromagnetic bodies only when the magnetising field is so large that saturation is reached.

This method has been modified for determinations of the value of χ for liquids and gases by Quincke and others.

MODIFICATIONS OF THE GOUY METHOD: SONÉ'S APPARATUS.

The direct application of Gouy cylinder method for the determination of magnetic susceptibility *of gases* becomes difficult on account of small density of the gases, except in cases where they have high specific susceptibilities (*e.g.*, O_2). To avoid this difficulty Soné* improved this method substantially and was able to attain sufficient sensitiveness so that accurate determinations of susceptibility for gases became possible. The gas under investigation is enclosed in a cylindrical glass tube T (Fig. 10) which is divided into two halves by a glass partition P. The lower half of the tube is evacuated and the upper half filled with the compressed gas. This tube takes the place of the cylinder in Gouy's method. Now the magnetic field is applied. If the tube were empty, there would be no resultant thrust, since the thrust on the upper part is equal and opposite to that on the lower part. When the upper part is filled with compressed gas, the resultant thrust measures only the force on the gas. *The method is thus a differential one.* The thrust is balanced, as in Gouy method, by placing weights on the other pan of the balances. The pointer of the balance is replaced by an elaborate system of bifiliar suspension. This enables very small forces to be measured. A few of Soné's results are given below in Table 1.

---

* T. Soné, *Sci. Rep.*, 8, 115, 1919; **11**, 139, 1922.

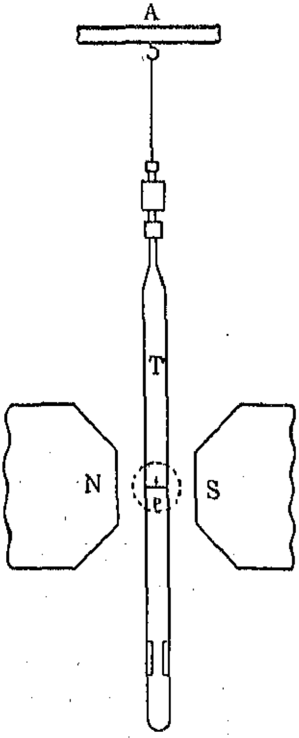

Fig. 10. Soné's balance.

QUINCKE'S CAPILLARY ASCENSION METHOD FOR LIQUIDS

The Gouy method was modified by Quincke for measuring the susceptibilities of liquids and gases. The substance was enclosed in a U-tube (Fig. 11) one limb

Table 1.—Magnetic susceptibility of gases at 20° C and 760 mm (Soné).

Gas	$\chi_m \times 10^6$	$k \times 10^6$
Air	23·85	0·03084
Oxygen, O_2	104·1	0·0488
Carbondioxide, CO_2 ...	—0·423	—0·000836
Nitrogen, N_2 (chemical)...	—0·265	—0·000331
" (atmospheric)	—0·360	—0·000452
Hydrogen, H_2 ...	—1·982	—0·0001781
Nitric oxide, NO ...	48·80	
Nitrous oxide, N_2O ...	—0·429	
Nitrogen peroxide, NO_2...	4·54	
Nitrogen tetroxide, N_2O_4	—0·276	
Nitrogen trioxide, N_2O_3	—0·206	
Nitrogen pentoxide, N_2O_5	—0·332	

of which is wider than the other. A uniform magnetic field is applied across the meniscus in the narrow limb, the other limb being fairly distant. The meniscus rises under the force, through a height h given by $hg\rho=\frac{1}{2}(k-k_0)H^2$, where $\rho=$ density of the liquid and k, k_0 the susceptibilities of the liquid and of the gas above it. If χ represents the mass-susceptibility, we have $\chi=k/\rho$, $\chi_0=k_0/\rho_0$

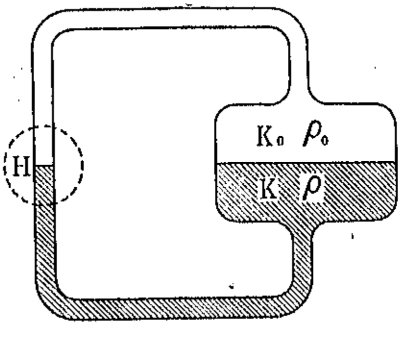

Fig. 11. Quincke's apparatus.

Hence $$\chi=\frac{\rho_0}{\rho}\chi_0+\frac{2hg}{H^2} \quad . \quad . \quad . \quad . \quad . \quad . \quad . \quad . \quad . \quad . \quad (4)$$

The method is convenient inasmuch as the blank experiment is dispensed with, and the presence of impurities of higher susceptibilities does not affect the result. For accurate measurement it is preferable to bring back the meniscus to its original position by applying pressure, in which case the necessity of making the field uniform may be done away with.

BAUER AND PICCARD'S METHOD

357. Modifications of Quincke's Method.—A modified form of Quincke's method has been employed by Bauer and Piccard* in their investigation on the magnetic susceptibility of oxygen and nitric oxide. The gas under investigation was enclosed under high pressure in the capillary limb of the U-tube, the other limb being filled with water. As on applying the magnetic field the liquid-gas meniscus was displaced, it was brought back to its original position by raising a reservoir attached to the other limb, by means of micrometer screws. The amount of elevation could be accurately read, and making preliminary blank experiments on water, the magnetic susceptibility of the gas could be calculated. The temperature of the gas was determined by a silver-constantan-couple.

The accuracy of the above method was however nullified by the effect of gas contained in water in the dissolved state, and Bauer and Piccard therefore devised a second method. The apparatus for the later method is shown in Fig. 12.

---

* Bauer and Piccard, *Journ de Phys.*, **1**, 97, 1920.

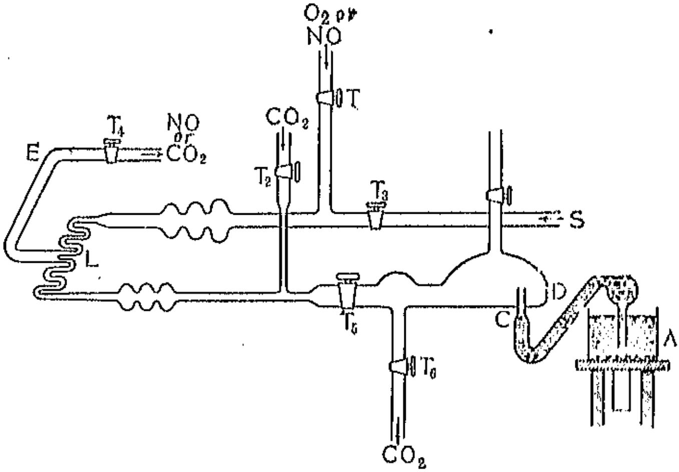

Fig. 12. Bauer and Piccard's apparatus.

The gas under investigation (O_2 or NO) was contained in the tube LS which was kept open to the atmosphere by means of the stopcock T_3. The side tubes T_1 and T_4 served as the inlet and outlet for the gas. The other part LD of the apparatus was filled with CO_2-gas which is only very feebly diamagnetic. The side tubes T_2 and T_6 were respectively inlet and outlet for CO_2. The part L was a labyrinth which was specially designed to prevent interdiffusion of the two gases. The pressure of the experimental gas at L was transmitted to the water manometer A through the CO_2-gas. The field was applied at L the place of separation of the two gases, and the resulting change in pressure, was recorded by the displacement of C the gas-water meniscus as before. This eliminates the error due to solution of the experimental gas in water. In this method however the homogeneity of the field over the zone of mixture of the two gases is essential.

Table 2.—Magnetic moments of O_2 and NO.

Gases	$\chi \times 10^6$	$\chi \times 10^6$	p
O_2	107·8	·1434	14·12
NO	48·7	·0609	9·20

Thus the difference of pressure was measured between two points on a column of gas, one of which was exposed to the magnetic field and the other was outside of it. Bauer and Piccard's result for O_2 and NO are shown opposite.

WILLS AND HECTOR'S METHOD.

More recently (1924) the Quincke method has been ingeniously modified by Wills and Hector* for the determination of magnetic susceptibilities of the inert gases. In this the gas to be tested is enclosed under high pressure in an O-shaped tube (Fig. 13). The gas occupies the part C to F and is in contact at F with a solution of the paramagnetic salt nickel-chloride of known susceptibility. Magnetic field is applied at F. The two are then magnetically balanced first by varying the concentration of the salt solution at a known pressure of the gas, and then accurately by changing the pressure of the enclosed gas or the common temperature of the gas and the solution. The gas pressure is noted by means of a manometer connected at M. The movement of the meniscus is not directly observed at F, but at the constricted part G by means of a microscope. Gum-mastic particles are put in the solution which serve as a sensitive indicator for the movement of the meniscus. From this observation the susceptibility of the gas at any other temperature is calculated by using Curie's law. The following table shows some of their results.

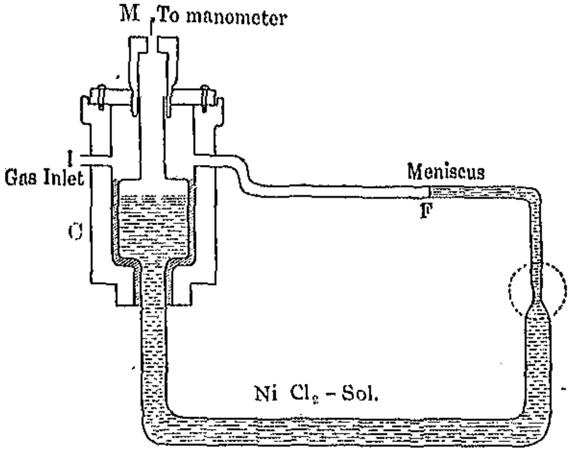

Fig. 13. Wills and Hector's magnetic balance.

Table 3.—Magnetic susceptibility of inert gases.

Gases	$\chi \times 10^6$ at 20°C and 1 atm. press.	$k \times 10^6$
Argon	-0.452	-0.000752
Helium	-0.473	-0.0000780
Neon	-0.334	-0.000277

In all these methods which depend upon the measurement of the forces acting on the substance when placed in a homogeneous or non-homogeneous magnetic field, the necessity of measuring field strength is often avoided by making the measurements relative to a substance of which the absolute value of susceptibility is known. Water is generally chosen for this purpose for which $\chi = -0{\cdot}72 \times 10^{-6}$ at 20°C as determined by Sevè, Piccard and Piccard and Johner. *

---

* Wills and Hector, *Phys. Rev.*, 23, 209, 1924; Hector, *ibid*, 24, 418, 1924.

The fact that the force on a substance in a magnetic field is proportional to the difference in volume susceptibilities of the material and the surrounding medium, has often been utilised to measure the susceptibilities of solutions and of gases. The experimental liquid or gas forms the medium in which a test piece is suspended, and magnetic field is applied to the latter. The force on this piece is measured in different media.

Interpretation of the results of paramagnetic measurements always requires the susceptibility values to be known over as large a range of temperature as possible. An arrangement for varying the temperature is therefore kept in all the methods. For temperatures higher than the room temperature an electric furnace is used. Lower temperatures are obtained by immersing the test piece in a liquified gas, or by cooling with cold gas or vapour. For details of experiments the publications from the Cryogenic Laboratory at Leiden may be consulted. The temperature is measured by a thermocouple or a resistance thermometer.

Finally, brief mention may be made to a dynamical method used for the measurement of the principal susceptibilities of crystals. A suitably cut crystal is suspended with one of its principal axes parallel to the lines of force of a magnet. When it is displaced slightly from the position of equilibrium it executes simple harmonic oscillations. The time period depends upon the susceptibility, and absolute measurements may be made if the field strengths at different parts are known.

358. Summary of Experimental Results on Diamagnetism.

—The experimental study of diamagnetism has shown that the mass susceptibility is :

(1) almost always independent of temperature, and
(2) very often independent of the physical state.

While a very large number of substances obeys law (1) over a considerable range of temperature, there are also several cases of exception. χ for substances like Bi, Sb, Te diminishes in value as

---

* Piccard and Johner, *Helv. Phys. Acta*, 4, 238, 1931.

the temperature is raised and undergoes a remarkable diminution at the melting point.

Graphite presents very peculiar features. When the cleavage plane is perpendicular to the magnetic field, χ has the exceptionally high value -15×10^{-6}, while with the above plane parallel to the field, χ is $-4{\cdot}7\times10^{-6}$. This phenomenon of *diamagnetic anisotropy* is shown by all anisotropic crystals in general and its study sheds considerable light in elucidating the structure of such crystals.

Accurate measurements always reveal a more or less pronounced difference between the χ-values of the same substance in different physical states. The same also holds for allotropic modifications of a substance. Metallic tin is remarkable in this respect, for while the grey variety, which is stable below 18°C, is diamagnetic, the white variety is paramagnetic. On fusion it is diamagnetic again.

359. Langevin's Theory of Diamagnetism.—The interpretation of magnetism as an atomic phenomenon began practically with Weber's idea of molecular currents. But a real mathematical theory was first worked out by Langevin* in 1905 who started from the ideas introduced by Lorentz on the electron theory of matter: (1) material substances consist of assemblages of electrons which rotate in closed orbits about a centre of force, (2) as an electron rotates in an orbit, it behaves like a magnetic shell having the moment $es/c\tau$, where e = charge, s = area of the orbit, c = velocity of light, τ = periodic time. If, on the whole, the different electronic orbits be magnetically balanced, the system will have no resultant magnetic moment, that is, it will be diamagnetic. We shall now proceed to show how starting from these ideas the theory of diamagnetism can be worked out.

According to the classical electron theory, an electron moving in a circular orbit of radius r_1 and period τ possesses the magnetic moment

$$\mu_e = \frac{e\pi r_1{}^2}{c\tau} = \frac{er_1{}^2}{2c}\,\omega \quad . \quad . \quad . \quad . \quad . \quad . \quad . \quad . \qquad (5)$$

where ω = angular velocity.

The moment is directed perpendicularly to the plane of the orbit. The sense of the moment can be easily fixed with the aid of the usual rules. Now the moving electron is subjected to a centrifugal force which is equal and opposite to the attraction of the nucleus, and is given by

---

* Langevin, *Jour. de Phys.*, 4, 678, 1905.

$$F = m\omega^2 r \quad . \quad . \quad . \quad . \quad . \quad . \quad . \quad . \quad . \quad (6)$$

What happens when a magnetic field perpendicular to the plane of the orbit is applied? The electron in motion is equivalent to an electric current of magnitude $e\omega r_i/c$ and on applying the magnetic field it experiences a force $He\omega r_i/c$, directed along the radius, the sense depending upon the direction of the magnetic field and of the moving electron. If the equivalent magnetic moment and the field have the same directions, the force is directed away from the nucleus, but when the field and the moment are oppositely directed, the force is towards the nucleus. These are illustrated in Fig. 14 (*a*) and (*b*) respectively.

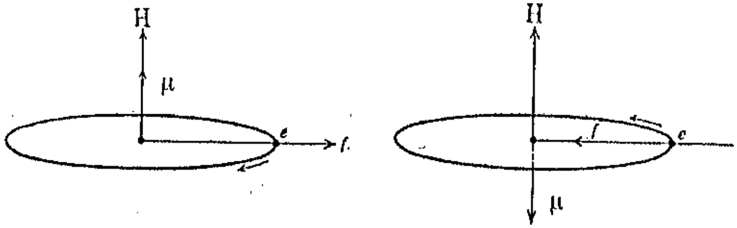

(*a*) Fig. 14. (*b*)

As long as the force $He\omega r_i/c$ acts on the electron, its angular velocity undergoes a change $\Delta\omega$, and the modified value of the centrifugal force is equivalent to the resultant of the radial forces. Hence

$$F \pm \frac{He\omega r_i}{c} = m(\omega \pm \Delta\omega)^2 r_i \quad . \quad . \quad . \quad . \quad . \quad . \quad . \quad . \quad (6')$$

We can assume $\Delta\omega$ to be small compared to ω. Comparing equations (6) and (6′), we get

$$\Delta\omega = -\frac{He\omega r_i}{2\,me\omega r_i} = -\frac{He}{2mc}$$

This causes a variation in the magnetic moment of the electron by an amount $\Delta\mu_e$ given by

$$\Delta\mu_e = \frac{e}{2c} r_i^2 \Delta\omega = -\frac{e^2 H}{4mc^2} r_i^2 \quad . \quad . \quad . \quad . \quad . \quad . \quad (6'')$$

When there are more than one electron in the atom, a summation is to be made over them, and r_i^2 should be replaced by Σr_i^2.

And as the orbits are not all circular, r_i^2 values are to be replaced by an average value $\overline{r_i^2}$. Instead of the orbital planes being perpendicular to the field, they can have all possible orientations with respect to it. Let r_1 be the radius of the projection of the orbit on a plane at right angles to the magnetic field. Then for an atom containing N electrons,

$$\Delta\mu_e = -\frac{e^2 H}{4mc^2} \Sigma r_1^2 \, * \quad . \quad . \quad . \quad . \quad . \quad . \quad . \quad . \quad (7)$$

where the summation extends over all the electrons.

For a diamagnetic atom, therefore, the atomic diamagnetic susceptibility is given by

$$\chi_{At} = \frac{\Delta\mu_{At}}{H} = -\frac{e^2}{4mc^2} \Sigma \overline{r_1^2} \quad . \quad . \quad . \quad . \quad . \quad . \quad . \quad (8)$$

For spherically symmetrical atoms $\Sigma r_1^2 = \frac{2}{3} \Sigma \overline{r^2}$. And for a gm-atom which contains N (Avagadro number) atoms

$$\chi_A = \chi_m \times A = \chi_{At} \times N = -\frac{e^2 N}{6mc^2} \Sigma \overline{r^2} \quad . \quad . \quad . \quad . \quad . \quad (9)$$

where χ_m denotes mass susceptibility and A the atomic weight.

It is clear from Fig. 14 that in (*a*) the angular velocity of the electron is diminished, and the moment μ therefore suffers a reduction. In case (*b*) the reverse holds. In both cases the change in moment is directed opposite to the field. This induction effect immediately follows from Lenz's law. The entire atom undergoes a change in moment of the magnitude $\Delta\mu_e$, irrespective of the fact whether initially the magnetic moments of the individual orbits compensated each other or not. When compensation is wanting, there is a resulting magnetic moment, and the substance is paramagnetic.

Thus diamagnetism appears to be a universal property of matter, and, as the above formula shows, is independent of temperature and field strength. Even in the case of para or ferromagnetic bodies, the diamagnetism is present, but is obscured by the much more intensive phenomena of an opposite kind.

---

* The formula (7) can be much more easily deduced by using Larmor's theorem of precession, *i.e.*, the induced angular velocity of precession of the electronic orbit due to the magnetic field H is $\Delta\omega = -He/2mc$. But here we have preferred a deduction from fundamental principles, because this method gives an insight into the mechanism of diamagnetism.

The essential condition for an atom or an ion to be wholly diamagnetic is that the electronic orbits of the system of electrons composing it must be symmetrically distributed around the nucleus, so that the initial resultant magnetic moment of the orbital electrons vanishes. From the spectroscopic point of view this amounts to the fact that the atom or ion should be in the $^1S_0$ -state, in which the resultant spin moment and the orbital moment of the system vanish. The diamagnetic susceptibility for such an atom or ion is given by equation (9). Such are, for example, the inert gases, He, Ne, A, Kr, Xe and Niton and atoms of the second group Be, Mg, Ca, Sr, Ba, Zn, Cd and Hg.

360. Discussion of Results on Determinations of the Diamagnetic Susceptibility.—As emphasised already, the theory of diamagnetic susceptibility sketched above is strictly applicable only to mononuclear systems. The ideal case where the theory is expected to hold good is the family of inert gases, *e.g.*, He, Ne, A, etc., which form monatomic molecules and are characterised by closed shell electronic structure. But from the standpoint of experimental study inert gases offered for a long time a problem of great uncertainty. Joos* pointed out that the susceptibility of an inert gas atom like Ne should be greater than that of the positively charged ions just following it in the periodic table as Na^+, and less than that of the negatively charged ion just preceding it, $\bar{F}$ in this case; because the nuclear charge of the inert gas atom is intermediate between the two, and greater nuclear charge is associated with smaller radius of electron orbit, and *vice versa*. Direct measurement of χ of inert gases has now been possible by the improved methods of Wills and Hector as already described, and the above conclusion has been verified.

We shall now describe how the susceptibility of other mononuclear structures (ions) with inert gas shells has been determined. It is not possible to get ions in the free state, hence an indirect method is employed.

Suppose we take a substance like CsI in solution. According to very probable hypothesis, CsI or most alkali halides are *ionic* compounds, *i.e.*, are supposed to consist of a positively charged alkali ion, and a negatively charged halogen ion. It is assumed that the alkali loses one electron which attaches to the halogen atom. The molecule is thus made up of two mononuclear systems Cs^+ and $\bar{I}$ each with an inert gas structure like Xe and each containing 54 electrons in the outer shells. It is assumed further that diamagnetic χ of the compound is the sum of the χ's of the individual ions. This is a direct consequence of *Pascal's law* which states that the χ of a diamagnetic molecule is equal to the sum of the χ's of its constituent atoms and ions each of which is independently diamagnetic. The problem is then to determine χ for the compound CsI and to partition it in a suitable way between its two constituent ions.

---

* Joos, *Zs. f. Phys.*, 19, 347, 1923.

The χ-value for CsI and most other salts is best determined in their solution. Water is diamagnetic having its susceptibility $\chi_w = -·72\times10^{-6}$. Hence the susceptibility of a salt is obtained from that of its solution by applying the additive law

$$\chi = c_s\,\chi_s + (1-c_s)\,\chi_w \qquad . \quad . \quad . \quad . \quad . \quad (10)$$

where χ, χ_s and χ_w denote respectively the susceptibility of solution, salt and water, and c_s = the concentration of the salt. A determination of χ and c_s enables us to obtain χ_s. Ikenmeyer[*] obtained in this way for CsI, $\chi_m = -95\times10^{-6}$, ($\chi_m$ = molecular susceptibility).

We now consider the method of partitioning χ_s between the ions. Cs^+ and $\bar{I}$ both contain 54 electrons in the outer shells. Ikenmeyer takes χ's for the ions Cs^+ and $\bar{I}$ to be inversely proportional to the square of their nuclear charges, and hence obtain

$\chi_{Cs^+} = -45·75\times10^{-6}$,

$\chi_{I^-} = -49·25\times10^{-6}$

Taking these as standard, χ's for singly charged ions of alkali elements and of doubly charged ions of alkaline earth elements can be easily measured from the determination of χ for compounds of these ions with $\bar{I}$. The χ-values of single negatively charged halogen ions also can then be easily determined from those of their compounds with alkalies. This has been done by Ikenmeyer and others as shown in Table 4.

Table 4.—Diamagnetic susceptibilities of ions. ($\chi\times10^6$)

$Z\rightarrow$ No. of electrons N	$N-1$		$N+1$		$N+2$	
10	F^-	13·9	Na^+	10·4	Mg^{++}	4·5
18	Cl^-	20·4	K^+	16·9	Ca^{++}	11·0
36	Br^-	34·8	Rb^+	31·3	Sr^{++}	25·4
54	I^-	49·3	Cs^+	45·7	Ba^{++}	39·9

It was further found that a linear relation existed between χ, and N the number of electrons of the ions of elements in the same vertical column of periodic table. The relation is

$$-\chi\times10^6 = a_1\,N + a_2 \quad . \quad . \quad . \quad . \quad . \quad . \quad . \quad . \quad (11)$$

---

[*] K. Ikenmeyer, *Ann. d. Phys.*, **1**, 169, 1929.

where c_1 is a constant for different series, and c_2 another constant which however is different for different series. For heavy elements c_2 is negligible in comparison with $c_1 N$. Thus for alkali ions $c_1 = 0{\cdot}80 \times 10^{-6}$, $c_2 = 2{\cdot}4$; for alkaline earth ions $c_2 = -3{\cdot}5$.

We can make an estimate of radius of the electronic orbit from magnetic data in the following way: from (9) we have

$$\chi_M = -\frac{Ne^2}{6mc^2}\sum_N \overline{r^2} = -2{\cdot}85\times 10^{10} \sum_N \overline{r^2} = -0{\cdot}80\times 10^{-6}\, N$$

Hence

$$\overline{r^2} = \frac{0{\cdot}80\times 10^{-6}}{2{\cdot}85\times 10^{10}} = ({\cdot}53\times 10^{-8})^2. \quad . \quad . \quad . \quad . \qquad (12)$$

This shows that the root mean square value of the radius of electronic orbit for heavy orbits is roughly equal to that of the innermost orbit of hydrogen ($r = {\cdot}532\times 10^{-8}$ cm.). But this deduction has very little significance beyond showing that $\overline{r^2}$ is of the reasonable order or magnitude. In general the agreement is much less striking for other ions, as it naturally should be, for $\overline{r^2}$ gives only mean value of the radii.

In recent years attempts have been made by Hartree,* Pauling,† Slater‡ and others to calculate χ-values theoretically with the help of equation (9) by assuming continuous electronic charge distribution of ions as postulated by the new quantum mechanics. As the methods are in controversial stage, we shall not enter into their discussions here.

361. Langevin's Theory of Paramagnetism.—As already remarked on p. 787, Langevin§ gave a mathematical precision to Weber's ideas, and worked out a theory of paramagnetism which has been highly successful in explaining Curie's result $\chi = C/T$. The fundamental assumptions in Weber's picture are (i) the ultimate constituents of matter are each a small magnet, (ii) they are haphazardly arranged when no magnetising field acts on them.

The first assumption has been completely vindicated in Bohr's picture of the atom, and by the direct experimental proof by Stern and Gerlach, which showed that all atoms possess magnetic moments of $\mu_B gj$, where $\mu_B = eh/4\pi mc$ is the Bohr-magneton or the magnetic moment of an electron rotating in an orbit. But when Langevin worked out his theory, such definite pictures were absent.

---

* Hartree, *Proc. Camb. Phil. Soc.*, 24, 89, 1928.
† Pauling, *Proc. Roy. Soc. A.*, **114**, 181, 1927.
‡ Slater, *Phys. Rev.*, **36**, 57, 1930.
§ Langevin, *Jour. de Phys.*, 4, 678, 1905.

He proceeded only with general ideas. He supposed that when the substance is placed in a magnetic field the constituent particles tend to set themselves with their axes parallel to the magnetic field. But this is resisted by the chaotic heat motion of the particles, and ultimately a condition of equilibrium is established. The mathematical theory is as follows :

Let θ be the inclination of the magnetic axis of a particle to the direction of the external magnetic field. Its potential energy in the field is

$$\int_{\theta}^{0} \mu H \sin\theta \, d\theta = \mu H(1-\cos\theta) \quad . \quad . \quad . \quad . \quad . \quad (13)$$

where μ = the molecular magnetic moment. According to Maxwell's law, the number of molecular magnets possessing the moment within a solid angle $d\omega$ is

$$dn = Ce^{-\frac{\mu H}{kT}(1-\cos\theta)} d\omega = Ae^{\alpha\cos\theta} \sin\theta \, d\theta \quad . \quad . \quad . \quad (14)$$

where $\alpha = \mu H/kT$ and A is a new constant $= 2\pi Ce^{-\alpha}$

Then the number of molecules per unit volume is obtained by integrating the expression (14) between $\theta = 0$ to $\theta = \pi$; we have

$$n = A\int_{0}^{\pi} e^{\alpha\cos\theta} \sin\theta \, d\theta = A\frac{e^{\alpha} - e^{-\alpha}}{\alpha}$$

The maximum magnetic moment due to n molecules is given by the expression

$$\sigma_0 = n\mu$$

Again let $\bar{\mu}$ = mean resolved magnetic moment of the particles along the field direction. Let $\sigma = n\bar{\mu}$. We have then

$$\sigma = \int \mu \cos\theta \, dn = \mu A\int_{0}^{\pi} e^{\alpha\cos\theta} \cos\theta \sin\theta \, d\theta = \mu \frac{\partial n}{\partial \alpha}$$

Therefore
$$\frac{\bar{\mu}}{\mu} = \frac{\sigma}{\sigma_0} = \frac{\mu}{\mu n} \frac{\partial n}{\partial \alpha} = \coth\alpha - \frac{1}{\alpha} = L(\alpha) \quad . \quad (15)$$

The function $L(\alpha)$ is known as the *Langevin function.* For small values of α, we can have a power-series expansion of $L(\alpha)$ as

$$L(\alpha) = \frac{\alpha}{3} - \frac{\alpha^3}{45} + \frac{\alpha^5}{473} \quad . \quad . \quad . \quad . \quad . \quad . \quad . \quad (16)$$

For large values of α

$$L(\alpha) = 1 - \frac{1}{\alpha} + 2e^{-2\alpha} \quad . \quad . \quad . \quad . \quad . \quad . \quad . \quad (17)$$

If α be very small, as is usually the case when $\mu H << kT$, we can neglect powers of α higher than unity in the expansion (16), and the expression (15) reduces to $\frac{\alpha}{3}$, so that

$$\frac{\bar{\mu}}{\mu} = \frac{\alpha}{3} = \frac{\mu H}{3kT} \text{ or } \bar{\mu} = \frac{\mu^2 H}{3kT} \cdot \quad . \quad . \quad . \quad . \quad (18)$$

Thus the *gm-molecular susceptibility* χ_M *is given by*

$$\chi_M = \frac{\bar{\mu}N}{H} = \frac{\mu^2 N}{3kT} = \frac{\sigma_0^{\,2}}{3RT} \quad . \quad . \quad . \quad . \quad . \quad . \quad . \quad (19)$$

where $\sigma_0 = \mu N =$ gm-molecular magnetic moment.

The justification for the above approximation becomes very clear from the curve in Fig 15. This is obtained by plotting the function $L(\alpha)$ against α. It will be seen that over an extended range the curve coincides with its tangent at the origin. For large values of α, the curve shows that there is saturation, the numerical value of $\bar{\mu}/\mu$ approaching unity. This also follows from the expansion (17).

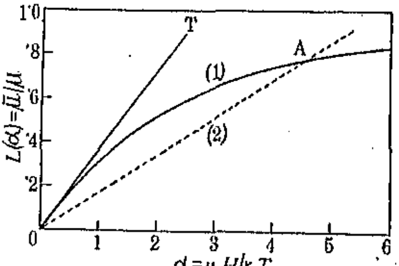

Fig. 15

At ordinary temperature, with the magnetic field usually available, even the strongest paramagnetics give a very low value of α. Thus for Mg, for which μ=32,800 for a gm-atom at about 27°C, taking H=20,000 Gauss, we have

$$\alpha = \frac{\mu_{\text{atom}} H}{kT} = \frac{\mu_{\text{gm. at.}} H}{NkT} = \frac{32800 \times 20000}{8{\cdot}3 \times 10^7 \times 300} = 0{\cdot}026.$$

While for $\alpha = 100$, $\bar{\mu}/\mu$ is within 1% of its saturation value 1. So for the paramagnetics in general, α is much smaller than its saturation value, and we may replace the Langevin-function by its tangent at the origin. From the geometry of the curve $L(\alpha) = \coth\alpha - 1/\alpha$, the tangent to it at the origin is $\alpha/3$, which justifies our approximation $\bar{\mu}/\mu = \alpha/3$.

We can further conclude from (19) that the paramagnetic susceptibility varies inversely as the absolute temperature. This explains the result first obtained by Curie from extensive experimental researches (*vide supra*) and expressed in the form $\chi_M T = C_M$, where C_M = the Curie constant for a gm-molecule. Most of the paramagnetic gases and solutions obey this law over a wide range of temperature. Among the solids gadolinium sulphate $Gd_2(SO_4)_3, 8H_2O$ is one of the few substances which has been found to obey Curie's law accurately down to the lowest temperature of 1·3°K.

Further we obtain from (19) that the gm-molecular moment

$$\sigma_0 = \sqrt{3R\chi_M T} = \sqrt{3RC_M} \quad . \quad . \quad . \quad . \quad . \quad . \quad (20)$$

which enables us to calculate the magnetic moment μ from a knowledge of Curie's constant C_M.

An example will perhaps help the student towards a better understanding of the principles set forth above. Take the case of $FeCl_2$. It is a highly paramagnetic substance, and its magnetic susceptibility at 10°C is given by

$$\chi_m = 91\times10^{-6},\quad \chi_M = 91\times127\times10^{-6} = 1{\cdot}156\times10^{-2}$$

Hence the gm-molecular magnetic moment

$$\sigma_0 = \sqrt{3RT\chi_M} = \sqrt{3\times8{\cdot}3\times10^7\times283\times1{\cdot}156\times10^{-2}} = 2{\cdot}8\times10^4$$

Therefore the molecular magnetic moment $\mu = \dfrac{\sigma_0}{N} = 4{\cdot}5\times10^{-20}$ units.

It should be noted here that the $FeCl_2$ molecule is supposed to consist of Fe^{++} and two $\overline{Cl}$-ions. Since $\overline{Cl}$ is diamagnetic by constitution, the above magnetic moment is contributed wholly by Fe^{++}, which is the active ion in this case. The magnetic moment of Fe^{++}-ion in the solid state may be expressed in terms of Bohr-magneton. It is $4{\cdot}5\times10^{-20}/9{\cdot}23\times10^{-21} = 4{\cdot}87$ Bohr-magnetons.

362. Weiss's Extension of Langevin's Theory.—The result of extended investigations shows however that very few substances strictly obey the theoretical Curie law $\chi_M T = C_M$, but the results agree tolerably well if we take a slightly modified law

$$\chi = \frac{C}{T-\theta} \quad \text{or} \quad \frac{C}{T+\theta} \quad . \quad . \quad . \quad . \quad . \quad . \quad (21)$$

where θ is a constant which depends upon the nature of the substance.

Most paramagnetic solids as well as ferromagnetic substances above Curie point follow the Weiss law (21). For example, investigations of Jackson[*] shows that anhydrous, hydrated and double sulphates of Fe, Co and Ni follow the law

$$\chi = \frac{C}{T-\theta} \quad . \quad . \quad . \quad . \quad . \quad . \quad . \quad . \quad . \quad (21')$$

between 290°K to 70°K (temperature of liquid nitrogen). The values of magnetic moment p and Weiss constant θ for a number of these sulphates over this range of temperature is given in Table 5.

Table 5.

Substance	θ	p
$Fe\,SO_4$	−31	25·53
$Fe\,SO_4.7H_2O$	− 1	25·84
$Fe\,SO_4.(NH_4)_2SO_4.6H_2O$	− 3	27·5
$Co\,SO_4$	−44·9	25·2
$Co\,SO_4.7H_2O$	−13·9	25·04
$Co\,SO_4.(NH_4)_2SO_4.6H_2O$	−22	24·75
$Ni\,SO_4$	−79·4	16·9
$Ni\,SO_4.7H_2O$	+59	14·62
$Ni\,SO_4.(NH_4)_2SO_4.6H_2O$	− 4	15·9

A similar law is followed by $MnSO_4$ ($C = 0{\cdot}0283$, $\theta = -28{\cdot}3$) down to about 70°K. But below this temperature it is found that the relation between $1/\chi$ and T is no longer linear, the increase in χ being less rapid than that given by (21). This deviation is known as *cryomagnetic anomaly*[†] and is exhibited by many substances at low temperatures.

Weiss[‡] has tried to account for the modified Curie law in the following way. He suggested that for these solids the effective magnetising field causing orientation of the particles is not merely the external magnetising field H, but it is supplemented by an internal field H_i due to the surrounding ions. Weiss took this inner field to be proportional to the intensity of magnetisation I. Thus the effective magnetising field

$$H_e = H + H_i = H + AI \quad . \quad . \quad . \quad . \quad . \quad . \quad . \quad (22)$$

where A is the constant of proportionality. Though the internal field is supposed to be due to the magnetic particles surrounding the particle in question, its real nature is still a matter of speculation. (See, for example, Van Vleck, *Electric and Magnetic Susceptibilities*, p. 304).

---

[*] Jackson, *Phil. Trans. A*, 224, 1, 1923.

[†] The effect was discovered in the Cryogenic Laboratory at Leiden by K. Onnes and his callaborators in their low temperature investigations.

[‡] Weiss, *Jour. de Phys.*, 6 (4), 661, 1907; 1, 134, 1914.

Assuming the existence of such a field we can now revise the equations (18) to (20). We have consequently

$$\frac{\bar{\mu}}{\mu} = \frac{\mu(H+AI)}{3kT} \quad . \quad . \quad . \quad . \quad . \quad . \quad . \quad . \quad . \quad (23)$$

We use $\sigma = N\bar{\mu}$, $\sigma_0 = N\mu$ in the same sense as before. Further if ρ = density, and m = molecular weight, the intensity of magnetisation $I = \rho\sigma/m$. Then we have

$$\frac{\sigma}{\sigma_0} = \frac{\bar{\mu}}{\mu} = \frac{\mu}{3kT}\left(H + \frac{A\rho\sigma}{m}\right)$$

or

$$\sigma\left(1 - \frac{\mu\sigma_0 A\rho}{3kTm}\right) = \frac{\mu\sigma_0}{3kT} H$$

Therefore, $\chi_M = \sigma/H = \dfrac{\mu\sigma_0/3kT}{1 - \mu\sigma_0 A\rho/3kTm} = \dfrac{\sigma_0{}^2/3R}{T - \sigma_0{}^2 A\rho/3Rm}$. . (24)

or, $\chi_M = \dfrac{C_M}{T - \theta}$, where $\theta = A\rho\sigma_0{}^2/3Rm$ . . . . (25)

For substances which obey the Weiss law, there arises a probability for the spontaneous magnetisation in the absence of any external field acting. For when the external field is zero, we have

$$a = \frac{\mu H_e}{kT} = \frac{\mu AI}{kT} = \frac{\sigma_0 A\sigma}{RTm} = \frac{\sigma_0{}^2 A\rho}{RTm} \cdot \frac{\sigma}{\sigma_0}$$

Therefore

$$\frac{\sigma}{\sigma_0} = \frac{mRT}{\sigma_0{}^2 A\rho}\,a \quad . \quad . \quad . \quad . \quad . \quad . \quad . \quad . \quad . \quad (26)$$

In such a case, the magnetisation is entirely due to the interaction field. Also in general, we have

$$\frac{\sigma}{\sigma_0} = \coth a - \frac{1}{a} \quad . \quad . \quad . \quad . \quad . \quad . \quad . \quad . \quad . \quad (27)$$

Thus at the particular temperature which satisfies simultaneously the two relations (26) and (27) the phenomenon of spontaneous magnetisation must occur. These equations are best solved graphically as shown in Fig. 15. The dotted line (2) represents the relation (26) and the full line (1) the usual Langevin function. The two curves intersect at the origin as well as at A, where the slope of the curve is much less than that at the origin. This gives the condition for spontaneous magnetisation

$$\frac{\sigma}{\sigma_0} < \tfrac{1}{3}a, \qquad \text{or } T < \frac{\sigma_0{}^2 A\rho}{3mR}, \qquad i.e., \; T < \theta$$

This temperature may be regarded as a transition temperature below which the substance becomes ferromagnetic. Thus Weiss hypothesis predicts the existence of a Curie point.

Though in this way, an *ad hoc* explanation of the modified Curie law $\chi = C/(T-\theta)$ has been given, the theory is not capable of explaining why θ sometimes takes a negative value. This can be explained only if we assume that $H_e = H - AI$, *i.e.,* the induced molecular field acts in an opposite direction to the external field. But such an assumption is contrary to classical ideas as this yields a negative value of the Curie temperature, as expression (25) shows.

Weiss's assumption of molecular fields led to some understanding of the phenomenon of Ferromagnetism.

THE WEISS MAGNETON.

Weiss and his co-workers carried out a large number of experiments on paramagnetic salts and solutions, chiefly of the transitional groups of elements (Sc to Cu), to verify the correctness or otherwise of formula (21). He found that the relation was generally correct; further he deduced the important conclusion that the magnetic moment M appeared to occur in multiples of a fundamental unit, thus pointing to the existence of atomicity in magnetic phenomena. The numerical value of this unit was found to be

$$M = 1123{\cdot}5 \text{ gauss} \times \text{cm.}$$

for a gm-molecule, and $1{\cdot}85 \times 10^{-21}$ gauss × cm. for a single molecule.

This quantity received the name of the *Weiss-magneton*, but as we shall presently see, it has got no theoretical basis.

Thus in the numerical example of $FeCl_2$ given above, we have $\mu = 4{\cdot}5 \times 10^{-20}$. The moment expressed in the corresponding Weiss-magneton number, which is usually denoted by p is given by

$$p = \frac{4{\cdot}5 \times 10^{-20}}{1{\cdot}85 \times 10^{-21}} = 25{\cdot}9$$

The Weiss-magneton numbers calculated for a number of compounds are shown in table on p. 796.

363. Application of the Quantum Theory.—The Weiss-magneton was so far a purely hypothetical physical unit and lacked theoretical basis. After the successful explanation of the hydrogen spectrum by Bohr, it was natural to suppose that an electron revolving in an one-quantum orbit may correspond to the Weiss-magneton. But no quantitative agreement could be found on this basis, as can be shown from the following calculation;

The magnetic moment of an electron revolving in a circle of radius r has been shown [*vide* eqn. (5)] to be

$$\mu = \frac{e\omega r^2}{2c}$$

Now according to Bohr

$$mr^2\omega = \frac{nh}{2\pi}$$

Hence
$$\mu = \frac{neh}{4\pi cm} \quad . \quad . \quad . \quad . \quad . \quad . \quad . \quad . \quad . \quad (28)$$

or μ is an integral multiple of the elementary quantity $eh/4\pi cm$, to which the name of *Bohr magneton* is usually given. It is generally denoted by μ_B.

But on substituting the values of e, h and c it is found that

$$\mu_B \times N = 5593 \text{ gauss} \times \text{cm.}$$

Thus we see that the magnetic moment possessed by a normal H-atom is not identical with the Weiss-magneton. In fact we have taking $\mu_W = 1123{\cdot}5$

$$\frac{\mu_B}{\mu_W} = 4{\cdot}967 \text{ (\textit{i.e.} nearly 5)} \quad . \quad . \quad . \quad . \quad (29)$$

The cause of this failure is quite apparent. The atoms and ions whose magnetic moments were measured by Curie, Weiss and others cannot be represented by the hydrogen model. For example, when we measure the paramagnetic susceptibility of $FeCl_2$, we suppose that $FeCl_2$ is an ionic compound, consisting of one Fe^{++} ion, and two $\overline{Cl}$ ions. The $\overline{Cl}$-ion is magnetically neutral (diamagnetic), hence the magnetic moment measured is that of Fe^{++} ion. Apparently a complex structure like Fe^{++} cannot be represented by a hydrogen model, which is the basis of the above theoretical calculation.

The difficulties have gradually been cleared up as our knowledge in atomic physics has advanced. The reader can easily see that for a successful theory of paramagnetism, a knowledge of the electronic structure of atoms and ions, and of the coupling relations amongst the constituent electrons is necessary. Hence a study of complex spectra, and of complex Zeeman effect should first be made. It is known from these studies that every atom can be regarded as a magnet with the magnetic moment $\mu_B\, gj$ where j=inner quantum number, and g=Landé factor.

This atom, when it is placed in a magnetic field, cannot place itself at any inclination θ to the field as was supposed in Langevin's theory. It is oriented only at some definite angles, given by the relation $\cos\theta = m/j$, where $m = j, j-1, \ldots\ldots -j$ (*vide* Fig. 7, p. 405, where these orientations are graphically shown). The hypothesis received confirmation from Stern and Gerlach's experiments which have already been described (*vide* §214). In the light of this hypothesis, Langevin's theory now requires a complete modification.

Let us now calculate the average magnetic moment of a system of such atoms when they are placed in a magnetic field*.

The energy of an atomic magnet with a given m (magnetic quantum number) is now

$$E = \mu_B\, g\, j\, H(1-\cos\theta) = \mu_B\, g\, j\, H - \mu_B\, g m H$$

We now find the probability W_m of the atomic magnets of possessing the magnetic quantum number m. This is

$$W_m = C\, e^{-E/kT} = A\, e^{\frac{m\mu_B g H}{kT}} = A\, e^{m\alpha} \quad . \quad . \quad . \quad . \quad . \quad . \quad (30)$$

where $\quad A = C\, e^{-\frac{\mu_B g j H}{kT}} \quad$ and $\quad \alpha = \dfrac{\mu_B g H}{kT}$

Now A can be obtained from the condition that $\sum\limits_{m=-j}^{m=j} W_m = 1$.

The average magnetic moment is given by

$$\bar{\mu} = \frac{kT}{H}\frac{\Sigma W_m\, m\,\alpha}{\Sigma W_m} = \frac{kT}{H}\sum \alpha\, W_m\, m \quad . \quad . \quad . \quad . \quad (31)$$

Since $mg\mu_B H$ is small compared to kT, we replace $e^{\frac{mg\mu_B H}{kT}}$ by $1 + \dfrac{Hmg\mu_B}{kT}$. Then (30) gives

$$\Sigma W_m/A = \Sigma 1 + \alpha\Sigma m = (2j+1) \quad . \quad . \quad . \quad . \quad . \quad (32)$$

where the summation is taken over $m=j$ to $m=-j$, so that the second term vanishes.

Hence

$$A = 1/(2j+1)$$

and

$$\bar{\mu} = \frac{kT}{H(2j+1)}\,\Sigma\, \alpha m\,(1+\alpha m) = \frac{kT}{H(2j+1)}\,(\alpha\,\Sigma m + \alpha^2 \Sigma m^2)$$

Now $\Sigma m = 0$, and

$$\sum_{-j}^{j} m^2 = \frac{j(j+1)\,(2j+1)}{3}$$

---

* This calculation was first given by Hund, *Zs. f. Phys.*, 33, 855, 1925.

Hence
$$\bar{\mu} = \frac{H(\mu_B\, g)^2}{3kT}\, j(j+1) \quad \ldots\ldots \quad (33)$$

The gm-molecular susceptibility χ_M is now given by
$$\chi_M = \frac{(g\mu_B)^2}{3kT}\, j(j+1)\, N \quad \ldots\ldots \quad (34)$$

We can put this in Langevin's form if we substitute
$$\sigma' = N g\, \mu_B \sqrt{j(j+1)} \quad \ldots\ldots \quad (35)$$

Then
$$\chi_M = \frac{\sigma'^2}{3RT} \quad \ldots\ldots \quad (36)$$

Expressing the moment σ' in terms of the Weiss-unit μ_W, we get the Weiss-magneton number
$$p = \frac{\sqrt{3RT\chi_M}}{\mu_W N} \quad \ldots\ldots \quad (37)$$

Substituting for χ_M from the modified relation (36), we get
$$p = \frac{\mu_B}{\mu_W}\, g\, \sqrt{j(j+1)} = 4{\cdot}97\, g\, \sqrt{j(j+1)} \quad \ldots\ldots \quad (38)$$

This is the quantum mechanical expression for paramagnetic moment first obtained by Hund. Later on it was variously modified by Sommerfeld, Laporte, Van Vleck, D. M. Bose and Stoner for obtaining better agreement with experimental values. We shall consider these in the following sections.

364. Discussion of Results.—The theories sketched above can apply only to assemblies of monatomic gases or ions. But such a paramagnetic gas is rarely known or has yet been investigated. The only monatomic paramagnetic vapour that has been so far investigated is that of potassium by Gerlach*. It has been found that between 600°C and 800°C the vapour obeys Curie's Law and $\chi_M = 0{\cdot}38/T$. The normal state of K is $^2S_{\frac{1}{2}}$, and the theoretical value according to (34) is $\chi_M = 0{\cdot}372/T$. Though the agreement between experiment and theory is quite good, Gerlach does not claim an accuracy of more than 10%. As regards diatomic or triatomic molecules like O_2 or NO the above results cannot be applied without suitable modification.

Let us therefore apply these equations to the measurement of magnetic moments of paramagnetic bodies in the form of solutions or crystals given in Table 6. In these bodies the gaseous condition

---

* Gerlach, *Atti. de Congress Int. dei Fisici*, **1**, 119, 1927.

Table 6.—Magnetic moments (p-values) of Ions of the First transitional group.

Electron structure		19 d	20 d^2	21 d^3	22 d^4	23 d^5	24 d^6	25 d^7	26 d^8	27 d^9
Ground term		$^2D_{\frac{3}{2}}$	$^3F_2$	$^4F_{\frac{3}{2}}$	$^5D_0$	$^6S_{\frac{5}{2}}$	$^5D_4$	$^4F_{\frac{9}{2}}$	$^3F_4$	$^2D_{\frac{5}{2}}$
$4{\cdot}97\, g\sqrt{j(j+1)}$ … (Hund)		7·7	8·1	3·9	0	29·4	33·6	33·2	28·0	17·7
$4{\cdot}97\sqrt{4s(s+1)}$ …. (Bose)		8·6	14·1	19·3	24·4	29·4	24·4	19·3	14·1	8·6
$4{\cdot}97\sqrt{4s(s+1)+l(l+1)}$ (Van Vleck)		14·9	22·2	25·8	27·2	29·4	27·2	25·8	22·2	14·9
Observed values of p	Solution			Cr³ 18·2 – 19·1	Cr² 23·8 – 24‡	Fe³ 26 – 29·5	Fe² 26·5	Co² 23 – 25	Ni² 16 – 17	Cu² 9 – 10
		V⁴ 8·6*	Ti²	V² 19·0*	Mn³ 25	Mn² 29·4				
			V³ 12·6*† – 14·0 (eff.)	Mn⁴ 19·9						
	Solid Salts	V⁴ 7·9 – 8·9	V³ 9·5	Cr³ 17·9 – 18·9		Fe³ 28·7 – 29·1	Fe² 25 – 27·5	Co² 22 – 26	Ni² 14·5 – 17	Cu² 9 – 11
				Mn⁴ 19·8	Mn³ 25	Mn² 27 – 30				

Row 3 gives the p-numbers calculated according to Hund.
… 4 . . . . . numbers calculated according to D. M. Bose.
… 5 . . . . . numbers calculated according to Van-Vleck.
… 6, 7, 8, . . experimental values when the salt is in solution.
… 9, 10, . . … … when the salt is in the solid state

may be supposed to hold good as a first approximation. Taking the case of $FeCl_2$, if we suppose this to consist of Fe^{++}-ion bound to two $\overline{Cl}$-ions, then since $\overline{Cl}$ is diamagnetic, the paramagnetism of $FeCl_2$ must arise wholly from the Fe^{++}-ion. We find that according to measurements $p = 26{\cdot}5$. Let us compare it with the magnetic moment of Fe^{++}-ion calculated from spectroscopic principles.

The composition of Fe^{++} is … $3d^6$. The lowest state is $^5D_4$ for which $j = 4$, $g = \frac{3}{2}$. If we suppose that all Fe^{++}-ions in the compound are in this state we should have

$$p = 4{\cdot}97\, g\, \sqrt{j(j+1)} = 33{\cdot}56$$

This is very much different from the experiment value 26·5. The failure of Hund's formula is not only confined to Fe^{++}, but it extends to other ions of the first transitional group, as a glance at Table 6 shows.

---

* S. Freed, *Jour. Am. Chem. Soc.*, **49**, 2456, 1927.

† Bose and Bhar, *Zs. f. Phys*, **48**, 716, 1928. Both Freed and Bose, and Bhar measures χ at one temp. in 293°K, hence the symbol (eff.)

‡ Cabrera and Pina, *An. Soc. Esp. Fis. y Quim*, **17**, 149, 1919. Other data have been collected from Van Vleck's and Stoner's books.

The value of p has been found to vary to some extent on the state of dilution, the nature of chemical combination etc. . . . . Thus Chantillon* found for Co^{++}-ions p-values varying from 22 to 26. The consideration of such cases is beyond the scope of this book (*vide* Van-Vleck, *Electric and Magnetic Susceptibilities*, p. 298).

The results are better displayed in Fig. 16 in which the number of d-electrons in the incomplete shell is taken as abscissa and the corresponding p-values as ordinates. The thick vertical lines denote experimental values.

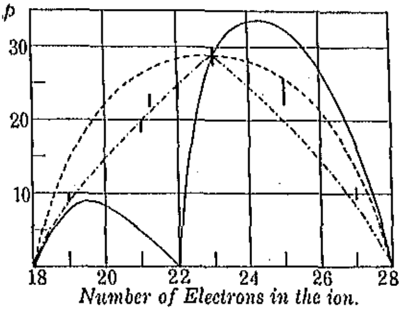

Fig. 16. Magnetic moment of elements of the first transitional group.

———— Hund,
- - - - Bose,
- - - - Van-Vleck.

It is seen from Table 6 and Fig. 16, that there is absolutely no agreement between experimental values, and the p-values calculated from Hund's formula (38). We shall return to the discussion of other formulæ mentioned in Table 6 presently.

PARAMAGNETISM OF RARE EARTH COMPOUNDS.

But better agreement was found by Hund in the case of compounds of rare earths. As mentioned on p. 585, these compounds are mostly trivalent, as illustrated by $GdCl_3$, and if we suppose that the binding is ionic, the compound consists of triply ionised Gd^{+++} surrounded by 3 chlorine ions. The paramagnetism is entirely due to the triply ionised rare earth ions. According to §289, these in the gaseous form have the electron structure $4f^x$ where x varies from 0 in La to 14 in Lu. We suppose the RS-coupling to hold good, and calculate p-values according to formula (38). The results are shown in Table 7, and Fig. 17, where the atomic number of the

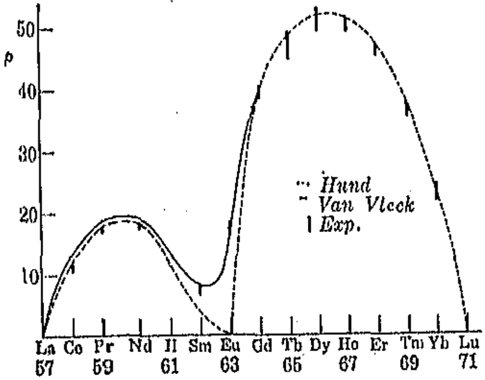

Fig. 17. Magnetic moments of elements of the rare earth group.

---

* Chantillon, *Ann. de Phys.*, 9, 187, 1928.

elements from 57 La to 71 Lu have been plotted as abscissa, and the corresponding p-values as the ordinates. The thick vertical lines represent the experimental values, the dotted curve shows the values calculated according to Hund's theory and the full curve those according to Van Vleck's.

Table 7.—Magnetic moment (p-values) of rare earth ions.

+++Ion	Term	Theoretical value of p		Observed value of p		
		Hund	Van Vleck*	Cabrera (*sulphate*)	Decker† (*solution*)	Williams (*oxide*)
57 La	$^1S_0$	0·00	...	...	...	Diamag.
58 Ce $4f$	$^2F_{\frac{5}{2}}$	12·65	11·9	11·89	10·45	1·143(?)
59 Pr $4f^2$	$^3H_4$	17·83	17·9	17·90	16·98	11·40(?)
60 Nd $4f^3$	$^4I_{\frac{9}{2}}$	18·03	18·0	17·99	17·18	17·06
61 Il $4f^4$	$^5I_4$	13·34	?	...	...	...
62 Sm $4f^5$	$^6H_{\frac{5}{2}}$	4·179	7·6	7·65	8·091	7·816
63 Eu $4f^6$	$^7F_0$	0	18·0	17·96	...	...
64 Gd $4f^7$	$^8S_{\frac{7}{2}}$	39·54	39	40·84	39·08	37·07
65 Tb $4f^8$	$^7F_6$	48·30	47·9	47·75	48·75	...
66 Ds $4f^9$	$^6H_{\frac{15}{2}}$	52·72	52·2	52·24	54·20	...
67 Ho $4f^{10}$	$^5I_8$	52·72	52·0	52·24	51·76	50·24
68 Er $4f^{11}$	$^4I_{\frac{15}{2}}$	47·75	47·0	47·21	47·21	45·82
69 Tu $4f^{12}$	$^3H_6$	37·85	35·8	35·82	...	...
70 Yb $4f^{13}$	$^2F_{\frac{7}{2}}$	22·39	21·6	21·88	22·30	..
71 Lu	^1S	0	0	...	5·970(?)	2·44(?)

EXPLANATION OF THE TABLE.

Column 1 . . . . contains the number of electrons in the ion, and the structure of incomplete shells.

. . . . 2 . . . . Lowest term due to the given electron structure.

---

* J. Van Vleck and A. Frank, *Phys. Rev.*, 34, 1494, 1929.

† H. Decker, *Ann. d. Phys.*, 79, 324, 1926.

Columns 3 and 4 give theoretical values of Hund and Van Vleck. The last three columns show the values experimentally observed by Cabrera, Decker and Williams. A few words of explanation are necessary on the experimental values of magnetic moments of the paramagnetic ions as given above. Decker† used solutions of sulphates dissolved in suitable solvents in all cases except for La, Ce and Pr for which he used nitrates of these elements. Cabrera,* St. Meyer† and Zernicke‡ experimented directly upon the hydrated solid sulphates in all cases. We have given in Table 7, only the values due to Cabrera, as those due to other two authors are also in fair agreement in most cases with these. Williams§ on the other hand made measurements on oxides.

It will be seen that the values obtained from solutions as well as pure solids are in good agreement with those theoretically calculated. This shows that under both these circumstances, ions exist in free states at least with respect to their 4f-shells. The values for Ce and Pr obtained by Williams are however specially low. Van Vleck is of opinion that in the case of oxide of Ce perhaps a large percentage of $Ce\,O_2$ was present in the sample rather than $Ce_2\,O_3$. The former contains Ce^{+4}-ion which should be diamagnetic like La^{+3}. The binding of Ce which is stronger in oxides than in most other compounds may also affect the shell by interatomic affinity. Impurity also probably plays an important part specially in the case of Pr_2O_3 and $Lu_2\,O_3$.

But even in this table it is found the p-numbers for Eu and Sm have no pretence of agreement with Hund's theoretical values. We shall come to these cases later on.

Attempts have been made in recent years to account for the anomalous results in the iron and in the rare earth group of elements. A short account of them is given below.

(a) D. M. Bose‖ showed empirically that the formula

$$p = 4{\cdot}97\sqrt{4s\,(s+1)} \quad \ldots\ldots\ldots \quad (39)$$

agreed better as far as the first transitional elements are concerned. The p-values calculated from this formula are shown in row 4 of Table 6. There is good agreement up to d^6 after which however the disagreement is rather large. The formula does not hold good for rare earths.

(b) Sommerfeld and Laporte¶ argued that when the multiplet intervals calculated for the lowest configuration are small compared to kT, we are not justified in assuming that all ions are in the lowest level. We should rather postulate a Maxwellian distribution amongst the levels obtained from the lowest value of state. They obtained in this way the formula

---

* B. Cabrera, *Compt. Rend.*, **180**, 668, 1925.

† St. Meyer, *Phys. Zeits.*, **26**, 51, 478, 1925.

‡ Zernicke and James, *Journ. Am. Chem. Soc.*, **48**, 28, 27, 1926.

§ E. H. Williams, *Phys. Rev.*, **12**, 158, 1918; **27**, 484, 1926.

‖ D. M. Bose, *Zs. f. Phys.*, **43**, 864, 1927.

¶ Sommerfeld and Laporte, *Zs. f. Phys.*, **40**, 33, 1926; Laporte, *ibid.*, **74**, 761, 1928.

$$p = 4{\cdot}97 \sqrt{\frac{\overset{j}{\Sigma}\,(2j+1)\,j\,(j+1).\,e^{-ch\nu_j/kT}\,g^2}{\Sigma\,(2j+1).\;e^{-ch\,\Delta\nu/kT}}} \quad . \quad . \quad . \quad . \quad . \qquad (40)$$

where $h\nu_j$ is the energy difference between the particular j-level concerned and the ground state.

From this they worked out two cases, first when the multiplet separation is supposed to be very large compared to kT, and the second when this is very small compared to kT. The first reduces to Hund's case. The formula however fails to give any agreement with the observed values.

Van Vleck* gave a very complete treatment of paramagnetism on the basis of new quantum mechanics, and obtained the expressions:

(*a*) When the multiplet interval is large compared to kT

$$\chi = \frac{N g^2 \mu_B^2\, j\,(j+1)}{3\,kT} + N\alpha\,(j) \quad . \quad . \quad . \quad . \quad . \qquad (41)$$

where $\mu_B = eh/4\pi m_0 c$ and $\alpha\,(j)$ is a contribution from second order Zeeman terms, *i.e.*, a term due to the component of the magnetic moment perpendicular to the angular momentum vector.

(*b*) When the multiplet interval is comparable to kT

$$\chi = \frac{N\overset{j}{\Sigma}\,[g^2 \mu_B^2\; j\,(j+1)/3\,kT + \alpha\,(j)]\;(2j+1)\;e^{-W/kT}}{\Sigma(2j+1)\;e^{-W/kT}} \quad . \quad . \quad . \qquad (42)$$

The additional term $\alpha\,(j)$ is generally negligible, but becomes quite important in the cases where l and s are large, the resultant j being small. Such cases arise for Sm^{+++} and Eu^{+++} to which this formula has been applied with complete success.

(*c*) When the multiplet interval is very small and it is assumed that l and s are not coupled to form a resultant j, but they are quantised separately with respect to the field, the magneton number is given by

$$p = 4{\cdot}97\;\sqrt{4s\,(s+1) + l\,(l+1)} \quad . \quad . \quad . \quad . \quad . \quad . \quad . \quad . \qquad (43)$$

This formula, as a glance at Table 6 shows, is also not in agreement with experimental facts. The results of this discussion seem to be that Hund's formula gives good results for rare earth ions, while Bose's formula holds for the first half of the transitional elements. Bose has tried to justify his formula on the supposition that for the Fe-group it is only the spin moment of the electron that is effective in producing paramagnetism. The l-moment for some reason disappears.

---

*Van Vleck, *Phys. Rev.*. 31, 587, 1928; 34, 1494, 1625, 1929.

Stoner* has offered an explanation along the line developed below. He thinks it necessary to take into account the possibility of a definite interaction between the paramagnetic ion, and the surrounding ions and molecules.

According to him the ideal RS-coupling between the spin vector and l-vectors of d^x-electrons assumed implicitly in Hund's formula is not applicable to salts of the iron group, as the free ion interacts with the ions and molecules surrounding it. Under these conditions, the ion (or the shells of d^x-electrons) can no longer be regarded as free. What will be the nature of the influence exerted by the interaction of the foreign ions and molecules? Stoner thinks that for the iron group at least, the influence on the resultant s-vector will be negligible, but the l-vectors of the d-electrons will be strongly influenced. The ion may still behave as relatively free as far as the resultant s is concerned.

The effect of l-moments therefore largely disappears, thus justifying D. M. Bose's assumptions.

But for the rare earths, the paramagnetism arises from the $4f^x$-shell. Now the incomplete $4f$-electron shell may be supposed to be surrounded by the $5s^2$, $5p^6$-shells which *shield* it from the influence of the foreign ions and molecules. The usual coupling relations between the electrons in the $4f$-shell remain undisturbed.

In support of this view, attention may be drawn to the fact that while salts and solutions of the Fe-group show continuous absorption of light, the rare earth compounds and salts show approximate line absorptions whose positions do not vary much with the nature of the compound or the solvent. This may be explained by the assumptions that the lines are due to intertransition amongst the metastable levels of the fundamental electron configuration $4f^x$.

The disagreement between the experimental values and the theoretical values calculated according to Hund's formula for the cases of Sm^{+++} and Eu^{+++} has been removed by Van Vleck and Frank†. Approximate calculations show that the separation of the lowest levels is about 930 cm^{-1} for Sm^{+++}, and 250 cm^{-1} for Eu^{+++}, while the value of kT at room temperatures is about 200 cm^{-1}. Hence χ-value should be calculated out not on formula (41) which applies to multiplet intervals large compared to kT, but on formula (42) which is for intermediate multiplet intervals. Van Vleck and Frank's calculations show that the disagreement disappears under this condition.

---

* Stoner, *Phil. Mag.*, 8, 250, 1929.

† *Vide Theory of Electric and Magnetic Susceptibilities*, by J. H. Van Vleck, p. 245.

PARAMAGNETISM INDEPENDENT OF TEMPERATURE.

Quite a number of solids shows a feeble paramagnetism independent of temperature and comparable with diamagnetism in order of magnitude. To this class belong a great many pure solid elements, *e.g.*, the alkalies and the alkaline earths, as also a number of salts like $KMnO_4$, $K_2Cr_2O_7$, $K_4Fe(CN)_6$, etc. In many cases, as, *e.g.*, in the Pt and Pd metals and in many ferromagnetics above the Curie point a constant paramagnetism* is superposed on the variable paramagnetism. Theoretically the existence of this feeble paramagnetism may be understood on the basis of the degeneracy phenomena in Fermi-Dirac Statistics† or of interatomic interactions proposed by Van Vleck.‡ Consideration of this phenomenon is beyond the scope of this chapter.

365. Dia and Paramagnetism of Molecules.—We have seen that the diamagnetism of a number of atoms and of mononuclear ions having inert gas structure and spherically symmetrical charge distribution can be explained by the Langevin theory at least to a first degree of approximation. In the case of paramagnetism also, the susceptibilities of the ions of the rare earth and transitional groups of elements can be calculated with fair accuracy from the theories of Hund, D. M. Bose and Van Vleck. But coming to the cases of dia and paramagnetism of molecules we find that the above theories no longer hold. The reason is that the electronic charge distribution of molecules is considerably modified by their vibrational and rotational motions as well as by the nature of the couplings involved. Thus a molecule should be diamagnetic when its resultant orbital and spin moments vanish, but as we shall see presently, the simple theory of diamagnetism when applied to such a molecule gives only an upper limit to its susceptibility, and that with greater approximation, the more its charge-distribution approaches the condition of spherical symmetry. In the case of paramagnetic molecules, the calculation of their susceptibilities involves the knowledge of their spectroscopic states depending on the coupling relations, as well as on the multiplet intervals on those states.

---

* Mlle A. Serreo, *Dissertation*, *Strassbourg*, 1931.

† W. Pauli, *Zs. f. Phys.*, **41**, 81, 1927 ; J. Frenkel, *ibid.* **49**, 31, 1928.

‡ Van Vleck, *The Theory of Electric and Magnetic Susceptibilities*, p. 347.

DIAMAGNETIC MOLECULES.

Experimental investigations on the diamagnetism of molecules were carried on by Pascal,* and more recently by Bhatnagar and others. Pascal from an extensive series of measurements on organic molecules concluded that the gram-molecular diamagnetic susceptibility of a molecule, χ_M, can be expressed as the sum of those of its constituent atoms as

$$\chi_M = \Sigma\, \chi_A + \lambda$$

where λ is a correcting factor which depends upon the nature of the chemical binding of the atoms. Further, Bhatnagar and others have shown that for molecules forming electronic isomers, the diamagnetic susceptibilities bear a simple relationship with the molecular radius calculated from the radii of the atoms on the assumption that the packing is close. These empirical laws however do not elucidate the problem in any way, except showing merely a few regularities.

On the basis of the new quantum mechanics, Van Vleck† has shown that the gram-molecular susceptibility of a polyatomic molecule with resultant spin and orbital moments zero, is given by the expression

$$\chi_M = -\frac{Ne^2}{6mc^2}\Sigma\overline{r^2} + \tfrac{2}{3}N \sum_{n'=n} \frac{|\, m\,(n', n)\,|^2}{h\nu\ (n', n)} \quad . \quad . \quad . \quad . \quad . \quad . \qquad (44)$$

Both the terms on the right hand side are independent of the temperature, the first term being the one which for mononuclear systems in the $^1S_0$-state gives the diamagnetism. The origin of the second term is difficult to conceive in terms of models. $m^0\,(n'n)$ is a nondiagonal term in the angular momentum matrix and corresponds to the transition n' to n. For diatomic molecules this part may be supposed to arise from the rapid precession of the perpendicular component of the orbital angular momentum vector about the axis of the molecule. It thus appears that Langevin's formula represents only an upper limit to the diamagnetism of molecules, and estimates of $\overline{r^2}$ made with its help are liable to be too high.

But the fact that such estimates are generally of the right order of magnitude as also the fact that diamagnetism of many organic molecules may be found by adding together the contributions of the constituent atoms (as found by Pascal and known as *Pascal's law*) show that the second term is in general much smaller in magnitude than the first. Van Vleck and Frank have made a rough theoretical calculation of the second term for the hydrogen molecule and found it to be about 10% of the first.

---

* P. Pascal, *Ann. de Chim. et Phys.*, 1908—13; also later papers in *Comp. Rend.*

† Van Vleck, *Phys. Rev.*, **32**, 880, 1928.

When the nuclear field departs more and more from central symmetry, we have reasons to believe that the second term increases in magnitude. That some molecules have a constant paramagnetism independent of temperature may be explained by saying that the second term mentioned above is in these cases greater than the first.

PARAMAGNETISM OF DIATOMIC MOLECULES*

When the multiplet intervals are small compared to kT, Van Vleck has shown that, regardless of the fact whether the coupling† is of the Hund-type (a) or (b) or intermediate, the molar susceptibility is given by

$$\chi = \frac{N\mu_B^2}{3kT}[4S(S+1) + \Lambda^2] \quad . \quad . \quad . \quad . \quad . \quad . \quad (45)$$

where μ_B is the Bohr-magneton, S is the resultant spin and Λ the total orbital quantum number for the molecular state.

When the multiplet intervals are large compared to kT

$$\chi = \frac{N\mu_B^2}{3kT}[\Lambda + 2\Sigma]^2 \quad . \quad . \quad . \quad . \quad . \quad . \quad . \quad (46)$$

Here the coupling is in general of the type (a).

Diatomic molecules have generally ${}^1\Sigma_0$- normal states, except O_2 and NO. Mulliken‡ has shown from band spectrum analysis that the ground state for O_2 is ${}^3\Sigma$. Since ${}^3\Sigma$- states are practically devoid of fine structure, we apply formula (45) above and putting $S = 1$, $\Lambda = 0$, find

$$\chi = \frac{8N\mu_B^2}{3kT} = \frac{\cdot 993}{T} \quad . \quad . \quad . \quad . \quad . \quad . \quad . \quad . \quad (47)$$

At 20°C, χ from above is $3{\cdot}39 \times 10^{-3}$. The observed values range from $3{\cdot}31.10^{-3}$ to $3{\cdot}45.10^{-3}$. The agreement is thus very good.

The NO-molecule offers a very convenient example for the study of the finer points in Van Vleck's theory. Birge finds the normal state to be ${}^2\pi$ with $h\Delta\nu$ approximately 120 cm^{-1}. The interval thus becomes comparable to kT and none of the above two formulæ can be applied. Van Vleck‖ shows that the effective magneton number is given as a

---

[*] The student should read this section after he has acquired a knowledge of molecular spectra. Note that Σ in eqn. (46) stands for parallel component of the spin angular quantum number S.

[†] These refer to Hund's (a), (b) types of coupling. See Hund, *Zs. f. Phys.*, 36, 657, 1926.

[‡] *Nature*, Feb. 27, 1926; also Jenkins, Barton and Mulliken, *Phys. Rev.*, 30, 150, 1927.

[‖] *Theory of Electric and Magnetic Susceptibilities*, p. 269.

function of temperature by

$$\mu_{\text{eff}} = 2\sqrt{\left(\frac{1-e^{-x}+xe^{-x}}{x+e^{-x}}\right)}, \text{ where } x = \frac{h\Delta\nu}{kT} = \frac{173}{T} \quad . \quad (48)$$

At 20°C, this gives 1·836. The experimental value of Bauer and Piccard is 1·86.

The above formula for the temperature variation of NO has been tested experimentally by a number of observers of whom Wiersma, De Haas and Capel used the longest range of temperatures, *viz.*, from 112·8°C to 292·1°C. The relative variations calculated theoretically and found experimentally are in perfect agreement.

POLYATOMIC MOLECULES.

The analysis of spectra for such molecules is not far advanced. We can in general assume that the entire orbital angular momentum is of the same nature as the perpendicular component of the orbital angular momentum for diatomic molecules. Hence there is no first order contribution to the magnetic moment of the molecule. If, however, there is a resultant spin, the susceptibility may be expressed by

$$\chi = \frac{4N\mu_B^2\, S(S+1)}{3kT} + N\alpha \quad . \quad . \quad . \quad . \quad . \quad . \quad (49)$$

where $N\alpha$ is the small residual effect of the orbital moment. The above formula assumes small energy of coupling between the spin and the rest of the molecule, which is justified.

Gases are mostly diamagnetic. Cases where magnetic measurements are available for polyatomic molecules with resultant spin (*i.e.*, with odd number of electrons) are not very common. As far as is known to the authors the only cases are ClO_2 and NO_2 for which the values are given below:

Table 8.

	χ_M at 20°C		Author	Remarks
	Calc.	Obs.		
ClO_2 ($S=\frac{1}{2}$, $\alpha=0$)	$1{\cdot}27\times10^{-4}$	$1{\cdot}34\times10^{-4}$	Taylor	Solution
NO_2 ($S=\frac{1}{2}$)	$\sim10\times10^{-4}$	$2{\cdot}1\times10^{-4}$	Soné	

It is very likely that ionisation or polymerisation changes the value for the free molecule.

366. The Gyromagnetic Effect.

—A brief description of gyromagnetic effect has already been outlined earlier in this chapter. The subject will now be studied a little more closely, both from the theoretical and experimental points of view.

---

* *J. Amer. Chem. Soc.*, **48**, 859, 1926.

As mentioned in §355, the ratio of the mechanical to the magnetic moment for the orbital motion of the electron is

$$R = \frac{\Omega}{\mu} = \frac{2mc}{e} \quad . \quad . \quad . \quad . \quad . \quad . \quad . \quad . \quad . \quad (50)$$

Substituting the values of m, c, e we get $R = -1{\cdot}16 \times 10^{-7}$. In a paramagnetic body, we may suppose that atoms are themselves magnets, and the effect of magnetisation consists in the partial fixing of the axes of the orbits along the line of the magnetising field. The total gain in magnetisation due to this process, therefore, also produces an equivalent gain of angular momentum of carriers. In a solid body, as the atoms are not free to move, the effect of magnetisation will be a rotation of the body as a whole with the reaction momentum in the opposite direction. The ratio of the total mechanical momentum $J = \Sigma\, \Omega$ to the total magnetic moment $M = \Sigma\, \mu$ is therefore given by

$$J = MR \quad . \quad . \quad . \quad . \quad . \quad . \quad . \quad . \quad . \quad . \quad . \quad (51)$$

Richardson[*] in 1908 obtained a correct idea of the amount of rotational motion which accompanies magnetisation, but his experiments were inconclusive. The first successful experiments on this line were performed by Einstein and de Haas in 1915 though the reverse experiment on the gyromagnetic effect was successfully carried out a year earlier by S. J. Barnett (§369). As the moment is extremely small, Einstein and De Haas devised out an ingenious method of amplifying the deflections by resonance. We give below an account of this and subsequent improved experiments.

367. Experiments on Gyromagnetic Effect.—It is seen from (51), that the rotational couple is proportional to the intensity of magnetisation, hence though theoretically the gyromagnetic effect may be observed for all dia, para and ferromagnetic solids alike yet it is far too small for the para and diamagnetics, and the measurements are not practicable. It is only for the ferromagnetics which acquire large magnetic moments even in weak fields, that the effect can be observed with any accuracy. The experimental method is directly suggested by the theory. A rod of some ferromagnetic material is to be suspended vertically and magnetised suddenly, say by means of a current-bearing solenoid surrounding it. The resulting rotation of the rod is to be noted by some sensitive arrangement. The difficulties in such experiments are however numerous. For instance, the magnetic axis of the suspended wire may not be exactly vertical, so that a small horizontal component of the magnetic moment may exist which will be affected by the earth's horizontal magnetic field. To eliminate this, the effect of the earth's field on the specimen must be neutralised and the horizontal component of the moment must be reduced to a minimum. In the same way, various disturbing forces may come into play masking entirely the effect which is already very small.

---

[*] O. W. Richardson, *Phys. Rev.*, **26**, 248, 1908.

The first successful experiments of Einstein and De Haas* were as follows. An alternating current was used in the magnetising coil, and its frequency was adjusted to be the same as the natural frequency of the suspended system. The specimen was magnetised by quick reversals of the current and the maximum amplitude of rotation of the system was noted. If T denotes the moment of the rotational couple and θ the amplitude, the equation of motion is given by

$$I\ddot{\theta} + K\dot{\theta} + C\theta = T \,. \quad . \quad . \quad . \quad . \quad . \quad . \qquad (52)$$

But
$$T = dJ/dt = R\,\chi m_0 \frac{\partial H}{\partial t}$$

where χ = mass susceptibility and m_0 = mass of the specimen. Now the periodic magnetic field can be represented as a Fourier series. But at resonance, all terms excepting that corresponding to $n = 1$ can be neglected. We may put

$$H = \sum_{1}^{n} H_0 \cos n\omega t = \frac{4}{\pi} H_0 \cos \omega t$$

Then equation (52) becomes

$$I\ddot{\theta} + K\dot{\theta} + C\theta + R\chi\, m_0\, H_0 \sin \omega t = 0$$

Solution of this equation gives the resonance amplitude

$$\theta_M = \frac{4}{\pi} R \frac{\chi m_0 H_0}{K} \quad . \quad . \quad . \quad . \quad . \quad . \quad . \qquad (53)$$

We have now to evaluate K and H_0. K can be easily obtained by observing the damping of the suspended system, for taking t = the period of oscillations, and α_1, α_2 two successive maximum amplitudes on the same side, the logarithmic damping $\lambda = ln\,(\alpha_1/\alpha_2)$ is given by

$$\lambda = Kt/2I, \qquad K = 2I\lambda/t$$

---

* A. Einstein and De Haas, *Verh. d. D. Phys. Ges.*, **17**, 152; Einstein, *ibid.*, 18, 173, 1916; De Haas, *ibid.*, 18, 423, 1916.

Hence from the value of θ_M and λ, R can be calculated. Using this method Einstein and De Haas obtained $R=0{\cdot}98\ R_0$, *i.e.*, within 2% of the theoretical value, where R=experimental and R_0=theoretical ratio.

This original method of Einstein and De Haas was repeated by Beck* (1919) with great improvements in technique, and both iron and nickel were experimented upon. He found the value $R=0{\cdot}53\ R_0$ which is nearly half of Einstein and De Haas's value. Stewart† and later Arvidsson‡ repeated these experiments using resonance methods and obtained the results $R=0{\cdot}49\ R_0$ and $0{\cdot}47\ R_0 \pm 5\%$ respectively.

The next accurate experiment for the determination of gyromagnetic ratio was performed by Chattock and Bates§ by using a more direct method. They magnetised a vertically suspended iron wire by means of a solenoid carrying a current which surrounded the wire. The magnetic moment was measured by a standardised magnetometer. The amplitude of rotation of the wire due to sudden magnetisation was observed by a reflecting mirror arrangement. The torsional coefficient of the suspending fibre and time of swing of the system being known, the mechanical moment was calculated from the observed deflection as explained. Thus the ratio R was determined. They obtained the same result as Beck, *viz.*, $R=0{\cdot}5\ R_0$.

More recently Sucksmith and Bates‖ have repeated the experiment on rotation by magnetisation using a null method (1925). Their apparatus is shown in Fig. 18.

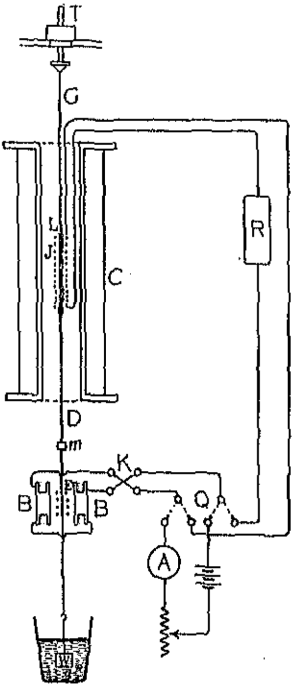

Fig. 18. Sucksmith and Bates's apparatus.

---

* E. Beck, *Ann. d. Phys.*, **60**, 109, 1919.

† J. Q. Stewart, *Phys. Rev.*, **11**, 100, 1918.

‡ G. Arvidsson, *Phys. Zeits.*, **21**, 88, 1920.

§ A. P. Chattock and L. F. Bates, *Phil. Trans. A*, **233**, 257, 1923.

‖ W. Sucksmith and L. F. Bates, *Proc. Roy. Soc. A*, **108**, 638, 1925; **104**, 499, 1932.

L .... the rod to be tested. It is suspended from the torsionhead T by means of a thin German-silver wire G.

C .... the magnetising coil through which an A. C. current passes. The rod L is suspended symmetrically along the axis of C.

D .... an aluminium wire attached to the lower end of L. It carries a small mirror m and a number of small magnetised needles E.

BB ... a small pair of Helmholtz coils, so situated that the needles E lie at their centre.

J .... a coil placed inside the magnetising coil C coaxially with L. It forms a part of the secondary circuit containing the resistance R, the Helmholtz coil BB, the commutator K and the switches Q.

A .... an ammeter which may be connected to the Helmholtz coil with the help of the switches Q, and the H-coil may be calibrated by using a known current from the battery.

An A. C. current is passed through C, its frequency being adjusted very nearly to the natural frequency of the suspended system. The magnetisation of the rod L is thus periodically reversed, and the rod oscillates about its axis with a maximum amplitude. It induces a current in the coil J the magnitude of which is regulated by means of the resistance R. This current flows through BB, and as a result a momentum is imparted to the needle magnets E which exactly balances the momentum of the system due to the gyromagnetic effect.

The flux through the secondary coil, due to the intensity of magnetisation I in the primary, and a magnetic field H is given by

$$N = (H + 4\pi I)\, s\, l\, n$$

where s = area of cross-section and l = length of the specimen rod and n = number of turns per cm. of the coil J. The induced current is

$$i = \frac{1}{r} \cdot \frac{dN}{dt} = \frac{s\,l\,n}{r}\left(4\pi \frac{dI}{dt} + \frac{dH}{dt}\right)$$

The angular momentum imparted to the magnets is

$$J = \int \tau\, i dt = \frac{\tau\, s\, l\, n}{r}\,(4\pi\, I + H)$$

where τ = the couple due to unit current. The magnetic moment of the specimen is

$$M = Isl$$

Neglecting H compared to I, we at once get

$$R = \frac{J}{M} = \frac{4\pi\tau n}{r} \quad . \quad . \quad . \quad . \quad . \quad . \quad . \quad . \qquad (54)$$

τ may be determined by passing a known current i_0 through BB and noting the deflection θ of the system from the relation $-\tau i = c\theta$, where c = torsional constant of the suspending wire.

Using this method Sucksmith and Bates obtained the values of $R/R_0 = 0{\cdot}503$ for iron, $0{\cdot}501$ for Ni, and $0{\cdot}515$ for Co.

368. The Gyromagnetic Anomaly: Application of Quantum Theory.—From all the experiments described above, except one due to Einstein and De Haas, a consistent discrepancy ($R/R_0 = 0{\cdot}5$) is observed between the experimental and the theoretical values of R. This is sometimes known as the *gyromagnetic anomaly*. It called for a modification of the simple formulation of the gyromagnetic effect in equation (50), as given by Richardson. This was achieved by the application of quantum theory to the phenomenon.

From the quantum theory of Zeeman effect, the resolved magnetic moment of the atom is given by

$$\mu = mg\,\frac{eh}{4\pi m_0 c}$$

and the mechanical moment $\Omega = \dfrac{mh}{2\pi}$. Thus we get

$$\frac{\mu}{\Omega} = g\,\frac{e}{2mc} \quad . \quad . \quad . \quad . \quad . \quad . \quad . \quad . \quad . \qquad (55')$$

where g = Landé's splitting factor (see §222). Thus the modified relation between the mechanical and magnetic moments become

$$R = \frac{J}{M} = \frac{1}{g} \cdot \frac{2mc}{e} \quad . \quad . \quad . \quad . \quad . \quad . \quad . \quad . \qquad (55)$$

Thus the determination of R enables us to calculate g for the normal paramagnetic or ferromagnetic atoms, and thereby to gain direct knowledge regarding the magnetic condition of the carriers.

The quantum theory makes it clear that R/R_0 should be equal to the reciprocal of the Landé factor (eqn. 55), so that the anomaly disappears if for Fe and Ni, we assume $g = 2$. A reference to the quantum mechanical expression for g on page 425 at once shows that this is the case when $l = 0$. The gyromagnetic experiment therefore leads us to the conclusion that for the ferromagnetics, only the spin moments of electrons contribute to magnetic moment, and the orbital moments are inoperative.* This view is supported also by recent gyromagnetic experiments of Sucksmith and others.

Thus D. P. Ray Chaudhuri† has performed experiments on oxides of iron and nickel by using these substances in powdered form packed inside thin glass tubes. He used a resonance method similar to Sucksmith's, with apparatus highly evacuated, so as to get large resonance oscillations, and obtained the results $R = 1{\cdot}008$, $1{\cdot}016$ and $1{\cdot}022$ me/e (R_0 being $2me/e$) for Fe_3O_4, Fe_2O_3 and $NiO.Fe_2O_3$ respectively.

Coeterier and Scherrer‡ have obtained a value of $R = 1{\cdot}01$ me/e for iron in powder form.

All these results support the value $g = 2$ for iron. But an experiment of Coeterier on pyrrhotite in powder form which shows well-known ferromagnetic properties gives $g = 0{\cdot}63$. This value is surprisingly low.

If ferromagnetism arises entirely from electron-spin, we expect $g = 2$, if however the electron system is supposed to be distorted by the fields of the neighbouring atoms, g may lie between 1 and 2, the value of R being correspondingly increased. Van Vleck's§ suggestion that two types of ions with g-values $\frac{3}{2}$ and 2 may be simultaneously present in the iron lattice may be noted in this connection.

Sucksmith‖ has recently developed a method for measuring R for paramagnetic substances of rare-earth series. He has obtained for Dy^{+3}-ion in Dy_2O_3, $g = 1{\cdot}36$ experimentally. Hund¶ gives the ground term of the ion as $^6H_{15/2}$ which leads to the theoretical value $g = \frac{4}{3}$. The experiment is therefore in excellent agreement with the theory.

Sucksmith$ has extended his method to ions of the first transitional group and to other rare-earth ions. His results are summed up in Table 9.

---

* This was first pointed out by D. M. Bose from a study of the magnetic moments of ions of the first transitional group (*vide* p. 805).

† Ray Chaudhuri, *P.R.S. Dissertation.*

‡ Coeterier and Scherrer, *Helvetica Physica Acta,* 1932.

§ Van Vleck *Electric and Magnetic Susceptibilities.*

‖ Sucksmith, *Proc. Roy. Soc. A*, **128**, 276, 1930.

¶ Hund, *Zs. f. Phys.*, **33**, 855, 1925.

$ W. Sucksmith, *Proc. Roy. Soc. A.*, **133**, 179, 1931; **135**, 276, 1932.

Table 9.—Values of g for ions of the first transitional and rare-earth groups of elements as determined from the gyromagnetic ratio, and calculated from theory (Sucksmith).

Ion	Ground Term	*g* (Experimental)	*g* (Theoretical)	Remarks
Cr^{+++}	$^4F_{\frac{3}{2}}$	2·0	2·0 D. M. (Bose)	Agreement with theory: *l*-moment inoperative.
Mn^{++}	$^6S_{\frac{5}{2}}$	2·0	2·0 ”	”
Fe^{++}	$^5D_4$	1·9	2·0 ”	”
Co^{++}	$^4F_{\frac{9}{2}}$	1·5	2·0 ” 1·27 (Sommerfeld-Laporte)	No agreement with theory. *l*-moment may be partially operative.
Gd^{+3}	$^8S_{\frac{7}{2}}$	2·12	2·0	Agreement with all theories, since here $l=0$.
Nd^{+3}	$^4I_{\frac{9}{2}}$	0·77	0·752 (Van Vleck)	Agreement with Van Vleck's theory (*vide* p. 806, eqn. 43).
Eu^{+3}	$^7F_0$	>4·5	”	Result inconclusive on account of experimental difficulties.
Dy^{+3}	$^6H_{\frac{15}{2}}$	1·36	1·33 (Hund)	Agreement with Hund's theory.

As explained on p. 805, various formulae have been proposed by Sommerfeld, Laporte, D. M. Bose and Stoner, Van Vleck and others to account for the paramagnetic moments of these ions. In D. M. Bose and Stoner's theories the *l*-moment is assumed to be inoperative. It will be noticed that this hypothesis is supported by the results of gyromagnetic experiments for ions of the first transitional group. The only exception is Co^{++} which agrees with none of the theories. It is supposed that in this case the *l*-moment may only be partially operative. The ions of the rare-earth group give results in agreement with Hund or Van Vleck's theory, in which both *l* and *s*-moments are taken to be operative. These conclusions are exactly similar to those arrived at from considerations of paramagnetic moments.

369. Barnett's Experiment.—In the foregoing sections we have discussed the experiments in which an angular momentum is produced by magnetisation of ferro and paramagnetic substances, and have studied how it throws light on the nature of the elementary magnets constituting them. We shall now consider another effect which demonstrates the intimate connection between magnetisation and mechanical motion. This effect consists in the observation of magnetisation of substances produced by their uniform rotation round an axis. This phenomenon is not to be regarded however as the converse of the first phenomenon, as its underlying reason is a little different.

Consider an electron revolving in an orbit with an angular velocity ω. If we now impose a further rotation by some external agent, so that the angular velocity now be $\omega+\Delta\omega$, the additional rotation will be equivalent to a precessional motion of the orbit with angular velocity $\Delta\omega$. We have seen in §207 that the effect of applying an external magnetic field H on the electron revolving in a closed orbit is the precessional motion of the orbit with an angular velocity $\Delta\omega = eH/2mc$, which is the famous *Larmor theorem.* In the present case we may consider the reverse effect to be taking place, so that the precession of the orbit set up by the external rotation will result in the generation of a magnetic field H given by the Larmor theorem

$$H = \frac{2mc}{e} . \Delta\omega \quad . \quad . \quad . \quad . \quad . \quad . \quad . \quad . \quad (56)$$

If n = number of revolutions per second, $\Delta\omega = 2\pi n$, and we get

$$H/n = \frac{4\pi mc}{e} = 7{\cdot}1 \times 10^{-7} \text{ gauss/r. p. s.} \quad . \quad . \quad . \quad (57)$$

Expressing this in terms of ratio of the magnetic field and the angular velocity of rotation, we have

$$R = H/\Delta\omega = 2 . \frac{mc}{e} \quad . \quad . \quad . \quad . \quad . \quad . \quad . \quad (58)$$

This effect was first observed by S. J. Barnett * in 1914, and in fact constitutes the first experimental observation in the whole domain of gyromagnetism.

In the experiment two iron rods about 7 cms. in diameter and 84 cms. long were taken. Each of these rods was surrounded with a solenoid, the two solenoids being exactly alike. The number of turns in each was about 5000. The solenoids were connected in opposition to a fluxmeter, whose deflections were read to tenths of mm. at the scale distance of 8 meters. Any change in the earth's field generated equal and opposite e. m. f.'s. in the two solenoids and thus the fluxmeter was not affected. One of the rods was then rapidly rotated at a rate of about 3000 revolutions per minute. The rotation of the rod generated a magnetic field H, which magnetised the rod and the flux thus produced was measured by the fluxmeter. The field H was determined by comparing this change of flux with that produced by the application of a small uniform magnetic field on the specimen parallel to the axis of rotation. By using this method Barnett obtained a result of $R=0{\cdot}98\ me/e$, or $H/n=3{\cdot}1\times10^{-7}$ gauss/r. p. s. within an error of 15%. This value is about half the value to be expected from the theory described above.

---

* S. J. Barnett, *Phys. Rev.*, **6**, 171, 239, 1915; *Journ. Wash. Acad. Sci.*, **11**, 162, 1921; *Phys. Rev.*, **17**, 404, 1921; **20**, 90, 1922.

S. J. Barnett and L. J. H. Barnett* made in 1925 a careful redetermination of the ratio by using a magnetometer method. In this an astatic magnetometer was mounted with the centre of the lower magnet system in the axis of the rod under investigation. The magnetometer deflection produced by reversing the direction of rotation of the rod or the rotor driven at a constant speed was noted. The corresponding magnetic field was determined by comparing this deflection with that produced by reversing a known magnetic field in the rod parallel to its axis. The substances investigated by Barnett are Co, Ni, some Heusler alloys, Fe-Ni, and Fe-Co alloys. The mean value of $R=H/n$ obtained for all these substances is $1{\cdot}06\ me/e$ with an error estimated as not greater than 2%. There is no certain evidence of any difference between the gyromagnetic ratios of the elementary magnets in different substances.

The ratio thus obtained is again almost half the theoretical value. This anomaly has been explained exactly in the same way as in the Einstein-De Haas effect already described. It arises because of the fact that the magnetisation of iron—as Heisenberg has shown—is produced by the free electron, that is, the electron possessing the spin only, and no orbital moment. For a spinning electron Larmor's theorem is modified and the precessional velocity is not given by eqn. (56), but by the expression

$$H=\frac{1}{g}\,\frac{2mc}{e}\,\triangle\omega \quad . \quad . \quad . \quad . \quad . \quad . \quad . \quad . \qquad (59)$$

---

* S. J. Barnett and L. J. H. Barnett, *Proc. Amer. Acad. of Arts and Sciences*, 60, 125, 1925. See also *ibid.*, 66, 273, 1931.

where g is the Landé factor. If the spin alone is present and the l moment is imperative, we get $g=2$. Hence

$$R = H/\triangle\omega = J/M = \frac{1}{g}\frac{2mc}{e} = mc/e \quad . \quad . \quad . \quad (60)$$

If on the other hand, the spin is absent and the electron possesses only orbital motion, $g=1$, and $R=2mc/e$ as given by (58).

This effect has so far been measured only in the case of ferromagnetic substances.*

Books Recommended

1. J. H. Van Vleck, *Electric and Magnetic Susceptibilities*, 1932.
2. E. C. Stoner, *Magnetism and Atomic Structure*, 1926.
3. E. C. Stoner, *Magnetism*, 1930.
4. K. Honda, *Magnetic Properties of Matter*, 1928.
5. G. Foëx, *Le Magnetisme*, 1926.
6. P. Debye, *H. d. Radiologie*, **6**, 1925.
7. *H. d. Physik*, **15** and **16**, 1927.

---

* For a complete discussion see S. J. Barnett, *Phys. Zeits.*, **35**, 203, March 1, 1934; L. F. Bates, *Nature*, **134**, 50, July 14, 1934.

APPENDIX

Note 1.—Comparison between Different Systems of Electrical units.

In our studies of the phenomena of Electricity and Magnetism, we are confronted with two systems of units corresponding to the two main divisions in which such phenomena occur. These are: (1) electrostatic, in which electricity is supposed to be at rest, (2) electro-dynamic, in which electricity is in motion and is detected by the magnetic effect which it produces in the space about it. Thus we find that if two pith balls, each 1 cm. in radius, be charged with equal quantities of electricity and placed at 1 cm. apart, then if they repel each other with a force of 1 dyne, each pith ball is said to possess one unit quantity of electricity. But we define the same quantity from the standpoint of current electricity in a widely different way. A unit quantity of dynamical electricity is that which deposits $\frac{1}{9645}$ gm-atoms of a positive monovalent electrolyte (say, Ag) from a solution of silver salt. It is difficult at first sight to see the connection between the two quantities. But electricity, whether measured by its statical effect or dynamical effect, is one and the same ; the two units should differ only in a numerical ratio. Let us suppose that the e.m. unit is x times larger than the e.s. unit. We have now to find out the value of x.

It is clear that in order to find the value of x, we must produce the same effect by known quantities of (1) static electricity and (2) current electricity and compare the magnitudes of these effects. A number of methods can be suggested. According to experience, when 10 coulombs (1 e. m. u. unit) of electricity pass through a silver salt solution, $\frac{1}{9645}$ gm-atoms of Ag is deposited. Now suppose we take a condenser of capacity C and charge it to the e. s. potential V. The quantity of electricity stored is $Q = CV$. Let this condenser be now discharged through an electrolytic tube containing some silver salt, and measure the amount of silver deposited. Let it be y gm-atoms.

Then in e.m. units the measure of the amount of electricity is $9645\,y$. Hence we have

$$9645\,y = Q/x, \qquad x = Q/9645\,y$$

This experiment, though simple in theory, cannot be practically realized under laboratory condition as x is too large. Hence some practicable method should be devised.

It can be shown that static electricity bound in a condenser can produce steady deflexion in a galvanometer, *i.e.*, if the condenser is alternately charged from a source of e.m.f. and discharged through the galvanometer, the latter would show a steady deflection.

We can calculate the equivalent resistance as follows: we have the current = quantity of electricity flowing per unit time = (quantity discharged at each contact) × (n the number of chargings per sec.). Denoting the current by i, we have $i = CVn$ e.s. units. The equivalent resistance $R = V/i = 1/nC$ e.s. units.

Now let the corresponding resistance measured in e.m. units be R'. Generally R' is very large, hence it is measured by a Wheatstone bridge arrangement.

Now what will be the magnitude of R'? We can calculate it as follows. Since CV^2 is the energy, it has got the same magnitude on both systems of units. But CV being the charge in the e.s. units, it is equal to CV/x e.m. units of charge. Hence the e.m.f. V must be equal to Vx e.m. units. Hence R', the resistance in e.m. units is given by $R' = Vx \Big/ \frac{CVn}{x}$ $= x^2/Cn$. Thus we get

$$x^2 = R'/R = nCR'$$

Further since the dimensions of the quantities on the right hand side are $[n] = T^{-1}$, $[C] = L$, $[R'] = LT^{-1}$, hence dimensions of $[x] = LT^{-1}$; thus the ratio x has the dimensions of velocity. In fact it was found first by Weber and Kohlrausch, and later confirmed by the accurate determinations of Rossa, Thomson, Abraham, Pallat, and Glazebrook that $x = 3{\cdot}0001 \times 10^{10}$, which is identical, within the limits of experimental error, with the *velocity of light*. This identity, as is well-known, led Maxwell to his famous theories correlating the phenomenon of light propagation with the propagation of electromagnetic waves.

Starting from the ratio of these two fundamental units, *viz.*, the unit quantity of electricity in e.m. units, and that in e.s. units, we can calculate the ratio between units of other derived quantities, *e.g.*, potential, resistance, capacity, inductance, etc. . . . which occur in the measurements of electrical and magnetic phenomena. Thus for electric resistance we have calculated the ratio to be $1/x^2$.

We next consider the ratio of e.m. units to practical units. The practical units are based on two assumptions which were introduced for the sake of convenience. These assumptions are: (1) one practical unit of quantity of electricity = 10^{-1} e.m. units; (2) one practical unit of energy = 10^7 ergs (*Joule*). From these the practical units for other quantities have also been evolved. We collect in the table below the dimensions and ratios of e.s., e.m. and practical units of various quantities.

Comparison of different systems of units.

Quantity	e.s. dimension	e.m. dimension	$\frac{\text{e.m. units}}{\text{e.s. units}}$	Practical unit	$\frac{\text{P. unit}}{\text{e.m. unit}}$	$\frac{\text{e.s. unit}}{\text{P. unit}}$
Charge of electricity e	$M^{\frac{1}{2}}L^{\frac{3}{2}}\ T^{-1}$	$M^{\frac{1}{2}}L^{\frac{1}{2}}$	x	Coulomb	10^{-1}	3×10^{9}
Current i	$M^{\frac{1}{2}}L^{\frac{3}{2}}\ T^{-2}$	$M^{\frac{1}{2}}L^{\frac{1}{2}}\ T^{-1}$	x	Ampère	10^{-1}	3×10^{9}
Electro motive force E	$M^{\frac{1}{2}}L^{\frac{1}{2}}\ T^{-1}$	$M^{\frac{1}{2}}L^{\frac{3}{2}}\ T^{-2}$	$1/x$	Volt/cm	10^{8}	$\frac{1}{300}$
Potential V	$M^{\frac{1}{2}}L^{\frac{1}{2}}\ T^{-1}$	$M^{\frac{1}{2}}L^{\frac{3}{2}}\ T^{-2}$	$1/x$	Volt	10^{8}	$\frac{1}{300}$
Capacity C	L	$L^{-1}T^{2}$	x^{2}	Farad	10^{-9}	9×10^{11}
Resistance R	$L^{-1}T$	$L\ \ T^{-1}$	$1/x^{2}$	Ohm	10^{9}	$\frac{1}{9\times10^{11}}$
Inductance L	$L^{-1}T^{2}$	L	$1/x^{2}$	Henry	10^{9}	
Electric intensity F	$M^{\frac{1}{2}}L^{-\frac{1}{2}}T^{-1}$	$M^{\frac{1}{2}}L^{\frac{1}{2}}\ T^{-2}$	$1/x$			
Electric Polarisation P	$M^{\frac{1}{2}}L^{-\frac{1}{2}}T^{-1}$	$M^{\frac{1}{2}}L^{-\frac{3}{2}}$	x			
Magnetic pole strength m	$M^{\frac{1}{2}}L^{\frac{1}{2}}$	$M^{\frac{1}{2}}L^{\frac{3}{2}}\ T^{-1}$	$1/x$			
Magnetic Induction B	$M^{\frac{1}{2}}L^{-\frac{3}{2}}$	$M^{\frac{1}{2}}L^{-\frac{1}{2}}T^{-1}$	$1/x$	Maxwell	1	
Inductive Capacity k	1	$L^{-2}T^{2}$	x^{2}			
Magnetic Permeability μ	$L^{-2}\ T^{2}$	1	$1/x^{2}$			
Magnetic field H	$M^{\frac{1}{2}}L^{\frac{1}{2}}\ T^{-2}$	$M^{\frac{1}{2}}L^{-\frac{1}{2}}T^{-1}$	x	Gauss	1	
Magnetic moment μ	$M^{\frac{1}{2}}L^{\frac{3}{2}}$	$M^{\frac{1}{2}}L^{\frac{5}{2}}\ T^{-1}$	$1/x$			

The unit of capacity in the e.s. measure has the dimension of length, and is measured in *centimeters*. This is the capacity of a sphere of radius one cm. Hence one e.m. unit of capacity $= x^2 = 9\times10^{20}$ cms. This is the capacity of a sphere of radius 9×10^{15} km. which is nearly equal to the distance from the sun to the nearest star. The practical unit is *Farad* $=10^{-9}$ e.m. units $= 9\times10^{11}$ cm. Very often a still smaller unit, the *microfarad*, is used. 1 microfarad (μF) $= 10^{-6}$. Farad $= 10^{-15}$ e.m. units $= 9\times10^{5}$ cm.

The unit of inductance in the e.m. units is also a *centimeter* as $L = \int ds\, ds' \cos\theta/r$, where ds and ds' are two elements of length, r is the distance between them, and θ is the angle which their directions make with each other.

Note 2.—Methods for the Determination of *e/mc* for Electron.

For these see the account by. W. Gerlach in *Handbuch der Physik.* 22, 1, 1926.

Note 3.—Motion of the Nucleus (p. 335).

Let G be the centre of gravity of the two particles the electron E and the proton p, and let (x, y, z) and (X, Y, Z) be their coordinates referred to any axes. Then we have

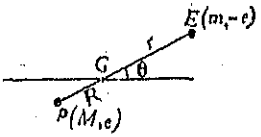

Fig. 1.

$$m\frac{d^2x}{dt^2} = F_x, \quad M\frac{d^2X}{dt^2} = -F_x$$

and two other pair of such equations in Y and Z-coordinates.

The forces are equal and opposite, and directed along the joining line. Hence we have

$$m\frac{d^2x}{dt^2} + M\frac{d^2X}{dt^2} = 0 \qquad \text{or} \qquad \frac{d^2}{dt^2}(mx + MX) = 0$$

But $mx + MX = (m+M)\bar{X}$, where $\bar{X}, \bar{Y}, \bar{Z}$ are the coordinates of the centre of gravity of the two particles.

Hence we have $\frac{d^2}{dt^2}\bar{X} = 0, \ldots .$ etc. $\ldots .$

i.e., $\bar{X} = \alpha_x t + \beta_x, \quad \bar{Y} = \alpha_y t + \beta_y, \quad \bar{Z} = \alpha_z t + \beta_z \quad . \quad . \quad (1)$

i.e., the c.g., of the system moves with uniform velocity. We can without loss of any generality, suppose the c.g., to be at rest.

Let us now take G as the origin of coordinates (r, θ), and let $r = \text{GE}$, $R = \text{G}p$, and let $\text{E}p = r + R = a$.

Then we have

$$r = a\frac{M}{M+m}, \quad R = a\frac{m}{m+M} \quad . \quad . \quad . \quad . \quad . \quad . \quad . \quad . \quad (2)$$

The equation of motion of the electron E is

$$m(\ddot{r} - r\dot{\theta}^2) = -f(a) = -e^2/a$$

$$r^2\dot{\theta} = k \text{ (const.)}$$

Then using (2), we get

$$\frac{mM}{m+M}(\ddot{a} - a\dot{\theta}^2) = -e^2/a$$

$$a^2\dot{\theta} = k \text{ (const.)}$$

Thus the motion of E is the same as if p is fixed, and m is replaced by $\mu = mM/\overline{m+M}$. The quality μ is known as the "reduced mass."

The kinetic energy of the system is

$$T = \tfrac{1}{2}m(\dot{r}^2 + r^2\dot{\theta}^2) + \tfrac{1}{2}M(\dot{R}^2 + R^2\dot{\theta}^2)$$

Using (2), we easily see that it reduces to

$$T = \tfrac{1}{2}\,\mu\,(\dot{a}^2 + a^2\dot{\theta}^2)$$

The angular momentum of the system about G is

$$mr^2\dot{\theta} + MR^2\dot{\theta} = \mu\, a^2\dot{\theta}$$

Hence all that we are required to do is to substitute $mM/(m+M)$ in place of m in Bohr's equations given in §164.

Note 3-A.—Relativity Form of the Orbit (p. 356).

In § 180, in the discussion of the energy of the electron when the relativity correction for energy was taken into account, the form of the orbit was not calculated. This can be done by proceeding from eqn. (36) on p. 356. We have

$$p_r^2 + p^2_\theta / r^2 = \frac{E + e^2 Z/r}{c^2} - (mc)^2 \; . \; . \; . \; . \; . \quad (36)$$

We have $p_\theta = \text{const.} = p$ (Kepler's Law), and if we put $u = 1/r$, it can be easily seen that $p_r / p_\theta = - \partial u/\partial\theta$. Equation (36) transforms into

$$u^2 + \left(\frac{\partial u}{\partial \theta}\right)^2 = \frac{(E + e^2 Z u)^2}{p^2 c^2} - \left(\frac{mc}{p}\right)^2 \; . \; . \; . \; . \quad (A)$$

This can be simplified into the form

$$\left(\frac{\partial u}{\partial \theta}\right)^2 = - f^2 (u - \beta)^2 + \delta^2 \; . \; . \; . \; . \; . \; . \; . \quad (A')$$

where $f^2 = 1 - \left(\frac{e^2 Z}{pc}\right)^2$, and if we put $p = kh/2\pi$, we have $f^2 = 1 - \alpha^2 Z^2/k^2$, where α is the Sommerfeld fine-structure constant; and

$$\beta = \frac{E}{pc} \, \frac{\sqrt{1-f^2}}{f^2}, \quad \delta = \frac{\sqrt{E^2 - (fmc^2)^2}}{fpc} \; . \; . \; . \; . \quad (B)$$

Integrating (A′), we have

$$u = \beta + \frac{\delta}{f} \cos (f\theta) = \beta \left[1 + \varepsilon \cos (f\theta)\right] \; . \; . \; . \; . \quad (C)$$

where $$\varepsilon^2 = \left[1 - (fmc^2/E)^2\right] / (1 - f^2). \; . \; . \; . \; . \; . \; . \; . \quad (C')$$

It can be seen with a little labour that when f is little different from unity, we get all the results on p. 342, for

$$l = \frac{1}{\beta} = \frac{pc}{E} \, \frac{f^2}{\sqrt{1-f^2}}$$

Now putting $p = kh/2\pi$, $\sqrt{1-f^2} = \alpha Z/k$, $f = 1$, $E = mc^2 + W \cong mc^2$, we have

$$= k^2 . \frac{h^2}{4\pi^2 e^2 m Z}$$, which is eqn. (25) of p. 342.

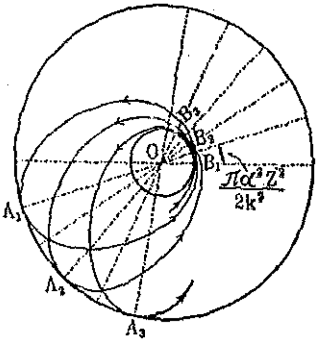

Fig. 2.

Again from (B), we have

$$1 - \varepsilon^2 = \frac{f^2}{1-f^2} \left\{ \left(\frac{mc^2}{E}\right)^2 - 1 \right\}$$

Now E cannot be put mc^2, but $mc^2 + W$, where W is small compared to mc^2, and equal to $-\frac{1}{2}\, m\alpha^2 Z^2 c^2/(n'+k)^2$.

Hence $(1-\varepsilon^2) = \dfrac{k^2}{\alpha^2 Z^2}\ \dfrac{-2W}{mc^2} = \left(\dfrac{k}{n'+k}\right)^2$ which is eqn. (23) of p. 342.

The Form of the Orbit.

The form of the orbit is given by

$$u = 1/r = \beta\,(\,1 + \varepsilon \cos f\,\theta\,) \quad . \quad . \quad . \quad . \quad . \quad . \quad . \quad . \qquad (C'')$$

which differs from the equation of a conic section $u = (1+\varepsilon \cos\ \theta)/l$ only in $f\theta$ being substituted for θ.

We see from (C'') that r is maximum when

$$f\theta = \pi,\ 3\pi,\ 4\pi,\ \ .\ .\ .\ .\ \overline{2n+1}\,\pi.$$

We have then $\qquad r = 1/\beta\,(1-\varepsilon)$.

On the other hand, r is minimum, if

$$f\theta = 0,\ 2\pi,\ \ .\ \ .\ \ .\ \ .\ \ .\ \ .\ \ 2n\,\pi.$$

We have then $\qquad r = 1/(1+\varepsilon)\beta$.

The angle between the two apses are

$$\pi/f = \pi\left(1 - \frac{\alpha^2 Z^2}{k^2}\right)^{-\frac{1}{2}} = \pi\left(1 + \frac{\alpha^2 Z^2}{2k^2}\right) \text{ approximately.}$$

Thus the angle between the successive lines to the perihelion are $\pi\,\alpha^2 Z^2/k^2$.

With the aid of these results, we can visualize the form of the orbit. Let the centre of force be denoted by O, and draw two circles of radii $r = 1/\beta\,(1-\varepsilon)$ and $1/\beta\,(1+\varepsilon)$ (Fig. 2) where these circles are denoted in thick. The dotted lines represent the perihelion lines, and the points $A_1, A_2, \ldots$ denote the points at which the perihelion line touches the outer circle, and the points $B_1, B_2 \ldots$, denote the corresponding points at which the aphelion line touches the inner circle, at successive revolutions. Thus the apse line is advancing, and the electron is describing a spiral curve limited between the two circles, which are envelopes of the perihelion and aphelion respectively.

The angular velocity of the perihelion motion is

$$\Omega = \frac{\pi\alpha^2 Z^2}{k^2} \Big/ T = \frac{\omega}{2} \cdot \frac{\alpha^2 Z^2}{k^2}$$

The orbit is thus an ellipse whose perihelion is advancing with the velocity Ω, or more rigorously with the angular velocity $\omega\ (1/f - 1)$.

Note 4.—Thomas Precession. For an account of this see Birtwistle, *The New Quantum Mechanics*, p. 194.

Note 5.—A Few General Informations.

1. We have mentioned on p. 589 the recent announcement of the discovery of element number 93 by Koblic* in pitchblende. But in a subsequent issue of the Nature he has contradicted the announcement, as his further searches for the element have yielded negative results. (*Nature*, August, 1934).

2. On p. 749 it was mentioned that the nebular lines λ 4959 and 5007 ascribed by Bowen to the O^{++} transition $^3P_1-^1D_2$ have not been produced in the laboratory. In a recent paper Nagaoka and Futagami claim to have produced these lines in the laboratory by sending a disruptive discharge through oxygen. [*Proc. Imp. Acad. Tokyo*, 9, (4), 1933].

3. The auroral lines λ 5577, 6300, 6363 due to forbidden transitions of oxygen have also been found by Grotrian in the spectra of nebulae. (*Zs. f. Astr.*, 2, 78, 1930).

---

* O. Koblic, *Nature*, 134, 55, July 14, 1934.

PHYSICAL CONSTANTS*

Angular momentum unit $h/2\pi = (1{\cdot}0420 \pm 0{\cdot}0013).10^{-27}$ erg. sec.

Avagadro-Loschmidt number $N = (6{\cdot}064 \pm 0{\cdot}006).\ 10^{23}$

Bohr-magneton $\mu = eh/4\pi mc = (0{\cdot}9175 \pm 0{\cdot}0013)\ 10^{-20}$ erg/gauss.

Boltzmann constant $k = (1{\cdot}3709 \pm 0{\cdot}0014).\ 10^{-16}$ erg/degree.

Compton Wavelength $h/mc = (2{\cdot}417 \pm 0{\cdot}005).\ 10^{-10}$ cm.

Electronic charge $e = (4{\cdot}770 \pm 0{\cdot}005).\ 10^{-10}$ abs. e. s. u.

Faraday $F = 96494 \pm 5$ int. Coulombs per gm.-equiv.

Fine-structure constant $\alpha = 2\pi e^2/hc = (7{\cdot}284 \pm 0{\cdot}006).\ 10^{-3}$.
$\alpha^2 = (5{\cdot}305 \pm 0{\cdot}008).\ 10^{-5},\ \ 1/\alpha = 137{\cdot}29 \pm 0{\cdot}11.$

Grating constant for calcite at 20°C $d = (3{\cdot}0283 \pm 0{\cdot}0010).\ 10^{-8}$ cm.

Mass of electron $m = (9{\cdot}035 \pm 0{\cdot}010).\ 10^{-28}$ grammes.

Mass of proton $M = (1{\cdot}6609 \pm 0{\cdot}0017).\ 10^{-24}$ grammes.

Mass of α-particle $M_\alpha = (6{\cdot}598 \pm 0{\cdot}002).\ 10^{-24}$ grammes.

Magnetic moment of proton $eh/4\pi Mc = (0{\cdot}4967 \pm 0{\cdot}0010).\ 10^{-23}$ erg/gauss.

Planck's constant $h = (6{\cdot}547 \pm 0{\cdot}008).\ 10^{-27}$ erg. sec.

Quantum constant $h/k = (4{\cdot}7757 \pm 0{\cdot}0019).\ 10^{-11}$ sec. degree.

Radius of the normal H-atom $a_0 = h^2/4\pi^2e^2m = (0{\cdot}5285 \pm 0{\cdot}0004).\ 10^{-8}$ cm.

Ratio of charge to mass of an electron $e/mc = (1{\cdot}761 \pm 0{\cdot}001).10^7$ abs. e.m.u./gram.

Ratio of masses of proton and electron $M/m = 1838 \pm 1$.

Rydberg constant $R_\infty = 2\pi^2me^4/h^3c = 109737{\cdot}42 \pm 0{\cdot}06\ \text{cm}^{-1} = 13{\cdot}54$ volts.

$R_\infty\alpha^2 = 5{\cdot}822 \pm 0{\cdot}009\ \text{cm}^{-1}$

Stefan-Boltzmann constant $\sigma = (5{\cdot}714 \pm 0{\cdot}006)\ 10^{-5}$. erg. cm.$^{-2}$ sec.$^{-1}$ degr.$^{-4}$.

Velocity of light in vacuum $c = (2{\cdot}99796 \pm 0{\cdot}00004).\ 10^{10}$ cm/sec.

1 Å. U. $= 10^{-8}$ cm. 1 X. U. $= 10^{-11}$ cm.; $1\ \mu = 10^{-4}$ cm.; $1\mu\mu = 10^{-7}$ cm.
If ν = wave number, V = volts, $h\nu c = eV$. $10^8/c = kT$ ergs.

To convert wavelength λ into electron-volts, divide 12340 by λ in Å. U.
To convert electron-volts into wave-numbers, multiply by 8106.
To convert wavelength λ into kilocalories, divide 286000 by λ in Å. U.
To convert volts into kilocalories, multiply by 23·018.
To convert ergs into electron-volts, multiply by $0{\cdot}6285 \times 10^{12}$.
To convert electron-volts into ergs, multiply by $1{\cdot}5911 \times 10^{-12}$.

---

* Adopted from the compilations of R. T. Birge, *Phys. Rev. Suppl.*, 1, 1, 1929; and those of F. Göpel, F. Henning, W. Jaeger and others, *Handbuch der Physik*, 2, 1926.

AUTHOR INDEX

[The figures refer to pages]

Abraham, 69, 417
Adams, E. F. 646
Aitken, 26
Akker, Van der, 37, 405
Albertson, 675
Allen, 220
Allison, 273
Ampère, 403
— and Weber, 770
Anderson, 99, 100, 101
Ångstrom, K 165
Antonoff, 130
Arcadiewa, 182
Arvidsson, 277, 314
Astbury, 251
Aston, F. W. 44, 88, 89, 92, 95, 102, 105, 106, 108, 131
Auger, 485, 492, 516
Ayers, 300

Babcock, H. D. 393, 646, 761
Bacher, 759, 762
Back, E. 395, 403, 426, 427, 430, 752, 754
—, E. and Landé, A. 403
—, E. and Paschen, F. 686
—, and Wulf, 762
Backhurst, 510
Bäcklin, E. 65, 67, 278
Bainbridge, 97, 102, 103
Balmer, 320
Baly, E. 395, 430
Bär, R. 62
Barkla, C. G., 196, 206, 207, 208, 210, 213, 217, 221, 299, 300, 303
Barnes, H. T. 165
Barnett, L. J. H. 820
—, S. J. 774, 812, 819, 820
—, S. J. and Barnett, L. J. H. 820
Barret, 301
Barton and Mulliken, 810
Bassler, 305
Bates, 314
Bauer and Piccard, 783
Bearden, J. A. 65, 67, 277
Beatty, 293
Becher, R. F. 589
Beck, 774
Becquerel, 109, 116, 117
Berg, O. 587
Bergmann, 368
Berkey, 517
Bethe, 563
Beutler, 736
Bevan, 308
Bhar, 802
Bhatnagar, S. S. 779
Birge, R. T. 65, 103
Birtwistle, G. 430
Blackett, P. M. S. 81, 100
Blake, 290
Bleakney, 615
Böhme, 104
Bohr, N. 160, 202, 319, 321, 324, 332, 333, 334 341, 367, 369, 402, 403, 404, 419, 449, 525, 528, 531, 562, 582, 584, 586, 659, 734, 799.
—, and Van der Bijl, 594
Boltwood, 122
Born, M. 546, 589
Bosanquet, 259
Bose, D. M. 805, 818
—, and Bhar, 802
—, J. C. 178, 182
—, de M. H. 739
Bothe, W. 164, 201, 202, 203, 491
Bowen, I. S., 536, 538, 569, 571, 675, 735, 736, 745, 748, 749
Brace, 180
Brackett, 323, 326
Bragg, W. H. 229, 258, 259, 260, 261, 263, 271
—, W. L. 229, 241, 248, 259, 260, 497
—, and Kleeman, 140
—, and Pierce, 497
Braun, 51
Bravais, 223, 237
Brickwedde, F. G. 94, 336, 337
Briggs, 136, 147

F. 105

Broek, Van der, 160
Brück, 768
Bruygmans, 771
Bubb, 492, 493
Bucherer, A. H. 70
Buisson, 676
Burger, 564
Burrau, 618

Cabrera, B. 805
—, and Piña, 802
Campbell, 110
Carlsson, 273
Casimir, 768
Cassie, 487
Catalan, 677, 740
Cauchois, 273
Chadwick, 103, 159, 160, 162, 164
—, and Mercier, 164
Chantillon; 809
Chattock and Bates, 814
Coade, 218
Cockroft, 102
Coeterier and Scherrer, 817
Compton, A. H. 8, 11, 198, 258, 259, 262, 273, 301, 312, 517
Constable, 103
Cooksey, 490
Coolidge, 280
Costa, 102
Coster, 283, 444, 449, 477, 480, 586
Crawford, M. F. 738
Crookes, W. 42, 49, 114, 116
Crowther, 163
Curie, I. 141
—, Madame, 110, 112, 116, 130, 140
—, P. 110, 114, 122, 165, 772, 775
—, Joliot, 101
—, and Laborde, 114

Dalton, 40, 179
Darwin, 258, 308, 685
Datta, S. 366, 368
Dauvillier, 198, 271, 473
Davidson and Stratton, 323
Davis, 272, 310
— and Goucher, F. 599
De Broglie, 198, 498, 482, 484, 513, 531
— Kronig, 318
Debierne, 112
Debye, P. 194, 250, 261, 302, 399
Decker, H. 804
Democritus, 39
Dempster, 95, 97, 611
Descartes, 175
Dewar, 165
Dingle, 745
Dirac, P. 101, 420
Doan, 262, 273
Dolezalek, F. 8, 11
Doljsek, 479
Dorgelo, 626
Dorn, 206, 481
Duane, 288, 289, 290
Dumas, 87
Dunlop, 219

Eddington, 66
Eder, 586
Edlén, B. 277, 467, 565, 625
Eggert, J. 632
Ehrenhaft, 61
Einsporn, 599
Einstein, A. 70, 186, 189, 190, 331, 345, 441, 619, 778.
— and de Haas 774, 812, 818
Ekefors, 277
Ellis, and Wooster, 166
Elster, J. 1, 18
— and Geitel, 1
Emelius, 85
Empedocles, 39
Epstein, 658, 659, 671
Erickson, 565
Ettinghausen von, 781
Eves, A. S. 166
Evershed, J. 330
Ewald, 308

Fabry and Buisson, 676
Fajans, K. 87, 131, 548
Faraday, M. 41, 42, 180, 391, 771, 774
Feather, 141
Fedorov, 223
Fermi, 470, 589, 697, 768
Flint, 589
Foëx, 779
Foote, Meggers and Mohler, 605, 606
Foster, 658, 671, 672
Fowler, A. 333, 334, 367, 374, 381, 571, 643, 698, 722

Fowler, R. H. 91, 635
—, and Milne, 644, 645, 646
—, and Payne, 652
Franck, 599
—, and Hertz, 590, 595
Frank, 804
Fraser, R. G. J. 411
Fraunhofer, 177
Freed, S. 802
Frerichs, 751
Fresnel, 176, 179, 180
Friedrich, 226

Garrett, 626
Gehrcke, 88
—, and Lau, 753
—, and Reichenheim, 95
Geiger, H. 6, 32, 95, 96, 125, 136, 142, 145, 146, 147, 202, 203
Geiger and Bothe, 164
—, and Marsden, 153, 157, 158, 159
—, and Nuttall, 144, 147
Gieseler, 740
Geitel, H. 1, 2, 3, 13
Gerlach, 409, 801
Ghosh, R. N. 371
Giaque, 103
Gibbs, R. C. and White, H. E. 675
—, R. C., Wilber, D. T. and White, H. E. 697
Giesel, 112
Goldstein, 49
Goucher, F. 599
Goudsmith, S. 350, 352, 417, 418, 420, 430, 539, 557, 687, 720, 752, 754, 765
—, and Bacher, 759, 762
Gould, 102
Gouy, 780
Gräetz, 56, 286
Graffunder, 626
Graham, W. P. 44
Grimaldi, 176
Grotrian, W. 540, 589

Haas de, 774, 812, 813
Hadding, 270
Haga, 222
Hahn, 129
—, and Soddy, 112
Hale, G. E. 333
Hallwachs, 186
Hamer, 608
Hansen, G. 339, 564, 586, 753, 756
Hargreaves, 768
Harnwell, 615
Harris, J. H. 587
Hartley, 320, 361
Hartree, 301, 470, 792
Haüy, 233
Hector, 785
Heisenberg, W. 420, 546, 555, 568, 820
Helmholtz, R. von, 27, 41, 182
Henderson, 127, 141
Hertz, G. von, 181, 182, 183, 186, 459, 538, 590, 002
Herzog, 301
Hess, 165, 166
—, and Lawson, 168
Hettemer, 104
Heussler, 772
Hevesy, G. 281, 283, 582, 589
Hewlett, 217, 219, 200
Heydweiller, A. 548
Hicks, 367
Hognes, 98, 615
Holweck, 449
Honda, K. 779
—, and Ishiwara, 779
Hönigschmidt, 87
Hopfield, 650, 751
Hopkins, B. S. 587
Hornbostel, 85
Houston, 322, 564
Howe, 475
Huggins, 320
Hull, 250
Humphreys, C. Y. 557
Hund, F. 589, 692, 702 800, 810, 817
Hunt, 274, 288, 289
Huygens, 176, 179
Hylleras, 467, 565

Ingram, 745
Ikenmeyer, 791
Ishiwara, 779

Jackson, 796
James, 259, 805
Jeans, 185
Jog, 744
Johann, 278

Johnston, 103
Johner, 786
Joliot, 101
Jönsson, 441, 498, 507
Joos, G. 548, 790.
Jordan, P. 420

Kallmann, 103, 198, 315, 615
Kanad, 39
Kapitza, 134, 396
—, and Skinner, 396
Kaufmann, 54, 67
Kayser, 558, 676
Kellner, 467, 565
Kellström, 316, 475
Kelvin, 26, 169
Keussler, 338, 354
Keyston, 764
Kichlu, P. K. 538, 571, 579, 745
Kiess, 408, 745
King, A. S. 103, 655, 656, 729.
Kingdon, 655
Kirchhoff, 178
Kirchner, 492
Kleeman, 140
Knipping, 226, 599
Koch, 315
Kohlrausch, 40, 180
Kokubu, 671
Konen, 676
Kossel, 375, 444
Kramers, H. A. 202, 289, 562, 670
Krishnamurti, 675
Kulenkampff, 291, 295
Kurth, 608
Kustner, 515
Kutzner, 35
Kvalnes, 98

Laborde, 114
Laby, 13, 283
Ladenberg, 327
Lambert, 87
Lampa, 182
Langevin, 19, 21, 738, 787
Langmuir and Kingdon, 655
Landé, A. 405, 408, 412, 424, 428, 430, 548, 686
Laporte, 680, 805, 818
Larmor, J. 391, 392, 397
Larsson, 313
Lasareff, 103
Lattey, R. T. 22
Lau, 338, 753
Laub, 481
Laue, 205, 222, 224, 253
Laurence, 147
Lavoisier, 39
Lawrence, E.O. 739
Lawson, 168, 171
Lebedew, 182, 192
Le Bon, 112
Leu, 411
Lenard, P. 27, 50, 186, 188, 189, 590, 594
Leucippus, 39
Lindberg, 477
Lo Surdo, 658, 672
Löbe, 294
Locher, 517
Lockyer, Norman, 40, 374, 557, 698
Lonsdale, 261
Lorentz, H. A. 69, 182, 183, 185, 391, 392
Loria, 327
Lotharmeyer, 527
Loyarte, R. G. and de Bose, M.H., 739
Lozier, 618
Lummer, 184
Lummer and Gehrcke, 184
Lunn, 615
Lutz, 13
Lyman, 322, 326, 558

Magnusson, 275, 449, 475, 478
Mainsmith, J. D. 592, 672
Makower, 6
Marckwald, 132
Mark, 198, 315
Mark and Wierl, 657, 666
Marsden, 141, 158
Martin, 517
Marx, 206
Matuyama, 626
Maxwell, 40, 181, 191, 770, 773
Mayer, 590, 655
Mazumdar, K. 658, 744, 745
Mc Coy and Ross, 131
McLay, A. V. 738,
Mc Lennan, J.C. 751
Mc Lennan and Mc Lay, 769
—, Mc Lay and Crawford, M.F., 738
Meggers, F. 408, 605, 606, 729, 730

Meissner, 626
Meitner, L. 101, 143
—, and Freitag, 143
Mendeléef, 527, 587
Menzel, 639
Mercier, 164
Merrill, 639, 749, 750
Messenger, 623
Meyer, St. 805
—, and Hess, 166, 167
Michelson, A. A. 65, 338, 399, 752
Millikan, R. A. 58, 62, 186, 188, 189, 322, 536, 538, 571
—, and Bowen, 735, 736, 748
Milne, 623, 630
Mishima, 756
Mogendorff, 367
Mohler, 605, 606
Moore, D. E. 646
Moseley 160, 262, 269, 481, 482, 486, 487
—, and Robinson, 166
Mott, 164
Mukherjee, J. B. 480
Mulder, 477
Müller, 36, 271, 282
Mulliken, 810
Murphy, G.M., 94, 336, 337

Nagaoka, H. 153, 321, 756
Nardroff, 314
Naudé, 103
Neufeldt, 34, 37
Newton, 177
Nicholas, 293
Nichols, 182
Nicholson, 324
Nickerson, J. L. 127
Nimmo, 141
Noddack, W. 587, 589
—, and Tacke, 587
Nuttall, 401

O' Bryan, 474, 481
Occhialini, 100
Oersted, 40, 402, 770
Onnes, K. 116
Ornstein, 564
Orthmann, 167
Osgood, 277
Ott, 281
Owen, 779

Paneth, F. 585, 589
Pannekoek, 646
Parker, 102
Pascal, P. 809
Paschen, F. 17, 165, 323, 326, 333, 348, 349, 395, 399, 426, 427, 650, 677, 686, 691, 724, 725, 736, 738, 751
Paschen and Back, 395
Pauli, 404, 417, 445, 462, 558, 572, 690, 753, 756, 808
Pauling, L. 430, 548, 589, 792
Paulson, 677
Payne, C.H., 646, 652
Perkins, 141
Perrin, 50, 492
Petrova, 168
Pfund, 323, 326
Philipp, 144
Phipps, 411
Piccard, 783
—, and Johner, 786
Piccardy, 675
Pickering, 333, 638
Pierce, 497
Piña, 802
Piper, 261
Planck, M. 184, 185
Plaskett, 630
Plessner, 776
Plücker, 49
Poetker, 323
Pol, Van der, 46
Pollard, 103
Poole, 165
Precht, 165
Preston, 399, 401
Prins, 315, 474, 477
Prout, 40, 87

Quincke, 781

Raman, C. V. 261
Ramanatham, 261
Ramsauer, 500, 530
Ramsay, W. 558
Rao and Krisnamurti, 675
Rasmussen, 675
Ray Chaudhuri, 817
Rayleigh, 185
Regener, 136
Reichenheim, 88.
Reynolds, 367

Richards, 87
Richardson, O. W. 494, 589, 774, 812
Richarz, 27
Richtmeyer, 505
Righi, 182, 186
Ritschl, 754
Ritz, 332, 366
Robinson, 133, 166, 482, 485, 487, 489
Rojansky, 670
Rolla, 587
—, and Piccardi, 675
Römer, 174
Röntgen, 204
Ross, P. A., 131, 200, 305
Rosseland, S. 420
Rowland, H. A., 319, 646
—, and Jacques, 775
Ruark, A., 130, 322, 605, 608
—, and Sommerfeld, A., 756
Rump, 293
Runge, 395, 397, 399, 401, 558
650, 333, 368, 676
Runge and Paschen, 395
Russell, H. N., 534, 633, 638, 639,
640, 646, 649, 717, 726, 729, 742
—, and Meggers, 730
—, Saunders, 733, 734
Rutherford, E. 18,32, 112, 117, 120,
125, 133, 136, 152, 155
—, and Barnes, 165
—, and Chadwick, 162
—, and Geiger, 137
—, and Mme Curie, 140
—, and Robinson, 133, 134, 136
—, and Royds, 139
—, and Soddy, 117, 118
—, and Wood, 143
Rydberg, 332, 361, 362, 363, 369, 677

Sadler, 208
Saha, M. N., 480, 538, 630, 653
Saha and Mazumdar, 744
Sandström, 443
Saunders, 534, 639, 733
Sawyer, R. A. 569
Scherrer, 250, 817
Schiebold, 256
Schlapp and Rojansky, 670
Schmidt, 110
Schmutzer, 85
Schoenfliess, 223, 240
Schonland, 169
Schrödinger, E. 540, 542, 543
Schüler, 565, 754
—, and Brück, 768
—, and Eastermann, 757
—, and Keyston, 764
Schur, 496
Schuster, 363, 364
Schwarzschild, 499, 658, 659
Schweidler, von, 16
—, von and Hess, 165
Seeman, 267, 438
Sellmeyer, 182
Serreo, A., 808
Shearer, 271
Shenstone, A. G., 578, 730, 630
Shimizu, T., 30
Sidgwick, N. V. 589
Siegbahn, M., 264, 268, 269, 275, 277,
436, 438, 449, 466, 474, 475, 476, 478
Simon, W., 200
Simpson, 10
Singh, 608
Skinner, 396, 474, 481
Skobelzyn, 100, 104
Slater, J. C. 202, 698, 702, 792
Smekal, A., 480, 548
Smith, P.T., 730
Smyth, 612, 615
Snellius, 175
Soddy, 87, 112, 117, 132
Soddy and Boltwood, 122
Soddy and Fajans, 131, 132
Söderman, 274, 449
Söderqvist, 675, 745
Sohncke, 240
Sommer, L.A., 752
Sommerfeld, A., 294, 207, 340, 341,
342, 344, 345, 371, 375, 384, 390,
402, 404, 415, 430, 446, 460, 466,
468, 469, 493, 494, 496, 671, 680,
756, 818
Sommerfeld and Laporte, 805
Soné, T. 780
St. John, C. E., 646, 647, 651
Stark, J., 294, 656
Stas, 87
Stempel, 272
Stenström, 308
Stern, 408, 649
—, and Gerlach, 408
Stewart, 261, 646, 814

Stokes, 206, 287
Stoner, E.C., 59, 470, 532, 672, 807, 818
Strutt (Lord Rayleigh II), 170, 171
Stratton, 823
Stuckelberg, 615
Sucksmith, 817
—, and Bates, 814
Sur, N. K., 371, 653, 748
Swinne, 148

Tacke, I. 587
Takamine and Kokubu, 671
Takens, 477
Taylors, 411
Tears, 182
Théodoridès, 779
Thibaud, 274, 312, 449, 473, 474, 477
Thomas, 421, 608
Thomson, G. P., 88
—, J.J., 3, 27, 44, 47, 51, 53, 74, 81, 94, 152, 183, 196, 205, 214, 511, 611
—, and Rutherford, E., 169
Thomson, 527, 577
Thoraeus, 271, 470, 473, 475
Thorsen, V. 755
Tizard, H. T., 22
Toshniwal, G. R., 755
Turner, 724
Townsend, 16, 22, 73, 590, 774

Uhlenbeck, 350, 352, 417, 418, 420, 687
Ulrey, 290
Urbain, 582, 586
Urey, H. C., 94, 336, 337
—, and Fermi, 687

Valenta, 586
Van der Bijl, 594
Van der Broek, 160
Van Urk, 543, 544
Van Vleck, 806, 817, 818
Van Vleck, and Frank, 804, 808
Vegard, 751
Villard, 48

Wadlund, A. P. R., 65
Wagner, 290, 295, 438, 439, 531
Waller, I. 548, 671
Wali Mohammed, 756
Walter, 222
Walton, 102
Ware, L. M. 646
Wasastjerna, I.A., 548
Watson, H. E., 44
Watson, 87, 102, 493, 495
Webb, 625
—, and Messenger, 623
Weber, 40, 180. 770
Webster, 290, 293, 297, 441
Weiss, P., 773, 796
Wellisch, 21
Welsbach, Auer von, 582
Wentzel, 164, 671, 734
Werner, 34, 565, 586
Western and Ruark, 130
White, H. E., 675, 697
Wiechert, 206, 287
Wiedemann and Plessner, 776
Wien, 81, 184, 293, 622
Wierl, 657, 666
Wilbert, D. T. 697
Williams, E. H. 805
Wills, 771
—, and Hector, 785, 790
Wilson, C.T.R., 2, 3, 9, 26, 28, 29, 201
—, H. A., 45, 47, 75
Wilson, W. 342
Wind, 222
Wollan, 301
Woo, Y. H. 200
Wood, R. W. 321, 322, 368, 395
Wooston, 441
Wooster, 166
Wrede, 411
Wright, 10
Wulf, 8, 10
Wyckoff, 252

Yntema, L. F. 587
Young, T. 176, 177

Zeleny, 21
Zeeman, 391, 395, 656
—, Back and Goudsmit, 752, 754
Zernicke and James, 805
Ziegert, H. 142

SUBJECT INDEX

A, the separation factor, **717**
  for equivalent electrons, **718**
  for non-equivaloent electrons, **718**
  observed and calculated values of, 720 (table)
A and B Coefficients of Einstein, 619
Absorption,
  experiments on, 140
  mechanism of, 140, 326
  negative, 621
  selective, 198
Absorption coefficient of X-rays
  atomic, 212
  mass, 212, 498 (table)
  mathematical relations of, 504
  variations of, with wave length, **500**
  variations with At no., 501
Absorption edge, 439
  explanation of, **439**
Absorption filters, 502
  half-value thickness of, 503 (table)
  selective, 504
Absorption jumps, 507
  empirical relations in, 511
  values of, 509 (table)
Absorption of X-rays, 209, 497
  experimental methods, 497
  in the long wave length region, 474, **498**
  levels in, 444
  study of, **513**
  universal curve of, 509
Absorption spectra
  due to excitation of inner electrons, 736
  of Hg, 737
Actinium,
  constants, 126 (table)
  discovery of, 112
  genealogy related to, 131
  series—chart of, 124, 130
  structure of, 588
Actino-lead, 131
Actino-uranium, 130
Aether, 179
Age of earth, Kelvin's calculation of, 169
Age of minerals
  from He contents, 170
  from lead contents, 171
  from radioactive data, 168
  table for, 172
Air, conductivity of, 1, 2
Alkali elements,
  effective quantum no. for, 542
  excited states of, **535**
  explanation of ionisation potential of, 369, 376
  hydrogenic and non-hydrogenic terms of, 514
  isotopes of, 95, 97
  resonance lines, 376
  resonance potential, 376
  spectra of, 361
Alkali spectra, **534**
  doubling of levels in, **423**
  Zeeman-splitting in, 396, 400, **407** 426, **429**
Alpha particles,
  absorption of, **140**
  and Helium atom, identity of, 139
  charge on, **137**, 138
  chemical actions of, 114
  counting of, by Regener's method, **136**,
  curved tracks of in high
  magnetic field, 134, 149
  deflection of, under electric field, 134, 135
  distance of nearest approach of, 154, 162
  e/m of, 135
  heat evolved by, 166
  ionisation produced by, 142
  magnetic deflection,
  — accurate measurement of, 134
  magnetic deviation of, 133
  mass and charge of, 136
  $\frac{MUc}{E}$ of, 134
  $\frac{MU^2c}{E}$ of, 134

Alpha particles—(*contd.*)
  nature of, 31
  range of, 140
  rate of emission of, 137
  scattering of, 152
  — large angle, 158
  — small angle, 143
  scintillations produced by, 114
  stoppage of, 164
  stopping power of substances for, 142
  straight collison of, 162
  tracks of, 31
  velocity of, 113
  — Bragg's determination of, 147
Ampere's theorem, 403
Anode
  composite, 88
  hot, discharge tube, 88, 95
  rays, 88
Anomalous dispersion of X-rays, 314
Anomalous terms of Ca, 783
Anomalous Zeeman effect, **399**
Arc lines of He I, 559
Argon, isotopes of, 98
Atom, as a magnet, 402
  average life of, 110
  directional quantisation of, **408**
  electronic composition of **531, 583** (chart)
  factor, 258
  in a magnetic field, 403, 404
  life in the excited state, **621**
  — Webbs and Messenger's experiment, **623**
  — Wien's experiments, **622**
  life in the metastable state, 626
  — Matuyama's experiment, **626**
  magnetic moment of an, 405
  of positive electricity, 78
  Rutherford's picture of, 159
  structure of, 152
  Vector model of, 416
Atom core
  polarisation of, **546**
  radius of, 580
Atomic number, 98, 160
Atomic structure factor, 258
Atomic weights
  constancy of, 87
  law of integral multiples of, 40 87, 98
Auger effect, **485**
  explanation of, 486
  experimental investigation of, 486
Aurora
  Austrealis, 751
  Borealis, 751
Auroral lines, green, 751
Axial ratios, 233
Azoic rocks, 169

Balmer's discovery, 320
Balmer's law, 320
Balmer lines
  fine-structure of, **337,** 420 423
  — explanation of, 340
  — relativity correction for, **345**
  — intensity of components, **353**
Balmer-series, 321, **322,** 323
Barium, interval rule for, 682
Becquerel-rays, 110
Beryl, helium contents of, 173
Berrylium, isotopes of, 97
Exchange resonance, 464
Beta-rays
  from RaC, e/me of, 67, 69
  heat evolved by, 166
  nature of, 133, 114
  properties of, **163**
  range of, 168
  scattering of, 168
  scintillations produced by, 114
  stoppage of, 164
  tracks of, from RaD, 163
  velocity of, 113, 114
Bismuth, susceptibility of, variation with temperature, 777
Bohr-Coster diagram, **449**
Bohr-diagram, for NaI, 367
Bohr-Grotrian-diagram
  for HeI, 560, 561
  for AlI, **568**
  for Na I, 378
  for MgI, 388
Bohr-magneton, 402, **403, 799**
Bohr's orbits for hydrogen, 325
Bohr's theory of hydrogen atom, **321**
  insufficiency of, **331**
  Sommerfeld's generalisation of, 341
Brackett-series, 323, 326
Bragg's law, 281
  deviation from, 308

Bragg's method for crystal structure determination, 421
Bragg's spectrograph, 243
Bragg's theory of X-ray reflection, 229
Braun tube, 51
Bravis lattice, 287
Breadth of X-ray lines, 466

Calcium
  anomalous terms of, 733, isotopes of, 97
Canal rays, 79
Cathode, 42
Cathode ray,
  discharge, nature of, 48
  e/mc of, J. J. Thomson's method, 53
  — Bucherer's method, 70
  — Kaufmann's method, 54
  furnaces, 50
  maximum velocity of, 55
Ceylon thorianite, time of deposit of, 171
Chadwick's measurement of nuclear charge, 150
Characteristic X-rays
  breadth of lines of, 466
  conditions of excitation of K-lines in, 436
  excitation potentials of, 441
  explanation of, 445
  origin of lines in, 434, 445
  origin of L-lines in, 445
  theoretical explanation of, 461
Chlorine, isotopes of, 98
Chromosphere, 192
Clevite, Norwegian, 87
Closed shells, 528
Cloud-chamber
  applications of, 31, 74
  method of Blackett, 31
  method of C. T. R. Wilson, 26
  method of Shimizu, 30
Coefficient
  of diffusion, 23
  of interdiffusion, 25
  of mobility, 21
Collision, elastic, 590
  inelastic, 593
Complex spectra, 676
Compton's theory, experimental verification of, 196
Condensation, rain-like and cloud-like, 28
Conductivity, electrical, of gases,
  measurement of, by Elster and Geitel, 1
  — by C. T. R. Wilson, 2
  distriution of, in the discharge tube 43, 47
  interpretation of, 3
Constant
  auxiliary, 65
  decay, 118
  fine structure, Sommerfeld's, 66
  fundamental, 66
  Planck's, 65, 66
Contact potential, 598
Continuous X-rays, 287
  distribution of energy in the spectrum of, 291
  efficiency of production of, 293
  polarisation of, 303
  — estimation of, 305
  pulse theory of, 287
  Short wave limit of, 289
  — experimental measurements of, 289
  Sommerfeld's theory of, 297
  space-distribution of, 294
Convergence frequency, 366
Convergence limit, 321
Copper, chemical and physical properties of, 578
Corpuscular theory, revival of, 183
Cosmic rays, 99
  tracks of, 100
Counters,
  action of point, various theories of, 35
  arrangements of connections in, 33
  difficulties of working with, 34
  eletrical, Rutherford and Geiger's 32
  point, Geiger's, 33
  record of, 37
  the Geiger-Müller tube, 36
  use of amplifiers in, 34
  uses of, 35
Coupling,
  JJ— 638, nature of terms in, 685
  Russell-Saunders' 682
  —departure from, 682
Critical potential
  for soft X-ray emission, 608
  of Fe, Co, Ni, Cu, by electron

    bombardment method, 610
  of molecular hydrogen, 614
  —secondary effects in, 615, 618
  of He, Ne and Hg, 608
  of Hg, 600
Critical potential of elements,
  Davis and Goucher's experiment, 599
  Einsporn's method, 599
  Franck and Hertz' experiment, 595
  Hertz' method, 602
  Hertz' method of residual current 608
  Lenard's experiment, 594
Critical potential of molecules, **610**
  Bleakney's apparatus, 616
  modern experimental arrangement for, **611**
  Smyth's apparatus, 612
Crookes dark space, 42, 44, 48
Crystal
  atomic structure factor of, 258
  classes, 234
  diffraction of X-rays in, 22
  dispersive power of, 265
  ionic, molecular and atomic, 260
  reflection of X-rays in, 229
  resolving power of, 265
  structure factor of, 256
  symmetry in, 234
Crystalline theory, Classical, 232
Crystal structure, determination of
  Bragg's method, 241
  complete determination of, 256
  Debye and Hull method, 250
  powder method, 250
  Schiebold-method, 256
Curie, one, defined, 122
Curie's balance, **775**
Curie's law, **772**, 778
  Weiss's extension of, 778
Curie point, 778
  of soft iron, Ni and Co, 778

Dark space
  Crookes, 42
  Faraday, 42
Decay of radioactivity, **116**
  curve for ThX, 117
Debye factor, 258
Debye-Hull method, 250
Deuton, 336
Diamagnetic anisotropy, 787
  of graphite, 787
Diamagnetic susceptibility
  discussion of results on, determination of, **790**
  of irons, 790 (table)
  of salt-solution, 791
Diamagnetism
  condition for, 790
  discovery of, 771
  Langevin's theory of, **787**
  of molecules, 808, **809**
  — Van Vleck's theory, 809
  Pascal's law of, 791
  summary of experimental results on, **786**
Diffuse triplet, 382
Diplogen, 336
Discharge tube
  distribution of electric field and conductivity in the **43**, **45**, 47
  Hot anode, 88, 95
  phenomena in, **41**
  secondary phenomena in, 47
Disintegration of radio active bodies
  Dual (branch), 129, 131
  half value- period of, 119
  successive, extension to, 120
  theory of Rutherford and Soddy, 118
Dispersion of X-rays, 313
  anomalous, 314
Dispersive power of crystal, 265
Displacement law, Soddy and Fajans' 131
Distribution of electrons round atom, 259
Double electron transition, **732**
Doublet laws
  application of, **570**
  irregular, **536**
  regular, **548**
Doublet separation
  for single electron, 708
  for Al-like ions, 571
  for B-like ions, 570
  for halogens, 724
  for Li-like ions, 424
  for Na-like ions, 424
Doubling of levels, 372
  separations due to, 372
Duane and Hunt's experiment, 289

Duplicity phenomena, 378
Dwi-manganese, 587

"e," early determinations of,
  Townsend's, 73
  J. J. Thomson's 74
  Wilson's, by balanced drop method, 75
  independent methods of determination, 65
  Millikan's determination, 58
  on the absolute value of, 65
Electricity, atom of positive, 78
  elementary quantum of, 56
Earth
  age of, Kelvin's calculation, 169
  temperature of interior, 169
Einsporn's method, 599
Einstein's A and B coefficients, 619
Einstein's transition probability, 331
Eka-ceasium, 587
Eka-manganese, 587
Electrolysis, Faraday's law, interpretation of, 41
  studies in, 40
Electrometers
  adjustments and calibrations of, 59
  Compton's, 11
  Comparison of different types of 14
  Dolezalek, 10, 11
  Lindemann, 11
  — arrangement for using, 12
  — principle of , 12
  — sensitivity of, 13
  other types of, 9
  string, 13
  use of, 5
Electron
  as an oscillator, 183
  as wave 78
  charge on the, Millikan's determination of, 58
  contractile, of Lorentz, 69, 70
  dimensions of, 75
  isolation of, 41
  magnectic moment of, 403
  mass of, 57
  maximum velocity of, 55
  motion of, under electric and magnetic fields, 52
  recoil, experimental evidence regarding, 200
Electron—(*contd.*)
  rigid, of Abraham, 69, 70
  spinning, 78, 417, 774
  — in the magnetic field of the nucleus, 420
  Sub, Ehrenhaft's hypothesis of 61
  swift, e/mc for
    Kaufmann's experiment, 67
    Bucherer's experiment, 70
Electron-composition of elements, 529
  Bohr's theory of, 531
  calculation of optical levels due to, 692
  of alkali metals, 534
  He to Ne, 533
  of Mg, 549
Electron-pressure
  from maximum intensity of subordinate series lines and enhanced lines, 644, 645
Electroscope
  alpha, beta and gamma-ray, 115
  Arrangement for use of, 8
  comparison of different types of, 14
  emanation, 116
  other types of, 9
  the tilted, 9
  Wulf's, 10
Element, 93, 589
Elements, maximum number of, 588
  of atomic number 43, 61, 75
  — discovery of, 586
Eman, defined, 122
Emanation, radioactive, 121
Emission
  mechanism of, 326
  stimulated, 621
Emission of X-rays, 441
Energy-formula, general, 707
Energy-levels, 444
  Calculation of, from absorption and emission spectra, 448
  — from magnetic spectroscopy, 487, 488
  determination of, from magnetic spectroscopy, 481
  of AlI, 568
  of HeI, 560, 561
  of HgI, 595
  of MgI, 388
  of NaI, 378
  tables for, 450 (X-rays)

Epoch, 169
  tertiary, secondary, palaeozoic, protozoic, archaean, **172**
Equivalent electrons, **693**
  in jj—coupling, 702
  highest terms of, 717
  p, d and f, 697
Evolution of heat by radioactive substances, 167
  — theory of, 167
Excitation potential of X-ray lines, 441
Exclusion principle, Pauli's 553, **572**

f-the hyperfine structure quantum number, 756, 758
Faraday effect, 391
Filters
  absorption, for X-rays, 503
  selective, 504
Fine-structure constant, Sommerfeld's, 347
Fine structure
  of Balmer lines, 337
  of He—lines, 348
  of hydrogen lines, 350
Fluorescent X-rays, 208, 212, 485, **512**
  efficiency of production, **516**
Forbidden lines, 371, 746
  in He I spectrum, 562
  Red, of oxygen, 751
Forbidden transition, 748
  due to O in nebulae, 749
  in nebulae and Wolf Rayet stars, 748
  in Fe specturm, 749
  in Pb and Bi spectra, 748
  list of lines due to, in astrophysical sources (table), 750
Formation of elements
  after argon, **574**
  after copper, **579**
  after Hafnium, **587**
  after Radium, **588**
  of the fifth period, **580**
  of transitional group, **577**
Franck and Hertz' experiment, **595**, 596
  sources of error in, 597.

g, the Landé factor, 405, 412
  for a pd-combination, 688
  for strong fields, 689
  for several electrons, 690
  for two electron systems, 687
  for singlet, doublet terms, 412 (tables)
  for triplet, quartet terms, 413 (tables)
  for a given multiplet, 691 (table)
  in RS-coupling and jj-coupling, 686
  interpretation of, **424**
g(i) the nuclear Landé factor, 757
G—permanence rule, 688, **691**
G—sum rule, **688**
  illustration of, 690
Gamma factors, 707
  for many electrons on RS-coupling, **709**
  for more than two electrons, 712
  for strong fields, 710
Gamma permanence rule, **711**
  applications of, 712
Gamma sum rule, **711**
  applications of, 712
Gamma rays,
  heat envolved by, 166, 167
  nature of, 113, 114
  properties of, **163**
  stoppage of, 146
  tracks of, 164, 201
  wave length of, 164
Geiger and Nuttall's law, 147
Geiger and Nuttall's method for determination of range, 144
Giegor relation, 142, 150
Geological epochs, 169
Goniometer, 234
Growth of radioactivity, **116**
  curve for Th, 117
Gyromagnetic anomaly, 816
  applications of quantum theory to, **816**
Gyromagnetic effect, 773, **811**
  experiments on, **812**
  — Barnett's experiment, **819**
  — Beck's method, 814
  — Einstein-de Haas method, **813**
  — Ray Chaudhuri's experiment, 817
  — Sucksmith and Bates' experiment, **814**
Gyromagnetic ratio, 774, 812
  determination by magnetometer method, 820

Gyromagnetic ratio—(*contd.*)
  for Fe, Ni, Dy, 817
  for ions of the first transitional group (table), 818

h—Planck's universal constant, 190
Hafnium, discovery of, 585
  name of, 586
Half value period, 119
Helios, 558
Helium
  contents of, in old minerals, 170
  ionisation potential of, 565
  ionised, lines of, 333
  — fine structure of, 348
  — — intensity of components of, 355
  Stark-effect of, 672
  mass analysis of, 94
Helium spectrum
  arc lines in, 559 (table)
  forbidden lines in, 562
  general description, 557
  intensity anomaly of, 564
  inter-combination lines in, 559
  interval rule in, 564
  resonance lines in, 558
  theoretical explanation of, 562
Heusler alloys, 772
Hertzian oscillator, 391
Highest term
  for equivalent d and f electrons, 704
  for many electrons, 705
Hydrogen
  atom, radius of, 326
  atom, higher states of, 392
  heavy isotopes of, 94
  — spectrum of, 336
  negative ion of 86
  second order spectra of, 94
Hydrogen spectra
  Bohr's theory of, 319, 821
  Sommerfeld's generalisations of, 341
  continuous, 330
  fine structure in (see under Balmer lines).
  series of, 322 (table).
Hydrogenic orbit, 540
Hyperfine structure
  due to isotopic effect, 764
  — of Tl λ 5351 line, 764
  experimental methods of, 753
Hyperfine structure—(*contd.*)
  explanation of results, 756
  interval rules in, 755
  of Bi lines, 745, 763
  of Bi λ 4722, 752
  of Bi 2898 line, 755
  of elements possessing more than one istope (Tl), 763
  of spectral lines, 752
  physical nature and importance of, 753.
  quantum number, 756, 758
  selection rules and intensity rules in multiplets of 759
  splitting of Bi levels, 756 (table)
  terms, direct and inverted in, 759
  Zeeman effect of lines possessing
  — (Bismuth), 759
  — λ 4722 of Bi, 761
  — — comparison with experiment, 762
Hyperfine-structure-separation, 758
  comparison with doublet separation, 768
  for positive and negative intervals for, 759
  of S-terms, 768
  — of Na, 768
  theoretical calculation of, 765
Hypothesis
  nebular, of Kant and Laplace, 168
  of spontaneous disintegration, 118
  of sub-electrons, Ehrenhaft's, 61
  Prout's, 87

i—the nuclear quantum number, 756
Inner conversion of X-rays, 485
Inert gases, 565
  spectra of 724
Inner quantum number, 405, 412, 680
  mechanical interpretation of, 430
  significance of, 680
Inner transition, 571, 735
  for Al 736
Insulating power of gases, 1, 3
  comparison of bad conductors and good conductors, 4
Inter-action energy between a single electron and a nucleus (regarded as a magnet) 766
Interaction of the magnetic nucleus

with the extranuclear electrons 758
Intercombination lines, 387
Interference of X-rays, 317
  effect of scattering on, 300
Interval ratio, for triplet P, D, F, G. H terms, 710
Interval rule, 684, **710**
  proof of, **714**
Inverse square law, validity of, 162
  Rutherford and Chadwick's experiments on, 126
Inverted terms, 696
  occurrence of, **714**
Ionisation
  by collision, 16
  chamber **4**, 5
  current, 4
  — saturation, 15
  hypothesis, J. J. Thomson's, 3
  mechanism of, 25
  nature of, 14
  of H 618
  — probability of different modes of, 619
  process of, 4
  ultra, 739
  variation of, with voltage, 14
  various agents of, 3
Ionisation potential
  calculation of 780
  Davis and Goucher's experiment on, 599
  of alkali elements 376
  of elements and ions of the transitional group I, 743 (table).
  of elements and ions of the transitional groups, **742**
  of helium 565
  of three valence elements 569
  of two valence elements 387
  principal, 744
  — of elements and ions of the first transitional group, 743, 744
Ionium, discovery of, 111
Ionometer, 8
Ions
  charge on the, 24
  defined, 3
  diffusion of, **22**
  — coefficients of, 23
  mass of, 25
  mobility of 17 (see under mobility).
Ions—(*contd.*)
  photographing the **26** (see under cloud-chamber).
  physical nature of, 17
  positive, 79
  — production of 88
Iron, soft, variation of magnetisation with temperature, 778
  soft, variation of magnetic susceptibility with temperature, 778
Irregular doublet law, 446, 449 **536, 570**
  illustration of 537
Isochromats, 291
Isotherms 291
Isotopes
  laws of, discussion on **98**
  problems of **87**
  radioactive 104, 106, 108
  table of **102, 108**

J—the inner quantum number, 384, 405 412, **680** (see under inner quantum number).
  selection principles for, 384
jj-coupling, **683**
  equivalent electrons in, **705**
  for Pb and Sn, 6687
  nature of terms in, 685
  terms in 688
  Zeeman effect for, **685**

k, the azimuthal quantum number 343
K—series, 432
  absorption edges in 440
  calculation of absorption frequency for 466
  condition of excitation, 436
  dependence of structuure of, on electrical conductivity 474
  excitation potential of 441
  in soft X-ray region 478
  origin of 431, 462
Kainozoic rocks, 169
Kenotrons 285
Kepler orbits, orientation of, 358
Krypton,
  ionisation potential of 604
  isotopes of 95
Kulenkampff's experiment, 295

l—quantum number, 349
  transition rules for, 722
L—spectrum, 436
  absorption edges in 443
  absorption in very soft X-ray region 477
  causes of multiplicities in 437
  dependence of, on electrical conductivity, 476
  in soft X-ray region 475
  probability of inter-level transition in 480
  term values in 470
Landé-factor g 405, 412 (see under *g*).
  from gyromagnetic effect 816
  for Fe and Ni 816
  of ions of the first transitional and rare earth groups 818
Langevin-function 793
Langevin's theorem 789
Langevin's theory 792
  Weiss's extension of, 795
Lanthanum 112
  structure of 584
Larmor's theorem 391, 819
Laue--diagram
  interpretation of, 254
  symmetry in, 254
Laue's discovery, 222
  experimental verification of, 226
  — result of 227
Laue's theory of X-ray diffraction, 224
Lead
  atomic weights of, 87
  isotopes of, 108, 131
  thoric-and uranic, 87
Lenard's experiment, 590
Life of metastable states, 622
  Matuyama's experiment on 626 (neon).
Life of atom in the excited state, 621
  Webb and Messenger's experiment (Hg 2696, 1849) 623
  Wien's experiment 622
Light, connection with magnetism, 391
  corpuscular theory of 174
  electromagnetic theory of 180
  heterogeneity of 177
  physical properties of, 174
  pressure of, 191
Light—(*contd.*)
  — from quantum theory 192
  wave-theory of 176
Lutecium, structure of, 585
Lyman series, 326

m, the magnetic quantum number, 405
  for strong fields 573
  for *pd*-combination, 689
  selection principles for 406
M-series, 438
  absorption edges in, 444
  in soft region, 477
  interlevel transitions in 478
MM-transitions, 478
Magma, fluid, 168
Magnesium,
  controlled excitation of spectrum, 606
  609 (table).
  isotopes of, 97
  the triplet spectrum of 381
Magnetic field
  in Zeeman effect, 396
  non-homogeneous, 409
Magnetic moment, of O_2 and NO, 784
Magnetic properties, discovery of
  universality of, dia, para and ferro, 771
Magnetic shell, equivalence to a current, 770
Magnetic spectrum of photoelectrons
  emitted by X-ray, 481
  calculation of levels from, 487
Magnetic susceptibilities
  dependence of, on physical state, 787
  of Bi, 777
  of gases, 782
  of inert gases, 785
  of O_2 and NO, 784
  of soft iron, 778
  of water, 780
Magnetic susceptibility, determination of
  Bhatnagar's method, 779
  Bauer and Piccard's method, 783
  Curie's method 775
  Faraday's method 774
  — modification of, 779
  Foëx-method 779
  for liquids, 780

- Magnetic susceptibility—(*contd.*)
  - Gouy's method, **780**
  - interpretation of results on 786
  - Quincke's method, 782
  - — modification of 783
  - Soné's method, **781**
  - — results of, 782
  - Wills and Hector's method **785**
  - for crystals, dynamical method, 786
- Magnetisation, of soft iron, 778
- Magnetism,
  - connection with electricity, 770
  - dia, para and ferro, distribution of, 772
  - experimental studies in, **774**
  - natural, explanation of, 770
  - Weber's theory of, 771
- Magneton,
  - Bohr-402, **403**, 709
  - Weiss, 773, 798
- Manganese, lines of, Catalan's classification of, 677
- Many-electron-problems, **709**
- Mass-number, 98, 99
- Mass-spectra,
  - discussions of, **98**
  - explanation of, **93**
- Mass-spectrograph,
  - Aston's **89**
  - Dempster's **95**
  - resolving power and accuracy of, 92
- Masurium, discovery of, 587
- Matrix mechanics, 420
- Matter, earlier theories of, 89
  - fourth state of, 49
- Maxwell's field equations, **181**
- Median plane, 231
- Mercury ions, multiply charged, 86
- Mesozoic rocks, 169
- Metastable states, 725, (see under life).
- Metastable levels 746, 748
- Method of comparison of isotope masses, **91**
- Method of horizontal comparison **744**
  - illustration of, 745
- Millerian indices, 233
- Minerals, age of,
  - from He-contents, 170
  - from Pb-contents, 171
  - from radioactive data, 168
- Mobility of ions,
  - coefficients of 21
- Mobility—(*contd.*)
  - determination of, experimental
  - —, Langevin's method, **19**
  - —, Rutherford's method, **18**
  - of positive and negative ions, 22
  - relation with coefficient of diffusion, **23**
  - variation of, with pressure **22**
- Moseley curve, 432
  - for K, Ca II, etc. 576
  - in very soft X-rays 476
- Moseley's discovery, 431
- Moseley's work on K-series, 432
- Multiplets *pp*., of Mg-like elements, **734**
- Multiplet separation, calculation of 716
  - for Ti, d^3-configuration, 716

- **N**-series, 438
  - in ultra soft regions, 479
- NN-transitions, 479
- Natural magnetism, explanation of, 770
- Nebulium, 749
- Needle valve, 280
- Negative absorption, 621
- Neon,
  - ionisation potential of, 604
  - isotopes of, 86, 88
  - life of metastable states of 626
- Neutron, 79, 101
- Non-hydrogenic orbits, 540
- Non-penetrating orbits, **538**, **546**
- Nuclear charge,
  - measurement of, 150
  - equal to atomic number, 160, 162
- Nuclear Landé-factor, $g(i)$ 757
- Nuclear moment, 756
  - of proton, 757
  - resultant, 757
- Nuclear quantum number i, 756
- Nuclear theory of atom, 153
  - experimental verification of, **155**, **157**
  - —, mathematical working of **156**
- Nucleus,
  - interaction energy between a single electron and, **766**
  - magnetic, interaction of, with extra-nuclear electrons, 758
  - motion of, 334, see also appendix.
  - radius of, 155

O-series, 481
Optical levels, calculation for any electron composition, 692
Orbit,
  electrical centre of 666
  Keplerian, orientation of, 358
  non-penetrating 538, 546
  penetrating, 538, 548
  precession of 398, 819
Orthoterms, 555
Oxygen, isotopes of, 86

pp-multiplet, 734
  —, of Mg I, Al II, Si III, P IV, S V, Cl VI, 735
Par-terms, 555
Parabola,
  positive rays 85
  method, application of, 86
  — extension of, 88
Paramagnetic moment,
  D. M. Bose's theory, 805
  Hund's theory, 800
  of Fe Cl_2 802
  of ions of the first transitional group (table) 802
  of NO, calculation of, 810
  of NO_2 ClO, calculation of, 811
  of rare-earth ions 804 (table).
  of Sm +++ and Eu+++, 807
  Sommerfeld and Laporte's theory, 805
  Stoner's theory, 807
  Van Vleck's theory, 806
Paramagnetism,
  application of quantum theory on, 798
  Cryomagnetic anomaly in, 796
  discussion of results on, 801
  independent of temperature 808
  Langevin's theory of, 792
  —Weiss's extension of 795
  of diatomic molecules, Van Vleck's theory of, 810
  of molecules, 808
  of polyatomic molecules, Van Vleck's theory, 811
  of rare earth compounds 803
  probability of spontaneous magnetisation in, 797
Particle,
  path of, under a central force, 148
Particle—(*contd.*)
  — application of 152
Parametric face, 233
Pascal's law, for diamagnetism of molecules, 791, 809
Paschen's law, 17
Paschen-Back effect, 396, 401, 426
  explanation of, 427
Pauli's principle, 462, 553, 572
Penetrating orbit, 538, 543
Periodic classification, 525, 526
  Bohr's theory, 531
  Mendeleef's, 526
  Thomson's, 527
Periodicity of spectra, 530
Phosphorescence, 109
Phosphorescent light, 51
Phosphorescent substances, 109
Photoelectric effect, 186
  in X-rays, 440
Photo electrons, 57
  calculation of energy of, 483
  conditions of emissions of 484
  magnetic spectrum of, 481
  space distribution of, 490
  — forward component of, 494
  — lateral, 492
  — longitudinal, 491
  — of K, L, M, 496
  — theoretical explanation of, 492
Photon, 194
Photosphere, 192
Pitch blende, 110
Planck's constant, 190
Point-group, 235
Polarisation,
  estimation of, 809
  — with different values of λ, 805
  of atomic core, 546
  of continuous X-rays, 303
  of scattered X-ray, 221
Polonium, activity of,
  discovery of, radiations emitted by 112
Positive ray,
  analysis of 85, 95, 97
  experimental study of, 80
  method, applications of, 87
  — extension of, 88
  multiply charged, 86
  parabola, J.J. Thomson's, 85
Positron, discovery of, 99
  confirmation of, 100

Positron—(*contd.*)
  production, 101
  tracks of, 86
Potassium,
  isotopes of 95, 97
  — radioactive, 104
Potential,
  cathode fall of, 448
  sparking, 18
  variation of sparking, with pressure, 17
Powder method of crystal structure determination, 250
  calculation of spacings from, 252
Precession,
  of orbit in a magnetic field, 398, 810
  Thomas, 421, 422
Predissociation, 780
Preston's rule, 401
Protactinium, 112
  production of, 130
  structure of, 588
Proton, 78, 757
Protozoic rocks, 169
Protyle, 49
Prout's hypothesis, 87
Pulse theory, 287

Quantum, 183
Quantum conditions, 341
Quantum defect, 546, 548
  for alkali elements, 542
  for d-terms of Na 548
Quantum number,
  azimuthal, 343
  effective, 370
  hyperfine structure, 756, 758
  inner, 384, 405, 412, 680
  — for terms of alkali elements, 385
  — sigificance of, 680
  magnetic, 405
  nuclear, 756
  spin, 416
  total, 343
Quantum theory of light, evidence in favour of, 190
Quantum theory of Zeeman effect, 399

Radiation from radioactive bodies.
  Physical nature of, 112
  Properties of 110, 116
  three types of, alpha, beta, gamma, 112
  — difference in properties of, 113
  — heating effect of, 114
  — ionisation, penetrability photographic and physiological actions of, 114
  — ionisation produced by, 110
  — isolation of, 113
  — magnetic deflections of 113
  — scintillations produced by, 114
Radiation Pressure, Selective, 192
Radio-active constants,
  charts for 123, 124, 128
  Tables for 125, 127
Radio-active data, age of minerals from 168
Radio-active emanation, 121
Radio-active isotopes, 131, 132
Radio-active recoil, 122
Radio-active substances,
  activity, measurement of, 115
  evolution of heat by 164
  — experimental verification of, 165
  — rate of, 166
  proportions in the earth's interior of, 170
Radio-activity,
  discovery and nature of, 109
  growth and decay of 116
  induced 121, 589
  of potassium and rubidium, 110, 104, 106
  of Tl, Pb, Bi, 108
  recovery of, 120
  simple measuring instruments in, 114
Radio-lead, 112, 130
Radium,
  activity of, 111
  atomic weight and atomic number of, 111
  branch products of, 130
    range of alpha-particles from, 144
  discovery of, 110
  disintegration product of, 121
  elements after (Ac, Th, U) 588
  isolation of, 111
  number of Ra-em atoms emitted by, 121
  products of disintegration of, 129
  series, 122, 120

Radium—(*contd.*)
  — charts showing the, 123
  — constants, 125
  structure of, 588
Radium emanation, 121
  atomic number of, 121
  atomic weight of, 121
  number emitted per second, 121
  one curie of, 122
  properties of, 121
Raman effect, 203
Range of alpha-particles
  determination of, Geiger and Nuttall's method, 144
  early experiments on, 140
  extrapolated, 141
  Geiger's method of determination of, 145
  maximum, 141
  — direct determination of, 143
  — — other methods of, 144
  relation with velocity, 142
  Relation with life, 147
  Tables for, 146
Rare earths, 581
  trebly ionised, composition of, 585
Rectification of high tension current by Kenotrons 285
  By mechanical means, 285
  Full wave, 286
Reflexion of X-rays, 229
Refraction of X-rays, 307
Regular doublet law, 446, 460, 468, 548, 550, 570
  modified, 548
Relative abundance of isotopes 98, 102, 108
Relativity doublets, 461
Resonance lines,
  of alkali metals, 376
  of aluminium, 567
  of B, Al, Ga, In, Tl, 569
  of Helium, 558
  of stripped atoms, identification of, 538
  of two valency elements, 387
Resonance potential of alkali metals, 376
  of three valency elements, 387
  of two valency elements, 569
Reversing layer, 198
Rhenium, discovery of, 587
Röntgen rays, 204
  story of discovery of, 204
Rocks,
  Archaean, 173
  division of, 169
  mean conductivity of, 169
Rotating electron, 417
  in the field of nucleus, 420
Runge denominator, 402
Runge's rule, 401
Russell-Saunders coupling 557, 682, 692
Russell-Saunders noation, 536, 550
Rydberg constant, 325
  variation in the value of, 334
Rydberg correction for alkali elements, 547
Rydberg-Schuster law, 362
  failure of, 382
Rydberg sequence,
  in inner electron excitation spectra, 738
  in Ne-spectrum, 725

Scattering, Compton, 193
  change of wavelength at different angles, 158
  experimental evidence regarding recoil electrons, 200
  Geiger and Bothe's experiment, 202
  Modified and unmodified lines, 199
Scattering of alpha particles, 152
  Ideal picture of, 155
  large angle, 153
  — mathematical theory of, 154
  laws of, 157
  small angle, 153
  variation with angle, 158
  variation with thickness, 158
Scattering of beta-rays, 163
Scattering of X-rays, 213
  Compton's theory of, 301
  Debye's theory of 301
  Distribution of intensity of, 299
  effect of interference in 301
Screening constant, 423, 435, 535
  calculation of, 715
  for K-levels 466
  for L-levels, 470
  variation of, with atomic number, 464
Secondary electrons, 481

Selection Principles, 344, 371
  for inner quantum number, 384
Selection rules, 722
  in X-ray spectra, 446
Separation factor A, 717
  for equivalent electron 718
  for non-equivalent electrons 718
  observed and calculated values of, 720 (table)
Series,
  Balmer, 322, 323
  Brackett, 323, 326
  Convergence of (for Ne) 725
  Diffuse 362, 365
  Lyman 322, 326
  Paschen, 326
  Pfund, 323
  Pickering, 333, 335
  Principal 364, 365
  — Importance of, 368
  Ritz, Paschen, 323
  Sharp, 361, 365
Shells of electrons, 528
Singlet spectrum, 380
Slater's diagrammatic method, 698
  for ss-electrons, 699
  for sp-electrons, 700
  for equivalent p-electrons, 701
Solar chromosphere, appearance of He lines in, 652
Sommerfeld and Kossel's displacement law, 375
Sommerfeld's fine structure constant, 347
Space charge-effect, 602
Space groups, 240
Spectra,
  absorption, due to excitation of inner electrons, 736
  — of Hg I, 737
  Complex, definition of, 676
  — History and method of classification of lines, 676
  Controlled excitation of, 605
  due to removal of electrons from inner shells, 736
  Enhanced, 374
  — Systematisation of, 374
  Fraunhofer, of the sun 193, 646
  Multiplet, definition of, 670
  of alkali elements, 534
  of alkali metals, 361
Spectra—(*contd.*)
  — family of terms in, 364
  of atoms and ions with d-shell 726
  of atoms and ions with p-shell, 721
  of aurora, 751
  of bismuth, 754
  of cerium, 731
  of chromium, 740
  of elements belonging to individual periods, 721
  of elements, general explanation of, 332
  of elements of group 2, 380
  — general features of, 381
  of elements of the first transitional group, 728 (Fe I, Fe II, III, IV)
  of faculae, 751
  of Helium, 557
  of inert gases, 724
  of La I, 730
  of La II, 731
  of Li II and Be III, 566
  of Magnesium II in Vacuum arc, 652
  of Manganese, Catalan's classification of 677
  of night sky, 725
  of O III (lines and terms), 723
  of rare earths, 729
  of solar chromosphere, influence of pressure on, 651
  of stars, explanation by ionisation formula, 638
  — general features of variations, 639
  of three-valence elements 566
  of Ti I, 728
  of Ti II, 717, 727
  of Ti II and Ca I, due to double electron transitions, 732
  of Ti III, 727
  of Ti IV, 726
  of transitional elements of groups II and III, 729
  of two-valence elements, 549, 554
  recombination, 331
  second stage, 656
Spectral lines, Breadth of, 338
  Half-width of, 339
Spectrograph, X-ray,
  Bragg, 243
  Double crystal, 271
  Seeman, 267
  Siegbahn, 264

- Spectroscopes, interference, 395
- Spectroscopy of X-rays,
  - absolute method of, 273
  - Bragg's focussing method, 268
  - Concave grating, 277
  - Curved Crystal, 273
  - Double-Crystal, 271
  - in hard region, 268
  - in soft-region, 269
  - Moseley's fixed crystal method, 262
  - Plane grating, 276
  - Seeman, Schneiden and Loch-camera, 267
  - Siegbahn's precision, 264
- Spin doublet, 461
- Spinning electron, 774
- Spinthariscope, 114, 144
- *Spitzentladung*, 33
- Stark effect,
  - Bohr's treatment of, 666
  - Components of H_α, microphotograms of 664
  - experimental arrangement, 657
  - for non-hydrogenic atoms, 671
  - Physical explanation of results, 672
  - further works on, 670
  - intensity distribution of components of Balmer lines in, 665
  - of hydrogen lines for weak fields, 670
  - quantum numbers, 664
  - results on, 687
  - second order, 671
  - selection rules for, 668
  - separation compared to fine structure, 666
  - Theories of, 658
  - —, Epstein's, 659
  - Transition diagram for H_α, 668
- Stars,
  - temperature of, 644
  - types of, 638, 639
- Stellar atmosphere, pressure of, 644
- Stellar spectra,
  - general features of variation, 639
  - of astro-physical importance, 640 (table)
  - variation of intensity, Lockyer's diagram, 642
  - variation of intensity with temperature of subordinate series and enhanced lines, 645
- Stern and Gerlach's experiment, 408
- Stokes' Law, 59, 62, 73
- Stokes' theory of X-ray production, 278
- Straggling of α-rays, 141
- Stripped atoms, 598
- Structure
  - of crystals (see under crystal structure).
  - of hair wool and celluloid, 251
  - of liquids, 261
- Structure diagram,
  - of aluminium, 560
  - of magnesium, 549
  - of sodium, 535
- Structure factor,
  - atomic, 256
  - electronic, 258
- Structure of the atom, 142
  - Planetary, theory of, 153
  - Rutherford's picture, 153
  - Thomson's picture, 152
- Sublevels, electrons to, 532
- Sun,
  - Elements in 647 (table)
  - Fraunhofer's spectrum of 646
  - percentage ionisation of elements of groups I and II in 648 (table)
- Sun spots, percentage of ionisation of elements in 648.
- Symmetry in crystals, 234
  - in Laue diagrams, 253

- Temperature, of recalescence, 771
- Term formula, quantitative, 706
- Term intervals, in spectra of two valence elements, 553, 554
- Terms,
  - anomalous, of Ca, 733
  - arising from equivalent p-electron configuration, 722
  - families of, in the alkali spectrum, 364, 367, 371
  - — absolute value, calculation of, 366
  - — representation of, 366
  - — Sommerfeld's representation of, 371
  - Normal and excited for Ti I, Ti II, Ti III, Ti IV, 726
  - Primed and unprimed, 723

Term Values, 446
  absolute calculation of, 740
  alternative way of designating, 741
  calculation of, 448, 538, 739
  definition of 739
  for barium, 581
  for hydrogenic and non-hydrogenic
    orbits of alkali elements, 541, 546
  for highest and lowest multiplicities
    with largest l-values, 702
  for Na-spectrum, 540
  for penetrating orbits, 543
  highest, for equivalent f and d-
    electrons, 704
  — for many electrons, 705
  S, P, D, for two equivalent p-electrons
  706
  Tables of, 450 (X-ray)
Term values of,
  Al I, 567 (with table)
  Ba 581
  Ba II 851
  Ca II 575
  Cs I, 581
  H, 322, 323
  He I, 559
  K, 575
  L-levels, 470
  Mg I, 550 (table)
  Mg II, 375
  O III 694
  Sc III 575
  Ti IV 575
Theorem of,
  Ampère, 403
  Larmor, 397
Thermal excitation of gases, 628
Thermal Ionisation,
  as a case of reversible reaction,
    calculation of percentage of 633
  in a mixture of gases, 655
  influence of pressure on, 651
  multiple, 637
  Saha's theory of, 630
  — applications of, towards a physical
    explanation of the spectra of stars,
  368
  — Darwin and Fowler's modification
    of 635
  — experimental verification of, 653
  — further modifications of 638
  — Russell's modification, 632
Thermal Ionisation—(*contd.*)
  some apparent difficulties in 649
Thermions, 57
  — velocity distribution of, 596
Thomas precession, 422
Thompson factor, 226
Thomson's theory
  of absorption of X-ray, 513
  of scattering of X-ray, 214
Thorianite, Ceylon, 87
Thorio-lead, 131
Thorium,
  activity of, 117
  branch products, 131
  helium yield of, 171
  lead, 87
  series, 130
  — chart showing the, 124
  — constants of, 127
  structure of, 588
Thorium X, activity of, 117
  ThC, range of α-particles from, 143
  long range groups of α-particles
    from, 143
Threshold frequency, 189
Total reflexion of X-rays, 312
Tracks of alpha-particles 31, 141
  of beta-rays from Ra.D, 163
  of X-rays, 201
  of gamma-rays from Ra.C, 164
Transitional groups, formation of
  first, 577
  of second, 580
Transitions,
  forbidden 372, 748
  rules of, 722
Triangle of vectors, 415
Triplet separation,
  for Be-like ions, 557
  for C, 706
  for Ge, 706
  for Mg like ions, 557
  for Pb, 706
  for Sc to Fe, 710
  for Si, 706
  for Sn, 706
Two electrons problem, 681
  — energy relation for, 682

Ultra ionisation, 780
  for mercury, 789
Uncertainty Principle, 410

Unit cell, 237
  dimension of, 249
Uranio-lead, 87, 130
Uranium,
  Activity of, 117
  Compound, 109
  Helium yield of, 171
  Isotopes of, 130, 131
  Rate of evolution of heat by, 170
  Structure of, 588
Uranium I and II, range of α-particles from, 147
Uranium-radium series, 122, 129
  chart showing the 123
  constants of, 125
Uranium X
  Discovery of, 117

Vacuum in positive ray apparatus, 82
Vacuum spark, 395
Valency, 529
Valve-rectifiers, 285
Vector model of an atom, 416
  of two electrons system, 555
Vector sum,
  of l vectors, 682
  of l-s vectors, 681
  of s vectors, 683

Weight factor, 681
Weiss' hypothesis of internal field, 796
Weiss' law, 796
Weiss' Magneton, 773, 798
Willemite, screen, 51

X-Rays,
  absorption of, 209, 497
  absorption spectrum of, 438
  anomalous dispersion of, 314
  characteristic, 207
  continuous, 287
  diffraction of, 212, 215
  discovery of, 109, 214
  dispersion of, 318
  fluorescent 208, 213, 485, 515
  History, 205
  inner conversion of, 485
  interaction with matter, 206
  interference of, 317
  methods of spectroscopy of, 262
  monochromators for, 515
  optics of, 208
X-rays—(*contd.*)
  photo-electric effect by, 440
  production of, by high tension, 284, 285
  reflection of, 229
  refraction of, 306
  scattering of, 219 (see under scattering of X-rays)
  soft, 473
  term-values in, 450 (table)
  total reflection, 318
X-rays, spectrograph, (see under spectrograph).
X-ray tubes, electron type, 250
  for chemical analysis, 283
  gas filled (ion type), 205, 278

Ytterbium, electron composition of, 685

Zeeman components, calculation of, 406
Zeeman effect, 391
  anomalous, 396, 399
  classical theory of, 391, 392
  experimental verification of, 395
  for jj-coupling, 685
  — expression for, 686
  in high fields 426, 429
  intensity of lines in 408
  Larmor's treatment of, 397
  normal, 393, 394, 396
  of Bi line 4772, 760
  of doublet spectrum 396, 400, 406
  of lines possessing hyper-fine structure 759
  — Bi line 4772, 761
  — comparison with experiments, 762
  of triplet spectrum, 396, 401, 407
  photographs of, 396
  polarisation of lines in normal, 394
  Preston's rule, 401
  Quantum theory of, 399
  — Sommerfeld's generalisation of, 402
  Separation in 406
  transverse view of, 393
Zeeman pattern,
  Regularities in, 401
Zeeman, separations for neon, 686
Zinc, isotopes of, 97

ERRATA

p. 28, last line, *read* B *for* A.

p. 86, line 7, *read* 'largest' *for* 'smallest.'

p. 91, para 1, *read*:

It is now easy to see that if we draw a line ZB, so that it makes an angle θ with $S_1 S_2 Z$, then ZB is the locus of the point (r, θ), *i.e.*, all particles having the same value of e/m, whatever the value of v may be, are focussed on some point in ZB. To prove this we draw a line OX parallel to ZB through O. Let OF cut ZB at F. Then we have $\angle FOX = \phi - 2\theta$, and $OF\,(\phi - 2\theta) = ON = 2b\theta$.

p. 324, equ. (5), *read* h^2 *for* h^3 in the denominator.

p. 335, equ. (16), second line from the bottom, *read* e^4 in the numerator *for* c^4.

p. 356, line 12, *read* $m_0/\sqrt{1-\beta^2}$ *for* $m_0/1\sqrt{-\beta^2}$.

p. 356, equ. (40) *read* $n' + \sqrt{k^2 - \alpha^2 Z^2}$ *for* $n' - \sqrt{k^2 - \alpha^2 Z^2}$.

p. 376, line 6, *read* 'P of four and S of five' *for* 'P of five and S of six.

p. 422, line 14, *read* $-\cos \widehat{sl}$ *for* $\cos \widehat{sl}$.

" equ. (45), *read* $-sl. \cos \widehat{sl}$ *for* $sl. \cos \widehat{sl}$.

p. 583, table 20, *read* 28 Ni . . . $3d^8\, 4s^2$ / $3d^9\, 4s$ *for* 28 Ni . . . $3d^8\, 4s$ / $3d^9\, 4s^2$.

" last column, *read* 90Th *for* 99Th.

p. 677, last line, *add* 'and shown in Fig. 2*a*, Plate XII.'

p. 803, below Fig. 16, *read* '—·—·— Bose' *for* '. . . . Bose.'

p. 809, equ. (44), *read* $n' \neq n$ *for* $n' = n$.